

CE-QUAL-W2: A Two-Dimensional, Laterally Averaged, Hydrodynamic and Water Quality Model, Version 3.72

User Manual

by Thomas M. Cole
Environmental Laboratory
U.S. Army Corps of Engineers
Waterways Experiment Station
Vicksburg, MS 39180-6199

and

Scott A. Wells
Department of Civil and Environmental Engineering
Portland State University
Portland, OR 97207-0751

Department of Civil and Environmental Engineering
Portland State University
Portland, OR 97207-0751

March 2015

CONTENTS

Contents

Contents	ii
Preface.....	xii
List of Figures	xiii
List of Tables.....	xix
Model Release Package	1
1 Introduction	2
Model Overview	2
Terminology used in the CE-QUAL-W2 model.....	2
Model Background	3
Manual	10
2 Capabilities and Limitations.....	11
Capabilities	11
Potential Limitations.....	13
Theoretical.....	13
Numerical.....	14
Input Data	15
3 Model Application.....	16
Overview.....	16
Data Preparation	16
Geometric Data.....	16
Initial Conditions	20
Boundary Conditions.....	20
Hydraulic Parameters (required).....	23
Kinetic Parameters (optional)	23
Calibration Data (required).....	23
Simulations.....	28
Model Preparation.....	28
Calibration.....	28
Lake/Reservoir.....	31
Water budget.....	31
Hydrodynamics and Temperature.....	33
Water Quality.....	46
Estuary	70
Boundary conditions.....	70
Water surface elevations and flows	70
Time of Travel	73
Temperature and Salinity	73
Water Quality.....	76
River	78
Channel Slope.....	78
Channel bottom.....	79
Hydrodynamics and Temperature.....	85

CONTENTS

Water Quality.....	90
Summary.....	99
References.....	100
CE-QUAL-W2 Publications.....	125
Peer Reviewed Publications and Proceedings.....	125
Presentations at Scientific Meetings	129
Reports and Miscellaneous Articles	136
Appendix A Hydrodynamics and Transport	A-1
Coordinate System.....	A-1
Turbulent Time-Averaged Equations	A-2
Continuity	A-3
x-Momentum Equation	A-3
y-Momentum Equation	A-4
z-Momentum Equation	A-5
Coriolis Effect.....	A-6
Adjusting the Coordinate System	A-6
Governing Equations for General Coordinate System	A-9
Continuity	A-9
x-Momentum Equation	A-9
y-Momentum Equation	A-9
z-Momentum Equation	A-9
Simplification of z-Momentum Equation	A-9
Lateral Averaging	A-10
Continuity Equation.....	A-11
x-Momentum Equation	A-13
Shear stresses.....	A-15
Summary of Laterally Averaged Equations.....	A-15
Continuity Equation.....	A-15
x-Momentum Equation	A-15
z-Momentum Equation	A-15
Simplification of Pressure Term	A-16
Free Water Surface.....	A-17
Equation of State.....	A-20
Summary of Governing Equations.....	A-20
Branch Linkage with Internal Head Boundary Conditions	A-21
Linkage of Mainstem Branches.....	A-21
Linkage of Tributary Branches	A-23
Longitudinal Momentum	A-24
Cross-shear of Tributary Inflow	A-25
River Basin Theory.....	A-26
Free-Water Surface Numerical Solution.....	A-26
Horizontal Momentum Numerical Solution.....	A-32
Explicit Solution.....	A-32
Implicit Solution.....	A-34
Computation of Initial Water Surface Slope and Velocity Field for River	A-35
Turbulent Advection-Diffusion Equation	A-37
Water Quality Transport	A-39
Determination of Dz and Dx.....	A-42

CONTENTS

Numerical Solution	A-42
Non-Uniform Grid QUICKEST Formulation	A-45
ULTIMATE/QUICKEST Numerical Transport Solution Scheme	A-47
Vertical Implicit Transport	A-55
Auxiliary Functions	A-56
Surface Shear Stress	A-56
Bottom Shear Stress	A-61
Vertical Shear Stress	A-62
Formulation	A-65
RNG Turbulent Eddy Viscosity Formulation	A-68
Nikuradse Formulation	A-70
Parabolic Formulation	A-71
W2N Formulation	A-71
TKE Formulation	A-72
Algorithm	A-73
Explicit Vertical Convection	A-74
Implicit Vertical Convection	A-78
Boundary and initial conditions for k- ϵ model	A-81
Effect of Vertical Layer Numbers on Vertical Turbulence	A-85
Longitudinal Shear Stress	A-89
Hydraulic Structures	A-89
Internal Weirs	A-93
Water Level Control	A-93
Outlet Structures	A-93
Spillways/Weirs	A-96
Gates	A-103
Branch Momentum Exchange	A-106
Lateral Inflows	A-107
Heat Exchange	A-108
Surface Heat Exchange	A-108
Evaporation	A-111
Equilibrium Temperature	A-114
Sediment Heat Exchange	A-114
Dynamic Shading	A-115
Solar Altitude and Azimuth	A-115
Topographic Shading	A-117
Vegetative Shading	A-117
Data Requirements	A-120
Ice Cover	A-121
Initial Ice Formation	A-122
Air-Ice Flux Boundary Condition and Ice Surface Temperature	
Approximation	A-123
Absorbed Solar Radiation by Water Under Ice	A-123
Ice Melt at Air-Ice Interface	A-124
Ice-Water Flux Boundary Condition Formulation	A-124
Freezing Temperature of Ice	A-125
Density	A-125

CONTENTS

Selective Withdrawal.....	A-126
Sediment Resuspension	128
Appendix B Water Quality.....	B-1
Overview of Kinetic Source/Sink Term	B-1
Generic Constituent	B-3
Conservative Tracer.....	B-4
Coliform Bacteria.....	B-4
Water Age or Residence time	B-5
Inorganic Suspended Solids.....	B-6
Total Dissolved Solids or Salinity.....	B-7
Labile DOM	B-7
Refractory DOM.....	B-8
Labile Particulate Organic Matter	B-9
Refractory Particulate Organic Matter.....	B-10
Carbonaceous Biochemical Oxygen Demand (CBOD).....	B-11
Carbonaceous Biochemical Oxygen Demand - Phosphorus (CBODP)	B-13
Carbonaceous Biochemical Oxygen Demand - Nitrogen (CBODN)	B-14
Algae	B-15
Epiphyton.....	B-20
Macrophytes.....	B-24
Modeling Frictional Force	B-27
Modeling Porosity	B-28
Changes to Governing Equations	B-28
Zooplankton.....	B-30
Phosphorus	B-32
Ammonium	B-35
Nitrate-Nitrite.....	B-37
Dissolved Silica.....	B-39
Organic Matter Variable Stoichiometry	B-40
Labile Dissolved Organic Matter – Phosphorus (LDOM-P)	B-41
Refractory Dissolved Organic Matter – Phosphorus (RDOM-P).....	B-41
Labile Particulate Organic Matter – Phosphorus (LPOM-P).....	B-42
Refractory Particulate Organic Matter – Phosphorus (RPOM-P)	B-43
Labile Dissolved Organic Matter – Nitrogen (LDOM-N)	B-43
Refractory Dissolved Organic Matter – Nitrogen (RDOM-N).....	B-44
Labile Particulate Organic Matter – Nitrogen (LPOM-N).....	B-44
Refractory Particulate Organic Matter – Nitrogen (RPOM-N)	B-45
Particulate Biogenic Silica.....	B-46
Total Iron.....	47
Dissolved Oxygen	B-48
River Reaeration Equations	B-50
Lake Reaeration Equations	B-53
Estuarine Equations.....	B-57
Reaeration Temperature Dependence	B-58
Dam Reaeration.....	B-59
Small Dams or Weirs	B-59
Large Dam Spillways/Gates	B-60
DO Impacts of Spillways	B-61

CONTENTS

Dissolved Oxygen Saturation Computations.....	B-62
Sediments.....	B-62
Sediment Variable Stoichiometry and Kinetics.....	B-65
Sediment Phosphorus.....	B-65
Sediment Nitrogen.....	B-66
Sediment Carbon.....	B-66
Total Inorganic Carbon.....	B-67
Alkalinity.....	B-70
pH and Carbonate Species.....	B-70
Temperature Rate Multipliers.....	B-74
Appendix C Input/Output Data Description.....	C-1
Input Files.....	C-1
Control File.....	C-1
Title (TITLE C).....	C-2
Grid Dimensions (GRID).....	C-3
Inflow/Outflow Dimensions (IN/OUTFLOW).....	C-4
Constituent Dimensions (CONSTITUENTS).....	C-5
Miscellaneous (MISCELL).....	C-6
Time Control (TIME CON).....	C-8
Timestep Control (DLT CON).....	C-9
Timestep Date (DLT DATE).....	C-10
Maximum Timestep (DLT MAX).....	C-11
Timestep Fraction (DLT FRN).....	C-12
Timestep Limitations (DLT LIMIT).....	C-13
Branch Geometry (BRANCH G).....	C-14
Waterbody Definition (LOCATION).....	C-16
Initial Conditions (INIT CND).....	C-18
Calculations (CALCULAT).....	C-21
Dead Sea (DEAD SEA).....	C-23
Interpolation (INTERPOL).....	C-24
Heat Exchange (HEAT EXCH).....	C-26
Ice Cover (ICE COVER).....	C-28
Transport Scheme (TRANSPORT).....	C-30
Hydraulic Coefficients (HYD COEF).....	C-31
Vertical Eddy Viscosity (EDDY VISC).....	C-33
Number of Structures (N STRUC).....	C-36
Structure Interpolation (STR INT).....	C-37
Structure Top Selective Withdrawal Limit (STR TOP).....	C-38
Structure Bottom Selective Withdrawal Limit (STR BOT).....	C-39
Sink Type (SINK TYPE).....	C-40
Structure Elevation (E STRUC).....	C-41
Structure Width (W STRUC).....	C-42
Pipes (PIPES).....	C-43
Upstream Pipe (PIPE UP).....	C-46
Downstream Pipe (PIPE DOWN).....	C-47
Spillways (SPILLWAYS).....	C-48
Upstream Spillways (SPILL UP).....	C-51

CONTENTS

Downstream Spillways (SPILL DOWN)	C-52
Spillway Dissolved Gas (SPILL GAS)	C-53
Gates (GATES).....	C-56
Gate Weir (GATE WEIR).....	C-60
Upstream Gate (GATE UP)	C-62
Downstream Gate (GATE DOWN)	C-63
Gate Dissolved Gas (GATE GAS)	C-64
Pumps 1 (PUMPS 1).....	C-67
Pumps 2 (PUMPS 2).....	C-70
Internal Weir Segment Location (WEIR SEG)	C-71
Internal Weir Top Layer (WEIR TOP).....	C-73
Internal Weir Bottom Layer (WEIR BOT).....	C-74
Withdrawal Interpolation (WD INT)	C-75
Withdrawal Segment (WD SEG)	C-76
Withdrawal Elevation (WD ELEV).....	C-77
Withdrawal Top Layer (WD TOP)	C-78
Withdrawal Bottom Layer (WD BOT)	C-79
Tributary Inflow Placement (TRIB PLACE)	C-80
Tributary Interpolation (TRIB INT).....	C-81
Tributary Segment (TRIB SEG)	C-82
Tributary Inflow Top Elevation (TRIB TOP).....	C-83
Tributary Inflow Bottom Elevation (ELEV BOT)	C-84
Distributed Tributaries (DST TRIB).....	C-85
Hydrodynamic Output Control (HYD PRINT)	C-86
Snapshot Print (SNP PRINT)	C-88
Snapshot Dates (SNP DATE).....	C-89
Snapshot Frequency (SNP FREQ).....	C-90
Snapshot Segments (SNP SEG)	C-91
Screen Print (SCR PRNT).....	C-92
Screen Dates (SCR DATE).....	C-93
Screen Frequency (SCR FREQ).....	C-94
Profile Plot (PRF PLOT)	C-95
Profile Date (PRF DATE)	C-96
Profile Frequency (PRF FREQ).....	C-97
Profile Segment (PRF SEG)	C-98
Spreadsheet Profile Plot (SPR PLOT)	C-99
Spreadsheet Profile Date (SPR DATE)	C-100
Spreadsheet Profile Frequency (SPR FREQ).....	C-101
Spreadsheet Profile Segment (SPR SEG)	C-102
Vector Plot (VPL PLOT)	C-103
Vector Plot Date (VPL DATE).....	C-104
Vector Plot Frequency (VPL FREQ).....	C-105
Contour Plot (CPL PLOT)	C-106
Contour Plot Dates (CPL DATE).....	C-108
Contour Plot Frequency (CPL FREQ).....	C-109
Kinetic Flux Output (FLUXES).....	C-110
Kinetic Flux Date (KFL DATE).....	C-111
Kinetic Flux Frequency (FLX FREQ).....	C-112

CONTENTS

Time Series Plot (TSR PLOT)	C-113
Time Series Date (TSR DATE)	C-114
Time Series Frequency (TSR FREQ).....	C-115
Time Series Segment (TSR SEG)	C-116
Time Series Elevation (TSR ELEV)	C-117
Withdrawal Output (WITH OUT)	C-118
Withdrawal Output Date (WDO DATE)	C-120
Withdrawal Output Frequency (WDO FREQ)	C-121
Withdrawal Output Segment (WITH SEG)	C-122
Restart (RESTART)	C-123
Restart Date (RSO DATE)	C-124
Restart Frequency (RSO FREQ)	C-125
Constituent Computations (CST COMP)	C-126
Active Constituents (CST ACTIVE)	C-128
Derived Constituents (CST DERIVE)	C-130
Constituent Fluxes (CST FLUX).....	C-132
Constituent Initial Concentration (CST ICON)	C-134
Constituent Output (CST PRINT).....	C-136
Inflow Active Constituent Control (CIN CON)	C-138
Tributary Active Constituent Control (CTR CON).....	C-140
Distributed Trib Active Constituent (CDT CON).....	C-142
Precipitation Active Constituent Control (CPR CON)	C-144
Extinction Coefficient (EX COEF)	C-146
Algal Extinction (ALG EX)	C-149
Zooplankton Extinction (ZOO EX).....	C-150
Macrophyte Extinction (MAC EX)	C-151
Generic Constituent (GENERIC).....	C-152
Suspended Solids (S SOLIDS)	C-154
Algal Rates (ALGAL RATE).....	C-155
Algal Temperature Rate Coefficients (ALG TEMP)	C-169
Algal Stoichiometry (ALG STOICH).....	C-171
Epiphyte/Periphyton Control (EPIPHYTE).....	C-174
Epiphyte/Periphyton Print (EPI PRINT)	C-175
Epiphyte/Periphyton Initial Density (EPI INI).....	C-176
Epiphyte/Periphyton Rate (EPI RATE).....	C-177
Epiphyte/Periphyton Half-Saturation (EPI HALF).....	C-178
Epiphyte/Periphyton Temperature Rate Coefficients (EPI TEMP)	C-180
Epiphyte/Periphyton Stoichiometry (EPI STOICH)	C-182
Zooplankton Rate (ZOO RATE)	C-183
Zooplankton Algal Preference (ZOO ALGP)	C-184
Zooplankton Zooplankton Preference (ZOO ZOO).....	C-185
Zooplankton Temperature Rate Coefficients (ZOO TEMP)	C-186
Zooplankton Stoichiometry (ZOO STOICH)	C-188
Macrophyte Control (MACROPHYT).....	C-189
Macrophyte Print (MAC PRINT)	C-190
Macrophyte Initial Concentration (MAC INI).....	C-191
Macrophyte Rate (MAC RATE)	C-192

CONTENTS

Macrophyte Sediments (MAC SED)	C-194
Macrophyte Distribution (MAC DIST)	C-195
Macrophyte Drag (MAC DRAG)	C-196
Macrophyte Temperature Rate Coefficients (MAC TEMP)	C-197
Macrophyte Stoichiometry (MAC STOICH)	C-199
Dissolved Organic Matter (DOM)	C-200
Particulate Organic Matter (POM)	C-201
Organic Matter Stoichiometry (OM STOICH)	C-203
Organic Matter Temperature Rate Multipliers (OM RATE)	C-204
Carbonaceous Biochemical Oxygen Demand (CBOD)	C-205
CBOD Stoichiometry (CBOD STOICH)	C-206
Inorganic Phosphorus (PHOSPHOR)	C-207
Ammonium (AMMONIUM)	C-208
Ammonium Temperature Rate Multipliers (NH4 RATE)	C-210
Nitrate (NITRATE)	C-211
Nitrate Temperature Rate Multipliers (NO3 RATE)	C-212
Silica (SILICA)	C-213
Iron (IRON)	C-214
Sediment Carbon Dioxide Release (SED CO2)	C-215
Oxygen Stoichiometry 1 (STOICH 1)	C-216
Oxygen Stoichiometry 2 (STOICH 2)	C-217
Oxygen Stoichiometry 3 (STOICH 3)	C-218
Oxygen Stoichiometry 4 (STOICH 4)	C-219
Oxygen Stoichiometry 5 (STOICH 5)	C-220
Oxygen Limit (O2 LIMIT)	C-221
Sediment Compartment (SEDIMENT)	C-222
SOD Temperature Rate Multipliers (SOD RATE)	C-224
Zero-Order Sediment Oxygen Demand (S DEMAND)	C-225
Reaeration (REAERAT)	C-226
Restart Input Filename (RSI FILE)	C-230
Withdrawal Filename (QWD FILE)	C-231
Gate Outflow Filename (QGT FILE)	C-232
Wind Sheltering Filename (WSC FILE)	C-233
Dynamic Shading Filename (SHD FILE)	C-234
Bathymetry Filename (BTH FILE)	C-235
Meteorology Filename (MET FILE)	C-236
Light Extinction Filename (EXT FILE)	C-237
Vertical Profile Filename (VPR FILE)	C-238
Longitudinal Profile Filename (LPR FILE)	C-239
Branch Inflow Filename (QIN FILE)	C-240
Branch Inflow Temperature Filename (TIN FILE)	C-241
Branch Inflow Constituent Filename (CIN FILE)	C-242
Branch Outflow Filename (QOT FILE)	C-243
Tributary Inflow Filename (QTR FILE)	C-244
Tributary Inflow Temperature Filename (TTR FILE)	C-245
Tributary Inflow Concentration Filename (CTR FILE)	C-246
Distributed Tributary Inflow Filename (QDT FILE)	C-247
Distributed Tributary Inflow Temperature Filename (TDT FILE)	C-248

CONTENTS

Distributed Tributary Inflow Concentration Filename (CDT FILE)	C-249
Precipitation Filename (PRE FILE)	C-250
Precipitation Temperature Filename (TPR FILE)	C-251
Precipitation Concentration Filename (CPR FILE)	C-252
External Upstream Head Filename (EUH FILE)	C-253
External Upstream Head Temperature Filename (TUH FILE)	C-254
External Upstream Head Concentration Filename (CUH FILE)	C-255
External Downstream Head Filename (EDH FILE)	C-256
External Downstream Head Temperature Filename (TDH FILE)	C-257
External Downstream Head Concentration Filename (CDH FILE)	C-258
Snapshot Filename (SNP FILE)	C-259
Profile Plot Filename (PRF FILE)	C-260
W2 Linkage Output Filename (VPL FILE)	C-261
Contour Plot Filename (CPL FILE)	C-262
Spreadsheet Profile Plot Filename (SPR FILE)	C-263
Flux Filename (FLX FILE)	C-264
Time Series Plot Filename (TSR FILE)	C-265
Withdrawal Output Filename (WDO FILE)	C-266
Sample Control Input File	C-267
Bathymetry File	C-295
Comma Delimited Bathymetry File Format	C-301
Fish Habitat Volumes and Volume-Weighted Averages of Eutrophication State	
Variables	C-303
Fish habitat volumes	C-304
Volume weighted segment and surface averages	C-308
Output of overall organic matter accumulation at the bottom of each layer	
and summed for each segment	C-310
Automatic Port Selection and Reservoir Volumes at Specified Temperatures....	C-311
Temperature of outlet releases	C-311
Automatic selection of outlet port to control temperature	C-312
Volume of Reservoir at a Temperature Threshold	C-318
Environmental Performance Criteria	C-323
Hypolimnetic Aeration	C-328
Meteorology File	C-332
Dynamic Elevation for Structure Outflows	C-334
Dynamic Pump Input File	C-335
Dynamic Pipe Input File	C-336
Gate File	C-337
Light Extinction File	C-340
Wind Sheltering Coefficient File	C-341
Shade Input File	C-343
Branch Inflow File	C-349
Branch Inflow Temperature File	C-350
Branch Inflow Constituent Concentration File	C-351
Branch Outflow File	C-354
Withdrawal File	C-356
Tributary Inflow File	C-357

CONTENTS

Tributary Inflow Temperature File	C-358
Tributary Inflow Concentration File	C-359
Branch Distributed Tributary Inflow File	C-360
Branch Distributed Tributary Inflow Temperature File	C-361
Branch Distributed Tributary Inflow Concentration File	C-362
Branch Precipitation File	C-363
Branch Precipitation Temperature File	C-364
Branch Precipitation Concentration File	C-365
Branch External Upstream Head Elevation File	C-366
Branch External Upstream Head Temperature File	C-367
Branch External Upstream Head Constituent Concentration File	C-368
Branch External Downstream Head Elevation File	C-370
Branch External Downstream Head Temperature File	C-371
Branch External Downstream Head Concentration File	C-372
Vertical Profile File	C-373
Longitudinal Profile File	C-375
Graph Input File	C-380
Output FilesSnapshot	C-382
Title Cards	C-382
Time Parameters	C-382
Meteorological Parameters	C-383
Inflow/Outflow Parameters	C-383
Balances	C-385
Geometry	C-387
Water Surface	C-388
Temperature/Water Quality	C-388
Time Series	C-390
Preprocessor	C-393
Command-line working directory specification	C-393
Output (pre.opt)	C-393
Warning Messages (pre.wrn)	C-409
Error Messages (pre.err)	C-410
Spreadsheet Profile Plot	C-411
Profile Plot	C-412
Vector Plot	C-416
Contour Plot	C-416
Kinetic Fluxes	C-419
Withdrawal Outflow	C-421
Flow Balance Output File	C-422
Water Level Output File	C-423
Run-time Warnings	C-424
Run-time Errors	C-426
Command-line working directory specification for w2 windows executable	C-429

PREFACE

Preface

This manual documents the two-dimensional, laterally averaged, hydrodynamic and water quality model CE-QUAL-W2.

The principal investigator for the CE-QUAL-W2 and the User Manual was Mr. Thomas M. Cole of the Water Quality and Contaminant Modeling Branch (WQCMB), Environmental Processes and Effects Division (EPED), Environmental Laboratory. Since his retirement around 2005, Dr. Scott Wells has been responsible for all manual updates and changes.

This report supercedes the earlier model version 3.6. Revisions to this manual since the Version 3.2 manual were made under the direction of Dr. Scott Wells at Portland State University (PSU). Dr. Chris Berger at PSU contributed significantly to V3.5. Dr. Berger's macrophyte algorithm was one of the many new features starting with V3.5. The assistance of Dr. Robert Annear is also gratefully acknowledged in the shading algorithm and general support and assistance. Samuel Gould, a Master's student at PSU, contributed to the write-up and development of the $k-\epsilon$ turbulence model.

Version 3.72 includes a new automatic port selection algorithm from the USGS (Rounds and Buccola, 2015). Details are shown in the new section on the `w2_selective.npt` file.

This report should be cited as follows:

Cole, T.M., and Wells, S. A. (2015) "CE-QUAL-W2: A two-dimensional, laterally averaged, hydrodynamic and water quality model, version 3.72," Department of Civil and Environmental Engineering, Portland State University, Portland, OR.

List of Figures

Figure 1. Sample computational grid in the x-z plane showing active and inactive cells.	18
Figure 2. Sample computational grid in the x-y plane showing cell numbering and branch and water body connections.	19
Figure 3. Allatoona Reservoir computed (lines) vs. observed (symbols) water surface elevations for 1992, 1993, 1996, and 1997.....	33
Figure 4. 1989 Pineflat Reservoir computed versus observed temperatures.	38
Figure 5. 1993 Pineflat Reservoir computed versus observed temperatures.	38
Figure 6. 1981 Bluestone Reservoir computed versus observed temperatures.	39
Figure 7. 1983 Bluestone Reservoir computed versus observed temperatures.	39
Figure 8. 1988 Richard B. Russell computed versus observed temperatures.	40
Figure 9. 1994 Richard B. Russell computed versus observed temperatures.	41
Figure 10. 1996 Richard B. Russell computed versus observed temperatures.	41
Figure 11. Paintsville Reservoir computed versus observed temperatures.	42
Figure 12. 1992 Brownlee Reservoir computed versus observed temperatures.	43
Figure 13. 1995 Brownlee Reservoir computed versus observed temperatures.	44
Figure 14. C.J. Strike Reservoir computed versus observed temperatures.	45
Figure 15. Allatoona Reservoir computed vs. observed DO.	47
Figure 16. Brownlee Reservoir computed vs. observed DO.	48
Figure 17. C.J. Strike Reservoir computed vs. observed DO.	48
Figure 18. DeGray Reservoir computed vs. observed DO.	49
Figure 19. Richard B. Russell Reservoir computed vs. observed DO, March through June, 1988.	49
Figure 20. Richard B. Russell Reservoir computed vs. observed DO, June through October, 1988.	50
Figure 21. 1996 Richard B. Russell computed vs. observed DO.	50
Figure 22. Neely Henry Reservoir computed vs. observed DO.	51
Figure 23. J. Strom Thurmond Reservoir computed vs. observed DO.	51
Figure 24. Monroe Reservoir computed vs. observed DO.	52
Figure 25. Rimov Reservoir computed vs. observed DO.	52
Figure 26. Shepaug Reservoir computed vs. observed DO.	53
Figure 27. Shepaug Reservoir computed vs. observed DO.	53
Figure 28. Weiss Reservoir computed vs. observed DO.	54
Figure 29. West Point Reservoir computed vs. observed DO.	55
Figure 30. Walter F. George Reservoir computed vs. observed DO.	55
Figure 31. Rimov Reservoir computed vs. observed phytoplankton biomass.	57
Figure 32. Rimov Reservoir computed vs. observed phytoplankton biomass.	58
Figure 33. Rimov Reservoir computed vs. observed phytoplankton biomass.	59
Figure 34. Rimov Reservoir computed vs. observed phytoplankton biomass.	59

LIST OF FIGURES

Figure 35. Rimov Reservoir computed vs. observed phytoplankton biomass.....	60
Figure 36. Rimov Reservoir computed vs. observed phytoplankton biomass.....	61
Figure 37. Rimov Reservoir computed vs. observed phytoplankton with wind rotated 90°.....	62
Figure 38. Rimov Reservoir computed vs. observed phytoplankton with wind rotated 90°	63
Figure 39. Rimov Reservoir computed vs. observed phytoplankton with wind rotated 90°.....	63
Figure 40. Rimov Reservoir computed vs. observed phytoplankton with wind rotated 90°.....	64
Figure 41. Rimov Reservoir computed vs. observed phytoplankton with wind rotated 90°.....	64
Figure 42. Rimov Reservoir computed vs. observed phytoplankton with wind rotated 90°.....	65
Figure 43. Rimov Reservoir computed vs. observed phytoplankton with no inflowing phytoplankton.....	66
Figure 44. Rimov Reservoir computed vs. observed phytoplankton with no inflowing phytoplankton.....	67
Figure 45. Rimov Reservoir computed vs. observed phytoplankton with no inflowing phytoplankton.....	67
Figure 46. Rimov Reservoir computed vs. observed phytoplankton with no inflowing phytoplankton.....	68
Figure 47. Rimov Reservoir computed vs. observed phytoplankton with no inflowing phytoplankton.....	69
Figure 48. Rimov Reservoir computed vs. observed phytoplankton with no inflowing phytoplankton.....	69
Figure 49. Water level data versus model predictions for Longview, WA during a 20-day period in 1993.....	72
Figure 50. Model flow predictions versus data for a 20-day period during 1998 at Beaver Army Terminal near Quincy, OR.....	72
Figure 51. Patuxent River computed versus observed vertical salinity distributions.....	74
Figure 52. Patuxent River computed versus observed vertical temperature distributions.	75
Figure 53. Patuxent River computed versus observed nutrient, dissolved oxygen, and chl <i>a</i> time series.....	77
Figure 54. Snake River water level comparison between CE-QUAL-W2 V3 and USGS field data.....	79
Figure 55. Channel vertical grid where every slope change is a new branch.....	79
Figure 56. Snake River channel slope determination.....	80
Figure 57. Channel slope for the Bull Run system.....	82
Figure 58. Vertical grid for W2 model of Bull Run Lower River.....	83
Figure 59. Bull Run River computed versus observed tracer at three stations progressing downstream.....	85
Figure 60. Spokane River computed versus observed water surface elevations at Spokane.....	86
Figure 61. Spokane River computed versus observed flows at the city of Spokane.....	86
Figure 62. Snake River computed versus observed temperature at six stations.....	88

LIST OF FIGURES

Figure 63. Computed versus observed temperatures for the Spokane River at Stateline Bridge (upstream boundary), City of Spokane, Fort Wright Bridge, and Riverside State Park.....	89
Figure 64. Spokane River computed versus observed conductivity below Nine Mile Dam.....	90
Figure 65. Snake River computed versus observed dissolved oxygen at six stations....	91
Figure 66. Snake River computed versus observed orthophosphorus at six stations. ...	93
Figure 67. Snake River computed versus observed nitrate-nitrite at six stations.	94
Figure 68. Snake River computed versus observed chlorophyll a at six stations.	95
Figure 69. Snake River computed versus total organic carbon.....	96
Figure 70. Spokane River computed versus observed dissolved oxygen at Riverside State Park.....	96
Figure 71. Spokane River computed versus observed dissolved oxygen below Nine Mile Dam.....	97
Figure 72. Spokane River computed versus observed pH upstream of Nine Mile Dam.	97
Figure 73. Spokane River computed versus observed nitrate-nitrite at Riverside State Park.....	98
Figure 74. Spokane River computed versus observed soluble reactive phosphorus below Nine Mile Dam.....	98
Figure 75. Spokane River computed versus observed total nitrogen below Nine Mile Dam.....	99
Figure A-1. Definition sketch of coordinate system for governing equations where x is oriented east, y is oriented north, and z is oriented upward.....	A-1
Figure A-2. Definition sketch of turbulent time averaging for velocity.	A-2
Figure A-3. Definition sketch of turbulent shear stresses in x-direction.	A-4
Figure A-4. Sketch of turbulent shear stresses in y-direction.	A-5
Figure A-5. Sketch of turbulent shear stresses in z-direction.	A-6
Figure A-6. General coordinate system with z-axis compatible with original derivation of W2 model.	A-7
Figure A-7. Sketch of channel slope and coordinate system for W2 where the x-axis is oriented along the channel slope.....	A-8
Figure A-8. Lateral average and deviation from lateral average components of longitudinal velocity.....	A-11
Figure A-9. Schematization for simplification of pressure term.	A-16
Figure A-10. Coordinate system without channel slope.	A-18
Figure A-11. Coordinate system with channel slope.	A-18
Figure A-12. Definition sketch for channel slope.	A-21
Figure A-13. Computational grid variable definitions for arbitrary channel slope.	A-22
Figure A-14. Transfer of mass and momentum between branches with unequal vertical grid spacing.....	A-23
Figure A-15. Linkage of tributary branch coming in at an angle to main branch.....	A-24
Figure A-16. Schematic of x and y velocity components.	A-25
Figure A-17. Velocity variability with time.....	A-37
Figure A-18. Concentration variability with time.....	A-37
Figure A-19. Lateral average of the velocity field.....	A-39
Figure A-20. Lateral average of the concentration field.....	A-40
Figure A-21. Variable locations in computational grid.....	A-43
Figure A-22. ULTIMATE schematization for positive flow.	A-48

LIST OF FIGURES

Figure A-23. ULTIMATE schematization for negative flow.....	A-49
Figure A-24. Definition sketch for monotonic solution domain.....	A-51
Figure A-25. Comparison of UPWIND, QUICKEST, and ULTIMATE/QUICKEST schemes for conservative tracer transport.	A-52
Figure A-26. Definition sketch for variable velocity.....	A-54
Figure A-27. Shear stress at the air-water surface.....	A-57
Figure A-28. Segment orientation.	A-58
Figure A-29. Wind orientation.	A-59
Figure 30. Comparison of current W2 model computation of CD and that recommended as a lower limit by Wuest and Lorke (2003).....	A-60
Figure 31. Surface shear stress for V3.6 and later compared to V3.5 and earlier.....	A-61
Figure A-32. Variation of turbulent vertical eddy viscosity for flow of $2574 \text{ m}^3 \text{ s}^{-1}$ flow down a channel of length 30 km and width of 100 m at $x=15 \text{ km}$	A-64
Figure A-33. Variation of turbulent vertical eddy viscosity for flow of $2574 \text{ m}^3 \text{ s}^{-1}$ flow down a channel of length 30 km and width of 100 m measured at $x=15 \text{ km}$	A-65
Figure A-34. Comparison of vertical velocity predictions of W2 model with various eddy viscosity models compared to theory.	A-65
Figure A-35. Conceptual diagram of wind induced motion.....	A-66
Figure A-36. Mixing length as a function of depth for the Nikuradse formulation.	A-70
Figure A-37. Variation of A_z with depth for the parabolic model of Englund (1976).	A-71
Figure 38. CE-QUAL-W2 computational grid. Width, density, pressure and water quality state variables are defined at cell centers. Horizontal velocity, longitudinal eddy viscosity and diffusivity, and longitudinal shear stress are defined at the right hand side of the cell. Vertical velocity and vertical diffusivity is defiend at the bottom of the cell, and the vertical eddy viscosity is defined at the lower right corner of the cell. .A-	74
Figure A-39. Variation of Manning's friction factor using formulae from Limerinos (1970) and Jarrett (1984) for a channel slope, S , of 0.0005 and 84 th pecentile diameter of the bed material, d_{84} , of 50.	A-86
Figure A-40. Comparison of vertical velocity predictions with one, three, and seven vertical layers	A-87
Figure A-41. Comparison of elevation drop of W2 model with one, three, and seven vertical layers with same Manning's friction factor.	A-88
Figure A-42. Schematic of linkage of model segments with a culvert.	A-89
Figure A-43. Linkage schematic of model segments with a culvert.	A-92
Figure A-44. Computed versus observed flow using dynamic culvert model.....	A-92
Figure A-45. Schematic representation of internal weirs.	A-93
Figure A-46. Radial gates and spillway flow.	A-94
Figure A-47. Flow rate over a spillway or weir for submerged and free flowing conditions.	A-101
Figure A-48. Flow at a submerged weir.....	A-102
Figure A-49. Flow rate variation with gate opening.	A-104
Figure A-50. Selective withdrawal with outflow connected to a valve with a gate.	A-105
Figure A-51. Schematic of branch connection.	A-106
Figure A-52. Comparison of the wind speed formualtion for Ryan-Harleman and W2 default (for $T_{\text{air}}=15^\circ\text{C}$, $T_{\text{dew}}=-5^\circ\text{C}$, $T_{\text{surface}}=25^\circ\text{C}$).....	A-113
Figure A-53. Schematic of solar altitude, A_o , and azimuth, AZ	A-116

LIST OF FIGURES

Figure A-54. Schematic of topographic and vegetative shading, solar altitude (α_0), and vegetation height (T) and their affect on shadow length.	A-117
Figure A-55. Azimuth angle, α_{AZ} , and stream orientation, Θ_0	A-119
Figure A-56. Relationship between azimuth, stream orientation, and shadow length. ...	A-119
Figure B-1. Internal flux for generic constituent compartment.	B-3
Figure B-2. Internal flux for coliform bacteria.	B-4
Figure 3. Water age in Chester Morse Lake, WA.	B-5
Figure B-4. Internal flux for inorganic suspended solids.	B-6
Figure B-5. Internal flux between labile DOM and other compartments.	B-7
Figure B-6. Internal flux between refractory DOM and other compartments.	B-8
Figure B-7. Internal flux between Labile POM and other compartments.	B-9
Figure B-8. Internal flux between refractory POM and other compartments.	B-11
Figure B-9. Internal flux between CBOD and other compartments in Version 3.6 and earlier.	B-12
Figure B-10. Internal flux between CBOD and other compartments in Version 3.7 and later.	B-12
Figure 11. Internal flux between CBODP and other compartments.	B-14
Figure 12. Internal flux between CBODN and other compartments.	B-15
Figure B-13. Internal flux between algae and other compartments.	B-16
Figure B-14. Internal flux between epiphyton and other compartments.	B-20
Figure 15. Nutrient fluxes for the macrophyte compartment in CE-QUAL-W2.	B-25
Figure 16. Zooplankton source/sinks.	B-31
Figure B-17. Internal flux between phosphorus and other compartments.	B-33
Figure B-18. Internal flux between ammonium and other compartments.	B-36
Figure B-19. Internal flux between nitrate + nitrite and other compartments.	B-38
Figure B-20. Internal flux between dissolved silica and other compartments.	B-39
Figure B-21. Internal flux between particulate biogenic silica and other compartments.	B-46
Figure B-22. Internal flux between total iron and other compartments.	47
Figure B-23. Internal flux between dissolved oxygen and other compartments.	B-48
Figure B-24. Reaeration coefficient as a function of flow rate.	B-53
Figure B-25. Variation of wind speed and K_L for lake/reservoir equations.	B-55
Figure B-26. Wind speed of 5 m s^{-1} and a fetch of 5 km corrected to 10 m as a function of measuring height on land.	B-56
Figure B-27. Wind speed of 5 m s^{-1} corrected to 10 m as a function of fetch.	B-56
Figure B-28. Wind corrected to 10 m based on wind measured on land.	B-57
Figure B-29. Variation of K_{LT}/K_{L20} as a function of temperature.	B-59
Figure B-30. Internal flux between 0-order sediment compartment and other compartments.	B-63
Figure B-31. Internal flux between 1st-order sediment compartment and other compartments.	B-63
Figure B-32. Internal flux between inorganic carbon and other compartments.	B-67
Figure B-33. Temperature rate multiplier function.	B-75
Figure C-34. Layer numbers and segments for a sloping waterbody where segment 9 is the last active segment of the waterbody. EBOT is 268.82 m, which is the lowest elevation in the waterbody and is the bottom elevation of layer 13 or KMX-1 (where KMX=14).	C-17

LIST OF FIGURES

Figure C-35. Layer numbers and segments for a branch with a zero slope where segment 37 is the last active segment of the branch. EBOT for this waterbody is 261.21 m and is the bottom elevation of layer 13 or KMX-1 (where KMX=14).	C-17
Figure 36. Cross-section of current rectangular grid system.....	C-19
Figure 37. Various solutions to fitting a cross-section –trapezoidal layers compared to multiple rectangular layers.....	C-19
Figure 38. Description of internal weir in CE-QUAL-W2 at downstream side of segment.	C-72
Figure 39. Growth rate as a function of temperature.....	C-169
Figure 40. Growth rate as a function of temperature.....	C-181
Figure 41. Growth rate as a function of temperature.....	C-186
Figure 42. Growth rate as a function of temperature.....	C-197
Figure 43. Organic matter decay as a function of temperature.	C-204
Figure 44. Ammonia decay as a function of temperature.	C-210
Figure 45. Denitrification as a function of temperature.	C-212
Figure 46. Illustration of sediment focusing rate.	C-223
Figure 47. SOD rate as a function of temperature.	C-224
Figure 48. New bathymetry file format in csv format within Excel.	C-302
Figure 49. Small mouth bass habitat in DeGray reservoir for 1980.	C-308
Figure 50. Outlet temperature as a function of time illustrating selective withdrawal meeting temperature target of 15°C between Julian day 1 and 45.	C-317
Figure 51. Environmental performance for 3 different scenario runs comparing dissolved oxygen in a eutrophic system Eucha Reservoir in OK.	C-328
Figure 52. Side view of DeGray Lake grid used for hypolimnetic aeration.	C-330
Figure 53. Dissolved oxygen at probe location and cumulative oxygen added in kg over period of aeration (Julian day 1-125). Target dissolved oxygen at probe location was between 11 and 12.5 mg/l.....	C-331
Figure C-1. Tree top elevation and vegetation offset from a river.....	C-345
Figure C-2. The influence of topographic shading along a river.....	C-347
Figure C-3. Topographic slices at three segments along a river.....	C-347
Figure C-4. Diagram illustrating unstable water surface elevation solution.....	C-424

List of Tables

Table 1. General guidelines for in-pool water quality sampling.....	25
Table 2. Constituent levels and names.	26
Table 3. Coefficients affecting thermal calibration.....	34
Table 4. Reservoir thermal simulations with error statistics for station closest to dam...	36
Table A-5. Governing equations with and without channel slope.....	A-20
Table A-6. Vertical eddy viscosity formulations.....	A-62
Table A-7. HEC-RAS flow rates through weirs and sluice gates.....	A-95
Table A-8. List of weir types (French, 1985; USBR, 1999)	A-97
Table A-9. Typical Evaporation Formulae for Lakes and Reservoirs	A-113
Table A-10. Criteria for determining sunward bank	A-120
Table B-11. CE-QUAL-W2 Water Quality State Variables	B-2
Table B-15. River reaeration equations.....	B-51
Table B-16. Lake reaeration equations as a function of wind speed at 20°C.....	B-53
Table B-17. Reaeration equations for estuarine waterbody at 20°C.....	B-57
Table B-18. Formulae for small dam or weir reaeration effects.....	B-59
Table B-19. Equations used in CRiSP model for gas production.....	B-60
Table B-20. Equations used in CRiSP model for gas production.....	B-61
Table B-21. Spillways and weirs reaeration.....	B-61
Table C-23. Vertical Eddy Viscosity Formulations.....	C-33
Table C-24. Equations used in CRiSP model for gas production.....	C-53
Table C-25. Equations used in CRiSP model for gas production at Columbia basin dams.....	C-54
Table C-26. Reaeration Effects of Spillways, Weirs, and Gates	C-54
Table C-27. Equations used in CRiSP model for gas production.....	C-64
Table C-28. Equations used in CRiSP model for gas production at Columbia basin dams.....	C-64
Table C-29. Reaeration effects of gates	C-65
Table C-30. Hydraulic Print Parameters.....	C-86
Table C-31. Extinction Coefficient Literature Values	C-147
Table C-32. Values of BETA (TVA, 1972).....	C-148
Table 33. Literature values for light extinction due to macrophyte plant tissue concentration.	C-151
Table C-34. <i>In Situ</i> Coliform Decay Rates	C-152
Table C-35. Gross Production Rates of Phytoplankton.	C-155
Table C-57. Maximum Algal Excretion Rate Literature Values.....	C-164
Table C-58. Algal Dark Respiration Rate Literature Values	C-164
Table C-59. Algal settling Velocity Literature Values	C-165
Table C-60. Phosphorus Half-Saturation Constant Literature Values	C-166

LIST OF TABLES

Table C-61. Nitrogen Half-Saturation Constant Literature Values	C-166
Table C-62. Literature values for saturating light intensity	C-167
Table C-63. Freshwater algae minimum and optimum elemental contents in percentages of dry-weight (Reynolds, 1984).	C-172
Table 64. Coefficients used in CE-QUAL-R1 to simulate macrophytes (from Collins and Wlosinski, 1989).	C-192
Table 65. Values for the ratio between dry weight to wet volume ratio.	C-196
Table 66. Literature values for the ration of dry weight to surface area.	C-196
Table C-67. Labile DOM Decay Rate Literature Values.	C-200
Table C-68. Detritus Decay Rate Literature Values.....	C-201
Table C-69. Detritus Settling Velocity Literature Values	C-201
Table C-70. Ammonium Decay Rate Literature Values	C-208
Table 71. Nitrification rates measured by McCutcheon (1987).....	C-208
Table C-72. Sediment Oxygen Demand Literature Values	C-225
Table C-73. River Reaeration Equations.....	C-226
Table C-74. Lake Reaeration Equations	C-227
Table C-75. Estuarine Reaeration Equations	C-228
Table 76. Fish temperature and dissolved oxygen criteria from Cooke and Welch (2008).	C-306
Table 77. General fish temperature criteria from Hondzo and Stefan (1996).....	C-306
Table 78. Rules for selective withdrawal when there are 2 outlets where flow is being split.	C-316
Table 79. Description of user-specified inputs in the w2_selective.npt file for blending when SELECTC='USGS' (Rounds and Buccola, 2015)	C-321
Table C-80. Description of Dynamic Shading Input Variables	C-344

Model Release Package

All files on the CE-QUAL-W2 web site (<http://www.ce.pdx.edu/w2>) are archived in compressed zip files. To install CE-QUAL-W2, follow directions on the web site. All model files are provided in zipped format and are provided in directories that contain the source code, executables, user manual, and example applications. The download page describes the files available and how they are organized in the zip file. The example applications include DeGray Lake, the Spokane River, and the Columbia Slough. DeGray Lake is a reservoir with a single branch and a complete water quality application. The Spokane River is an example of a river system with multiple river sections. The Columbia Slough is a fresh-water estuary example.

1 Introduction

Model Overview

CE-QUAL-W2 is a two-dimensional, longitudinal/vertical, hydrodynamic and water quality model. Because the model assumes lateral homogeneity, it is best suited for relatively long and narrow waterbodies exhibiting longitudinal and vertical water quality gradients. The model has been applied to rivers, lakes, reservoirs, estuaries, and combinations thereof including entire river basins with multiple reservoirs and river segments.

The application of CE-QUAL-W2 requires knowledge in the following areas:

1. Hydrodynamics
2. Aquatic biology
3. Aquatic chemistry
4. Numerical methods
5. Computers and FORTRAN coding
6. Statistics
7. Data assembly and reconstruction

Water quality modeling is in many ways an art requiring not only knowledge in these areas but also experience in their integration. *A word of caution to the first time user* - model application is a complicated and time-consuming task.

Terminology used in the CE-QUAL-W2 model

The CE-QUAL-W2 model discretization uses the following definitions:

- Waterbodies: a collection of model branches that have similar turbulence closure and water quality parameter values and the same meteorological forcing. A typical example would be a reservoir and a river as separate waterbodies. One can also have one reservoir with separate waterbodies designated by different meteorological forcing.
- Branches: a collection of model segments with variable model slope. In a river waterbody, there can be multiple branches of variable slope; or in a reservoir, the sidearms of the reservoir can be different model branches.
- Segments: a longitudinal segment of length Δx .
- Layers: a vertical layer of height Δz .

Model Background

Version 1.0. CE-QUAL-W2 has been under continuous development since 1975. The original model was known as LARM (*L*aterally *A*veraged *R*eservoir *M*odel) developed by Edinger and Buchak (1975). The first LARM application was on a reservoir with no branches. Subsequent modifications to allow for multiple branches and estuarine boundary conditions resulted in the code known as GLVHT (*G*eneralized *L*ongitudinal-*V*ertical *H*ydrodynamics and *T*ransport Model). Addition of the water quality algorithms by the Water Quality Modeling Group at the US Army Engineer Waterways Experiment Station (WES) resulted in CE-QUAL-W2 Version 1.0 (Environmental and Hydraulic Laboratories, 1986).

Version 2.0. Version 2.0 was a result of major modifications to the code to improve the mathematical description of the prototype and increase computational accuracy and efficiency. Numerous new capabilities were included in Version 2.0, including:

1. an algorithm that calculated the maximum allowable timestep and adjusted the timestep to ensure hydrodynamic stability requirements were not violated (autostep-ping)
2. a selective withdrawal algorithm that calculated a withdrawal zone based on out-flow, outlet geometry, and upstream density gradients
3. a higher-order transport scheme (QUICKEST) that reduced numerical diffusion (Leonard, 1979)
4. time-weighted vertical advection and fully implicit vertical diffusion
5. step function or linear interpolation of inputs
6. improved ice-cover algorithm
7. internal calculation of equilibrium temperatures and coefficients of surface heat exchange or a term-by-term accounting of surface heat exchange
8. variable layer heights and segment lengths
9. surface layer extending through multiple layers
10. generalized time-varying data input subroutine with input data accepted at any frequency
11. volume and mass balances to machine accuracy
12. sediment/water heat exchange

Version 3.0. Version 3.0 is a result of additional improvements to the numerical solution scheme and water quality algorithms, as well as extending the utility of the model to provide state-of-the-art capabilities for modeling entire waterbasins in two-dimensions. The new capabilities included in Version 3 include:

1. an implicit solution for the effects of vertical eddy viscosity in the horizontal momentum equation
2. addition of Leonard's ULTIMATE algorithm that eliminates over/ under-shoots in the numerical solution scheme
3. inclusion of momentum transfer between branches

INTRODUCTION

4. the ability to model multiple waterbodies in the same computational grid including multiple reservoirs, steeply sloping riverine sections between reservoirs, and estuaries
5. additional vertical turbulence algorithms more appropriate for rivers
6. additional reaeration algorithms more appropriate for rivers
7. variable vertical grid spacing between waterbodies
8. numerical algorithms for pipe, weir, and pump flow
9. internal weir algorithm for submerged or skimmer weirs
10. three algal groups
11. arbitrary constituents defined by a decay rate, settling rate, and temperature rate multiplier
12. nine inorganic suspended solids groups
13. dissolved and particulate biogenic silica
14. age of water
15. derived constituents such as total DOC, organic nitrogen, organic phosphorus, etc. that are not state variables
16. a graphical pre/postprocessor
17. converted to FORTRAN 90/95 with Dynamic Array Allocation eliminating the need to recompile the code for each application
18. user defined evaporation models including the Ryan-Harleman model

Version 3.1. Version 3.1 is a result of additional improvements to the numerical solution scheme and water quality algorithms, as well as extending the utility of the model to provide state-of-the-art capabilities for modeling entire waterbasins in two-dimensions. The new capabilities include:

1. any number of user defined arbitrary constituents defined by a decay rate, settling rate, and temperature rate multiplier that can include
 - a. conservative tracers
 - b. coliform bacteria
 - c. water age
 - d. contaminants
2. any number of user defined phytoplankton groups
3. any number of user defined epiphyton groups
4. any number of user defined CBOD groups
5. any number of user defined inorganic suspended solids groups
6. dissolved and particulate biogenic silica
7. derived constituents such as total DOC, organic nitrogen, organic phosphorus, etc. that are not state variables
8. kinetic fluxes
9. graphical preprocessor

Version 3.2. Version 3.2 is a result of additional improvements to the model. These new capabilities include:

1. Internal code rewrite to reduce code size, simplify code maintenance, and improve model execution speed
2. New screen display during model run-time. The new screen display allows for controlling the processor usage, examining output variables, and stopping, starting and

restarting a model run on the fly. This allows the model user to stop a code, then make changes in the control file or any input file, and then restart the model at the point that it was stopped.

3. Addition of a new algorithm to estimate suspended solids resuspension as a result of wind-wave action.
4. Reorganization of the graph.npt file to allow more output control formatting possibilities.
5. New turbulent kinetic energy-turbulent dissipation turbulence closure model was added to the model.

Version 3.5. Version 3.5 is a result of significant enhancements to the model. These new capabilities include:

1. Addition of the macrophyte model of Berger and Wells (2008) with a user-defined # of species
2. Addition of a zooplankton model with a user-defined # of species based on an updated version of the CE-QUAL-R1 model (Environmental Laboratory, 1995)
3. Addition of a new focusing or settling velocity for sediments that accumulate in the first order sediment model. In earlier versions, sediment focusing occurred at the velocity given for POM. In this version, a user can specify that focusing velocity. This means that sediments can still migrate toward the bottom of the channel over time even after they have hit the sidewalls of the channel.
4. User-defined time-variable input of P and N associated with organic matter inputs. In earlier versions, the P or N associated with organic matter was based on a static stoichiometric coefficient specified in the control file. Now, the user provides in the input files the dynamic P and N associated with organic matter inputs from tributaries or inflows. This is essentially allowing for variable stoichiometry in the input boundary conditions.
5. Based on the above refinement, the organic matter fractions within the model now have variable stoichiometry for P and N. This preserves P and N mass balances. The stoichiometry given in the input files is merely the initial value of the C-N-P stoichiometry of POM and DOM compartments. Hence, organic P and organic N are tracked correctly in the code.
6. The first order sediment model also tracks C-N-P correctly and has a dynamic stoichiometry as it accumulates organic matter in the sediment. Prior versions of W2 had a user-defined value of fixed stoichiometry for the 1st order sediment model. Also, instead of a fixed decay rate for the sediments, the decay rate is dynamic based on the decay rates of the accumulated organic material. A mass weighted average is used.
7. CBOD groups now have a user-defined settling velocity. Hence, the user can define organic matter groups as particulate and dissolved based on specification of the settling velocity. As in prior versions, CBOD has associated stoichiometry and if there is settling, it will accumulate in the 1st order sediment compartment.
8. A Monod formulation was implemented for the initiation of anaerobic processes and reduction of aerobic processes. In earlier model versions there was a specified oxygen concentration that acted like a step function turning these processes on or off.

INTRODUCTION

Version 3.6. This version is file compatible with version 3.5. Hence no changes need to be made to any input files. Even though there are some new features in the input files, these are not required for users of V3.5 and can be kept blank. The primary change is allowing the code to run on multiple processors. The following changes have been made in the code from V3.5 to V3.6:

1. The code has been rewritten into smaller subroutines to allow better code compilation and optimization.
2. The code has been revised with the goal of improving the computational speed. This new compiled code using Intel Visual Fortran 11 should be faster on a single processor than the V3.5 code compiled on a PC with CVF 6.6.
3. The code now has OPENMP commands embedded to allow for limited parallelization of some of the routines. Current tests show that going from 1 processor to 2 can result in up to 20-40% speed improvement. The user can specify the # of processors the code will use in NPROC.
4. The TKE algorithm has been updated with new algorithms that match experimental tank data for kinetic energy and dissipation. This is based on a Master's degree project by Sam Gould at Portland State University. A new user option is the TKE1 algorithm, in addition to the legacy algorithm TKE.
5. The roughness height of the water for correction of the vertical velocity wind profile is now a user-defined input, z_0 . Prior to this the model had hardwired the value of $z_0=0.003$ m for wind speed correction at 2m (for evaporation where wind height at 2 m is typical) and $z_0=0.01$ m for wind at 10 m (for shear stress calculations where wind height of 10 m is typical). For consistency, both conversions now use the same value of roughness height. If the user does not specify the value of z_0 (for example if he/she leaves the spaces blank for z_0 using a V3.5 control file), the code uses 0.001 m.
6. The Windows user interface no longer uses Array Viewer. The dialog box and PC executable no longer require installation of Array Viewer (which is now obsolete) nor do they need the Array Viewer DLL. The Dialog box has some minor improvements: model run directory displayed and a progress bar.
7. Fixed error with Algae/chlorophyll a ratio in user manual and fixed pre-processor. The earlier language in the user manual discussed an Algae/Chlorophyll a ratio but presented information that was the ratio of chlorophyll a/algae – this has been revised and fixed in User Manual and in preprocessor.
8. Spreadsheet output: in earlier versions put in an alphanumeric character as a space for the spreadsheet to preserve the formatting. This was changed to a default value of -99 to facilitate numeric data processing. Also, the “-Depth” output value was changed to just “Depth” since modern plotting programs can reverse an axis.
9. Preprocessor improvements. Added variable checks for new parameters, fixed bugs, new check for wsc.npt file (not checked in earlier versions).

10. For the generic constituent, added temperature dependence on 0th order decay and fixed errors in User Manual for units of zero order decay coefficient.
11. Added the kinetic flux rates to the TSR file output for easier analysis using a spreadsheet of the flux terms for specific locations in the modeled system.
12. Revised the computation of the drag coefficient for low wind speeds so that the model now agrees better with theory in this wind speed range.
13. The light extinction coefficient (in m⁻¹) is now included as an output variable in the TSR opt file. Because the model internally computes the light extinction coefficient based on water, SS, POM, algae, zooplankton, and macrophytes, this is an important parameter understanding the internal light transmission predicted by the model. This variable replaces the equilibrium temperature as an output variable.
14. A new option for output is in the format required for TECPLOT. For TECPLOT animation there is only a flag in the CPL output line. This allows for easy model animation of the variables U, W, T, RHO, and all active constituents at the frequency specified by the CPL file as a function of distance and elevation.
15. A new variable for determining the fraction of NO₃-N that is diffused into the sediments that becomes organic matter, or SED-N was introduced.
16. In V3.5 the model computed an average decay coefficient of the sediments based on what was deposited. The user now has the option to dynamically compute that decay rate or to have it fixed and controlled by the model user. A new variable was introduced called DYNSEDK which is either ON/OFF to allow or not allow dynamic computation of the sediment decay rate.
17. Added Kinetic flux output that sums up fluxes for all cells of a waterbody at the output frequency specified in the kinetic flux output. The output filenames are called "kflux_jw#.opt" where # is the waterbody number. All active fluxes are summed for the waterbody. This is an important overall diagnostic tool to evaluate the important fluxes in the waterbody over time. Instantaneous fluxes are output in the TSR file for individual cells and a series of fluxes at given segments are shown in the Flux output file which is similar in format as the SNP file. This new file is easy to import into a spreadsheet for analysis.
18. The selective withdrawal algorithm computation was adjusted to more closely follow the Corps' model code SELECT (based on personal communication with Gary Hauser, 2008). The variable DLRHOMAX is used to compute the relative velocity profile. In V3.5 and earlier, this variable was the maximum for the entire profile above and below the outlet, i.e., DLRHOMAX=MAX(DLRHOT, DLRHOB). In V3.6 and later, DLRHOT is used above the outlet and DLRHOB is used below the outlet.
19. Command-line working directory specification is now active for the preprocessor, GUI, and W2 windows versions. Also, the Windows box can now be closed after a run is finished by specifying CLOSEC=ON in the control file. This makes it easier to use the Windows executable in batch file processing.

INTRODUCTION

Version 3.7. This version is not file compatible with version 3.6 because of the addition of several more state variables. The release notes show where the control file differs from Version 3.6. Many of the new features to Version 3.7 are accessed through additional control files separate from the main control file, w2_con.npt. The following changes have been made in the code from V3.6 to V3.7:

1. The model has been improved to handle river flow regimes. These model enhancements for river systems include the following:
 - a. The initial water surface elevation of a river system based on the normal depth of the river is computed within the model. This allows the model to run more smoothly from the start and eliminates trying to guess an initial water surface elevation for a river system.
 - b. The model in earlier versions assumed that the initial velocity regime was 'zero'. By computing an initial velocity regime based on the initial conditions of the flows, the river model then starts with a non-zero velocity. This allows the model to run more smoothly from the very beginning of the model simulation.
 - c. The model user can choose 'Trapezoidal' or 'Rectangular' model segments. This will allow for a smoother transition as water levels move up and down in a river channel. This should also allow for a larger maximum time step for stability in the river system.
 - d. The model user can now specify 2 slopes for a model branch. One slope is the slope of the elevation grid for which all elevations are tied together. The other slope is the hydraulic equivalent slope of a channel. In other words, if a model branch includes riffles and pools, the actual grid slope may not be the equivalent hydraulic slope.
2. There is a new bathymetry file input format in comma delimited format (csv) that is easily developed using 'Excel'. This simplifies setting up the initial grid and debugging it.
3. Temperature and dissolved oxygen habitat volumes are now computed within the model for user-specified fish species.
4. There is a new automatic selection of a withdrawal port algorithm that will select the elevation of the withdrawal necessary to meet temperature targets including splitting flows between outlets to reach a target temperature.
5. Since each BOD group can have a different BOD-P, BOD-C and BOD-N stoichiometric equivalent, it was necessary to add to the model new state variables, BOD-P, BOD-N, and BOD-C that allowed for time variable inputs of BOD-P, BOD-C and BOD-N from a point or non-point source.
6. Environmental performance criteria were developed to evaluate time and volume averages over the system of state variables chosen for analysis. This is an easy method for looking at water quality differences between model runs.
7. The model now has a module for adding dissolved oxygen, such as hypolimnetic aeration, to specific locations based on a dynamic dissolved oxygen probe monitoring the dissolved oxygen levels.

8. The model has a dynamic pipe algorithm allowing a pipe to be turned ON or OFF over time, as if a gate was closed.
9. The model also has a dynamic pump algorithm that allows the model user to set dynamic parameters for the water level control over time. This is very useful in setting rule curves for operation of the reservoir water levels over time.
10. The maximum time step can now be set to interpolate its value over time rather than suddenly changing the maximum time step. This allows for a smoother change in the model time step.
11. The computation of the temperature at which ice freezes has been adjusted to account for salt water impacts. [Courtesy of Dr. Ray Walton]
12. New model output includes volume weighted averages of eutrophication water quality variables as a function of segment and for only surface conditions as specified by the model user. Other new output includes output of flows, concentrations, and temperatures from a segment for all individual withdrawals.

Version 3.71. This version is file compatible with version 3.7 but does add one new variable to the control file w2_con.npt.

1. New model input formats (free format) for many input files that were in fixed format. The new files allow for much easier model file development in Excel. These new files include the following files:
 - a. All concentration input files for inflows, tributaries, distributed tributaries and precipitation:
 - i. Cin files
 - ii. Ctrib files
 - iii. Cdtrib files
 - iv. Cpre files
 - b. Wind sheltering file
 - i. Wsc file
 - c. Meteorological input file
 - i. Met file
 - d. Vertical profile file for initial condition
 - i. Vpr file
 - e. Longitudinal-vertical profile initial condition
 - i. Lpr file
 - f. Withdrawal flow file
 - i. Qwd file
 - g. Structure outflow file
 - i. Qot file
 - h. Flow and temperature input files for
 - i. Qin and Tin
 - ii. Qtrib and Ttrib
 - iii. Qdtrib and Tdtrib

INTRODUCTION

2. New option for dynamic outlet structure elevation for each model structure. Hence, the centerline elevation of the structure can be variable over time. In the control file, there is an ON/OFF option after declaring the # of structures for each branch.
3. The release of a new post-processor from DSI, Inc. that uses the vector output in w2_con.npt to specify frequency of output for this post-processor.

Version 3.72. This version is file compatible with version 3.71 unless one uses the new USGS automatic port selection algorithm where the w2_selective.npt format is changed. This new version allows for using the algorithm of Rounds and Buccola (2015) for trying to meet downstream temperature targets from reservoirs.

Manual

Organization. Chapter 1 consists of an introduction to the model and the user manual. Chapter 2 describes the model's capabilities and limitations. Chapter 3 provides an overview of the steps involved in applying the model including data preparation and model application.

The appendices provide the user with the information necessary to understand the model details. Appendix A describes the theoretical, numerical, and computational basis for the hydrodynamic portion of the model. Appendix B describes the theoretical and computational basis for the water quality algorithms. Appendix C describes input file preparation. References include a partial bibliography of CE-QUAL-W2 applications.

The following concepts have been used in the writing of the User's Manual:

1. Page headers are used to allow the user to easily find major areas in the manual.
2. Where applicable, paragraphs contain descriptive headings for easy reference.
3. Hyperlinks are used when related information is contained elsewhere.

Conventions. References to FORTRAN variables in the manual are made in English and are followed by their FORTRAN name enclosed by brackets (e.g., surface layer [KT]). The user need not first memorize the variable names to comprehend the manual. Potential problem areas in applying the model are emphasized with ***bold italic*** type.

2 Capabilities and Limitations

Capabilities

Hydrodynamic. The model predicts water surface elevations, velocities (longitudinal and vertical), and temperatures. Temperature is included in the hydrodynamic calculations because of its effect on water density and cannot be turned off. Water quality computations are done after a hydrodynamic computation allowing for feedback between water quality and hydrodynamic variables.

Water quality. Any combination of constituents can be included/excluded from a simulation. The effects of salinity or total dissolved solids/salinity on density and thus hydrodynamics are included only if they are simulated in the water quality module. The water quality algorithm is modular allowing constituents to be easily added as additional subroutines. The current version includes the following water quality state variables in addition to temperature:

1. any number of generic constituents defined by a 0 and/or a 1st order decay rate and/or a settling velocity and/or an Arrhenius temperature rate multiplier that can be used to define any number of the following:
 - a. conservative tracer(s)
 - b. water age or hydraulic residence time
 - c. coliform bacteria(s)
 - d. contaminant(s)
2. any number of inorganic suspended solids groups
3. any number of phytoplankton groups
4. any number of periphyton/epiphyton groups
5. any number of CBOD groups, including CBOD-N and CBOD-P
6. ammonium
7. nitrate+nitrite
8. bioavailable phosphorus (commonly represented by orthophosphate or soluble reactive phosphorus)
9. labile dissolved organic matter
10. refractory dissolved organic matter
11. labile particulate organic matter
12. refractory particulate organic matter
13. total inorganic carbon
14. alkalinity
15. total iron
16. dissolved oxygen

CAPABILITIES

17. organic sediments
18. gas entrainment
19. any number of macrophyte groups
20. any number of zooplankton groups
21. labile dissolved organic matter-P
22. refractory dissolved organic matter-P
23. labile particulate organic matter-P
24. refractory particulate organic matter-P
25. labile dissolved organic matter-N
26. refractory dissolved organic matter-N
27. labile particulate organic matter-N
28. refractory particulate organic matter-N

Additionally, over 60 derived variables including pH, TOC, DOC, TON, TOP, DOP, etc. can be computed internally from the state variables and output for comparison to measured data.

Long term simulations. The water surface elevation is solved implicitly, which eliminates the surface gravity wave restriction on the timestep. This permits larger timesteps during a simulation resulting in decreased computational time. As a result, the model can easily simulate long-term water quality responses. The vertical diffusion criteria from stability requirements has also been eliminated allowing for even larger timesteps.

Head boundary conditions. The model can be applied to estuaries, rivers, or portions of a waterbody by specifying upstream or downstream head boundary conditions.

Multiple branches. The branching algorithm allows application to geometrically complex waterbodies such as dendritic reservoirs or estuaries.

Multiple waterbodies. The model can be applied to any number of rivers, reservoirs, lakes, and estuaries linked in series.

Multiple turbulence closure schemes. The model user can choose several different turbulence closure schemes. The preferred scheme for both estuary, river and lake/reservoir systems is the $k-\epsilon$ turbulence model.

Variable grid spacing. Variable segment lengths and layer thicknesses can be used allowing specification of higher resolution where needed. Vertical grid spacing can vary in thickness between waterbodies.

Water quality independent of hydrodynamics. Water quality can be updated less frequently than hydrodynamics thus reducing computational requirements. However, water quality is *not* decoupled from the hydrodynamics (i.e., separate, standalone code for hydrodynamics and water quality where output from the hydrodynamic model is stored on disk and then used to specify advective fluxes for the water quality computations). Storage requirements for long-term hydrodynamic output to drive the water quality model are prohibitive for anything except very small grids. Additionally, reduction in computer time is minimal when hydrodynamic data used to drive water quality are input every timestep.

Autostepping. The model includes a variable timestep algorithm that attempts to help ensure stability requirements for the hydrodynamics imposed by the numerical solution scheme are not violated.

Restart provision. The user can output results during a simulation that can subsequently be used as input. Execution can then be resumed at that point.

Layer/segment addition and subtraction. The model will adjust surface layer and upstream segment locations for a rising or falling water surface during a simulation.

Multiple inflows and outflows. Provisions are made for inflows and inflow loadings from point/nonpoint sources, branches, and precipitation. Outflows are specified either as releases at a branch's downstream segment or as lateral withdrawals. Although evaporation is not considered an outflow in the strictest sense, it can be included in the water budget.

Ice cover calculations. The model can calculate onset, growth, and breakup of ice cover.

Selective withdrawal calculations. The model can calculate the vertical extent of the withdrawal zone based on outlet geometry, outflow, and density.

Multiple hydraulic structure algorithms. The model can be set up to allow multiple pumps, spillways, pipes and gates between model segments.

Dynamic shading. The model computes topographic and vegetative shading for each model segment.

Automatic vertical port selection in a reservoir. The model can compute what vertical layer to extract water from a reservoir to meet an imposed temperature standard.

Time-varying boundary conditions. The model accepts a given set of time-varying inputs at the frequency they occur independent of other sets of time-varying inputs.

Outputs. The model allows the user considerable flexibility in the type and frequency of outputs. Output is available for the screen, hard copy, plotting, and restarts. The user can specify what is output, when during the simulation output is to begin, and the output frequency. Version 3.71 now includes a graphical pre- and postprocessor for plotting/ visualization.

Details of these capabilities are discussed in Appendix C.

Potential Limitations

Theoretical

Hydrodynamics and transport. The governing equations are laterally and layer averaged. Lateral averaging assumes lateral variations in velocities, temperatures, and constituents are negligible. This assumption may be inappropriate for large waterbodies exhibiting significant lateral variations in water quality. Whether this assumption is met is often a judgment call on the user and depends in large part on the questions being addressed. Eddy coefficients are used to model turbulence.

Chapter 2 Capabilities and Limitations

LIMITATIONS

Currently, the user must decide among several vertical turbulence schemes the one that is most appropriate for the type of waterbody being simulated. The equations are written in the conservative form using the Boussinesq and hydrostatic approximations. Since vertical momentum is not included, the model may give inaccurate results where there is significant vertical acceleration.

Water quality. Water quality interactions are, by necessity, simplified descriptions of an aquatic ecosystem that is extremely complex. Improvements will be made in the future as better means of describing the aquatic ecosystem in mathematical terms and time for incorporating the changes into the model become available in this one area.

Sediment oxygen demand. The model includes a user-specified sediment oxygen demand that is not coupled to the water column. SOD only varies according to temperature. The first order sediment model is tied to the water column settling of organic matter. But this models only labile, oxic, sediment decay. The model does not have a sediment compartment that models kinetics in the sediment and at the sediment-water interface, i.e., a complete sediment diagenesis model. This places a limitation on long-term predictive capabilities of the water quality portion of the model.

Future releases will include the following additional capabilities:

1. sediment diagenesis algorithm that will compute SOD and sediment to water column nutrient fluxes based on organic matter delivery to the sediments
2. sediment transport including both cohesive and non-cohesive sediments
3. toxics
4. simultaneous water surface elevation solution among all branches in a waterbody
5. downstream segment addition/subtraction between a river and a reservoir and/or estuary

Numerical

Solution scheme. The model provides three different numerical transport schemes for temperature and constituents - upwind differencing, the higher-order QUICKEST (Leonard, 1979), and Leonard's ULTIMATE algorithm. Upwind differencing introduces numerical diffusion often greater than physical diffusion. The QUICKEST scheme reduces numerical diffusion, but in areas of high gradients generates overshoots and undershoots which may produce small negative concentrations. ULTIMATE, Leonard's solution to the over/undershoots, has been incorporated into Version 3. In addition, discretization errors are introduced as the finite difference cell dimensions or the timestep increase. This is an important point to keep in mind when evaluating model predictions that are spatially and temporally averaged versus observed data collected at discrete points in time and space. A more thorough discussion of the numerical solution and its implementation is found in Appendix A.

Computer limits. A considerable effort has been invested in increasing model efficiency including a vertically implicit solution for vertical turbulence in the horizontal momentum equation. However, the model still places computational and storage burdens on a computer when making long-term simulations. Year long water quality simulations for a single reservoir can take from a few minutes to days for multiple waterbodies in a large river basin. Applications to dynamic river

systems can take considerably longer than reservoirs because of much smaller timesteps needed for river numerical stability.

Since the model uses dynamic allocation memory, the memory required for a simulation is determined at run-time. In cases where the user is running on a Windows 32-bit operating system, the virtual memory is limited to 2GB. If your system requires more memory, you will need to recompile the code using a 64-bit operating system and compiler that can address more memory.

Input Data

The availability of input data is not a limitation of the model itself. However, it is most often the limiting factor in the application or misapplication of the model. This cannot be stressed enough. The user should always keep in mind the adage "garbage in equals garbage out".

3 Model Application

This chapter is intended to present the user with a general overview of the steps involved in a model application. The initial user should read the chapter once to gain a general understanding of these steps setting aside questions that might arise upon initial reading. The user should then reread the chapter and explore the hyperlinks to clarify any questions that arose during the first reading. File-names are referred to generically (i.e., inflow file, outflow file, withdrawal file). Actual filenames are specified by the user in the control file.

Overview

Data Preparation

The following data are needed for model application:

1. geometric data
2. initial conditions
3. boundary conditions
4. hydraulic parameters
5. kinetic parameters
6. calibration data

A detailed discussion of these data follows.

Geometric Data

The first input task involves assembling geometric data. These data will be used to define the finite difference representation of the waterbody. The following data are needed for setting up input geometry:

1. topographic map and/or sediment range surveys
2. project volume-area-elevation table

The topographic map or sediment range surveys are used to generate bathymetric cross-sections that are input into the model. The project volume-area-elevation table is used for comparison with the volume-area-elevation table generated by the model.

Computational grid. The computational grid is the term used for the finite difference representation of the waterbody. Grid geometry is determined by four parameters:

- | | |
|---|---------|
| 1. longitudinal spacing (segment length) | [DLX] |
| 2. vertical spacing (layer height) | [H] |
| 3. average cross-sectional width (cell width) | [B] |
| 4. waterbody slope | [SLOPE] |

The longitudinal and vertical spacing may vary from segment to segment and layer to layer, but should vary gradually from one segment or layer to the next to minimize discretization errors.

Factors affecting computational grid. A number of factors must be evaluated and weighed against each other when determining longitudinal and vertical spacing. These include:

1. **Areas of strongest gradients.** This factor applies particularly to the metalimnion in freshwater and the pycnocline in saltwater. If the model is not capturing water quality gradients in these regions, then vertical resolution may have to be increased. Similar reasoning applies to areas of longitudinal gradients.
2. **Computational and memory requirements.** The model penalizes the user in two ways when increasing grid resolution. As the number of grid cells goes up, so do computational and memory requirements. In addition, as the dimensions of a grid cell **decrease**, the timestep must also decrease to maintain numerical stability. As a rule of thumb, it is always desirable to err on the side of greater grid resolution, but at some point the user must give way to the reality of the available computer resources and the money and time available for completing the project.
3. **Bottom slope.** For reservoirs and some estuaries, the waterbody bottom slope is more accurately modeled as the ratio of cell thickness to cell length $[H]/[DLX]$ approaches the overall bottom slope. For sloping streams/rivers, the ratio is accurately represented by the slope and is typically not of concern.
4. **Results.** Results should not be a function of the computational grid's resolution. With the development of the bathymetry editor, finely discretized grids can be easily coarsened. The coarser grid will have fewer computational cells and larger average timesteps resulting in decreased runtimes. The computational grid should initially be of high resolution and, if runtimes are excessive, reduced in resolution until the results change substantially. Results should never be a function of the grid resolution.

Previous applications have used a horizontal grid spacing of 100 to 10,000 *m* and a vertical grid spacing of 0.2 to 5 *m*. Regardless of the grid spacing used, the user should check to make certain that model predictions are grid independent. This is usually performed by making model simulations with varying grid resolution and using the largest grid that reproduces essentially the same results as those using the smallest grid.

Bathymetric data. The next step after determining horizontal and vertical cell dimensions is to determine average cross-sectional widths for each cell. This is an iterative procedure whereby initial bathymetry is input into the preprocessor and the volume-area-elevation table is then generated by the preprocessor. This table is compared to the project table and widths are adjusted to better match the project table.

Several methods have been used for determining average widths. Transects along the waterbody centerline can be drawn on a topographic map. A contour at the elevation corresponding to the **center** of a grid cell is located and the area encompassed by the contour line and the upstream and

DATA PREPARATION

downstream transect is determined by planimeter. This area divided by the segment length is the average width of the grid cell. The process is repeated for each grid cell.

When no topographic information is available, the user can determine average widths from sediment range surveys for existing waterbodies. However, this method is generally not as accurate as data obtained from topographic maps since the number of available transects are usually insufficient to adequately describe the complex shape of most waterbodies. If available, sediment range surveys should be used to refine the grid generated from topographic information - particularly where significant sedimentation has occurred.

Other methods by individual investigators have been developed for generating grids using contour plotting packages such as Surfer and AUTOCAD. Eventually, the preprocessor will incorporate an algorithm that will automatically generate the bathymetry based on lateral transects or x-y-z coordinate data.

Sample computational grid. A sample computational grid in the longitudinal/vertical plane with four branches is shown in [Figure 1](#). The FORTRAN variables associated with the grid are also included. The grid consists of 25 longitudinal segments [IMX] and 22 vertical layers [KMX]. They constitute the total number of cells in the computational grid. This is exactly how the model sees the grid layout even though this is not the correct physical representation of the system. In reality, branch two and branch three join branch one. Branch setup is described in more detail below.

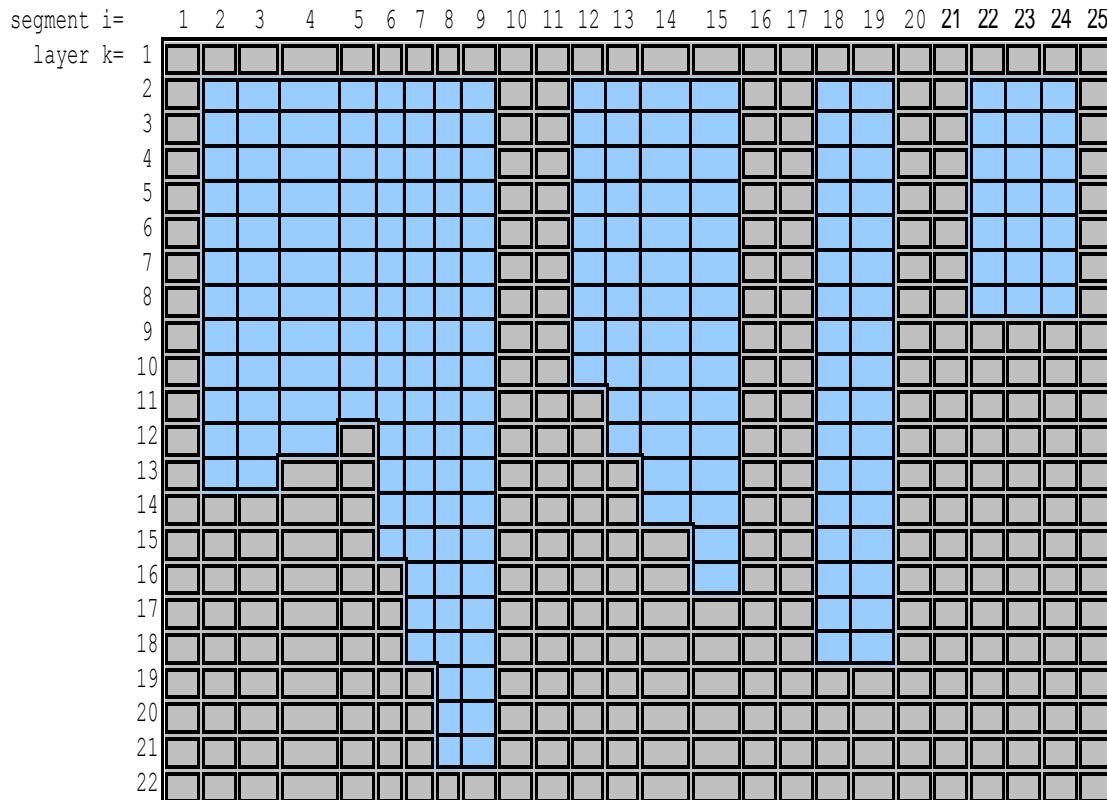


Figure 1. Sample computational grid in the x-z plane showing active and inactive cells.

DATA PREPARATION

Grid cell types. [Figure 1](#) contains two kinds of cells - ones with either a single or a double line border. Cells with a single line border represent cells that may contain water during the simulation. The **active cells** are defined in the bathymetry input as having **non-zero widths**. Cells with a double border represent boundary cells located at or beyond the waterbody boundaries. The **boundary cells** are defined in the bathymetry input as having **zero widths**.

Boundary cells. There are four types of boundary cells:

1. top
2. bottom
3. upstream
4. downstream

Each segment must have a zero width for the cell in layer 1 and a zero width for every cell located below the bottom active cell. For example, cells 1 and 12-22 in segment five would have zero widths. In addition, each branch must have zero widths for upstream boundary and downstream boundary segments. Note this requirement results in **two segments** of boundary cells between each branch (segments 10-11 & 16-17).

Branches. CE-QUAL-W2 can simulate a system with any number of waterbodies containing any number of branches. [Figure 2](#) shows a plan view of the same three branch grid of [Figure 1](#) along with the FORTRAN variables defining the geometry for each branch. For each branch, the upstream segment [US] and the downstream segment [DS] must be defined. The current upstream segment [CUS] is calculated by the model and may vary over time to meet restrictions imposed by the solution scheme. Typically segment numbers increase going from upstream to downstream in the branch.

A branch may connect to other branches at its upstream [UHS] and/or downstream segment [DHS]. In [Figure 2](#), the downstream segment of branch 2 ([DS]=15) connects to branch 1 at segment 7 ([DHS]=7).

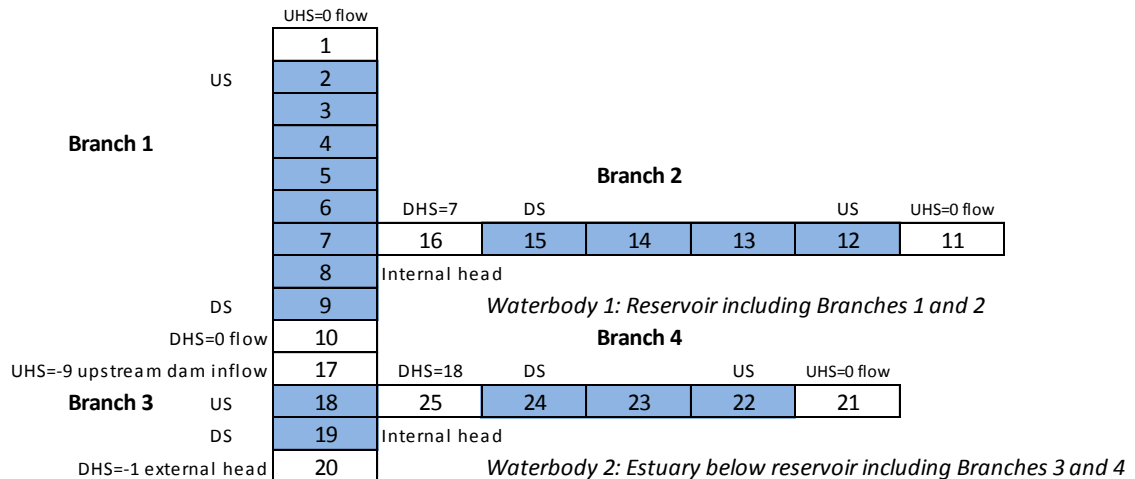


Figure 2. Sample computational grid in the x-y plane showing cell numbering and branch and water body connections.

DATA PREPARATION

Grid restrictions. The grid must satisfy the following restrictions:

1. Cell widths *cannot increase* with depth.
2. A **branch** may connect to other branches at its upstream or downstream segment, but a branch *may not enter or leave* itself.
3. Two branches may not connect at the same segment of another branch.

The bathymetry input file contains the longitudinal grid spacing [DLX], initial water surface elevation [WSEL], segment orientations [PHI0], vertical grid spacing [H], bottom friction [FRICT], and average cell widths [B].

After the bathymetry is generated, it should be checked to ensure the bottom elevation varies smoothly and represents the average slope over appropriate portions of the waterbody for reservoirs and estuaries. Oftentimes, minimum bottom widths are set at 5-15 *m*. This helps increase timesteps with minimal impact on the volume-area-elevation curves. However, increasing widths in the bottom layers can affect water quality since sediment oxygen demand and nutrient fluxes are dependent on bottom surface areas. Refer to the [bathymetry file](#) and [preprocessor output](#) in the sample applications for additional guidance in setting up the bathymetry.

Initial Conditions

Initial conditions are specified in the control, bathymetry, and vertical and/or longitudinal profile input files. The control file specifies the following initial conditions:

1. **Time (required).** Starting [TMSTRT] and ending time [TMEND] of the simulation.
2. **Temperatures (required) and concentrations** (optional). The initial temperature [IT2] and constituent concentrations [IC2]. If the grid is not initialized to a single value, then a grid-wide vertical profile can be specified in the vertical profile input file [VPRFN]. The option is also available to specify a longitudinally and vertically varying initial concentration for temperature and constituents via the longitudinal profile file [LPRFN].
3. **Inflows/outflows** (optional). The number and location of inflows and outflows.
4. **Restart** (optional). If a previous run with the model was made specifying restart conditions were to be written [RSOC] to an output file, then the user can specify the model read the file [RSIC] and continue the simulation from that point.
5. **Waterbody type (required).** The waterbody can be specified as either saltwater or freshwater [WTYPE].
6. **Ice thickness** (optional). The initial ice thickness [ICETHI].

Boundary Conditions

Inflows. The model recognizes the following inflows:

1. **Upstream inflows** (optional). Upstream inflows occur only at a branch's current upstream segment [CUS], which may vary during a simulation. The model provides the option to distribute inflows evenly throughout the inflow segment or place inflows according to density [PQC]. *If* the upstream inflow option is used, then a

separate file for inflow **[QIN]**, a separate file for temperature **[TIN]**, and, *if* constituents are modeled, a separate file containing constituent concentrations **[CIN]** for *each* branch is required.

2. **Tributary inflows** (optional). Tributary inflows or point source loadings **[QTR]** may enter any segment of the computational grid. If the current upstream segment **[CUS]** number is greater than the segment the tributary enters, then the tributary inflows are added into the current upstream segment to maintain the waterbody water balance. As in upstream inflows, the model provides the option to distribute tributary inflows evenly throughout the inflow segment or place inflows according to their density **[PTRC]**. An additional option to place inflows between two specified elevations is also included to better describe point source inflows such as wastewater effluent discharged from a pipe. The number of tributaries **[NTR]** and their segment location **[ITR]** are specified in the control file. *If* this option is used, then file requirements for *each* tributary are the same as for upstream inflows.
3. **Distributed tributary inflows** (optional). Distributed tributary inflows or nonpoint source loadings **[DTRC]** may be specified for any branch. The flow is distributed throughout a branch weighted by segment surface areas. *If* this option is used, then file requirements for *each* distributed tributary are the same as for upstream inflows.
4. **Precipitation** (optional). Precipitation **[PRC]** can be specified for each branch and is distributed according to the segment surface areas. *If* this option is used, then file requirements for *each* branch are the same as for upstream inflows.
5. **Internal inflows** (optional). Flows from gates, pipes, and pumps and over spillways and weirs can now be routed internally in the computational grid from one segment to another. This allows application of the model to highly engineered systems.

Outflows. The model recognizes the following outflows:

1. **Downstream outflows** (optional). Downstream outflows **[QOUT]** occur only at the downstream segment **[DS]** of a branch. Selective withdrawal where the vertical extent of and flow distribution in the withdrawal zone is calculated by the model is used for all outflows. Additionally, the bottom **[KBSTR]** and top layers **[KTSTR]** below and above which outflow cannot occur can be specified by the user to include the effects of upstream structures that restrict the selective withdrawal zone. Outflow will occur even if the outlet location is above the current water surface layer **[KT]**. This is a necessity when calibrating water surface elevations. A separate file for *each* branch is required.
2. **Lateral withdrawals** (optional). Lateral withdrawals **[QWD]** may be specified for any active cell. The number of withdrawals **[NWD]**, their segment location **[IWD]**, and their centerline elevation **[EWD]** must be specified in the control file. *If* this option is used, a separate file for *each* withdrawal is required. Version 3 now uses selective withdrawal for lateral withdrawals.
3. **Evaporation** (optional). Evaporation is calculated by the model from air **[TAIR]** and dewpoint **[TDEW]** temperature and wind speed **[WIND]**. If a waterbody loses a significant amount of water from evaporation that is not accounted for in the inflows, then the user should include evaporation. Evaporative heat loss is *always* included in the heat budget.
4. **Internal outflows** (optional). Flows from gates, pipes, and pumps and over spillways and weirs can now be routed internally in the computational grid from one

DATA PREPARATION

segment to another. This allows application of the model to highly engineered systems.

Head Boundary Conditions (optional). The model recognizes the following head boundary

1. **External.** The user may specify an external upstream [UHS] and/or downstream head [DHS] boundary condition for each branch. This boundary specification is intended primarily for estuarine simulations although it has also been used for river and reservoir applications. *If* this option is used, a separate file for time-varying elevations, [EUH] and/or [EDH], a separate file for vertical temperature profiles, [TUH] and/or [TDH], and, if constituents are modeled, a separate file containing vertical profiles for each constituent modeled, [CUH] and/or [CDH], *must* be specified for *each* external head boundary condition.
2. **Internal.** Internal head boundary conditions are specified wherever one branch connects with another branch. The boundary surface elevation, temperatures, and constituent concentrations are calculated internally by the model.

Surface Boundary Conditions (required). The model requires the following surface boundary conditions:

1. **Surface heat exchange.** Surface heat exchange is calculated by either of two methods using the input variable [SLHTC] in the control file. The first method uses equilibrium temperatures [ET] and coefficients of surface heat exchange [CSHE] to calculate surface heat exchange (Brady and Edinger, 1975). The second method uses a term-by-term accounting for calculating surface heat exchange. For both methods, latitude [LAT] and longitude [LONG] are specified in the control file and values for air temperature [TAIR], dew point temperature [TDEW], wind speed [WIND] and direction [PHI], and cloud cover [CLOUD] *must* be included in the meteorological file. If available, short wave solar radiation can be input directly into the model.
2. **Solar radiation absorption.** Distribution of solar radiation in the water column is controlled by the fraction of solar radiation absorbed in the surface layer [BETA] and the attenuation rate due to water [EXH2O], inorganic suspended solids [EXINOR], and organic suspended solids [EXORG]. Values for [EXINOR] and [EXORG] affect solar radiation only if constituents are modeled. These values are specified in the control file.
3. **Wind stress.** Wind speed [WIND] and direction [PHI] *must* be supplied in the meteorological file [METFN]. Wind stress is an extremely important physical process and should be included in all applications. The model allows the user to specify a wind sheltering coefficient [WSC] which, when multiplied with the wind speed, reduces effects of the wind to take into account differences in terrain from the met station and the prototype site. The sheltering coefficient is specified in the wind sheltering file [WSCFN].
4. **Gas exchange.** The wind speed [WIND] supplied in the meteorological file is also used for computing gas exchange at the water surface if dissolved oxygen and/or total inorganic carbon are simulated. Gas exchange is also affected by the wind sheltering coefficient [WSC].

Temperature transport cannot be turned off in the model. Temperature can be treated conservatively by turning off heat exchange computations [\[HEATC\]](#).

Hydraulic Parameters (required)

Dispersion/diffusion coefficients. The horizontal dispersion coefficients for momentum [\[AX\]](#) and temperature/constituents [\[DX\]](#) are specified in the control file. They are presently time and space invariant. Sensitivity analyses on numerous applications have shown the model is relatively insensitive to variations in the default values for reservoirs, but can be important in rivers and estuaries.

The vertical diffusion coefficients for momentum [\[AZ\]](#) and temperature/constituents [\[DZ\]](#) vary in space and time and are computed by the model. The current version allows for a number of different vertical turbulence algorithms for sloping river sections and estuaries. Work is underway on a k-ε vertical turbulence algorithm that will hopefully replace the various options now available.

Bottom friction. The latest version now allows the user the option of specifying longitudinally varying values for the Chezy coefficient or Manning's N for bottom friction. The friction type is specified in the control file [\[FRICC\]](#). They are used in calculating boundary friction that varies spatially as a function of exposed bottom area and temporally as a function of the flow field. The values are specified in the bathymetry file.

Kinetic Parameters (optional)

There are more than 120 coefficients affecting constituent kinetics, although less than 10 are normally adjusted during water quality calibration. The values are specified in the control file. If simulations include water quality, then the user should see [Appendix C](#) for a detailed discussion of these coefficients.

Calibration Data (required)

Calibration data are used to provide initial and boundary conditions and assess model performance during calibration. A great deal of thought should go into assessing the amount and type of data necessary to adequately characterize and understand the limnology of a waterbody and to develop the database required to support a water quality modeling effort. Gaugush (1986; 1987; 1993) provides detailed information on sampling design and frequency. ***Determining the availability of adequate calibration data should be done as early in the study as possible.*** If the user determines calibration data are inadequate, then immediate steps should be taken to collect sufficient data. Results will be suspect at best and will not withstand scrutiny at worst if the model is applied with insufficient and/or inadequate calibration data. The following discussion provides an overview of data required for the proper application of CE-QUAL-W2.

In-Pool. Proper application of mechanistic water quality models requires at least one set of in-pool observed data. The preferred method is *at least* two sets of data encompassing different extremes in the prototype (i.e., high and low flow years, warm and cold years, spring phytoplankton bloom and no spring phytoplankton bloom, etc.). In-pool data is used to set initial conditions and assess the model's ability to reproduce observed conditions. Given sufficient time and funding, *all years* in which sufficient data are available should be included during model calibration.

DATA PREPARATION

Time-Varying Boundary Conditions. It cannot be overemphasized that data used to drive the model needs to be as accurate as possible. For temperature calibration, this typically means using continuous inflow temperatures or developing regression relationships for inflow temperatures based on flow and air or equilibrium temperature to generate at least daily inflow temperatures (see Ford & Stein, 1984). Equilibrium temperature is preferred since it includes more of the mechanisms affecting water temperature.

For meteorological data, use the most frequent data available. Previously, daily average values were used to drive the model because earlier 1-D models used daily timesteps. Many modelers still take hourly or three-hourly data and generate daily averages for model input. *Any time data is averaged, information is lost.* For most reservoirs, thermocline depth and shape are a function of two physical mechanisms - wind mixing and convective cooling. Using daily average air temperatures eliminates nighttime convective mixing that can be a very important physical process affecting epilimnetic depths and thermocline shapes for reservoirs. As another example, applying a daily average wind speed and direction can generate an artificial water surface slope that incorrectly drives hydrodynamics. Daily averaging of wind speeds can also result in much less energy input into the model since the energy input by wind is a function of the wind speed cubed.

For water quality simulations, it is important the user provide accurate initial and time-varying boundary conditions. If nutrient loadings are not adequately characterized, then it will be impossible for the model to accurately reproduce phytoplankton/nutrient/DO dynamics. It is a waste of time and effort to collect in-pool data in support of water quality modeling when inflow concentrations/loadings have not been adequately characterized since they often drive the system. As in the development of inflow temperatures, regressions relating concentration/loadings with flow and possibly refined for season should be developed for tributary inflows. Ideally, several storm events should be intensively sampled since this is when loadings are generally highest to a waterbody. Also, point source loadings should be identified and loading estimates obtained. Some estimate of non-point source loadings should also be made. In some cases, meteorological loading estimates should be obtained. A software package, FLUX (Walker, 1986), is useful for generating loadings over time from intermittent samples. [Table 1](#) gives general guidelines for data collection.

Kinetic Rates. Because water quality modeling is still very much an art with numerous rate coefficients available for adjustment during calibration, it is highly preferable to obtain actual measurements of these coefficients used in the water quality formulations. If all of the rate coefficients have been determined for a waterbody, then any discrepancies between computed and observed data highlight the model's shortcomings, help to identify the bounds of the model's predictive capabilities, and provide direction for efficient use of resources to provide a better understanding of the system's water quality dynamics.

Ideally, a model should be used as a starting point for limnological investigations of a waterbody, with the data and formulations continuously refined to reflect the increased understanding of the system and processes gained over time. Unfortunately, this approach is rarely taken in practice due in large part to the expense involved, but also, even more unfortunately, due to the inability of aquatic biologists/limnologists and engineers to collaborate.

This cooperative approach between experimentalists and theoreticians is the main impetus behind the tremendous advances in physics, chemistry, and, to some extent, biology (e.g., genetic research)

DATA PREPARATION

during the last century, but is seldom seen in the field of water quality modeling. A notable exception is the Chesapeake Bay Modeling Study (Cерco and Cole, 1994). Researchers in the Chesapeake Bay region, including both biologists and engineers, were actively involved in data acquisition and water quality formulations and provided invaluable knowledge and feedback during the course of the study. This cooperative arrangement is continuing and should be a model for all future water quality model development.

Table 1. General guidelines for in-pool water quality sampling.

Boundary Conditions		
Minimum parameters	Additional parameters	Frequency
inflow/outflow temperature	conductivity dissolved oxygen pH total dissolved solids ¹	daily or continuous
total organic carbon	dissolved and/or particulate organic carbon BOD ²	weekly w/ storm sampling
soluble reactive phosphorous total phosphorous	total dissolved phosphorus total inorganic phosphorus dissolved inorganic phosphorus	weekly w/ storm sampling
nitrate+nitrite nitrogen ammonium nitrogen	total Kjeldahl nitrogen filtered total Kjeldahl nitrogen	weekly w/ storm sampling
	total suspended solids ³ inorganic and/or volatile suspended solids	weekly w/ storm sampling
	chlorophyll a dissolved silica ⁴ alkalinity	weekly w/ storm sampling
In-Pool		
Minimum parameters	Additional parameters	Frequency
Temperature ⁵ Dissolved oxygen ⁵ pH ⁵ Conductivity ⁵	total dissolved solids ¹	monthly ⁶
Chlorophyll a ⁷	phytoplankton biomass and type	monthly
Total organic carbon ⁷	dissolved and/or particulate organic carbon BOD ²	monthly
Soluble reactive phosphorus Total phosphorus ⁷	total dissolved phosphorus total inorganic phosphorus dissolved inorganic phosphorus	monthly
nitrate + nitrite nitrogen ammonium nitrogen ⁷	total Kjeldahl nitrogen filtered total Kjeldahl nitrogen	monthly
	secchi depth/light transmission	monthly
	total inorganic carbon alkalinity	monthly
	total suspended solids ³ inorganic and/or volatile suspended solids	monthly

DATA PREPARATION

	dissolved/total iron ⁸ dissolved/total manganese ⁸ dissolved/total silica ⁸ total dissolved sulfide ⁸ sulfate ⁸ iron sulfide ⁸	monthly
¹ enough samples to correlate to conductivity - important for density effects ² used to characterize decay rates of organic matter ³ suspended solids affect phosphorus partitioning, light penetration, and density ⁴ can be limiting for diatom growth ⁵ preferably bi-weekly - samples should be taken at 1m intervals ⁶ 1m intervals ⁷ minimum number of samples includes one each in epilimnion, metalimnion, and hypolimnion - preferred number of samples (depending on depth) would be at 3m intervals with more frequent metalimnetic sampling ⁸ when concerned about sediment release during anoxic periods		

Since water quality compartments are coupled, calibration of one compartment may affect other compartments making calibration difficult. *An understanding of the processes modeled as well as knowledge of the system being simulated is an absolute must if the modeling effort is to succeed.* A complete description of kinetic coefficients along with guidelines for appropriate default and a range of literature values is given in Appendix C.

Constituents are grouped into four levels ([Table 2](#)). Level **I** includes constituents that have no interaction with phytoplankton/nutrient/DO dynamics. Level **II** includes constituents affecting phytoplankton/nutrient/DO dynamics. Level **III** includes constituents that interact with level II constituents, but that are not transported. In level **IV**, alkalinity and total inorganic carbon are transported by the model and are thus state variables. They are necessary for computing pH and carbonate species.

Table 2. Constituent levels and names.

Level	Constituent
I	Total dissolved solids (or salinity)
	Generic constituents
	Inorganic suspended solids
II	Dissolved inorganic phosphorus
	Ammonium
	Nitrate-nitrite
	Dissolved silica
	Particulate biogenic silica
	Total Iron
	Labile DOM
	Refractory DOM
	Labile POM
	Refractory POM
	CBOD
	Dissolved oxygen

Level	Constituent
	Zooplankton
	Phytoplankton
III	Epiphyton
	Organic sediments
	Macrophytes
IV	Total inorganic carbon
	Alkalinity

The user should spend time familiarizing himself with the water quality formulations in [Appendix B](#) taking note of the assumptions used.

Data Analysis. An often overlooked step in model applications is plotting and analyzing observed data for all stations and times for which data are available. Do not plot up just the data chosen for calibration as the additional data may reveal important information about the prototype. Unfortunately, most mechanistic water quality modelers come from an engineering background with only cursory exposure to limnology. If a limnologist is available, they should be consulted during this stage to help in identifying the dominant processes occurring in the system. Once these have been identified, then efforts should be made to ensure the dominant forcing functions are represented as accurately as possible in the model, either as accurate boundary conditions or as additional water quality formulations.

For example, phosphorus coprecipitation with calcite is not currently included in the model. If this is known to be an important mechanism for phosphorus removal from the photic zone resulting from pH changes due to phytoplankton primary production, then this mechanism should be included in the kinetic formulations. This is a common mechanism for many freshwater systems located in limestone topography, such as Texas, Tennessee, and Florida. Another example would be the presence of macrophytes that affect hydrodynamics, nutrient uptake rates, phytoplankton primary production, and water column oxygen dynamics. Since macrophytes are not in the current release, then they would have to be included in the hydrodynamic and kinetic formulations.

Another important task in data development and analysis is to analyze the data for reasonableness. Checks for reasonableness should go beyond outlier checks to include checks to see if changes in concentrations over space and time make limnological sense. For example, if reservoir hypolimnetic nitrate concentrations increase during anoxic conditions and inflow temperatures are warmer than epilimnetic temperatures and/or inflow nitrate concentrations are less than the hypolimnetic concentrations, then there is no way for nitrate concentrations to increase during this time in either the prototype or in the model. So, there is no use wasting time during calibration trying to reproduce this behavior and the failure of the model to reproduce this behavior should not be viewed as a shortcoming of the model. Another example would be observed reservoir hypolimnetic release temperatures that were greater than the hypolimnetic temperatures. It would be impossible for the model to match these temperatures during calibration

CALIBRATION

Simulations

Once the necessary data have been assembled into proper input format, then simulations can begin. This section describes the recommended steps for obtaining meaningful model results.

Model Preparation

Input checks. A preprocessor program, `pre.exe`, performs checks of the control file for many errors that can be detected by the preprocessor. Errors are written to the file [PRE.ERR](#) and warnings are written to the file [PRE.WRN](#). If no errors are detected, then input from the control file is written to the file [PRE.OPT](#). All errors should be corrected before proceeding any further. Warnings should be investigated to ensure that what is being input into the model is what is intended. The preprocessor should be run periodically during the calibration phase to ensure that errors have not been introduced into the input files. However, do not assume that all is necessarily well if no warnings or errors are reported.

Additionally, the user should check preprocessor output against inputs to ensure they are correct. Further evaluation of control file input data must be performed by the user to ensure data the user thinks he has input into the model is what the model is actually receiving. Additionally, *all* time-varying input data should be plotted and screened for errors. These plots will need to be included in any final report and can eliminate a number of problems early on in the project.

Calibration

The next step is to begin calibration runs. Much of the literature refers to this step as calibration and verification in which model coefficients are adjusted to match an observed data set (calibration) and then the model is run on another “independent” data set without adjusting model coefficients to see if the model reproduces observed data in the prototype (verification in most circles, but variously called confirmation, validation, substantiation, etc. as numerous water quality modelers object to the word verification).

This separation is artificial and wrong. If a model does not reproduce observed data (and, more importantly, trends in data) for the “verification” data, then any good modeler will adjust coefficients, review model assumptions, include new processes, or collect additional data to adequately match both sets of data. Often, application to additional sets of data improves the fit to the first. The artificiality of this concept has led to applications in which modelers have used May, June, and July data for “calibration” and August, September, and October data of the same year for “verification” so they can state the model has been “calibrated/verified”.

The following examples will further illustrate the artificiality of the current concept of “calibration/verification”. Consider the following summary of observed data.

CALIBRATION

Year	Flow	Stratification	Fall algal bloom	Minimum DO at dam
1989	high	weak	yes	0 ppm
1990	low	strong	no	3 ppm
1991	average	medium	yes	1 ppm
1992	average	medium	yes	1 ppm
1993	low	strong	yes	1 ppm
1994	high	weak	no	3 ppm

Based on the currently accepted definition of calibration/verification, which of the years should be chosen for calibration and which should be chosen for verification? A case could be made for 1989 for calibration and 1994 for verification because of a fall phytoplankton bloom in 1989 and its absence in 1994. Additionally, the minimum dissolved oxygen at the dam was different between the years. If the model were to reproduce this behavior, then confidence could be placed in the model's ability to reproduce dissolved oxygen and phytoplankton blooms for the correct reasons. However, both years were years of high flow and using them would not test the model's ability to reproduce prototype behavior under different flow regimes.

Cases could be made for other combinations of calibration/verification years and different modelers would probably choose different calibration/verification years, so there doesn't appear to be one "correct" answer. In actuality, there is a correct answer. Model all the years and model them continuously. Modeling them continuously would eliminate separate calibration and verification years or data sets so the model could not be considered "calibrated and verified". However, if the model reproduces the wide variation in prototype behavior between all the years, a lot more confidence can be placed in the model's ability to reproduce prototype behavior for the "right" reasons than if the model were calibrated for one year and verified for another year.

Another example of the problems with the currently accepted "calibration/verification" approach to establishing model credibility is illustrated in the following table.

Year	Dominant algae	Flow	Minimum DO at dam
1979	diatoms	average	5 ppm
1986	greens	average	3 ppm
1994	bluegreens	average	0 ppm

Which year should be used for calibration and which year should be used for verification? Again, the best approach would be to model all three years, but since data do not exist for all the intervening years from 1979 to 1994, the simulation could not be continuous. An analysis of the data indicates a clear progression of eutrophication from 1979 to 1994 based on phytoplankton progression and increasing hypoxia. According to the current concept of "calibration/verification", all kinetic coefficients should be the same for all simulation years. However, the different dominant phytoplankton groups will have different growth, mortality, respiration, excretion, and settling rates and different light and nutrient growth rate half-saturation constants between the years. Keeping these values constant between calibration years would fly in the face of reality.

Additionally, the sediment oxygen demand has clearly changed because of eutrophication, so the values used in the zero-order sediment compartment should be different for the three years. As can be seen from just these two examples, all years should be considered calibration years and rate coefficients in some cases should change between different calibration data sets if the prototype is to be represented accurately.

CALIBRATION

Another concept associated with “calibration/verification” of a model is a post audit. Post audits are recommended whenever management changes are made as a result of modeling studies. A post audit involves making the management changes and then collecting data to see if the hoped for changes in prototype behavior based on model guidance have taken place. This appears to be a very reasonable concept and straightforward test of a given model’s simulation capabilities and, if the hoped for changes occur, then a great deal of confidence can be placed in the model’s simulative capabilities.

But what if the changes in water quality such as an improvement in minimum dissolved oxygen or extent of hypoxia does not occur? Can one then conclude that the model is not very good and little confidence can be placed in model results? The answer is no and the reason why is that no model can be used to predict the future. A model can only be used to determine what might have occurred if a particular set of boundary forcing functions were to occur in the prototype.

For example, hypoxia in Chesapeake Bay is a result of not only nutrient and organic matter loading, but also the degree of stratification that inhibits vertical mixing and reaeration. The degree of stratification is in large part a function of freshwater inflow. The higher the inflow, the greater the areal extent of density stratification in the Bay resulting in a greater areal extent of hypoxic waters. Suppose a model of the Bay “predicted” that a 40% nitrogen loading reduction decreased the areal extent of hypoxia by 20%. Based on this result, loadings were then reduced by 40% for five years and hypoxia did not decrease but actually increased during this time period.

Since the exact opposite occurred from what the model predicted, can the modeling study be concluded to be a failure? The answer is no. Suppose that the model results assume average freshwater river inflows and the five years after implementing loading reductions were high flow years, which increased the extent of hypoxia compared to an average flow year due strictly to physical effects. The only way to tell if the conclusions based on the model study were erroneous would be to model the five years using observed boundary conditions for this period and see if the model reproduced the observed increase rather than decrease in hypoxia. Thus, if a post audit yielded water quality different from expected water quality based on model results, this has no reflection on a given model’s ability to reproduce water quality in the prototype. Again, models cannot be used to predict the future, only what might have been.

Ideally, calibration should involve multiple data sets encompassing as many variations and extremes as possible in the prototype. A model’s ability to reproduce prototype behavior under a variety of conditions gives the modeler more confidence in the model’s ability to accurately simulate the prototype under proposed conditions. To put it very simply, a model is a theory about behavior in the real world. A theory is continuously tested against *all* observed data, and, if it does not match the data, then the theory should either be modified or a new one developed that more closely agrees with observed data.

Model data/comparison. The model produces the following output files for displaying results:

1. [Profile file \[PRFFN\]](#). This file is used to plot observed versus predicted vertical profiles for temperature and constituents at a given segment.
2. [Time series file \[TSRFN\]](#). This file is used to plot time histories of water surface elevations, flows, temperatures and constituent concentrations for user specified

computational cells. This file also contains information to plot out the time history of the variable timestep and average timestep.

3. [Contour plot file \[CPLFN\]](#). This file is used to plot contours of temperature and constituents along the waterbody length.
4. [Vector plot file \[VPLFN\]](#). This file is used to plot velocity vectors determined from horizontal and vertical velocities. The output is useful in analyzing flow patterns in the waterbody.
5. [Spreadsheet file \[SPRFN\]](#). This file is similar to the profile except the output is suitable for importing into a spreadsheet type database for subsequent plotting.

A description of the output from each file and how to use the information is given in [Appendix C](#). The current release version requires the user to develop plotting capabilities from these files. This is most often done using the [spreadsheet output file](#) and [time series output file](#) and developing macros to process the data.

Calibration is an iterative process whereby model coefficients are adjusted until an adequate fit of observed versus predicted data is obtained. Unfortunately, there are no hard and fast guidelines for determining when an adequate fit is obtained. The user must continually ask himself "is the model giving useful results based on model formulations, assumptions and input data?". If it is not, then the user must determine if the inability of the model to produce useful results is due to the use of the model in an inappropriate manner (i.e., hydrostatic approximation is invalid, one phytoplankton group is not sufficient to capture phytoplankton/nutrient/DO interactions, wind speed function for evaporation is inappropriate for the waterbody, etc.), model formulations are insufficient to describe known prototype behavior, or if input data are insufficient to describe the system dynamics.

Another important point to keep in mind during calibration is that a model may give inadequate results for a given spatial and/or temporal scale, but at another scale may reasonably represent the dynamics of the prototype. For example, the model may fail to predict a short-term phytoplankton bloom using monthly inflowing phytoplankton and nutrient concentrations, but may adequately represent phytoplankton production over the summer stratification period. The model may thus be useful in determining a waterbody's long-term response to nutrient loading reductions but be inadequate in addressing short-term responses to a nutrient reduction strategy. In summary, it is not always necessary for model output to match all of the observed data for the model to provide meaningful results.

The usual sequence for calibration is to first calibrate the water budget (or water surface elevation), then calibrate temperature (preferably salinity for estuarine applications), and finally water quality. Keep in mind water quality calibration can affect temperature/salinity calibration. A description of each follows. Calibration is separated into different sections for river, lake/reservoir, and estuarine applications.

Lake/Reservoir

Water budget

The water budget is checked by comparing predicted elevations with observed elevations. Errors in the water budget are generated by the following:

CALIBRATION

1. **Incorrect bathymetry.** The user should carefully check the volume-area-elevation table produced by the model to ensure it closely matches the project volume-area-elevation table. If it does not, then the bathymetry should be checked carefully to ensure there are no errors. In some cases, additional sediment range surveys may be necessary to adequately define the bathymetry. It may also be necessary to include branches that were not included in the initial bathymetry. Also, keep in mind that development of the original volume-area-elevation table was subject to the same errors used in developing the volume-area-elevation table for the application. In some applications, the new volume-area-elevation table was deemed more accurate than the original.
2. **Storm events.** Errors in the water budget due to storm events can be determined by comparing predicted with observed elevations using output from the time series plots. If the error is generated during storm events, then the user should check to see if precipitation must be included and/or if more tributaries need to be included than were originally specified. The user may need to use a hydrologic model to determine inflows during storm events for ungaged tributaries. An alternative method is to apportion inflows for ungaged tributaries based on their watershed areas.
3. **Incomplete inflow data.** A substantial amount of inflow is often unaccounted for when using gauged inflows. The unaccounted inflows can include minor tributary, precipitation, stormwater, and wastewater treatment plant contributions. The distributed tributary option provides the user with a means to account for these contributions. This option distributes inflows into every branch segment weighted by the segment surface area.
4. **Evaporation.** If evaporation in the region is significant and is not accounted for in inflows, then it should be included using the evaporation option [\[EVC\]](#).
5. **Seepage.** Seepage gains or losses can be significant for some waterbodies. The model does not explicitly handle seepage at present, but the coding is such that seepage can be readily included in the calculations as an additional rate term in the flow source/sink array [QSS]. Several applications required specifying seepage losses through the dam in order to properly calibrate temperature.
6. **Inaccurate Inflow/Outflow Measurements.** Gauged inflows and reservoir outflows are notoriously inaccurate with typical measurement errors of 5-10%. The model is very sensitive to inflow/outflow error measurements that can result in significant errors in water level predictions.

Typically, the user will first plot observed versus predicted water surface elevations for the simulation period after all the inflow/outflow data have been collected and the model is running to completion. The latest version contains a program for computing reservoir water balances that will initially compute the additional flows necessary for reproducing observed water surface elevations, but it will not normally generate a perfect water balance. The computed flows can then be manually adjusted to more closely match observed water surface elevations. Normally, the computed flows are initially incorporated using the distributed tributary option in the model with interpolation turned off so that the model sees the flows as a step function since this is how the flow is computed by the utility. Using this option, the flows necessary to compute the water balance are distributed into the surface layer weighted according to segment surface area.

CALIBRATION

Keep in mind that this method only provides the necessary flows to complete the water balance. The user must decide how to incorporate them into the model in a realistic fashion as the method of incorporation can have a large impact on temperature and water quality calibration – another fork in the road in the “art” of water quality modeling. The recommended procedure is to first plot up and analyze the computed flows to see if they provide any information as to the source of the error.

For example, if the majority of the computed flows are negative and the inflows are deemed accurate, then this would indicate that the outflow has been underestimated. It could be due to seepage into groundwater or seepage through the dam. If the hypolimnetic temperatures were also being underpredicted, which would indicate that the hypolimnetic residence time was being overpredicted, then incorporating the computed flows into an additional outflow could solve both problems at once. The point to be made is that various methods of incorporating the computed flows during temperature and water quality calibration should be tried to determine if they have an affect on temperature or water quality. Whichever method improves the calibration is the method to use. The following plot illustrates the accuracy normally expected for a reservoir water surface elevation calibration. The computed elevations overlay the observed elevations.

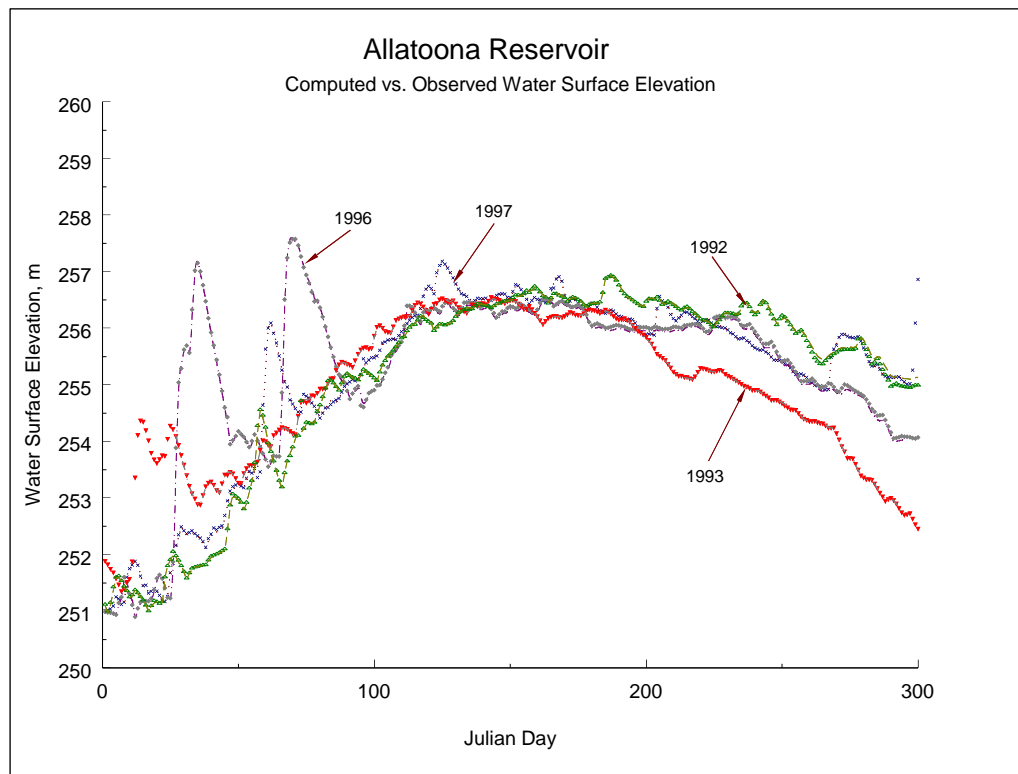


Figure 3. Allatoona Reservoir computed (lines) vs. observed (symbols) water surface elevations for 1992, 1993, 1996, and 1997.

Hydrodynamics and Temperature

The earliest one-dimensional mechanistic reservoir models included only temperature. As a result, temperature was the only model prediction that could be used for hydrodynamic calibration. Since

CALIBRATION

temperature is affected by surface and bottom heat exchange and is therefore nonconservative, it is not the best parameter for calibrating hydrodynamics. Salinity, which is conservative, has historically been considered the ideal constituent for hydrodynamic calibration. However, this is generally feasible only for estuarine applications where salinity is routinely monitored. Dissolved solids are not conservative and are generally *not* a good substitute for salinity during calibration except in waterbodies where the conservative assumption is appropriate. The previous three sentences echo the prevailing sentiment of hydrodynamic modelers. In reality, there is no “ideal” constituent that should be used for hydrodynamic calibration. Each constituent can contribute knowledge about the system and can have an impact on the hydrodynamic calibration.

Experience has shown that dissolved oxygen and phytoplankton are often much better indicators of proper hydrodynamic calibration than either temperature or salinity. There are several reasons for this. First, gradients in dissolved oxygen and phytoplankton are often present at different locations in the water column than either temperature or salinity gradients. Consequently, they can provide additional information as to the correctness of the hydrodynamic calibration beyond either temperature and/or salinity alone. Second, dissolved oxygen is much more dynamic than either temperature or salinity and readily responds to wind events including seiching, with the anoxic zone often moving several kilometers over a day in response to the hydrodynamics. Phytoplankton distributions are also affected by the hydrodynamics. Further discussion and examples will be presented in the section on water quality calibration. Nevertheless, temperature and/or salinity should always be the first step during hydrodynamic calibration, with the hydrodynamic calibration further refined during water quality calibration.

Computed velocities can be compared with velocity and flow measurements obtained from an acoustic Doppler current profiler (ADCP) to additionally evaluate the model’s hydrodynamic performance. However, care must be taken when comparing model velocities with observed velocities to ensure ADCP measurements are comparable to the laterally averaged velocities generated by the model.

Coefficients affecting temperature and their default values are given in [Table 3](#). The eddy viscosities, Chezy coefficient, and wind sheltering coefficient directly affect hydrodynamics that affect heat and constituent transport. The remaining coefficients directly affect temperature that affects hydrodynamics. Of these, the last two coefficients affect temperature only if constituents are modeled. See [Appendix C](#) for a more detailed description of these coefficients and their effects.

Table 3. Coefficients affecting thermal calibration

Coefficient	FORTRAN Name	Default
Longitudinal eddy viscosity	[AX]	1 m ² sec ⁻¹
Longitudinal eddy diffusivity	[DX]	1 m ² sec ⁻¹
Chezy coefficient or Manning’s N	[FRICT]	70 m ² sec ⁻¹
Wind sheltering coefficient	[WSC]	Calibration parameter
Solar radiation absorbed in surface layer	[BETA]	0.45
Extinction coefficient for pure water	[EXH20]	0.45 m ⁻¹
Extinction coefficient for inorganic solids	[EXINOR]	0.01 m ⁻¹

Extinction coefficient for organic solids	[EXORG]	0.2 m ⁻¹
---	-------------------------	---------------------

In addition to the above coefficients, temperature predictions are also affected by the surface heat exchange algorithm specified, mainstem and tributary inflows, inflow temperatures and their placement, outlet and withdrawal specifications, the numerical solution scheme, and bathymetric and meteorological data. Again, always represent the prototype as accurately as possible.

Applications on over 400 waterbodies under a wide variety of conditions have shown the model generates remarkably accurate temperature predictions using default values when provided accurate geometry and boundary conditions. The wind-sheltering coefficient [\[WSC\]](#) has the most effect on temperature during calibration and should be adjusted first. Previous applications varied the wind sheltering coefficient from 0.5-0.9 for mountainous and/or dense vegetative canopy and 1.0 for open terrain. In a very few cases, the wind-sheltering coefficient [\[WSC\]](#) has been increased above 1.0 to account for funneling effects on systems with steep banks. The user should also run sensitivity analyses on the other coefficients to gain a "feel" for how they affect temperature predictions.

Calibration problems. Difficulties during temperature calibration can often be traced to the following:

1. **Inflows and Inflow temperatures.** Accurate inflows and inflow temperatures are desirable for all applications, but they are critical for waterbodies with short residence times or during high inflow periods. Temperature calibration will be difficult using monthly inflow temperatures for a waterbody with a one week residence time. Methods exist for generating more frequent inflow temperatures based on flow and meteorological data (Ford and Stein, 1986), but there is no substitute for actual measurements.
2. **Meteorological data.** Many difficulties are associated with extrapolating weather station meteorological data to a waterbody site. Weather stations are typically located in different terrain and at large distances from the prototype. Frontal movements can occur at different times over the waterbody and meteorological station resulting in model predictions that are in closer agreement either earlier or later than the actual comparison date. Methods for addressing these problems include adjustment of the wind sheltering coefficient [\[WSC\]](#), use of an alternative meteorological station, averaging data from several meteorological stations, separating a waterbody into regions applying data from different meteorological stations, and comparison of observed data using model output either before or after the observed date. If the user has the luxury of obtaining calibration data before applying the model, portable weather stations exist which can be deployed on the waterbody. Obviously, this is the preferred method.
3. **Outflow data.** The addition of the selective withdrawal algorithm in Version 2.0 has reduced many of the previous problems of accurately representing outflows. However, problems still arise. In the application of CE-QUAL-W2 to Bluestone Reservoir, Tillman and Cole (1994) were unable to reproduce observed temperature stratification without limiting the lower withdrawal layer. Subsequent investigation showed that withdrawal was limited by trash accumulation that effectively acted as a submerged weir. This was a problem generated by inadequate knowledge of the

CALIBRATION

prototype and not a problem with the model. Indeed, this is an example of a model giving insight into the behavior of the prototype.

4. **Bathymetry.** Several previous applications of the model encountered difficulties during temperature calibration until the bathymetry was revisited. Check the assumptions made during the development of the bathymetry to ensure they are not the source of the problem. Starting points include grid resolution that affects the models ability to define sharp thermal gradients and bottom slope, volume-area-elevation accuracy that can have a marked effect on hypolimnetic temperatures since the volumes are generally small near the bottom, and water surface areas that affect the area available for surface heat exchange. Branch definition has also been found to have an effect on temperature predictions.

In order to illustrate how accurate reservoir temperature modeling has become with CE-QUAL-W2, [Table 4](#) lists calibration results for 70 reservoir thermal simulations. The statistic presented is the absolute mean error (AME) computed as follows:

$$AME = \frac{\sum |Predicted - Observed|}{\text{number of observations}}$$

Although a number of other statistics have been used when evaluating model results, the AME provides the best indication of model performance since it is directly interpretable. For example, an AME of 0.5 °C means that the model results are, on the average, within °0.5 EC of the observed data. As can be seen, model predictions for all the reservoirs are within °1 °C and most of them are much less.

Table 4. Reservoir thermal simulations with error statistics for station closest to dam.

	Reservoir	# years	AME, °C		Reservoir	# years	AME, °C
1	Allatoona	4	0.6	36	Monroe	4	0.7
2	Alum Creek	1	0.5	37	Neely Henry	2	0.6
3	Barklay	1	0.5	38	Neversink	3	0.4
4	Bluestone	2	0.5	39	Norman	3	0.7
5	Brownlee	2	0.6	40	Oxbow	1	0.3
6	Bull Run 1	2	0.5	41	Oahe	2	0.9
7	Bull Run 2	2	0.7	42	Occoquan	1	0.9
8	Burnsville	1	0.9	43	Paint Creek	1	0.4
9	Caesar Creek	1	0.6	44	Paintsville	1	0.4
10	Cannonsville	5	0.7	45	Patoka	3	0.7
11	Cave Run	4	0.8	46	Pepacton	3	0.6
12	C.J. Strike	2	0.7	47	Pineflat	5	0.6
13	Croton	1	0.7	48	Powell	1	0.7
14	Cumberland	1	0.5	49	J. Percy Priest	3	0.8
15	Deer Creek, OH	1	0.4	50	Quabbin	1	0.7
16	Deer Creek, ID	5	0.8	51	Richard B. Russell	3	0.5
17	DeGray	8	0.9	52	Rhodiss	2	0.6
18	Fishtrap	1	0.8	53	Riffe	1	0.7
19	Fort Peck	2	0.7	54	Rimov	1	0.5
20	Francis Case	2	0.7	55	Rondout	3	0.5
21	Herrington	1	0.7	56	Sakakawea	2	0.7
22	Hickory	1	0.5	57	Schoharie	2	0.8
23	J.W. Flanagan	1	0.5	58	Shasta	1	0.6
24	Jordanelle	3	0.7	59	Shepaug	1	0.6
25	J. Strom Thurmond	5	0.9	60	Stonewall Jackson	2	0.5

CALIBRATION

26	James	1	0.6	61	Toledo Bend	1	0.7
27	Houston	6	0.5	62	Taylorville	2	0.9
28	Lanier	2	0.9	63	Tolt	1	0.5
29	Loch Raven	1	0.9	64	Travis	1	0.3
30	Long Lake	1	0.5	65	Wabush	1	0.6
31	Lost Creek	1	0.6	66	Wachusett	4	0.7
32	Maumelle	2	0.7	67	Weiss	2	0.6
33	Mayfield	1	0.6	68	West Point	3	0.8
34	Moehnetalsperre	1	0.4	69	Walter F. George	2	0.6
35	Mountain Island	1	0.7	70	Youghiogheny	2	0.8

The following examples illustrate CE-QUAL-W2's ability to reproduce observed temperatures on a variety of systems with widely varying temperature regimes. On all plots, x 's represent observed data and their widths are scaled to represent $\pm 0.5^\circ\text{C}$. The dotted lines represent computed model values. The absolute mean error (AME) and root mean square error (RMS) are also included for each date in order to help in interpreting the predictive capability of the model. These statistics should always be included in plots of computed versus observed data since plots can often be misleading depending upon the scale of the x and y axes and the size of the marker used to represent the observed data (a common technique used to make model results appear better than they actually are).

Pineflat Reservoir. Pineflat Reservoir is located in California near the base of the Sierra Madre mountain range. One of its primary uses is for providing irrigation water during the summer growing season. Consequently, the reservoir is drawn down as much as 70 *m* over the summer during drought years. The model was used to provide operational guidance for a temperature control device that will be installed in the reservoir to optimize the storage of cold water for downstream releases at the end of summer.

Figure 4 shows the results of temperature predictions for 1989. The thermal regime exhibits two thermoclines starting in early spring. As can be seen, the reservoir was drawn down over 40 *m* during the summer. During 1993, the development of the two thermoclines was delayed until the end of summer (**Figure 5**). CE-QUAL-W2 correctly captured the thermal regimes for both years and the differences in the thermal regimes between the two years.

Sensitivity analyses showed that temperature predictions were very sensitive to inflow temperatures. Calibration consisted of adjusting inflow temperatures to more closely match in-pool temperature profiles. Because calibration showed the importance of accurate inflow temperatures in order to properly calibrate the model, additional fieldwork was done to obtain accurate inflow temperatures. During this effort, it was discovered that the location where inflow temperatures were taken showed a lateral variation in the river of over 5°C due to hypolimnetic discharges from an upstream reservoir that did not completely mix laterally. Additionally, during extreme drawdown, it was shown that inflow temperatures increased by nearly 2°C from measured temperatures as the upstream boundary of the model moved downstream approximately 10 *km* due to the large drawdowns that the reservoir was periodically subjected to.

CALIBRATION

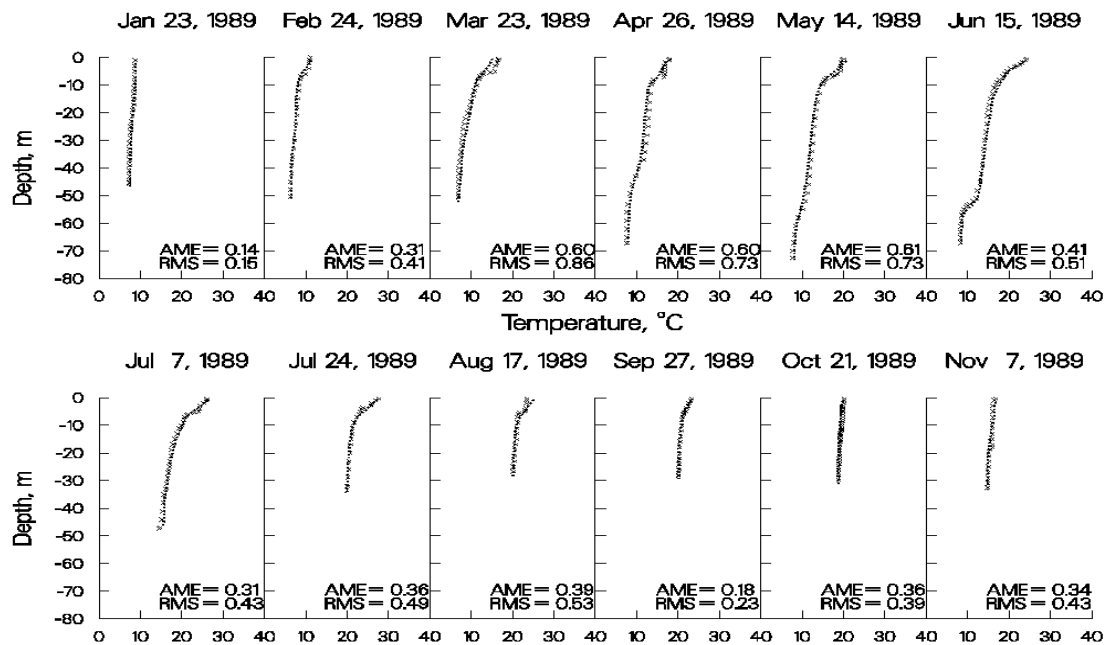


Figure 4. 1989 Pineflat Reservoir computed versus observed temperatures.

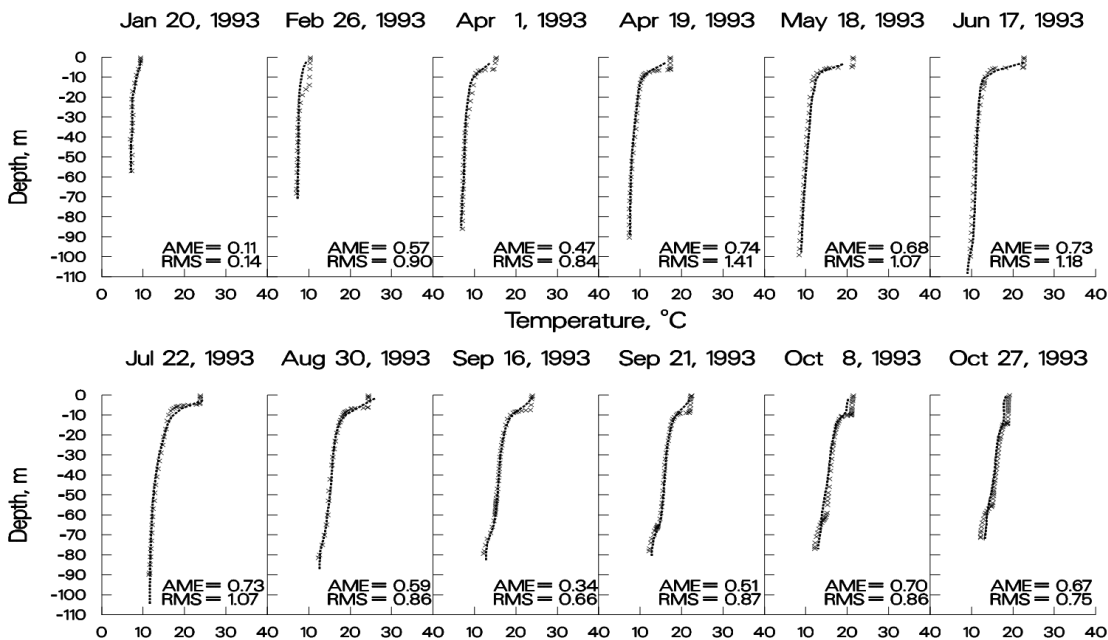


Figure 5. 1993 Pineflat Reservoir computed versus observed temperatures.

Bluestone. Bluestone Reservoir is located in the mountains of West Virginia. The reservoir has an average hydraulic retention time of less than a week during the summer. When first calibrating for temperature, the model predicted essentially no thermal stratification during the summer whereas the observed data showed strong stratification beginning at a depth of about eight meters. Based on the short residence time during the summer, model predictions seemed quite reasonable.

However, stratification was present in both 1981 and 1983 indicating that stratification was not a rare occurrence.

A number of mechanisms were proposed to explain the observed stratification including ground-water seepage and extreme wind sheltering. Including these in the model did not result in any improvements in model predictions. Finally, the lower limit of selective withdrawal was set at the depth corresponding to the outlet elevation. Results of the simulation are shown in [Figure 6](#) and [Figure 7](#). Subsequent investigations at the reservoir revealed that accumulated debris at the level of the trash racks was acting like a submerged weir that limited the bottom of the withdrawal zone to the elevation of the trash racks. This is an example of a model providing insight into previously unknown behavior of the prototype.

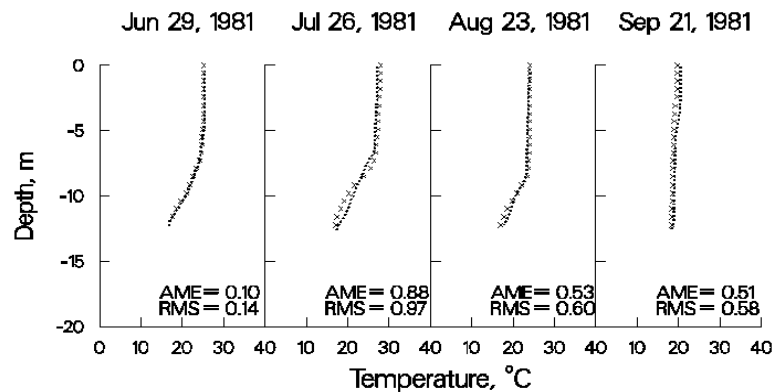


Figure 6. 1981 Bluestone Reservoir computed versus observed temperatures.

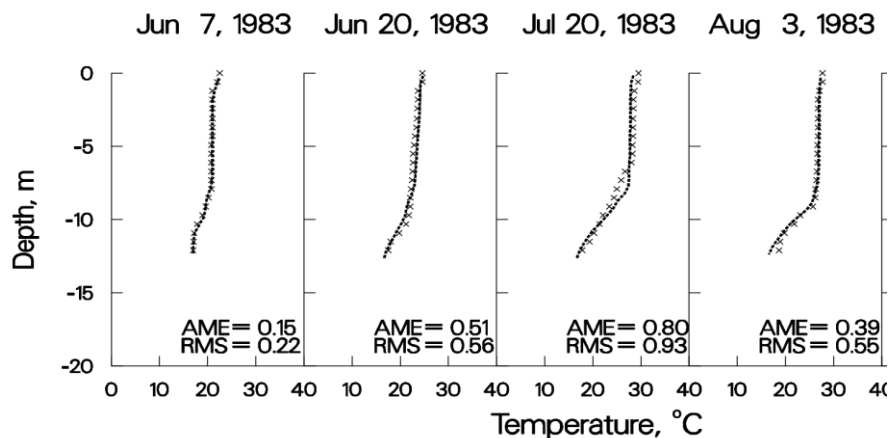


Figure 7. 1983 Bluestone Reservoir computed versus observed temperatures.

Richard B. Russell. Richard B. Russell (RBR) is located immediately upstream of J. Strom Thurmond Reservoir (JST) on the Savannah River bordering Georgia and South Carolina. The model was used to investigate the effects of proposed pump-storage operations in which water would be pumped into RBR from JST and reused for hydropower operations during peak energy demands. An important concern was what effect pump-storage operations would have on the thermal regime in RBR. The model was subsequently applied to 1996, a year in which extensive pump-storage

CALIBRATION

operations occurred. In order to simulate the effects of pump-storage, the model code was altered to allow dynamic linkage of RBR and JST reservoirs.

This is a stringent test of the model's simulation capabilities because the dynamic linkage required accurate temperature simulations in RBR in order to provide accurate inflow temperatures to JST. Likewise, accurate temperature predictions were required in JST in order to provide accurate temperatures entering RBR during pumpback.

[Figure 8](#) [Figure 10](#) show the results of the simulations. The model correctly predicted the approximately 4 °C increase in hypolimnetic temperatures compared to previous years that did not have pump-storage operations. No calibration was involved for this simulation. Results are from the first run of the model for 1996 using default hydrodynamic/temperature calibration parameters and a wind-sheltering coefficient determined from calibration to two previous years that did not include pump-storage operations.

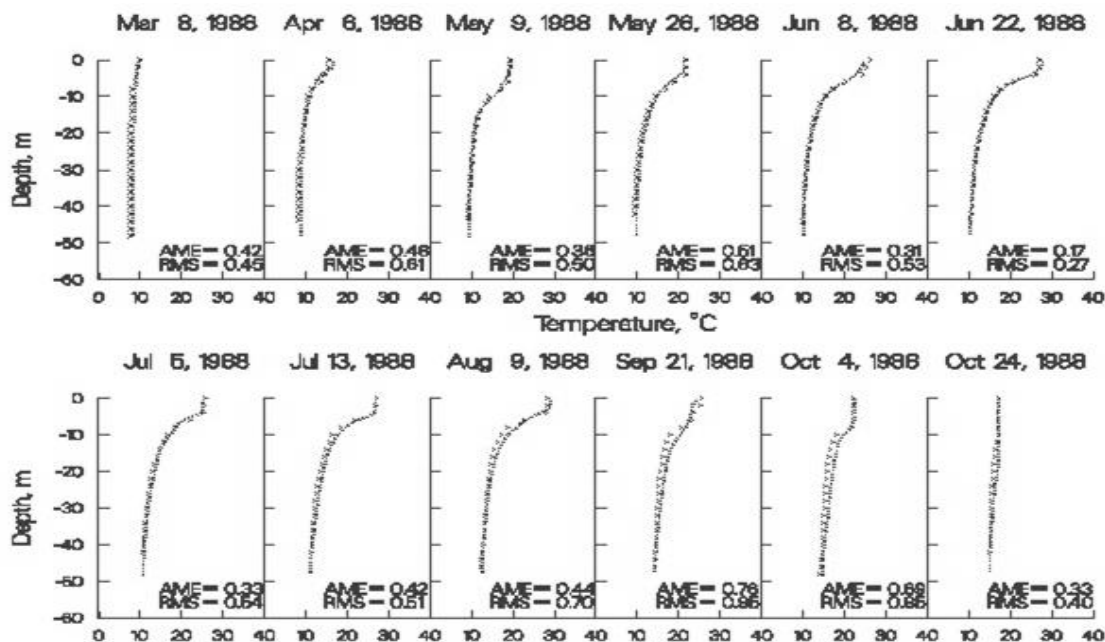


Figure 8. 1988 Richard B. Russell computed versus observed temperatures.

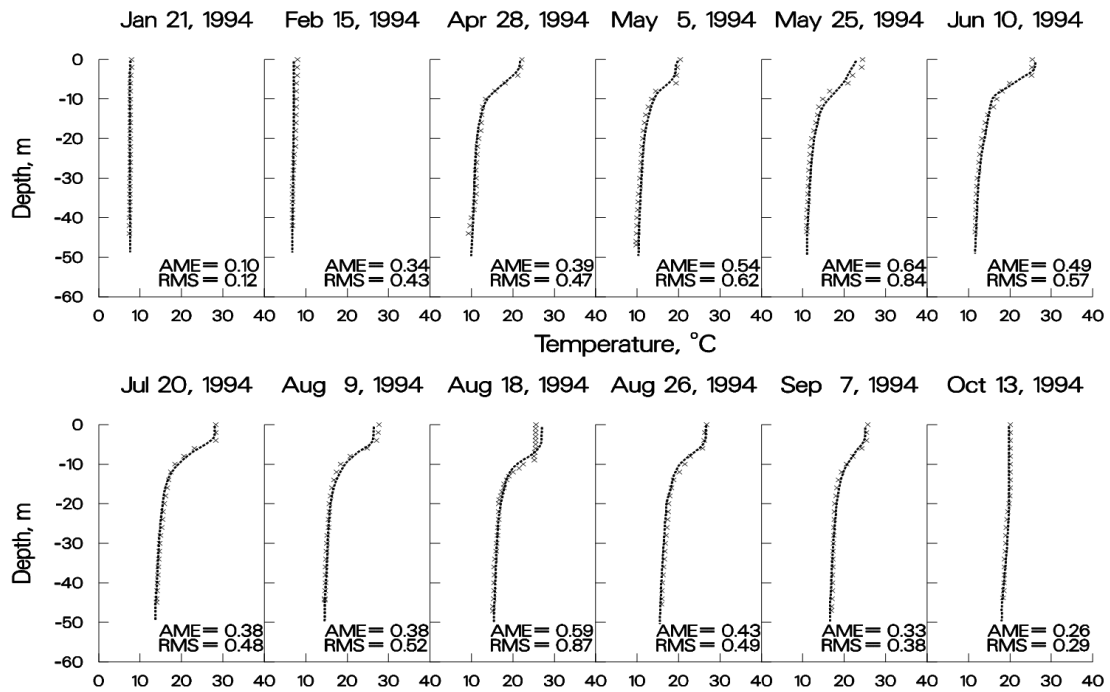


Figure 9. 1994 Richard B. Russell computed versus observed temperatures.

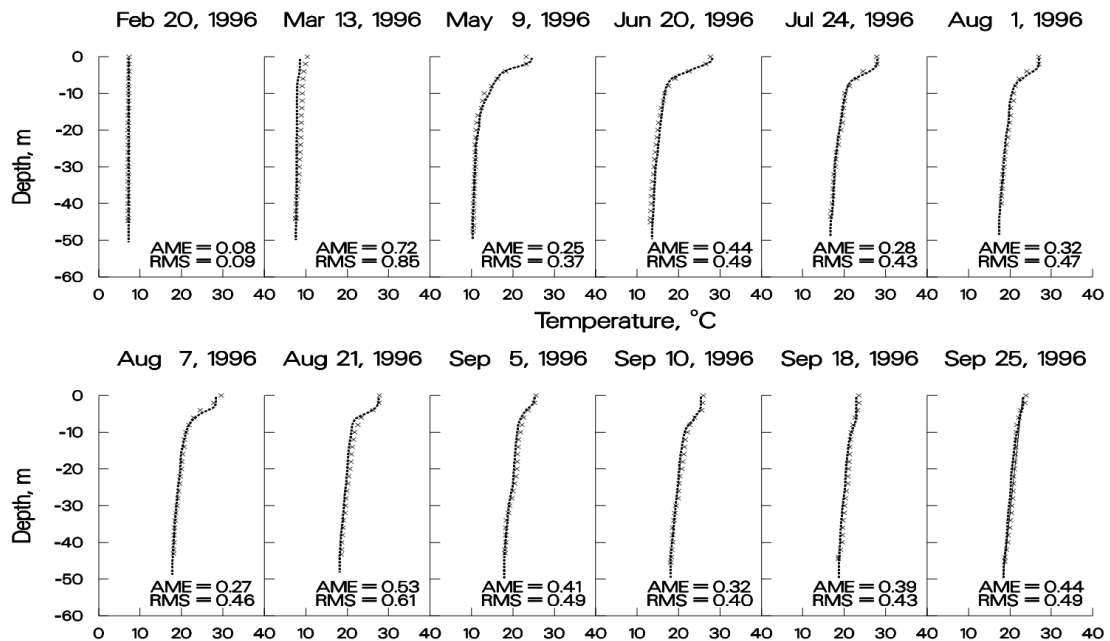


Figure 10. 1996 Richard B. Russell computed versus observed temperatures.

Paintsville Reservoir. Paintsville Reservoir is a US Army Corps of Engineers reservoir located in Kentucky. The reservoir's thermal regime is typical of deep-storage reservoirs with hydraulic retention times greater than four months. [Figure 11](#) illustrates the model's ability to reproduce the

CALIBRATION

springtime development of the thermocline, the strong thermocline present in late summer, and fall overturn.

During initial calibration, the model consistently overpredicted hypolimnetic temperatures. No parameter adjustment (wind-sheltering or light absorption/extinction) resulted in an acceptable calibration. Realizing that hypolimnetic temperatures are influenced by residence time, a sensitivity analysis was performed in which the widths were increased uniformly (thus increasing hypolimnetic residence time) until the predicted hypolimnetic temperatures matched the observed temperatures. Subsequently, it was determined that the original development of the bathymetry did not include two branches that accounted for approximately 15% of the storage in the reservoir. In this case, calibration consisted of ensuring that the volume-elevation relationship was accurately described.

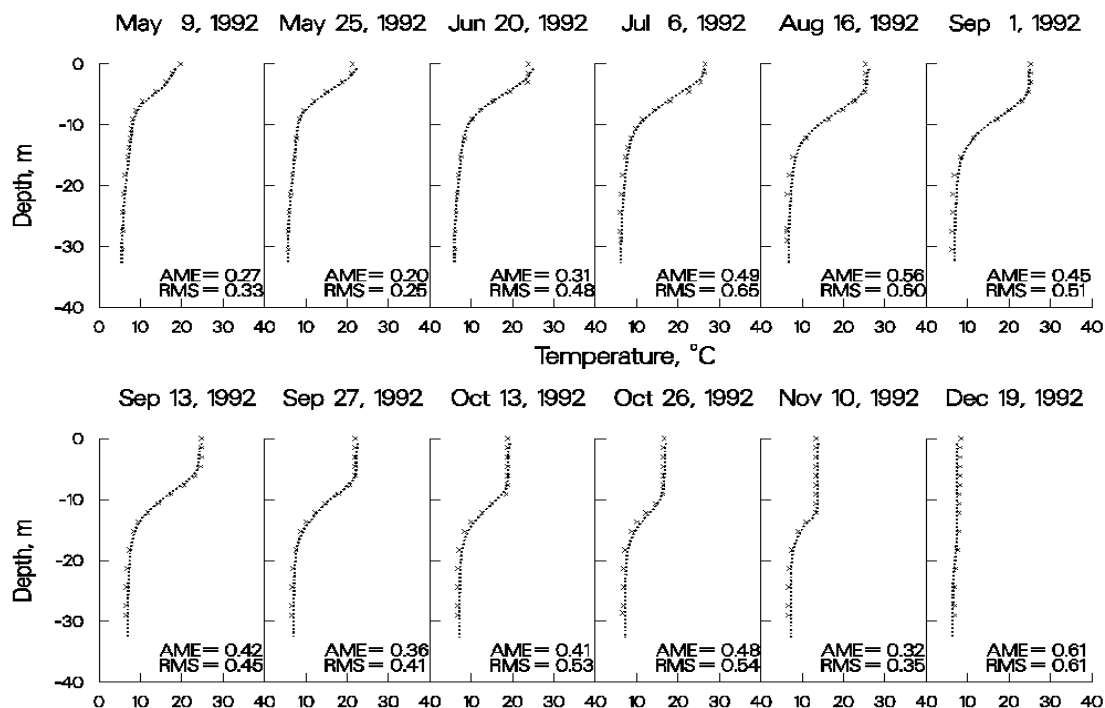


Figure 11. Paintsville Reservoir computed versus observed temperatures.

Brownlee Reservoir. Brownlee Reservoir is located on the Snake River in Idaho and is operated by Idaho Power. Brownlee's thermal regime is very distinctive with the thermocline starting at approximately 30 m below the water surface. [Figure 12](#) and [Figure 13](#) illustrate the model's ability to simulate the thermal regime in Brownlee.

During initial temperature calibration, the model predicted hypolimnetic temperatures greater than 15°C, whereas the observed temperatures were always near 5°C. No parameter adjustment allowed for adequate temperature calibration. An analysis of the system showed that the theoretical residence time during the summer was less than two months indicating that model predictions of warmer hypolimnetic temperatures were more reasonable than the observed data.

CALIBRATION

Additionally, the thermal structure in Brownlee exhibits a well-mixed epilimnion approximately 30 m in depth. Wind mixing could not supply sufficient energy to account for the depth of the epilimnion. Therefore, it was concluded that outflow dynamics had to be responsible for the observed thermal regime. As in the Bluestone application, the bottom layer for selective withdrawal was set at approximately the same depth as the thermocline. Subsequent investigations revealed the presence of a ledge below the outlet that was limiting the outflow to the level of the observed thermocline.

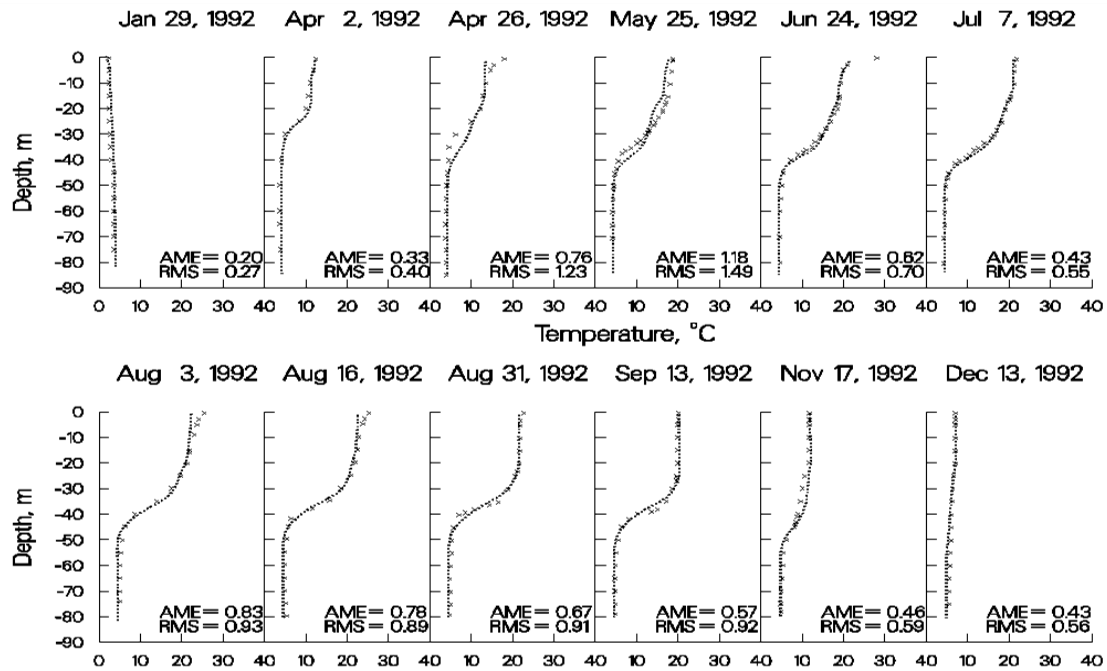


Figure 12. 1992 Brownlee Reservoir computed versus observed temperatures.

CALIBRATION

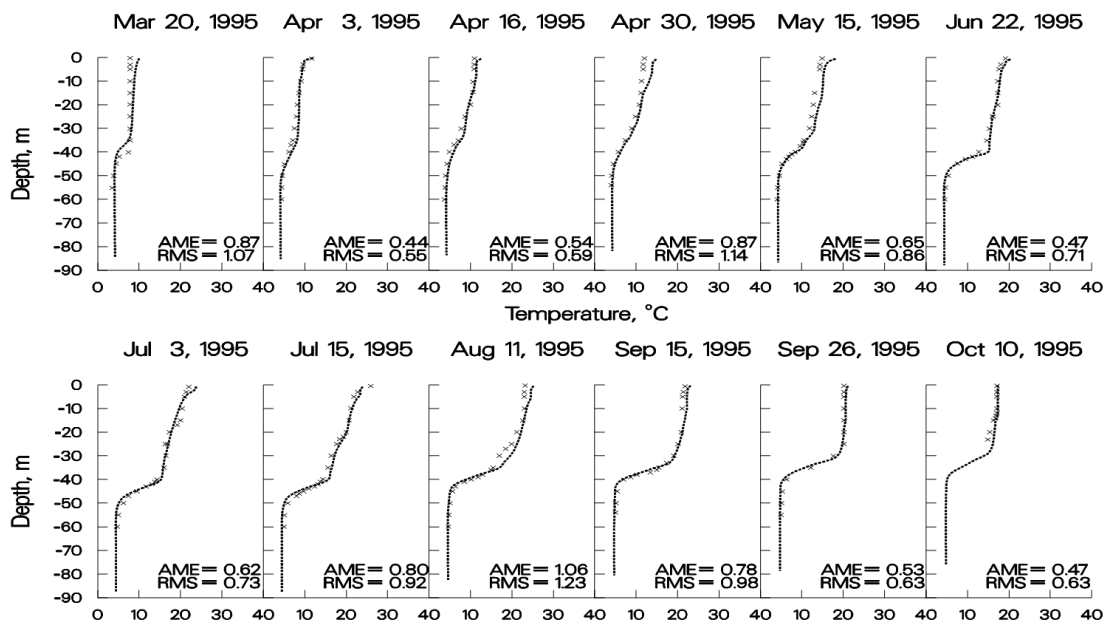


Figure 13. 1995 Brownlee Reservoir computed versus observed temperatures.

C.J. Strike Reservoir. C.J. Strike Reservoir is located on the Snake River in Idaho upstream of Brownlee Reservoir and is also operated by Idaho Power. Stratification is not nearly as pronounced as in Brownlee Reservoir due to the smaller volume of C.J. Strike and subsequent shorter residence time.

As noted in the discussion for Brownlee Reservoir, the relatively short residence time during the summer should result in considerable hypolimnetic heating as cold water is withdrawn and replaced by warmer waters from above. Temperature calibration consisted of adjusting the wind-sheltering coefficient until adequate agreement was obtained between computed and observed temperatures.

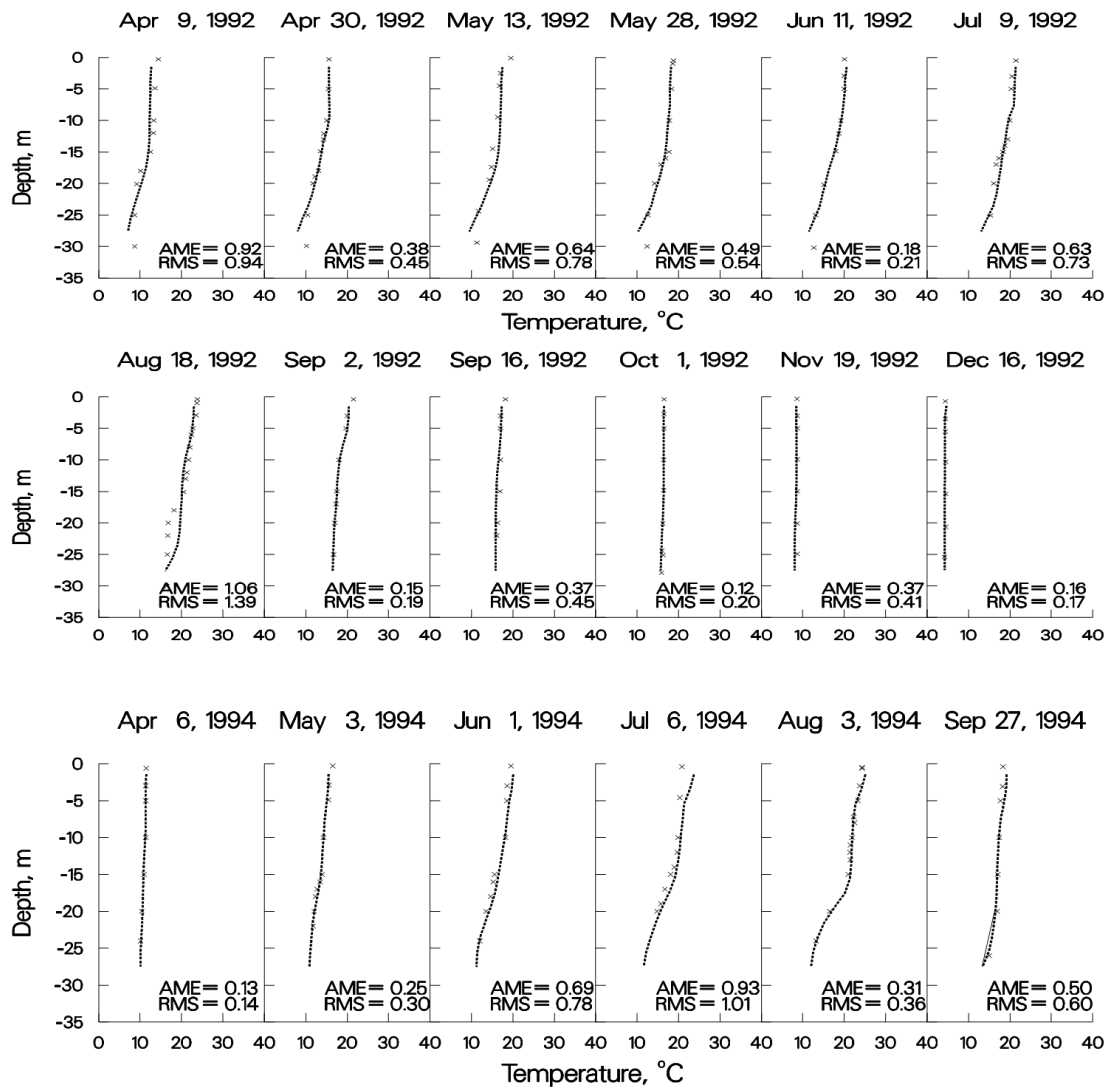


Figure 14. C.J. Strike Reservoir computed versus observed temperatures.

These examples illustrate the models ability to reproduce complex thermal regimes that differ widely depending upon a particular reservoir's morphometry, location, surrounding terrain, and operations with a minimum of parameter adjustment. The only parameter adjusted was the wind-sheltering coefficient that was used to adjust wind speeds taken at a given meteorological station to the reservoir surface. Values ranged from 0.6 for small reservoirs located in mountainous terrains to 1.0 for large reservoirs located in open terrain.

The preceding discussion is not meant to imply that the model is "plug and play" and requires no calibration with regards to temperature. Greater discrepancies between computed and observed temperature profiles were always present at the beginning of thermal calibration for all the presented examples.

Aside from adjustment of wind sheltering, calibration consisted of determining whether known inaccuracies in a given forcing function could be responsible for the discrepancies in the computed

CALIBRATION

temperature profiles and then describing the forcing function more accurately. This procedure included the following:

1. Adjustment of volume-elevation relationship to ensure that residence time was accurately represented
2. Adjustment of bottom elevation to ensure that computed and observed bottom elevations for the deepest station were at least as deep as the observed data
3. Adjustment of inflow temperatures to more closely match temperatures at the most upstream station
4. Generation of more frequent inflow temperatures based on equilibrium temperature
5. Using more frequent outflow data than daily average values, particularly for peaking hydropower systems
6. Ensuring that the outflow distribution for multi-level outlets was accurately described
7. Ensuring sufficient longitudinal/vertical grid resolution
8. Obtaining more frequent meteorological data than daily average values
9. Limiting the bottom zone for selective withdrawal (all instances were eventually physically justified in the prototype)
10. Including additional sources of outflow due to dam leakage or seepage to groundwater
11. Ensuring multiple branch descriptions were accurately represented
12. Using the most accurate numerical scheme (ULTIMATE with [THETA] set to 0) and including the effects of vertical turbulence [VISC] and internal gravity waves [CELC] in the autosteping stability requirements

As a result of the numerous thermal applications of the model, an important concept that has emerged is that the more accurately the behavior of the prototype is described, the more accurately the model responds. Always keep this in mind during model calibration.

Water Quality

The following discussion can serve as a starting point for reservoir water quality calibration. However, each application is different and requires knowledge about prototype behavior and the dominant water quality processes that are occurring in the prototype before ever attempting to model water quality. Black box application of any model is a recipe for failure.

Dissolved Oxygen. Once the user has a good understanding of the dominant water quality processes occurring in the prototype and ensures they are accurately represented in the model, then the user should begin dissolved oxygen calibration. The zero-order SOD should be used initially as it is essentially a pure calibration parameter that allows for back calculating the oxygen uptake rate in the water column. If dissolved oxygen profiles in the water column are exactly matched, then the values for SOD used in calibration are very close to the actual uptake rates of dissolved oxygen in the water column. The problem with using only the zero-order SOD for water column DO calibration is that the model will not be sensitive to load increases/decreases that directly affect water column DO uptake and sediment nutrient recycling that affect phytoplankton primary production.

However, this is seldom the case, particularly where loadings to the system in the form of allochthonous organic matter (or CBOD), autochthonous organic matter due to phytoplankton production, and/or ammonium are important forcing functions for water column dissolved oxygen that are subject to change over time. Unfortunately, for systems where allochthonous loadings of organic matter are important, rarely are there sufficient boundary condition data to adequately represent the loadings to the system.

Particular care should be paid to the timing and duration of events involving phytoplankton, epiphyton, and dissolved oxygen. If the model does not represent the onset, extent, and duration of anoxic conditions, then nutrient dynamics will not be represented either. They in turn affect phytoplankton production that affects dissolved oxygen. Timing of the onset of dissolved oxygen depletion is greatly influenced by the temperature rate multipliers used for organic matter and the sediments. A change in the lower temperature [OMT1] of 1°C in the temperature rate formulation can shift the initial uptake of water column dissolved oxygen by as much as two weeks. The same effect can be obtained by adjusting the value of the multiplier [OMK1]. Much of the art in water quality modeling is involved in calibrating phytoplankton/nutrient/DO dynamics.

The following plots illustrate the model's ability to reproduce widely varying reservoir dissolved oxygen regimes. With the exception of the zero-order SOD rates, all kinetic coefficients were set to their default values thus ensuring that the model was applied with a minimum of "curve fitting". In all likelihood, using the same values for kinetic parameters such as phytoplankton growth and settling rates is not correct. However, the point to be made is that the model is capable of reproducing very different water quality regimes without having to resort to extensive, site-specific parameter manipulations.

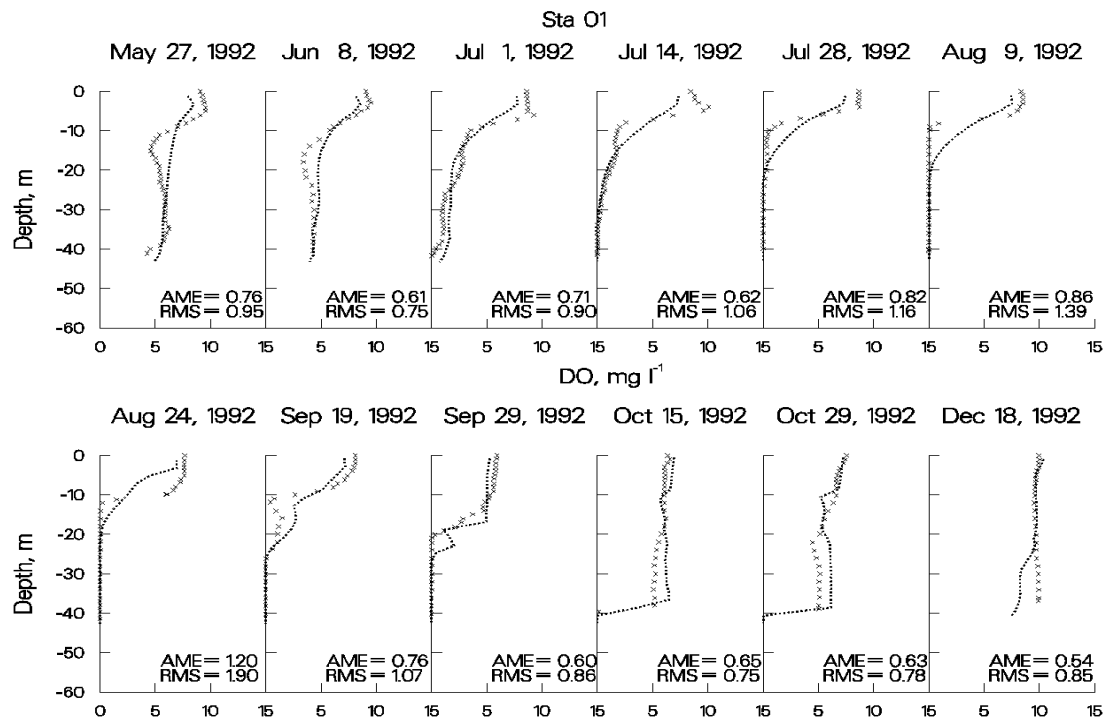


Figure 15. Allatoona Reservoir computed vs. observed DO.

CALIBRATION

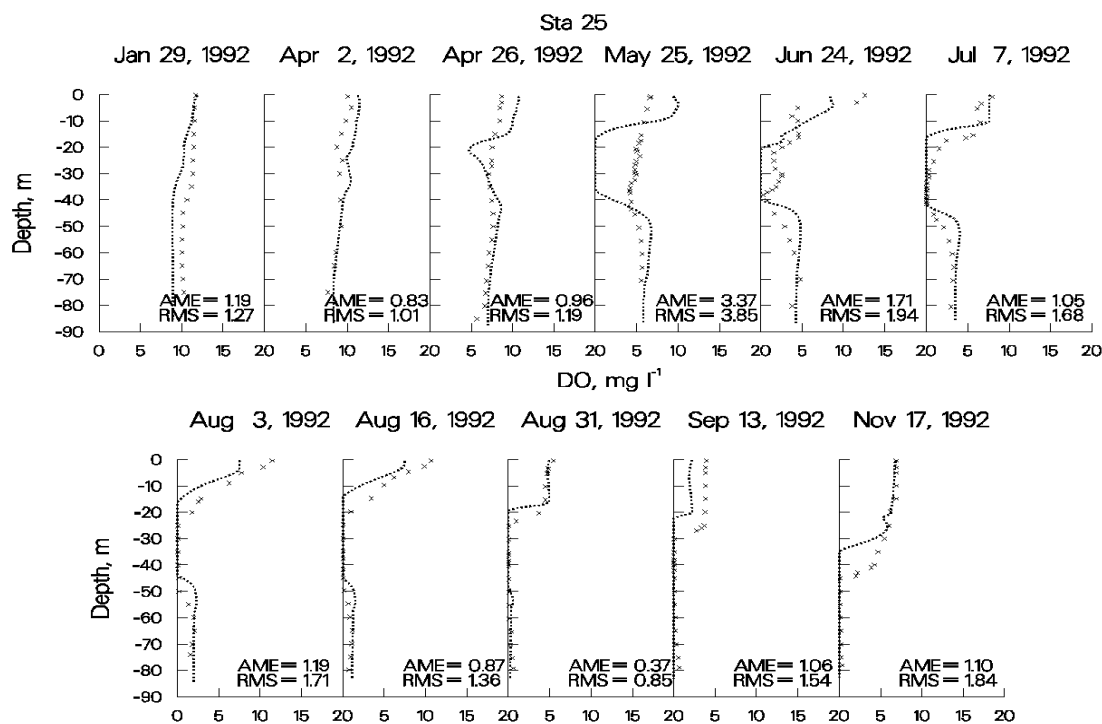


Figure 16. Brownlee Reservoir computed vs. observed DO.

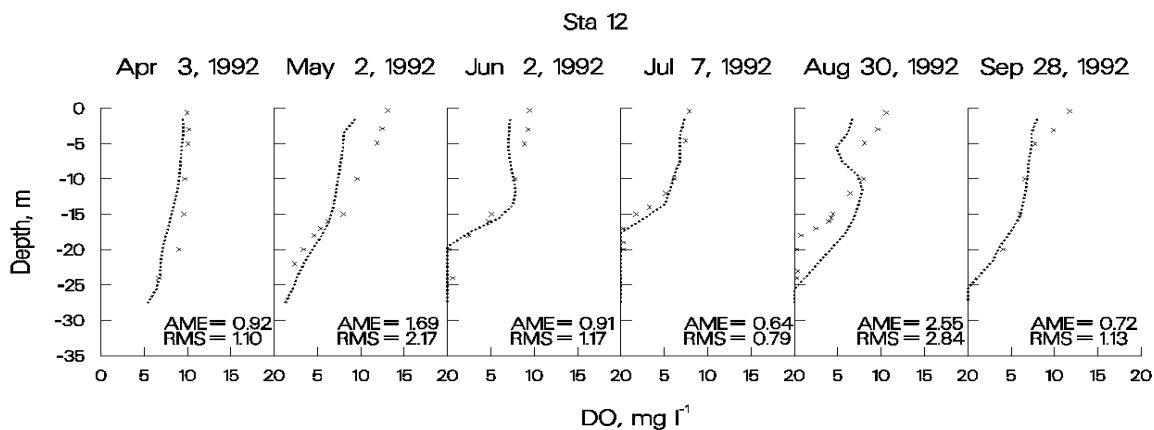


Figure 17. C.J. Strike Reservoir computed vs. observed DO.

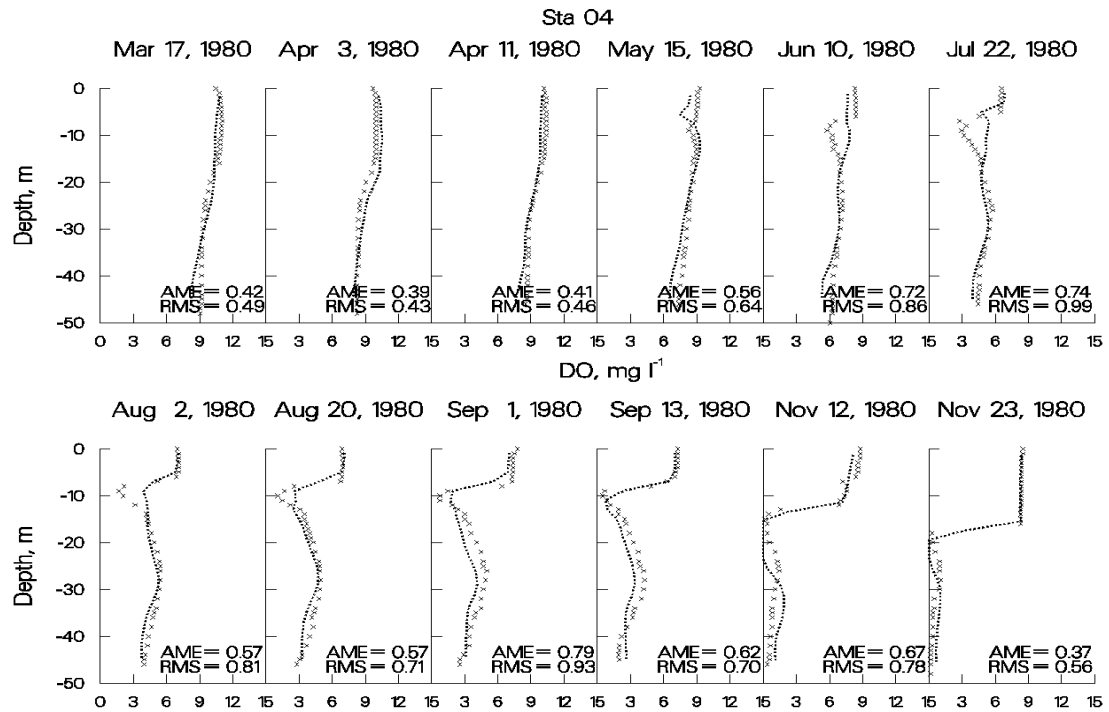


Figure 18. DeGray Reservoir computed vs. observed DO.

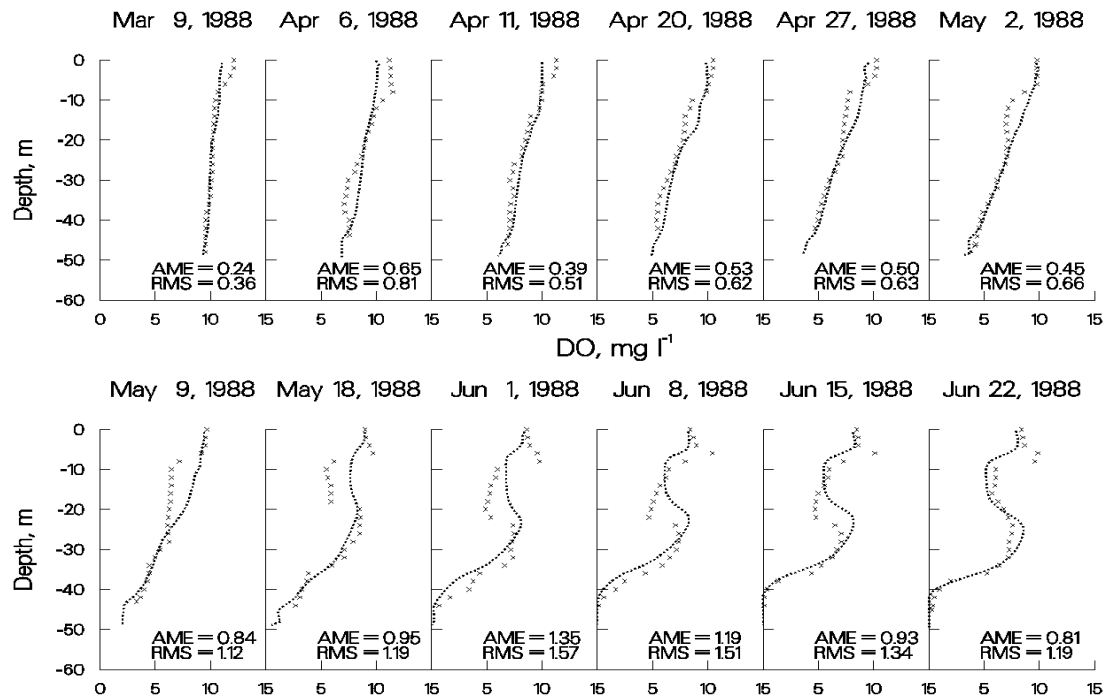


Figure 19. Richard B. Russell Reservoir computed vs. observed DO, March through June, 1988.

CALIBRATION

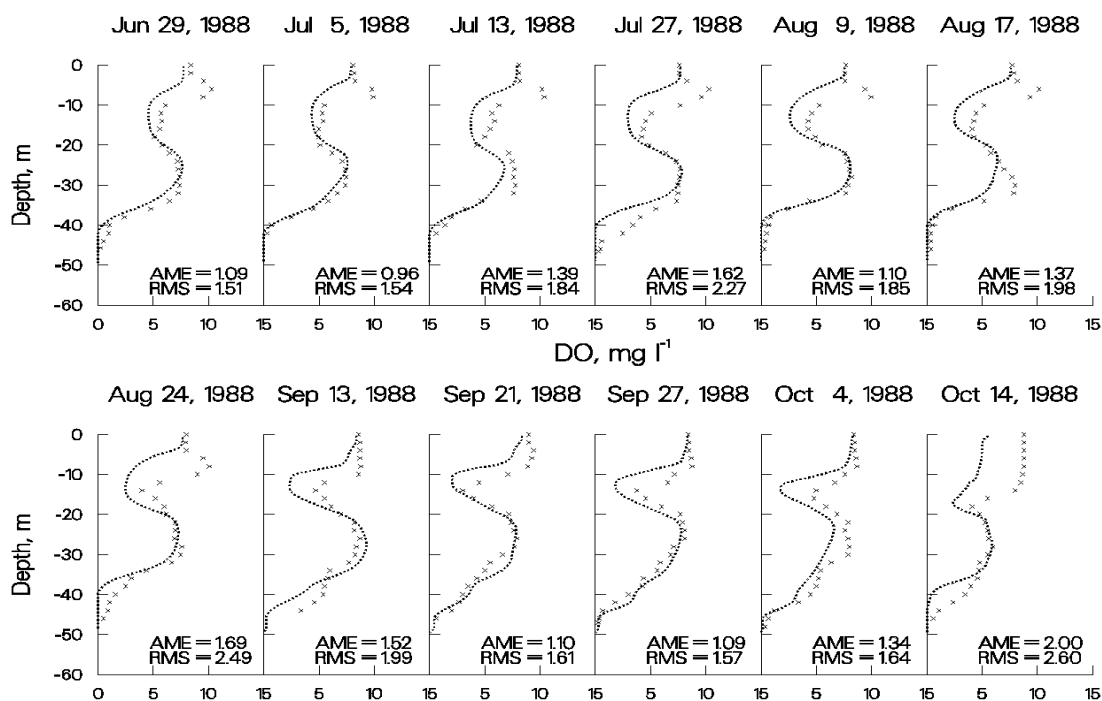


Figure 20. Richard B. Russell Reservoir computed vs. observed DO, June through October, 1988.

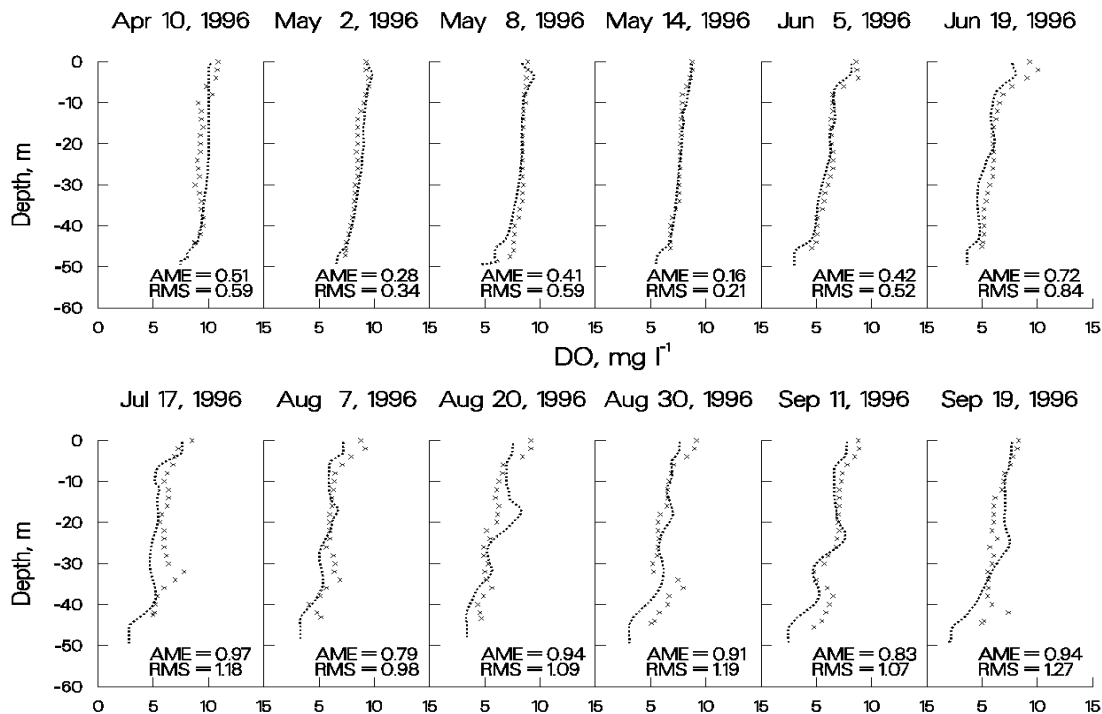


Figure 21. 1996 Richard B. Russell computed vs. observed DO.

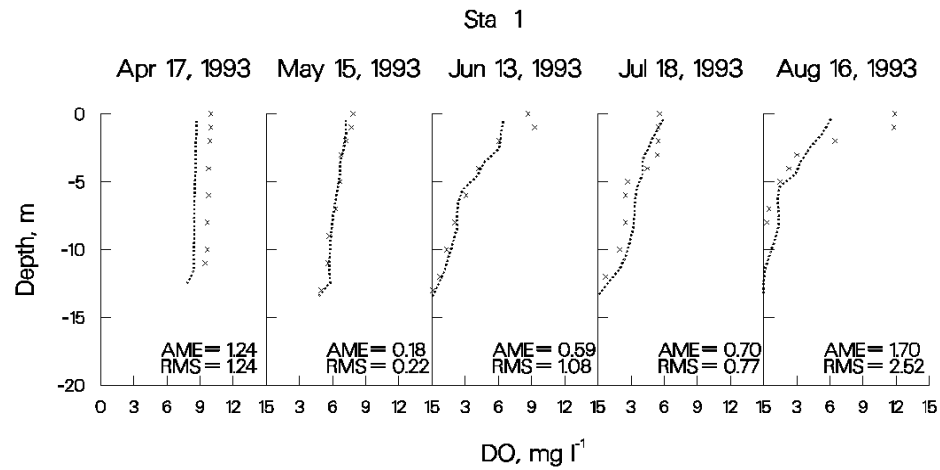


Figure 22. Neely Henry Reservoir computed vs. observed DO.

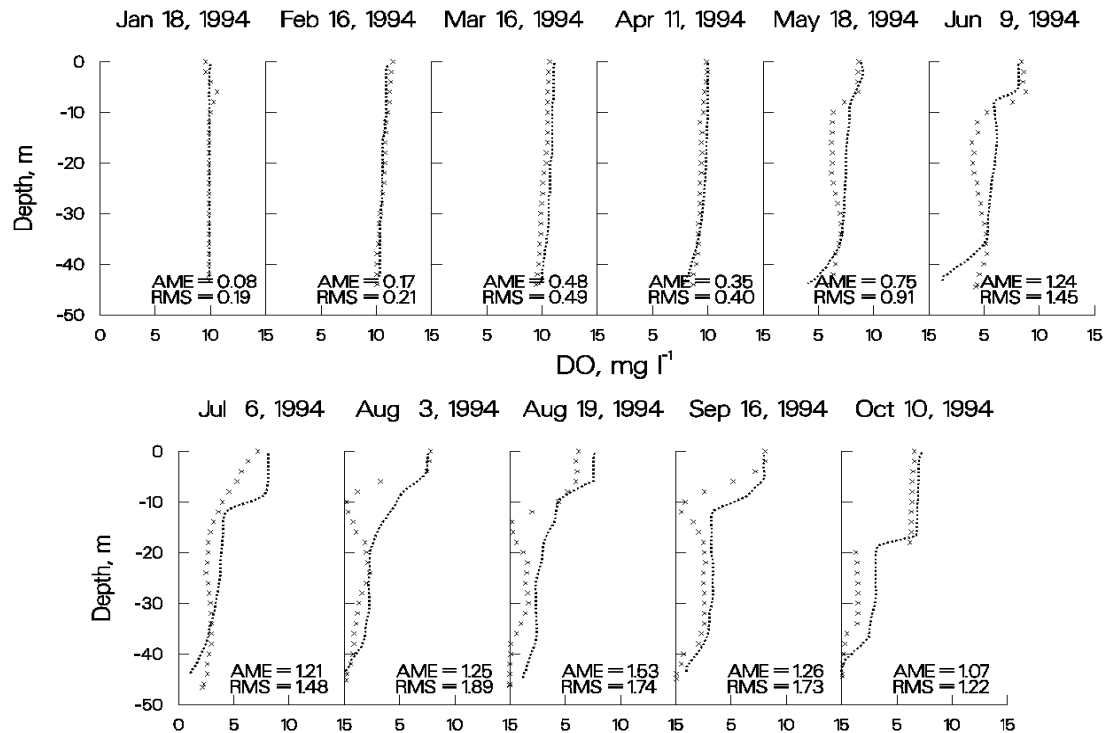


Figure 23. J. Strom Thurmond Reservoir computed vs. observed DO.

CALIBRATION

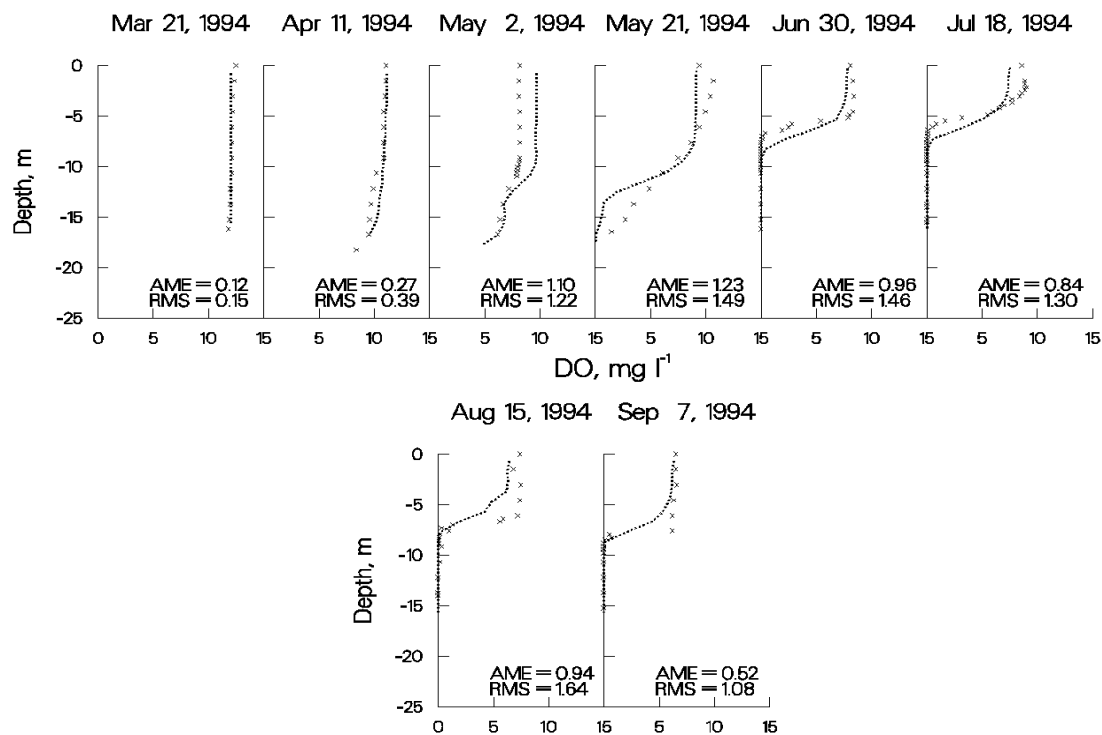


Figure 24. Monroe Reservoir computed vs. observed DO.

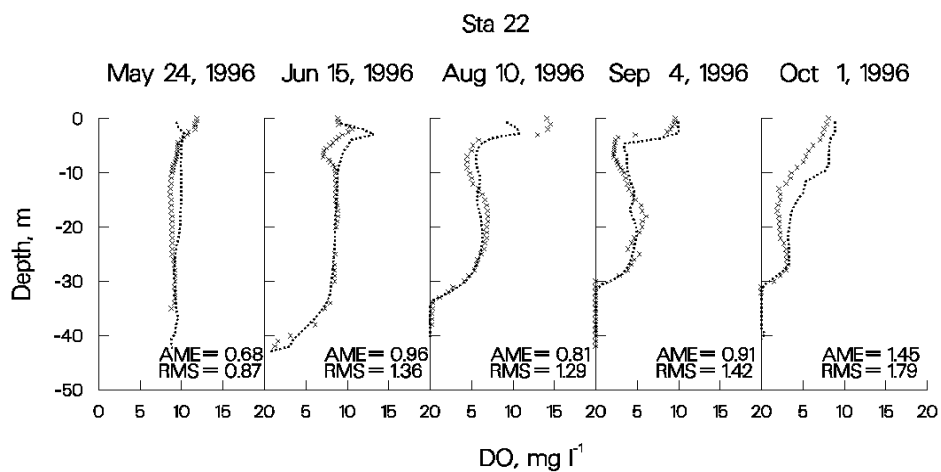


Figure 25. Rimov Reservoir computed vs. observed DO.

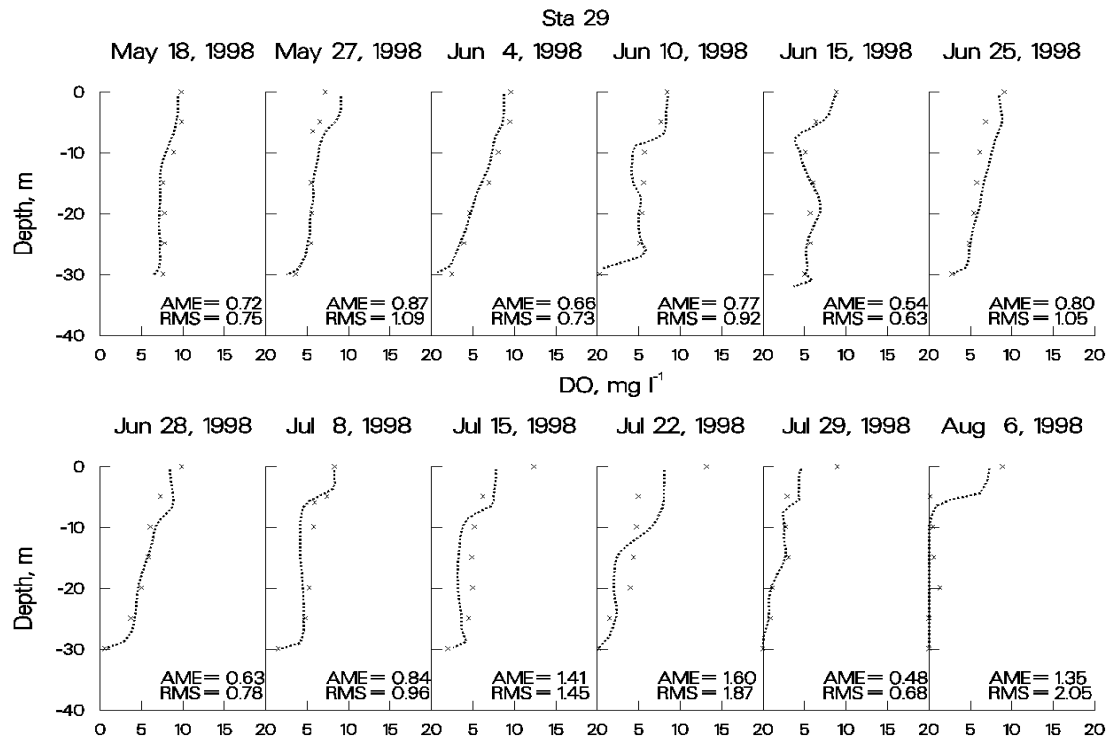


Figure 26. Shepaug Reservoir computed vs. observed DO.

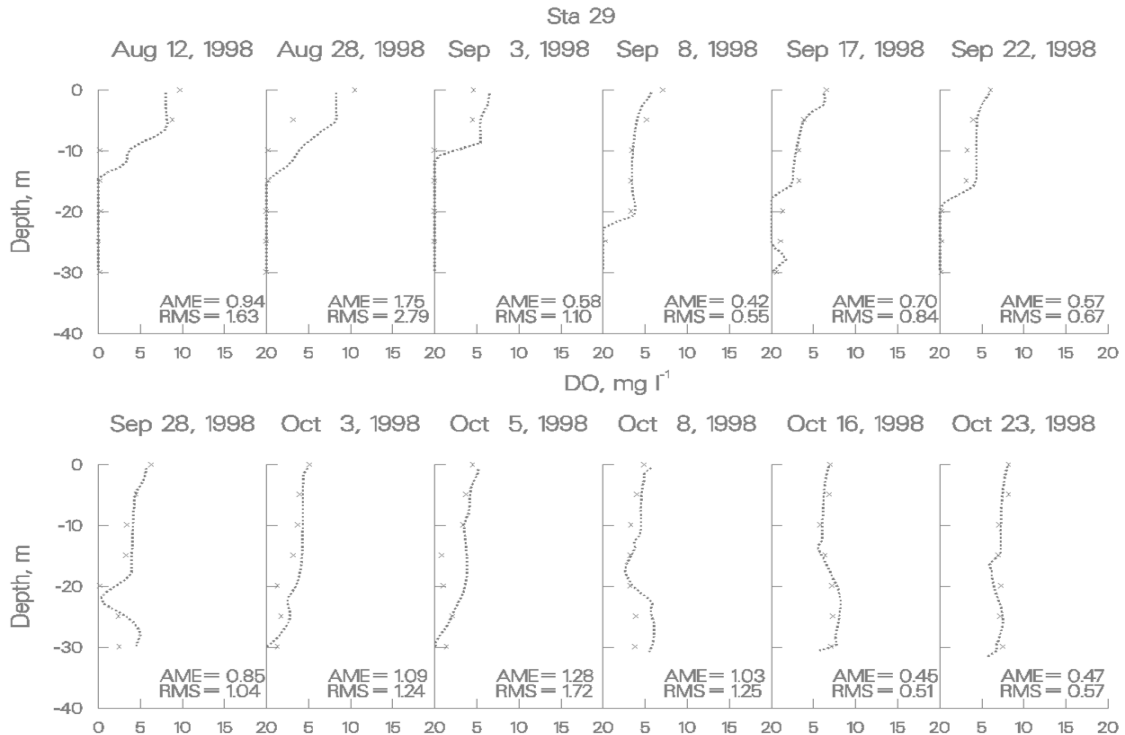


Figure 27. Shepaug Reservoir computed vs. observed DO.

CALIBRATION

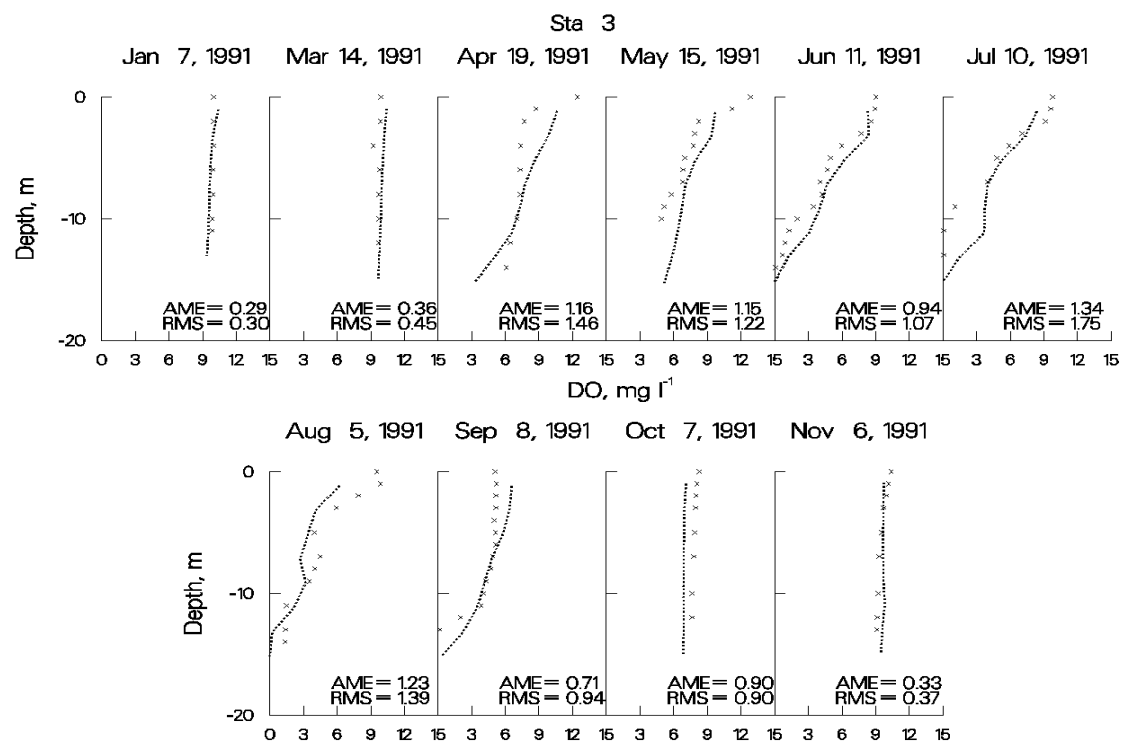


Figure 28. Weiss Reservoir computed vs. observed DO.

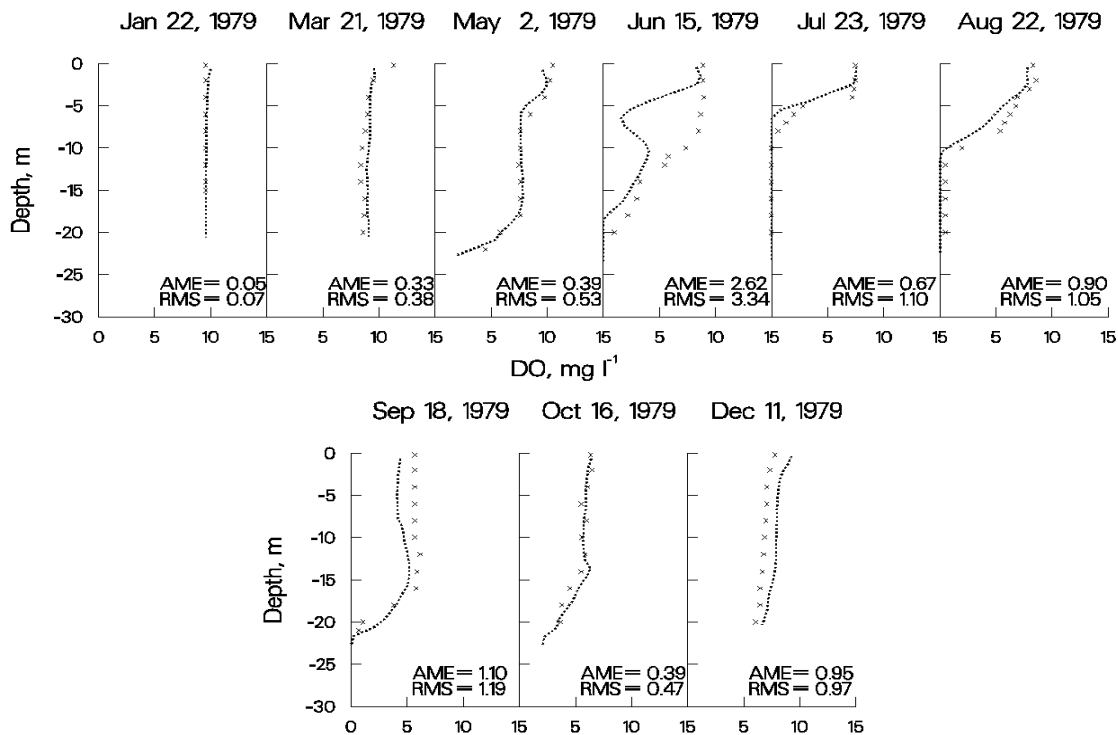


Figure 29. West Point Reservoir computed vs. observed DO.

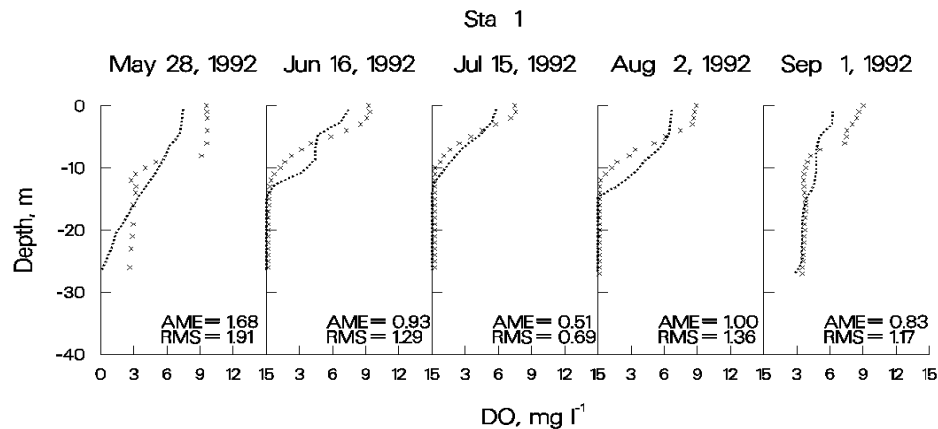


Figure 30. Walter F. George Reservoir computed vs. observed DO.

As can be seen from the previous figures for computed versus observed DO comparisons, the model has reproduced a wide range of DO regimes with a high degree of accuracy using mostly default kinetic parameters. The largest discrepancies between computed and observed DO occur in the epilimnion during middle to late summer where the model consistently underpredicts supersaturated DO. The problem is that if the model is correctly predicting very low nutrient levels during these times (typically at detection levels), then there are insufficient nutrients in the water column to support the observed levels of primary production indicated by supersaturated conditions. This is a shortcoming of all currently used water quality models and indicates insufficient understanding

CALIBRATION

of phytoplankton/nutrient dynamics in the photic zone. A great deal of research needs to be done in this area in order to improve our ability to model phytoplankton primary productivity.

Another possible problem during dissolved oxygen calibration is during fall overturn when anoxic hypolimnetic water mixes with epilimnetic water. For the most part, the model reproduces dissolved oxygen fairly well during overturn ([Figure 29](#)), but in some applications the model has consistently underpredicted dissolved oxygen and in other applications the model has consistently overpredicted hypolimnetic concentrations.

There are three possible causes for this behavior. The first is the reaeration formula is not appropriate for the waterbody. For reservoirs, the model has accurately reproduced epilimnetic dissolved oxygen concentrations on so many systems that this is probably not the case. The second possibility is that the volumes of epilimnetic and hypolimnetic volumes are sufficiently off to affect the final mixed dissolved oxygen concentration. Depending upon the direction of the volume error, this can result in either over or underprediction. The third possibility in the case of overprediction is that reduced substances including ammonium, iron, manganese, and sulfides have been released from the sediments in sufficient quantities to exert an appreciable oxygen demand. The model includes only the affect of ammonium on dissolved oxygen. In this case, the code would need to be altered to include their effects on dissolved oxygen. All of these scenarios should be investigated if accurate reproduction of dissolved oxygen during fall overturn is important to simulate.

Nutrients. Given accurate boundary conditions for phosphorus, ammonium, and iron and accurate simulations of metalimnetic/hypolimnetic dissolved oxygen, hypolimnetic concentrations of these nutrients are relatively easy to reproduce. Again, this is basically a back calculation of the sediment fluxes to match observed hypolimnetic concentrations.

Epilimnetic concentrations of phosphorus during the growing season are typically at or below detection levels in both the model and the prototype, so they are also relatively easy to reproduce. Fall concentrations can be more complicated, particularly if iron and manganese have built up during the summer in an anoxic hypolimnion. In this case, the iron compartment should be turned on so that iron is released in the hypolimnion. The model includes phosphorus sorption onto iron hydroxides that form during fall overturn and settle into the sediments, thus removing phosphorus from the water column.

Epilimnetic ammonium and nitrate levels are more difficult to reproduce as some phytoplankton show a preference for ammonium over nitrate and the degree to which they exhibit this preference is different between groups. In addition, water column nitrate undergoes denitrification when the water column goes anoxic and also diffuses into the sediments where it undergoes denitrification in the anaerobic layer under both oxic and anoxic conditions. The ammonium preference factor [\[ANPR\]](#), the water column denitrification rate [\[NO3DK\]](#), and the sediment nitrate uptake rate [\[NO3S\]](#) are calibration parameters that can be adjusted to better match observed concentrations of these nutrients.

Phytoplankton. The following plots illustrate the model's ability to reproduce a spring phytoplankton bloom in Rimov Reservoir, Czech Republic. Tremendous amounts of data were collected to analyze the spring bloom. Chlorophyll *a* samples were taken at 1 m depth intervals over upper 10 m of the water column at six stations approximately every three days for over a month. The

CALIBRATION

plots include six stations along the length of the reservoir starting upstream and progressing towards the dam.

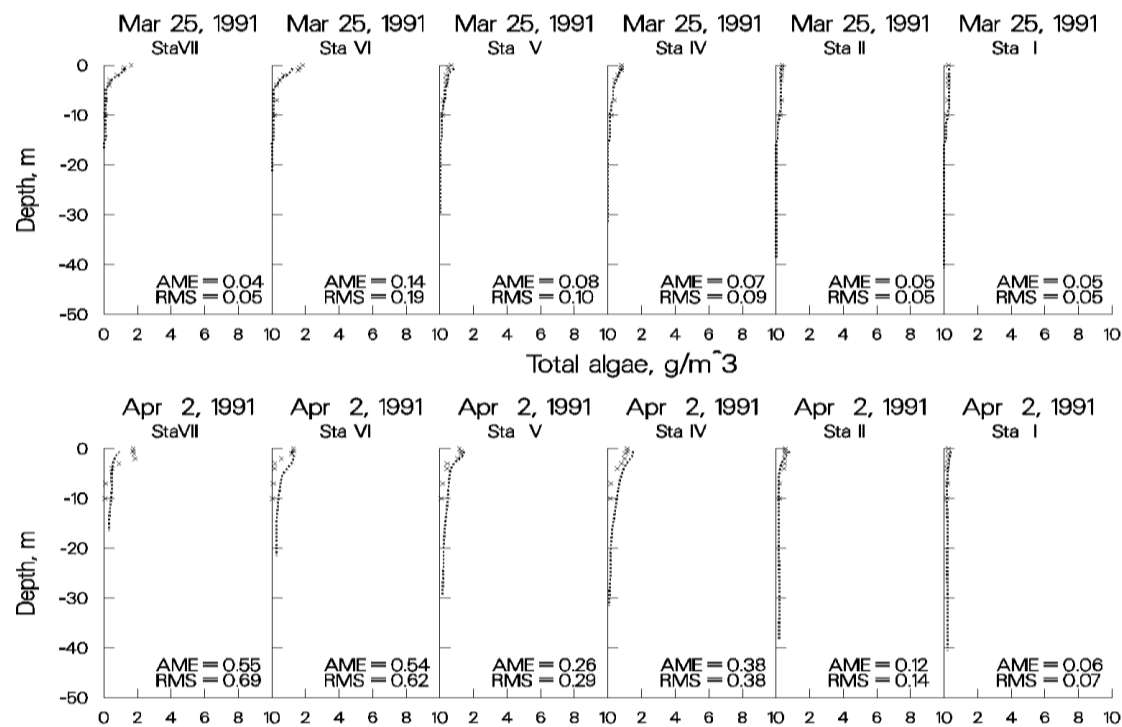


Figure 31. Rimov Reservoir computed vs. observed phytoplankton biomass.

CALIBRATION

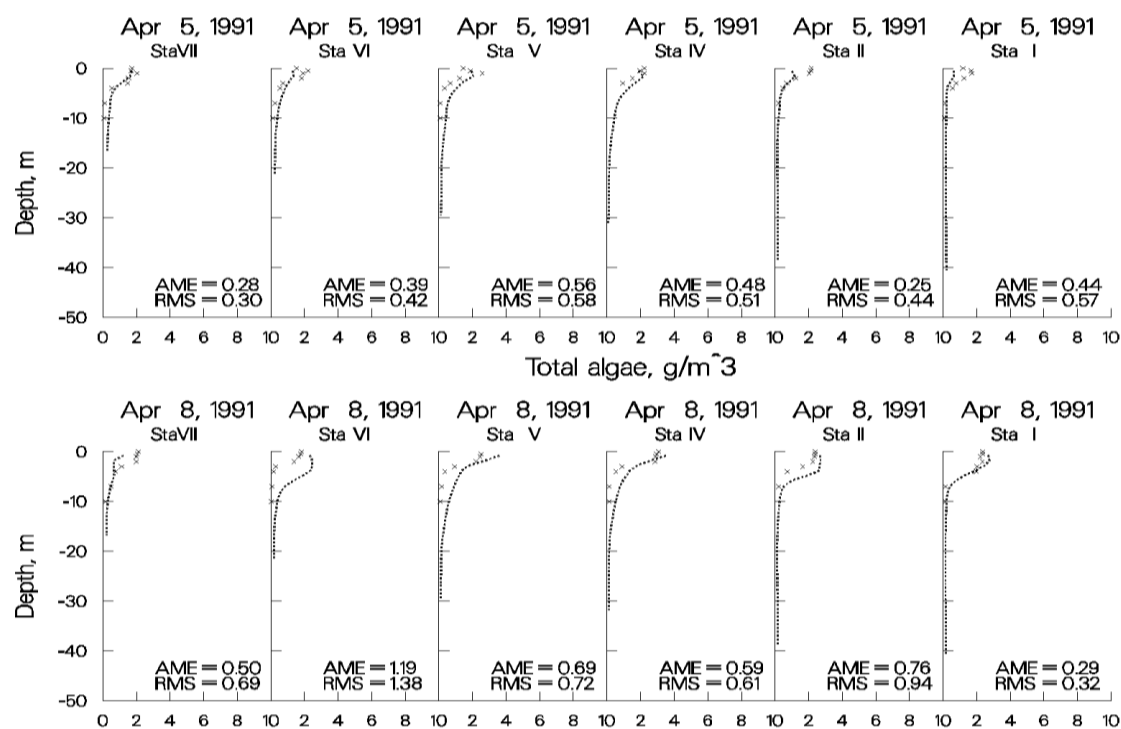


Figure 32. Rimov Reservoir computed vs. observed phytoplankton biomass.

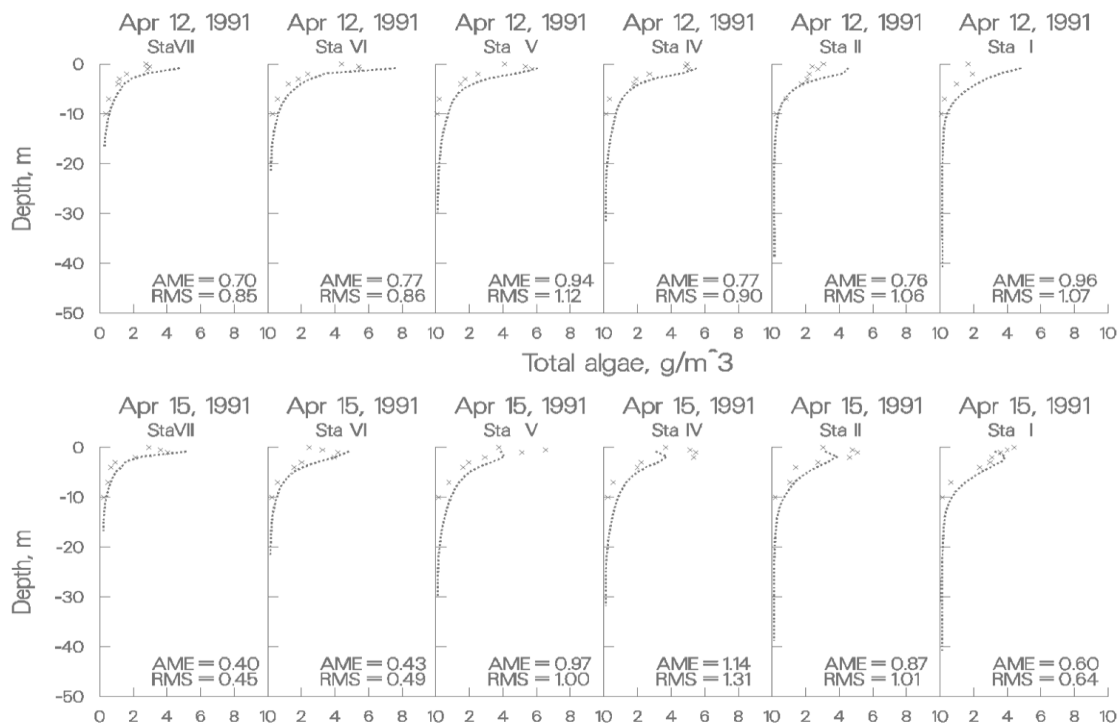


Figure 33. Rimov Reservoir computed vs. observed phytoplankton biomass.

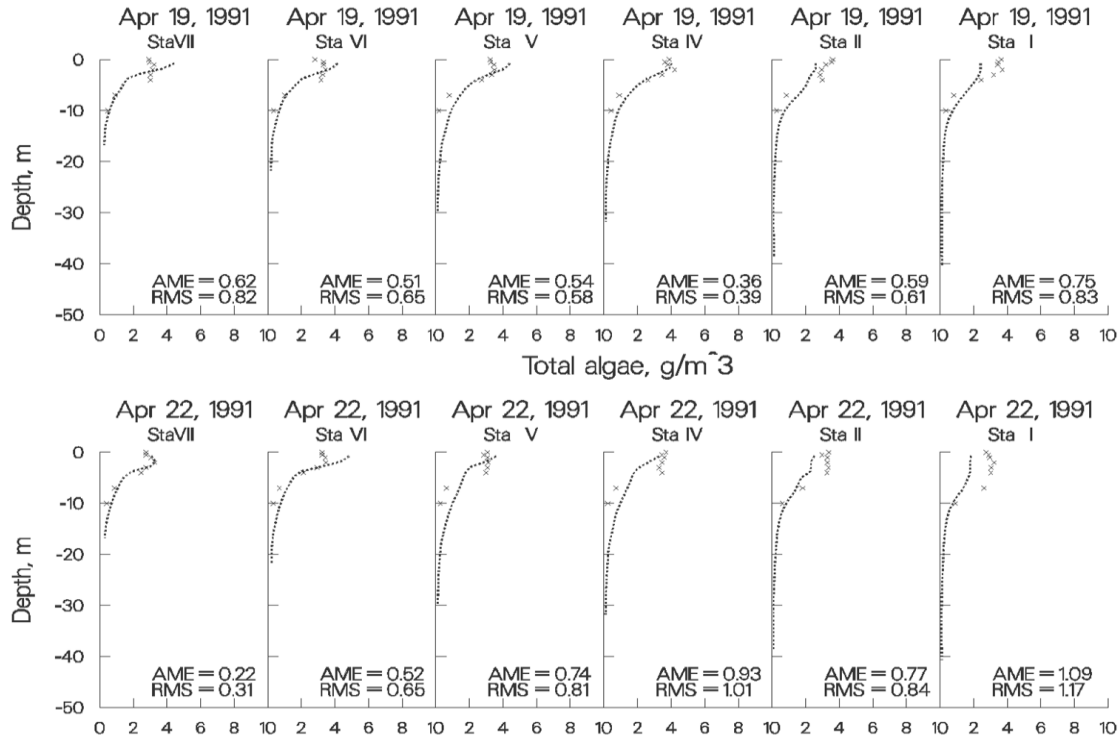


Figure 34. Rimov Reservoir computed vs. observed phytoplankton biomass.

CALIBRATION

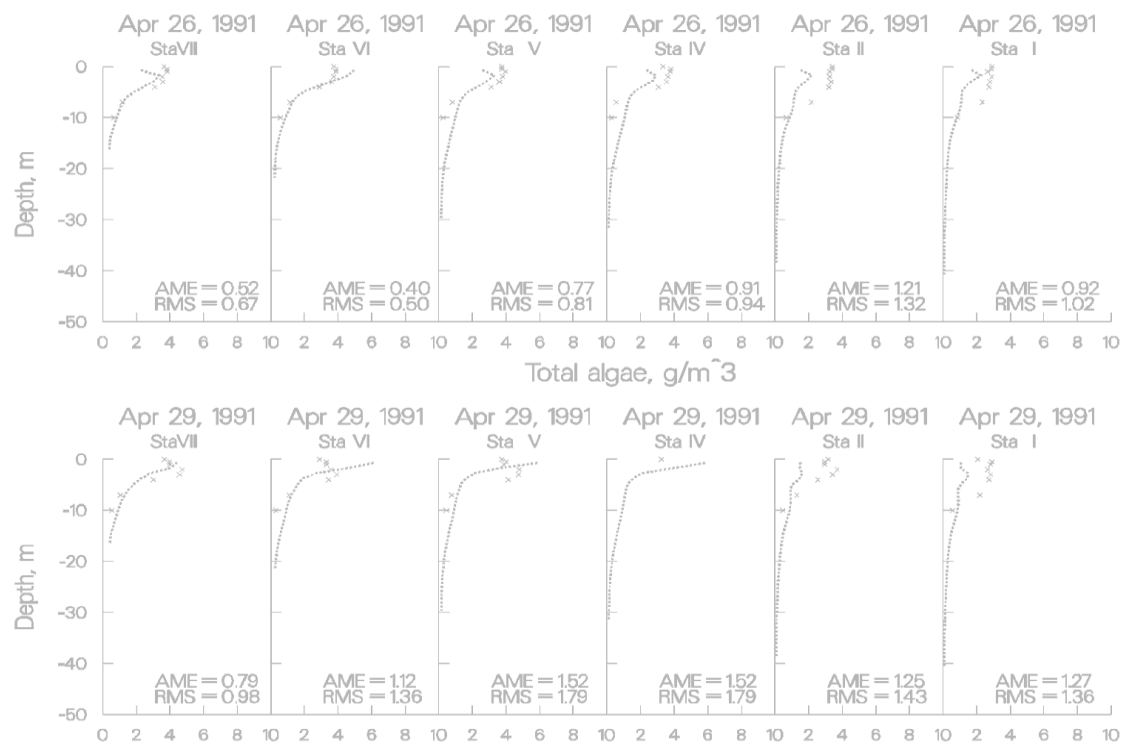


Figure 35. Rimov Reservoir computed vs. observed phytoplankton biomass.

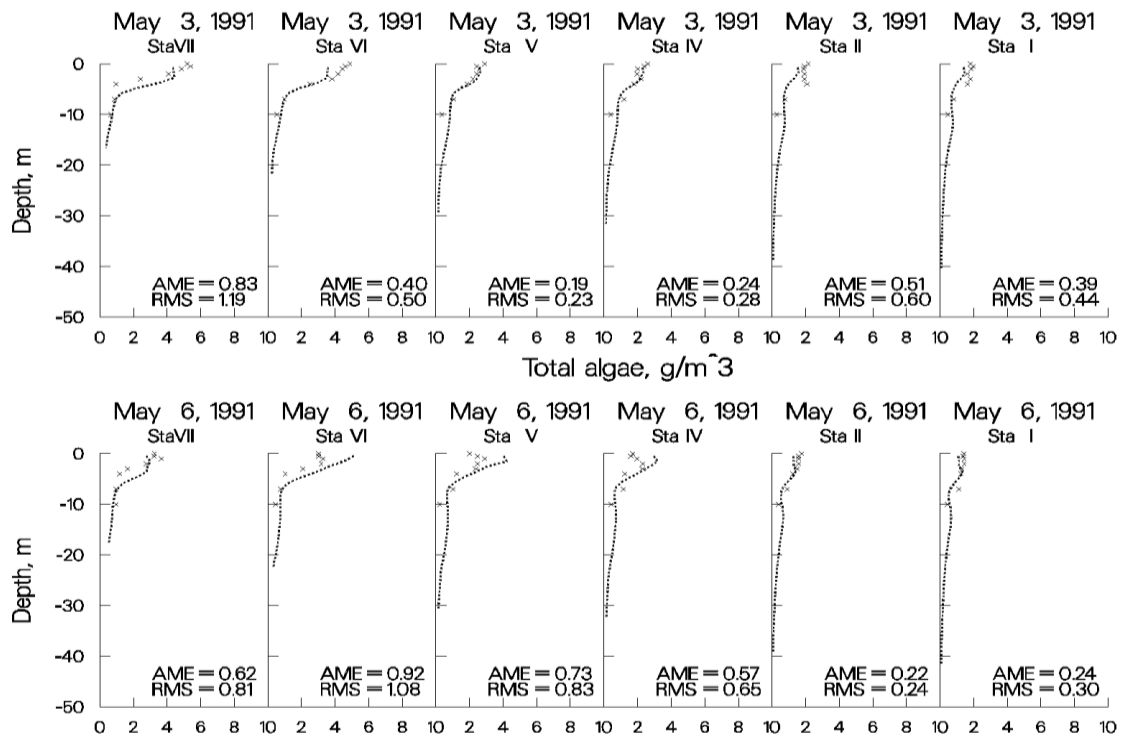


Figure 36. Rimov Reservoir computed vs. observed phytoplankton biomass.

The following plots illustrate how important it is to describe the system accurately. The plots show results of the Rimov phytoplankton simulation in which the wind direction was inadvertently changed by 90°. The importance of wind direction and its influence on the spring phytoplankton bloom was noted by limnologists who originally collected the 1991 data. Note the difference at the most downstream station on April 8 compared to the previous plot of April 8 using the correct wind direction. This also illustrates that the model can be a powerful limnological investigative tool when trying to determine how important different forcing functions are to the limnology of a reservoir.

CALIBRATION

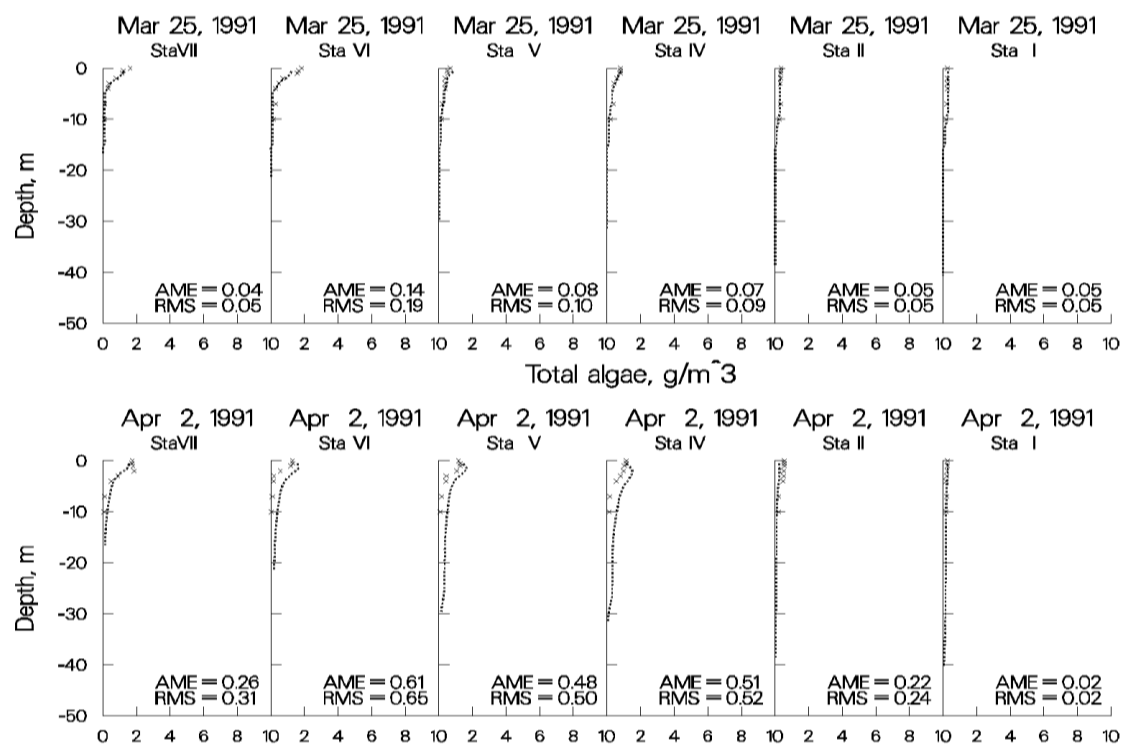


Figure 37. Rimov Reservoir computed vs. observed phytoplankton with wind rotated 90°.

CALIBRATION

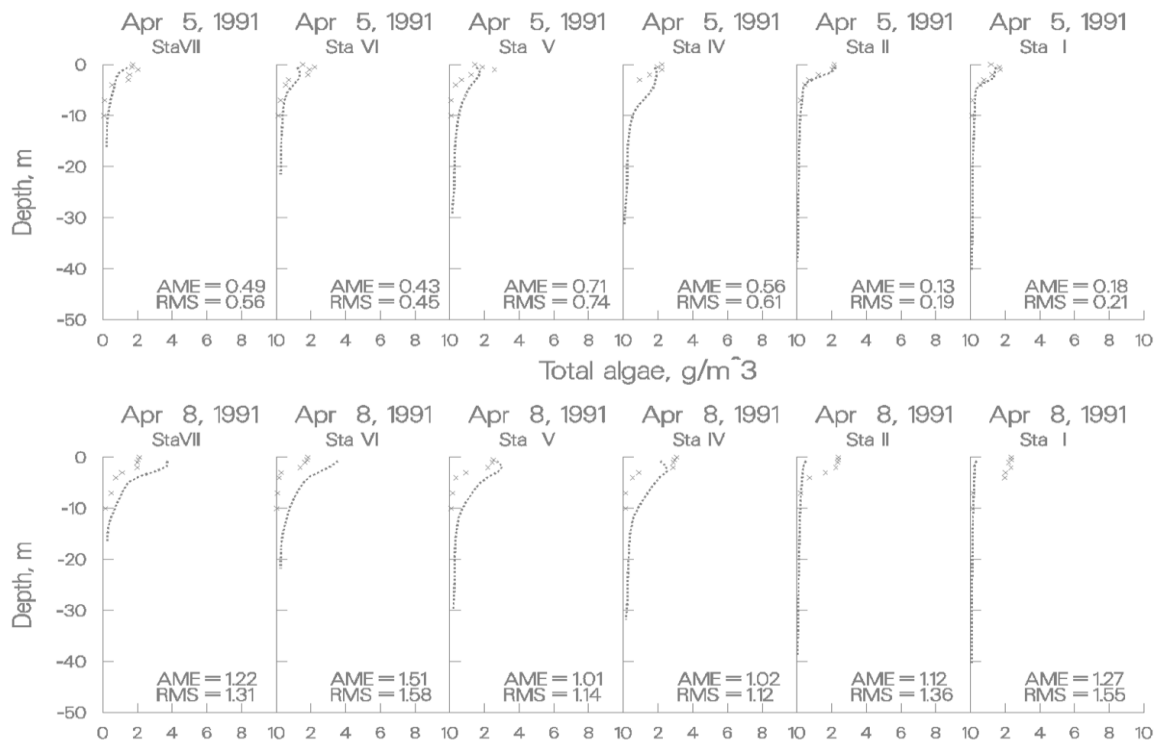


Figure 38. Rimov Reservoir computed vs. observed phytoplankton with wind rotated 90°

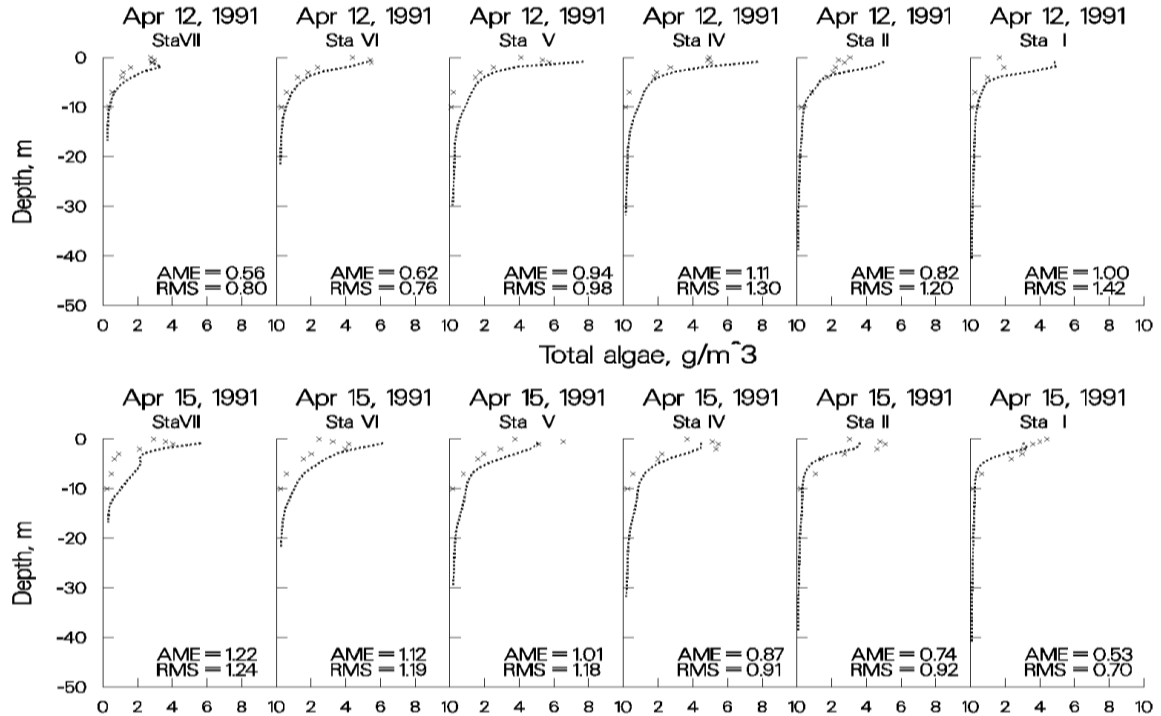


Figure 39. Rimov Reservoir computed vs. observed phytoplankton with wind rotated 90°.

CALIBRATION

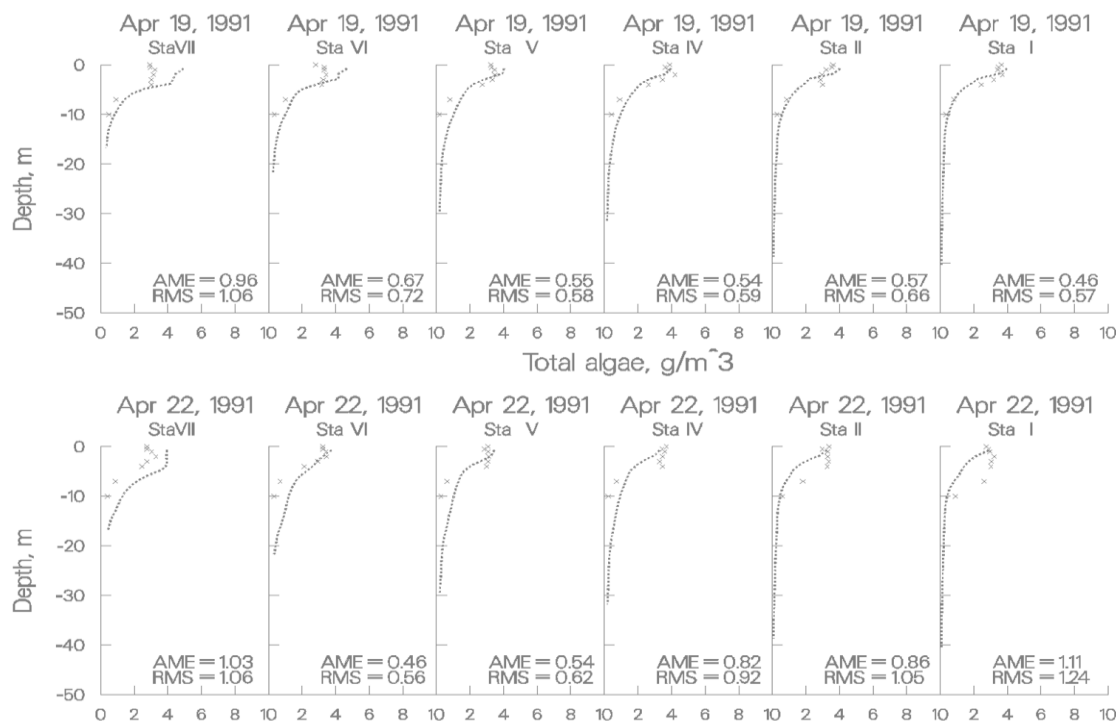


Figure 40. Rimov Reservoir computed vs. observed phytoplankton with wind rotated 90°.

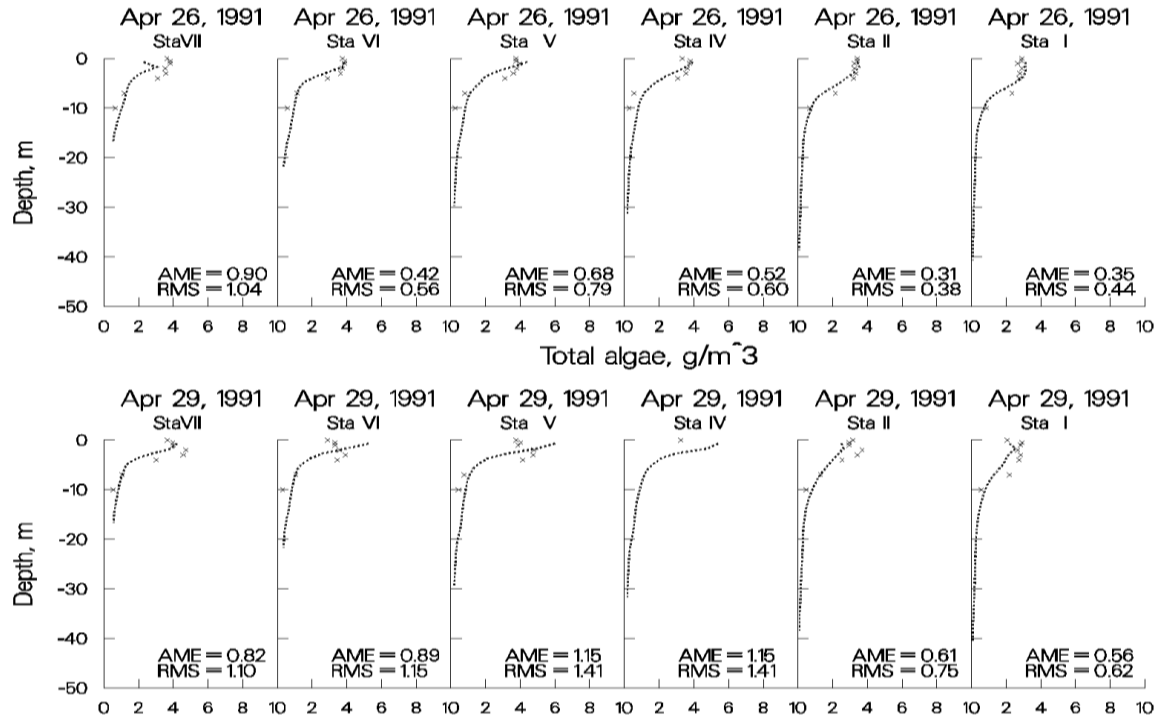


Figure 41. Rimov Reservoir computed vs. observed phytoplankton with wind rotated 90°.

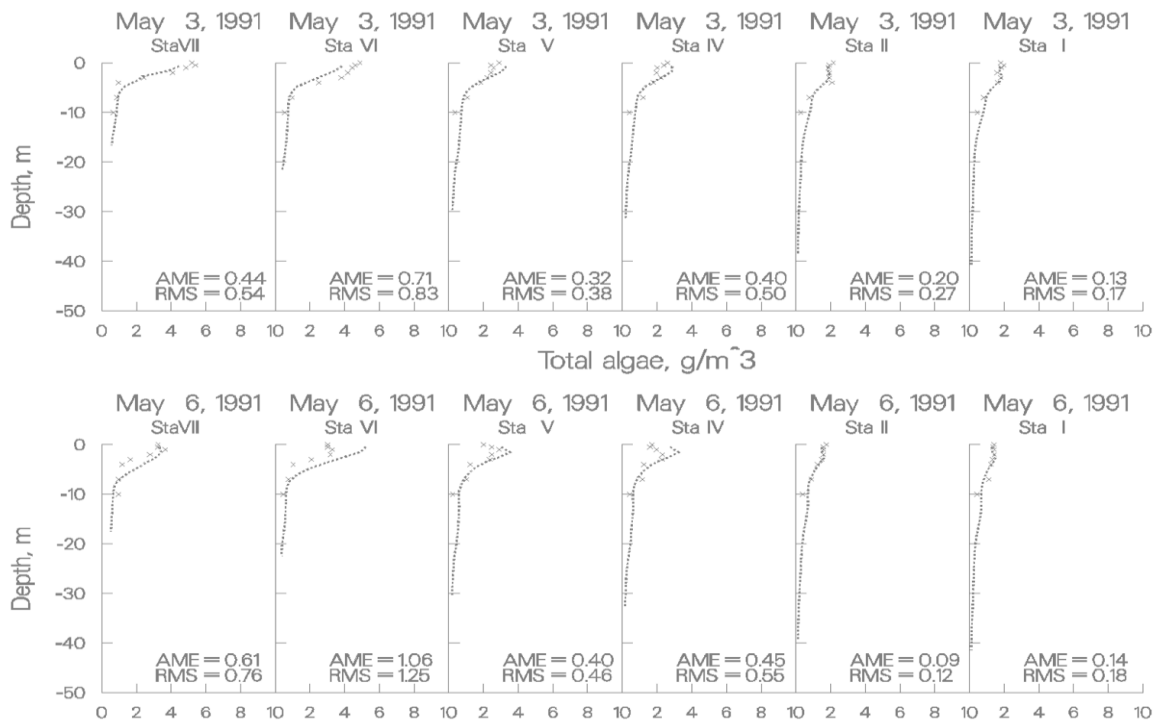


Figure 42. Rimov Reservoir computed vs. observed phytoplankton with wind rotated 90°.

The following plots illustrate the importance of accurate inflow boundary conditions for phytoplankton in Rimov Reservoir. Inflow phytoplankton concentrations were inadvertently set to $0.05 g m^{-3}$ rather than the observed concentrations when converting from V2 to V3. Again, the researchers who collected the original data concluded that the spring phytoplankton bloom was first initiated in Rimov because of inflowing phytoplankton. The model concurs with this conclusion and again illustrates how powerful a limnological investigative tool the model can be.

CALIBRATION

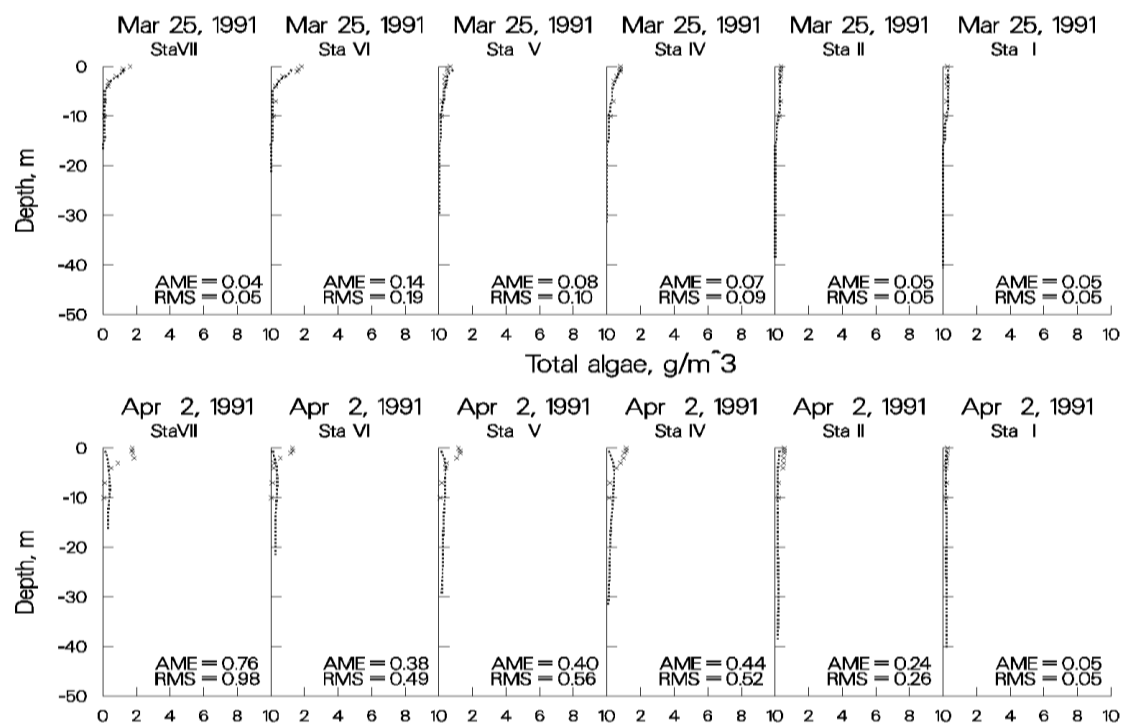


Figure 43. Rimov Reservoir computed vs. observed phytoplankton with no inflowing phytoplankton.

CALIBRATION

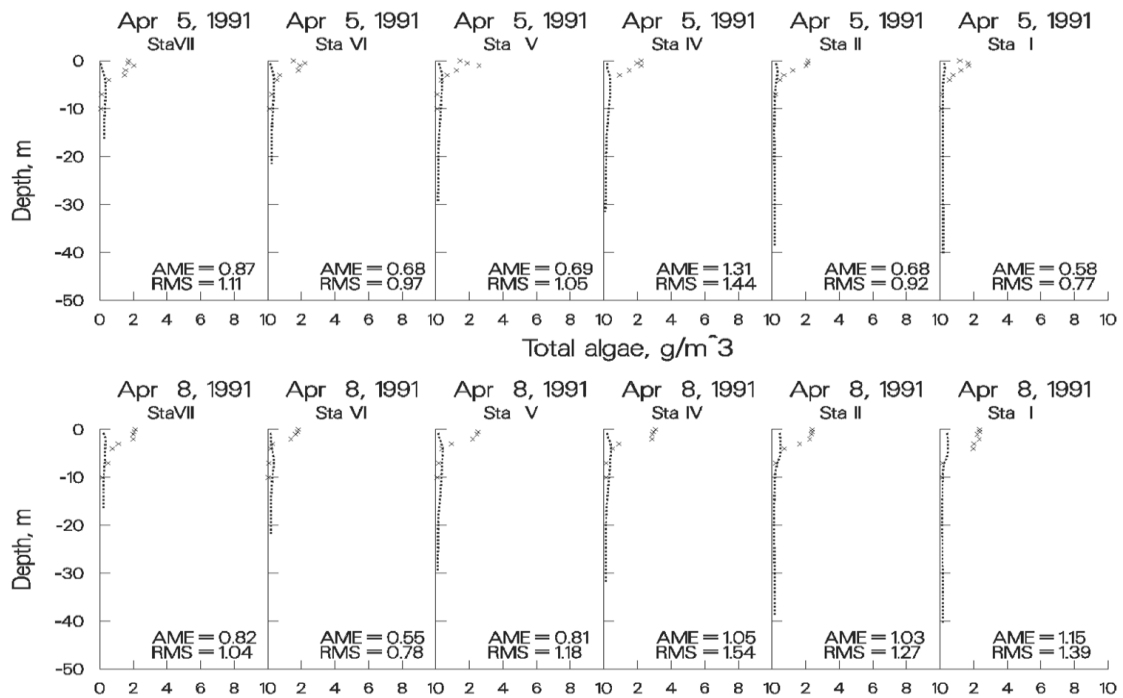


Figure 44. Rimov Reservoir computed vs. observed phytoplankton with no inflowing phytoplankton.

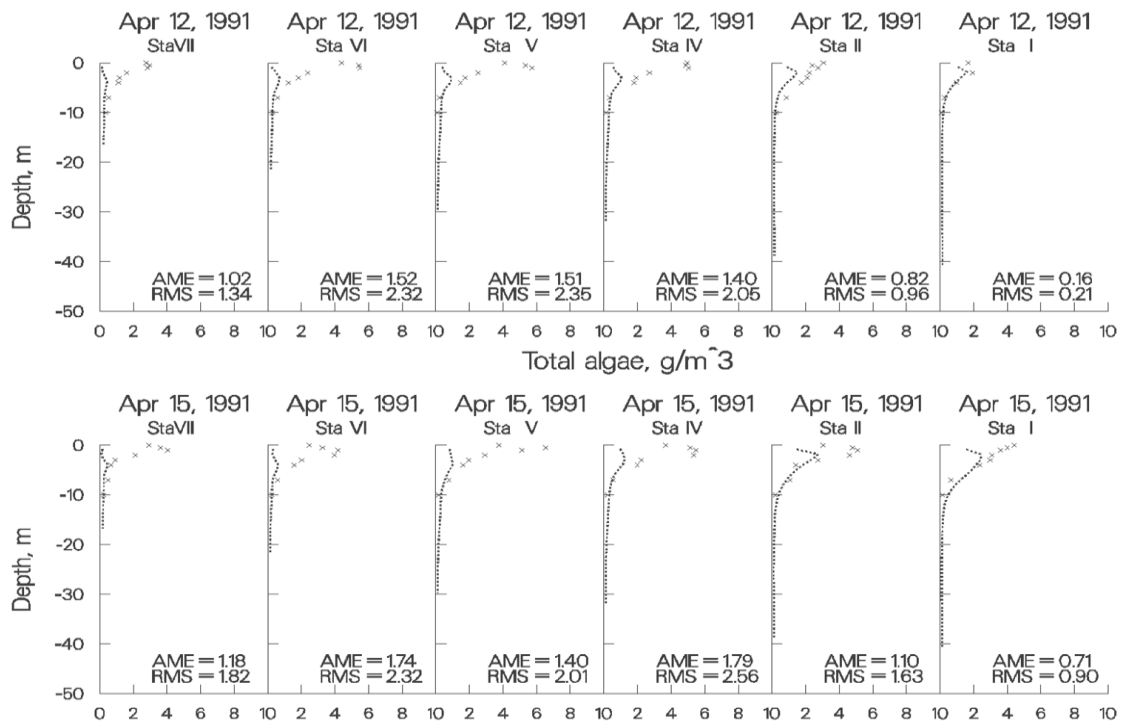


Figure 45. Rimov Reservoir computed vs. observed phytoplankton with no inflowing phytoplankton.

CALIBRATION

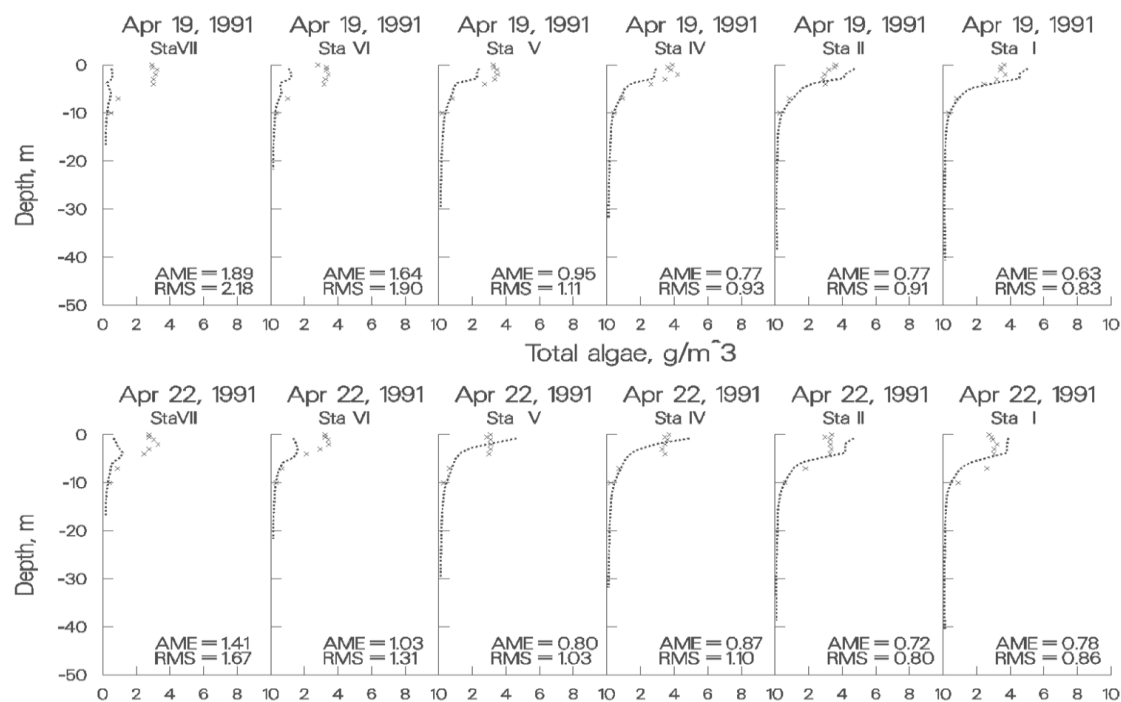


Figure 46. Rimov Reservoir computed vs. observed phytoplankton with no inflowing phytoplankton.

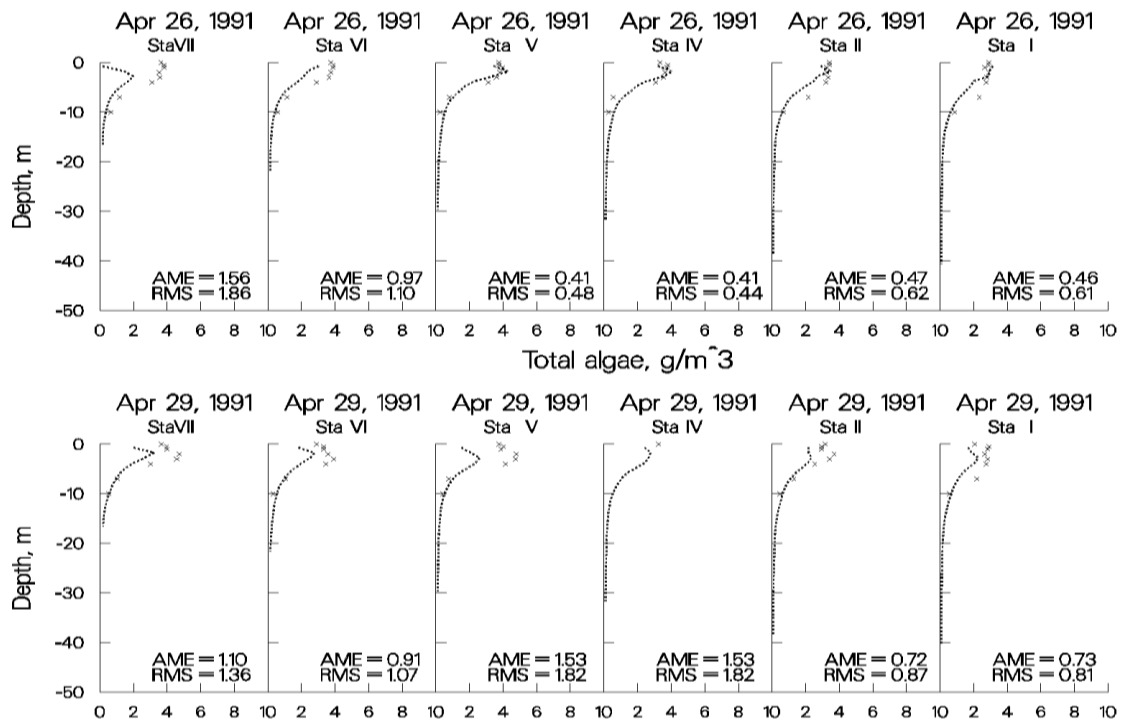


Figure 47. Rimov Reservoir computed vs. observed phytoplankton with no inflowing phytoplankton.

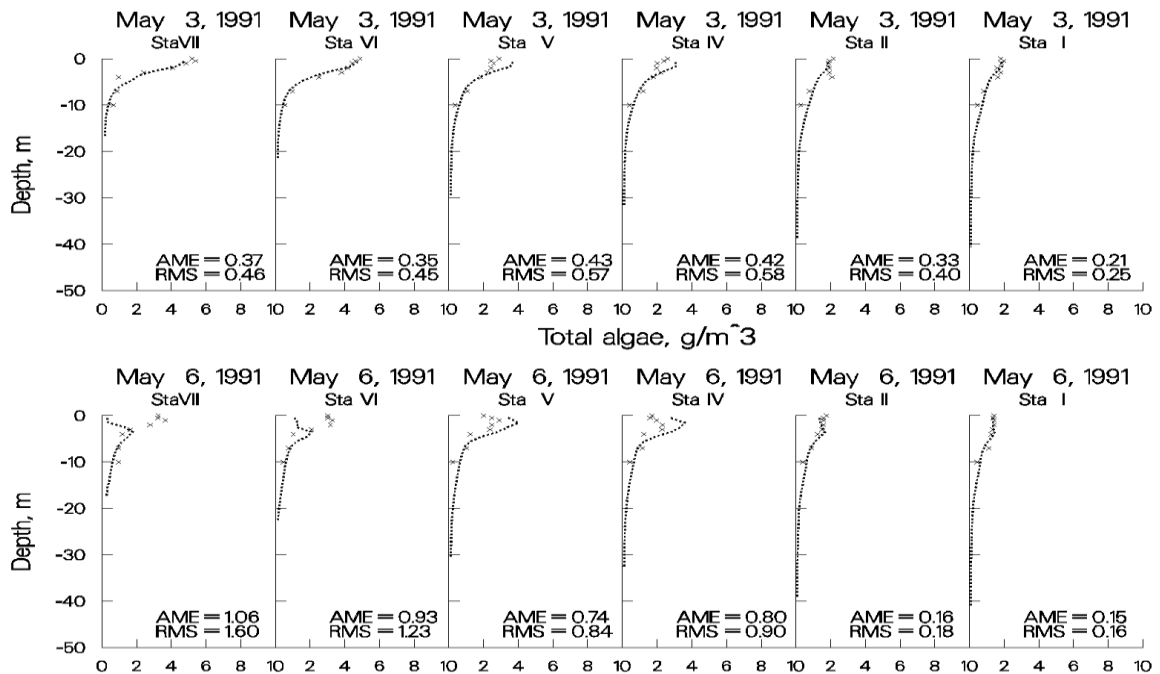


Figure 48. Rimov Reservoir computed vs. observed phytoplankton with no inflowing phytoplankton.

CALIBRATION

Estuary

Estuarine modeling is similar to reservoir and lake modeling for both bathymetry development and water quality modeling, but there are a few important differences in the hydrodynamic calibration. Salinity is commonly used to assess model hydrodynamic performance. However, as with reservoirs, water quality variables such as dissolved oxygen and phytoplankton can be used to also assess the accuracy of the hydrodynamics. When calibrating salinity, it is common practice to plot predicted versus observed time-series of surface and bottom salinity. While plots such as these are useful, vertical plots of computed versus observed salinity, if available, should always be included as part of the calibration process.

Boundary conditions

Ocean boundary conditions play a critical role in estuarine modeling and the data should be frequent and of high quality. At a minimum, downstream head boundary elevations should be available on an hourly basis. The model can be used to linearly interpolate [\[HDIC\]](#) between observed elevations. Alternatively, formulas can be used to compute elevations at any frequency based on various components of the tidal cycle.

Equally important are salinity concentrations specified at the downstream boundary. It is always preferable to set the boundary sufficiently downstream so that there is no vertical variation in salinity and hopefully only small temporal changes. However, the boundary needs to be set where the head elevations are measured, and oftentimes there are significant vertical and temporal variations in salinity at the site. Weekly vertical profiles are usually of insufficient frequency to reproduce the hydrodynamics of the estuary with any accuracy in this case. The same will hold true for temperature and constituents if they exhibit vertical and temporal variations.

Upstream freshwater inflows need to be accurately gaged and evaporation and precipitation should be included in the simulation if possible. Because of the inaccuracies associated with gaged inflows, sensitivity analyses should be run by increasing and decreasing upstream inflows to determine their impacts on hydrodynamics and water quality rather than initially turning to a model “knob” to adjust model results, particularly for vertical salinity distributions in a stratified estuary. Many times the model has provided information as to where forcing functions need to be more accurately measured for a successful model application.

Water surface elevations and flows

In an estuarine system, the first step is to make certain the model correctly replicates tidal elevations and flows at various stations along the length of the system. Usually these stations have continuous data for comparison. Problems in water level and flow calibration can be caused by the following:

1. **Incorrect or inadequate bathymetry.** The user should ensure that the model correctly reproduces cross-sections where these are measured. The model is very sensitive to small changes in the cross-section and more frequent cross-sectional data may be necessary for accurate water level and flow simulations.
2. **Incomplete inflow/outflow data.** A substantial amount of flow can often be unaccounted for as a result of not including tributaries, point sources, precipitation,

stormwater, irrigation users, and groundwater. Although precipitation and evaporation will normally be minor sources and sinks, they should be included by turning on the precipitation [PRC] and evaporation options [EVC]. In an estuary, flow is very dependent on the cross-sectional area at a given location, so grid evaluation should also be part of the calibration process.

3. **Bottom friction.** Bottom friction values [FRICT] for an estuary significantly affect the water level. Bottom friction can be used to calibrate the model to observed water levels at gages along the length of the estuary.

In most cases, the initial water level [WSEL] in the estuary is specified as flat with a velocity field of zero. The model should be run for several days with steady-state inflows [QIN], inflow temperature [TIN], inflow salinity [CIN], [meteorology](#), and downstream head boundary conditions for temperature [TDH] and salinity [CDH]. Once the temperature and salinity distributions are no longer changing, the simulation can continue with observed boundary conditions.

The initial water surface elevation should be the same elevation as the external downstream elevation [EDH] at the start of the simulation. If there is a large elevation difference between the initial condition water level and the first head boundary condition, the model can quickly become unstable because of large flows generated as a result of the water level differences at the head boundary.

Typically, the user will first plot observed versus computed water surface elevations for the simulation period after all the inflow/outflow data have been collected and the model is running to completion. Distributed tributary flows [DTRC] may need to be added or subtracted if the mean flows over a tidal period are not correct. The model user should also check not only instantaneous flow rates, but tidal average rates to make sure the total flow coming into the system at the upstream boundary condition agrees with the net residual flow at different locations downstream. This could point to unaccounted inflows or outflows.

The model user should always take the model segment next to the downstream boundary and compare it to the actual water level data used and the flow rate at the gage, if measured. This checks that the water level in the model is correct and the flow rate predicted by the model agrees with the field data at that location. If the water level matches and the flow does not, this could point to channel bathymetry errors or too high or too low a channel friction near the head boundary condition.

A typical comparison of field data to model predictions of water level are shown in [Figure 49](#) for the Columbia River at Longview, Washington approximately 110 km from the Pacific Ocean. The absolute and root mean square errors were 0.12 m and 0.18 m, respectively, over the period of record with a maximum tidal range of 1.5 m.

CALIBRATION

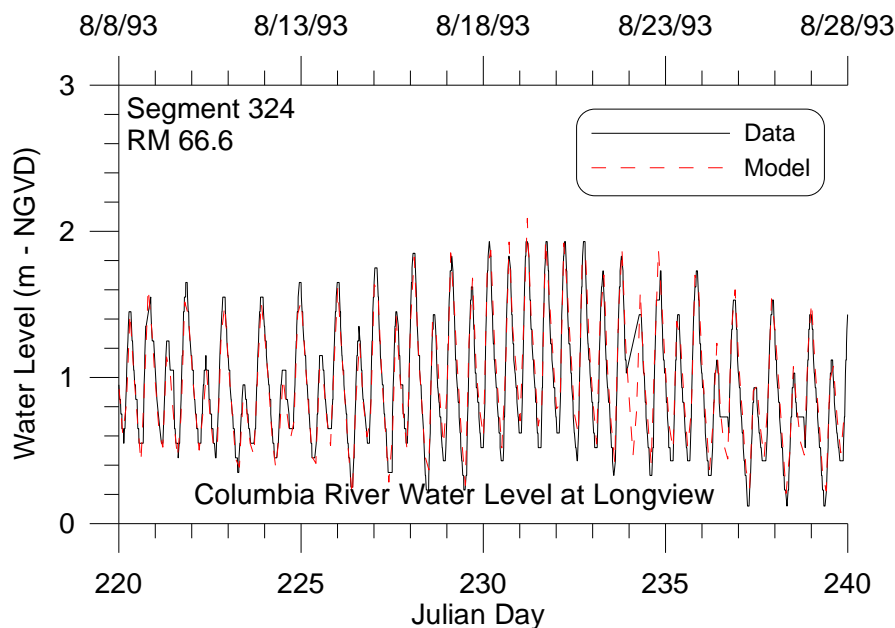


Figure 49. Water level data versus model predictions for Longview, WA during a 20-day period in 1993.

Similarly, a typical comparison of model predictions and field data of flow rate is shown in [Figure 50](#) for the Columbia River approximately 90 km from the Pacific Ocean.

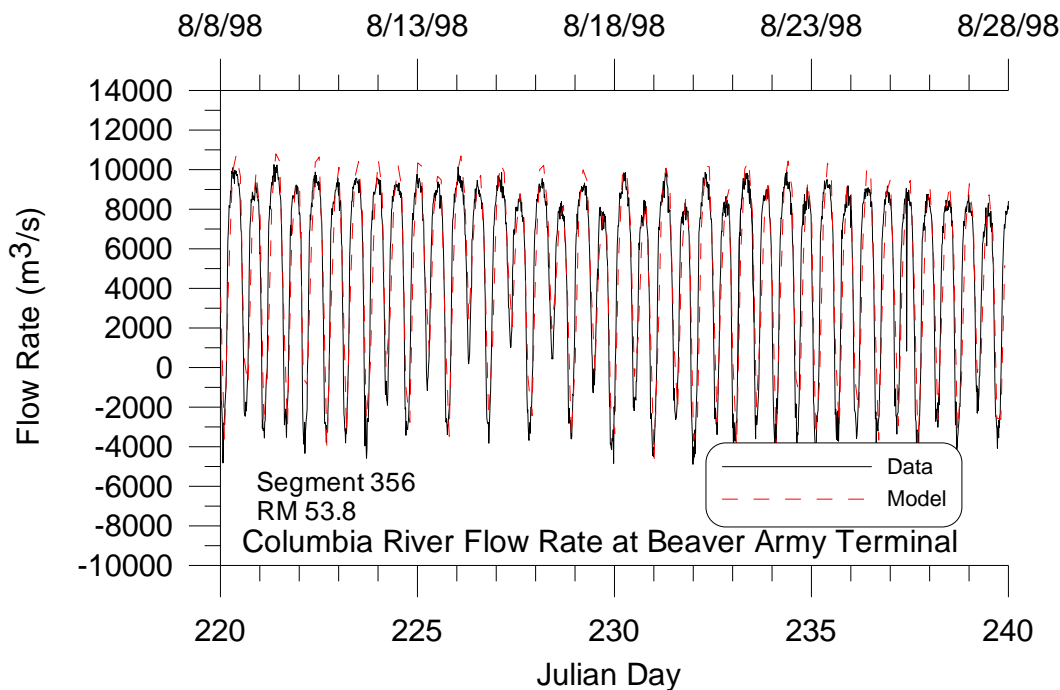


Figure 50. Model flow predictions versus data for a 20-day period during 1998 at Beaver Army Terminal near Quincy, OR.

Time of Travel

If at all possible, the model should be calibrated to a time-of-travel or dye study. This is important to ensure the model represents transport and mixing characteristics of the estuary accurately. Usually, the adjustment of bottom friction is the primary calibration parameter, but in some cases the bathymetry may need revision. The longitudinal eddy viscosity [AX] and diffusivity [DX] can also be adjusted during calibration. Since CE-QUAL-W2 uses a constant value for these coefficients for each waterbody, the user may need to include a longitudinal dispersion algorithm based on theoretical formulae if the constant value is not appropriate.

In many cases a dye release will also vary vertically as a result of stratification. The model internally computes the vertical diffusion coefficient based on the eddy diffusivity using the Reynolds analogy. The model user should ensure that they are using the implicit solution technique for the transport of vertical momentum, [AZSLC]=IMP, and that the maximum value of the vertical eddy viscosity [AZMAX] is at least $1 \text{ m}^2 \text{ s}^{-1}$ for estuarine systems.

Temperature and Salinity

Calibrating the model for estuarine temperature and salinity includes the same caveats as for reservoirs with, as previously mentioned, the additional need for accurate boundary conditions at the ocean boundary. If the user has developed a good hydrodynamic calibration for water surface elevations and flows, then temperature and salinity calibrations should require a minimal effort. However, keep in mind that water surface elevation, flow, and time of travel calibrations are all affected by the adequacy of the temperature and salinity calibration.

[Figure 51](#) and [Figure 52](#) are from an application of CE-QUAL-W2 to the estuarine portion of the Patuxent River that feeds into Chesapeake Bay (Lung and Bai, 2002). They illustrate the model's ability to reproduce vertical profiles of salinity and temperature over time.

CALIBRATION

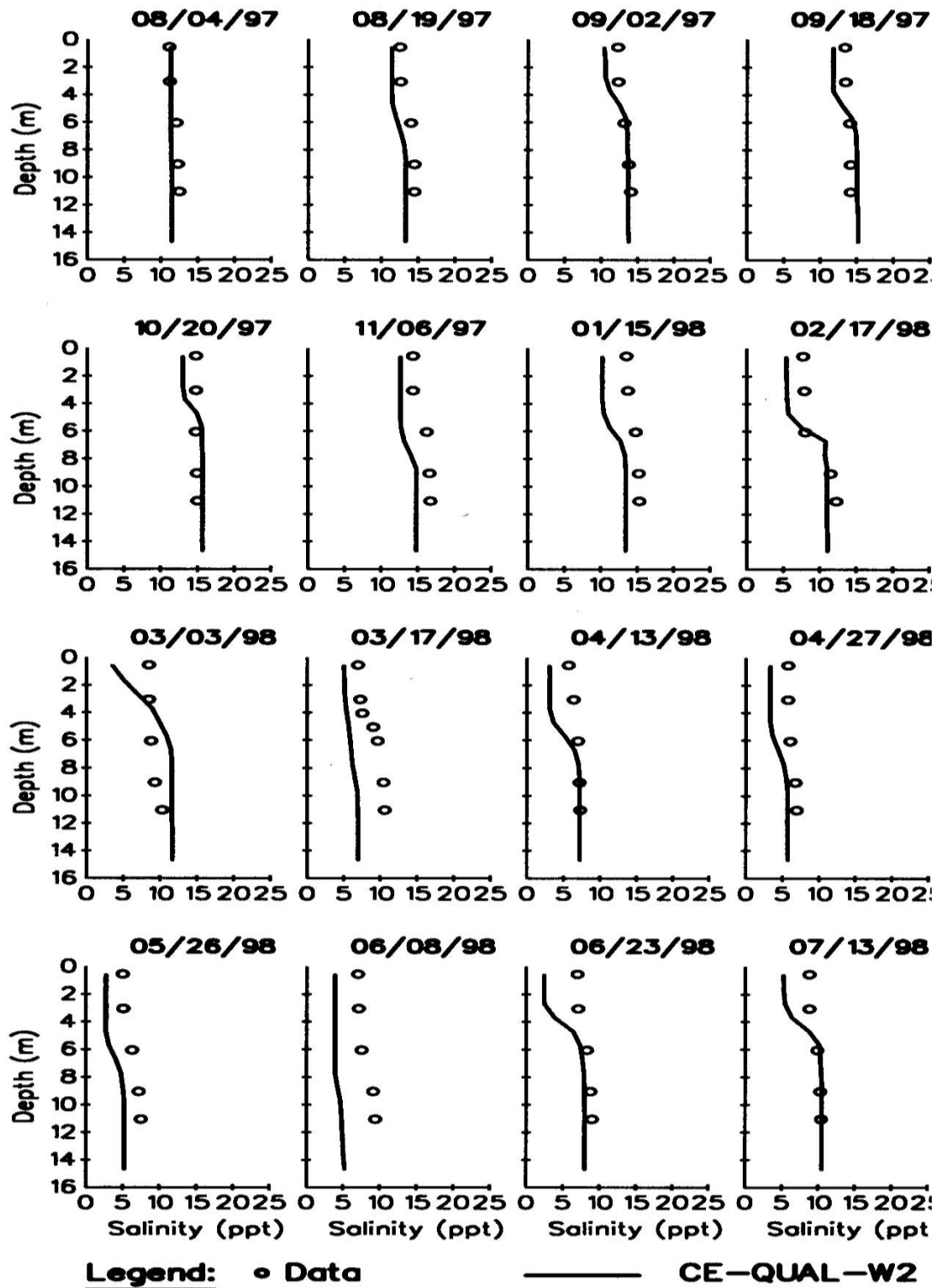


Figure 51. Patuxent River computed versus observed vertical salinity distributions.

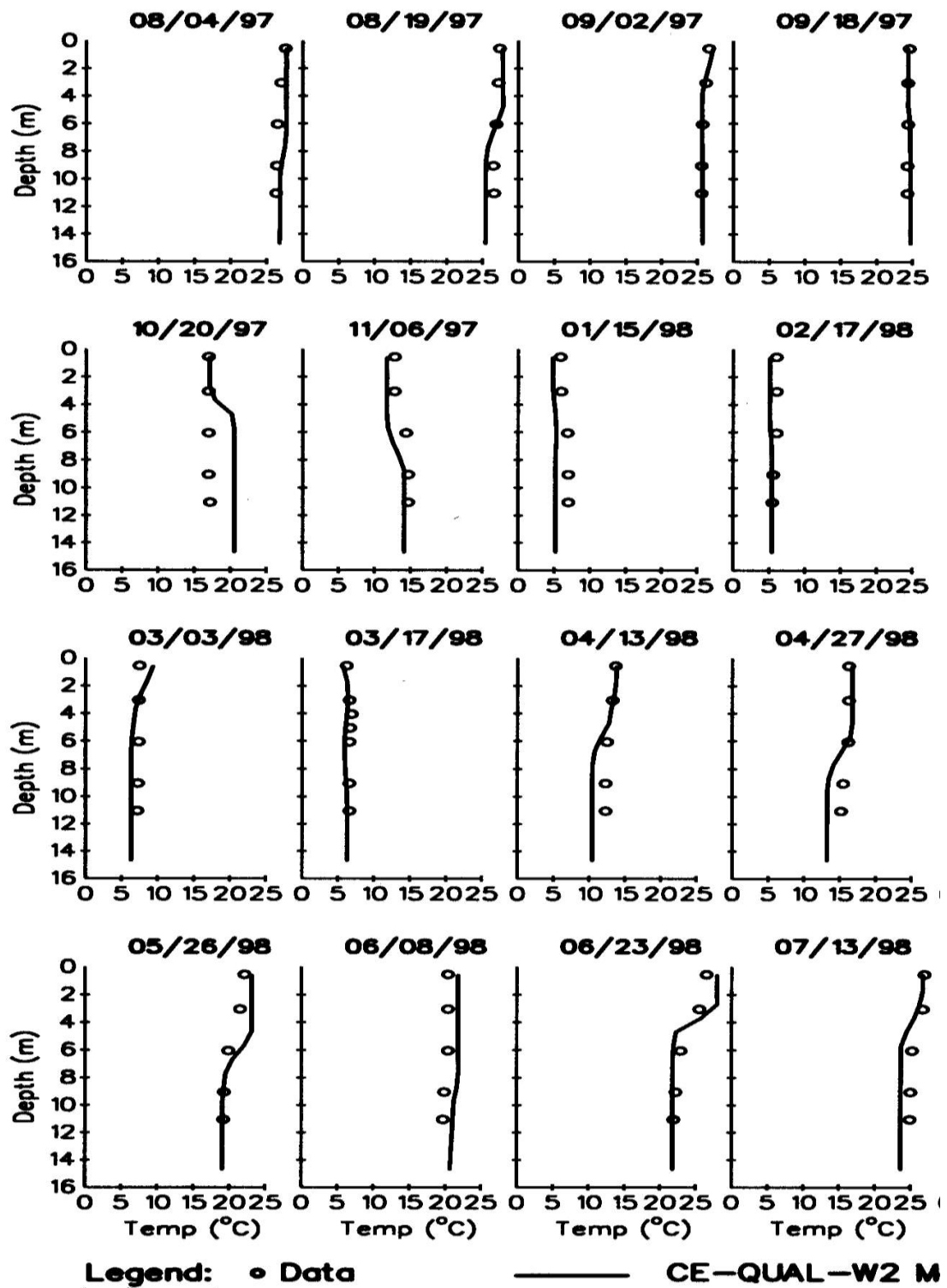


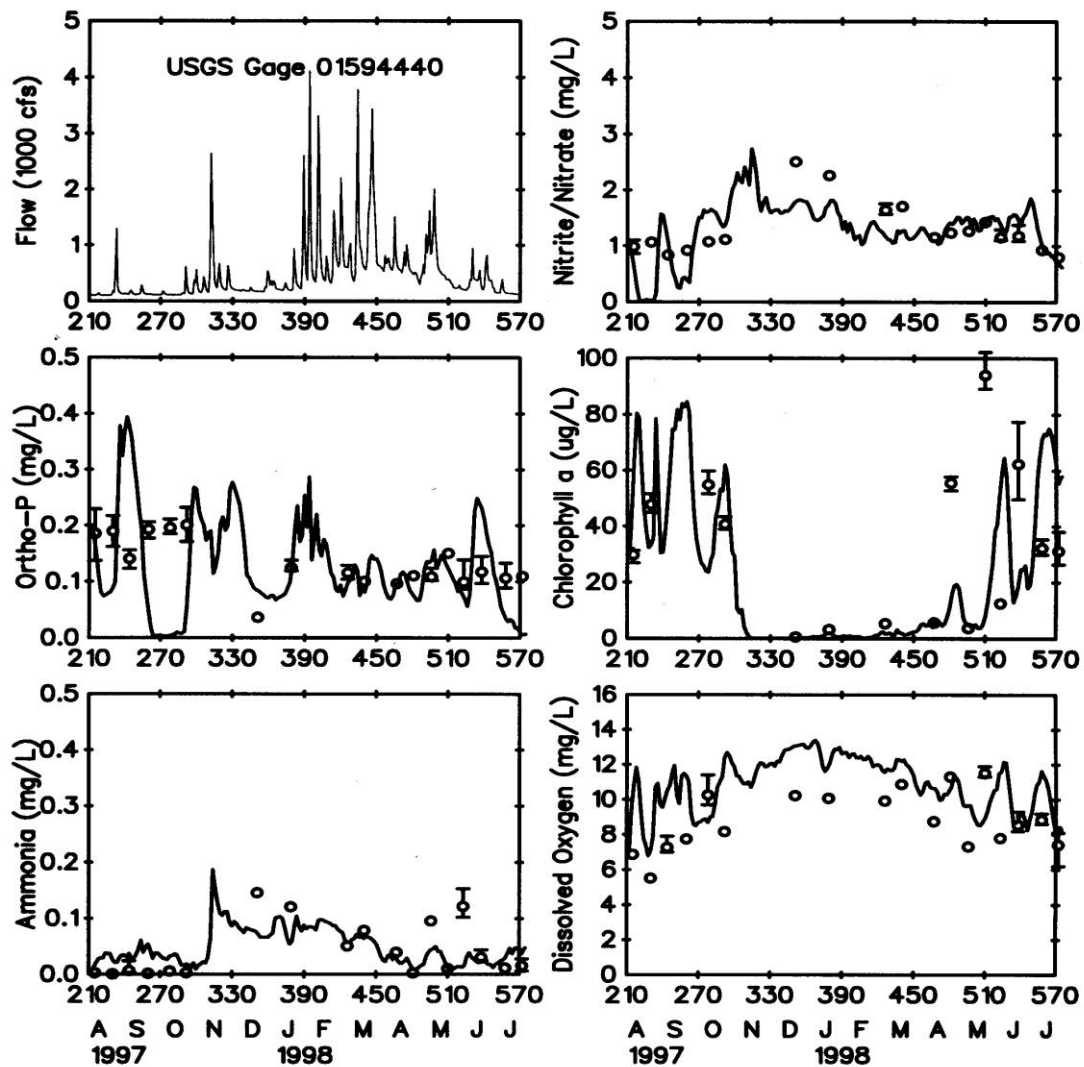
Figure 52. Patuxent River computed versus observed vertical temperature distributions.

CALIBRATION

Water Quality

Water quality calibration for estuaries is again subject to the same caveats as for reservoirs with the additional importance of accurate downstream boundary conditions. Again, if at all possible, the downstream boundary should be located sufficiently downstream where vertical variations in water quality are negligible.

[Figure 53](#) presents results for nutrients, dissolved oxygen, and chl *a* concentrations for Lung and Bai's Patuxent River application of the model.



LEGEND: \circ Observed Data (Water Column Average and Range)
 — Model Results

Figure 53. Patuxent River computed versus observed nutrient, dissolved oxygen, and chl *a* time series.

Calibration Problems Modeling an estuarine system requires a tremendous amount of data, expertise, and patience for proper calibration. In previous estuarine applications, calibration consisted mainly of determining whether known inaccuracies in a given forcing function could be responsible for the discrepancies in the model predictions and then describing the forcing function more accurately. This procedure included the following:

1. Ensuring the model reproduces flow and water level at various control points in the model domain and involved detailed evaluation of inflows and outflows, head boundary conditions, channel bathymetry, and channel friction.

CALIBRATION

3. Adjusting channel friction or longitudinal dispersivity to match time-of-travel data or dye study field data
4. Ensuring accurate vertical profiles for the downstream boundary
5. Ensuring grid refinement does not affect the model results
6. Ensuring accurate meteorological data for the estuary especially if the model domain extends over a large geographical area. Wind variability is extremely important and can be reflected in the wind sheltering coefficient that varies by segment and time.
7. Using an implicit eddy viscosity solution scheme, [\[AZSLC\]=IMP](#), and a maximum vertical eddy viscosity [\[AZMAX\]](#) of $1 \text{ m}^2 \text{ s}^{-1}$.

Since the model can be susceptible to accuracy issues using an implicit water surface solution scheme with a large time step, the user should ensure results are not impacted by using a smaller maximum time step [\[DLTMAX\]](#). Again, keep in mind that the more accurately the behavior of the prototype is described, the more accurately the model responds.

River

Dynamic river modeling can be a challenging endeavor because:

1. Velocities are generally high resulting in a lower time step for numerical stability
2. Shear and bottom friction effects are significant requiring a considerable calibration effort
3. Channel slopes accelerate the fluid
4. Changes in river bathymetry can dramatically affect the velocity field
5. Dynamic flow rates at low flows can dry up segments causing the model to stop running

One of the original motivations for development of the capability of modeling sloping rivers was to eliminate vertical accelerations in the fluid since the model does not solve the full vertical momentum equation. Keeping this in mind, the grid slope should be chosen to minimize the vertical fluid acceleration.

Channel Slope

The channel slope is used to compute the gravity force of the channel. This slope should be the slope of the water surface as that is the slope used to accelerate fluid parcels, or the energy grade line, rather than the bottom slope from segment to segment. As an example, consider the slope of a section of the Snake River shown in [Figure 54](#).

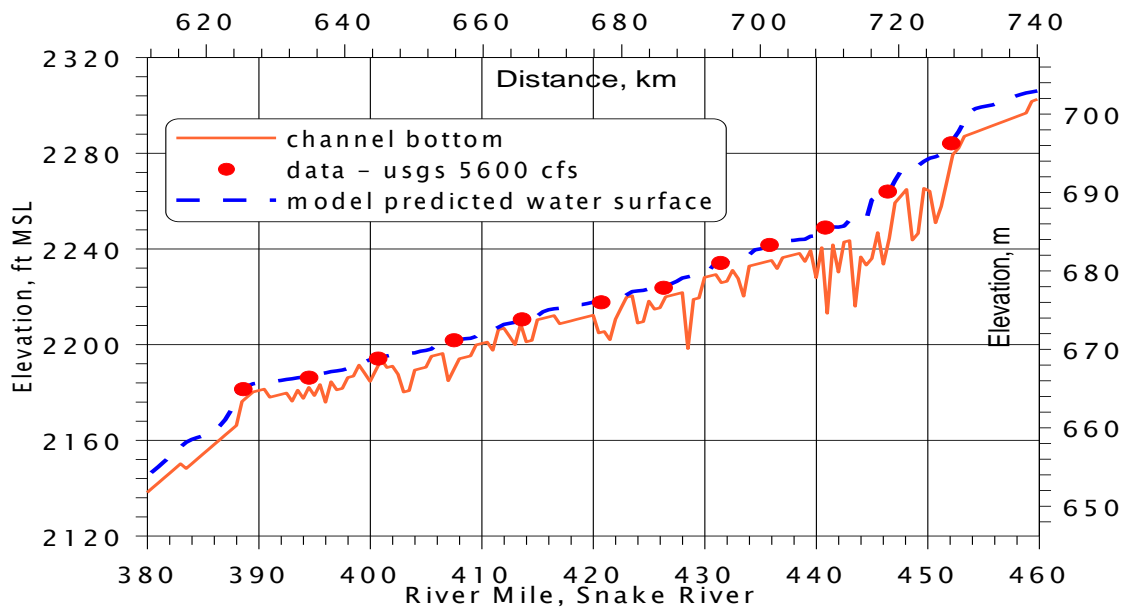


Figure 54. Snake River water level comparison between CE-QUAL-W2 V3 and USGS field data.

The slope of the vertical grid as well as the different branch slopes is shown in [Figure 55](#).

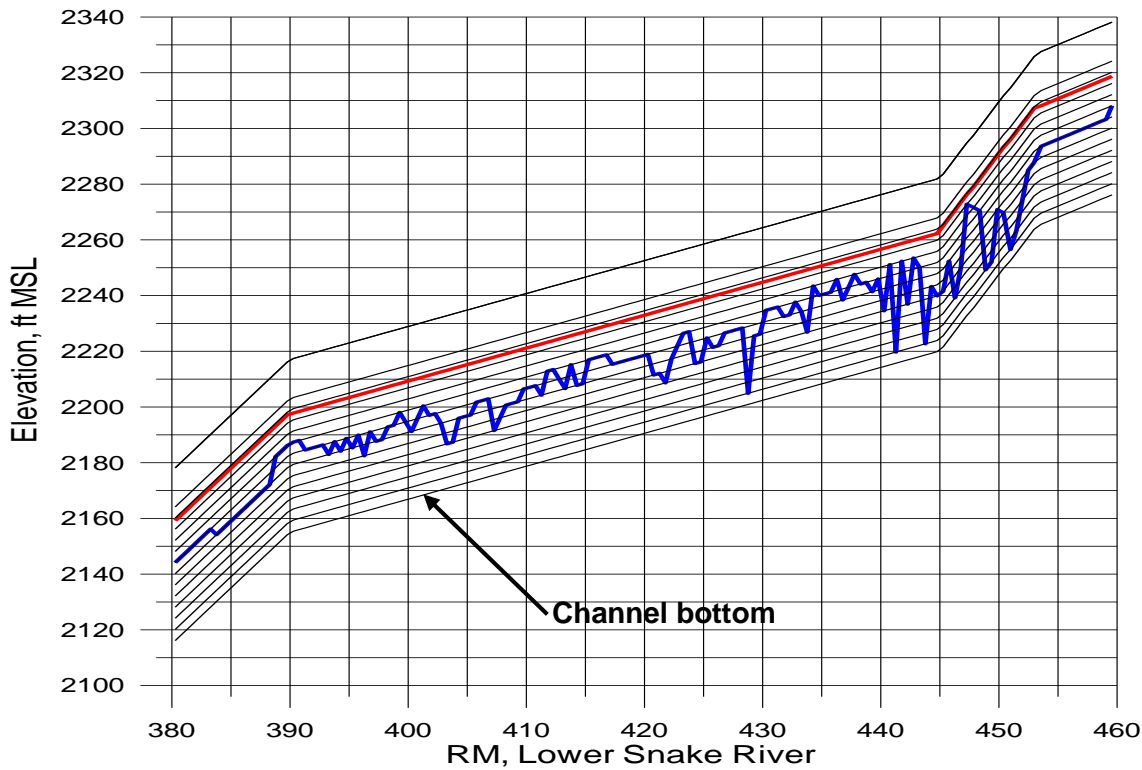


Figure 55. Channel vertical grid where every slope change is a new branch.

CALIBRATION

Rather than going from segment to segment with varying slopes, a general channel slope is used for a collection of segments with similar water slope. As the variability in water slope changes, so does the grid slope. How can one obtain this slope? [Figure 56](#) illustrates the use of a regression line to fit the channel slope for the section between RM 390 and 445 for the Snake River.

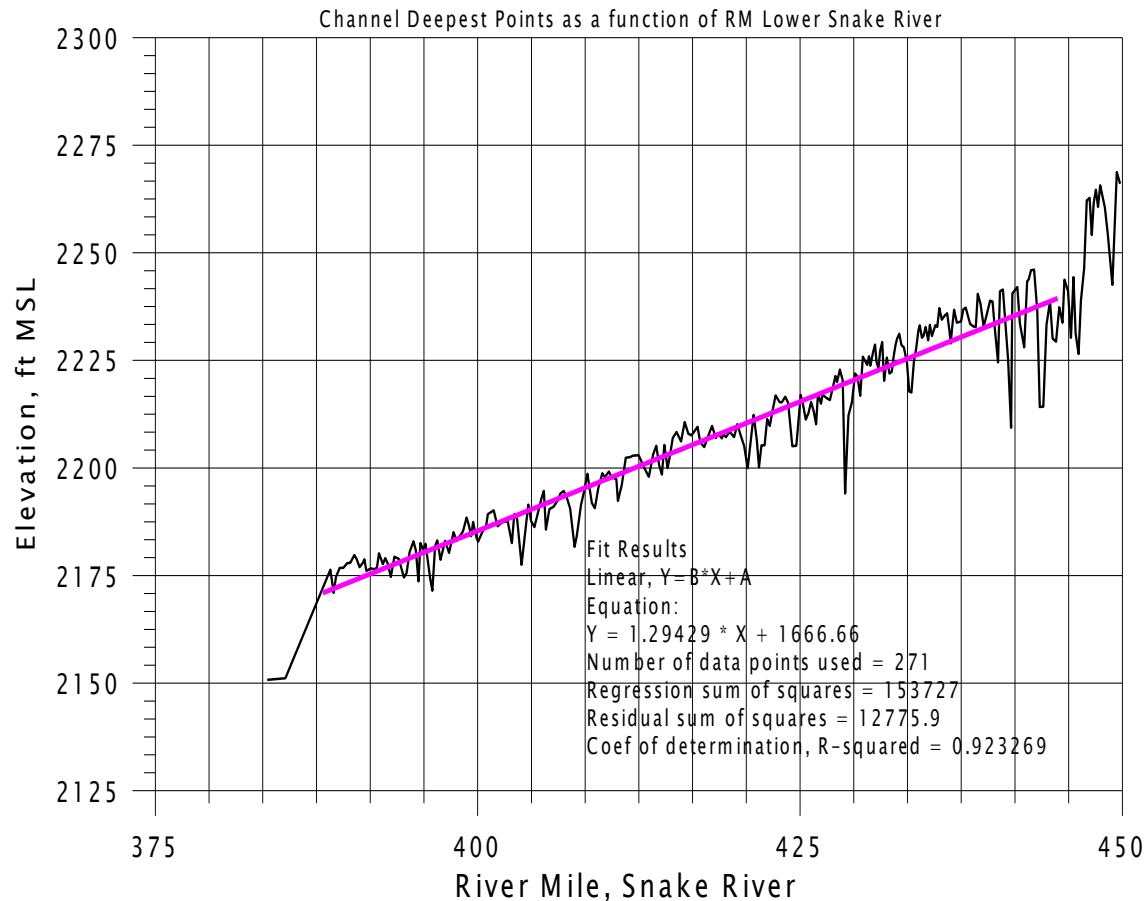


Figure 56. Snake River channel slope determination.

Why does W2 not use a segment-by-segment slope? Consider the “noise” in the cross-sections in [Figure 56](#). Even though the geometry could be set up with a variable channel slope for each segment (in the current application this means creating multiple waterbodies or branches for each slope), setting a general channel grade is often simpler and one still has the noise of the bathymetry represented as shown in [Figure 56](#). Computing the slope from one segment to a deep hole would not be correct since the water is flowing along its energy grade line and not the channel slope. Bottom elevations for many of the channel segments rise or have a negative channel slope following a depression. In using a segment-by-segment slope, these variations become unrealistic when represented using a slope for each segment. Therefore, the proper channel slope should be that of the water surface.

In estuarine flow, one usually uses a channel slope of zero and considers fluid accelerations as a result of water surface elevation changes rather than gravity flow down a slope, at least in the

estuary section below the head of tide. This is similar in a reservoir, which may have a sloping channel, but a relatively flat water surface.

In some cases, the average channel slope changes and the user must separate the different sections into separate branches or waterbodies. The model can be set up to have almost continuous changes in channel slope by making branches with two segments and changing the slope where it is required. If the choice is to create separate branches, then the surface layer and grid will be the same for all branches. If the choice is to create separate waterbodies, then each waterbody computes a surface layer independently of the other and there can be different vertical grids between water bodies.

When there are problems keeping water in upstream segments, which is a very common problem, the model takes the lowest water level in a waterbody and subtracts layers such that the lowest water level resides in the surface layer. If the surface layer is below the bottom layer in a segment, the model will subtract that segment and all segments above it from the active computational grid. If this occurs in a shallow location in the middle of a branch, the model will not run since it dries up a segment in the middle of a branch.

How can this be corrected? One way is to decouple one branch from another by splitting them into waterbodies. By splitting the system into more than one waterbody, water can be maintained at various levels throughout the domain since each waterbody has its own separate surface layer.

This is another reason why the model does not use segment-by-segment slopes since the surface layer defines the upper layer for a waterbody and in many cases these need to be broken apart into waterbodies to keep water in all segments. In addition, the translation from one waterbody to another introduces some small error into the solution since concentrations, temperatures, and velocities are interpolated from one 2D grid onto another. If the model were run in 1D mode with only one vertical layer, then this problem would not exist.

Consider another case study, the Bull Run system shown in [Figure 57](#).

CALIBRATION

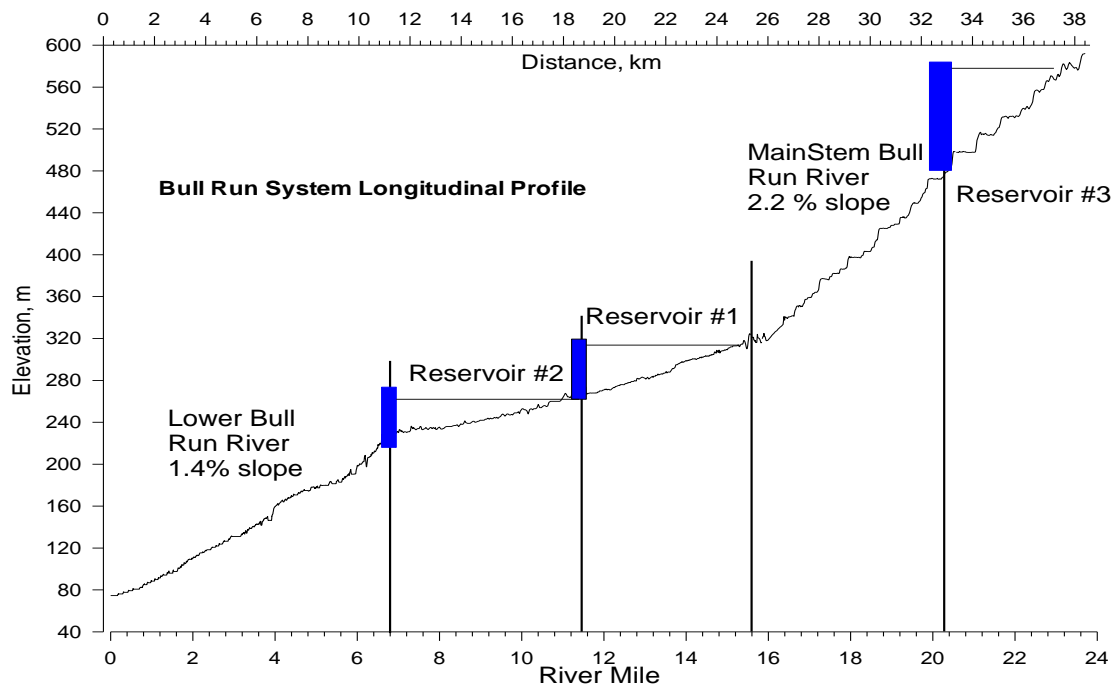


Figure 57. Channel slope for the Bull Run system.

The reservoirs were modeled with a channel slope of zero. Instead of a constant slope of 1.4%, the river is really divided into a large number of small-scale changes including pools and riffles. A section of the river is shown in Figure 58 with the assumed model grid divided into branches and waterbodies. In most cases, different waterbodies were used between branches of different slope. This allowed the water surface layer determination to be based on the water level in the branch with the given slope. However, the steeply sloping section may not have a slope equal to the grid slope shown. This may occur because if the steeply sloping section were modeled in more detail, it would really be a series of “flat” pools with small water drops (or falls) between the pools. If all the fine scale variability is ignored and the system is modeled on a larger scale, the problem becomes one of trying to estimate the “equivalent” channel slope that represents the channel.

This is similar to modeling a network of pipes and ignoring all the details but inserting pipes of “equivalent” slope and diameter. In this case, the channel slope is used as a calibration tool to match water level or dye study data. If channel friction were used to hold the water back, the values would have to be enormous to reproduce the complicated pool-waterfall system.

In addition, if the grid is broken into different waterbodies, discontinuities in the water surface such as waterfalls can be simulated.

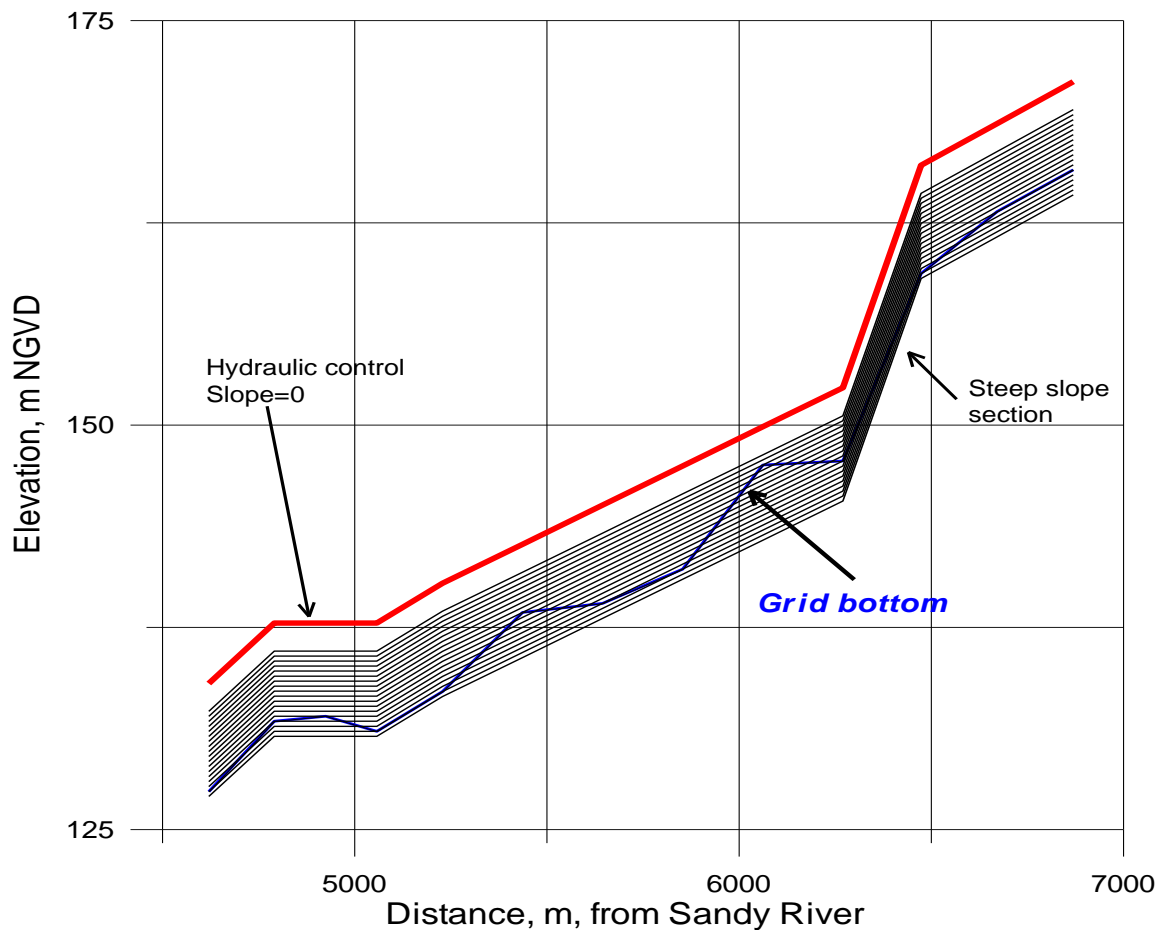


Figure 58. Vertical grid for W2 model of Bull Run Lower River.

Modeling of shallow streams with large slopes is difficult and takes patience. The model drying out at intermediate sections is often the cause of problems and can be remedied by breaking the system into smaller pieces or waterbodies and/or by adding additional computational cells below the bottom layer at a given segment. Matching river data is accomplished by adjusting friction factors, refining the geometry, and in some cases refining the “equivalent” channel slope if detail has been sacrificed in setting up the model. The quality of the model geometry is essential for good model-data reproducibility in a river system, especially one that is highly irregular in slope and channel width.

Developing a river model is also difficult at low flows since the model may become either unstable during the initial time steps or become dry in a segment. The reason for this is that, in the beginning, an initial water surface elevation is set and the river is “frozen” at that elevation until the model is started, at which point the water starts moving downstream. If a conservative high water is set initially in all segments, a wall of water will be sent downstream. If inflows are so small that at the upstream edge of this wave there is too little water, segments can dry out. The model includes a warning [w2.wrn] and error file [w2.err] that contains information for debugging a river model problem.

CALIBRATION

The following are suggestions for setting up a river model:

1. For the first 0.1 JDAY or so of the simulation, choose a maximum timestep **[DLTMAX]** that is small (10 s or less). This should be done only if the code seems to go unstable soon after starting the model. Alternatively, one can lower the fraction of the timestep **[DLTF]** used as this can provide numerical stability and allow for higher timesteps. The maximum timestep should be lowered if the number of time step violations is greater than 10% for an extended period of time.
2. Start with high flow rates gradually approaching the lower flow regime if model stability is a problem at low flows.
3. In order to keep water in the model, friction factors and geometry are very important considerations. The goal is to have sufficient model friction so that water does not quickly drain out of the system.
4. Add active computational cells at the bottom of the grid using small widths to prevent the section of the river from drying up or subtracting segments unnecessarily because the water surface layer **[KT]** is below the bottom **[KB]**.
4. For a river that has sloping sections followed by flat sections (slope=0), you may want to set the slope to a non-zero value of 0.000001. This activates in the code the ability of the model for **[KT]** to be below **[KB]** when the segment is still hydrated.
5. If the water surface elevation becomes unstable as evidenced by a negative surface layer thickness, try reducing the maximum timestep **[DLTMAX]** to 5-10 seconds or less during the unstable time period. Alternatively, the fraction of the timestep **[DLTF]** can be set to 0.5 or less during this period.
6. For the end of the river, often a weir/spillway condition is used. This allows the specification of the stage-discharge relationship for the river. See the **Spillways/Weirs** description for an example of how to do this.
7. Set **AZSLC=IMP** and **AZMAX=1.0**. Do not use **ASC=W2**; use one of the other formulations.

The following discussion illustrates the model's ability to accurately simulate river hydrodynamics, temperature, and water quality and includes a synopsis of the model's application to the Bull Run River, Snake River, and Spokane River

Bull Run River. The Bull Run River is located in Oregon and the two existing reservoirs located on the river provide water for the city of Portland ([Figure 57](#)). A third reservoir upstream of the existing reservoirs is in the planning stage. The two portions of the free flowing river that were modeled had slopes of 1.4% and 2.2%. The model was used to address temperature and suspended solids questions about the system.

Snake River. The Lower Snake River from C.J. Strike to Brownlee Reservoir suffers from eutrophication problems below the city of Boise. Chlorophyll *a* concentrations in the river often exceed $100 \mu\text{g l}^{-1}$ and ultimately can cause severe dissolved oxygen depletion in the upper reaches of Brownlee Reservoir leading to fish kills. The model was used to determine how inflowing algae and nutrients affect chl *a* and dissolved oxygen concentrations in Brownlee Reservoir.

Spokane River. The Spokane River from the Idaho border to Long Lake was modeled as part of a Total Maximum Daily Load allocation study and was conducted by Portland State University, the Washington State Department of Ecology, and the U.S Army Corps of Engineers. Epiphyton

were added to the model because of their importance on nutrient and dissolved oxygen dynamics in the River.

The system is complex hydraulically with three run-of-the-river impoundments used for power generation, significant groundwater inflows during low flow periods, a water fall, and Long Lake, a deep storage impoundment. Although Long Lake is a long and fairly deep reservoir, residence times during the summer are relatively short (< 1 month). Therefore, accurate inflow temperatures and constituent concentrations were crucial for accurate simulations of temperature and water quality in Long Lake, which required accurate simulations of over 40 miles of the Spokane River upstream of Long Lake.

The system is also complex with respect to water quality as epiphyton dominate nutrient and dissolved oxygen dynamics in the river and phytoplankton dominate their dynamics in Long Lake. Additionally, there are four point source discharges including the City of Spokane's wastewater effluent.

Hydrodynamics and Temperature

[Figure 59](#) shows results of a dye study conducted as part of the hydrodynamic calibration for the Bull Run River. Results show that the QUICKEST/ULTIMATE transport algorithm does not suffer from excessive numerical dispersion nor does it generate over/undershoots and that the model is capable of accurate river hydrodynamic simulations.

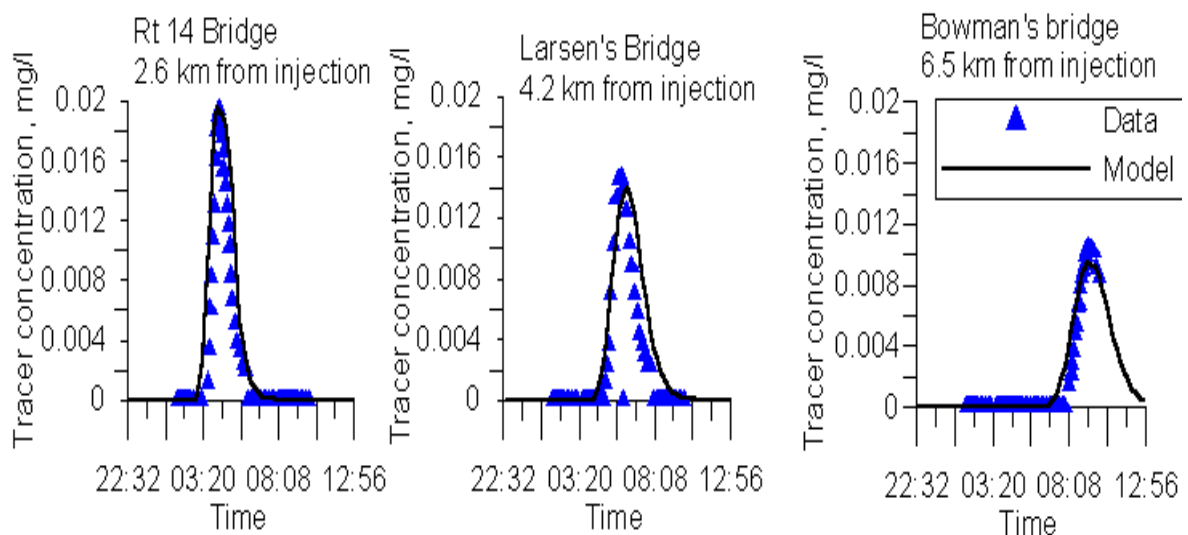


Figure 59. Bull Run River computed versus observed tracer at three stations progressing downstream.

[Figure 60](#) illustrates the accuracy of the water balance at the City of Spokane and [Figure 61](#) shows the accuracy of the computed flows at the same location.

CALIBRATION

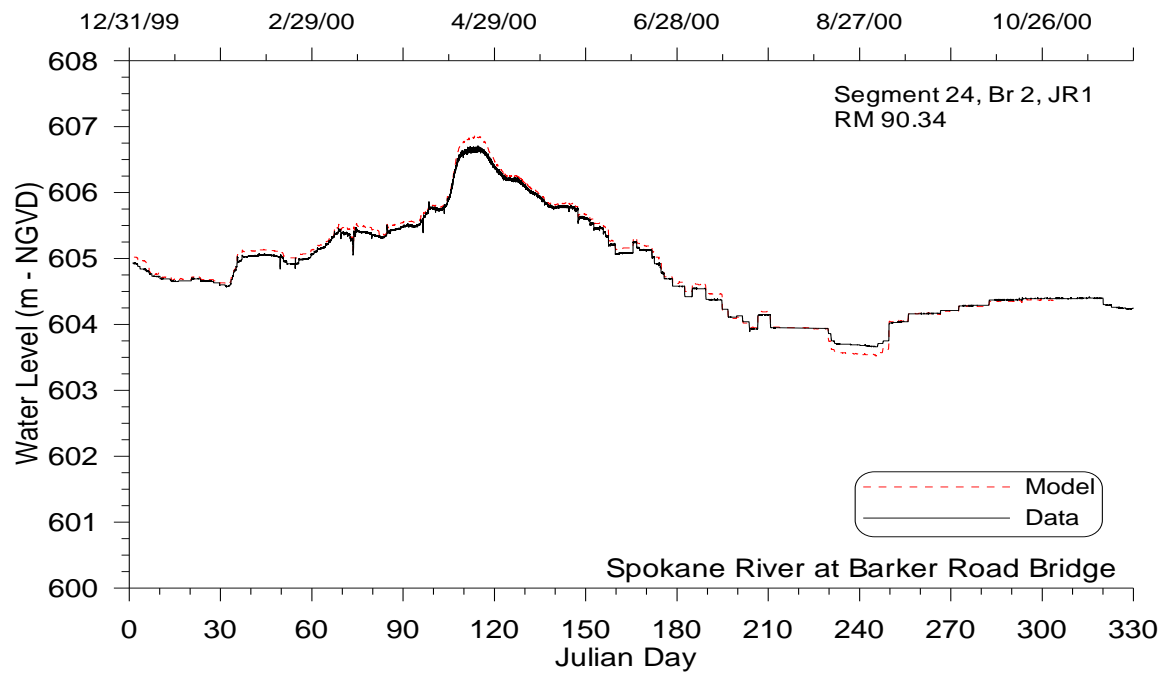


Figure 60. Spokane River computed versus observed water surface elevations at Spokane.

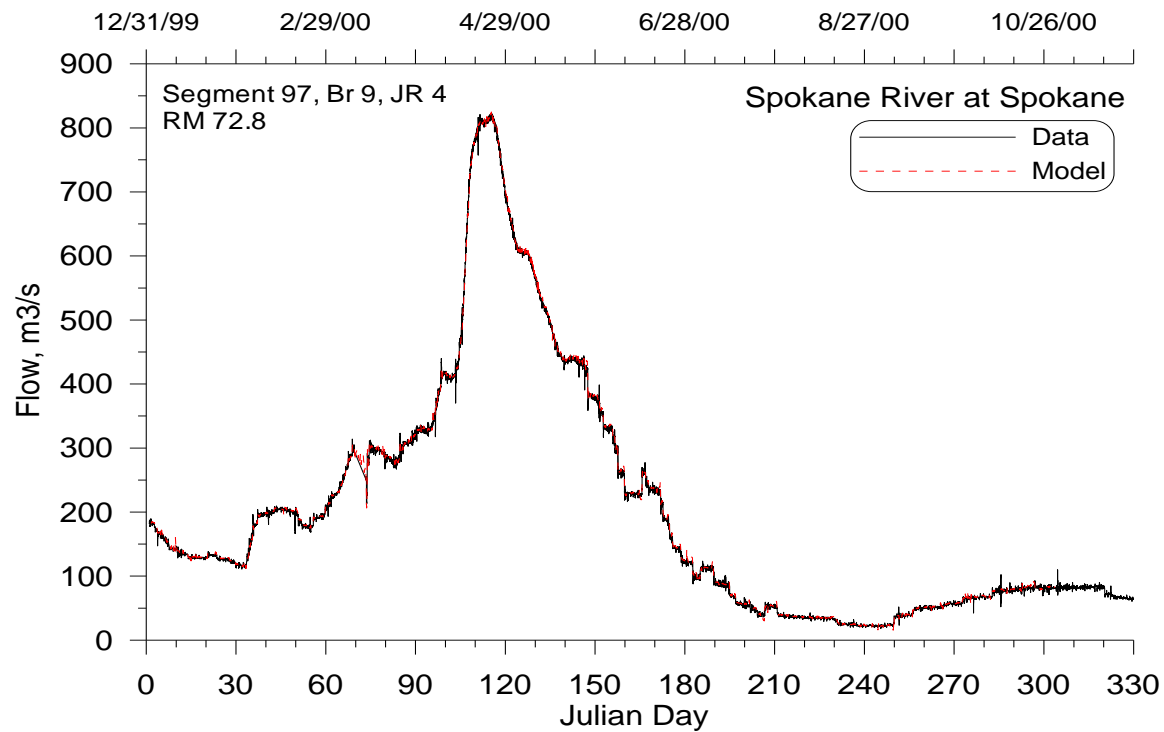


Figure 61. Spokane River computed versus observed flows at the city of Spokane.

CALIBRATION

Computed versus observed temperatures are shown in [Figure 62](#) and [Figure 63](#) for the Snake and Spokane rivers. As for reservoirs, temperature predictions are in close agreement with observed data.

CALIBRATION

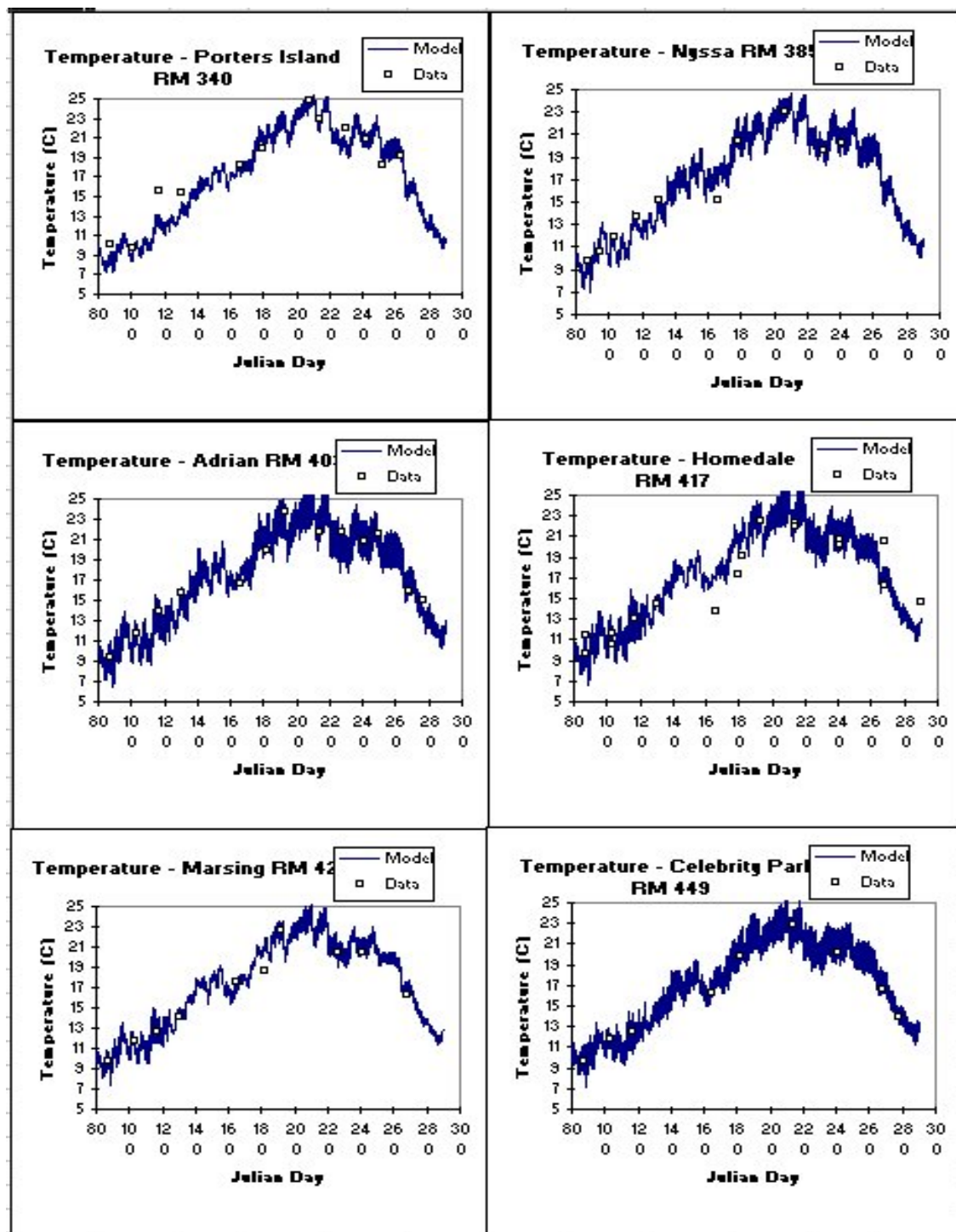


Figure 62. Snake River computed versus observed temperature at six stations.

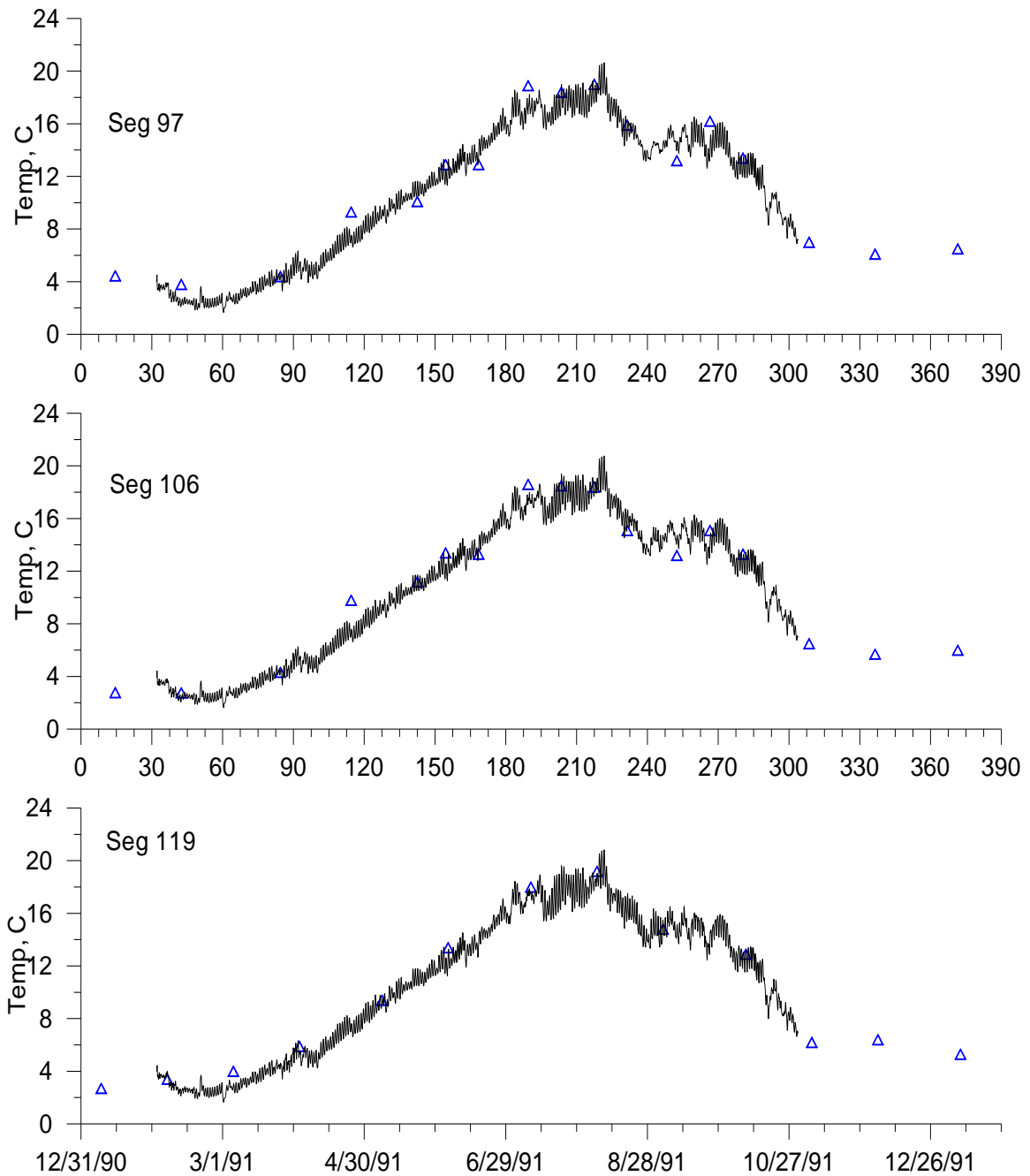


Figure 63. Computed versus observed temperatures for the Spokane River at Stateline Bridge (upstream boundary), City of Spokane, Fort Wright Bridge, and Riverside State Park.

For the Spokane study, conductivity was an important indicator of not only the hydrodynamics but also of the groundwater portion of the water balance. The model is accurately reproducing the temporal variation in conductivity ([Figure 64](#)) and is probably more accurate than any other method for determining groundwater inflows.

CALIBRATION

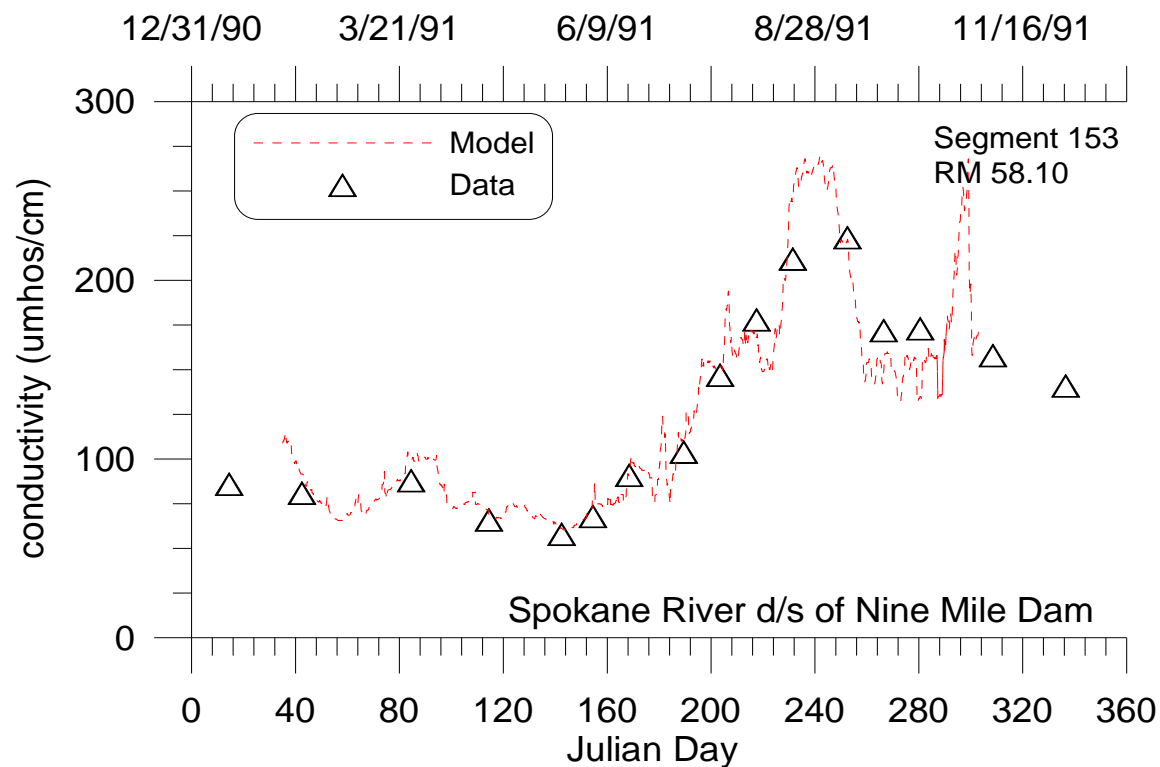


Figure 64. Spokane River computed versus observed conductivity below Nine Mile Dam.

Water Quality

Results for nutrients, dissolved oxygen, and chlorophyll *a* are given in [Figure 65-Figure 69](#) for the Snake River. The model is capturing much of the spatial and temporal changes in water quality for the river section where, unlike the Spokane River, phytoplankton rather than epiphyton dominate dissolved oxygen and nutrient dynamics.

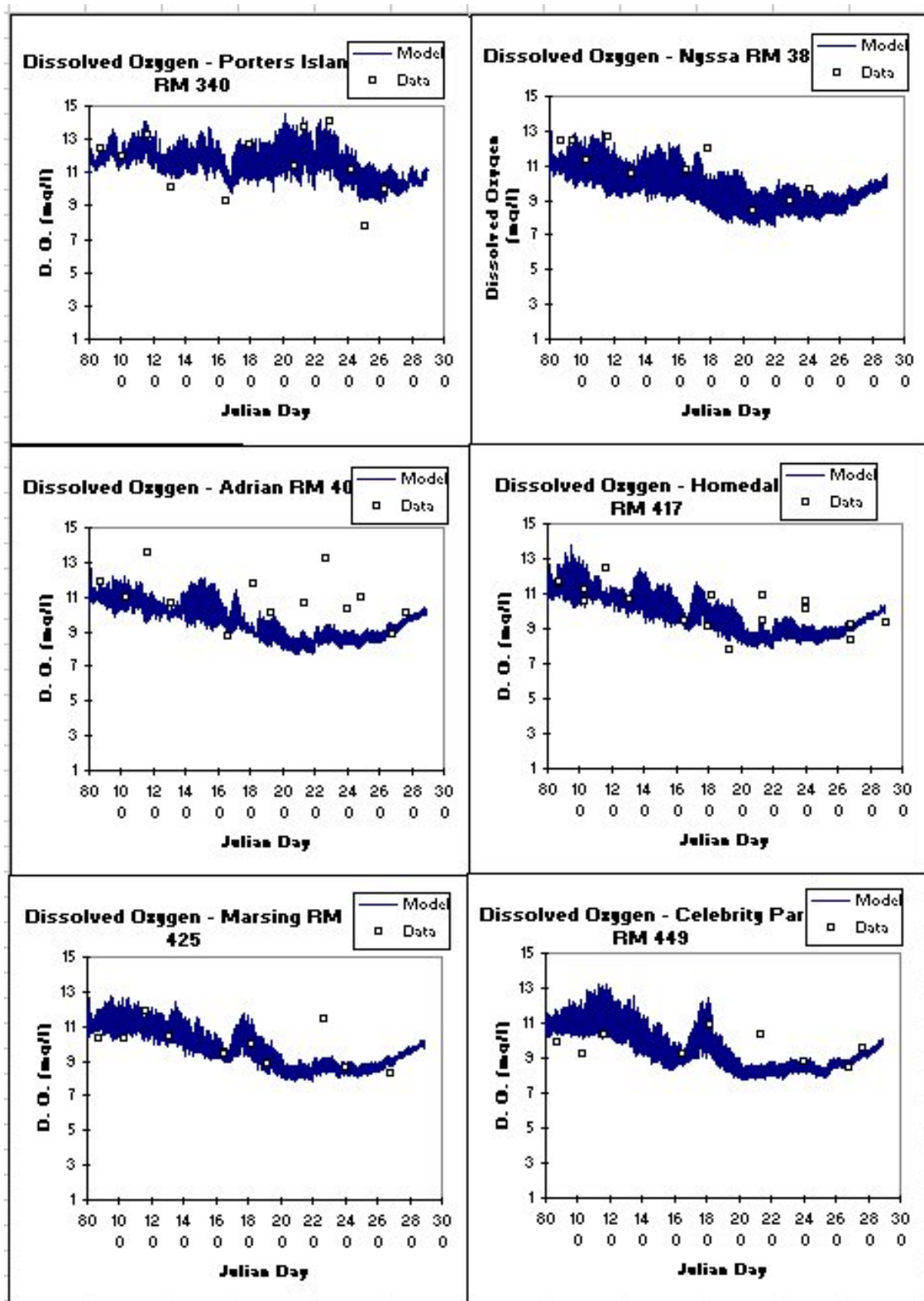


Figure 65. Snake River computed versus observed dissolved oxygen at six stations.

CALIBRATION

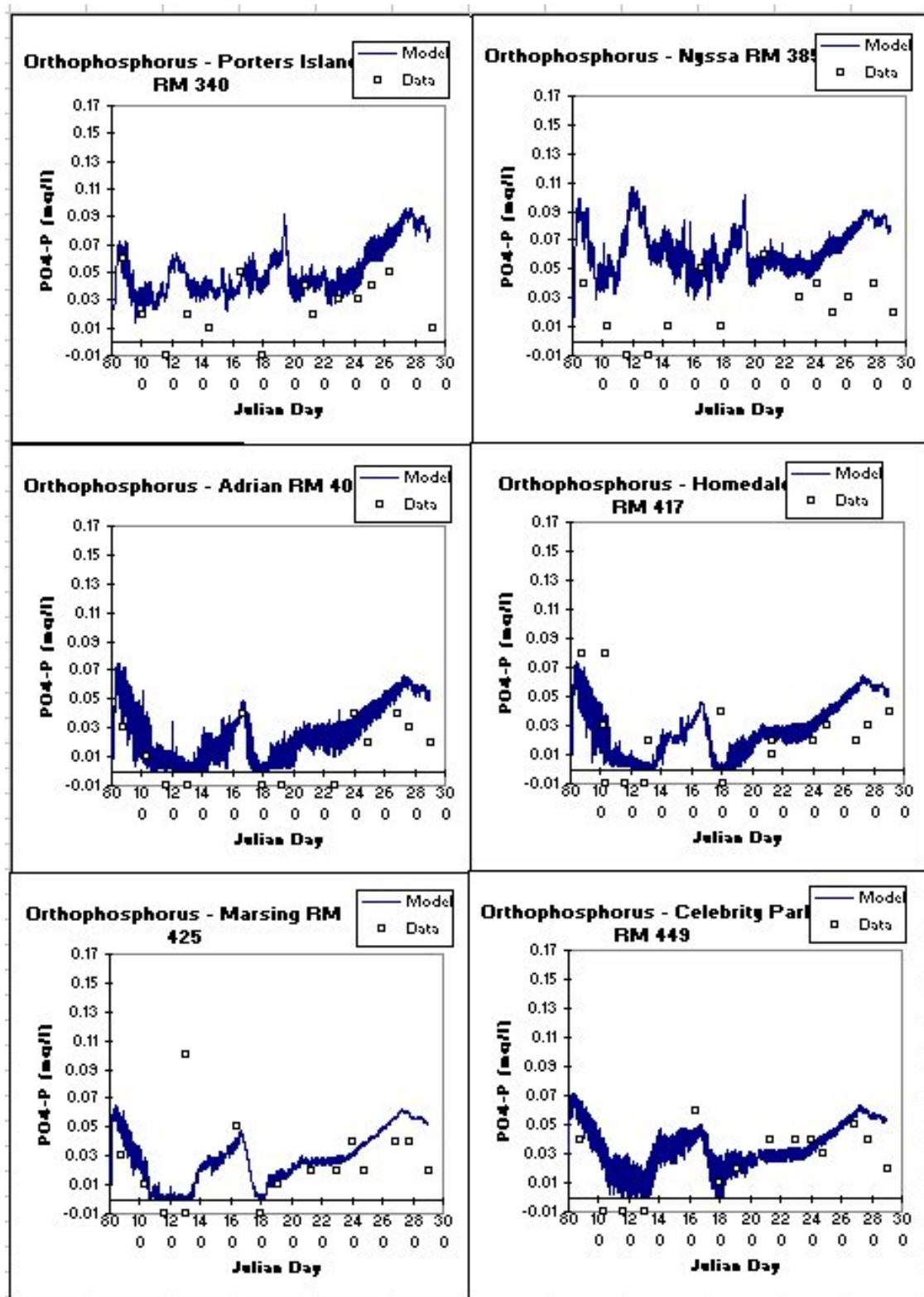


Figure 66. Snake River computed versus observed orthophosphorus at six stations.

CALIBRATION

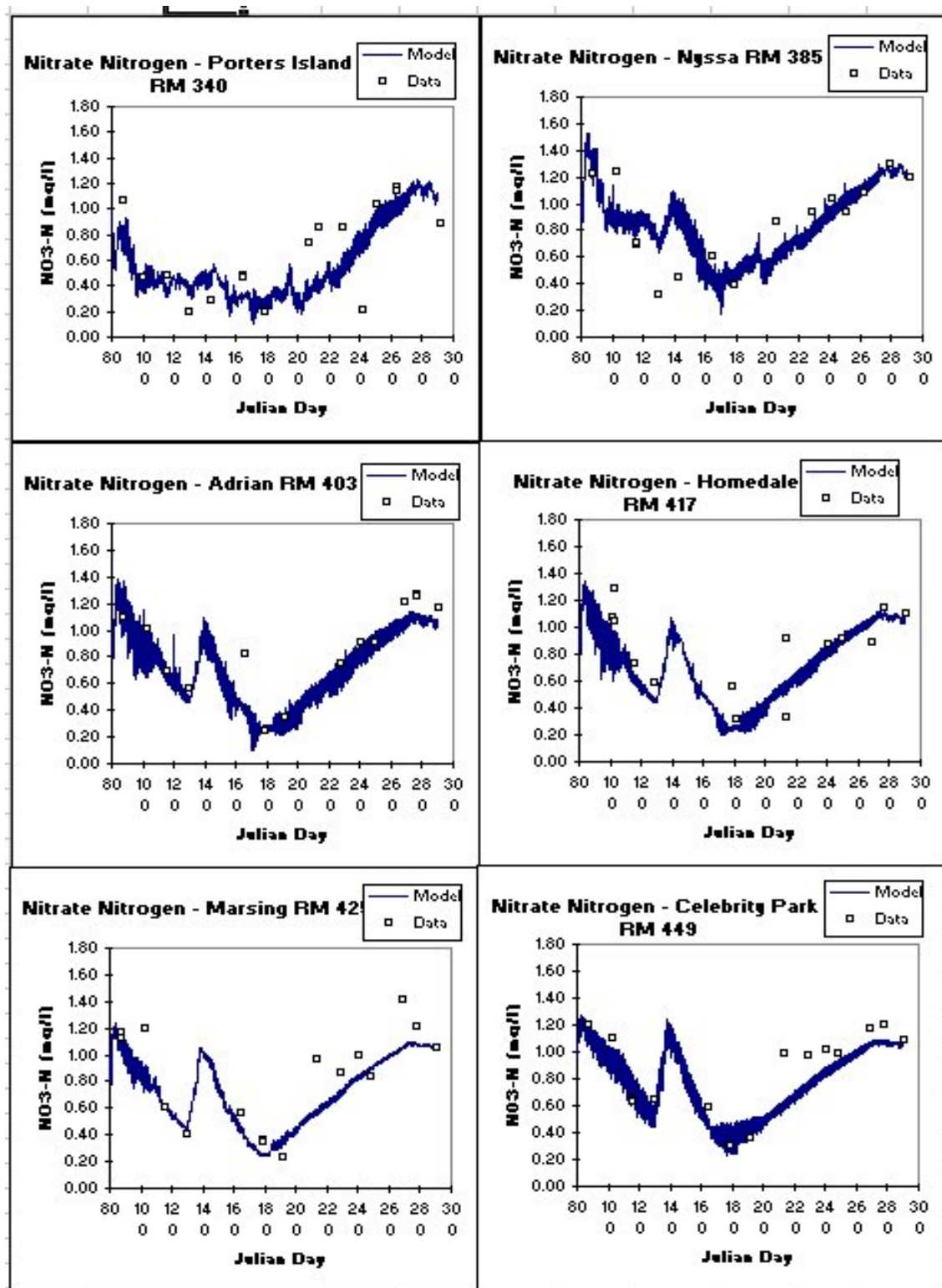


Figure 67. Snake River computed versus observed nitrate-nitrite at six stations.

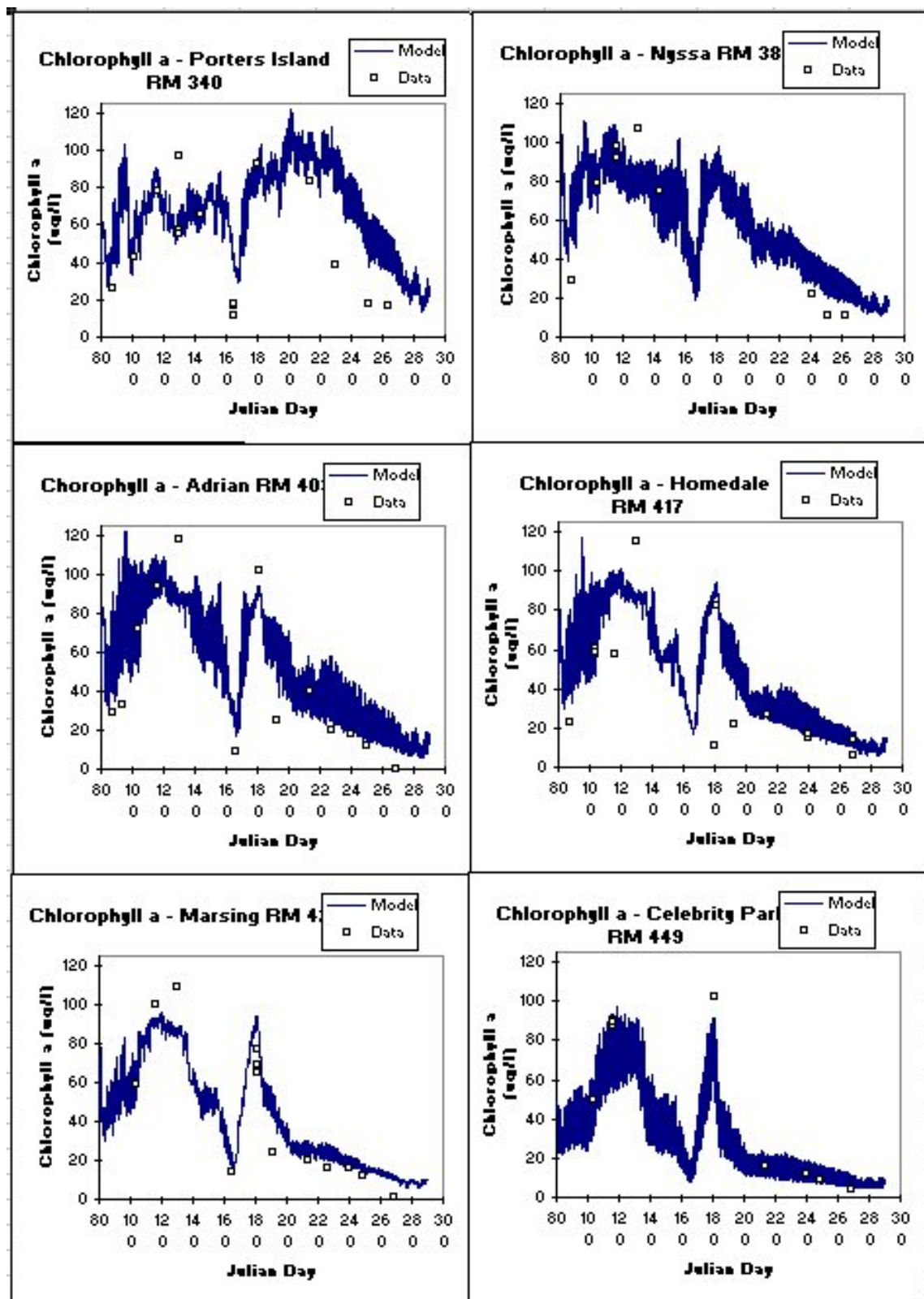


Figure 68. Snake River computed versus observed chlorophyll a at six stations.

CALIBRATION

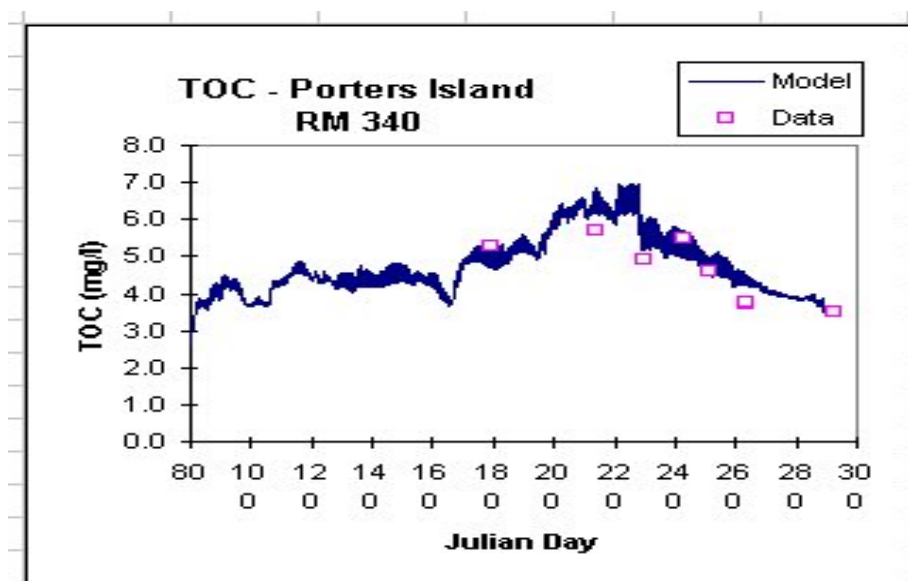


Figure 69. Snake River computed versus total organic carbon.

[Figure 70](#) and [Figure 71](#) illustrate the models ability to reproduce changes in dissolved oxygen over a year and also on a diel basis on the Spokane River. Note how the model has captured not only the diel swings in dissolved oxygen, but also the decrease in the magnitude of the diel variation, which indicates that the model is accurately reproducing epiphyton primary production. This is reinforced in [Figure 72](#) where the model is reproducing diel variations in pH due to epiphyton growth and respiration and the decrease in diel variation over time

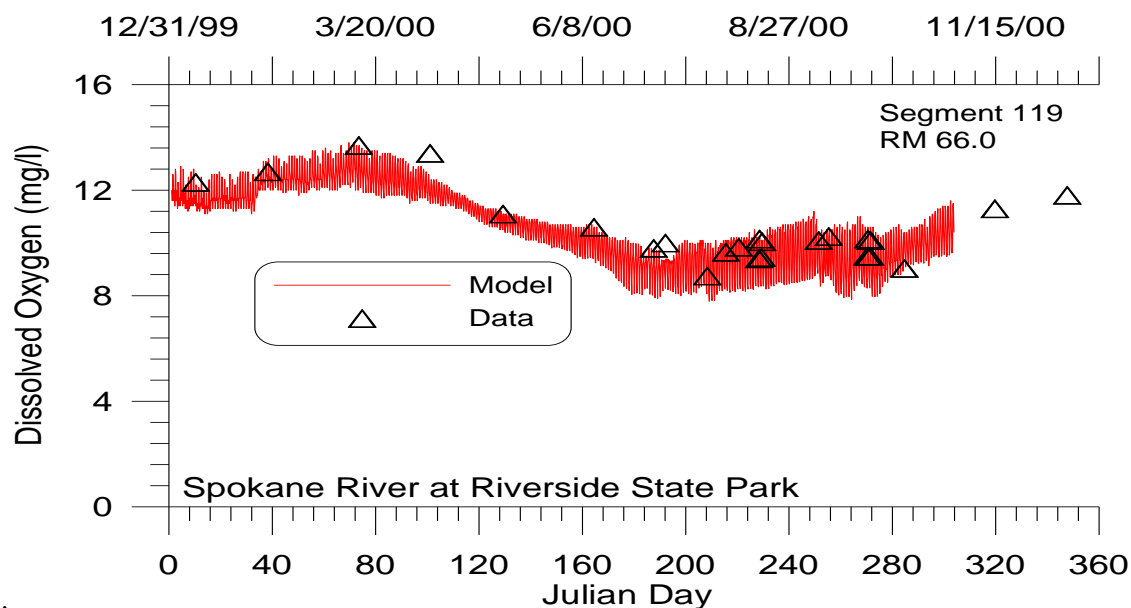


Figure 70. Spokane River computed versus observed dissolved oxygen at Riverside State Park.

CALIBRATION

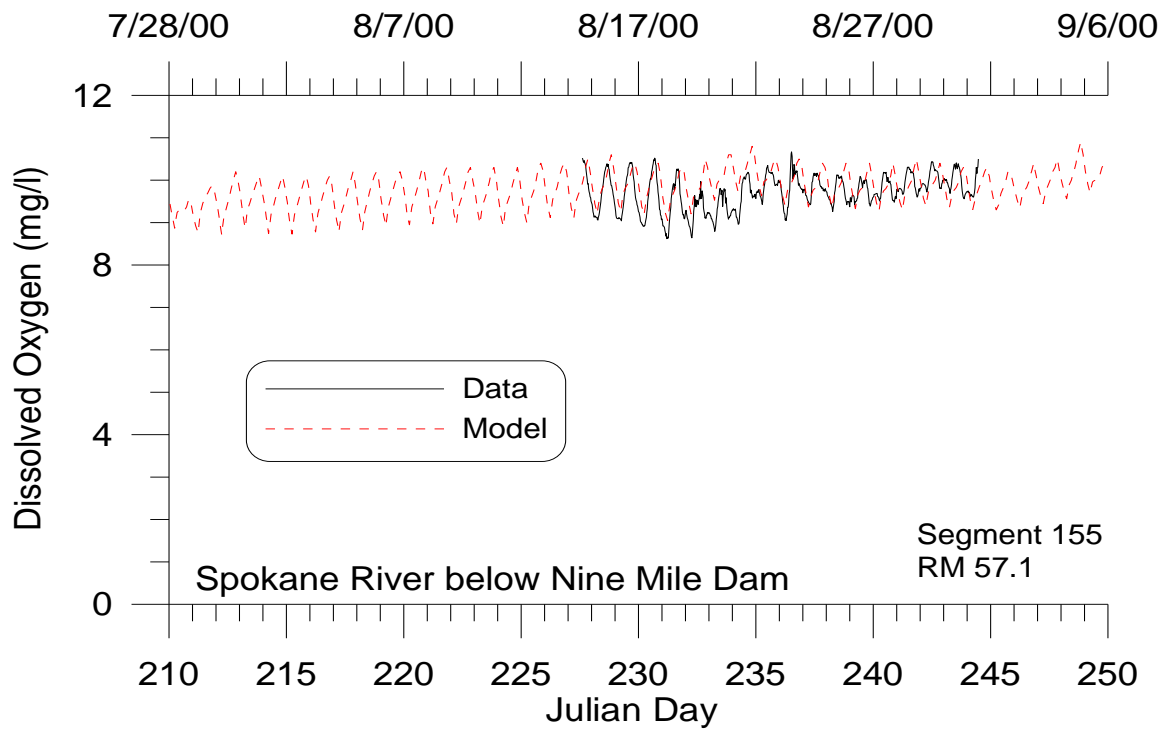


Figure 71. Spokane River computed versus observed dissolved oxygen below Nine Mile Dam.

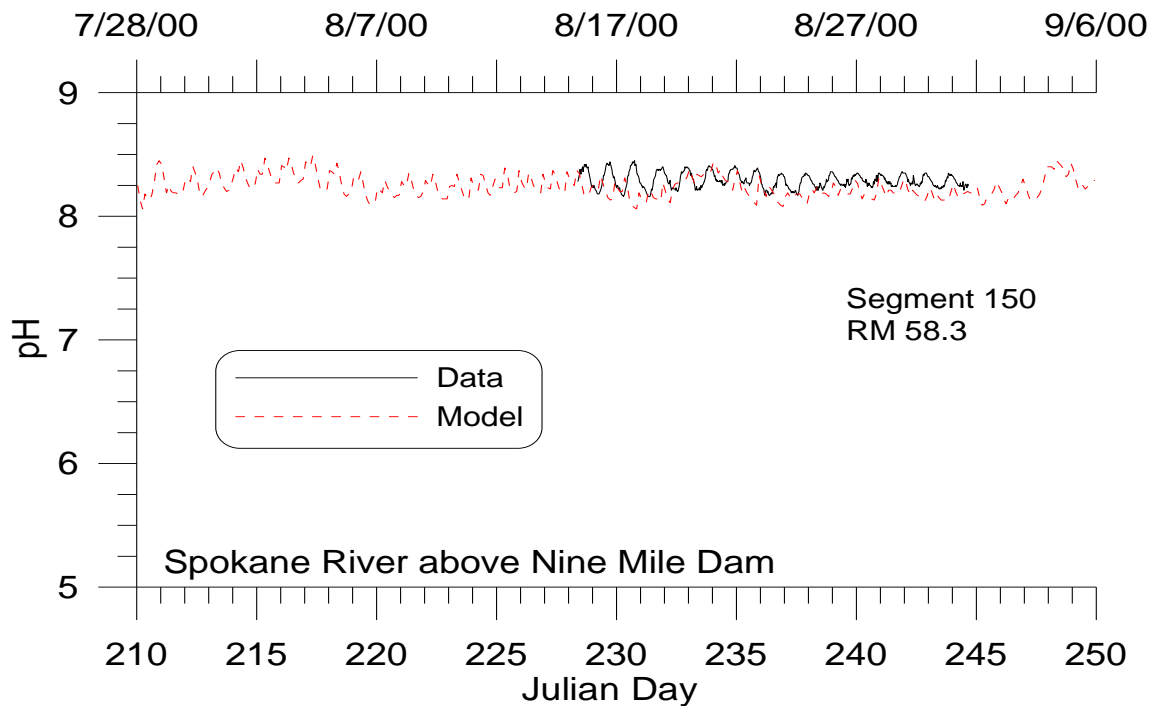


Figure 72. Spokane River computed versus observed pH upstream of Nine Mile Dam.

CALIBRATION

[Figure 73-Figure 75](#) illustrate the model's ability to reproduce nutrient dynamics that are impacted by upstream inflows, groundwater inflows, point source loadings, and epiphyton interactions.

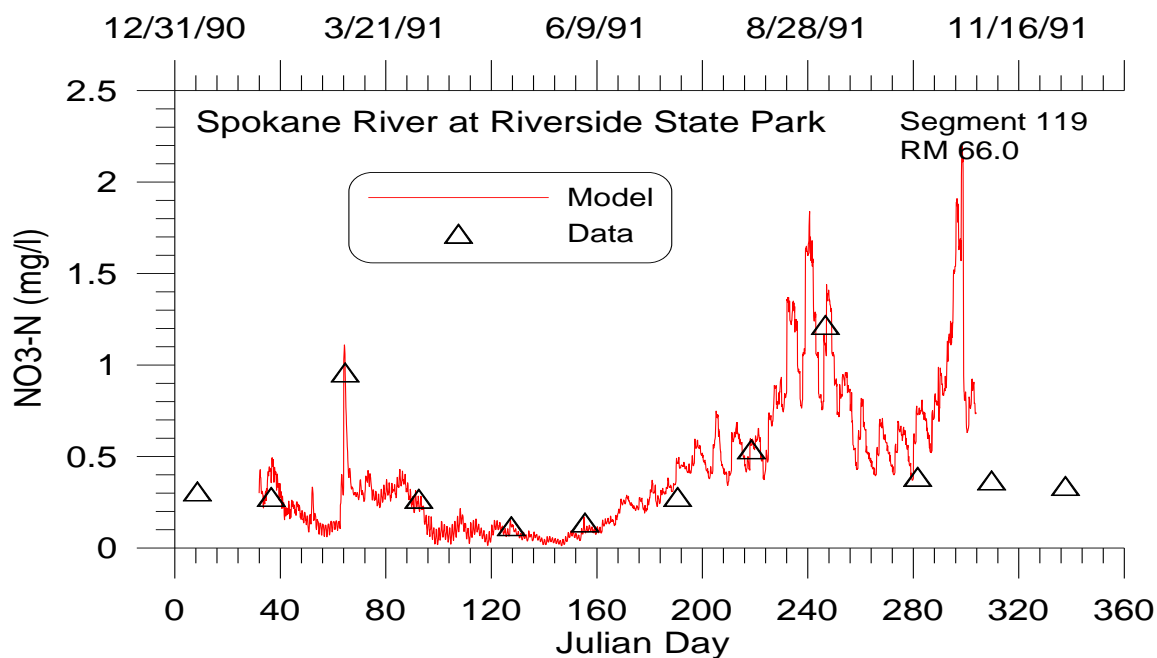


Figure 73. Spokane River computed versus observed nitrate-nitrite at Riverside State Park.

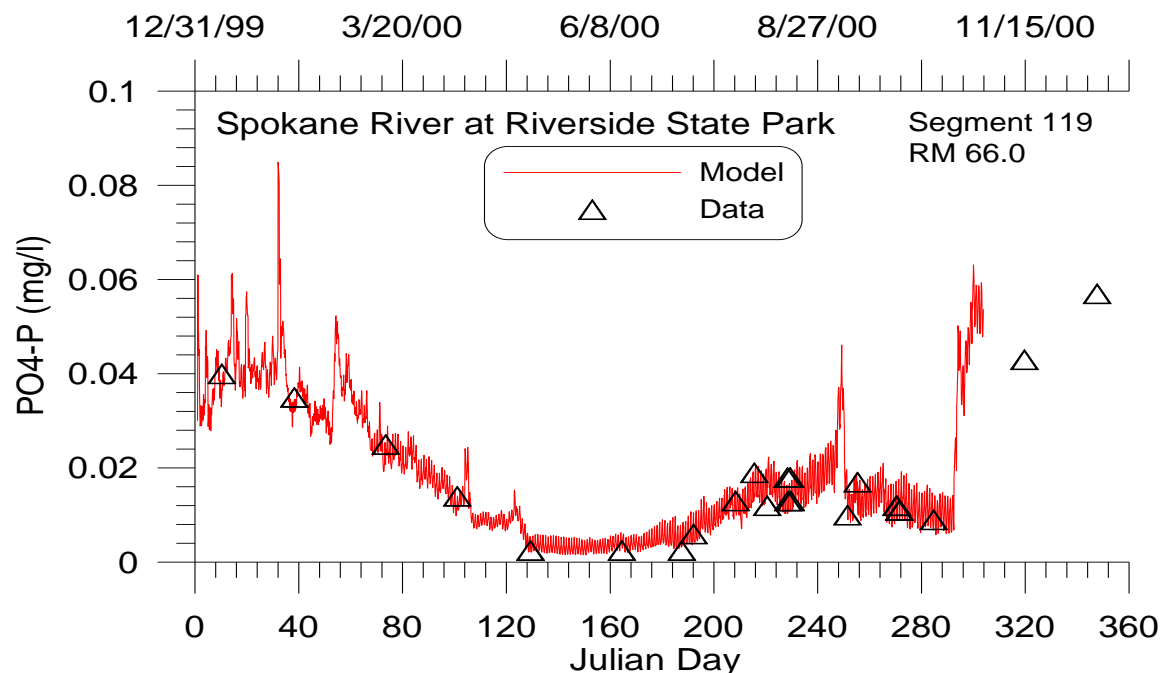


Figure 74. Spokane River computed versus observed soluble reactive phosphorus below Nine Mile Dam.

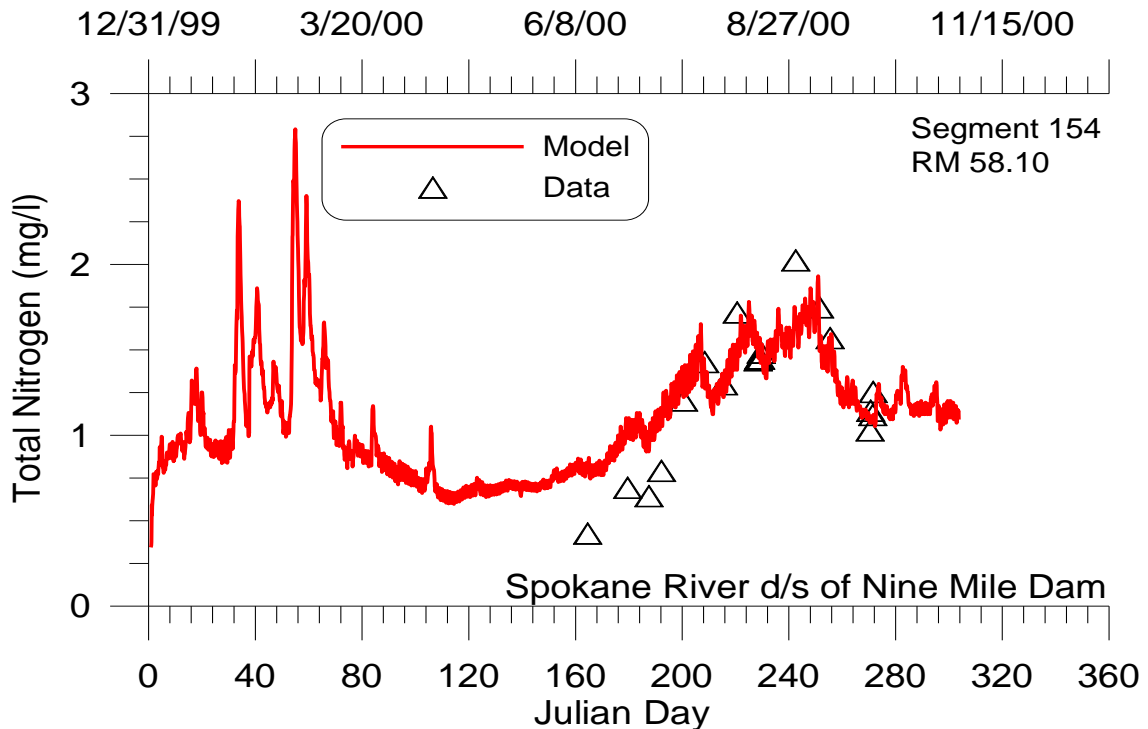


Figure 75. Spokane River computed versus observed total nitrogen below Nine Mile Dam.

Summary

As the preceding figures illustrate, CE-QUAL-W2 is capable of reproducing a wide range of complex hydrodynamics, temperature, dissolved oxygen, nutrient, and phytoplankton and epiphyton regimes in rivers, lakes, reservoirs, and estuaries. If the model is not adequately reproducing prototype behavior, the reason is most likely that the bathymetry or important boundary conditions are not being described with sufficient accuracy. The saying “You cannot make a silk purse out of a sow’s ear” applies equally well to water quality modeling.

A few final words about model calibration. For some applications, no amount of model adjustment or data reconstruction will provide acceptable calibration if data are insufficient to describe the dominant forcing functions in the prototype. For these cases, the model can still be used to provide information about the prototype by pointing out data inadequacies, important mechanisms not included in the model but important in the prototype, or inappropriate assumptions used in the model. In these cases, further fieldwork will be necessary to successfully apply the model.

References

- Alexander, M. 1965. *Microbial Ecology*, John Wiley and Sons, New York.
- Allen, W.E. 1932. "Marine Plankton Diatom of Lower California in 1931", *Botanical Gazette*, Vol 95, pp 485-492.
- Ambrose, R. B.; Wool, T.; Connolly, J. P.; and Schanz, R. W. 1988. "WASP4, A Hydrodynamic and Water Quality Model: Model Theory, User's Manual, and Programmer's Guide," Environmental Research Laboratory, Environmental Protection Agency, EPA 600/3-87/039, Athens, Ga.
- Annear, R., Berger, C. and Wells, S. 2001. "CE-QUAL-W2 Version 3.1 Shading Algorithm," *Technical Report EWR-3-01*, Dept. of Civil and Environmental Engineering, Portland State University, 39 pp.
- Annear, R., Wells, S. and Berger, C. 2005. "Upper Spokane River Model in Idaho: Boundary Conditions and Model Setup and Calibration for 2001 and 2004," *Technical Report EWR-2-05*, Dept. of Civil and Environmental Engineering, Portland State University, 187 pp.
- Annear, R. and Wells, S. A. 2007. A comparison of five models for estimating clear-sky solar radiation, *Water Resources Research*, 43, W10415, doi:10.1029/2006WR005055.
- APHA 1985. *Standard Methods for the Examination of Water and Wastewater*, APHA, Washington, DC.
- Apstein, C. 1910. "Hat ein Organisms in der Tiefe Gelebt, in der er gefischt ist?", *Internat. Rev. Ges. Hydrobiol. Hydrograph*, Vol 3, pp 17-33.
- Armengol, J., Caputo, L., Comerma1, M., Feijoó, C., García, J., Marcé, R., Navarro, E. and Ordoñez, J. 2003. Sau reservoir's light climate: relationships between Secchi depth and light extinction coefficient, *Limnetica* 22(1-2): 195-210.
- Ashton, G.D. 1979. "Suppression of River Ice by Thermal Effluents", *CRREL Rpt. 79-30*, US Army Engineer Cold Regions Research and Engineering Laboratory, Hanover, NH.
- ASCE 1988. "Turbulence Modeling of Surface Water Flow and Transport," *Journal of Hydraulic Engineering*, *ASCE Committee on Turbulence Models in Hydraulic Computations*, 114(9),970-1073.

REFERENCES

- Auer, M. T., M.T.; Johnson, N. A., Penn, M. R. and Effler, S. 1993. Measurement and verification of rates of sediment phosphorus release for a hypereutrophic urban lake. *Hydrobiologia*, Volume 253, Numbers 1-3 / March, 1993 DOI:10.1007/BF00050750.
- Baca, R.G. and R.C. Arnett. 1976. A Limnological Model for Eutrophic Lakes and Impoundments, Batelle Inc., Pacific Northwest Laboratories, Richland, Washington.
- Banks, R.B. 1975. "Some Features of Wind Action on Shallow Lakes," *ASCE, J. Env. Engr. Div.*, 101(E3), pp. 489-504.
- Banks, R. B. and Herrera, F. F. 1977. Effect of Wind and Rain on Surface Reaeration. *J. Envir. Engr. Div. ASCE*, 101(E5):813-827.
- Bannister, T.T. 1979. "Quantitative Description of Steady State, Nutrient-Saturated Algal Growth, Including Adaptation", *Limnology and Oceanography*, Vol 24, pp 76-96.
- Bansal, M.K. 1976. "Nitrification in Natural Streams", *Water Pollution Control Federation Journal*, Vol 48, pp 2380-2393.
- Barkau, R. 1997. "UNET One-Dimensional Unsteady Flow Through a Full Network of Open Channels, User's Manual, US Army Corps of Engineers, Hydrologic Engineering Center, Davis, Ca.
- Barrett, M.J.; Gameson, A.L.; and Ogden, C.G. 1960. Aeration Studies of Four Weir Systems, *Water and Water Engineering*, London.
- Batchelor, G. K. 1967. An Introduction to Fluid Dynamics, Cambridge University Press, NY.
- Belay, A. 1981. "An Experimental Investigation of Inhibition of Phytoplankton Photosynthesis at Lake Surfaces", *New Phytologist*, Vol 89, pp 61-74.
- Bella, D. 1970. "Dissolved Oxygen Variations in Stratified Lakes", *ASCE J. of the Sanitary Engineering Division*, Vol 96, No. SA5, pp 1129-1146.
- Berger, C. (2000). "Modeling Macrophytes of the Columbia Slough." Phd. dissertation, Portland State University, Portland, Oregon.
- Berger, C. and Wells, S. A. 1995. "Effects of Management Strategies to Improve Water Quality in the Tualatin River, Oregon," in *Water Resources Engineering, Vol. 2*, ed. by W, Espey Jr. and P. Combs, ASCE, 1360-1364.
- Berger, C. and Wells, S. A. (in-review) "A Macrophyte Water Quality and Hydrodynamic Model," *ASCE, Journal of Environmental Engineering*.
- Bernard, F. 1963. "Vitesses de chute chez *Cyclococcolithus fragilis* Lohm", *Consequences Pour le Cycle Vital Des Mers Chaudes*.
- Beutel, M. 2006. Inhibition of ammonia release from anoxic profundal sediments in lakes using hypolimnetic oxygenation. doi:10.1016/j.ecoleng.2006.05.009.

REFERENCES

- Bloss, S., and Harleman, D.R.F. 1979. "Effect of Wind Mixing on the Thermocline Formation in Lakes and Reservoirs", *R.M. Parsons Laboratory Rpt. 249*, Department of Civil Engineering, Massachusetts Institute of Technology, Cambridge, MA.
- Blum, J.J. 1966. "Phosphate Uptake by Phosphate-Starved Euglena", *J. of General Physiology*, Vol 49, pp 1125-1137.
- Bohan, J.P., and Grace, J.L., Jr. 1973. "Selective Withdrawal from Man-Made Lakes: Hydraulic Laboratory Investigation", *Technical Rpt. H-73-4*, US Army Engineer Waterways Experiment Station, Vicksburg, MS.
- Borchardt, J.A. 1966. "Nitrification in the Activated Sludge Process", The Activated Sludge Process, Division of Sanitary and Water Resources Engineering, University of Michigan, Ann Arbor, MI.
- Bott, T.L. 1975. "Bacterial Growth Rates and Temperature Optima in a Stream with a Fluctuating Thermal Regime", *Limnology and Oceanography*, Vol 20, pp 191-197.
- Boylen, C.W., and Brock, T.D. 1973. "Bacterial Decomposition Processes in Lake Wingra Sediments During Winter", *Limnology and Oceanography*, Vol 18, pp 628-634.
- Brady, D.K., Graves, W.L., and Geyer, J.C. 1969. "Surface Heat Exchange at Power Plant Cooling Lakes", *Cooling Water 2, Discharge Project No. 5, Publication No. 69-901*, Edison Electric Institute, New York, NY.
- Bramlette, M.N. 1961. In. *Oceanography*, No. 67, M. Sears, ed., American Association of Science, Washington, DC., pp 345-366
- Broecker, H. C., Petermann, J., and Siems, W. 1978. The Influence of Wind on CO₂ Exchange in a Wind-Wave Tunnel, *J. Marine Res.*, 36(4):595-610.
- Brown, L. C. and Barnwell, T. O. 1987. "The Enhanced Stream water Quality Models QUAL2E and QUAL2E-UNCAS: Documentation and User Manual," *Environmental Research Laboratory, EPA/600/3-87/007*, Athens, Ga.
- Butler, D.; Rock, S. P.; and West, J. R. 1978) "Friction Coefficient Variation with Flow in an Urban Stream," *J. of the Institution of Water Engineers and Scientists*, Vol 32, No 3, pp. 227-232.
- Butts, T.A. and Evans, R.L. 1983. "Small Stream Channel Dam Aeration Characteristics," *ASCE J. Env. Engr.*, Vol 109, No 3, pp. 555-573, June 1983.
- Buchak, E.M., and Edinger, J.E. 1982a. "Hydrothermal Simulation of Quabbin Reservoir Using Longitudinal-Vertical Hydrodynamics, Interim Report", prepared for Wallace, Floyd Associates, Inc., Cambridge, MA.
- 1982b. "User's Guide for LARM2: A Longitudinal-Vertical, Time-Varying Hydrodynamic Reservoir Model", *Instruction Rpt. E-82-3*, US Army Engineer Waterways Experiment Station, Vicksburg, MS.

REFERENCES

- _____. 1984. "Generalized Longitudinal-Vertical Hydrodynamics and Transport: Development, Programming and Applications", *Contract No. DACW39-84-M-1636*, prepared for US Army Engineer Waterways Experiment Station, Vicksburg, MS.
- Burns, N.M. 1976. "Nutrient Budgets for Lake Erie", *J. of the Fisheries Research Board of Canada*, Vol 33, pp 520-536.
- Burns, N.M., and Rosa, F. 1980. "In situ Measurement of Settling Velocity of Organic Carbon Particles and 10 Species of Phytoplankton", *Limnology and Oceanography*, Vol 25, pp 855-864.
- Caffrey, A., Hoyer, M., and Canfield, D. 2006. Factors Affecting the Maximum Depth of Colonization by Submersed Macrophytes in Florida Lakes, Southwest Florida Water Management District, 46 pp.
- Caperon, J., and Meyer, J. 1972. "Nitrogen-Limited Growth of Marine Phytoplankton; I. Changes in Population Characteristics with Steady-State Growth Rate", *Deepsea Research with Oceanography*, Vol 9, pp 601-618.
- Carney, J.F., and Colwell, R.R. 1976. "Heterotrophic Utilization of Glucose and Glutamate in an Estuary: Effect of Season and Nutrient Load", *Applied and Environmental Microbiology*, Vol. 31, pp 227-233.
- Carpenter, E.J., and Guillard, R.R.L. 1971. "Intraspecific Differences in Nitrate Half-Saturation Constants for Three Species of Marine Phytoplankton", *Ecology*, Vol 52, pp 183-185.
- Castenholz, R.W. 1964. "The Effect of Daylength and Light Intensity on the Growth of Littoral Marine Diatoms in Culture", *Physiological Plant*, Vol 17, pp 951-963.
- Castenholz, R.W. 1969. "The Thermophilic Cyanophytes of Iceland and the Upper Temperature Limit", *J. of Phycology*, Vol 5, pp 360-368.
- Celik I., Rodi W. 1984. "Simulation of Free-Surface Effects in Turbulent Channel Flow", *PhysicoChemical Hydrodynamics*, Vol. 5, No 3 / 4, 1984, pp 217-227.
- Celik I., Rodi W. 1988. "Modeling Suspended Sediment Transport in Nonequilibrium Situations", *Journal of Hydraulic Engineering*, Vol. 114, No. 10, October, 1988, pp 1157-1191.
- Cerco, C. F.; and Cole, T. M. (1994) "Three-dimensional eutrophication model of Chesapeake Bay. Volume 1." U.S. Army Engineer Waterways Experiment Station, Vicksburg, Mississippi. 1994-05.
- Chapman, R.S. 1988. "Analysis and Improvement of the Numerical and Physical Mixing Characteristics of the WASP Box Model", Contract Report Submitted to the US Army Waterway Experiment Station, Vicksburg, MS.
- Chapman, R. 1989. "Review and Recommendation of Estuarine Mixing Parameterizations, with Specific Reference to Vertical Mixing in Multi-Dimensional Boxes," Report prepared for USACE, Waterways Experiments Station, Vicksburg, MS.

REFERENCES

- Chapman, R.S. and T.M. Cole. 1992. "Improved Thermal Predictions in CE-QUAL-W2", in *Hydraulic Engineering Saving a Threatened Resource - In Search of Solutions Proceedings of the Hydraulic Engineering sessions at Water Forum '92*, M. Jennings and N. G. Bhowmik, eds.), August 2-6, 1992, Baltimore, MD. American Society of Civil Engineers. New York, NY.
- Chapra, S. 1997. *Surface Water Quality Modeling*, McGraw-Hill, NY
- Chapra, S.C., and Reckhow, K.W. 1983. *Engineering Approaches for Lake Management, Vol 12: Mechanistic Modeling*, Butterworth Publishers, Boston, MA.
- Chen, R.L., Brannon, J.M., and Gunnison, D. 1984. "Anaerobic and Aerobic Rate Coefficients for Use in CE-QUAL-RI", *Miscellaneous Paper E-84-5*, US Army Engineer Waterways Experiment Station, Vicksburg, MS.
- Chen, Yongoin. 1996. "Hydrologic and Water Quality Modeling for Aquatic Ecosystem Protection and Restoration in Forest Watersheds: A Case Study of Stream Temperature in the Upper Grande Ronde River, Oregon," Dissertation submitted to The University of Georgia, Doctor of Philosophy, 268 pp.
- Chiaro, P.S., and Burke, D.A. 1980. "Sediment Oxygen Demand and Nutrient Release", *ASCE J. Env. Engr.*, Vol 106, No. EE1, pp 177-195.
- Chow, V. T. 1959. *Open Channel Hydraulics*, McGraw-Hill, NY.
- Churchill, M.A., Elmore, H. L., and Buckingham, R.A. 1962. "Prediction of Stream Reaeration Rates," *J. San. Engr. Div., ASCE*, SA4:1, Proc. Paper 3199.
- Clark, Darren R. and Kevin J. Flynn. 2000. "The relationship between the dissolved inorganic carbon concentration and growth rate in marine phytoplankton." *Proceedings of the Royal Society of London, Series B: Biological Sciences*, Vol. 267, No. 1447, pp. 953-959.
- Clay, C.H. 1995. *Design of Fishway and Other Fish Facilities*, Lewis Publishers, Ann Arbor.
- Clendenning, K.A., Brown, T.E., and Eyster, H.C. 1956. *Canadian J. of Botany*, Vol 34, pp 943-966.
- Cloern, J.E. 1977. "Effects of Light Intensity and Temperature on *Cryptomonas* Cryptophyceae. Growth and Nutrient Uptake Rates", *J. of Phycology*, Vol 13, pp 389-395.
- Cole, T. and Buchak, E. 1995. CE-QUAL-W2: A Two-Dimensional, Laterally Averaged, Hydrodynamic and Water Quality Model, Version 2.0, Technical Report EI-95-1, U.S. Army Engineer Waterways Experiment Station, Vicksburg, MS.
- Collins, C.D., and Boylen, C.W. 1982a. "Physiological Responses of *Anabaena variabilis* Cyanophyceae. to Instantaneous Exposure to Various Combinations of Light Intensity and Temperature", *J. of Phycology*, Vol 18, pp 206-211.

REFERENCES

- _____. 1982b. "Ecological Consequences of Long-Term Exposure of *Anabaena variabilis* to Shifts in Environmental Conditions", *Applied and Environmental Microbiology*, Vol 44, pp 141-148.
- Columbia Basin Research 1998. University of Washington, http://www.cqs.washington.edu/d_gas/papers/tdg_manual.html
- Cotton, M., Reedha, D., Stansby, P. 2005. "Low-Reynolds Number two-equation turbulence modeling for open channel flow: development and evaluation of free surface boundary conditions on the dissipation rate equation", *Journal of Hydraulic Research*, Vol 43, No 6, pp. 632-643.
- Courchaine, R.J. 1968. "Significance of Nitrification in Stream Analysis--Effects on the Oxygen Balance", *J. of the Water Pollution Control Federation*, Vol 40, p 835.
- Covar, A. P. 1976. "Selecting the Proper Reaeration Coefficient for Use in Water Quality Models," presented at the US EPA Conference on Environmental Simulation and Modeling, April 19-22, Cincinnati, OH.
- Cushman-Roisin, B. 1994. *Introduction to Geophysical Fluid Dynamics*, Prentice-Hall, Englewood Cliffs, NJ.
- Davis, J. E., et al. 1987. "SELECT: A Numerical, One-dimensional Model for Selective Withdrawal", *Instruction Rpt. E-87-2*, US Army engineer Waterways Experiment Station, Vicksburg, MS.
- DiLaura, D.L. 1984. "IES Calculation Procedures Committee Recommended practice for the calculation of daylight availability." *Journal of the Illuminating Engineering Society of North America*, 13 (4) p. 381-392.
- Downing, A.L., and G.A. Truesdale 1955. Some factors affecting the rates of solution of oxygen in water. *J. Applied Chemistry*, Vol. 5, pp.570-581.
- Edinger, J.E., Brady, D.K., and Geyer, J.C. 1974. "Heat Exchange and Transport in the Environment", *Rpt. No. 14, EPRI Publication No. 74-049-00-34*, prepared for Electric Power Research Institute, Cooling Water Discharge Research Project RP-49), Palo Alto, CA.
- Edinger, J.E., and Buchak, E.M. 1975. "A Hydrodynamic, Two-Dimensional Reservoir Model: The Computational Basis", prepared for US Army Engineer Division, Ohio River, Cincinnati, Ohio.
- _____. 1978. "Reservoir Longitudinal and Vertical Implicit Hydrodynamics", *Environmental Effects of Hydraulic Engineering Works*, Proceedings of an International Symposium, Knoxville, TN.
- _____. 1980. "Numerical Hydrodynamics of Estuaries", *Estuarine and Wetland Processes with Emphasis on Modeling*, P. Hamilton and K.B. Macdonald, eds., Plenum Press, New York, pp. 115-146.

REFERENCES

- _____. 1983. "Developments in LARM2: A Longitudinal-Vertical, Time-Varying Hydrodynamic Reservoir Model", *Technical Rpt. E-83-1*, US Army Engineer Waterways Experiment Station, Vicksburg, MS.
- Edinger, J. E., D. K. Brady and J. C. Geyer. 1974. "Heat Exchange and Transport in the Environment", *Research Project RP-49, Rpt. 14, EPRI Publication Number 74-049-00-3*, Cooling Water Studies for the Electric Power Research Institute, Palo Alto, CA.
- Edinger, J.E., Buchak, E.M., and Merritt, D.H. 1983. "Longitudinal-Vertical Hydrodynamics and Transport with Chemical Equilibria for Lake Powell and Lake Mead", *Salinity in Watercourses and Reservoirs*, R.H. French, ed., Butterworth Publishers, Stoneham, MA, pp 213-222.
- Edinger, J.E., and Geyer, J.C. 1965. "Heat Exchange in the Environment", *Publication No. 65-902*, Edison Electric Institute, New York, NY.
- Engelund, F. 1978. Effect of Lateral Wind on Uniform Channel Flow. *Progress Report 45*, Inst. of Hydrodynamic and Hydraulic Engr., Tech. Univ. of Denmark.
- Environmental Laboratory. 1985. "CE-QUAL-R1: A Numerical One-Dimensional Model of Reservoir Water Quality; User's Manual", *Instruction Rpt. E-82-1*, US Army Engineer Waterways Experiment Station, Vicksburg, MS.
- Environmental Laboratory 1995. "CE-QUAL-RIV1: A Dynamic, One-Dimensional Longitudinal Water Quality Model for Streams: User's Manual," *Instruction Report EL-95-2*, USACE Waterways Experiments Station, Vicksburg, MS.
- EPA 1971. "Effect of Geographical Location on Cooling Pond Requirements and Performance," in Water Pollution Control Research Series. Report No. 16130 FDQ, Environmental Protection Agency, Water Quality Office, Washington, District of Columbia, 160 pp.
- EPA 1985. Rates, Constants and Kinetics in Surface Water Quality Modeling, Environmental Research Laboratory, EPA/600/3-85/040, Athens, Ga.
- Eppley, R.W., Holmes, R.W., and Strickland, J.D.H. 1967b. "Sinking Rates of Marine Phytoplankton Measured with a Fluorometer", *J. of Experimental Marine Biology and Ecology*, Vol 1, pp 191-208.
- Eppley, R.W., Rogers, J.N., and McCarthy, J.J. 1969. "Half-Saturation Constants for Uptake of Nitrate and Ammonia by Marine Phytoplankton", *Limnology and Oceanography*, Vol 14, pp. 912-920.
- Eppley, R.W., and Sloan, P.R. 1966. "Growth Rates of Marine Phytoplankton: Correlation with Light Adsorption by Cell Chlorophyll-a", *Physiological Plant*, Vol 19, pp 47-59.
- Eppley, R.W., and Thomas, W.H. 1969. "Comparison of Half-Saturation Constants for Growth and Nitrate Uptake of Marine Phytoplankton", *J. of Phycology*, Vol 5, pp 375-379.

REFERENCES

- Evans, F.C., Goldreich, E.C., Weibel, S.R., and Robeck, G.G. 1968. "Treatment of Urban Storm Runoff", *J. of the Water Pollution Control Federation*, Vol 40, pp 162-170.
- Fang, X. and Stefan, H. G. 1994. "Modeling Dissolved Oxygen Stratification Dynamics in Minnesota Lakes under Different Climate Scenarios," *Project Report 339*, St. Anthony Falls Hydraulic Laboratory, University of Minnesota, Minneapolis.
- Fenchel, T. 1970. "Studies of the Decomposition of Organic Detritus Derived from Turtle Grass *Thalassia testudinum*", *Limnology and Oceanography*, Vol 15, pp 14-20.
- Ferziger J., Peric, M. 2002. *Computational Methods for Fluid Dynamics*, Springer Verlag.
- Finenko, Z.Z., and Krupatkina-Aki-Nina, D.K. 1974. "Effect of Inorganic Phosphorus on the Growth Rate of Diatoms", *Marine Biology*, Vol 26, pp. 193-201.
- Fischer, H. B.; E. List; R. Koh; J. Imberger; N. Brooks 1979. *Mixing in Inland and Coastal Waters*, Academic Press, NY.
- Fitzgerald, G.P. 1964. "The Effect of Algae on BOD Measurements", *National Pollution Control Federation J.*, Vol 36, pp 1524-1542.
- Fogg, G.E. 1969. "The Physiology of an Algal Nuisance", *Proc. R. Soc.B.*, Vol 173, pp 175-189.
- _____. 1973. "Phosphorus in Primary Aquatic Plants", *Water Research*, Vol 7, pp 77-91.
- Ford, B. and A. B. Stein. 1984. "The Hydrometeorology of DeGray Lake, Arkansas", *Miscellaneous Paper E-84-3*, U.S. Army Engineer Waterways Experiment Station, Vicksburg, MS.
- Ford, D.E., and Johnson, M.C. 1983. "An Assessment of Reservoir Density Currents and Inflow Processes", *Technical Rpt. E-83-7*, US Army Engineer Waterways Experiment Station, Vicksburg, MS.
- Fowler, S.W., and Small, L.F. 1972. *Limnology and Oceanography*, Vol 17, pp 293-296.
- French, R. H. 1985. *Open-Channel Hydraulics*, McGraw-Hill, New York.
- Frost, W.H., and Streeter, H.W. 1924. "Bacteriological Studies", *Public Health Bulletin 143*, US Public Health Service, Washington, DC.
- Fuhs, G.W., Demmerle, S.D., Canelli, E., and Chen, M. 1972. "Characterization of Phosphorus--Limited Plankton Algae", *Limnol. Oceanogr. Special Symposia*, Vol 1, pp 113-133.
- Gaudy, A. F. and Gaudy, E. T. (1980) Microbiology for Environmental Engineers and Scientists, Mc-Graw-Hill, N.Y.
- Gaugush, R. F., tech. ed. 1986. "Statistical Methods for reservoir water quality investigations", *Instruction Rpt. E-86-2*, U.S. Army Engineer Waterways Experiment Station, Vicksburg, MS.

REFERENCES

- _____. 1987. "Sampling Design for Reservoir Water Quality Investigations", *Instruction Report E-87-1*, U.S. Army Engineer Waterways Experiment Station, Vicksburg, MS.
- _____. 1993. "Sampling Design Software User's Manual", *Instruction Report W-93-1*, U.S. Army Engineer Waterways Experiment Station, Vicksburg, MS.
- Gebhart, B.; Jaluria, Y.; Mahajan, R.; and Sammakia, B. 1988. *Buoyancy-Induced Flows and Transport*, Hemisphere Publishing Co., NY.
- Gelda, R. K., Auer, M. T., Effler, S. W., Chapra, S. C., and Storey, M. L. 1996. Determination of Reaeration Coefficients: A Whole Lake Approach. *ASCE J. Envir. Engr.*
- Geldreich, E.E., Best, L.C., Kenner, B.A., and Van Donsel, D.J. 1968. "The Bacteriological Aspects of Stormwater Pollution", *J. of the Water Pollution Control Federation*, Vol 40, p 1861.
- Giese, A.C. 1968. *Cell Physiology*, 3d ed., W.B. Saunders Co., Philadelphia, PA.
- Gill, A.E. 1982. "Appendix 3, Properties of Seawater", *Atmosphere-Ocean Dynamics*, Academic Press, New York, NY, pp 599-600.
- Goldman, J.C., and Graham, S.J. 1981. "Inorganic Carbon Limitation and Chemical Composition of Two Freshwater Green Microalgae", *Applied and Environmental Microbiology*, Vol 41, pp 60-70.
- Goldman, J.C., Porcella, D.B., Middlebrooks, E.J., and Toerien, D.F. 1972. "The Effects of Carbon on Algal Growth--Its Relationship to Eutrophication", *Water Research*, Vol 6, pp 637-679.
- Golterman, H.L. 1975. *Physiological Limnology*, Elsevier, Amsterdam.
- Gordon, J.A. 1980. "An Evaluation of the LARM Two-Dimensional Model for Water Quality Management Purposes", *Proceedings of the Symposium on Surface-Water Impoundments*, Minneapolis, MN, June 2-5, 1980, Vol 1, Paper 4-34, pp 518-527, American Society of Civil Engineers, New York, NY.
- _____. 1981. "LARM Two-Dimensional Model: An Evaluation", *ASCE J. of the Environmental Engineering Division*, 107(EE5), pp 877-886.
- _____. 1983. "Short-Term Hydrodynamics in a Stratified Reservoir", *Environmental Engineering, Proceedings of the ASCE Specialty Conference, Hilton Harvest House, Boulder, Colo.*, July 6-8, 1983, pp 524-531, American Society of Civil Engineers, New York, NY.
- Gould, S. 2006. "k- ϵ turbulence model in CE-QUAL-W2", Master's research report in partial fulfillment for the degree Master of Science, Department of Civil and Environmental Engineering, Portland State University, Portland, OR.
- Green, D.B., Logan, J., and Smeck, N.E. 1978. "Phosphorus Adsorption-Desorption Characteristics of Suspended Sediments in the Maumee River of Ohio", *J. of Environmental Quality*, Vol 7, pp 208-212.

REFERENCES

- Guillard, R.R.L., and Ryther, J.H. 1962. "Studies on the Marine Planktonic Diatoms; I. *Cyclotella nana* Hustedt and *Detonula confervacea* Cleve)", *Canadian J. of Microbiology*, Vol 8, pp 229-239.
- Gunnison, D., and Alexander, M. 1975. "Resistance and Susceptibility of Algae to Decomposition by Natural Microbial Communities", *Limnology and Oceanography*, Vol 20, pp 64-70.
- Gunnison, D., Chen, R.L., and Brannon, J.M. 1983. "Relationship of Materials in Flooded Soils and Sediments to the Water Quality of Reservoir; I. Oxygen Consumption Rates", *Water Research*, Vol 17, No. 11, pp 1609-1617.
- Hall, G.H. 1982. "Apparent and Measured Rates of Nitrification in the Hypolimnion of a Mesotrophic Lake", *Applied and Environmental Microbiology*, Vol 43, pp 542-547.
- Halmann, M., and Stiller, M. 1974. "Turnover and Uptake of Dissolved Phosphate in Freshwater; A Study in Lake Kinneret", *Limnology and Oceanography*, Vol 19, pp 774-783.
- Hanlon, R.D.G. 1982. "The Breakdown and Decomposition of Allochthonous and Autochthonous Plant Litter in an Oligotrophic Lake Llyn Frongoch)", *Hydrobiologia*, Vol 88, pp 281-288.
- Harbeck, G.E., Koberg, G.E., and Hughes, G.H. 1959. "The Effect of Addition of Heat...on Lake Colorado City, Texas", *USGS Professional Paper 272-B*, US Government Printing Office, Washington, DC.
- Hargrave, B.T. 1972a. "Aerobic Decomposition of Sediment and Detritus as a Function of Particle Surface Area and Organic Content", *Limnology and Oceanography*, Vol 17, pp 582-597.
- Hargrave, B.T. 1972b. "Oxidation-Reduction Potentials, Oxygen Concentration and Oxygen Uptake of Profundal Sediments in a Eutrophic Lake", *Oikos*, Vol 23, pp 167-177.
- Hattori, A. 1962. "Light-Induced Reduction of Nitrate, Nitrite and Hydroxylamine in a Blue-green Alga, *Anabaena cylindrica*", *Plant Cell Physiology*, Vol 3, pp 355-369.
- HEC 1997a. "UNET One-Dimensional Unsteady-Flow Through a Full Network of Open Channels, User's Manual," US Army Corps of Engineers, Hydrologic Engineering Center, Davis, CA.
- HEC 1997b. "HEC-RAS River Analysis System Hydraulic Reference Manual Version 2.0," US Army Corps of Engineers, Hydrologic Engineering Center, Davis, CA.
- HEC 1977. "HEC-6 Scour and Deposition in Rivers and Reservoirs," US Army Corps of Engineers, Hydrologic Engineering Center, Davis, CA.
- Hecky, R.E., and Kilham, P. 1974. "Environmental Control of Phytoplankton Cell Size", *Limnology and Oceanography*, Vol 19, No. 2, pp 361-365.
- Henderson, H. 1966. *Open Channel Flow*, The MacMillan Company, NY.

REFERENCES

- Hendry, G.R., and Welch, E. 1973. "The Effects of Nutrient Availability and Light Intensity on the Growth Kinetics of Natural Phytoplankton Communities", presented at American Society of Limnology and Oceanography, 36th Annual Meeting, Salt Lake City, UT.
- Henrici, P. 1964. *Elements of Numerical Analysis*, John Wiley & Sons, Inc., New York.
- Holley, E. R. and Jirka, G. 1986. "Mixing in Rivers," *Technical Report E-86-11*, US Army Engineer Waterways Experiment Station, Vicksburg, MS.
- Holm, N.P., and Armstrong, D.E. 1981. "Role of Nutrient Limitation and Competition in Controlling the Populations of *Asterionella formosa* and *Microcystis aeruginosa* in Semicontinuous Culture", *Limnology and Oceanography*, Vol 26, pp 622-634.
- Hoogenhout, H., and Ames, J. 1965. "Growth Rates of Photosynthetic Microorganisms in Laboratory Studies", *Archives of Microbiology*, Vol 50, pp 10-24.
- Hoskins, J.K., Ruchhoft, C.C., and Williams, L.G. 1927. "A Study of the Pollution and Natural Purification of the Illinois River; I. Surveys and Laboratory Studies", *Public Health Bulletin No. 171*, Washington, DC.
- Hutchinson, G.E. 1957. *A Treatise on Limnology; I. Geography, Physics and Chemistry*, John Wiley and Sons, New York, NY.
- Hwang, C.P., Lackie, T.H., and Huang, P.M. 1976. "Adsorption of Inorganic Phosphorus by Lake Sediments", *J. of the Water Pollution Control Federation*, Vol 48, pp 2754-2760.
- Hydrologic Engineering Center. 1981. "Geometric Elements from Cross Section coordinates", Computer program description.
- Ignatiades, L., and Smayda, T.J. 1970. "Autecological Studies on the Marine Diatom *Rhizosolenia fragilissima* Bergon; I. The Influence of Light, Temperature, and Salinity", *J. of Phycology*, Vol 6, pp 332-229.
- Jacoby, G.C., Jr., et al. 1977. "Evaporation, Bank Storage and Water Budget at Lake Powell", *Lake Powell Research Project Bulletin No. 48*, Institute of Geophysics and Planetary Physics, University of California, Los Angeles, CA.
- James, William F. ; Berko, John W. ; Eakin, Harry L. 1995. Phosphorus Loading in Lake Pepin (Minnesota-Wisconsin). Final report ADA304855. Army Engineer Waterways Experiment Station, Vicksburg MS.
- Janik, J.J., Taylor, W.D., and Lambou, V.W. 1981. "Estimating Phytoplankton Biomass and Productivity", *Miscellaneous Paper E-81-2*, US Army Engineer Waterways Experiment Station, Vicksburg, MS.
- Jeanjean, R. 1969. "Influence de la Carence en Phosphore sur les Vitesses d'Absorption du Phosphate Par les Chlorelles", *Bull. Soc. Fr. Physiol. Veg.*, Vol 15, pp 159-171.

REFERENCES

- Jewell, W.J., and McCarty, P.L. 1971. "Aerobic Decomposition of Algae", *Environment Science and Technology*, Vol 5, pp 1023-1031.
- Jitts, H.R., McAllister, C.D., Stephens, K., and Strickland, J.D.H. 1964. "The Cell Division Rates of Some Marine Phytoplankton as a Function of Light and Temperature", *J. of the Fisheries Research Board of Canada*, Vol 21, pp 139-157.
- Johnson, M.C., et al. 1981 Oct. "Analyzing Storm Event Data from DeGray Lake, Arkansas Using LARM", presented at the American Society of Civil Engineers 1981 Convention and Exposition, St. Louis, MO.
- Jorgensen, E.G. 1968. "The Adaptation of Plankton Algae; II. Aspects of the Temperature and the Temperature Adaptation of *Skeletonema costatum*", *Physiological Plant*, Vol 21, pp 423-427.
- Kamp-Nielson, L. 1974. "Mud-Water Exchange of Phosphate and Other Ions in Undisturbed Sediment Cores and Factors Affecting Exchange Rates", *Archives of Hydrobiologia*, Vol 73, pp 218-237.
- Kanwisher, J. 1963. "On the Exchange of Gases Between the Atmosphere and the Sea", *Deepsea Research with Oceanography*, Vol 10, pp 195-207.
- Ketchum, B.H. 1939. "The Absorption of Phosphate and Nitrate by Illuminated Cultures of *Nitzschia closterium*", *American J. of Botany*, Vol 26, pp 399-407.
- Kim, Lee-Hyung; Choi, Euiso; Gil, Kyung-Ik; and Stenstrom, M. K.. 2003. Phosphorus release rates from sediments and pollutant characteristics in Han River, Seoul, Korea. doi:10.1016/j.scitotenv.2003.08.018.
- Kinsman, B. 1979. *Wind Waves: Their Generation and Propagation*, Prentice-Hall, Englewood Cliffs, N.J.
- Kirk, J.T.O. 1975. "A Theoretical Analysis of the Contribution of Algal Cells to the Attenuation of Light Within Natural Waters; I. General Treatment of Suspensions of Pigmented Cells", *New Phytology*, Vol 75, pp 11-20.
- Kittrell, F.W., and Furfari, S.A. 1963. "Observations of Coliform Bacteria in Streams", *J. of the Water Pollution Control Federation*, Vol 35, p 1361.
- Kittrell, F.W., and Koschitzky, O.W., Jr. 1947. "Natural Purification Characteristics of a Shallow Turbulent Stream", *Sewage Works J.*, Vol 19, p 1031.
- Klock, J.W. 1971. "Survival of Coliform Bacteria in Wastewater Treatment Lagoons", *J. of the Water Pollution Control Federation*, Vol 43, p 2071.
- Knowles, G., Downing, A.L., and Barrett, M.J. 1965. "Determination of Kinetic Constants for Nitrifying Bacteria in Mixed Culture, with the Aid of an Electronic Computer", *J. of General Microbiology*, Vol 38, pp 263-278.

REFERENCES

- Knudsen, G. 1965. "Induction of Nitrate Reductase in Synchronized Cultures of *Chlorella pinnatifida*", *Biochem. Biophys. Acta.*, Vol 103, pp 495-502.
- Konopka, A. 1983. "The Effect of Nutrient Limitation and Its Interaction with Light upon the Products of Photosynthesis in *Merismopedia tenuissima* (Cyanophyceae)", *J. Phycology*, Vol 19, pp 403-409.
- Koutitas, C. G. 1978. Numerical Solution of the Complete Equations for Nearly Horizontal Flows. *Advances in Water Resources*, 1(4), 213.
- Krishnappan, B., Lau, Y. 1986. "Turbulence Modeling of Flood Plain Flow", *Journal of Hydraulic Engineering*, Vol. 112, No. 4, April, pp 251-266.
- Ku, W.C., Di Giano, F.A., and Feng, T.H. 1978. "Factors Affecting Phosphate Adsorption Equilibria in Lake Sediments", *Water Research*, Vol 12, pp 1069-1074.
- Lane, E.W. 1938. "Notes on Formation of Sand", *Transactions of the American Geophysical Union*, Vol 18, pp 505-508.
- Langbien, W. B. and Durum, W. H. 1967. "The Aeration Capacity of Streams," USGS, Washington, D.C. Circ. 542.
- Laws, E.A., and Wong, D.C. 1978. "Studies of Carbon and Nitrogen Metabolism by Three Marine Phytoplankton Species in Nitrate-Limited Continuous Culture", *J. of Phycology*, Vol 14, pp 406-416.
- Leendertse, J.J., and Liu, S-K. 1977. "Turbulent Energy for Computation; Volume IV, A Three-Dimensional Model for Estuaries and Coastal Seas", Rpt. No. 2-2187-OWRT, The Rand Corporation, Santa Monica, CA.
- Leonard, B. P. 1979. "A Stable and Accurate Convective Modelling Procedure Based on Upstream Interpolation", *Computer Methods in Applied Mechanics and Engineering*, Vol 19, pp. 59-98.
- Leonard, B. P. 1991. "The ULTIMATE conservative difference scheme applied to unsteady one-dimensional advection," *Computer Methods in Applied Mechanics and Engr*, 88 (1991), 17-74.
- Li, W.K.W., and Morris, I. 1982. "Temperature Adaptation in *Phaeodactylum tricornutum* Bohlin: Photosynthetic Rate Compensation and Capacity", *J. of Experimental Marine Biology and Ecology*, Vol 58, pp 135-150.
- Libby, P. A. 1996. *Introduction to Turbulence*, Taylor and Francis, Washington D.C.
- Lighthill, J. 1978. *Waves in Fluids*, Cambridge University Press, NY.
- Liggett, J. A. 1970. "Cell Method for Computing Lake Circulation," *J. of the Hydraulics Div., ASCE*, 96(HY3), 725.

REFERENCES

- Lin, B., and Falconer, R. A. 1997. "Tidal Flow and Transport Modeling Using ULTIMATE QUICKEST Scheme", *J. of Hydraulic Engineering, ASCE*, 123(4), 303-314.
- Lindijer, G. H. 1979. "Three-Dimensional Circulation Models for Shallow Lakes and Seas; Semi-Analytical Steady-State Analysis of Wind-Driven Current Including the effect of Depth-Dependent Turbulent Exchange Coefficient," *Report R 900-11*, Delft Hydraulics Laboratory, Netherlands.
- Liss, P.S. 1973. "Processes of gas exchange across an air-water interface," *Deep Sea Research*, Vol. 20, pp 221-238.
- Litchman, Elena. 2000. "Growth rates of phytoplankton under fluctuating light." *Freshwater Biology*, Volume 44, pp. 223-235.
- MacIsaac, J.H., and Dugdale, R.C. 1969. "The Kinetics of Nitrate and Ammonia Uptake by Natural Populations of Marine Phytoplankton", *Deepsea Research with Oceanography*, Vol 16, pp 16-27.
- Mackay, D. 1980. "Solubility, Partition Coefficients, Volatility, and Evaporation Rates", *Reactions and Processes Handbook*, Vol 2, Part A, Springer-Verlag, New York, NY.
- Madsen, O. S. 1977. A Realistic Model of the Wind-Induced Ekman Boundary Layer. *J. Physical Oceanography*, 7(2), 248.
- Mahloch, J.L. 1974. "Comparative Analysis of Modeling Techniques for Coliform Organisms in Streams", *Applied Microbiology*, Vol 27, p 340.
- Mann, K.H. 1972. "Ecology Energetics of the Seaweed Zone in a Marine Bay on the Atlantic Coast of Canada; I. Zonation and Biomass of Seaweeds", *Marine Biology Berlin*, Vol 12, pp 1-10.
- Marais, G.V.R. 1974. "Faecal Bacterial Kinetics in Stabilization Ponds", *ASCE J. of the Sanitation Engineering Division*, Vol 100, No. EEI, p 119.
- Margalef, R. 1961. "Velocidad de Sedimentation de Organismos Pasivos del Fitoplancton", *Investigacion Pesq.*, Vol 18, pp 3-8.
- Martin, J.L. 1987. "Application of a Two-Dimensional Model of Hydrodynamics and Water Quality CE-QUAL-W2. to DeGray Lake, Arkansas", *Technical Rpt. E-87-1*, US Army Engineer Waterways Experiment Station, Vicksburg, MS.
- Martin, J. L., McCutcheon, S.C. 1999. *Hydrodynamics and Transport for Water Quality Modeling*, Lewis Publishers, NY.
- Mastropietro, M. A. 1968. "Effects of Dam Reaeration on Waste Assimilation Capacities of the Mohawk River," *Proceedings of the 23rd Industrial Waste Conference, Purdue University*.
- Maykut, G. N. and N. Untersteiner. 1971. "Some results from a time dependent, thermodynamic model of sea ice", *J. Geophys. Res.*, 83: 1550-1575.

REFERENCES

- McCutcheon, Steve. 1987. "Laboratory and instream nitrification rates for selected streams." *Journal of Environmental Engineering*, Vol. 113, No. 3, pp. 628-646.
- Megard, R. O., Comles, W.S., Smith, P.D., and Knoll, A.S. 1980. "Attenuation of Light and Daily Integral Rates of Photosynthesis Attained by Planktonic Algae", *Limnology and Oceanography*, Vol 24, pp 1038-1050.
- Melching, C. and Flores, H. 1999. "Reaeration Equations Derived from USGS Database," *J. Envir. Engr., ASCE*, 125(5), 407-414.
- Meyer, A.F. 1928. *The Elements of Hydrology*, John Wiley and Sons, New York, NY.
- Mills, W.B.; Porcella, D.; Unga, M.; Gherini, S.; Summers, K.; Lingfung, M.; Rupp, G.; Bowie, G. Haith, D. 1985. "A Screening Procedure for Toxic and Conventional Pollutants in Surface and Ground Water," *EPA/600/6-85/002a*, Environmental Research Laboratory, Athens, GA.
- Mitchell, R., and Chamberlain, C. 1978. "Survival of Indicator Organisms", *Indicators of Enteric Contamination in Natural Waters*, G. Berg, ed.), Ann Arbor Science Publ., Inc., Ann Arbor, MI, pp 15-38.
- Moog, D.B. and Jirka, G.H. 1998. "Analysis of reaeration equations using multiplicative error," *J. Environ Engr, ASCE*, 124(2), 104-110.
- Mortimer, C.H. 1981. "The Oxygen Content of Air Saturated Fresh Waters over Ranges of Temperature and Atmospheric Pressure of Limnological Interest", *International Vereinigung Theoretische and Angewandte Limnologie*, Vol 22, pp 2-23.
- Morton, F.I. 1965. "Potential Evaporation and River Basin Evaporation", *ASCE J. of the Hydraulics Division*, Vol 91, No. HY6, pp 67-97.
- Munk, W. H. and Anderson, E. R. 1948. "Notes on the Theory of the Thermocline," *Journal of Marine Research*, Vol 1, p.276.
- Myers, J., and Graham, J. 1961. "On the Mass Culture of Algae; III. Light Diffusers: High vs. Low Temperature Chlorellas", *Plant Physiology*, Vol 36, pp 342-346.
- Nakagawa H., Nezu I., Ueda H. 1975. "Turbulence of Open Channel Flow Over Smooth and Rough Beds", *Proceedings of the Japan Society of Civil Engineers*, No 241 September, pp. 155-168.
- Nalewajko, C. 1966. "Photosynthesis and Excretion in Various Planktonic Algae", *Limnology and Oceanography*, Vol 11, pp 1-10.
- Neumann, G. and Pierson, W. J. 1966. *Principles of Physical Oceanography*. Prentice-Hall Inc. Englewood Cliffs, N. J.
- Newbold, J.D., and Liggett, D.S. 1974. "Oxygen Depletion Model for Cayuga Lake", *ASCE J. of the Environmental Engineering Division*, Vol 100, No. EE1, pp 41-59.

REFERENCES

- O'Connor, D. J. and Dobbins, W.E. 1958. "Mechanism of Reaeration in Natural Streams," *ASCE Trans.*, 86(SA3):35-55.
- O'Connor, D.J. 1983. "Wind Effects on Gas-Liquid Transfer Coefficients" *J. Envir Engr ASCE*, Vol. 109, pp. 731-752.
- Odum, E.P., and de la Cruz, A.A. 1967. "Particulate Organic Detritus in a Georgia Salt Marsh--Estuarine Ecosystem", *Estuaries*, G.H. Lauff, ed., American Association for the Advancement of Sciences, Washington, DC, pp 383-388.
- Okubo, 1971. Oceanic Diffusion Diagrams, *Deep-Sea Research*, 18:789.
- Olson, R. M. and Wright, S. J. 1990. *Essentials of Engineering Fluid Mechanics*, 5th edition, Harper and Row, NY.
- Osterberg, C., Casey, A.G., and Curl, H. 1963. In *Nature*, Vol 200, pp 1276-1277.
- Otsuki, A., and Hanya, T. 1972. "Production of Dissolved Organic Matter from Dead Green Algal Cells; I. Aerobic Microbial Decomposition", *Limnology and Oceanography*, Vol 17, pp 248-257.
- Owens, M., Edwards, R., and Gibbs, J. 1964. "Some Reaeration Studies in Streams," *Int. J. Air Water Poll.*, 8:469-486.
- Paasche, E. 1968. "Marine Plankton Algae Grown with Light-Dark Cycles; II. *Ditylum brightwellii* and *Nitzschia turgidula*", *Physiological Plant*, Vol 21, pp 66-77.
- Parson, T.R., and Strickland, J.D.H. 1963. "On the Production of Particulate Organic Carbon by Heterotrophic Processes in Sea Water", *Deepsea Research with Oceanography*, Vol 8, pp 211-222.
- Patterson, J.C. and Hamblin, P.F., "Thermal Simulation of a Lake with Winter Ice Cover", *Limnology and Oceanography*, 33(3), 1988, P. 323-338.
- Pauer, James J. and Martin T. Auer. 2000. "Nitrification in the water column and sediment of a hypereutrophic lake and adjoining river system." *Water Resources*, Volume 34, No. 4, pp. 1247-1254.
- Pickett, J.M. 1975. "Growth of *Chlorella* in a Nitrate-Limited Chemostat", *Plant Physiology*, Vol 55, pp 223-225.
- Piecznska. 1972. *Wiadomosci Ekologiczne*, Vol 18, pp 131-140.
- Prakash, S., Vandenberg, J. A., E. M. Buchak. 2015. Sediment Diagenesis Module for CE-QUAL-W2. Part 2: Numerical Formulation. Environmental Modeling & Assessment. Print ISSN 1420-2026. Online ISSN 1573-2967. <http://dx.doi.org/10.1007/s10666-015-9459-1>. Springer International Publishing. April.

REFERENCES

- Press W., Teukolsky S., Vetterling W., Flannery B. 1996. Numerical Recipes in Fortran: The Art of Scientific Computing, Cambridge University Press.
- Quasim, S.Z., Bhattathiri, P.M.A., and Dovassoy, V.P. 1973. *Marine Biology*, Vol 21, pp 299-304.
- Reay, David S., Nedwell, David B., Priddle, Julian, and Ellis-Evans, J. Cynan. 1999. "Temperature dependence of inorganic nitrogen uptake: reduced affinity for nitrate at suboptimal temperatures in both algae and bacteria." *Applied and Environmental Microbiology*, June, p. 2577-2584.
- Reynolds, C. S. (1984) *The ecology of freshwater phytoplankton*. Cambridge University Press.
- Rhee, G-Yull. 1973. "A Continuous Culture Study of Phosphate Uptake, Growth Rate and Polyphosphate in *Scenedesmus sp.*", *J. of Phycology*, Vol 9, pp 495-506.
- Rhee, G-Yull, and Gotham, I.J. 1981a. "The Effects of Environmental Factors on Phytoplankton Growth: Temperature and the Interaction of Temperature with Nutrient Limitation", *Limnology and Oceanography*, Vol 26, pp 635-648.
- _____. 1981b. "The Effects of Environmental Factors on Phytoplankton Growth: Light and the Interaction of Light with Nitrate Limitation", *Limnology and Oceanography*, Vol 26, pp 649-659.
- Riley, G.A. 1943. *Bulletin of the Bingham Oceanography College*, Vol 8, Art. 4, p 53.
- Riley, G.A., H. Stommel, and D.F. Bumpus. 1949. "Quantitative Ecology of the Plankton of the Western North Atlantic", *Bulletin of the Bingham Oceanography College*, Vol 12, pp 1-169.
- Riley, G.A., and von Aux, R. 1949. In. *J. of Marine Research*, Vol 8, No. 11, pp 60-72.
- Roache, P.J. 1982. *Computational Fluid Dynamics*, Hermosa Publishers, Albuquerque, NM.
- Rodi, W. 1993. *Turbulence Models and Their Application in Hydraulics*, 3rd edition, IAHR, A.A. Balkema, Rotterdam.
- Rogers, K.H., and C.M. Breen. 1982. "Decomposition of *Potamogeton crispus*; I. Effects of Drying on the Pattern of Mass and Nutrient Loss", *Aquatic Botany*, Vol 12, pp 1-12.
- Rounds, S.A., and Buccola, N.L., 2015, Improved algorithms in the CE-QUAL-W2 water-quality model for blending dam releases to meet downstream water-temperature targets: U.S. Geological Survey Open-File Report 2015-1027, 40 p., <http://dx.doi.org/10.3133/ofr20151027>.
- Ruane, Jim (2014) Personal communication, Portland, OR.
- Ryan, P.J. and D.R.F. Harleman. 1974. "Surface Heat Losses from Cooling Ponds," *Water Resources Research*, Vol 10, No 5, Oct 1974, pp. 930-938.

REFERENCES

- Ryan, Patrick J. and Keith D. Stolzenbach. 1972. Chapter 1: "Environmental Heat Transfer" in *Engineering Aspects of Heat Disposal from Power Generation*, D. R. F. Harleman, ed.. R. M. Parson Laboratory for Water Resources and Hydrodynamics, Department of Civil Engineering, Massachusetts Institute of Technology, Cambridge, MA.
- Ryding, S.O., and C. Forsberg. 1977. "Sediments as a Nutrient Source in Shallow Polluted Lakes", *Interactions Between Sediments and Freshwater*, H.L. Golterman, ed.), Junk, The Hague.
- Ryther, J.H. 1954. "Inhibitory Effects of Phytoplankton upon the Feeding of *Daphnia magna* with Reference to Growth, Reproduction, and Survival", *Ecology*, Vol 35, pp 522-533.
- Sabersky, R.; A. Acosta, E. Haupmann 1989. *Fluid Flow A First Course in Fluid Mechanics*, Macmillan Publishing Co., NY.
- Saunders, G.W. 1972. "The Transformation of Artificial Detritus in Lake Water", *Mem. Ist. Ital. Idrobiol. Dott Marco de Marchi*, Pallanza, Italy 29 (Suppl), pp 261-288.
- Sawyer, C.N., and McCarty, P.L. 1967. *Chemistry for Sanitary Engineers*, 2d ed., McGraw-Hill, St. Louis, MO.
- Schindler, D.W. 1971. "Food Quality and Zooplankton Nutrition", *J. of Animal Ecology*, Vol 40, pp 598-595.
- Schindler, D.W., et al. 1973. "Eutrophication of Lake 227 by Addition of Phosphate and Nitrate: The Second, Third and Fourth Years of Enrichment, 1970, 1971, 1972", *J. of the Fisheries Research Board of Canada*, Vol 30, pp 1415-1428.
- Schlichting, H. 1962. *Boundary Layer Theory*, McGraw-Hill, NY.
- Schnoor, J.L., and Fruh, E.G. 1979. "Dissolved Oxygen Model of a Short Detention Time Reservoir with Anaerobic Hypolimnion", *Water Resources Bulletin*, Vol 15, No. 2, pp 506-518.
- Sedell, J.R., Triska, F.J., and Triska, N.S. 1975. "The Processing of Conifer and Hardwood Leaves in Two Coniferous Forest Streams; I. Weight Loss and Associated Invertebrates", *Verh. Internat. Verein. Limnol.*, Vol 19, pp 1617-1627.
- Sen, S., Haggard, B.E., Chaubey, I., Brye, K.R., Matlock, M.D., Costello, T.A. 2004. Preliminary estimation of sediment phosphorus flux in Beaver Lake, Northwest Arkansas. In: Proceedings of American Society of Agricultural Engineers, August 1-4, 2004, Ottawa, Ontario, Canada. 2004 CDROM.
- Shanahan, P. and Harleman, D. 1982. "Linked Hydrodynamic and Biogeochemical Models of Water Quality in Shallow Lakes," *Technical Report 268*, R. M. Parson Laboratory, MIT, Cambridge, MA.
- Shelef, G. 1968. "Kinetics of Algal Systems in Waste Treatment; Light Intensity and Nitrogen Concentration as Growth-Limiting Factors", Ph.D. Thesis, University of California, Berkeley, CA.

REFERENCES

- Sher-Kaul, S., Oertli, B., Castella, E. and J. Lachavanne (1995), "Relationship between biomass and surface area of six submerged aquatic plant species." *Aquatic Botany*, 51, 147-154.
- Simoes, F. 1998. "An Eddy Viscosity Model for Shallow-Water Flows," *Water Resources Engineering* 98, ASCE, NY, 1858-1863.
- Smayda, T.J. 1969. "Experimental Observations on the Influence of Temperature, Light, and Salinity on Cell Division of the Marine Diatom *Detonula confervacea* Cleve. Gran", *J. of Phycology*, Vol 5, pp 150-157.
- _____. 1971. "Normal and Accelerated Sinking of Phytoplankton in the Sea", *Marine Geology*, Vol 11, pp 105-122.
- _____. 1974. "Some Experiments on the Sinking Characteristics of Two Freshwater Diatoms", *Limnology and Oceanography*, Vol 19, No. 4, pp 628-635.
- Smayda, T.J., and Boleyn, B.J. 1965. "Experimental Observations on the Flotation of Marine Diatoms; I. *Thalassiosira* cf. *nana*, *Thalassiosira rotula* and *Nitzschia seriata*", *Limnology and Oceanography*, Vol 10, pp 499-509.
- _____. 1966. "Experimental Observations on the Flotation of Marine Diatoms; III. *Bacteriastrium hyalinum* and *Chaetoceros lauderi*", *Limnology and Oceanography*, Vol 11, pp 35-43.
- Smith, D.J. 1978. "WQRRS, Generalized computer program for River-Reservoir systems," *USACE Hydrologic Engineering Center HEC*, Davis, California. User's Manual 401-100, 100A, 210 pp.
- Smith, W.O. 1979. "A Budget for the Autotrophic Ciliate *Mesodinium rubrum*", *J. of Phycology*, Vol 15, pp 27-33.
- Smith, R.C., and Baker, K.S. 1978. "The Bio-optical State of Ocean Waters and Remote Sensing", *Limnology and Oceanography*, Vol 23, pp 247-259.
- Snow, P.D., and Di Giano, F.A. 1976. "Mathematical Modeling of Phosphorus Exchange Between Sediments and Overlaying Water in Shallow Eutrophic Lakes", *Rpt. 54-76-3*, Department of Civil Engineering, University of Massachusetts, Amherst, MA.
- Sorokin, C., and Krauss, R.W. 1962. "Effects of Temperature and Illumination on *Chorella* Growth Uncoupled from Cell Division", *Plant Physiology*, Vol 37, pp 37-42.
- Sorokin, C., and Meyers, J. 1953. "A High Temperature Strain of *Chlorella*", *Science*, Washington, D.C., Vol 117, pp 330-331.
- Soong, T. W., DePue, M.; D. Anderson 1995. "The Changes of Manning's Roughness Coefficient with River Stages," *Water Resources Engineering*, ed. by W. H. Epsey and P. Combs, ASCE, pp.1759-1763.

REFERENCES

- Spears, Bryan M.; Carvalho, Laurence; Perkins, Rupert; Kirika, Alex; Paterson, David M.. 2007. Sediment phosphorus cycling in a large shallow lake: spatio-temporal variation in phosphorus pools and release. *Hydrobiologia*, 584. 37-48. doi:10.1007/s10750-007-0610-0
- Spence, D.H.N. 1981. "Light Quality and Plant Responses Underwater", *Plants and the Daylight Spectrum*, H. Smith, ed., Academic Press, New York, NY, pp 245-276.
- Spencer, J. W. 1971. "Fourier series representation of the position of the sun." *Search* 2(5), 172.
- Spencer, D.F., and Lembi, C.A. 1981. "Factors Regulating the Spatial Distribution of the Filamentous Alga *Pithophora oedoga* Chlorophyceae. in an Indiana Lake", *J. of Phycology*, Vol 17, pp 168-173.
- Steele, J.H. 1962. "Environmental Control of Photosynthesis in the Sea", *Limnology and Oceanography*, Vol 7, pp 137-150.
- Steemann-Nielsen, E. 1952. "On Detrimental Effects of High Light Intensities on the Photosynthetic Mechanism", *Physiological Plant*, Vol 5, pp 334-344.
- Steemann-Nielsen, E., and Jorgensen, E.G. 1968. "The Adaptation of Plankton Algae; I. General Part", *Physiological Plant*, Vol 21, pp 401-413.
- St. John, J. P., T. W. Gallagher, and P. R. Paquin, 1984. "The Sensitivity of the Dissolved oxygen Bahnce to Predictive Reaeration Equations", in *Gas Transfer at Water Surfaces*, W. Brutsaert and G. H. Jirka (Eds.), D. Reidel Publishing Co., Boston, 577-589.
- Stumm, W., and Morgan, J.J. 1981. *Aquatic Chemistry*, Wiley Interscience, New York, NY.
- Swean, T., Leighton, R., Handler, R., Swearingen J. 1991. "Turbulence Modeling Near the Free Surface in an Open Channel Flow", AIAA 91-0613, 29th Aerospace Sciences Meeting, Reno, Nevada, January 7-10.
- Tailing, J.F. 1955. "The Relative Growth Rates of Three Plankton Diatoms in Relation to Underwater Radiation and Temperature", *Ann. Bot. N. S.*, Vol 19, pp 329-341.
- Tamiya, H.T., Sasa, T., Nikei, T., and Ishibashi, S. 1965. "Effects of Variation of Daylength, Day and Night Temperatures, and Intensity of Daylight on the Growth of *Chlorella*", *J. of General and Applied Microbiology*, Vol 4, pp 298-307.
- Tanaka, N., Nakanishi, M., and Kadota, H. 1974. "Nutritional Interrelation Between Bacteria and Phytoplankton in a Pelagic Ecosystem", *Effects of the Ocean Environment on Microbial Activities*, R.R. Colwell and R.V. Mouta, eds., University Park Press, Baltimore, MD, pp 495-509.
- Thackston, E. L. and Krenkel, P. A. 1966. "Reaeration Predictions in Natural Streams," *J. San. Engr. Div., ASCE*, 89(SA5):1-30.
- Thackston, E., L. and Dawson, J. W. 2001. "Recalibration of a Reaeration Equation," *J. Envir. Engr., ASCE*, 127(4), 317-321.

REFERENCES

- Thibodeaux, L. 1996. *Environmental Chemodynamics*, Wiley-Interscience, NY.
- Thomann, R.V. 1971. "The Effect of Nitrification on the Dissolved Oxygen of Streams and Estuaries", Environmental Engineering and Scientific Program, Manhattan College, Bronx, New York, NY.
- Thomann, R. V. and Fitzpatrick, J. F. 1982. "Calibration and Verification of a Mathematical Model of the Eutrophication of the Potomac Estuary," report by HydroQual, Inc. Mahwah, NJ, to DES, District of Columbia.
- Thomann, R. V. and Mueller, J. A. 1987. *Principles of Surface Water Quality Modeling and Control*, Harper and Row, NY.
- Thomas, J. H. 1975. "A Theory of Steady Wind-Driven Current in Shallow Water with Variable Eddy Viscosity," *J. Physical Oceanography*, 5(1), 136.
- Thomas, W.H., and Dodson, A.N. 1968. "Effects of Phosphate Concentration on Cell Division Rates and Yield of a Tropical Oceanic Diatom", *Biological Bulletin*, Vol 134, pp 199-208.
- Thompson, J.R., and Bernard, R.S. 1985. "WESSEL: Code for Numerical Simulation of Two-Dimensional Time-Dependent, Width-Averaged Flows with Arbitrary Boundaries", *Technical Rpt. E-85-8*, US Army Engineer Waterways Experiment Station, Vicksburg, MS.
- Thornton, K.W., and Lessem, A.S. 1978. "A Temperature Algorithm for Modifying Biological Rates", *Transactions of the American Fisheries Society*, Vol 107, No. 2, pp 284-287.
- Thornton, K.W., Nix, J.F., and Bragg, J.D. 1980. "Coliforms and Water Quality: Use of Data in Project Design and Operation", *Water Resources Bulletin*, No. 16, pp 86-92.
- Tison, D.L., and Pope, D.H. 1980. "Effect of Temperature on Mineralization by Heterotrophic Bacteria", *Applied and Environmental Microbiology*, Vol 39, pp 584-587.
- Tison, D.L., Pope, D.P., and Boylen, C.W. 1980. "Influence of Seasonal Temperature on the Temperature Optima of Bacteria in Sediments of Lake George, New York", *Applied and Environmental Microbiology*, Vol 39, pp 675-677.
- Titman, D., and Kilham, P. 1976. "Sinking in Freshwater Phytoplankton: Some Ecological Implications of Cell Nutrient Status and Physical Mixing Processes", *Limnology and Oceanography*, Vol 21, No. 3, pp 109-117.
- Toerien, D.F., and Cavari, B. 1982. "Effect of Temperature on Heterotrophic Glucose Uptake, Mineralization, and Turnover Rates in Lake Sediment", *Applied and Environmental Microbiology*, Vol 43, pp 1-5.
- Toetz, D., Varga, L., and Loughran, D. 1973. "Half-Saturation Constants for Uptake of Nitrate and Ammonia by Reservoir Plankton", *Ecology*, Vol 54, pp 903-908.

REFERENCES

- Trussell, R.P. 1972. "The Percent Un-ionized Ammonia in Aqueous Ammonia Solutions at Different pH Levels and Temperature", *J. of the Fisheries Research Board of Canada*, Vol 29, pp 1505-1507.
- Tsivoglou, E. C. and Wallace, S. R. 1972. "Characterization of Stream Reaeration Capacity," *USEPA, Report No. EPA-R3-72-012*.
- Turner, J. S. 1979. *Buoyancy Effects in Fluids*, Cambridge University Press, NY.
- Turner, J.T. 1977. "Sinking Rates of Fecal Pellets from the Marine Copepod *Pontella meadii*", *Marine Biology*, Vol 40, No. 3, pp 249-259.
- Tennessee Valley Authority (TVA) 1972. Heat and Mass Transfer between a water surface and the atmosphere, Water Resources Report 0-6803, Lab Report #14, Norris, TN.
- Underhill, P.A. 1977. "Nitrate Uptake Kinetics and Clonal Variability in the Neritic Diatom *Biddulphia aurita*", *J. of Phycology*, Vol 13, pp 170-176.
- Ugarte, A. and M. Madrid 1994. "Roughness Coefficient in Mountain Rivers," *Proceedings National Conference on Hydraulic Engineering, ASCE*, pp. 652-656.
- USBR 1999. Water Measurement Manual, <http://ogee.do.usbr.gov/fmt/wmm>.
- US Army Engineer District, Baltimore. 1977. "Thermal Simulation of Lakes; User's Manual for Program Numbers 722-F5-E1010 and 722-F5-E1011", Baltimore, MD.
- Vaccaro, R.F. 1969. "The Response of Natural Microbial Populations in Seawater to Organic Enrichment", *Limnology and Oceanography*, Vol 14, pp 726-735.
- van Lierre, L., Zevenboom, W., and Mur, L.R. 1977. "Nitrogen as a Limiting Factor for the Growth of the Blue Green Alga *Oscillatoria*", *Progressive Water Technology*, Vol 8, pp 301-312.
- Vandenberg, J. A., S. Prakash, E. M. Buchak. 2014. Sediment Diagenesis Module for CE-QUAL-W2. Part 1: Conceptual Formulation. Environmental Modeling & Assessment. DOI 10.1007/s10666-014-9428-0. Print ISSN 1420-2026. Online ISSN 1573-2967. <http://link.springer.com/article/10.1007%2Fs10666-014-9428-0>. Springer International Publishing. November.
- Verduin, J. 1952. "Photosynthesis and Growth Rates of Live Diatom Communities in Western Lake Erie", *Ecology*, Vol 33, pp 163-169.
- _____. 1982. "Components Contributing to Light Extinction in Natural Waters: Methods of Isolation", *Archives of Hydrobiology*, Vol 93, pp 303-312.
- Verity, P.G. 1981. "Effects of Temperature, Irradiance and Daylength on the Marine Diatom *Lep-
tocyldrus danicus* Cleve; I. Photosynthesis and Cellular Composition", *J. of Experimental Marine Biology and Ecology*, Vol 55, pp 79-91.

REFERENCES

- Vollenweider, R.A. 1968. "Scientific Fundamentals of the Eutrophication of Lakes and Flowing Waters, with Particular Reference to Nitrogen and Phosphorus as Factors in Eutrophication", *Tech. Rept. OECD, DAS/CSI/68.27*, Paris, France.
- _____. 1976. "Advances in Defining Critical Loading Levels for Phosphorus in Lake Eutrophication", *Mem. Inst. Ital. Idrobiol.*, Vol 33, pp 53-83.
- Von Muller, H. 1972. "Wachstum und Phosphatbedarf von *Nitzschia octinastroides* Lemm.. V. Goor in Statischer und Homokontinuierlicher Kultur unter Phosphatlimitierung", *Arch. Hydrobiol. Suppl.*, Vol 38, pp 399-484.
- Wallen, D.G., and Cartier, L.D. 1975. "Molybdenum Dependence, Nitrate Uptake and Photosynthesis of Freshwater Plankton Algae", *J. of Phycology*, Vol 11, pp 345-349.
- Wake, A. 1977. "Development of a Thermodynamic Simulation Model for the Ice Regime of Lake Erie", Ph.D. thesis, SUNY at Buffalo, Buffalo, NY.
- Wang, L.K., Poon, C.P., Wang, M.H., and Bergenthal, J. 1978. "Chemistry of Nitrification-Denitrification Process", *J. of Environmental Sciences*, Vol 21, pp 23-28.
- Wannikof, R., Ledwell, J. R., and Crusius, J. 1991. "Gas Transfer Velocities on Lakes measured with Sulfur Hexafluoride," In *Symposium Volume of the Second International Conference on Gas Transfer at Water Surfaces*, S. C. Wilhelms and J. S. Gulliver, eds., Minneapolis, MN.
- Watts, F. J. 1993. "n Values for Shallow Flow in Rough Channels," *Proceedings National Conference on Hydraulic Engineering, Part 1*, ASCE, pp. 995-1000.
- Weiler, R.R. 1974. "Carbon dioxide exchange between water and atmosphere," *Journal of Fisheries Research, Board Committee*, Vol. 31, pp. 329-332.
- Wells, S. A. and Berger, C. J. 1995. "Hydraulic and Water Quality Modeling of Wahiawa Reservoir," prepared for R. M. Towill Corporation, Honolulu, HA.
- Wells, S. A. 1997. "Theoretical Basis for the CE-QUAL-W2 River Basin Model," Department of Civil Engineering, *Technical Report EWR-6-97*, Portland State University, Portland, OR.
- Wells, S. A. and Berger, C. 1997. "Modeling the Lower Snake River," report prepared for HDR Engineering, Inc., Boise, ID.
- Wells, S. A. and Berger, C. 1998. "The Lower Snake River Model," report prepared for HDR Engineering, Inc., Boise, ID.
- WES. 1996. Evaluation and Analysis of Historical Dissolved Gas Data from the Snake and Columbia Rivers, Waterways Experiments Station, *ACOE Dissolved Gas Abatement Study Phase 1 Technical Report*, Vicksburg, MS.

REFERENCES

- WES. 1997. "Total Dissolved Gas Production at Spillways on the Snake and Columbia Rivers, Memorandum for Record," Waterways Experiments Station, *ACOE Dissolved Gas Abatement Study Phase I Technical Report*, Vicksburg, MS.
- Wetzel, R.G. 1975. *Limnology*, W.B. Saunders, Philadelphia, PA.
- Wetzel, R.G., Rich, P.H., Miller, M.C., and Allen, H.L. 1972. "Metabolism of Dissolved Particulate Detrital Carbon in a Temperate Hardwater Lake", *Mem. Ist Ital. Idrobiol. Suppl.*, Vol 29, pp 185-243.
- Whittaker, R.H. 1975. *Communities and Ecosystems*, MacMillan, New York, NY.
- Wiegel, R.L. 1964. *Oceanographical Engineering*, Prentice-Hall, Englewood Cliffs, NJ.
- Wild, H.E., Sawyer, C.N., and McMahon, T.C. 1971. "Factors Affecting Nitrification Kinetics", *J. of the Water Pollution Control Federation*, Vol 43, pp 1845-1854.
- Williams, D.T.; Drummond, G.R.; Ford, D.E.; and Robey, D.L. 1980. "Determination of Light Extinction Coefficients in Lakes and Reservoirs", *Surface Water Impoundments, Proceedings of the Symposium on Surface Water Impoundments*, American Society of Civil Engineers, H.G. Stefan, ed..
- Williams, P.J., Yentsch, L.B., and Yentsch, C.S. 1976. "An Examination of Photosynthetic Production, Excretion of Photosynthetic Products and Heterotrophic Utilization of Dissolved Organic Compounds with Reference to Results from a Coastal Subtropical Sea", *Marine Biology*, Vol 35, pp 31-40.
- Witten, A. J. and J. H. Thomas 1976. "Steady Wind-Driven Currents in a Large Lake with Depth Dependent Eddy Viscosity," *J. Physical Oceanography*, 6(1), 85.
- Wright, R.T. 1975. "Studies on Glycolic Acid Metabolism by Freshwater Bacteria", *Limnology and Oceanography*, Vol 20, pp 626-633.
- Wuest, A. and Lorke, A. 2003. Small-Scale Hydrodynamics In Lakes. *Annu. Rev. Fluid Mech.* 2003. 35:373–412, doi: 10.1146/annurev.fluid.35.101101.161220.
- Wuhrmann, K. 1972. "Stream Purification", *Water Pollution Microbiology*, R. Mitchell, ed.), Interscience, New York, NY.
- Wunderlich, W. 1972. "Heat and Mass Transfer between a Water Surface and the Atmosphere", *Rpt. No. 14, Rpt. Publication No. 0-6803*, Water Resources Research Laboratory, Tennessee Valley Authority, Division of Water Control Planning, Engineering Laboratory, Norris, TN.
- Zimmerman, U. 1969. "Okologische and Physiologische Untersuchungen an der Planktonischen Blaualge *Oscillatoria Rubescens*, D.C., unter Besonderer Beruchlschtlung von Licht und Temperatur", *Schweiz. Z. Hydrol.*, Vol 31, pp 1-58.
- Yakhot, V. and Orszag, S. 1986. "Renormalization Group Analysis of Turbulence 1: Basic Theory," *J. Sci. Comput.* 1(1), 3-51.

REFERENCES

- Yen, B. C. 1992. *Hydraulic Resistance of Open Channels in Channel Flow: Centennial of Manning's Formula*, ed. B.C. Yen, Water Resources Publications, Littleton, CO.
- Yu, S.L., T.J. Tuffy, and D.S. Lee. 1977. "Atmosphere Reaeration in a lake," *Office of Water Resources and Technology*, U.S. Department of the Interior.
- Zison, S.W., Mills, W.B., Deimer, B., and Chen, C.W. 1978. "Rates, Constants, and Kinetics Formulations in Surface Water Quality Modeling", *EPA-600/3-68-105*, US Environmental Protection Agency, Washington, DC.

CE-QUAL-W2 Publications

Peer Reviewed Publications and Proceedings

- Annear, R. L., and Wells, S. A. 2007. A comparison of five models for estimating clear-sky solar radiation, *Water Resources Research*, 43, W10415, doi:10.1029/2006WR005055.
- Bartholow, J., R.B. Hanna, L. Saito, D. Lieberman, and M. Horn. 2001. "Simulated Limnological Effects of the Shasta Lake Temperature Control Device". *Environmental Management*, Vol. 27, No. 4, pp. 609-626. http://smig.usgs.gov/SMIG/uo/features_0999/shasta_tcd.html.
- Bath, A.J., and T.D. Timm. 1994. "Hydrodynamic Simulation of Water Quality in Reservoirs of South Africa", *Commission Internationale Des Grands Barrages*, Q.69 R. 39, 625-633.
- Berger, C. and Wells, S. A. 2007. "Modeling Effects of Channel Complexity and Hyporheic Flow on Stream Temperatures," Proceedings, National TMDL 2007 Conference, Water Environment Federation, Bellevue, WA, June 24-27.
- Berger, C. and Wells, S. A. 2007. "Development and Calibration Of Lake Whatcom Water Quality Model," Proceedings, National TMDL 2007 Conference, Water Environment Federation, Bellevue, WA, June 24-27.
- Berger, C. and Wells, S. 2008. "A Macrophyte Water Quality and Hydrodynamic Model," ASCE, *Journal of Environmental Engineering*, 134:778-788.
- Berger, C.; McKillip, M.; Annear, R.; Wells, V., and Wells, S. 2009. "Modeling the Spokane River-Lake Roosevelt System," *Proceedings IAHR 33rd Congress*, Vancouver, BC, August 9-14, pp. 6223-6230.
- Berger, C., Wells, S. A., and Wells, V. I. 2012. Modeling of Water Quality and Greenhouse Emissions of Proposed South American Reservoirs, *Proceedings World Environmental and Water Resources Congress*, EWRI, ASCE, Albuquerque, NM, pp. 911-923.
- Berger, C. J., Bigham, G., and Wells, S. A. 2014. Prediction of GHG Emissions from a New Reservoir, *Proceedings World Environmental and Water Resources Congress*, EWRI, ASCE, Portland, OR, pp. 1010-1019.
- Boatman, C.D., and E.M. Buchak. 1987. "Application of an Ecosystem/Water Quality Model as a Tool for Managing Estuarine Water Quality". In *Proceedings Fifth Symposium on Coastal Ocean Management*, ASCE, Vol. 3, Seattle, Washington, 3932-3945.

CE-QUAL-W2 BIBLIOGRAPHY

- Boegman, L., M.R. Loewen, D.A. Culver, P.F. Hamblin and M.N. Charlton. 2002. "A two-dimensional model coupling pelagic dynamics to benthic grazing by zebra mussels in western Lake Erie: Relative impacts of nutrient load abatement and mussel invasion, 1960s to 1994". (Under consideration for submission to *Can. J. Fish. Aquat. Sci.*).
- Boegman, L., M.R. Loewen, P.F. Hamblin and D.A. Culver. 2002. "A Two-Dimensional Model Coupling Pelagic Dynamics to Benthic Grazing by Zebra Mussels in Western Lake Erie: Spatial-Dynamic Responses". (Under consideration for submission to *Canadian Journal of Fisheries and Aquatic Sciences*).
- Boegman, L., M.R. Loewen, P.F. Hamblin and D.A. Culver. 2001. Application of a Two-Dimensional Hydrodynamic Reservoir Model to Lake Erie". *Canadian Journal of Fisheries and Aquatic Sciences*, 58: 858-869.
- Crain, A. S., G. L. Jarrett, and P. A. Bukaveckas. 1997. "Development And Calibration Of A Water Quality Model For Herrington Lake". *Waterworks* 3(1):1-3.
- Deliman, P.N. and J.A. Gerald. 2002. "Application of the Two-Dimensional Hydrothermal and Water Quality Model, CE-QUAL-W2, to the Chesapeake Bay – Conowingo Reservoir". *Journal of Lake and Reservoir Management*, Vol. 18, No. 1, pp. 1-9.
- Dortch, M. S., and W. L. Boyt. 1983. "Simulating Advective Transport in Reservoirs". In *Proceedings of the Conference on Frontiers in Hydraulic Engineering*, H. T. Shen, ed., August 9-12, 1983. Hydraulics Division of the American Society of Civil Engineers in conjunction with Massachusetts Institute of Technology and the Boston Society of Civil Engineers. Cambridge, MA.
- Edinger, J. E., and E. M. Buchak. 1980. "Numerical Hydrodynamics of Estuaries" in *Estuarine and Wetland Processes with Emphasis on Modeling*, P. Hamilton and K. B. MacDonald eds., Plenum Press, New York, NY, 115-146.
- Edinger, J. E., E. M. Buchak, and D. H. Merritt. 1983. "Longitudinal-Vertical Hydrodynamics and Transport with Chemical Equilibria for Lake Powell and Lake Mead", in *Salinity in Watercourses and Reservoirs*, R. H. French, ed., Butterworth Publishers, Stoneham, MA, pp. 213-222.
- Edinger, J. E., E. M. Buchak, and S. Rives. 1987. "GLVHT Model Verification Using Field Data", in *Proc. 1987 National Conference on Hydraulic Engineering*, R. M. Ragan, ed., August 3-7, 1987. Hydraulics Division of the American Society of Civil Engineers. Williamsburg, VA.
- Garvey, E., J.E. Tobiasson, M. Hayes, E. Wolfram, D.A. Reckhow, and J.W. Male. 1998. "Coliform Transport in a Pristine Reservoir: Modeling and Field Studies". *Water Science and Technology*, Vol. 37, No. 2, pp. 137-144.
- Gelda, R. K. and S. W. Effler. 2000. "A River Water Quality Model for Chlorophyll and Dissolved Oxygen that Accommodates Zebra Mussel Metabolism". *Water Quality and Ecosystem Modeling* 1:271-309.

CE-QUAL-W2 BIBLIOGRAPHY

- Gelda, R. K., S. W. Effler and E. M. Owens. 2001. "River Dissolved Oxygen Model with Zebra Mussel Oxygen Demand (ZOD)". *Journal of Environmental Engineering Division, ASCE* 127:790-801.
- Gelda, R. K. and S. W. Effler. 2007. Testing and application of a two-dimensional hydrothermal model for a water supply reservoir: Implications of sedimentation. *J. Environ. Eng. Sci.* 6:73-84.
- Gelda, R. K. and S. W. Effler. 2007. Modeling turbidity in a water supply reservoir: Advancements and issues. *J. Environ. Eng.* 133:139-148.
- Gelda, R. K., S. W. Effler, F. Peng, E. M. Owens and D. C. Pierson. 2009. Turbidity model for Ashokan Reservoir, New York: Case Study. *J. Environ. Eng.* 135:885-895.
- Gelda, R. K., E. M. Owens and S. W. Effler. 1998. "Calibration, Verification, and an Application of a Two-Dimensional Hydrothermal Model [CE-QUAL-W2] for Cannonsville Reservoir". *Journal of Lake and Reservoir Management*, 14:186-196.
- Gordon, J. A. 1980. "An Evaluation of the LARM Two-Dimensional Model for Water Quality Management Purposes", in *Proceedings of the Symposium on Surface-Water Impoundments*, H. G. Stefan, ed., Minneapolis, Minnesota, June 2-5, 1980, Vol. 1, Paper 4-34, pp. 518-527. American Society of Civil Engineers, New York, NY.
- Gordon, J. A. 1981. "LARM Two-Dimensional Model: An Evaluation". *Journal of Environmental Engineering*, 107(5), 77-886.
- Gordon, J. A., and J. S. Lane. 1983. "Short-Term Hydrodynamics in a Stratified Reservoir", in *Proceedings of the 1983 National Conference on Environmental Engineering*, A. Medine and M. Anderson, eds.), Boulder, Colorado, July 6-8, 1983, pp. 524-531. American Society of Civil Engineers, New York, NY.
- Gündüz, O., S. Soyupak, and C. Yurteri. 1998. Development of Water Quality Management Strategies for the Proposed Isikli Reservoir". *Water Science and Technology*, Vol. 37, No. 2, pp. 369-376
- Hanna, R.B., L. Saito, J.M. Bartholow, and J. Sandelin. 1999. "Results of Simulated Temperature Control Device Operations on In-Reservoir and Discharge Water Temperatures Using CE-QUAL-W2. *Journal of Lake and Reservoir Management* 15(2):87-102. <http://www.fort.usgs.gov/>.
- Johnson, B. H., M. B. Boyd and R. R. Copeland. 1987. "Lower Mississippi River Salt Intrusion Modeling", in *Proceedings 1987 National Conference on Hydraulic Engineering*, R. M. Ragan, ed.), 3-7 August 1987. Hydraulics Division of the American Society of Civil Engineers. Williamsburg, VA.
- Kim, B. R., J. M. Higgins and D. J. Bruggink. 1983. "Reservoir Circulation Patterns and Water Quality". *Journal of Environmental Engineering, ASCE*, 109(6), 1284-1294.

CE-QUAL-W2 BIBLIOGRAPHY

- Kurup, R.G., D.P. Hamilton, and R.L. Phillips. 2000. "Comparison of Two 2-Dimensional, Laterally Averaged Hydrodynamic Model Applications to the Swan River Estuary". *Mathematics and Computers in Simulation*, 51(6): 627-639. <http://www.cwr.uwa.edu.au/cwr/publications/papers1500/1536.html>
- Martin, J. L. 1988. "Application of Two-Dimensional Water Quality Model". *Journal of Environmental Engineering, ASCE*, 114(2), 317-336.
- Martinez, V. I., Wells, S. A. and R. C. Addley. 2014. Meeting Temperature Requirements for Fisheries Downstream of Folsom Reservoir, California, Proceedings World Environmental and Water Resources Congress, EWRI, ASCE, Portland, OR, pp. 1081-1092.
- McKillip, M. and Wells, S. 2006. Hydrodynamic, water quality and fish bioenergetics modeling in Lake Roosevelt Washington USA using CE-QUAL-W2, *Proceedings, 5th International Conference on Reservoir Limnology and Water Quality*, Brno, Czech Republic, August 27-September 2, 2006, pp. 145-148.
- Mooij WM, Trolle D, Jeppesen E, Arhonditsis G, Belolipetsky PV, Chitamwebwa DBR, Degermendzhy AG, DeAngelis DL, De Senerpont Domis LN, Downing AS, Elliott JA, Fragoso Jr CR, Gaedke U, Genova SN, Gulati RD, Håkanson L, Hamilton DP, Hipsey MR, 't Hoen J, Hülsmann S, Los FJ, Makler-Pick V, Petzoldt T, Prokopkin IG, Rinke K, Schep SA, Tominaga K, Van Dam AA, Van Nes EH, Wells SA and Janse JH. 2010. "Challenges and opportunities for integrating lake ecosystem modelling approaches," *Aquatic Ecology*: DOI:10.1007/s10452-010-9339-3, 44(3): 633-667.
- O'Donnell, S. M., R. K. Gelda and S. W. Effler. 2011. Modeling the fate of runoff events density currents in a reservoir with a two-dimensional framework. *Lake and Reserv. Manage.* (in press).
- P.Yu. Pushistov, V.N. Danchev. 2012. Experience in development and results of informational-computational complexes application in modeling of hydrodynamic variables and thermal regime in water bodies of the Ob River basin. Part 1 – ICC "Severnaya Sosva". Part 2 – ICC "Lake Teletskoye", Russian Academy Of Sciences, Siberian Branch, Institute For Water And Environmental Problems, Federal Service for Hydrometeorology and Environmental Monitoring, Siberian Regional Hydrometeorological Research Institute.
- Saito, L. B.M. Johnson, J. Bartholow, R. B. Hanna. 2001. "Assessing Ecosystem Effects of Reservoir Operations Using Food Web-Energy Transfer and Water Quality Models". *Ecosystems* 4(2):105-125. <http://link.springer-ny.com/link/service/journals/10021/bibs/1004002/10040105.html>
- Saito, Laurel, Brett M. Johnson, John M. Bartholow, and Darrell G. Fontane. 2001. Interdisciplinary modeling to assess ecosystem effects of reservoir operations. Pp. 373-377 in Marino, Miguel A., and Slobodan P. Simonovic, editors. *Integrated Water Resources Management*. IAHS Publication no. 272. Oxfordshire (UK): International Association of Hydrologic Sciences Press.
- Shoajei, N. and Wells, S. A. 2014. Automatic Calibration of Water Quality Models for Reservoirs and Lakes, *Proceedings World Environmental and Water Resources Congress*, EWRI, ASCE, Portland, OR, pp. 1020-1029.

- Wells, S. A., J. R. Manson, and J. L. Martin 2007. "Numerical Hydrodynamic and Transport Models for Reservoirs," Chapter 4 in Energy Production and Reservoir Water Quality, ASCE.
- Wells, S. 2009. Hydrodynamic Compressible and Incompressible Modeling of the Density Structure and Hydrodynamics of Hypersaline Systems, *Proceedings IAHR 33rd Congress*, Vancouver, BC, August 9-14, pp. 4345-4352.
- Wells, S. A., Wells, V. I., and Berger, C. 2012. Impact of Phosphorus Loading from the Watershed on Water Quality Dynamics in Lake Tenkiller, Oklahoma, USA, *Proceedings World Environmental and Water Resources Congress*, EWRI, ASCE, Albuquerque, NM, pp. 888-899.
- Wells, V. I. and Wells, S. A. 2012. CE-QUAL-W2 Water Quality and Fish-bioenergetics Model of Chester Morse Lake and the Cedar River, *Proceedings World Environmental and Water Resources Congress*, EWRI, ASCE, Albuquerque, NM, pp. 2756-2767.

Presentations at Scientific Meetings

- Annear, R. and S. Wells. 2002. "The Bull Run Reservoir River System Model". *Proceedings Research and Extension Regional Water Quality Conference 2002* [on CD], Vancouver, Washington.
- Annear, R. and S. Wells. 2002. "The Bull Run River – Reservoir System Model". *Proceedings 2nd Federal InterAgency Hydrologic Modeling Conference*, Las Vegas, July 28-Aug 1, 2002.
- Atkins, D., T. Martin, and M. Bennett. 1998. "Pitlake Limnology". In *Proceedings of the 1998 Conference on Hazardous Waste Research: Bridging Gaps in Technology and Culture*, Snowbird, Utah, May 18-21, 1998.
- Atkins, D., J.H. Kempton, T. Martin, and P. Maley. 1997. "Limnologic Conditions in Three Existing Nevada Pit Lakes: Observations and Modeling Using CE-QUAL-W2". in *Proceedings - Fourth International Conference on Acid Rock Drainage*, Vancouver, B.C., Canada, May 31 - June 6, 1997.
- Bales, J.D. 2001. "Data Quality and Uncertainty in Reservoir Water-Quality Modeling Carolina". In Warwick, J.J., ed., *Water Quality Monitoring and Modeling—Proceedings of the AWRA Annual Spring Specialty Conference*, p. 113.
- Bales, J.D. 2001. Dynamic Water-Quality Models of Catawba River Basin Reservoirs, North Carolina". In *NALMS 10th Annual Southeastern Lakes Conference*, Knoxville, TN, p. 28.
- Bales, J.D. 1998. "Dynamic Water-Quality Modeling of Catawba River Reservoirs". In *Water resources protection: understanding and management, Institute Proceedings Series No. 11*, Raleigh, NC, University of North Carolina Water Resources Research Institute, p. 23 [abs].

CE-QUAL-W2 BIBLIOGRAPHY

- Bales, J.D. 1997. "Modeling estuarine effects of nitrogen loading reduction". In *Tanner, J., ed., Nutrients in the Neuse River--Working Toward Solutions*. New Bern, NC, Confere, North Carolina State University, p. 11 [abs].
- Bales, J.D., and M.L. Jaynes. 1995. "Dynamic Modeling of Circulation and Water Quality in a Narrow Piedmont Reservoir". *4th Annual Southeastern Lakes Management Conference*, North American Lake Management Society, Charlotte, North Carolina.
- Bales, J.D. 1993. U.S. Geological Survey Reservoir Studies in North Carolina". *2nd Annual Southeastern Lakes Management Conference*, North American Lake Management Society Chattanooga, Tennessee.
- Bales, J.D., 1993, The role of models in evaluating water quality in *Proceedings of the Conference on Water Issues in the 1990's*: Hickory, NC, Environmental Policy Studies Center, Catawba Valley Community College, p. 1-2.
- Bales, J.D. and M.J. Diorgino. 1998. "Dynamic Modeling of Water Supply Reservoir Physical and Chemical Processes". In *Proceedings of the First Federal Interagency Hydrologic Modeling Conference*, April 19-23, 1998, Las Vegas, NV: Subcommittee on Hydrology of the Interagency Advisory Committee on Water Data, p. 2-61 to 2-67. http://smig.usgs.gov/SMIG/features_0998/rhodhiss.html.
- Bartholow, J., L. Saito, B. Hanna, B. Johnson, D. Lieberman, and M. Horn. 2000. "Predicting the Effects of Shasta's Temperature Control Device on In-Reservoir Limnology and Fish". *Bay Delta Modeling Forum/Interagency Ecological Program*, Pacific Grove, California, February 29-March 3, 2000.
- Bartholow, J.M., B. Hanna, L. Saito, D. Lieberman, and M. Horn. 1999. "Simulated effects of a temperature control device on Shasta Lake". *North American Lake Management Society Symposium '99*. Reno, Nevada, December 1-4, 1999.
- Bartholow, J., D. Lieberman, M. Horn, B. Hanna, and L. Saito. 1998. "Effects of Dam Reoperation on Reservoir Limnology and Fishery Energetics". *North American Lake Management Society Conference*, Banff, Alberta, Canada.
- Berger, C. and S. Wells. 1995. "Effects of Management Strategies to Improve Water Quality in the Tualatin River, Oregon," in *Water Resources Engineering*, Vol. 2, ed. by W. Espey Jr. and P. Combs, ASCE, 1360-1364.
- Berger, C. and S. Wells. 1999. "Macrophyte Modeling in the Columbia Slough," *Proceedings International Water Resources Engineering Conference*, ASCE, Seattle, Wa, Aug.8-11.
- Berger, C., R. Annear, and S. Wells. 2002. "Willamette River and Columbia River Waster Load Allocation Model". In *Proceedings 2nd Federal InterAgency Hydrologic Modeling Conference*, Las Vegas, July 28-Aug 1, 2002.

CE-QUAL-W2 BIBLIOGRAPHY

- Berger, C. and Wells, S. A. 2007. "Modeling Effects of Channel Complexity and Hyporheic Flow on Stream Temperatures," Proceedings, National TMDL 2007 Conference, Water Environment Federation, Bellevue, WA, June 24-27.
- Berger, C. and Wells, S. A. 2007. "Development And Calibration Of Lake Whatcom Water Quality Model," Proceedings, National TMDL 2007 Conference, Water Environment Federation, Bellevue, WA, June 24-27.
- Berger, C., Wells, S. A., and Wells, V. I. 2012. "Modeling of Water Quality and Greenhouse Emissions of Proposed South American Reservoirs," Proceedings World Environmental and Water Resources Congress, EWRI, ASCE, Albuquerque, NM, pp. 911-923.
- Berger, C. J., Bigham, G., and Wells, S. A. 2014. "Prediction of GHG Emissions from a New Reservoir," Proceedings World Environmental and Water Resources Congress, EWRI, ASCE, Portland, OR.
- Bowen, J.D. 1998. "Using Eutrophication Modeling to Predict the Effectiveness of River Restoration Efforts". In *Proceedings Wetlands Engineering and River Restoration Conference*", ASCE.
- Buchak, E. M., and J. E. Edinger. 1989. "Comparison of Computed and Observed Velocities at Three Estuarine Sites". Presented at the *Estuarine and Coastal Circulation and Pollutant Transport Modeling: Model-Data Comparison*. Waterway, Port, Coastal and Ocean Division, American Society of Civil Engineers, November 17, Newport, RI.
- Buchak, E.M., J.E. Edinger, J.J. Loos and E.S. Perry. 1989. "Larval Transport and Entrainment Modeling for the Patuxent Estuary". Presented at the *Tenth Biennial International Estuarine Research Conference*, Estuarine Research Federation, October 11, Baltimore, MD.
- Buchak, E. M., C. B. James and A. C. Mitchell. 1991. "Nechako Reservoir Mathematical Modeling Studies". Presented at the *1991 Annual Conference of the Canadian Society for Civil Engineering, 10th Canadian Hydrotechnical Conference and Engineering Mechanics Symposium*, May 29, Vancouver, BC.
- Boegman, L., P.F. Hamblin and M.R. Loewen. Two-Dimensional Modelling of Zebra Mussel Effects in Lake Erie, Stage One: Validation of Temperature, Currents and Water Levels. In *Proceedings of the 42nd Conference of the International Association of Great Lakes Research*, May 24-28, 1999, Case Western Reserve University, Cleveland, Ohio USA.
- Boegman, L., M.R. Loewen, P.F. Hamblin and D.A. Culver. Application of a Two-Dimensional Hydrodynamic and Water Quality Model to Lake Erie. Abstract in proceedings 2000 Ocean Sciences Meeting, Jan. 24-28, 2000, San Antonio, Texas USA.
- Chapman, R.S. and T.M. Cole. 1992. "Improved Thermal Predictions in CE-QUAL-W2". In *Hydraulic Engineering: Saving a Threatened Resource—In Search of Solutions*, Water Forum '92, Baltimore, Maryland.

CE-QUAL-W2 BIBLIOGRAPHY

- Cheslak, E; Berger, C; Annear, R., and Wells, S. 2009. "Protecting Spring-Run Chinook Salmon: The Use of a Two-dimensional Water Temperature Model to Evaluate Alternative Hydroelectric Operations," *WaterPower XVI Proceedings*, Spokane, WA, July 27-30, 2009
- Chow, I.B. 2002 "A Two-Dimensional Model Application for Manatee Protection". *Charlotte Harbor Watershed Summit*, IMPAC University in Punta Gorda, Florida, February 7-9, 2002.
- Cole, T. M., and Hannan, H. H. 1979. "Computer Simulations of Canyon Reservoir". Presented at the *Texas Academy of Sciences Annual Meeting*. Austin, TX.
- Cole, T.M. 1995. "The Future Role of Sophisticated Models in Reservoir Management". *Lake and Reservoir Management V9 No. 2, NALMS 14th Annual International Symposium*, Orlando, FL.
- Cole, T. M. 2000. "Temperature Modeling Using CE-QUAL-W2". In *Proceedings_HydroInformatics 2000, IAHR*, CDROM EW4.
- Cole, T.M. 2002. "CE-QUAL-W2 – A 2D Hydrodynamic and Water Quality Model for Rivers, Lakes, Reservoirs, and Estuaries". In *4th International Conference on Reservoir Limnology and Water Quality*, Ceshe Budejovice, Czech Republic, August 12-16, 2002.
- Devine, G., M. French, And G. L. Jarrett. 1997. "Neural Networks As A Tool To Calibrate Reservoir Water Quality Models". In *Proceedings Of The Kentucky Water Resources Research Institute*.
- Easley, W.S., L.E. Barness-Walz, P.L. Neichter, and J.A. Bohannon. 1995. "Evaluation of Water Quality in Taylorsville Lake, Kentucky: Using CE-QUAL-W2 Water Quality Model". *Lake and Reservoir Management V9 No. 2, NALMS 14th Annual International Symposium*, Orlando, FL.
- Edinger, J. E., and E. M. Buchak. 1978. "Reservoir Longitudinal and Vertical Implicit Hydrodynamics". Presented at the international conference *Environmental Effects of Hydraulic Engineering Works*, ASCE, September, Knoxville, TN.
- Goodwin, R.A., J.M. Nestler, and D. Degan. 2000. "Simulating Movement of Cool Water Fish in a Stratified Southern Impoundment". *American Fisheries Society Annual Meeting: Reflections*, St. Louis, Missouri, August 20-24, 2000.
- Hanna, B., L. Saito, J. Bartholow, and J. Sandelin. 1997. "Results of Mock 1995 Shasta TCD Operations on In-Reservoir and Discharge Water Quality Parameters using CE-QUAL-W2". *17th International Symposium of the North American Lake Management Society*, Houston, TX. page 54. <http://www.fort.usgs.gov/>.
- Johnson, M. C., D. E. Ford, J. E. Edinger and E. M. Buchak. 1981. "Analyzing Storm Event Data from DeGray Lake, Arkansas Using LARM". Presented at the *American Society of Civil Engineers Convention and Exposition*, October, St. Louis, MO.

CE-QUAL-W2 BIBLIOGRAPHY

- Hejzlar J., M. Růžička, and P. A. Diogo. 1999. "The Use of water quality modelling for optimising operation of a drinking water reservoir" *Proceedings International Conference on Fluid Mechanics and Hydrology*, June 23-26, 1999, Prague, Czech Republic, Institute of Hydrodynamics AS CR, Prague, 475-482.
- Jain, R., G. L. Jarrett, and E. M. Buchak. 2002. "Watershed and Reservoir Modeling in the Crum Creek Watershed". *AWRA Annual 2002 Conference*. Philadelphia, Pennsylvania. November 3-7.
- Jarrett, G. L., L. Curry, and J. Overing. 2001. Herrington Lake - Dix River Watershed (HSPF CEQUAL-W2 linkage). *Kentucky Water Resources Symposium*, Lexington, KY, Feb. 23.
- Kennedy, R.H., T. Cole, W. Boyd, K. Barko. 2002. Operational Influences on the Limnological Characteristics of Reservoirs: A Model Study. 2002. In *4th International Conference on Reservoir Limnology and Water Quality*, Ceshe Budejovice, Czech Republic, August 12-16, 2002.
- Lieberman, D., J. Bartholow, M. Horn, B. Hanna, and L. Saito. 1999. "Effects of Dam Reoperation on Reservoir Limnology and Fishery Energetics". *North American Lake Management Society Conference*, Banff, Alberta, Canada.
- Little, J.C. and McGinnis, D. F. "Hypolimnetic Oxygenation: Predicting Performance Using a Discrete-Bubble Model". In *Proceedings of 1st World Water Congress, International Water Association (IWA)*, Paris, France, July 3-7, 2000.
- Makinia, J., Wells, S. A., Crawford, D., and Kulbik, M. 1998. "Application of Mathematical Modeling and Computer Simulation for Solving Water Quality Problems," *Proceedings of the Fourth International Symposium and Exhibition on Environmental Contamination in Central and Eastern Europe Warsaw '98*, Warsaw, Poland, September 15-17, #233 CD-ROM.
- Martinez, V. I., Wells, S. A. and R. C. Addley. 2014. "Meeting Temperature Requirements for Fisheries Downstream of Folsom Reservoir, California," *Proceedings World Environmental and Water Resources Congress*, EWRI, ASCE, Portland, OR
- McGinnis, D.F., Little, J.C. and Wüest, A. "Hypolimnetic oxygenation: Coupling bubble-plume and reservoir models" submitted to *Asian Waterqual 2001, First IWA Asia-Pacific Regional Conference*, Fukuoka, Japan. http://www.eawag.ch/research_e/apec/Scripts/IWA%20Japan%20v6.pdf
- McGinnis, D., J. Little, A. Wuest. 2002. Coupling Bubble-Plume and Reservoir Models for Optimization of Hypolimnetic Oxygenation". In *4th International Conference on Reservoir Limnology and Water Quality*, Ceshe Budejovice, Czech Republic, August 12-16, 2002.
- McKillip, M. and Wells, S. 2006. "Hydrodynamic, water quality and fish bioenergetics modeling in Lake Roosevelt Washington USA using CE-QUAL-W2," *Proceedings, 5th International Conference on Reservoir Limnology and Water Quality*, Brno, Czech Republic, August 27 September 2, 2006, pp. 145-148.

CE-QUAL-W2 BIBLIOGRAPHY

- Müller M., F. Werner, and L. Luckner. 2002. "A Tool for Conjunctive Groundwater and Surface Water Quality Modeling in Post Mining Areas". In *Proceedings of Third International Conference on Water Resources and Environment Research*, Dresden, Germany. Vol. I. pp.136-141.
- Růžicka, M., J. Hejzlar, and T.M. Cole. 2002. "Impacts of Climate Change on the Water Quality in a Dimictic Reservoir". In *4th International Conference on Reservoir Limnology and Water Quality*, Ceshe Budejovice, Czech Republic, August 12-16, 2002.
- Růžicka M., J. Hejzlar, P. Mikešová, and T. M. Cole. 2000. "2-D Water Quality Modelling of a Drinking Water Reservoir: Římov Reservoir, Czech Republic". In *Proceedings 5th International Symposium on Systems Analysis and Computing in Water Quality Management WATERMATEX 2000*, Gent, Belgium, 18-20 September 2000. Gent University, Gent, pp. 1.59-1.66.
- Ruzicka, M., J. Hejzlar, M. Dubrovsky, J. Buchtele, T.M. Cole. 2001. "A Scenario Study of Water Quality in a Drinking Water Supply Reservoir in Response to Climate Change". In *Detecting Environmental Change*, London, 17-20 July 2001, London, UK. <http://www.ufa.cas.cz/dub/dub.htm>
- Rounds, S.A. 2001. "Modeling water quality in the Tualatin River: Achievements and limitations". In *AWRA Annual Spring Specialty Conference Proceedings, "Water Quality Monitoring and Modeling"*. Warwick, John J., ed., American Water Resources Association, Middleburg, Virginia, TPS-01-1, p. 115-120.
- Saito, L., B. Johnson, J. Bartholow, and Blair Hanna. 2001. "Assessing Effects of Reservoir Operations on the Reservoir Ecosystem Using Food Web-Energy Transfer and Water Quality Models". *21st Annual American Geophysical Union Hydrology Days*, April 2-5, 2001, Colorado State University, Fort Collins, Colorado, USA.
- Saito, L., B. Johnson, J. Bartholow, and D. Fontane. 2000. "Interdisciplinary modeling to assess ecosystem effects of reservoir operations". *International Symposium on Integrated Water Resources Management*. Davis, CA. April 2000.
- Shoajei, N. and Wells, S. A. 2014. "Automatic Calibration of Water Quality Models for Reservoirs and Lakes," *Proceedings World Environmental and Water Resources Congress*, EWRI, ASCE, Portland, OR.
- Smemoe, C.M., E.J. Nelson, and T.M. Cole. 2000. "A Conceptual Modeling Approach to CEQUAL-W2 Using the Watershed Modeling System". In *Proceedings of the Hydroinformatics Conference*, Iowa City, Iowa, July 2000.
- Wells, S.A. 1995. "Management of the Water Quality of the North Slough Adjacent to the St. John's Landfill". In *Proceedings First Annual Pacific Northwest Water Issues and 1995 Pacific Northwest/Oceania Conference*, Portland, Oregon.
- Wells, S.A. and C. Berger. 1995. "Management Strategies to Improve Water Quality in the Tualatin River, Oregon". In *Proceedings NCASI Conference*, September 27-28, 1995, Portland, OR.

CE-QUAL-W2 BIBLIOGRAPHY

- Wells, S.A. and C. Berger. 1995. "Management of the Water Quality of the Upper and Lower Columbia Slough System". In *Proceedings First Annual Pacific Northwest Water Issues and 1995 Pacific Northwest/Oceania Conference*, Portland, OR.
- Wells, S. A., C. Berger, and M. Abrams. 1996. "Winter Storm Event Impacts on Dissolved Oxygen Levels in the Columbia Slough System". In *The Pacific Northwest Floods of February 6-11, 1996, Proceedings of the Pacific Northwest Water Issues Conference*, ed. by A. Laenen, American Institute of Hydrology, pp.107-126.
- Wells, S.A. and C. Berger. 1998. "Water Quality Impacts of Urban Stormwater Runoff from the Portland International Airport on the Columbia Slough". In *Proceedings Gdanska Fundacja Wody, Podczyszczanie Wod Opadowych Wymagania Formalnoprprawne I Mozliwosci Technicne*, [in Polish], Gdansk, Poland.
- Wells, S.A. 1999. "River Basin Modeling Using CE-QUAL-W2". In *Proceedings International Water Resources Engineering Conference, ASCE*, Seattle, WA, Aug.8-11.
- Wells, S.A. 2000. "Hydrodynamic and Water Quality River Basin Modeling Using CE-QUAL-W2 Version 3". In *Development and Application of Computer Techniques to Environmental Studies VIII*, ed. G. Ibarra-Berastegi, C. Brebbia, P. Zannetti, WIT Press, Boston, 195-204.
- Wells, S. A. 2000. "CE-QUAL-W2 Version 3: Hydrodynamic and Water Quality River Basin Modeling". In *Proceedings HydroInformatics 2000, IAHR*, CDROM EW4.
- Wells, S.A. 2002. "Validation of the CE-QUAL-W2 Version 3 River Basin Hydrodynamic and Water Quality Model". *Proceedings HydroInformatics 2002, IAHR*, Cardiff, England.
- Wells, S.A. 2002. "Basis of the CE-QUAL-W2 Version 3 River Basin Hydrodynamic and Water Quality Model.". In *Proceedings 2nd Federal InterAgency Hydrologic Modeling Conference*, Las Vegas, July 28-Aug 1, 2002.
- Wells, S. A. and Annear, R. A. 2002. "River Basin Modeling Using CE-QUAL-W2 Version 3: The Bull Run River-Reservoir System Model". In *Proceedings 4th International Conference on Reservoir Limnology and Water Quality*, Ceske Budejovice, Czech Republic, August 12-16, 2002.
- Wells, S.A. and T.M. Cole. 2002. "TMDLS: Statistical Correlations or Mechanistic Modeling?". In *Proceedings National TMDL Science and Policy Conference*, Phoenix, AR, November 13-16, 2002.
- Wells, S.A. and R. Annear. 2002. "River Basin Modeling Using CE-QUAL-W2 V3: The Bull Run River-Reservoir System Model". In *4th International Conference on Reservoir Limnology and Water Quality*, Ceshe Budejovice, Czech Republic, August 12-16, 2002.
- Wells, S. A., Berger, C. J., Annear, R. L., McKillip, M. and Jamal, S. 2003. "Willamette River Basin Temperature TMDL Modeling Study," *Proceedings National TMDL Science and Policy Conference*, Chicago, IL, November 16-19, 2003.

CE-QUAL-W2 BIBLIOGRAPHY

- Wells, S. A., Berger, C. J., Annear, R. L., McKillip, M. and Jamal, S. 2004. "Willamette River Basin Temperature Modeling Study," Proceedings Watershed 2004, Dearborn, MI, July 11-14, 2004.
- Wells, S. A., Wells, V. I., and Berger, C. 2012. "Impact of Phosphorus Loading from the Watershed on Water Quality Dynamics in Lake Tenkiller, Oklahoma, USA," Proceedings World Environmental and Water Resources Congress, EWRI, ASCE, Albuquerque, NM, pp. 888-899.
- Wells, V. I. and Wells, S. A. 2012. "CE-QUAL-W2 Water Quality and Fish-bioenergetics Model of Chester Morse Lake and the Cedar River," Proceedings World Environmental and Water Resources Congress, EWRI, ASCE, Albuquerque, NM, pp. 2756-2767.
- Wood, T.M. and Rounds, S.A. 1998. "Using CE-QUAL-W2 to Assess the Effect of Reduced Phosphorus Loads on Chlorophyll-a and Dissolved Oxygen in the Tualatin River, Oregon". In *Proceedings of the First Federal Interagency Hydrologic Modeling Conference*, Las Vegas, Nevada, April 19-23, 1998: U.S. Geological Survey, p. 2-149 - 2-156. http://smig.usgs.gov/SMIG/features_0398/phos_tual.html
- Rounds, S.A. and Wood, T.M. 1998. "Using CE-QUAL-W2 to Assess the Ammonia Assimilative Capacity of the Tualatin River, Oregon". In *Proceedings of the First Federal Interagency Hydrologic Modeling Conference*, Las Vegas, Nevada, April 19-23, 1998: U.S. Geological Survey, p. 2-133 - 2-140. http://smig.usgs.gov/SMIG/features_0398/ammonia_tual.html
- Yager, R.E. B.R. Hayes, and M.J. Sale. 1995. "Modeling of Reservoir Release Temperature for Protecting Downstream Fish Habitat". In *Lake and Reservoir Management V9 No. 2, NALMS 14th Annual International Symposium*, Orlando, FL.
- Young, W.S., B.R. Schachte, and J.D. Bales. 1996. "Customized Software for Model Calibration and Visualization of Reservoir Water-Quality Model Results". In *Babcock, C.A., ed., Proceedings 1996 USGS National Computer Technology Meeting*.

Reports and Miscellaneous Articles

- Adams, R. W., Thackston, E. L., Speece, R. E., Wilson, D. J., and Cardozo, R. 1993. "Effect of Nashville's Combined Sewer Overflows on the Water Quality of the Cumberland River", *Technical Rpt. No. 42*, Environmental and Water Resources Engineering, Vanderbilt University, Nashville, TN.
- Bales, J.D., K.M. Sarver, and M.J. Giorgino. 2001. "Mountain Island Lake, North Carolina: Analysis of Ambient Conditions and Simulation of Hydrodynamics, Constituent Transport, and Water-Quality Characteristics, 1996-97". *U.S. Geological Survey Water-Resources Investigations Report 01-4138*.
- Bales, J.D., and J.C. Robbins. 1999. "A Water-Quality Modeling Framework for the Neuse River Estuary, North Carolina". *U.S. Geological Survey Water-Resources Investigations Report 99-4017*, 35 p.

CE-QUAL-W2 BIBLIOGRAPHY

- Bales, J.D., and M.J. Giorgino. 1998. "Lake Hickory, North Carolina: Analysis of Ambient Conditions and Simulation of Hydrodynamics, Constituent Transport, and Water-Quality Characteristics, 1993-94". *U.S. Geological Survey Water-Resources Investigations Report 98-4189*, 62 p.
- Barnese, Lisa E., Neichter, Patrick L., and Bohanon, Joseph A. 1993. "Evaluation of Water Quality in Caesar Creek Lake, Ohio using the CE-QUAL-W2 Water Quality Model", U.S. Army Corps of Engineers, Louisville, KY.
- Bartholow, J. 1998. "Animation of 'Age of Water' in Shasta Lake for 1995". <http://www.fort.usgs.gov/>.
- Buchak, E. M. and J. E. Edinger. 1982. "Hydrothermal Simulation of Quabbin Reservoir Using Longitudinal-Vertical Hydrodynamics", Final Report, prepared for Wallace, Floyd Associates, Inc., Cambridge, MA.
- _____. 1982. "Hydrothermal Simulations of Pool 3, Monongahela River Using Longitudinal-Vertical Numerical Hydrodynamics", prepared for Energy & Environmental Management, Inc., Murrysville, PA 15668-1809. Prepared by J. E. Edinger Associates, Inc., Wayne, Pennsylvania 19087-3226.
- _____. 1982. "User Guide for CE-QUAL-ELV2: A Longitudinal-Vertical, Time-Varying Estuarine Water Quality Model", *Instruction Rpt. EL-82-1*, U.S. Army Engineer Waterways Experiment Station, Vicksburg, MS.
- _____. 1982. "User Guide for LARM2: A longitudinal-Vertical, Time-Varying Hydrodynamic Reservoir Model", *Instruction Rpt. E-82-3*, U.S. Army Engineer Waterways Experiment Station, Vicksburg, MS.
- _____. 1985. "Simulation of Cooling Operations at Oak Knoll Reservoir, Phase II of Cooling Reservoir Modeling Program", *Document No. 85-41-R*, prepared for Environmental Department, Texas Utilities Generating Company, Dallas, Texas 75201 by J. E. Edinger Associates, Inc., Wayne, PA.
- _____. 1988. "Hydrothermal Analysis of Jersey Central Power and Light Sayreville and Werner Generating Stations", *Document No. 88-103-R/L*, prepared for EA Engineering, Science, and Technology, Inc., Hunt Valley/Loveton Center, Sparks, Maryland by J. E. Edinger Associates, Inc., Wayne, PA.
- Buchak, E. M., J. E. Edinger, and N. C. Huang. 1989. "Hydrothermal Analysis of Public Service Electric and Gas Linden and Sewaren Generating Stations", *Document No. 89-79-R*, prepared for EA Engineering, Science, and Technology, Inc., Hunt Valley/Loveton Center, Sparks, Maryland by J. E. Edinger Associates, Inc., Wayne, PA.
- _____. 1990. "Stationary State Dilution Studies of Lake Sinclair and Plant Harlee Branch", *Document No. 90-068-R*, prepared for Georgia Power Company Environmental Affairs, Atlanta, Georgia 30302. Prepared by J. E. Edinger Associates, Inc., Wayne, PA.

CE-QUAL-W2 BIBLIOGRAPHY

- Chu, C. and Jirka, G. (2003) "Wind and Stream Flow Induced Reaeration," *Journal of Environmental Engineering*, ASCE, Vol 129, No 12, 1129-1136.
- Cole, T. M. 1982. "Application of the LARM Two-Dimensional Computer Model to Canyon Reservoir", M.S. Thesis, Southwest Texas State University, San Marcos, TX.
- Cole, T.M. and D.H. Tillman. 2001. "Water Quality Modeling of Allatoona and West Point Reservoirs Using CE-QUAL-W2". ERDC/EL SR-01-3, U.S. Army Engineer Research and Development Center, Vicksburg, MS.
- Crain, A. S., A. A. Shipp, T. Mesko, and G. L. Jarrett. 1999. Modeling Hydrodynamics and Water Quality in Herrington Lake, Kentucky. U.S. Geological Survey, *Water-Resources Investigations Report*, 99-4281. pp. 84.
- EA Engineering, Science, and Technology, Inc. 1987. "Perryman Site Cooling Water Alternatives Study", *Rpt. No. BSC43D*, prepared for Baltimore Gas and Electric Company, Baltimore, MD.
- EA Engineering, Science, and Technology, Inc. 1993. "Lake Intrusion Modeling Study of the Black River", prepared for USS/KOBE, Loraine, OH.
- EA Engineering, Science, and Technology, Inc. 1994. "Shellfish Harvesting Exclusion Zone for the proposed Tolchester Outfall", prepared for McCrone, Inc., Annapolis, MD.
- _____. 1993. "Comparison of the Lake Sinclair GLVHT Model Predictions with Current Meter Measurements", *EA Project No. 11987.01*, prepared for Georgia Power Company.
- Edinger, J. E. and E. M. Buchak. 1978. "Hydrodynamics and Transport of Chlorine in Panther Branch Arm, Squaw Creek Reservoir for Comanche Peak S. E. S., Development Document", prepared for Texas Utilities Services, Inc., Dallas, TX.
- _____. 1981. "Estuarine Laterally Averaged Numerical Dynamics: The Development and Testing of Estuarine Boundary conditions in the LARM Code", *Miscellaneous Paper EL-81-9*, U.S. Army Engineer Waterways Experiment Station, CE, Vicksburg, MS.
- _____. 1982. "Analysis and Development of Carbonate-Bicarbonate Chemical Subroutine", Phase II, Development, Verification, and Use of Methods to Model Chemical and Thermal Processes for Lakes Mead and Powell. *Contract No. 2-07-DV-00131*, United States Department of the Interior, Bureau of Reclamation, Denver, CO.
- _____. 1983. "Developments in LARM2: A Longitudinal-Vertical, Time-Varying Hydrodynamic Reservoir Model", *Technical Rpt. E-83-1*, U.S. Army Engineer Waterways Experiment Station, Vicksburg, MS.
- _____. 1987. "Summary of Plant Hammond Coosa River - Weiss Reservoir Hydrothermal Analysis and Compliance Temperatures Reporting Procedures", *Document No. 87-119-R*, prepared for Georgia Power Company by J. E. Edinger Associates, Inc., Wayne, PA.

CE-QUAL-W2 BIBLIOGRAPHY

- _____. 1989. "Probabilistic Hydrothermal Modeling Study of Clinton Lake, Exhibit D", *Document No. 89-15-R*, prepared for Illinois Power Company, Decatur, IL 62525. Prepared by J. E. Edinger Associates, Inc., Wayne, PA.
- _____. 1993. "Harlee Branch Impact on Dissolved Oxygen of Lake Sinclair", *Document No. January 18*, prepared for Georgia Power Company Environmental Affairs, Atlanta, Georgia. Prepared by J. E. Edinger Associates, Inc., Wayne, PA.
- Edinger, J. E., E. M. Buchak, J. Loos, and E. Krueger. 1986. "Effects of the Chalk Point Steam Electric Station on BOD and DO in the Patuxent Estuary", *Document No. 86-56-R*, Potomac Electric Power Company, Environmental Affairs Group, Water and Land Use Department, Washington, DC 20068, prepared by J. E. Edinger Associates, Inc., Wayne, PA.
- Edinger, J.E., E.M. Buchak, and N.C. Huang. 1988. "Chalk Point Steam Electric Station Patuxent Estuary Hydrodynamic and Transport Model Verification and Real Time Intake Entrainment Rates for 1985 Larval Sampling", *Document No. 88-77-R*, prepared for Potomac Electric Power Company, Environmental Affairs Group, Water and Land Use Department, Washington, D.C. 20068. Prepared by J. E. Edinger Associates, Inc., Wayne, PA.
- _____. 1989. "Verification of Nechako Reservoir Hydrothermal Model", *Document No. 89-130-R*, prepared for Triton Environmental Consultants, Ltd., Burnaby, British Columbia V5M 3Z3. Prepared by J. E. Edinger Associates, Inc., Wayne, PA.
- Edward K. Noda and Associates, Inc. 1992. "Ala Wai Canal Improvement, Feasability Report", prepared for Hawaii Department of Land and Natural Resources, Division of Water and Land Development.
- Energy & Environmental Management, Inc. 1990. "Gorge Power Station Load Management Project", prepared for Ohio Edison Company, Ohio.
- Envirocon Pacific Limited and J. E. Edinger Associates, Inc. 1989. "Nechako Reservoir Mathematical Modeling Program Preliminary Results and Conclusions", prepared for Alcan Smelters & Chemicals Ltd., Vancouver, British Columbia.
- Environmental Consulting & Technology, Inc. 1999. "Thermal Modeling Report: Fort Myers Power Plant Repowering Project". ECT No. 98615-0100. Prepared for Florida Power & Light Company, Juno Beach, FL.
- Environmental Consulting & Technology, Inc. 1999. "Thermal Impact Study for S-79 Lock Operation: Fort Myers Power Plant Repowering Project". ECT No. 98615-0100. Prepared for Florida Power & Light Company, Juno Beach, FL.
- Environmental Consulting & Technology, Inc. 1999. "Manatee Protection Modeling Report: Fort Myers Power Plant Repowering Project". ECT No. 98615-0100. Prepared for Florida Power & Light Company, Juno Beach, FL.
- Environmental and Hydraulics Laboratory. 1986. "CE-QUAL-W2: A Numerical Two-Dimensional, Laterally Averaged Model of Hydrodynamics and Water Quality; User's Manual", *Instruction Rpt. E-86-5*. U.S. Army Engineer Waterways Experiment Station, Vicksburg, MS.

CE-QUAL-W2 BIBLIOGRAPHY

- EPA. 1994. "Alaska Juneau Gold Mine Project", Technical Assistance Report for the U.S. Army Corps of Engineers Alaska District, EPA 910/B-94-007.
- FERC. 1992. "Proposed Modifications to the Lower Mokelumne River Project, California", Draft Environmental Impact Statement, Federal Energy Regulatory Commission Office of Hydro-power Licensing, FERC Project No. 2916-004.
- Flowers, J.D., L.M. Hauch, and R.L. Kiesling. 2001. "Water Quality Modeling of Lake Waco Using CE-QUAL-W2 for Assessment of Phosphorus Control Strategies". *TR0114*, Texas Institute for Applied Environmental Research, Tarleton State University, Stephenville, Texas.
- FTN Associates. 2001. "Center Hill Lake CE-QUAL-W2 Water Quality Model". Prepared for U.S. Army Corps of Engineers, Nashville District, Contract DACW 62-98-D-0002, Delivery Order No. 0011.
- FTN Associates. 1998. "Taylorsville Lake Water Quality Model Study". Prepared for U.S. Army Corps of Engineers, Louisville District, Louisville, KY.
- Georgia Power Company. 1992. "Hydrological and Limnological Study of Lake Sinclair in Support of Application for Renewal and Modification of a Thermal Variance for Plant Branch NPDES Permit No. GA00026051", prepared for Georgia Power Company, Atlanta, Georgia by EA Engineering Science and Technology, Atlanta, Georgia and J. E. Edinger Associates, Inc., Wayne, PA.
- Giorgino, M.J., J.D. and Bales. 1997. "Rhodhiss Lake, North Carolina: Analysis of Ambient Conditions and Simulation of Hydrodynamics, Constituent Transport, and Water-Quality Characteristics, 1993-94". *U.S. Geological Survey Water-Resources Investigations Report 97-4131*, 62 p.
- Gorgens, A.H.M, A.J. Bath, A. Venter, K. De Smidt, G.v.R. Marais. 1993. "The Applicability of Hydrodynamic Reservoir Models for Water Quality Management of Stratified Water Bodies in South Africa", Report to the Water Research Commission, WRC Report No. 304/1/93.
- Green, W.R. 2001. "Analysis of Ambient Conditions and Simulation of Hydrodynamics, Constituent Transport, and Water-Quality Characteristics in Lake Maumelle, Arkansas, 1991-92. *USGS Water-Resources Investigations Report 01-4045*.
- Hall, R. W. 1987. "Application of CE-QUAL-W2 to the Savannah River Estuary", *Technical Rpt. EL-87-4*, U.S. Army Engineer Waterways Experiment Station, Vicksburg, MS.
- Jain, R., G. A. Krallis and E. M. Buchak. 2000. "Sammamish River Temperature Study: 1998 and 1999 CE-QUAL-W2 Calibration and Management Scenarios". Prepared for Seattle District, Corps of Engineers, Seattle, Washington. Prepared by J. E. Edinger Associates, Inc., Wayne, Pennsylvania. 15 September.
- Johnson, B. H. 1981. "A Review of Numerical Reservoir Hydrodynamic Modeling", *Technical Rpt. E-81-2*, U.S. Army Engineer Waterways Experiment Station, Vicksburg, MS.

CE-QUAL-W2 BIBLIOGRAPHY

- Johnson, B. H., M. J. Trawle and P. G. Kee. 1989. "A Numerical Model Study of the Effect of Channel Deepening on Shoaling and Salinity Intrusion in the Savannah Estuary", *Technical Rpt. HL-89-26*, Hydraulics Laboratory, Department of the Army, Waterways Experiment Station, Vicksburg, MS.
- Kinhill Cameron McNamara Pty Ltd. 1991. Proposed Third Runway Sydney Kingsford-Smith. Airport, Botany Bay Borrow Pit, Water Quality", Milton Queensland, Australia.
- Martin, J. L. 1988. "Application of a Two-Dimensional Model of Hydrodynamics and Water Quality CE-QUAL-W2. to DeGray Lake, Arkansas", *Technical Rpt. E-87-1*, U.S. Army Engineer Waterways Experiment Station, Vicksburg, MS.
- McKee, C. P., Thackston, E. L., Speece, R. E., Wilson, D. J., Cardozo, R. J. 1992. "Modeling of Water Quality in Cheatham Lake", *Technical Rpt. No. 42*, Environmental and Water Resources Engineering, Vanderbilt University, Nashville, TN.
- Mobley, M.H., D. McGinnis, and R.J. Ruane. 1999. "Conceptual Design Report for the Shepaug Oxygen Diffuser System". Tennessee Valley Authority report WR99-1-760-128.
- Ormsbee, L., L. Jarrett, and B. Perkins. 1998. Kentucky River Basin Water Quality Assessment Study. *Kentucky Water Resources Institute (KWRI) Technical Report*. pp. 110.
- Owoputi, L. 1998. "Water Quality Model Development for Stonewall Jackson Lake and the West Fork River". Prepared for USACE Pittsburg District, Contract No. DACW59-96-D-0005, Delivery Order No. 6.
- Risley, J.C. 2000. "Effects of Hypothetical Management Scenarios on Water Temperatures in the Tualatin River, Oregon", U.S. Geological Survey Water-Resources Investigations Report 00-4071 (supplement to Water-Resources Investigations Report 97-4071), 110 p. http://oregon.usgs.gov/pubs_dir/Online/Pdf/00-4071.pdf
- Risley, J.C. 1997. Relations of Tualatin River Water Temperatures to Natural and Human-Caused Factors: U.S. Geological Survey Water-Resources Investigations Report 97-4071, 143 p. http://oregon.usgs.gov/pubs_dir/Online/Pdf/97-4071.pdf
- Rounds, S.A. and T.M. Wood. 2001. "Modeling Water Quality in the Tualatin River, Oregon, 1991-1997". USGS Water Resources Investigations Report 01-4041.
- Rounds, S.A., T.M. Wood, and D.D. Lynch. 1998. "Modeling Discharge, Temperature, and Water Quality in the Tualatin River, Oregon". USGS Open-File Report 98-186.
- Tetra Tech. 2002. "Pineview Reservoir TMDL". Prepared for Utah Department of Environmental Quality.
- Tillman, D. H., and Cole, T. M. 1993. "Bluestone Phase 2 Temperature and Dissolved Oxygen Modeling Study", *Technical Rpt. EL-93-*, U.S. Army Engineer Waterways Experiment Station, Vicksburg, MS.

CE-QUAL-W2 BIBLIOGRAPHY

- Tillman, D.H., T.M. Cole, and B.W. Bunch. 1999. "Detailed Reservoir Water Quality Modeling (CE-QUAL-W2), Alabama-Coosa-Tallapoosa/Apalachicola-Chattahoochee-Flint (ACT-ACF) Comprehensive Water Resource Study". Technical Report EL-99-XXX, U.S. Army Engineer Waterways Experiment Station, Vicksburg, MS.
- URS Corporation. 1986. "Southern Puget Sound Water Quality Assessment Study, Final Report, Comprehensive Circulation and Water Quality Study of Budd Inlet", prepared for Washington State Department of Ecology. By URS Corporation, Seattle, WA.
- Waide, J. B., Dortch, M. S., and Cole, T. M., 1984. "Two-Dimensional Reservoir Model", *EWQOS Information Exchange Bulletin*, Vol. E-84-3, U.S. Army Engineer Waterways Experiment Station, Vicksburg, MS.
- Wells, S. A. 1992. "Assessment of Management Alternatives for Water Quality Improvement in the Columbia Slough System, Volume 1: Technical Report", *Technical Rpt. EWR-001-92*, Department of Civil Engineering, Portland State University, Portland, OR.
- _____. 1992. "User Manual for the Columbia Slough Model using CE-QUAL-W2", *Technical Rpt. EWR-003-92*, Department of Civil Engineering, Portland State University, Portland, OR.
- Wells, S. A., Berger, C., and Knutson, M. 1992. "Modeling the Tualatin River System Including Scoggins Creek and Hagg Lake: Model Description, Geometry, and Forcing Data", *Technical Rpt. EWR-010-92*, Department of Civil Engineering, Portland State University, Portland, OR.
- Wells, S.A. and T.M. Cole. 2000. "Theoretical Basis for the CE-QUAL-W2 River Basin Model." ERDC/EL TR-00-7, U.S. Army Engineer Research and Development Center, Vicksburg, MS.
- Yager, R.E. 1996. "Application of CE-QUAL-W2 to Lake Cumberland". Report prepared by Environmental Consulting Engineers for U.S. Army Corps of Engineers, Nashville District, Nashville, Tennessee.

Appendix A Hydrodynamics and Transport

CE-QUAL-W2 uses the laterally averaged equations of fluid motion derived from the three dimensional equations, which consist of six equations and six unknowns. Their development is described below.

Coordinate System

The general coordinate system used in the development of the laterally averaged equations of fluid motion is shown in [Figure A-1](#).

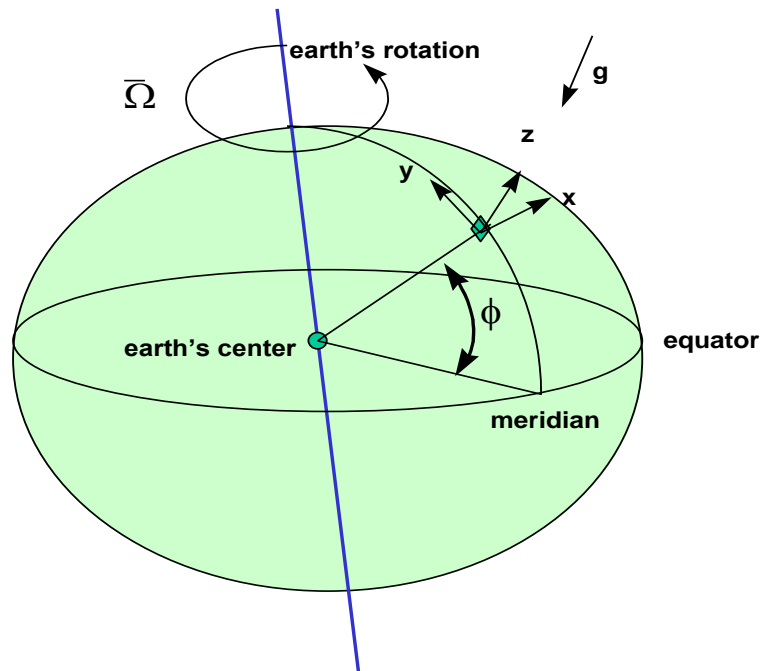


Figure A-1. Definition sketch of coordinate system for governing equations where x is oriented east, y is oriented north, and z is oriented upward.

Note that Ω is a vector that represents the angular velocity of the earth spinning on its axis. The rotation of the coordinate system can result in significant horizontal accelerations of fluids. This

is usually restricted to large water bodies such as large lakes and ocean systems. The force that causes horizontal accelerations because of the spinning coordinate system is termed the Coriolis force.

Turbulent Time-Averaged Equations

The governing equations are obtained by performing a mass and a momentum balance of the fluid phase about a control volume. The resulting equations are the continuity (or conservation of fluid mass) and the conservation of momentum equations for a rotating coordinate system (Batchelor, 1967; Sabersky et al., 1989; Cushman-Roisin, 1994). After using the coordinate system in [Figure A-1](#), applying the following assumptions:

1. incompressible fluid
2. centripetal acceleration is a minor correction to gravity
3. Boussinesq approximation
4. $\frac{1}{\rho} = \frac{1}{\rho_o + \Delta\rho} \approx \frac{1}{\rho_o}$ where $\rho = \rho_o + \Delta\rho$; ρ_o is a base value
and $\Delta\rho$ has all variations in ρ

and substituting the turbulent time averages of velocity and pressure as defined below:

all velocities and pressure are considered the sum of turbulent time averages and deviations from that average, i.e., $u = \bar{u} + u'$, where $\bar{u} = \frac{1}{T} \int_t^{t+T} u dt$ as shown in [Figure A-2](#). The other terms are $v = \bar{v} + v'$; $w = \bar{w} + w'$ and $p = \bar{p} + p'$ where the overbar represents time averaged and the prime represents deviation from the temporal average;

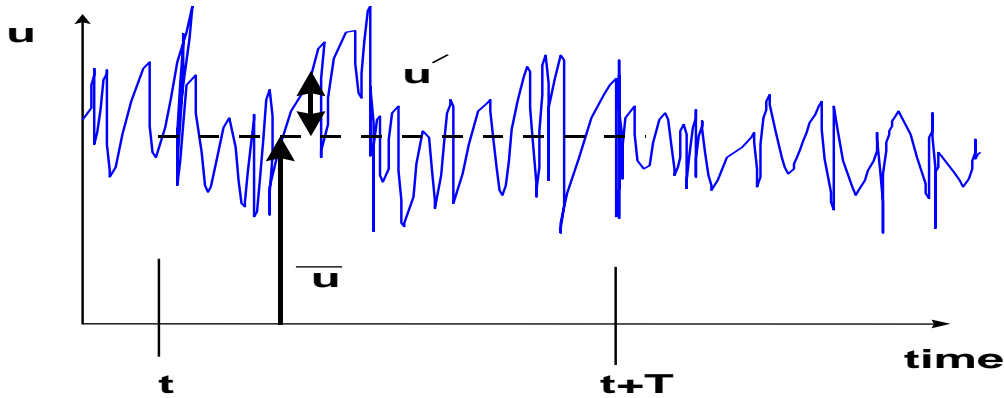


Figure A-2. Definition sketch of turbulent time averaging for velocity.

The governing equations become after simplification:

Continuity

$$\frac{\partial \bar{u}}{\partial x} + \frac{\partial \bar{v}}{\partial y} + \frac{\partial \bar{w}}{\partial z} = 0 \quad (\text{A-1})$$

where:

\bar{u} = x-direction velocity

\bar{v} = y-direction velocity

\bar{w} = z-direction velocity

x-Momentum Equation

$$\underbrace{\frac{\partial \bar{u}}{\partial t}}_{\text{unsteady acceleration}} + \underbrace{\bar{u} \frac{\partial \bar{u}}{\partial x} + \bar{v} \frac{\partial \bar{u}}{\partial y} + \bar{w} \frac{\partial \bar{u}}{\partial z}}_{\text{convective acceleration}} - \underbrace{2\Omega_z \bar{v} + 2\Omega_y \bar{w}}_{\text{Coriolis acceleration}} = -\underbrace{\frac{1}{\rho} \frac{\partial \bar{p}}{\partial x}}_{\text{pressure gradient}} + \underbrace{\frac{\mu}{\rho} \left(\frac{\partial^2 \bar{u}}{\partial x^2} + \frac{\partial^2 \bar{u}}{\partial y^2} + \frac{\partial^2 \bar{u}}{\partial z^2} \right)}_{\text{viscous stresses}} + \underbrace{\frac{1}{\rho} \left(\frac{\partial \tau_{xx}}{\partial x} + \frac{\partial \tau_{xy}}{\partial y} + \frac{\partial \tau_{xz}}{\partial z} \right)}_{\text{turbulent stresses}} \quad (\text{A-2})$$

where:

τ_{xx} = turbulent shear stress acting in x direction on the x-face of control volume

τ_{xy} = turbulent shear stress acting in x direction on the y-face of control volume

τ_{xz} = turbulent shear stress acting in x direction on the z-face of control volume

μ = dynamic viscosity

Ω = component of Coriolis acceleration where:

$$\Omega_z = \Omega_E \sin \phi$$

$$\Omega_y = \Omega_E \cos \phi$$

ϕ = latitude

Ω_E = earth's rotation rate

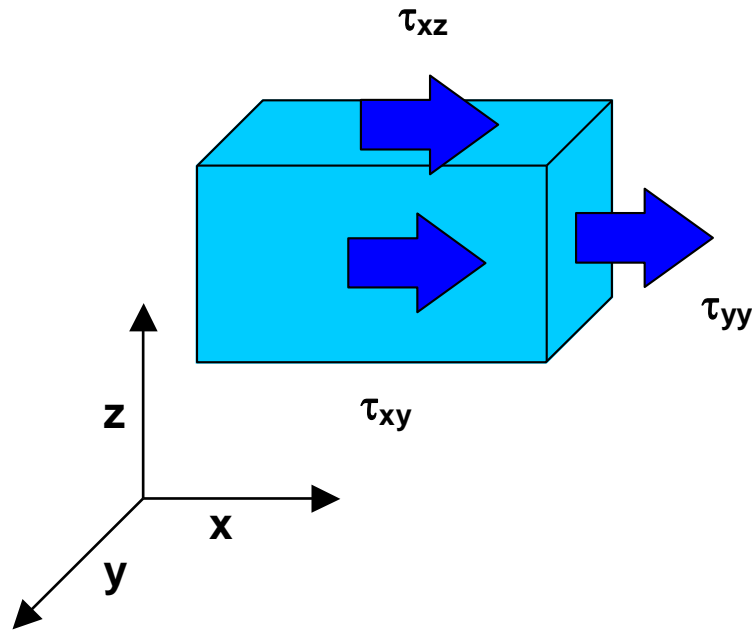


Figure A-3. Definition sketch of turbulent shear stresses in x-direction.

y-Momentum Equation

$$\begin{aligned} \frac{\partial \bar{v}}{\partial t} + \bar{u} \frac{\partial \bar{v}}{\partial x} + \bar{v} \frac{\partial \bar{v}}{\partial y} + \bar{w} \frac{\partial \bar{v}}{\partial z} + 2\Omega_x \bar{u} - 2\Omega_x \bar{w} = \\ -\frac{1}{\rho} \frac{\partial \bar{p}}{\partial y} + \frac{\mu}{\rho} \left(\frac{\partial^2 \bar{v}}{\partial x^2} + \frac{\partial^2 \bar{v}}{\partial y^2} + \frac{\partial^2 \bar{v}}{\partial z^2} \right) + \frac{1}{\rho} \left(\frac{\partial \tau_{yx}}{\partial x} + \frac{\partial \tau_{yy}}{\partial y} + \frac{\partial \tau_{yz}}{\partial z} \right) \end{aligned} \quad (\text{A-3})$$

where:

τ_{yx} = turbulent shear stress acting in y direction on the x-face of control volume

τ_{yy} = turbulent shear stress acting in y direction on the y-face of control volume

τ_{yz} = turbulent shear stress acting in y direction on the z-face of control volume

$\Omega_x = 0$

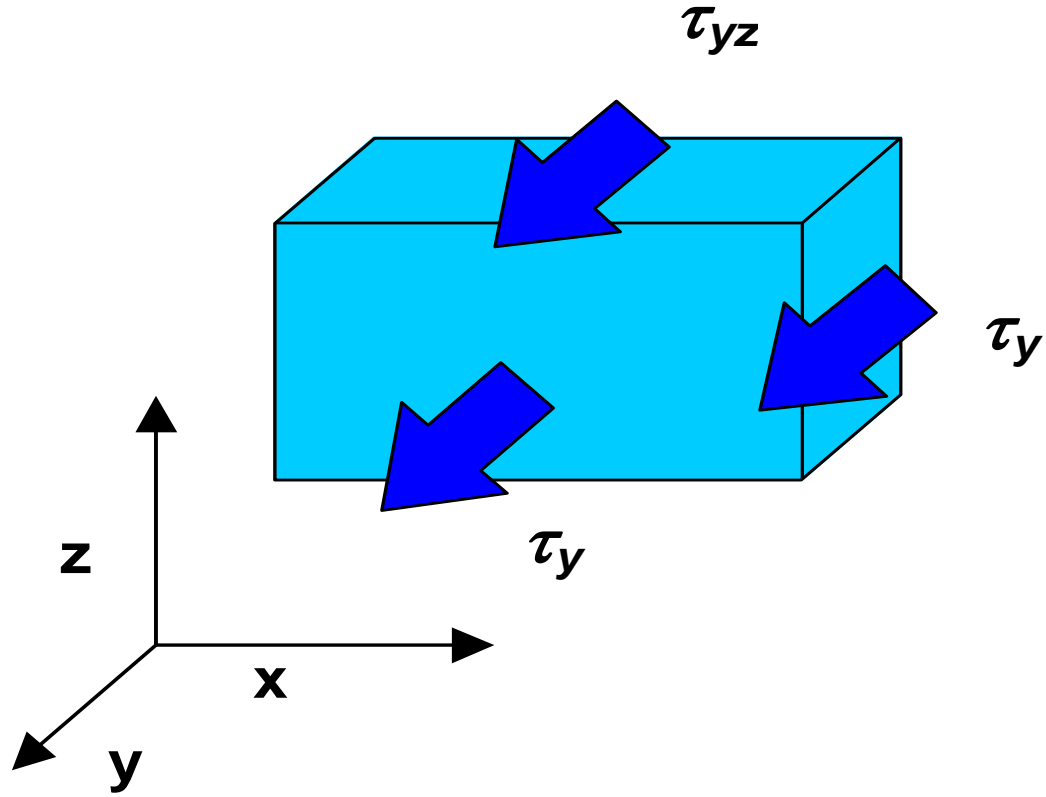


Figure A-4. Sketch of turbulent shear stresses in y-direction.

z-Momentum Equation

$$\begin{aligned} \frac{\partial \bar{w}}{\partial t} + \bar{u} \frac{\partial \bar{w}}{\partial x} + \bar{v} \frac{\partial \bar{w}}{\partial y} + \bar{w} \frac{\partial \bar{w}}{\partial z} - 2\Omega_y \bar{u} + 2\Omega_x \bar{v} = -g \\ - \frac{1}{\rho} \frac{\partial \bar{p}}{\partial z} + \frac{\mu}{\rho} \left(\frac{\partial^2 \bar{w}}{\partial x^2} + \frac{\partial^2 \bar{w}}{\partial y^2} + \frac{\partial^2 \bar{w}}{\partial z^2} \right) + \frac{1}{\rho} \left(\frac{\partial \tau_{zx}}{\partial x} + \frac{\partial \tau_{zy}}{\partial y} + \frac{\partial \tau_{zz}}{\partial z} \right) \end{aligned} \quad (\text{A-4})$$

where:

τ_{zx} = turbulent shear stress acting in z direction on the x-face of control volume

τ_{zy} = turbulent shear stress acting in z direction on the y-face of control volume

τ_{zz} = turbulent shear stress acting in z direction on the z-face of control volume

$\Omega_x = 0$

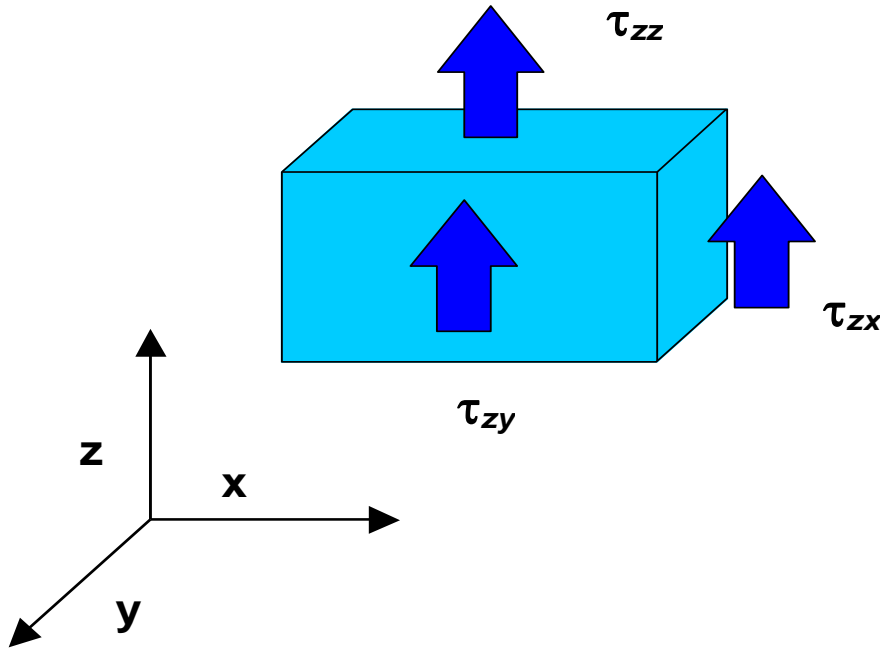


Figure A-5. Sketch of turbulent shear stresses in z-direction.

Note that the turbulent shear stresses are defined as follows:

$$\tau_{xx} = \overline{\rho u' u'}$$

$$\tau_{xy} = \overline{\rho u' v'} \text{ is the same as } \tau_{yx} = \overline{\rho v' u'}$$

$$\tau_{xz} = \overline{\rho u' w'} \text{ is the same as } \tau_{zx} = \overline{\rho w' u'}$$

$$\tau_{yy} = \overline{\rho v' v'}$$

$$\tau_{yz} = \overline{\rho v' w'} \text{ is the same as } \tau_{zy} = \overline{\rho w' v'}$$

$$\tau_{zz} = \overline{\rho w' w'}$$

Coriolis Effect

As noted above, all the Ω_x terms are zero and can be eliminated from the y and z-momentum equations. If one integrates over the y-direction (therefore assuming the net velocity in y is zero) and assumes that the horizontal length scale is much greater than vertical length scale, it can be shown by using scaling arguments that the Coriolis acceleration forces are negligible (Cushman-Roisin, 1994). Hence, prior to lateral averaging, the Coriolis acceleration terms will be neglected.

Adjusting the Coordinate System

The coordinate system is transformed into a form compatible with the original W2 development where the vertical axis is in the direction of gravity. In addition, as shown in [Figure A-6](#), the coordinate system is oriented along an arbitrary slope.

Coordinate System

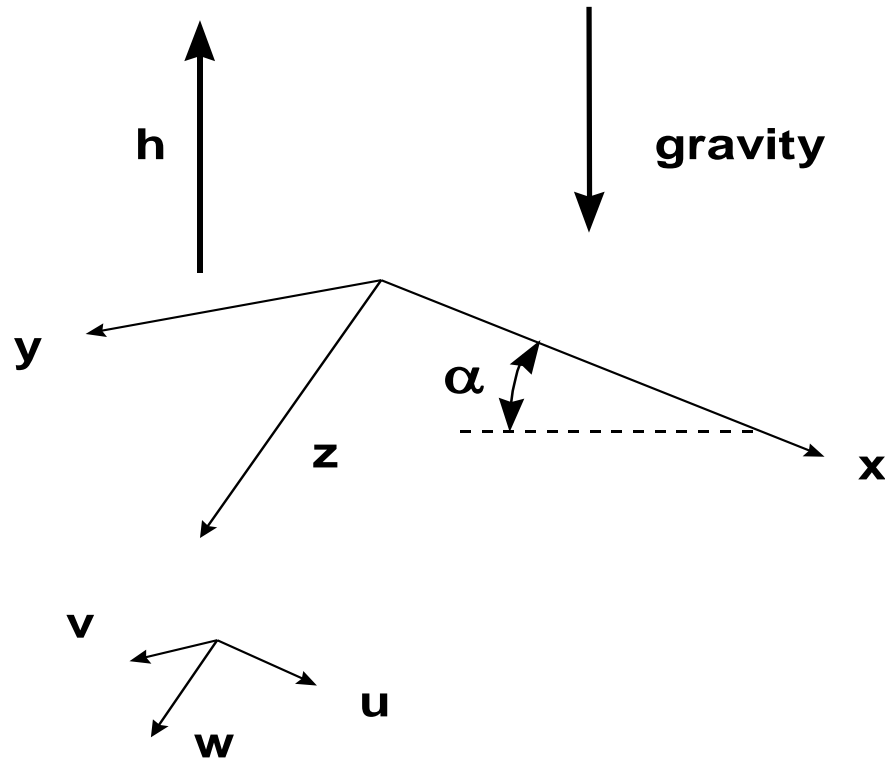


Figure A-6. General coordinate system with z-axis compatible with original derivation of W2 model.

The gravity acceleration is a body force that is then represented by a vector:

$$\vec{g} = -g\vec{\nabla}h \quad (\text{A-5})$$

where:

h = surface normal from the earth's surface

g = gravitational acceleration, 9.8 m s^{-2} .

This term can be written as three vector components:

$$g_x = -g \frac{\partial h}{\partial x} \quad (\text{A-6})$$

$$g_y = -g \frac{\partial h}{\partial y} \quad (\text{A-7})$$

$$g_z = -g \frac{\partial h}{\partial z} \quad (\text{A-8})$$

These gravity components can be applied to an arbitrary channel slope as shown in [Figure A-7](#).

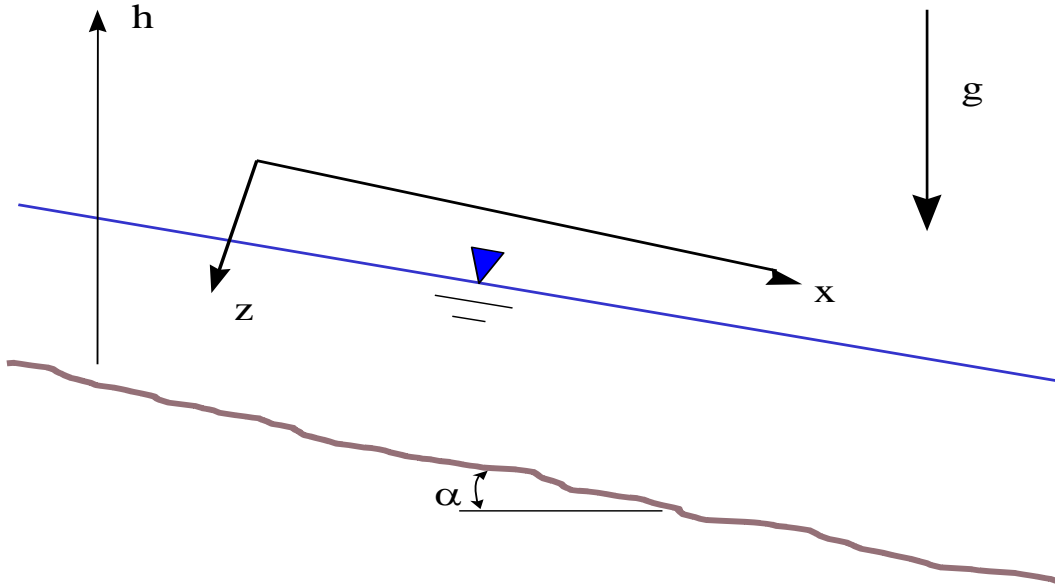


Figure A-7. Sketch of channel slope and coordinate system for W2 where the x-axis is oriented along the channel slope.

The channel slope can also be incorporated into the definition of the gravity vector if the x-axis is chosen parallel to the channel slope as:

The channel slope is defined as:

$$S_o = \tan \alpha \quad (\text{A-9})$$

and also:

$$g_x = -g \frac{\partial h}{\partial x} = g \sin \alpha \quad (\text{A-10})$$

$$g_z = -g \frac{\partial h}{\partial z} = g \cos \alpha \quad (\text{A-11})$$

The gravity acceleration in y is assumed negligible since $\frac{\partial h}{\partial y} = 0$ in the lateral direction of the channel.

Governing Equations for General Coordinate System

After redefining the coordinate system, eliminating Coriolis effects, and neglecting viscous shear stresses the governing equations become:

Continuity

$$\frac{\partial \bar{u}}{\partial x} + \frac{\partial \bar{v}}{\partial y} + \frac{\partial \bar{w}}{\partial z} = 0 \quad (\text{A-12})$$

x-Momentum Equation

$$\underbrace{\frac{\partial \bar{u}}{\partial t}}_{\text{unsteady acceleration}} + \underbrace{\bar{u} \frac{\partial \bar{u}}{\partial x} + \bar{v} \frac{\partial \bar{u}}{\partial y} + \bar{w} \frac{\partial \bar{u}}{\partial z}}_{\text{convective acceleration}} = \underbrace{g \sin \alpha}_{\text{gravity}} - \underbrace{\frac{1}{\rho} \frac{\partial \bar{p}}{\partial x}}_{\text{pressure gradient}} + \underbrace{\frac{1}{\rho} \left(\frac{\partial \tau_{xx}}{\partial x} + \frac{\partial \tau_{xy}}{\partial y} + \frac{\partial \tau_{xz}}{\partial z} \right)}_{\text{turbulent shear stresses}} \quad (\text{A-13})$$

y-Momentum Equation

$$\underbrace{\frac{\partial \bar{v}}{\partial t}}_{\text{unsteady acceleration}} + \underbrace{\bar{u} \frac{\partial \bar{v}}{\partial x} + \bar{v} \frac{\partial \bar{v}}{\partial y} + \bar{w} \frac{\partial \bar{v}}{\partial z}}_{\text{convective acceleration}} = - \underbrace{\frac{1}{\rho} \frac{\partial \bar{p}}{\partial y}}_{\text{pressure gradient}} + \underbrace{\frac{1}{\rho} \left(\frac{\partial \tau_{yx}}{\partial x} + \frac{\partial \tau_{yy}}{\partial y} + \frac{\partial \tau_{yz}}{\partial z} \right)}_{\text{turbulent shear stresses}} \quad (\text{A-14})$$

z-Momentum Equation

$$\underbrace{\frac{\partial \bar{w}}{\partial t}}_{\text{unsteady acceleration}} + \underbrace{\bar{u} \frac{\partial \bar{w}}{\partial x} + \bar{v} \frac{\partial \bar{w}}{\partial y} + \bar{w} \frac{\partial \bar{w}}{\partial z}}_{\text{convective acceleration}} = \underbrace{g \cos \alpha}_{\text{gravity}} - \underbrace{\frac{1}{\rho} \frac{\partial \bar{p}}{\partial z}}_{\text{pressure gradient}} + \underbrace{\frac{1}{\rho} \left(\frac{\partial \tau_{zx}}{\partial x} + \frac{\partial \tau_{zy}}{\partial y} + \frac{\partial \tau_{zz}}{\partial z} \right)}_{\text{turbulent shear stresses}} \quad (\text{A-15})$$

Simplification of z-Momentum Equation

If the longitudinal length scale is much greater than the vertical length scale, then this makes all vertical velocities \ll horizontal velocities. A result of this assumption is that vertical velocities are very small such that the z-momentum equation becomes the hydrostatic equation:

$$\frac{1}{\rho} \frac{\partial \bar{p}}{\partial z} = g \cos \alpha \quad (\text{A-16})$$

This assumption prevents the model from accurately modeling vertical accelerations of the fluid because of convective cooling at night and other such vertical accelerations.

Lateral Averaging

The governing equations above will be laterally averaged after decomposing all velocities and pressure into a lateral average and a deviation from the lateral average. The lateral, longitudinal, and vertical velocities and pressure are defined as follows:

$$\bar{v} = \bar{\bar{v}} + v'' \quad (\text{A-17})$$

$$\bar{u} = \bar{\bar{u}} + u'' \quad (\text{A-18})$$

$$\bar{w} = \bar{\bar{w}} + w'' \quad (\text{A-19})$$

$$\bar{p} = \bar{\bar{p}} + p'' \quad (\text{A-20})$$

where:

$$\bar{\bar{u}} = \frac{1}{B} \int_{y_1}^{y_2} \bar{u} dy$$

B = control volume width, *m*

y₁ = left bank coordinate

y₂ = right bank coordinate

The double overbars represent the spatial average of the temporal average quantity. The double prime represents the deviation from the lateral average and is a function of *y*. This is shown in [Figure A-8](#).

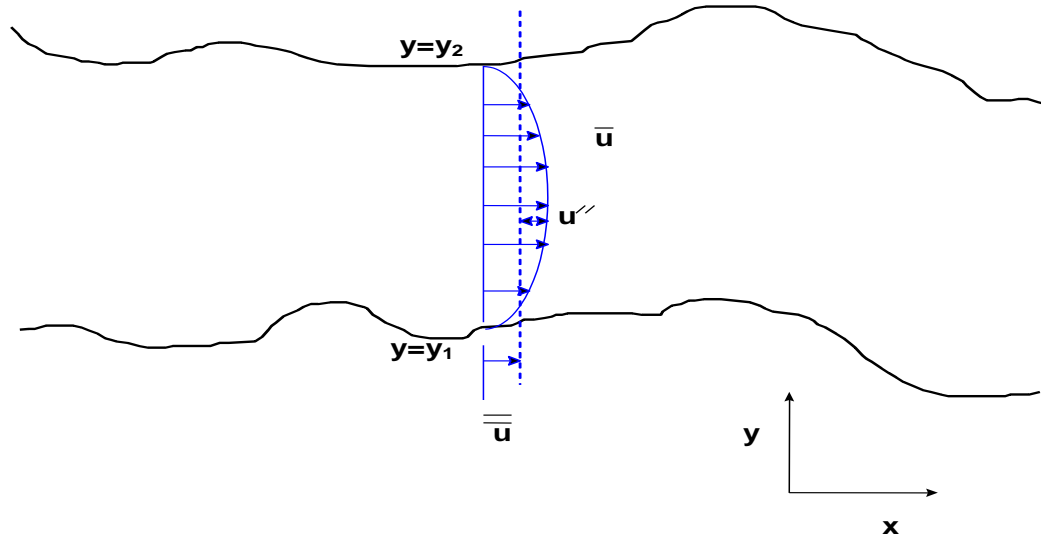


Figure A-8. Lateral average and deviation from lateral average components of longitudinal velocity.

These definitions are substituted into the turbulent time-average governing equations and then laterally averaged. The y-momentum equation is neglected since the average lateral velocities are zero ($\bar{v} = 0$) and cross shear stresses that contribute to vertical mixing will be computed from the analysis of wind stress. The equations that remain are the continuity, x-momentum, and z-momentum equations.

Continuity Equation

The continuity equation becomes after substituting the above velocity components and laterally averaging

$$\frac{\partial(\bar{\bar{u}} + u'')}{\partial x} + \frac{\partial(\bar{\bar{v}} + v'')}{\partial y} + \frac{\partial(\bar{\bar{w}} + w'')}{\partial z} = 0 \quad (\text{A-21})$$

The lateral average of a double primed variable is by definition zero:

$$\bar{\bar{u}}'' = \frac{1}{B} \int_{y1}^{y2} u'' dy = 0 \quad (\text{A-22})$$

Also, note that:

$$\begin{aligned}
 \frac{\partial(\bar{\bar{v}} + v'')}{\partial y} &= \frac{1}{B} \int_{y1}^{y2} \frac{\partial(\bar{\bar{v}} + v'')}{\partial y} dy \\
 &= \frac{(\bar{\bar{v}} + v'')}{B} \Big|_{y1}^{y2} \\
 &= \frac{v''}{B} \Big|_{y1}^{y2} \\
 &= q
 \end{aligned} \tag{A-23}$$

where q is defined as the net lateral inflow per unit volume of cell [T⁻¹], and:

$$\begin{aligned}
 \frac{\partial(\bar{\bar{u}} + u'')}{\partial x} &= \frac{1}{B} \int_{y1}^{y2} \frac{\partial(\bar{\bar{u}} + u'')}{\partial x} dy \\
 &= \frac{1}{B} \int_{y1}^{y2} \frac{\partial \bar{\bar{u}}}{\partial x} dy + \frac{1}{B} \int_{y1}^{y2} \frac{\partial u''}{\partial x} dy \\
 &= \frac{1}{B} \frac{\partial}{\partial x} \int_{y1}^{y2} \bar{\bar{u}} dy \\
 &= \frac{1}{B} \frac{\partial \bar{\bar{B}u}}{\partial x}
 \end{aligned} \tag{A-24}$$

and:

$$\begin{aligned}
 \frac{\partial(\bar{\bar{w}} + w'')}{\partial z} &= \frac{1}{B} \int_{y1}^{y2} \frac{\partial(\bar{\bar{w}} + w'')}{\partial z} dy \\
 &= \frac{1}{B} \int_{y1}^{y2} \frac{\partial \bar{\bar{w}}}{\partial z} dy + \frac{1}{B} \int_{y1}^{y2} \frac{\partial w''}{\partial z} dy \\
 &= \frac{1}{B} \frac{\partial}{\partial z} \int_{y1}^{y2} \bar{\bar{w}} dy \\
 &= \frac{1}{B} \frac{\partial \bar{\bar{B}w}}{\partial z}
 \end{aligned} \tag{A-25}$$

Combining terms, the continuity equation becomes:

$$\frac{\partial \bar{\bar{B}u}}{\partial x} + \frac{\partial \bar{\bar{B}w}}{\partial z} = qB \tag{A-26}$$

x-Momentum Equation

The laterally-averaged x-momentum equation is more easily simplified by writing it in conservative form (this can be verified by using the continuity equation with the x-momentum equation),

$$\begin{aligned} \frac{\partial(\bar{u} + u'')}{\partial t} + \frac{\partial(\bar{u} + u'')(\bar{u} + u'')}{\partial x} + \frac{\partial(\bar{v} + v'')(\bar{u} + u'')}{\partial y} + \frac{\partial(\bar{w} + w'')(\bar{u} + u'')}{\partial z} \\ = \overline{g \sin \alpha} - \frac{1}{\rho} \frac{\partial(\bar{p} + p'')}{\partial x} + \frac{1}{\rho} \left(\frac{\partial \tau_{xx}}{\partial x} + \frac{\partial \tau_{xy}}{\partial y} + \frac{\partial \tau_{xz}}{\partial z} \right) \end{aligned} \quad (\text{A-27})$$

27)

Each term in this equation can be simplified as follows (note that the spatial average of any double primed variable goes to zero by definition).

The unsteady acceleration term:

$$\begin{aligned} \frac{\partial(\bar{u} + u'')}{\partial t} &= \frac{1}{B} \int_{y1}^{y2} \frac{\partial(\bar{u} + u'')}{\partial t} dy \\ &= \frac{1}{B} \int_{y1}^{y2} \frac{\partial \bar{u}}{\partial t} dy + \frac{1}{B} \int_{y1}^{y2} \frac{\partial u''}{\partial t} dy \\ &= \frac{1}{B} \frac{\partial}{\partial t} \int_{y1}^{y2} \bar{u} dy + \frac{1}{B} \frac{\partial}{\partial t} \int_{y1}^{y2} u'' dy \\ &= \frac{1}{B} \frac{\partial B \bar{u}}{\partial t} \end{aligned} \quad (\text{A-28})$$

The convective acceleration terms:

$$\begin{aligned} \frac{\partial(\bar{u} + u'')(\bar{u} + u'')}{\partial x} &= \frac{1}{B} \int_{y1}^{y2} \frac{\partial(\bar{u} + u'')(\bar{u} + u'')}{\partial x} dy \\ &= \frac{1}{B} \int_{y1}^{y2} \frac{\partial \bar{u} \bar{u}}{\partial x} dy + \frac{1}{B} \int_{y1}^{y2} \frac{\partial 2\bar{u} u''}{\partial x} dy + \frac{1}{B} \int_{y1}^{y2} \frac{\partial u'' u''}{\partial x} dy \\ &= \frac{1}{B} \frac{\partial}{\partial x} \int_{y1}^{y2} \bar{u} \bar{u} dy + \frac{1}{B} \frac{\partial}{\partial x} \int_{y1}^{y2} u'' u'' dy \\ &= \frac{1}{B} \frac{\partial B \bar{u} \bar{u}}{\partial x} + \frac{1}{B} \frac{\partial}{\partial x} \underbrace{\int_{y1}^{y2} u'' u'' dy}_{\text{dispersion term}} \end{aligned} \quad (\text{A-29})$$

Similarly for the other two terms:

$$\frac{\overline{\partial(\bar{u} + u'')(\bar{w} + w'')}}{\partial z} = \frac{1}{B} \frac{\partial \overline{B u \bar{w}}}{\partial z} + \underbrace{\frac{1}{B} \frac{\partial}{\partial z} \int_{y1}^{y2} u'' w'' dy}_{\text{dispersion term}} \quad (\text{A-30})$$

$$\frac{\partial(\bar{u} + u'')(\bar{v} + v'')}{\partial y} = u'' v''|_{y2} - u'' v''|_{y1} = 0 \quad (\text{A-31})$$

The gravity term:

$$\overline{g \sin \alpha} = \frac{1}{B} \int_{y1}^{y2} g \sin \alpha dy = \frac{1}{B} (g \sin \alpha) \int_{y1}^{y2} dy = g \sin \alpha \quad (\text{A-32})$$

The pressure gradient term:

$$\begin{aligned} \frac{\overline{\partial(\bar{p} + p'')}}{\partial x} &= \frac{1}{B} \int_{y1}^{y2} \frac{\partial(\bar{p} + p'')}{\partial x} dy \\ &= \frac{1}{B} \int_{y1}^{y2} \frac{\partial \bar{p}}{\partial x} dy + \frac{1}{B} \int_{y1}^{y2} \frac{\partial p''}{\partial x} dy \\ &= \frac{1}{B} \frac{\partial}{\partial x} \int_{y1}^{y2} \bar{p} dy + \frac{1}{B} \frac{\partial}{\partial x} \int_{y1}^{y2} p'' dy \\ &= \frac{1}{B} \frac{\partial \overline{B \bar{p}}}{\partial x} \end{aligned} \quad (\text{A-33})$$

or the above equation can be written, assuming that the derivative of the lateral average pressure gradient in the x-direction is not a function of y:

$$\begin{aligned} \frac{\overline{\partial(\bar{p} + p'')}}{\partial x} &= \frac{1}{B} \int_{y1}^{y2} \frac{\partial(\bar{p} + p'')}{\partial x} dy \\ &= \frac{1}{B} \frac{\partial \bar{p}}{\partial x} \int_{y1}^{y2} dy + \frac{1}{B} \int_{y1}^{y2} \frac{\partial p''}{\partial x} dy \\ &= \frac{1}{B} \frac{\partial \bar{p}}{\partial x} B + \frac{1}{B} \frac{\partial}{\partial x} \int_{y1}^{y2} p'' dy \\ &= \frac{\partial \bar{p}}{\partial x} \end{aligned} \quad (\text{A-34})$$

Shear stresses

$$\begin{aligned}
 \overline{\left(\frac{\partial \tau_{xx}}{\partial x} + \frac{\partial \tau_{xy}}{\partial y} + \frac{\partial \tau_{xz}}{\partial z} \right)} &= \frac{1}{B} \int_{y1}^{y2} \frac{\partial \tau_{xx}}{\partial x} dy + \frac{1}{B} \int_{y1}^{y2} \frac{\partial \tau_{xy}}{\partial y} dy + \frac{1}{B} \int_{y1}^{y2} \frac{\partial \tau_{xz}}{\partial z} dy \\
 &= \frac{1}{B} \frac{\partial}{\partial x} \int_{y1}^{y2} \tau_{xx} dy + \frac{1}{B} \frac{\partial}{\partial x} \int_{y1}^{y2} \tau_{xy} dy + \frac{1}{B} \frac{\partial}{\partial z} \int_{y1}^{y2} \tau_{xz} dy \\
 &= \frac{1}{B} \left(\frac{\partial \overline{\tau_{xx}}}{\partial x} + \frac{\partial \overline{\tau_{xy}}}{\partial y} + \frac{\partial \overline{\tau_{xz}}}{\partial z} \right) = \frac{1}{B} \left(\frac{\partial \overline{\tau_{xx}}}{\partial x} + \frac{\partial \overline{\tau_{xz}}}{\partial z} \right)
 \end{aligned} \tag{A-35}$$

Collecting all terms and neglecting all dispersion terms, the final x-momentum equation is:

$$\frac{\partial \overline{B\bar{u}}}{\partial t} + \frac{\partial \overline{B\bar{u}\bar{u}}}{\partial x} + \frac{\partial \overline{B\bar{u}\bar{w}}}{\partial z} = Bg \sin \alpha - \frac{B}{\rho} \frac{\partial \bar{p}}{\partial x} + \frac{1}{\rho} \left(\frac{\partial \overline{\tau_{xx}}}{\partial x} + \frac{\partial \overline{\tau_{xz}}}{\partial z} \right) \tag{A-36}$$

Summary of Laterally Averaged Equations

In the development of CE-QUAL-W2 in Cole and Buchak (1995), the lateral average terms were represented by uppercase characters, such that $\bar{u} = U$, $\bar{w} = W$, and $\bar{p} = P$. The shear stress terms will be assumed lateral averages and the double overbars will be dropped for convenience. Making these simplifications, the governing equations become:

Continuity Equation

$$\frac{\partial UB}{\partial x} + \frac{\partial WB}{\partial z} = qB \tag{A-37}$$

x-Momentum Equation

$$\frac{\partial UB}{\partial t} + \frac{\partial UUB}{\partial x} + \frac{\partial WUB}{\partial z} = gB \sin \alpha - \frac{B}{\rho} \frac{\partial P}{\partial x} + \frac{1}{\rho} \frac{\partial B\tau_{xx}}{\partial x} + \frac{1}{\rho} \frac{\partial B\tau_{xz}}{\partial z} \tag{A-38}$$

z-Momentum Equation

$$\frac{1}{\rho} \frac{\partial P}{\partial z} = g \cos \alpha \tag{A-39}$$

There are now three equations and three unknowns - U , W , and P .

Simplification of Pressure Term

The z-momentum equation reduces to:

$$P = P_a + g \cos \alpha \int_{\eta}^z \rho dz \quad (\text{A-40})$$

after integration from a depth z to the water surface defined as $z=\eta$. P_a is the atmospheric pressure at the water surface ([Figure A-9](#)).

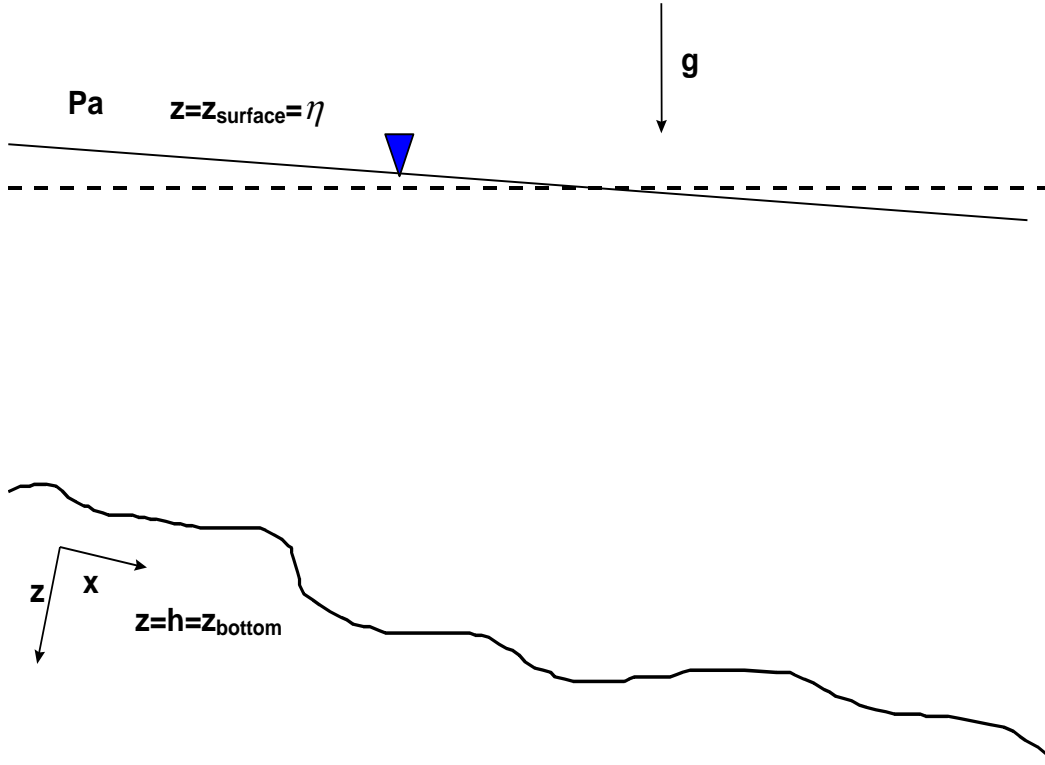


Figure A-9. Schematization for simplification of pressure term.

This equation for pressure is now substituted into the x-momentum equation and simplified using Leibnitz rule. The pressure gradient term in the x-momentum equation then becomes:

$$-\frac{1}{\rho} \frac{\partial P}{\partial x} = -\frac{1}{\rho} \frac{\partial P_a}{\partial x} + g \cos \alpha \frac{\partial \eta}{\partial x} - \frac{g \cos \alpha}{\rho} \int_{\eta}^z \frac{\partial \rho}{\partial x} dz \quad (\text{A-41})$$

The first term on the RHS is the atmospheric pressure term (accelerations due to atmospheric pressure changes over the water surface), the second is the barotropic pressure term (accelerations due to water surface variations), and the third is the baroclinic pressure term (accelerations due to density driven currents).

In CE-QUAL-W2, the atmospheric pressure term is assumed zero and is neglected. This implies that for long systems during severe storms the model will not be able to account for accelerations because of atmospheric changes. For a large physical domain, variations in meteorological forcing may be significant. This is discussed in the section on Variability in Meteorological Forcing. The pressure term then becomes:

$$-\frac{1}{\rho} \frac{\partial P}{\partial x} = g \cos \alpha \frac{\partial \eta}{\partial x} - \frac{g \cos \alpha}{\rho} \int_{\eta}^z \frac{\partial \rho}{\partial x} dz \quad (\text{A-42})$$

The revised form of the x-momentum equation is then:

$$\begin{aligned} \frac{\partial UB}{\partial t} + \frac{\partial UUB}{\partial x} + \frac{\partial WUB}{\partial z} = & gB \sin \alpha + g \cos \alpha B \frac{\partial \eta}{\partial x} - \frac{g \cos \alpha B}{\rho} \int_{\eta}^z \frac{\partial \rho}{\partial x} dz \\ & + \frac{1}{\rho} \frac{\partial B \tau_{xx}}{\partial x} + \frac{1}{\rho} \frac{\partial B \tau_{xz}}{\partial z} \end{aligned} \quad (\text{A-43})$$

Effectively, pressure has been removed from the unknowns by combining the z-momentum and x-momentum equations, but η has been added as an unknown.

Free Water Surface

This equation is a simplification of the continuity equation. The continuity equation integrated over the depth from the water surface to the bottom is called the free water surface equation. [Figure A-10](#) and [Figure A-11](#) are definition sketches for the computational grid without and with a channel slope, respectively.

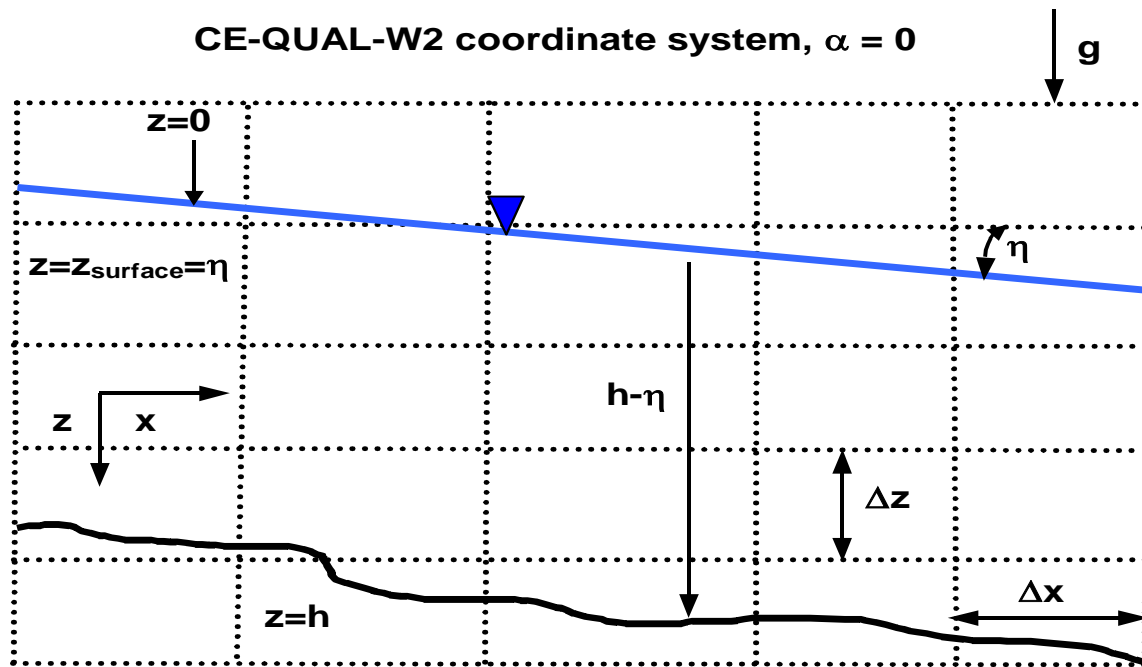


Figure A-10. Coordinate system without channel slope.

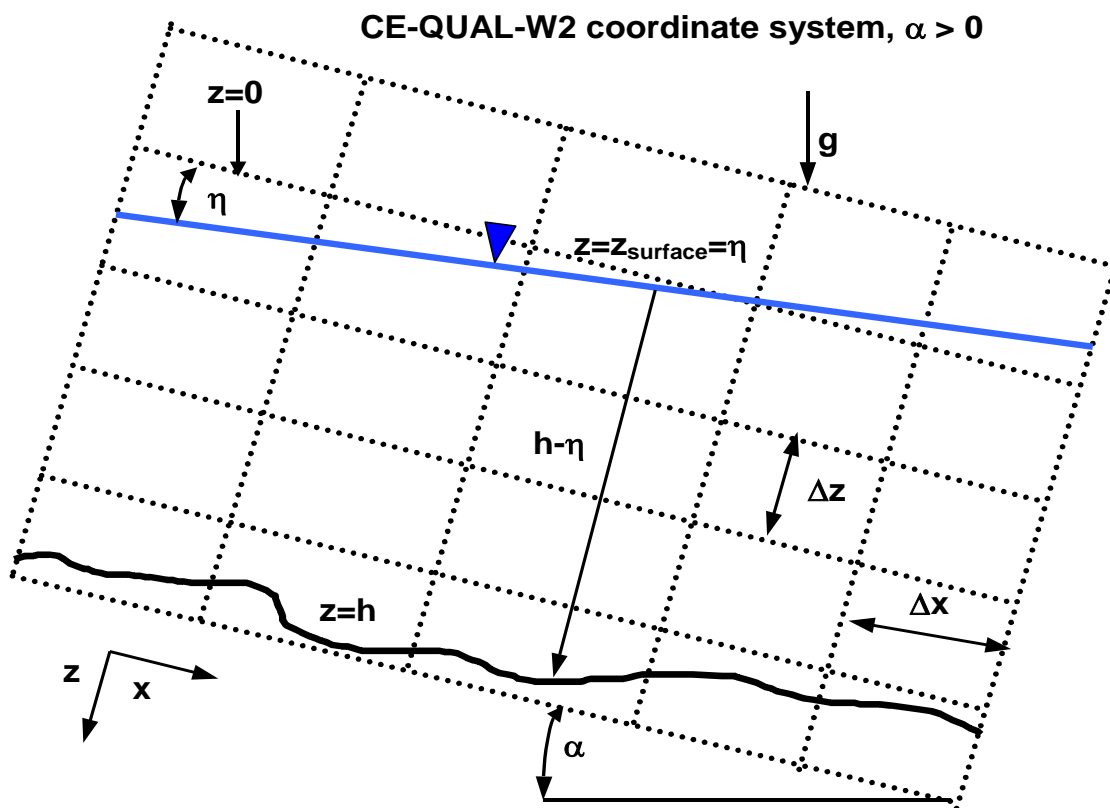


Figure A-11. Coordinate system with channel slope.

The continuity equation is integrated over the depth as follows:

$$\int_{\eta}^h \frac{\partial UB}{\partial x} dz + \int_{\eta}^h \frac{\partial WB}{\partial z} dz = \int_{\eta}^h qB dz \quad (\text{A-44})$$

The first term can be expanded as follows using Leibnitz's rule:

$$\int_{\eta}^h \frac{\partial UB}{\partial x} dz = \frac{\partial}{\partial x} \int_{\eta}^h UB dz - \frac{\partial h}{\partial x} UB|_h + \frac{\partial \eta}{\partial x} UB|_{\eta} \quad (\text{A-45})$$

The integral of the vertical flow rate over z relates to changes in water surface elevation as shown below:

$$\int_{\eta}^h \frac{\partial WB}{\partial z} dz = WB|_h - WB|_{\eta} \quad (\text{A-46})$$

where:

$$W_h = \frac{\partial h}{\partial t} + U_h \frac{\partial h}{\partial x}$$

$$W_{\eta} = \frac{\partial \eta}{\partial t} + U_{\eta} \frac{\partial \eta}{\partial x}$$

Combining these terms together, the free surface equation becomes:

$$\begin{aligned} \int_{\eta}^h qB dz &= \frac{\partial}{\partial x} \int_{\eta}^h UB dz - \frac{\partial h}{\partial x} UB|_h + \frac{\partial \eta}{\partial x} UB|_{\eta} + U_h B_h \frac{\partial h}{\partial t} + U_h B_h \frac{\partial h}{\partial x} \\ &\quad - B_{\eta} \frac{\partial \eta}{\partial t} - B_{\eta} U_{\eta} \frac{\partial \eta}{\partial x} \end{aligned} \quad (\text{A-47})$$

Canceling out terms and applying the no-slip boundary condition that U_h is zero:

$$\frac{\partial}{\partial x} \int_{\eta}^h UB dz - B_{\eta} \frac{\partial \eta}{\partial t} = \int_{\eta}^h qB dz \quad (\text{A-48})$$

or

$$B_{\eta} \frac{\partial \eta}{\partial t} = \frac{\partial}{\partial x} \int_{\eta}^h UB dz - \int_{\eta}^h qB dz \quad (\text{A-49})$$

where B_η is the width at the surface.

Equation of State

The density must be known for solution of the momentum equations. The equation of state is an equation that relates density to temperature and concentration of dissolved substances. This equation is given by:

$$\rho = f(T_w, \Phi_{TDS}, \Phi_{ISS}) \quad (\text{A-50})$$

where $f(T_w, \Phi_{TDS}, \Phi_{ISS})$ is a density function dependent upon temperature, total dissolved solids or salinity, and inorganic suspended solids.

Summary of Governing Equations

Table A-5 shows the governing equations after lateral averaging for a channel slope of zero (original model formulation) and for an arbitrary channel slope. Parameters used in [Table A-5](#) are illustrated in [Figure A-12](#).

Table A-5. Governing equations with and without channel slope.

Equation	Governing equation assuming no channel slope and no momentum conservation at branch intersections	Governing equation assuming an arbitrary channel slope and conservation of momentum at branch intersections
x-momentum	$\frac{\partial UB}{\partial t} + \frac{\partial UUB}{\partial x} + \frac{\partial WUB}{\partial z} =$ $gB \frac{\partial \eta}{\partial x} - \frac{gB}{\rho} \int_{\eta}^z \frac{\partial \rho}{\partial x} dz +$ $\frac{1}{\rho} \frac{\partial B \tau_{xx}}{\partial x} + \frac{1}{\rho} \frac{\partial B \tau_{xz}}{\partial z}$	$\frac{\partial UB}{\partial t} + \frac{\partial UUB}{\partial x} + \frac{\partial WUB}{\partial z} = gB \sin \alpha$ $+ g \cos \alpha B \frac{\partial \eta}{\partial x} - \frac{g \cos \alpha B}{\rho} \int_{\eta}^z \frac{\partial \rho}{\partial x} dz +$ $\frac{1}{\rho} \frac{\partial B \tau_{xx}}{\partial x} + \frac{1}{\rho} \frac{\partial B \tau_{xz}}{\partial z} + qBU_x$
z-momentum	$0 = g - \frac{1}{\rho} \frac{\partial P}{\partial z}$	$0 = g \cos \alpha - \frac{1}{\rho} \frac{\partial P}{\partial z}$
continuity	$\frac{\partial UB}{\partial x} + \frac{\partial WB}{\partial z} = qB$	$\frac{\partial UB}{\partial x} + \frac{\partial WB}{\partial z} = qB$
state	$\rho = f(T_w, \Phi_{TDS}, \Phi_{ss})$	$\rho = f(T_w, \Phi_{TDS}, \Phi_{ss})$
free surface	$B_\eta \frac{\partial \eta}{\partial t} = \frac{\partial}{\partial x} \int_{\eta}^h UB dz - \int_{\eta}^h qB dz$	$B_\eta \frac{\partial \eta}{\partial t} = \frac{\partial}{\partial x} \int_{\eta}^h UB dz - \int_{\eta}^h qB dz$
U = horizontal velocity, $m s^{-1}$ τ_x = x-direction lateral average shear stress W = vertical velocity, $m s^{-1}$ τ_y = y-direction lateral average shear stress B = channel width ρ = density P = pressure η = water surface		

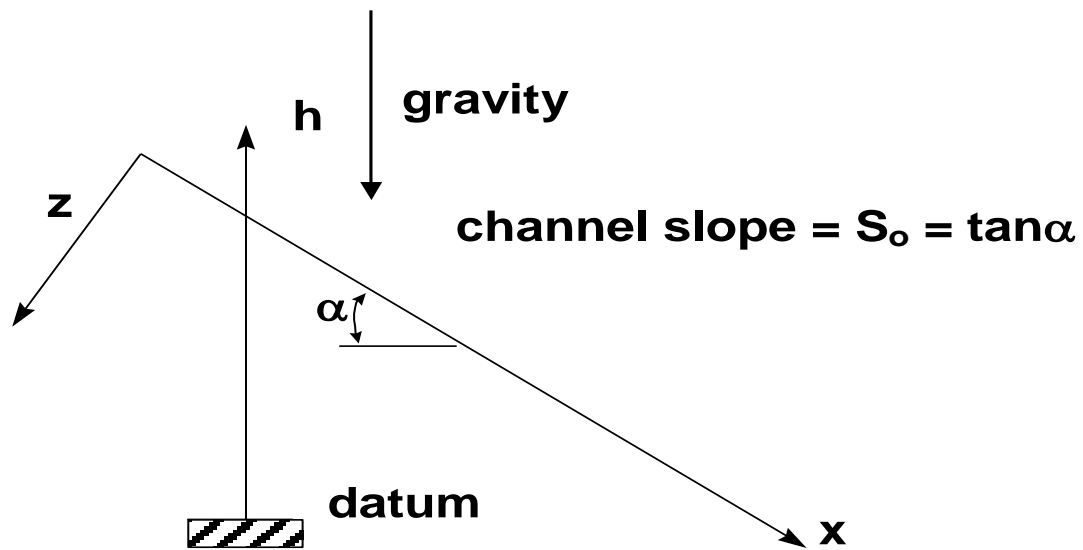


Figure A-12. Definition sketch for channel slope.

Branch Linkage with Internal Head Boundary Conditions

Linkage of Mainstem Branches

One issue in the development of the river basin model is the linkage of branches with different vertical grids. [Figure A-13](#) shows variable definitions for a sloping channel.

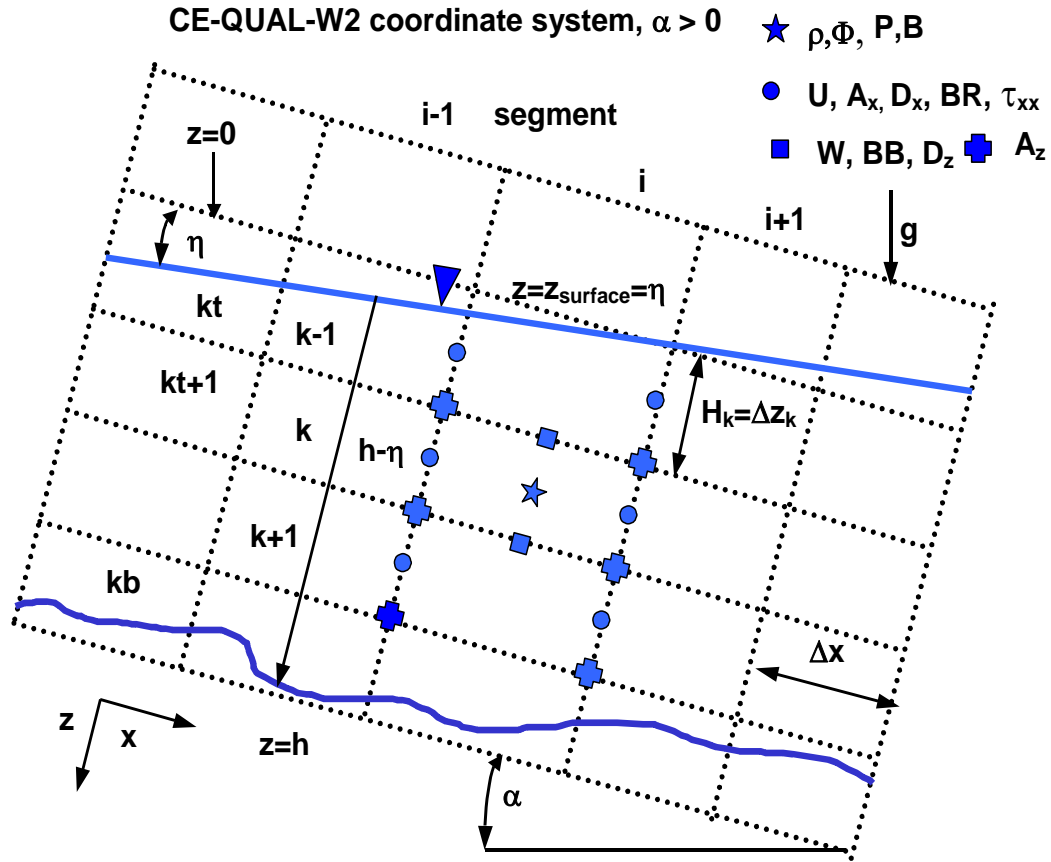


Figure A-13. Computational grid variable definitions for arbitrary channel slope.

However, the vertical velocity of a cell is not determined at the side edge of a segment, but at the bottom of the segment. In order for all the volume to be passed from one cell to another, all the flow from the downstream segment [ID] should be transferred to the upstream segment [IU]. Since the model does not assume strong vertical accelerations, we may be forced to neglect the vertical component of velocity at this transition and assume that the longitudinal velocity entering the upstream segment is U_{ID} .

The model ensures that flow and mass are conserved between branches when the vertical spacing is different between the upstream and downstream grid. Spatial averaging to conserve flow, heat, and mass is illustrated in [Figure A-14](#).

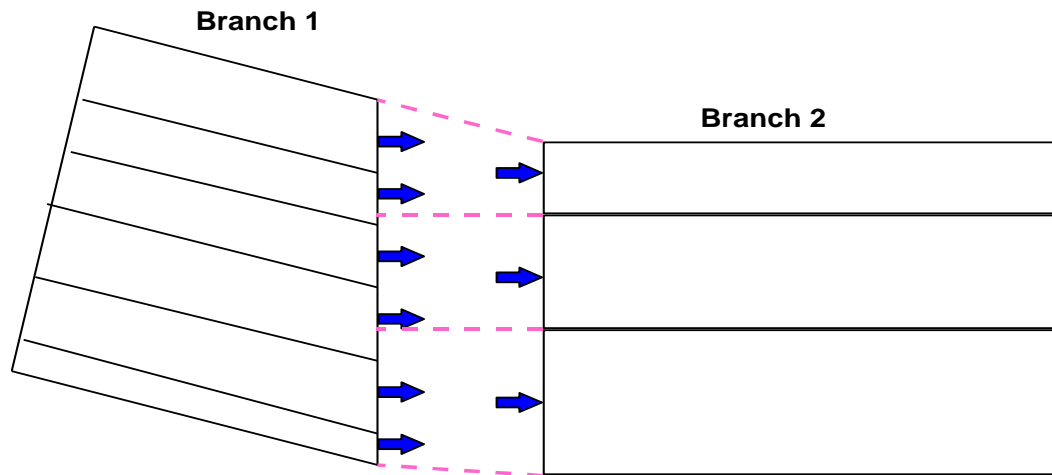


Figure A-14. Transfer of mass and momentum between branches with unequal vertical grid spacing.

Linkage of Tributary Branches

Version 2 assumed all tributary branches came in at right angles to the main channel resulting in no longitudinal momentum exchange between the branches. In many cases, this was appropriate, but in certain cases prevented a realistic depiction of the physics of the prototype. Version 3 now includes momentum transfer between branches that do not enter perpendicular to each other ([Figure A-15](#)).

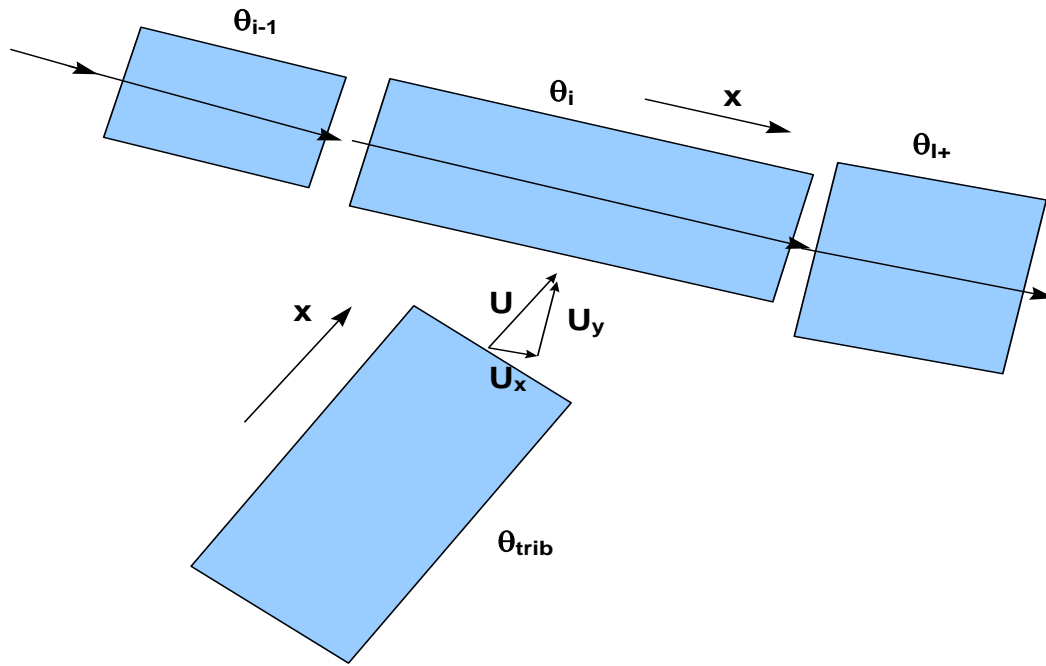


Figure A-15. Linkage of tributary branch coming in at an angle to main branch.

The tributary inflow can create shear stress along both the longitudinal axis of the main stem branch and along the y-axis of the segment. For the new formulation, the cross-shear mixing has been added to the cross-shear wind stress for the computation involving the vertical eddy viscosity and vertical diffusivity. This involves determining the y and x velocity components of the entering branch ([Figure A-16](#)).

Longitudinal Momentum

The vector component of velocity in the x-direction of the main channel, U_x , can be computed by analysis of the channel orientations. This component in the x-direction would be:

$$U_x = U \cos \beta \quad (\text{A-51})$$

where:

U = longitudinal velocity of the tributary at segment ID for the tributary branch

β = difference in the angle between the main stem and tributary segments ([Figure A-16](#)).

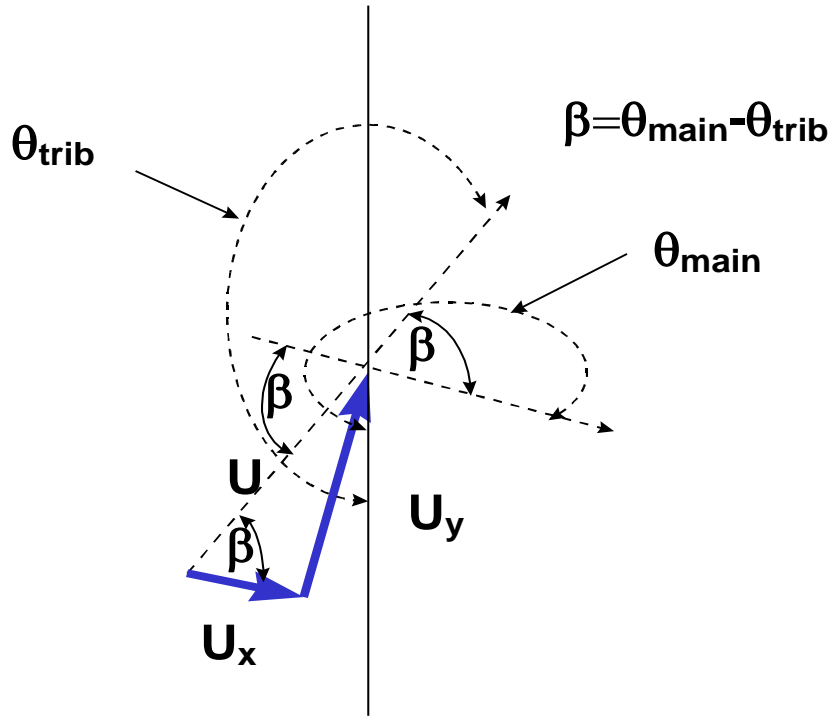


Figure A-16. Schematic of x and y velocity components.

The conservation of momentum about a control volume, the main stem segment, would result in an additional source of momentum. Lai (1986) shows that the correction to the x-momentum equation would be:

$$qBU_x \quad (\text{A-52})$$

where:

q = lateral inflow per unit length.

This arises from re-deriving the momentum equations and assuming that all the fluid (q) entering the segment is moving at the velocity U_x . This correction to the x-momentum equation would be

$$\begin{aligned} \frac{\partial UB}{\partial t} + \frac{\partial UUB}{\partial x} + \frac{\partial WUB}{\partial z} = & gB \sin \alpha + g \cos \alpha B \frac{\partial \eta}{\partial x} - \frac{g \cos \alpha B}{\rho} \int_{\eta}^z \frac{\partial \rho}{\partial x} dz \\ & + \frac{1}{\rho} \frac{\partial B \tau_{xx}}{\partial x} + \frac{1}{\rho} \frac{\partial B \tau_{xz}}{\partial z} + \underbrace{qBU_x}_{\text{momentum from side tributaries}} \end{aligned} \quad (\text{A-53})$$

Cross-shear of Tributary Inflow

The y-velocity coming into a reservoir may also contribute to vertical mixing. The y component of a tributary inflow is $U_y = U \sin \beta$ (Figure A-16). Since there is no y-momentum equation, the only

mechanism for mixing energy with the present formulation of the vertical shear stress is the cross-shear stress from the wind given as $\tau_{wy} \cong C_D \rho_a W_h^2 \sin(\Theta_1 - \Theta_2)$. The cross-shear stress accounts for the shear stress and mixing that results from wind blowing across the y-axis of the segment. The lateral branch inflow at a velocity, U_y , could be thought of as an additional component of the stress under the current context of the turbulence closure approximations.

If the water in the y-direction has zero velocity, the additional shear stress can be parameterized as an interfacial shear:

$$\tau_{ytrib} \cong \rho \frac{f}{8} U_y^2 \quad (\text{A-54})$$

where:

f = interfacial friction factor

For two-layer flow systems, f has been found to be of order 0.01. The value of f for this non-ideal approach could be determined by numerical computation. Therefore, the value of the cross-shear term would be increased by a lateral tributary inflow. This can be evaluated by numerical experiments computing the magnitude of the cross-shear term from wind and from lateral inflow. A more robust theoretical approach may be needed to account for this increase in lateral shear, but that may be necessary only if the model includes the y-momentum equation.

River Basin Theory

The corrections to the governing equations incorporating the sloping channel and the transfer of momentum from a side tributary are incorporated in the new solution technique as described below.

Free-Water Surface Numerical Solution

The free surface equation:

$$B_\eta \frac{\partial \eta}{\partial t} = \frac{\partial}{\partial x} \int_\eta^h U B dz - \int_\eta^h q B dz \quad (\text{A-55})$$

is solved by substituting the momentum equation:

$$\begin{aligned} \frac{\partial U B}{\partial t} + \frac{\partial U U B}{\partial x} + \frac{\partial W U B}{\partial z} &= g B \sin \alpha + g \cos \alpha B \frac{\partial \eta}{\partial x} - \frac{g \cos \alpha B}{\rho} \int_\eta^z \frac{\partial \rho}{\partial x} dz \\ &+ \frac{1}{\rho} \frac{\partial B \tau_{xx}}{\partial x} + \frac{1}{\rho} \frac{\partial B \tau_{xz}}{\partial z} + q B U_x \end{aligned} \quad (\text{A-56})$$

in finite difference form and then simplifying. The finite difference form of the momentum equation is:

$$UB_i^{n+1} = UB_i^n + \Delta t \left[-\frac{\partial UUB}{\partial x} - \frac{\partial WUB}{\partial z} + gB \sin \alpha + g \cos \alpha B \frac{\partial \eta}{\partial x} - \frac{g \cos \alpha B}{\rho} \int_{\eta}^z \frac{\partial \rho}{\partial x} dz + \frac{1}{\rho} \frac{\partial B \tau_{xx}}{\partial x} + \frac{1}{\rho} \frac{\partial B \tau_{xz}}{\partial z} + qBU_x \right]_i^n \quad (\text{A-57})$$

Defining for simplicity the term F as:

$$F = -\frac{\partial UUB}{\partial x} - \frac{\partial WUB}{\partial z} + \frac{1}{\rho} \frac{\partial B \tau_{xx}}{\partial x} \quad (\text{A-58})$$

and substituting in for τ_{xx} , F becomes:

$$F = -\frac{\partial UUB}{\partial x} - \frac{\partial WUB}{\partial z} + \frac{\partial \left(BA_x \frac{\partial U}{\partial x} \right)}{\partial x} \quad (\text{A-59})$$

Substituting in the term UB_i^{n+1} in the free surface equation for UB , the free surface equation becomes:

$$\begin{aligned} B_{\eta} \frac{\partial \eta}{\partial t} &= \frac{\partial}{\partial x} \int_{\eta}^h UB_i^n dz + \Delta t \frac{\partial}{\partial x} \int_{\eta}^h F^n dz + \Delta t \frac{\partial}{\partial x} \int_{\eta}^h gB \sin \alpha dz \\ &+ \Delta t \frac{\partial}{\partial x} \int_{\eta}^h g \cos \alpha B \frac{\partial \eta}{\partial x} dz - \Delta t \frac{\partial}{\partial x} \int_{\eta}^h \frac{g \cos \alpha B}{\rho} \int_{\eta}^z \frac{\partial \rho}{\partial x} dz dz \\ &+ \Delta t \frac{\partial}{\partial x} \int_{\eta}^h \frac{1}{\rho} \frac{\partial B \tau_{xz}}{\partial z} dz + \Delta t \frac{\partial}{\partial x} \int_{\eta}^h qBU_x^n dz \\ &- \int_{\eta}^h q^n B dz \end{aligned} \quad (\text{A-60})$$

Some of these terms can be simplified as follows:

$$\frac{\partial}{\partial x} \int_{\eta}^h gB \sin \alpha dz = g \sin \alpha \frac{\partial}{\partial x} \int_{\eta}^h B dz \quad (\text{A-61})$$

$$\frac{\partial}{\partial x} \int_{\eta}^h g \cos \alpha B \frac{\partial \eta}{\partial x} dz = g \cos \alpha \frac{\partial}{\partial x} \left(\frac{\partial \eta}{\partial x} \int_{\eta}^h B dz \right) \quad (\text{A-62})$$

$$\frac{\partial}{\partial x} \int_{\eta}^h \frac{g \cos \alpha B}{\rho} \int_{\eta}^z \frac{\partial \rho}{\partial x} dz dz = \frac{g \cos \alpha}{\rho} \frac{\partial}{\partial x} \int_{\eta}^h B \int_{\eta}^z \frac{\partial \rho}{\partial x} dz dz \quad (\text{A-63})$$

$$\frac{\partial}{\partial x} \int_{\eta}^h \frac{1}{\rho} \frac{\partial B \tau_{xz}}{\partial z} dz = \frac{1}{\rho} \frac{\partial}{\partial x} \left(B \tau_{xz} \Big|_h - B \tau_{xz} \Big|_{\eta} \right) \quad (\text{A-64})$$

Then substituting these into the above equation:

$$\begin{aligned} B_{\eta} \frac{\partial \eta}{\partial t} &= \frac{\partial}{\partial x} \int_{\eta}^h U B_i^n dz + \Delta t \frac{\partial}{\partial x} \int_{\eta}^h F^n dz + \Delta t g \sin \alpha \frac{\partial}{\partial x} \int_{\eta}^h B dz \\ &+ \Delta t g \cos \alpha \frac{\partial}{\partial x} \left(\frac{\partial \eta}{\partial x} \Big|_{\eta} \int_{\eta}^h B dz \right) - \Delta t \frac{g \cos \alpha}{\rho} \frac{\partial}{\partial x} \int_{\eta}^h B \int_{\eta}^z \frac{\partial \rho}{\partial x} \Big|_{\eta}^n dz dz \\ &+ \Delta t \frac{\partial}{\partial x} \frac{1}{\rho} \left(B \tau_{xz} \Big|_h - B \tau_{xz} \Big|_{\eta} \right)^n + \Delta t \frac{\partial}{\partial x} \int_{\eta}^h q B U_x^n dz - \int_{\eta}^h q^n B dz \end{aligned} \quad (\text{A-65})$$

All terms with η are grouped on the LHS such that:

$$\begin{aligned} B_{\eta} \frac{\partial \eta}{\partial t} - \Delta t g \cos \alpha \frac{\partial}{\partial x} \left(\frac{\partial \eta}{\partial x} \Big|_{\eta} \int_{\eta}^h B dz \right) &= \frac{\partial}{\partial x} \int_{\eta}^h U B_i^n dz + \Delta t \frac{\partial}{\partial x} \int_{\eta}^h F^n dz \\ &+ \Delta t g \sin \alpha \frac{\partial}{\partial x} \int_{\eta}^h B dz \\ &- \Delta t \frac{g \cos \alpha}{\rho} \frac{\partial}{\partial x} \int_{\eta}^h B \int_{\eta}^z \frac{\partial \rho}{\partial x} \Big|_{\eta}^n dz dz \\ &+ \Delta t \frac{\partial}{\partial x} \frac{1}{\rho} \left(B \tau_{xz} \Big|_h - B \tau_{xz} \Big|_{\eta} \right)^n \\ &+ \Delta t \frac{\partial}{\partial x} \int_{\eta}^h q B U_x^n dz \\ &- \int_{\eta}^h q^n B dz \end{aligned} \quad (\text{A-66})$$

The first term on the LHS can be put into a backward finite difference form as:

$$B_{\eta} \frac{\partial \eta}{\partial t} \approx B_{\eta} \frac{\eta_i^n - \eta_i^{n-1}}{\Delta t} \quad (\text{A-67})$$

The second term, $-\Delta t g \cos \alpha \frac{\partial}{\partial x} \left(\frac{\partial \eta}{\partial x} \int_{\eta}^h B dz \right)^n$, can be simplified using the chain rule for partial differential equations to:

$$-\Delta t g \cos \alpha \left. \frac{\partial \eta}{\partial x} \right|^n \frac{\partial}{\partial x} \int_{\eta}^h B dz - \Delta t g \cos \alpha \int_{\eta}^h B dz \left. \frac{\partial^2 \eta}{\partial x^2} \right|^n \quad (\text{A-68})$$

Then using a second-order central difference for the second derivative and a first order backward difference for the first derivative such that:

$$\begin{aligned} & -\Delta t g \cos \alpha \left. \frac{\partial \eta}{\partial x} \right|^n \frac{\partial}{\partial x} \int_{\eta}^h B dz - \Delta t g \cos \alpha \int_{\eta}^h B dz \left. \frac{\partial^2 \eta}{\partial x^2} \right|^n \\ & \approx -\Delta t g \cos \alpha \frac{\eta_i^n - \eta_{i-1}^n}{\Delta x} \frac{\partial}{\partial x} \int_{\eta}^h B dz \\ & \quad - \Delta t g \cos \alpha \int_{\eta}^h B dz \frac{\eta_{i+1}^n - 2\eta_i^n + \eta_{i-1}^n}{\Delta x^2} \end{aligned} \quad (\text{A-69})$$

Also using a backward difference:

$$\frac{\partial}{\partial x} \int_{\eta}^h B dz = \frac{1}{\Delta x} \left(\int_{\eta}^h B dz \Big|_i - \int_{\eta}^h B dz \Big|_{i-1} \right). \quad (\text{A-70})$$

Grouping and collecting terms and multiplying through by $\Delta t \Delta x$, the LHS becomes after simplification:

$$\begin{aligned} & \eta_{i-1}^n \left[\frac{-g \cos \alpha \Delta t^2}{\Delta x} \int_{\eta}^h B dz \Big|_{i-1} \right] + \eta_i^n \left[B_{\eta} \Delta x + \frac{g \cos \alpha \Delta t^2}{\Delta x} \left\{ \int_{\eta}^h B dz \Big|_i + \int_{\eta}^h B dz \Big|_{i-1} \right\} \right] \\ & + \eta_{i+1}^n \left[\frac{-g \cos \alpha \Delta t^2}{\Delta x} \int_{\eta}^h B dz \Big|_i \right] = (RHS)_i^n \Delta x \Delta t + B_{\eta} \eta_i^{n-1} \Delta x \end{aligned} \quad (\text{A-71})$$

where the RHS is defined as:

$$\begin{aligned}
 RHS = & \frac{\partial}{\partial x} \int_{\eta}^h UB_i^n dz + \Delta t \frac{\partial}{\partial x} \int_{\eta}^h F dz + \Delta t g \sin \alpha \frac{\partial}{\partial x} \int_{\eta}^h B dz \\
 & - \Delta t \frac{g \cos \alpha}{\rho} \frac{\partial}{\partial x} \int_{\eta}^h B \int_{\eta}^z \frac{\partial \rho}{\partial x} dz dz + \Delta t \frac{\partial}{\partial x} \frac{1}{\rho} \left(B \tau_{xz}|_h - B \tau_{xz}|_{\eta} \right) \\
 & + \Delta t \frac{\partial}{\partial x} \int_{\eta}^h q B U_x dz - \int_{\eta}^h q B dz
 \end{aligned} \tag{A-72}$$

and is evaluated at time level n.

The integral of the cell widths can be put into a summation over the vertical layers as:

$$\int_{\eta}^h B dz \Big|_i = \sum_{kb}^{kt} BH_{ri} \tag{A-73}$$

$$\int_{\eta}^h B dz \Big|_{i-1} = \sum_{kb}^{kt} BH_{ri-1} \tag{A-74}$$

where BH_r is the value of the width times the layer depth for the right-hand side of a cell. In the code, this is the variable BR(I,K) times H(K), or the derived variable BHR(I,K).

Some of the right hand side terms can be put into a format compatible with the model schematization such as:

$$\begin{aligned}
 \frac{\partial}{\partial x} \int_{\eta}^h (UB)_i^n dz & \approx \frac{\partial}{\partial x} \sum_{kt}^{kb} UBH_r \\
 & \approx \frac{1}{\Delta x} \left(\sum_{kt}^{kb} UBH_r \Big|_i - \sum_{kt}^{kb} UBH_r \Big|_{i-1} \right) \\
 & = \frac{1}{\Delta x} \sum_{kt}^{kb} \left(UBH_r \Big|_i - UBH_r \Big|_{i-1} \right)^n
 \end{aligned} \tag{A-75}$$

$$\begin{aligned}
 \Delta t \frac{\partial}{\partial x} \int_{\eta}^h F^n dz & \approx \Delta t \frac{\partial}{\partial x} \sum_{kt}^{kb} FH_r \\
 & \approx \frac{\Delta t}{\Delta x} \left(\sum_{kt}^{kb} FH_r \Big|_i - \sum_{kt}^{kb} FH_r \Big|_{i-1} \right) \\
 & = \frac{\Delta t}{\Delta x} \sum_{kt}^{kb} \left(FH_r \Big|_i - FH_r \Big|_{i-1} \right)^n
 \end{aligned} \tag{A-76}$$

$$\begin{aligned}
\Delta t g \sin \alpha \frac{\partial}{\partial x} \int_{\eta}^h B dz &\approx \Delta t g \sin \alpha \frac{\partial}{\partial x} \sum_{kt}^{kb} B H_r \\
&\approx \frac{\Delta t g \sin \alpha}{\Delta x} \left(\sum_{kt}^{kb} B H_r \Big|_i - \sum_{kt}^{kb} B H_r \Big|_{i-1} \right) \\
&= \frac{\Delta t g \sin \alpha}{\Delta x} \sum_{kt}^{kb} (B H_r \Big|_i - B H_r \Big|_{i-1})
\end{aligned} \tag{A-77}$$

$$\begin{aligned}
\Delta t \frac{g \cos \alpha}{\rho} \frac{\partial}{\partial x} \int_{\eta}^h B \int_{\eta}^z \frac{\partial \rho}{\partial x} dz dz &\approx \Delta t \frac{g \cos \alpha}{\rho} \frac{\partial}{\partial x} \int_{\eta}^h B \sum_{kt}^{kb} \frac{\partial \rho}{\partial x} H_r dz \\
&\approx \Delta t \frac{g \cos \alpha}{\rho \Delta x} \sum_{kt}^{kb} \frac{\partial \rho}{\partial x} H_r \sum_{kt}^{kb} (B H_r \Big|_i - B H_r \Big|_{i-1})
\end{aligned} \tag{A-78}$$

$$\Delta t \frac{\partial}{\partial x} \frac{1}{\rho} (B \tau_{xz} \Big|_h - B \tau_{xz} \Big|_{\eta}) \approx \frac{\Delta t}{\rho \Delta x} \left\{ (B \tau_{xz} \Big|_h - B \tau_{xz} \Big|_{\eta})_i - (B \tau_{xz} \Big|_h - B \tau_{xz} \Big|_{\eta})_{i-1} \right\} \tag{A-79}$$

The lateral inflow of momentum term represents the gradient over x of the inflow momentum:

$$\Delta t \frac{\partial}{\partial x} \int_{\eta}^h q B U_x dz \approx \Delta t \frac{\partial}{\partial x} \sum_{kt}^{kb} q U_x B H_r \tag{A-80}$$

$$\int_{\eta}^h q B dz \approx \sum_{kt}^{kb} q B H_r \tag{A-81}$$

Combining these terms into one equation:

$$A \eta_{i-1}^n + X \eta_i^n + C \eta_{i+1}^n = D \tag{A-82}$$

where:

$$\begin{aligned}
A &= \left[\frac{-g \cos \alpha \Delta t^2}{\Delta x} \sum_{kt}^{kb} B H_r \Big|_{i-1} \right] \\
X &= \left[B_{\eta} \Delta x + \frac{g \cos \alpha \Delta t^2}{\Delta x} \left\{ \sum_{kt}^{kb} B H_r \Big|_i + \sum_{kt}^{kb} B H_r \Big|_{i-1} \right\} \right] \\
C &= \left[\frac{-g \cos \alpha \Delta t^2}{\Delta x} \sum_{kt}^{kb} B H_r \Big|_i \right]
\end{aligned}$$

$$\begin{aligned}
D = & \Delta t \sum_{kt}^{kb} (UBH_r|_i - UBH_r|_{i-1}) + B_\eta \eta_i^{n-1} \Delta x + \Delta t^2 \sum_{kt}^{kb} (FH_r|_i - FH_r|_{i-1}) \\
& + \Delta t^2 g \sin \alpha \sum_{kt}^{kb} (BH_r|_i - BH_r|_{i-1}) + \Delta t^2 \frac{g \cos \alpha}{\rho} \sum_{kt}^{kb} (BH_r|_i - BH_r|_{i-1}) \sum_{kt}^{kb} \frac{\partial \rho}{\partial x} H_r \\
& + \Delta x \Delta t \sum_{kt}^{kb} q BH_r + \Delta x \Delta t^2 \frac{\partial}{\partial x} \sum_{kt}^{kb} q U_x BH_r \\
& + \frac{\Delta t^2}{\rho} \left[(B\tau_{xz}|_h - B\tau_{xz}|_\eta)_i - (B\tau_{xz}|_h - B\tau_{xz}|_\eta)_{i-1} \right]
\end{aligned}$$

This equation is solved for the water surface elevation at the $n+1$ time level using the Thomas algorithm. The boundary condition implementation is the same as described in Cole and Buchak (1995).

Horizontal Momentum Numerical Solution

The x-momentum equation:

$$\begin{aligned}
\frac{\partial UB}{\partial t} + \frac{\partial UUB}{\partial x} + \frac{\partial WUB}{\partial z} = & gB \sin \alpha + g \cos \alpha B \frac{\partial \eta}{\partial x} - \frac{g \cos \alpha B}{\rho} \int_\eta^z \frac{\partial \rho}{\partial x} dz \\
& + \frac{1}{\rho} \frac{\partial B \tau_{xx}}{\partial x} + \frac{1}{\rho} \frac{\partial B \tau_{xz}}{\partial z} + qBU_x
\end{aligned} \tag{A-83}$$

is solved using either a fully explicit or an explicit/implicit finite difference solution technique specified by the user.

Explicit Solution

This scheme is based on solving the partial differential terms using an explicit finite difference technique where:

$$\begin{aligned}
U_i^{n+1} B_i^{n+1} = & U_i^n B_i^n + \Delta t \left\{ -\frac{\partial UUB}{\partial x} - \frac{\partial WUB}{\partial z} + gB \sin \alpha + g \cos \alpha B \frac{\partial \eta}{\partial x} \right. \\
& \left. - \frac{g \cos \alpha B}{\rho} \int_\eta^z \frac{\partial \rho}{\partial x} dz - \frac{1}{\rho} \frac{\partial B \tau_{xx}}{\partial x} + \frac{1}{\rho} \frac{\partial B \tau_{xz}}{\partial z} + qBU_x \right\}_i^n
\end{aligned} \tag{A-84}$$

The various terms are put into finite difference form as follows. The longitudinal advection of momentum is an upwind difference scheme where the order of differencing is dependent on the sign of U , e.g., for $U > 0$

$$\left. \frac{\partial UUB}{\partial x} \right|_{i,k} \cong \frac{1}{\Delta x_i} [B_{i,k}^n U_{i,k}^n U_{i,k}^n - B_{i-1,k}^n U_{i-1,k}^n U_{i-1,k}^n] \tag{A-85}$$

The vertical advection of momentum is also an upwind scheme based on the velocity of W. For $W > 0$ or downward flow

$$\left. \frac{\partial WUB}{\partial z} \right|_{i,k} \cong \frac{1}{\Delta z_k} \left[(W_{i,k}^n U_{i,k}^n B_{i,k}^n) - (W_{i,k-1}^n U_{i,k-1}^n B_{i,k-1}^n) \right] \quad (\text{A-86})$$

The gravity force is:

$$gB \sin \alpha = g \sin \alpha B_i^n \quad (\text{A-87})$$

The pressure gradient is:

$$\begin{aligned} g \cos \alpha B \frac{\partial \eta}{\partial x} - \frac{g \cos \alpha B}{\rho} \int_{\eta}^z \frac{\partial \rho}{\partial x} dz &= \frac{g \cos \alpha B_i^n}{\Delta x} (\eta_{i+1} - \eta_i)^n \\ &\quad - \frac{g \cos \alpha B_i^n}{\rho \Delta x} \sum (\rho_{i+1,k} - \rho_{i,k})^n \Delta z_k \end{aligned} \quad (\text{A-88})$$

The horizontal advection of turbulent momentum is:

$$\begin{aligned} \frac{1}{\rho} \frac{\partial B \tau_{xx}}{\partial x} &= \frac{\partial B A_x}{\partial x} \frac{\partial U}{\partial x} = \left(\frac{B_{i+1/2}^n A_x}{\Delta x_i \Delta x_{i+1/2}} \right) (U_{i+1,k}^n - U_{i,k}^n) \\ &\quad - \left(\frac{B_{i-1/2}^n A_x}{\Delta x_i \Delta x_{i-1/2}} \right) (U_{i,k}^n - U_{i-1,k}^n) \end{aligned} \quad (\text{A-89})$$

The contribution to longitudinal momentum by lateral branch inflows is:

$$qBU_x = qBU_x|_{i,k}^n \quad (\text{A-90})$$

Using the definition of the shear stress:

$$\tau_{xz} = \left[\tau_w + \tau_b + \rho A_z \frac{\partial U}{\partial z} \right] \quad (\text{A-91})$$

where A_z is the turbulent kinematic viscosity, the vertical transport of momentum is:

$$\begin{aligned} \frac{1}{\rho} \frac{\partial B \tau_{xz}}{\partial z} = \frac{\partial}{\partial z} \frac{B}{\rho} \left[\tau_w + \tau_b + \rho A_z \frac{\partial U}{\partial z} \right] = & \left(\frac{B_{i,k+1/2}^n}{\Delta z_k \Delta z_{k+1/2} \rho} \right) \\ & \left[\tau_w^n|_{i,k+1/2} + \tau_b^n|_{i,k+1/2} + \frac{\rho A_{zi,k+1/2}}{\Delta z_{k+1/2}} (U_{i,k+1}^n - U_{i,k}^n) \right] \\ & - \left(\frac{B_{i,k-1/2}^n}{\Delta z_k \Delta z_{k-1/2} \rho} \right) \left[\tau_w^n|_{i,k-1/2} + \tau_b^n|_{i,k-1/2} + \frac{\rho A_{zi,k-1/2}}{\Delta z_{k-1/2}} (U_{i,k}^n - U_{i,k-1}^n) \right] \end{aligned} \quad (\text{A-92})$$

Implicit Solution

The implicit technique was utilized to reduce the time step limitation for numerical stability when values of A_z were large, as for an estuary or a river system. This occurs because the time step limitation is a function of A_z . Only the vertical transport of momentum term was solved implicitly. All other terms for the solution of the horizontal momentum equation were the same as the explicit scheme.

The horizontal momentum equation can be separated into the following two equations:

$$\begin{aligned} \frac{\partial UB}{\partial t} + \frac{\partial UUB}{\partial x} + \frac{\partial WUB}{\partial z} = & gB \sin \alpha + g \cos \alpha B \frac{\partial \eta}{\partial x} - \frac{g \cos \alpha B}{\rho} \int_{\eta}^z \frac{\partial \rho}{\partial x} dz \\ & + \frac{1}{\rho} \frac{\partial B \tau_{xx}}{\partial x} + \frac{1}{\rho} \frac{\partial B(\tau_b + \tau_w)}{\partial z} + qBU_x \end{aligned} \quad (\text{A-93})$$

$$\frac{\partial UB}{\partial t} = \frac{1}{\rho} \frac{\partial}{\partial z} \left(BA_z \frac{\partial U}{\partial z} \right) \quad (\text{A-94})$$

Equation A-93 is written as:

$$\begin{aligned} U_i^* B_i^{n+1} = U_i^n B_i^n + \Delta t \{ & - \frac{\partial UUB}{\partial x} - \frac{\partial WUB}{\partial z} + gB \sin \alpha + g \cos \alpha B \frac{\partial \eta}{\partial x} \\ & - \frac{g \cos \alpha B}{\rho} \int_{\eta}^z \frac{\partial \rho}{\partial x} dz + \frac{1}{\rho} \frac{\partial B \tau_{xx}}{\partial x} + \frac{1}{\rho} \frac{\partial B(\tau_b + \tau_w)}{\partial z} + qBU_x \}_i^n \end{aligned} \quad (\text{A-95})$$

where U^* is the velocity at the new time level before the application of equation A-94. Equation A-92 is solved similarly to the solution of the fully explicit technique outlined above.

Equation A-94 is then solved using a fully implicit technique as:

$$\begin{aligned}\frac{\partial UB}{\partial t} &= \frac{(U_i^{n+1} B_i^{n+1} - U_i^* B_i^{n+1})}{\Delta t} \\ &= \frac{1}{\rho} \frac{\partial}{\partial z} \left(B^{n+1} A_z \frac{\partial U^{n+1}}{\partial z} \right)\end{aligned}\quad (\text{A-96})$$

This can be rewritten as:

$$\begin{aligned}U_i^{n+1} B_i^{n+1} &= U_i^* B_i^{n+1} + \left(\frac{\Delta t B_{i,k+1/2}^{n+1}}{\Delta z_k \rho} \right) \left[\frac{A_{z,i,k+1/2}}{\Delta z_{k+1/2}} (U_{i,k+1}^{n+1} - U_{i,k}^{n+1}) \right] \\ &\quad - \left(\frac{\Delta t B_{i,k-1/2}^{n+1}}{\Delta z_k \rho} \right) \left[\frac{A_{z,i,k-1/2}}{\Delta z_{k-1/2}} (U_{i,k}^{n+1} - U_{i,k-1}^{n+1}) \right]\end{aligned}\quad (\text{A-97})$$

Regrouping terms at n+1 time level on the LHS, the equation can be written as

$$AU_{i,k-1}^{n+1} + VU_{i,k}^{n+1} + CU_{i,k+1}^{n+1} = DU_{i,k}^* \quad (\text{A-98})$$

where:

$$\begin{aligned}A &= \left(\frac{-\Delta t B_{i,k-1/2}^{n+1}}{B_{i,k}^{n+1} \Delta z_k \rho} \right) \left[\frac{A_{z,i,k-1/2}}{\Delta z_{k-1/2}} \right] \\ V &= 1 + \left(\frac{\Delta t B_{i,k+1/2}^{n+1}}{B_{i,k}^{n+1} \Delta z_k \rho} \right) \left[\frac{A_{z,i,k+1/2}}{\Delta z_{k+1/2}} \right] + \left(\frac{\Delta t B_{i,k-1/2}^{n+1}}{B_{i,k}^{n+1} \Delta z_k \rho} \right) \left[\frac{A_{z,i,k-1/2}}{\Delta z_{k-1/2}} \right] \\ C &= \left(\frac{-\Delta t B_{i,k+1/2}^{n+1}}{B_{i,k}^{n+1} \Delta z_k \rho} \right) \left[\frac{A_{z,i,k+1/2}}{\Delta z_{k+1/2}} \right] \\ D &= 1\end{aligned}$$

The resulting simultaneous equations are solved for U^{n+1} using the Thomas algorithm.

Computation of Initial Water Surface Slope and Velocity Field for River

Within the CE-QUAL-W2 model, initial water levels and horizontal velocities are computed using Manning's normal depth equation for sloping branches. The program reads model bathymetry and flow files to determine the normal depth and horizontal velocities at the beginning of a simulation. The model user can turn this feature on for river systems. This feature should allow for much smoother running of the river model initially and avoids somewhat difficult setting of the initial water surface elevation before a model simulation.

The initial water level/horizontal velocity first determines the flow through each model segment. All tributaries, withdrawals, distributed tributaries, upstream branch inflows, internal head boundaries, and dam outflows are considered. Once the flow through each segment has been estimated, the normal depth for each segment is calculated using Manning's equation:

$$Q_i = \frac{1}{n_i} A_i R_i^{2/3} S^{1/2}$$

where

Q_i : Flow through segment i

n_i : Manning's friction coefficient for segment i

A_i : Cross-sectional area of segment i

R_i : Hydraulic Radius of segment i

S : Branch slope

The cross-sectional area A_i and hydraulic radius R_i are a function of depth. The hydraulic radius is calculated using

$$R_i = \frac{A_i}{P_i}$$

P_i is the wetted perimeter. To calculate the normal depth, the root to the following function is found:

$$Q_i - \frac{1}{n_i} A_i R_i^{2/3} S^{1/2} = 0$$

The method of bisection (Press et al., 1992) is used to find the root, or normal depth, because the function is discontinuous (has corners).

Once the normal depth for every segment has been calculated, the water surface of each sloping branch is smoothed. If the predicted water level of a segment is less than the water level of a downstream segment, the downstream segment is considered controlling and the water level is increased to match that of the downstream segment. The effect of spillways and gates is considered by calculating the head necessary to convey the flow of the segment on the upstream side of the gate or spillway. If the normal depth predicted water levels of segments upstream of the gate/spillway are less than the necessary water level at the gate/spillway, water levels of upstream segments are set to that of the segment immediately upstream of the gate/spillway.

Once water levels have been smoothed and spillway/gates accounted for, the average horizontal velocity U_{avg} in each segment will be estimated with

$$U_{avg} = \frac{Q_i}{A_i}$$

If a branch is a "loop branch", or a branch with upstream and downstream ends that are internal head boundaries attached to segments of another, single branch, the initial velocity water level tool will set initial velocities of this branch equal to zero and estimate water levels by interpolating between the water levels in upstream and downstream boundary condition segments.

Turbulent Advection-Diffusion Equation

As in the momentum equation, time-averaged variables for velocity are introduced ([Figure A-17](#)) and concentration ([Figure A-18](#)).

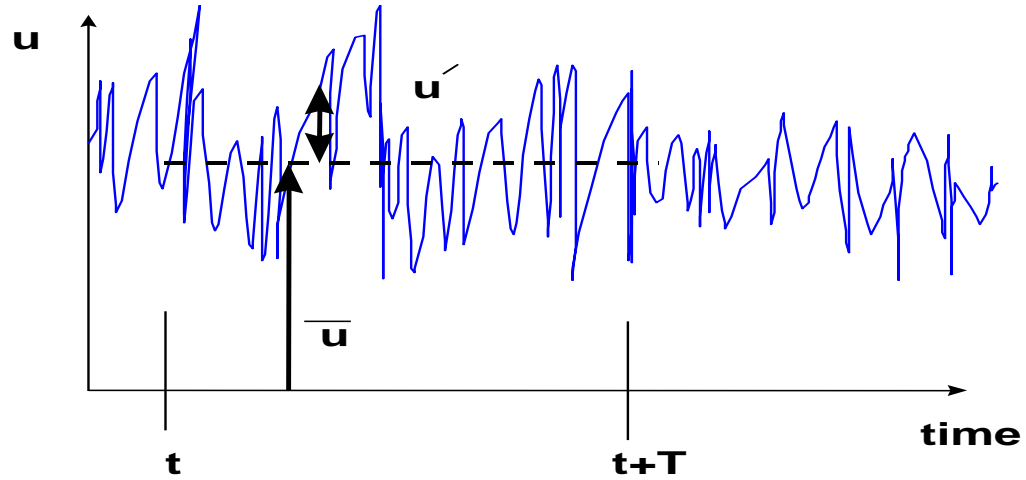


Figure A-17. Velocity variability with time.

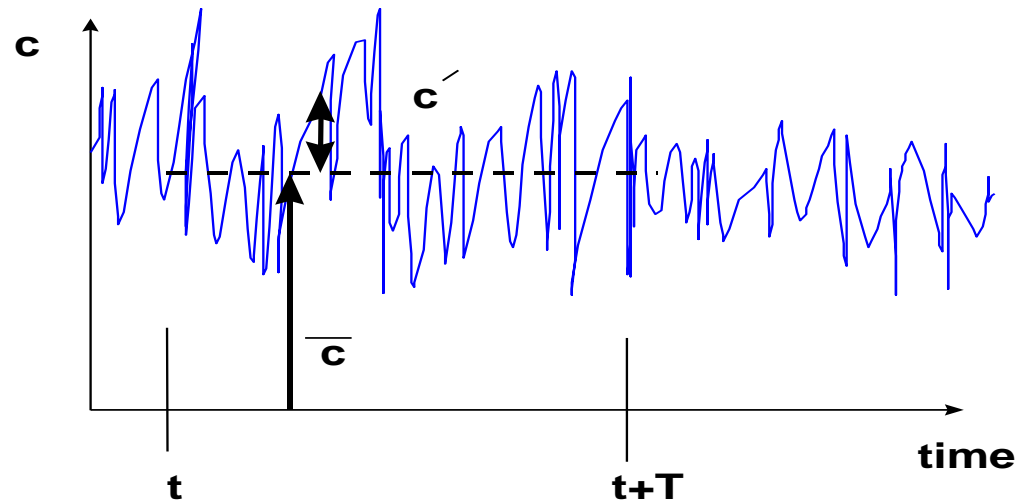


Figure A-18. Concentration variability with time.

The instantaneous velocity and concentration are decomposed into a mean and an unsteady component:

$$u(t) = \bar{u} + u'(t) \text{ where } \bar{u} = \frac{1}{T} \int_t^{t+T} u(t) dt \quad (\text{A-99})$$

Similarly for w , v , and c :

$$\begin{aligned}
v &= \bar{v} + v' \\
w &= \bar{w} + w' \\
c &= \bar{c} + c'
\end{aligned}
\tag{A-100}$$

Substituting these into the 3D governing equation and time averaging:

$$\begin{aligned}
\frac{\partial \bar{c}}{\partial t} + \underbrace{\bar{u} \frac{\partial \bar{c}}{\partial x} + \bar{v} \frac{\partial \bar{c}}{\partial y} + \bar{w} \frac{\partial \bar{c}}{\partial z}}_{\text{transport by mean advection}} &= D \underbrace{\left[\frac{\partial^2 \bar{c}}{\partial x^2} + \frac{\partial^2 \bar{c}}{\partial y^2} + \frac{\partial^2 \bar{c}}{\partial z^2} \right]}_{\text{molecular diffusive transport}} \\
&\quad - \underbrace{\frac{\partial}{\partial x} (\overline{u'c'}) - \frac{\partial}{\partial y} (\overline{v'c'}) - \frac{\partial}{\partial z} (\overline{w'c'})}_{\text{turbulent mass transport}} + \bar{S}
\end{aligned}
\tag{A-101}$$

The new terms in the governing equation represent mass transport by turbulent eddies. As the intensity of turbulence increases, turbulent mass transport increases. Notice also that all velocities and concentrations are time averaged. The following turbulent mass fluxes are defined as:

$$\bar{J}_i = (\overline{u'c'}, \overline{v'c'}, \overline{w'c'})
\tag{A-102}$$

where:

$$\begin{aligned}
(\overline{u'c'}) &= -E_x \frac{\partial \bar{c}}{\partial x} \\
(\overline{v'c'}) &= -E_y \frac{\partial \bar{c}}{\partial y} \\
(\overline{w'c'}) &= -E_z \frac{\partial \bar{c}}{\partial z}
\end{aligned}$$

Substituting into the above equation:

$$\begin{aligned}
\frac{\partial \bar{c}}{\partial t} + \bar{u} \frac{\partial \bar{c}}{\partial x} + \bar{v} \frac{\partial \bar{c}}{\partial y} + \bar{w} \frac{\partial \bar{c}}{\partial z} &= \frac{\partial}{\partial x} \left[(E_x + D) \frac{\partial \bar{c}}{\partial x} \right] + \frac{\partial}{\partial y} \left[(E_y + D) \frac{\partial \bar{c}}{\partial y} \right] \\
&\quad + \frac{\partial}{\partial z} \left[(E_z + D) \frac{\partial \bar{c}}{\partial z} \right] + \bar{S}
\end{aligned}
\tag{A-103}$$

In turbulent fluids, E_x , E_y , and $E_z \gg D$, and D can be neglected except at interfaces where turbulence goes to zero. The turbulent diffusion coefficients can be thought of as the product of the velocity scale of turbulence and the length scale of that turbulence. These coefficients are related to the turbulent eddy viscosity. One is turbulent mass transport, the other is turbulent momentum

transport between adjacent control volumes. In general, these turbulent diffusion coefficients are non-isotropic and non-homogeneous.

Water Quality Transport

Spatial averages across the lateral dimension of the channel of the turbulent time-averaged quantities can now be introduced:

$$\begin{aligned}\bar{c} &= \overline{\overline{c}} + c'' \\ \bar{u} &= \overline{\overline{u}} + u'' \\ \bar{w} &= \overline{\overline{w}} + w''\end{aligned}\tag{A-104}$$

where the double overbar is a spatial average over y and the double prime is the deviation from the spatial mean as illustrated in [Figure A-19](#) for velocity and [Figure A-20](#) for constituent concentrations.

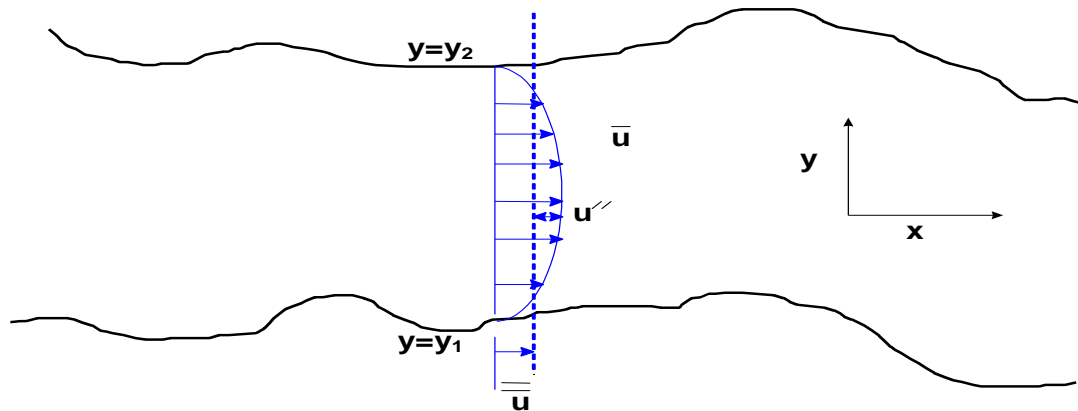


Figure A-19. Lateral average of the velocity field.

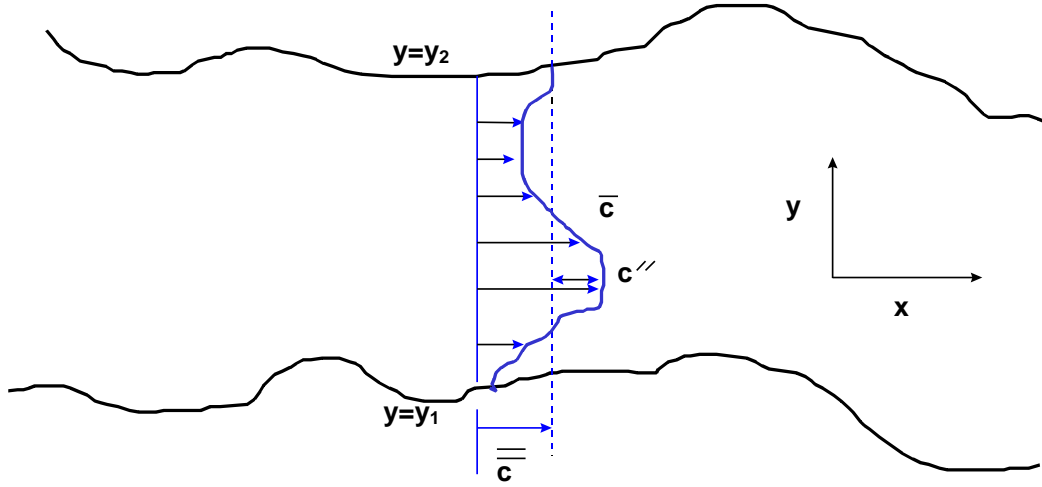


Figure A-20. Lateral average of the concentration field.

These are substituted into the governing equation and then the governing equation is integrated over the width such that:

$$\begin{aligned}
 \frac{\partial \bar{c}}{\partial t} + \frac{\partial \bar{u} \bar{c}}{\partial x} + \frac{\partial \bar{w} \bar{c}}{\partial z} = & \overbrace{-B \left(\bar{v} \bar{c} \Big|_{y_2} - \bar{v} \bar{c} \Big|_{y_1} + \bar{c}' v' \Big|_{y_2} - \bar{c}' v' \Big|_{y_1} \right)}^{\text{mass transfer at side boundaries}} \\
 & + \frac{\partial}{\partial x} \left((D + E_x) B \frac{\partial \bar{c}}{\partial x} \right) + \frac{\partial}{\partial z} \left((D + E_z) B \frac{\partial \bar{c}}{\partial z} \right) \\
 & - \left[\frac{\partial \bar{u} c''}{\partial x} + \frac{\partial \bar{w} c''}{\partial z} \right] + rB
 \end{aligned} \quad (\text{A-105})$$

Note how the following terms are simplified:

$$\begin{aligned}
 \frac{1}{B} \int_{y_1}^{y_2} \frac{\partial (\bar{c} + c'')}{\partial t} dy &= \frac{1}{B} \int_{y_1}^{y_2} \frac{\partial \bar{c}}{\partial t} dy + \frac{1}{B} \int_{y_1}^{y_2} \frac{\partial (c'')}{\partial t} dy \\
 &= \frac{1}{B} \frac{\partial}{\partial t} \int_{y_1}^{y_2} \bar{c} dy + \frac{1}{B} \frac{\partial}{\partial t} \int_{y_1}^{y_2} c'' dy \\
 &= \frac{1}{B} \frac{\partial \bar{c}}{\partial t}
 \end{aligned} \quad (\text{A-106})$$

$$\begin{aligned}
\frac{1}{B} \int_{y1}^{y2} \frac{\partial(\bar{u} + u'')(\bar{c} + c'')}{\partial x} dy &= \frac{1}{B} \int_{y1}^{y2} \frac{\partial(\bar{c}\bar{u})}{\partial t} dy + \frac{1}{B} \int_{y1}^{y2} \frac{\partial(c''u'')}{\partial t} dy \\
&= \frac{1}{B} \frac{\partial}{\partial x} \int_{y1}^{y2} \bar{c}\bar{u} dy + \frac{1}{B} \frac{\partial}{\partial x} \int_{y1}^{y2} c''u'' dy \\
&= \frac{1}{B} \frac{\partial \bar{B}\bar{u}\bar{c}}{\partial t} + \frac{1}{B} \frac{\partial \bar{B}u''c''}{\partial x}
\end{aligned} \tag{A-107}$$

The spatial average of any double primed variable goes to zero by definition.

The turbulent dispersion coefficients are defined as:

$$\begin{aligned}
\overline{u''c''} &= -D_x \frac{\partial \bar{c}}{\partial x} \\
\overline{w''c''} &= -D_z \frac{\partial \bar{c}}{\partial z}
\end{aligned} \tag{A-108}$$

The dispersion terms are a result of lateral averaging of the velocity field. In general, except at an interface, $D_x \gg E_x \gg D$ and similarly for $D_z \gg E_z \gg D$. Substituting in for the dispersion coefficients and using q to be the net mass transport from lateral boundaries, this equation becomes:

$$\frac{\partial \bar{c}}{\partial t} + \frac{\partial \bar{B}\bar{u}\bar{c}}{\partial x} + \frac{\partial \bar{B}\bar{w}\bar{c}}{\partial z} = qB + \frac{\partial}{\partial x} \left(D_x B \frac{\partial \bar{c}}{\partial x} \right) + \frac{\partial}{\partial z} \left(D_z B \frac{\partial \bar{c}}{\partial z} \right) + \bar{r}B \tag{A-109}$$

If the overbars are dropped and replaced with capitals, c is replaced with Φ , then the following equation is obtained:

$$\frac{\partial B\Phi}{\partial t} + \frac{\partial UB\Phi}{\partial x} + \frac{\partial WB\Phi}{\partial z} - \frac{\partial \left(BD_x \frac{\partial \Phi}{\partial x} \right)}{\partial x} - \frac{\partial \left(BD_z \frac{\partial \Phi}{\partial z} \right)}{\partial z} = q_\Phi B + S_\Phi B \tag{A-110}$$

where:

Φ = laterally averaged constituent concentration, $g \, m^{-3}$

D_x = longitudinal temperature and constituent dispersion coefficient, $m^2 \, sec^{-1}$

D_z = vertical temperature and constituent dispersion coefficient, $m^2 \, sec^{-1}$

q_Φ = lateral inflow or outflow mass flow rate of constituent per unit volume, $g \, m^{-3} \, sec^{-1}$

S_Φ = laterally averaged source/sink term, $g \, m^{-3} \, sec^{-1}$

Note that this can be concentration or temperature since the concentration of heat can be determined to be $\rho c_p T$ where ρ is the fluid density, c_p is the specific heat of water, and T is the temperature.

The following must be determined in order to solve the equation:

1. laterally-averaged velocity field the from momentum equations
2. appropriate boundary and initial conditions
3. D_x and D_z
4. laterally-averaged source/sink terms

Determination of D_z and D_x

The specification of D_x , the longitudinal dispersion coefficient, is a user-defined input. The preprocessor though does a check on the magnitude of this value by computing D_x based on an approach by Okubo (1971):

$$D_x = 5.84 \times 10^{-4} \Delta x^{1.1}$$

where D_x is in m^2/s and the longitudinal grid spacing Δx is in m. D_x is currently space and time invariant.

D_z is internally computed within the CE-QUAL-W2 model using the Reynold's analogy, where D_z is computed from A_z , the vertical eddy viscosity, from

$$D_z = 0.14 A_z$$

Numerical Solution

The first step in the numerical solution is to define the computational grid ([Figure A-21](#)). The grid is space-staggered since some variables are defined at one location and the remainder are displaced by $\Delta x/2$ or $\Delta z/2$. The grid discretizes a waterbody into computational cells whose locations are defined by their segment [I] and layer number [K], i.e., cell (K,I). Variables are located at either the center or boundary of a cell. Variables defined at the boundary include the horizontal and vertical velocities, U and W , longitudinal eddy viscosity and diffusivity, A_x and D_x , vertical eddy viscosity and diffusivity, A_z and D_z , and internal shear stress τ_x . The density, ρ , temperature, T , constituent concentration, Φ , pressure, P , and average cell width, B are defined at the cell center.

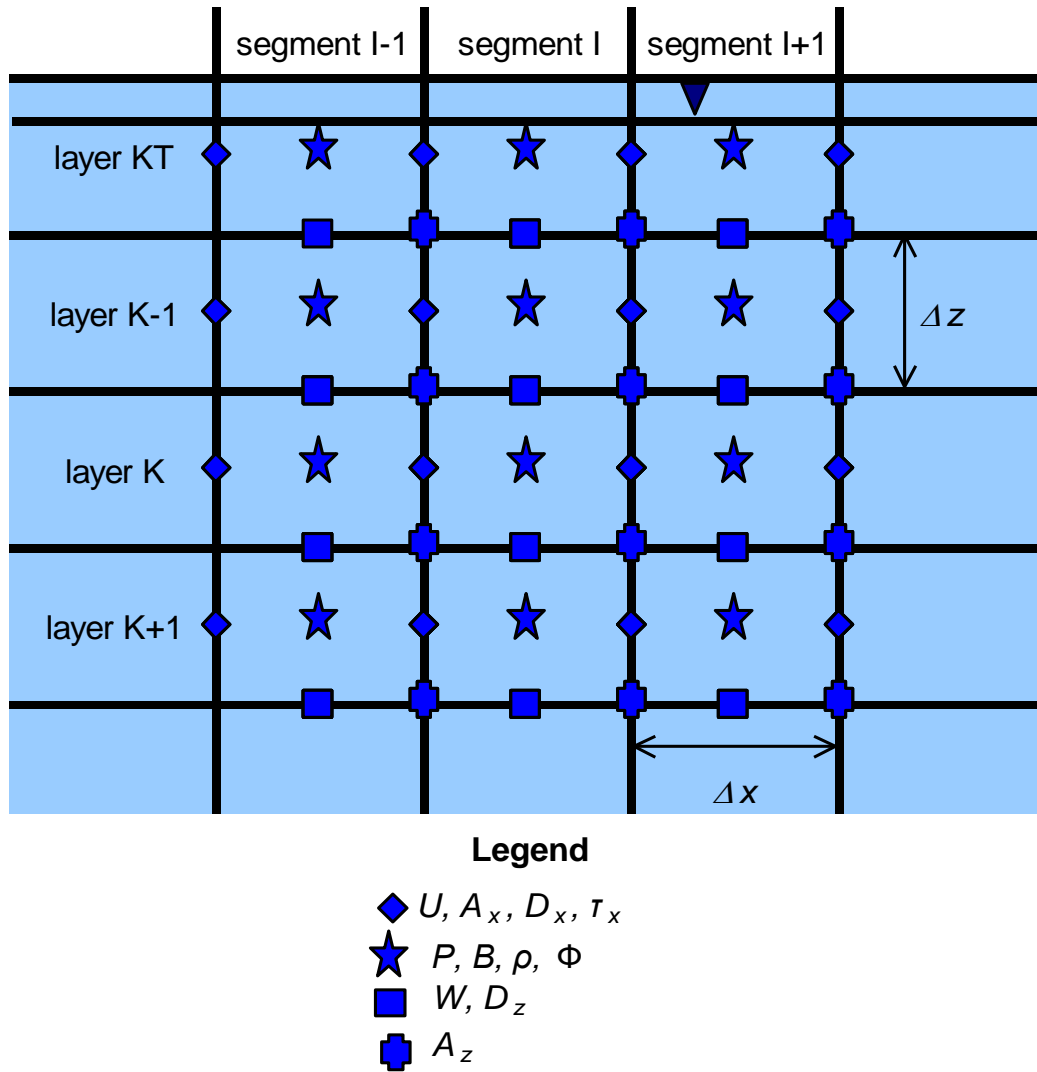


Figure A-21. Variable locations in computational grid.

There is a rational basis for choosing variable locations. Since the constituent concentration is defined at the center and velocities are defined at the boundaries, spatial averaging of velocities is not required to determine changes in concentration over time. In addition, the horizontal velocity is surrounded by a cell with water surface elevations and densities defined on either side. Thus, the horizontal velocity is computed from horizontal gradients of the surface slope and densities without requiring spatial averaging of these variables.

The geometry is specified by a cell width, B , thickness, H , and length, Δx . Several additional geometric variables are used in the calculations. These include the average cross-sectional area between two cells (k,i) and ($k,i+1$)

$$BH_{r_{k,i}} = \frac{B_{k,i} H_{k,i} + B_{k,i} H_{k,i+1}}{2} \quad (\text{A-111})$$

the average widths between two cells (k,i) and (k+1,i)

$$B_{b_{ki}} = \frac{B_{k,i} + B_{k+1,i}}{2} \quad (\text{A-112})$$

and the average layer thickness between layers k and k+1

$$\overline{H}_{k,i} = \frac{H_k + H_{k+1}}{2} \quad (\text{A-113})$$

The numerical procedure for solving the six unknowns at each timestep is to first compute water surface elevations. With the new surface elevations, new horizontal velocities can be computed. With new horizontal velocities, the vertical velocities can be found from continuity. New constituent concentrations are computed from the constituent balance. Using new horizontal and vertical velocities, the water surface elevation equation can be solved for η simultaneously. The solution for η is thus spatially implicit at the same time level and eliminates the surface gravity wave speed criterion:

$$\Delta t < \frac{\Delta x}{\sqrt{g H_{max}}} \quad (\text{A-114})$$

that can seriously limit timesteps in deep waterbodies.

Version 1.0 used upwind differencing in the constituent transport advective terms in which the cell concentration immediately upstream of the velocity is used to calculate fluxes. A major problem with upwind differencing is the introduction of numerical diffusion given by (for longitudinal advection):

$$\alpha_e = \frac{u \Delta x}{2} (1 - c) \quad (\text{A-115})$$

where:

α_e = numerical diffusion

$c = \frac{U \Delta t}{\Delta x}$ = Courant number

A similar condition holds for vertical advection. In many cases, numerical diffusion can overwhelm physical diffusion producing inaccurate results when strong gradients are present. The problem is particularly pronounced for stratified reservoirs and estuaries.

Numerical diffusion has been reduced by implementing an explicit, third-order accurate QUICKEST horizontal/vertical transport scheme (Leonard, 1979), and time-weighted, implicit vertical advection. Tests of this scheme are reported in Chapman and Cole (1992).

QUICKEST uses an additional spatial term to estimate concentrations used in computing horizontal and vertical fluxes. A nonuniform grid QUICKEST scheme was developed using a three-point

Lagrangian interpolation function to estimate constituent values at grid cell interfaces. Specifically, advective multipliers for each of three upstream weighted grid cells are derived in terms of cell lengths and the local cell interface velocity. Time invariant parts of the interpolation functions are calculated once thus minimizing computations for additional constituents.

Implicit vertical transport including variable layer heights has also been implemented. Vertical diffusion is fully implicit and advection employs a time-weighted, central difference, implicit scheme. A unique feature of vertical advection, in the explicit part of the time-weighted scheme, is QUICKEST which increases overall accuracy.

As implemented in the code, the new transport scheme is a two-part solution for constituent concentrations at the new timestep. First, horizontal advection is computed using QUICKEST and diffusion is computed using central differencing. This part also includes the explicit vertical advection contribution (which utilizes QUICKEST) and all sources and sinks.

Next, the implicit part of vertical advection and diffusion are included. Diffusion is always fully implicit. The user can time-weight advection by specifying a value for **[THETA]** which varies from 0 to 1. For **[THETA]** equal to 0, the solution is explicit in time and vertical advection is accounted for in the first part of the algorithm. For **[THETA]** equal to 1, the solution is fully implicit in time and vertical advection is accounted for in this part of the algorithm. A Crank-Nicholson scheme where vertical advection is time-weighted between the explicit (using QUICKEST) and implicit parts results if **[THETA]** is set to 0.5 or greater. The following is a description of QUICKEST, the preferred transport scheme.

Non-Uniform Grid QUICKEST Formulation

In one dimension, the conservative control volume advective transport of a constituent Φ integrated over a timestep is:

$$\Phi_i^{n+1} = \Phi_i^n - \frac{\Delta t}{\Delta x} (U_r \Phi_r^n - U_l \Phi_l^n) \quad (\text{A-116})$$

where:

Φ_i = constituent concentration at a grid point, $g\ m^{-3}$

$\Phi_{r,l}$ = right and left cell face constituent concentrations, $g\ m^{-3}$

$U_{r,l}$ = right and left cell face velocity, $m\ s^{-1}$

t = time, s

The QUICKEST algorithm was originally derived using an upstream weighted quadratic interpolation function defined over three uniformly spaced grid points. This interpolation function estimates cell face concentrations required by the conservative control volume transport scheme. For example, the right cell face concentration estimate for a flow positive to the right is:

$$\Phi_r = T_{i-1} \Phi_{i-1} + T_i \Phi_i + T_{i+1} \Phi_{i+1} \quad (\text{A-117})$$

where T are advective multipliers which weight the contribution of three adjacent grid point concentrations.

The advective multipliers are obtained by collecting terms associated with each constituent defined by the QUICKEST advection operator. For a non-uniform grid, a combination of two and three point Lagrangian interpolation functions (Henrici, 1964) are used to compute the QUICKEST estimate for the right cell face concentration centered about cells i and $i+1$:

$$\Phi_r = P_1(x) - \frac{U \Delta t}{2} P_2(x) + \left[D_x \Delta t - \frac{1}{6} \left[\Delta x^2 - (U \Delta t)^2 \right] \right] P_2''(x) \quad (\text{A-118})$$

where:

x = the local right cell face position

D_x = diffusion coefficient

Defining a local coordinate system of three non-uniformly spaced grid cells denoted by x_{i-1} , x_i , and x_{i+1} with corresponding constituent values, the interpolation functions required in equation A-118 are:

$$P_1(x) = \frac{(x - x_i)}{(x_{i+1} - x_i)} \Phi_{i+1} + \frac{(x_{i+1} - x)}{(x_{i+1} - x_i)} \Phi_i \quad (\text{A-119})$$

$$P_2(x) = \frac{(x - x_i)(x - x_{i-1})}{(x_{i+1} - x_i)(x_{i+1} - x_{i-1})} \Phi_{i+1} + \frac{(x - x_{i+1})(x - x_{i-1})}{(x_i - x_{i+1})(x_i - x_{i-1})} \Phi_i \quad (\text{A-120})$$

$$+ \frac{(x - x_{i+1})(x - x_i)}{(x_{i-1} - x_{i+1})(x_{i-1} - x_i)} \Phi_{i-1}$$

Taking the first derivative of $P_1(x)$ and the second derivative of $P_2(x)$ and substituting into equation A-118, it is then possible to group terms and obtain the advective multipliers. For example, the T_{i+1} multiplier is:

$$T_{i+1} = \frac{(x - x_i)}{(x_{i+1} - x_i)} - \frac{U \Delta t}{2} \frac{[(x - x_i) + (x - x_{i-1})]}{(x_{i+1} - x_i)(x_{i+1} - x_{i-1})} \quad (\text{A-121})$$

$$+ \frac{2 \left(D_x \Delta t - \frac{1}{6} \left[\Delta x_i^2 - (U \Delta t)^2 \right] \right)}{(x_{i+1} - x_i)(x_{i+1} - x_{i-1})}$$

Similar functions are obtained for T_i and T_{i-1} multipliers that complete the formulation for the QUICKEST algorithm.

From a computational standpoint, most geometric components of the multipliers are time-invariant and are computed once and stored in arrays. The time-varying part of the multipliers (U , Δt , D_x) are updated each timestep during computation of the T arrays. However, when the QUICKEST

scheme is applied vertically, the spatial part of the multipliers for layers [KT] and [KT]+1 are updated each timestep to accommodate the surface elevation fluctuation.

ULTIMATE/QUICKEST Numerical Transport Solution Scheme

In Version 2, the QUICKEST numerical scheme replaced the upwind numerical scheme used in Version 1 for solving the advective terms in the advection-diffusion equation. Compared to the upwind scheme, QUICKEST resulted in improved numerical accuracy in simulating sharp fronts since the upwind transport scheme adds excessive numerical diffusion.

A problem with the QUICKEST scheme is that it can give rise to spurious oscillations at the leading and trailing edge of a sharp front or gradient. This can occur where there are fresh/salt water interfaces, point source discharges, or cases of strong temperature stratification. Even though the upwind scheme always gives physically realistic solutions, it introduces numerical diffusion that artificially reduces sharp gradients.

An improvement was introduced by Leonard (1991) that eliminated spurious oscillations but preserved the higher-order solution scheme of QUICKEST. This technique is a universal (in the sense that it can be applied to numerical schemes other than QUICKEST) limiter for maintaining monotonic profiles near a gradient and is called the ULTIMATE solution scheme.

In order to illustrate the scheme, consider the solution of the unsteady advective equation:

$$\frac{\partial B\Phi}{\partial t} + \frac{\partial BU\Phi}{\partial x} = 0 \quad (\text{A-122})$$

where:

- Φ = concentration, $g\ m^{-3}$
- B = width, m
- U = velocity, $m\ s^{-1}$
- x = longitudinal coordinate, m
- t = time, s

The finite difference scheme for this based on a positive flow ($U > 0$) is:

$$\Phi_i^{n+1} = \frac{1}{B_i^{n+1}} \left(B_i^n \Phi_i^n - \left\{ \left[\frac{UB\Delta t}{\Delta x} \right]_R \Phi_R - \left[\frac{UB\Delta t}{\Delta x} \right]_L \Phi_L \right\} \right) \quad (\text{A-123})$$

The value i refers to the center grid point, R is the right-hand face value, and L is the left hand face value ([Figure A-22](#)).

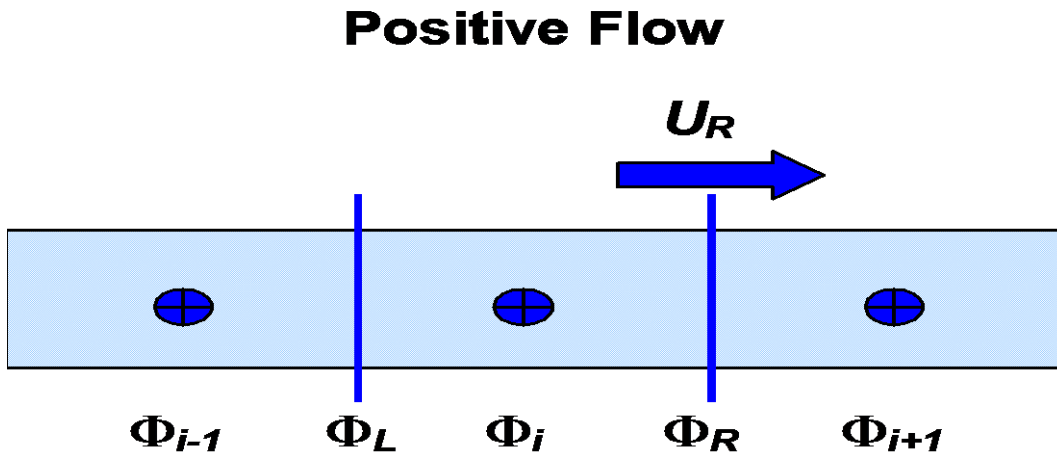


Figure A-22. ULTIMATE schematization for positive flow.

where:

- Φ_{i-1} = upstream concentration, $g\ m^{-3}$
- Φ_i = center concentration, $g\ m^{-3}$
- Φ_{i+1} = downstream concentration, $g\ m^{-3}$
- Φ_L = left face concentration, $g\ m^{-3}$
- Φ_R = right face concentration, $g\ m^{-3}$
- U_r = right face horizontal velocity, $m\ s^{-1}$

[Figure A-23](#) shows a sketch of variables used for a negative flow. The term $U\Delta t / \Delta x$ is called the Courant number. The problem to resolve is how to choose the concentrations at the “face” values since concentrations are defined at the center of a cell. An upwinding scheme would say that the concentration at the left face is Φ_{i-1} and the concentration at the right face is Φ_i for positive flow. In order to improve numerical accuracy, there are other higher-order numerical techniques, such as QUICKEST (Leonard, 1979), to estimate these face values. In CE-QUAL-W2, Φ_R and Φ_L are initially computed based on the QUICKEST method. However, if the criteria for a monotonic solution are violated, the values for Φ_R and Φ_L are revised to assure a monotonic solution. This is the essence of the ULTIMATE algorithm that eliminates over/undershoots in the numerical transport scheme.

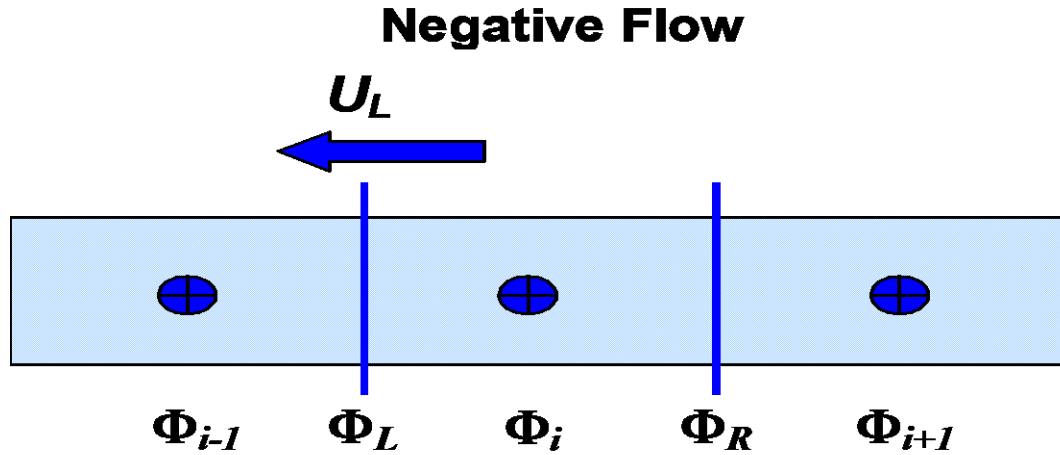


Figure A-23. ULTIMATE schematization for negative flow.

where:

- Φ_{i-1} = downstream concentration, $g\ m^{-3}$
- Φ_i = center concentration, $g\ m^{-3}$
- Φ_{i+1} = upstream concentration, $g\ m^{-3}$
- Φ_L = left face concentration, $g\ m^{-3}$
- Φ_R = right face concentration, $g\ m^{-3}$
- U_L = left face horizontal velocity, $m\ s^{-1}$

To outline the procedure for simple conditions, the velocity, segment spacing and segment widths are assumed constant, so that Equation A-123 can be written as:

$$\Phi_i^{n+1} = \left(\Phi_i^n - \left[\frac{U\Delta t}{\Delta x} \right] \Phi_R - \left[\frac{U\Delta t}{\Delta x} \right] \Phi_L \right) \quad (\text{A-124})$$

Defining normalized variables based on:

$$\tilde{\Phi} = \frac{\Phi - \Phi_{i-1}^n}{\Phi_{i+1}^n - \Phi_{i-1}^n}, \quad (\text{A-125})$$

for location i (the center location) and the right face value for positive flow as in [Figure A-22](#), we have the following:

$$\tilde{\Phi}_i^n = \frac{\Phi_i^n - \Phi_{i-1}^n}{\Phi_{i+1}^n - \Phi_{i-1}^n} \quad (\text{A-126})$$

$$\tilde{\Phi}_R = \frac{\Phi_R - \Phi_{i-1}^n}{\Phi_{i+1}^n - \Phi_{i-1}^n} \quad (\text{A-127})$$

$$\text{If } \tilde{\Phi}_R \leq \left[\frac{\tilde{\Phi}_i^n}{U\Delta t / \Delta x} \right]_R \text{ for } 0 < \tilde{\Phi}_i^n \leq 1 \quad (\text{A-128})$$

$$\tilde{\Phi}_i^n \leq \tilde{\Phi}_R \leq 1 \text{ for } 0 < \tilde{\Phi}_i^n \leq 1 \quad (\text{A-129})$$

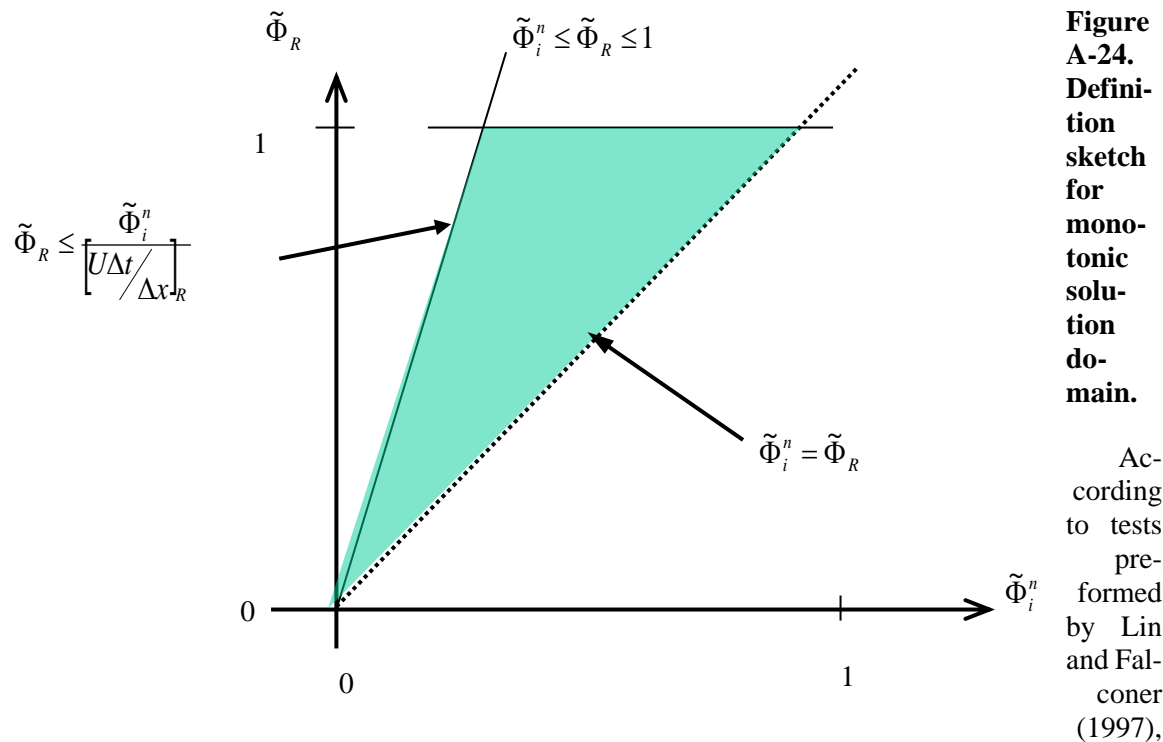
$$\tilde{\Phi}_i^n = \tilde{\Phi}_R \text{ for } \tilde{\Phi}_i^n < 0 \text{ or } \tilde{\Phi}_i^n > 1 \quad (\text{A-130})$$

The face value is unadjusted from that computed by the numerical scheme and the QUICKEST value of Φ_R is used without alteration. These conditions are shown as the shaded region in [Figure A-24](#).

If these conditions are not met, then Φ_R is adjusted to force a monotonic solution. The value of the face is replaced with the nearest allowable value of $\tilde{\Phi}_R$ based on the above criteria that will ensure these criteria are met. The face value is determined by using:

$$\Phi_R = \Phi_{i-1}^n + \tilde{\Phi}_R (\Phi_{i+1}^n - \Phi_{i-1}^n) \quad (\text{A-131})$$

This procedure is applied to all the faces and then Equation A-124 is solved to update the concentration at the next time level. This means that the right face concentration will be the left face concentration for the next segment thus ensuring mass conservation.



the QUICKEST-ULTIMATE scheme with splitting of the diffusion and source/sink terms conserved mass and eliminated numerical oscillations. Leonard (1991) also indicated that the QUICKEST scheme coupled with the ULTIMATE scheme was numerically accurate and cost-effective in terms of computational time.

[Figure A-25](#) shows the results of a square pulse of 100 g m^{-3} moving downstream using the UPWIND, QUICKEST, and ULTIMATE/QUICKEST numerical transport schemes. The UPWIND scheme has a large amount of numerical diffusion whereas the QUICKEST scheme has non-physical oscillations about the leading and trailing edge of the solution. The ULTIMATE/QUICKEST numerical solution greatly reduces numerical diffusion and eliminates the over and undershoots.

For any case of unequal grid spacing, the order of accuracy diminishes. Leonard (1991) recommends that if used with non-uniform grid spacing, the formal accuracy of the method is only preserved if the grid does not expand or contract more than about 125%.

Even though the ULTIMATE scheme can be used with any suitable numerical technique, Leonard (1991) indicates that when coupled with the 3rd order QUICKEST scheme and a 2nd order central difference diffusion operator, the results are virtually indistinguishable from other higher-order advection solvers.

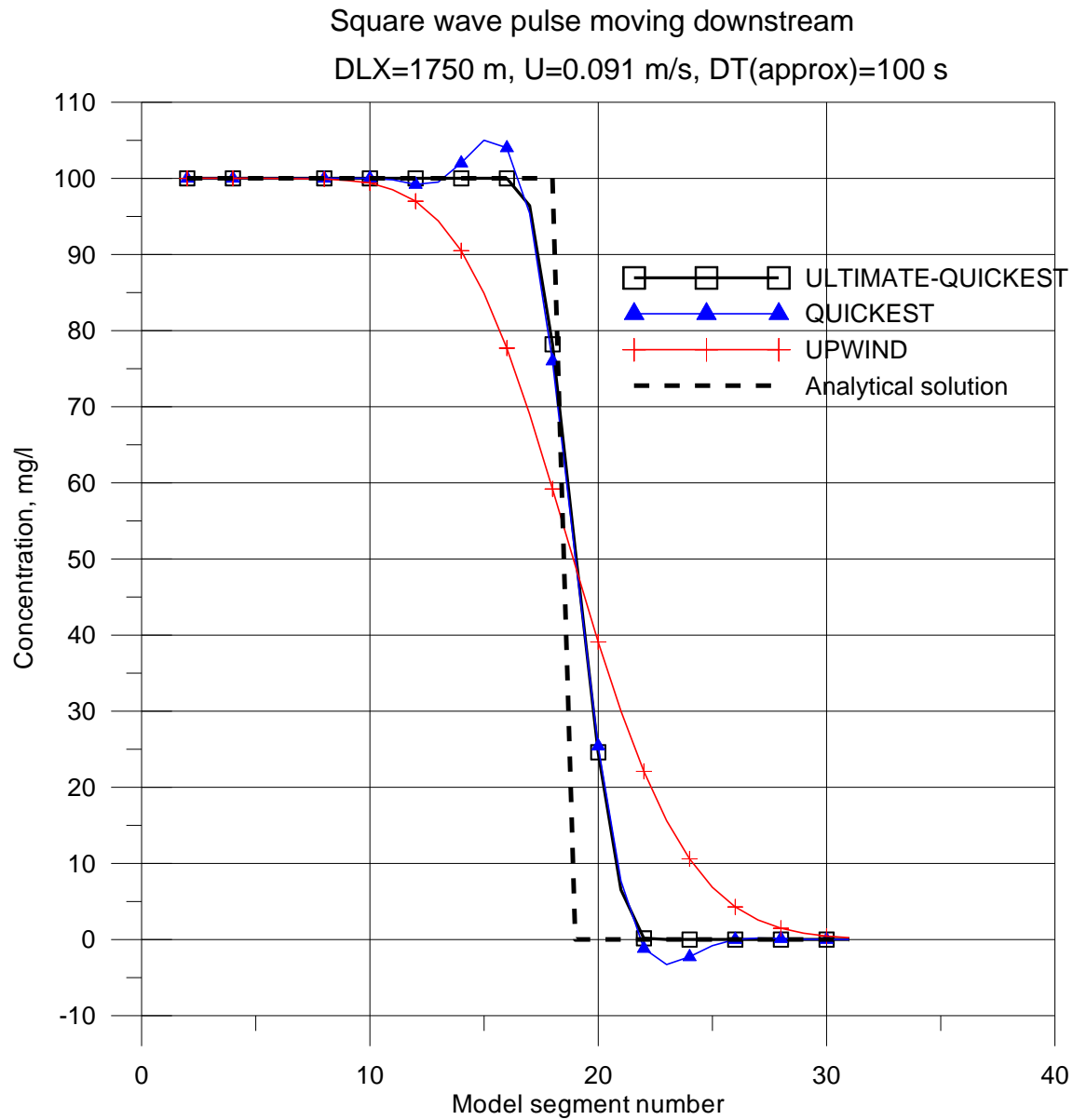


Figure A-25. Comparison of UPWIND, QUICKEST, and ULTIMATE/QUICKEST schemes for conservative tracer transport.

The following shows a straightforward procedure by Leonard to compute the right and left face values if they do not meet the monotonic criteria, as well as a procedure for variable velocities.

Based on the sign of the velocity for each face, compute DEL:

$$DEL = \Phi_{i+1}^n - \Phi_{i-1}^n \quad (\text{A-132})$$

If $|DEL| < 10^{-5}$ set $\Phi_{face} = \Phi_i^n$ and proceed to the next face (the face value is the L or R face as shown in). Otherwise, compute:

$$\tilde{\Phi}_i^n = \frac{\Phi_i^n - \Phi_{i-1}^n}{\Phi_{i+1}^n - \Phi_i^n} = \frac{\Phi_i^n - \Phi_{i-1}^n}{DEL} \quad (\text{A-133})$$

If $\tilde{\Phi}_i^n < 0$ or $\tilde{\Phi}_i^n > 1$, set $\Phi_{face} = \Phi_i^n$ and proceed to the next face. If not, compute:

$$\tilde{\Phi}_{face} = \frac{\Phi_{face} - \Phi_{i-1}^n}{\Phi_{i+1}^n - \Phi_{i-1}^n} = \frac{\Phi_{face} - \Phi_{i-1}^n}{DEL} \quad (\text{A-134})$$

where Φ_{face} is computed based on the user's chosen numerical scheme (such as QUICKEST or another scheme).

1. If $\tilde{\Phi}_{face} < \tilde{\Phi}_i^n$, $\tilde{\Phi}_{face} = \tilde{\Phi}_i^n$
2. if $\tilde{\Phi}_{face} > \frac{\tilde{\Phi}_i^n}{\left(\frac{U\Delta t}{\Delta x}\right)}$, $\tilde{\Phi}_{face} = \frac{\tilde{\Phi}_i^n}{\left(\frac{U\Delta t}{\Delta x}\right)}$
3. if $\tilde{\Phi}_{face} > 1$, $\tilde{\Phi}_{face} = 1$

Then recompute the face value according to $\Phi_{face} = \tilde{\Phi}_{face} DEL + \Phi_i^n$.

Once all the face values are determined, use the finite difference form of the solution to determine the solution (Equation A-123)

Leonard (1991) also showed a numerical technique that minimized the computational burden when using ULTIMATE with the QUICKEST scheme. This technique is described as follows.

Based on the sign of the velocity for each face, define C, D, and U nodes (center, downstream, and upstream) corresponding for positive flow to i, i+1, and i-1, respectively.

Compute DEL and $CURV$, where $DEL = \Phi_{i+1}^n - \Phi_i^n$ and $CURV = \Phi_{i+1}^n - 2\Phi_i^n + \Phi_{i-1}^n$

1. If $|CURV| \leq 0.6|DEL|$, then use the QUICKEST computed value for the face value, Φ_{face} (the face value is the R or L face as shown in).
2. If not, and if $|CURV| \geq |DEL|$, then set $\Phi_{face} = \Phi_i^n$
3. If not, and $DEL > 0$, limit Φ_{face} by Φ_i^n below, or the smaller of

$$\Phi_{reference} = \Phi_{i-1}^n + \frac{(\Phi_i^n - \Phi_{i-1}^n)}{\left(\frac{U\Delta t}{\Delta x}\right)} \text{ and } \Phi_{i+1}^n$$

4. If not, and $DEL < 0$, limit Φ_{face} by Φ_i^n , or the larger of

$$\Phi_{reference} = \Phi_{i-1}^n + \frac{(\Phi_i^n - \Phi_{i-1}^n)}{\left(\frac{U\Delta t}{\Delta x}\right)} \text{ and } \Phi_{i+1}^n$$

5. Once all the face values are determined, use Equation A-123 to obtain the solution

The procedure outlined above is based on unidirectional and uniform magnitude velocity and segment widths. If the velocity regime and widths are variable, then the following procedure is followed in order to maintain a monotonic solution. Consider the following limitations based on definitions shown in [Figure A-26](#).

Positive flow at right face, $U > 0$

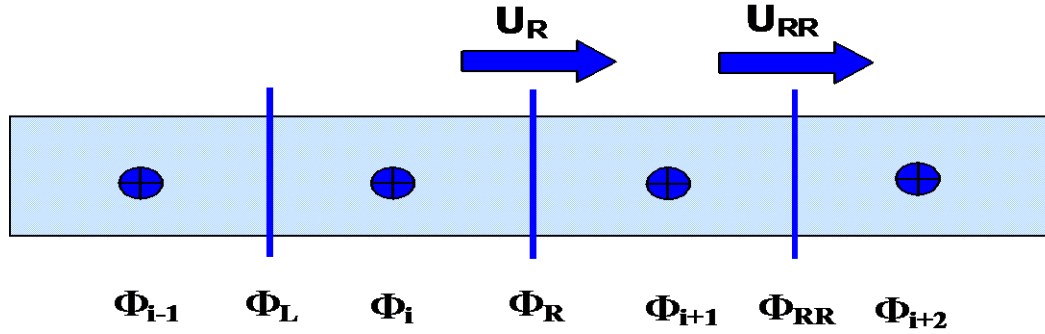


Figure A-26. Definition sketch for variable velocity.

where:

- Φ_{i-1} = upstream concentration
- Φ_i = center concentration
- Φ_{i+1} = center concentration
- Φ_L = left face concentration at i
- Φ_R = right face concentration at i
- Φ_{RR} = right face concentration at $i+1$

Assuming that U_R is positive and the concentration times width (ΦB) increases monotonically, i.e., $(B\Phi)_{i-1}^n < (B\Phi)_i^n < (B\Phi)_{i+1}^n < (B\Phi)_{i+2}^n$, between segment $i-1$ and $i+2$, then the goal of the technique is to estimate Φ_R , or really $B_R \Phi_R$, and to update the concentration using Equation A-123. Equation A-123 can be written as a condition for Φ_R as:

$$\left[\frac{UB\Delta t}{\Delta x} \right]_R \Phi_R = B_i^n \Phi_i^n - \Phi_i^{n+1} B_i^{n+1} + \left[\frac{UB\Delta t}{\Delta x} \right]_L \Phi_L \quad (\text{A-135})$$

If it is assumed that $B_i^n \Phi_i^n \leq B_R \Phi_R \leq B_{i+1}^n \Phi_{i+1}^n$, then this is equivalent to saying that $B_i^n U_i^n \Phi_i^n \leq B_R^n U_R^n \Phi_R \leq B_{i+1}^n U_{i+1}^n \Phi_{i+1}^n$ or that the net flux into a segment is increasing.

Using the monotonic limitation that $B_i^{n+1} \Phi_i^{n+1} \geq B_{i-1}^n \Phi_{i-1}^n$ then Equation A-135 becomes:

$$\left[\frac{UB\Delta t}{\Delta x} \right]_R \Phi_R \leq B_i^n \Phi_i^n - \Phi_{i-1}^n B_{i-1}^n + \left[\frac{UB\Delta t}{\Delta x} \right]_L \Phi_L \quad (\text{A-136})$$

Then making a conservative assumption that $B_L \Phi_L \geq B_{i-1}^n \Phi_{i-1}^n$, Equation A-136 becomes:

$$\left[\frac{UB\Delta t}{\Delta x} \right]_R \Phi_R \leq B_i^n \Phi_i^n - \Phi_{i-1}^n B_{i-1}^n + \left[\frac{UB\Delta t}{\Delta x} \right]_{i-1}^n \Phi_{i-1}^n \quad (\text{A-137})$$

Another condition is also imposed on $B_R \Phi_R$ by looking at the control volume segment centered at $i+1$. Using similar reasoning as above and assuming that $U_{RR} > 0$, the other criterion for $B_R \Phi_R$ is

$$\left[\frac{UB\Delta t}{\Delta x} \right]_R \Phi_R \leq B_{i+2}^n \Phi_{i+2}^n - \Phi_{i+1}^n B_{i+1}^n + \left[\frac{UB\Delta t}{\Delta x} \right]_{RR} \Phi_{i+1}^n \quad (\text{A-138})$$

These criteria would be altered appropriately if the function were monotonically decreasing rather than increasing.

Vertical Implicit Transport

Focusing on vertical advective and diffusive transport, constituent transport can be written as:

$$\frac{\partial B\Phi}{\partial t} + \frac{\partial WB\Phi}{\partial z} - \frac{\partial}{\partial z} \left(BD_z \frac{\partial \Phi}{\partial z} \right) = RHS \quad (\text{A-139})$$

where RHS represents horizontal transport and all sources/sinks. Integrating the transport equation vertically and over time gives:

$$BH \Phi^{n+1} + \theta H \Delta t \delta_z (WB \Phi^{n+1}) - H \Delta t \delta_z \left(BD_z \frac{\partial \Phi^{n+1}}{\partial z} \right) = BH \Phi^* \quad (\text{A-140})$$

where:

Φ^* = all n-time level horizontal and explicit vertical transport and sources/sinks

θ = time-weighting for vertical advection; 0 for fully explicit, 0.55 for Crank-Nicholson, and 1 for fully implicit

Expanding the differential operators in terms of central differences and collecting terms, the above equation can be recast as:

$$A_{t_i} \Phi_{i-1}^{n+1} + V_{t_i} \Phi_i^{n+1} + C_{t_i} \Phi_{i+1}^{n+1} = D_{t_i} \quad (\text{A-141})$$

where:

$$V_{t_i} = 1 + \frac{\Delta t}{BH_{k,i}} \left[\theta \left(\frac{W_{k,i} B_{b_{k,i}} - W_{k-1,i} B_{b_{k-1,i}}}{2} \right) + \frac{B_{b_{k,i}} D_{z_{k,i}}}{\bar{H}_k} + \frac{B_{b_{k-1,i}} D_{z_{k-1,i}}}{\bar{H}_{k-1}} \right]$$

$$A_{t_i} = \frac{\Delta t B_{b_{k,i}}}{BH_{k,i}} \left(\theta \frac{W_{k,i}}{2} - \frac{D_{z_{k,i}}}{\bar{H}_k} \right)$$

$$C_{t_i} = - \frac{\Delta t B_{b_{k-1,i}}}{BH_{k,i}} \left(\theta \frac{W_{k-1,i}}{2} + \frac{D_{z_{k-1,i}}}{\bar{H}_{k-1}} \right)$$

The coefficients are computed once, stored in arrays, and used to update each constituent. This is accomplished by loading the explicit part of the solution, Φ^* , with each successive constituent and inverting the resulting matrix via a Thomas tridiagonal solver.

Auxiliary Functions

Auxiliary functions are relationships that describe processes independent of basic hydrodynamic and transport computational schemes in the model. Auxiliary functions include turbulent dispersion and wind shear processes, heat exchange (including ice cover), evaporation, hydraulic structures, density, and selective withdrawal.

Surface Shear Stress

Referring to [Figure A-27](#), the shear stress at the water surface is defined as

$$\tau_s = C_D \rho_a (W_h - u_s)^2 \cong C_D \rho_a (W_h)^2 \quad (\text{A-142})$$

where:

τ_s = surface shear stress at water surface, kg/m/s²

u_s = surface velocity in water, m/s

W_h = wind velocity measured at a distance h above water surface in direction of shear, m/s

C_D = drag coefficient, [-]

ρ_a = air density, kg/m³

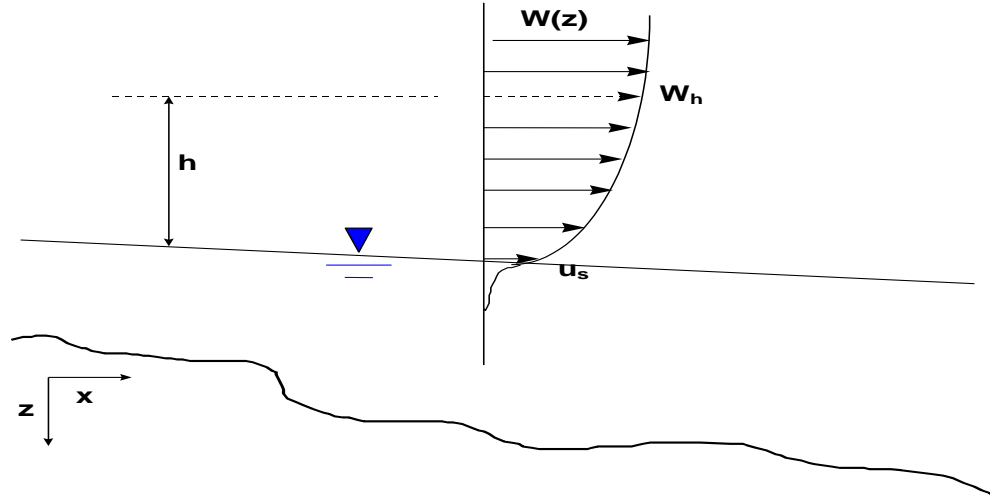


Figure A-27. Shear stress at the air-water surface.

Note that this relationship leads to the “3% rule” for surface currents:

$$\tau_s = \underbrace{C_D \rho_a (W_h - u_s)^2}_{\text{air}} = \underbrace{C_D \rho_w u_s^2}_{\text{water}} \quad (\text{A-143})$$

if $C_{D_{\text{air}}} \sim C_{D_{\text{water}}}$, then $\underbrace{u_s \sim 0.03 W_h}_{\text{3\% rule}}$

Usually the drag coefficient is a function of the measurement height, h , above the water surface. Most drag coefficient formulae have been determined based on a 10 m wind speed measurement height. If wind speeds are taken at other measurement heights for the shear stress calculation, these are corrected in the model to a 10 m height.

The wind speed is a function of measurement height. To correct the measurement height to an elevation z , use the following approach.

Assuming a logarithmic boundary layer:

$$\frac{W_z}{W_{z1}} = \frac{\ln(\frac{z}{z_0})}{\ln(\frac{z1}{z_0})} \quad (\text{A-144})$$

where:

W_z = desired wind speed at elevation z

W_{z1} = known wind speed at height z_1

z_0 = wind roughness height (some assume 0.003 ft for wind < 5 mph and 0.015 for wind > 5 mph, range 0.0005 to 0.03 ft, this is a user-defined coefficient in the CE-QUAL-W2 model)

This term can then be used to compute the surface stress in the direction of the x-axis and the cross-shear (the cross-shear term will be used in the turbulent shear stress algorithm) as follows:

$$\tau_{wx} \cong C_D \rho_a W_h^2 \cos(\Theta_1 - \Theta_2) \quad (\text{A-145})$$

$$\tau_{wy} \cong C_D \rho_a W_h^2 \sin(\Theta_1 - \Theta_2) \quad (\text{A-146})$$

where:

τ_{wx} = surface shear stress along x-axis due to wind

τ_{wy} = surface shear stress along lateral direction due to wind

Θ_1 = wind orientation relative to North, radians

Θ_2 = segment orientation relative to North, radians

Segment and wind orientation are illustrated in [Figure A-28](#) and [Figure A-29](#). The angles are measured in radians clockwise from north. A wind from the east would have an angle of $\pi/2$ radians, π radians from the south, $3\pi/2$ radians from the west, and 0 or 2π radians from the north.

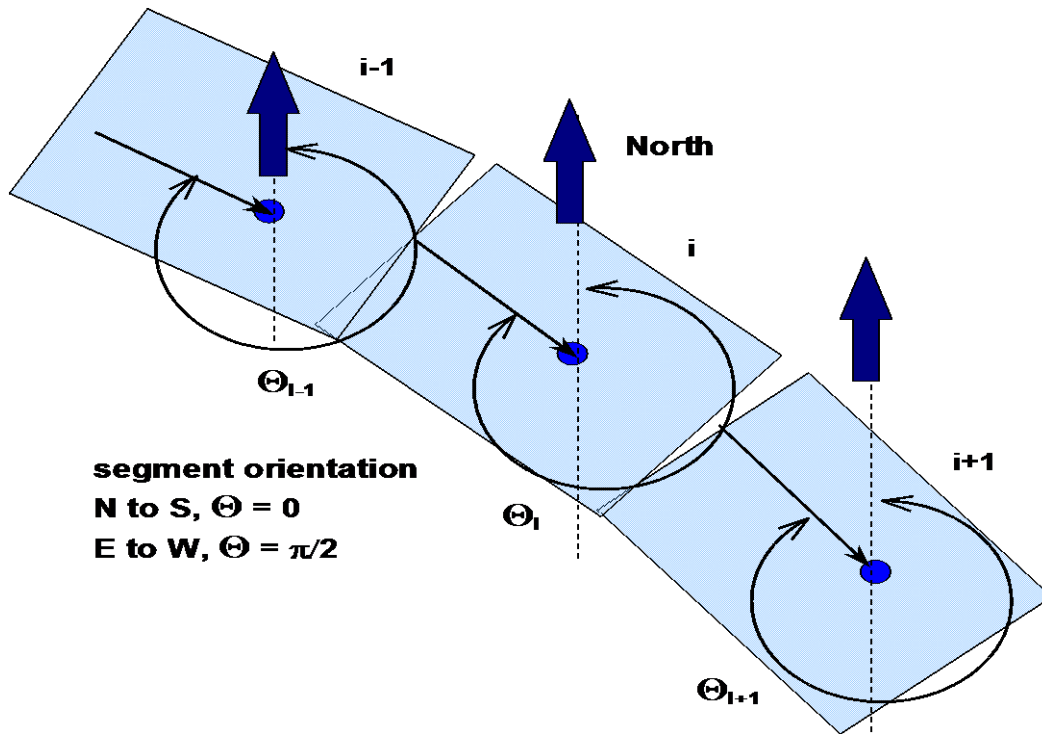


Figure A-28. Segment orientation.

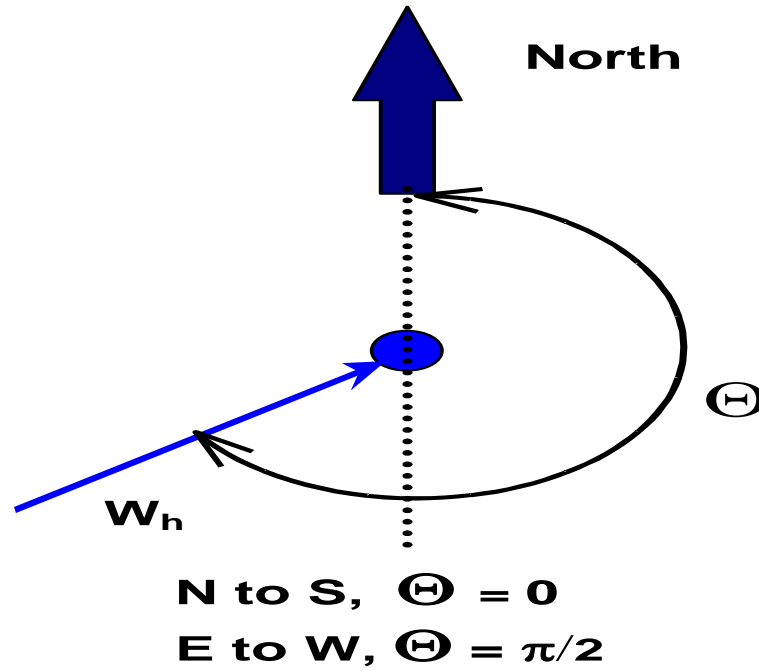


Figure A-29. Wind orientation.

The CE-QUAL-W2 model V3.5 and earlier included a drag coefficient, C_D , that was based on the following formulae:

$$\begin{aligned} CD &= 0.0 \text{ if } W_{10} < 1 \text{ m/s} \\ CD &= 0.005W_{10}^{0.5} \text{ if } 1 \text{ m/s} \leq W_{10} < 15 \text{ m/s} \\ CD &= 0.0026 \text{ if } W_{10} \geq 15 \text{ m/s} \end{aligned}$$

where W_{10} is the wind speed in m/s at 10 m.

This formulation shows that C_D decreases as wind speed decreases. It has been observed though that for wind speeds below 5 m/s, C_D increases with lowering wind speed. According to Wuest and Lorke (2003), the drag coefficient for a smooth surface (below 5 m/s) follows the following equation:

$$CD = 0.0044W_{10}^{-1.15}$$

Above a wind speed of 5 m/s, C_D can be calculated from the following implicit equation:

$$CD = \left\{ k^{-1} \ln \left[\frac{10g}{CDW_{10}^2} \right] + 11.3 \right\}^{-2}$$

where k is von Karman constant ($=0.41$), and the '10' in the above equation has units of m. The above equation for winds greater than 5 m/s are thought to be a lower limit to the drag coefficient since the wind-wave effects at higher wind speeds probably increase the value of C_D higher than that predicted by the above implicit equation. The difference between these 2 equations is shown below in Figure 30.

Since the W2 approximation for wind speeds above 4 m/s is reasonable, for V3.6 and later versions the following drag coefficient formulation is being used:

$$CD = 0.01 \text{ if } W_{10} < 0.5 \text{ m/s}$$

$$\begin{aligned}
 CD &= 0.0044W_{10}^{-1.15} \text{ if } W_{10} < 4 \text{ m/s} \\
 CD &= 0.005W_{10}^{0.5} \text{ if } 4 \text{ m/s} \leq W_{10} < 15 \text{ m/s} \\
 CD &= 0.0026 \text{ if } W_{10} \geq 15 \text{ m/s}
 \end{aligned}$$

This is shown as the dotted line in Figure 30.

This will have the effect of increasing the drag coefficient at low wind speeds. The impact of this on the wind shear stress at the surface, $\tau = \rho_a CD W_{10}^2$, is shown in Figure 31.

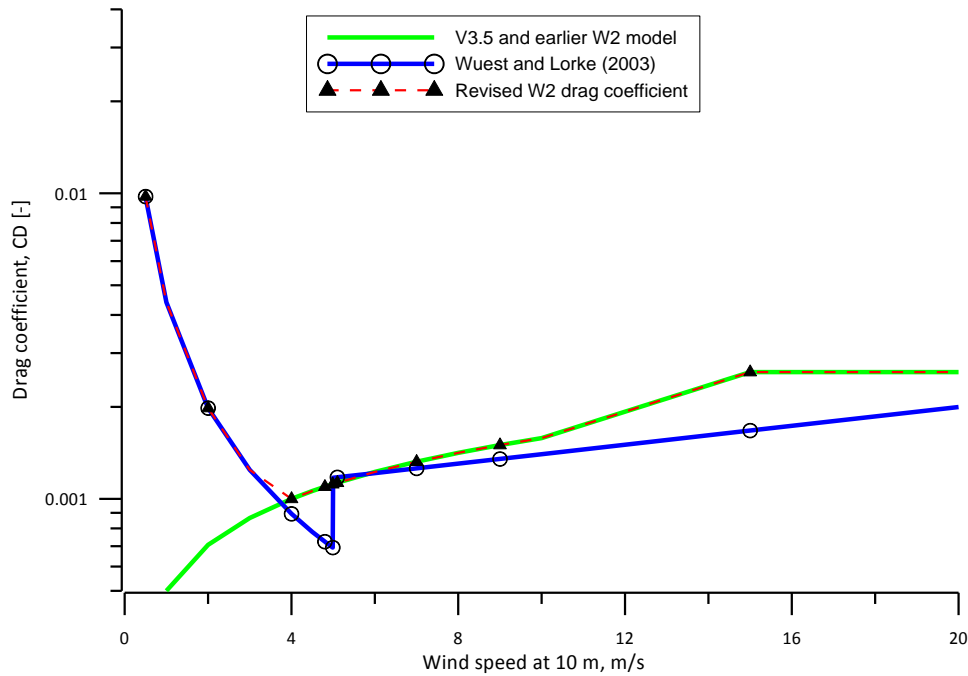


Figure 30. Comparison of current W2 model computation of CD and that recommended as a lower limit by Wuest and Lorke (2003).

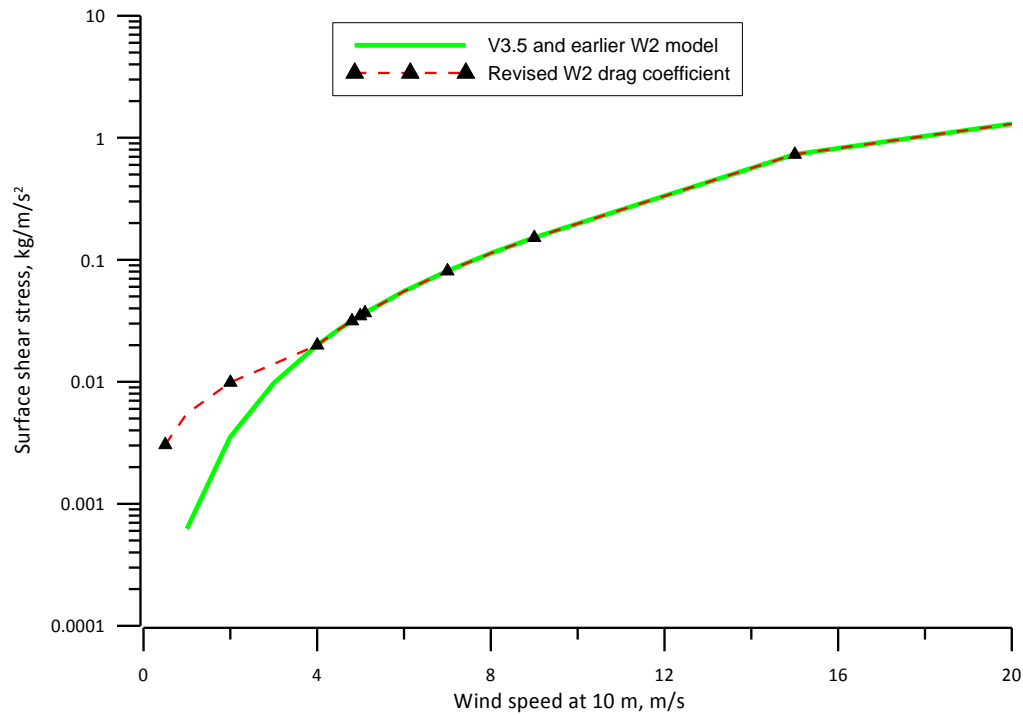


Figure 31. Surface shear stress for V3.6 and later compared to V3.5 and earlier.

In addition, a fetch correction to the wind velocity can be used as determined by Fang and Stefan (1994). This correction is described in Appendix B under [Dissolved Oxygen](#), but is not applicable to rivers.

Bottom Shear Stress

The shear stress is defined along the bottom of each cell (or for each cell in contact with side walls or channel bottom) as

$$\tau_b = \frac{\rho_w g}{C^2} U|U| \quad (\text{A-147})$$

where:

- C = Chezy friction coefficient
- U = longitudinal velocity
- ρ_w = density of water

Also, the model user can specify a Manning's friction factor where the Chezy coefficient is related to the Manning's friction factor (SI units) as

$$C = (1/n)R^{1/6} \quad (\text{A-148})$$

where:

n = Manning's friction factor

R = hydraulic radius

In Version 2, the bottom shear stress was applied only to the bottom of each layer. In Version 3 and later, the sidewall friction is accounted for because of its greater importance in river systems. The user can input either the Chezy or Manning's coefficient for each model segment.

Vertical Shear Stress

The algorithm for the vertical shear stress is

$$\frac{\tau_{xz}}{\rho} = \nu_t \frac{\partial U}{\partial z} = A_z \frac{\partial U}{\partial z} \quad (\text{A-149})$$

In Version 3, the user must specify which formulation to use for A_z or ν_t . The formulations are shown in [Table A-6](#).

Table A-6. Vertical eddy viscosity formulations.

Formulation	Formula	Reference
Nickuradse (NICK)	$\nu_t = \ell_m^2 \left \frac{\partial u}{\partial z} \right e^{-CRi}$ $\ell_m = H \left[0.14 - 0.08 \left(1 - \frac{z}{H} \right)^2 - 0.06 \left(1 - \frac{z}{H} \right)^4 \right]$	Rodi (1993)
Parabolic (PARAB)	$\nu_t = \kappa u_* z \left(1 - \frac{z}{H} \right) e^{-CRi}$	Engelund (1976)
W2 (used in Version 2)	$\nu_t = \kappa \left(\frac{l_m^2}{2} \right) \sqrt{\left(\frac{\partial U}{\partial z} \right)^2 + \left(\frac{\tau_{wy} e^{-2kz} + \tau_{y \text{ tributary}}}{\rho \nu_t} \right)^2} e^{(-CR_i)}$ $\ell_m = \Delta z_{\max}$	Cole and Buchak (1995)
W2 with mixing length of Nickuradse (W2N)	$\nu_t = \kappa \left(\frac{l_m^2}{2} \right) \sqrt{\left(\frac{\partial U}{\partial z} \right)^2 + \left(\frac{\tau_{wy} e^{-2kz} + \tau_{y \text{ tributary}}}{\rho \nu_t} \right)^2} e^{(-CR_i)}$ $\ell_m = H \left[0.14 - 0.08 \left(1 - \frac{z}{H} \right)^2 - 0.06 \left(1 - \frac{z}{H} \right)^4 \right]$	Cole and Buchak (1995) and Rodi (1993)
RNG (re-normalization group)	$\nu_t = \nu \left[1 + \psi \left(3\kappa \left(\frac{zu_*}{\nu} \right)^3 \left(1 - \frac{z}{H} \right)^3 - C_1 \right) \right]^{1/3} e^{-CRi}$	Simoes (1998)

Formulation	Formula	Reference
TKE (Turbulent kinetic energy)	$\nu_t = C_\mu \frac{k^2}{\varepsilon} \text{ where } k \text{ and } \varepsilon \text{ are defined from}$ $\frac{\partial k B}{\partial t} + \frac{\partial k B U}{\partial x} + \frac{\partial k B W}{\partial z} - \frac{\partial}{\partial z} \left(B \frac{\nu_t}{\sigma_k} \frac{\partial k}{\partial z} \right)$ $- \frac{\partial}{\partial x} \left(B \frac{\nu_t}{\sigma_k} \frac{\partial k}{\partial x} \right) = B(P + G - \varepsilon + P_k)$ $\frac{\partial \varepsilon B}{\partial t} + \frac{\partial \varepsilon B U}{\partial x} + \frac{\partial \varepsilon B W}{\partial z} - \frac{\partial}{\partial z} \left(B \frac{\nu_t}{\sigma_\varepsilon} \frac{\partial \varepsilon}{\partial z} \right)$ $- \frac{\partial}{\partial x} \left(B \frac{\nu_t}{\sigma_\varepsilon} \frac{\partial \varepsilon}{\partial x} \right) = B \left(C_{\varepsilon 1} \frac{\varepsilon}{k} P + C_{\varepsilon 2} \frac{\varepsilon^2}{k} + P_\varepsilon \right)$	Wells (2003)
<p>where:</p> <p> ℓ_m = mixing length C = constant (assumed 0.15) k = wave number (in W2 models) z = vertical coordiante u_* = shear velocity ρ = liquid density H = depth κ = von Karman constant $\Psi(x) = \max(0, x)$ u = horizontal velocity τ_{wy} = cross-shear from wind ν = molecular viscosity Ri = Richardson number Δz_{max} = maximum vertical grid spacing C_1 = empirical constant, 100 B = width ν_t = turbulent viscosity k = turbulent kinetic energy (in TKE model) ε = turbulent energy dissipation rate P = turbulent energy production from boundary friction U = longitudinal velocity (laterally averaged) W = vertical velocity (laterally averaged) σ = turbulent Prandlt number </p> $P = \nu_t \left[\left(\frac{\partial U}{\partial z} \right)^2 \right] \quad \text{Buoyancy term: } G = - \frac{\nu_t}{\sigma_t} N^2 \quad \text{Brunt-Vaisala frequency } N = \sqrt{-\frac{g}{\rho} \frac{d\rho}{dz}}$ <p> C_ε, C_μ = constants in the TKE model τ_{ytrib} = cross-shear from lateral tributaries </p>		

The model user can also specify the maximum value of the vertical eddy viscosity [\[AZMAX\]](#), but this value is only used with the W2N and W2 formulations. This value is specified because the time step for numerical stability is greatly reduced when solving the momentum equations using an explicit numerical technique. In addition, the model user can choose whether to compute the vertical momentum transfer with the longitudinal momentum equation using an implicit or an explicit numerical technique. The explicit formulation was used in Version 2 with a fixed [\[AZMAX\]](#) of $1.0 \times 10^{-5} \text{ m}^2 \text{ s}^{-1}$. The implicit solution code was originally developed by Chapman and Cole and revised/updated for Version 3.

Note that only the W2 and W2N include the effects of cross-shear from wind and from tributary or branch inflows. Hence, it is recommended to use either W2 or W2N for waterbodies with deep sections that could be stratified. The other formulations should be used for estuary or river systems where the maximum computed [\[AZMAX\]](#) could be as high as $1 \text{ to } 5 \text{ m}^2 \text{ s}^{-1}$. For the river model, the model user should use the implicit solution technique. To reproduce results from Version 2 in a stratified reservoir, set [\[AZMAX\]](#) to $1.0 \times 10^{-5} \text{ m}^2 \text{ s}^{-1}$ and use the explicit solution.

How does one know which turbulent closure scheme to use for τ_{xz} since, according to Hamblin and Salmon (1975), "the vertical diffusion of momentum is probably the most important internal parameter" for predicting internal circulation patterns? Because of the disarray in the literature over which formulation is best, Shanahan (1980) suggested that we "use theory and literature as a guide to develop alternative viscosity functions and then test those functions in calibration runs against field data." In the absence of expensive-to-obtain current velocity data, the use of temperature profiles is often used to test the adequacy of the hydrodynamic regime against different formulations.

Typical variations of these formulations as predicted by the model are shown in [Figure A-32](#) for Manning's friction factor and in [Figure A-33](#) for a Chezy friction factor. Comparison of the various turbulence closure theories to classical open channel flow theory for seven vertical layers is shown in [Figure A-34](#).

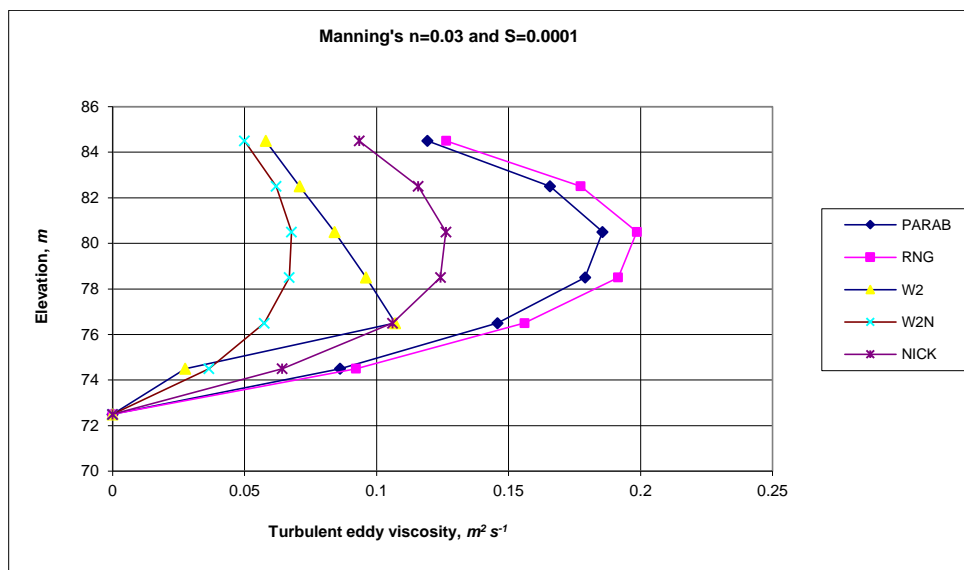


Figure A-32. Variation of turbulent vertical eddy viscosity for flow of $2574 \text{ m}^3 \text{ s}^{-1}$ flow down a channel of length 30 km and width of 100 m at $x=15 \text{ km}$.

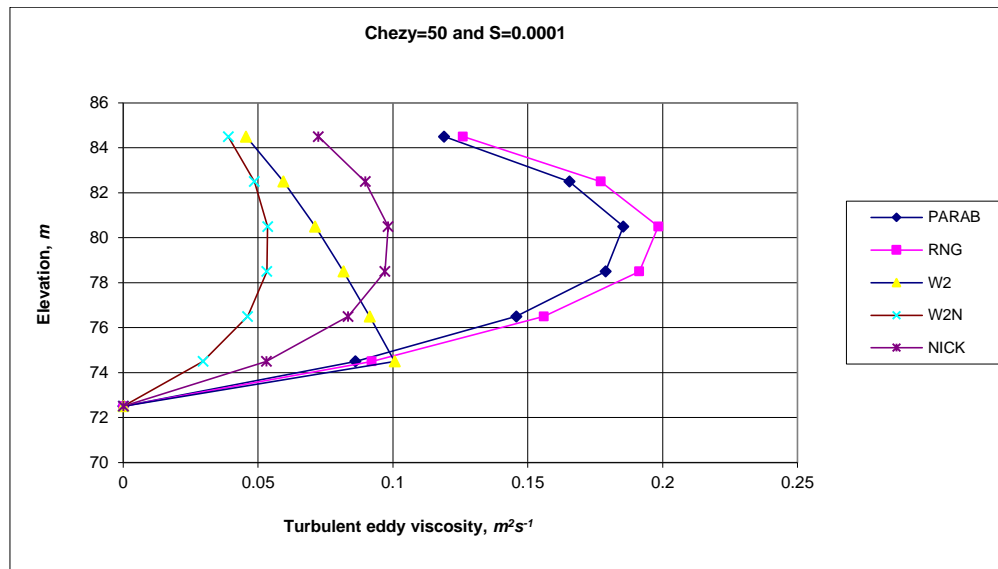


Figure A-33. Variation of turbulent vertical eddy viscosity for flow of $2574 \text{ m}^3 \text{ s}^{-1}$ flow down a channel of length 30 km and width of 100 m measured at $x=15 \text{ km}$.

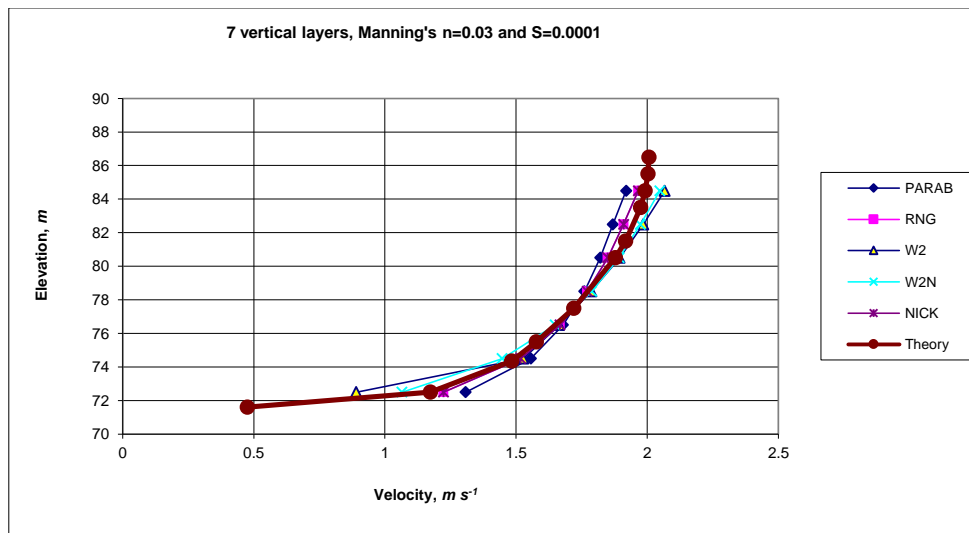


Figure A-34. Comparison of vertical velocity predictions of W2 model with various eddy viscosity models compared to theory.

Formulation

In CE-QUAL-W2, the shear stress term includes the contribution to the shear stress from surface waves induced by the wind. The wind can produce waves that produce decaying motions with depth ([Figure A-35](#)).

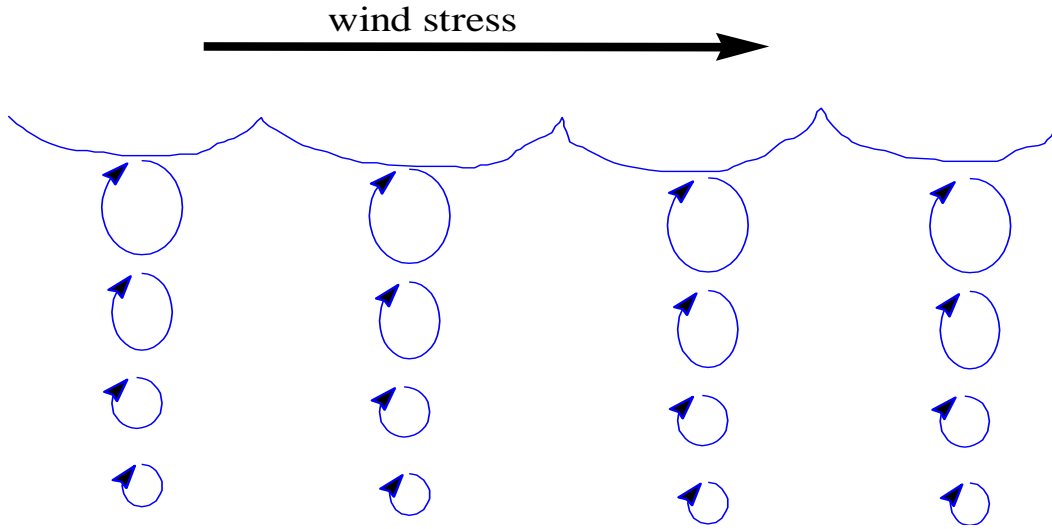


Figure A-35. Conceptual diagram of wind induced motion.

The total longitudinal shear stress for a layer is defined as having contributions from interfacial velocity shear, wind wave generated shear, and friction shear along boundaries:

$$\frac{\tau_{xz}}{\rho} = A_z \frac{\partial U}{\partial z} + \frac{\tau_{wx}}{\rho} e^{-2kz} + \frac{\tau_b}{\rho} \quad (\text{A-150})$$

where:

τ_{wx} = longitudinal wind shear at the surface

$$k = \text{wave number} = \frac{4\pi^2}{gT_w^2}$$

$$T_w = \text{wind wave period} = 6.95E - 2F^{0.233}|W|^{0.534}$$

F = fetch length, m

The turbulent eddy viscosity was conceptualized by Prandtl as:

$$\nu_{turbulent} = \ell^2 \left| \frac{dU}{dz} \right| \quad (\text{A-151})$$

where ℓ is defined as the mixing length and can be interpreted as being proportional to the average size of large eddies or the length scale of a turbulent eddy. This length is a function of distance from a boundary or wall since the eddy sizes vary as a function of distance from a boundary. The goal in most turbulence models is the determination of the mixing length as a function of position in the fluid. Because this concept is not firmly grounded in theory, there have been many published formulations for determination of A_z in the literature (Shanahan and Harleman, 1982).

The mechanism for transporting the wind stress on the surface in the model is based on:

$$A_z = \kappa \frac{\ell^2}{2} \left[\left(\frac{\partial U}{\partial z} \right)^2 + \left(\frac{\partial V}{\partial z} \right)^2 \right]^{1/2} e^{-CRi} \quad (\text{A-152})$$

where:

$$Ri = \text{Richardson number} = \frac{g \frac{\partial \rho}{\partial z}}{\rho \left(\frac{\partial U}{\partial z} \right)^2}$$

κ = von Karman constant, 0.4

C = constant, 1.5

ℓ = vertical length scale chosen as cell thickness, Δz

The formulation is a typical mixing length formulation that is decreased or increased based on the Richardson number. The Richardson number accounts for the impact of density stratification on transfer of momentum between fluid parcels. In regions where there is no stratification, the Richardson number is zero and the exponential term is one. For regions where there is strong stratification, the Richardson number becomes large and the exponential term approaches zero.

In the longitudinal-vertical model, the lateral velocity, V , and its gradient, $\partial V / \partial z$, are due to the lateral component of wind wave motion and are assumed to be zero when averaged laterally, but not necessarily the square $(\partial V / \partial z)^2$. It is assumed that cross wind shear, τ_{wy} , generates lateral wave components and decays exponentially with depth such that

$$\tau_{yz} = \tau_{wy} e^{(-2kz)} \quad (\text{A-153})$$

where:

τ_{wy} = lateral wind shear at the surface

Then using:

$$\frac{\tau_{yz}}{\rho} = A_z \frac{\partial V}{\partial z} \quad (\text{A-154})$$

The lateral velocity gradient squared becomes:

$$\left(\frac{\partial V}{\partial z} \right)^2 = \left[\frac{\tau_{wy} e^{(-2kz)}}{\rho A_z} \right]^2 \quad (\text{A-155})$$

The final equation for the vertical eddy viscosity is then:

$$A_z = \kappa \left(\frac{l^2}{2} \right) \sqrt{\left(\frac{\partial U}{\partial z} \right)^2 + \left(\frac{\tau_{wy} e^{-2kz}}{\rho A_z} \right)^2} e^{(-CR_t)} \quad (\text{A-156})$$

The above equation is implicit. In the model, this equation is explicit since the value of A_z in the lateral wind shear term is used from the previous time step. A_z is never less than the molecular kinematic viscosity for water.

The above formulation of wind shear in horizontal momentum and evaluation of A_z leads to wind driven surface currents that are three to ten percent of the surface wind velocity with higher values appearing at higher wind speeds. This is in accordance with the few attempts to relate wind speed and surface current velocity from field data appearing in the literature. With this formulation, the surface current does not reach abnormal values as it does for the case of wind shear applied only to the surface and as the surface layer thickness decreases. The depth of the wind driven surface layer increases with wind speed, and mass transport due to wind appears to be insensitive to the finite difference layer thickness.

RNG Turbulent Eddy Viscosity Formulation

The RNG model was derived from the RNG model of Yakhot and Orszag (1986) by Simoes (1998). The turbulent eddy viscosity is derived from Yakhot and Orszag (1986) as

$$\nu_t = \nu \left[1 + \Psi \left(a' \frac{\varepsilon \ell_m^4}{\nu^3} - C_1 \right) \right]^{1/3} \quad (\text{A-157})$$

where:

$$\Psi(x) = \max(0, x)$$

ν = molecular viscosity

ν_t = turbulent eddy viscosity

ℓ_m = mixing length

ε = turbulent energy dissipation rate

$a' \sim 1$

$C_1 \sim 100$

Two additional equations are necessary in determining the mixing length and the turbulent energy dissipation. For the mixing length:

$$\frac{\ell_m}{H} = \kappa \frac{z}{H} \sqrt{1 - \frac{z}{H}} \quad (\text{A-158})$$

and for the turbulent eddy dissipation:

$$\frac{\varepsilon H}{u_*^3} = \frac{3z}{H} \left(1 - \frac{z}{H} \right)^{3/2} \quad (\text{A-159})$$

where:

- u^* = shear velocity, $m\ s^{-1}$
- H = depth of the channel, m
- Z = vertical coordinate measured from the bottom of the channel, m
- κ = von Karman's constant, 0.41

Substituting these into equation A-157:

$$\nu_t = \nu \left[1 + \Psi \left(3\kappa \left(\frac{zu_*}{\nu} \right)^3 \left(1 - \frac{z}{H} \right)^3 - C_t \right) \right]^{1/3} \quad (\text{A-160})$$

Simoes (1998) states that this model better represents experimental data than the more traditional parabolic eddy viscosity model of

$$\nu_t = \kappa zu_* \left(1 - \frac{z}{H} \right) \quad (\text{A-161})$$

A value of ν was derived as a function of temperature based on values from Batchelor (1966) using a polynomial curve fit between 0 and 30°C.

This model was adjusted to account for stratified flow conditions by using the same Richardson number criteria as used in the original W2 model (the approach of Mamayev as quoted in French, 1985),

$$\nu_t = \max(\nu, \nu_{tRNG} e^{-CRi}) \quad (\text{A-162})$$

where:

$$Ri = \text{Richardson number} = \frac{g \frac{\partial \rho}{\partial z}}{\rho \left(\frac{\partial U}{\partial z} \right)^2}$$

C = empirical constant, 1.5 (French [1985] shows a value of 0.4)

The Richardson number accounts for the impact of density stratification on transfer of momentum between fluid parcels. In regions where there is no stratification, $Ri=0$, and the exponential term is

1. For regions where there is strong stratification (or as $\frac{d\rho}{dz} \rightarrow \infty$), the Richardson number becomes large and the exponential term approaches 0.

Nikuradse Formulation

This model, as noted in Rodi (1993), is a mixing length model where the mixing length, ℓ_m , and eddy viscosity, ν_t , are determined from

$$\nu_t = \ell_m^2 \left| \frac{\partial u}{\partial z} \right| \quad (\text{A-163})$$

$$\ell_m = H \left[0.14 - 0.08 \left(1 - \frac{z}{H} \right)^2 - 0.06 \left(1 - \frac{z}{H} \right)^4 \right] \quad (\text{A-164})$$

This results in a vertical distribution for the mixing length as shown in [Figure A-36](#).

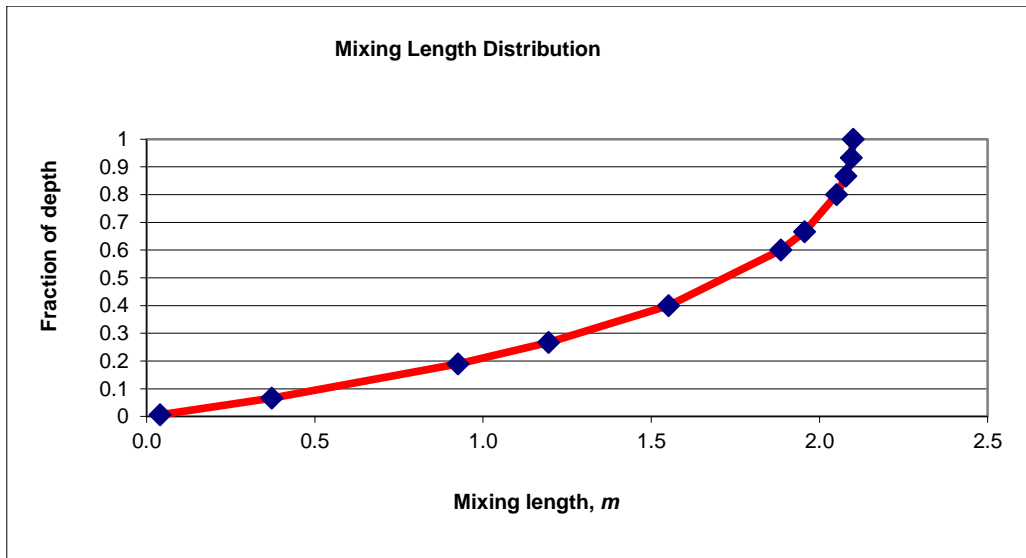


Figure A-36. Mixing length as a function of depth for the Nikuradse formulation.

The stability of the water column affects the mixing length. A Richardson number criteria has been applied to correct the mixing length for stability effects such as

$$\ell_m = \ell_{mo} (1 - 7 Ri) \quad \text{if } Ri \geq 0 \quad (\text{A-165})$$

$$\ell_m = \ell_{mo} (1 - 14 Ri)^{-0.25} \quad \text{if } Ri < 0 \quad (\text{A-166})$$

This is different from the approach of Munk and Anderson (1948) where the Richardson number correction was applied to the value of A_z and not the mixing length directly.

In order to be compatible with the original formulation, the computed value of A_z is corrected using the Mamayev formulation:

$$\nu_t = \max\left(\nu, \nu_{t_{NICK}} e^{-CR_i}\right) \quad (\text{A-167})$$

Parabolic Formulation

Another formulation is a parabolic distribution for A_z (Engelund, 1978):

$$\nu_t = \kappa u_* z \left(1 - \frac{z}{H}\right) \quad (\text{A-168})$$

[Figure A-37](#) shows the spatial distribution of A_z for the parabolic model.

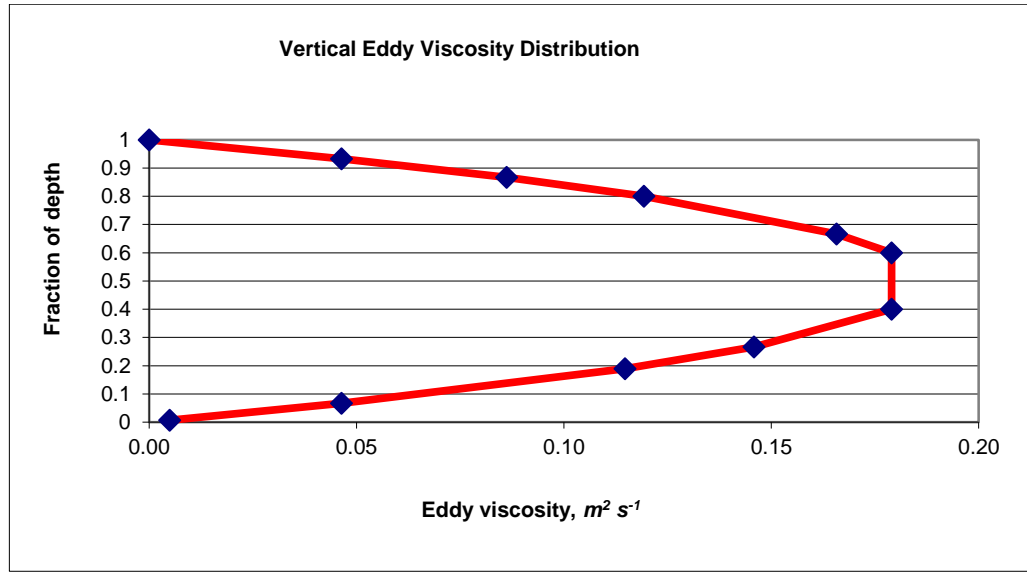


Figure A-37. Variation of A_z with depth for the parabolic model of Engelund (1976).

In order to be compatible with the original formulation in the model, the computed value of A_z is corrected using the Mamayev formulation:

$$\nu_t = \max\left(\nu, \nu_{t_{PARAB}} e^{-CR_i}\right) \quad (\text{A-169})$$

W2N Formulation

The W2N formulation is the same as the W2 model except that the mixing length is no longer the layer thickness, but is computed using Nickaradse's mixing length model. The equations for the W2N formulation are:

$$A_z = \kappa \left(\frac{\ell_m^2}{2} \right) \sqrt{\left(\frac{\partial U}{\partial z} \right)^2 + \left(\frac{\tau_{wy} e^{-2kz}}{\rho A_z} \right)^2} e^{(-CR_i)} \quad (\text{A-170})$$

$$\ell_m = H \left[0.14 - 0.08 \left(1 - \frac{z}{H} \right)^2 - 0.06 \left(1 - \frac{z}{H} \right)^4 \right] \quad (\text{A-171})$$

TKE Formulation

The TKE formulation is a typical application of the k- ε turbulence model. This model includes both vertical transport of kinetic energy and dissipation by advection and ‘diffusion’ but also horizontal transport by advection. The model solves 2 partial differential equations for k and ε in order to compute the turbulent eddy viscosity:

$$\nu_t = C_\mu \frac{k^2}{\varepsilon} \quad (\text{A-172})$$

$$\frac{\partial \varepsilon B}{\partial t} + \frac{\partial \varepsilon B U}{\partial x} + \frac{\partial \varepsilon B W}{\partial z} - \frac{\partial}{\partial z} \left(B \frac{\nu_t}{\sigma_\varepsilon} \frac{\partial \varepsilon}{\partial z} \right) - \frac{\partial}{\partial x} \left(B \frac{\nu_t}{\sigma_\varepsilon} \frac{\partial \varepsilon}{\partial x} \right) = B \left(C_{\varepsilon 1} \frac{\varepsilon}{k} P + C_{\varepsilon 2} \frac{\varepsilon^2}{k} + P_\varepsilon \right) \quad (\text{A-173})$$

$$\frac{\partial k B}{\partial t} + \frac{\partial k B U}{\partial x} + \frac{\partial k B W}{\partial z} - \frac{\partial}{\partial z} \left(B \frac{\nu_t}{\sigma_k} \frac{\partial k}{\partial z} \right) - \frac{\partial}{\partial x} \left(B \frac{\nu_t}{\sigma_k} \frac{\partial k}{\partial x} \right) = B (P + G - \varepsilon + P_k) \quad (\text{A-174})$$

where C_μ is an empirical constant

$$P = \nu_t \left[\left(\frac{\partial U}{\partial z} \right)^2 \right]$$

$$G = - \frac{\nu_t}{\sigma_t} N^2$$

$$P_k = \frac{C_f U^3}{(0.5B)} \quad \text{Production term from boundary friction}$$

$$P_\varepsilon = \frac{10 C_f^{1.25} U^4}{(0.5B)^2} \quad \text{Production term from boundary friction}$$

$$\text{Brunt-Vaisala frequency } N = \sqrt{-\frac{g}{\rho} \frac{d\rho}{dz}}$$

B is the width, U and W are the advective velocities in x and z respectively, and other terms are empirical constants.

Typical values of the above model constants that have been used in other studies are:

$$\sigma_k = 1.0$$

$$\sigma_\varepsilon = 1.3$$

$$C_\mu = 0.09$$

$$C_{1\varepsilon} = 1.44$$

$$C_{2\varepsilon} = 1.92$$

Turbulent Prandtl/Schmidt number, σ_t , = 1.0.

The solution of the above equations for k and ε used a split solution technique: explicit horizontal and source-sink term solution followed by an implicit vertical solution. A description of the solution algorithm below is from a Master's research project by Gould (2006).

Algorithm

The current algorithm is based on the laterally averaged k - ε turbulence model equations shown below:

$$\nu_t = C_\mu \frac{k^2}{\varepsilon} \quad [\text{eq 1}]$$

$$\underbrace{\frac{\partial k B}{\partial t}}_{\text{unsteady}} + \underbrace{\frac{\partial(kUB)}{\partial x} + \frac{\partial(kWB)}{\partial z}}_{\text{convection}} - \underbrace{\frac{\partial}{\partial z} \left(B \frac{\nu_t}{\sigma_k} \frac{\partial k}{\partial z} \right)}_{\text{diffusion}} = \underbrace{B(P + G - \varepsilon + P_k)}_{\text{source/sink}} \quad [\text{eq 2}]$$

$$\underbrace{\frac{\partial \varepsilon B}{\partial t}}_{\text{unsteady}} + \underbrace{\frac{\partial(\varepsilon UB)}{\partial x} + \frac{\partial(\varepsilon WB)}{\partial z}}_{\text{convection}} - \underbrace{\frac{\partial}{\partial z} \left(B \frac{\nu_t}{\sigma_\varepsilon} \frac{\partial \varepsilon}{\partial z} \right)}_{\text{diffusion}} = \underbrace{B \left(C_{\varepsilon 1} \frac{\varepsilon}{k} P - C_{\varepsilon 2} \frac{\varepsilon^2}{k} + P_e \right)}_{\text{source/sink}} \quad [\text{eq 3}]$$

Where ν_t , k , and ε are the eddy viscosity, turbulent kinetic energy and turbulent dissipation. P is the production term and is calculated using equation 4

$$P = \nu_t \left(\frac{\partial U}{\partial z} \right)^2 \quad [\text{eq 4}]$$

and G is the buoyancy term and is represented using equation 5.

$$G = -\frac{\nu_t}{\sigma_t} N^2 \quad [\text{eq 5}]$$

The production of turbulent kinetic energy and turbulent dissipation from boundary friction are represented by the terms P_k and P_e . These terms are calculated using equations 6 and 7.

$$P_k = \frac{C_f |U^3|}{(0.5B)} \quad [\text{eq 6}]$$

$$P_e = \frac{10C_f^{1.25} U^4}{(0.5B)^2} \quad [\text{eq 7}]$$

The friction coefficient C_f is defined in equation 8.

$$C_f = \frac{g}{C^2} = \frac{gn^2}{R_h^{1/3}} \quad [\text{eq 8}]$$

Where g is gravitational acceleration, C is a Chezy friction factor, n is a Manning's friction factor, and R_h is the hydraulic radius. The remaining terms C_μ , C_ε , $C_{\varepsilon 1}$, $C_{\varepsilon 2}$, σ_k , and σ_ε are empirical constants and the values used in the current model are shown in Table 1 below (Rodi, 1993).

Table 1 Constants in k - ε model (Rodi, 1993)

C_μ	$C_{\varepsilon 1}$	$C_{\varepsilon 2}$	σ_k	σ_ε
0.09	1.44	1.92	1.0	1.3

The equations above are solved using a split solution technique in a similar fashion to the horizontal momentum equation in CE-QUAL-W2. Two different methods for solving the equations were implemented. In the first method the vertical transport term was solved using an explicit finite difference along with the horizontal transport term. The second method involved integrating the vertical transport term into a fully implicit finite difference. Both methods are based on the solutions developed by Wells (2001). The computational grid used in these calculations is shown below.

CE-QUAL-W2 coordinate system

★ ρ, Φ, P, B

- U, A_x, D_x, τ_{xx}

 W, D_z
 A_z

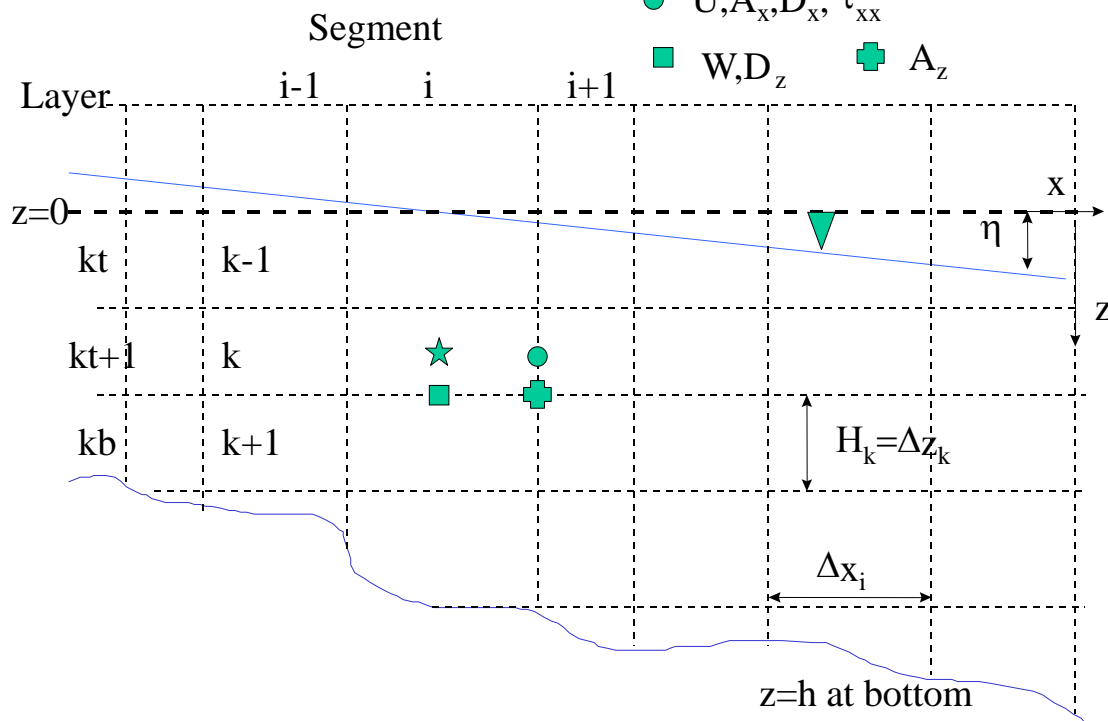


Figure 38. CE-QUAL-W2 computational grid. Width, density, pressure and water quality state variables are defined at cell centers. Horizontal velocity, longitudinal eddy viscosity and diffusivity, and longitudinal shear stress are defined at the right hand side of the cell. Vertical velocity and vertical diffusivity is defiend at the bottom of the cell, and the vertical eddy viscosity is defined at the lower right corner of the cell.

Explicit Vertical Convection

The first method developed for implementing the convective terms involved using an explicit finite difference for the vertical convection term. The first step in this method is to split the turbulent kinetic energy transport equation, equation 2, into the two equations shown below as equations 9a and 9b.

$$\frac{\partial k B}{\partial t} + \frac{\partial(kUB)}{\partial x} + \frac{\partial(kWB)}{\partial z} = B(P + G - \varepsilon + P_k) \quad [\text{eq 9a}]$$

$$\frac{\partial k B}{\partial t} = \frac{\partial}{\partial z} \left(B \frac{\nu_t}{\sigma_k} \frac{\partial k}{\partial z} \right) \quad [\text{eq 9b}]$$

Next each equation is averaged over a layer.

$$\underbrace{\frac{1}{\Delta z} \frac{\partial}{\partial t} (kB\Delta z)}_{\text{unsteady}} + \underbrace{\frac{1}{\Delta z} \frac{\partial}{\partial x} (kUB\Delta z)}_{\text{convection}} + \underbrace{\frac{1}{\Delta z} \frac{\partial}{\partial z} (kWB\Delta z)}_{\text{convection}} = \underbrace{\frac{1}{\Delta z} B\Delta z (P + G - \varepsilon + P_k)}_{\text{source/sink}} \quad [\text{eq 10a}]$$

$$\underbrace{\frac{1}{\Delta z} \frac{\partial}{\partial t} (kB\Delta z)}_{\text{unsteady}} = \underbrace{\frac{1}{\Delta z} \left[B \frac{\nu_t}{\sigma_k} \frac{\partial k}{\partial z} \right]_{z+\Delta z} - B \frac{\nu_t}{\sigma_k} \frac{\partial k}{\partial z} \Big|_z}_{\text{diffusion}} \quad [\text{eq 10b}]$$

The partial derivatives in equation 10a can be replaced by the finite difference schemes below. The unsteady term is represented as an explicit finite difference, where k^* is the kinetic turbulent energy at the next time step before the application of equation 10b.

$$\left. \frac{\partial}{\partial t} (kB\Delta z) \right|_{i,k} = \frac{k_{i,k}^* B_{i,k}^{n+1} \Delta z_{i,k}^{n+1} - k_{i,k}^n B_{i,k}^n \Delta z_{i,k}^n}{\Delta t} \quad [\text{eq 11}]$$

The horizontal convective term is represented by an upwind difference scheme. The order of differencing depends on the direction of the horizontal component of the velocity. The difference shown below is for $U > 0$.

$$\left. \frac{\partial}{\partial x} (kUB\Delta z) \right|_{i,k} = \frac{k_{i,k}^n U_{i,k}^n B_{i,k}^n \Delta z_{i,k}^n - k_{i-1,k}^n U_{i-1,k}^n B_{i-1,k}^n \Delta z_{i-1,k}^n}{\Delta x_{i,k}^n} \quad [\text{eq 12}]$$

The vertical convective term is also represented by an upwind difference scheme. The order of differencing depends on the direction of the vertical component of the velocity. The difference shown below is for $W > 0$.

$$\left. \frac{\partial}{\partial z} (kWB\Delta z) \right|_{i,k} = \frac{k_{i,k}^n W_{i,k}^n B_{i,k}^n \Delta z_{i,k}^n - k_{i-1,k}^n W_{i-1,k}^n B_{i-1,k}^n \Delta z_{i-1,k}^n}{\Delta z_{i,k}^n} \quad [\text{eq 13}]$$

These differences can be inserted into equation 9a and rearranged to give the following explicit solution for k^* .

$$\begin{aligned}
k^* = & \frac{k_{i,k}^n B_{i,k}^n \Delta z_{i,k}^n}{B_{i,k}^{n+1} \Delta z_{i,k}^{n+1}} - \frac{\Delta t}{\Delta x_{i,k} B_{i,k}^{n+1} \Delta z_{i,k}^{n+1}} \left(k_{i,k}^n U_{i,k}^n B_{i,k}^n \Delta z_{i,k}^n - k_{i-1,k}^n U_{i-1,k}^n B_{i-1,k}^n \Delta z_{i-1,k}^n \right) \\
& - \frac{\Delta t}{\Delta x_{i,k} B_{i,k}^{n+1} \Delta z_{i,k}^{n+1}} \left(k_{i,k}^n W_{i,k}^n B_{i,k}^n \Delta z_{i,k}^n - k_{i-1,k}^n W_{i-1,k}^n B_{i-1,k}^n \Delta z_{i-1,k}^n \right) \\
& + \frac{\Delta t B_{i,k}^n \Delta z_{i,k}^n}{B_{i,k}^{n+1} \Delta z_{i,k}^{n+1}} \left(P_{i,k}^n + G_{i,k}^n - \varepsilon_{i,k}^n + P_{k,i,k}^n \right)
\end{aligned} \tag{eq 14}$$

Where the terms P and G are calculated using the explicit differences shown below.

$$P_{i,k}^n = \nu_t \left(\frac{\left(0.5 \cdot (U_{k,i}^n + U_{k,i-1}^n) - 0.5 \cdot (U_{k+1,i}^n + U_{k+1,i-1}^n) \right)}{\Delta z_{k+1/2,i}^n} \right)^2 \tag{eq 15}$$

$$G_{i,k}^n = \nu_t g \left(\frac{\rho_{k+1,i}^n - \rho_{k,i}^n}{\Delta z_{k,i}^n \rho_w} \right) \tag{eq 16}$$

Equation 14 is calculated for all of the layers in a segment except for the top and bottom layer.

Next the partial derivatives in equation 10b are replaced with the following differences.

$$\left. \frac{\partial}{\partial t} (kB\Delta z) \right|_{i,k} = \frac{k_{i,k}^{n+1} B_{i,k}^{n+1} \Delta z_{i,k}^{n+1} - k_{i,k}^* B_{i,k}^{n+1} \Delta z_{i,k}^{n+1}}{\Delta t} \tag{eq 17}$$

$$\begin{aligned}
& \left[B \frac{\nu_t}{\sigma_k} \frac{\partial k}{\partial z} \right]_{i,k}^{z+\Delta z} - B \frac{\nu_t}{\sigma_k} \frac{\partial k}{\partial z} \bigg|_{i,k}^z = \\
& B_{i,k+1/2}^n \frac{\nu_{ti,k+1/2}^n}{\sigma_k} \left(\frac{k_{i,k+1}^{n+1} - k_{i,k}^{n+1}}{\Delta z_{i,k+1/2}^{n+1}} \right) + B_{i,k-1/2}^n \frac{\nu_{ti,k-1/2}^n}{\sigma_k} \left(\frac{k_{i,k}^{n+1} - k_{i,k-1}^{n+1}}{\Delta z_{i,k-1/2}^{n+1}} \right)
\end{aligned} \tag{eq 18}$$

The resulting equation can then be simplified to a tridiagonal matrix solution format,

$$AT \cdot k_{k-1}^{n+1} + VT \cdot k_k^{n+1} + CT \cdot k_{k+1}^{n+1} = DT \tag{eq 19}$$

where

$$\begin{aligned}
AT &= - \frac{\Delta t}{B_{i,k}^{n+1} \Delta z_{i,k}^{n+1}} \left(\frac{B_{i,k-1/2}^n \nu_{ti,k-1/2}^n}{\Delta z_{i,k-1/2}^{n+1} \sigma_k} \right) \\
VT &= \frac{\Delta t}{B_{i,k}^{n+1} \Delta z_{i,k}^{n+1}} \left(1 + \frac{B_{i,k+1/2}^n \nu_{ti,k+1/2}^n}{\Delta z_{i,k+1/2}^{n+1}} + \frac{B_{i,k-1/2}^n \nu_{ti,k-1/2}^n}{\Delta z_{i,k-1/2}^{n+1}} \right) \\
CT &= - \frac{\Delta t}{B_{i,k}^{n+1} \Delta z_{i,k}^{n+1}} \left(\frac{B_{i,k+1/2}^n \nu_{ti,k+1/2}^n}{\Delta z_{i,k+1/2}^{n+1} \sigma_k} \right)
\end{aligned}$$

$$DT = k_{i,k}^* \frac{B_{i,k}^n \Delta z_{i,k}^n}{B_{i,k}^{n+1} \Delta z_{i,k}^{n+1}}$$

and $\frac{B_{i,k}^n \Delta z_{i,k}^n}{B_{i,k}^{n+1} \Delta z_{i,k}^{n+1}} = 1$ except at the top layer. The boundary conditions at the top and bottom layers are implemented using the method shown in Appendix A. Then k^{n+1} can be found by solving the equations using the Thomas algorithm.

The turbulent dissipation is found using the same procedure. Equation 3 is split as shown in equations 20a and 20b below.

$$\frac{\partial \varepsilon B}{\partial t} + \frac{\partial (\varepsilon U B)}{\partial x} + \frac{\partial (\varepsilon W B)}{\partial z} = B \left(C_{\varepsilon 1} \frac{\varepsilon}{k} P - C_{\varepsilon 2} \frac{(\varepsilon)^2}{k} + P_e \right) \quad [\text{eq 20a}]$$

$$\frac{\partial \varepsilon B}{\partial t} = \frac{\partial}{\partial z} \left(B \frac{\nu_t}{\sigma_\varepsilon} \frac{\partial \varepsilon}{\partial z} \right) \quad [\text{eq 20b}]$$

These equations are then averaged over a layer.

$$\underbrace{\frac{1}{\Delta z} \frac{\partial}{\partial t} (\varepsilon B \Delta z)}_{\text{unsteady}} + \underbrace{\frac{1}{\Delta z} \frac{\partial}{\partial x} (\varepsilon U B \Delta z)}_{\text{convection}} + \underbrace{\frac{1}{\Delta z} \frac{\partial}{\partial z} (\varepsilon W B \Delta z)}_{\text{convection}} = \underbrace{\frac{1}{\Delta z} B \Delta z \left(C_{\varepsilon 1} \frac{\varepsilon}{k} P - C_{\varepsilon 2} \frac{(\varepsilon)^2}{k} + P_e \right)}_{\text{source/sink}} \quad [\text{eq 21a}]$$

$$\underbrace{\frac{1}{\Delta z} \frac{\partial}{\partial t} (\varepsilon B \Delta z)}_{\text{unsteady}} = \underbrace{\frac{1}{\Delta z} \left[B \frac{\nu_t}{\sigma_k} \frac{\partial \varepsilon}{\partial z} \Big|_{z+\Delta z} - B \frac{\nu_t}{\sigma_k} \frac{\partial \varepsilon}{\partial z} \Big|_z \right]}_{\text{diffusion}} \quad [\text{eq 21b}]$$

The partial derivatives in equation 21a are replaced with finite differences using similar schemes to those used in the turbulent kinetic energy solution. This results in the explicit solution for ε^* shown below.

$$\begin{aligned} \varepsilon^* = & \frac{\varepsilon_{i,k}^n B_{i,k}^n \Delta z_{i,k}^n}{B_{i,k}^{n+1} \Delta z_{i,k}^{n+1}} - \frac{\Delta t}{\Delta x_{i,k} B_{i,k}^{n+1} \Delta z_{i,k}^{n+1}} \left(\varepsilon_{i,k}^n U_{i,k}^n B_{i,k}^n \Delta z_{i,k}^n - \varepsilon_{i-1,k}^n U_{i-1,k}^n B_{i-1,k}^n \Delta z_{i-1,k}^n \right) \\ & - \frac{\Delta t}{\Delta x_{i,k} B_{i,k}^{n+1} \Delta z_{i,k}^{n+1}} \left(\varepsilon_{i,k}^n W_{i,k}^n B_{i,k}^n \Delta z_{i,k}^n - \varepsilon_{i-1,k}^n W_{i-1,k}^n B_{i-1,k}^n \Delta z_{i-1,k}^n \right) \\ & + \frac{\Delta t B_{i,k}^n \Delta z_{i,k}^n}{B_{i,k}^{n+1} \Delta z_{i,k}^{n+1}} \left(C_{\varepsilon 1} \frac{\varepsilon_{i,k}^n}{k_{i,k}^n} P_{i,k}^n + C_{\varepsilon 2} \frac{(\varepsilon_{i,k}^n)^2}{k_{i,k}^n} + P_{e,i,k}^n \right) \end{aligned} \quad [\text{eq 22}]$$

Where ε^* is the turbulent dissipation at the next time step before the application of equation 21b. Equation 22 is calculated for all of the layers in a segment except for the top and bottom layer.

Next the partial derivatives in equation 21b are replaced with finite differences

using similar schemes to those used in the turbulent kinetic energy solution. This again results in a set of equations in a tridiagonal format.

$$AT \cdot \varepsilon_{k-1}^{n+1} + VT \cdot \varepsilon_k^{n+1} + CT \cdot \varepsilon_{k+1}^{n+1} = DT \quad [\text{eq 23}]$$

where

$$AT = -\frac{\Delta t}{B_{i,k}^{n+1} \Delta z_{i,k}^{n+1}} \left(\frac{B_{i,k-1/2}^n v_{ti,k-1/2}^n}{\Delta z_{i,k-1/2}^{n+1} \sigma_k} \right)$$

$$VT = \frac{\Delta t}{B_{i,k}^{n+1} \Delta z_{i,k}^{n+1}} \left(1 + \frac{B_{i,k+1/2}^n v_{ti,k+1/2}^n}{\Delta z_{i,k+1/2}^{n+1}} + \frac{B_{i,k-1/2}^n v_{ti,k-1/2}^n}{\Delta z_{i,k-1/2}^{n+1}} \right)$$

$$CT = -\frac{\Delta t}{B_{i,k}^{n+1} \Delta z_{i,k}^{n+1}} \left(\frac{B_{i,k+1/2}^n v_{ti,k+1/2}^n}{\Delta z_{i,k+1/2}^{n+1} \sigma_k} \right)$$

$$DT = \varepsilon_{i,k}^* \frac{B_{i,k}^n \Delta z_{i,k}^n}{B_{i,k}^{n+1} \Delta z_{i,k}^{n+1}}$$

and $\frac{B_{i,k}^n \Delta z_{i,k}^n}{B_{i,k}^{n+1} \Delta z_{i,k}^{n+1}} = 1$ except at the top layer. These equations are solved for ε^{n+1} using the Thomas algorithm.

Implicit Vertical Convection

The second method is very similar to the technique developed above. The only difference is that the vertical convection term is integrated into the implicit part of the solution. First equation 3 is split into horizontal and vertical components as shown in equations 24a to 24b.

$$\frac{\partial k B}{\partial t} + \frac{\partial (k U B)}{\partial x} = B(P + G - \varepsilon + P_k) \quad [\text{eq 24a}]$$

$$\frac{\partial k B}{\partial t} + \frac{\partial (k W B)}{\partial z} = \frac{\partial}{\partial z} \left(B \frac{v_t}{\sigma_k} \frac{\partial k}{\partial z} \right) \quad [\text{eq 24b}]$$

Next each equation is averaged over a layer.

$$\underbrace{\frac{1}{\Delta z} \frac{\partial}{\partial t} (k B \Delta z)}_{\text{unsteady}} + \underbrace{\frac{1}{\Delta z} \frac{\partial}{\partial x} (k U B \Delta z)}_{\text{convection}} = \underbrace{\frac{1}{\Delta z} B \Delta z (P + G - \varepsilon + P_k)}_{\text{source/sink}} \quad [\text{eq 25a}]$$

$$\underbrace{\frac{1}{\Delta z} \frac{\partial}{\partial t} (k B \Delta z)}_{\text{unsteady}} + \underbrace{\frac{1}{\Delta z} \frac{\partial}{\partial z} (k W B \Delta z)}_{\text{convection}} = \underbrace{\frac{1}{\Delta z} B \frac{v_t}{\sigma_k} \frac{\partial k}{\partial z} \bigg|_z^{z+\Delta z}}_{\text{diffusion}} \quad [\text{eq 25b}]$$

Then the differences developed in the previous section, equations 11 and 12, are substituted into equation 25a. The resulting equation can then be rearranged and simplified in order to explicitly solve for k^* as shown in the equation below.

$$k^* = \frac{k_{i,k}^n B_{i,k}^n \Delta z_{i,k}^n}{B_{i,k}^{n+1} \Delta z_{i,k}^{n+1}} - \frac{\Delta t}{\Delta x_{i,k} B_{i,k}^{n+1} \Delta z_{i,k}^{n+1}} \left(k_{i,k}^n U_{i,k}^n B_{i,k}^n \Delta z_{i,k}^n - k_{i-1,k}^n U_{i-1,k}^n B_{i-1,k}^n \Delta z_{i-1,k}^n \right) + \frac{\Delta t B_{i,k}^n \Delta z_{i,k}^n}{B_{i,k}^{n+1} \Delta z_{i,k}^{n+1}} \left(P_{i,k}^n + G_{i,k}^n - \varepsilon_{i,k}^n + P_{k i,k}^n \right) \quad [\text{eq 26}]$$

Where k^* is the kinetic turbulent energy at the next time step before the application of equation 25b. Equation 26 is calculated for all of the layers in a segment except for the top and bottom layer.

Next the finite differences developed in the previous section, equations 17 and 18, along with the finite difference for the vertical convective term, equation 27, are substituted into equation 25b.

$$\frac{\partial}{\partial z} (kWB\Delta z) = \frac{k_{i,k+1/2}^{n+1} W_{i,k}^n B_{i,k}^n \Delta z_{i,k}^{n+1} - k_{i,k-1/2}^{n+1} W_{i,k}^n B_{i,k}^n \Delta z_{i,k}^{n+1}}{\Delta z_k^{n+1}} \quad [\text{eq 27}]$$

$$k_{i,k+1/2}^{n+1} = \frac{k_{i,k+1}^{n+1} + k_{i,k}^{n+1}}{2} \quad [\text{eq 28}]$$

$$k_{i,k-1/2}^{n+1} = \frac{k_{i,k}^{n+1} + k_{i,k-1}^{n+1}}{2} \quad [\text{eq 29}]$$

The resulting equation can then be simplified to a tridiagonal matrix solution format,

$$AT \cdot k_{k-1}^{n+1} + VT \cdot k_k^{n+1} + CT \cdot k_{k+1}^{n+1} = DT \quad [\text{eq 30}]$$

where

$$AT = -\frac{\Delta t}{B_{i,k}^{n+1} \Delta z_{i,k}^{n+1}} \left(\frac{W_{i,k-1/2}^n B_{i,k-1/2}^n}{2} + \frac{B_{i,k-1/2}^n v_{t,i,k-1/2}^n}{\Delta z_{i,k-1/2}^{n+1} \sigma_k} \right)$$

$$VT = \frac{\Delta t}{B_{i,k}^{n+1} \Delta z_{i,k}^{n+1}} \left(1 + \frac{B_{i,k}^{n+1} \Delta z_{i,k}^{n+1}}{\Delta t} + \frac{W_{i,k+1/2}^n B_{i,k+1/2}^n}{2} - \frac{W_{i,k-1/2}^n B_{i,k-1/2}^n}{2} + \frac{B_{i,k+1/2}^n v_{t,i,k+1/2}^n}{\Delta z_{i,k+1/2}^{n+1}} + \frac{B_{i,k-1/2}^n v_{t,i,k-1/2}^n}{\Delta z_{i,k-1/2}^{n+1}} \right)$$

$$CT = -\frac{\Delta t}{B_{i,k}^{n+1} \Delta z_{i,k}^{n+1}} \left(\frac{W_{i,k+1/2}^n B_{i,k+1/2}^n \Delta z_{i,k}^{n+1}}{2 \Delta z_{i,k}^{n+1}} - \frac{B_{i,k+1/2}^n v_{t,i,k+1/2}^n}{\Delta z_{i,k+1/2}^{n+1} \sigma_k} \right)$$

$$DT = k_{i,k}^* \frac{B_{i,k}^n \Delta z_{i,k}^n}{B_{i,k}^{n+1} \Delta z_{i,k}^{n+1}}$$

and $\frac{B_{i,k}^n \Delta z_{i,k}^n}{B_{i,k}^{n+1} \Delta z_{i,k}^{n+1}} = 1$ except at the top layer. The boundary conditions at the top and bottom layers

are implemented using the method shown in Appendix A. Then k^{n+1} is found by solving the equations using the Thomas algorithm.

The turbulent dissipation is found using the same procedure. Equation 3 is split as shown in equations 31a and 31b below.

$$\frac{\partial \varepsilon B}{\partial t} + \frac{\partial(\varepsilon UB)}{\partial x} = B \left(C_{\varepsilon 1} \frac{\varepsilon}{k} P - C_{\varepsilon 2} \frac{(\varepsilon)^2}{k} + P_e \right) \quad [\text{eq 31a}]$$

$$\frac{\partial \varepsilon B}{\partial t} + \frac{\partial(\varepsilon WB)}{\partial z} = \frac{\partial}{\partial z} \left(B \frac{\nu_t}{\sigma_\varepsilon} \frac{\partial \varepsilon}{\partial z} \right) \quad [\text{eq 31b}]$$

These equations are then averaged over a layer.

$$\underbrace{\frac{1}{\Delta z} \frac{\partial}{\partial t} (\varepsilon B \Delta z)}_{\text{unsteady}} + \underbrace{\frac{1}{\Delta z} \frac{\partial}{\partial x} (\varepsilon UB \Delta z)}_{\text{convection}} = \underbrace{\frac{1}{\Delta z} B \Delta z \left(C_{\varepsilon 1} \frac{\varepsilon}{k} P - C_{\varepsilon 2} \frac{(\varepsilon)^2}{k} + P_e \right)}_{\text{source/sink}} \quad [\text{eq 32a}]$$

$$\underbrace{\frac{1}{\Delta z} \frac{\partial}{\partial t} (\varepsilon B \Delta z)}_{\text{unsteady}} + \underbrace{\frac{1}{\Delta z} \frac{\partial}{\partial z} (\varepsilon WB \Delta z)}_{\text{unsteady}} = \underbrace{\frac{1}{\Delta z} B \frac{\nu_t}{\sigma_\varepsilon} \frac{\partial \varepsilon}{\partial z}}_{\text{diffusion}} \bigg|_z^{z+\Delta z} \quad [\text{eq 32b}]$$

The partial derivatives in equation 21a are replaced with finite differences using similar schemes to those used in the turbulent kinetic energy solution. This results in the explicit solution for ε^* shown below.

$$\begin{aligned} \varepsilon^* = & \frac{\varepsilon_{i,k}^n B_{i,k}^n \Delta z_{i,k}^n}{B_{i,k}^{n+1} \Delta z_{i,k}^{n+1}} - \frac{\Delta t}{\Delta x B_{i,k}^{n+1} \Delta z_{i,k}^{n+1}} \left(\varepsilon_{i,k}^n U_{i,k}^n B_{i,k}^n \Delta z_{i,k}^n - \varepsilon_{i-1,k}^n U_{i-1,k}^n B_{i-1,k}^n \Delta z_{i-1,k}^n \right) \\ & + \frac{\Delta t B_{i,k}^n \Delta z_{i,k}^n}{B_{i,k}^{n+1} \Delta z_{i,k}^{n+1}} \left(C_{\varepsilon 1} \frac{\varepsilon_{i,k}^n}{k_{i,k}^n} P_{k,i}^n + C_{\varepsilon 2} \frac{(\varepsilon_{i,k}^n)^2}{k_{i,k}^n} + P_{e,i,k}^n \right) \end{aligned} \quad [\text{eq 33}]$$

Where ε^* is the turbulent dissipation at the next time step before the application of equation 32a. Equation 33 is calculated for all of the layers in a segment except for the top and bottom layer.

Next the partial derivatives in equation 32b are replaced with finite differences using similar schemes to those used in the turbulent kinetic energy solution. This again results in a set of equations in a tridiagonal format.

$$AT \cdot \varepsilon_{k-1}^{n+1} + VT \cdot \varepsilon_k^{n+1} + CT \cdot \varepsilon_{k+1}^{n+1} = DT \quad [\text{eq 34}]$$

where

$$\begin{aligned} AT = & - \frac{\Delta t}{B_{i,k}^{n+1} \Delta z_{i,k}^{n+1}} \left(\frac{W_{i,k-1/2}^n B_{i,k-1/2}^n}{2} + \frac{B_{i,k-1/2}^n \nu_{t,i,k-1/2}^n}{\Delta z_{i,k-1/2}^{n+1} \sigma_k} \right) \\ VT = & \frac{\Delta t}{B_{i,k}^{n+1} \Delta z_{i,k}^{n+1}} \left(1 + \frac{B_{i,k}^{n+1} \Delta z_{i,k}^{n+1}}{\Delta t} + \frac{W_{i,k+1/2}^n B_{i,k+1/2}^n}{2} - \frac{W_{i,k-1/2}^n B_{i,k+1/2}^n}{2} + \frac{B_{i,k+1/2}^n \nu_{t,i,k+1/2}^n}{\Delta z_{i,k+1/2}^{n+1}} + \frac{B_{i,k-1/2}^n \nu_{t,i,k-1/2}^n}{\Delta z_{i,k-1/2}^{n+1}} \right) \end{aligned}$$

$$CT = -\frac{\Delta t}{B_{i,k}^{n+1} \Delta z_{i,k}^{n+1}} \left(\frac{W_{i,k+1/2}^n B_{i,k+1/2}^n}{2} - \frac{B_{i,k+1/2}^n v_{ti,k+1/2}^n}{\Delta z_{i,k+1/2}^{n+1} \sigma_k} \right)$$

$$DT = \varepsilon_{i,k}^* \frac{B_{i,k}^n \Delta z_{i,k}^n}{B_{i,k}^{n+1} \Delta z_{i,k}^{n+1}}$$

and $\frac{B_{i,k}^n \Delta z_{i,k}^n}{B_{i,k}^{n+1} \Delta z_{i,k}^{n+1}} = 1$ except at the top layer. These equations are then solved for ε^{n+1} using the

Thomas algorithm.

Boundary and initial conditions for k-ε model

In order to be able to apply the algorithm developed above to the typical hydraulic problems investigated using CE-QUAL-W2 the appropriate boundary conditions for the bed, free surface, inlet and outlet as well as initial conditions must be specified. This section outlines the boundary conditions and initial conditions implemented in the current version of the k -ε algorithm.

At the bed steep gradients of turbulent kinetic energy and turbulent dissipation are present in the viscous sublayer. To accurately calculate these steep gradients a large number of grid points are needed in the viscous sublayer and a low Reynolds number version of the k -ε turbulence model must be used. To avoid this problem an empirical law can be used to construct a simple wall function.

To construct a wall function several assumptions must be made about flow in the inner region near the wall. The largest assumption is that the flow parallel to the wall obeys the law of the wall shown below.

$$\frac{U}{U_*} = \frac{1}{\kappa} \ln \left(E \frac{y U_*}{\nu} \right) \quad [\text{eq 35}]$$

Where U_* is the bed friction velocity, κ is the von Karman constant, y is the distance of the grid point from the bed, E is the roughness coefficient and ν is the kinematic viscosity. In addition to the assumption that the flow has a logarithmic velocity profile it is necessary to assume that the total shear stress remains constant in the inner region and is equal to the bed stress. These assumptions can normally be made if the first grid point is in the range of $30 < y^+ < 100$ from the wall (Rodi, 1993).

$$y^+ = \frac{y U_*}{\nu} \quad [\text{eq 36}]$$

In the range of y^+ specified above the Reynolds stresses are relatively constant. In this region local equilibrium prevails, so if buoyancy effects are negligible then the production equals dissipation which implies that $P = \varepsilon$. It is also assumed that the total shear stress remains constant and is approximately equal to the wall shear stress in this region. Using these assumptions and equation 1 it is possible to derive the equation for turbulent kinetic energy at the first grid point shown below (Rodi, 1993).

$$k = \frac{U_*^2}{\sqrt{c_\mu}} \quad [\text{eq 37}]$$

The boundary condition for turbulent dissipation can be determined using $\varepsilon = P = U_*^2 \frac{\partial U}{\partial y}$

where $\frac{\partial U}{\partial y}$ is determined from equation 35 and is given below.

$$\varepsilon = \frac{U_*^3}{\kappa y} \quad [\text{eq 38}]$$

Since y , U , E , κ , ν and E are known, a very simple wall function can be implemented by solving equation 35 for U_* [5]. In the current version of the k - ε model U_* was found using a root solver based on the bisection method from Press et al. (1996). Then equations 37 and 38 are used to determine the turbulent kinetic energy and the turbulent dissipation at the first grid point. This simple approach has some limitations, such as not being able to handle separated flow, but seemed a reasonable starting point for this project [5].

The wall function outlined above is valid for both smooth and rough boundaries. For hydraulically smooth beds the roughness coefficient E is set to 9.535 (Ferziger, 2002). For rough boundaries a smaller value of E is used. Two options are available in the current algorithm for specifying the roughness coefficient. A uniform constant roughness coefficient value can be applied to all segments or the roughness coefficient can be calculated based on the Manning's coefficients specified in the bathymetry file.

In the first option the user specifies the roughness coefficient and this value is used to calculate the bed friction velocity using equation 35. After the bed friction velocity has been determined a new Manning's coefficient is calculated using equation 39 below. This method was used primarily for experimental channel test cases where the bed was hydraulically smooth and had a roughness coefficient equal to 9.535.

$$n = \frac{R_h^{1/6}}{\sqrt{\left(\frac{U_*}{U_m}\right)^2}} \quad [\text{eq 39}]$$

In the second option the roughness coefficient is calculated using a Strickler relationship and an approximation of the Nikuradse's data shown in equations 40 below 42 (Krishnappan and Lau, 1986).

$$E = \exp\left(\frac{(\kappa B_s)}{\left(\frac{U_* k_s}{\nu}\right)}\right) \quad [\text{eq 40}]$$

$$B_s = \left[5.50 + 2.5 \ln \left(\frac{U_* k_s}{\nu} \right) \right] \exp \left\{ -0.217 \left[\ln \left(\frac{U_* k_s}{\nu} \right) \right]^2 \right\} \quad [\text{eq 41}]$$

$$+ 8.5 \left(1 - \exp \left\{ -0.217 \left[\ln \left(\frac{U_* k_s}{\nu} \right) \right]^2 \right\} \right) \quad [\text{eq 42}]$$

$$k_s = (n \cdot 24.04)^6 \quad (k_s \text{ in m})$$

The appropriate boundary condition for the free surface is harder to determine. Unfortunately there is very little experimental data available for turbulent statistics at the free surface (Rodi, 1993). It is difficult to make such measurements because hot wire anemometers tend to disturb the surface and laser Doppler anemometry systems, LDA, have issues with reflections and refraction caused by the free surface (Swean et al., 1991). In many cases researchers have turned to Direct Navier Stokes simulations for more information on the relationship between turbulent kinetic energy and turbulent dissipation and the free surface (Swean et al., 1991, Cotton et al., 2005).

A first approximation for the boundary conditions at the free surface in absence of a wind induced shear is to use a symmetry plane where both turbulent kinetic energy and turbulent dissipation are found using a zero gradient condition (Rodi, 1993). However it is generally thought that the presence of the free surface should reduce the length scale of turbulence and reduce the turbulent dissipation. An attempt to take this into account was made in the empirically determined boundary conditions shown in equations 43 and 44 (Celik and Rodi, 1984).

$$\frac{\partial k}{\partial y} = 0 \quad [\text{eq 43}]$$

$$\varepsilon = \frac{k^{3/2}}{aH} \quad [\text{eq 44}]$$

Where a is an empirical constant and H is the depth of the shear layer, in this case the depth of the channel. The coefficient a was originally set to a value of 0.18 by Celik and Rodi (1984) and then later changed to a value of 0.43 by Celik and Rodi (1988).

For a free surface with wind induced surface shear, the boundary conditions similar to those used for wall boundaries are appropriate, equations 35, 37, and 38. The free surface can be seen as a moving wall. So the bed friction velocity in equations 37 and 38 can be replaced with the wind induced surface friction velocity (Rodi, 1993).

Rodi presented a set of boundary conditions that could be used for free surfaces with or without wind induced surface shear in reference 4. When the wind induced surface shear is large then the following boundary condition is used for turbulent kinetic energy.

$$k = \frac{U_*^2}{\sqrt{C_\mu}} \quad [\text{eq 45}]$$

When the surface shear is small, $k_s \sqrt{C_\mu} > U_*^2$, then the symmetry condition for turbulent kinetic energy shown in equation 43 is used. Where U_{*s} is the wind induced surface friction velocity. In

a similar fashion the turbulent dissipation boundary condition for a free surface with and without wind induced surface shear was developed and is given in equation 46.

$$\varepsilon = \frac{(k_s \sqrt{C_\mu})^{3/2}}{\kappa \left[y + aH \left(1 - \frac{U_{*s}^2}{k_s \sqrt{C_\mu}} \right) \right]} \quad [\text{eq 46}]$$

The coefficient a was set to a value of 0.07 by Rodi in 1983. When surface shear is present equation 45 reduces to $\varepsilon = \frac{U_{*s}^3}{\kappa \cdot y}$. When surface shear is not present equation 46 becomes

$$\varepsilon = \frac{k^{3/2}}{\kappa [y + aH]} \text{ which is similar to equation 44 above.}$$

The original CE-QUALW2 free surface boundary conditions are shown below

$$k = \frac{(U_{*s}^2 + U_{*boundary}^2)}{\sqrt{C_\mu}} \quad [\text{eq 47}]$$

$$\varepsilon = \frac{(U_{*s}^3 + U_{*boundary}^3)}{\kappa \cdot y} \quad [\text{eq 48}]$$

These are similar to the boundary conditions presented in equations 45 and 46 when wind induced shear is present. The only difference is that both the turbulent kinetic energy and turbulent dissipation boundary conditions include an additional term for the friction velocity of the lateral boundaries.

The initial conditions and inlet boundary conditions are specified by setting the eddy viscosity, turbulent kinetic energy, and turbulent dissipation terms to the following values.

$$\begin{aligned} \nu_t &= 1.4 \cdot 10^{-6} \\ k &= 1.25 \cdot 10^{-7} \\ \varepsilon &= 1.0 \cdot 10^{-9} \end{aligned}$$

The outlet values of turbulent kinetic energy and turbulent dissipation are determined using a zero gradient approach shown in equations 49 and 50.

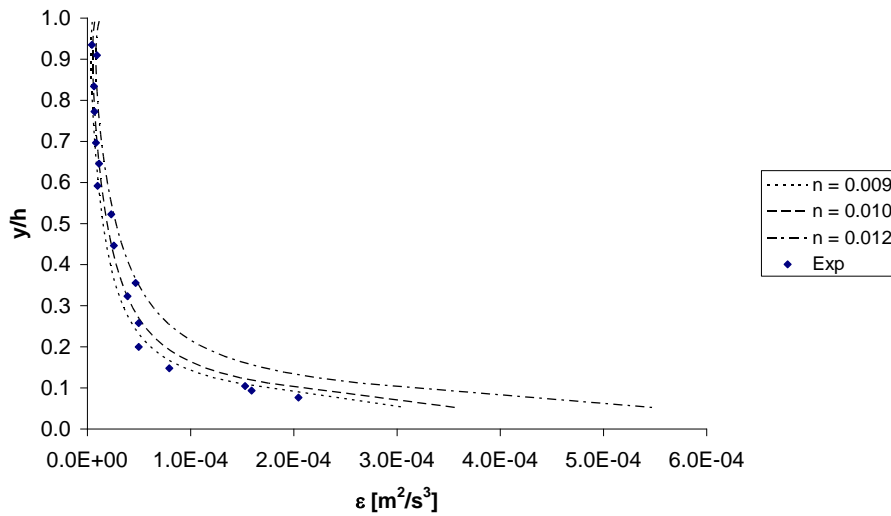
$$\frac{\partial k}{\partial x} = 0 \quad [\text{eq 49}]$$

$$\frac{\partial \varepsilon}{\partial x} = 0 \quad [\text{eq 50}]$$

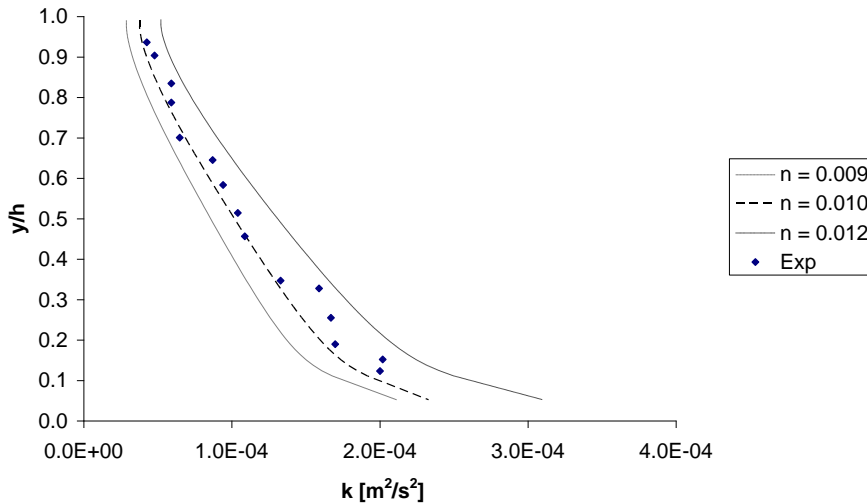
This is done by setting the value of turbulent kinetic energy and turbulent dissipation at the outlet cell equal to the value of the cell in the upstream segment.

Computations of k and ε compared to experimental data are shown in Gould (2006). The experimental data were taken from a uniform open channel experiment conducted by Nakagawa, Neuzu, and Ueda (1975). The figures below show CE-QUAL-W2 model comparisons to the experimental data varying Manning's friction factor. As shown in Gould (2006), the number of vertical layers used in the model application was very important in being able to match experimental laboratory data.

Turbulent Dissipation



Turbulent Kinetic Energy



Effect of Vertical Layer Numbers on Vertical Turbulence

In contrast to other riverine models that assume vertically well-mixed systems, CE-QUAL-W2 accounts for the vertical variation of velocity in a riverine reach. Even though there is an added computational burden of computing the 2D velocity profile, the advantage of making this computation is that the friction factor (Manning's or Chezy) for a segment can be flow or stage invariant depending on the number of vertical layers schematized.

Many 1D hydraulic flow models, such as CE-QUAL-RIV1 and UNET (Barkau, 1997), allow the model user to specify how Manning's friction factor changes with depth. The Manning's friction factor, n , has been thought to vary as a function of depth, Reynolds number, and roughness factor or scale of bed grain size (Ugarte and Madrid, 1994; Soong, et. el., 1995). Some of these formulations for variation of Manning's friction factor with hydraulic radius, R , are shown in [Figure A-39](#):

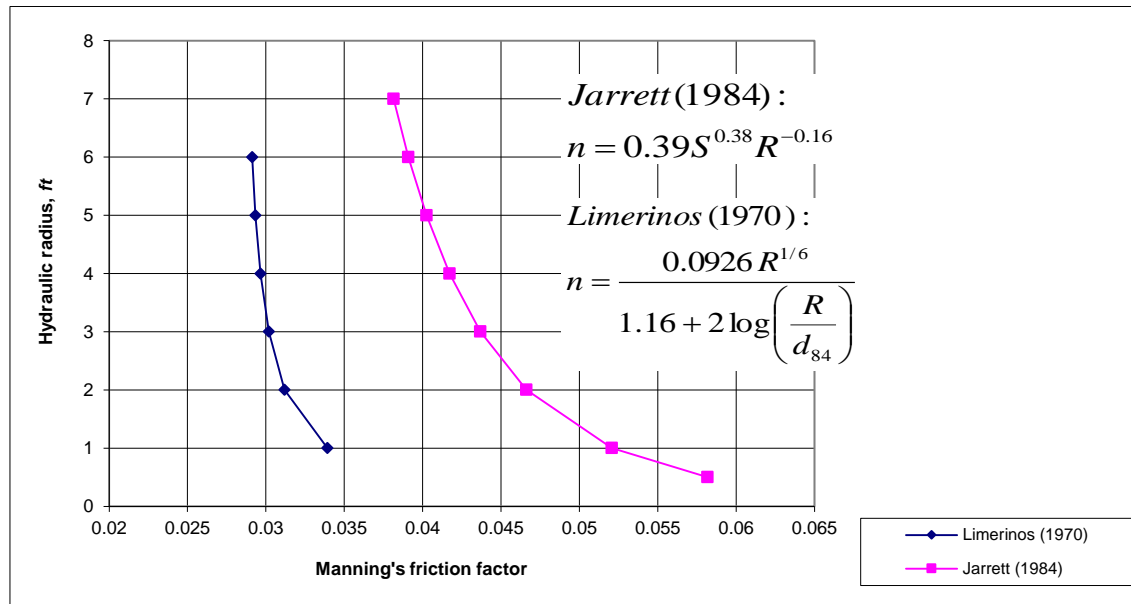


Figure A-39. Variation of Manning's friction factor using formulae from Limerinos (1970) and Jarrett (1984) for a channel slope, S , of 0.0005 and 84th percentile diameter of the bed material, d_{84} , of 50.

Researchers understand that the friction factor, when representing a hydraulic element with uniform roughness, should be flow invariant with depth (Henderson 1966). However, many assert that the friction factor changes with depth because the friction coefficient is variable with the wetted perimeter. Some investigators reason that it is to be expected that at shallow depths the larger size of the bed material produces a higher overall friction factor than a deeper flow where the sidewalls may have a smaller friction.

Since most researchers used 1D, cross-sectionally averaged flow equations such as Manning's Equation or 1D dynamic hydraulic models, this parameterization itself has been responsible for the seeming variation of Manning's friction factor with depth. For example, all 1D hydraulic models implicitly assume that the rate of transfer of momentum from the bottom of the channel to the top is infinite. For these hydraulic models, even as the depth of the channel increases, they still assume an infinite momentum transfer rate over the depth of the channel. Therefore, as the water depth increases, the apparent friction factor must be reduced because of the assumption of infinite momentum transfer between the bottom and the surface.

However, in a longitudinal-vertical river model, Manning's friction factor does not have to vary with stage in order to produce the effect that as the river stage increases, the apparent friction decreases. The water surface set-up changes significantly as the layer numbers increase. In general, the water surface slope increases as the number of computational layers decreases. This is because the average eddy viscosity in the water column increases as the number of layers decrease until at

the limit of a one-layer system, the average vertical eddy viscosity is infinite. The fact that the Manning's friction factor seems to decrease with depth in 1D models is accounted for in modeling the river channel as a 2D, longitudinal-vertical system.

Version 3 allows choosing between five different vertical eddy viscosity formulations. These formulations are shown in [Table A-6](#). Typical variation of these formulations is shown in [Figure A-34](#) for Manning's friction factor for an open-channel, non-stratified flow regime as compared to theory of steady, uniform channel flow.

The number of vertical layers significantly affects model predictions. For example, [Figure A-40](#) shows a comparison of vertical velocity profiles from a model with one, three, and seven vertical layers using the parabolic eddy viscosity model.

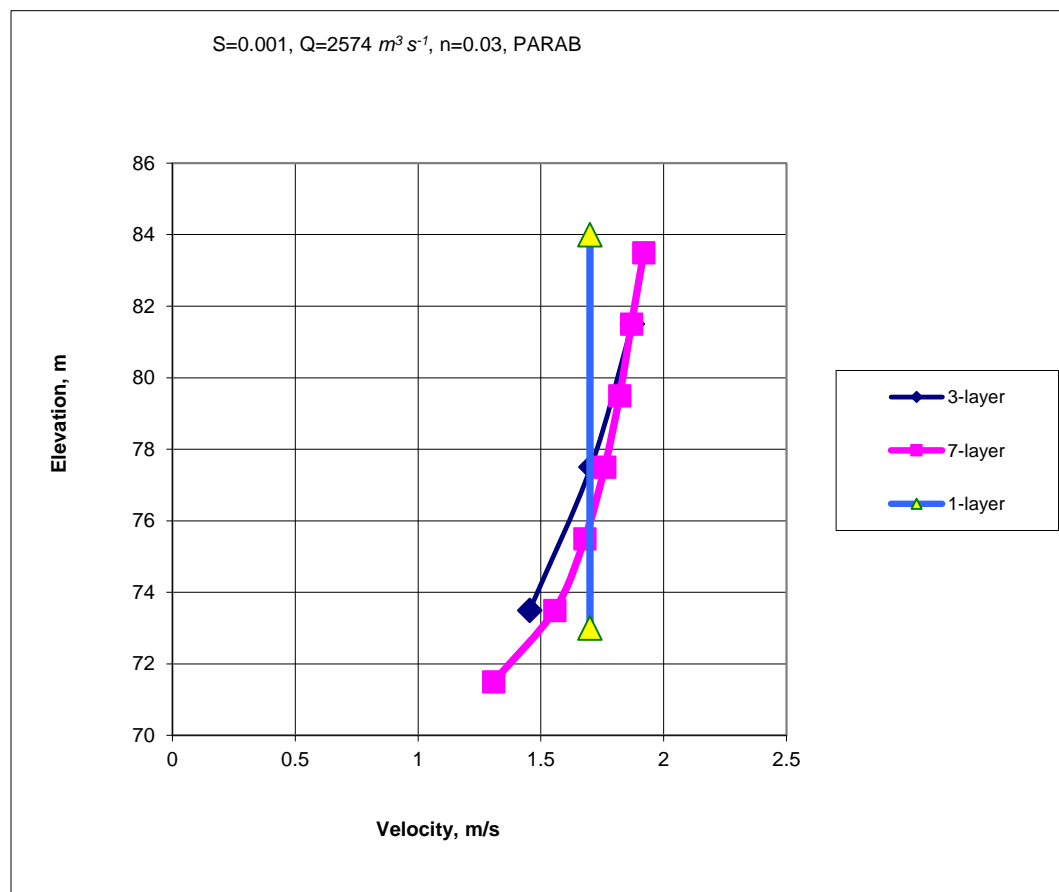


Figure A-40. Comparison of vertical velocity predictions with one, three, and seven vertical layers

[Figure A-41](#) shows how the change in the number of vertical layers affects the water surface slope over the domain length for a steady-state flow. In order to model the water surface slope of the 1-layer model with the 7-layer model, the apparent value of Manning's friction factor would have to be reduced. Hence, the apparent friction decreases as the number of layers increase.

CE-QUAL-W2 V3 has also been compared to the 1D models DYNHYD (Ambrose et al., 1988) and CE-QUAL-RIV1 (Environmental Laboratory, 1995) by running W2 with only a single vertical layer.

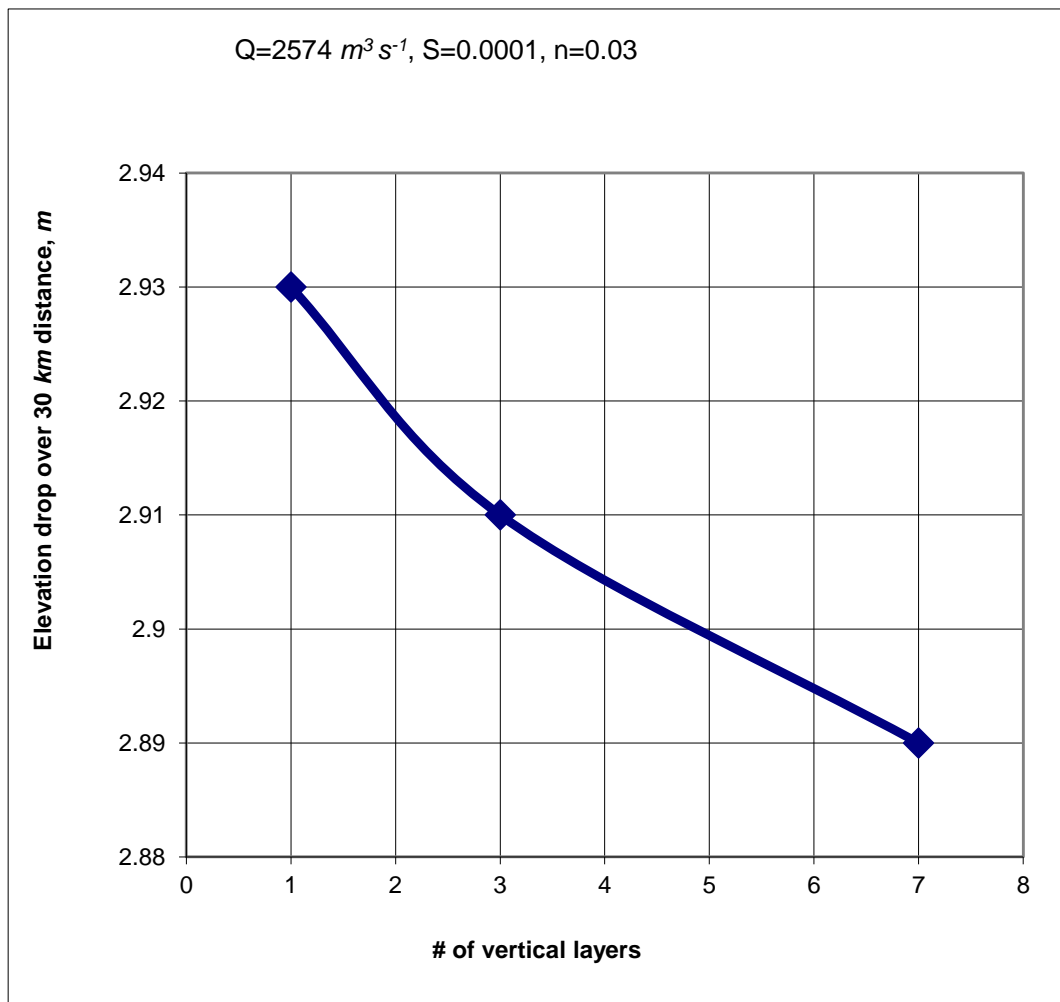


Figure A-41. Comparison of elevation drop of W2 model with one, three, and seven vertical layers with same Manning's friction factor.

The average velocities between the three models agreed well with theory but the water surface slopes are different. W2 predicts an elevation difference of 2.93 m, compared to 2.07 m for DYNHYD and 2.05 m for RIV1 over 30 km for a flow of 2574 m³ s⁻¹, a Manning's n of 0.03, a slope of 0.001, and a channel width of 100 m. Based on steady-state theory, the actual difference should be 2.9 m. Both the DYNHYD and RIV1 models require friction factors greater than expected to correspond to classical theory. This may be a result of these models not incorporating sidewall friction that was important during these test runs where the depth was 15 m and the width was 100 m.

Longitudinal Shear Stress

The longitudinal turbulent shear stress is defined as

$$\frac{\tau_{xx}}{\rho} = \nu_t \frac{\partial U}{\partial x} = A_x \frac{\partial U}{\partial x} \quad (\text{A-175})$$

where:

$A_x = \nu_t$ = longitudinal eddy viscosity

A_x is a user-defined constant in the model. This turbulence closure approximation is termed a zero-order closure model since no further equations are necessary to solve for the transmission of shear stress within the fluid.

This term is usually of very low magnitude except in areas near boundaries such as at a dam face where the longitudinal velocity goes to zero.

Hydraulic Structures

The model user can specify a pipe or culvert between model segments (Berger and Wells, 1999) and uses a 1D, unsteady hydraulic submodel that computes the flow between the two linked segments. The model computes the selective withdrawal outflow from the upstream segment with the model user specifying whether the inflow to the downstream segment is treated as mixed over the depth, inflow depth is determined from inflow density, or inflow depth is specified between an upper and lower elevation. The flow between an upstream segment and a downstream segment is shown in [Figure A-42](#).

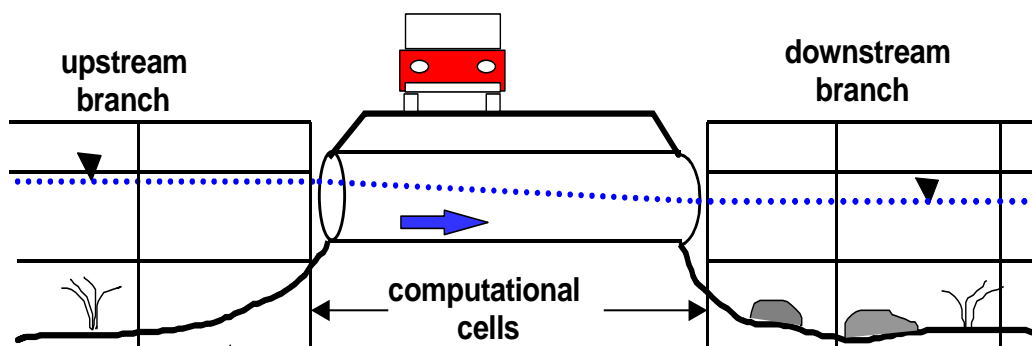


Figure A-42. Schematic of linkage of model segments with a culvert.

This model is only appropriate for simple piping systems that are not suddenly under a large hydraulic head. The governing equations for computing the flow and the numerical solution technique are shown below.

The governing equations used to predict flow through culverts are the 1D, time-dependent conservation of momentum and continuity equations (Yen, 1973).

$$\frac{\partial u}{\partial t} + u \frac{\partial u}{\partial x} + g \cos \phi \frac{\partial h}{\partial x} - g(S_o - S_f - S_m) = 0 \quad (\text{A-176})$$

$$\frac{\partial h}{\partial t} + u \frac{\partial h}{\partial x} + \frac{A}{T} \frac{\partial u}{\partial x} = 0 \quad (\text{A-177})$$

where:

u = velocity, $m \ s^{-1}$

t = time, s

h = piezometric head, m

g = gravitational acceleration, $m^2 \ s^{-1}$

x = distance along axis of culvert, m

A = cross-sectional area of culvert filled with water, m^2

T = width of water level surface, m

ϕ = angle between culvert axis and horizontal

S_o = culvert slope

S_f = friction slope.

S_m = minor loss slope

The friction slope S_f is estimated using the Manning formula:

$$S_f = \frac{n^2}{R^{4/3}} u |u| \quad (\text{A-178})$$

where:

n = Mannings roughness factor

R = hydraulic radius.

Minor losses due to entrance configuration, gates, valves, and corners are accounted for in the minor loss term S_m :

$$S_m = k \frac{u |u|}{2g} \frac{1}{L} \quad (\text{A-179})$$

where:

k = sum of minor loss coefficients

L = length

Pressurized or full culvert flow is modeled assuming a fictitious water surface width called a Preissmann slot (Yen, 1986). If the culvert is full, the surface width T is zero and the governing equations become singular. Using a Preissmann slot avoids having to switch between the open channel and pressurized flow equations. The slot must be narrow enough to minimize error in the mass and

momentum balance but large enough to maintain numerical stability when solving the open channel St. Venant equations. A top width of 0.5% of the diameter is assumed for culverts flowing full.

The advantages of using a Preissmann slot are (Yen, 1986):

1. uses only Saint-Venant equations and avoids switching between the surcharge equation and open-channel flow equations and avoids the associated separate treatment of the boundary conditions
2. no need to define surcharge criteria
3. not necessary to keep inventory of the pipes that are surcharged at different times
4. permits the flow transition to progress computationally reach by reach in a sewer, as in the open-channel case, and hence it can account for the situation when only part of the length of the pipe is full
5. requires few additional assumptions than the standard approach to achieve numerical stability
6. simpler to program

The disadvantages are:

1. introduces a potential accuracy problem in the mass and momentum balance of the flow if the slot is too wide, and stability problems if it is too narrow
2. requires computation of two equations (continuity and momentum) for each of the reaches of the sewer when the sewer is full surcharged, whereas in the standard surcharge computation only one equation is applied to the entire length of the sewer
3. hypothetical rather than real

The Preissmann slot concept has been applied to other models for surcharged flow including the model described by Abbot (1982) and SWMM EXTRAN (Roesner et al. 1988).

The boundary condition used for solving the governing equations is the head or water level at each end of the culvert. However, if the water level at the downstream end of the culvert is less than the critical depth, the critical depth is used. Momentum is not transferred between model segments and the culverts. Initial conditions are the calculated velocities and heads at the previous time step.

The governing equations cannot be solved analytically and an implicit finite difference scheme is used to approximate the solution. The solution method employs the “leap-frog scheme” which calculates the head and velocity at alternating computational nodes (Anderson, et. al., 1984). The finite difference forms of the continuity and momentum equations are:

$$\begin{aligned}
 0 = & \frac{h_i^{n+1} - h_i^n}{\Delta t} + \theta u_i^n \frac{h_{i+2}^{n+1} - h_{i-2}^{n+1}}{2\Delta x} + (1 - \theta) u_i^n \frac{h_{i+2}^n - h_{i-2}^n}{2\Delta x} + \theta \frac{A_i^n}{T_i^n} \frac{u_{i+1}^{n+1} - u_{i-1}^{n+1}}{\Delta x} \\
 & + (1 - \theta) \frac{A_i^n}{T_i^n} \frac{u_{i+1}^n - u_{i-1}^n}{\Delta x}
 \end{aligned} \tag{A-180}$$

$$\begin{aligned}
0 = & \frac{u_i^{n+1} - u_i^n}{\Delta t} + \theta u_{i+1}^n \frac{u_{i+1}^{n+1} - u_{i+1}^n}{\Delta x} + (1 - \theta) u_{i+1}^n \frac{u_{i+1}^n - u_{i+1}^{n+1}}{\Delta x} + \theta g \frac{h_{i+2}^{n+1} - h_i^{n+1}}{\Delta x} \\
& + (1 - \theta) g \frac{h_{i+2}^n - h_i^n}{\Delta x} + \theta g \frac{n^2}{R^{4/3}} u_{i+1}^{n+1} |u_{i+1}^n| + (1 - \theta) g \frac{n^2}{R^{4/3}} u_{i+1}^n |u_{i+1}^n| \\
& + \theta \frac{k}{L} u_{i+1}^{n+1} |u_{i+1}^n| + (1 - \theta) \frac{k}{L} u_{i+1}^n |u_{i+1}^n|
\end{aligned} \quad (\text{A-181})$$

where n refers to the time level and i references the spatial node ([Figure A-43](#)).

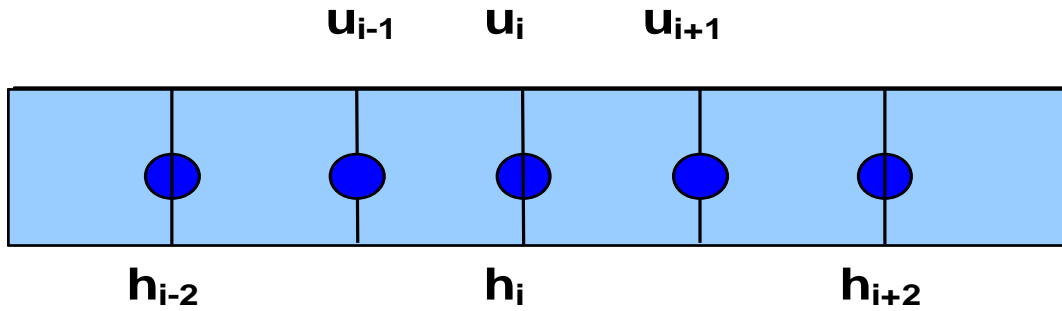


Figure A-43. Linkage schematic of model segments with a culvert.

[Figure A-44](#) compares flow predictions using the dynamic culvert model with flow data taken within a culvert at NE 47th bridge in the Upper Columbia Slough, Portland, Oregon. Data was recorded using a flow meter placed directly in a culvert. The cyclical flows are the result of turning pumps on and off at a downstream pump station. The culvert was calibrated by adjusting the minor loss parameter.

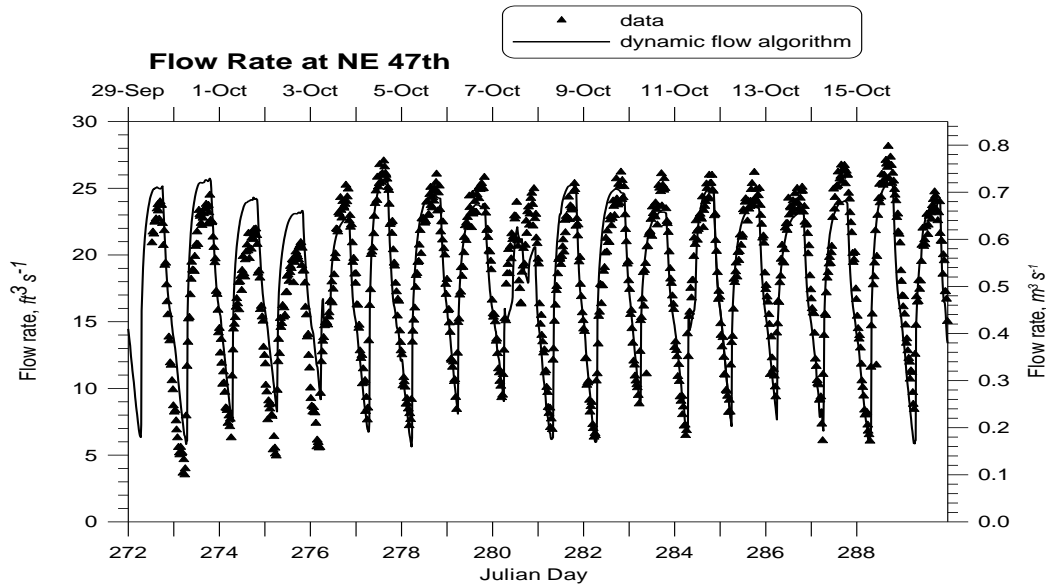


Figure A-44. Computed versus observed flow using dynamic culvert model.

Internal Weirs

The model can be used to set internal weirs at specified cell locations. The user specifies the location of the internal weir by providing a segment and layer number. The weir effectively acts as a barrier to flow and diffusion of mass/heat across the width of the waterbody as shown in [Figure A-45](#). This can be used to simulate submerged and curtain weirs within a waterbody.

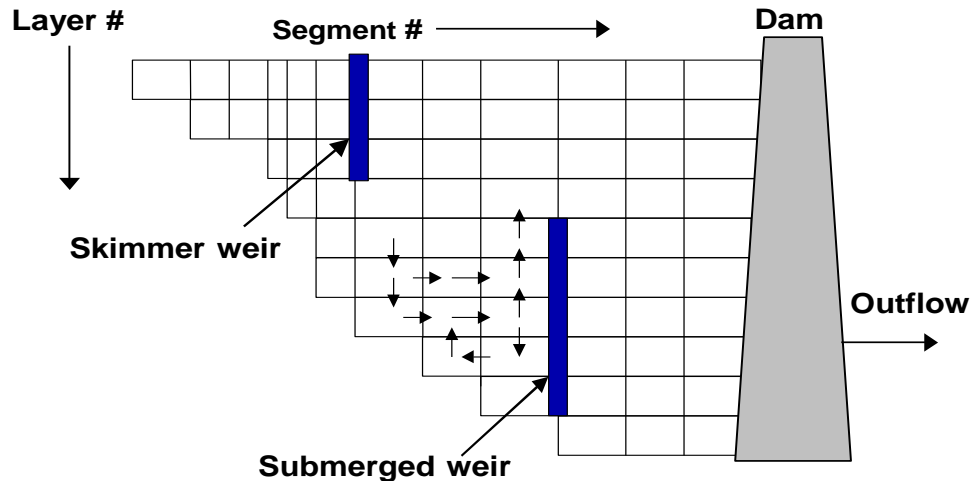


Figure A-45. Schematic representation of internal weirs.

Water Level Control

Many times, outflows in reservoirs are controlled by water levels. In order to facilitate management of the water body, a water level control algorithm was added to the code. Essentially, this is a pump based on a float controller.

The algorithm allows the user to specify the upstream and downstream segment for water to be transferred at a given flow rate based on the water level at the upstream segment. Reverse flow is not allowed. The withdrawal is treated as a lateral selective withdrawal and the segment that receives the inflow is treated as a tributary.

Outlet Structures

Outflows through hydraulic structures ([Figure A-46](#)) can either be specified or computed by the model based on user-supplied rating curves.

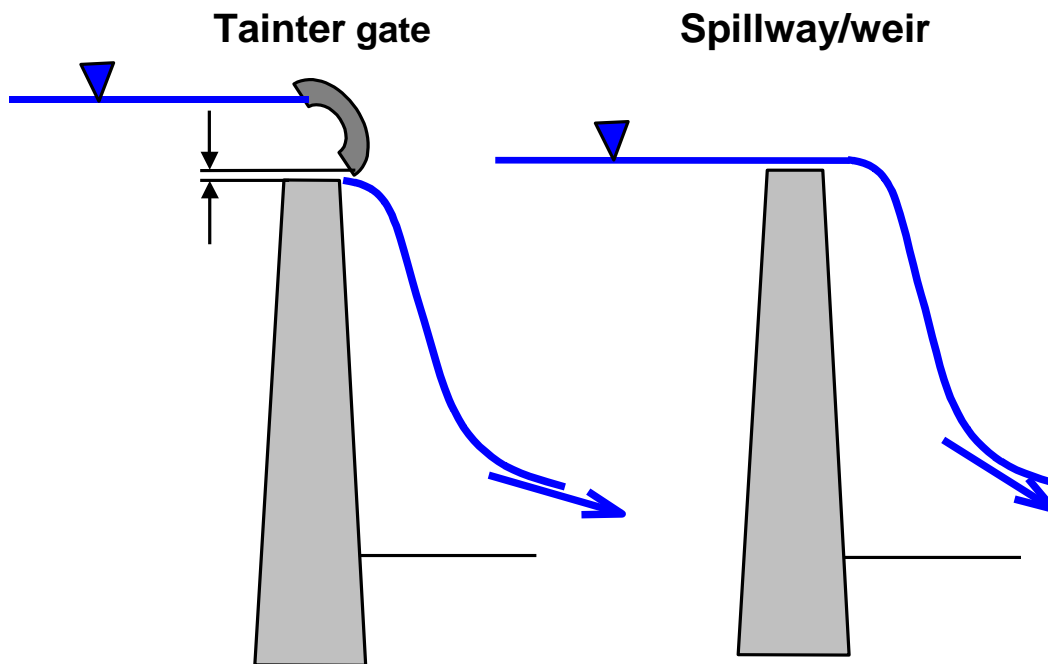


Figure A-46. Radial gates and spillway flow.

The UNET model (HEC, 1997a), a one-dimensional unsteady hydraulic model, formally accounts for spillway flow from weirs and spillways. For free or submerged flow from a spillway with a radial gate, UNET uses a general equation of the form:

$$Q_{sp} = CWA^{\alpha} B^{\beta} H^{\eta} \quad (\text{A-182})$$

where:

- α = empirical coefficient
- β = empirical coefficient
- η = empirical coefficient
- Q_{sp} = flow rate, $m^3 s^{-1}$
- A = trunnion height, m
- B = gate opening, m
- C = empirical coefficient
- W = gate width, m

and

$$H = Z_u - KZ_d - (1 - K)Z_{sp} \quad (\text{A-183})$$

where:

Z_u = headwater elevation

Z_d = tailwater elevation

K = 1 for submerged flow and 0 for free flow

Z_{sp} = spillway elevation

This equation was developed based on rating curves for hydraulic control structures in Arizona. Submergence is defined as:

$$\frac{Z_d - Z_{sp}}{Z_u - Z_{sp}} > \frac{2}{3} \quad (\text{A-184})$$

Note that weir flow is assumed to occur whenever $B = 0.8H$ and is computed as:

$$Q_{weir} = C_w F W \left((1 - K) Z_u + K Z_d - Z_{sp} \right) H^{1/2} \quad (\text{A-185})$$

where:

C_w = weir coefficient

$$F = 3 \left(1 - \frac{Z_d - Z_{sp}}{Z_u - Z_{sp}} \right) \text{ when } K = 1$$

$$F = 1 \text{ when } K = 0$$

For a concrete spillway, HEC (1997a) suggests using a weir coefficient value of 4. Note that the above two equations are considered equivalent whenever $B = 0.8H$.

HEC-RAS, a one-dimensional, steady-state hydraulic model, (HEC, 1997b), includes the ability to model flow over spillways including tainter and sluice gates, broad-crested weirs, and an ogee crest. Ineffective flow area, that area below the weir or gate opening, is used to block a part of the channel until it reaches the level of a spillway or weir.

A summary of the equations used by HEC-RAS (HEC, 1997b) as well as explanations are shown in [Table A-7](#).

Table A-7. HEC-RAS flow rates through weirs and sluice gates.

Condition	Equation	Description
Radial flow gate, flowing freely	$Q = C \sqrt{2g} W T^{T_E} B^{B_E} H^{H_E}$	<p>When the upstream water surface is ≥ 1.25 times the gate opening height (above the spillway crest),</p> <p> Q = flow, <i>cfs</i> C = discharge coefficient (between 0.6 and 0.8) W = gated spillway width, <i>ft</i> T = trunnion height (from spillway crest to trunnion pivot point), <i>ft</i> B = gate opening height, <i>ft</i> H = upstream energy head above spillway crest, $Z_u - Z_{sp}$, <i>ft</i> Z_u = upstream energy grade line elevation, <i>ft</i> Z_d = downstream water surface elevation, <i>ft</i> Z_{sp} = spillway crest elevation, <i>ft</i> T_E = empirical trunnion height exponent, 0.16 B_E = gate opening coefficient, 0.72 H_E = head exponent, 0.62 </p>

Condition	Equation	Description
radial gate flowing under submerged conditions	$Q = 3C\sqrt{2g} WT^{T_E} B^{B_E} H^{H_E}$	When the upstream water surface is ≥ 1.25 times the gate opening height (above the spillway crest), whenever the tailwater depth divided by the energy depth above the spillway is greater than 0.67 $H = Z_u - Z_d$
freely flowing sluice gate	$Q = C\sqrt{2gH} WB$	When the upstream water surface is ≥ 1.25 times the gate opening height above the spillway crest H = upstream energy head above the spillway, $Z_u - Z_{sp}$ C = discharge coefficient, 0.5 to 0.7
submerged sluice gate	$Q = 3C\sqrt{2gH} WB$	When the upstream water surface is ≥ 1.25 times the gate opening height above the spillway crest, whenever the tailwater depth divided by the energy depth above the spillway is greater than 0.67 $H = Z_u - Z_d$
Low flow through gated structure	$Q = CLH^{\frac{3}{2}}$	When upstream water level is equal to or less than the top of the gate opening, weir flow equation is used C = weir coefficient, 2.6-4.0 depending on broad crested or Ogee spillway and length of spillway crest H = upstream energy head above spillway crest, for an Ogee spillway the value of C is adjusted according to a 1977 Bureau of Reclamation study on variability of C for Ogee spillways, suggested values of C are 2.6 for bridge decks and 3.0 for flow over elevated roadways

Spillways/Weirs

Analysis of flow over weirs has been studied extensively. Martin and McCutcheon (1999) show that a typical relationship between the pool depth and flow over a weir is:

$$Q = C_e W_c h_w^\eta \quad (\text{A-186})$$

where C_e and η are empirical coefficients, W_c is the length of the weir crest, and h_w is the height of the pool above the weir crest. Theoretical calculations of steady-state flow over a weir can be complex depending on whether the weirs are sharp-crested, broad-crested, V-notched, rectangular, Cipolletti, parabolic, or some other type. [Table A-8](#) shows some examples from French (1985) and USBR (1999) on typical equations used for the different weir types. For many regular weir types, formulae exist for accurate estimation of the flow. However, in most cases a rating curve for a given installation is necessary because of the uncertainty of end effects, flow alignments, shallowness in the upstream pool, and other unique features of the installation (Martin and McCutcheon, 1999).

Table A-8. List of weir types (French, 1985; USBR, 1999)

Weir type	Weir Equation	Description
Rectangular broad crested weir	$Q = C_D C_v \frac{2}{3} \sqrt{\frac{2}{3}} g W H^{3/2}$	<p>Valid when $0.08 < H/L < 0.5$ Q = flow rate C_D = discharge coefficient (0.84 to 1.06) C_v = velocity coefficient accounting for neglecting the velocity head in the approach channel (between 1.0 and 1.2)</p> <p>W = gated spillway width, ft W = width at surface H = upstream head above spillway crest</p> <p>Z_u = upstream energy grade line elevation, ft g = gravity acceleration</p> <p>H_E = head exponent, 0.62</p> <p>H_1 = total head upstream of the weir (energy + static head)</p> <p>L = weir block length</p> <p>W = weir width from edge to edge</p> <p>C_v = coefficient, 1-1.2</p> <p>C_D = coefficient, 0.85-1.06\</p>

Weir type	Weir Equation	Description
Rectangular, sharp crested weir	$Q = C_e \frac{2}{3} \sqrt{2g} B H^{3/2}$	Where B = width at bottom of weir crest Olson and Wright (1990) show that C_e depends on the approach velocity head, $V^2/2g$, and the contraction of streamlines just beyond the weir crest and show that $C_e = 0.611 + 0.075^*(H/Z)$ H = weir head, ft Z = weir crest head measured from the channel bottom, ft Clay (1995) suggests a simple equation of $Q=3.33BH^{6/2}$ of this form when approach velocities are less than 1 fps or $Q=3.33B[(H+h)^{3/2} - h_v^{3/2}]$ $h_v = V^2/2g$ V = approach velocity, $ft\ s^{-1}$
Parabolic, broad-crested	$Q = C_D C_v \sqrt{\frac{3}{4} f g} H^2$	f = distance from the bottom point of the weir to the weir focal point, ft
Parabolic, sharp-crested	$Q = C_e \frac{1}{2} \pi \sqrt{f g} H^2$	C_e = effective discharge coefficient
Triangular, broad-crested	$Q = C_D C_v \frac{16}{25} \sqrt{\frac{2}{5} g} \tan(0.5\Theta) H^{5/2}$	Θ = half angle of the triangular notch Θ = angle of half of the triangular weir
Triangular, sharp-crested	$Q = C_e \frac{8}{25} \sqrt{2g} \tan(0.5\Theta) H^{5/2}$	C_e = function of notch angle and varies from 0.59 to 0.57 for angles between 20 and 100 degrees
Trapezoidal, broad-crested	$Q = C_D (W y_c + m y_c^2) [2g(H - y_c)]^{1/2}$	W = top width of trapezoidal weir T = top width m = slope of trapezoidal weir y_c = depth of water at the weir m = slope y_c = water surface elevation at the weir H_1 = energy head upstream of the spillway
Trapezoidal, sharp-crested	$Q = C_e \frac{2}{3} \sqrt{2g} (B + \frac{4}{5} H \tan 0.5\Theta) H^{1/2}$	B = bottom width of trapezoidal weir Θ = angle of the trapezoid at a convergence point of the 2 sides
Truncated triangular, broad-crested	$Q = C_D C_v \frac{2}{3} \sqrt{\frac{2}{3} g} W (H - 0.5H_b)^{3/2}$	Use when $H > 1.25H_b$, otherwise use equation for broad crested triangular weir H_b = depth from the bottom of the truncated triangular weir to the top of the triangle and the beginning of the rectangular section

Weir type	Weir Equation	Description
Truncated triangular, sharp-crested	$Q = C_e \frac{4}{15} \sqrt{2g} \frac{W}{H_b} (H^{2.5} - (H - H_b)^{2.5})$	Use when $H > H_b$, otherwise use equation for sharp crested triangular weir
Cipoletti	$Q = C_D C_v \frac{2}{3} \sqrt{2g} W H^{3/2}$	A modification of the contracted, rectangular, sharp-crested weir with a trapezoidal control section and sides sloping outward with slopes of 4:1 W = top width of weir $C_D \approx 0.63$ C_v varies from 1 to 1.2 and is a function of C_D and the ratio of area upstream of the control section and at the control section
Proportional or sutro weir	$Q = C_D B \sqrt{2ga} \left(H - \frac{1}{3}a \right)$	a = height of the rectangular portion of the weir above the base B = bottom width of weir a = distance from weir bottom to top of the rectangular weir section b = bottom width of sutro weir C_D = coefficient, 0.597-0.619 for symmetrical Suto weir, 0.625- 0.603 for unsymmetrical Suto weir

Since all weirs in practice are calibrated and a head discharge relationship is usually determined, the flow versus head relationship is used rather than an equation from [Table A-8](#). The user must then analyze the weir or spillway and input a relationship based on the weir or spillway geometry. The model accepts equations in the form of a power function for freely flowing conditions:

$$Q = \alpha_1 \Delta h^{\beta_1} \quad (\text{A-187})$$

where:

α_1 = empirical parameter
 β_1 = empirical parameter
 $\Delta h = Z_u - Z_{sp}$
 Z_u = upstream head
 Z_{sp} = spillway crest elevation

and for submerged conditions

$$Q = \alpha_2 \Delta h^{\beta_2} \quad (\text{A-188})$$

where:

α_2 = empirical parameter
 β_2 = empirical parameter

$$\Delta h = Z_u - Z_d$$

Z_u = upstream head

Z_d = downstream head

Submerged conditions are defined when the tailwater depth over the upstream energy head (static head and velocity head) is greater than 0.67 (HEC, 1997b). Even though negative flow rates are possible using the second equation whenever $Z_d > Z_u$, these results should be used with caution since rarely are rating curves done for reverse flow over a spillway. The user needs to ensure there is a smooth transition between submerged flow conditions and free flowing conditions by proper choice of model coefficients. The following discussion shows how to generate a smooth flow transition from free flowing to submerged flow conditions ([Figure A-47](#)).

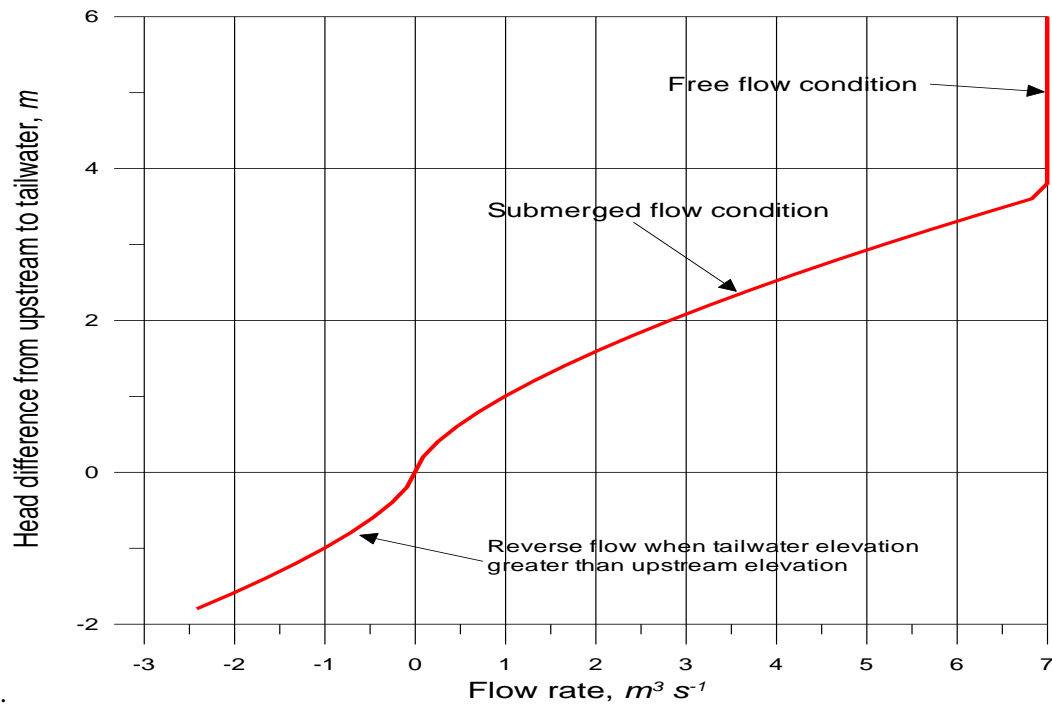


Figure A-47. Flow rate over a spillway or weir for submerged and free flowing conditions.

Consider the following weir flow condition in [Figure A-48](#).

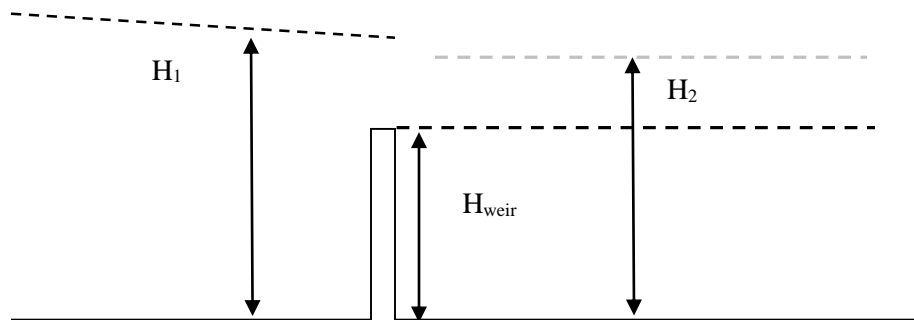


Figure A-48. Flow at a submerged weir.

In order to have a smooth transition, the two flows must be equal at the transition point. Using

$$H_2 - H_{weir} = 0.67(\Delta h_1 + \frac{u^2}{2g}) \approx 0.67(H_1 - H_{weir}) \quad (\text{A-189})$$

and substituting the rating curves for free flow and submerged conditions and solving for α_2 results in:

$$\alpha_2 = \frac{\alpha_1 (H_1 - H_{weir})^{\beta_1 - \beta_2}}{(0.33)^{\beta_2}} \quad (\text{A-190})$$

In many cases a weir can be set as the downstream boundary condition of a river. In CE-QUAL-W2, the user can specify the weir crest as the channel bottom elevation, such that the weir equation is of the form:

$$Q = \alpha_1 H^{\beta_1} \quad (\text{A-191})$$

where H is the depth of the water at the weir. Setting this in the form of a stage-discharge relationship:

$$H = aQ^b = \left(\frac{Q}{\alpha_1} \right)^{\frac{1}{\beta_1}} \quad (\text{A-192})$$

where a and b are empirical coefficients. Writing this equation in a form compatible with the stage discharge relationship using the a and b coefficients,

$$H = \left(\frac{1}{\alpha_1} \right)^{\frac{1}{\beta_1}} Q^{\frac{1}{\beta_1}} \quad (\text{A-193})$$

Then the a and b coefficients become

$$a = \left(\frac{1}{\alpha_1} \right)^{\frac{1}{\beta_1}} \quad (\text{A-194})$$

$$b = \frac{1}{\beta_1} \quad (\text{A-195})$$

or vice versa:

$$\alpha_1 = a^{-\beta_1} \quad (\text{A-196})$$

$$\beta_1 = \frac{1}{b} \quad (\text{A-197})$$

allows the user to set a weir-rating curve that reproduces the stage discharge relationship at a downstream boundary.

A dynamic weir or spillway crest elevation can also be used to simulate dynamic raising of flashboards. These are designated in the model as gates.

Gates

For a gated structure or sluice gate, a more complex rating curve is required based on the opening and the head difference between the upstream and downstream condition (the spillway crest if free flow and the tailwater elevation if submerged flow).

The following equation is used for freely flowing conditions:

$$Q = \alpha_1 \Delta h^{\beta_1} B^{\gamma_1} \quad (\text{A-198})$$

where:

α_1 = empirical coefficient

β_1 = empirical coefficient

γ_1 = empirical coefficient

$\Delta h = Z_u - Z_{sp}$

Z_u = upstream head

Z_{sp} = spillway crest elevation

and the following equation is used for submerged flow:

$$Q = \alpha_2 \Delta h^{\beta_2} B^{\gamma_2} \quad (\text{A-199})$$

where:

α_2 = empirical coefficient

β_2 = empirical coefficient

γ_2 = empirical coefficient

$\Delta h = Z_u - Z_d$

Z_d = downstream head

B = gate opening, m

In defining these parameters, the user also has to generate a time series file with the gate opening in m where a gate opening of $0\ m$ is closed. Whenever the gate opening is equal to or greater than $0.8\Delta h$, a weir equation is used with no functional dependency on the gate opening. In this case, a rating curve must be supplied when the gate acts like a weir. [Figure A-49](#) shows the flow rate dependence on the gate opening.

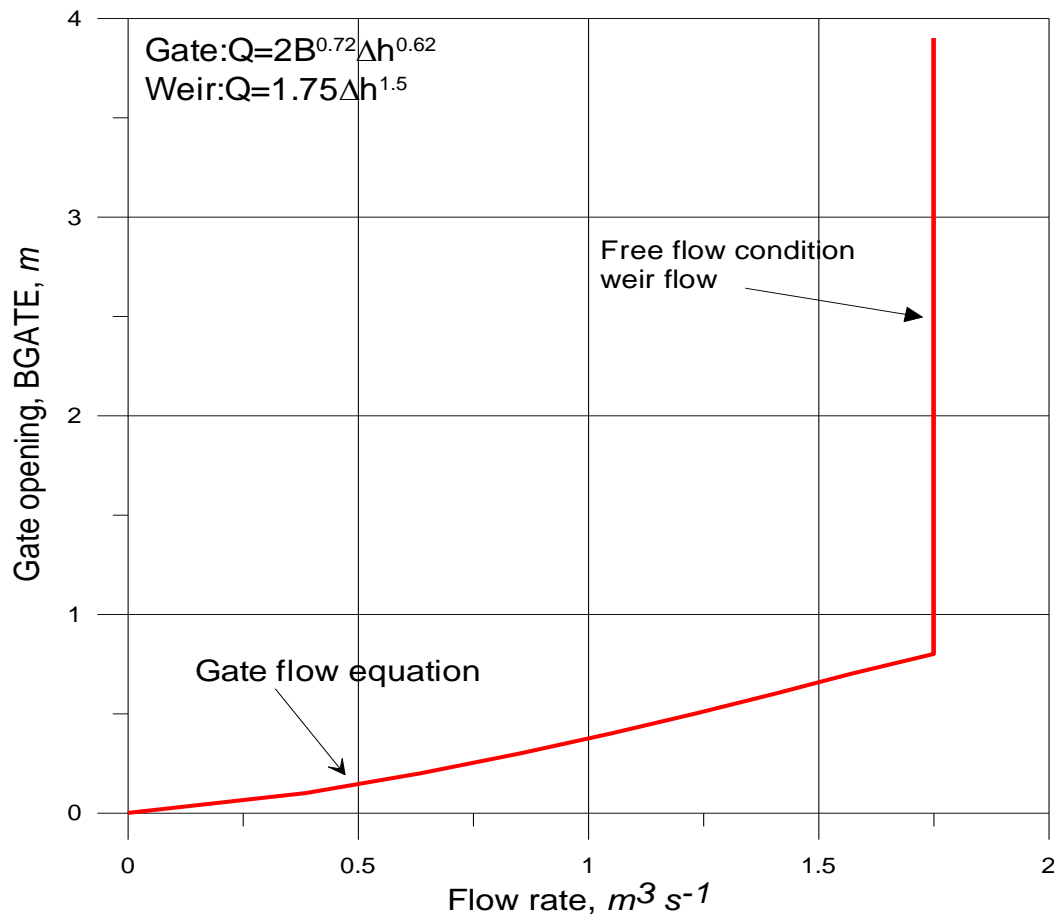


Figure A-49. Flow rate variation with gate opening.

In some reservoir systems, an outlet valve is connected to the reservoir and a head-discharge relationship is used based on the gate opening or number of gate turns. In this case, the outlet level is usually at a different elevation than the withdrawal elevation. The above gate formulation can still be used if no reverse flow occurs through the needle valve. This situation is illustrated in [Figure A-50](#). In this case, the elevation of the outflow is required in addition to the elevation at which the outflow is taken if a rating curve is used in the model. This use is described in the section on changes to the control file.

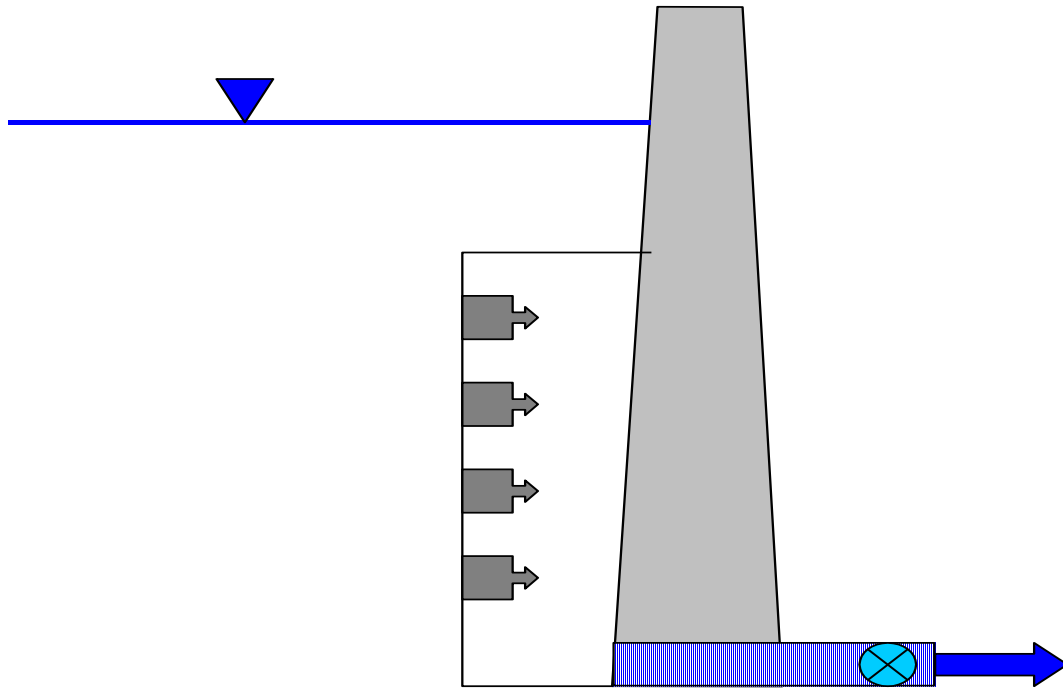


Figure A-50. Selective withdrawal with outflow connected to a valve with a gate.

The user can insert weirs and/or spillways, specify connectivity to other model segments, and insert the ratings curve parameters for each weir/spillway. The model treats each spillway, weir, or gate as a selective withdrawal outflow and uses the selective withdrawal algorithm for determining water flow from each vertical layer adjacent to the structure. Inflows from hydraulic control structures are treated as tributary inflows where the user must specify whether the inflow is placed according to density, equally distributed between all vertical layers, or distributed between a given elevation range.

Weir equations are used when gates are open and the open gate does not interfere with the flow (when $B \geq 0.8\Delta h$).

Gates can also be used to move flows around to different parts of the model domain – different branches. In that case the specification of gate openings are interpreted as specification of flow rates.

Branch Momentum Exchange

Version 3 conserves longitudinal momentum at branch intersections ([Figure A-51](#)). The vector component of velocity in the x-direction of the main channel, U_x , can be computed from the channel orientations. The x-direction component is $U_x = U \cos \beta$ where U is the longitudinal velocity of the tributary at the downstream segment that intersects the main branch and β is the difference in the angle between the main stem and tributary segments.

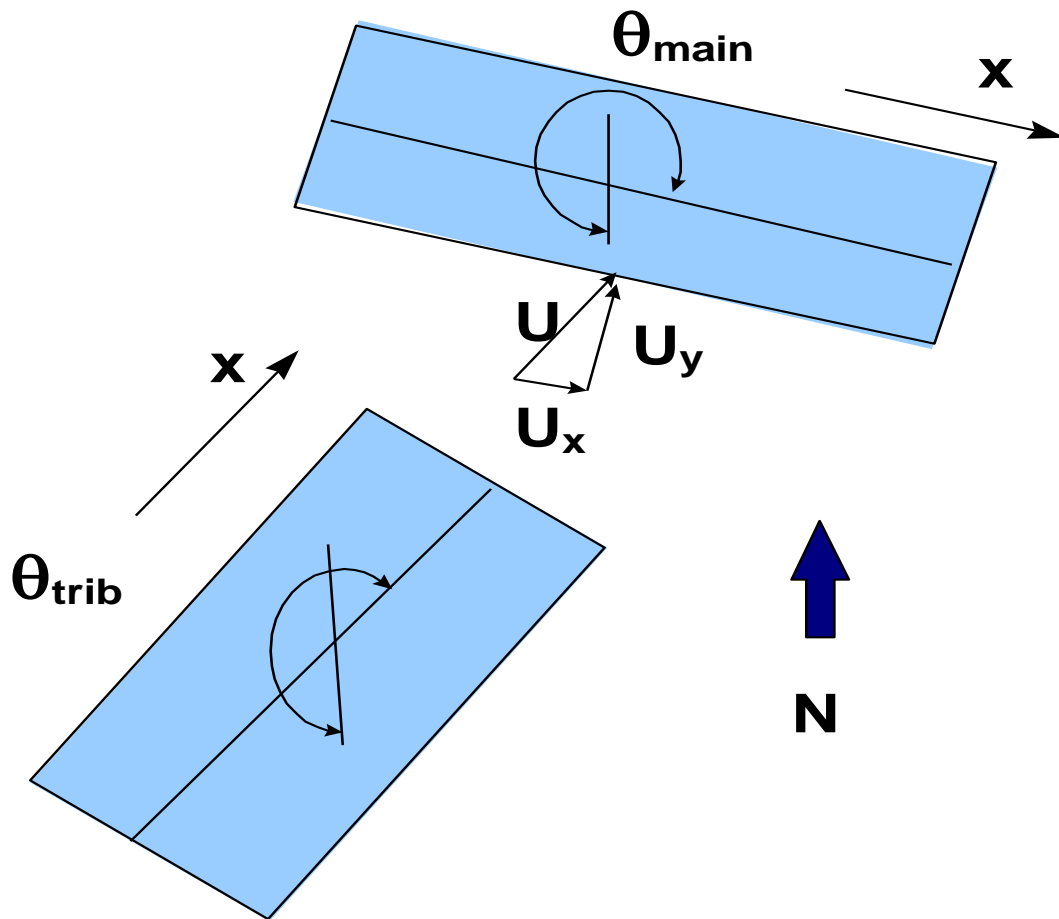


Figure A-51. Schematic of branch connection.

The conservation of momentum about a control volume, the main stem segment, would result in an additional source of momentum. Lai (1986) shows that the correction to the x-momentum equation would be:

$$200) \quad qBU_x \quad (\text{A-})$$

where:

q = lateral inflow per unit length

This arises from re-deriving the momentum equations and assuming that all the fluid entering the segment is moving at the velocity U_x . The correction to the x-momentum equation is:

$$\begin{aligned} \frac{\partial UB}{\partial t} + \frac{\partial UUB}{\partial x} + \frac{\partial WUB}{\partial z} = & gB \sin \alpha + g \cos \alpha B \frac{\partial \eta}{\partial x} - \frac{g \cos \alpha B}{\rho} \int_{\eta}^z \frac{\partial \rho}{\partial x} dz \\ & + \frac{1}{\rho} \frac{\partial B \tau_{xx}}{\partial x} + \frac{1}{\rho} \frac{\partial B \tau_{xz}}{\partial z} + \underbrace{qBU_x}_{\text{side tributary momentum}} \end{aligned} \quad (\text{A-201})$$

Lateral Inflows

Wells (1997) proposed accounting for the cross-shear as a result of the y component of the velocity of a side branch in the computation of the vertical eddy viscosity. This was implemented by increasing the cross-shear velocity gradient. In Version 2, wind shear across the lateral axis of a segment also increased the vertical mixing by affecting the computation of A_z . Analogous to wind shear, an additional side shear is included in the calculation of the vertical eddy viscosity:

$$A_z = \kappa \left(\frac{l^2}{2} \right) \sqrt{\left(\frac{\partial U}{\partial z} \right)^2 + \left(\frac{\tau_{wy} e^{-2kz} + \tau_{trib}}{\rho A_z} \right)^2} e^{(-CR_t)} \quad (\text{A-202})$$

where:

$$\tau_{trib} \cong \rho \frac{f_i}{8} U_y^2$$

f_i = is an interfacial friction factor, ≈ 0.01

$$U_y = \frac{\sum Q_{in_y}}{\Delta z \Delta x}$$

$$\sum Q_{in_y} = [U_{br} \Delta z B] + [\sum Q_{trib}]$$

$$U_{br} = U_{br} \sin(\Theta_{\text{main}} - \Theta_{\text{branch}})$$

Δz = inflow cell layer height

B = inflow cell width

Δx = inflow cell segment length

Q_{trib} = tributary flow rate assumed to be at right angles to the main channel

This side shear effect is only computed when the vertical mixing algorithm chosen by the user is W2 or W2N.

Heat Exchange

Surface Heat Exchange

Surface heat exchange can be formulated as a term by-term process using the explicit adjacent cell transport computation as long as the integration timestep is shorter than or equal to the frequency of the meteorological data. Surface heat exchange processes depending on water surface temperatures are computed using previous timestep data and are therefore lagged from transport processes by the integration timestep.

Term-by-term surface heat exchange is computed as:

$$H_n = H_s + H_a + H_e + H_c - (H_{sr} + H_{ar} + H_{br}) \quad (\text{A-203})$$

where:

- H_n = the net rate of heat exchange across the water surface, $W m^{-2}$
- H_s = incident short wave solar radiation, $W m^{-2}$
- H_a = incident long wave radiation, $W m^{-2}$
- H_{sr} = reflected short wave solar radiation, $W m^{-2}$
- H_{ar} = reflected long wave radiation, $W m^{-2}$
- H_{br} = back radiation from the water surface, $W m^{-2}$
- H_e = evaporative heat loss, $W m^{-2}$
- H_c = heat conduction, $W m^{-2}$

The short wave solar radiation is either measured directly or computed from sun angle relationships and cloud cover. Annear and Wells (2007) provide an overview of formulae for short wave solar radiation. If the model user chooses the internally computed short wave solar, the model computes the clear sky solar radiation φ_s (H_s , short wave solar radiation in Btu/ft²/day) using the EPA (1971) relationship:

$$\varphi_s = 24(2.044A_o + 0.1296A_o^2 - 1.941E - 3A_o^3 + 7.591E - 6A_o^4) * 0.1314 \quad (\text{A-204})$$

Note that this equation includes the average reflection loss of short wave solar radiation. The total clear sky solar radiation was calculated using a least squares fit polynomial regression of the solar altitude A_o (degrees), which is the angle of inclination of the sun relative to the horizon from an observer's perspective (Wunderlich, 1972) using

$$A_o = A \sin[\sin(Lat)\sin(\delta) + \cos(Lat)\cos(\delta)\cos(H)] \quad (\text{A-205})$$

where Lat is the latitude, δ is the solar declination, and H is the local hour angle. The local hour angle H (radians), is the angular position of the sun for a given location at a specific time during the day and was calculated from Ryan and Stolzenbach (1972) using

$$H = \frac{2\pi}{24} \left[HOUR - (Long - \phi) \frac{24}{360} + EQT - 12.0 \right] \quad (\text{A-206})$$

where $HOUR$ is the local hour, ϕ is standard meridian, $Long$ is the longitude, and EQT is the equation of time. The equation of time EQT (hours), represents the difference between true solar time and mean solar time due to seasonal variations in the orbital velocity of the earth (Ryan and Stolzenbach, 1972). DiLaura (1984) calculated EQT as

$$\begin{aligned} EQT = & 0.170 \sin[4\pi(INT(Jday) - 80)/373] \\ & - 0.129 \sin[2\pi(INT(Jday) - 8)/355] \end{aligned} \quad (\text{A-207})$$

where $Jday$ is the Julian day as a floating-point value on a scale of 1 to 365 days for a year (366 for a leap year) and INT is the integer function. The local hour $HOUR$ (hours), was calculated using the time during the day (Wunderlich, 1972), such as

$$HOUR = 24(Jday - INT(Jday)) \quad (\text{A-208})$$

EPA (1971) calculated the standard meridian ϕ (degrees), as

$$\phi = 15.0 * INT\left(\frac{Long}{15.0}\right) \quad (\text{A-209})$$

where $Long$ is the longitude. The time zones calculate a more appropriate standard meridian than the longitude, so the variable TZ (hours), the time zone relative to Greenwich Mean Time (GMT) was used to improve the calculation of the standard meridian in the above equation, such that

$$\phi = -15.0 * INT(TZ) \quad (\text{A-210})$$

The solar declination angle δ (radians) was calculated by Spencer (1971) as:

$$\begin{aligned} \delta = & 0.006918 - 0.399912 \cos(\tau_d) + 0.070257 \sin(\tau_d) \\ & - 0.006758 \cos(2\tau_d) + 0.000907 \sin(2\tau_d) \\ & - 0.002697 \cos(3\tau_d) + 0.001480 \sin(3\tau_d) \end{aligned} \quad (\text{A-211})$$

where τ_d is the angular fraction of the year which Spencer (1971) calculated as

$$\tau_d = \frac{2\pi(INT(Jday) - 1)}{365} \quad (\text{A-212})$$

AUXILIARY FUNCTIONS

HEAT EXCHANGE

Cloud cover reduction of clear sky solar radiation uses the following relationship (Wunderlich, 1972): $\varphi_{s_net} = \varphi_{s_clearsky}(1 - 0.65C^2)$ where C is the cloud cover fraction between 0 and 1.

The long wave atmospheric radiation is computed from air temperature and cloud cover or air vapor pressure using Bruns formula. The right-hand terms are all water surface temperature dependent.

Water surface back radiation is computed as:

$$H_{br} = \varepsilon \sigma^* (T_s + 273.15)^4 \quad (\text{A-213})$$

where:

ε = emissivity of water, 0.97

σ^* = Stephan-Boltzman constant, $5.67 \times 10^{-8} \text{ W m}^{-2} \text{ }^\circ\text{K}^{-4}$

T_s = water surface temperature, $^\circ\text{C}$

Like the remaining terms, it is computed for each surface layer cell on each iteration timestep.

Evaporative heat loss is computed as:

$$H_e = f(W) (e_s - e_a) \quad (\text{A-214})$$

where:

$f(W)$ = evaporative wind speed function, $\text{W m}^{-2} \text{ mm Hg}^{-1}$

e_s = saturation vapor pressure at the water surface, mm Hg

e_a = atmospheric vapor pressure, mm Hg

Evaporative heat loss depends on air temperature and dew point temperature or relative humidity. Surface vapor pressure is computed from the surface temperature for each surface cell on each iteration.

Surface heat conduction is computed as:

$$H_c = C_c f(W) (T_s - T_a) \quad (\text{A-215})$$

where:

C_c = Bowen's coefficient, $0.47 \text{ mm Hg } ^\circ\text{C}^{-1}$

T_a = air temperature, $^\circ\text{C}$

Short wave solar radiation penetrates the surface and decays exponentially with depth according to Bears Law:

$$H_s(z) = (1 - \beta) H_s e^{-\eta z} \quad (\text{A-216})$$

where:

$H_s(z)$ = short wave radiation at depth z , $W m^{-2}$

β = fraction absorbed at the water surface

η = extinction coefficient, m^{-1}

H_s = short wave radiation reaching the surface, $W m^{-2}$

Aside from the problems of measuring meteorological data relative to a large waterbody and translating data from oftentimes distant weather stations, the most uncertain parameter in the surface heat exchange computations is the evaporative wind speed function, $f(W)$. Various formulations of $f(W)$ have been catalogued and examined in Edinger, et al. (1974). The different formulations result from the empirical determination of $f(W)$ for waterbodies of different size and shape with data from different locations and averaged over different periods of time.

Evaporation

The model allows the user the freedom to include different evaporation formulations via a user defined evaporation wind speed formula of the form

$$f(W) = a + b W^c \quad (\text{A-217})$$

where:

$f(W)$ = wind speed function, $W m^{-2} mm Hg^{-1}$

a = empirical coefficient, 9.2 default

b = empirical coefficient, 0.46 default

c = empirical coefficient, 2 default

W = wind speed measure at 2 m above the ground, $m s^{-1}$

The function is used in computing both evaporative water and heat loss. The default values for a , b , and c are the ones suggested in Edinger, et. al. (1974). The model assumes that the wind is measured at a 2m height. The following equation converts b from any measurement height to 2 m :

$$b_{2m} = \alpha^c b_z \quad (\text{A-218})$$

where b_z is b measured at z m and α is the conversion factor between the wind at z and the wind at 2m using

$$\frac{W_{2m}}{W_z} = \frac{\ln\left(\frac{2}{z_0}\right)}{\ln\left(\frac{z}{z_0}\right)} = \frac{1}{\alpha} \quad (\text{A-219})$$

where:

W_{2m} = wind speed at elevation 2 m , $m s^{-1}$

W_z = wind speed at height z , $m s^{-1}$

z_o = wind roughness height (this is a model input parameter from Version 3.6, typical values include assuming 0.003 *ft* (0.001 m) for wind < 5 *mph* (2.3 m/s) and 0.015 for wind > 5 *mph* (2.3 m/s), range 0.0005 to 0.03 *ft* (0.00015-0.01 m), note that z_o is in m as input to the model)

The Ryan-Harleman (1974) formulation has also been included :

$$f(W_z) = a + bW_z \quad (\text{A-220})$$

where:

$$b = 4.1 \text{ W m}^{-2} \text{ mm Hg}^{-1} \text{ m}^{-1} \text{ s}^{-1}$$

$$a = \lambda (T_{sv} - T_{av})^{1/3}$$

$$\lambda = 3.59 \text{ W m}^2 \text{ mm Hg } ^\circ\text{C}^{-1/3}$$

$$T_v = T^* \left(1 - 0.378 \left[\frac{e}{p} \right] \right)^{-1}, \text{ } ^\circ\text{K}$$

$$p = 760 \text{ mm Hg}$$

For the Lake Hefner model, $a = 0$ and $b = 4.99 \text{ W m}^{-2} \text{ mm Hg}^{-1} \text{ m}^{-1} \text{ s}^{-1}$.

If the virtual temperature difference, T_v , is negative or less than that computed using the Lake Hefner model, $f(W)$ reverts to the Lake Hefner evaporation model. [Figure A-52](#) shows a comparison of the Ryan-Harleman model with the model's default formulation.

Adams et al. (1981) recommended that the Lake Hefner model be used for natural lakes ([Table A-9](#)).

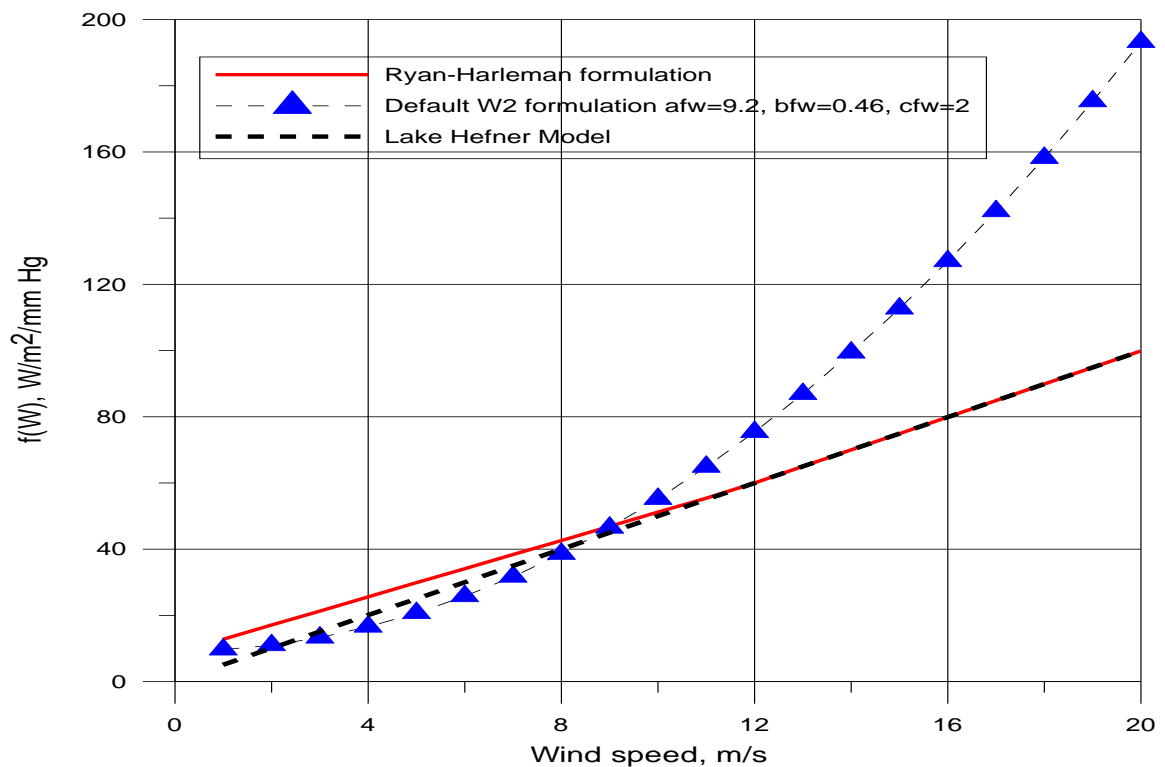


Figure A-52. Comparison of the wind speed formulation for Ryan-Harleman and W2 default (for $T_{\text{air}}=15^{\circ}\text{C}$, $T_{\text{dew}}=-5^{\circ}\text{C}$, $T_{\text{surface}}=25^{\circ}\text{C}$).

Summaries of several evaporation formulations are shown below in [Table A-9](#) as adapted from Adams, et al. (1981).

Table A-9. Typical Evaporation Formulae for Lakes and Reservoirs

Name	Time	Waterbody	ϕ_e	$f(W)$	Remarks
Lake Hefner	3 hrs and day	Lake Hefner, OK, 2587 acres	$17.2W_2(e_s - e_2)$	$5.06W_2$	good agreement with lake data from several lakes in US and Russia
Kohler	day	Lake Hefner OK, 2587 acres	$17.5W_2(e_s - e_2)$	$5.14W_2$	essentially the same as Lake Hefner formula
Zaykov	-	ponds and small reservoirs	$(1.3+14W_2)(e_s - e_2)$	$0.1708 + 4.11W_2$	based on Russian work
Meyer	month	small lakes and reservoirs	$(80+10W_2)(e_s - e_2)$	$10.512+2.94W_2$	e_a obtained daily from mean morning and evening measurements of air temperature and relative humidity
Morton	month	Class A pan	$(73.5+14.7W_2)(e_s - e_2)$	$9.658+4.32W_2$	data from meteorological stations, measurement heights assumed
Rohwer	day	pans, 85 ft dia tank, 1300 acre reservoir	$(67+10W_2)(e_s - e_2)$	$8.8+2.94W_2$	extensive pan measurements using different pans, correlated with tank and reservoir data
ϕ_e = evaporation at sea-level with wind corrected to 2 m, $\text{BTU ft}^2 \text{ day}^{-1}$ W = wind, mph e = vapor pressure, mm Hg $W m^2 = 0.1314 \text{ BTU ft}^2 \text{ day}^{-1}$ $10 \text{ mb} = 7.5006151 \text{ mm Hg}$					

Equilibrium Temperature

Since some of the terms in the term-by-term heat balance equation are surface temperature dependent and others are measurable or computable input variables, the most direct route is to define an equilibrium temperature, T_e , as the temperature at which the net rate of surface heat exchange is zero.

Linearization of the term-by-term heat balance along with the definition of equilibrium temperature allows expressing the net rate of surface heat exchange, H_n , as:

$$H_{aw} = -K_{aw}(T_w - T_e) \quad (\text{A-221})$$

where:

H_{aw} = rate of surface heat exchange, $W m^{-2}$

K_{aw} = coefficient of surface heat exchange, $W m^{-2} ^\circ C^{-1}$

T_w = water surface temperature, $^\circ C$

T_e = equilibrium temperature, $^\circ C$

Seven separate heat exchange processes are summarized in the coefficient of surface heat exchange and equilibrium temperature. The linearization is examined in detail by Brady, et al. (1968), and Edinger et al. (1974).

The definition of the coefficient of surface heat exchange can be shown to be the first term of a Taylor series expansion by considering the above equation as:

$$H_{aw} = -\frac{dH_{an}}{dT_s}(T_s - T_e) \quad (\text{A-222})$$

where the derivative of H_{aw} with respect to surface temperature is evaluated from equation A-191 to give K_{aw} , the coefficient of surface heat exchange. All approximations of the individual surface heat exchange terms enter into the evaluation of the coefficient of surface heat exchange and the equilibrium temperature.

The mass evaporation rate is computed by dividing evaporative heat loss by the latent heat of evaporation of water. Surface heat exchange always includes evaporative heat loss in the heat budget, but the user may choose to exclude it in the water budget. For many reservoirs, inflow rates are determined from storage estimates that implicitly include evaporation.

Sediment Heat Exchange

Sediment heat exchange with water is generally small compared to surface heat exchange and many previous modelers have neglected it. Investigations on several reservoirs have shown the process must be included to accurately reproduce hypolimnetic temperatures primarily because of the reduction in numerical diffusion that previously swamped the numerical solution. The formulation is similar to surface heat exchange:

$$H_{sw} = -K_{sw}(T_w - T_s) \quad (\text{A-223})$$

where:

H_{sw} = rate of sediment/water heat exchange, $W m^{-2}$

K_{sw} = coefficient of sediment/water heat exchange, $W m^{-2} ^\circ C^{-1}$

T_w = water temperature, $^\circ C$

T_s = sediment temperature, $^\circ C$

Previous applications used a value of $0.3 W m^{-2} ^\circ C^{-1}$ for K_{sw} that is approximately two orders of magnitude smaller than the surface heat exchange coefficient. Average yearly air temperature is a good estimate of T_s .

Dynamic Shading

Solar Altitude and Azimuth

The declination angle, δ , is computed from Spencer (1971):

$$\begin{aligned} \delta = & 0.006918 - 0.399912 \cos(\tau_d) + 0.070257 \sin(\tau_d) - 0.006758 \cos(2\tau_d) \\ & + 0.000907 \sin(2\tau_d) - 0.0022697 \cos(3\tau_d) + 0.001480 \sin(3\tau_d) \end{aligned} \quad (A-224)$$

where:

$$\tau_d = \frac{2\pi(JD_i - 1)}{365}$$

JD_i = Julian date integer value

The local hour is calculated as:

$$HOUR = 24(JD_r - JD_i) \quad (A-225)$$

where:

JD_i = Julian date integer value

JD_r = Julian date floating-point value

An equation of time, EQT , correction is needed to calculate the local hour angle. The equation of time represents the difference between true and mean solar time due to seasonal variations in the earth's orbital velocity (DiLaura, D.L 1984) and is given as:

$$EQT = 0.17 \sin \frac{4\pi(JD_i - 80)}{373} - 0.129 \sin \frac{2\pi(JD_i - 8)}{355} \quad (A-226)$$

where:

JD_i = Julian date integer value

The local hour angle, H , is calculated as:

$$H = \frac{2\pi}{24} \left[HOUR + (Long - \phi) \frac{24}{360} + EQT - 12 \right] \quad (\text{A-227})$$

The solar altitude, A_o , is the angle of inclination of the sun relative to the horizon from an observer's perspective as shown in [Figure A-53](#).

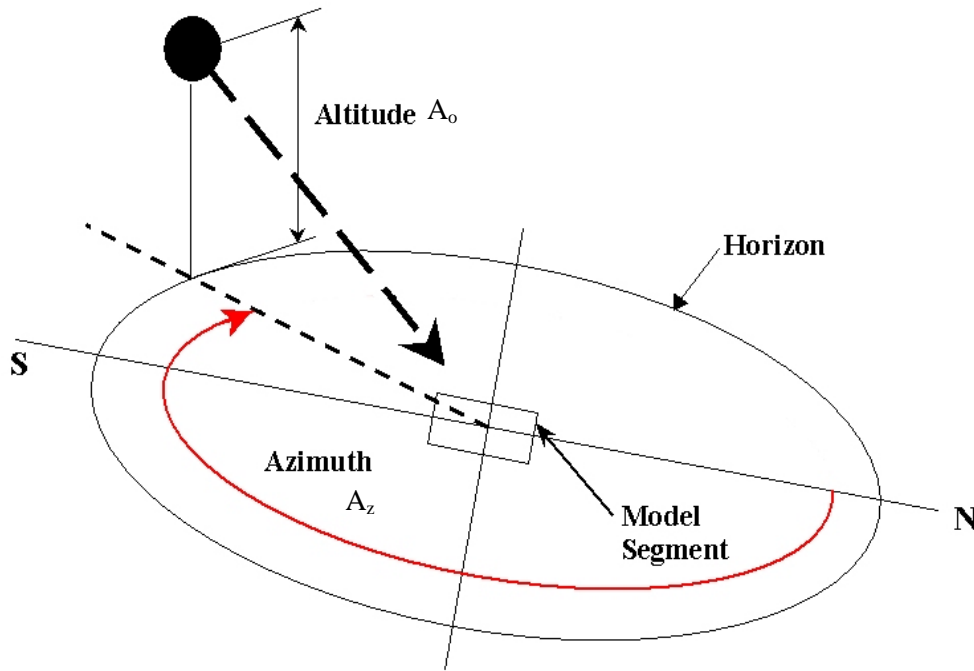


Figure A-53. Schematic of solar altitude, A_o , and azimuth, A_z

A_o is calculated from Wunderlich (1972):

$$A_o = A \sin \left[\sin \left(lat * \frac{\pi}{180} \right) \sin(\delta) + \cos \left(lat * \frac{\pi}{180} \right) \cos(\delta) \cos(H) \right] \quad (\text{A-228})$$

The solar azimuth is the direction of the sun with respect to a North-South axis measured clockwise from the North as shown in [Figure A-54](#). The solar azimuth is computed as (Annual Nautical Almanac, 2001):

$$X = \frac{\sin(\delta) \cos \left(\frac{Lat * \pi}{180} \right) - \cos(\delta) \cos(H) \sin \left(\frac{Lat * \pi}{180} \right)}{\cos A_o} \quad (\text{A-229})$$

$$\begin{aligned} \text{If } X > 1, \quad X &= 1 \\ \text{If } X < -1, \quad X &= -1 \end{aligned} \quad (\text{A-230})$$

$$A = A \cos X \quad (\text{A-231})$$

$$\begin{aligned} AZ &= 2\pi - A \\ \text{If } H < 0, \quad AZ &= A \end{aligned} \quad (\text{A-232})$$

After computing the solar altitude and azimuth, the impact of shading ([Figure A-54](#)) on short-wave solar radiation is computed as follows.

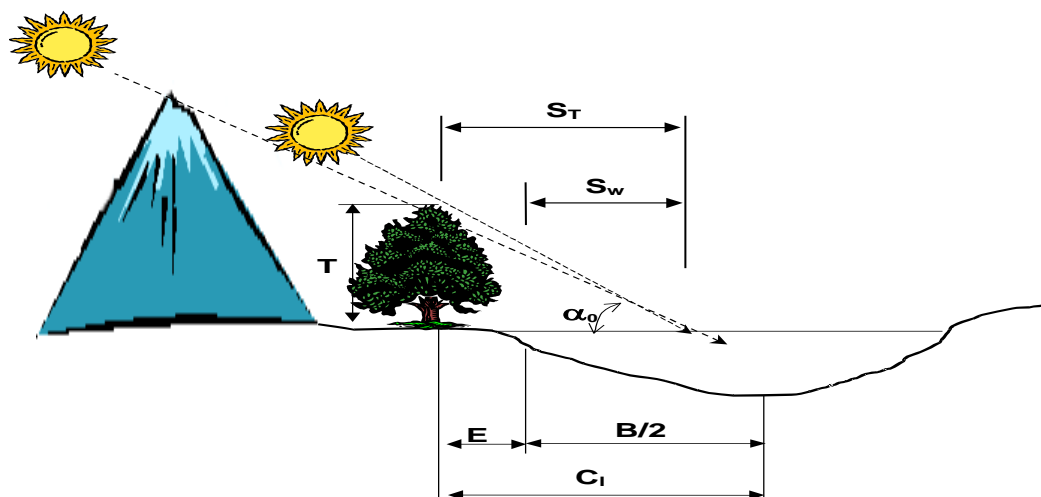


Figure A-54. Schematic of topographic and vegetative shading, solar altitude (α_0), and vegetation height (T) and their affect on shadow length.

Topographic Shading

The algorithm uses the position of the sun to determine which topographic inclination angle coincides with the direction of incoming solar radiation. The algorithm determines the closest two inclination angles in the direction of the incoming solar radiation and uses them to linearly interpolate an inclination angle for the specific direction of the incoming solar radiation. The calculated inclination angle is then used to determine if vegetative or topographic shading dominates at that time. If the solar altitude is below the calculated topographic inclination angle, then topographic shading dominates and the short wave solar radiation is reduced by 90% for complete shade. This allows for 10% of the incoming solar radiation as a result of diffuse radiation even when in the shade. If the solar altitude is above the calculated inclination angle, then vegetative shading dominates.

Vegetative Shading

If the topographic angle is less than the solar altitude, vegetative shade dominates and the algorithm calculates the shading influence by determining how far the shadow extends over the water. [Figure A-55](#) and [Figure A-56](#) show schematics of the azimuth angle, segment orientation and computed

shadow lengths. The tree shadow length, S_T , is calculated using the tree height, T , and solar altitude, A_0 , using Equation A-206. Then the length of the shadow cast over the water is calculated using Equation A-207 where E is the distance between the tree and the edge of water and Θ_0 is the segment orientation. The shadow length, S_N , perpendicular to the edge of the water is then calculated using Equation A-208. Refer to [Figure A-55](#) and [Figure A-56](#) for diagrams showing the distance calculated in Equations A-206 to A-208.

$$S_T = \frac{T}{\tan A_0} \quad (\text{A-233})$$

$$S_w = S_T - \frac{E}{\sin(\Theta_0 - \alpha_A)} \quad (\text{A-234})$$

$$S_N = S_w \sin(\Theta_0 - \alpha_A) \quad (\text{A-235})$$

Simplifying Equations A-206 to A-208:

$$S_N = \frac{T * \sin(\Theta_0 - \alpha_A)}{\tan A_0} - E \quad (\text{A-236})$$

A shading reduction factor is applied in cases where a model segment has potential shading along only part of its segment length or the vegetation density is low. For example, if shade-producing vegetation exists along only half the length of a segment and is 100% opaque, a shade reduction factor of 0.5 is used. If shading is due to vegetation along only half of a segment with 80% opaque-ness, a value of 0.4 is used.

The shade factor, $sfact$, is the shadow length perpendicular to the edge of the water, S_N , multiplied by the shade reduction factor, SRF , and divided by the segment width:

$$sfact = SRF \frac{S_N}{B} \quad (\text{A-237})$$

The amount of shade that should be applied to the incoming short wave solar radiation is calculated as:

$$Shade = (1 - sfact) \quad (\text{A-238})$$

The short wave solar radiation [SRO] computed by the model is reduced by the shade variable:

$$SRO_{net} = SRO * Shade \quad (\text{A-239})$$

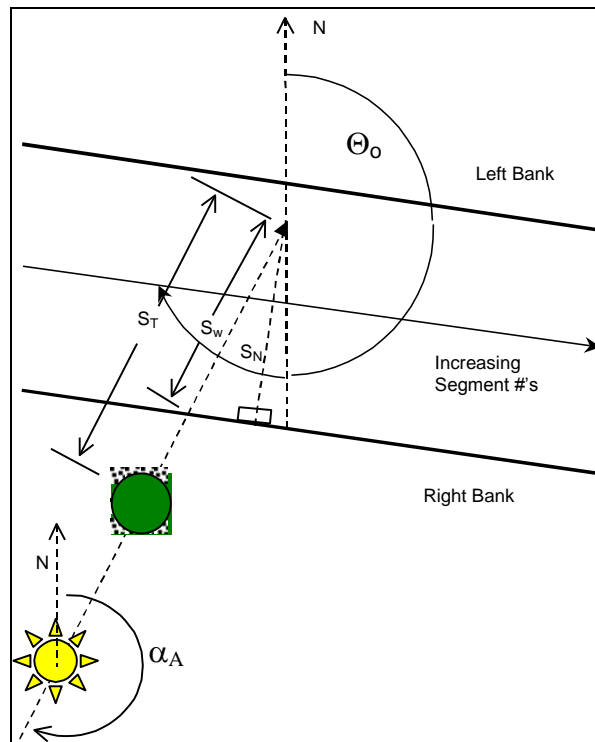


Figure A-55. Azimuth angle, α_{AZ} , and stream orientation, Θ_0 .

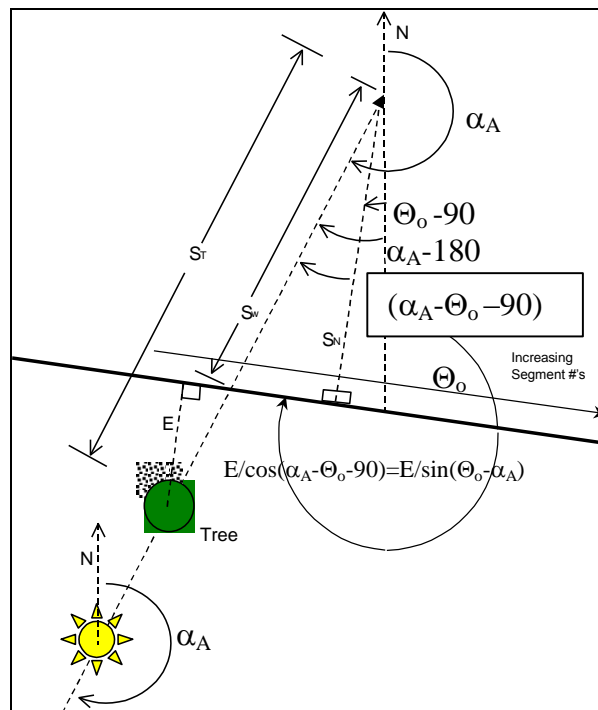


Figure A-56. Relationship between azimuth, stream orientation, and shadow length.

Data Requirements

Topography and vegetation data are stored in a user-defined input file. An example input file is shown in Appendix C. The file includes tree top elevations for both stream banks. The file also includes the distance from the centerline of the river to the controlling vegetation and the shade reduction factor (explained below) for both stream banks. The shade file has vegetation characteristics recorded by the left and right banks of the stream. The convention used for defining left or right bank is dependent on looking downstream in the system, the 'Left Bank' is on the left and the 'Right Bank' is to the right.

The shade algorithm reads in 18 topographic inclination angles surrounding each segment center-point. The inclination angles can be determined using topographical maps, Digital Elevation Models (DEM), or contour plots. The steepest inclination angle for each of the 18 locations surrounding a segment should be selected since this angle will control the topographic shading. The first inclination angle is taken from directly North of a segment (orientation angle 0.0) and moves clockwise to the East with increasing orientation angles around the segment in 20° increments.

How far away from the centerline of the river the topography should be analyzed will depend on the system. Wide flat river systems will utilize longer distances for identifying influencing topography than a narrow river canyon. In addition, rather than restricting the code to orientation angles only toward the south appropriate for the Northern hemisphere, using orientation angles that surround a segment allows the algorithm to be used in both the northern and southern hemispheres.

In addition, the user can specify dynamic shading reduction factors as a function of time. Usually, these would correspond to the times for leaf growth and fall for deciduous trees.

The topography and vegetation information is first read in from the input file. Then, using the segment orientation angle, Θ_0 , and the solar azimuth, α_A , the bank that has the sun behind it is computed. The criteria used for determining the bank with the sun behind it was modified from Chen (1996) because the segment orientation angle is determined differently in CE-QUAL-W2. [Table A-10](#) shows the criteria used in the model.

Table A-10. Criteria for determining sunward bank

Sunward Bank	$0^\circ < \Theta_0 \leq 180^\circ$	$180^\circ < \Theta_0 \leq 360^\circ$
Left	$\alpha_A < \Theta_0$ or $\alpha_A > \Theta_0 + 180^\circ$	$\Theta_0 - 180^\circ < \alpha_A < \Theta_0$
Right	$\Theta_0 < \alpha_A < \Theta_0 + 180^\circ$	$\alpha_A > \Theta_0$ or $\alpha_A < \Theta_0 - 180^\circ$

Ice Cover

Ice thickness, onset, and loss of ice cover play an important role in the heat budget of northern waterbodies. At high latitudes, ice cover may remain until late spring or early summer and prevent warming due to absorption of short wave solar radiation.

The ice model is based on an ice cover with ice-to-air heat exchange, conduction through the ice, conduction between underlying water, and a "melt temperature" layer on the ice bottom (Ashton, 1979). The overall heat balance for the water-to-ice-to-air system is:

$$\rho_i L_f \frac{\Delta h}{\Delta t} = h_{ai} (T_i - T_e) - h_{wi} (T_w - T_m) \quad (\text{A-240})$$

where:

ρ_i = density of ice, $kg\ m^{-3}$

L_f = latent heat of fusion of ice, $J\ kg^{-1}$

$\Delta h/\Delta t$ = change in ice thickness (h) with time (t), $m\ sec^{-1}$

h_{ai} = coefficient of ice-to-air heat exchange, $W\ m^{-2}\ ^\circ C^{-1}$

h_{wi} = coefficient of water-to-ice heat exchange through the melt layer, $W\ m^{-2}\ C$

T_i = ice temperature, $^\circ C$

T_{ei} = equilibrium temperature of ice-to-air heat exchange, $^\circ C$

T_w = water temperature below ice, $^\circ C$

T_m = melt temperature, $0^\circ C$

The ice-to-air coefficient of surface heat exchange, h_{ai} , and its equilibrium temperature, T_{ei} , are computed the same as for surface heat exchange in Edinger, et al. (1974) because heat balance of the thin, ice surface water layer is the same as the net rate of surface heat exchange presented previously. The coefficient of water-to-ice exchange, h_{wi} , depends on turbulence and water movement under ice and their effect on melt layer thickness. It is a function of water velocity for rivers but must be empirically adjusted for reservoirs.

Ice temperature in the ice-heat balance is computed by equating the rate of surface heat transfer between ice and air to the rate of heat conduction through ice:

$$h_{ai} (T_i - T_{ei}) = \frac{-k_i (T_i - T_m)}{h} \quad (\text{A-241})$$

where:

k_i = molecular heat conductivity of ice, $W\ m^{-1}\ ^\circ C^{-1}$

When solved for ice temperature, T_i , and inserted in the overall ice-heat balance, the ice thickness relationship becomes:

$$\frac{\rho_i L_f \Delta h}{\Delta t} = \frac{(T_M - T_{ei})}{\frac{h}{k_i} + \frac{1}{h_{ia}}} - h_{wi} (T_w - T_m) \quad (\text{A-242})$$

from which ice thickness can be computed for each longitudinal segment. Heat from water to ice transferred by the last term is removed in the water temperature transport computations.

Variations in the onset of ice cover and seasonal growth and melt over the waterbody depend on locations and temperatures of inflows and outflows, evaporative wind variations over the ice surface, and effects of water movement on the ice-to-water exchange coefficient. Ice will often form in reservoir branches before forming in the main pool and remain longer due to these effects.

A second, more detailed algorithm for computing ice growth and decay has been developed for the model. The algorithm consists of a series of one-dimensional, quasi steady-state, thermodynamic calculations for each timestep. It is similar to those of Maykut and Untersteiner (1971), Wake (1977) and Patterson and Hamblin (1988). The detailed algorithm provides a more accurate representation of the upper part of the ice temperature profile resulting in a more accurate calculation of ice surface temperature and rate of ice freezing and melting.

The ice surface temperature, T_s , is iteratively computed at each timestep using the upper boundary condition as follows. Assuming linear thermal gradients and using finite difference approximations, heat fluxes through the ice, q_i , and at the ice-water interface, q_{iw} , are computed. Ice thickness at time t , $\theta(t)$, is determined by ice melt at the air-ice interface, $\Delta\theta_{ai}$, and ice growth and melt at the ice-water interface, $\Delta\theta_{iw}$. The computational sequence of ice cover is presented below.

Initial Ice Formation

Formation of ice requires lowering the surface water temperature to the freezing point by normal surface heat exchange processes. With further heat removal, ice begins to form on the water surface. This is indicated by a negative water surface temperature. The negative water surface temperature is then converted to equivalent ice thickness and equivalent heat is added to the heat source and sink term for water. The computation is done once for each segment beginning with the ice-free period:

$$\theta_0 = \frac{-T_{wn} \rho_w C_{pw} h}{\rho_i L_f} \quad (\text{A-243})$$

where:

θ_0 = thickness of initial ice formation during a timestep, m

T_{wn} = local temporary negative water temperature, $^{\circ}C$

h = layer thickness, m

ρ_w = density of water, $kg\ m^{-3}$

C_{pw} = specific heat of water, $J\ kg^{-1}\ ^{\circ}C^{-1}$

ρ_i = density of ice, $kg\ m^{-3}$

L_f = latent heat of fusion, $J\ kg^{-1}$

Air-Ice Flux Boundary Condition and Ice Surface Temperature Approximation

The ice surface temperature, T_s , must be known to calculate the heat components, H_{br} , H_e , H_c , and the thermal gradient in the ice since the components and gradient all are either explicitly or implicitly a function of T_s . Except during the active thawing season when ice surface temperature is constant at 0°C , T_s must be computed at each timestep using the upper boundary condition. The approximate value for T_s is obtained by linearizing the ice thickness across the timestep and solving for T_s .

$$T_s^n \approx \frac{\theta^{n-1}}{K_i} \left[H_{sn}^n + H_{an}^n - H_{br}(T_s^n) - H_e(T_s^n) - H_c(T_s^n) \right] \quad (\text{A-244})$$

$$H_{sn} + H_{an} - H_{br} - H_e - H_c + q_i = \rho_i L_f \frac{d\theta_{ai}}{dt}, \text{ for } T_s = 0^\circ\text{C} \quad (\text{A-245})$$

$$q_i = K_i \frac{T_f - T_s(t)}{\theta(t)} \quad (\text{A-246})$$

where:

K_i = thermal conductivity of ice, $\text{W m}^{-1} ^\circ\text{C}^{-1}$

T_f = freezing point temperature, $^\circ\text{C}$

n = time level

θ = thickness of ice, m

q_i = heat flux through ice, W m^{-2}

Absorbed Solar Radiation by Water Under Ice

Although the amount of penetrated solar radiation is relatively small, it is an important component of the heat budget since it is the only heat source to the water column when ice is present and may contribute significantly to ice melting at the ice-water interface. The amount of solar radiation absorbed by water under the ice cover may be expressed as:

$$H_{ps} = H_s (1 - ALB_i) (1 - \beta_i) e^{-\gamma_i \theta(t)} \quad (\text{A-247})$$

where:

H_{ps} = solar radiation absorbed by water under ice cover, W m^{-2}

H_s = incident solar radiation, W m^{-2}

ALB_i = ice albedo

β_i = fraction of the incoming solar radiation absorbed in the ice surface

γ_i = ice extinction coefficient, m^{-1}

Ice Melt at Air-Ice Interface

The solution for T_s holds as long as net surface heat exchange, $H_n(T_s)$, remains negative corresponding to surface cooling, and surface melting cannot occur. If $H_n(T_s)$ becomes positive corresponding to a net gain of heat at the surface, q_i must become negative and an equilibrium solution can only exist if $T_s > T_f$. This situation is not possible as melting will occur at the surface before equilibrium is reached (Patterson and Hamblin, 1988). Because of a quasi-steady approximation, heat, which in reality is used to melt ice at the surface, is stored internally producing an unrealistic temperature profile. Stored energy is used for melting at each timestep and since total energy input is the same, net error is small. Stored energy used for melting ice is expressed as:

$$\rho_i C_{pi} \frac{T_s(t)}{2} \theta(t) = \rho_i L_f \Delta \theta_{ai} \quad (\text{A-248})$$

where:

C_{pi} = specific heat of ice, $J kg^{-1} ^\circ C^{-1}$

θ_{ai} = ice melt at the air-ice interface, m^{-1}

Ice-Water Flux Boundary Condition Formulation

Both ice growth and melt may occur at the ice-water interface. The interface temperature, T_f , is fixed by the water properties. Flux of heat in the ice at the interface therefore depends on T_f and the surface temperature T_s through the heat flux q_i . Independently, heat flux from the water to ice, q_{iw} , depends only on conditions beneath the ice. An imbalance between these fluxes provides a mechanism for freezing or melting. Thus,

$$q_i - q_{iw} = \rho_i L_f \frac{d \theta_{iw}}{dt} \quad (\text{A-249})$$

where:

θ_{iw} = ice growth/melt at the ice-water interface

The coefficient of water-to-ice exchange, K_{wi} , depends on turbulence and water movement under the ice and their effect on melt layer thickness. It is known to be a function of water velocity for rivers and streams but must be empirically adjusted for reservoirs. The heat flux at the ice-water interface is:

$$q_{iw} = h_{wi} (T_w(t) - T_f) \quad (\text{A-250})$$

where:

T_w = water temperature in the uppermost layer under the ice, $^\circ C$

Finally, ice growth or melt at the ice-water interface is:

$$\Delta \theta_{iw}^n = \frac{I}{\rho_i L_f} \left[K_i \frac{T_f - T_s^n}{\theta^{n-1}} - h_{wi} (T_w^n - T_f) \right] \quad (\text{A-251})$$

Freezing Temperature of Ice

In general, the temperature at which water freezes, T_f , is set to 0°C for fresh water. If the model is set to SALT [See WTYPEC input], the freezing temperature is affected by the salinity. In the model, when WTYPEC=SALT, the TDS state variable is in units of ppt and the equations used for computing the freezing temperature are computed from the following equations:

For TDS < 35 ppt,

$$T_f = -0.0545TDS$$

For TDS > 35 ppt:

$$T_f = -0.3146 - 0.0417TDS - 0.000166TDS^2$$

Density

Accurate hydrodynamic calculations require accurate water densities. Water densities are affected by variations in temperature and solids concentrations given by :

$$\rho = \rho_T + \Delta \rho_S \quad (\text{A-252})$$

where:

ρ = density, $kg\ m^{-3}$

ρ_T = water density as a function of temperature, $kg\ m^{-3}$

$\Delta \rho_S$ = density increment due to solids, $kg\ m^{-3}$

A variety of formulations has been proposed to describe water density variations due to temperatures. The following relationship is used in the model (Gill, 1982):

$$\begin{aligned} \rho_{T_w} = & 999.8452594 + 6.793952 \times 10^{-2} T_w \\ & - 9.095290 \times 10^{-3} T_w^2 + 1.001685 \times 10^{-4} T_w^3 \\ & - 1.120083 \times 10^{-6} T_w^4 + 6.536332 \times 10^{-9} T_w^5 \end{aligned} \quad (\text{A-253})$$

Suspended and dissolved solids also affect density. For most applications, dissolved solids will be in the form of total dissolved solids. For estuarine applications, salinity should be specified. The effect of dissolved solids on density is calculated using either of these variables with the choice specified by the variable [WTYPE]. Density effects due to total dissolved solids are given by Ford and Johnson (1983):

$$\Delta \rho_{TDS} = (8.221 \times 10^{-4} - 3.87 \times 10^{-6} T_w + 4.99 \times 10^{-8} T_w^2) \Phi_{TDS} \quad (\text{A-254})$$

where:

Φ_{TDS} = TDS concentration, $g\ m^{-3}$

and for salinity (Gill, 1982):

$$\begin{aligned} \Delta \rho_{sal} = & (0.824493 - 4.0899 \times 10^{-3} T_w + 7.6438 \times 10^{-5} T_w^2 \\ & - 8.2467 \times 10^{-7} T_w^3 + 5.3875 \times 10^{-9} T_w^4) \Phi_{sal} \\ & + (-5.72466 \times 10^{-3} + 1.0227 \times 10^{-4} T_w \\ & - 1.6546 \times 10^{-6} T_w^2) \Phi_{sal}^{1.5} + 4.8314 \times 10^{-4} \Phi_{sal}^2 \end{aligned} \quad (A-255)$$

where:

Φ_{sal} = salinity, $kg\ m^{-3}$

The suspended solids effects are given by Ford and Johnson (1983):

$$\Delta \rho_{ss} = \Phi_{ss} \left(1 - \frac{1}{SG} \right) \times 10^{-3} \quad (A-256)$$

where:

Φ_{ss} = suspended solids concentration, $g\ m^{-3}$

SG = specific gravity of suspended solids

Assuming a specific gravity of 2.65, the above relationship is simplified to:

$$\Delta \rho_{ss} = 0.00062 \Phi_{ss} \quad (A-257)$$

The total effect of solids is then:

$$\Delta \rho_s = (\Delta \rho_{sal} \text{ or } \Delta \rho_{tds}) + \Delta \rho_{ss} \quad (A-258)$$

Selective Withdrawal

The latest version includes selective withdrawal for all outflows where layer locations and outflows at each layer are calculated based on the total outflow [\[QOUT\]](#), structure type [\[SINKC\]](#), elevation [\[ESTRI\]](#), and computed upstream density gradients. The selective withdrawal computation uses these values to compute vertical withdrawal zone limits and outflows. It also sums the outflows for multiple structures.

Outflow distribution is calculated in the subroutine SELECTIVE_WITHDRAWAL. This routine first calculates limits of withdrawal based on either a user specified point or line sink approximation for outlet geometry [SINKC]. The empirical expression for point sink withdrawal limits is:

$$d = (c_{bi} Q/N)^{0.3333} \quad (\text{A-259})$$

and for a line sink:

$$d = (c_{bi} 2q/N)^{0.5} \quad (\text{A-260})$$

where:

- d = withdrawal zone half height, m
- Q = total outflow, $m^3 s^{-1}$
- N = internal buoyancy frequency, Hz
- q = outflow per unit width, $m^2 s^{-1}$
- c_{bi} = boundary interference coefficient

The width is the outlet width. The point sink approximation assumes approach flow is radial both longitudinally and vertically while the line sink approximation assumes flow approaches the outlet radially in the vertical. The boundary interference coefficient is two near a physical boundary and one elsewhere.

Velocities are determined using a quadratic shape function:

$$V_k = I - \left[\frac{(\rho_k - \rho_o)}{(\rho_l - \rho_o)} \right]^2 \quad (\text{A-261})$$

where:

- V_k = normalized velocity in layer k
- ρ_k = density in layer k, $kg m^{-3}$
- ρ_o = density in the outlet layer, $kg m^{-3}$
- ρ_l = density of the withdrawal limit layer, $kg m^{-3}$

The shape function generates a maximum velocity at the outlet level with velocities approaching zero at withdrawal limits. During non-stratified periods, outflow from top to bottom is uniform. Uniform flows also result from large outflows during periods of mild stratification. As stratification develops, withdrawal limits decrease and outflow is weighted towards the outlet elevation.

Withdrawal limits can be varied by specifying a line sink and changing the effective width. Small outlet widths result in nearly uniform outflows, while large widths limit outflows to the outlet layer.

Sediment Resuspension

This algorithm is based on work from Kang et al. (1982) where the bottom shear stress is computed based on wind speed, wind fetch and depth. The wind blowing across a water surface creates wind waves that have orbital motion that decays with depth. The model user inputs a critical shear stress for detachment of the particles. If the critical shear stress is exceeded, then particles are resuspended. The approach of Kang et al. (1982) consists of the following steps:

1. Computation of the wave height, H_s in m,

$$H_s = \frac{W^2}{g} 0.283 \tanh \left[0.53 \left(\frac{gH}{W^2} \right)^{0.75} \right] \tanh \left[\frac{0.0125 \left(\frac{gF}{W^2} \right)^{0.42}}{\tanh \left[0.53 \left(\frac{gH}{W^2} \right)^{0.75} \right]} \right] \quad (\text{A-262})$$

where W is the wind velocity (m/s), F is the fetch (m), H is the mean depth (m)

2. Computation of wave period, T_s in s,

$$T_s = \frac{2\pi W}{g} 1.2 \tanh \left[0.833 \left(\frac{gH}{W^2} \right)^{0.375} \right] \tanh \left[\frac{0.077 \left(\frac{gF}{W^2} \right)^{0.25}}{\tanh \left[0.833 \left(\frac{gH}{W^2} \right)^{0.375} \right]} \right] \quad (\text{A-263})$$

3. Computation of the wavelength, L in m, iteratively from the following equation:

$$L = \frac{gT_s^2}{2\pi} \tanh \left[\frac{2\pi H}{L} \right] \quad (\text{A-264})$$

4. Computation of the orbital velocity, \bar{U} in cm/s,

$$\bar{U} = \frac{\pi H_s}{T_s} \frac{100}{\sinh(2\pi H / L)} \quad (\text{A-265})$$

5. Computation of bottom shear stress, τ in dynes/cm²,

$$\tau = 0.003 \bar{U}^2 \quad (\text{A-266})$$

6. Computation of actual bottom scour rate of suspended solids, ε in mass of sediments scoured per area or g/m²,

AUXILIARY FUNCTIONS

SEDIMENT RESUSPENSION

$$\varepsilon = 0 \quad \tau \leq \tau_c \quad (\text{A-267})$$

$$\varepsilon = \frac{\alpha_o}{t_d^2} (\tau - \tau_c)^3 \quad \tau > \tau_c \quad (\text{A-268})$$

where α_o is an empirical constant=0.008, $t_d=7$, and τ_c is the user-defined critical shear stress in dynes/cm². Resuspension supposedly only occurs during the first hour of the wind shear greater than the critical shear stress. Hence, the rate of resuspension per time, E in g/m²/hour, would be

$E = \frac{\varepsilon}{1hr}$ for the first hour and nothing after that. The resulting concentration of suspended solids

in the entire water column, c in mg/l, if distributed evenly over the entire volume would then be

$$c = \frac{10000\varepsilon A_{bottom}}{V} = \frac{10000\varepsilon}{H}.$$

where A_{bottom} is the surface area of the bottom and V is the volume of the water column above the bottom ($=HA_{bottom}$). Chapra (1997) also uses this approach and provides an example calculation.

Appendix B Water Quality

The constituent transport relationships described in Appendix A compute the transport of constituents with their kinetic reaction rates expressed in source and sink terms. All sources/sinks (both internal and external) for water temperature are contained in the array [TSS]. The sources/sinks for constituents are separated into two arrays, [CSSB] and [CSSK]. [CSSB] contains boundary sources/sinks. [CSSK] contains internal sources/sinks due to kinetic interactions. The division of terms allows kinetic sources/sinks to be updated at different frequencies than boundary sources/sinks - consistent with coarser time scales associated with biological and chemical processes as opposed to hydrodynamics. Computational time is also reduced. The frequency at which kinetic sources/sinks [CSSK] are updated is specified by the parameter [\[CUF\]](#).

The source/sink term [CSSK] represents a mass rate of change ($grams\ sec^{-1}$) of a constituent due to kinetic reactions where concentrations are expressed as $grams\ meter^{-3}$. The kinetic reactions can be depicted graphically by considering each constituent as a compartment. Arrows represent mass transfer rates between compartments, with a source represented by a blue arrow leading to the compartment and a sink by a red arrow leading away. All of the rate terms in the following discussion are in units of sec^{-1} and these are the units used in the code. However, all rate units input into the model from the control file are in units of day^{-1} and are then converted to sec^{-1} before being used in the code. Both graphical and mathematical descriptions of the rate equation for each constituent are provided.

Overview of Kinetic Source/Sink Term

In order to solve the 2D advection-diffusion equation, the source/sink term, S_ϕ , must be specified. The model solves for temperature and a user specified number of water quality variables. Water quality state variables along with their kinetic source/sink terms are shown in [Table B-11](#). The user can specify any number of generic constituents [\[NGC\]](#), suspended solids groups [\[NSS\]](#), CBOD groups [\[NBOD\]](#), algal groups [\[NAL\]](#), macrophyte groups [\[NMC\]](#), zooplankton groups [\[NZP\]](#), and epiphyton groups [\[NEP\]](#).

Table B-11. CE-QUAL-W2 Water Quality State Variables

Constituent	Internal Source	Internal Sink
Total dissolved solids		
generic constituent, no interactions with other state variables bacteria tracer water age contaminants	0 order decay	settling 0 and 1 st order decay
Inorganic suspended solids		sedimentation
bioavailable P measured as one of the following ortho-P dissolved P SRP	algal/epiphyton respiration labile/refractory particulate/dissolved organic matter sediment release CBOD decay	algal/epiphyton growth adsorption onto inorganic suspended solids
ammonium	sediment release algal/epiphyton/macrophyte excretion labile/refractory dissolved/particulate organic matter decay CBOD decay	algal/epiphyton/macrophyte growth nitrification
nitrate-nitrite	nitrification	denitrification algal/epiphyton/macrophyte growth
dissolved silica	anoxic sediment release particulate biogenic silica decay	algal/epiphyton growth adsorption onto suspended solids
particulate biogenic silica	algal/epiphyton mortality	settling decay
Iron	anoxic sediment release	oxic water column settling
labile dissolved organic matter	algal/epiphyton/macrophyte mortality excretion	Decay
refractory dissolved organic matter	labile dissolved organic matter decay	Decay
labile particulate organic matter	algal/epiphyton/macrophyte mortality	settling decay
refractory particulate organic matter	labile particulate organic matter decay	settling decay
Total P in labile dissolved organic matter	algal/epiphyton/macrophyte mortality excretion	Decay
Total P in refractory dissolved organic matter	labile dissolved organic matter decay	Decay
Total P in labile particulate organic matter	algal/epiphyton/macrophyte mortality	settling decay
Total P in refractory particulate organic matter	labile particulate organic matter decay	settling decay
Total N in labile dissolved organic matter	algal/epiphyton/macrophyte mortality excretion	Decay
Total N in refractory dissolved organic matter	labile dissolved organic matter decay	Decay
Total N in labile particulate organic matter	algal/epiphyton/macrophyte mortality	settling decay
Total N in refractory particulate organic matter	labile particulate organic matter decay	settling decay
CBOD		decay, settling
CBOD-P (Total P in organic matter represented by CBOD)		decay, settling
CBOD-N (Total N in organic matter represented by CBOD)		decay, settling
algae	algal growth	respiration excretion mortality settling

Constituent	Internal Source	Internal Sink
Epiphyton	epiphyton growth	respiration excretion mortality settling
zooplankton	zooplankton growth	transport settling excretion mortality
macrophytes	macrophyte growth	respiration mortality excretion
dissolved oxygen	surface exchange algal/epiphyton growth	surface exchange algal/epiphyton/macrophyte/zooplankton respiration nitrification CBOD decay 0 and 1 st order SOD labile/refractory dissolved/ particulate organic matter decay
total inorganic carbon	labile/refractory dissolved/ particulate organic matter decay sediment release surface exchange algal respiration	surface exchange algal/epiphyton growth CBOD decay
alkalinity		
Sediment (1 st order sediment model)	settling of algae, LPOM, RPOM, epiphyton burial	decay, focusing of sediments

In addition to these water quality state variables, the model also solves for pH and the carbonate cycle (CO_2 , HCO_3^- , H_2CO_3) as part of the set of derived water quality variables.

Generic Constituent

Any number of generic constituents [\[NGC\]](#) can be defined that can settle and decay. The user supplies a zero and/or 1st order decay coefficient with or without an Arrhenius temperature dependence function, and/or a settling velocity. Generic constituents do not interact with the hydrodynamics nor any other water quality state variables.

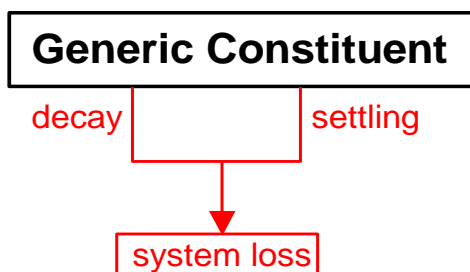


Figure B-1. Internal flux for generic constituent compartment.

Referring to [Figure B-1](#), the source/sink term for a generic constituent is:

$$S_g = \underbrace{-K_0 \theta_g^{(T-20)}}_{\text{0-order decay}} - \underbrace{K_1 \theta_g^{(T-20)} \Phi_g}_{\text{1st-order decay}} - \underbrace{\omega_g \frac{\partial \Phi_g}{\partial z}}_{\text{settling}} \quad (\text{B-1})$$

where:

Y_g = temperature rate multiplier

T = water temperature, °C

ω_g = settling velocity, $m\ s^{-1}$

K_0 = zero order decay coefficient, $g\ m^{-3}\ s^{-1}$ at 20°C

K_1 = first order decay coefficient, s^{-1} at 20°C

Φ_g = generic constituent concentration, $g\ m^{-3}$

A conservative tracer, coliform bacteria, and water age are some of the state variables that can be modeled using the generic constituent and are described further below.

Conservative Tracer

A conservative constituent is included to allow dye study simulations, movements of conservative materials through the waterbody, and as an aid in calibrating and testing flow regimes. As a conservative material, this constituent has no internal sources or sinks and the rate term [CSSK] is set to zero.

$$S_{tracer} = 0 \quad (\text{B-2})$$

Coliform Bacteria

Coliform bacteria is commonly used as an indicator of pathogen contamination. Safety standards and criteria for drinking and recreational purposes are based upon coliform concentrations. Predictions of coliform bacteria are important because of their impact on recreation and water supply.

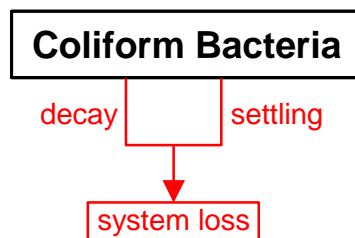


Figure B-2. Internal flux for coliform bacteria.

Total coliform, fecal coliform, fecal streptococci, and/or any other type of bacteria that do not interact with other state variables can be simulated with this generic constituent formulation. Referring to [Figure B-2](#), the rate equation for coliform bacteria is:

$$S_{col} = - \underbrace{K_{col} \theta^{(T-20)} \Phi_{col}}_{\text{1st-order decay}} - \underbrace{\omega_{col} \frac{\partial \Phi_{col}}{\partial z}}_{\text{settling}} \quad (\text{B-3})$$

where:

θ = temperature factor (Q10)

T = water temperature, °C

K_{col} = coliform mortality rate, sec^{-1} at 20°C

Φ_{col} = coliform concentration, g m^{-3}

The Q_{10} formulation arises from a doubling of the reaction rate with each 10°C increase in temperature. This doubling rate has not been found at lower temperatures (Hargrave 1972b) and is quite variable for various reactions (Giese 1968). Modeling coliform bacteria is discussed in detail in Zison, et al. (1978).

Water Age or Residence time

Setting the zero-order decay rate to -1 day^{-1} and zeroing out all other generic constituent kinetic parameters results in a state variable that increases by 1 day^{-1} , which is an exact representation of water age or hydraulic residence time. This is a very useful state variable when looking at hydrodynamics.

$$S_{age} = -1 \text{ day}^{-1} \quad (\text{B-4})$$

An example of water age for a reservoir in Washington, USA is shown below.

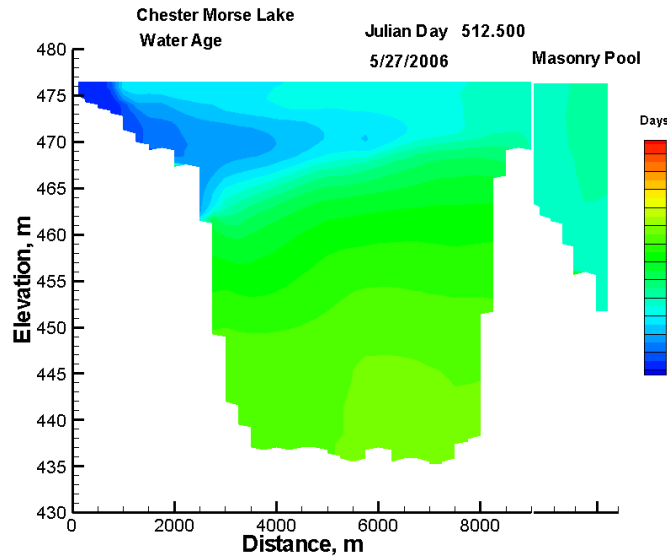


Figure 3. Water age in Chester Morse Lake, WA.

Inorganic Suspended Solids

Inorganic suspended solids [ISS] are important in water quality simulations because of their influence on density, light penetration, and nutrient availability. Increased solids concentrations reduce light penetration in the water column thus affecting temperature that in turn affects biological and chemical reaction rates. Dissolved phosphorus and silica concentrations can also be affected by solids through sorption and settling. Light and nutrient availability largely control algal production.

The settling velocity of each inorganic suspended solids compartment is a user-defined parameter. Usually this is determined from Stoke's settling velocity for a particular sediment diameter and specific gravity. Any number of inorganic suspended solids groups can now be modeled.

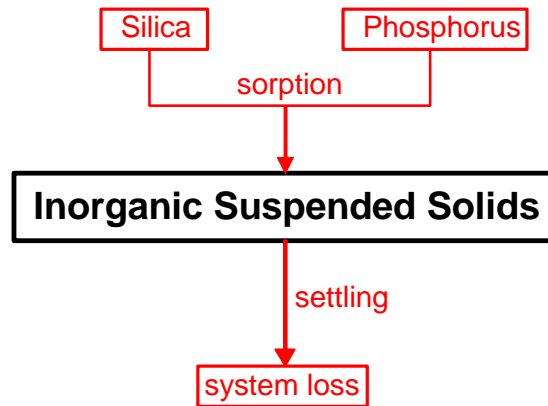


Figure B-4. Internal flux for inorganic suspended solids.

Referring to [Figure B-4](#), the rate equation for inorganic suspended solids is:

$$S_{ISS} = \omega_{ISS} \frac{\partial \Phi_{ISS}}{\partial z} \quad (\text{B-5})$$

where:

z = layer thickness, m

ω_{ISS} = settling velocity, $m \text{ sec}^{-1}$

Φ_{ISS} = inorganic suspended solids concentration, $g \text{ m}^{-3}$

In the finite difference representation of suspended solids concentrations, solids settling from layer [K]-1 serve as a source for the layer below it [K]. No provision is made to accumulate inorganic solids or allow resuspension in the sediments. A later version of the model will include these processes in a sediment transport compartment. Lateral averaging results in homogeneous solids concentrations laterally. In reality, concentrations generally decrease with distance away from the dominant flow path. This effect is not included. The rate term for inorganic suspended solids is evaluated in the subroutine SUSPENDED_SOLIDS.

Total Dissolved Solids or Salinity

Total dissolved solids (TDS) affect water density and ionic strength, thereby affecting water movements, pH, and the distribution of carbonate species. Dissolved solids are normally expressed as TDS in freshwater applications. Estuarine applications normally use salinity. Either TDS or salinity can be used with the choice indicated by the parameter [\[WTYPEC\]](#) specified in the control file. The choice is then reflected in the computation of density and ionic strength. If TDS is used, the units are $g\ m^{-3}$, while salinity is $kg\ m^{-3}$. It is important to keep in mind TDS and salinity are not equivalent - salinity is conservative while TDS is not. In the model, however, both are treated conservatively with the rate term set to zero.

Labile DOM

Because of the importance of dissolved oxygen in aquatic systems, all constituents exerting an oxygen demand must be included in kinetic formulations. This demand is often measured in rivers as the biochemical oxygen demand (BOD), which includes microbial respiration and metabolism of various organic and inorganic compounds. However, production of these materials occurs as well as decomposition, requiring the major components of BOD be modeled individually. One of these constituents is dissolved organic matter (DOM), which is composed of labile and refractory components. DOM is modeled as two separate compartments because of the different decomposition rates of the two groups.

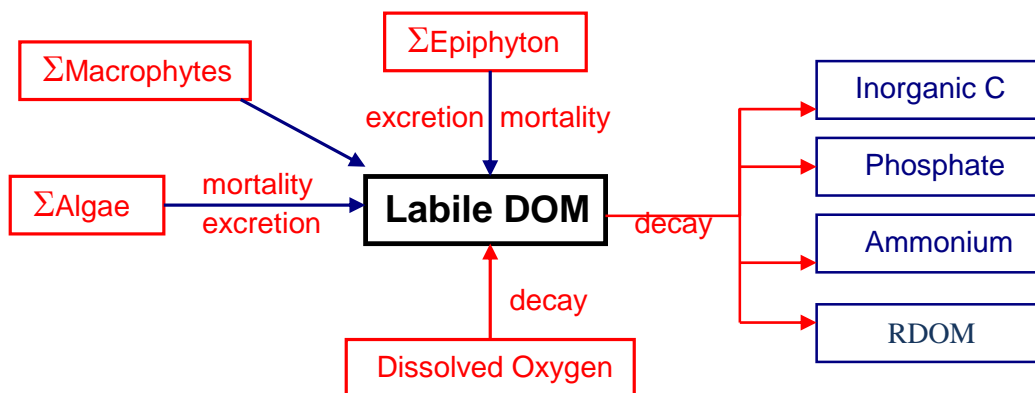


Figure B-5. Internal flux between labile DOM and other compartments

Referring to

Figure B-5, the rate equation for labile DOM is:

$$\begin{aligned}
 S_{LDOM} = & \underbrace{\sum K_{ae} \Phi_a}_{\text{algal excretion}} + \underbrace{\sum (1 - P_{am}) K_{am} \Phi_a}_{\text{algal mortality}} + \underbrace{\sum K_{ee} \Phi_e}_{\text{epiphyton excretion}} \\
 & + \underbrace{\sum (1 - P_{em}) K_{em} \Phi_e}_{\text{epiphyton mortality}} - \underbrace{\gamma_{OM} K_{LDOM} \Phi_{LDOM}}_{\text{labile DOM decay}} - \underbrace{K_{L \rightarrow R} \Phi_{LDOM}}_{\text{labile to refractory DOM decay}} + \underbrace{\sum (1 - P_{mm}) K_{mm} \Phi_{macro}}_{\text{macrophyte mortality/excretion}}
 \end{aligned}
 \tag{B-6}$$

where:

- P_{am} = pattern coefficient for algal mortality
- P_{em} = pattern coefficient for epiphyton mortality
- P_{mm} = partitioning coefficient for macrophyte mortality
- γ_{OM} = temperature rate multiplier for organic matter decay
- K_{ae} = algal excretion rate, sec^{-1}
- K_{am} = algal mortality rate, sec^{-1}
- K_{ee} = epiphyton excretion rate, sec^{-1}
- K_{em} = epiphyton mortality rate, sec^{-1}
- K_{mm} = macrophyte mortality rate, sec^{-1}
- K_{LDOM} = labile DOM decay rate, sec^{-1}
- $K_{L \rightarrow R}$ = labile to refractory DOM transfer rate, sec^{-1}
- Φ_a = algal concentration, $g\ m^{-3}$
- Φ_e = epiphyton concentration, $g\ m^{-3}$
- Φ_{LDOM} = labile DOM concentration, $g\ m^{-3}$
- Φ_{macro} = macrophyte concentration, $g\ m^{-3}$

Refractory DOM

Refractory DOM is composed of compounds in the aquatic environment that slowly decompose exerting oxygen demand over long periods. Internally, refractory DOM is produced from the decomposition of labile DOM.

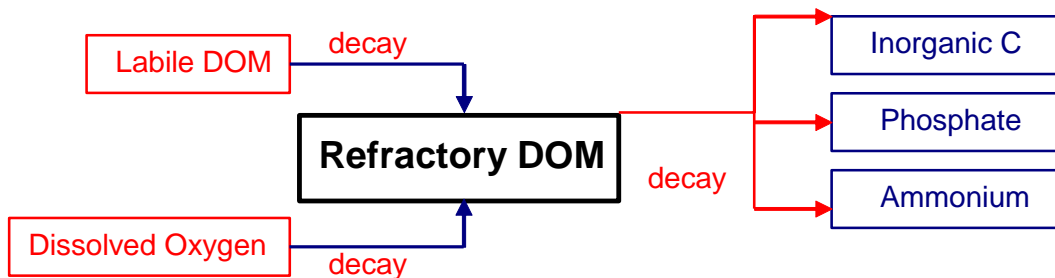


Figure B-6. Internal flux between refractory DOM and other compartments.

Referring to [Figure B-6](#), the rate equation for refractory DOM is:

$$S_{RDOM} = \underbrace{K_{L \rightarrow R} \Phi_{LDOM}}_{\text{labile to refractory DOM decay}} - \underbrace{\gamma_{OM} K_{RDOM} \Phi_{RDOM}}_{\text{decay}} \quad (\text{B-7})$$

where:

- γ_{OM} = temperature rate multiplier
- K_{RDOM} = refractory DOM decay rate, sec^{-1}
- $K_{L \rightarrow R}$ = transfer rate from labile DOM, sec^{-1}
- Φ_{LDOM} = labile DOM concentration, g m^{-3}
- Φ_{RDOM} = refractory DOM concentration, g m^{-3}

and the rate terms are evaluated in subroutine REFRACTORY_DOM.

Labile Particulate Organic Matter

Labile particulate organic matter (LPOM) represents particulate organic material in the water column. When decaying, particulate organic matter is a source of refractory particulate organic matter, nitrogen, phosphorus, and inorganic carbon. A stoichiometric relationship is used for mineralization of ammonium, phosphorus, and inorganic carbon, and an oxygen demand is exerted as LPOM decomposes. When LPOM settles to the bottom, it accumulates and decays in the sediment compartment if the 1st order sediment compartment is included in the simulation.

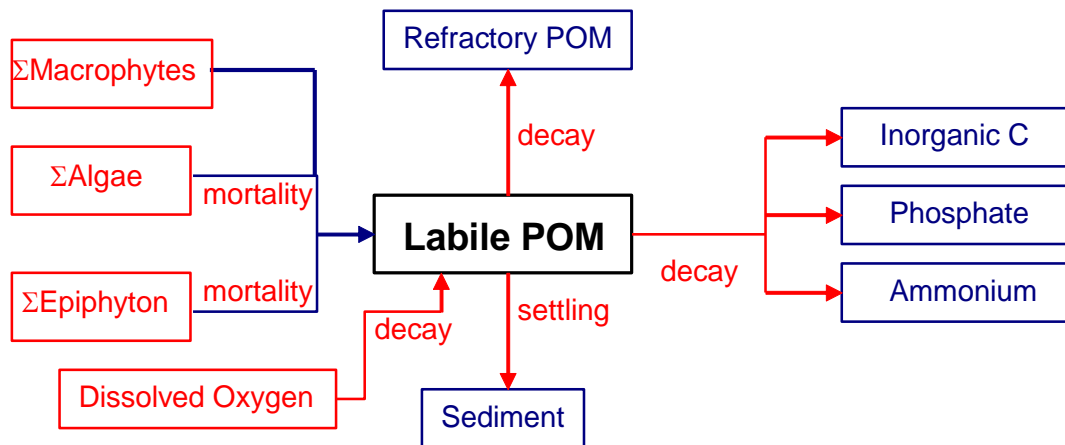


Figure B-7. Internal flux between Labile POM and other compartments.

Referring to [Figure B-7](#), the rate equation for LPOM is:

$$\begin{aligned}
 S_{LPOM} = & \underbrace{\sum P_{am} K_{am} \Phi_a}_{\text{algal mortality}} + \underbrace{\sum P_{em} K_{em} \Phi_e}_{\text{epiphyton mortality}} - \underbrace{K_{LPOM} \gamma_{OM} \Phi_{LPOM}}_{\text{decay}} \\
 & - \underbrace{K_{L \rightarrow R} \Phi_{LPOM}}_{\substack{\text{labile to refractory} \\ \text{POM decay}}} - \underbrace{\omega_{POM} \frac{\partial \Phi_{LPOM}}{\partial z}}_{\text{settling}} + \underbrace{\sum P_{mm} K_{mm} \Phi_{macro}}_{\text{macrophyte mortality}}
 \end{aligned} \tag{B-8}$$

where:

- P_{am} = partition coefficient for algal mortality
- P_{em} = partition coefficient for epiphyton mortality
- P_{mm} = partition coefficient for macrophyte mortality
- γ_{OM} = temperature rate multiplier for organic matter
- ω_{POM} = POM settling rate, $m \text{ sec}^{-1}$
- K_{am} = algal mortality rate, sec^{-1}
- K_{em} = epiphyton mortality rate, sec^{-1}
- K_{mm} = macrophyte mortality rate, sec^{-1}
- K_{LPOM} = labile POM decay rate, sec^{-1}
- $K_{L \rightarrow R}$ = transfer rate from labile POM to refractory POM, sec^{-1}
- Φ_a = algal concentration, $g \text{ m}^{-3}$
- Φ_e = epiphyton concentration, $g \text{ m}^{-3}$
- Φ_{macro} = macrophyte concentration, $g \text{ m}^{-3}$
- Φ_{LPOM} = detritus concentration, $g \text{ m}^{-3}$

and the rate terms are evaluated in subroutine POM. POM settling and accumulation in the sediment compartment is handled identically to the algal compartment.

Refractory Particulate Organic Matter

Refractory POM is slowly decaying non-living, organic matter that settles. The source/sink terms are first order decay, the conversion of LPOM to RPOM, and sedimentation:

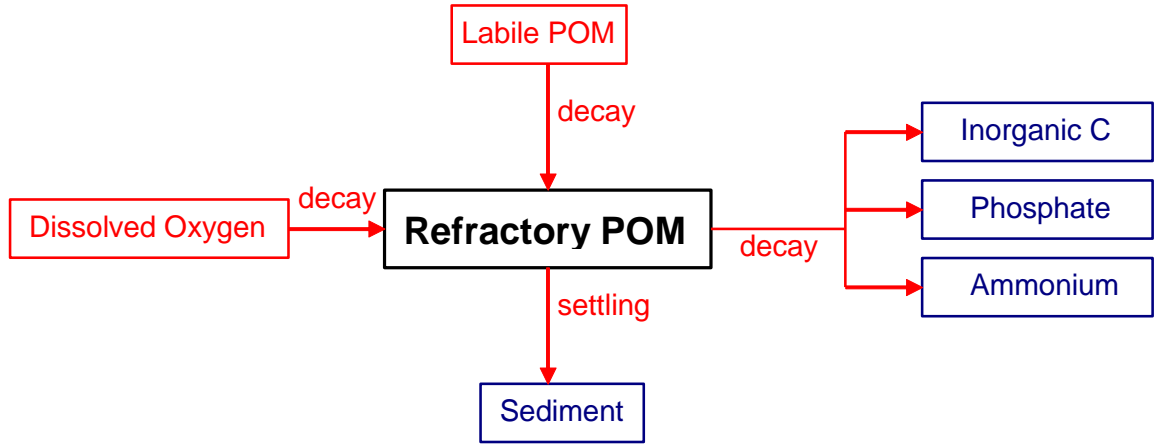


Figure B-8. Internal flux between refractory POM and other compartments.

Referring to [Figure B-8](#), the rate equation for labile POM is:

$$S_{RPOM} = \underbrace{K_{L \rightarrow R} \Phi_{LPOM}}_{\text{labile to refractory POM decay}} - \underbrace{\gamma_{OM} K_{RPOM} \Phi_{RPOM}}_{\text{decay}} - \underbrace{\omega_{RPOM} \frac{\partial \Phi_{RPOM}}{\partial z}}_{\text{settling}} \quad (\text{B-9})$$

where:

γ_{OM} = temperature rate multiplier

$K_{L \rightarrow R}$ = transfer rate from labile POM to refractory POM, sec^{-1}

K_{RPOM} = refractory POM decay rate, sec^{-1}

ω_{RPOM} = POM settling velocity, m/sec^{-1}

Φ_{LPOM} = labile POM concentration, g m^{-3}

Φ_{RPOM} = refractory POM concentration, g m^{-3}

Carbonaceous Biochemical Oxygen Demand (CBOD)

Any number of CBOD groups with varying decay rates can be modeled allowing the user to more accurately characterize various CBOD sources to the prototype. Additionally, different CBOD sources can be tracked separately in the model to determine what affect they have at different locations in the system.

Care must be taken when including CBOD in the simulation to ensure that CBOD, DOM, POM, and algal biomass are properly accounted for. CBOD is typically specified as allochthonous inputs and the forms of autochthonous organic matter are kept track of in the various organic matter compartments. This ensures that no “double dipping” occurs. This group can also model dissolved or

particulate CBOD by specifying a zero or a finite settling velocity, respectively, for the group. The settled CBOD goes into the 1st order sediment compartment.

In Version 3.6 and earlier, [Figure B-9](#) described the CBOD cycle with fixed stoichiometry of the CBOD in terms of C:N:P. Starting with Version 3.7, code changes were made such that for each CBOD group, the nitrogen and phosphorus corresponding to the CBOD group were modeled as separate constituents. One can still though use the V3.6 and earlier fixed N and P stoichiometry for the BOD groups if one wishes. CBOD-C though is still based on a fixed C stoichiometry.

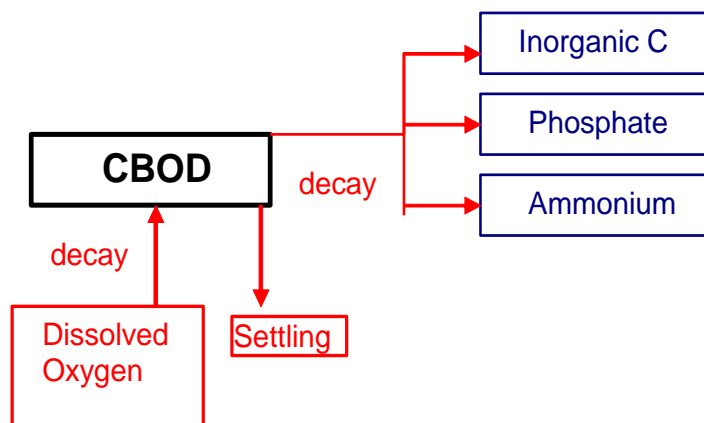


Figure B-9. Internal flux between CBOD and other compartments in Version 3.6 and earlier.

The following figure illustrates the CBOD cycle for Version 3.7 and later.

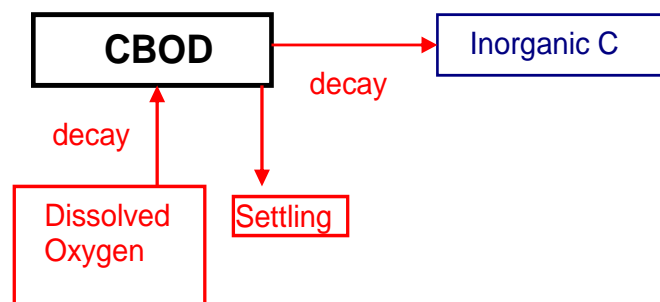


Figure B-10. Internal flux between CBOD and other compartments in Version 3.7 and later.

The rate equation for CBOD is:

$$S_{CBOD} = - \underbrace{\Theta^{T-20} K_{BOD} R_{BOD} \Phi_{CBOD}}_{\text{decay}} - \underbrace{\omega_{CBOD} \frac{\partial R_{BOD} \Phi_{CBOD}}{\partial z}}_{\text{settling}} \quad (\text{B-10})$$

where:

Θ = BOD temperature rate multiplier

T = temperature, °C

ω_{CBOD} = CBOD settling velocity, m/sec^{-1}

K_{BOD} = CBOD decay rate, sec^{-1}

R_{BOD} = CBOD conversion from input CBOD to CBOD-ultimate (CBOD_u)

Φ_{BOD} = CBOD concentration, $g\ m^{-3}$

Note that the user can enter CBOD5 or CBOD10 or whatever into the CE-QUAL-W2 model. The R_{BOD} term converts to CBOD_u internally in the model. The model though will output CBOD5 if you entered CBOD5 as input - not CBOD_u. If you use CBOD_u as the input CBOD, then $R_{BOD}=1$ and the output would be CBOD_u.

Typical determination of R_{BOD} is based on the following standard CBOD equation:

$$R_{BOD} = \frac{CBOD_u}{CBOD_t} = \frac{1}{(1 - \exp[-K_{BOD}t])} \quad \text{where } t \text{ is the time (5 days, for example) and } CBOD_t \text{ is the CBOD at that time.}$$

Carbonaceous Biochemical Oxygen Demand - Phosphorus (CBODP)

The phosphorus associated with a specific CBOD group is modeled as a separate constituent.

Sources and sinks for carbonaceous biochemical oxygen demand - phosphorus (CBODP) are shown in Figure 11.

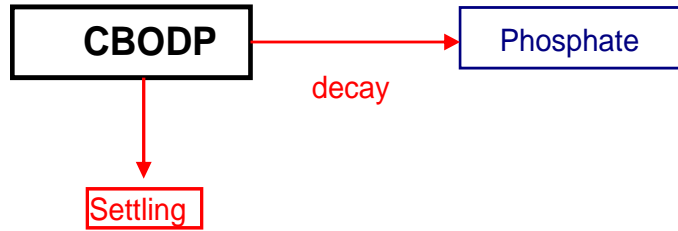


Figure 11. Internal flux between CBODP and other compartments.

The rate equation for CBODP is:

$$S_{CBODP} = - \underbrace{\Theta^{T-20} K_{BOD} \Phi_{CBODP}}_{\text{decay}} - \underbrace{\omega_{CBOD} \frac{\partial \Phi_{CBODP}}{\partial z}}_{\text{settling}}$$

where:

Θ = BOD temperature rate multiplier

T = temperature, $^{\circ}\text{C}$

ω_{CBOD} = CBOD settling velocity, m/sec^{-1}

K_{BOD} = CBOD decay rate, sec^{-1}

Φ_{CBODP} = CBODP concentration, g m^{-3}

Carbonaceous Biochemical Oxygen Demand - Nitrogen (CBODN)

The nitrogen associated with a specific CBOD group is modeled as a separate constituent. Figure 12 shows the CBODN sources and sinks.

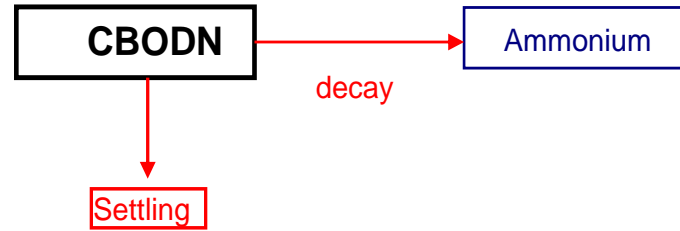


Figure 12. Internal flux between CBODN and other compartments.

The rate equation for CBODN is:

$$S_{CBODN} = - \underbrace{\Theta^{T-20} K_{BOD} \Phi_{CBODN}}_{\text{decay}} - \underbrace{\omega_{CBOD} \frac{\partial \Phi_{CBODN}}{\partial z}}_{\text{settling}}$$

where:

Θ = BOD temperature rate multiplier

T = temperature, $^{\circ}\text{C}$

ω_{CBOD} = CBOD settling velocity, $m\ s^{-1}$

K_{BOD} = CBOD decay rate, sec^{-1}

Φ_{CBODN} = CBODN concentration, $g\ m^{-3}$

Algae

Typically, the algal community is represented as a single assemblage or is broken down into diatoms, greens, and cyanobacteria (blue-greens). However, the current formulation now gives the user complete freedom in how many and what kinds of algal groups can be included in the simulation through careful specification of the kinetic rate parameters that define the characteristics of each algal group.

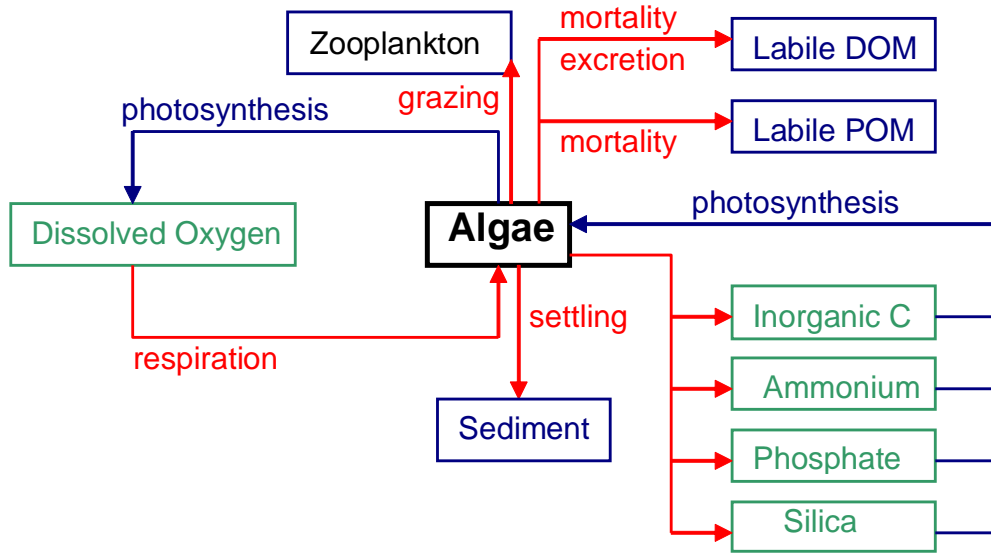


Figure B-13. Internal flux between algae and other compartments.

Referring to [Figure B-13](#), the rate equation for each algal group is:

$$\begin{aligned}
 S_a = & \underbrace{K_{ag} \Phi_a}_{\text{growth}} - \underbrace{K_{ar} \Phi_a}_{\text{respiration}} - \underbrace{K_{ae} \Phi_a}_{\text{excretion}} - \underbrace{K_{am} \Phi_a}_{\text{mortality}} - \underbrace{\omega_a \frac{\partial \Phi_a}{\partial z}}_{\text{settling}} \\
 & - \underbrace{\sum \left(\frac{Z_\mu \Phi_{zoo} \sigma_{alg} \Phi_a}{\sum \sigma_{alg} \Phi_a + \sigma_{pom} \Phi_{lpom} + \sum \sigma_{zoo} \Phi_{zoo}} \right)}_{\text{net loss to grazing}}
 \end{aligned} \tag{B-11}$$

where:

z = cell height

Z_μ = net growth rate of a zooplankton species

σ = zooplankton grazing preference factors

K_{ag} = algal growth rate, sec^{-1}

K_{ar} = algal dark respiration rate, sec^{-1}

K_{ae} = algal excretion rate, sec^{-1}

K_{am} = algal mortality rate, sec^{-1}

ω_a = algal settling rate, $m \text{ sec}^{-1}$

Φ_a = algal concentration, $g \text{ m}^{-3}$

Chlorophyll *a* (chl *a*) is most commonly available as an estimate of algal biomass. To convert chl *a* to algal biomass, chl *a* is typically multiplied by the given algae (as $g \text{ m}^{-3}$ or mg/l dry weight OM)/chl *a* (as μg chlorophyll *a*/l) ratio. This value can vary widely depending on the makeup of

the algal population. Some previous studies determined the conversion factor by regressing particulate organic matter with chl *a*.

Algal growth rate is computed by modifying a maximum growth rate affected by temperature, light, and nutrient availability:

$$K_{ag} = \gamma_{ar} \gamma_{af} \lambda_{min} K_{agmax} \quad (\text{B-12})$$

where:

γ_{ar} = temperature rate multiplier for rising limb of curve

γ_{af} = temperature rate multiplier for falling limb of curve

λ_{min} = multiplier for limiting growth factor (minimum of light, phosphorus, silica, and nitrogen)

K_{ag} = algal growth rate, sec^{-1}

K_{agmax} = maximum algal growth rate, sec^{-1}

Rate multipliers for algal growth are computed based upon available light, phosphorus, nitrogen, and silica. The rate multiplier for light is based upon the Steele (1962) function:

$$\lambda_l = \frac{I}{I_s} e^{\left(-\frac{I}{I_s} + 1\right)} \quad (\text{B-13})$$

where:

I = available light, $W m^{-2}$

I_s = saturating light intensity at maximum photosynthetic rate, $W m^{-2}$

λ_l = light limiting factor

The above expression allows for simulation of photoinhibition at light intensities greater than the saturation value. However, light penetration decreases with depth:

$$I = (1 - \beta) I_0 e^{-\alpha z} \quad (\text{B-14})$$

where:

I_0 = solar radiation at the water surface, $W m^{-2}$

α = attenuation coefficient, m^{-2}

z = depth, m

β = fraction of solar radiation absorbed at the water surface

The average effect of light on algal growth in a particular model cell can be obtained by combining the above two expressions and integrating over the cell depth to obtain (Chapra and Reckhow, 1983):

$$\lambda_l = \frac{e}{\alpha \Delta z} \left[e^{-\gamma_2} - e^{-\gamma_1} \right] \quad (\text{B-15})$$

where:

$$\gamma_1 = \frac{(1 - \beta) I_0}{I_s} e^{-\alpha d}$$

$$\gamma_2 = \frac{(1 - \beta) I_0}{I_s} e^{\alpha(d + \Delta z)}$$

d = depth at top of model cell, m

The fraction of solar radiation, β_{10} , is added directly to the surface layer. The attenuation coefficient, α , consists of a baseline value [\[EXH2O\]](#) to which the effects of inorganic [\[EXINOR\]](#) and organic [\[EXORG\]](#) suspended solids, and algae [\[EXA\]](#) are added.

Rate multipliers limiting maximum algal growth due to nutrient limitations are computed using the Monod relationship:

$$\lambda_i = \frac{\Phi_i}{P_i + \Phi_i} \quad (\text{B-16})$$

where:

Φ_i = phosphorus or nitrate + ammonium concentration, $g\ m^{-3}$

P_i = half-saturation coefficient for phosphorus or nitrate + ammonium, $g\ m^{-3}$

The algal nitrogen preference for ammonium is based upon the following (Thomann and Fitzpatrick, 1982).

$$P_{NH4} = \Phi_{NH4} \frac{\Phi_{NOx}}{(K_{NH4} + \Phi_{NH4})(K_{NH4} + \Phi_{NOx})} + \Phi_{NH4} \frac{K_{NH4}}{(\Phi_{NH4} + \Phi_{NOx})(K_{NH4} + \Phi_{NOx})} \quad (\text{B-17})$$

where:

P_{NH4} = ammonium preference factor

K_{NH4} = ammonia preference half-saturation coefficient, $g\ m^{-3}$

Φ_{NH4} = ammonium concentration, $g\ m^{-3}$

Φ_{NOx} = nitrate-nitrite concentration, $g\ m^{-3}$

This allows algae to use primarily ammonium and gradually switch to nitrate as ammonium concentrations decrease.

Algal dark respiration is computed using the rising limb of the temperature function:

$$K_{ar} = \gamma_{ar} \gamma_{af} K_{armax} \quad (\text{B-18})$$

where:

γ_{ar} = temperature rate multiplier for rising limb of curve

γ_{af} = temperature rate multiplier for falling limb of curve

K_{armax} = maximum dark respiration rate, sec^{-1}

Algal photorespiration (excretion) is evaluated using an inverse relation to the light rate multiplier:

$$K_{ae} = (1 - \lambda_l) \gamma_{ar} \gamma_{af} K_{aemax} \quad (\text{B-19})$$

where:

γ_{ar} = temperature rate multiplier for rising limb of curve

γ_{af} = temperature rate multiplier for falling limb of curve

K_{aemax} = maximum excretion rate constant, sec^{-1}

λ_l = light limiting factor

Excretion rates increase at both low and high light intensities, with excretion products contributing to labile DOM.

Algal mortality is defined as:

$$K_{am} = \gamma_{ar} \gamma_{af} K_{amax} \quad (\text{B-20})$$

where:

γ_{ar} = temperature rate multiplier for rising limb of curve

γ_{af} = temperature rate multiplier for falling limb of curve

K_{amax} = maximum mortality rate, sec^{-1}

This mortality rate represents both natural and predator mortality. Algal growth does not occur in the absence of light. Algal growth is not allowed to exceed the limit imposed by nutrient supply over a given timestep. Algal excretion is not allowed to exceed algal growth rates.

Similar to inorganic solids, settling algae serve as a source for the layer below. Unlike inorganic solids, algae passing to the sediments accumulate within the sediment compartment. POM is also accumulated in this sediment compartment.

Epiphyton

Any number of user defined epiphyton groups can be modeled. Similar to the 1st order sediment compartment, epiphyton are not transported in the water column and are thus not state variables.

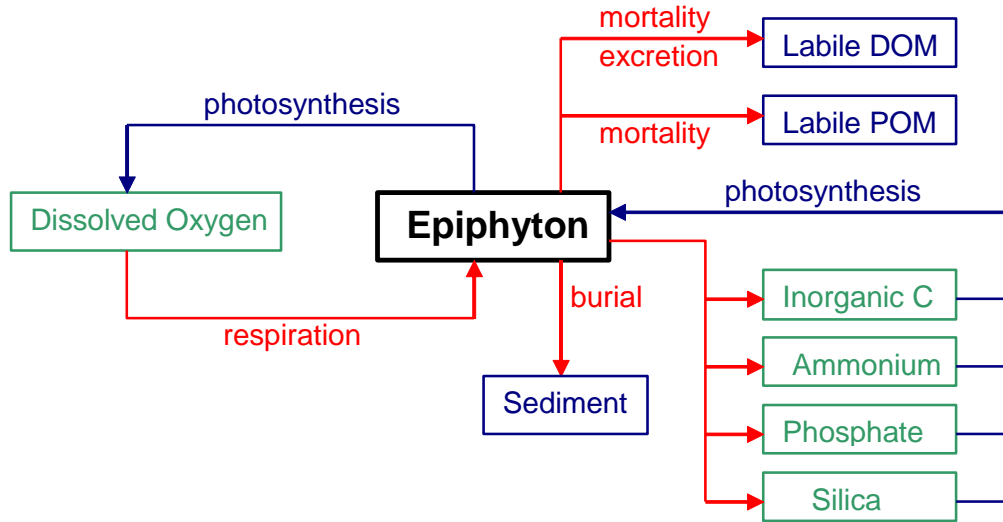


Figure B-14. Internal flux between epiphyton and other compartments.

Referring to [Figure B-14](#), the rate equation for each epiphyton group is:

$$S_e = \underbrace{K_{eg} \Phi_e}_{\text{growth}} - \underbrace{K_{er} \Phi_e}_{\text{respiration}} - \underbrace{K_{ee} \Phi_e}_{\text{excretion}} - \underbrace{K_{em} \Phi_e}_{\text{mortality}} - \underbrace{K_{eb} \Phi_e}_{\text{burial}} \quad (\text{B-21})$$

where:

- K_{eg} = epiphyton growth rate, sec^{-1}
- K_{er} = epiphyton dark respiration rate, sec^{-1}
- K_{ee} = epiphyton excretion rate, sec^{-1}
- K_{em} = epiphyton mortality rate, sec^{-1}
- K_{eb} = epiphyton burial rate, $m \text{ sec}^{-1}$
- Φ_e = epiphyton concentration, $g \text{ m}^{-3}$

Epiphyton growth rate is computed by modifying a maximum growth rate affected by epiphyton biomass, temperature, and nutrient availability:

$$K_{eg} = \gamma_{er} \gamma_{ef} \lambda_{min} K_{eg \text{ max}} \quad (\text{B-22})$$

where:

γ_{er} = temperature rate multiplier for rising limb of curve

γ_{ef} = temperature rate multiplier for falling limb of curve

λ_{min} = multiplier for limiting growth factor (minimum of phosphorus, silica, nitrogen, and epiphyton biomass)

K_{eg} = epiphyton growth rate, sec^{-1}

K_{egmax} = maximum epiphyton growth rate, sec^{-1}

Rate multipliers for epiphyton growth are computed based upon available light, phosphorus, nitrogen, silica, and epiphyton biomass. Epiphyton biomass is included as a surrogate for light limited epiphyton self-shading and will be discussed in greater detail below.

The rate multiplier for light is based upon the Steele (1962) function:

$$\lambda_l = \frac{I}{I_s} e^{\left(\frac{I}{I_s} + 1\right)} \quad (\text{B-23})$$

where:

I = available light, $W m^{-2}$

I_s = saturating light intensity at maximum photosynthetic rate, $W m^{-2}$

λ_l = light limiting factor

The above expression allows for simulation of photoinhibition at light intensities greater than the saturation value. However, light penetration decreases with depth:

$$I = (1 - \beta) I_0 e^{-\alpha z} \quad (\text{B-24})$$

24)

where:

I_0 = solar radiation at the water surface, $W m^{-2}$

α = attenuation coefficient, m^{-2}

z = depth, m

β = fraction of solar radiation absorbed at the water surface

The average effect of light on epiphyton growth in a particular model cell can be obtained by combining the above two expressions and integrating over the cell depth to obtain (Chapra and Reckhow, 1983):

$$\lambda_l = \frac{e}{\alpha \Delta z} \left[e^{-\gamma_2} - e^{-\gamma_1} \right] \quad (\text{B-25})$$

where:

$$\gamma_1 = \frac{(1 - \beta) I_o}{I_s} e^{-\alpha d}$$

$$\gamma_2 = \frac{(1 - \beta) I_o}{I_s} e^{\alpha(d + \Delta z)}$$

d = depth at the top of computational cell, m

The attenuation coefficient, λ , is computed from a baseline value [\[EXH2O\]](#) to which the effects of inorganic [\[EXINOR\]](#) and organic [\[EXORG\]](#) suspended solids, as well as the extinction of each algal group, are added. Epiphyton self-shading are accounted for in the biomass limitation formulation.

Rate multipliers limiting epiphyton growth due to nutrient limitations are computed using the Monod relationship:

$$\lambda_i = \frac{\Phi_i}{P_i + \Phi_i} \quad (\text{B-26})$$

26)

where:

Φ_i = phosphorus or nitrate + ammonium concentration, $g\ m^{-3}$

P_i = half-saturation coefficient for phosphorus or nitrate + ammonium, $g\ m^{-3}$

The epiphyton preference for ammonium is modeled using the following (Thomann and Fitzpatrick, 1982).

$$P_{NH4} = \Phi_{NH4} \frac{\Phi_{NOx}}{(K_{NH4} + \Phi_{NH4})(K_{NH4} + \Phi_{NOx})} + \Phi_{NH4} \frac{K_{NH4}}{(\Phi_{NH4} + \Phi_{NOx})(K_{NH4} + \Phi_{NOx})} \quad (\text{B-27})$$

P_{NH4} = ammonium preference factor

K_{NH4} = ammonia preference half-saturation coefficient, $g\ m^{-3}$

Φ_{NH4} = ammonium concentration, $g\ m^{-3}$

Φ_{NOx} = nitrate-nitrite concentration, $g\ m^{-3}$

Epiphyton dark respiration is computed using the rising limb of the temperature function:

$$K_{er} = \gamma_{er} \gamma_{ef} K_{ermax} \quad (\text{B-28})$$

where:

γ_{er} = temperature rate multiplier for rising limb of the curve

γ_{ef} = temperature rate multiplier for falling limb of the curve

K_{armax} = maximum dark respiration rate, sec^{-1}

Epiphyton excretion is evaluated using an inverse relation to the light rate multiplier:

$$K_{ee} = (1 - \lambda_l) \gamma_{er} \gamma_{ef} K_{ee max} \quad (B-29)$$

where:

λ_l = light limiting factor

γ_{er} = temperature rate multiplier for rising limb of the curve

γ_{ef} = temperature rate multiplier for falling limb of the curve

K_{eemax} = maximum excretion rate constant, sec^{-1}

Excretion rates increase at both low and high light intensities, with excretion products contributing to labile DOM.

Epiphyton mortality is defined as:

$$K_{em} = \gamma_{er} \gamma_{ef} K_{em max} \quad (B-30)$$

where:

γ_{er} = temperature rate multiplier for rising limb of the curve

γ_{ef} = temperature rate multiplier for falling limb of the curve

K_{emmax} = maximum mortality rate, sec^{-1}

This mortality rate represents both natural and predator mortality. Epiphyton growth does not occur in the absence of light. Epiphyton growth is not allowed to exceed the limit imposed by nutrient supply over a given timestep. Epiphyton excretion is not allowed to exceed epiphyton growth rates.

The epiphyton burial rate represents the burial of dead epiphyton to the organic sediment compartment. The epiphyton become part of the 1st-order sediment compartment. Epiphyton though that die (mortality) become a part of the labile particulate organic matter and the labile dissolved organic matter pool. The user defines the fraction of the dead epiphyton (EPOM) that goes to the LPOM pool. This POM is then transported in the water column. Currently, there is no sloughing of epiphyton into the water column as a function of velocity shear. This is a function of the biomass limitation term.

The epiphyton biomass is controlled by a biomass limitation equation based on Monod kinetics. The biomass limitation function, f , varies from 0 to 1 and is multiplied with the growth rate. This function is defined as

$$f = \left[1 - \frac{B}{B + K_B} \right] \quad (\text{B-31})$$

where:

B = epiphyton areal biomass, g/m^2

K_b = epiphyton areal biomass half-saturation coefficient, g/m^2

The areal biomass is calculated as follows:

$$B = \Phi_e \frac{V}{A} \quad (\text{B-32})$$

where:

A = computational cell surface area, m^2

V = computational cell volume, m^3

Φ_e = epiphyton concentration, $g\ m^{-3}$

The biomass limitation is a surrogate calibration parameter for light limitation due to self-shading.

Macrophytes

The macrophyte model consists of two parts: a section describing the water quality compartment and a section describing the hydrodynamic compartment.

The macrophyte model was designed to simulate multiple submerged macrophyte species. It does not differentiate between plant parts. The nutrient fluxes for the water quality component of the macrophyte compartment are shown in Figure 15. Light, temperature, carbon dioxide, ammonia-nitrogen (only ammonia is used as a N source for macrophytes), and ortho-phosphorus may limit growth. Depending on the macrophyte species, nitrogen and phosphorus may be obtained from the sediments or the water column. If they are obtained from the sediments, the sediments are assumed to be an infinite pool that cannot limit growth. Plants grow upwards from the sediment through model layers. Growth upward is accomplished by moving the growth of a layer to the layer above if the concentration in the layer is greater than a threshold concentration and the concentration in the upper layer is less than the same threshold concentration. Macrophyte shading is modeled by making light attenuation a function of macrophyte concentration.

KINETICS

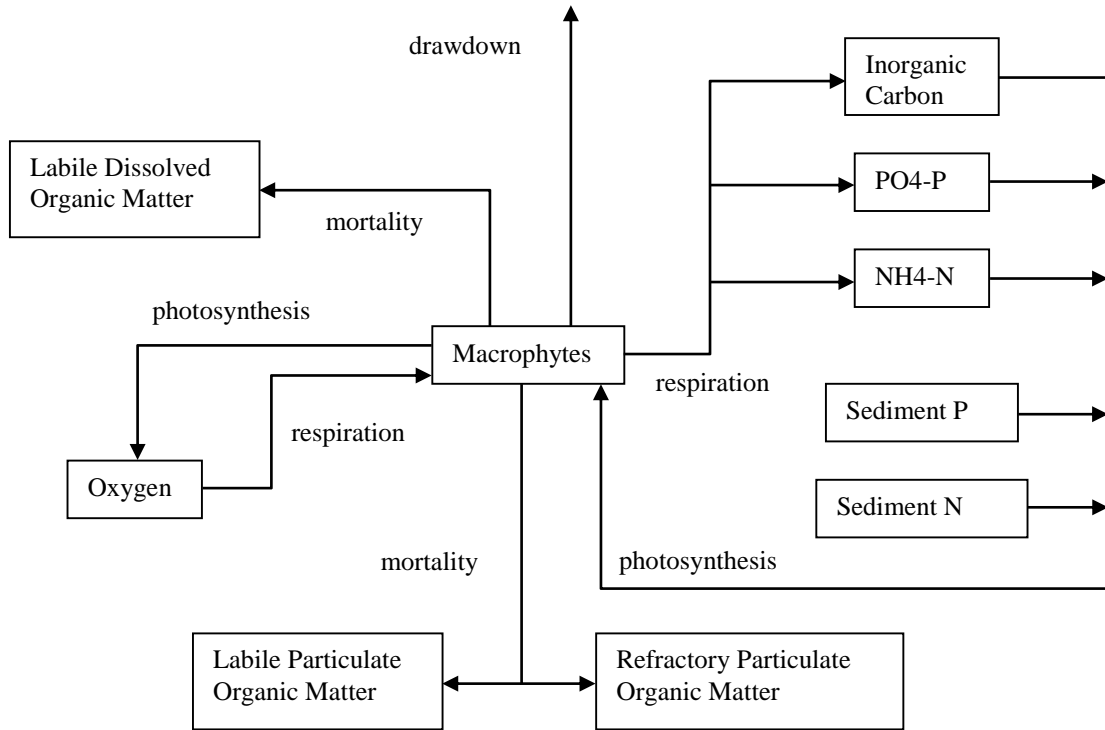


Figure 15. Nutrient fluxes for the macrophyte compartment in CE-QUAL-W2.

The macrophyte growth rate is modeled as follows:

$$S_{macro} = \underbrace{\mu_{mmax} f(I, N, P, C) \gamma_1 \gamma_2 \Phi_{macro}}_{\text{growth}} - \underbrace{K_{mr} \gamma_1 \Phi_{macro}}_{\text{respiration}} - \underbrace{K_{mm} \Phi_{macro}}_{\text{mortality}}$$

where

S_{macro} : macrophyte growth rate density (g/m³/s)

I : solar radiation (W/m²)

$f(I, N, P, C)$: Growth limiting function between 0 and 1

μ_{mmax} : maximum macrophyte growth rate (day⁻¹)

K_{mr} : maximum respiration rate (day⁻¹)

K_{mm} : mortality/excretion rate (day⁻¹)

γ_1 : ascending temperature rate multiplier

γ_2 : descending temperature rate multiplier

γ_3 : growth limiting factor due to photosynthesis

Φ_{macro} : macrophyte concentration (g/m³)

Growth rate, respiration rate, and mortality/excretion rate are temperature dependent. Temperature effects are modeled using the equations developed by Thornton and Lessem (1978) which are currently used in the phytoplankton compartment of CE-QUAL-W2. The growth limiting function $f(I, N, P, C)$ is the minimum of the light $f(I)$, nitrogen $f(N)$, phosphorus $f(P)$, and carbon $f(C)$ limiting functions such that $f(I, N, P, C) = \text{minimum}(f(I), f(N), f(P), f(C))$.

All the limiting functions are unit-less and have a value between 0 and 1. The limiting functions for the nutrients have the following Michaelis-Menten form

$$f(S) = \frac{S}{K_s + S}$$

where S (mg/l) is the nutrient concentration and K_s (mg/l) is the half-saturation concentration. Light limitation was modeled with a hyperbolic equation which has the same form as the Michaelis-Menten function:

$$f(I) = \frac{I}{I_h + I}$$

where

I : solar radiation (W/m²)

I_h : half-saturation coefficient for solar radiation (W/m²)

This function is frequently used in the absence of photo-inhibition (Carr et al., 1997).

The net light extinction coefficient γ (m⁻¹) was modeled as a function of macrophyte plant tissue concentration giving

$$\gamma = \varepsilon_{H_2O} + \varepsilon_{iss} \Phi_{iss} + \varepsilon_{oss} \Phi_{oss} + \sum_{\substack{\# \text{ of} \\ \text{macrophyte} \\ \text{groups}}} \varepsilon_{mac} \Phi_{mac} + \sum_{\substack{\# \text{ of} \\ \text{algae} \\ \text{groups}}} \varepsilon_{algae} \Phi_{algae}$$

where:

ε_{H_2O} = light extinction exclusive of suspended solids, m⁻¹

ε_{iss} = light extinction due to inorganic suspended solids, m³ m⁻¹ g⁻¹

ε_{oss} = light extinction due to non-living organic suspended solids, m³ m⁻¹ g⁻¹

ε_{mac} = light extinction due to macrophytes, m³ m⁻¹ g⁻¹

ε_{algae} = light extinction due to algae, m³ m⁻¹ g⁻¹

Φ_{iss} = inorganic suspended solids concentration, g m⁻³

Φ_{oss} = organic suspended solids concentration, g m⁻³

Φ_{mac} = macrophyte plant tissue concentration, g m⁻³

Φ_{algae} = algae concentration, g m⁻³

Modeling of flow through macrophytes incorporated the following concepts:

- Porosity of the macrophytes was calculated through determination of the blockage area of the vegetation normal to the direction of flow
- The drag of individual stems and leaves were totaled to determine the total drag force in a model cell
- The effective Mannings n was calculated by combining the effect of bed shear and the drag force on the plants

KINETICS

Modeling Frictional Force

The total frictional force f was partitioned into a bottom friction component f_b and a vegetation drag component f_v giving

$$f = f_b + f_v$$

Bottom shear τ_b was simulated using Manning's friction factor

$$\tau_b = \frac{\rho_w g n^2}{R^{1/3}} U |U|$$

where

ρ_w : density of water

g : gravitational constant

U : water velocity

R : hydraulic radius

n : Manning's friction factor

The Columbia Slough model has already been calibrated for the no macrophytes condition. Manning's friction factor for the model segments was typically around 0.03.

Vegetative drag caused by macrophytes was modeled in a manner similar to that used by Petryk and Bosmajian (1975) where the drag force D_i on the i^{th} plant is

$$D_i = C_d A_i \left(\frac{\rho_w U^2}{2} \right)$$

with

A_i : area of plant projected normal to the direction of flow

C_d : drag coefficient

The total drag force in a model cell due to vegetation is

$$\sum D_i = C_d \left(\frac{\rho_w U^2}{2} \right) \sum A_i$$

The total plant area normal to the direction of flow $\sum A_i$ was estimated using biomass to surface area ratios from Sher-Kaul et al. (1995) and surface area to volume ratios from Sand-Jensen and Borum (1991).

The projected area normal to flow would then be $\varepsilon \sum A_i$ and the total drag was then

$$\sum D_i = C_d \left(\frac{\rho_w U^2}{2} \right) \sum A_i$$

The drag coefficient C_d was a calibration parameter but has been shown to be of the order of 1.0 for vegetation (Hsi and Nath, 1968; Hoerner, 1965; Petryk, 1969).

The effective Mannings n of each model cell was calculated in the manner used by Petryk and Bosmajian (1975) with

$$n = n_b \sqrt{1 + \frac{C_d \sum A_i}{2gAL} \frac{1}{n_b^2} R^{4/3}}$$

where

n_b : Mannings friction factor due to bed shear only.

This derivation is shown in more detail in Berger and Wells (in-print).

Modeling Porosity

The volume V_m of macrophytes can be estimated by dividing the macrophyte mass in a model cell m by density ρ_m

$$V_m = \frac{m}{\rho_m}$$

The porosity ϕ was estimated by dividing volume within a cell free of macrophytes by the cell total volume V giving

$$\phi = \left(\frac{V - V_m}{V} \right)$$

The cross-sectional area of each model cell was multiplied by the porosity to calculate the effective cross-sectional area. The porosity affected both the continuity and momentum equations.

Changes to Governing Equations

Several of the governing equations have been altered to account for porosity and the frictional effects of macrophytes. Equations affected include the x-momentum equation, the continuity equation, the free water surface equation, and the constituent transport equation. The new x-momentum equations is

$$\frac{\partial U \phi B}{\partial t} + \frac{\partial U U \phi B}{\partial x} + \frac{\partial W U \phi B}{\partial z} = - \frac{\phi B}{\rho} \frac{\partial P}{\partial x} + \frac{1}{\rho} \frac{\partial \phi B \tau_{xx}}{\partial x} + \frac{1}{\rho} \frac{\partial \phi B \tau_{xz}}{\partial z}$$

where

U - x-direction velocity, m/sec

W - z-direction velocity, m/sec

B - channel width, meters

ρ - density, mg/l

P - Pressure, Newtons/m²

τ_{xz} - vertical shear stress, Newtons/m²

τ_{xx} - longitudinal shear stress, Newtons/m²

Vertical shear stress τ_{xz} is a function of interfacial shear stress, shear stress due to wind, and bottom and plant shear stress. It was determined from

$$\frac{\tau_{xz}}{\rho} = A_z \frac{\partial U}{\partial z} + \frac{\tau_{wx}}{\rho} e^{-dkz} + \frac{\tau_{bm}}{\rho}$$

where

τ_{bm} -bottom and plant shear stress

A_z - turbulent eddy viscosity

τ_{wx} -wind shear stress

k-wave number

Bottom and plant shear stress is calculated using the effective Mannings n determined above

KINETICS

$$\tau_{bm} = \frac{\rho \, g n^2}{R^{1/3}} U|U|$$

The continuity equation was changed to

$$\frac{\partial U\phi B}{\partial x} + \frac{\partial W\phi B}{\partial z} = q\phi B$$

where

q - lateral inflow/outflow per unit volume (T^{-1})

The new free water surface equation is

$$\frac{\partial B_\eta \phi \eta}{\partial t} = \frac{\partial}{\partial x} \int_\eta^h U \phi B dz - \int_\eta^h q \phi B dz$$

with

B_η – time and spatially varying surface width, meters

η - free water surface elevation, meters

The constituent transport equation could also be affected by the reduction of cross-sectional area due to macrophytes giving

$$\frac{\partial \phi BC}{\partial t} + \frac{\partial U \phi BC}{\partial x} + \frac{\partial W \phi BC}{\partial z} - \frac{\partial}{\partial x} \phi B D_x \frac{\partial C}{\partial x} - \frac{\partial}{\partial z} \phi B D_z \frac{\partial C}{\partial z} = q_\phi \phi B + S_K \phi B$$

with

C - constituent concentration, mg/l

D_x - longitudinal temperature and constituent dispersion coefficient, m^2/sec

D_z - vertical temperature and constituent dispersion coefficient, m^2/sec

q_ϕ - lateral inflow or outflow mass flow rate of constituent per unit volume, mg/l/sec

S_K - kinetics source/sink term for constituent concentration, mg/l/sec

The parameter coefficients used in the first application of this model to the Columbia Slough are shown below in Table 12. Descriptions of the input data fields are included in Appendix C.

Table 12. Parameters and values used for macrophytes in the Columbia Slough model.

Variable name in input data file	CE-QUAL-W2 Model value	Coefficient definition (units)
PRNMC	ON or OFF	Macrophyte snapshot output on or off
MACROC	ON or OFF	Macrophyte compartment on or off
EXM	0.01	Light extinction coefficient for organic particles (m/mg/l)
MBMP	40.0	Threshold macrophyte concentration for which growth is moved to the above layer (mg/l)
MMAX	500.0	Maximum macrophyte concentration (mg/l)
MG	0.30	Maximum macrophyte growth rate (day^{-1})
MR	0.05	Macrophyte respiration rate (day^{-1})
MM	0.05	Macrophyte mortality rate (day^{-1})
SATM	20.0	Macrophyte half-saturation light intensity at the maximum photosynthetic rate (Watts/ m^2)
MT1	7	Lower temperature bound for macrophyte growth (Celsius)

KINETICS

Variable name in input data file	CE-QUAL-W2 Model value	Coefficient definition (units)
MT2	15	Lowest temperature at which macrophyte growth processes are near the maximum rate (Celsius)
MT3	24	Upper temperature at which macrophyte growth processes are near the maximum rate (Celsius)
MT4	34	Upper lethal temperature for macrophytes(Celsius)
MK1	0.1	Temperature rate multiplier for MT1
MK2	0.99	Temperature rate multiplier for MT2
MK3	0.99	Temperature rate multiplier for MT3
MK4	0.01	Temperature rate multiplier for MT4
MPOM	0.9	Fraction of dead macrophytes which becomes POM, the fraction (1-MPOM) becomes labile DOM
LRPMAC	0.2	Fraction of POM which originates as dead macrophytes becoming labile POM
PSED	0.5	Fraction of phosphorus uptake by macrophytes obtained from sediments
NSED	0.5	Fraction of nitrogen uptake by macrophytes obtained from sediments
MHSP	0	Half-saturation constant for P uptake by macrophytes (mg/l)
MHSN	0	Half-saturation constant for N uptake by macrophytes (mg/l)
MHSC	10	Half-saturation constant for carbon uptake by macrophytes (mg/l)
MACP	0.005	Stoichiometric equivalent between macrophyte biomass and orthophosphate
MACN	0.08	Stoichiometric equivalent between macrophyte biomass and nitrogen
MACC	0.45	Stoichiometric equivalent between macrophyte biomass and carbon
02MR	1.1	Dissolved oxygen requirement for macrophyte respiration
02MG	2.0	Stoichiometric equivalent for dissolved oxygen production during macrophyte photosynthesis
CD	3.0	Macrophyte drag coefficient

Zooplankton

A multiple zooplankton compartment was adapted from the U.S. Army Corps of Engineers reservoir model CE-QUAL-R1 (Environmental Laboratory, 1995) for the CE-QUAL-W2 model. Zooplankton are assumed to be non-motile and are transported only by advection and dispersion. Zooplankton can graze algae, detritus (POM), and other zooplankton. Losses occur through mortality and respiration. The source/sink term for zooplankton is shown below:

$$S_{zoo} = \underbrace{\gamma_1 \gamma_2 Z_e K_{zmax} \left(\frac{\left(\sum \sigma_{alg} \Phi_a + \sigma_{pom} \Phi_{lpom} + \sum \sigma_{zoo} \Phi_{zoo} \right) - Z_L}{\left(\sum \sigma_{alg} \Phi_a + \sigma_{pom} \Phi_{lpom} + \sum \sigma_{zoo} \Phi_{zoo} \right) + Z_{1/2}} \right)}_{\text{growth}} \Phi_{zoo} - \underbrace{(1 - \gamma_2) K_{zm} \Phi_{zoo}}_{\text{mortality}} - \underbrace{\gamma_1 K_{zr} \Phi_{zoo}}_{\text{respiration}}$$

Φ_{lpom} = Labile particulate organic matter concentration (mg/l)

Φ_{rpom} =Refractory particulate organic matter concentration(mg/l)

Φ_a = Algae concentration (mg/l)

Φ_{zoo} = Zooplankton concentration (mg/l)

KINETICS

K_{zm} = Zooplankton mortality rate (d^{-1})

K_{zmax} = Maximum ingestion rate for zooplankton (d^{-1})

K_{zr} = Zooplankton respiration rate (d^{-1})

$Z_{1/2}$ = Half-saturation coefficient for zooplankton ingestion (mg/l)

Z_e = Zooplankton ingestion efficiency

Z_L = Low threshold concentration for zooplankton feeding (mg/l)

γ_1 = Temperature coefficient for rising limb of curve for zooplankton

γ_2 = Temperature coefficient for falling limb of curve for zooplankton

σ_{alg} = Zooplankton preference fraction for algae

σ_{zoo} = Zooplankton preference fraction for zooplankton

σ_{pom} = Zooplankton preference fraction for particulate organic matter

The zooplankton source/sinks are also illustrated in Figure 16. The growth rate is a function of temperature, the maximum growth rate, and a modified Michaelis-Menten equation which includes a low threshold concentration below which zooplankton do not feed. At dissolved oxygen concentrations below 2 mg/l feeding stops and the mortality rate is doubled. The zooplankton model coefficients described in Table 13.

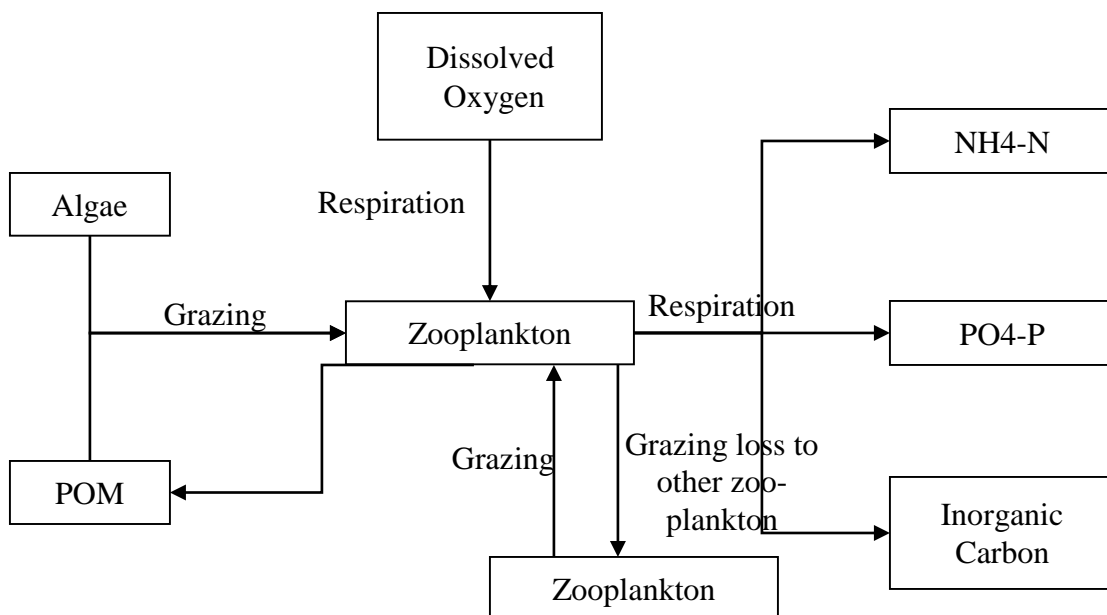


Figure 16. Zooplankton source/sinks.

Table 13. Parameters used in the zooplankton model.

Name	Description
ZMAX	Maximum ingestion rate for zooplankton (1/day)
ZMORT	Maximum nonpredatory mortality rate for zooplankton (1/day).
ZEFFIC	Zooplankton assimilation efficiency or the proportion of food assimilated to food consumed (dimensionless).
PREFA	Preference factor of zooplankton for algae (dimensionless).

KINETICS

Name	Description
PREFP	Preference factor of zooplankton for detritus (dimensionless).
ZRESP	Maximum zooplankton respiration rate (1/day).
ZOOMIN	Threshold food concentration at which zooplankton feeding begins (mg/l).
ZS2P	Zooplankton half-saturation constant for food concentration (mg/l)
ZOOT1	Lower temperature for zooplankton growth (Celsius)
ZOOT2	Lower temperature for maximum zooplankton growth (Celsius)
ZOOT3	Upper temperature for maximum zooplankton growth (Celsius)
ZOOT4	Upper temperature for zooplankton growth (Celsius)
ZOOK1	Fraction of zooplankton growth rate at ZOOT1 (dimensionless)
ZOOK2	Fraction of zooplankton growth rate at ZOOT2 (dimensionless)
ZOOK3	Fraction of zooplankton growth rate at ZOOT3 (dimensionless)
ZOOK4	Fraction of zooplankton growth rate at ZOOT4 (dimensionless)
EXZ	Zooplankton light extinction (m^{-1})
O2ZR	Oxygen stoichiometry for zooplankton respiration
ZP	Stoichiometric equivalent between zooplankton biomass and phosphorus
ZN	Stoichiometric equivalent between zooplankton biomass and nitrogen
ZC	Stoichiometric equivalent between zooplankton biomass and carbon

Phosphorus

Phosphorus is an important element in aquatic ecosystems since it serves as one of the primary nutrients for phytoplankton growth. In many fresh waters, phosphorus is considered to be the nutrient limiting maximum production of phytoplankton biomass (Schindler, 1971; Schindler et al., 1973; Vollenweider, 1968, 1976).

Phosphorus is assumed to be completely available as ortho-phosphate (PO_4) for uptake by phytoplankton. Measurements of soluble reactive phosphorus are closest to the form used in the model. Macrophytes are specified as either taking P from the sediments or from the water column.

KINETICS

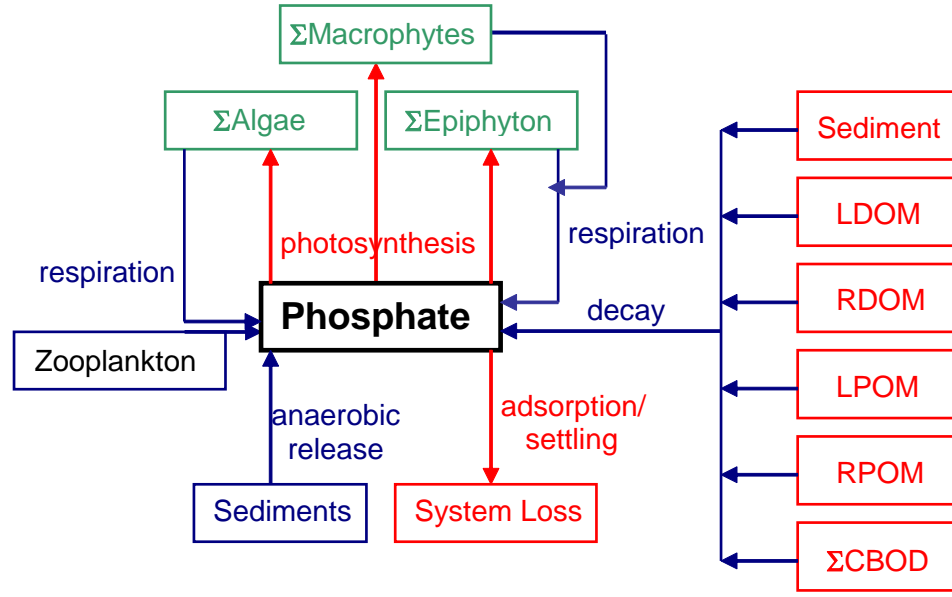


Figure B-17. Internal flux between phosphorus and other compartments.

Referring to [Figure B-17](#), the rate equation for phosphorus is:

$$\begin{aligned}
 S_p = & \underbrace{\sum (K_{ar} - K_{ag}) \delta_{Pa} \Phi_a}_{\text{algal net growth}} + \underbrace{\sum (K_{er} - K_{eg}) \delta_{Pe} \Phi_e}_{\text{epiphyton net growth}} + \underbrace{K_{LDOM} \delta_{POM} \gamma_{OM} \Phi_{LDOM}}_{\text{labile DOM decay}} \\
 & + \underbrace{K_{RDOM} \delta_{POM} \gamma_{OM} \Phi_{RDOM}}_{\text{refractory DOM decay}} + \underbrace{K_{LPOM} \delta_{POM} \gamma_{OM} \Phi_{LPOM}}_{\text{labile POM decay}} + \underbrace{K_{RPOM} \delta_{POM} \gamma_{OM} \Phi_{RPOM}}_{\text{refractory POM decay}} \\
 & + \underbrace{\sum K_{CBOD} R_{CBOD} \delta_{P-CBOD} \Theta^{T-20} \Phi_{CBOD}}_{\text{CBOD decay}} + \underbrace{K_s \delta_{POM} \gamma_{OM} \Phi_s}_{\text{1st-order sediment release}} + \underbrace{SOD \gamma_{OM} \frac{A_{sed}}{V}}_{\text{0-order sediment release}} \\
 & - \underbrace{\frac{(\sum \varpi_{ISS} \Phi_{ISS} + \omega_{Fe} \Phi_{Fe}) P_P}{\Delta Z}}_{\text{inorganic solids adsorption}} \Phi_P + \underbrace{\sum (K_{mr} - (1 - f_{psed}) K_{mg}) \delta_{Pm} \Phi_{macro}}_{\text{macrophyte net growth}} + \underbrace{\sum K_{zr} \delta_{Pz} \Phi_{zoo}}_{\text{zooplankton respiration}}
 \end{aligned} \tag{B-33}$$

where:

- Δz = model cell thickness, m
- A_{sed} = sediment surface area, m^2
- V = cell volume, m^3
- P_P = adsorption coefficient, $m^3 g^{-1}$
- f_{psed} = fraction of macrophyte phosphorus uptake from sediments
- δ_{Pe} = epiphyton stoichiometric coefficient for phosphorus
- δ_{Pa} = algal stoichiometric coefficient for phosphorus
- δ_{Pm} = macrophyte stoichiometric coefficient for phosphorus
- δ_{Pz} = zooplankton stoichiometric coefficient for phosphorus

KINETICS

δ_{POM} = organic matter stoichiometric coefficient for phosphorus
 δ_{P-CBOD} = phosphorus/CBOD stoichiometric ratio
 γ_{OM} = temperature rate multiplier for organic matter decay
 Θ = temperature rate multiplier for CBOD decay
 R_{BOD} = conversion ratio for 5-day CBOD to CBOD ultimate
 ω_{ISS} = inorganic suspended solids settling velocity, $m\ sec^{-1}$
 ω_{Fe} = particulate organic matter settling velocity, $m\ sec^{-1}$
 K_{ag} = algal growth rate, sec^{-1}
 K_{ar} = algal dark respiration rate, sec^{-1}
 K_{eg} = epiphyton growth rate, sec^{-1}
 K_{er} = epiphyton dark respiration rate, sec^{-1}
 K_{mg} = macrophyte growth rate, sec^{-1}
 K_{mr} = macrophyte respiration rate, sec^{-1}
 K_{zr} = macrophyte respiration rate, sec^{-1}
 K_{LDOM} = labile DOM decay rate, sec^{-1}
 K_{RDOM} = refractory DOM decay rate, sec^{-1}
 K_{LPOM} = labile POM decay rate, sec^{-1}
 K_{RPOM} = refractory POM decay rate, sec^{-1}
 K_{CBOD} = CBOD decay rate, sec^{-1}
 K_{sed} = sediment decay rate, sec^{-1}
 SOD = anaerobic sediment release rate, $g\ m^{-2}\ s^{-1}$
 Φ_P = phosphorus concentration, $g\ m^{-3}$
 Φ_{Fe} = total iron concentration, $g\ m^{-3}$
 Φ_{ISS} = inorganic suspended solids concentration, $g\ m^{-3}$
 Φ_a = algal concentration, $g\ m^{-3}$
 Φ_e = epiphyton concentration, $g\ m^{-3}$
 Φ_{LDOM} = labile DOM concentration, $g\ m^{-3}$
 Φ_{LPOM} = labile POM concentration, $g\ m^{-3}$
 Φ_{RDOM} = refractory DOM concentration, $g\ m^{-3}$
 Φ_{RPOM} = refractory POM concentration, $g\ m^{-3}$
 Φ_{CBOD} = CBOD concentration, $g\ m^{-3}$
 Φ_{sed} = organic sediment concentration, $g\ m^{-3}$
 Φ_{macro} = macrophyte concentration, $g\ m^{-3}$
 Φ_{zoo} = zooplankton concentration, $g\ m^{-3}$

and the rate terms are evaluated in subroutine PHOSPHORUS. In the model, the PO_4 concentration is in units of PO_4 as P.

The contribution of algae, POM, and DOM to phosphorus is given in the rate equations and [Figure B-7](#). However, effects due to settling and contribution from sediments require some additional explanation.

KINETICS

Dissolved inorganic phosphorus adsorbs onto inorganic particulates under oxic conditions and is lost when these materials settle. Loss may be rapid in the upper end of reservoirs in the riverine and transition zones due to greater concentrations of allochthonous particulates. A Langmuir isotherm describes this process. Since phosphorus concentrations are generally small, only the isotherm's linear region is utilized and is represented by the product $P_p\Phi_p$. The adsorbed solids settle at a rate equal to the solids' settling velocity. Adsorption is not allowed to occur if dissolved oxygen concentrations are less than a minimum value [\[O2LIM\]](#).

Phosphorus adsorption onto inorganic suspended solids should be used cautiously. In most systems, available phosphorus sites for adsorption onto inflowing inorganic suspended solids are generally already in use, so little adsorption takes place when inorganic suspended solids enter into a reservoir or estuary. The phosphorus formulation needs to be recast with inorganic phosphorus as the state variable that is then partitioned between dissolved and particulate forms. This will be done in a future version. However, phosphorus sorption onto iron hydroxides that form when anoxic waters come into contact with oxygen can be an important mechanism of phosphorus removal from the water column for certain waterbodies and should be included.

Sediment contribution of phosphorus to overlying waters can be simulated in three ways. In the first, the sediment compartment accumulates particulate organic matter and algae, which then decay. This is modeled as a 1st-order process. However, sediment phosphorus release depends upon sediment age, chemistry, overlying phosphorus concentrations, and other factors not included in the sediment compartment. In the second, sediments can be assigned a release rate for phosphorus that is independent of sediment concentrations. Sediments are modeled as a "black box" using a zero-order rate. Phosphorus release is only allowed to occur if the overlying water dissolved oxygen concentration is less than a minimum value [\[O2LIM\]](#). The third method is a combination of the first two where organic materials accumulate and decay in the sediments along with a background decay rate independent of organic matter accumulation in the sediments.

Ammonium

Algae use ammonium during photosynthesis to form proteins. In many estuarine applications, nitrogen is the limiting nutrient for algal growth. Macrophytes can prefer taking N from the sediments versus the water column.

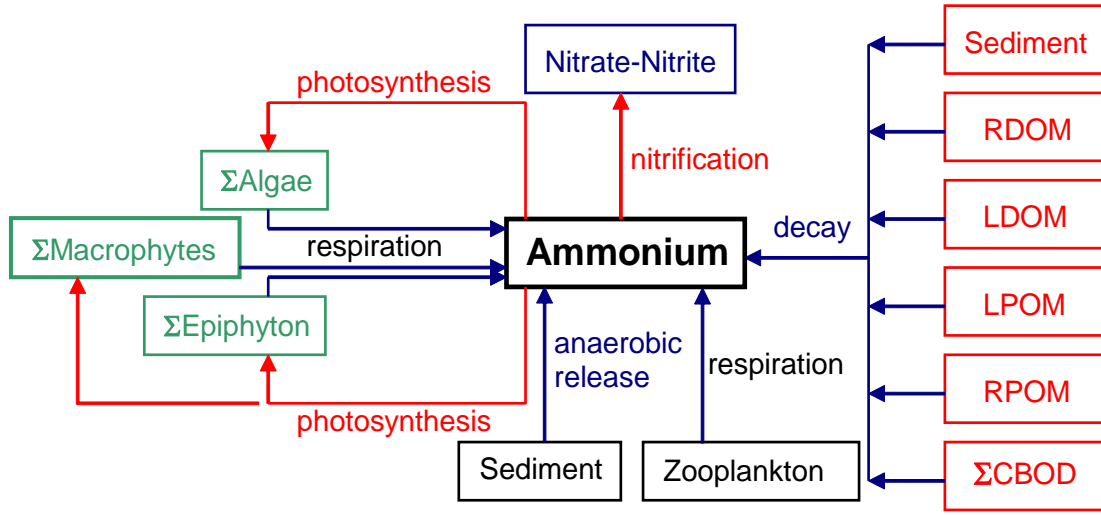


Figure B-18. Internal flux between ammonium and other compartments.

Referring to [Figure B-18](#), the rate equation for ammonium is:

$$\begin{aligned}
 S_{NH4} = & \underbrace{\sum K_{ar} \delta_{Na} \Phi_s}_{\text{algal respiration}} - \underbrace{\sum K_{ag} \delta_{Na} \Phi_a P_{NH4}}_{\text{algal growth}} + \underbrace{\sum K_{er} \delta_{Ne} \Phi_e}_{\text{epiphyton respiration}} - \underbrace{\sum K_{eg} \delta_{Ne} \Phi_e P_{NH4}}_{\text{epiphyton growth}} \\
 & + \underbrace{K_{LDOM} \delta_{NOM} \gamma_{OM} \Phi_{LDOM}}_{\text{labile DOM decay}} + \underbrace{K_{RDOM} \delta_{NOM} \gamma_{OM} \Phi_{RDOM}}_{\text{refractory DOM decay}} + \underbrace{K_{LPOM} \delta_{NOM} \gamma_{OM} \Phi_{LPOM}}_{\text{labile POM decay}} \\
 & + \underbrace{K_{RPOM} \delta_{NOM} \gamma_{OM} \Phi_{RPOM}}_{\text{refractory POM decay}} + \underbrace{K_s \delta_{NOM} \gamma_{OM} \Phi_s}_{\text{1st-order sediment release}} + \underbrace{SOD_{NH4} \gamma_{OM} \frac{A_{sed}}{V}}_{\text{0-order sediment release}} \\
 & + \underbrace{\sum K_{CBOD} R_{CBOD} \delta_{N-CBOD} \Theta^{T-20} \Phi_{CBOD}}_{\text{CBOD decay}} - \underbrace{K_{NH4} \gamma_{NH4} \Phi_{NH4}}_{\text{nitrification}} \\
 & + \underbrace{\sum (K_{mr} - (1 - f_{nsed}) K_{mg}) \delta_{Nm} \Phi_{macro}}_{\text{net macrophyte growth}} + \underbrace{\sum K_{zr} \delta_{Nz} \Phi_{zoo}}_{\text{zooplankton respiration}}
 \end{aligned}
 \tag{B-34}$$

where:

A_{sed} = sediment area, m^2

V = volume of cell, m^3

f_{nsed} = fraction of macrophyte nitrogen uptake from sediments

δ_{Na} = algal stoichiometric coefficient for nitrogen

δ_{Ne} = epiphyton stoichiometric coefficient for nitrogen

δ_{Nm} = macrophyte stoichiometric coefficient for nitrogen

δ_{Nz} = zooplankton stoichiometric coefficient for nitrogen

δ_{NOM} = organic matter stoichiometric coefficient for nitrogen

δ_{N-CBOD} = CBOD stoichiometric coefficient for nitrogen

γ_{NH4} = temperature rate multiplier for nitrification

γ_{NOx} = temperature rate multiplier for denitrification

γ_{OM} = temperature rate multiplier for organic matter decay

Θ = temperature rate multiplier for CBOD decay

R_{CBOD} = ratio of 5-day CBOD to ultimate CBOD

P_{NH4} = ammonium preference factor

K_{NOx} = nitrate-nitrogen decay rate, sec^{-1}

K_{NH4} = ammonium decay rate, sec^{-1}

K_{ar} = algal dark respiration rate, sec^{-1}

K_{ag} = algal growth rate, sec^{-1}

K_{mg} = macrophyte growth rate, sec^{-1}

K_{mr} = macrophyte respiration rate, sec^{-1}

K_{zr} = zooplankton respiration rate, sec^{-1}

K_{LDOM} = labile DOM decay rate, sec^{-1}

K_{RDOM} = refractory DOM decay rate, sec^{-1}

K_{LPOM} = labile POM decay rate, sec^{-1}

K_{RPOM} = refractory POM decay rate, sec^{-1}

K_{CBOD} = CBOD decay rate, sec^{-1}

K_{sed} = sediment decay rate, sec^{-1}

SOD_{NH4} = sediment ammonium release rate, $g\ m^{-2}\ sec^{-1}$

Φ_{ISS} = inorganic suspended solids concentration, $g\ m^{-3}$

Φ_{NH4} = ammonium concentration, $g\ m^{-3}$

Φ_a = algal concentration, $g\ m^{-3}$

Φ_{LDOM} = labile DOM concentration, $g\ m^{-3}$

Φ_{RDOM} = refractory DOM concentration, $g\ m^{-3}$

Φ_{LPOM} = labile POM concentration, $g\ m^{-3}$

Φ_{RPOM} = refractory POM concentration, $g\ m^{-3}$

Φ_{CBOD} = CBOD concentration, $g\ m^{-3}$

Φ_{macro} = macrophyte concentration, $g\ m^{-3}$

Φ_{zoo} = zooplankton concentration, $g\ m^{-3}$

Φ_{sed} = organic sediment concentration, $g\ m^{-3}$

and the rate terms are evaluated in subroutine AMMONIUM. As with phosphorus, 0-order sediment release only occurs when dissolved oxygen is less than a minimum value [\[O2LIM\]](#). Either a 0- or 1st-order process or a combination of both may be used for sediment ammonium release. In the model, the ammonia concentration is in units of NH_4 as N.

Nitrate-Nitrite

This compartment represents nitrate plus nitrite. Nitrite is an intermediate product in nitrification between ammonium and nitrate. Nitrate is used as a source of nitrogen for algae and epiphyton

during photosynthesis. Preferential uptake of ammonium over nitrate by algae and periphyton is now included.

Nitrogen may be the limiting nutrient for algae in systems with high phosphorus loadings or in estuaries. Some species of blue-green algae are capable of fixing atmospheric nitrogen for use in photosynthesis. This process can be included by setting the nitrogen half-saturation concentration for algal growth to zero.

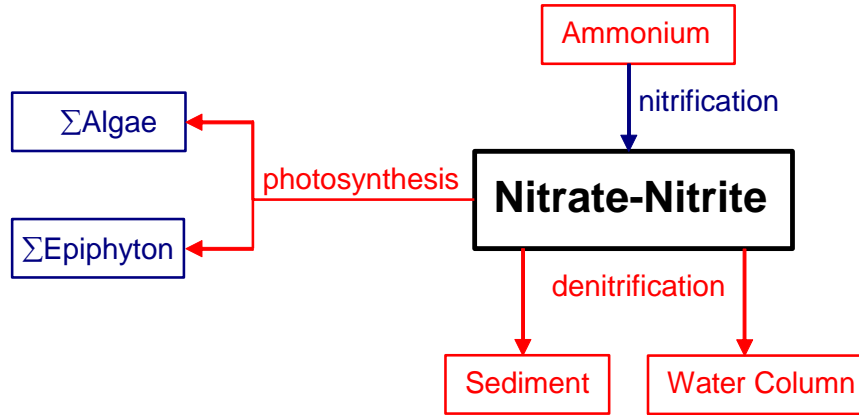


Figure B-19. Internal flux between nitrate + nitrite and other compartments.

Referring to [Figure B-19](#), the rate equation for nitrate-nitrite is:

$$\begin{aligned}
 S_{NOx} = & \underbrace{K_{NH4} \gamma_{NH4} \Phi_{NH4}}_{\text{nitrification}} - \underbrace{K_{NOx} \gamma_{NOx} \Phi_{NOx}}_{\text{water column denitrification}} - \underbrace{\omega_{NOx} \frac{\partial \Phi_{NOx}}{\partial z}}_{\text{sediment denitrification}} \\
 & - \underbrace{\sum K_{ag} \delta_{Na} \Phi_a (1 - P_{NH4})}_{\text{algal uptake}} - \underbrace{\sum K_{eg} \delta_{Ne} \Phi_e (1 - P_{NH4})}_{\text{epiphyton uptake}}
 \end{aligned} \tag{B-35}$$

where:

- γ_{NH4} = temperature rate multiplier for nitrification
- γ_{NOx} = temperature rate multiplier for denitrification
- δ_{Ne} = epiphyton stoichiometric coefficient for nitrogen
- δ_{Na} = algal stoichiometric coefficient for nitrogen
- P_{NH4} = ammonium preference factor
- K_{NH4} = nitrification rate, sec^{-1}
- K_{NOx} = denitrification rate, sec^{-1}
- K_{ag} = algal growth rate, sec^{-1}
- ω_{NOx} = sediment transfer velocity, $m sec^{-1}$
- Φ_{NH4} = ammonia-nitrogen concentration, $g m^{-3}$
- Φ_{NOx} = nitrate-nitrogen concentration, $g m^{-3}$
- Φ_a = algal concentration, $g m^{-3}$

and the rate terms are evaluated in subroutine NITRATE. Nitrification is only allowed to occur if oxygen is present, and denitrification is allowed only if dissolved oxygen is less than a specified minimum value [O2LIM]. In the model, the nitrate+nitrite concentration is in units of $\text{NO}_3 + \text{NO}_2$ as N.

Dissolved Silica

Dissolved silica is an important component of diatoms, providing the structural skeleton. In many cases diatoms can be silica limited. Dissolved silica is taken up by algae based on stoichiometric relationships and is produced by the decay of organic matter containing particulate biogenic silica. Also, dissolved silica is adsorbed onto inorganic suspended solids based on a partitioning coefficient.

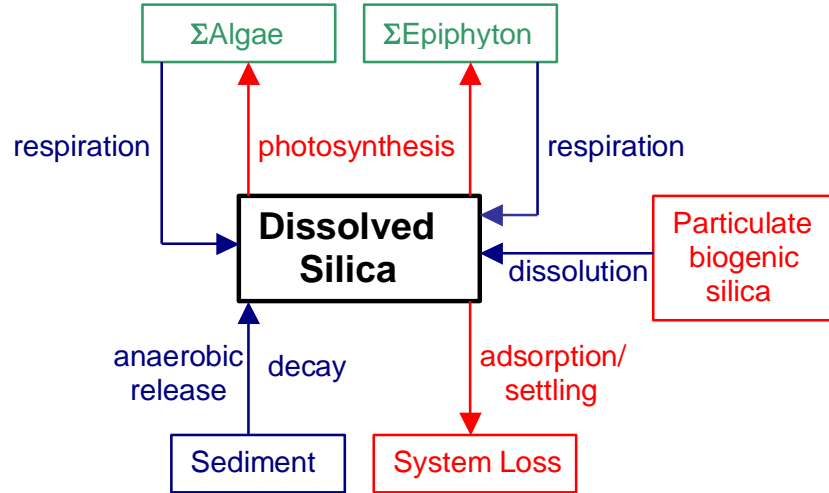


Figure B-20. Internal flux between dissolved silica and other compartments.

Referring to [Figure B-20](#), the rate equation for dissolved silica is:

$$\begin{aligned}
 S_{DSi} = & - \sum \underbrace{(K_{ag} - K_{ar}) \delta_{Si a} \Phi_a}_{\text{algal uptake}} - \sum \underbrace{(K_{eg} - K_{er}) \delta_{Si e} \Phi_e}_{\text{epiphyton uptake}} \\
 & + \underbrace{K_{sed} \delta_{Si OM} \gamma_{OM} \Phi_{sed}}_{\text{1st order sediment release}} + \underbrace{SOD \phi_{Si} \gamma_{OM} \frac{A_{sed}}{V}}_{\text{0-order sediment release}} + \underbrace{K_{PSi} \gamma_{OM} \Phi_{PSi}}_{\text{particulate biogenic decay}} \\
 & - \underbrace{\frac{P_{Si} (\sum \omega_{ss} \Phi_{ss} + \omega_{POM} \Phi_{POML} + \omega_{POM} \Phi_{POMR} + \omega_{Fe} \Phi_{Fe})}{\Delta z}}_{\text{inorganic solids adsorption and settling}} \Phi_{DSi}
 \end{aligned} \tag{B-36}$$

where:

θ = temperature rate factor for BOD decay

- γ_{OM} = temperature rate multiplier for organic matter decay
 φ_{Si} = fraction of SOD for silica release
 Δz = computational cell height, m
 δ_{Sie} = epiphyton stoichiometric ratio for silica
 δ_{Sia} = algal stoichiometric ratio for silica
 δ_{SiOM} = sediment organic matter stoichiometric ratio for silica
 A_{sed} = sediment area, m^2
 V = computational cell volume, m^3
 P_{Si} = silica adsorption coefficient, $m^3 g^{-1}$
 SOD = sediment oxygen demand, $g m^{-2} sec^{-1}$
 ω_{ISS} = inorganic suspended solids settling velocity, $m sec^{-1}$
 K_{ag} = algal growth rate, sec^{-1}
 K_{eg} = epiphyton growth rate, sec^{-1}
 K_{sed} = sediment decay rate, sec^{-1}
 Φ_a = algal concentration, $g m^{-3}$
 Φ_e = epiphyton concentration, $g m^{-3}$
 Φ_{sed} = organic sediment mass, g
 Φ_{ISS} = inorganic suspended solids concentration, $g m^{-3}$
 Φ_{DSi} = dissolved silica concentration, $g m^{-3}$
 Φ_{Fe} = total iron concentration, $g m^{-3}$

Organic Matter Variable Stoichiometry

The CE-QUAL-W2 model includes a feature starting with V3.5 which allows for the variable stoichiometry of organic matter. Past versions of W2 models have used fixed stoichiometric constants for the ratios of nitrogen and phosphorus to organic matter.

Eight new constituents were required to simulate the amount of nitrogen and phosphorus in labile dissolved organic matter (LDOM), refractory organic matter (RDOM), labile particulate organic matter (LPOM), and refractory particulate organic matter (RPOM). These constituents were summarized in Table 14. Hence, all inputs of organic matter accumulate N and P according to the stoichiometry of the incoming organic matter.

Table 14. Constituents used for variable stoichiometry of organic matter.

Abbreviation	Constituent
LDOM-P	Labile Dissolved Organic Matter – Phosphorus
RDOM-P	Refractory Dissolved Organic Matter – Phosphorus
LPOM-P	Labile Particulate Organic Matter – Phosphorus
RPOM-P	Refractory Particulate Organic Matter – Phosphorus
LDOM-N	Labile Dissolved Organic Matter – Nitrogen
RDOM-N	Refractory Dissolved Organic Matter – Nitrogen
LPOM-N	Labile Particulate Organic Matter – Nitrogen

RPOM-N	Refractory Particulate Organic Matter – Nitrogen
--------	--

These state variables are used in the model when that constituent is active.

Labile Dissolved Organic Matter – Phosphorus (LDOM-P)

LDOM-P is the amount of phosphorus in labile dissolved organic matter.

The rate equation of LDOM-P is:

$$\begin{aligned}
 S_{\text{LDOM-P}} = & \underbrace{\sum K_{ae} \delta_{Pa} \Phi_a}_{\text{algal excretion}} + \underbrace{\sum (1 - P_{am}) K_{am} \delta_{Pa} \Phi_a}_{\text{algal mortality}} + \underbrace{\sum K_{ee} \delta_{Pe} \Phi_e}_{\text{epiphyton excretion}} \\
 & + \underbrace{\sum (1 - P_{em}) K_{em} \delta_{Pe} \Phi_e}_{\text{epiphyton mortality}} + \underbrace{\sum (1 - P_{mm}) K_{mm} \delta_{Pm} \Phi_m}_{\text{macrophyte mortality}} - \underbrace{K_{\text{LDOM}} \gamma_{\text{OM}} \Phi_{\text{LDOM-P}}}_{\text{labile DOM-P decay}} - \underbrace{K_{\text{L} \rightarrow \text{R}} \gamma_{\text{OM}} \Phi_{\text{LDOM-P}}}_{\text{labile to refractory DOM-P decay}}
 \end{aligned}$$

where:

P_{am} = pattern coefficient for algal mortality

P_{em} = pattern coefficient for epiphyton mortality

γ_{OM} = temperature rate multiplier for organic matter decay

$\delta_{\text{P-LDOM}}$ = LDOM stoichiometric ratio for phosphorus

δ_{Pe} = epiphyton stoichiometric coefficient for phosphorus

δ_{Pa} = algal stoichiometric coefficient for phosphorus

δ_{Pm} = macrophyte stoichiometric coefficient for phosphorus

K_{ae} = algal excretion rate, sec^{-1}

K_{am} = algal mortality rate, sec^{-1}

K_{ee} = epiphyton excretion rate, sec^{-1}

K_{em} = epiphyton mortality rate, sec^{-1}

K_{mm} = macrophyte mortality rate, sec^{-1}

K_{LDOM} = labile DOM decay rate, sec^{-1}

$K_{\text{L} \rightarrow \text{R}}$ = labile to refractory DOM transfer rate, sec^{-1}

Φ_a = algal concentration, g m^{-3}

Φ_m = macrophyte concentration, g m^{-3}

Φ_e = epiphyton concentration, g m^{-3}

$\Phi_{\text{LDOM-P}}$ = labile DOM-P concentration, g m^{-3}

Refractory Dissolved Organic Matter – Phosphorus (RDOM-P)

RDOM-P is the amount of phosphorus in refractory dissolved organic matter.

The rate equation of LDOM-P is:

$$S_{RDOM-P} = \underbrace{K_{L \rightarrow R} \Phi_{L DOM-P}}_{\substack{\text{labile to refractory} \\ \text{DOM decay}}} - \underbrace{\gamma_{OM} K_{R DOM} \Phi_{R DOM-P}}_{\text{decay}}$$

$\Phi_{L DOM-P}$ = labile DOM-P concentration, $g\ m^{-3}$

Labile Particulate Organic Matter – Phosphorus (LPOM-P)

LPOM-P is the amount of phosphorus in refractory dissolved organic matter.

The rate equation of LPOM-P is:

$$\begin{aligned} S_{LPOM-P} = & \underbrace{\sum P_{am} K_{am} \delta_{Pa} \Phi_a}_{\text{algal mortality}} + \underbrace{\sum P_{em} K_{em} \delta_{Pe} \Phi_e}_{\text{epiphyton mortality}} + \underbrace{\sum P_{mm} P_{mpom} K_{mm} \delta_{Pm} \Phi_m}_{\text{macrophyte mortality}} + \underbrace{K_{zm} \delta_{Pz} \Phi_{zoo}}_{\text{zooplankton mortality}} \\ & - \underbrace{K_{LPOM} \gamma_{OM} \Phi_{LPOM-P}}_{\text{decay}} - \underbrace{K_{L \rightarrow R} \Phi_{LPOM-P}}_{\substack{\text{labile to refractory} \\ \text{POM decay}}} + \underbrace{K_{zg} (1 - Z_{effic}) \delta_{Pz} \Phi_{zoo}}_{\text{zooplankton}} \\ & - \underbrace{K_{zg} \frac{\Phi_{LPOM-P}}{\Phi_{LPOM}} \left(\frac{\sigma_{pom} \Phi_{LPOM}}{\sigma_{alg} \sum \Phi_a + \sigma_{pom} \Phi_{LPOM}} \right) \Phi_{zoo}}_{\text{zooplankton ingestion}} - \underbrace{\omega_{POM} \frac{\partial \Phi_{LPOM-P}}{\partial Z}}_{\text{settling}} \end{aligned}$$

where:

P_{am} = partition coefficient for algal mortality

P_{em} = partition coefficient for epiphyton mortality

P_{mm} = partition coefficient for macrophyte mortality

P_{mpom} = partition coefficient for RPOM and LPOM from macrophyte mortality

γ_{OM} = temperature rate multiplier for organic matter

σ_{alg} = Zooplankton preference fraction for algae

σ_{pom} = Zooplankton preference fraction for particulate organic matter

ω_{POM} = POM settling rate, $m\ sec^{-1}$

K_{am} = algal mortality rate, sec^{-1}

K_{em} = epiphyton mortality rate, sec^{-1}

K_{zm} = zooplankton mortality rate, sec^{-1}

K_{mm} = macrophyte mortality rate, sec^{-1}

K_{LPOM} = labile POM decay rate, sec^{-1}

$K_{L \rightarrow R}$ = transfer rate from labile POM to refractory POM, sec^{-1}

Φ_a = algal concentration, $g\ m^{-3}$

Φ_{zoo} = algal concentration, $g\ m^{-3}$

Φ_e = epiphyton concentration, $g\ m^{-3}$

Φ_{LPOM} = LPOM concentration, $g\ m^{-3}$

Φ_{LPOM-P} = LPOM-P concentration, $g\ m^{-3}$

Refractory Particulate Organic Matter – Phosphorus (RPOM-P)

RPOM-P is the amount of phosphorus in refractory dissolved organic matter.

The rate equation of LPOM-P is:

$$S_{RPOM} = \underbrace{K_{L \rightarrow R} \Phi_{LPOM-P}}_{\text{labile to refractory POM decay}} - \underbrace{\gamma_{OM} K_{RPOM} \Phi_{RPOM-P}}_{\text{decay}} + \underbrace{\sum P_{mm} (1 - P_{mpom}) K_{mm} \delta_{Pm} \Phi_m}_{\text{macrophyte mortality}} - \underbrace{\omega_{POM} \frac{\partial \Phi_{RPOM-P}}{\partial z}}_{\text{settling}}$$

where:

P_{mm} = partition coefficient for macrophyte mortality

P_{mpom} = partition coefficient for RPOM and LPOM from macrophyte mortality

δ_{Pm} = macrophyte stoichiometric coefficient for phosphorus

γ_{OM} = temperature rate multiplier

$K_{L \rightarrow R}$ = transfer rate from labile POM to refractory POM, sec^{-1}

K_{RPOM} = refractory POM decay rate, sec^{-1}

K_{mm} = macrophyte mortality rate, sec^{-1}

ω_{RPOM} = POM settling velocity, m/sec^{-1}

Φ_{LPOM-P} = labile POM concentration, $g\ m^{-3}$

Φ_{RPOM-P} = refractory POM phosphorus concentration, $g\ m^{-3}$

Labile Dissolved Organic Matter – Nitrogen (LDOM-N)

LDOM-N is the amount of nitrogen in labile dissolved organic matter.

The rate equation of LDOM-N is:

$$S_{LDOM-N} = \underbrace{\sum K_{ae} \delta_{Na} \Phi_a}_{\text{algal excretion}} + \underbrace{\sum (1 - P_{am}) K_{am} \delta_{Na} \Phi_a}_{\text{algal mortality}} + \underbrace{\sum K_{ee} \delta_{Ne} \Phi_e}_{\text{epiphyton excretion}} + \underbrace{\sum (1 - P_{em}) K_{em} \delta_{Ne} \Phi_e}_{\text{epiphyton mortality}} + \underbrace{\sum (1 - P_{mm}) K_{mm} \delta_{Nm} \Phi_m}_{\text{macrophyte mortality}} - \underbrace{K_{LDOM} \gamma_{OM} \Phi_{LDOM-N}}_{\text{labile DOM-N decay}} - \underbrace{K_{L \rightarrow R} \gamma_{OM} \Phi_{LDOM-N}}_{\text{labile to refractory DOM-N decay}}$$

where:

- P_{am} = pattern coefficient for algal mortality
 P_{em} = pattern coefficient for epiphyton mortality
 γ_{OM} = temperature rate multiplier for organic matter decay
 δ_{P-LDOM} = LDOM stoichiometric ratio for nitrogen
 δ_{Ne} = epiphyton stoichiometric coefficient for nitrogen
 δ_{Na} = algal stoichiometric coefficient for nitrogen
 δ_{Nm} = macrophyte stoichiometric coefficient for nitrogen
 K_{ae} = algal excretion rate, sec^{-1}
 K_{am} = algal mortality rate, sec^{-1}
 K_{ee} = epiphyton excretion rate, sec^{-1}
 K_{em} = epiphyton mortality rate, sec^{-1}
 K_{mm} = macrophyte mortality rate, sec^{-1}
 K_{LDOM} = labile DOM decay rate, sec^{-1}
 $K_{L \rightarrow R}$ = labile to refractory DOM transfer rate, sec^{-1}
 Φ_a = algal concentration, $g\ m^{-3}$
 Φ_m = macrophyte concentration, $g\ m^{-3}$
 Φ_e = epiphyton concentration, $g\ m^{-3}$
 Φ_{LDOM-N} = labile DOM-N concentration, $g\ m^{-3}$

Refractory Dissolved Organic Matter – Nitrogen (RDOM-N)

RDOM-N is the amount of nitrogen in refractory dissolved organic matter.

The rate equation of LDOM-N is:

$$S_{RDOM-N} = \underbrace{K_{L \rightarrow R} \Phi_{LDOM-N}}_{\text{labile to refractory DOM decay}} - \underbrace{\gamma_{OM} K_{RDOM} \Phi_{RDOM-N}}_{\text{decay}}$$

Where

Φ_{LDOM-N} = labile DOM-N concentration, $g\ m^{-3}$

Labile Particulate Organic Matter – Nitrogen (LPOM-N)

LPOM-N is the amount of nitrogen in refractory dissolved organic matter.

The rate equation of LPOM-N is:

$$\begin{aligned}
S_{LPOM-N} = & \underbrace{\sum P_{am} K_{am} \delta_{Na} \Phi_a}_{\text{algal mortality}} + \underbrace{\sum P_{em} K_{em} \delta_{Ne} \Phi_e}_{\text{epiphyton mortality}} + \underbrace{\sum P_{mm} P_{mpom} K_{mm} \delta_{Nm} \Phi_m}_{\text{macrophyte mortality}} + \underbrace{K_{zm} \delta_{Nz} \Phi_{zoo}}_{\text{zooplankton mortality}} \\
& - \underbrace{K_{LPOM} \gamma_{OM} \Phi_{LPOM-N}}_{\text{decay}} - \underbrace{K_{L \rightarrow R} \Phi_{LPOM-N}}_{\text{labile to refractory POM decay}} + \underbrace{K_{zg} (1 - Z_{effic}) \delta_{Nz} \Phi_{zoo}}_{\text{zooplankton}} \\
& - \underbrace{K_{zg} \frac{\Phi_{LPOM-N}}{\Phi_{LPOM}} \left(\frac{\sigma_{pom} \Phi_{LPOM}}{\sigma_{alg} \sum \Phi_a + \sigma_{pom} \Phi_{LPOM}} \right) \Phi_{zoo}}_{\text{zooplankton ingestion}} - \underbrace{\omega_{POM} \frac{\partial \Phi_{LPOM-N}}{\partial Z}}_{\text{settling}}
\end{aligned}$$

where:

- P_{am} = partition coefficient for algal mortality
- P_{em} = partition coefficient for epiphyton mortality
- P_{mm} = partition coefficient for macrophyte mortality
- P_{mpom} = partition coefficient for RPOM and LPOM from macrophyte mortality
- γ_{OM} = temperature rate multiplier for organic matter
- σ_{alg} = Zooplankton preference fraction for algae
- σ_{pom} = Zooplankton preference fraction for particulate organic matter
- ω_{POM} = POM settling rate, $m \text{ sec}^{-1}$
- K_{am} = algal mortality rate, sec^{-1}
- K_{em} = epiphyton mortality rate, sec^{-1}
- K_{zm} = zooplankton mortality rate, sec^{-1}
- K_{mm} = macrophyte mortality rate, sec^{-1}
- K_{LPOM} = labile POM decay rate, sec^{-1}
- $K_{L \rightarrow R}$ = transfer rate from labile POM to refractory POM, sec^{-1}
- Φ_a = algal concentration, $g \text{ m}^{-3}$
- Φ_{zoo} = algal concentration, $g \text{ m}^{-3}$
- Φ_e = epiphyton concentration, $g \text{ m}^{-3}$
- Φ_{LPOM} = LPOM concentration, $g \text{ m}^{-3}$
- Φ_{LPOM-N} = LPOM-N concentration, $g \text{ m}^{-3}$

Refractory Particulate Organic Matter – Nitrogen (RPOM-N)

RPOM-N is the amount of nitrogen in refractory dissolved organic matter.

The rate equation of LPOM-N is:

$$\begin{aligned}
S_{RPOM} = & \underbrace{K_{L \rightarrow R} \Phi_{LPOM-N}}_{\text{labile to refractory POM decay}} - \underbrace{\gamma_{OM} K_{RPOM} \Phi_{RPOM-N}}_{\text{decay}} + \underbrace{\sum P_{mm} (1 - P_{mpom}) K_{mm} \delta_{Nm} \Phi_m}_{\text{macrophyte mortality}} \\
& - \underbrace{\omega_{POM} \frac{\partial \Phi_{RPOM-N}}{\partial z}}_{\text{settling}}
\end{aligned}$$

where:

P_{mm} = partition coefficient for macrophyte mortality

P_{mpom} = partition coefficient for RPOM and LPOM from macrophyte mortality

γ_{OM} = temperature rate multiplier

δ_{Nm} = macrophyte stoichiometric coefficient for nitrogen

$K_{L \rightarrow R}$ = transfer rate from labile POM to refractory POM, sec^{-1}

K_{RPOM} = refractory POM decay rate, sec^{-1}

K_{mm} = macrophyte mortality rate, sec^{-1}

ω_{RPOM} = POM settling velocity, m/sec^{-1}

Φ_{LPOM-N} = labile POM-N concentration, $g\ m^{-3}$

Φ_{RPOM-N} = refractory POM-N concentration, $g\ m^{-3}$

Particulate Biogenic Silica

Particulate biogenic silica results from diatom mortality and settles and also dissolves to form dissolved silica.

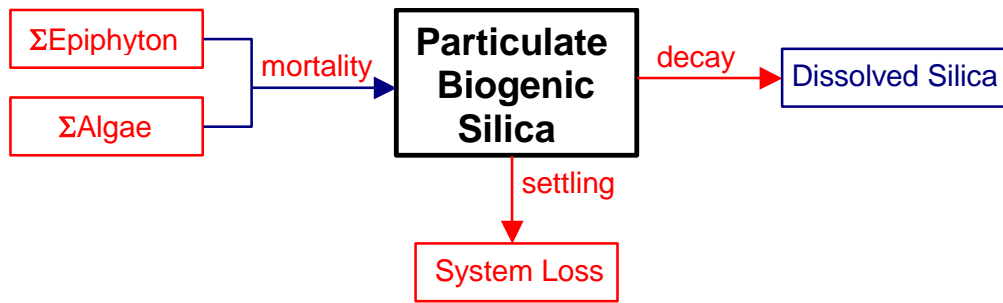


Figure B-21. Internal flux between particulate biogenic silica and other compartments

Referring to [Figure B-21](#), the rate equation for particulate biogenic silica is:

$$S_{PSi} = \underbrace{P_{am} \delta_{Sia} K_{am} \Phi_a}_{\text{algae mortality}} + \underbrace{P_{em} \delta_{Sie} K_{em} \Phi_e}_{\text{epiphyton mortality}} - \underbrace{K_{PSi} \gamma_{OM} \Phi_{PSi}}_{\text{decay}} - \underbrace{\omega_{PSi} \frac{\partial \Phi_{PSi}}{\partial z}}_{\text{settling}} \quad (\text{B-37})$$

where:

- P_{am} = partition coefficient for algal mortality
- δ_{sie} = epiphyton stoichiometric coefficient for silica
- δ_{sia} = algal stoichiometric coefficient for silica
- γ_{OM} = temperature rate multiplier for organic matter
- P_{em} = partition coefficient for epiphyton mortality
- K_{am} = algal mortality rate, sec^{-1}
- K_{em} = epiphyton mortality rate, sec^{-1}
- K_{PSi} = particulate biogenic silica decay rate, sec^{-1}
- ω_{PSi} = particulate biogenic silica settling rate, $m\ sec^{-1}$
- Φ_e = epiphyton concentration, $g\ m^{-3}$
- Φ_a = algal concentration, $g\ m^{-3}$
- Φ_{PSi} = particulate biogenic silica concentration, $g\ m^{-3}$

Total Iron

Total iron is included in the model primarily because of its effect on nutrient concentrations through adsorption and settling. Iron is commonly released from anoxic sediments and may influence nutrient dynamics in many reservoirs. Iron may also contribute to dissolved oxygen depletions, but the model does not presently include these effects. Iron sediment release is modeled as a zero-order process.

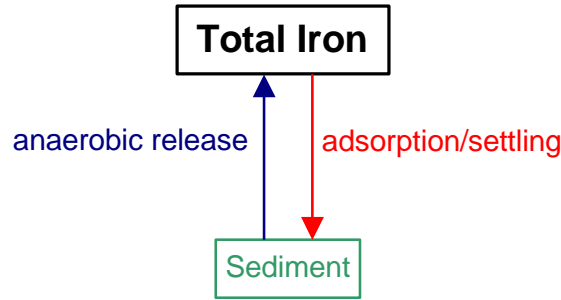


Figure B-22. Internal flux between total iron and other compartments.

Referring to [Figure B-22](#), the rate equation for total iron is:

$$S_{Fe} = \underbrace{SOD \gamma_{om} A_s}_{\text{0-order sediment release}} - \underbrace{\frac{\omega_{Fe} \partial \Phi_{Fe}}{\partial z}}_{\text{oxic water column settling}} \quad (\text{B-38})$$

where:

$$A_s = \text{sediment area, } m^2$$

γ_{OM} = temperature rate multiplier
 ω_{Fe} = settling velocity, $m\ sec^{-1}$
 Φ_{Fe} = total iron concentration, $g\ m^{-3}$
 SOD = sediment oxygen demand, $g\ m^{-2}\ sec^{-1}$.

Dissolved Oxygen

Oxygen is one of the most important elements in aquatic ecosystems. It is essential for higher forms of life, controls many chemical reactions through oxidation, and is a surrogate variable indicating the general health of aquatic systems.

CE-QUAL-W2 includes both aerobic and anaerobic processes. The ability to model anaerobic periods is important since it provides information on potential problems with water quality. Simulations can be used to identify possibilities for both metalimnetic and hypolimnetic oxygen depletion and its impact on various water control management alternatives. If a single variable were to be measured in aquatic systems that would provide maximum information about the system state, it would be dissolved oxygen.

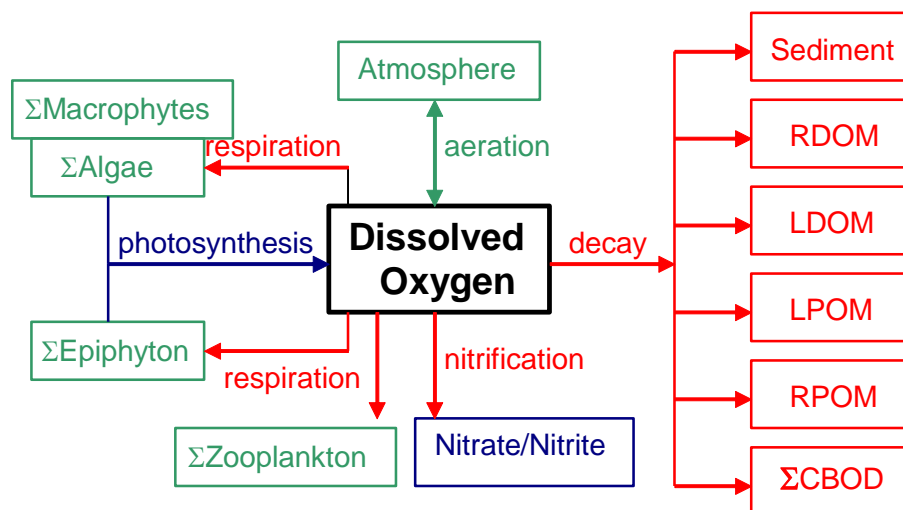


Figure B-23. Internal flux between dissolved oxygen and other compartments.

Referring to [Figure B-23](#), the rate equation for dissolved oxygen is:

$$\begin{aligned}
S_{DO} = & \underbrace{\sum (K_{ag} - K_{ar}) \delta_{OMa} \Phi_a}_{\text{algal net production}} + \underbrace{\sum (K_{eg} - K_{er}) \delta_{OMe} \Phi_e}_{\text{epiphyton net production}} + \underbrace{A_{sur} K_L (\Phi'_{DO} - \Phi_{DO})}_{\text{aeration}} \\
& - \underbrace{K_{RPOM} \delta_{OM} \gamma_{OM} \Phi_{RPOM}}_{\text{refractory POM decay}} - \underbrace{K_{LPOM} \delta_{OM} \gamma_{OM} \Phi_{LPOM}}_{\text{labile POM decay}} - \underbrace{K_{LDOM} \gamma_{OM} \delta_{OM} \Phi_{LDOM}}_{\text{labile DOM decay}} \\
& - \underbrace{K_{RDOM} \delta_{OM} \gamma_{OM} \Phi_{RDOM}}_{\text{refractory DOM decay}} - \underbrace{K_s \delta_{OM} \gamma_{OM} \Phi_{sed}}_{\text{1st-order sediment decay}} - \underbrace{SOD \gamma_{OM} \frac{A_{sed}}{V}}_{\text{0-order SOD}} \\
& - \underbrace{\sum K_{CBOD} R_{CBOD} \Theta^{T-20} \Phi_{CBOD}}_{\text{CBOD decay}} - \underbrace{K_{NH4} \delta_{NH4} \gamma_{NH4} \Phi_{NH4}}_{\text{nitrification}} + \underbrace{\sum (K_{mg} - K_{mr}) \delta_{OMmac} \Phi_{macro}}_{\text{macrophyte net production}} \\
& - \underbrace{\sum \gamma_{zoo} K_{zr} \delta_{OMzoo} \Phi_{zoo}}_{\text{zooplankton respiration}}
\end{aligned}
\tag{B-39}$$

where:

δ_{OMa} = oxygen stoichiometric coefficient for algal organic matter

δ_{OMe} = oxygen stoichiometric coefficient for epiphyton organic matter

δ_{OMmac} = oxygen stoichiometric coefficient for macrophyte organic matter

δ_{OM} = oxygen stoichiometric coefficient for organic matter

δ_{NH4} = oxygen stoichiometric coefficient for nitrification

δ_{OMzoo} = oxygen stoichiometric coefficient for zooplankton

γ_{NH4} = temperature rate multiplier for nitrification

γ_{OM} = temperature rate multiplier for organic matter decay

γ_{zoo} = temperature rate multiplier for zooplankton

R_{BOD} = conversion from CBOD in the model to CBOD ultimate

Θ = BOD temperature rate multiplier

V = volume of computational cell, m^3

T = temperature, $^{\circ}C$

A_{sed} = sediment surface area, m^2

A_{sur} = water surface area, m^2

K_{ag} = algal growth rate, sec^{-1}

K_{ar} = algal dark respiration rate, sec^{-1}

K_{eg} = epiphyton growth rate, sec^{-1}

K_{er} = epiphyton dark respiration rate, sec^{-1}

K_{mg} = macrophyte growth rate, sec^{-1}

K_{mr} = macrophyte dark respiration rate, sec^{-1}

K_{zr} = zooplankton respiration rate, sec^{-1}

K_{NH4} = ammonia decay (nitrification) rate, sec^{-1}

K_{LDOM} = labile DOM decay rate, sec^{-1}

K_{RDOM} = refractory DOM decay rate, sec^{-1}

K_{LPOM} = labile POM decay rate, sec^{-1}

K_{RPOM} = refractory POM decay rate, sec^{-1}

K_{BOD} = CBOD decay rate, sec^{-1}

- K_{sed} = sediment decay rate, sec^{-1}
 SOD = sediment oxygen demand, $g\ m^{-2}\ sec^{-1}$
 K_L = interfacial exchange rate for oxygen, $m\ sec^{-1}$
 Φ_{NH4} = ammonia-nitrogen concentration, $g\ m^{-3}$
 Φ_a = algal concentration, $g\ m^{-3}$
 Φ_e = epiphyton concentration, $g\ m^{-3}$
 Φ_{zoo} = zooplankton concentration, $g\ m^{-3}$
 Φ_{macr} = macrophyte concentration, $g\ m^{-3}$
 Φ_{LDOM} = labile DOM concentration, $g\ m^{-3}$
 Φ_{RDOM} = refractory DOM concentration, $g\ m^{-3}$
 Φ_{LPOM} = labile POM concentration, $g\ m^{-3}$
 Φ_{RPOM} = refractory POM concentration, $g\ m^{-3}$
 Φ_{BOD} = CBOD concentration, $g\ m^{-3}$
 Φ_{sed} = organic sediment concentration, $g\ m^{-3}$
 Φ_{DO} = dissolved oxygen concentration, $g\ m^{-3}$
 Φ'_{DO} = saturation DO concentration, $g\ m^{-3}$

and the rate terms are evaluated in subroutine DISSOLVED_OXYGEN. Decay is not allowed to occur when dissolved oxygen concentrations are zero. A Monod formulation is used though to move gradually from oxic to anoxic conditions. This is accomplished by reducing temperature rate multipliers eventually to zero as dissolved oxygen concentrations are zero.

This reduction of oxic reactions as dissolved oxygen levels approach zero is based on specification of a dissolved oxygen half-saturation constant in the following equation:

$$Rate\ Reduction = \frac{\Phi_{DO}}{K_{DO} + \Phi_{DO}} \text{ where } \Phi_{DO} \text{ is the concentration of dissolved oxygen and } K_{DO} \text{ is}$$

a half-saturation dissolved oxygen concentration when oxic reactions are half of their maximum without limitation of oxygen conditions.

Since the river basin model will encompass waterbodies that are dependent on boundary shear in river segments and wind stress for lake or reservoir segments for turbulence, the reaeration formulae for these systems must be different. In the following sections, formulae for reaeration as a function of wind speed and boundary shear are presented. The user has the ability to select a different formulation for each waterbody type selected. The reason for selecting a waterbody type is to force the user to select a system that best approximates the theory being used. The possible water body types are RIVER, LAKE, or ESTUARY.

River Reaeration Equations

Reaeration equations for rivers are given in [Table B-15](#). Most of these equations are based on field studies of selected streams or laboratory channels. Equations 7 and 8 were developed from Melting and Flores (1999) for a large data set of reaeration coefficients. These may be the best choice for rivers even though other equations have been used extensively.

Recently, Moog and Jirka (1998) suggested that formulations that do not account for channel slope should not be used. Therefore, equations 7 and 8 may again be the best selection of equations for river sections.

Thomann and Mueller (1987) suggested using Equation 1 except for small streams where Equation 3 for flow less than 10 cfs should be used. They also suggested a minimum value of K_L of 0.6 m day⁻¹. This value has been implemented as a lower limit in the code.

Mills et al. (1985) in a review of water quality reaeration coefficients used a different formulation than equation 3 in [Table B-15](#) based on a 1978 reference at 25°C:

$$\begin{aligned} K_a &= 7776US \quad \text{for } Q < 10 \text{ cfs} \\ K_a &= 4665.6US \quad \text{for } 10 < Q < 3000 \text{ cfs} \\ K_a &= 2592US \quad \text{for } Q > 3000 \text{ cfs} \end{aligned} \quad (\text{B-40})$$

where S is the slope in ft/ft and U is velocity in ft/s

However, Mills et al. (1985) only recommend its use for shallow low-flow streams. Therefore, equation 3 in [Table B-15](#) is exactly the same as the above formulation in the low flow regime (note that the slopes in Equation 3 are in ft/mile and in the above equation are unitless).

Covar (1976) used an approach where the equations of O'Connor-Dobbins, Churchill, and Owens were used together based on the applicability of each equation. The applicability of each equation was based on the velocity of the stream and its depth. This is equation 0 in the following table.

Table B-15. River reaeration equations.

#	Equation	Comments	Applicability	Reference
0	Either Eq 1, 2 or 4	K_a – evaluated based on applicability criteria of these equations		Covar (1976)
1	$K_a = \frac{K_L}{H} = \frac{(D_{O_2} U)^{1/2}}{H^{3/2}}$	D_{O_2} = H ₂ O molecular diffusion, m ² s ⁻¹ U = average velocity, m s ⁻¹ H = average channel depth, m	depths between 1-30 ft and velocities between 0.5-1.6 fps	O'Connor and Dobbins (1958)
2	$K_a = \frac{K_L}{H} = \frac{11.6U}{H^{1.67}}$	U, ft s ⁻¹ H, ft K_a , day ⁻¹	depths between 2-11 ft and velocities between 1.8-5 fps	Churchill, Elmore and Buckingham (1962)
3	$K_a = 0.88US \text{ for } 10 < Q < 300 \text{ cfs}$ $K_a = 1.8US \text{ for } 1 < Q < 10 \text{ cfs}$	S, ft mile ⁻¹ U, ft s ⁻¹ K_a , day ⁻¹	suggested for use when Q < 10cfs	Tsivoglou and Wallace (1972)
4	$K_a = \frac{K_L}{H} = \frac{21.6U^{0.67}}{H^{1.85}}$	U, ft s ⁻¹ H, ft	depths between 0.4-2.4 ft and velocities between 0.1-1.8 fps	Owens et al. (1964)
5	$K_a = \frac{K_L}{H} = \frac{25u^*}{H} (1 + F^{0.5})$	u^* = shear velocity, (HSg) ^{0.5} S = slope of energy grade line F = Froude number, U/(gH) ^{0.5}		Thackston and Krenkel (1966)

#	Equation	Comments	Applicability	Reference
6	$K_a = \frac{K_L}{H} = \frac{7.62U}{H^{1.33}}$	$U, \text{ ft s}^{-1}$ $H, \text{ ft}$		Langbien and Durum (1967)
7	$K_a = 517(US)^{0.524} Q^{-0.242} \text{ for } Q < 0.556$ $K_a = 596(US)^{0.528} Q^{-0.136} \text{ for } Q > 0.556$	$U, \text{ m s}^{-1}$ $S, \text{ m m}^{-1}$ $Q, \text{ m}^3 \text{ s}^{-1}$ $K_a, \text{ day}^{-1}$	for pool and riffle streams	Melching and Flores (1999)
8	$K_a = 88(US)^{0.313} D^{-0.353} \text{ for } Q < 0.556$ $K_a = 142(US)^{0.333} D^{-0.66} W^{-0.243} \text{ for } Q > 0.556$	$U, \text{ m s}^{-1}$ $S, \text{ m m}^{-1}$ $W = \text{stream top width, m}$ $D = \text{average depth, m}$ $K_a, \text{ day}^{-1}$	for channel-control streams	Melching and Flores (1999)
9	w/ channel slope - $K_a = C_1 U^{C_2} H^{C_3} S^{C_4}$ w/o channel slope - $K_a = C_1 U^{C_2} H^{C_3}$	$U, \text{ m s}^{-1}$ $H, \text{ m}$ $S, \text{ non-dimensional}$ $K_a, \text{ day}^{-1}$ $C_1, C_2, C_3, C_4 = \text{user defined parameters}$	User defined relationship	
10	$K_a = \frac{K_L}{H} = \frac{5.0u^*}{H} (1 + 9F^{0.25})$	$u^* = \text{shear velocity, (HSg)}^{0.5}$ $S = \text{slope of energy grade line}$ $F = \text{Froude number, } U/(gH)^{0.5}$ $K_a, \text{ day}^{-1}$		Thackston and Dawson (2001)

Figure B-24 shows the functional dependence of these formulae assuming the following relationship between flow (Q , ft^3/s), velocity (V , ft/s) and depth (H , ft) (St. John et al., 1984):

$$V = 0.033 Q^{0.5}$$

$$H = 0.475 Q^{0.4}$$

$$S = 5.2 \text{ ft/mile}$$

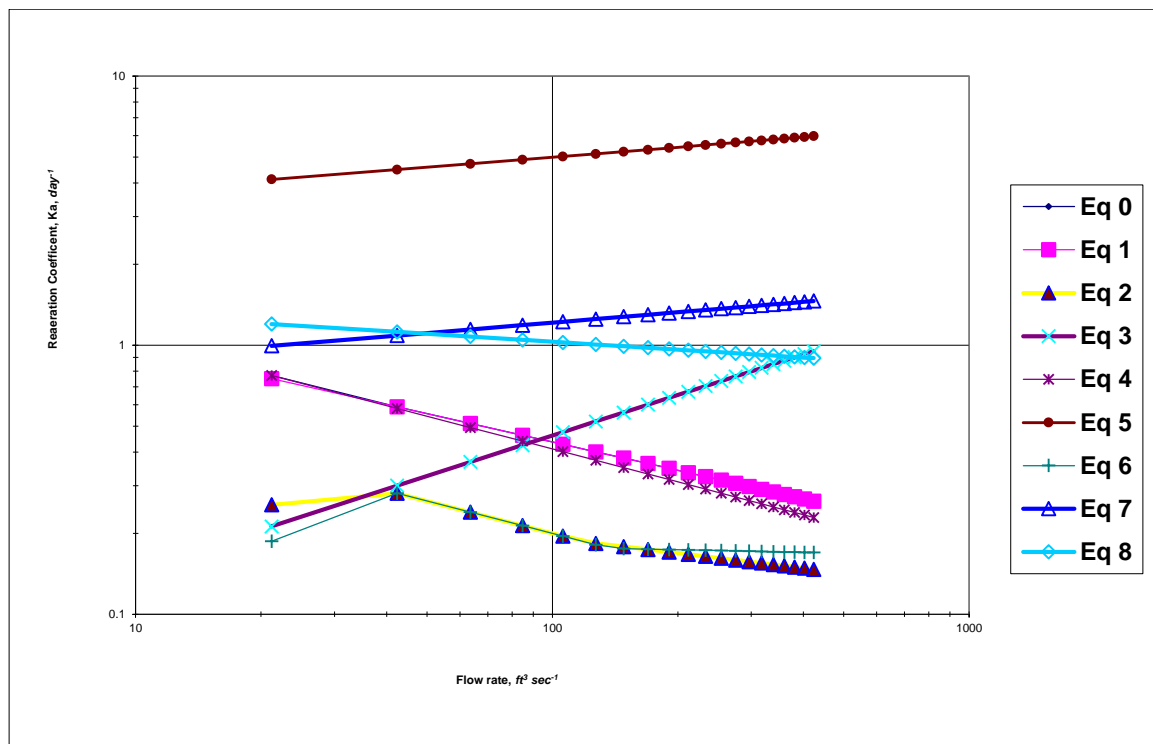


Figure B-24. Reaeration coefficient as a function of flow rate.

Lake Reaeration Equations

Wind effects rather than boundary shear more often control reaeration in lakes, reservoirs, and estuarine systems. There have been many wind studies for lakes (e.g., O'Connor, 1983) and open ocean systems. A summary of wind speed formulae for predicting reaeration is shown in [Table B-16](#) based on a 10 m wind measuring height.

Table B-16. Lake reaeration equations as a function of wind speed at 20°C.

#	Equation	Comments	Reference
1	$K_a = \frac{K_L}{H} = \frac{0.864W}{H}$	W, $m s^{-1}$ at 10 m H, m K_L , $m day^{-1}$	Broecker et al (1978)
2	$K_a = \frac{K_L}{H} = \frac{\alpha W^\beta}{H}$	$\alpha = 0.2$, $\beta = 1$ for $W < 3.5 m s^{-1}$ $\alpha = 0.057$, $\beta = 2$ for $W > 3.5 m s^{-1}$ where W is a daily average wind speed	Gelda et al (1996)
3	$K_a = \frac{K_L}{H} = \frac{0.728W^{0.5} - 0.317W + 0.0372W^2}{H}$	W, $m s^{-1}$ at 10 m K_L , $m day^{-1}$	Banks and Herrera (1977)
4	$K_a = \frac{K_L}{H} = \frac{0.0986W^{1.64}}{H} \text{ [at } 20^\circ\text{C]}$ or $K_a = \frac{K_L}{H} = \frac{0.0986W^{1.64}}{H} \left(\frac{600}{Sc} \right)^{0.5}$	The latter equation was the original equation used where W is measured at 10 m and Sc is the Schmidt number $Sc = (\nu/D) = 13750[0.10656 \exp(-0.0627T) + 0.00495]$ T = temperature, °C ν = kinematic viscosity D = diffusivity	Wanninkhof et al. (1991)

#	Equation	Comments	Reference
5	$K_a = \frac{K_L}{H} = \frac{\frac{D_{O_2}}{(200 - 60W^{0.5})10^{-6}}}{H}$	D_{O_2} = oxygen molecular diffusivity, $m^2 s^{-1}$ W , $m s^{-1}$ K_L , $m s^{-1}$	Chen, Kanwisher (1963)
6	$K_a = \frac{K_L}{H} = \frac{0.5 + 0.05W^2}{H}$		Cole and Buchak (1995)
7	$K_a = \frac{K_L}{H} = \frac{0.362\sqrt{W}}{H} \quad W < 5.5 m/s$ $K_a = \frac{K_L}{H} = \frac{0.0277W^2}{H} \quad W > 5.5 m/s$		Banks (1975)
8	$K_a = \frac{K_L}{H} = \frac{0.64 + 0.128W^2}{H}$	Recommended form for WQRSS reservoir model	Smith (1978)
9	$K_a = \frac{K_L}{H} = \frac{0.156W^{0.63}}{H} \quad W \leq 4.1 m/s$ $K_a = \frac{K_L}{H} = \frac{0.0269W^{1.9}}{H} \quad W > 4.1 m/s$		Liss (1973)
10	$K_a = \frac{K_L}{H} = \frac{0.0276W^2}{H}$		Downing and Truesdale (1955)
11	$K_a = \frac{K_L}{H} = \frac{0.0432W^2}{H}$		Kanwisher (1963)
12	$K_a = \frac{K_L}{H} = \frac{0.319W}{H}$		Yu et al (1977)
13	$K_a = \frac{K_L}{H} = \frac{0.398}{H} \quad W < 1.6$ $K_a = \frac{K_L}{H} = \frac{0.155W^2}{H} \quad W \geq 1.6$	W = wind speed, $m s^{-1}$	Weiler (1974)
14	$K_a = \frac{K_L}{H} = \frac{C_1 + C_2W^{C_3}}{H}$	User defined relationship where: W , $m s^{-1}$ at 10 m K_a , day^{-1} C_1, C_2, C_3 are user defined	

Figure B-25 shows how these formulations vary with wind speed.

The definition of wind speed was usually taken at an elevation of 10 m for these formulations. The wind speed at 10 m elevation in the middle of a lake or reservoir, W_{10m} , can be computed from that measured at 10 m on land by using an approach from Fang and Stefan (1994).

$$W_{10m} = W_z f(\text{fetch}) \quad (\text{B-41})$$

where:

W_z = wind speed measured at 10 m height on land, m/s

$$f(fetch) = \frac{\ln \frac{10}{z_{o2}} \ln \frac{\delta}{z_{o1}}}{\ln \frac{10}{z_{o1}} \ln \frac{\delta}{z_{o2}}} \cong \frac{5ZB + 4.6052}{3ZB + 9.2103} \quad (\text{B-42})$$

where:

z_{o1} = roughness of land (assume 0.01 m) (Kraus, 1972)

z_{o2} = roughness of water surface (assume 0.0001 m) (Ford and Stefan, 1980)

δ = thickness of wind boundary layer over smooth surface that is a function of the fetch length (Elliot, 1958), m

$$ZB = 0.8 \ln \frac{fetch}{2} - 1.0718$$

The function $f(fetch)$ varies from 1.056 for small lakes to 1.123 for large lakes. The fetch is the length in m of the wind over the water surface from one bank to the other.

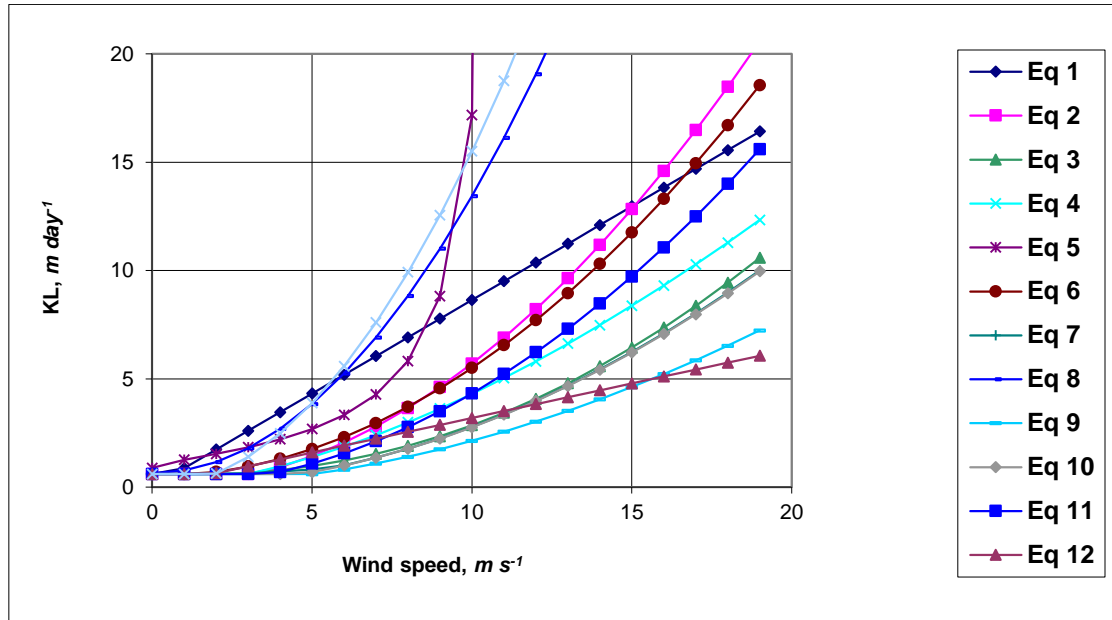


Figure B-25. Variation of wind speed and KL for lake/reservoir equations.

Equations for correcting the wind speed to 10 m and accounting for fetch dependence are included in the model. This dependence on measuring height, fetch, and wind speed is shown in [Figure B-26](#) and [Figure B-27](#).

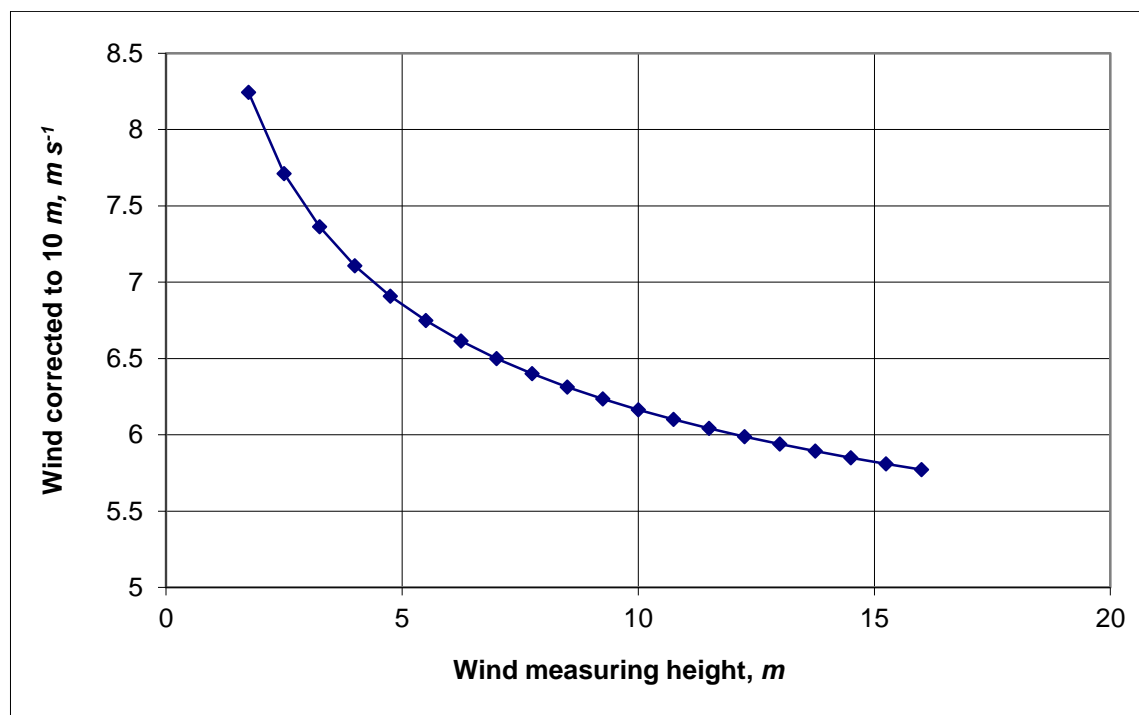


Figure B-26. Wind speed of 5 m s^{-1} and a fetch of 5 km corrected to 10 m as a function of measuring height on land.

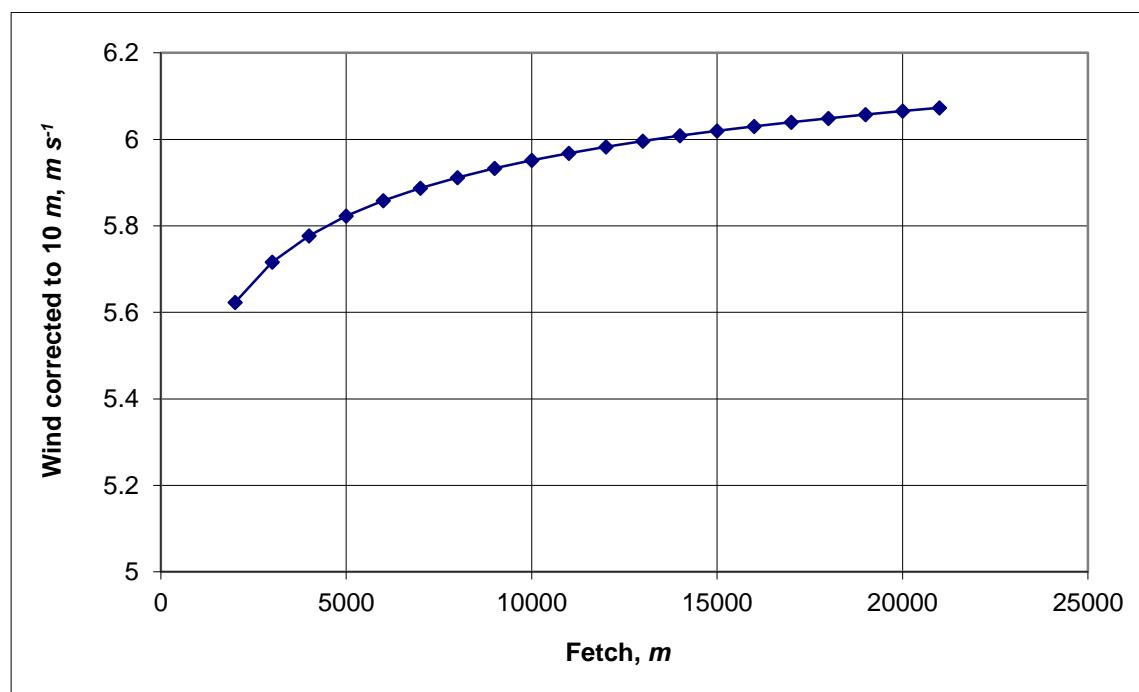


Figure B-27. Wind speed of 5 m s^{-1} corrected to 10 m as a function of fetch.

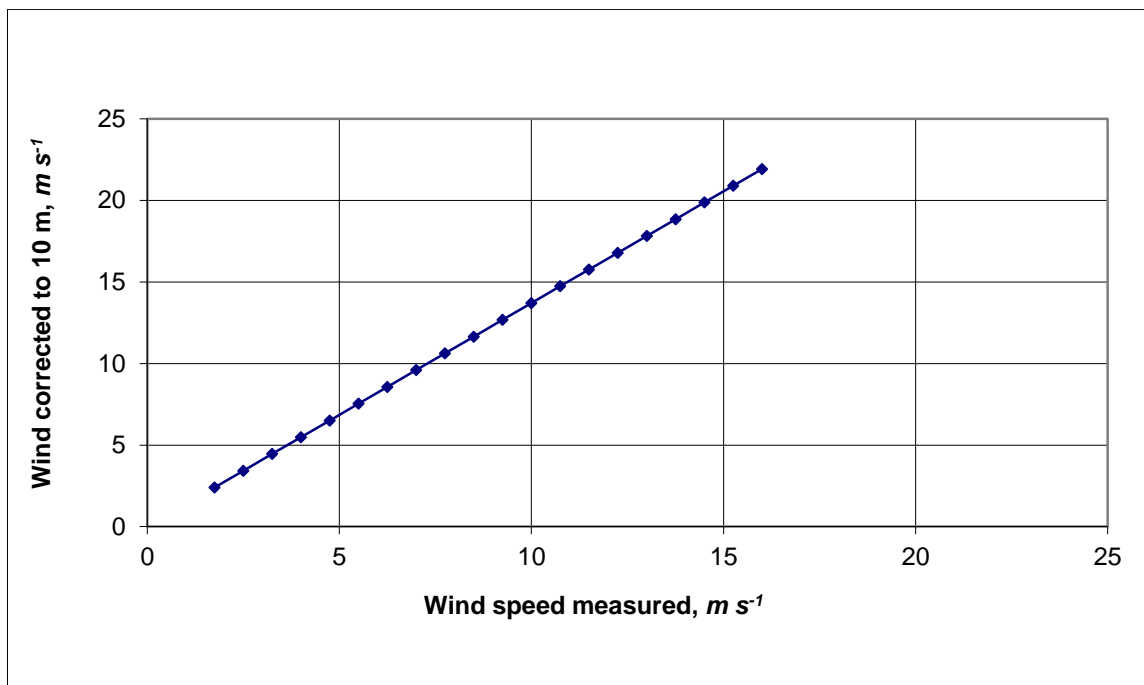


Figure B-28. Wind corrected to 10 m based on wind measured on land.

Estuarine Equations

For estuarine systems, Thomann and Mueller (1987) and Chapra (1997) suggest using any of the wind formulations in [Table B-17](#) or Equation 1 in [Table B-15](#) using the mean tidal velocity over a tidal cycle for the horizontal velocity. Table B-17 shows an additional formulation from Thomann and Fitzpatrick (1982) for estuaries, as well as the approach of Covar (1976) for rivers. Since many texts suggest using the mean tidal velocity, caution should be exercised in using these equations since they are based on the instantaneous velocity in the model.

Table B-17. Reaeration equations for estuarine waterbody at 20°C.

#	Equation	Comments	Reference
0	Either Eq 1, 2 or 4 from Table B-15	K_a is determined based on applicability criteria of each of these 3 formulations	Covar (1976)
1	$K_a = \frac{K_L}{H} = \frac{0.728W^{0.5} - 0.317W + 0.0372W^2}{H} + 3.93 \frac{\sqrt{U}}{H^{1.5}}$	U , $m s^{-1}$ this formula combines the effect of wind from Banks and Herrera (1977) and estuary tidal flow	Thomann and Fitzpatrick (1982)
2	$K_a = C_1 U^{C_2} H^{C_3} + \frac{0.5 + C_4 W^2}{H}$	U , $m s^{-1}$ H , m W , $m s^{-1}$ at 10 m K_a , day^{-1} C_1 , C_2 , C_3 , and C_4 - user defined parameters	User defined relationship

Chu and Jirka (2003) reported on wind and stream flow induced reaeration and showed that for cases where the time scale tidal flow is \gg the time scale for reaeration, then the reaeration process can be described as a steady process and the impacts of stream flow and wind can be additive using:

$$K_L = K_{Lb} + K_{Lw}$$

Where K_{Lb} is the reaeration coefficient (or transfer velocity) due to bottom shear and K_{Lw} is the reaeration coefficient due to wind in m/day.

$$K_{Lb} = 2.150 \left(\frac{u_{*b}^3}{h} \right)^{0.25}$$

Where h is the depth in cm, $u_{*b} = \sqrt{\frac{f}{8}} U$, U is the mean water velocity, f is approximately 0.04.

$$K_{Lw} = \alpha u_{*a} \text{ for smooth surfaces } (u_{*a} < 20 \text{ cm/s})$$

$$\alpha = 4.38E - 5 \text{ when } u_{*a} \text{ is in units of cm/s}$$

$$K_{Lw} = \beta u_{*a}^2 \text{ for rough surfaces}$$

$$\beta = 1.83E - 3 \text{ when } u_{*a} \text{ is in units of cm/s}$$

$$u_{*a} = 0.01U_{10} (8 + 0.65U_{10})^{1/2} \text{ from Wu (1980) and } U_{10} \text{ is wind speed at 10 m in m/s and } u_{*a} \text{ is in m/s.}$$

Reaeration Temperature Dependence

Reaeration temperature dependence is usually based upon an Arrhenius formulation:

$$K_T = K_{20} \Theta^{T-20} \quad (\text{B-43})$$

where Θ is 1.024. This dependency is based on the variation in molecular diffusivity as a function of temperature. The molecular diffusivity of oxygen varies according to temperature based on the following equation:

$$D_{O_2} = 4.58E - 11T + 1.2E - 9 \quad (\text{B-44})$$

where:

$$D_{O_2} = \text{molecular diffusivity of oxygen, } m^2 \text{ sec}^{-1}$$

$$T = \text{temperature, } ^\circ\text{C}$$

Using Equation 1 in Table B-2, the variation of K_L as a function of temperature using Equation B-43 (assuming D is a constant) and B-44 yield similar results ([Figure B-29](#)).

No temperature correction was made to the calculated value of K_L in earlier versions of the model. The latest version includes the correction with theta set to 1.024.

Variation of K_L with Temperature

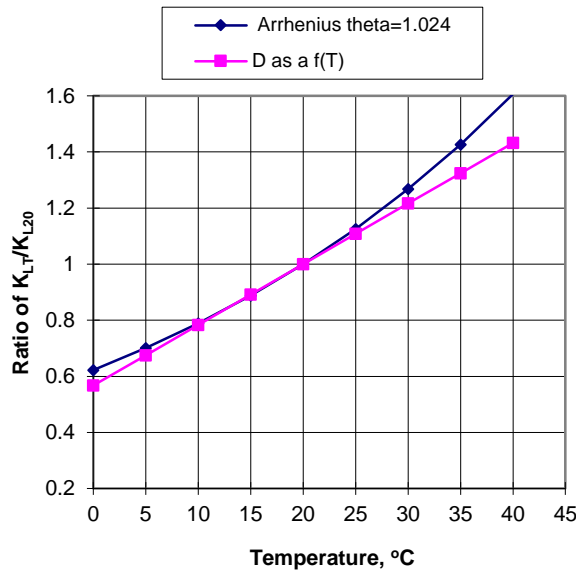


Figure B-29. Variation of K_{LT}/K_{L20} as a function of temperature.

Dam Reaeration

Many rivers and reservoirs have spillways or weirs over which water entrains oxygen into a pool below the dam. This section outlines the approach for including oxygen entrainment at dams and weirs.

Small Dams or Weirs

Many rivers have small spillways or weirs over which water flows that entrains oxygen. [Table B-18](#) lists formulae for predicting the entrainment of dissolved oxygen based on empirical data.

Table B-18. Formulae for small dam or weir reaeration effects.

Equation	Comments	Reference
$D_a - D_b = \left[1 - \frac{1}{1 + 0.11ab(1 + 0.046T)H} \right] D_a$ <p>or</p> $\frac{D_a}{D_b} = 1 + 0.11ab(1 + 0.046T)H$	D_a = DO deficit above dam, $g\ m^{-3}$ D_b = DO deficit below dam, $g\ m^{-3}$ T = temperature, °C H = height of water fall, ft a = 1.25 in clear to slightly polluted water to 1.00 in polluted water b = 1.00 for weir with free flow b = 1.3 for step weirs or cascades	Barrett et al. (1960)
$D_a - D_b = 0.037HD_a$	D_a = DO deficit above dam, $g\ m^{-3}$ D_b = DO deficit below dam, $g\ m^{-3}$ H = height of water fall, ft only valid for dams less than 15 ft and T between 20 and 25°C	Mastropietro (1968)

Equation	Comments	Reference
$\frac{D_a}{D_b} = 1 + 0.38ab(1 - 0.11H)(1 + 0.046T)H$	D_a = DO deficit above dam, $g\ m^{-3}$ D_b = DO deficit below dam, $g\ m^{-3}$ T = temperature, °C H = height of water fall, m a = 1.8 for clean water to 0.65 for gross polluted water b = 0.05 for sluice gates b = 1.0 for sharp crested straight faced weir b = 0.45 for flat broad crested curved face weir b = 0.7 for flat broad crested weir with regular step b = 0.8 for sharp crested vertical face weir b = 0.6 for flat broad crested weir vertical face	Butts and Evans (1983)

Most of these equations have been used for dams or weirs with heights of fall between 3 and 10 m . These equations do not generally predict supersaturation.

Large Dam Spillways/Gates

The USACE has been involved in gas abatement studies on the Columbia and Snake River system for many years (WES, 1996, 1997). Some of their research efforts have been focused on development of models of gas generation from spillways. These empirical models have been called CriSP 1.6 (Columbia Basin Research, 1998). The gas production equations used in CriSP are empirical correlations between total dissolved gas (TDG), usually measured a mile downstream of the dam after turbulence from the spillway had subsided, and discharge, usually measured in kcfs. The form of these equations is shown in [Table B-19](#).

Table B-19. Equations used in CRiSP model for gas production.

Equation type	Equation	Description of empirical coefficients
Linear function of total spill	$\%TDG = mQ_s + b$	Q_s = total spill, $kcfs$ m = empirical coefficient b = empirical coefficient
Bounded exponential of total spill	$\%TDG = a + be^{cQ_s}$	Q_s = total spill, $kcfs$ a = empirical coefficient b = empirical coefficient c = empirical coefficient
Bounded exponential of the spill on a per spillway basis	$\%TDG = a + be^{cq_s}$	q_s = spill through an individual spillway, $kcfs$ a = empirical coefficient b = empirical coefficient c = empirical coefficient

Examples of some of these correlations are shown in [Table B-20](#). In many cases, the %TDG in these correlations was constrained to a maximum of 145% and when the flow reached only a few kcfs, there was assumed to be no change in TDG from the forebay to the tailrace. Also, the correlations in [Table B-20](#) sometimes changed from year to year based on changes in operating conditions or structural changes in the spillway or deflectors.

Table B-20. Equations used in CRiSP model for gas production.

Dam	Equation	Coefficients
Bonneville	$\%TDG = mQ_s + b$	$m = 0.12, b = 105.61$
Lower Granite	$\%TDG = a + be^{cq_s}$	$a = 138.0; b = -35.8; c = -0.10$
Dworshak	$\%TDG = a + be^{cQ_s}$	$a = 135.9; b = -71.1; c = -0.4787$
Ice Harbor	$\%TDG = a + be^{cQ_s}$	$a = 136.8; b = -42.0; c = -0.0340$ 1995 $a = 138.7; b = -79.0; c = -0.0591$ 1996 $a = 130.9; b = -26.5; c = -0.0220$ 1997 $a = 120.9; b = -20.5; c = -0.0230$ 1998
Hell's Canyon	$\%TDG = a + be^{cQ_s}$	$a = 138; b = -36; c = -0.02$ [Assumed relationship - no data]

DO Impacts of Spillways

For each spillway, weir, or gate, the user now has the choice of equation to use for computing the effects of hydraulic structures on downstream dissolved oxygen. The equations chosen are shown in [Table B-21](#). These equations are based on equations from [Table B-18](#) and [Table B-19](#).

Table B-21. Spillways and weirs reaeration

#	Equation type	Equation	Description of empirical coefficients
1	Linear function of spill on a per spillway basis	$\%TDG = aq_s + b$ DO concentration, Φ_{O_2} , is determined from $\Phi_{O_2} = \%TDG \Phi_s$	$\%TDG$ = % total dissolved gas saturation q_s = spill through an individual spillway, kcfs a = empirical coefficient Φ_s = dissolved oxygen saturation
2	empirical coefficients a and b	$\%TDG = a + be^{q_s}$ Φ_{O_2} , is then determined from $\Phi_{O_2} = \%TDG \Phi_{sat}$	q_s = spill through an individual spillway, kcfs a = empirical coefficient b = empirical coefficient c = empirical coefficient Φ_{sat} = dissolved oxygen saturation
3	Reaeration effect for a small height weir or dam (<10 m) empirical coefficients a, b, and c	$\frac{D_a}{D_b} = 1 + 0.38ab(1 - 0.11c)(1 + 0.046T)c$ Φ_{O_2} below the dam is then computed from: $\Phi_{O_2} = \Phi_{sat} - D_b$	D_a = DO deficit above dam, $g\ m^{-3}$ D_b = DO deficit below dam T = temperature in $^{\circ}C$ H = height of water fall, m a = 1.8 for clean water to 0.65 for gross polluted water b = 0.05 for sluice gates 1.0 for sharp crested, straight faced weir 0.45 for flat, broad crested, curved face weir 0.7 for flat, broad crested weir with regular step 0.8 for sharp crested, vertical face weir 0.6 for flat, broad crested weir with vertical face Φ_{sat} = dissolved oxygen saturation, $g\ m^{-3}$

Note that for equations 1 and 2, the maximum TDG allowed is 145%. If TDG is computed to be less than 100%, there is no effect of the spillway or gate on reaeration. For each spillway or gate defined in the model, there is a section to define whether gas effects for dissolved oxygen are computed and, if so, by which formula.

For each spillway or weir, the user turns on the computations and then selects an equation number from [Table B-21](#). This algorithm only computes gas effects for flow from upstream to downstream. There is no adjustment of dissolved oxygen for reverse flow.

Dissolved Oxygen Saturation Computations

The dissolved oxygen saturation is computed from Mortimer's (1981) formulation:

$$\Phi_{O2sat} = P_{alt} e^{(7.7117 - 1.31403[\ln\{T + 45.93\}])} \quad (\text{B-45})$$

where:

T = water temperature, °C

P_{alt} = altitude correction factor = $\left(1 - \frac{H}{44.3}\right)^{5.25}$,

H = elevation of the waterbody, *km above sea level*

The saturation value is also a function of the chlorinity in saline environments. The following equation is used to compute DO saturation for a saltwater waterbody type that includes salinity effects (APHA, 1985; EPA 1985; Thomann and Mueller, 1987).

$$\Phi^*_{O2sat} = e^{\left(\ln(\Phi_{O2sat}) - S \left[1.7674 \times 10^{-2} - \frac{1.0754 \times 10^1}{T} + \frac{2.1407 \times 10^3}{T^2} \right] \right)} \quad (\text{B-46})$$

where:

S = salinity, $kg\ m^{-3}$

T = temperature, °K

Sediments

Organic sediment contributions to nutrients and dissolved oxygen demand are simulated using two methods. The first method uses a constant, or zero-order, release and demand. This method has been frequently used to model sediment demands and nutrient release rates. It does not depend on sediment concentrations or require a separate sediment compartment. However, the formulation is not predictive as the rates do not vary over time except as a result of temperature dependence of the decay rate. As a consequence, results should be interpreted cautiously when evaluating effects of different nutrient loadings on dissolved oxygen in a waterbody.

KINETICS

TOTAL INORGANIC CARBON

The second method uses a sediment compartment to accumulate organic sediments and allow their decay. Nutrient releases and oxygen demand are thus dependent upon sediment accumulation – a 1st-order process. However, there is no release of phosphorus or other diagenesis products when overlying water is anoxic since this sediment compartment is labile, oxic decay of organics on the sediment surface. A later version will include a fully predictive sediment diagenesis model. Either of these methods, or a combination, may be used to simulate effects of organic sediments upon water quality. However, caution must be exercised to avoid errors if both methods are used.

The 0-order process uses a specified sediment oxygen demand and anoxic release rates for phosphorus, ammonium, inorganic carbon, and iron that are temperature dependent. Nutrient releases do not occur when dissolved oxygen concentrations are above a minimum value [\[O2LIM\]](#) nor do they occur if the SOD is set to zero. The sediment contribution to inorganic carbon is computed as a fraction of the sediment oxygen demand.

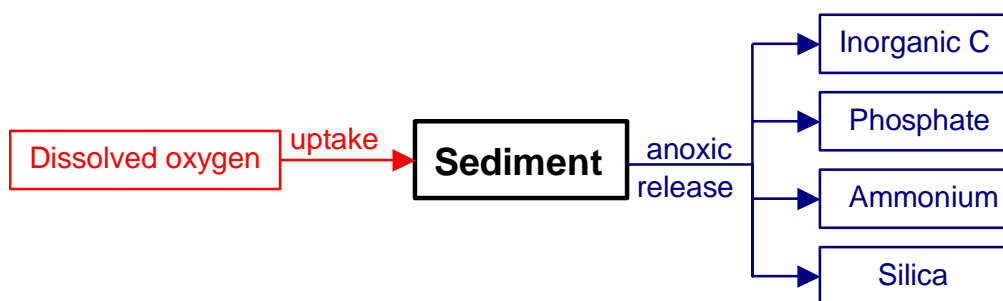


Figure B-30. Internal flux between 0-order sediment compartment and other compartments.

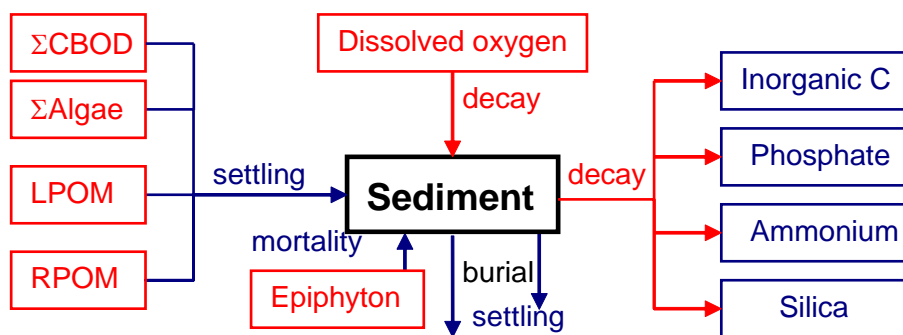


Figure B-31. Internal flux between 1st-order sediment compartment and other compartments.

The 1st-order sediment compartment requires specifying inclusion of this compartment in the simulation, a decay rate, and initial conditions. The sediment compartment is not transported, except for focusing of sediments to the bottom by a user-defined settling velocity. Instead, a compartmental equation is written for the sediment compartment that is solved in the subroutine SEDIMENT.

Referring to [Figure B-31](#), the equation for the 1st-order sediment compartment is:

$$\begin{aligned}
S_{sed} = & \underbrace{\frac{\omega_{POMR} A_{bottom}}{Vol_{cell}} \Phi_{POMR}}_{\text{POMR sedimentation}} + \underbrace{\frac{\omega_{POML} A_{bottom}}{Vol_{cell}} \Phi_{POML}}_{\text{POML sedimentation}} + \sum \underbrace{\frac{\omega_a A_{bottom}}{Vol_{cell}} \Phi_a}_{\text{algae sedimentation}} - \underbrace{\gamma_{om} K_s \Phi_s}_{\text{sediment decay}} + \underbrace{K_{epom} K_{eb} \Phi_e}_{\text{epiphyton burial}} - \\
& \underbrace{\frac{\omega_{SED} A_{bottom}}{Vol_{cell}} \Phi_s}_{\text{sediment sedimentation}} + \underbrace{\frac{\omega_{CBOD} A_{bottom}}{Vol_{cell}} \Phi_{CBOD}}_{\text{CBOD sedimentation}} - \underbrace{K_{burial} \Phi_s}_{\text{sediment burial}}
\end{aligned}
\tag{B-47}$$

where:

- γ_{OM} = rate multiplier for organic matter
- Δz = model cell thickness, m
- ω_{POM} = POM settling velocity, $m \text{ sec}^{-1}$
- ω_a = algal settling velocity, $m \text{ sec}^{-1}$
- ω_{SED} = sediment settling velocity, $m \text{ sec}^{-1}$
- K_{sed} = sediment decay rate, sec^{-1}
- Φ_a = algal concentration, $g \text{ m}^{-3}$
- Φ_{LPOM} = POM labile concentration, $g \text{ m}^{-3}$
- Φ_{RPOM} = POM refractory concentration, $g \text{ m}^{-3}$
- Φ_s = organic sediment concentration, $g \text{ m}^{-3}$
- Vol_{cell} = volume of computational cell, m^3
- A_{bottom} = Area of bottom, m^2
- Φ_e = epiphyton concentration, $g \text{ m}^{-3}$
- K_{epom} = fraction of epiphyton that go to particulate fraction and settle into sediment at death
- K_{em} = epiphyton mortality rate
- K_{burial} = sediment burial rate, sec^{-1}

Pauer and Auer (2000) claim that nitrification is generally a sediment based phenomena rather than one existing in the water column. Their argument is based on the study of a samples obtained from a hypereutrophic lake-river system which had extremely high ammonia concentrations (2-10 mg/l $\text{NH}_3\text{-N}$) and where cell counts indicated much higher nitrifier populations in the sediments rather than in the water column. They question if nitrification is being modeled correctly in many water quality models, where nitrification is treated as occurring in the water column rather than the sediments.

Nitrification rates of water column samples were measured in 2.5 L bottles kept in the dark at 20° Celsius. Rates of nitrification were to be determined by tracking concentrations of nitrogen species in the bottles. Since no change in ammonia or nitrate-nitrite concentrations were noted, the authors assumed that the lack of observable nitrification was due to low nitrifier populations occurring in the water column of the lake and river. Sediment nitrification rates were measured using sediment core samples under similar conditions. Changes in the concentrations of nitrogen species were apparent and an average sediment nitrification rate of 0.34 g N/m²/day was determined. Table 22 summarizes the nitrification rates.

Table 22. Areal nitrification rates of sediment nitrifiers of Onondaga Lake and the Seneca River, New York (Pauer and Auer, 2000).

Reaction	Source	Growth Temperature (Celsius)	Nitrification rate (g N/m ² /day)
Nitrification	Onondaga Lake, Seneca River, New York	20°	0.21 to 0.67 (mean=0.34)

Sediment Variable Stoichiometry and Kinetics

Variable stoichiometry of sediments is done automatically within the W2 model. In addition to sediment phosphorus and sediment nitrogen, there is also a sediment carbon compartment. The sediment carbon stoichiometry is variable because organic matter, algae and epiphyton may have differing carbon stoichiometry. The initial sediment stoichiometry for P, N, and C is based on the given initial stoichiometry for organic matter. The decay rate of sediment in a model cell is the mass averaged decay rate of the LPOM, RPOM, and the CBOD groups.

Sediment Phosphorus

$$S_{P_{sed}} = \underbrace{\frac{\omega_{POMR} A_{bottom}}{Vol_{cell}} \Phi_{RPOM-P}}_{RPOM-P \text{ sedimentation}} + \underbrace{\frac{\omega_{POML} A_{bottom}}{Vol_{cell}} \Phi_{LPOM-P}}_{LPOM-P \text{ sedimentation}} + \underbrace{\sum \frac{\omega_a A_{bottom}}{Vol_{cell}} \delta_{Pa} \Phi_a}_{\text{algae sedimentation}} - \underbrace{\gamma_{om} K_s \Phi_{s-P}}_{\text{sediment decay}} + \underbrace{\sum \frac{K_{epom} K_{em} \delta_{Pe} \Phi_e}{epiphyton \text{ mortality}}}_{\text{epiphyton mortality}}$$

$$\underbrace{\frac{\omega_{SED} A_{bottom}}{Vol_{cell}} \Phi_{s-P}}_{\text{sediment sedimentation}}$$

where:

γ_{OM} = rate multiplier for organic matter

δ_{Pe} = epiphyton stoichiometric coefficient for phosphorus

δ_{Pa} = algal stoichiometric coefficient for phosphorus

Δz = model cell thickness, m

ω_{POM} = POM settling velocity, $m \text{ sec}^{-1}$

ω_a = algal settling velocity, $m \text{ sec}^{-1}$

ω_{SED} = sediment settling velocity, $m \text{ sec}^{-1}$

K_{sed} = sediment decay rate, sec^{-1}

Φ_a = algal concentration, $g \text{ m}^{-3}$

Φ_{LPOM-P} = labile POM labile concentration, $g \text{ m}^{-3}$

Φ_{RPOM-P} = refractory POM concentration, $g \text{ m}^{-3}$

Φ_{s-P} = sediment phosphorus concentration, $g \text{ m}^{-3}$

Vol_{cell} = volume of computational cell, m^3

A_{bottom} = Area of bottom, m^2

Φ_e = epiphyton concentration, $g \text{ m}^{-3}$

K_{epom} = fraction of epiphyton that go to particulate fraction and settle into sediment at death

K_{em} = epiphyton mortality rate

Sediment Nitrogen

$$S_{Nsed} = \underbrace{\frac{\omega_{POMR} A_{bottom}}{Vol_{cell}} \Phi_{RPOM-N}}_{\text{RPOM-N sedimentation}} + \underbrace{\frac{\omega_{POML} A_{bottom}}{Vol_{cell}} \Phi_{LPOM-N}}_{\text{LPOM-N sedimentation}} + \underbrace{\sum \frac{\omega_a A_{bottom}}{Vol_{cell}} \delta_{Na} \Phi_a}_{\text{algae sedimentation}} - \underbrace{\gamma_{om} K_s \Phi_{s-N}}_{\text{sediment decay}} + \underbrace{\sum K_{epom} K_{em} \delta_{Ne} \Phi_e}_{\text{epiphyton mortality}} - \underbrace{\frac{\omega_{SED} A_{bottom}}{Vol_{cell}} \Phi_{s-N}}_{\text{sediment sedimentation}} + \underbrace{\frac{\omega_{NO3SED} A_{bottom}}{Vol_{cell}} \Phi_{NO3-N} f_{NO3-SED}}_{\text{diffusion of NO3 into sediments}}$$

where:

γ_{OM} = rate multiplier for organic matter

δ_{Ne} = epiphyton stoichiometric coefficient for nitrogen

δ_{Na} = algal stoichiometric coefficient for nitrogen

Δz = model cell thickness, m

ω_{POM} = POM settling velocity, $m \text{ sec}^{-1}$

ω_a = algal settling velocity, $m \text{ sec}^{-1}$

ω_{SED} = sediment settling velocity, $m \text{ sec}^{-1}$

ω_{NO3} = $\text{NO}_3\text{-N}$ diffusion rate into sediments, $m \text{ sec}^{-1}$

K_{sed} = sediment decay rate, sec^{-1}

Φ_a = algal concentration, $g \text{ m}^{-3}$

Φ_{LPOM-N} = labile POM concentration, $g \text{ m}^{-3}$

Φ_{RPOM-N} = refractory POM concentration, $g \text{ m}^{-3}$

Φ_{NO3-N} = $\text{NO}_3\text{-N}$ concentration, $g \text{ m}^{-3}$

Φ_{s-N} = sediment nitrogen concentration, $g \text{ m}^{-3}$

Vol_{cell} = volume of computational cell, m^3

A_{bottom} = Area of bottom, m^2

Φ_e = epiphyton concentration, $g \text{ m}^{-3}$

K_{epom} = fraction of epiphyton that go to particulate fraction and settle into sediment at death

K_{em} = epiphyton mortality rate

$f_{\text{NO3-SED}}$ = fraction of $\text{NO}_3\text{-N}$ diffused into sediments that is incorporated into organic matter in the sediments (the rest, $1 - f_{\text{NO3-SED}}$, is denitrified into N_2)

Sediment Carbon

$$S_{Csed} = \underbrace{\frac{\omega_{POMR} A_{bottom}}{Vol_{cell}} \gamma_{OM} \Phi_{RPOM}}_{\text{RPOM sedimentation}} + \underbrace{\frac{\omega_{POML} A_{bottom}}{Vol_{cell}} \gamma_{OM} \Phi_{LPOM}}_{\text{LPOM sedimentation}} + \underbrace{\sum \frac{\omega_a A_{bottom}}{Vol_{cell}} \delta_{Ca} \Phi_a}_{\text{algae sedimentation}} - \underbrace{\gamma_{om} K_s \Phi_{s-C}}_{\text{sediment decay}} + \underbrace{\sum K_{epom} K_{em} \delta_{Ce} \Phi_e}_{\text{epiphyton mortality}} - \underbrace{\frac{\omega_{SED} A_{bottom}}{Vol_{cell}} \Phi_{s-C}}_{\text{sediment sedimentation}}$$

where:

γ_{OM} = rate multiplier for organic matter

- δ_{Ce} = epiphyton stoichiometric coefficient for carbon
 δ_{Ca} = algal stoichiometric coefficient for carbon
 δ_{COM} = organic matter stoichiometric coefficient for carbon
 Δz = model cell thickness, m
 ω_{POM} = POM settling velocity, $m\ sec^{-1}$
 ω_a = algal settling velocity, $m\ sec^{-1}$
 ω_{SED} = sediment settling velocity, $m\ sec^{-1}$
 K_{sed} = sediment decay rate, sec^{-1}
 Φ_a = algal concentration, $g\ m^{-3}$
 Φ_{LPOM} = labile POM carbon concentration, $g\ m^{-3}$
 Φ_{RPOM} = refractory POM carbon concentration, $g\ m^{-3}$
 Φ_{s-C} = sediment carbon concentration, $g\ m^{-3}$
 Vol_{cell} = volume of computational cell, m^3
 A_{bottom} = Area of bottom, m^2
 Φ_e = epiphyton concentration, $g\ m^{-3}$
 K_{epom} = fraction of epiphyton that go to particulate fraction and settle into sediment at death
 K_{em} = epiphyton mortality rate

Total Inorganic Carbon

Carbon, hydrogen, and oxygen are the most abundant elements in living matter and form the essential backbone of organic material. Inorganic carbon directly influences pH.

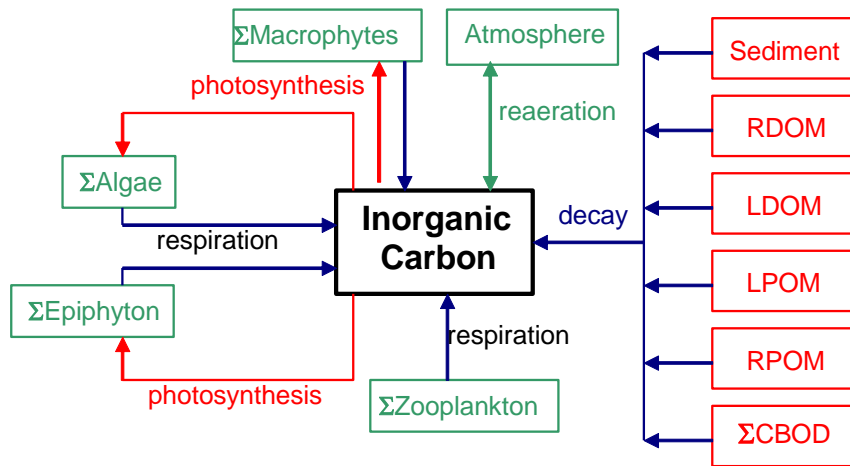


Figure B-32. Internal flux between inorganic carbon and other compartments.

Referring to [Figure B-32](#), the rate equation for total inorganic carbon is:

$$\begin{aligned}
S_{TIC} = & \underbrace{\sum (K_{ar} - K_{ag}) \delta_{Ca} \Phi_a}_{\text{net algal production}} + \underbrace{\sum (K_{er} - K_{eg}) \delta_{Ce} \Phi_e}_{\text{net epiphyton production}} + \underbrace{K_{LPOM} \delta_{COM} \gamma_{OM} \Phi_{LPOM}}_{\text{labile POM decay}} \\
& + \underbrace{K_{LDOM} \gamma_{OM} \delta_{COM} \Phi_{LCOM}}_{\text{labile DOM decay}} + \underbrace{K_{RDOM} \gamma_{OM} \delta_{COM} \Phi_{RDOM}}_{\text{refractory DOM decay}} + \underbrace{K_{RPOM} \delta_{COM} \gamma_{OM} \Phi_{RPOM}}_{\text{refractory POM decay}} \\
& + \underbrace{K_{sed} \gamma_{OM} \delta_{COM} \Phi_{sed}}_{\text{1st-order sediment release}} + \underbrace{SOD \gamma_{OM} \delta_{COM} \frac{A_{sed}}{V}}_{\text{0-order sediment release}} + \underbrace{A_{sur} K_{Lc} (\Phi'_{CO2} - \Phi_{CO2})}_{\text{reaeration}} \\
& + \underbrace{\sum K_{CBOD} R_{CBOD} \delta_{C-CBOD} \Theta^{T-20} \Phi_{CBOD}}_{\text{CBOD decay}} + \underbrace{\sum (K_{mr} - K_{mg}) \delta_{Cm} \Phi_{macro}}_{\text{net macrophyte production}} \\
& + \underbrace{K_{zr} \delta_{Czoo} \gamma_{zoo} \Phi_{zoo}}_{\text{zooplankton respiration}}
\end{aligned}$$

(B-48)

where:

- θ = temperature rate multiplier for BOD decay
- γ_{OM} = organic matter temperature rate multiplier
- δ_{Ce} = epiphyton stoichiometric coefficient for carbon
- δ_{Ca} = algal stoichiometric coefficient for carbon
- δ_{COM} = organic matter stoichiometric coefficient for carbon
- δ_{C-CBOD} = CBOD stoichiometric coefficient for carbon
- R_{BOD} = 5-day CBOD to ultimate CBOD ratio
- A_{sed} = sediment surface area, m^2
- A_{sur} = surface area of surface computational cell, m^2
- SOD = sediment oxygen demand, $g\ m^{-2}\ sec^{-1}$
- K_{Lc} = inorganic carbon interfacial exchange rate, $m\ sec^{-1}$
- K_{ar} = algal dark respiration rate, sec^{-1}
- K_{ag} = algal growth rate, sec^{-1}
- K_{er} = epiphyton dark respiration rate, sec^{-1}
- K_{eg} = epiphyton growth rate, sec^{-1}
- K_{LDOM} = labile DOM decay rate, sec^{-1}
- K_{RDOM} = refractory DOM decay rate, sec^{-1}
- K_{LPOM} = labile POM decay rate, sec^{-1}
- K_{RPOM} = refractory POM decay rate, sec^{-1}
- K_{CBOD} = CBOD decay rate, sec^{-1}
- K_{sed} = sediment decay rate, sec^{-1}
- Φ_a = algal concentration, $g\ m^{-3}$
- Φ_e = epiphyton concentration, $g\ m^{-3}$
- Φ_{LDOM} = labile DOM concentration, $g\ m^{-3}$
- Φ_{RDOM} = refractory DOM concentration, $g\ m^{-3}$
- Φ_{LPOM} = labile POM concentration, $g\ m^{-3}$
- Φ_{RPOM} = refractory POM concentration, $g\ m^{-3}$
- Φ_{CBOD} = CBOD concentration, $g\ m^{-3}$

KINETICS

TOTAL INORGANIC CARBON

- Φ_{sed} = organic sediment concentration, $g\ m^{-3}$
 Φ_{TIC} = inorganic carbon concentration, $g\ m^{-3}$
 Φ_{CO_2} = carbon dioxide concentration, $g\ m^{-3}$
 Φ'_{CO_2} = carbon dioxide saturation concentration, $g\ m^{-3}$

and the rate terms are evaluated in subroutine INORGANIC_CARBON.

The basic physics of gas transfer are the same for CO_2 and O_2 . Using Higbie penetration theory, the gas transfer coefficient for CO_2 is related to that of oxygen by:

$$KL_{CO_2} = KL_{O_2} \sqrt{\frac{D_{CO_2}}{D_{O_2}}} \quad (B-49)$$

where:

- KL_{CO_2} = reaeration coefficient for CO_2
 KL_{O_2} = reaeration coefficient for oxygen
 D_{CO_2} = molecular diffusion coefficient for CO_2
 D_{O_2} = molecular diffusion coefficient for oxygen

Using the fact that the ratio of molecular diffusion coefficients of two gases A and B are related to their molecular weights, MW (Thibedoux, 1996)

$$\frac{D_A}{D_B} = \sqrt{\frac{MW_B}{MW_A}} \quad (B-50)$$

then

$$KL_{CO_2} = KL_{O_2} \left(\frac{MW_{O_2}}{MW_{CO_2}} \right)^{0.25} = 0.923 KL_{O_2} \quad (B-51)$$

Hence, the reaeration rate equations presented for oxygen transfer are applicable to CO_2 transfer using a factor of 0.923.

Carbon dioxide concentration for the interfacial exchange rate is determined from total inorganic carbon and alkalinity in subroutine PH_CO2. The saturation concentration of carbon dioxide is determined from:

$$\Phi'_{CO_2} = 0.286 e^{(-0.0314T_s)} P_a \quad (B-52)$$

where:

- Φ'_{CO_2} = carbon dioxide saturation concentration, $g\ m^{-3}$
 P_a = altitude correction factor
 T_s = surface cell water temperature, $^{\circ}C$

Altitude correction is from Mortimer, 1981:

$$P_a = \left(1 - \frac{H}{44.3} \right)^{5.25} \quad (\text{B-53})$$

where:

H = reservoir elevation from sea level, km

TIC is in units of mg/l as C.

Alkalinity

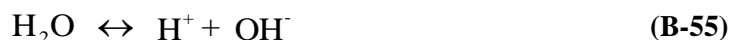
Alkalinity provides an indication of the buffering capacity of aquatic systems and their resistance to pH changes from acidic or alkaline loadings. Alkalinity is treated as conservative in the model and its internal rate term is set to zero. Alkalinity, along with total inorganic carbon, is used to determine pH and concentrations of carbonate species in subroutine PH_CO2.

In reality, alkalinity variations are common in most aquatic systems. Whittings, or large precipitations of carbonates, may occur. Sediment release of carbonates may increase alkalinity in the anoxic zones of many reservoirs. If these effects are important, a non-conservative model of alkalinity should be added. Alkalinity is in units of mg/l as $CaCO_3$.

pH and Carbonate Species

The pH and carbonate species are computed using water temperature, TDS or salinity, alkalinity, and total inorganic carbon concentrations using basic carbonate relationships. Computed carbonate species are carbon dioxide, bicarbonates, and carbonates. The pH and carbonate species are computed in subroutine PH_CO2. These materials are not subject to transport and are computed at each water quality update interval.

Calculations performed by subroutine PH_CO2 are based on the carbonate-bicarbonate equilibrium reaction (Stumm and Morgan 1981):



These equilibria express the source of bicarbonate and carbonate ions, alkaline constituents, and dissolution of atmospheric CO_2 in water. Contribution of calcium and magnesium carbonate to alkalinity is not included. The equilibrium state in terms of the equilibrium constants K_i is:

$$K_1 = \frac{[H^+] [HCO_3^-]}{[H_2CO_3]} \quad (B-56)$$

$$K_2 = \frac{[H^+] [CO_3^{2-}]}{[HCO_3^-]} \quad (B-57)$$

$$K_w = \frac{[H^+] [OH^-]}{[H_2O]} \quad (B-58)$$

where:

[X] = molar concentration, *moles liter⁻¹*

[H₂O] = unity (by definition)

Alkalinity is defined as:

$$[ALK] = [HCO_3^-] + 2[CO_3^{2-}] + [OH^-] - [H^+] \quad (B-59)$$

The following condition prevails for the dissolution of carbonic acid:

$$[H_2CO_3] + [HCO_3^-] + [CO_3^{2-}] = \text{CONSTANT} = C_T \quad (B-60)$$

By combining equations B-53, B-54, and B-57, the quantities [HCO₃⁻] and [CO₃²⁻] can be expressed in terms of [H⁺] and the constant C_T. In addition, equation B-55 allows for [OH⁻] to be expressed in terms of [H⁺]. When these expressions are included in equation B-56, the result is:

$$[ALK] = \frac{C_T [H^+] K_1}{[H^+] K_1 + K_1 K_2 + [H^+]^2} \frac{[H^+] + 2 K_2}{[H^+]} + \frac{K_w}{[H^+]} - [H^+] \quad (B-61)$$

The model interprets the constant C_T as moles per liter of total inorganic carbon and assumes [ALK] is known. Equation B-58 is iteratively solved in subroutine PH_CO2 until the value of [H⁺] converges. The negative logarithm of [H⁺] is, by definition, pH.

Once equation B-58 has been solved for [H⁺], then [H₂CO₃] is given by:

$$[H_2CO_3] = \frac{C_T}{1 + \frac{K_1}{[H^+]} + \frac{K_1 K_2}{[H^+]^2}} \quad (B-62)$$

and is the same as [CO₂]. Bicarbonate concentration is computed from:

$$[\text{HCO}_3^-] = \frac{C_T}{1 + \frac{[\text{H}^+]}{K_1} + \frac{K_2}{[\text{H}^+]}} \quad (\text{B-63})$$

and carbonate from:

$$[\text{CO}_3^{2-}] = \frac{C_T}{1 + \frac{[\text{H}^+]}{K_1} + \frac{[\text{H}^+]^2}{K_1 K_2}} \quad (\text{B-64})$$

which are then converted to grams per cubic meter.

Equilibrium constants in the preceding equations are obtained by first expressing a thermodynamic temperature dependence for a related constant, K_i^* :

$$\log K_i^* = a + \frac{b}{T} + cT + d \log T \quad (\text{B-65})$$

The constants a, b, c, and d are:

	a	b	c	d
K_w^*	35.3944	-5242.39	-0.00835	11.8261
K_1^*	14.8435	-3404.71	-0.03278	0
K_2^*	6.4980	-2902.39	-0.02379	0

The relation between K_i and K_i^* is obtained from the definition of the activity of a chemical species:

$$\{X\} = \gamma [X] \quad (\text{B-66})$$

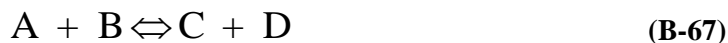
where:

$\{X\}$ = activity of species X, *moles liter⁻¹*

γ = dimensionless activity coefficient

$[X]$ = concentration, *moles liter⁻¹*

For the reaction:



the equilibrium constant K^* is:

$$K^* = \frac{\{C\} \{D\}}{\{A\} \{B\}} \quad (\text{B-68})$$

thus:

$$K^* = \frac{\gamma_C [C] \gamma_D [D]}{\gamma_A [A] \gamma_B [B]} = \frac{\gamma_C \gamma_D}{\gamma_A \gamma_B} K \quad (\text{B-69})$$

$$K = \frac{\gamma_A \gamma_B}{\gamma_C \gamma_D} K^* \quad (\text{B-70})$$

Activity coefficients are obtained from an extension of Debye-Huckel theory as:

$$\text{Log } \gamma = \frac{-AZ^2\sqrt{I}}{1 + 0.33a\sqrt{I}} + k_1 + k_2 I + k_3 I^2 \quad (\text{B-71})$$

where:

- I = ionic strength
- Z = ionic charge
- A = approximately 0.5 for water at 25°C
- a = ionic size parameter
- k_i = empirical coefficients

Ionic strength is approximated as (Sawyer and McCarty 1967):

$$I = 2.5 \times 10^{-5} \Phi_{TDS} \quad (\text{B-72})$$

or for salinity:

$$I = 0.00147 + 0.019885 \Phi_{sal} + 0.000038 \Phi_{sal}^2 \quad (\text{B-73})$$

where:

- Φ_{TDS} = total dissolved solids, $g\ m^{-3}$
- Φ_{sal} = salinity, $kg\ m^{-3}$

Values of the other parameters are:

	Z	a	k ₁	k ₂	k ₃
HCO ₃ ⁻	1	4	0.0047	0.042	-0.0093

CO ₃ ⁼	2	4.5	0.0121	0.0972	-0.0207
------------------------------	---	-----	--------	--------	---------

Activity coefficients for [H⁺], [OH⁻], [H₂CO₃], and [H₂O] are treated as special cases:

$$[H^+] \gamma = [H_2O] \gamma = 1 \quad (\text{B-74})$$

$$[H_2CO_3] \gamma = [OH^-] \gamma = 0.07551 \quad (\text{B-75})$$

Temperature Rate Multipliers

Most biological and chemical rates are temperature dependent. Subroutine RATE_MULTIPLIERS calculates the temperature dependence for all rates. It is called after the temperature solution so the temperature of the current computational interval is used.

A representative rate multiplier function is shown in [Figure B-33](#) with its K and T parameters. The curve represents how biological process rates exhibit an optimum range and diminish asymmetrically at higher and lower temperatures (Thornton and Lessem, 1978).

$$\lambda_T = 0 \quad \text{where } T \leq T_1$$

$$\lambda_T = \underbrace{\frac{K_1 e^{\gamma_1(T-T_1)}}{1 + K_1 e^{\gamma_1(T-T_1)} - K_1}}_{\gamma_{ar}} \underbrace{\frac{K_4 e^{\gamma_2(T_4-T)}}{1 + K_4 e^{\gamma_2(T_4-T)} - K_4}}_{\gamma_{af}} \quad \text{where } T_1 < T < T_4 \quad (\text{B-76})$$

$$\lambda_T = 0 \quad \text{where } T \geq T_4$$

where:

$$\gamma_{ar} = \frac{1}{T_2 - T_1} \ln \frac{K_2(1 - K_1)}{K_1(1 - K_2)}$$

$$\gamma_{af} = \frac{1}{T_4 - T_3} \ln \frac{K_3(1 - K_4)}{K_4(1 - K_3)}$$

γ_{ar} and γ_{af} are the rising and falling limb temperature multipliers.

KINETICS

TEMPERATURE RATE MULTIPLIERS

The user supplies temperatures T_1 to T_4 and multiplier factors K_1 to K_4 . Temperatures T_1 and T_4 represent mortality limits, and T_2 and T_3 are used to define the optimum range. Maximum reaction rates supplied by the user are multiplied by λT to determine rates corresponding to the water temperature of a model cell. For non-algae temperature rate multipliers, only the K_1 and K_2 corresponding to T_1 and T_2 are used.

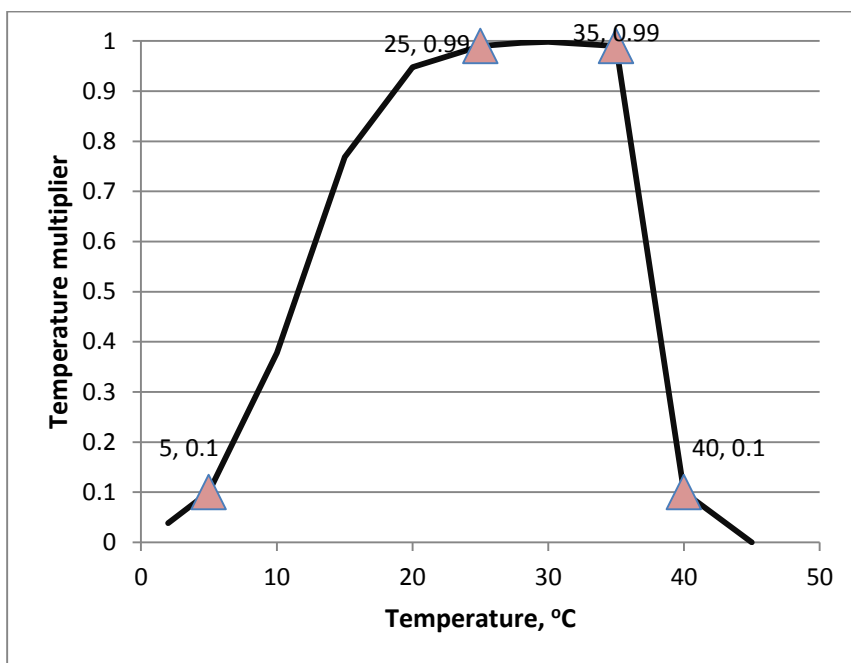


Figure B-33. Temperature rate multiplier function.

Appendix C Input/Output Data Description

Input file format has been developed for a full-screen text editor. Each input file begins with two lines used for file identification that are ignored by the program. The rest of the input file consists of groups of three lines - the first line is blank serving as a separator, the second line contains the card identification and the FORTRAN variable names associated with the input card, and the third line contains the input values. The identifier card is only checked by the pre-processor code. FORTRAN names are right justified according to the field widths associated with the input variable. There are 10 input fields associated with each card although the first field is not used in several of the input files. Each field has a length of eight characters.

Input Files

Control File

The control file [CONFN] contains the variables used to run the model. There are no optional cards in the control file - each card is ***required*** although there may be either zero or no values associated with the card. The following pages contain a description of each card. ***All character inputs must be capitalized except the TITLE cards and input/output filenames*** or the variable will take on the default value. An example of a portion of a control file is given with each card description and a complete control file is given at the end of the control file description. Hyperlinks to related input cards are included at the bottom of each card description.

Title (TITLE C)

FIELD	NAME	VALUE	DESCRIPTION
1			(Ignored by code)
2-10	TITLE	Character	Text for identification of simulation

There are 10 title cards for each a simulation that can be used to identify various types of output. Each line may contain up to 72 characters of text. Title cards appear in every output file except for the restart file. Uses for the title cards include identifying the simulation, the simulation time frame, the date the simulation was run, and other information specific to the simulation. A few words of wisdom - the user should be conscientious in updating the title cards for each simulation.

Example

```

TITLE C .....TITLE.....
Card 1  Version 3 Example Model
Card 2  PSU CE-QUAL-W2 Workshop Problem 7
Card 3  River with 2 branches
Card 4  Reservoir
Card 5  Estuary
Card 6  River Sloping Channels 2 Branches
Card 7  Temperature Mitigation Problem
Card 8  Temperature and residence time simulation
Card 9  Scott Wells - PSU
Card 10 Tom Cole - WES

```

Grid Dimensions (GRID)

FIELD	NAME	VALUE	DESCRIPTION
1			(Ignored by code)
2	NWB	Integer	Number of waterbodies in the computational grid
3	NBR	Integer	Number of branches in the computational grid
4	IMX	Integer	Number of segments in the computational grid
5	KMX	Integer	Number of layers in the computational grid
6	NPROC	Integer	Number of processors to use for computation
7	CLOSEC	ON or OFF	Close the W2 Windows dialog box at the end of simulation (ON) or keep it open (OFF)

This card defines the computational grid including the total number of waterbodies [NWB], branches [NBR], segments [IMX], and layers [KMX]. These values are used to define the array dimensions in the code since the code has been converted over to FORTRAN 90 and now takes advantage of dynamic array allocation. This eliminates the need to recompile the code for each application.

Since Version 3.6, the code uses some OPENMP commands for parallelization. In recent testing, the code achieves up to a 20% improvement in speed by choosing 2 processors over 1 processor. Using more than 2 can often degrade system performance. You may want to test to see if your model runs faster using any number of processors. [NPROC] sets the number of physical processors the model uses. We recommend starting with [NPROC]=1.

[CLOSEC] is a control that allows the W2 windows dialog box to remain open at the end of a simulation (OFF) or to close at the end of a run (ON). Setting [CLOSEC]=OFF, at the end of a windows run, the windows dialog box waits for the user to press 'close' to exit the window. This allows the user to examine the final run parameters. Setting [CLOSEC]=ON allows the window dialog box to close when the run has completed. This allows for efficient batch processing of the model, especially in conjunction with command line processing. When [CLOSEC] is set to ON, then the dialog box will disappear once the run finishes. If it is set to OFF, then the dialog box will remain until the user clicks 'close'.

Example

GRID	NWB	NBR	IMX	KMX	NPROC	CLOSEC
	3	4	43	24	2	OFF

Related Cards and Files

[Inflow/Outflow Dimensions](#)
[Constituent Dimensions](#)
[Miscellaneous Dimensions](#)

Inflow/Outflow Dimensions (IN/OUTFLOW)

FIELD	NAME	VALUE	DESCRIPTION
1			(Ignored by code)
2	NTR	Integer	Number of tributaries
3	NST	Integer	Number of structures
4	NIW	Integer	Number of internal weirs
5	NWD	Integer	Number of withdrawals
6	NGT	Integer	Number of gates
7	NSP	Integer	Number of spillways
8	NPI	Integer	Number of pipes
9	NPU	Integer	Number of pumps

This card defines the variables used to dimension the arrays for tributaries, internal weirs, and in-flow/outflow hydraulic structures including lateral withdrawals, outlet gates, spillways, pipes, and pumps. All variables should be set to zero if they are not used.

Example

IN/OUTFLOW	NTR	NST	NIW	NWD	NGT	NSP	NPI	NPU
	1	3	1	0	1	2	1	0

Related Cards and Files

[Grid Dimensions](#)

[Constituent Dimensions](#)

[Miscellaneous Dimensions](#)

[Tributaries](#)

[Structures](#)

[Weirs](#)

[Withdrawals](#)

[Gates](#)

[Spillways](#)

[Pipes](#)

[Pumps](#)

Constituent Dimensions (CONSTITUENTS)

FIELD	NAME	VALUE	DESCRIPTION
1			(Ignored by code)
2	NGC	Integer	Number of generic constituents
3	NSS	Integer	Number of inorganic suspended solids
4	NAL	Integer	Number of algal groups
5	NEP	Integer	Number of epiphyton/periphyton groups
6	NBOD	Integer	Number of CBOD groups
7	NMC	Integer	Number of macrophyte groups
8	NZP	Integer	Number of zooplankton groups

This card defines the array dimensions for the number of generic constituents, inorganic suspended solids groups, algal groups, CBOD groups, macrophyte groups and zooplankton groups. The user has complete freedom to include as many of these groups as data are available for and the application warrants.

The generic constituent allows the user the freedom to model any number of constituents that can be defined using a 0-order decay rate and/or a 1st- order decay rate and/or a settling velocity and/or an Arrhenius temperature rate multiplier. Version 2 state variables that fall into the generic category include tracer and coliform. Thus, any number of tracers or coliform groups can be modeled. Additionally, residence time can be modeled in this group by setting the 0-order decay rate to -1.0 and setting all other kinetic parameters to zero.

The ability to model any number of CBOD groups now allows the model to characterize and track any number of point sources of CBOD. This should prove useful in determining which point source(s) is/are contributing to depressed dissolved oxygen levels or violations in a system and allow better understanding of what management strategies could be used to improve dissolved oxygen.

Care should be taken when including multiple algal, epiphyton, zooplankton, and macrophyte groups to ensure that the data are sufficient to describe their variation in the system. As a general rule, it is better to start with as simple a description of the kinetics in a system that still allows the model to capture the important temporal and spatial changes in water quality.

Example

CONSTITU	NGC	NSS	NAL	NEP	NBOD	NMC	NZP
	3	1	3	1	1	1	1

Related Cards and Files

[Grid Dimensions](#)
[Inflow/Outflow Dimensions](#)
[Miscellaneous Dimensions](#)

Miscellaneous (MISCELL)

FIELD	NAME	VALUE	DESCRIPTION
1			(Ignored by code)
2	NDAY	Integer	Maximum number of output dates or timestep related changes
3	SELECTC	Character	Turn ON/OFF/USGS automatic port selection from a multiple outlet structure where level is chosen by model to reach temperature target
4	HABTATC	Character	Turn ON/OFF habitat analyses for fish and eutrophication variables
5	ENVIRPC	Character	Turn ON/OFF environmental performance criteria
6	AERATEC	Character	Turn ON/OFF aeration to waterbody with dissolved oxygenprobe control
7	INITUWL	Character	Turn ON/OFF initial water surface slope and velocity calculation for a river system

This card defines several variables that turn ON or OFF features of the code first implemented in Version 3.7. NDAY is the maximum number of output dates that will be used in the simulation. This should be the maximum of timestep, snapshot, screen, profile, vector, contour, time series, withdrawal, and restart number of dates that are used to define when output frequencies, or, in the case of the timestep related cards, when the maximum timestep or the fraction of the timestep change. This can easily be set to a value greater than any anticipated number of dates without any impact as the memory used by these variables is trivial. The user should use 100 as a default. There often is no reason to ever change this value.

SELECTC is a control that turns ON or OFF the use of the automatic port selection for a multiple outlet withdrawal structure at a downstream end of a branch. If this is ON, the model then reads the control file for this feature, "w2_selective.npt". Another option new in Version 3.72 is to set SELECTC='USGS'. Either of these options allows the user to let the model decide what outlet to use to meet temperature targets. Please see the section on the automatic port selection control file in Appendix C for a description of its features. If SELECTC='OFF', then this algorithm is not used.

HABTATC is a control that turns ON or OFF the fish habitat analysis and other useful analyses for eutrophication studies. If this is ON, the model then reads the control file for this feature, "w2_habitat.npt". Please see the section on the habitat control file in Appendix C for a description of its features.

ENVIRPC is a control that turns ON or OFF the environmental performance analysis for user-chosen model state variables. This feature allows for temporal and volume-weighted averages of and histograms of specified state variables. If this is ON, the model then reads the control file for this feature, "w2_envirpc.npt". Please see the section on the environmental performance control file in Appendix C for a description of its features.

AERATEC is a control that turns ON or OFF aeration at specified segments and layers. If this is ON, the model then reads the control file for this feature, "w2_aerate.npt". Please see the section on the aeration control file in Appendix C for a description of its features.

CONTROL FILE

ARRAY DIMENSIONS

INITUWL is a control that turns ON or OFF a computation of the initial water level and the initial velocity of the river. A computation of the normal depth and initial velocity is made for any branch with a non-zero slope. This normal depth profile is used instead of the water surface profile given in the bathymetry file. The theory for this is described in Appendix A in the User Manual. A typical CE-QUAL-W2 application starts with velocity set to zero in the domain at the initial time. If INITUWL is ON, then the velocity at normal depth is computed and used as the initial velocity. This allows smoother running of the river models. When INITUWL is turned ON, the CE-QUAL-W2 model also writes out a file that shows the initial water surface elevations, normal depths, and velocities it computed for the first time step. These are found in an output file called, "init_wl_u_check.dat".

Example

```
MISCELL      NDAY SELECTC HABTATC ENVIRPC AERATEC INITUWL
              100      USGS      ON      ON      ON      OFF
```

Related Cards and Files

[Grid Dimensions](#)

[Inflow/Outflow Dimensions](#)

[Constituent Dimensions](#)

[Control File for selective withdrawal](#)

[Control File for habitat](#)

[Control File for environmental performance](#)

[Control File for aeration](#)

Time Control (TIME CON)

FIELD	NAME	VALUE	DESCRIPTION
1			(Ignored by code)
2	TMSTRT	Real	Starting time, <i>Julian day</i>
3	TMEND	Real	Ending time, <i>Julian day</i>
4	YEAR	Integer	Starting year

The simulation starting and ending times are specified with this card. When making a simulation extending into another year, the ending time is calculated as 365 (or 366 for a leap year) + Julian date of ending time. Midnight, January 1 starts at Julian day 1.0 in the model.

Example

TIME CON	TMSTRT	TMEND	YEAR
	63.5	64.5	1980

Timestep Control (DLT CON)

FIELD	NAME	VALUE	DESCRIPTION
1			(Ignored by code)
2	NDT	Integer	Number of timestep intervals
3	DLTMIN	Real	Minimum timestep, sec
4	DLTINTR	Character	Turn ON or OFF time step interpolation between DLTMIN time steps

The number of timestep intervals, minimum timestep, and whether interpolation is used between those time steps [NDT] are specified on this card.

The autostepping algorithm calculates a maximum timestep based on an estimate of hydrodynamic numerical stability requirements and then uses a fraction of this value for the actual timestep. The user can specify any number of intervals up to the value specified for [\[NDAY\]](#) on the [Miscellaneous Dimensions](#) card in which the maximum timestep and fraction of the timestep can vary. The values are specified on the next three cards.

This option is useful during periods of very low flow where the timestep is very large. Under these conditions, small changes in flow will result in large timestep changes that can lead to an excessive number of timestep violations detected by the autostepping algorithm. The model automatically adjusts the timestep to ensure that it is never greater than the next time varying update, so the maximum timestep can be set to a value greater than the minimum time varying data update frequency.

The minimum timestep is useful during periods of extremely high flows. In these instances, the timestep could become too small to economically run the model. Care should be taken when using this variable as the model may become numerically unstable if the minimum value is set too high. The default value of 1 sec should not be increased unless the user is absolutely certain that this will not affect numerical stability. Minimum values as low as 0.1 s have been used for river systems.

In Version 3.7 and forward, the option of interpolating the maximum time steps [DLTMAX] and DLTF by setting DLTINTR to ON is available. For V3.6 and before, only step changes were available in the specifying DLTMAX and DLTF. Turning interpolation on, DLTINTR=' ON', allows for a smoother transition between changes in DLTMAX and DLTF.

Example

```
DLT CON      NDT  MINDLT  DLTINTR
              2      1.0      ON
```

Related Cards and Files

[Timestep Date](#)
[Maximum Timestep](#)
[Timestep Fraction](#)
[Timestep Limitation](#)

Timestep Date (DLT DATE)

FIELD	NAME	VALUE	DESCRIPTION
1			(Ignored by code)
2-10	DLTD	Real	Beginning of timestep interval, <i>Julian day</i>

The intervals for the maximum timestep are specified on this card. Any number of intervals up to the value of **[NDAY]** on the [Miscellaneous Dimensions](#) card can be specified. If there are more intervals than can be specified on one line, then they are continued on the next line without another **DLT DATE** card being specified.

Example

DLT DATE	DLTD	DLTD	DLTD	DLTD	DLTD	DLTD	DLTD	DLTD	DLTD
	63.5	63.52							

Related Cards and Files

[Timestep Control](#)
[Maximum Timestep](#)
[Timestep Fraction](#)
[Timestep Limitation](#)

Maximum Timestep (DLT MAX)

FIELD	NAME	VALUE	DESCRIPTION
1			(Ignored by code)
2-10	DLTMAX	Real	Maximum timestep, <i>sec</i>

The maximum timestep for intervals provided on the timestep interval card are specified with this card. If there are more intervals than can be specified on one line, then they are continued on the next line without another **DLT MAX** card being specified.

Example

```
DLT MAX      DLTMAX  DLTMAX  DLTMAX  DLTMAX  DLTMAX  DLTMAX  DLTMAX  DLTMAX  DLTMAX
              30.0    100.0
```

Related Cards and Files

[Timestep Control](#)
[Timestep Date](#)
[Timestep Fraction](#)
[Timestep Limitation](#)

Timestep Fraction (DLT FRN)

FIELD	NAME	VALUE	DESCRIPTION
1			(Ignored by code)
2-10	DLTF	Real	Fraction of calculated maximum timestep necessary for numerical stability

The fraction of the calculated maximum timestep for intervals given on the timestep interval card is specified here. If there are more intervals than can be specified on one line, then they are continued on the next line without another **DLT FRN** card being specified. If the number of timestep violations exceeds 5%, either [[DLTMAX](#)] on the [Maximum Timestep](#) card or [[DLTF](#)] should be decreased.

Decreasing [[DLTF](#)] usually decreases the number of timestep violations without affecting the maximum timestep that the model can use. Thus, during times of low velocities, the model can still use the maximum timestep, but during periods of high velocities, the model will use a smaller timestep than if [[DLTF](#)] were set to a higher value.

Example

DLT FRN	DLTF	DLTF	DLTF	DLTF	DLTF	DLTF	DLTF	DLTF	DLTF
	0.9	0.9							

Related Cards and Files

[Timestep Control](#)
[Timestep Date](#)
[Maximum Timestep](#)
[Timestep Limitation](#)

Timestep Limitations (DLT LIMIT)

FIELD	NAME	VALUE	DESCRIPTION
1			(Ignored by code)
2	VISC	Character	Turns ON/OFF vertical eddy viscosity limitation on timestep calculated in autostepping algorithm
3	CELC	Character	Turns ON/OFF internal gravity wave limitation on timestep calculated in autostepping algorithm

This card specifies whether the effects of the vertical eddy viscosity and/or the internal gravity wave are included in the autostepping algorithm. Separate values are specified on a separate card for each waterbody.

If the average timestep is very small, these can be turned **OFF** to decrease runtimes. However, care should be taken when using this option as experience has shown that, in certain applications, turning these **OFF** can affect the results. If either of these variables are turned **OFF**, the user should also make a run with them turned **ON** to see if this option affects the results. Results should never be a function of the timestep or grid spacing.

Example

DLT LIMIT	VISC	CELC
Wb 1	ON	ON
Wb 2	ON	ON
Wb 3	ON	ON

Related Cards and Files

[Timestep Control](#)

[Timestep Date](#)

[Maximum Timestep](#)

[Timestep Fraction](#)

Branch Geometry (BRANCH G)

FIELD	NAME	VALUE	DESCRIPTION
1			(Ignored by code)
2	US	Integer	Branch upstream segment
3	DS	Integer	Branch downstream segment
4	UHS	Integer	Upstream boundary condition
5	DHS	Integer	Downstream boundary condition
6	UQB	Integer	Upstream internal flow boundary condition - IGNORE
7	DQB	Integer	Downstream internal flow boundary condition - IGNORE
6	NLMIN	Integer	Minimum number of layers for a segment to be active
7	SLOPE	Real	Branch bottom slope (actual)
8	SLOPEC	Real	Hydraulic equivalent branch slope

This card specifies the branch location in the grid and branch boundary conditions. No distinction is made between waterbodies. The mainstem of the first waterbody is always branch 1 and the mainstem of subsequent waterbodies is always the next branch after all branches have been numbered for the previous waterbody. Side branches for a given waterbody can be ordered in any fashion, but it is good practice to order the remaining branches starting with the most upstream branch and continuing downstream.

The branch upstream segment number **[US]** is the most upstream potentially active segment. For branch 1, this would always be segment 2. The branch downstream segment number **[DS]** is the most downstream *active* segment. The boundary segment is *never* included for either the upstream or downstream segment.

Four upstream and downstream boundary conditions can be specified. Boundary conditions along with the upstream head segment **[UHS]** and downstream head segment **[DHS]** values that specify these conditions are:

Boundary type [UHS] and/or [DHS]

External head -1

External/internal flow 0

Internal head >0

Dam flow-only for [UHS] <-1 [only for receiving a structure flow from another branch]

For internal head boundary conditions between branches or dam flow boundary conditions between waterbodies, **[UHS]** and/or **[DHS]** correspond to the branch segment the branch attaches to. In the following example, branch 1 consists of segments 2 through 6 and attaches to branch 2 at segment 9. Branch 2 consists of segments 9 through 14 and attaches at segment 6 in branch 1 and segment 17 at branch 3. See [Chapter 3](#) for additional information on the computational grid setup. The current version does not use the **[UQB]** and **[DQB]** variables – ignore these fields. A later version may use these to define internal flow boundary conditions. Any internal flow such as a structure flow will have a 0 value for **[DHS]**. For the receiving branch, a negative number corresponding to the structure segment number is specified for **[UHS]**. This is only when there is a structure flow specified as the downstream outflow of a corresponding branch, in other words you must specify the DS value of a corresponding branch. This allows that specified structure flow to go into the upstream segment of a downstream branch. If you use any hydraulic elements, such as spillways,

CONTROL FILE

GRID DEFINITION

pumps, pipes, gates, you would not use a negative value. You would use a flow boundary condition, i.e., zero for UHS or DHS. The spillways, pumps, pipes, and gates have their own specification for where the flow is directed.

The following example is taken from the example [control file](#) of the Spokane River/Long Lake in Washington, USA. Branches one through four represent sloping river sections that are linked in series since the downstream head segment number [DHS=13 for branch one] is the upstream segment number [US=13 for branch 2] of the next branch and the upstream head segment number [UHS=10 for branch 2] is the downstream segment number [DS=10 for branch 1] of the preceeding branch. Similar linkage occurs for branches two to three and three to four. Branch four, however, has a downstream head [DHS] set to 0, indicating either an internal (spillway or gate) or external (outlet structure) flow boundary condition. Branch 6 inflow is from the structure release from Branch 5; this structure outflow is a given, known flow rate, not one computed in the model.

In this example, branch four is connected to branch 5 via an internal flow from a spillway and the linkage is specified on the spillway card in the sample control file. Note though that branch 5 must be a separate waterbody with its own value of EBOT (see next card) since there is no way to define the elevations of the grid with another branch since it has no linkage specified.

SLOPEC is the hydraulic equivalent slope of the model branch. In many cases the actual slope of the channel (SLOPE) is not the correct equivalent hydraulic slope, since this may be punctuated by falls and riffles. SLOPEC is used in the momentum equation to determine the acceleration of a parcel of fluid for that branch rather than SLOPE. SLOPE is though critical for linking the model system together with correct elevations.

Example

BRANCH	G	US	DS	UHS	DHS	UQB	DQB	NL	SLOPE	SLOPEC
Br 1		2	10	0	13	0	0	1	0.00181	0.00181
Br 2		13	24	10	27	0	0	1	0.00152	0.00100
Br 3		27	36	24	39	0	0	1	0.00328	0.00200
Br 4		39	48	36	0	0	0	1	0.00142	0.00142
Br 5		51	64	0	0	0	0	1	0.00000	0.00000
Br 6		67	73	-64	76	0	0	1	0.00000	0.00000
Br 7		76	86	73	0	0	0	1	0.00000	0.00000
Br 8		89	94	-86	97	0	0	1	0.00256	0.00150
Br 9		97	128	94	0	0	0	1	0.00208	0.00100
Br 10		131	135	0	138	0	0	1	0.00000	0.00000
Br 11		138	151	135	0	0	0	1	0.00000	0.00000
Br 12		154	188	-151	0	0	0	1	0.00000	0.00000

Related Cards and Files

[Bathymetry File](#)

[Branch Inflow File](#)

[Branch Inflow Temperature File](#)

[Branch Inflow Concentration File](#)

[Branch Outflow File](#)

[Branch External Upstream Head Elevation File](#)

[Branch External Upstream Head Temperature File](#)

[Branch External Upstream Head Concentration File](#)

[Branch External Downstream Head Elevation File](#)

[Branch External Downstream Head Temperature File](#)

[Branch External Downstream Head Concentration File](#)

Waterbody Definition (LOCATION)

FIELD	NAME	VALUE	DESCRIPTION
1			(Ignored by code)
2	LAT	Real	Latitude, <i>degrees</i>
3	LONG	Real	Longitude, <i>degrees</i>
4	EBOT	Real	Bottom elevation of waterbody, <i>m</i>
5	BS	Integer	Starting branch of waterbody
6	BE	Integer	Ending branch of waterbody
7	JBDN	Integer	Downstream branch of waterbody

This card specifies the waterbody latitude and longitude, bottom reference elevation, starting and ending branches of the waterbody, and the downstream most branch of the waterbody that connects to the next waterbody. The bottom elevation is used to tie computed water surface elevations to an external benchmark (e.g., *m* above sea level) and represents the elevation at the bottom of the bottommost active cell. This elevation is defined at the mid-point of a model cell.

The model was set up for LONG W and LAT N coordinates as being positive. Hence one would start at Greenwich as 0 and go 360 deg toward the West, or go negative toward the east - either approach is OK. Remember that this specification of LONG and LAT only affects internal short wave solar calculation and shading calculations. Hence, if one reads in short wave solar radiation and does not have dynamic shading calculations, LAT and LONG will not be used.

[JBDN] specifies the downstream branch from which [EBOT] is referenced. In the case of a complicated grid, this is the starting elevation for tying the rest of the elevation of the grid together. [EBOT] is the elevation of the bottom of the bottommost active layer in the computational grid [KMX]. Figure C-34 and Figure C-35 show [EBOT] for a sloping river and a reservoir, respectively. For a sloping river, [EBOT] would generally be located at the most downstream segment in the section. [EBOT] is defined as the elevation of KMX-1 of DS(JBDN). EBOT would be defined at the segment center for a sloping domain.

Example

LOCATION	LAT	LONG	EBOT	BS	BE	JBDN
WB 1	45.44	122.18	36.00	1	2	2
WB 2	45.44	122.18	0.00	3	3	3
WB 3	45.44	122.18	-8.00	4	4	4

CONTROL FILE

GRID DEFINITION

Segment	4		5		6		7		8		9		10
DLX	33.49		149.18		108.37		196.35		306.19		87.04		87.04
ELWS	271		271		271		271		271		271		271
PHI0	3.5		3.5		4.71		4.71		3.14		3.14		3.14
Friction	0.04		0.05		0.05		0.05		0.05		0.05		0.05
Layer	Width	Elev-top	Width	Elev-top	Width	Elev-top	Width	Elev-top	Width	Elev-top	Width	Elev-top	Width
1	.00	276.83	.00	276.71	.00	276.55	.00	276.35	.00	276.02	.00	275.77	.00
2	90.00	276.23	90.00	276.11	90.00	275.95	90.00	275.75	90.00	275.42	90.00	275.17	.00
3	90.00	275.63	90.00	275.51	90.00	275.35	90.00	275.15	90.00	274.82	90.00	274.57	.00
4	90.00	275.03	90.00	274.91	90.00	274.75	90.00	274.55	90.00	274.22	90.00	273.97	.00
5	90.00	274.43	90.00	274.31	90.00	274.15	90.00	273.95	90.00	273.62	90.00	273.37	.00
6	90.00	273.83	90.00	273.71	90.00	273.55	90.00	273.35	90.00	273.02	90.00	272.77	.00
7	90.00	273.23	90.00	273.11	90.00	272.95	90.00	272.75	90.00	272.42	90.00	272.17	.00
8	60.00	272.63	60.00	272.51	60.00	272.35	60.00	272.15	60.00	271.82	60.00	271.57	.00
9	45.00	272.03	45.00	271.91	45.00	271.75	45.00	271.55	45.00	271.22	45.00	270.97	.00
10	30.00	271.43	30.00	271.31	30.00	271.15	30.00	270.95	30.00	270.62	30.00	270.37	.00
11	17.50	270.83	17.50	270.71	17.50	270.55	17.50	270.35	17.50	270.02	17.50	269.77	.00
12	10.00	270.23	10.00	270.11	10.00	269.95	10.00	269.75	10.00	269.42	10.00	269.17	.00
13	7.00	269.93	7.00	269.81	7.00	269.65	7.00	269.45	7.00	269.12	7.00	268.87	.00
14	.00	269.88	.00	269.76	.00	269.6	.00	269.4	.00	269.07	.00	268.82	.00

Figure C-34. Layer numbers and segments for a sloping waterbody where segment 9 is the last active segment of the waterbody. EBOT is 268.82 m, which is the lowest elevation in the waterbody and is the bottom elevation of layer 13 or KMX-1 (where KMX=14).

Segment		29		30		31		32		33		34		35		36		37		38
DLX		117.988		28.3495		136.98		146.072		157.852		109.728		99.06		91.44		147.549		147.549
ELWS		264.5		264.5		264.5		264.5		264.5		264.5		264.5		264.5		264.5		264.5
PHI0		3.6		3.6		3.6		3.6		3.6		3.6		3.6		3.6		4.3		4.3
Friction		0.04		0.04		0.04		0.04		0.04		0.04		0.04		0.05		0.05		0.05
Layer	Elev-top	Width	Elev-top	Width	Elev-top	Width	Elev-top	Width	Elev-top	Width	Elev-top	Width	Elev-top	Width	Elev-top	Width	Elev-top	Width	Elev-top	Width
1	264.41	.00	264.41	.00	264.41	.00	264.41	.00	264.41	.00	264.41	.00	264.41	.00	264.41	.00	264.41	.00	264.41	.00
2	264.16	33.00	264.16	32.00	264.16	25.00	264.16	38.00	264.16	161.00	264.16	211.00	264.16	52.00	264.16	51.00	264.16	30.00	264.16	.00
3	263.91	20.00	263.91	30.00	263.91	20.00	263.91	20.00	263.91	90.00	263.91	120.00	263.91	40.00	263.91	40.00	263.91	20.00	263.91	.00
4	263.66	20.00	263.66	20.00	263.66	12.00	263.66	12.00	263.66	70.00	263.66	80.00	263.66	30.00	263.66	30.00	263.66	15.00	263.66	.00
5	263.41	.00	263.41	15.00	263.41	10.00	263.41	10.00	263.41	50.00	263.41	50.00	263.41	20.00	263.41	20.00	263.41	9.00	263.41	.00
6	263.16	.00	263.16	.00	263.16	10.00	263.16	10.00	263.16	30.00	263.16	30.00	263.16	18.00	263.16	13.00	263.16	8.00	263.16	.00
7	262.91	.00	262.91	.00	262.91	.00	262.91	10.00	262.91	20.00	262.91	20.00	262.91	15.00	262.91	12.00	262.91	7.00	262.91	.00
8	262.66	.00	262.66	.00	262.66	.00	262.66	.00	262.66	15.00	262.66	10.00	262.66	10.00	262.66	11.00	262.66	6.00	262.66	.00
9	262.41	.00	262.41	.00	262.41	.00	262.41	.00	262.41	10.00	262.41	10.00	262.41	10.00	262.41	10.00	262.41	.00	262.41	.00
10	262.16	.00	262.16	.00	262.16	.00	262.16	.00	262.16	.00	262.16	10.00	262.16	10.00	262.16	9.00	262.16	.00	262.16	.00
11	261.91	.00	261.91	.00	261.91	.00	261.91	.00	261.91	.00	261.91	.00	261.91	10.00	261.91	8.00	261.91	.00	261.91	.00
12	261.66	.00	261.66	.00	261.66	.00	261.66	.00	261.66	.00	261.66	.00	261.66	.00	261.66	7.00	261.66	.00	261.66	.00
13	261.41	.00	261.41	.00	261.41	.00	261.41	.00	261.41	.00	261.41	.00	261.41	.00	261.41	6.00	261.41	.00	261.41	.00
14	261.21	.00	261.21	.00	261.21	.00	261.21	.00	261.21	.00	261.21	.00	261.21	.00	261.21	.00	261.21	.00	261.21	.00

Figure C-35. Layer numbers and segments for a branch with a zero slope where segment 37 is the last active segment of the branch. EBOT for this waterbody is 261.21 m and is the bottom elevation of layer 13 or KMX-1 (where KMX=14).

Initial Conditions (INIT CND)

FIELD	NAME	VALUE	DEFAULT	DESCRIPTION
1				(Ignored by code)
2	T2I	Real		Initial temperature, °C
3	ICETHI	Real		Initial ice thickness, <i>m</i>
4	WTYPEC	Character	FRESH	Waterbody type
5	GRIDC	Character	RECT	Either 'RECT' or 'TRAP' specifying the interpretation of the bathymetry as either rectangular cells or trapezoidal cells

This card specifies the initial temperature and ice thickness, and waterbody type. Initial temperature can be specified as either a single value, a single vertical profile used to initialize every segment, or a vertical profile for each segment.

Initial condition	[T2I]
1. Isothermal	> or =0
2. Single vertical profile	-1.0
3. Vertical profile at each segment	-2.0

If option 2 or 3 is chosen, then the user must specify input files **[VPRFN]** or **[LPRFN]** containing the profile(s).

Initial ice thickness **[ICETHI]** is ignored if ice computations are turned off.

The waterbody type **[WTYPEC]** is either FRESH or SALT. If **[WTYPEC]** is set to SALT, then constituent computations **[CCC]** should be turned on and **salinity** should be included in the computations. This affects the equation of state used in the model and the units of TDS (if FRESH, g/m³ or mg/l) or SALINITY (if SALT, kg/m³). The equation of state for both FRESH and SALT is shown in Appendix A.

Starting with Version 3.7, the model user can specify that the grid can be interpreted as trapezoidal rather than rectangular. Trapezoidal cells have the advantage of smoother water level change especially in a river leading to faster run times and stability.

The computational grid system used by CE-QUAL-W2 prior to Version 3.7 was a rectangular grid system, a basic cross-section of which is shown in Figure 36. This grid system is ideal for waterbodies characterized by gradual changes in surface area with depth, such as lakes, reservoirs, and some larger rivers. In cases where small changes in water elevation result in large changes in surface area, however, the rectangular grid system can lead to numerical instability issues that require low maximum time steps and can impact processes on the air-water interface.

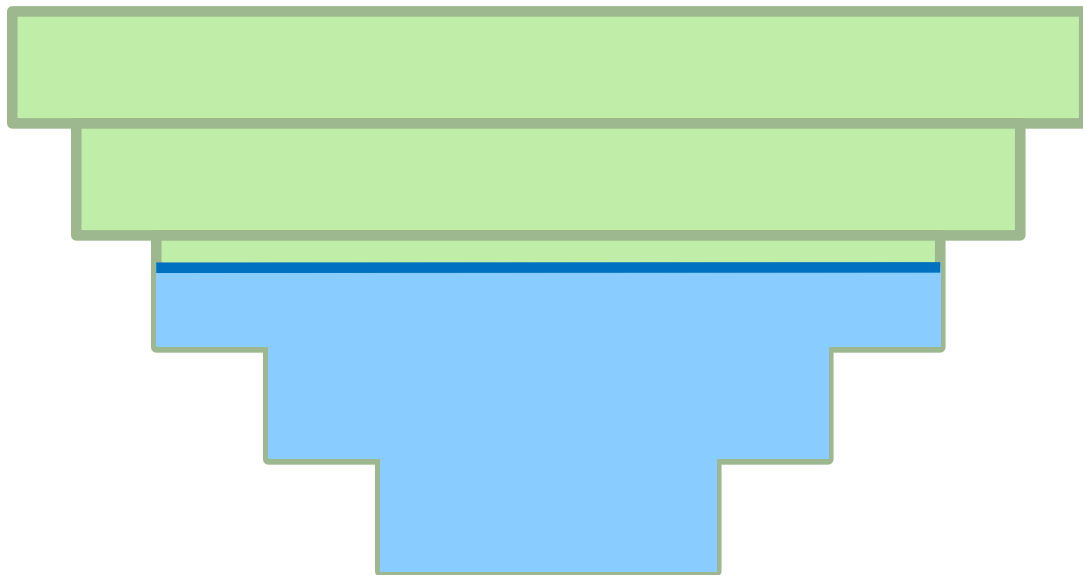


Figure 36. Cross-section of current rectangular grid system

Two possible solutions to make the layer change smoother is illustrated in Figure 37. The first approach involves decreasing layer thickness to create a more gradually sloping shoreline. This would entail increasing the number of layers which could considerably increase computational time. The second approach involves converting the rectangular grid to a trapezoidal grid. This solution not only results in increased stability and more realistic bank geometry, but it also allows for smooth changes in surface area while maintaining the same volume-elevation relationship in the channel as the original rectangular grid. (This approach makes it possible to “retrofit” older models without the necessity of recreating all the bathymetry and grid files.)



Figure 37. Various solutions to fitting a cross-section –trapezoidal layers compared to multiple rectangular layers.

Hence, the bathymetry will still be based on average widths at cell centers as shown above, but will be interpreted as either rectangles or trapezoids.

Example

INIT CND	T2I	ICETHI	WTYPEC	GRIDC
Wb 1	-1.0	0.0	FRESH	RECT
Wb 2	-1.0	0.0	FRESH	RECT
Wb 3	-1.0	0.0	FRESH	RECT

INITIAL CONDITIONS

CONTROL FILE

Related Cards and Files

[Constituent Computations](#)
[Constituent Initial Concentration](#)
[Vertical Profile File](#)
[Longitudinal Profile File](#)
[Ice Cover](#)

Calculations (CALCULAT)

FIELD	NAME	VALUE	DEFAULT	DESCRIPTION
1				(Ignored by code)
2	VBC	Character	ON	Volume balance calculation, ON or OFF
3	EBC	Character	ON	Thermal energy balance calculation, ON or OFF
3	MBC	Character	ON	Mass balance calculation, ON or OFF
4	PQC	Character	OFF	Density placed inflows, ON or OFF
5	EVC	Character	ON	Evaporation included in water budget, ON or OFF
6	PRC	Character	OFF	Precipitation included, ON or OFF

This card specifies whether the model performs certain optional calculations. Calculations are turned on or off by right justifying ON or OFF in the input field.

Volume balance calculations are useful during initial runs as a check to ensure the model is preserving continuity and should always be used as a check if the user modifies the code. In order to reduce roundoff errors, the volume balance algorithm accumulates spatial and temporal changes in volume over time and uses these for comparison. Once the user is satisfied the model is running correctly, volume balance calculations should be turned off to reduce computational time.

Thermal energy and mass balance calculations are similar in use to volume balance calculations. They should be used initially to ensure the model is running properly and turned off for further calculations. When this option is used, mass balances are performed for each constituent if constituent computations are turned on. Mass balances are not computed if only temperature is modeled. These balances are only written out to the Snapshot [SNP] file.

There are two options for distributing mainstem and branch inflows. The default is inflows distributed evenly into each layer from top to bottom. If [PQC] is turned ON, then inflows are matched up with the layer(s) whose density most closely corresponds to inflow density.

If precipitation is specified, then the user must supply input files for precipitation and precipitation temperature. If constituents are being modeled, then the user must supply an input file for constituent concentrations included in the simulation. The [Precipitation Active Constituent Control](#) card specifies which concentrations are included. If all precipitation constituents are turned OFF, then the precipitation constituent concentration input file is not required.

Evaporation rates are sometimes accounted for in estimating the inflow record, such as when net inflows are computed from outflows and water surface elevations. If so, then [EVC] should be set to OFF. Evaporation is always considered in the surface heat exchange calculations.

INITIAL CONDITIONS

CONTROL FILE

Example

CALCULAT	VBC	EBC	MBC	PQC	EVC	PRC
Wb 1	ON	ON	ON	OFF	OFF	OFF
Wb 2	ON	ON	ON	OFF	OFF	OFF
Wb 3	ON	ON	ON	OFF	OFF	OFF

Related Cards and Files

[Precipitation Active Constituent Control](#)

[Branch Inflow File](#)

[Tributary Inflow File](#)

[Precipitation File](#)

Dead Sea (DEAD SEA)

FIELD	NAME	VALUE	DEFAULT	DESCRIPTION
1				(Ignored by code)
2	WINDC	Character	ON	Turn ON/OFF wind
3	QINC	Character	ON	Turn ON/OFF all sources of water
4	QOUTC	Character	ON	Turn ON/OFF all sinks of water
5	HEATC	Character	ON	Turn ON/OFF heat exchange

This card has been used primarily during model development debugging. It is in the release version because it can be useful in evaluating relative effects of the hydrodynamic forcing functions and also as a debugging tool if the user decides to modify the code. Occasionally in estuarine applications, temperature is treated conservatively with the initial and boundary conditions set at a constant temperature with bottom and surface heat exchange turned off, although it is not recommended.

Example

DEAD SEA	WINDC	QINC	QOUTC	HEATC
Wb 1	ON	ON	ON	ON
Wb 2	ON	ON	ON	ON
Wb 3	ON	ON	ON	ON

Interpolation (INTERPOL)

FIELD	NAME	VALUE	DEFAULT	DESCRIPTION
1				(Ignored by code)
2	QINIC	Character	ON	Interpolate inflows, inflow temperatures, and inflow constituent concentrations, ON or OFF
3	DTRIC	Character	ON	Interpolate distributed tributary inflows and inflow temperatures and constituent concentrations, ON or OFF
4	HDIC	Character	ON	Interpolate head boundary elevations and boundary temperatures and constituent concentrations, ON or OFF

These options control whether time-varying data are input as a step function or linearly interpolated between data points. The latest version now gives the user control over inflow, distributed tributary inflow, and external head boundary elevations for each branch. If interpolation is used, then the user must ensure it is appropriate and the input data supply correct information. Many reservoirs have periods of no releases. If outflow interpolation is turned on, then input data must be set up so no outflow occurs during these periods. This is accomplished by including extra dates in the outflow file with zero outflows to ensure the interpolation routine yields zero outflows. For example, given the following outflow time-series in the branch [outflow file \[QOTFN\]](#):

JDAY	QOT
100.00	50.0
110.00	0.0
120.00	50.0

If interpolation is not used, then outflow from Julian day 100 to 110 is $50 \text{ m}^3 \text{ sec}^{-1}$, from Julian day 110 to 120 is $0.0 \text{ m}^3 \text{ sec}^{-1}$, and $50 \text{ m}^3 \text{ sec}^{-1}$ thereafter. If interpolation is turned on, then outflow linearly decreases from Julian day 100 to 110 and then increases from Julian day 110 to 120. To ensure no outflow occurs between day 110 and 120 with interpolation on, the outflow file should be setup as follows:

JDAY	QOT
100.0000	50.0
109.9999	50.0
110.0000	0.0
119.9999	0.0
120.0000	50.0

Example

INTERPOL	QINIC	DTRIC	HDIC
Br 1	ON	OFF	ON
Br 2	ON	OFF	ON
Br 3	ON	OFF	ON
Br 4	ON	OFF	ON

CONTROL FILE

INITIAL CONDITIONS

Related Cards and Files

[Branch Inflow File](#)

[Branch Distributed Tributary Inflow File](#)

[Branch Distributed Tributary Inflow Temperature File](#)

[Branch Distributed Tributary Inflow Concentration File](#)

[Branch External Upstream Head Elevation File](#)

[Branch External Upstream Head Temperature File](#)

[Branch External Upstream Head Concentration File](#)

[Branch External Downstream Head Elevation File](#)

[Branch External Downstream Head Temperature File](#)

[Branch External Downstream Head Concentration File](#)

Heat Exchange (HEAT EXCH)

FIELD	NAME	VALUE	DEFAULT	DESCRIPTION
1				(Ignored by code)
2	SLHTC	Character	TERM	Specify either term-by-term (TERM) or equilibrium temperature computations (ET) for surface heat exchange
3	SROC	Character	OFF	Read in observed short wave solar radiation, ON or OFF
4	RHEVC	Character	OFF	Turns ON/OFF Ryan-Harleman evaporation formula only for TERM (ignored if ET is chosen)
5	METIC	Character	ON	Turns ON/OFF meteorological data interpolation
6	FETCHC	Character	OFF	Turns ON/OFF Fang and Stefan (1994) fetch calculation
7	AFW	Real	9.2	a coefficient in the wind speed formulation, $\text{Wm}^{-2} \text{mm Hg}^{-1}$
8	BFW	Real	0.46	b coefficient in the wind speed formulation, $\text{Wm}^{-2} \text{mm Hg}^{-1} (\text{ms}^{-1})^{-\text{cfw}}$
9	CFW	Real	2.0	c coefficient in the wind speed formulation, [-]
10	WINDH	Real		Wind speed measurement height, m

This card specifies various parameters affecting surface heat exchange. [SLHTC] allows the user to specify whether a term-by-term accounting or the equilibrium temperature approach is used in the computation of surface heat exchange. Although the term-by-term approach is more theoretically sound, equilibrium temperatures have consistently given better results for the systems presented in Chapter 3. Predictions for a number of reservoirs in the Northeast underpredicted epilimnetic temperatures during the fall overturn period using the term-by-term method. The reasons for this are still being investigated.

The [METIC] variable turns ON/OFF linear interpolation of meteorological input data. The [SROC] variable allows the user to specify whether or not short wave solar radiation data are computed from cloud cover (the default), or whether the user specifies observed short wave solar radiation in the meteorological input file [METFN]. In the [meteorological data file](#), short wave solar radiation data are in units of W/m^2 and include only incident short-wave solar radiation on the water surface.

The [FETCHC] variable turns ON/OFF a technique of Fang and Stefan (1994) to compute fetch effects on wind. This should not be used for river sections and should be used with caution for reservoir/lake systems. A description is outlined in Appendix B under Dissolved Oxygen and reaeration coefficients. Note that internal fetch calculations are always on, but that you can choose the Fang and Stefan approach if desired.

The variables [AFW], [BFW], and [CFW] specify the coefficients to be used in the wind function used in computing surface heat exchange (for both term-by-term and equilibrium approaches) and evaporation (see Appendix A). The function has been generalized in the model to the following:

$$f(W_z) = afw + bfw W_z^{\text{cfw}}$$

CONTROL FILE

INITIAL CONDITIONS

where afw is in units of $Wm^{-2} mm Hg^{-1}$, bfw is in units of $Wm^{-2} mm Hg^{-1} (ms^{-1})^{-cfw}$, and cfw has no units. The default formulation is the recommended form of the function taken from Edinger, et. al. (1974), although there are several other forms that can be used. For systems that are thermally loaded such as cooling lakes, the Ryan-Harleman formulation that takes into account forced convection should be used with [RHEVC] set to ON. This only affects the term-by-term model and not the equilibrium temperature model. All of the wind speed formulations are referenced to a height at which wind speeds were measured. The variable [WINDH] allows the user to specify the height at which wind speed measurements were taken, and the model converts them to the appropriate wind speed at the height the wind speed formulation is based on.

Example

HEAT EXCH	SLHTC	SROC	RHEVC	METIC	FETCHC	AFW	BFW	CFW	WINDH
Wb 1	TERM	OFF	OFF	ON	OFF	9.2	0.46	2.0	2.0
Wb 2	TERM	OFF	OFF	ON	OFF	9.2	0.46	2.0	2.0
Wb 3	TERM	OFF	OFF	ON	OFF	9.2	0.46	2.0	2.0

Related Cards and Files

[Meteorology file](#)

Ice Cover (ICE COVER)

FIELD	NAME	VALUE	DEFAULT	DESCRIPTION
1				(Ignored by code)
2	ICEC	Character	OFF	Allow ice calculations
3	SLICEC	Character	DETAIL	Specifies the method of ice cover calculations - either SIMPLE or DETAIL
4	ALBEDO	Real	0.25	Ratio of reflection to incident radiation (albedo of ice)
5	HWI	Real	10.0	Coefficient of water-ice heat exchange, $W m^{-2} ^\circ C^{-1}$
6	BETAI	Real	0.6	Fraction of solar radiation absorbed in the ice surface
7	GAMMAI	Real	0.07	Solar radiation extinction coefficient, m^{-1}
8	ICEMIN	Real	0.05	Minimum ice thickness before ice formation is allowed, m
9	ICET2	Real	3.0	Temperature above which ice formation is not allowed, $^\circ C$

Ice calculations are controlled with this card. The variable [ICEC] turns ON/OFF ice calculations. Two different methods for computing ice cover are available. The first method ([SLICEC] = SIMPLE) was included in version 1.0 and is available for backwards compatibility. The second method, DETAIL, is the preferred method.

The coefficient of water-ice heat exchange [HWI], $W m^{-2} C^{-1}$, is a user specified calibration parameter that determines the rate of heat exchange between water and ice (see Appendix A). [BETAI] is the fraction of solar radiation absorbed at the ice surface and is similar to [BETA] in the surface heat exchange computations. [GAMMAI] is the solar radiation extinction coefficient through ice and is also similar to [GAMMA] in the surface heat exchange computations.

Albedo is the ratio of reflection to incident radiation. It is normally expressed by the albedo of a surface and varies widely depending on the solar altitude and the waterbody surface properties.

For free water surfaces, Anderson (1954), in his Lake Hefner studies, derived the following empirical formula for the water surface albedo, ALB_w , as a function of average solar altitude:

$$ALB_w = 1.18 A_s^{-0.77}$$

where A_s is average solar altitude in degrees. Anderson found the coefficient 1.18 and the exponent -0.77 to vary only slightly with cloud height and coverage.

For ice surface, a functional representation of albedo has not been established. Reported values for ice surface albedo vary greatly from about 10% for clear lake ice (Bolsenga, 1969) to almost 70% for snow free Arctic sea ice (Krutskih, et al., 1970). Krutskih, et al. suggest ice albedo is more dependent on air temperature than on solar altitude. Based on their extensive Arctic sea observations, ice surface albedo for solar radiation was determined as:

CONTROL FILE

INITIAL CONDITIONS

$$ALB_i = \varepsilon \quad \text{for } T_a \leq 0^\circ\text{C}$$

$$ALB_i = \xi + \omega e^{\Psi T_a} \quad \text{for } T_a > 0^\circ\text{C}$$

where ε , ξ , ω , and Ψ are empirical constants, and T_a is air temperature, $^\circ\text{C}$. Equation [\(A-53\)](#) is an empirical fit to the observed data given by Krutskih, et al. for Arctic ice.

The ice-water surface heat exchange coefficient for rivers was evaluated by Ashton (1979):

$$HWI = CWI \frac{U^{0.8}}{D^{0.2}}$$

Where U is the river velocity in m/s, D is the river depth in m, and CWI is an empirical coefficient ranging from 1622 to 2433 $\text{W s}^{0.8} \text{m}^{-2.6} ^\circ\text{C}^{-1}$.

Note that the ice cover algorithm does not take into account snow accumulation on the ice surface.

Example

ICE COVER	ICEC	SLICEC	ALBEDO	HWI	BETAI	GAMMAI	ICEMIN	ICET2
Wb 1	OFF	DETAIL	0.25	10.0	0.6	0.07	0.05	3.0
Wb 2	OFF	DETAIL	0.25	10.0	0.6	0.07	0.05	3.0
Wb 3	OFF	DETAIL	0.25	10.0	0.6	0.07	0.05	3.0

Related Cards and Files

[Initial Conditions](#)

Transport Scheme (TRANSPORT)

FIELD	NAME	VALUE	DEFAULT	DESCRIPTION
1				(Ignored by code)
2	SLTRC	Character	ULTIMATE	Transport solution scheme, ULTIMATE, QUICKEST, or UPWIND
3	THETA	Real	0.55	Time-weighting for vertical advection scheme

This card specifies the transport solution scheme used by the model. There are three options for [SLTRC] – UPWIND, QUICKEST, or ULTIMATE with the latter being the recommended option. The older solution schemes are retained in this version of the model mainly as a means of comparing the different solution schemes. The QUICKEST option employs a higher-order solution scheme to reduce numerical diffusion present in the original UPWIND differencing scheme. The ULTIMATE option eliminates the physically unrealistic over/undershoots that QUICKEST generates near regions of sharp concentration gradients.

[THETA] specifies the amount of time weighting in the vertical advection scheme. A value of 0 specifies fully explicit vertical advection, 1 specifies fully implicit vertical advection, and 0.5 specifies a Crank-Nicholson scheme. The recommended value for [THETA] is 0.55. This ensures unconditional numerical stability for vertical transport. Vertical diffusion is always fully implicit.

It should be pointed out that while the addition of the ULTIMATE algorithm eliminates physically unrealistic over/undershoots due to longitudinal transport, the model could still generate over/undershoots when using implicit weighting for vertical transport. This is a result of phase errors generated when trying to resolve sharp vertical gradients over a few computational cells and can be eliminated completely by setting [THETA] to zero.

Example

```
TRANSPORT  SLTRC  THETA
Wb 1      ULTIMATE  0.55
Wb 2      ULTIMATE  0.55
Wb 3      ULTIMATE  0.55
```

Hydraulic Coefficients (HYD COEF)

FIELD	NAME	VALUE	DEFAULT	DESCRIPTION
1				(Ignored by code)
2	AX	Real	1.0	Longitudinal eddy viscosity, $m^2 sec^{-1}$
3	DX	Real	1.0	Longitudinal eddy diffusivity, $m^2 sec^{-1}$
4	CBHE	Real	0.3	Coefficient of bottom heat exchange, $W m^{-2} ^\circ C^{-1}$
5	TSED	Real	-	Sediment temperature, $^\circ C$
6	FI	Real	0.01	Interfacial friction factor
7	TSEDF	Real	1.0	Heat lost to sediments that is added back to water column
8	FRICC	Character	CHEZY	Bottom friction solution, MANN or CHEZY
9	Z0	Real	0.001	Water surface roughness height, m

This card specifies hydraulic and bottom heat exchange coefficients that can be varied during model calibration. The horizontal eddy viscosity [AX] specifies dispersion of momentum in the X-direction. Note that for estuaries the value of [AX] is often as high as 10-30 m^2/s . The horizontal eddy diffusivity [DX] specifies dispersion of heat and constituents in the X-direction. [DX] can vary significantly from the default value of 1 m^2/s in estuaries and rivers, with values as high as 10 to 100 m^2/s . Dye studies are often used to calibrate the value of [DX]. One approach by Okubo (1971) for estimating [DX] in units of m^2/s when the longitudinal grid spacing Δx is in m is:

$$D_x = 5.84 \times 10^{-4} \Delta x^{1.1}$$

Both values are presently time and space invariant. The Chezy coefficient is used in calculating effects of bottom friction. The coefficient of bottom heat exchange [CBHE] and the sediment temperature [TSED] are used to compute heat exchange at the ground-water interface. Sediment temperature can be estimated from average annual temperature at the site. Recommended values are given in the example.

[TSEDF] is a coefficient that varies from 0 to 1. This regulates how short-wave solar radiation that penetrates to the bottom of the grid is handled in the code. A value of 1.0 specifies that 100% of the incident short wave solar impinging on the channel bottom is re-radiated as heat to the water column. A value of 0 means that 0% of the shortwave solar radiation is reradiated into the water column resulting in a loss of the solar radiation from the system.

Previous experience has shown recommended values produce remarkably accurate temperature predictions for a wide variety of systems. The horizontal eddy viscosities and diffusivities and Chezy or Manning's n coefficient may need additional tuning especially in modeling rivers or estuaries. The Chezy or Manning's n coefficient is important in estuarine applications for calibrating tidal range and phase.

Typical values for the Chezy coefficient and Manning's friction factors have been 70 and 0.035, respectively. In estuaries and rivers, these values can vary widely, especially since often this friction factor incorporates errors in the bathymetry of the model. For Manning's friction factors, a range of values have been used in rivers and estuaries from 0.01 to 0.1 or higher. These are usually determined by calibrating the model to water surface elevation data.

INITIAL CONDITIONS

CONTROL FILE

Starting with Version 3.6, the user can specify the value of [Z0], the roughness height of the water. Typical values are less than 10% of the actual roughness height elements (often roughness height divided by 30 is used) and can range from 10^{-3} to 10^{-4} m.

Example

HYD COEF	AX	DX	CBHE	TSER	FI	TSERF	FRIC	Z0
Wb 1	1.0	1.0	0.3	11.5	0.01	1.00	MANN	0.001
Wb 2	1.0	1.0	0.3	11.5	0.01	1.00	MANN	0.001
Wb 3	1.0	1.0	0.3	11.5	0.01	1.00	MANN	0.001

Vertical Eddy Viscosity (EDDY VISC)

FIELD	NAME	VALUE	DEFAULT	DESCRIPTION
1				(Ignored by code)
2	AZC	Character	TKE	Form of vertical turbulence closure algorithm, NICK, PARAB, RNG, W2, W2N, TKE, or TKE1
3	AZSLC	Character	IMP	Specifies either implicit, IMP, or explicit, EXP, treatment of the vertical eddy viscosity in the longitudinal momentum equation.
4	AZMAX	Real	1.0	Maximum value for vertical eddy viscosity, $m^2 s^{-1}$
5	FBC	Integer	3	Only active if AZC=TKE1; Choice of boundary condition: =1 Celik Rodi 1988, =2 Rodi 1983, =3 Original CE-QUAL-W2 boundary condition
6	E	Real	9.535	Only active if AZC=TKE1; roughness coefficient
7	ARODI	Real	0.431	Only active if AZC=TKE1; choose typical Values of 0.43 if FBC=1 and 0.07 if FBC=2. Not used if FBC=3.
8	STRCKLR	Real	24.0	Only active if AZC=TKE1; If this is =0.0, then the the Strickler Nickuradse relationships are NOT used to calculate the roughness coefficient; if >0.0, then the Strickler Nickuradse relationships are used to calculate the roughness coefficient. The value of the coefficient sets the relationship between the surface roughness and the Manning's friction factor.
9	BOUNDFR	Real	10.0	Only active if AZC=TKE1; if =0.0, then Boundary production is OFF. If > 0.0, then boundary production is ON. The value of the boundary friction production constant is set by this constant.
10	TKECAL	Character	IMP	Only active if AZC=TKE1; select either the implicit or explicit vertical transport term formulation, options then are either IMP or EXP.

[AZC] specifies the vertical turbulence algorithm used in the horizontal momentum equation. The following table lists the options available in Version 3. For more information see Appendix A.

Table C-23. Vertical Eddy Viscosity Formulations

Formulation	Formula	Reference
Nickuradse [NICK]	$v_t = \ell_m^2 \left \frac{\partial u}{\partial z} \right e^{-CRi}$ $\ell_m = H \left[0.14 - 0.08 \left(1 - \frac{z}{H} \right)^2 - 0.06 \left(1 - \frac{z}{H} \right)^4 \right]$	Rodi (1993)
Parabolic [PARAB]	$v_t = \kappa u_* z \left(1 - \frac{z}{H} \right) e^{-CRi}$	Engelund (1976)

INITIAL CONDITIONS

CONTROL FILE

[W2] (used in V2)	$\nu_t = \kappa \left(\frac{l_m^2}{2} \right) \sqrt{\left(\frac{\partial U}{\partial z} \right)^2 + \left(\frac{\tau_{wy} e^{-2kz} + \tau_{y trib}}{\rho \nu_t} \right)^2} e^{(-CR_i)}$ $\ell_m = \Delta z_{max}$	Cole and Buchak (1995)
W2 with mixing length of Nickuradse [W2N]	$\nu_t = \kappa \left(\frac{l_m^2}{2} \right) \sqrt{\left(\frac{\partial U}{\partial z} \right)^2 + \left(\frac{\tau_{wy} e^{-2kz} + \tau_{y trib}}{\rho \nu_t} \right)^2} e^{(-CR_i)}$ $\ell_m = H \left[0.14 - 0.08 \left(1 - \frac{z}{H} \right)^2 - 0.06 \left(1 - \frac{z}{H} \right)^4 \right]$	Cole and Buchak (1995) and Rodi (1993)
[RNG] (renormalization group)	$\nu_t = \nu \left[1 + \Psi \left(3\kappa \left(\frac{zu_*}{\nu} \right)^3 \left(1 - \frac{z}{H} \right)^3 - C_1 \right) \right]^{1/3} e^{-CR_i}$	Simoes (1998)
TKE (Turbulent kinetic energy) also TKE1 but with special conditons	$\nu_t = C_\mu \frac{k^2}{\varepsilon}$ <p>where k and ε are defined from</p> $\frac{\partial k B}{\partial t} + \frac{\partial k B U}{\partial x} + \frac{\partial k B W}{\partial z} - \frac{\partial}{\partial z} \left(B \frac{\nu_t}{\sigma_k} \frac{\partial k}{\partial z} \right) - \frac{\partial}{\partial x} \left(B \frac{\nu_t}{\sigma_k} \frac{\partial k}{\partial x} \right) = B(P + G - \varepsilon + P_k)$ $\frac{\partial \varepsilon B}{\partial t} + \frac{\partial \varepsilon B U}{\partial x} + \frac{\partial \varepsilon B W}{\partial z} - \frac{\partial}{\partial z} \left(B \frac{\nu_t}{\sigma_\varepsilon} \frac{\partial \varepsilon}{\partial z} \right) - \frac{\partial}{\partial x} \left(B \frac{\nu_t}{\sigma_\varepsilon} \frac{\partial \varepsilon}{\partial x} \right) = B \left(C_{\varepsilon 1} \frac{\varepsilon}{k} P + C_{\varepsilon 2} \frac{\varepsilon^2}{k} + P_\varepsilon \right)$	Wells (2003)
<p>where:</p> <p> ℓ_m = mixing length C = constant (assumed 0.15) k = wave number (in W2 models) z = vertical coordiante u_* = shear velocity ρ = liquid density H = depth κ = von Karman constant Ψ(x) = max(0,x) u = horizontal velocity τ_{wy} = cross-shear from wind ν = molecular viscosity Ri = Richardson number Δz_{max} = maximum vertical grid spacing C_1 = empirical constant, 100 $\tau_{y trib}$ = cross-shear from lateral tributaries B = width ν_t = turbulent viscosity k = turbulent kinetic energy (in TKE model) ε = turbulent energy dissipation rate P = turbulent energy production from boundary friction U = longitudinal velocity (laterally averaged) W = vertical velocity (laterally averaged) σ = turbulent Prandlt number </p> $P = \nu_t \left[\left(\frac{\partial U}{\partial z} \right)^2 \right]$ <p>Production term: Buoyancy term: $G = -\frac{\nu_t}{\sigma_t} N^2$ Brunt–Vaisala frequency $N = \sqrt{-\frac{g}{\rho} \frac{d\rho}{dz}}$</p> <p>$C_\varepsilon, C_\mu$ = constants in the TKE model</p>		

CONTROL FILE

INITIAL CONDITIONS

The formulations PARAB, NICK, and RNG are appropriate for riverine/estuarine sections in which shear due to friction is dominant. The W2 is usually the choice for reservoirs and lakes where wind shear is dominant. The k-ε turbulence formulation is though general to any waterbody and was added to W2 in order to eliminate the choice of turbulence scheme for the model user. The k-ε model though is computationally expensive and similar results can often be obtained at less computational cost using another formulation.

To be backwards compatible with Version 2, set [AZC] to W2, [AZSLC] to EXP, and [AZMAX] to 1.0E-4 even though a value of 1.0E-3 is recommended as a minimum value of the maximum vertical eddy viscosity [AZ]. Note that for all model applications, we recommend using [AZC]=TKE, [AZSLC]=IMP and [AZMAX]= $1 \text{ m}^2 \text{ s}^{-1}$. Setting [AZSLC] to EXP and [AZMAX] greater than 1.0E-2 will result in very low model time steps. In this case, setting [AZSLC] to IMP will remove the time step limitation allowing for much larger timesteps.

Only by choosing [AZC]=TKE1 are the other variables [FBC], [E], [ARODI], [STRCKLR], [BOUNDFR], and [TKECAL] active. These variables are described in detail in Gould (2006).

[FBC] sets the boundary condition for the model. The choices are [FBC]=1 Celik and Rodi (1988) model, [FBC]=2 Celik and Rodi (1983) model, [FBC]=3 Original TKE formulation found in CE-QUAL-W2. The user has the option of specifying the boundary roughness by setting the value of [E], the boundary roughness coefficient. [ARODI] sets the value of the coefficient used in the [FBC]=1 and [FBC]=2 models for computing boundary friction. [STRCKLR] gives a coefficient (typical is 24.0) used when Strickler Nickuradse relationships are used to calculate the roughness coefficient in the equation $k_s = (n \cdot 24.04)^6$. [BOUNDFR] sets the boundary condition for production, a typical value is 10.0 and is used in the production term as shown below:

$$P_\varepsilon = \frac{[\text{BOUNDFR}]C_f^{1.25}U^4}{(0.5B)^2}$$

[TKECAL] sets the implicit or explicit solution of the vertical transport terms in the k-ε model.

Example

EDDY VISC	AZC	AZSLC	AZMAX	FBC	E	ARODI	STRCKLR	BOUNDFR	TKECAL
WB 1	TKE	IMP	1.00	3	9.535	0.430	24.0	10.00	IMP
WB 2	TKE	IMP	1.00	3	9.535	0.430	24.0	10.00	IMP
WB 3	W2	IMP	1.00	3	9.535	0.430	24.0	10.00	IMP

Related Cards and Files

[Timestep Limitations](#)

Number of Structures (N STRUC)

FIELD	NAME	VALUE	DESCRIPTION
1			(Ignored by code)
2	NSTR	Integer	Number of branch outlet structures
3	DYNELEV	Character	ON or OFF. If this field is blank the model will assume this is OFF.

This card specifies the number of outlet structures for each branch. Outflows are computed based on a selective withdrawal algorithm. DYNELEV tells the model to use dynamic centerline elevation for the structure. Usually the centerline elevation is fixed and specified with ESTR. If this is ON, the model will read a separate file for each branch called **dynselevX.npt** where X is the branch number. The format of this file is shown in the input file descriptions. If this file is supplied, the value of ESTR is ignored.

Example

```

N STRUC      NSTR DYNELEV
Br 1          0      OFF
Br 2          0      OFF
Br 3          3      ON
Br 4          0      OFF

```

Related Cards and Files

[Inflow/Outflow Dimensions](#)

[Sink Type](#)

[Structure Elevation](#)

[Structure Width](#)

[Structure Interpolation](#)

[Structure Top Selective Withdrawal Limit](#)

[Structure Bottom Selective Withdrawal Limit](#)

[Outflow file](#)

Structure Interpolation (STR INT)

FIELD	NAME	VALUE	DEFAULT	DESCRIPTION
1				(Ignored by code)
2-10	STRIC	Character	OFF	Turns ON/OFF interpolation of structure outflows

The outflows specified by the outflow file can either be assumed to be step functions with [STRIC] set to OFF, or can be linearly interpolated between values with [STRIC] set to ON.

Example

STR INT	STRIC	STRIC	STRIC	STRIC	STRIC	STRIC	STRIC	STRIC	STRIC
Br 1									
Br 2									
Br 3	ON	ON	ON						
Br 4									

Related Cards and Files

[Inflow/Outflow Dimensions](#)

[Number of Structures](#)

[Sink Type](#)

[Structure Elevation](#)

[Structure Width](#)

[Structure Top Selective Withdrawal Limit](#)

[Structure Bottom Selective Withdrawal Limit](#)

[Outflow file](#)

Structure Top Selective Withdrawal Limit (STR TOP)

FIELD	NAME	VALUE	DESCRIPTION
1			(Ignored by code)
2-10	KTSTR	Integer	Top layer above which selective withdrawal will not occur

The selective withdrawal algorithm calculates vertical withdrawal zone limits based on outlet geometry, outflows, and in-pool densities. The algorithm then assigns flows for each layer within the withdrawal zone. This card specifies the top elevation for which outflows are calculated in the selective withdrawal algorithm. This option can be used to mimic the effects of a curtain weir that limits the upper extent of the withdrawal zone. In the absence of any structure or topographic feature that limits the top of the selective withdrawal zone, the elevation should be set to the top elevation of the computational grid. If the structure centerline elevation is above KTSTR, then the value of KTSTR is raised to the centerline elevation.

As a default, the user should set this to layer 2 unless there is some reason to suspect that there is a restriction of the structure limiting its withdrawal above the centerline of the outlet.

Example

STR TOP	KTSTR	KTSTR	KTSTR	KTSTR	KTSTR	KTSTR	KTSTR	KTSTR	KTSTR
Br 1									
Br 2									
Br 3	2	2	2						
Br 4									

Related Cards and Files

[Inflow/Outflow Dimensions](#)

[Number of Structures](#)

[Sink Type](#)

[Structure Elevation](#)

[Structure Width](#)

[Structure Interpolation](#)

[Structure Bottom Selective Withdrawal Limit](#)

[Outflow file](#)

Structure Bottom Selective Withdrawal Limit (STR BOT)

FIELD	NAME	VALUE	DESCRIPTION
1			(Ignored by code)
2-10	KBSTR	Integer	Bottom layer below which selective withdrawal will not occur

The selective withdrawal algorithm calculates vertical withdrawal zone limits based on outlet geometry, outflows, and in-pool densities. The algorithm then assigns flows for each layer within the withdrawal zone. This card specifies the bottom elevation for which outflows are calculated in the selective withdrawal algorithm. This option can be used to simulate the effects of an upstream submerged weir, accumulation of debris at the trash racks, an upstream cofferdam, etc. In the absence of any structure or topographic feature limiting the bottom withdrawal layer, the value should be set to the bottommost active layer at the downstream segment. If the structure centerline elevation is below KBSTR, then the value of KBSTR is lowered to the centerline elevation.

As a default, the user should set this to layer KB (lowest active layer) at the location of the structure unless there is some reason to suspect that there is a restriction of the structure limiting its withdrawal below the centerline of the outlet.

Example

STR BOT	KBSTR	KBSTR	KBSTR	KBSTR	KBSTR	KBSTR	KBSTR	KBSTR	KBSTR
Br 1									
Br 2									
Br 3	22	22	22						
Br 4									

Related Cards and Files

[Inflow/Outflow Dimensions](#)

[Number of Structures](#)

[Sink Type](#)

[Structure Elevation](#)

[Structure Width](#)

[Structure Interpolation](#)

[Structure Top Selective Withdrawal Limit](#)

[Outflow file](#)

Sink Type (SINK TYPE)

FIELD	NAME	VALUE	DEFAULT	DESCRIPTION
1				(Ignored by code)
2-10	SINKC	Character	POINT	Sink type used in the selective withdrawal algorithm, LINE or POINT

This card specifies the sink type for each withdrawal. The options are LINE or POINT each of which has different selective withdrawal characteristics.

Line sinks are usually structures wide in relation to dam width ($> 1/10$). Point sinks are usually structures narrow in relation to dam width ($< 1/10$).

Example

SINK TYPE	SINKC	SINKC	SINKC	SINKC	SINKC	SINKC	SINKC	SINKC	SINKC
Br 1									
Br 2									
Br 3	POINT	POINT	POINT						
Br 4									

Related Cards and Files

[Inflow/Outflow Dimensions](#)

[Number of Structures](#)

[Structure Elevation](#)

[Structure Width](#)

[Structure Interpolation](#)

[Structure Top Selective Withdrawal Limit](#)

[Structure Bottom Selective Withdrawal Limit](#)

[Outflow file](#)

Structure Elevation (E STRUC)

FIELD	NAME	VALUE	DESCRIPTION
1			(Ignored by code)
2-10	ESTR	Real	Centerline elevation of structure, <i>m</i>

This card specifies the centerline elevation for each withdrawal structure by branch.

Example

E STRUC	ESTR	ESTR	ESTR	ESTR	ESTR	ESTR	ESTR	ESTR	WSTR
Br 1									
Br 2									
Br 3	45.0	25.00	15.00						
Br 4									

Related Cards and Files

[Inflow/Outflow Dimensions](#)

[Number of Structures](#)

[Sink Type](#)

[Structure Width](#)

[Structure Interpolation](#)

[Structure Top Selective Withdrawal Limit](#)

[Structure Bottom Selective Withdrawal Limit](#)

[Outflow file](#)

Structure Width (W STRUC)

FIELD	NAME	VALUE	DESCRIPTION
1			(Ignored by code)
2-10	WSTR	Real	Width of structure (line sink), <i>m</i>

This card specifies the width of the structures by branch if a line sink is specified as the sink type [[SINKC](#)]. The values are ignored if a point sink is specified. If there are more outlet structures than will fit on a line, then the widths are continued on the next line starting in field 2.

Example

W STRUC	WSTR	WSTR	WSTR	WSTR	WSTR	WSTR	WSTR	WSTR	WSTR
Br 1									
Br 2									
Br 3	10.0	10.0	10.0						
Br 4									

Related Cards and Files

[Inflow/Outflow Dimensions](#)

[Number of Structures](#)

[Sink Type](#)

[Structure Elevation](#)

[Structure Interpolation](#)

[Structure Top Selective Withdrawal Limit](#)

[Structure Bottom Selective Withdrawal Limit](#)

[Outflow file](#)

Pipes (PIPES)

FIELD	NAME	VALUE	DEFAULT	DESCRIPTION
1				(Ignored by code)
2	IUPI	Integer		Pipe upstream segment number
3	IDPI	Integer		Pipe downstream segment number
4	EUPI	Real		Upstream invert elevation, <i>m</i>
5	EDPI	Real		Downstream invert elevation, <i>m</i>
6	WPI	Real		Pipe diameter, <i>m</i>
7	DLXPI	Real		Pipe length, <i>m</i>
8	FPI	Real		Bottom roughness (Mannings' friction)
9	FMINPI	Real		Minor friction losses
10	LATPIC	Character		Downstream or lateral pipe withdrawal, DOWN or LAT
11	DYNPIPE	Character		Either ON or OFF. This turns OFF or ON the dynamic pipe switch

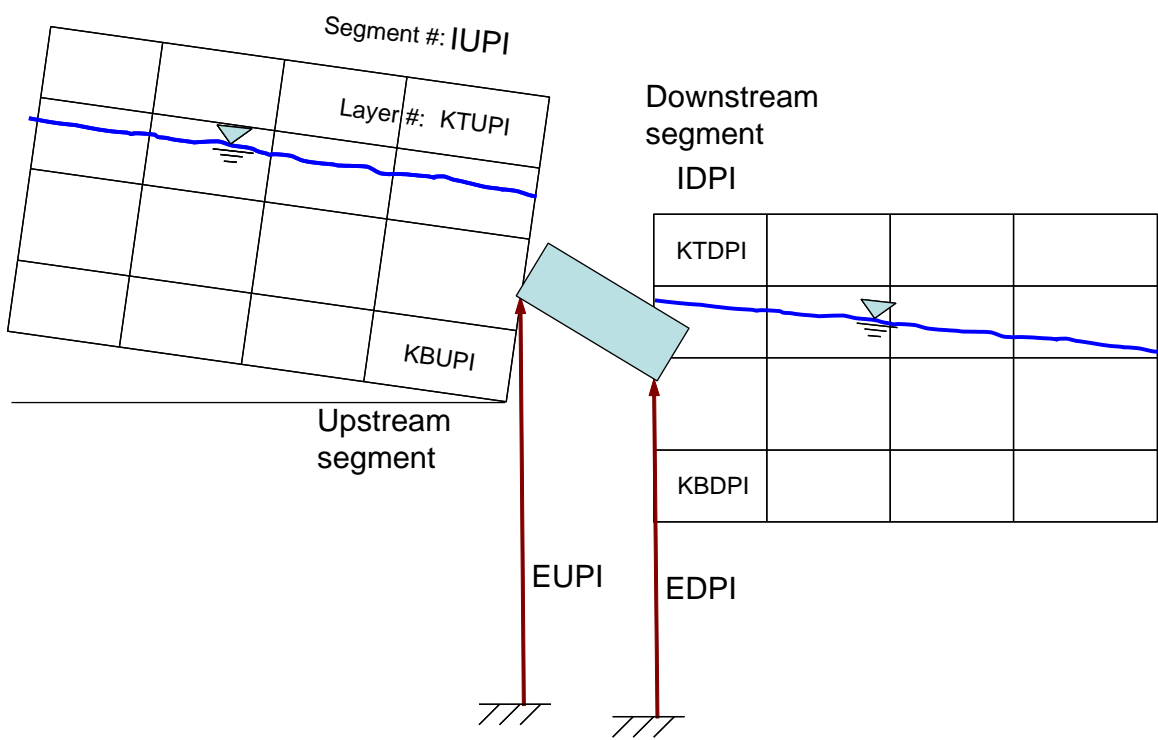
This card specifies the characteristics for each pipe included in the simulation. [IUSPI] and [IDPI] specify the upstream segment location and downstream segment location of the pipe, respectively. The user must also set an upstream [EUPI] and downstream [EDPI] invert elevation, diameter [WPI], and length [DLXPI] for each pipe. [FPI] sets the bottom roughness value (using a Manning's friction factor) and [FMINPI] specifies the minor friction losses.

Setting the pipe location [LATPIC] to DOWN specifies that the pipe is at the downstream end of the segment. In this case the water surface elevations are computed based on the right hand side water surface elevation of the segment. The elevation of the right hand side of the segment is estimated using the water surface slope of segment IUPI and IUPI-1. Also, momentum from the outflow is preserved as in a downstream structure withdrawal. If the pipe location [LATPIC] is set to LAT, it is assumed that the outflow is treated as a lateral withdrawal at the segment center elevation. In both cases selective withdrawal is used in the computations.

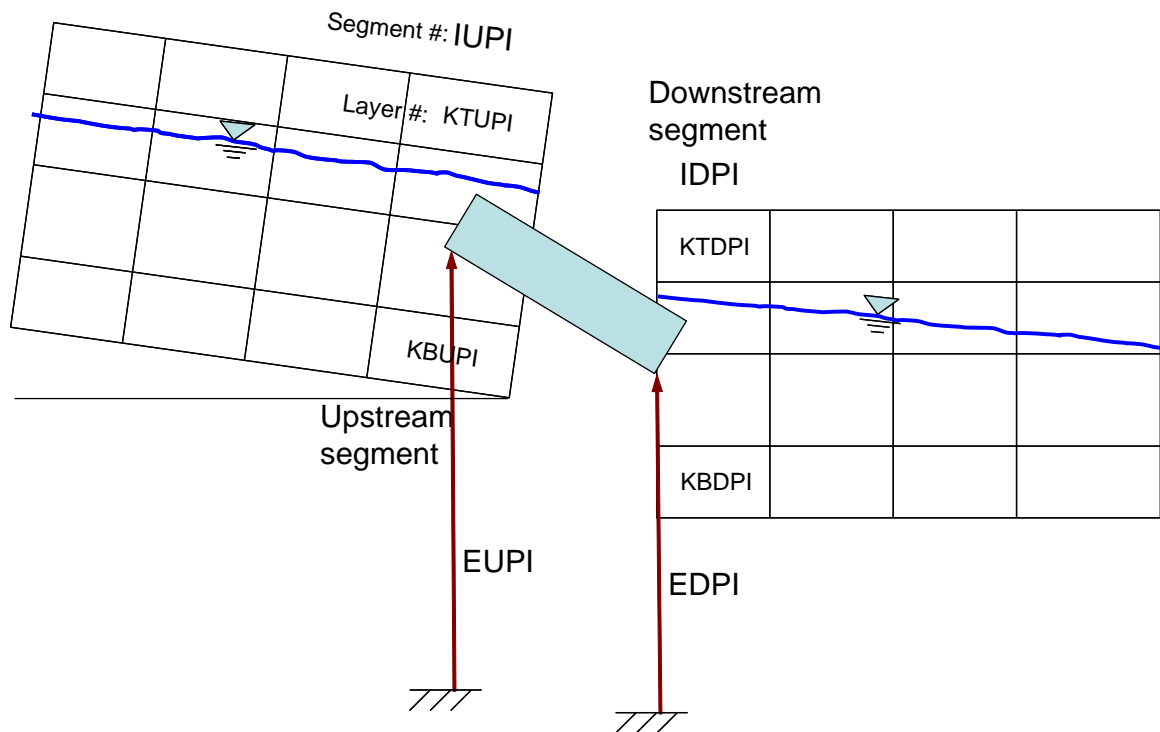
Note that for a downstream segment that is at the upstream end of a branch, this inflow is treated as an inflow. If it is input to a downstream segment that is not the upstream end, it is treated as a tributary inflow.

The following figures show the layout of pipes set as a downstream [DOWN] and a lateral [LAT] withdrawal from the upstream segment.

Downstream Pipe (DOWN)



Lateral Pipe (LAT)



When the DYNPIPE switch is ON, the CE-QUAL-W2 model reads a file called, **dynpipe.npt**. This file is in the same format as all time series files (see section on input files) with a time series of Julian day and a number usually from 0 to 1. The number is then multiplied by the flow rate computed for the pipe and has the effect of turning the pipe ON or OFF or reducing the flow for given periods of time. This input is treated as a step function, i.e., no linear interpolation between successive values. In many cases a gate valve is restricted to reduce the flow through the pipe over a certain time of year and later opened.

Example

PIPE	IUPI	IDPI	EUPI	EDPI	WPI	DLXPI	FPI	FMINPI	LATPIC	DYNPIPE
Pi 1	24	28	28.0	27.0	0.5	230.0	0.065	0.10	DOWN	ON

Related Cards and Files

[Inflow/Outflow Dimensions](#)

[Upstream Pipe](#)

[Downstream Pipe](#)

Upstream Pipe (PIPE UP)

FIELD	NAME	VALUE	DEFAULT	DESCRIPTION
1				(Ignored by code)
2	PUPIC	Character	DISTR	Specifies how inflows enter into the upstream pipe segment, DISTR, DENSITY, or SPECIFY
3	ETUPI	Real		Top elevation pipe inflows enter when using SPECIFY option, <i>m</i>
4	EBUPI	Real		Bottom elevation pipe inflows enter when using SPECIFY option, <i>m</i>
5	KTUPI	Integer		Top layer above which selective withdrawal will not occur
6	KBUPI	Integer		Bottom layer below which selective withdrawal will not occur

This card specifies how inflows/outflows for the upstream pipe location are handled. Setting [TRIBPL] to DISTR distributes the inflows evenly from the water surface to the bottom active layer, setting it to DENSITY places the inflows into a layer with similar density, and setting it to SPECIFY allows the user to specify a top and bottom elevation into which inflows enter. If the SPECIFY option is used, then [TRIBTOP] and [TRIBBOT] are used to specify the top and bottom elevations that the inflows are distributed over.

[KWTOP] and [KWBOT] are used to set the upper and lower layers above and below which outflow does not occur in the selective withdrawal algorithm.

Example

```
PIPE UP      PUPIC  ETUPI  EBUPI  KTUPI  KBUPI
Pi 1        DISTR              2      19
```

Related Cards and Files

[Inflow/Outflow Dimensions](#)
[Pipes](#)
[Downstream Pipe](#)

Downstream Pipe (PIPE DOWN)

FIELD	NAME	VALUE	DEFAULT	DESCRIPTION
1				(Ignored by code)
2	PDPIC	Character	DISTR	How inflows enter into the downstream pipe segment, DISTR, DENSITY, or SPECIFY
3	ETDPI	Real		Top elevation pipe inflows enter using SPECIFY option, <i>m</i>
4	EBDPI	Real		Bottom elevation pipe inflows enter using SPECIFY option, <i>m</i>
5	KTDPI	Integer		Top layer above which selective withdrawal will not occur
6	KBDPI	Integer		Bottom layer below which selective withdrawal will not occur

This card specifies how inflows/outflows for the downstream pipe location are handled. Setting [PDPIC] to DISTR distributes the inflows evenly from the water surface to the bottom active layer, setting it to DENSITY places the inflows into a layer with similar density, and setting it to SPECIFY allows the user to specify a top and bottom elevation into which inflows enter. If the SPECIFY option is used, then [ETDPI] and [EBDPI] are used to specify the top and bottom elevations that the inflows are distributed over.

[KTDPI] and [KBDPI] are used to set the upper and lower layers above and below which outflow does not occur in the selective withdrawal algorithm.

Example

```
PIPE DOWN  PDPIC  ETDPI  EBDPI  KTDPI  KBDPI
Pi 1      DISTR           2      23
```

Related Cards and Files

[Inflow/Outflow Dimensions](#)
[Pipes](#)
[Upstream Pipe](#)

Spillways (SPILLWAYS)

FIELD	NAME	VALUE	DEFAULT	DESCRIPTION
1				(Ignored by code)
2	IUSP	Integer		Spillway segment location
3	IDSP	Integer		Downstream segment spillway outflow enters
4	ESP	Real		Spillway elevation, m
5	A1SP	Real		α_1 , empirical coefficient for free-flowing conditions
6	B1SP	Real		β_1 , empirical coefficient for free-flowing conditions
7	A2SP	Real		α_2 , empirical coefficient for submerged conditions
8	B2SP	Real		β_2 , empirical coefficient for submerged conditions
9	LATSPC	Character		Downstream or lateral withdrawal, DOWN or LAT

This card specifies the spillway (or weir) characteristics. [IUSP] and [IDSP] specify the upstream and downstream segments for the spillway. Setting [IDSP] to 0 allows the user to spill water and have that water lost from the system. The model requires the user to specify a head (h) versus flow (Q) relationship in the following form for freely flowing conditions:

$$Q = \alpha_1 \Delta h^{\beta_1}$$

where:

α_1 = empirical parameter
 β_1 = empirical parameter
 $\Delta h = Z_u - Z_{sp}$, m
 Z_u = upstream head, m
 Z_{sp} = the spillway crest elevation, m

And for submerged conditions:

$$Q = \alpha_2 \Delta h^{\beta_2}$$

where:

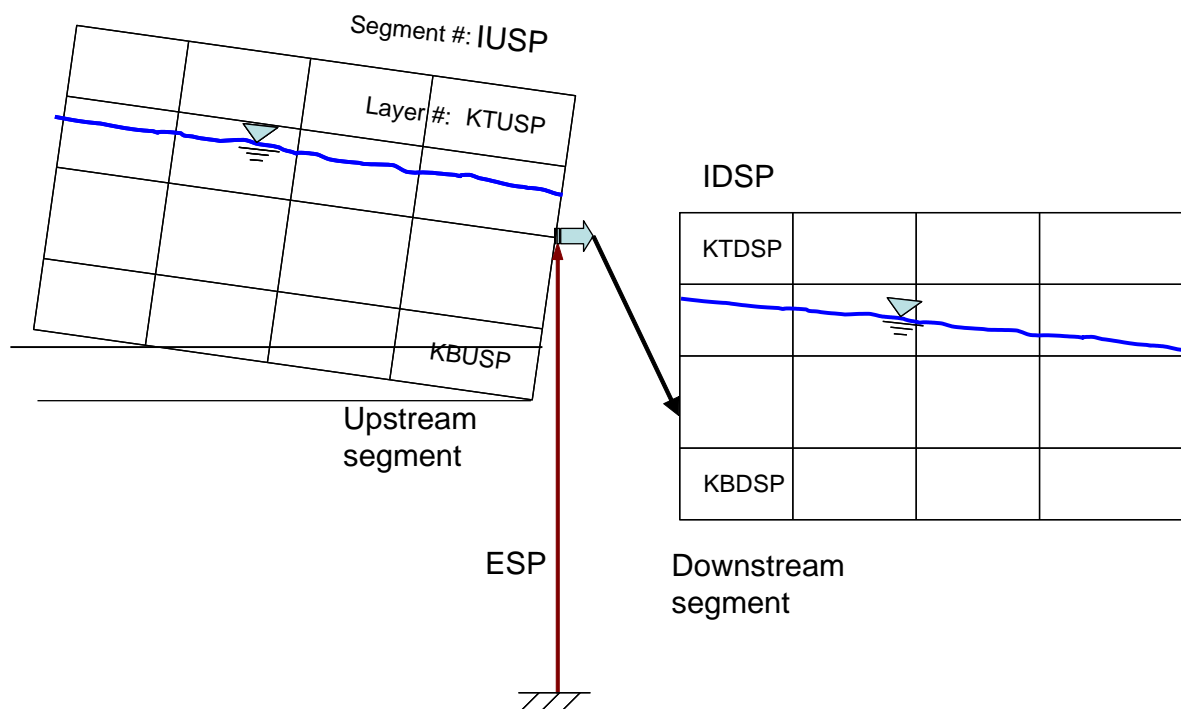
α_2 = empirical parameter
 β_2 = empirical parameter
 $\Delta h = Z_u - Z_d$, m
 Z_u = upstream head, m
 Z_d = downstream head, m

Submerged conditions are defined when the tailwater depth over the upstream energy head (static head and velocity head) is greater than 0.67. Even though negative flow rates are possible using the second equation when the downstream head is greater than the upstream head, these results should be used with caution since rarely are rating curves done for reverse flow. The user should ensure a smooth transition between submerged and free flowing conditions by proper choice of model coefficients. See [Appendix A](#) for further information.

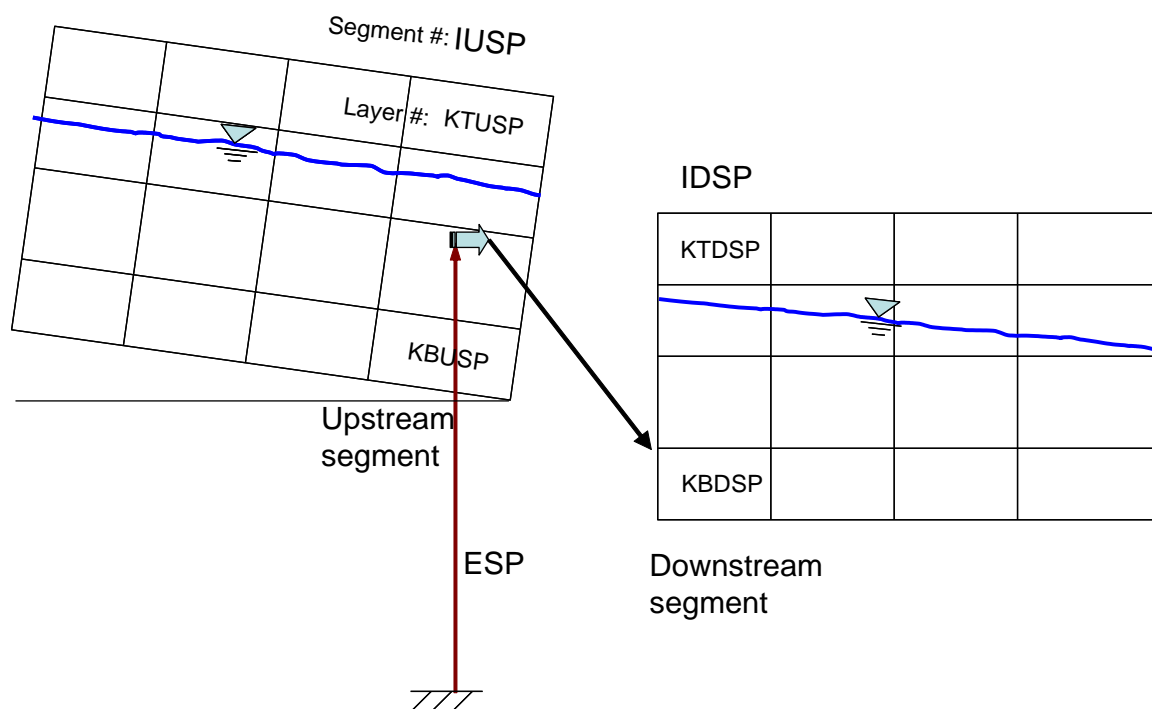
Setting the spillway location [LATSPC] to DOWN specifies that the spillway is at the downstream end of the segment. In this case the water surface elevations are computed based on the right hand side of segment IUSP. This water surface elevation is estimated based on the slope of the water surface at IUSP and IUSP-1. Also, momentum from the outflow is preserved as in a downstream structure withdrawal. If the spillway location [LATPIC] is set to LAT, it is assumed that the outflow is treated as a lateral withdrawal at the segment center elevation. In both cases selective withdrawal is used in the computations.

The following figures show the layout of spillways set as a downstream [DOWN] and a lateral [LAT] withdrawal from the upstream segment.

Downstream Spillway (DOWN)



Lateral Spillway (LAT)



Example

SPILLWAYS	IUSP	IDSP	ESP	A1SP	B1SP	A2SP	B2SP	LATSPC
Sp 1	30	33	45.5	45.33	1.5	34.45	1.0	DOWN
Sp 2	28	33	40.0	10.00	1.5	20.00	1.0	LAT

Related Cards and Files

[Inflow/Outflow Dimensions](#)
[Upstream Spillways](#)
[Downstream Spillways](#)
[Spillway Dissolved Gas](#)

Upstream Spillways (SPILL UP)

FIELD	NAME	VALUE	DEFAULT	DESCRIPTION
1				(Ignored by code)
2	PUSPC	Character	DISTR	How inflows enter into the upstream spillway segment, DISTR, DENSITY, or SPECIFY
3	ETUSP	Real		Top elevation spillway inflows enter using SPECIFY option, <i>m</i>
4	EBUSP	Real		Bottom elevation spillway inflows enter using SPECIFY option, <i>m</i>
5	KTUSP	Integer		Top layer above which selective withdrawal will not occur
6	KBUSP	Integer		Bottom layer below which selective withdrawal will not occur

This card specifies how inflows/outflows for the upstream spillway location are handled. Setting [PUSPC] to DISTR distributes the inflows evenly from the water surface to the bottom active layer, setting it to DENSITY places the inflows into a layer with similar density, and setting it to SPECIFY allows the user to specify a top and bottom elevation into which inflows enter. If the SPECIFY option is used, then [KTUSP] and [KBUSP] are used to specify the top and bottom elevations that the inflows are distributed over.

[KTUSP] and [KBUSP] are used to set the upper and lower layers above and below which outflow does not occur in the selective withdrawal algorithm.

Example

SPILL UP	PUSPC	ETUSP	EBUSP	KTUSP	KBUSP
Sp 1	DISTR			2	23
Sp 2	DISTR			2	23

Related Cards and Files

[Spillways](#)

[Downstream Spillways](#)

[Spillway Dissolved Gas](#)

Downstream Spillways (SPILL DOWN)

FIELD	NAME	VALUE	DEFAULT	DESCRIPTION
1				(Ignored by code)
2	PDSPC	Character	DISTR	How inflows enter into the downstream spillway segment, DISTR, DENSITY, or SPECIFY
3	ETDSP	Real		Top elevation spillway inflows enter using SPECIFY option, <i>m</i>
3	EBDSP	Real		Bottom elevation spillway inflows enter using SPECIFY option, <i>m</i>
5	KTDSP	Integer		Top layer above which selective withdrawal will not occur
5	KBDSP	Integer		Bottom layer below which selective withdrawal will not occur

This card specifies how inflows/outflows for the downstream spillway location are handled. Setting [PDSPC] to DISTR distributes the inflows evenly from the water surface to the bottom active layer, setting it to DENSITY places the inflows into a layer with similar density, and setting it to SPECIFY allows the user to specify a top and bottom elevation into which inflows enter. If the SPECIFY option is used, then [ETDSP] and [EBDSP] are used to specify the top and bottom elevations that the inflows are distributed over.

[KTDSP] and [KBDSP] are used to set the upper and lower layers above and below which outflow does not occur in the selective withdrawal algorithm.

Example

SPILL DOWN	PDSPC	ETDSP	EBDSP	KTDSP	KBDSP
Sp 1	DISTR			2	23
Sp 2	DISTR			2	23

Related Cards and Files

[Inflow/Outflow Dimensions](#)
[Spillways](#)
[Upstream Spillways](#)
[Spillway Dissolved Gas](#)

Spillway Dissolved Gas (SPILL GAS)

FIELD	NAME	VALUE	DEFAULT	DESCRIPTION
1				(Ignored by code)
2	GASSPC	Character	OFF	Dissolved gas computations, ON or OFF
3	EQSP	Integer		Equation number for computing dissolved gas
3	ASP	Real		a coefficient in dissolved gas equation
5	BSP	Real		b coefficient in dissolved gas equation
5	CSP	Real		c coefficient in dissolved gas equation

This card turns ON/OFF spillway gas computations [GASSPC] and specifies the parameters that define the dissolved gas relationship. If dissolved gas computations are turned ON, then an equation number must be supplied (1 to 3). Based on the equation number, two or three coefficients are required. These coefficients are *a*, *b*, and *c* as shown in [Table C-24](#). Note that if [IDSP] is 0, even if [GASSPC] is ON, the model will not compute any effects of gas transfer since the water exiting the spillway or weir is not accounted for in the system. This algorithm computes gas effects for flow from upstream to downstream and there is no adjustment of dissolved oxygen for reverse flow.

The Corps of Engineers has been involved in gas abatement studies on the Columbia and Snake River system for many years (WES, 1996, 1997). Some of their research efforts have been focused on development of models of spillway gas generations. These empirical models have been called CriSP 1.6 (Columbia Basin Research, 1998). The gas production equations used in CriSP are empirical correlations between total dissolved gas (TDG), usually measured a mile downstream of the dam after turbulence from the spillway had subsided, and discharge, usually measured in kcfs. The form of these equations is shown in [Table C-24](#).

Table C-24. Equations used in CriSP model for gas production

Equation type	Equation	Coefficient description
Linear function of total spill	$\%TDG = mQ_s + b$	%TDG = % total dissolved gas saturation Q _s = total spill, kcfs m = empirical coefficient b = empirical coefficient
Bounded exponential of total spill	$\%TDG = a + b^{cQ_s}$	Q _s = total spill, kcfs a = empirical coefficient b = empirical coefficient c = empirical coefficient
Bounded exponential of the spill on a per spillway basis	$\%TDG = a + b^{cq_s}$	q _s = individual spillway spill, kcfs a = empirical coefficient b = empirical coefficient c = empirical coefficient

Examples of some of these correlations are shown in [Table C-25](#). In many cases the %TDG in these correlations was constrained to a maximum of 145% and when the flow reached only a few kcfs, there was assumed to be no change in TDG from the forebay to the tailrace. Also, the correlations in [Table C-24](#) sometimes changed from year to year based on changes in operating conditions or structural changes in the spillway or deflectors.

Table C-25. Equations used in CRiSP model for gas production at Columbia basin dams

Dam	Equation	Coefficients
Bonneville	$\%TDG = mQ_s + b$	$m=0.12$ $b=105.61$
Lower Granite	$\%TDG = a + b^{cQ_s}$	$a = 138.0$ $b = -35.8$ $c = -0.10$
Dworshak	$\%TDG = a + b^{cQ_s}$	$a = 135.9$ $b = -71.1$ $c = -0.4787$
Ice Harbor	$\%TDG = a + b^{cQ_s}$	$a = 136.8; b = -42.0; c = -0.0340 - 1995$ $a = 138.7; b = -79.0; c = -0.0591 - 1996$ $a = 130.9; b = -26.5; c = -0.0220 - 1997$ $a = 120.9; b = -20.5; c = -0.0230 - 1998$
Hell's Canyon	$\%TDG = a + b^{cQ_s}$	$a = 138$ $b = -36$ $c = -0.02$ [Assumed relationship - no data]

For each spillway, the user now has a choice of equations to use for computing the effects of each hydraulic structure on downstream dissolved oxygen. The equations chosen are shown in [Table C-26](#). These equations are based on equations from [Table C-24](#) and [Table C-25](#).

Table C-26. Reaeration Effects of Spillways, Weirs, and Gates

Equation #	Equation	Coefficient description
1. Linear function of spill on a per spillway basis; 2 empirical coefficients a and b	$\%TDG = aq_s + b$ Once TDG is known below the spillway, the dissolved oxygen concentration, C_{O_2} , is determined from $C_{O_2} = \%TDG * C_{sO_2}$	$\%TDG$ = % total dissolved gas saturation q_s = individual spillway spill, $kcfs$ a = empirical coefficient b = empirical coefficient C_{sO_2} = dissolved oxygen saturation, $g\ m^{-3}$
2. Bounded exponential of the spill on a per spillway basis; 3 empirical coefficients a , b , and c	$\%TDG = a + be^{cq_s}$ Once TDG is known below the spillway, the dissolved oxygen concentration, C_{O_2} , is determined from $C_{O_2} = \%TDG * C_{sO_2}$	q_s = individual spillway spill, $kcfs$ a = empirical coefficient b = empirical coefficient c = empirical coefficient C_{sO_2} = dissolved oxygen saturation, $g\ m^{-3}$

CONTROL FILE

OUTPUT CONTROL

Equation #	Equation	Coefficient description
3. Reaeration effect for a small height weir or dam (<10 m); 3 empirical coefficients a , b , and c	$\frac{D_a}{D_b} = 1 + 0.38ab(1 - 0.11c)$ $(1 + 0.046T)^c$ <p>C_{O_2} below the dam is computed from:</p> $C_{O_2} = C_{sO_2} - D_b$	D_a = DO deficit above dam, $g\ m^{-3}$ D_b = DO deficit below dam, $g\ m^{-3}$ T = temperature, °C a = 1.8 for clean water to 0.65 for gross polluted water b = 0.05 for sluice gates b = 1.0 for sharp crested straight faced weir b = 0.45 for flat broad crested curved face weir b = 0.7 for flat broad crested weir with regular step b = 0.8 for sharp crested vertical face weir b = 0.6 for flat broad crested weir vertical face c = water fall height, m C_{sO_2} = dissolved oxygen saturation, $g\ m^{-3}$

Note that for equations 1 and 2, the maximum TDG allowed is 145%, and if TDG is computed to be less than 100%, there is no effect of the spillway or gate on reaeration.

Example

SPILL	GAS	GASSPC	EQSP	ASP	BSP	CSP
Sp 1		ON	2	110.0	-0.1	-0.1
Sp 2		ON	1	10.0	110.0	10.0

Related Cards and Files

[Inflow/Outflow Dimensions](#)

[Spillways](#)

[Upstream Spillways](#)

[Downstream Spillways](#)

[Spillway Dissolved Gas](#)

Gates (GATES)

FIELD	NAME	VALUE	DEFAULT	DESCRIPTION
1				(Ignored by code)
2	IUGT	Integer		Gate segment location
3	IDGT	Integer		Downstream segment gate outflow enters
4	EGT	Real		Gate elevation, m
5	A1GT	Real		α_1 coefficient in gate equation for free flowing conditions
6	B1GT	Real		β_1 coefficient in gate equation for free flowing conditions
7	G1GT	Real		γ_1 coefficient in gate equation for free flowing conditions
8	A2GT	Real		α_2 coefficient in gate equation for submerged conditions
9	B2GT	Real		β_2 coefficient in gate equation for submerged conditions
10	G2GT	Real		γ_2 coefficient in gate equation for submerged conditions
11	LATGTC	Character		Downstream or lateral withdrawal, DOWN or LAT

This card specifies the gate characteristics. [IUGT] and [IDGT] specify the upstream and downstream segments for the spillway. Setting the downstream spillway segment [IDSP] to 0 allows the user to spill water that is lost from the system. The following equation is used for freely flowing conditions:

$$Q = \alpha_1 \Delta h^{\beta_1} B^{\gamma_1}$$

where:

β_1 = empirical coefficient

γ_1 = empirical coefficient

$\Delta h = Z_u - Z_{sp}, m$

Z_u = upstream head, m

Z_{sp} = spillway crest elevation, m

B = gate opening, m

and the following equation is used for submerged flow:

$$Q = \alpha_2 \Delta h^{\beta_2} B^{\gamma_2}$$

where

α_2 = empirical coefficient

β_2 = empirical coefficient

γ_2 = empirical coefficient

$\Delta h = Z_u - Z_d, m$

Z_d = downstream head, m

B = gate opening, m

In defining these parameters, the model user also has to generate a time series file of the gate openings **[GATEFN]**. Whenever the gate opening, B , is equal to or greater than $0.8(Z_u - Z_{sp})$, a weir equation is used with no functional dependency on the gate width. In this case, the user must also supply a rating curve when the gate acts like a weir.

If a valve-rating curve is used as a “gate” and the outlet elevation to compute the head difference is not the same as the withdrawal elevation, the following changes need to be included in the input variables:

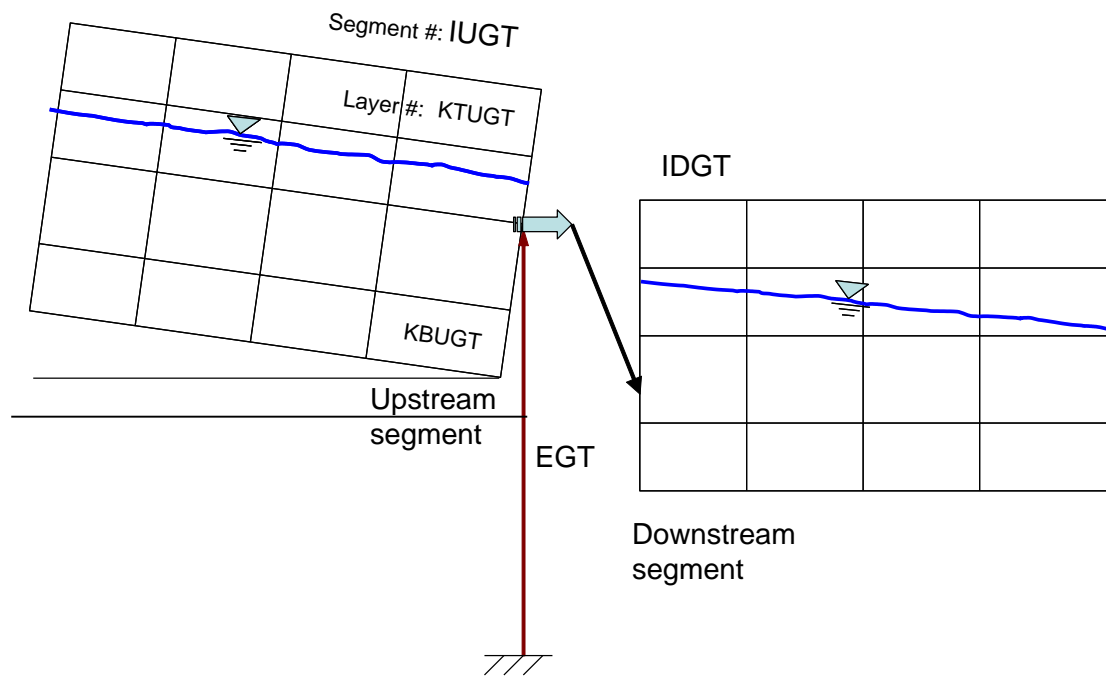
1. **[EGT]** is interpreted as the outlet level for the water being withdrawn
2. **[A2GT]** must be set to zero (no reverse flow equation is used)
3. **[G2GT]** is interpreted as the elevation used to compute the head on the outlet valve - whenever **[A2GT]** is set to zero and **[G2GT]** is non-zero, **[G2GT]** will be used to compute the head difference between the water level and the outlet rather than **[EGT]**, but **[EGT]** will still determine the location of the withdrawal.

In some reservoirs, an outlet valve is connected to the reservoir and a head-discharge relationship is used based on the gate opening or number of turns of the gate. In this case, the outlet level is usually at a different elevation than the withdrawal elevation. The gate formulation can still be used if there is no reverse flow through the needle valve.

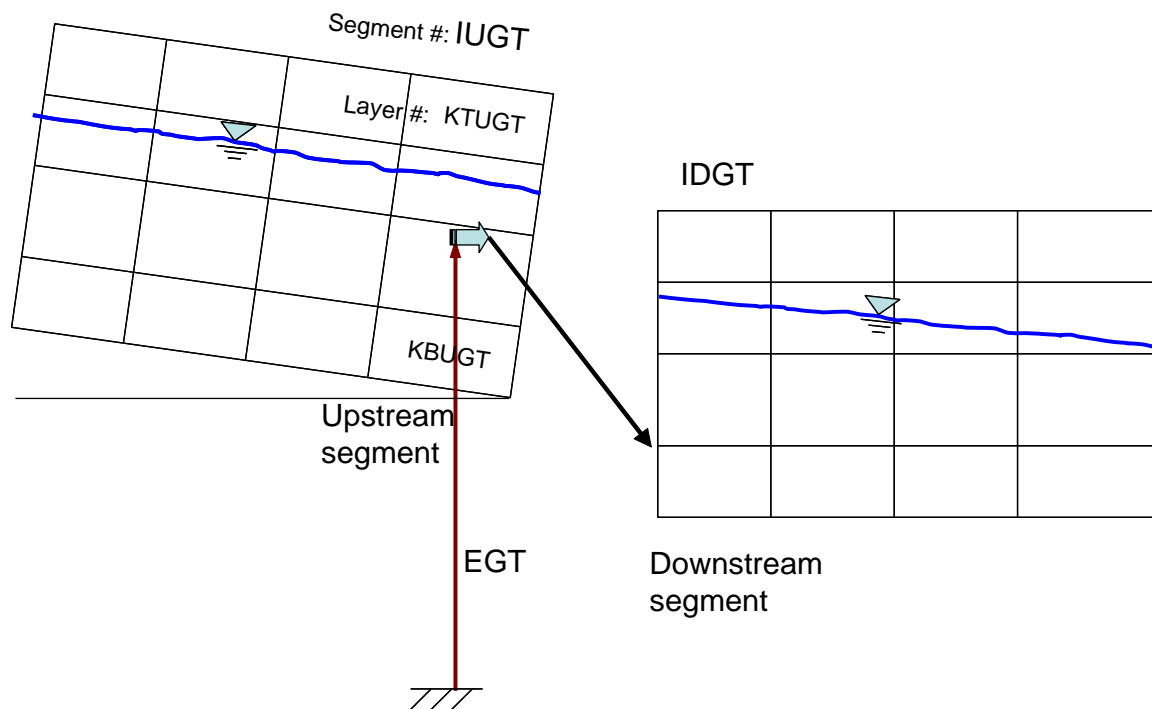
Setting the gate location **[LATGTC]** to **DOWN** specifies that the gate is located at the downstream end of the segment. In this case the water surface elevations are computed based on the right hand side of segment IUGT. This water surface elevation is estimated based on the slope of the water surface at IUGT and IUGT-1. Also, momentum from the outflow is preserved as in a downstream struture withdrawal. If **[LATGTC]** is set to **LAT**, it is assumed that the outflow is treated as a lateral withdrawal at the segment center elevation. In both cases selective withdrawal is used in the computations.

The following figures show the layout of gates set as a downstream **[DOWN]** and a lateral **[LAT]** withdrawal from the upstream segment.

Downstream Gate (DOWN)



Lateral Gate (LAT)



CONTROL FILE

OUTPUT CONTROL

Example

GATES	IUGT	IDGT	EGT	A1GT	B1GT	G1GT	A2GT	B2GT	G2GT	LATGTC
Gt 1	27	33	44.0	10.00	1.00	1.00	10.0	2.50	0.00	DOWN

Related Cards and Files

[Inflow/Outflow Dimensions](#)

[Gate Weir](#)

[Upstream Gate](#)

[Downstream Gate](#)

[Gate Dissolved Gas](#)

[Gate Filename](#)

Gate Weir (GATE WEIR)

FIELD	NAME	VALUE	DESCRIPTION
1			(Ignored by code)
2	GA1	Real	α_1 in gate equation for free flowing conditions
3	GB1	Real	β_1 in gate equation for free flowing conditions
4	GA2	Real	α_2 in gate equation for submerged conditions
5	GB2	Real	β_2 in gate equation for submerged conditions
6	DYNGTC	Character	Either 'B', 'ZGT', or 'FLOW'
7	GTIC	Character	Either 'ON' or 'OFF'

This card specifies the weir coefficients used when the gates are open and the open gate does not interfere with the flow (the gate opening, $B \geq 0.8\Delta h$). For [GA1] equal to zero, only the gated equations on the preceding card are used. For [GA2] equal to zero, only the freely flowing equation will be used even if submerged or reverse flow occurs.

The model requires the user to specify a head (h) versus flow (Q) relationship in the following form for freely flowing conditions:

$$Q = \alpha_1 \Delta h^{\beta_1}$$

where:

α_1 = empirical parameter [GA1]
 β_1 = empirical parameter [GB1]
 $\Delta h = Z_u - Z_{sp}$, m
 Z_u = upstream head, m
 Z_{sp} = the spillway crest elevation, m

And for submerged conditions:

$$Q = \alpha_2 \Delta h^{\beta_2}$$

where:

α_2 = empirical parameter [GA2]
 β_2 = empirical parameter [GB2]
 $\Delta h = Z_u - Z_d$, m
 Z_u = upstream head, m
 Z_d = downstream head, m

Submerged conditions are defined when the tailwater depth over the upstream energy head (static head and velocity head) is greater than 0.67. Even though negative flow rates are possible using the second equation when the downstream head is greater than the upstream head, these results should be used with caution since rarely are rating curves done for reverse flow. The user should

ensure a smooth transition between submerged and free flowing conditions by proper choice of model coefficients. See [Appendix A](#) for further information.

[DYNGC] is used to determine whether the gate inflow file represents dynamic gate opening heights (in that case, [DYNGC] is set to “B”), dynamic weir crest elevations ([DYNGC] is set to “ZGT”), or flow rates ([DYNGC] is set to “FLOW”). Using the dynamic gate opening results in use of the rating curves for gates as already described. Using the dynamic weir crest setting uses the rating curve for gates, but G1GT and G2GT are set equal to 0 – effectively changing the rating curve to the same one as for a spillway or weir. In this case though the inflow file is used to change the crest elevation. Using the flow rate setting allows the user to ignore all the rating curves on this card and the prior one. In this case dynamic flow rates are in the gate file and are used to move flow around the domain. For a pumped-storage project for example, the user can include one “gate” for flow out of Reservoir 1 to Reservoir 2 and another “gate” for flow from Reservoir 2 to Reservoir 1 (see descriptions of the GATE file).

With DYNGC=“ ZGT”, the model user can withdraw water using the dynamic weir crest (and weir rating curve) at the elevation of the dynamic weir crest or the user can withdraw water using the dynamic weir crest as before but specify a fixed elevation where that water is withdrawn. A description of this feature is shown in the GATE file description.

[GTIC] determines if the [DYNGTC] variable is to be interpolated or treated as a step function input. When [GTIC] is ‘ON’, then interpolation of the [DYNGTC] variable is ON and linear interpolation is used between data points in the input GATE file.

Example

GATE WEIR	GA1	GB1	GA2	GB2	DYNGC	GTIC
Gt 1	10.0	1.5	10.0	1.5	B	ON

Related Cards and Files

[Inflow/Outflow Dimensions](#)

[Gates](#)

[Upstream Gate](#)

[Downstream Gate](#)

[Gate Dissolved Gas](#)

[Gate Filename](#)

Upstream Gate (GATE UP)

FIELD	NAME	VALUE	DEFAULT	DESCRIPTION
1				(Ignored by code)
2	PUGTC	Character	DISTR	Specifies how inflows enter the upstream gate segment, DISTR, DENSITY, or SPECIFY
3	ETUGT	Real		Top elevation gate inflows enter using the SPECIFY option, <i>m</i>
4	EBUGT	Real		Bottom elevation gate inflows using the SPECIFY option, <i>m</i>
5	KTUGT	Integer		Top layer above which selective withdrawal will not occur
6	KBUGT	Integer		Bottom layer below which selective withdrawal will not occur

This card specifies how inflows/outflows for the upstream gate location are handled. Setting **[PUGTC]** to DISTR distributes the inflows evenly from the water surface to the bottom active layer, setting it to DENSITY places the inflows into a layer with similar density, and setting it to SPECIFY allows the user to specify a top and bottom elevation into which inflows enter. If the SPECIFY option is used, then **[KTUGT]** and **[KBUGT]** are used to specify the top and bottom elevations that the inflows are distributed over.

[KTUGT] and **[KBUGT]** are used to set the upper and lower layers above and below which outflow does not occur in the selective withdrawal algorithm.

Example

GATE UP	PUGTC	ETUGT	EBUGT	KTUGT	KBUGT
Gt 1	DISTR			2	23

Related Cards and Files

[Inflow/Outflow Dimensions](#)

[Gates](#)

[Gate Weir](#)

[Downstream Gate](#)

[Gate Dissolved Gas](#)

[Gate Filename](#)

Downstream Gate (GATE DOWN)

FIELD	NAME	VALUE	DEFAULT	DESCRIPTION
1				(Ignored by code)
2	PDGTC	Character	DISTR	Specifies how inflows enter the downstream gate segment, DISTR, DENSITY, or SPECIFY
3	ETDGT	Real		Top elevation gate inflows enter using the SPECIFY option, <i>m</i>
4	EBDGT	Real		Bottom elevation gate inflows enter using the SPECIFY option, <i>m</i>
5	KTDGT	Integer		Top layer above which selective withdrawal will not occur
6	KBDGT	Integer		Bottom layer below which selective withdrawal will not occur

This card specifies how inflows/outflows for the downstream gate location are handled. Setting **[PDGTC]** to DISTR distributes the inflows evenly from the water surface to the bottom active layer, setting it to DENSITY places the inflows into a layer with similar density, and setting it to SPECIFY allows the user to specify a top and bottom elevation into which inflows enter. If the SPECIFY option is used, then **[ETDGT]** and **[EBDGT]** are used to specify the top and bottom elevations that the inflows are distributed over.

[KTDGT] and **[KBDGT]** are used to set the upper and lower layers above and below which outflow does not occur in the selective withdrawal algorithm.

Example

```
GATE DOWN PDGTC ETDGT EBDGT KTDGT KBDGT
Gt 1      DISTR          2      23
```

Related Cards and Files

[Inflow/Outflow Dimensions](#)

[Gates](#)

[Gate Weir](#)

[Upstream Gate](#)

[Gate Dissolved Gas](#)

[Gate Filename](#)

Gate Dissolved Gas (GATE GAS)

FIELD	NAME	VALUE	DEFAULT	DESCRIPTION
1				(Ignored by code)
2	GASGTC	Character	OFF	Dissolved gas computations, ON or OFF
3	EQGT	Integer		Equation number for computing dissolved gas
3	AGASGT	Real		a coefficient in dissolved gas equation
5	BGASGT	Real		b coefficient in dissolved gas equation
5	CGASGT	Real		c coefficient in dissolved gas equation

For each gate, the model user activates or deactivates the computation by selecting ON or OFF for [GASGTC]. If the user activates this computation by choosing ON, then an equation number must be supplied (1 to 3). Based on the equation number, two or three coefficients are required. These coefficients are *a*, *b*, and *c* as shown in [Table C-27](#). Note that if [IDGT] is 0, even if [GASGTC] is ON, the model will not compute any effects of gas transfer since the water exiting the spillway or weir is not accounted for in the system. This algorithm only computes gas effects for upstream to downstream flow and there is no adjustment of dissolved oxygen for reverse flow.

The Corps of Engineers has been involved in Gas Abatement Studies on the Columbia and Snake River system for many years (WES, 1996, 1997). Some of their research efforts have been focused on development of models of gas generation from spillways. These empirical models have been called CriSP 1.6 (Columbia Basin Research, 1998). The gas production equations used in CriSP are empirical correlations between total dissolved gas (*TDG*), usually measured a mile downstream of the dam after turbulence from the spillway had subsided, and discharge, usually measured in kcfs. The form of these equations is shown in [Table C-27](#).

Table C-27. Equations used in CriSP model for gas production

Equation type	Equation	Coefficient Description
Linear function of total spill	$\%TDG = mQ_s + b$	$\%TDG$ = % total dissolved gas saturation Q_s = total spill, kcfs m, b = empirical coefficients
Bounded exponential of total spill	$\%TDG = a + be^{cQ_s}$	Q_s = total spill, kcfs a, b, c = empirical coefficients
Bounded exponential of the spill on a per spillway basis	$\%TDG = a + be^{cq_s}$	q_s = spill through individual spillway, kcfs a, b, c = empirical coefficients

Examples of some of these correlations are shown in [Table C-28](#). In many cases the $\%TDG$ in these correlations was constrained to a maximum of 145% and when the flow reached only a few thousand cfs, no change in *TDG* was assumed from the forebay to the tailrace. Also, the correlations in [Table C-28](#) sometimes changed from year to year based on changes in operating conditions or structural changes in the spillway or deflectors.

Table C-28. Equations used in CriSP model for gas production at Columbia basin dams

Dam	Equation	Coefficients
Bonneville	$\%TDG = mQ_s + b$	$m = 0.12$ $b = 105.61$

Dam	Equation	Coefficients
Lower Granite	$\%TDG = a + be^{cQ_s}$	$a = 138.0$ $b = -35.8$ $c = -0.10$
Dworshak	$\%TDG = a + be^{cQ_s}$	$a = 135.9$ $b = -71.1$ $c = -0.4787$
Ice Harbor	$\%TDG = a + be^{cQ_s}$	$a = 136.8; b = -42.0; c = -0.0340$ 1995; $a = 138.7; b = -79.0; c = -0.0591$ 1996; $a = 130.9; b = -26.5; c = -0.0220$ 1997; $a = 120.9; b = -20.5; c = -0.0230$ 1998
Hell's Canyon	$\%TDG = a + be^{cQ_s}$	$a = 138; b = -36; c = -0.02$ [Assumed relationship - no data]

For each gate, the user now has the choice of equation to use for computing the effects of each hydraulic structure on downstream dissolved oxygen. The equations chosen are shown in [Table C-29](#). These equations are based on equations from [Table C-27](#) and [Table C-28](#).

Table C-29. Reaeration effects of gates

#	Equation	Empirical Coefficient Description
1. Linear function of spill on a per spillway basis; 2 empirical coefficients: a and b	$\%TDG = aq_s + b$ Once %TDG is known below the spillway, the dissolved oxygen concentration, C_{O_2} , is determined from $C_{O_2} = \%TDG * C_{sO_2}$	$\%TDG$ = total dissolved gas saturation, % q_s = spill through an individual spillway, $kcfs$ a = empirical coefficient b = empirical coefficient C_{sO_2} = dissolved oxygen saturation, $g\ m^{-3}$
2. Bounded exponential of the spill on a per spillway basis; 3 empirical coefficients: a, b, c	$\%TDG = a + be^{cq_s}$ Once %TDG is known below the spillway, the dissolved oxygen concentration, C_{O_2} , is determined from $C_{O_2} = \%TDG * C_{sO_2}$	q_s = spill through an individual spillway, $kcfs$ a = empirical coefficient b = empirical coefficient c = empirical coefficient C_{sO_2} = dissolved oxygen saturation $g\ m^{-3}$
3. Reaeration effect for a small height weir or dam (<10 m); 3 empirical coefficients: a, b, c	$\frac{D_a}{D_b} = 1 + 0.38ab(1 - 0.11c)$ $(1 + 0.046T)c$ C_{O_2} below the dam is computed from: $C_{O_2} = C_{sO_2} - D_b$	D_a = DO deficit above dam, $g\ m^{-3}$ D_b = DO deficit below dam, $g\ m^{-3}$ T = temperature, $^{\circ}C$ c = height of water fall, m a = 1.8 for clean water to 0.65 for gross polluted water b = 0.05 for sluice gates b = 1.00 for sharp crested straight faced weir b = 0.45 for flat broad crested curved face weir b = 0.70 for flat broad crested weir with regular step b = 0.8 for sharp crested vertical face weir b = 0.60 for flat broad crested weir vertical face C_{sO_2} = dissolved oxygen saturation, $g\ m^{-3}$

Note that for equations 1 and 2, the maximum TDG allowed is 145%, and if TDG is computed to be less than 100%, there is no effect of the gate on reaeration.

OUTPUT CONTROL

CONTROL FILE

Example

GATE	GAS	GASGTC	EQGT	AGASGT	BGASGT	CGASGT
Gt	1	ON	1	10.0	120.0	1.0

Related Cards and Files

[Inflow/Outflow Dimensions](#)

[Gates](#)

[Gate Weir](#)

[Upstream Gate](#)

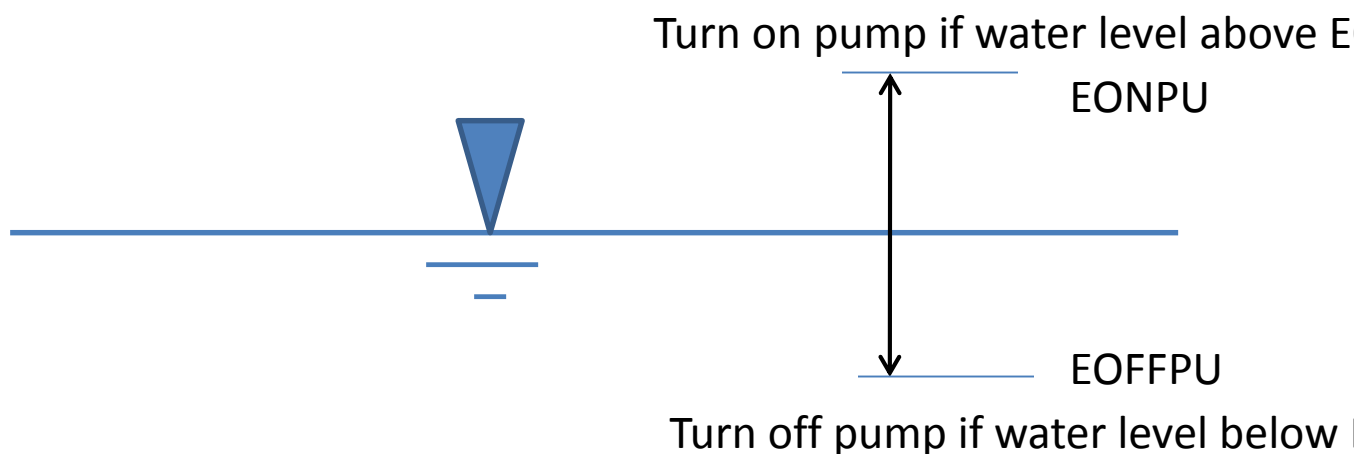
[Downstream Gate](#)

[Gate Filename](#)

Pumps 1 (PUMPS 1)

FIELD	NAME	VALUE	DEFAULT	DESCRIPTION
1				(Ignored by code)
2	IUPU	Integer		Upstream segment of pump where water is withdrawn
3	IDPU	Integer		Downstream segment of pump where water enters
4	EPU	Real		Elevation of pump, m
5	STRTPU	Real		Starting day of pumping, <i>Julian day</i>
6	ENDPU	Real		Ending day of pumping, <i>Julian day</i>
7	EONPU	Real		Pump starting elevation, m
8	EOFFPU	Real		Pump stopping elevations, m
9	QPU	Real		Pump flow rate, $m^3 \text{ sec}^{-1}$
10	LATPUC	Character	DOWN	Downstream or lateral withdrawal, DOWN or LAT
11	DYNPUMP	Character	OFF	Dynamic pump control ON or OFF. This allows dynamic changes in pump characteristics over time if ON. An external time series file is read in.

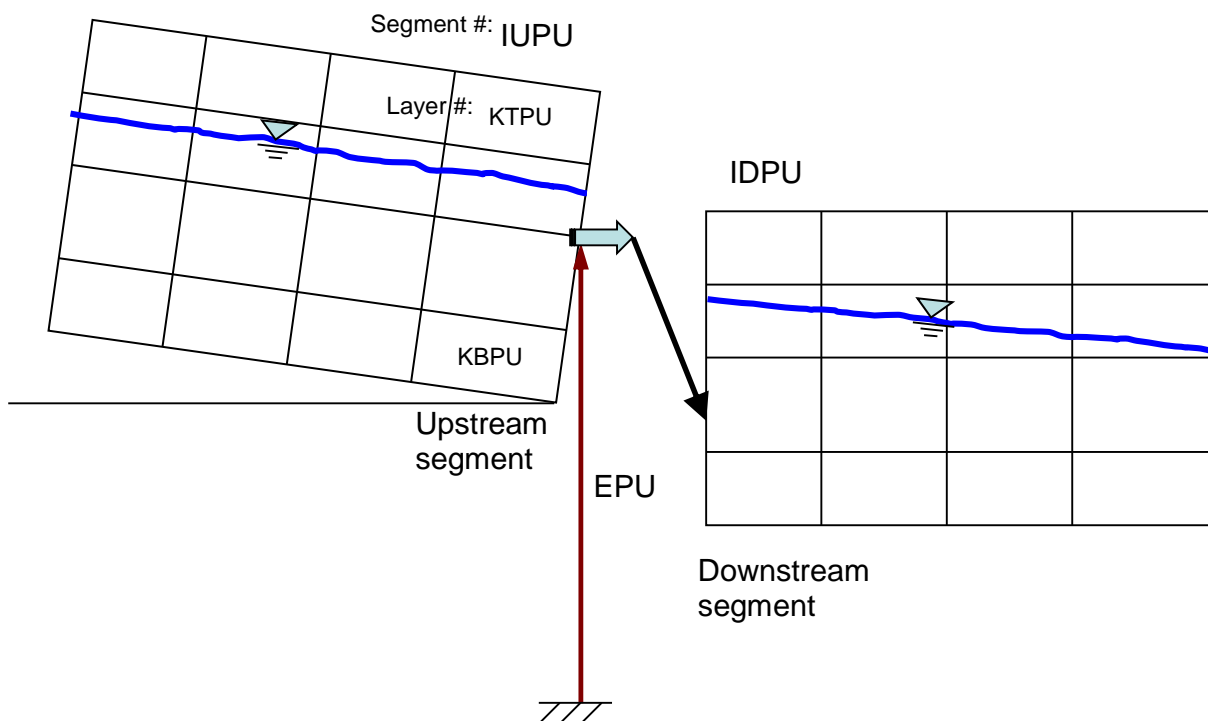
This card specifies the characteristics of the pumps in the system. [IUPU] and [IDPU] specify the segments from which water is withdrawn and added back to the system, respectively. IF [IDPU] is zero water is only withdrawn from the system. The elevation of the pump [EPU] is used to specify the vertical location of the pump for the selective withdrawal algorithm. [STRTPU] and [ENDPU] specify the starting and ending times during which pumping occurs, [EONPU] and [EOFFPU] specify the elevations at which pumping is activated/deactivated, and [QPU] specifies the pumping rate.



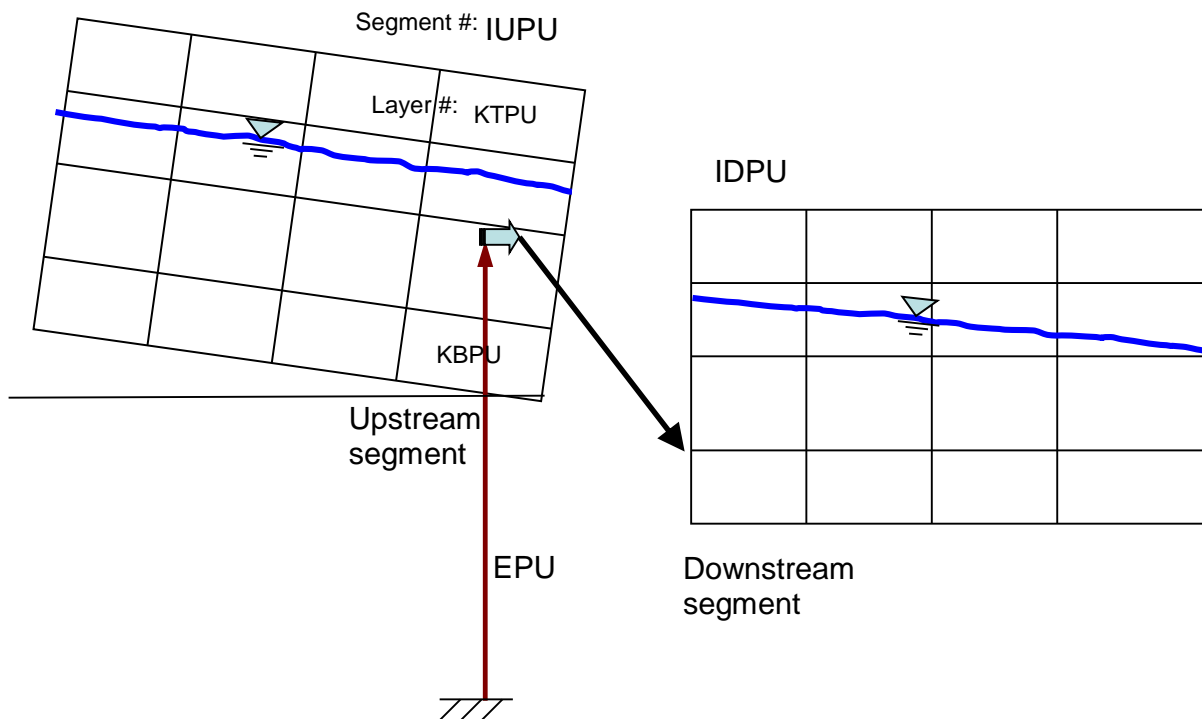
Setting the pump location [**LATPUC**] to **DOWN** specifies that the pump is at the downstream end of the segment. In this case the water surface elevations are computed based on the right hand side of segment IUPU. This water surface elevation is estimated based on the slope of the water surface at IUPU and IUPU-1.. Also, momentum from the outflow is preserved as in a downstream struture withdrawal. If [**LATPUC**] is set to **LAT**, it is assumed that the outflow is treated as a lateral withdrawal at the segment center elevation. In both cases selective withdrawal is used in the computations.

The following figures show the layout of pumps set as a downstream [**DOWN**] and a lateral [**LAT**] withdrawal from the upstream segment.

Downstream Pump (DOWN)



Lateral Pump (LAT)



When the DYNPUMP control is ON, an input file is read that has the variables: JDAY, EPU, EONPU, and EOFFPU as a time series. The name of the file will be 'dynpumpX.npt' where X is the Pump number. Hence, 'dynpump1.npt' is expected if DYNPUMP is ON for Pump #1. An example file is shown in the section on INPUT files. When reading a DYNPUMP file, the values are treated as step functions, i.e., there is no interpolation between values. This allows the user to dynamically change the location of the outflow, or the elevation targets or the flow rate dynamically.

Example

PUMPS	1	IUPU	IDPU	EPU	STRTPU	ENDPU	EONPU	EOFFPU	QPU	LATPUC	DYNPUMP
Pu 1		30	33	2.4	1.0	900.0	3.0	2.4	3.0	DOWN	OFF

Related Cards and Files

[Inflow/Outflow Dimensions](#)
[Pumps 2](#)

Pumps 2 (PUMPS 2)

FIELD	NAME	VALUE	DEFAULT	DESCRIPTION
1				(Ignored by code)
2	PPUC	Character	DISTR	How inflows enter into the downstream water level control segment, DISTR, DENSITY, or SPECIFY
3	ETPU	Real		Top elevation water level control inflows enter using SPECIFY option, <i>m</i>
4	EBPU	Real		Bottom elevation water level control inflows enter using SPECIFY option, <i>m</i>
5	KTPU	Integer		Top layer above which selective withdrawal does not occur
6	KBPU	Integer		Bottom layer below which selective withdrawal will not occur

This card specifies how inflows/outflows for the water level controls are handled. Setting [PPUC] to DISTR distributes the inflows evenly from the water surface to the bottom active layer, setting it to DENSITY places the inflows into a layer with similar density, and setting it to SPECIFY allows the user to specify a top and bottom elevation into which inflows enter. If the SPECIFY option is used, then [ETPU] and [EBPU] are used to specify the top and bottom elevations that the inflows are distributed over.

[KTPU] and [KBPU] are used to set the upper and lower layers above and below which outflow does not occur in the selective withdrawal algorithm. For the pumps algorithm, in contrast to gates, spillways (weirs), and pipes, flow is only in 1-direction, i.e., only outflow is allowed from the upstream segment.

Example

PUMPS 2	PPUC	ETPU	EBPU	KTPU	KBPU
Pu 1	DISTR			4	23

Related Cards and Files

[Inflow/Outflow Dimensions](#)
[Pumps 1](#)

Internal Weir Segment Location (WEIR SEG)

FIELD	NAME	VALUE	DESCRIPTION
1			(Ignored by code)
2-10	IWR	Integer	Weir segment location

This card specifies the segment location of the internal weir in the grid. If there are more internal weirs than can be specified on one line, then the segment locations are continued on the next line without another **WEIR SEG** card being specified.

The following figure illustrates the location of the internal weir. Note that the internal weir is always on the downstream side of a segment. The internal weir can simulate a skimmer (from the top down) or a curtain weir (from the bottom up).

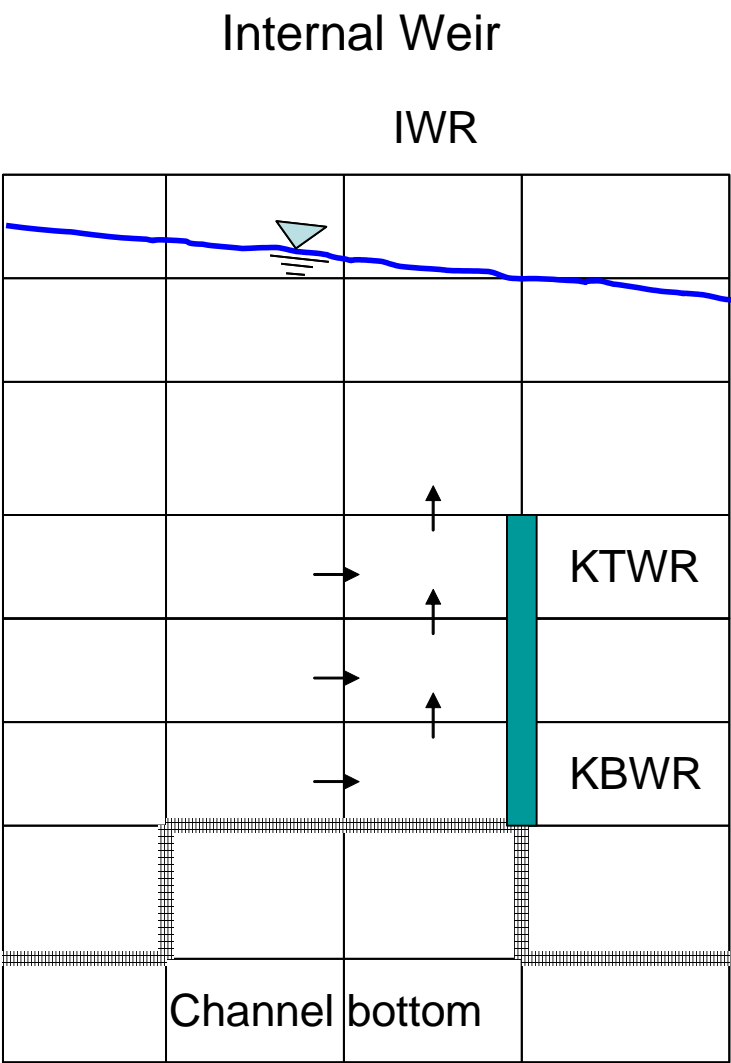


Figure 38. Description of internal weir in CE-QUAL-W2 at downstream side of segment.

Example

WEIR	SEG	IWR	IWR	IWR	IWR	IWR	IWR	IWR	IWR
		25							

Related Cards and Files

- [Inflow/Outflow Dimensions](#)
- [Weir Top Layer](#)
- [Weir Bottom Layer](#)

Internal Weir Top Layer (WEIR TOP)

FIELD	NAME	VALUE	DESCRIPTION
1			(Ignored by code)
2-10	KTWR	Integer	Weir top layer

This card specifies the top layer location of the internal weir. For a submerged weir, this should be set to the layer above which flow is allowed to occur between segments. If there are more internal weirs than can be specified on one line, then the top layer locations are continued on the next line without another WEIR TOP card being specified.

Example

WEIR TOP	KTWR	KTWR	KTWR	KTWR	KTWR	KTWR	KTWR	KTWR	KTWR
	25								

Related Cards and Files

[Inflow/Outflow Dimensions](#)

[Weir Segment Location](#)

[Weir Bottom Layer](#)

Internal Weir Bottom Layer (WEIR BOT)

FIELD	NAME	VALUE	DESCRIPTION
1			(Ignored by code)
2-10	KBWR	Integer	Weir bottom layer

This card specifies the bottom layer location of the internal weir. For a curtain weir, [KBWR] should be set to the bottommost layer above which flow between segments will not occur. For a submerged weir, [KBWR] should be set to the bottommost active layer for the segment specified in the [WEIR SEG](#) card. If there are more internal weirs than can be specified on one line, then the top layer locations are continued on the next line without another WEIR BOT card being specified.

Example

```
WEIR BOT      KBWR      KBWR      KBWR      KBWR      KBWR      KBWR      KBWR      KBWR
                25
```

Related Cards and Files

[Inflow/Outflow Dimensions](#)

[Weir Segment Location](#)

[Weir Top Layer](#)

Withdrawal Interpolation (WD INT)

FIELD	NAME	VALUE	DEFAULT	DESCRIPTION
1				(Ignored by code)
2-10	WDIC		OFF	Withdrawal outflow interpolation, ON or OFF

This card specifies whether interpolation is turned on for lateral withdrawal outflow. If there are *more* withdrawal interpolations than can be specified on one line, then they are continued on the next line without another WD INT card being specified.

If [WDIC] is turned ON, then flows are linearly interpolated between updates. If interpolation is used, then the user must ensure it is appropriate and the input data supply correct information. Withdrawals can have periods of no releases. If withdrawal interpolation is turned on, then input data must be set up so no outflow occurs during these periods. This is accomplished by including extra dates in the withdrawal file with zero outflows to ensure the interpolation routine yields zero outflows. For example, given the following withdrawal time-series in the withdrawal file [QWDFN]:

JDAY	QWD
100.00	50.0
110.00	0.0
120.00	50.0

If interpolation is not used, then outflow from Julian day 100 to 110 is $50 \text{ m}^3 \text{ sec}^{-1}$, from Julian day 110 to 120 is $0.0 \text{ m}^3 \text{ sec}^{-1}$, and $50 \text{ m}^3 \text{ sec}^{-1}$ thereafter. If interpolation is turned on, then outflow linearly decreases from Julian day 100 to 110 and then increases from Julian day 110 to 120. To ensure no outflow occurs between day 110 and 120 with interpolation on, the withdrawal file should be setup as follows:

JDAY	QWD
109.9999	50.0
110.0000	0.0
119.9999	0.0
120.0000	50.0

Example

WD INT	WDIC	WDIC	WDIC	WDIC	WDIC	WDIC	WDIC	WDIC	WDIC
	ON								

Related Cards and Files

[Inflow/Outflow Dimensions](#)
[Withdrawal Segment](#)
[Withdrawal Elevation](#)
[Withdrawal Top Layer](#)
[Withdrawal Bottom Layer](#)
[Withdrawal File](#)
[Withdrawal Filename](#)

Withdrawal Segment (WD SEG)

FIELD	NAME	VALUE	DESCRIPTION
1			(Ignored by code)
2-10	IWD	Integer	Withdrawal segment number

This card specifies the withdrawal segment location. If there are more withdrawal segments than can be specified on one line, then they are continued on the next line without another WD SEG card being specified.

Example

```
W SEGMENT      IWD      IWD      IWD      IWD      IWD      IWD      IWD      IWD
                4
```

Related Cards and Files

[Inflow/Outflow Dimensions](#)

[Withdrawal Interpolation](#)

[Withdrawal Elevation](#)

[Withdrawal Top Layer](#)

[Withdrawal Bottom Layer](#)

[Withdrawal File](#)

[Withdrawal Filename](#)

Withdrawal Elevation (WD ELEV)

FIELD	NAME	VALUE	DESCRIPTION
1			(Ignored by code)
2-10	EWD	Real	Withdrawal centerline elevation, <i>m</i>

This card specifies the centerline elevation of the withdrawal. If there are more withdrawal elevations than can be specified on one line, then they are continued on the next line without another WD ELEV card being specified.

Example

```
W EL      EWD      EWD      EWD      EWD      EWD      EWD      EWD      EWD
          40.0
```

Related Cards and Files

[Inflow/Outflow Dimensions](#)

[Withdrawal Interpolation](#)

[Withdrawal Segment](#)

[Withdrawal Top Layer](#)

[Withdrawal Bottom Layer](#)

[Withdrawal File](#)

[Withdrawal Filename](#)

Withdrawal Top Layer (WD TOP)

FIELD	NAME	VALUE	DESCRIPTION
1			(Ignored by code)
2-10	KTWD	Integer	Top layer above which selective withdrawal will not occur

This card specifies the layer above which no flows will be computed in the selective withdrawal algorithm. For most situations, this should be set to layer 2, which ensures that water can be withdrawn all the way to the surface layer. It should be set to something greater than 2 if a structure is somehow limiting the withdrawal of water, such as a curtain weir. If there are more withdrawal elevations than can be specified on one line, then they are continued on the next line without another WD TOP card being specified. If the structure centerline elevation is above KTWD, then the value of KTWD is raised to the centerline elevation.

Example

```
WD TOP      KTWD      KTWD      KTWD      KTWD      KTWD      KTWD      KTWD      KTWD      KTWD
              2
```

Related Cards and Files

[Inflow/Outflow Dimensions](#)
[Withdrawal Interpolation](#)
[Withdrawal Segment](#)
[Withdrawal Elevation](#)
[Withdrawal Bottom Layer](#)
[Withdrawal File](#)
[Withdrawal Filename](#)

Withdrawal Bottom Layer (WD BOT)

FIELD	NAME	VALUE	DESCRIPTION
1			(Ignored by code)
2-10	KBWD	Integer	Bottom layer below which selective withdrawal will not occur

This card specifies the layer below which no flows will be computed in the selective withdrawal algorithm. For most situations, this should be set to the bottommost active layer of the withdrawal segment, which ensures that water can be withdrawn all the way to the bottom layer. It should be set to something other than the bottommost active layer if a structure is somehow limiting the withdrawal of water, such as a submerged weir. If there are more bottom withdrawal layers than can be specified on one line, then they are continued on the next line without another WD BOT card being specified. If the structure centerline elevation is below KBWD, then the value of KBWD is lowered to the centerline elevation.

Example

```
WD BOT      KBWD      KBWD      KBWD      KBWD      KBWD      KBWD      KBWD      KBWD      KBWD
           10
```

Related Cards and Files

[Inflow/Outflow Dimensions](#)
[Withdrawal Interpolation](#)
[Withdrawal Segment](#)
[Withdrawal Elevation](#)
[Withdrawal Top Layer](#)
[Withdrawal File](#)
[Withdrawal Filename](#)

Tributary Inflow Placement (TRIB PLACE)

FIELD	NAME	VALUE	DESCRIPTION
1			(Ignored by code)
2-10	TRC	Character	Tributary inflow placement, DISTR, DENSITY, SPECIFY

This card specifies how tributary inflows are distributed into the model layers. There are three options. Inflows can be distributed evenly from top to bottom ([PTRC] = DISTR), placed according to density ([PTRC] = DENSITY), or the user may specify a range of layer elevations in which the tributary inflows are distributed evenly ([PTRC] = SPECIFY). This is similar to the branch inflows, but with the additional option allowing the user to specify the range of layer elevations in which to distribute the inflows. This option is particularly useful when trying to model discharges from a pipe such as wastewater treatment effluent.

If there are more tributaries than can be specified on one line, then they are continued on the next line without another TRIB PLACE card being specified.

Example

```
TRIB PLACE PTRC PTRC PTRC PTRC PTRC PTRC PTRC PTRC PTRC
          DENSITY DISTR SPECIFY DENSITY DENSITY DENSITY DENSITY DENSITY
```

Related Cards and Files

[Inflow/Outflow Dimensions](#)
[Tributary Interpolation](#)
[Tributary Segment](#)
[Tributary Inflow Top Elevation](#)
[Tributary Inflow Bottom Elevation](#)
[Tributary Active Constituent Control](#)
[Tributary Inflow File](#)
[Tributary Temperature File](#)
[Tributary Concentration File](#)
[Tributary Inflow Filename](#)
[Tributary Inflow Temperature Filename](#)
[Tributary Inflow Concentration Filename](#)

Tributary Interpolation (TRIB INT)

FIELD	NAME	VALUE	DEFAULT	DESCRIPTION
1				(Ignored by code)
2-10	TRIC	Character	ON	Turns ON/OFF interpolation of tributary inflows

The tributary inflow specified by the tributary files for flow, temperature, and concentration can either be assumed to be step functions, [TRIC] set to OFF, or can be linearly interpolated between values, [TRIC] set to ON.

Example

```

TRIB INT      TRIC      TRIC      TRIC      TRIC      TRIC      TRIC      TRIC      TRIC      TRIC
              ON        ON        ON

```

Related Cards and Files

[Inflow/Outflow Dimensions](#)
[Tributary Inflow Placement](#)
[Tributary Segment](#)
[Tributary Inflow Top Elevation](#)
[Tributary Inflow Bottom Elevation](#)
[Tributary Active Constituent Control](#)
[Tributary Inflow File](#)
[Tributary Temperature File](#)
[Tributary Concentration File](#)
[Tributary Inflow Filename](#)
[Tributary Inflow Temperature Filename](#)
[Tributary Inflow Concentration Filename](#)

Tributary Segment (TRIB SEG)

FIELD	NAME	VALUE	DESCRIPTION
1			(Ignored by code)
2-10	ITR	Integer	Segment tributary enters

This card specifies the segment that the tributary enters. Tributary flows are either placed into a layer whose density most closely corresponds to that of the tributary flows, are evenly distributed from top to bottom, or are specified to enter over a range of elevations (see [\[TRC\]](#)). Flows that enter segments upstream of the current upstream segment [\[CUS\]](#) for a branch are combined with the branch inflow.

If there are more tributary segments than can be specified on one line, then they are continued on the next line without another TRIB SEG card being specified.

Example

TRIB SEG	ITR	ITR	ITR	ITR	ITR	ITR	ITR	ITR	ITR
	2	3	4	3	4	5	6	7	

Related Cards and Files

[Inflow/Outflow Dimensions](#)
[Tributary Inflow Placement](#)
[Tributary Interpolation](#)
[Tributary Inflow Top Elevation](#)
[Tributary Inflow Bottom Elevation](#)
[Tributary Active Constituent Control](#)
[Tributary Inflow File](#)
[Tributary Temperature File](#)
[Tributary Concentration File](#)
[Tributary Inflow Filename](#)
[Tributary Inflow Temperature Filename](#)
[Tributary Inflow Concentration Filename](#)

Tributary Inflow Top Elevation (TRIB TOP)

FIELD	NAME	VALUE	DESCRIPTION
1			(Ignored by code)
2-10	ETRT	Real	Tributary inflow top elevation, <i>m</i>

This card specifies the upper elevation for each tributary inflow in which the user has specified that inflows will be placed over a range of elevations. Only tributaries that are specified as **SPECIFY** on the [Tributary Inflow Placement](#) card need top elevations specified on this card.

If there are more tributary top elevations than can be specified on one line, then they are continued on the next line without another TRIB TOP card being specified.

Example

```

TRIB TOP      ETRT      ETRT      ETRT      ETRT      ETRT      ETRT      ETRT      ETRT      ETRT
              116.0

```

Related Cards and Files

[Inflow/Outflow Dimensions](#)
[Tributary Inflow Placement](#)
[Tributary Interpolation](#)
[Tributary Segment](#)
[Tributary Inflow Top Elevation](#)
[Tributary Inflow Bottom Elevation](#)
[Tributary Active Constituent Control](#)
[Tributary Inflow File](#)
[Tributary Temperature File](#)
[Tributary Concentration File](#)
[Tributary Inflow Filename](#)
[Tributary Inflow Temperature Filename](#)
[Tributary Inflow Concentration Filename](#)

Tributary Inflow Bottom Elevation (ELEV BOT)

FIELD	NAME	VALUE	DESCRIPTION
1			(Ignored by code)
2-10	ETRB	Real	Tributary inflow bottom elevation, <i>m</i>

This card specifies the bottom elevation for each tributary inflow in which the user has specified that inflows will be placed over a range of elevations. Only tributaries that are specified as SPECIFY on the [Tributary Inflow Placement](#) card need bottom elevations specified on this card.

If there are more tributary bottom elevations than can be specified on one line, then they are continued on the next line without another TRIB BOT card being specified.

Example

```

TRIB BOT      ETRB      ETRB      ETRB      ETRB      ETRB      ETRB      ETRB      ETRB
              114.0

```

Related Cards and Files

[Inflow/Outflow Dimensions](#)
[Tributary Inflow Placement](#)
[Tributary Interpolation](#)
[Tributary Segment](#)
[Tributary Inflow Top Elevation](#)
[Tributary Inflow Bottom Elevation](#)
[Tributary Active Constituent Control](#)
[Tributary Inflow File](#)
[Tributary Temperature File](#)
[Tributary Concentration File](#)
[Tributary Inflow Filename](#)
[Tributary Inflow Temperature Filename](#)
[Tributary Inflow Concentration Filename](#)

Distributed Tributaries (DST TRIB)

FIELD	NAME	VALUE	DEFAULT	DESCRIPTION
1				(Ignored by code)
2	DTRC	Character	OFF	Distributed tributary option, ON or OFF

This card specifies whether or not a branch contains a distributed tributary inflow and whether or not the inflows, inflow temperatures, and inflow concentrations are linearly interpolated between input dates. A distributed tributary is equivalent to a non-point source loading. This option may be turned ON or OFF for each branch and is useful in accounting for ungaged flows for the water budget. The flow is distributed among the segments in each branch proportional to their surface areas. There is one value of [DTRC] for each branch. See the INTERPOL card for turning ON/OFF interpolation for distributed tributaries.

For each distributed tributary specified, the user must supply an inflow file [[QDTFN](#)], an inflow temperature file [[TDTFN](#)], and, if constituents are modeled, an inflow constituent concentration file [[CDTFN](#)].

If constituents are modeled, the user can select which constituents are included in the distributed tributary concentrations input file (see [Distributed Tributary Active Constituent Control](#) card).

Example

```
DST TRIB      DTRC
Br 1          ON
Br 2          ON
Br 3          OFF
Br 4          OFF
```

Related Cards and Files

[Distributed Tributary Active Constituent Control](#)
[Distributed Tributary Inflow File](#)
[Distributed Tributary Temperature File](#)
[Distributed Tributary Concentration File](#)
[Distributed Tributary Inflow Filename](#)
[Distributed Tributary Inflow Temperature Filename](#)
[Distributed Tributary Inflow Concentration Filename](#)

Hydrodynamic Output Control (HYD PRINT)

FIELD	NAME	VALUE	DEFAULT	DESCRIPTION
1				(Ignored by code)
2-10	HPRWBC	Character	OFF	Output hydrodynamic terms to the snapshot file, ON or OFF

This card specifies whether or not certain hydrodynamic terms are included as output in the snapshot file. The hydrodynamic terms include timestep violations, horizontal and vertical velocities, temperatures, and all the terms that comprise the horizontal momentum equation. The latest version allows the user to turn ON/OFF hydrodynamic output for each waterbody as shown in the example. Values for each waterbody continue across the line. If there are more than nine waterbodies, then additional values continue on the next line starting in field two. Output formatting and animation of these variables can be specified in the graph.npt file.

Table C-30. Hydraulic Print Parameters

Term	Explanation
[NLIM]	Location and number of limiting time steps in the model grid
[U]	Longitudinal velocity in m/s
[W]	Vertical velocity in m/s
[T]	Temperature in °C
[RHO]	Density in kg/m ³
[AZ]	Vertical turbulent eddy viscosity in m ² /s
[SHEAR]	Velocity shear stress squared [VSH] in 1/s ²
[ST]	Total shear stress at top of model layer (see Equation A-150) X width of cell in m ³ /s ² , ST=bottom and side-wall shear+velocity shear+wind induced shear
[SB]	Shear stress at bottom of model layer (see Equation A-147) X width of cell in m ³ /s ²
[ADMX]	Longitudinal advection of momentum in m ³ /s ² $[ADMX] \sim BH \frac{\Delta U^2}{\Delta x}$
[DM]	Longitudinal momentum transport by eddy viscosity in m ³ /s ² where approximately $[DM] \sim A_z BH \frac{\Delta U}{\Delta x^2}$
[HDG]	Horizontal density gradient in m ³ /s ² $[HDG] \sim BH \frac{\Delta P}{\rho \Delta x} *$
[ADMZ]	Vertical advection of momentum in m ³ /s ² $[ADMZ] \sim BWU$
[HPG]	Horizontal pressure gradient in m ³ /s ² $[HDP] \sim BH \frac{\Delta P}{\rho \Delta x} *$
[GRAV]	Gravity force term in m ³ /s ² $[GRAV] \sim BHg$
	g is acceleration due to gravity, B is cell width, H is average cell layer thickness, U is longitudinal velocity, W is vertical velocity, Δx is segment spacing, P is pressure, ρ is density. * Note HDG pressure is taken from horizontal elevation of layer KT and is used only in the water surface computation. HPG pressure is computed from actual water surface and is used in the velocity computation. The HDG pressure between the horizontal layer KT elevation and the water surface is already accounted for in the surface water layer computation for η.

Example

HYD PRINT	HPRWBC	HPRWBC	HPRWBC	HPRWBC	HPRWBC	HPRWBC	HPRWBC	HPRWBC	HPRWBC
NLIM	ON	ON	ON						
U	ON	ON	ON						
W	ON	ON	ON						
T	ON	ON	ON						
RHO	ON	ON	ON						
AZ	ON	ON	ON						
SHEAR	ON	ON	ON						
ST	ON	ON	ON						
SB	ON	ON	ON						
ADMX	ON	ON	ON						
DM	ON	ON	ON						
HDG	ON	ON	ON						

CONTROL FILE

ADMZ	ON	ON	ON
HPG	ON	ON	ON
GRAV	ON	ON	ON

OUTPUT CONTROL

Snapshot Print (SNP PRINT)

FIELD	NAME	VALUE	DEFAULT	DESCRIPTION
1				(Ignored by code)
2	SNPC	Character	OFF	Specifies if information is written to snapshot file, ON or OFF
3	NSNP	Integer		Number of snapshot dates
4	NISNP	Integer		Number of segments output

This card specifies if information is output to the snapshot file [SNPFN], number of snapshot intervals for specifying output dates and frequencies, and the number of segments that will be output to each snapshot file. Each water body has separate controls so that the user can include/suppress snapshot output for each waterbody.

Snapshot file output provides the user with a hard copy of computed values for hydrodynamic and constituent variables for user assigned segments. Output from this file can take up a tremendous amount of disk space and when printed can use up large quantities of computer paper in a short time. This option is generally used during initial runs and then turned off before the user becomes buried in computer output.

The number of snapshot dates [NSNP] refers to the option of writing information to the snapshot file for different dates and frequencies. For example, the user may specify output is to begin on Julian day 224.4 and output every 0.1 days until day 225.5. Information is then output every day until the end of the simulation. In this case, [NSNP] would be set to 2. Values for each waterbody start on a new line.

Example

SNP PRINT	SNPC	NSNP	NISNP
Wb 1	ON	3	11
Wb 2	ON	1	14
Wb 3	ON	1	10

Related Cards and Files

[Snapshot Dates](#)
[Snapshot Frequency](#)
[Snapshot Segments](#)
[Snapshot Filename](#)
[Constituent Output](#)

Snapshot Dates (SNP DATE)

FIELD	NAME	VALUE	DESCRIPTION
1			(Ignored by code)
2-10	SNPD	Real	Output dates, <i>Julian day</i>

This card specifies the dates that information is output to the snapshot file [SNPFN]. The total number of dates specified on this card must match [[NSNP](#)] on the [Snapshot Print](#) card.

If there are more dates than can be specified on one line, then the values for [SNPD] are continued on the next line without another SNP DATE card being specified. Values for each waterbody start on a new line.

Example

SNP DATE	SNPD	SNPD	SNPD	SNPD	SNPD	SNPD	SNPD	SNPD	SNPD
Wb 1	63.50	100.5	200.5						
Wb 2	63.50								
Wb 3	63.50								

Related Cards and Files

[Snapshot Print](#)
[Snapshot Frequency](#)
[Snapshot Segments](#)
[Snapshot Filename](#)
[Constituent Output](#)

Snapshot Frequency (SNP FREQ)

FIELD	NAME	VALUE	DESCRIPTION
1			(Ignored by code)
2-10	SNPF	Real	Output frequency, <i>days</i>

This card specifies the frequency information is output to the snapshot file [SNPFN]. Frequency can be changed at any time during the simulation by specifying appropriate dates on the [Snapshot Date](#) card and frequencies on the **Snapshot Frequency** card. If output is needed only for the date specified on the [Snapshot Date](#) card, then set the frequency to be greater than the number of days before the next output date.

If there are more frequencies than can be specified on one line, then they are continued on the next line without another SNP FREQ card being specified. Values for each waterbody start on a new line.

Example

SNP FREQ	SNPF	SNPF	SNPF	SNPF	SNPF	SNPF	SNPF	SNPF	SNPF
Wb 1	0.1	500.0	7.0						
Wb 2	0.1								
Wb 3	0.1								

Related Cards and Files

[Snapshot Print](#)
[Snapshot Dates](#)
[Snapshot Segments](#)
[Snapshot Filename](#)
[Constituent Output](#)

Snapshot Segments (SNP SEG)

FIELD	NAME	VALUE	DESCRIPTION
1			(Ignored by code)
2-10	ISNP	Integer	Output segments

This card specifies the segments to be included in the snapshot file for each waterbody. The user can include all segments in the computational grid. However, if the user wants to create a hardcopy that can be printed out, he should not specify more than 21 values for each waterbody. The user should also omit boundary segments that are not part of the computational grid.

If there are more dates than can be specified on one line, then the values for [ISNP] are continued on the next line without another **SNP SEG** card being specified. Values for each waterbody start on a new line.

Example

SNP SEG	ISNP	ISNP	ISNP	ISNP	ISNP	ISNP	ISNP	ISNP	ISNP
Wb 1	2	3	4	5	6	9	10	11	12
	13	14							
Wb 2	17	18	19	20	21	22	23	24	25
	26	27	28	29	30				
Wb 3	33	34	35	36	37	38	39	40	41
	42								

Related Cards and Files

[Snapshot Print](#)
[Snapshot Dates](#)
[Snapshot Frequency](#)
[Snapshot Filename](#)
[Constituent Output](#)

Screen Print (SCR PRNT)

FIELD	NAME	VALUE	DEFAULT	DESCRIPTION
1				(Ignored by code)
2	SCRC	Character	OFF	Specifies if information is written to the screen, ON or OFF
3	NSCR	Integer		Number of screen update intervals

This card specifies if information is output to the screen during the run and the number of intervals during which the frequency of updating the screen can change. The frequency at which the screen is updated should be large (at least 0.1 days). Experience has shown that updating the screen every timestep can easily *double* the runtime. Values for each waterbody start on a new line.

Example

SCR PRINT	SCRC	NSCR
Wb 1	ON	1
Wb 2	ON	1
Wb 3	ON	1

Related Cards and Files

[Screen Dates](#)

[Screen Frequency](#)

Screen Dates (SCR DATE)

FIELD	NAME	VALUE	DESCRIPTION
1			(Ignored by code)
2-10	SCRD	Real	Output dates, <i>Julian day</i>

This card specifies the dates information is output to the screen. The total number of dates specified on this card must match [NSCR] on the [Screen Print](#) card.

If there are more dates than can be specified on one line, then the values for [SCRD] are continued on the next line without another SCR DATE card being specified. Values for each waterbody start on a new line.

Example

SCR DATE	SCRD	SCRD	SCRD	SCRD	SCRD	SCRD	SCRD	SCRD	SCRD
Wb 1	63.5								
Wb 2	63.5								
Wb 3	63.5								

Related Cards and Files

[Screen Print](#)

[Screen Frequency](#)

Screen Frequency (SCR FREQ)

FIELD	NAME	VALUE	DESCRIPTION
1			(Ignored by code)
2-10	SCR F	Real	Output frequency, <i>days</i>

This card specifies the frequency information is output to the screen. Frequency can be changed at any time during the simulation by specifying appropriate dates on the [Screen Date](#) card and frequencies on the **Screen Frequency** card. The frequency at which the screen is updated should be large (at least 0.1 days and more often 1.0 days). Experience has shown that updating the screen every timestep can easily double the runtime. If output is needed only for the date specified on the [Screen Date](#) card, then set the frequency to be greater than the number of days before the next output date.

If there are more frequencies than can be specified on one line, then they are continued on the next line without another **Screen Frequency** card being specified. Values for each waterbody start on a new line.

Example

```
SCR FREQ      SCR F      SCR F      SCR F      SCR F      SCR F      SCR F      SCR F      SCR F      SCR F
Wb 1          0.15
Wb 2          0.15
Wb 3          0.15
```

Related Cards and Files

[Screen Print](#)
[Screen Dates](#)

Profile Plot (PRF PLOT)

FIELD	NAME	VALUE	DEFAULT	DESCRIPTION
1				(Ignored by code)
2	PRFC	Character	OFF	Specifies if information is written to the profile file, ON or OFF
3	NPRF	Integer		Number of profile dates
4	NIPRF	Integer		Number of segments output

This card specifies if information is output to the [profile output file \[PRFFN\]](#), the number of profile intervals for specifying output dates and frequencies, and the number of segments included in the output.

The [profile output file \[PRFFN\]](#) is used to plot vertical profiles of temperature and constituents at a specified model segment. This option is normally turned off during initial runs while the user is verifying the model is performing correctly. It is turned on to compare observed data with simulated data during calibration runs.

This file is in a form suitable for FORTRAN postprocessing. The [spreadsheet profile output file \[SPRFN\]](#) can be used for processing profile output data in a spreadsheet.

The [Constituent Output](#) card controls which constituents are output to the profile file. Temperature is always output to the profile file. Values for each waterbody start on a new line.

Example

PRF PLOT	PRFC	NPRF	NIPRF
Wb 1	ON	1	1
Wb 2	OFF	0	0
Wb 3	ON	1	1

Related Cards and Files

[Profile Date](#)

[Profile Frequency](#)

[Profile Segment](#)

[Profile Filename](#)

[Constituent Output](#)

Profile Date (PRF DATE)

FIELD	NAME	VALUE	DESCRIPTION
1			(Ignored by code)
2-10	PRFD	Real	Output dates, <i>Julian day</i>

This card specifies the dates that information is output to the [profile output file \[PRFFN\]](#). If there are more dates than can be specified on one line, then they are continued on the next line without another PRF DATE card being specified. Values for each waterbody start on a new line.

Example

PRF DATE	PRFD	PRFD	PRFD	PRFD	PRFD	PRFD	PRFD	PRFD	PRFD
Wb 1	63.5								
Wb 2									
Wb 3	63.5								

Related Cards and Files

[Profile Plot](#)

[Profile Frequency](#)

[Profile Segment](#)

[Profile Filename](#)

[Constituent Output](#)

Profile Frequency (PRF FREQ)

FIELD	NAME	VALUE	DESCRIPTION
1			(Ignored by code)
2-10	PRFF	Real	Output frequency, <i>days</i>

This card specifies the frequency information is output to the [profile output file \[PRFFN\]](#). Frequency can be changed at any time during the simulation by specifying appropriate dates on the [Profile Date](#) card and frequencies on the **Profile Frequency** card. If output is needed only for the date specified on the [Profile Date](#) card, then set the frequency to be greater than the number of days before the next output date.

If there are more frequencies than can be specified on one line, then they are continued on the next line without another **PRF FREQ** card being specified. Values for each waterbody start on a new line.

Example

PRF FREQ	PRFF	PRFF	PRFF	PRFF	PRFF	PRFF	PRFF	PRFF	PRFF
Wb 1	1.0								
Wb 2									
Wb 3	1.0								

Related Cards and Files

[Profile Plot](#)

[Profile Date](#)

[Profile Segment](#)

[Profile Filename](#)

[Constituent Output](#)

Profile Segment (PRF SEG)

FIELD	NAME	VALUE	DESCRIPTION
1			(Ignored by code)
2-10	IPRF	Integer	Output segments

This card specifies model segments for which information is output to the [profile output file PRFFN](#). If there are more segments than can be specified on one line, then they are continued on the next line without another **PRF SEG** card being specified. Values for each waterbody start on a new line.

Example

PRF SEG	IPRF	IPRF	IPRF	IPRF	IPRF	IPRF	IPRF	IPRF	IPRF
Wb 1	14								
Wb 2									
Wb 3	42								

Related Cards and Files

[Profile Plot](#)

[Profile Date](#)

[Profile Frequency](#)

[Profile Filename](#)

[Constituent Output](#)

Spreadsheet Profile Plot (SPR PLOT)

FIELD	NAME	VALUE	DEFAULT	DESCRIPTION
1				(Ignored by code)
2	SPRC	Character	OFF	Specifies if information is written to the spreadsheet profile file
3	NSPR	Integer		Number of spreadsheet dates
4	NISPR	Integer		Number of segments in output

This card specifies if information is output to the [spreadsheet profile output file \[SPRFN\]](#), the number of intervals for specifying output dates and frequencies, and the number of segments included in the output.

The [spreadsheet profile output file \[SPRFN\]](#) is used to plot vertical profiles of temperature and constituents at a specified model segment and is suitable as ASCII input into a spreadsheet type database. This option is normally turned off during initial runs while the user is verifying the model is performing correctly. It is turned on to compare observed data with simulated data during calibration. For output to null layers, the default output is -99.

The [Constituent Output](#) card controls which constituents are output to the spreadsheet file. Temperature is always output to the spreadsheet file. Values for each waterbody start on a new line.

Example

SPR PLOT	SPRC	NSPR	NISPR
Wb 1	OFF	0	0
Wb 2	OFF	1	1
Wb 3	OFF	1	1

Related Cards and Files

[Spreadsheet Date](#)
[Spreadsheet Frequency](#)
[Spreadsheet Segment](#)
[Spreadsheet Filename](#)
[Constituent Output](#)

Spreadsheet Profile Date (SPR DATE)

FIELD	NAME	VALUE	DESCRIPTION
1			(Ignored by code)
2-10	SPRD	Real	Output dates, <i>Julian Day</i>

This card specifies the dates that information is output to the [spreadsheet profile output file \[SPRFN\]](#). If there are more dates than can be specified on one line, then they are continued on the next line without another **SPR DATE** card being specified. Values for each waterbody start on a new line.

Example

SPR DATE	SPRD	SPRD	SPRD	SPRD	SPRD	SPRD	SPRD	SPRD	SPRD
Wb 1									
Wb 2	63.5								
Wb 3	63.5								

Related Cards and Files

[Spreadsheet Plot](#)
[Spreadsheet Frequency](#)
[Spreadsheet Segment](#)
[Spreadsheet Filename](#)
[Constituent Output](#)

Spreadsheet Profile Frequency (SPR FREQ)

FIELD	NAME	VALUE	DESCRIPTION
1			(Ignored by code)
2-10	SPRF	Real	Output frequency, <i>days</i>

This card specifies the frequency information is output to the [spreadsheet profile output file \[SPRFN\]](#). Frequency can be changed at any time during the simulation by specifying appropriate dates on the [Spreadsheet Date](#) card and frequencies on the **Spreadsheet Frequency** card. If output is needed only for the date specified on the [Spreadsheet Date](#) card, then set the frequency to be greater than the number of days before the next output date.

If there are more frequencies than can be specified on one line, then they are continued on the next line without another **SPR FREQ** card being specified. Values for each waterbody start on a new line.

Example

SPR FREQ	SPRF	SPRF	SPRF	SPRF	SPRF	SPRF	SPRF	SPRF	SPRF
Wb 1									
Wb 2	7.0								
Wb 3	7.0								

Related Cards and Files

[Spreadsheet Plot](#)
[Spreadsheet Date](#)
[Spreadsheet Segment](#)
[Spreadsheet Filename](#)
[Constituent Output](#)

Spreadsheet Profile Segment (SPR SEG)

FIELD	NAME	VALUE	DESCRIPTION
1			(Ignored by code)
2-10	ISPR	Integer	Output segments

This card specifies model segments for which information is output to the [spreadsheet output file \[SPRFN\]](#). If there are more segments than can be specified on one line, then they are continued on the next line without another **SPR SEG** card being specified.

Example

SPR SEG	ISPR	ISPR	ISPR	ISPR	ISPR	ISPR	ISPR	ISPR	ISPR
Wb 1									
Wb 2	14								
Wb 3	42								

Related Cards and Files

[Spreadsheet Plot](#)
[Spreadsheet Date](#)
[Spreadsheet Frequency](#)
[Spreadsheet Filename](#)
[Constituent Output](#)

Vector Plot (VPL PLOT)

FIELD	NAME	VALUE	DEFAULT	DESCRIPTION
1				(Ignored by code)
2	VPLC	Character	OFF	Specifies if information is written to the vector file, ON or OFF
3	NVPL	Integer		Number of vector plot dates

This card specifies if information is output to the [vector plot file \[VPLFN\]](#) and the number of vector plot intervals for specifying output dates and frequencies. Starting in Version 3.71, the VPL card is no longer the 'vector plot card'. This card will specify the frequency of output for the W2Tools post-processor. Hence, when VPL is ON, an output file will be created for the times and intervals specified in the vector plot frequency and the vector plot date. The vector plot filename specifies the binary file output. Be careful about high frequency output for a large system since the post-processor may not be able to process file sizes greater than 2 GB. For information on the W2Tools post-processor, please consult the user manual for the w2tools program. Also, note that only 1 output file is used even for multiple waterbodies. Hence, the value of VPLC for the 1st waterbody must be ON for output. The values of VPLC for other waterbodies are ignored.

Example

VPL PLOT	VPLC	NVPL	
Wb 1	ON	7	
Wb 2	ON	7	←This is ignored
Wb 3	ON	7	←This is ignored

Related Cards and Files

[Vector Plot Date](#)
[Vector Plot Frequency](#)
[Vector Plot Filename](#)

Vector Plot Date (VPL DATE)

FIELD	NAME	VALUE	DESCRIPTION
1			(Ignored by code)
2-10	VPLD	Real	Output dates, <i>Julian day</i>

This card specifies the dates that information is output to the [vector plot file](#) [VPLFN]. If there are more dates than can be specified on one line, then they are continued on the next line without another **VPL DATE** card being specified. This is the frequency of data written to the post-processing tool, w2tools. Only the value for the 1st waterbody is used to write out information for all waterbodies used by the W2tool post-processing program. The values for other waterbodies are ignored.

Example

VPL DATE	VPLD	VPLD	VPLD	VPLD	VPLD	VPLD	VPLD	VPLD	VPLD
Wb 1	224.5	225.5	226.5	227.5	228.5	229.5	230.5		
Wb 2	224.5	225.5	226.5	227.5	228.5	229.5	230.5	←This is ignored	
Wb 3	224.5	225.5	226.5	227.5	228.5	229.5	230.5	←This is ignored	

Related Cards and Files

[Vector Plot](#)

[Vector Plot Frequency](#)

[Vector Plot Filename](#)

Vector Plot Frequency (VPL FREQ)

FIELD	NAME	VALUE	DESCRIPTION
1			(Ignored by code)
2-10	VPLF	Real	Output frequency, <i>days</i>

This card specifies the frequency information is output to the [vector plot file](#) [**VPLFN**], the w2tools output file. Frequency can be changed at any time during the simulation by specifying the dates on the [Vector Plot Date](#) card and the frequencies on the **Vector Plot Frequency** card. If output is needed only for the date specified on the [Vector Plot Date](#) card, then set the frequency to be greater than the number of days before the next output date.

If there are more frequencies than can be specified on one line, then they are continued on the next line without another **VPL FREQ** card being specified.

Only the value for the 1st waterbody is used to write out information for all waterbodies used by the W2tool post-processing program. The values for other waterbodies are ignored.

Example

VPL FREQ	VPLF	VPLF	VPLF	VPLF	VPLF	VPLF	VPLF	VPLF	VPLF
Wb 1	100.0	100.0	100.0	100.0	100.0	100.0	100.0		
Wb 2	100.0	100.0	100.0	100.0	100.0	100.0	100.0		
Wb 3	100.0	100.0	100.0	100.0	100.0	100.0	100.0		

Related Cards and Files

[Vector Plot](#)

[Vector Plot Date](#)

[Vector Plot Filename](#)

Contour Plot (CPL PLOT)

FIELD	NAME	VALUE	DEFAULT	DESCRIPTION
1				(Ignored by code)
2	CPLC	Character	OFF	Specifies if information is output to the contour file, ON or OFF
3	NCPL	Integer		Number of contour plot dates
4	TECPLOT	Character	OFF	Turns ON or OFF TECPLOT output format

This card specifies if information is output to the [contour plot file \[CPLFN\]](#) and the number of contour plot intervals for specifying output dates and frequencies. The current version still requires the user to develop their own means of postprocessing data for contour plots. This also requires the user to “get under the hood” of the code in order to determine the data output and the format of the output to generate their own contour plots.

Turning ON TECPLOT output allows the user to quickly develop contour and vector animation of model output. TECPLOT output contains Elevation (m), Distance (m), U, W, T(C), RHO, HABITAT# (based on fish habitat criteria – see CPL file format) and all active constituents for the entire model grid at a frequency specified in CPL FREQ.

Instructions for using TECPLOT360 and creating an animation are shown below:

1. In control file, turn on contour output (CPLC='ON') and tecplot option (TECPLOT='ON'). Also set output frequency CPLF to desired value.
2. Run model
3. Start Tecplot, select 'File|Load Data File'. Select 'Tecplot Data Loader' and load contour output file (probably cpl.opt). It will probably take time for tecplot to convert the ascii file to binary. If the file is really big, this might take quite a while.
4. When the 'Select Initial Plot' window comes up, set initial plot time to “2D Cartesian” and select “Show First Zone Only”. A 2-D graph should be visible with Elevation being the y-axis and distance for the x-axis
5. In the “Zone Surfaces Layers” box at the upper left, select “Contour” and “deselect anything else.
6. Double Click on the y-axis, and a “Axis Details” box should come up. Select the Range tab and select “Independent” in the dependency box. Click on “Reset Range” and then select “reset to nice values” to reset the Min/Max values for the y-axis.. The contour plot for the first day should be visible now.
7. Select Plot|Contour to select the parameter for which you want to make an animation. It will likely be set to 'T' or temperature initially.
8. To set the contour plot intervals, select Plot|Contour and click on the “>>” button. Then select “New Levels”. A typical setting for temperature would be Minimum Level =0, Maximum Level=30, and Number of Levels=25
9. To show a legend, click on the “Legend” tab and click “Show Contour Legend”

CONTROL FILE

OUTPUT CONTROL

10. To blank out inactive cells, select Plot|Blanking|Value Blanking and click on “Include Value Blanking”. Then click on the “Active” box, and select “Blank when” temperature of ‘T’) is less than or equal to -0.1.
11. To create animation, select Animate|Zones and click animate. You have the option of animating on screen, to an AVI file, or to a rastermetafile (RM).
12. One can also add velocity vectors by turning on the vector map and adjusting the vector properties on top of the temperature contour plot. Other contour movies of other state variables can be performed by following these same steps.
13. Before exiting tecplot, save your work by selecting File|Save Layout.

Example

CPL PLOT	CPLC	NCPL	TECPLOT
Wb 1	ON	7	OFF
Wb 2	ON	7	OFF
Wb 3	ON	7	OFF

Related Cards and Files

[Contour Plot Date](#)
[Contour Plot Frequency](#)
[Contour Plot Filename](#)
[Constituent Output](#)

Contour Plot Dates (CPL DATE)

FIELD	NAME	VALUE	DESCRIPTION
1			(Ignored by code)
2-10	CPLD	Real	Output dates, <i>Julian day</i>

This card specifies the dates that information is output to the [contour plot file \[CPLFN\]](#). If there are more dates than can be specified on one line, then they are continued on the next line without another **CPL DATE** card being specified.

Example

CPL DATE	CPLD	CPLD	CPLD	CPLD	CPLD	CPLD	CPLD	CPLD	CPLD
Wb 1	224.5	225.5	226.5	227.5	228.5	229.5	230.5		
Wb 2	224.5	225.5	226.5	227.5	228.5	229.5	230.5		
Wb 3	224.5	225.5	226.5	227.5	228.5	229.5	230.5		

Related Cards and Files

[Contour Plot](#)

[Contour Plot Frequency](#)

[Contour Plot Filename](#)

[Constituent Output](#)

Contour Plot Frequency (CPL FREQ)

FIELD	NAME	VALUE	DESCRIPTION
1			(Ignored by code)
2-10	CPLF	Real	Output frequency, <i>days</i>

This card specifies the frequency information is output to the [contour plot file \[CPLFN\]](#). Frequency can be changed at any time during the simulation by specifying appropriate dates on the [Contour Plot Date](#) card and frequencies on the **Contour Plot Frequency** card. If output is needed only for the date specified on the [Contour Plot Date](#) card, then set the frequency to be greater than the number of days before the next output date.

If there are more frequencies than can be specified on one line, then they are continued on the next line without another **CPL FREQ** card being specified.

Example

CPL FREQ	CPLF	CPLF	CPLF	CPLF	CPLF	CPLF	CPLF	CPLF	CPLF
Wb 1	10.0	10.0	10.0	10.0	10.0	10.0	10.0		
Wb 2	10.0	10.0	10.0	10.0	10.0	10.0	10.0		
Wb 3	10.0	10.0	10.0	10.0	10.0	10.0	10.0		

Related Cards and Files

[Contour Plot](#)
[Contour Plot Date](#)
[Contour Plot Filename](#)
[Constituent Output](#)

Kinetic Flux Output (FLUXES)

FIELD	NAME	VALUE	DEFAULT	DESCRIPTION
1				(Ignored by code)
2	FLXC	Character	OFF	Specifies if information is sent to the kinetic flux output file, ON or OFF
3	NFLX	Integer		Number of kinetic flux dates

This card specifies if information is output to the [kinetic flux file \[KFLFN\]](#) and the number of kinetic flux intervals for specifying output dates and frequencies. Output of kinetic fluxes to the TSR file is dependent on the frequency of the TSR file. This file contains kinetic fluxes that allow the user to determine the dominant forcing function responsible for a given constituents increase/decrease in concentrations and is particularly useful during water quality calibration as the user can identify which kinetic processes are most responsible for the model behavior of a given constituent and adjust the rate coefficients correspondingly. The fluxes represent the average flux in kg/day over the time interval of flux output (FLX FREQ) and is in the same output format as the Snapshot [SNP] file. A summation of all active fluxes for each waterbody over all segments and layers is output to another file with a filename “KFLUX_JW#.OPT” where # is the waterbody number. This file is also output at the frequency specified for flux output (FLX FREQ).

Example

FLUXES	FLXC	NFLX
Wb 1	ON	1
Wb 2	OFF	0
Wb 3	OFF	0

Related Cards and Files

[Kinetic Flux Date](#)

[Kinetic Flux Frequency](#)

[Kinetic Flux Filename](#)

Kinetic Flux Date (KFL DATE)

FIELD	NAME	VALUE	DESCRIPTION
1			(Ignored by code)
2-10	KFLD	Real	Output dates, <i>Julian day</i>

This card specifies the dates that information is output to the [kinetic flux file \[KFLFN\]](#). If there are more dates than can be specified on one line, then they are continued on the next line without another **KFL DATE** card being specified.

Example

FLX DATE	FLXD	FLXD	FLXD	FLXD	FLXD	FLXD	FLXD	FLXD	FLXD
Wb 1	1.0								
Wb 2									
Wb 3									

Related Cards and Files

[Kinetic Flux Output](#)
[Kinetic Flux Frequency](#)
[Kinetic Flux Filename](#)

Kinetic Flux Frequency (FLX FREQ)

FIELD	NAME	VALUE	DESCRIPTION
1			(Ignored by code)
2-10	FLXF	Real	Output frequency, <i>days</i>

This card specifies the frequency information is output to the [kinetic flux file \[KFLFN\]](#). If there are more dates than can be specified on one line, then they are continued on the next line without another **KFL FREQ** card being specified. If output is needed only for the date specified on the [Kinetic Flux Date](#) card, then set the frequency to be greater than the number of days before the next output date.

Example

```
FLX FREQ      FLXF      FLXF      FLXF      FLXF      FLXF      FLXF      FLXF      FLXF
Wb 1          7.0
Wb 2
Wb 3
```

Related Cards and Files

[Kinetic Flux Output](#)

[Kinetic Flux Date](#)

[Kinetic Flux Filename](#)

Time Series Plot (TSR PLOT)

FIELD	NAME	VALUE	DEFAULT	DESCRIPTION
1				(Ignored by code)
2	TSRC	Character	OFF	Specifies if information is written to time series file, ON or OFF
3	NTSR	Integer		Number of time series dates
4	NITSR	Integer		Number of time series computational cells

This card specifies if information is output to the [times series file \[TSRFN\]](#) the number of time series intervals for specifying output dates and frequencies, and the number of time series computational cells for which information will be output.

Time series output consists of the Julian date, timestep, water surface elevation, temperature, flow rate (vertically integrated segment flow rate at the specified model segment), shortwave solar radiation (net) incident on the surface (i.e., it does not include the reflected solar), light extinction coefficient (m^{-1}), depth to bottom of channel (m), surface width (m), shade fraction (1.0 is no shade, 0.0 is 100% reduction in solar radiation), net radiation at surface of segment (W/m^2), short wave solar net at surface (W/m^2), long wave radiation in net at surface (W/m^2), back radiation at surface (W/m^2), evaporative heat flux at surface (W/m^2), conductive heat flux at surface (W/m^2), active constituents, derived constituents, and kinetic fluxes as specified in the CST flux card (fluxes are in units of kg/day). Note that the kinetic fluxes in the TSR file are instantaneous flux rates, whereas those fluxes shown in the kinetic flux file are averages over the time interval or frequency of output. The constituent concentrations output are the constituents specified for output on the [Constituent Output](#) card. The derived constituent concentrations output are the constituents specified on the [Derived Constituent](#) card.

Example

```
TSR PLOT      TSRC      NTSR      NITSR
              OFF        0          0
```

Related Cards and Files

[Time Series Date](#)
[Time Series Frequency](#)
[Time Series Segment](#)
[Time Series Elevation](#)
[Constituent Output](#)

Time Series Date (TSR DATE)

FIELD	NAME	VALUE	DESCRIPTION
1			(Ignored by code)
2-10	TSRD	Real	Output dates, <i>Julian day</i>

This card specifies the dates that information is output to the [times series file \[TSRFN\]](#). If there are more dates than can be specified on one line, then they are continued on the next line without another **TSR DATE** card being specified.

Example

TSR DATE	TSRD	TSRD	TSRD	TSRD	TSRD	TSRD	TSRD	TSRD	TSRD
	63.5								

Related Cards and Files

[Time Series Plot](#)
[Time Series Frequency](#)
[Time Series Segment](#)
[Time Series Elevation](#)
[Constituent Output](#)

Time Series Frequency (TSR FREQ)

FIELD	NAME	VALUE	DESCRIPTION
1			(Ignored by code)
2-10	TSRF	Real	Output frequency, <i>days</i>

This card specifies the frequency information is output to the [times series file \[TSRFN\]](#). Frequency can be changed at any time during the simulation by specifying the dates on the [Time Series Date](#) card and the frequencies on the **Time Series Frequency** card. If output is needed only for the date specified on the [Time Series Date](#) card, then set the frequency to be greater than the number of days before the next output date.

If there are more frequencies than can be specified on one line, then they are continued on the next line without another **TSR FREQ** card being specified.

Example

```
TSR FREQ      TSRF      TSRF      TSRF      TSRF      TSRF      TSRF      TSRF      TSRF
              1.00
```

Related Cards and Files

[Time Series Plot](#)
[Time Series Date](#)
[Time Series Segment](#)
[Time Series Elevation](#)
[Constituent Output](#)

Time Series Segment (TSR SEG)

FIELD	NAME	VALUE	DESCRIPTION
1			(Ignored by code)
2-10	ITSR	Integer	Output segments

This card, along with the [Time Series Elevation](#) card, defines which computational cells are output to the [times series file \[TSRFN\]](#). To specify multiple cells in a segment, the segment number must be duplicated for each computational cell to be output.

Example

TSR SEG	ITSR	ITSR	ITSR	ITSR	ITSR	ITSR	ITSR	ITSR	ITSR
	20	23	26	30	30				

Related Cards and Files

[Time Series Plot](#)
[Time Series Date](#)
[Time Series Frequency](#)
[Time Series Elevation](#)
[Constituent Output](#)

Time Series Elevation (TSR ELEV)

FIELD	NAME	VALUE	DESCRIPTION
1			(Ignored by code)
2-10	ETSR	Real	Depth below water surface in m (if positive) or layer number (if negative) corresponding to time series segment

This card specifies the elevation from the water surface that corresponds to the segment [[ITSR](#)] specified on the [Time Series Segment](#) card. Specifying a negative number results in the layer number being used for the vertical location. For example, setting [ETSR] to -5.0 results in output from layer 5; setting [ESTR] to 0.0 is at the water surface; and setting [ESTR] to 1.5 is 1.5 m below the water surface.

Example

TSR ELEV	ETSR	ETSR	ETSR	ETSR	ETSR	ETSR	ETSR	ETSR	ETSR
	1.0	5.0	10.0	-5.0	-8.0				

Related Cards and Files

[Time Series Plot](#)
[Time Series Date](#)
[Time Series Frequency](#)
[Time Series Segment](#)
[Constituent Output](#)

Withdrawal Output (WITH OUT)

FIELD	NAME	VALUE	DEFAULT	DESCRIPTION
1				(Ignored by code)
2	WDOC	Character	OFF	Specifies if information is written to withdrawal output file, ON or OFF
3	NWDO	Integer		Number of withdrawal output dates
4	NIWDO	Integer		Number of withdrawal output segments

This card specifies if information is output to a separate [withdrawal outflow file](#) [WDOFN] for outflow, outflow temperature, outflow constituent concentrations, and outflow derived constituent concentrations. This option is useful for comparing time series results of these variables and for providing input files for downstream models that are not run together. The names of the outflow files are appended with the segment number to differentiate each of the files.

The information can also be used to link output from one waterbody to a downstream waterbody. Currently, the model uses the minimum timestep necessary to maintain numerical stability throughout the entire system. In many cases, the riverine sections linking reservoirs and/or estuaries together in the system determine this. This option is provided to allow the user to break up the waterbasin so that each waterbody can be run separately. As a consequence, the separate waterbodies can now run at a timestep necessary to maintain numerical stability based on the limiting timestep criteria for the individual waterbody rather than the limiting criteria for the entire system.

When using this option, the user should investigate how the frequency of output affects the results by first running the model with a small output frequency and then increasing the frequency until the results change substantially. Model results should not be a function of the input frequency of boundary conditions. The user wants to make sure the instantaneous output frequency of this file matches the integrated response correctly.

If there is one output located at the withdrawal output segment [IWDO], like a structure, the output files will be called qwo_segXX.opt, two_segXX.opt, cwo_segXX.opt, and dwo_segXX.opt, where XX is the segment number, q is for flow, t is for temperature, c is for concentration, and d is for derived concentrations. If there is a structure, withdrawal and a 2 pumps at this segment, the combined flows and flow-averaged temperature and concentrations will be written to these files. In addition, output files are written for each separate outlet. In this case there will also be written the following files: qwo_str1_segXX.opt, qwo_wd1_segXX.npt, qwo_pmp1_segXX.opt, qwo_pmp2_segXX.opt, two_str1_segXX.opt, two_wd1_segXX.npt, two_pmp1_segXX.opt, two_pmp2_segXX.opt, cwo_str1_segXX.opt, cwo_wd1_segXX.npt, cwo_pmp1_segXX.opt, cwo_pmp2_segXX.opt, and similarly for the derived concentrations for the structure, withdrawal and two pump withdrawals. Similarly named output files are provided for gates, spillways and pipes if they are located at the withdrawal output segment [IWDO].

In the flow and temperature withdrawal files, in addition to the sum of flows and weighted temperature of all withdrawals/structures, a breakdown of individual flows and temperatures are given.

Example

```
WITH OUT      WDOC      NWDO      NIWDO
              ON        1        2
```

CONTROL FILE

OUTPUT CONTROL

Related Cards and Files

[Withdrawal Output Date](#)

[Withdrawal Output Frequency](#)

[Withdrawal Output Segment](#)

Withdrawal Output Date (WDO DATE)

FIELD	NAME	VALUE	DESCRIPTION
1			(Ignored by code)
2	WDOD	Real	Output dates, <i>Julian day</i>

This card specifies the dates information is output to the [withdrawal outflow file \[WDOFN\]](#). If there are more dates than can be specified on one line, then they are continued on the next line without another **WDO DATE** card being specified.

Example

WDO DATE	WDOD	WDOD	WDOD	WDOD	WDOD	WDOD	WDOD	WDOD	WDOD
	63.5								

Related Cards and Files

[Withdrawal Output](#)

[Withdrawal Output Frequency](#)

[Withdrawal Output Segment](#)

Withdrawal Output Frequency (WDO FREQ)

FIELD	NAME	VALUE	DESCRIPTION
1			(Ignored by code)
2-10	WDOF	Real	Output frequency, <i>days</i>

This card specifies the frequency information is output to the [withdrawal outflow file \[WDOFN\]](#). Frequency can be changed at any time during the simulation by specifying the dates on the [Withdrawal Output Date](#) card and the frequencies on the [Withdrawal Output Frequency](#) card. If output is needed only for the date specified on the [Withdrawal Output Date](#) card, then set the frequency to be greater than the number of days before the next output date.

If there are more frequencies than can be specified on one line, then they are continued on the next line without another **WDO FREQ** card being specified.

Example

```
WDO FREQ      WDOF      WDOF      WDOF      WDOF      WDOF      WDOF      WDOF      WDOF      WDOF
              0.2
```

Related Cards and Files

[Withdrawal Output](#)
[Withdrawal Output Date](#)
[Withdrawal Output Segment](#)

Withdrawal Output Segment (WITH SEG)

FIELD	NAME	VALUE	DESCRIPTION
1			(Ignored by code)
2-10	IWDO	Integer	Output segments

This card specifies model segments for which information is output to the withdrawal output file [[WDOFN](#)]. If a downstream segment of a reservoir is specified, then information is output at the frequency specified in the [Withdrawal Output Frequency](#) card that can be used as input files to a waterbody downstream of the reservoir.

If there are more segments than can be specified on one line, then they are continued on the next line without another **WITH SEG** card being specified.

Example

```
WITH SEG  IWDO  IWDO  IWDO  IWDO  IWDO  IWDO  IWDO  IWDO  IWDO
          30    32
```

Related Cards and Files

[Withdrawal Output](#)

[Withdrawal Output Date](#)

[Withdrawal Output Frequency](#)

Restart (RESTART)

FIELD	NAME	VALUE	DEFAULT	DESCRIPTION
1				(Ignored by code)
2	RSOC	Character	OFF	Specifies if information is output to the restart file, ON or OFF
3	NRSO	Integer		Number of restart dates
4	RSIC	Character	OFF	Specifies if information is input from the restart file, ON or OFF

This card specifies if information is output to the restart output file [[RSOFN](#)] or read into the model from a previously output restart file [[RSIFN](#)] and the number of restart dates.

Example

RESTART	RSOC	NRSO	RSIC
	ON	2	OFF

Related Cards and Files

[Restart Date](#)

[Restart Frequency](#)

Restart Date (RSO DATE)

FIELD	NAME	VALUE	DESCRIPTION
1			(Ignored by code)
2-10	RSOD	Real	Output dates, Julian day

This card specifies dates information is output to the restart file [[RSOFN](#)]. If there are more dates than can be specified on one line, then they are continued on the next line without another **RSO DATE** card being specified.

Example

RSO DATE	RSOD	RSOD	RSOD	RSOD	RSOD	RSOD	RSOD	RSOD	RSOD
	224.5	230.5							

Related Cards and Files

[Restart](#)
[Restart Frequency](#)

Restart Frequency (RSO FREQ)

FIELD	NAME	VALUE	DESCRIPTION
1			(Ignored by code)
2-10	RSOF	Real	Output frequency, <i>days</i>

This card specifies the frequency information is output to the restart plot file [[RSOFN](#)]. Frequencies can be changed at any time during the simulation by specifying the appropriate dates on the [Restart Date](#) card and frequencies on the Restart Frequency card. If output is needed only for the date specified on the [Restart Date](#) card, then set the frequency to be greater than the number of days before the next output date.

If there are more frequencies than can be specified on one line, then they are continued on the next line without another **RSO FREQ** card being specified.

Example

```
RSO FREQ      RSOF      RSOF      RSOF      RSOF      RSOF      RSOF      RSOF      RSOF      RSOF
              100.0     100.0
```

Related Cards and Files

[Restart](#)
[Restart Date](#)

Constituent Computations (CST COMP)

FIELD	NAME	VALUE	DEFAULT	DESCRIPTION
1				(Ignored by code)
2	CCC	Character	OFF	Specifies if constituents are computed, ON or OFF
3	LIMC	Character	OFF	Output algal growth limiting factor, ON or OFF
4	CUF	Integer	2	Frequency which constituent kinetics are updated

This card starts the specification of constituent computations. [CCC] determines if constituent computations are performed. If this variable is turned off, then constituent computations are not performed and all information specified on the remaining constituent control cards is ignored. Individual constituent computations are controlled on the [Active Constituents](#) card. During the initial calibration runs for freshwater systems, constituent computations are usually turned off until temperature, water surface elevations, and velocities are calibrated.

The [LIMC] variable specifies whether the factor limiting algal growth is output to the [snapshot file](#) [SNPFN].

The model allows the user to update constituent kinetics at a different frequency than constituent transport. The constituent update frequency [CUF] specifies how many transport iterations are performed before constituent kinetics are updated. This option is included primarily to reduce computation time. This variable should be set to one during initial calibration. If computation time is of concern, [CUF] can be increased until water quality results begin to deviate. Model results should not be a function of the timestep used during the simulation.

Active constituents must be in the following order in both the control file and the GRAPH.NPT file listing of constituents even if the constituents are not active.

Required Constituent order	Constituent
1	TDS (g/m ³ or mg/l) or salinity (kg/m ³) depending on variable waterbody type [WTYPEC]. If [FRESH], then TDS, or if [SALT], salinity.
2	Generic constituents, such as bacteria, water age, tracer, etc. – user defined number of groups set by [NGC]
3	Inorganic suspended solids, mg/l – user defined number of groups set by [NSS]
4	PO ₄ -P, mg/l as P
5	NH ₄ -N, mg/l as N
6	NO ₃ -N + NO ₂ -N, mg/l as N
7	Dissolved silica, mg/l as Si
8	Particulate silica, mg/l as Si
9	Iron, mg/l as Fe or divalent metal
10	LDOM, mg/l as organic matter
11	RDOM, mg/l as organic matter
12	LPOM, mg/l as organic matter
13	RPOM, mg/l as organic matter

CONTROL FILE**CONSTITUENT CONTROL**

Required Constituent order	Constituent
14	CBOD - user defined number of groups, mg/l as O ₂ , set by [NBOD]
15	CBOD-P – user defined number of groups, mg/l as P, set by [NBOD]
16	CBOD-N – user defined number of groups, mg/l as N, set by [NBOD]
17	Algae - user defined number of groups, mg/l as dry weight organic matter, set by [NAL]
18	Dissolved oxygen, mg/l
19	TIC, mg/l as C
20	Alkalinity, mg/l as CaCO ₃
21	Zooplankton - user defined number of groups, mg/l dry weight organic matter, set by [NZP]
22	LDOM-P, mg/l as P
23	RDOM-P, mg/l as P
24	LPOM-P, mg/l as P
25	RPOM-P, mg/l as P
26	LDOM-N, mg/l as N
27	RDOM-N, mg/l as N
28	LPOM-N, mg/l as N
29	RPOM-N, mg/l as N

Example

CST	COMP	CCC	LIMC	CUF
		ON	OFF	10

Related Cards and Files[Active Constituents](#)[Constituent Initial Concentration](#)[Constituent Output](#)[Inflow Active Constituent Control](#)[Tributary Active Constituent Control](#)[Distributed Tributary Active Constituent Control](#)[Precipitation Active Constituent Control](#)

Active Constituents (CST ACTIVE)

FIELD	NAME	VALUE	DEFAULT	DESCRIPTION
1				(Ignored by code)
2-10	CAC	Character	OFF	Specifies if calculations are to be performed for this constituent, ON or OFF

This card specifies which constituents are included in water quality calculations. The current version now allows the user the flexibility to include any number of generic, inorganic suspended solids, algal and/or epiphyton groups, and CBOD groups. The number of these groups is specified on the [Constituent Dimension](#) card. The generic constituent can be used to simulate any number of constituents that can be defined with a zero-order decay rate and/or a first order decay rate, and/or a settling velocity, and/or an Arrhenius temperature rate multiplier. This includes a conservative tracer with all kinetic coefficients set to zero, residence time with the zero-order decay rate set to -1.0 day^{-1} , and coliform bacteria where a temperature rate multiplier, first-order decay rate, and/or a settling velocity are defined.

The user has the flexibility of including/excluding any of the constituent state variables. The constituent kinetics are strongly coupled and failure to include one or more constituents can have far reaching effects that are hard to determine beforehand, so use this option carefully. Some previous applications have modeled only dissolved oxygen with the zero-order sediment oxygen demand used for calibration. This was deemed acceptable as the applications were looking only at how different reservoir operations and their impacts on hydrodynamics would affect temperature and dissolved oxygen.

Note that if the user has CBOD groups and if BODP and BODN are OFF, the model uses the stoichiometric coefficients in the CBOD STOICH card to compute the fixed N and P content of each CBOD organic matter group.

The [Constituents Computation](#) card goes over the required order of the active constituents, which is the same order required for the graph.npt file.

CONTROL FILE

CONSTITUENT CONTROL

Example

CST	ACTIVE	CAC	
TDS	ON		Total dissolved solids, mg/l
Age	ON		Water age
Tracer	ON		Conservative tracer
Coliform	ON		Coliform bacteria
ISS1	ON		inorganic suspended solids, mg/l
PO4	ON		phosphate-P, mg/l as P
NH4	ON		ammonia-N, mg/l as N
NO3	ON		nitrate-N, mg/l as N
DSI	OFF		dissolved silica
PSI	OFF		particulate silica
FE	OFF		iron, mg/l as Fe_total
LDOM	ON		labile dissolved organic matter, mg/l organic matter
RDOM	ON		refractory dissolved organic matter, mg/l organic matter
LPOM	ON		labile particulate organic matter, mg/l organic matter
RPOM	ON		refractory particulate organic matter, mg/l organic matter
BOD1	ON		CBOD group 1, mg/l O2
BOD1-P	ON		CBOD-P group 1, mg/l O2
BOD1-N	ON		CBOD-N group 1, mg/l O2
ALG1	ON		algal group 1, mg/l organic matter (dry weight)
ALG2	ON		algal group 2, mg/l organic matter (dry weight)
ALG3	ON		algal group 3, mg/l organic matter (dry weight)
DO	ON		dissolved oxygen, mg/l O2
TIC	ON		total inorganic carbon mg/l as C
ALK	ON		alkalinity mg/l as CaCO3
ZOO1	ON		zooplankton group 1
LDOM_P	ON		Total P in labile dissolved organic matter
RDOM_P	ON		Total P in refractory dissolved organic matter
LPOM_P	ON		Total P in labile particulate organic matter
RPOM_P	ON		Total P in refractory particulate organic matter
LDOM_N	ON		Total N in labile dissolved organic matter
RDOM_N	ON		Total N in refractory dissolved organic matter
LPOM_N	ON		Total N in labile particulate organic matter
RPOM_N	ON		Total N in refractory particulate organic matter

Related Cards and Files

[Constituent Computations](#)

[Constituent Initial Concentration](#)

[Constituent Output](#)

[Inflow Active Constituent Control](#)

[Tributary Active Constituent Control](#)

[Distributed Tributary Active Constituent Control](#)

[Precipitation Active Constituent Control](#)

Derived Constituents (CST DERIVE)

FIELD	NAME	VALUE	DEFAULT	DESCRIPTION
1				(Ignored by code)
2-10	CDWBC	Character	OFF	Specifies if derived variables are output for each waterbody, ON or OFF

This card allows the user to specify whether certain derived constituents are computed and output in order to compare with observed data. Derived constituents are constituents that are not state variables, but are useful for gaining a better understanding of how the water quality formulations are simulating the prototype. They are also useful for comparing computed versus observed data for water quality parameters that are not state variables, but that are routinely monitored, such as total Kjeldahl nitrogen.

In Version 2, pH computations were incorrectly included as a state variable. The current version now includes pH computations as a derived variable as pH is computed from the total inorganic carbon and alkalinity state variables (as well as temperature).

An example of the computation of the derived variable Total Suspended Solids (TSS) is shown below:

$$TSS, \frac{mg}{l} = \sum_i InorganicSuspendedSolids_i + \sum_j AlgaeDryWeightBiomass_j + \sum_k ZooplanktonDryWeightBiomass_k + ParticulateOrganicMatter_{labile} + ParticulateOrganicMatter_{refractory} + \sum_m ParticulateOrganicMatter - CBOD_m$$

Hence, the TSS output will include all the inorganic suspended solids fractions and all organic matter which includes algae, zooplankton, refractory and labile particulate organic matter (POM), and the particulate fractions of CBOD.

Example

CST	DERIVE	CDWBC	CDWBC	CDWBC	CDWBC	CDWBC	CDWBC	CDWBC	CDWBC	CDWBC	CDWBC
DOC		OFF	OFF	OFF							Dissolved organic carbon, mg/l as C
POC		OFF	OFF	OFF							Particulate organic carbon, mg/l as C
TOC		OFF	OFF	OFF							Total organic carbon, mg/l as C
DON		OFF	OFF	OFF							Dissolved organic nitrogen, mg/l as N
PON		OFF	OFF	OFF							Particulate organic nitrogen, mg/l N
TON		OFF	OFF	OFF							Total organic nitrogen, mg/l as N
TKN		OFF	OFF	OFF							Total Kjeldahl nitrogen, mg/l as N
TN		OFF	OFF	OFF							Total nitrogen, mg/l as N
DOP		OFF	OFF	OFF							Dissolved organic phosphorus, mg/l P
POP		OFF	OFF	OFF							Particulate organic phosphorus, mg/l P
TOP		OFF	OFF	OFF							Total organic phosphorus, mg/l as P
TP		OFF	OFF	OFF							Total phosphorus, mg/l as P
APR		OFF	OFF	OFF							Algal production
CHLA		OFF	OFF	OFF							Chlorophyll a, ug/l chlorophyll a
ATOT		OFF	OFF	OFF							Total algal biomass, mg/l organic matter

CONTROL FILE

%DO	OFF	OFF	OFF
TSS	OFF	OFF	OFF
TISS	OFF	OFF	OFF
CBODU	OFF	OFF	OFF
Ph	ON	OFF	OFF
CO2	OFF	OFF	OFF
HCO3	OFF	OFF	OFF
CO3	OFF	OFF	OFF

Related Cards and Files

[Constituent Computations](#)
[Active Constituents](#)

CONSTITUENT CONTROL

Dissolved oxygen saturation, %
Total suspended solids, mg/l
Total inorganic suspended solids, mg/l
Total carbonaceous BOD (ultimate)
pH
Carbon dioxide, mg/l as C
Bicarbonate, mg/l as C
Carbonate, mg/l as C

Constituent Fluxes (CST FLUX)

FIELD	NAME	VALUE	DEFAULT	DESCRIPTION
1				(Ignored by code)
2-10	CFWBC	Character	OFF	Specifies which kinetic fluxes are output for each waterbody, ON or OFF

This card allows the user to specify whether constituent advective, diffusive, and kinetic fluxes are computed and output in order to evaluate their importance on the resulting constituent state variable computed concentrations. For example, if all the fluxes associated with dissolved oxygen in the model are output, then the user can determine the most important fluxes affecting DO and adjust the kinetic rate coefficients accordingly during calibration. This should greatly reduce the time required for water quality calibration and provide a greater understanding of kinetic behavior in the model and the prototype. Only the kinetic fluxes are computed in the current release. Advective and diffusive fluxes will be included in a later release.

Example

CST FLUX	CFWBC	CFWBC	CFWBC	CFWBC	CFWBC	CFWBC	CFWBC	CFWBC	CFWBC
TISSIN	OFF	OFF	OFF	Total inorganic suspended solids settling, source					
TISSOUT	OFF	OFF	OFF	Total inorganic suspended solids settling, sink					
PO4AR	OFF	OFF	OFF	PO4 from algal respiration, source					
PO4AG	OFF	OFF	OFF	PO4 from algal growth, sink					
PO4AP	OFF	OFF	OFF	Net PO4 algal uptake, source/sink					
PO4ER	OFF	OFF	OFF	PO4 from epiphyton respiration, source					
PO4EG	OFF	OFF	OFF	PO4 from epiphyton growth, sink					
PO4EP	OFF	OFF	OFF	Net PO4 epiphyton uptake, source/sink					
PO4POM	OFF	OFF	OFF	PO4 from particulate organic matter, source					
PO4DOM	OFF	OFF	OFF	PO4 from dissolved organic matter, source					
PO4OM	OFF	OFF	OFF	PO4 from organic matter, source					
PO4SED	OFF	OFF	OFF	PO4 from sediment compartment, source					
PO4SOD	OFF	OFF	OFF	PO4 from 0-order sediment release, source					
PO4SET	OFF	OFF	OFF	Sorbed PO4 from settling, source/sink					
NH4NITR	OFF	OFF	OFF	NH4 from nitrification, sink					
NH4AR	OFF	OFF	OFF	NH4 from algal respiration, source					
NH4AG	OFF	OFF	OFF	NH4 from algal growth, sink					
NH4AP	OFF	OFF	OFF	Net NH4 from algal growth, sink					
NH4ER	OFF	OFF	OFF	NH4 from epiphyton respiration, source					
NH4EG	OFF	OFF	OFF	NH4 from epiphyton growth, sink					
NH4EP	OFF	OFF	OFF	Net NH4 from epiphyton growth, sink					
NH4ANET	OFF	OFF	OFF	Net NH4 algal uptake, source/sink					
NH4POM	OFF	OFF	OFF	NH4 from particulate organic matter, source					
NH4DOM	OFF	OFF	OFF	NH4 from dissolved organic matter, source					
NH4OM	OFF	OFF	OFF	NH4 from organic matter decay					
NH4SED	OFF	OFF	OFF	NH4 from sediment compartment, source					
NH4SOD	OFF	OFF	OFF	NH4 from 0-order sediment release, source					
NO3DEN	OFF	OFF	OFF	NO3 from denitrification, sink					
NO3AG	OFF	OFF	OFF	NO3 from algal growth, sink					
NO3EG	OFF	OFF	OFF	NO3 from epiphyton growth, sink					
NO3SED	OFF	OFF	OFF	NO3 loss to sediment compartment, sink					
DSIAG	OFF	OFF	OFF	Dissolved Si from algal growth, sink					
DSIEG	OFF	OFF	OFF	Dissolved Si from epiphyton growth, sink					
DSIPBSI	OFF	OFF	OFF	Dissolved Si from particulate biogenic Si, source					
DSISED	OFF	OFF	OFF	Dissolved Si from sediment compartment, source					
DSISOD	OFF	OFF	OFF	Dissolved Si from 0-order sediment release, source					
DSISET	OFF	OFF	OFF	Dissolved Si from sorbed Si settling, source/sink					
PBSIAM	OFF	OFF	OFF	Particulate biogenic Si from algal mortality, source					
PBSINET	OFF	OFF	OFF	Particulate biogenic Si from settling, source/sink					
PBSIDK	OFF	OFF	OFF	Particulate biogenic Si decay, sink					
FESET	OFF	OFF	OFF	Fe from settling, source/sink					

CONTROL FILE

CONSTITUENT CONTROL

FESED	OFF	OFF	OFF Fe from sediment release, source
LDOMDK	OFF	OFF	OFF Labile DOM decay, sink
LRDOM	OFF	OFF	OFF Labile to refractory DOM decay, sink
RDOMDK	OFF	OFF	OFF Refractory DOM decay, sink
LDOMAP	OFF	OFF	OFF Labile DOM from algal mortality, source
LDOMEF	OFF	OFF	OFF Labile DOM from epiphyton mortality, source
LPOMDK	OFF	OFF	OFF Labile POM decay, sink
LRPOM	OFF	OFF	OFF Labile to refractory POM decay, sink
RPOMDK	OFF	OFF	OFF Refractory POM decay, sink
LPOMAP	OFF	OFF	OFF Labile POM from algal mortality, source
LPOMSET	OFF	OFF	OFF Labile POM from settling, source/sink
RPOMSET	OFF	OFF	OFF Refractory POM from settling, source/sink
CBODDK	OFF	OFF	OFF CBOD decay, sink
DOAP	OFF	OFF	OFF DO from algal production, source
DOAR	OFF	OFF	OFF DO from algal respiration, sink
DOEP	OFF	OFF	OFF DO from epiphyton production, source
DOER	OFF	OFF	OFF DO from epiphyton respiration, sink
DOPOM	OFF	OFF	OFF DO from POM decay, sink
DODOM	OFF	OFF	OFF DO from DOM decay, sink
DOOM	OFF	OFF	OFF DO from OM decay, sink
DONITR	OFF	OFF	OFF DO from nitrification, sink
DOCBOD	OFF	OFF	OFF DO from CBOD decay, sink
DOREAR	OFF	OFF	OFF DO from reaeration, source
DOSED	OFF	OFF	OFF DO from sediment compartment decay, sink
DOSOD	OFF	OFF	OFF DO from 0-order sediment compartment, sink
TICAG	OFF	OFF	OFF Total inorganic carbon from algal growth, sink
TICEG	OFF	OFF	OFF Total inorganic carbon from epiphyton growth, sink
SEDDK	OFF	OFF	OFF Sediment compartment decay, sink
SEDAS	OFF	OFF	OFF Sediment compartment from algal settling, source
SEDLPOM	OFF	OFF	OFF Sediment compartment from LPOM settling, source
SEDSET	OFF	OFF	OFF Sediment compartment from net settling, source/sink
SODDK	OFF	OFF	OFF Sediment compartment from decay, sink

Related Cards and Files

[Constituent Computations](#)
[Active Constituents](#)

Constituent Initial Concentration (CST ICON)

FIELD	NAME	VALUE	DESCRIPTION
1			(Ignored by code)
2-10	C2IWB	Real	Initializes entire grid to this concentration, or specifies a vertical and/or longitudinal profile be used to initialize grid, $g\ m^{-3}$

This card allows the user to specify an initial concentration for each constituent. The user has three options. Initial concentrations can be specified as a single value, a single vertical profile which is used to initialize every segment, or a vertical profile for each segment.

Initial condition	[IC2]
Isoconcentration	>or =0.0
Single vertical profile	-1.0
Vertical profile at each segment	-2.0

Example

CST ICON	C2IWB	C2IWB	C2IWB	C2IWB	C2IWB	C2IWB	C2IWB	C2IWB	C2IWB
TDS	200.0	200.0	200.0	Total dissolved solids or salinity					
TRACER	-2.0	1000.0	1000.0	Generic constituent 1 - conservative tracer					
AGE	0.0	0.0	0.0	Generic constituent 2 - residence time					
COL1	1.0	1.0	1.0	Generic constituent 3 - coliform group 1					
COL2	1.0	1.0	1.0	Generic constituent 4 - coliform group 1					
ISS1	5.0	5.0	5.0	Inorganic suspended solids group 1					
ISS2	3.5	3.5	3.5	Inorganic suspended solids group 2					
ISS3	4.5	4.5	4.5	Inorganic suspended solids group 3					
PO4	0.1	0.1	0.1	Dissolved inorganic phosphorus mg/l as P					
NH4	0.1	0.1	0.1	Ammonium mg/l as N					
NO3	0.1	0.1	0.1	Nitrate-nitrite mg/l as N					
DSI	5.0	5.0	5.0	Dissolved silica mg/l as Si					
PSI	1.0	1.0	1.0	Particulate biogenic silica mg/l as Si					
FE	1.0	1.0	1.0	Iron mg/l					
LDOM	1.0	1.0	1.0	Labile dissolved organic matter mg/l					
RDOM	1.0	1.0	1.0	Refractory dissolved organic matter mg/l					
LPOM	2.0	2.0	2.0	Labile particulate organic matter mg/l					
RPOM	1.0	1.0	1.0	Refractory particulate organic matter mg/l					
CBOD1	1.0	1.0	1.0	Carbonaceous biochemical oxygen demand group 1					
CBOD2	1.0	1.0	1.0	Carbonaceous biochemical oxygen demand group 2					
CBOD3	1.0	1.0	1.0	Carbonaceous biochemical oxygen demand group 3					
CBOD1-P	0.01	0.01	0.01	Carbonaceous BOD-P group 1					
CBOD2-P	0.01	0.01	0.01	Carbonaceous BOD-P group 2					
CBOD3-P	0.01	0.01	0.01	Carbonaceous BOD-P group 3					
CBOD1-N	0.01	0.01	0.01	Carbonaceous BOD-N group 1					
CBOD2-N	0.01	0.01	0.01	Carbonaceous BOD-N group 2					
CBOD3-N	0.01	0.01	0.01	Carbonaceous BOD-N group 3					
ALG1	1.0	1.0	1.0	Algal group 1 mg/l dry weight biomass					
ALG2	1.0	1.0	1.0	Algal group 2 mg/l dry weight biomass					
ALG3	1.0	1.0	1.0	Algal group 3 mg/l dry weight biomass					
DO	-1.0	8.0	7.0	Dissolved oxygen mg/l					
TIC	3.5	3.5	3.5	Total inorganic carbon mg/l as C					
ALK	80.0	50.0	30.0	Alkalinity mg/l as CaCO ₃					
ZOO1	0.1000	0.10	0.10	Zooplankton mg/l dry biomass					
LDOM_P	0.0005	0.005	0.005	Total P in labile dissolved organic matter					
RDOM_P	0.0005	0.005	0.005	Total P in refractory dissolved organic matter					
LPOM_P	0.0005	0.005	0.005	Total P in labile particulate organic matter					
RPOM_P	0.0005	0.005	0.005	Total P in refractory particulate organic matter					
LDOM_N	0.0080	0.080	0.080	Total N in labile dissolved organic matter					
RDOM_N	0.0080	0.080	0.080	Total N in refractory dissolved organic matter					

CONTROL FILE

CONSTITUENT CONTROL

LPOM_N	0.0080	0.080	0.080	Total N in labile particulate organic matter
RPOM_N	0.0080	0.080	0.080	Total N in refractory particulate organic matter

Related Cards and Files

[Constituent Computations](#)

[Active Constituents](#)

[Vertical Profile File](#)

[Longitudinal Profile File](#)

Constituent Output (CST PRINT)

FIELD	NAME	VALUE	DEFAULT	DESCRIPTION
1				(Ignored by code)
2-10	CPRWBC	Character	OFF	Specifies which constituents are printed to output files, ON or OFF

This card specifies which constituents are printed to all the output files for water quality such as the [snapshot file](#) [[SNPFN](#)], [time series file](#) [[TSRFN](#)], [profile plot file](#) [[PRFFN](#)], spreadsheet plot file, withdrawal output, and [contour plot file](#) [[CPLFN](#)]. The user does not have control over which constituents will be sent to an individual file.

Example

CST PRINT	CPRWBC	CPRWBC	CPRWBC	CPRWBC	CPRWBC	CPRWBC	CPRWBC	CPRWBC	CPRWBC
TDS	ON	ON	ON	ON	ON	ON	ON	ON	ON
TRACER	ON	ON	ON	ON	ON	ON	ON	ON	ON
AGE	ON	ON	ON	ON	ON	ON	ON	ON	ON
COL1	ON	ON	ON	ON	ON	ON	ON	ON	ON
COL2	ON	ON	ON	ON	ON	ON	ON	ON	ON
ISS1	ON	ON	ON	ON	ON	ON	ON	ON	ON
ISS2	ON	ON	ON	ON	ON	ON	ON	ON	ON
ISS3	ON	ON	ON	ON	ON	ON	ON	ON	ON
PO4	ON	ON	ON	ON	ON	ON	ON	ON	ON
NH4	ON	ON	ON	ON	ON	ON	ON	ON	ON
NO3	ON	ON	ON	ON	ON	ON	ON	ON	ON
DSI	ON	ON	ON	ON	ON	ON	ON	ON	ON
PSI	ON	ON	ON	ON	ON	ON	ON	ON	ON
FEe	ON	ON	ON	ON	ON	ON	ON	ON	ON
LDOM	ON	ON	ON	ON	ON	ON	ON	ON	ON
RDOM	ON	ON	ON	ON	ON	ON	ON	ON	ON
LPOM	ON	ON	ON	ON	ON	ON	ON	ON	ON
RPOM	ON	ON	ON	ON	ON	ON	ON	ON	ON
CBOD1	ON	ON	ON	ON	ON	ON	ON	ON	ON
CBOD2	ON	ON	ON	ON	ON	ON	ON	ON	ON
CBOD3	ON	ON	ON	ON	ON	ON	ON	ON	ON
CBOD1-P	ON	ON	ON	ON	ON	ON	ON	ON	ON
CBOD2-P	ON	ON	ON	ON	ON	ON	ON	ON	ON
CBOD3-P	ON	ON	ON	ON	ON	ON	ON	ON	ON
CBOD1-N	ON	ON	ON	ON	ON	ON	ON	ON	ON
CBOD2-N	ON	ON	ON	ON	ON	ON	ON	ON	ON
CBOD3-N	ON	ON	ON	ON	ON	ON	ON	ON	ON
ALG1	ON	ON	ON	ON	ON	ON	ON	ON	ON
ALG2	ON	ON	ON	ON	ON	ON	ON	ON	ON
ALG3	ON	ON	ON	ON	ON	ON	ON	ON	ON
DO	ON	ON	ON	ON	ON	ON	ON	ON	ON
TIC	ON	ON	ON	ON	ON	ON	ON	ON	ON
ALK	ON	ON	ON	ON	ON	ON	ON	ON	ON
ZOO1	ON	ON	ON	ON	ON	ON	ON	ON	ON
LDOM_P	ON	ON	ON	ON	ON	ON	ON	ON	ON
RDOM_P	ON	ON	ON	ON	ON	ON	ON	ON	ON
LPOM_P	ON	ON	ON	ON	ON	ON	ON	ON	ON
RPOM_P	ON	ON	ON	ON	ON	ON	ON	ON	ON
LDOM_N	ON	ON	ON	ON	ON	ON	ON	ON	ON
RDOM_N	ON	ON	ON	ON	ON	ON	ON	ON	ON
LPOM_N	ON	ON	ON	ON	ON	ON	ON	ON	ON
RPOM_N	ON	ON	ON	ON	ON	ON	ON	ON	ON

CONTROL FILE

CONSTITUENT CONTROL

Related Cards and Files

[Snapshot Print](#)

[Profile Plot](#)

[Time Series Plot](#)

[Spreadsheet Plot](#)

[Contour Plot](#)

Inflow Active Constituent Control (CIN CON)

FIELD	NAME	VALUE	DEFAULT	DESCRIPTION
1				(Ignored by code)
2-10	CINBRC	Character	OFF	Specifies which constituents are included in inflow constituent file, ON or OFF

For some applications, inflow concentrations for a particular constituent may not be available. This card allows the user to include in the [inflow concentration file \[CINFN\]](#) only those constituents for which there is a concentration. For those excluded, the model uses a zero concentration for the inflow. As shown in the example, descriptions can be included after the input fields to aid in identifying a given constituent.

Example

CIN CON	CINBRC	CINBRC	CINBRC	CINBRC	CINBRC	CINBRC	CINBRC	CINBRC	CINBRC
TDS	ON	ON	ON	ON	ON	Total dissolved solids or salinity			
TRACER	ON	ON	ON	ON	ON	Generic constituent 1 - tracer			
AGE	OFF	OFF	OFF	OFF	OFF	Generic constituent 2 - residence time			
COL1	ON	ON	ON	ON	ON	Generic constituent 3 - coliform group 1			
COL2	ON	ON	ON	ON	ON	Generic constituent 4 - coliform group 2			
ISS1	ON	ON	ON	ON	ON	Inorganic suspended solids group 1			
ISS2	ON	ON	ON	ON	ON	Inorganic suspended solids group 2			
ISS3	ON	ON	ON	ON	ON	Inorganic suspended solids group 3			
PO4	ON	ON	ON	ON	ON	Inorganic dissolved phosphorus			
NH4	ON	ON	ON	ON	ON	Ammonium			
NO3	ON	ON	ON	ON	ON	Nitrate-nitrite			
DSI	ON	ON	ON	ON	ON	Dissolved silica			
PSI	ON	ON	ON	ON	ON	Particulate biogenic silica			
FE	ON	ON	ON	ON	ON	Iron			
LDOM	ON	ON	ON	ON	ON	Labile dissolved organic matter			
RDOM	ON	ON	ON	ON	ON	Refractory dissolved organic matter			
LPOM	ON	ON	ON	ON	ON	Labile particulate organic matter			
RPOM	ON	ON	ON	ON	ON	Refractory particulate organic matter			
CBOD1	ON	ON	ON	ON	ON	Carbonaceous BOD group 1			
CBOD2	ON	ON	ON	ON	ON	Carbonaceous BOD group 2			
CBOD3	ON	ON	ON	ON	ON	Carbonaceous BOD group 3			
CBOD1-P	ON	ON	ON	ON	ON	Carbonaceous BOD-P group 1			
CBOD2-P	ON	ON	ON	ON	ON	Carbonaceous BOD-P group 2			
CBOD3-P	ON	ON	ON	ON	ON	Carbonaceous BOD-P group 3			
CBOD1-N	ON	ON	ON	ON	ON	Carbonaceous BOD-N group 1			
CBOD2-N	ON	ON	ON	ON	ON	Carbonaceous BOD-N group 2			
CBOD3-N	ON	ON	ON	ON	ON	Carbonaceous BOD-N group 3			
ALG1	ON	ON	ON	ON	ON	Algal group 1			
ALG2	ON	ON	ON	ON	ON	Algal group 2			
ALG3	ON	ON	ON	ON	ON	Algal group 3			
DO	ON	ON	ON	ON	ON	Dissolved oxygen			
TIC	ON	ON	ON	ON	ON	Total inorganic carbon mg/l as C			
ALK	ON	ON	ON	ON	ON	Alkalinity mg/l as CaCO3			
ZOO1	ON	ON	ON	ON	ON	Zooplankton			
LDOM_P	ON	ON	ON	ON	ON	Total P in labile dissolved organic matter			
RDOM_P	ON	ON	ON	ON	ON	Total P in refractory dissolved organic matter			
LPOM_P	ON	ON	ON	ON	ON	Total P in labile particulate organic matter			
RPOM_P	ON	ON	ON	ON	ON	Total P in refractory particulate org matter			
LDOM_N	ON	ON	ON	ON	ON	Total N in labile dissolved organic matter			
RDOM_N	ON	ON	ON	ON	ON	Total N in refractory dissolved organic matter			
LPOM_N	ON	ON	ON	ON	ON	Total N in labile particulate organic matter			
RPOM_N	ON	ON	ON	ON	ON	Total N in refractory particulate org matter			

CONTROL FILE

CONSTITUENT CONTROL

Related Cards and Files

[Branch Inflow Constituent File](#)
[Branch Inflow Constituent Filename](#)

Tributary Active Constituent Control (CTR CON)

FIELD	NAME	VALUE	DEFAULT	DESCRIPTION
1				(Ignored by code)
2-10	CTRTRC	Character	OFF	Specifies which constituents are included in tributary inflow constituent file for each tributary, ON or OFF

For some applications, tributary inflow concentrations for a particular constituent may not be available. This card allows the user to include in the [tributary inflow concentration file](#) [CTR FN] only those constituents for which there is a concentration.

Example

CTR CON	CTRTRC	CTRTRC	CTRTRC	CTRTRC	CTRTRC	CTRTRC	CTRTRC	CTRTRC	CTRTRC
TDS	ON	Total dissolved solids or salinity							
TRACER	ON	Generic constituent 1 - tracer							
AGE	OFF	Generic constituent 2 - residence time							
COL1	ON	Generic constituent 3 - coliform group 1							
COL2	ON	Generic constituent 4 - coliform group 2							
ISS1	ON	Inorganic suspended solids group 1							
ISS2	ON	Inorganic suspended solids group 2							
ISS3	ON	Inorganic suspended solids group 3							
PO4	ON	Inorganic dissolved phosphorus							
NH4	ON	Ammonium							
NO3	ON	Nitrate-nitrite							
DSI	ON	Dissolved silica							
PSI	ON	Particulate biogenic silica							
FE	ON	Iron							
LDOM	ON	Labile dissolved organic matter							
RDOM	ON	Refractory dissolved organic matter							
LPOM	ON	Labile particulate organic matter							
RPOM	ON	Refractory particulate organic matter							
CBOD1	ON	Carbonaceous BOD group 1							
CBOD2	ON	Carbonaceous BOD group 2							
CBOD3	ON	Carbonaceous BOD group 3							
CBOD1-P	ON	Carbonaceous BOD-P group 1							
CBOD2-P	ON	Carbonaceous BOD-P group 2							
CBOD3-P	ON	Carbonaceous BOD-P group 3							
CBOD1-N	ON	Carbonaceous BOD-N group 1							
CBOD2-N	ON	Carbonaceous BOD-N group 2							
CBOD3-N	ON	Carbonaceous BOD-N group 3							
ALG1	ON	Algal group 1							
ALG2	ON	Algal group 2							
ALG3	ON	Algal group 3							
DO	ON	Dissolved oxygen							
TIC	ON	Total inorganic carbon mg/l as C							
ALK	ON	Alkalinity mg/l as CaCO3							
ZOO1	ON	Zooplankton							
LDOM_P	ON	Total P in labile dissolved organic matter							
RDOM_P	ON	Total P in refractory dissolved organic matter							
LPOM_P	ON	Total P in labile particulate organic matter							
RPOM_P	ON	Total P in refractory particulate organic matter							
LDOM_N	ON	Total N in labile dissolved organic matter							
RDOM_N	ON	Total N in refractory dissolved organic matter							
LPOM_N	ON	Total N in labile particulate organic matter							
RPOM_N	ON	Total N in refractory particulate organic matter							

CONTROL FILE

CONSTITUENT CONTROL

Related Cards and Files

[Tributary Inflow Concentration File](#)
[Tributary Inflow Concentration Filename](#)

Distributed Trib Active Constituent (CDT CON)

FIELD	NAME	VALUE	DEFAULT	DESCRIPTION
1				(Ignored by code)
2-10	CDTBRC	Character	OFF	Specifies which constituents are included in distributed tributary inflow constituent file for each branch, ON or OFF

For some applications, distributed tributary inflow concentrations for a particular constituent may not be available. This card allows the user to include in the [distributed tributary inflow concentration file](#) [[CDTFN](#)] only those constituents for which there is a concentration.

Example

CDT CON	CDTBRC	CDTBRC	CDTBRC	CDTBRC	CDTBRC	CDTBRC	CDTBRC	CDTBRC	CDTBRC
TDS	OFF	OFF	OFF	OFF	OFF	Total dissolved solids or salinity			
TRACER	OFF	OFF	OFF	OFF	OFF	Generic constituent 1 - tracer			
AGE	OFF	OFF	OFF	OFF	OFF	Generic constituent 2 - residence time			
COL1	OFF	OFF	OFF	OFF	OFF	Generic constituent 3 - coliform group 1			
COL2	OFF	OFF	OFF	OFF	OFF	Generic constituent 4 - coliform group 2			
ISS1	OFF	OFF	OFF	OFF	OFF	Inorganic suspended solids group 1			
ISS2	OFF	OFF	OFF	OFF	OFF	Inorganic suspended solids group 2			
ISS3	OFF	OFF	OFF	OFF	OFF	Inorganic suspended solids group 3			
PO4	OFF	OFF	OFF	OFF	OFF	Inorganic dissolved phosphorus			
NH4	OFF	OFF	OFF	OFF	OFF	Ammonium			
NO3	OFF	OFF	OFF	OFF	OFF	Nitrate-nitrite			
DSI	OFF	OFF	OFF	OFF	OFF	Dissolved silica			
PSI	OFF	OFF	OFF	OFF	OFF	Particulate biogenic silica			
FE	OFF	OFF	OFF	OFF	OFF	Iron			
LDOM	OFF	OFF	OFF	OFF	OFF	Labile dissolved organic matter			
RDOM	OFF	OFF	OFF	OFF	OFF	Refractory dissolved organic matter			
LPOM	OFF	OFF	OFF	OFF	OFF	Labile particulate organic matter			
RPOM	OFF	OFF	OFF	OFF	OFF	Refractory particulate organic matter			
CBOD1	OFF	OFF	OFF	OFF	OFF	Carbonaceous BOD group 1			
CBOD2	OFF	OFF	OFF	OFF	OFF	Carbonaceous BOD group 2			
CBOD3	OFF	OFF	OFF	OFF	OFF	Carbonaceous BOD group 3			
CBOD1-P	OFF	OFF	OFF	OFF	OFF	Carbonaceous BOD-P group 1			
CBOD2-P	OFF	OFF	OFF	OFF	OFF	Carbonaceous BOD-P group 2			
CBOD3-P	OFF	OFF	OFF	OFF	OFF	Carbonaceous BOD-P group 3			
CBOD1-N	OFF	OFF	OFF	OFF	OFF	Carbonaceous BOD-N group 1			
CBOD2-N	OFF	OFF	OFF	OFF	OFF	Carbonaceous BOD-N group 2			
CBOD3-N	OFF	OFF	OFF	OFF	OFF	Carbonaceous BOD-N group 3			
ALG1	OFF	OFF	OFF	OFF	OFF	Algal group 1			
ALG2	OFF	OFF	OFF	OFF	OFF	Algal group 2			
ALG3	OFF	OFF	OFF	OFF	OFF	Algal group 3			
DO	OFF	OFF	OFF	OFF	OFF	Dissolved oxygen			
TIC	OFF	OFF	OFF	OFF	OFF	Total inorganic carbon mg/l as C			
ALK	OFF	OFF	OFF	OFF	OFF	Alkalinity mg/l as CaCO3			
ZOO1	OFF	OFF	OFF	OFF	OFF	Zooplankton			
LDOM_P	OFF	OFF	OFF	OFF	OFF	Total P in labile dissolved organic matter			
RDOM_P	OFF	OFF	OFF	OFF	OFF	Total P in refractory dissolved organic matter			
LPOM_P	OFF	OFF	OFF	OFF	OFF	Total P in labile particulate organic matter			
RPOM_P	OFF	OFF	OFF	OFF	OFF	Total P in refractory particulate org matter			
LDOM_N	OFF	OFF	OFF	OFF	OFF	Total N in labile dissolved organic matter			
RDOM_N	OFF	OFF	OFF	OFF	OFF	Total N in refractory dissolved organic matter			
LPOM_N	OFF	OFF	OFF	OFF	OFF	Total N in labile particulate organic matter			
RPOM_N	OFF	OFF	OFF	OFF	OFF	Total N in refractory particulate org matter			

CONTROL FILE

CONSTITUENT CONTROL

Related Cards and Files

[Distributed Tributary Inflow Concentration File](#)
[Distributed Tributary Inflow Concentration Filename](#)

Precipitation Active Constituent Control (CPR CON)

FIELD	NAME	VALUE	DEFAULT	DESCRIPTION
1				(Ignored by code)
2-10	CPRBRC	Character	OFF	Specifies which constituents are included in the precipitation inflow constituent file for each branch, ON or OFF

For some applications, precipitation concentrations for a particular constituent may not be available. This card allows the user to include in the [precipitation concentration file](#) [CPRFN] only those constituents for which there is a concentration.

Example

CPR CON	CPRBRC	CPRBRC	CPRBRC	CPRBRC	CPRBRC	CPRBRC	CPRBRC	CPRBRC	CPRBRC
TDS	OFF	OFF	OFF	OFF	OFF	Total dissolved solids or salinity			
TRACER	OFF	OFF	OFF	OFF	OFF	Generic constituent 1 - tracer			
AGE	OFF	OFF	OFF	OFF	OFF	Generic constituent 2 - residence time			
COL1	OFF	OFF	OFF	OFF	OFF	Generic constituent 3 - coliform group 1			
COL2	OFF	OFF	OFF	OFF	OFF	Generic constituent 4 - coliform group 2			
ISS1	OFF	OFF	OFF	OFF	OFF	Inorganic suspended solids group 1			
ISS2	OFF	OFF	OFF	OFF	OFF	Inorganic suspended solids group 2			
ISS3	OFF	OFF	OFF	OFF	OFF	Inorganic suspended solids group 3			
PO4	OFF	OFF	OFF	OFF	OFF	Inorganic dissolved phosphorus			
NH4	OFF	OFF	OFF	OFF	OFF	Ammonium			
NO3	OFF	OFF	OFF	OFF	OFF	Nitrate-nitrite			
DSI	OFF	OFF	OFF	OFF	OFF	Dissolved silica			
PSI	OFF	OFF	OFF	OFF	OFF	Particulate biogenic silica			
FE	OFF	OFF	OFF	OFF	OFF	Iron			
LDOM	OFF	OFF	OFF	OFF	OFF	Labile dissolved organic matter			
RDOM	OFF	OFF	OFF	OFF	OFF	Refractory dissolved organic matter			
LPOM	OFF	OFF	OFF	OFF	OFF	Labile particulate organic matter			
RPOM	OFF	OFF	OFF	OFF	OFF	Refractory particulate organic matter			
CBOD1	OFF	OFF	OFF	OFF	OFF	Carbonaceous BOD group 1			
CBOD2	OFF	OFF	OFF	OFF	OFF	Carbonaceous BOD group 2			
CBOD3	OFF	OFF	OFF	OFF	OFF	Carbonaceous BOD group 3			
CBOD1-P	OFF	OFF	OFF	OFF	OFF	Carbonaceous BOD-P group 1			
CBOD2-P	OFF	OFF	OFF	OFF	OFF	Carbonaceous BOD-P group 2			
CBOD3-P	OFF	OFF	OFF	OFF	OFF	Carbonaceous BOD-P group 3			
CBOD1-N	OFF	OFF	OFF	OFF	OFF	Carbonaceous BOD-N group 1			
CBOD2-N	OFF	OFF	OFF	OFF	OFF	Carbonaceous BOD-N group 2			
CBOD3-N	OFF	OFF	OFF	OFF	OFF	Carbonaceous BOD-N group 3			
ALG1	OFF	OFF	OFF	OFF	OFF	Algal group 1			
ALG2	OFF	OFF	OFF	OFF	OFF	Algal group 2			
ALG3	OFF	OFF	OFF	OFF	OFF	Algal group 3			
DO	OFF	OFF	OFF	OFF	OFF	Dissolved oxygen			
TIC	OFF	OFF	OFF	OFF	OFF	Total inorganic carbon mg/l as C			
ALK	OFF	OFF	OFF	OFF	OFF	Alkalinity mg/l as CaCO3			
ZOO1	OFF	OFF	OFF	OFF	OFF	Zooplankton			
LDOM_P	OFF	OFF	OFF	OFF	OFF	Total P in labile dissolved organic matter			
RDOM_P	OFF	OFF	OFF	OFF	OFF	Total P in refractory dissolved organic matter			
LPOM_P	OFF	OFF	OFF	OFF	OFF	Total P in labile particulate organic matter			
RPOM_P	OFF	OFF	OFF	OFF	OFF	Total P in refractory particulate org matter			
LDOM_N	OFF	OFF	OFF	OFF	OFF	Total N in labile dissolved organic matter			
RDOM_N	OFF	OFF	OFF	OFF	OFF	Total N in refractory dissolved organic matter			
LPOM_N	OFF	OFF	OFF	OFF	OFF	Total N in labile particulate organic matter			
RPOM_N	OFF	OFF	OFF	OFF	OFF	Total N in refractory particulate org matter			

CONTROL FILE

CONSTITUENT CONTROL

Related Cards and Files

[Calculations](#)

[Precipitation Concentration File](#)

[Precipitation Concentration Filename](#)

Extinction Coefficient (EX COEF)

FIELD	NAME	VALUE	DEFAULT	DESCRIPTION
1				(Ignored by code)
2	EXH2O	Real	0.25 or 0.45	Extinction for pure water, m^{-1} [The 0.25 value is used when water quality constituents such as algae and suspended solids are 'ON' and the 0.45 value is used when only temperature is being simulated.]
3	EXSS	Real	0.1	ϵ_{ISS} : extinction due to inorganic suspended solids, $m^{-1}/(g/m^3)$
4	EXOM	Real	0.1	ϵ_{POM} : extinction due to organic suspended solids, $m^{-1}/(g/m^3)$
5	BETA	Real	0.45	Fraction of incident solar radiation absorbed at the water surface (longwave components of short-wave solar)
6	EXC	Character	OFF	Read extinction coefficients, ON or OFF
7	EXIC	Character	OFF	Interpolate extinction coefficients, ON or OFF

This card specifies the short wave solar radiation extinction coefficients and amount of solar radiation, β , absorbed in the surface layer. Extinction coefficients are used to calculate a net extinction coefficient, λ , which is determined from the following equation:

$$\lambda = \lambda_{H2O} + \lambda_{ISS} + \lambda_{POM} + \lambda_a + \lambda_{macro} + \lambda_{zoo}$$

where:

$$\lambda_{ISS} = \epsilon_{ISS} \sum_{\#ISS} \Phi_{ISS}$$

ϵ_{ISS} = extinction parameter for inorganic suspended solids, $m^{-1}/(g\ m^{-3})$ - user supplied parameter

Φ_{ISS} = inorganic suspended solids concentration for each size fraction (up to 9)

$$\lambda_{POM} = \epsilon_{POM} \sum \Phi_{POM}$$

ϵ_{POM} = extinction parameter for particulate organic matter, $m^{-1}/(g\ m^{-3})$ - user supplied parameter

Φ_{POM} = particulate organic matter concentration = particulate labile + particulate refractory organic matter concentration

$$\lambda_a = \sum \epsilon_a \Phi_a \text{ algae extinction, } m^{-1}$$

$$\lambda_{zoo} = \sum \epsilon_{zoo} \Phi_{zoo} \text{ zooplankton extinction, } m^{-1}$$

$$\lambda_{macro} = \sum \epsilon_{macro} \Phi_{macro} \text{ macrophyte extinction, } m^{-1}$$

ϵ_a = extinction coefficient for each algal group, $m^{-1}/(g\ m^{-3})$ - user supplied parameter

Φ_a = algal concentration for each algal group, $g\ m^{-3}$

ϵ_{zoo} = extinction coefficient for each zooplankton group, $m^{-1}/(g\ m^{-3})$ - user supplied parameter

Φ_{zoo} = zooplankton concentration for each zooplankton group, $g\ m^{-3}$

ϵ_{macro} = extinction coefficient for each macrophyte group, $m^{-1}/(g\ m^{-3})$ - user supplied parameter

Φ_{macro} = macrophyte concentration for each macrophyte group, $g\ m^{-3}$

λ_{H_2O} = extinction coefficient for water (for a wavelength of between 0.5 and 0.6 μm , the absorption coefficient for *pure water* is about 0.1 m^{-1}).

λ_{H_2O} varies greatly depending upon the dissolved substances in the water. [Table C-31](#) gives values reported in the literature that can be used as rudimentary guidelines for selecting a value of λ_{H_2O} .

Table C-31. Extinction Coefficient Literature Values

Location	Description	λ , m^{-1}	Reference
Lake Tahoe, CA	Oligotrophic	0.2	Wetzel, 1975
Crystal Lake, WI	Oligotrophic	0.2	Wetzel, 1975
Crater Lake, OR	Oligotrophic	0.18	Spence, 1981
Lake Borralie, Scotland	Calcareous water	0.34	Spence, 1981
Wintergreen Lake, MI	Eutrophic	0.46-1.68	Wetzel, 1975
Lake Paajarvi, Finland	Brown-stained	0.7	Verduin, 1982
Loch Unagan, Scotland	Brown-stained	1.53	Spence, 1981
Loch Leven, Scotland	Turbid, eutrophic	2.58	Spence, 1981
Neusiedlersee, Austria	Turbid	3.31	Spence, 1981
Highly stained lakes	Average	4.0	Wetzel, 1975

Megard et al. (1980) and Smith and Baker (1978) determined each gram per cubic meter of chlorophyll increased ϵ_{POM} by 22 and 16 m^{-1} , respectively. Averaging the two values and assuming a carbon to algal biomass ratio of 0.45 and a carbon to chlorophyll ratio of 50, then each gram per cubic meter of algal biomass should increase ϵ_{POM} by about 0.17 m^{-1} . However, the carbon to chlorophyll ratios vary from 25 to 150. Values for ϵ_{ISS} should be of the same order of magnitude as ϵ_{POM} .

If any constituents included in the above equation are not included in the simulation, then the value for λ_{H_2O} should be increased to account for the constituent left out.

In some cases Secchi disk data are available. There are different expressions for converting Secchi disk depth, z_{Secchi} in m, to a light extinction coefficient in m^{-1} , some of these include

$$\lambda = \frac{\alpha}{z_{\text{Secchi}}} \text{ (Chapra, 1997) where } \alpha \text{ varies from 1.4 to 1.9 (typical value of 1.7)}$$

$$\lambda = \frac{1.11}{z_{\text{Secchi}}^{0.73}} \text{ (Williams et al., 1980) for lakes and reservoirs in the Ohio River basin the 1970's}$$

$$\lambda = \frac{1.36}{z_{\text{Secchi}}^{0.86}} \text{ (Armenglo et al., 2003) for Sau Reservoir, Spain between 1995 and 2001}$$

$$\log \lambda = -0.96 \log(z_{\text{Secchi}}) + 0.30 \text{ (Caffrey et. al. 2006) for 32 Florida, USA lakes}$$

where:

$$\lambda = \text{net extinction coefficient, } \text{m}^{-1}$$

Caution should be used in transferring these results to reservoirs and lakes in other drainage basins.

The above equations converting Secchi disk depth to light extinction include the effects of ϵ_{ISS} and ϵ_{OSS} and should be used only when inorganic and organic suspended solids are not included in the simulation.

The fraction of incident solar radiation absorbed at the water surface, β , represents solar radiation absorbed in the surface layer. A study of 29 lakes and reservoirs in the Ohio River basin (USA) showed the following relationship between light extinction, λ in m^{-1} , and β (Williams et. al. 1980):

$$\beta = 0.265 \ln(\lambda) + 0.614$$

$$R^2 = 0.69 \text{ Standard error (SE)} = 0.0992$$

Again caution should be used in using a relationship developed for a different waterbody than your application. A typical value for [BETA] is 0.45, implying that 45% of the incident radiation is absorbed in the upper layer of the water body, assumed to be the surface layer of the model. This represents the long wave components of the solar spectrum which are readily absorbed.

Table C-32 shows values of BETA for a variety of systems. Note that in most cases these values assume that the water depth is between 0.5 to 2 m for the surface layer. The concept of using BETA in a shallow river system is not straightforward since the basic theory that we have a constant value of light extinction below the surface layer is probably not correct. The light extinction coefficient in a shallow system is constantly changing as a function of depth and light wavelength.

Table C-32. Values of BETA (TVA, 1972).

Location	β
Pure water	0.63
Clear oceanic water	0.64
Average oceanic water	0.68
Average coastal water	0.69
Turbid coastal water	0.69
Lake Mendota	0.58
Trout Lake	0.50
Big Ridge Lake, TVA	0.24
Fontana Lake, TVA	0.24

The model user can input a file of extinction coefficients as a function of time for each water body if [EXC] is ON. Interpolation of this input file is performed when [EXIC] is ON. The extinction coefficients can be derived from secchi disk or light photometer data. The input file is specified under the Extinction Coefficient file name. When the extinction coefficient is read in, all other calculations of light extinction are ignored.

Example

EX COEF	EXH2O	EXSS	EXOM	BETA	EXC	EXIC
WB 1	0.25	0.01	0.01	0.45	OFF	OFF
WB 2	0.25	0.01	0.01	0.45	OFF	OFF
WB 3	0.25	0.01	0.01	0.45	OFF	OFF

Related Cards and Files

[Algal Extinction](#)
[Light Extinction File](#)
[Light Extinction Filename](#)

Algal Extinction (ALG EX)

FIELD	NAME	VALUE	DEFAULT	DESCRIPTION
1				(Ignored by code)
2-10	EXA	Real	0.2	ε_a :algal light extinction, m^{-1}/gm^{-3}

This card specifies the effect of algae on short wave solar radiation extinction in the water column. See the [Extinction Coefficient](#) card for a more complete description.

Example

ALG EX	EXA	EXA	EXA	EXA	EXA	EXA	EXA	EXA	EXA
	0.2	0.2	0.2						

Related Cards and Files

[Extinction Coefficient](#)

Zooplankton Extinction (ZOO EX)

FIELD	NAME	VALUE	DEFAULT	DESCRIPTION
1				(Ignored by code)
2-10	EXZ	Real	0.2	ε_{zoo} :zooplankton light extinction, m^{-1}/gm^{-3}

This card specifies the effect of algae on short wave solar radiation extinction in the water column. See the [Extinction Coefficient](#) card for a more complete description.

Example

ZOO EX	EXZ	EXZ	EXZ	EXZ	EXZ	EXZ
	0.2	0.2	0.2			

Related Cards and Files

[Extinction Coefficient](#)

Macrophyte Extinction (MAC EX)

FIELD	NAME	VALUE	DEFAULT	DESCRIPTION
1				(Ignored by code)
2-10	EXM	Real	0.01	$\varepsilon_{\text{macro}}$: macrophyte light extinction, m^{-1}/gm^{-3}

This card specifies the effect of macrophytes on short wave solar radiation extinction in the water column. See the [Extinction Coefficient](#) card for a more complete description.

Berger (2000) compiled the following literature values of light extinction for macrophytes in the following table.

Table 33. Literature values for light extinction due to macrophyte plant tissue concentration.

Species	Light extinction due to macrophyte concentration, $m^3m^{-1}g^{-1}$	Reference
<i>Myriophyllum spicatum</i> L.	0.01	Ikusima, 1970
<i>Myriophyllum spicatum</i> L.	0.006	Titus and Adams, 1979
<i>Vallisneria americana</i> Michx.	0.013 to 0.019	Titus and Adams, 1979
<i>Potamogeton pectinatus</i>	0.024	Van der Bijl et al., 1989

Example

```
MACRO EX      EXM      EXM      EXM      EXM      EXM      EXM
          0.0100
```

Related Cards and Files

[Extinction Coefficient](#)

Generic Constituent (GENERIC)

FIELD	NAME	VALUE	DEFAULT	DESCRIPTION
1				(Ignored by code)
2	CGQ10	Real		Arrhenius temperature rate multiplier
3	CG0DK	Real		0-order decay rate, <i>with mass concentration</i> <i>units: gm³day⁻¹</i>
4	CG1DK	Real		1st -order decay rate, <i>day⁻¹</i>
5	CGS	Real		Settling rate, <i>m day⁻¹</i>

This card specifies the Arrhenius temperature rate multiplier, 0-order decay rate, 1st-order decay rate, and settling rate for a generic constituent. The ability to model any number of generic constituents whose kinetics can be described by these parameters has been a part of CE-QUAL-W2 since Version 3.1. These constituents can include tracers, residence time or water age, coliform bacteria, etc. For a tracer, all of the kinetic parameters should be set to zero. For residence time, the 0-order decay rate should be set to -1.0. In this case the units of [CG0DK] are [day/day] rather than [g/m³/day]. Since this is a decay rate, setting it to -1.0 specifies a growth rate of 1 day⁻¹.

Unlike other state variables, the generic constituent uses an Arrhenius temperature rate multiplier (or Q_{10}) formulation to modify the generic constituent decay rate (for both zero order and first order rates) as a function of temperature: $k_T = k_{20}\theta^{T-20}$, where $\theta = \text{CGQ10}$ and k_{20} is the decay rate (either CG0DK or CG1DK) at 20°C.

This decay as a function of temperature is what is most likely to be encountered in the literature, particularly for coliform bacteria. Care must be taken when using this formulation at low (< 6°C) temperatures. For coliform bacteria, the Q_{10} coefficient (CGQ10) is usually 1.04. A range of values for coliform can be found in Zison et al. (1978).

Coliform decay rate is a function of sedimentation, solar radiation, nutrient availability, predation, algae, bacterial toxins, and physicochemical factors. For studies in which bacterial contamination is of important concern, efforts should be made to obtain *in situ* decay rate measurements. Methods for obtaining decay rates can be found in Frost and Streeter (1924), Marais (1974), and Zison et al. (1978). [Table C-34](#) gives reported literature values for coliform decay rates.

Table C-34. *In Situ* Coliform Decay Rates

Location	Season/ Temperature	Rate, day ⁻¹	Reference
Ohio River	Summer, 20°C	1.18	Frost and Streeter, 1924
Ohio River	Winter, 5°C	1.08	Frost and Streeter, 1924
Upper Illinois River	June-September	2.04	Hoskins, et al, 1927
Upper Illinois River	October-May	2.52, 0.89	Hoskins, et al, 1927
Upper Illinois River	December-March	0.57, 0.62	Hoskins, et al, 1927
Upper Illinois River	April-November	1.03, 0.70	Hoskins, et al, 1927
Missouri River	Winter	0.48	Kittrell and Furfari, 1963
Tennessee River	Summer	1.03, 1.32	Kittrell and Furfari, 1963
Tennessee River	Summer	1.32	Kittrell and Furfari, 1963
Sacramento River	Summer	1.75	Kittrell and Furfari, 1963
Cumberland River	Summer	5.52	Kittrell and Furfari, 1963
Leaf River, MS		0.41	Mahloch, 1974
Wastewater lagoon	7.0-25.5°C	0.20-0.70	Klock, 1971
Maturation ponds	19°C	1.68	Marais, 1974

CONTROL FILE

KINETIC COEFFICIENTS

Location	Season/ Temperature	Rate, day^{-1}	Reference
Oxidation ponds	20 °C	2.59	Marais, 1974

Example

GENERIC	CGQ10	CG0DK	CG1DK	CGS
CG 1	0.00	0.0	0.0	0.0
CG 2	0.00	-1.0	0.0	0.0
CG 3	1.04	0.0	0.2	1.0

Suspended Solids (S SOLIDS)

FIELD	NAME	VALUE	DEFAULT	DESCRIPTION
1				(Ignored by code)
2-10	SSS	Real	1.0	Suspended solids settling rate, $m\ day^{-1}$
3	SEDRC	Real	OFF	Turns ON or OFF sediment resuspension
4	TAUCR	Real	1.0	Critical shear stress for sediment resuspension, $dynes/cm^2$

This card specifies the suspended solids settling rates for each inorganic suspended solids state variable specified in the [Constituent Dimensions](#) card. Currently, phosphorus partitioning as specified on the [Inorganic Phosphorus](#) card is the same for all inorganic suspended solids. New to V3.2 is the ability to resuspend inorganic suspended solids due to wind shear and the resulting wind waves that cause sediment resuspension (Chapra, 1997). The computations are included by turning [[SEDRC](#)] to ON. The critical shear stress is specified by [[TAUCR](#)]. Details of this computation for resuspension are found in Appendix A.

Example

S SOLIDS	SSS	SEDRC	TAUCR
SSS 1	1.5	ON	1.500
SSS 2	0.5	ON	1.000

Algal Rates (ALGAL RATE)

FIELD	NAME	VALUE	DEFAULT	DESCRIPTION
1				(Ignored by code)
2	AG	Real	2.0	Maximum algal growth rate, day^{-1}
3	AR	Real	0.04	Maximum algal respiration rate, day^{-1}
4	AE	Real	0.04	Maximum algal excretion rate, day^{-1}
5	AM	Real	0.1	Maximum algal mortality rate, day^{-1}
6	AS	Real	0.1	Algal settling rate, $m \text{ day}^{-1}$
7	AHSP	Real	0.003	Algal half-saturation for phosphorus limited growth, $g \text{ m}^{-3}$
8	AHSN	Real	0.014	Algal half-saturation for nitrogen limited growth, $g \text{ m}^{-3}$
9	AHSSI	Real	0.0	Algal half-saturation for silica limited growth, $g \text{ m}^{-3}$
10	ASAT	Real	100.0	Light saturation intensity at maximum photosynthetic rate, $W \text{ m}^{-2}$

This card specifies rates for algal growth, mortality, excretion, respiration, and settling. Additionally, values that affect the maximum algal growth rate including light and nutrient limited growth are also specified here.

[AG] is the maximum gross production rate that is not corrected for respiration, mortality, excretion, or sinking. Most literature values report net production rates that take into account respiration so care must be taken when using reported literature values. The user must evaluate the experimental design to determine if reported values represent gross or net production rates. Also, [AG] is temperature dependent. If the expected temperature in the photic zone is 25 °C, then the user should select rates measured near this temperature. The default value of 2 day^{-1} has given excellent results on previous studies.

Table C-35. Gross Production Rates of Phytoplankton.

Species	[AG], day^{-1}	Temperature, °C	Reference
<i>Diatoms</i>			
<i>Asterionella formosa</i>	0.81	20	Holm and Armstrong, 1981
<i>Asterionella Formosa</i>	0.69	10	Hutchinson, 1957
<i>Asterionella Formosa</i>	1.38	20	Hutchinson, 1957
<i>Asterionella Formosa</i>	1.66	25	Hutchinson, 1957
<i>Asterionella Formosa</i>	1.71	20	Fogg, 1969
<i>Asterionella Formosa</i>	0.28	4	Talling 1955
<i>Asterionella Formosa</i>	0.69	10	Talling 1955
<i>Asterionella Formosa</i>	1.38	20	Talling 1955
<i>Asterionella Formosa</i>	2.2	20	Hoogenhout and Ames, 1965
<i>Asterionella formosa</i>	1.9	18.5	Hoogenhout and Ames, 1965
<i>Asterionella japonica</i>	1.19	22	Fogg, 1969
<i>Asterionella japonica</i>	1.3	18	Hoogenhout and Ames, 1965
<i>Asterionella japonica</i>	1.7	25	Hoogenhout and Ames, 1965
<i>Biddulphia</i> sp.	1.5	11	Castenholz, 1964
<i>Coscinodiscus</i> sp.	0.55	18	Fogg, 1969
<i>Cyclotella meneghiniana</i>	0.34	16	Hoogenhout and Ames, 1965
<i>Cyclotella nana</i>	3.4	20	Hoogenhout and Ames, 1965
<i>Detonula confervacea</i>	0.62	2	Smayda, 1969
<i>Detonula confervacea</i>	1.4	10	Hoogenhout and Ames, 1965
<i>Ditylum brightwellii</i>	2.1	20	Paasche, 1968
<i>Fragilaria</i> sp.	0.85	20	Rhee and Gotham, 1981b

KINETIC COEFFICIENTS

CONTROL FILE

<i>Fragilaria</i> sp.	1.7	11	Castenholz, 1964
<i>Melosira</i> sp.	0.7	11	Castenholz, 1964
<i>Navicula minima</i>	1.4	25	Hoogenhout and Ames, 1965
<i>Navicula pelliculosa</i>	2.0	20	Hoogenhout and Ames, 1965
<i>Nitzschia palea</i>	2.1	25	Hoogenhout and Ames, 1965
<i>Nitzschia turgidula</i>	2.5	20	Paasche, 1968
<i>Phaedoactylum tricornutum</i>	1.66	25	Fogg, 1969
<i>Phaedoactylum tricornutum</i>	2.7	19	Hoogenhout and Ames, 1965
<i>Rhizosolenia fragillissima</i>	1.2	21	Ignatiades and Smayda, 1970
<i>Skeletonema costatum</i>	1.26	18	Fogg, 1969
<i>Skeletonema costatum</i>	2.30	20	Jorgensen, 1968
<i>Skeletonema costatum</i>	1.52	20	Steemann-Nielsen and Jorgensen, 1968
<i>Skeletonema costatum</i>	1.23	20	Jitts, et al., 1964
<i>Synedra</i> sp.	1.2	11	Castenholz, 1964
<i>Thalassiosira nordenskioldii</i>	0.77	12	Jitts, et al., 1964
Natural diatom community	3.1	20	Verduin, 1952
Greens			
<i>Ankistrodesmus braunii</i>	2.33	25	Hoogenhout and Ames, 1965
<i>Chlorella pyrenoidosa</i>	2.22	28	Shelef, 1968
<i>Chlorella ellipsoidea</i>	3.6	25	Hoogenhout and Ames, 1965
<i>Chlorella luteoviridis</i>	0.56	22.4	Hoogenhout and Ames, 1965
<i>Chlorella miniata</i>	0.87	25	Hoogenhout and Ames, 1965
<i>Chlorella pyrenoidosa</i>	2.14	25	Fogg, 1969
<i>Chlorella pyrenoidosa</i>	1.95	25.5	Sorokin and Meyers, 1953
<i>Chlorella pyrenoidosa</i>	9.00	39	Castenholz, 1969
<i>Chlorella pyrenoidosa</i>	9.2	39	Hoogenhout and Ames, 1965
<i>Chlorella seccharophila</i>	1.2	25	Hoogenhout and Ames, 1965
<i>Chlorella variegata</i>	0.86	25	Hoogenhout and Ames, 1965
<i>Chlorella vulgaris</i>	2.9	25	Hoogenhout and Ames, 1965
<i>Chlorella vulgaris</i>	1.59	20	Goldman and Graham, 1981
<i>Dunaliella tertiolecta</i>	1.0	16	Hoogenhout and Ames, 1965
<i>Dunaliella tertiolecta</i>	0.77	36	Jitts, et al., 1964
<i>Haematococcus pluvialis</i>	1.2	23	Hoogenhout and Ames, 1965
<i>Nanochloris atomus</i>	1.0	20	Hoogenhout and Ames, 1965
<i>Platymonas subcordiformia</i>	1.5	16	Hoogenhout and Ames, 1965
<i>Scenedesmus</i> sp.	1.34	20	Rhee and Gotham, 1981b
<i>Scenedesmus costulatus</i>	2.0	24.5	Hoogenhout and Ames, 1965
<i>Scenedesmus obliquus</i>	2.11	20	Goldman and Graham, 1981
<i>Scenedesmus obliquus</i>	2.2	25	Hoogenhout and Ames, 1965
<i>Scenedesmus quadricauda</i>	4.1	25	Hoogenhout and Ames, 1965
<i>Scenedesmus quadricauda</i>	2.29	27	Goldman, et al., 1972
<i>Selenastrum capricornutum</i>	2.45	27	Goldman, et al., 1972
<i>Selenastrum westii</i>	1.0	25	Hoogenhout and Ames, 1965
<i>Stichococcus</i> sp.	0.7	20	Hoogenhout and Ames, 1965
Golden-Brown			
<i>Botrydiopsis intercedens</i>	1.5	25	Hoogenhout and Ames, 1965
<i>Bumilleriopsis brevis</i>	2.9	25	Hoogenhout and Ames, 1965
<i>Cricosphaera carterae</i>	0.82	18	Fogg, 1969
<i>Isochrysis galbana</i>	0.55	20	Fogg, 1969
<i>Isochrysis galbana</i>	0.8	25	Hoogenhout and Ames, 1965
<i>Monochrysis lutheri</i>	1.5	15	Hoogenhout and Ames, 1965
<i>Monochrysis lutheri</i>	0.39	24	Jitts, et al., 1964
<i>Monodus subterraneus</i>	0.93	25	Hoogenhout and Ames, 1965
<i>Monodus subterraneus</i>	0.39	30	Fogg, 1969
<i>Tribonema aequale</i>	0.7	25	Hoogenhout and Ames, 1965
<i>Tribonema minus</i>	1.0	25	Hoogenhout and Ames, 1965
<i>Vischera stellata</i>	0.7	25	Hoogenhout and Ames, 1965
<i>Euglena gracilis</i>	2.2	25	Hoogenhout and Ames, 1965
Dinoflagellate			
<i>Amphidinium carteri</i>	1.88	18	Fogg, 1969
<i>Amphidinium carteri</i>	0.32	32	Jitts, et al., 1964
<i>Ceratium tropos</i>	0.20	20	Fogg, 1969
<i>Gonyaulax polyedra</i>	2.1	21.5	Hoogenhout and Ames, 1965

CONTROL FILE

KINETIC COEFFICIENTS

<i>Gymnodinium splendens</i>	0.92	20	Hoogenhout and Amesz, 1965
<i>Peridinium</i> sp.	0.9	18	Hoogenhout and Amesz, 1965
<i>Prorocentrum gracile</i>	0.83	18	Hoogenhout and Amesz, 1965
<i>Prorocentrum micans</i>	0.71	25	Hoogenhout and Amesz, 1965
<i>Prorocentrum micans</i>	0.3	20	Fogg, 1969
Cyanobacteria			
<i>Agmenellum quadriplaticum</i>	8.0	39	Hoogenhout and Amesz, 1965
<i>Anabaena cylindrical</i>	0.96	25	Hoogenhout and Amesz, 1965
<i>Anabaena variabilis</i>	3.9	34.5	Hoogenhout and Amesz, 1965
<i>Anacystis nidulans</i>	2.9	25	Hoogenhout and Amesz, 1965
<i>Anacystis nidulans</i>	11.0	40	Castenholz, 1969
<i>Chloropseudomonas ethylicum</i>	3.3	30	Hoogenhout and Amesz, 1965
<i>Cyanidium caldarium</i>	2.4	40	Hoogenhout and Amesz, 1965
<i>Cylindrospermum sphaerica</i>	0.17	25	Hoogenhout and Amesz, 1965
<i>Gloeotrichia echinulata</i>	0.2	26.5	Hoogenhout and Amesz, 1965
<i>Microcystis aeruginosa</i>	0.25	20	Holm and Armstrong, 1981
<i>Microcystis aeruginosa</i>	1.6	23	Hoogenhout and Amesz, 1965
<i>Microcystis luminmosis</i>	1.5	40	Castenholz, 1969
<i>Nostoc muscorum</i>	2.9	32.5	Hoogenhout and Amesz, 1965
<i>Oscillatoria prinsips</i>	0.5	40	Castenholz, 1969
<i>Oscillatoria terebriformis</i>	3.36	40	Castenholz, 1969
<i>Oscillatoria rubescens</i>	5.04	30	Zimmerman, 1969
<i>Rhodopseudomonas sphaeroides</i>	10.8	34	Hoogenhout and Amesz, 1965
<i>Rhodospirillum rubrum</i>	4.85	25	Hoogenhout and Amesz, 1965
<i>Schizothrix calcicola</i>	3.4	30	Hoogenhout and Amesz, 1965
<i>Synechococcus lividus</i>	4.98	40	Castenholz, 1969
<i>Synechococcus</i> sp.	8.0	37	Hoogenhout and Amesz, 1965
<i>Tolypothrix tenuis</i>	4.0	38	Hoogenhout and Amesz, 1965
<i>Leotocylindroc danicus</i>	0.67-2.0	10-20	Verity, 1981
<i>Anabaena variabilis</i>	0.07-2.0	10-35	Collins and Boylen, 1982a

Grover (1989) rated the competitiveness of 11 algal species in P limiting environment. Maximum growth rates and P half saturation constants were measured and confidence intervals given.

Mixed species batch cultures were used to measure the kinetics. Algae density was determined by counting cells and the coefficients were estimated by fitting data to the Monod model. Three types of models were fitted: one with a common maximum growth rate and half saturation constant, one with a common half saturation constant but individual growth rates, and one with a individual growth rate and common half saturation constant.

Grover found it difficult to measure the half saturation constant because growth occurred at low concentrations of the nutrient even when it only existed as a contaminant. Half saturation constant was measured in units of micromoles/liter. Soluble reactive phosphorus was form of P measured. Table 36 lists the maximum growth rates and Table 37 lists half-saturation constants determined by Grover. The source of the algae was Square Lake, Minnesota (Washington County). Temperature was maintained at 12° Celsius the photon supply rate was ~60 $\mu\text{moles}/\text{m}^2/\text{s}$ on a 14 hours light/10 hours dark cycle. The samples were grown over a period of 7 days.

Table 36. Maximum growth rates (1/day) determined by Grover (1989).

Species	Group	Maximum Growth Rate (1/day)		
		Estimate	95% Confidence Limit	
			Lower	Upper
<i>Chlamydomonas</i> sp.	Green	0.79	0.61	0.96
<i>Chlorella</i> sp.	Green	0.81	0.62	1.05
<i>Cryptomonas</i> sp.		0.49	0.39	0.58
<i>Oocystis</i> sp.		0.52	0.43	0.61

Species	Group	Maximum Growth Rate (1/day)		
		Estimate	95% Confidence Limit	
			Lower	Upper
<i>Scenedesmus quadricauda</i>		0.63	0.47	0.93
<i>Sphaerocystis Schroeteri</i>		0.48	0.28	0.71
<i>Nitzschia acicularis</i>	Diatom	0.35	0.24	0.46
<i>Nitzschia linearis</i>	Diatom	0.56	0.45	0.68
<i>Nitzschia palea</i>	Diatom	0.88	0.77	1.03
<i>Synedra radians</i>	Diatom	0.60	0.39	0.85
<i>Synedra rumpens</i>	Diatom	0.73	0.59	0.88

Table 37. Phosphorus half-saturation coefficients ($\mu\text{mol/liter}$) determined by Grover (1989).

Species	Group	P-half saturation coefficients ($\mu\text{mol/liter}$)		
		Estimate	95% Confidence Limit	
			Lower	Upper
<i>Chlamydomonas</i> sp.	Green	0.0071	0.00097	0.038
<i>Chlorella</i> sp.	Green	0.022	0.0047	0.23
<i>Cryptomonas</i> sp.		0.014	0.0043	0.096
<i>Oocystis</i> sp.		0.012	0.0037	0.067
<i>Scenedesmus quadricauda</i>		0.035	0.0043	0.50
<i>Sphaerocystis Schroeteri</i>		0.025	0.0011	0.34
<i>Nitzschia acicularis</i>	Diatom	0.0023	0	0.019
<i>Nitzschia linearis</i>	Diatom	0.019	0.0051	0.22
<i>Nitzschia palea</i>	Diatom	0.047	0.016	0.22
<i>Synedra radians</i>	Diatom	0.00014	0	0.012
<i>Synedra rumpens</i>	Diatom	0.0069	0.0014	0.026

Riebesell et. al. (1993) determined maximum growth rates (Table 38) and carbon half-saturation coefficients (Table 36) for 3 species of marine diatoms grown under optimal nutrient and light conditions. The carbon source of common marine diatoms is dissolved CO_2 although some microalgae can use bicarbonate. Temperatures were maintained at 17 degrees Celsius for *D. brightwellii* and *T. punctigera* and 5 degrees C for *R. cf. alata*. Light intensity was $120 \mu\text{E/m}^2/\text{second}$.

Table 38. Maximum growth rates and carbon half saturation constants of 3 marine diatoms (Riebesell et. al., 1993)

Species	Group	Temperature (Celsius)	Light Intensity ($\mu\text{E/m}^2/\text{second}$)	Maximum Growth Rate (1/day)	Carbon half-saturation constant (μM)
<i>Ditylum brightwellii</i>	Marine diatom	17°	120	1.46	1.4
<i>Thalassiosira punctigera</i>	Marine diatom	17°	120	1.30	1.2
<i>Rhizoselina cf. alata</i>	Marine diatom	5°	120	0.93	2.1

The common diatom *Skeletonema costatum* was studied by Samuel et. al. (1983). There is an abundance of literature out there regarding this diatom and are these references are listed in the article. In the East River *Skeletonema costatum* blooms during late winter early spring but does not do well in the summer months, perhaps because of pollution. The East River is saturated with $\text{NH}_3\text{-N}$, $\text{PO}_4\text{-P}$, and Silicon year round.

Source of water used in measuring growth rates was the East River. Salinity in laboratory was varied to simulate conditions found in East River. Temperature was 20° C and the photo period 14 hours light/10 hours dark at $2500 \mu\text{W/m}^2$. Maximum growth rates measured were 1.2 to 1.8 day^{-1} .

Table 39. Maximum growth rate of *Skeletonema costatum* (Samuel et. al., 1983).

Species	Group	Temperature (Celsius)	Light Intensity ($\mu\text{W}/\text{m}^2$)	Maximum growth rate (day^{-1})
<i>Skeletonema costatum</i>	diatom	20°	2500	1.2-1.8

Goldman et. al. (1974) determined the maximum growth rate and inorganic carbon half saturation coefficient for the freshwater algae *Selenastrum capricornutum* and *Scenedesmus quadricauda*. They are green algae of the order Chlorococcales.

Algae were grown in continuously stirred reactors at a constant inflow and outflow and constant nutrient concentration. Algae growth was limited by inorganic carbon. The steady state concentration and carbon concentration were fitted to the Monod equation to determine maximum growth rate and half-saturation concentration.

Cultures were grown at a constant temperature of $27^\circ \pm 1^\circ$ Celsius. Light was provided with “cool white” fluorescent tubes at an intensity of 4306 ± 431 lumens/meter². Concentrations were determined by counting algae cells.

The algae dry weight carbon fraction was 44.7% for *Scenedesmus quadricauda* and 48.9% for *Selenastrum capricornutum*.

Table 40. Maximum growth rates and carbon half-saturation coefficients of the green algae *Selenastrum capricornutum* and *Scenedesmus quadricauda* (Goldman et. al., 1974).

Species	Group	Temperature (Celsius)	Light Intensity (lumens/ meter ²)	Maximum growth rate (day^{-1})	Carbon Half-saturation coefficient (mg/l)
<i>Selenastrum capricornutum</i>	Green algae	27°	4306 ± 431	2.45	0.4-1.49
<i>Scenedesmus quadricauda</i>	Green algae	27°	4306 ± 431	2.29	0.1-0.7

Chalup and Laws (1990) calculated the nutrient saturated growth rate of the marine phytoplankter *Pavlova lutheri* at different light intensities. Algae were grown in batch cultures at a temperature between 21.9° - 22.1° Celsius. Predicted growth rates of 0.625 and 1.14 1/day for light intensities of 5.44 and 16.3 moles quanta/m²-day, respectively. The nutrient saturated growth rate prediction were calculated the following regression based on data:

$$\mu_s = \frac{1.95I}{I + 10.8} - 0.03$$

where μ_s and I have the dimensions day^{-1} and moles quanta $\text{m}^{-2} \text{d}^{-1}$. Table 36 shows the predicted growth rates.

Table 41. Nutrient saturated maximum growth rates of the marine algae *Pavlova lutheri* (Chalup and Laws, 1990).

Species	Group	Temperature (Celsius)	Light Intensity (moles quanta/m ² -day)	Growth rate (day^{-1})
<i>Pavlova lutheri</i>	marine	22°	5.44	0.625
<i>Pavlova lutheri</i>	marine	22°	16.3	1.14

The maximum growth rate (Table 42) and silicon half-saturation constant (Table 43) of two clones of the marine diatom *Thalassiosira Pseudonana* were calculated by Guillard et. al. (1973). One clone was from Saragossa Sea and the other was an estuarine clone from the Forge River, Moriches Bay, Long Island, New York. Batch cultures were grown at 20° Celsius and at 6500 lux. Growth was followed by counting cells.

Table 42. Maximum growth rate of two clones of the marine diatom *Thalassiosira Pseudonana* (Guillard et. al., 1973).

Species	Group	Source	Temperature (Celsius)	Light Intensity (lux)	Growth rate (doublings/day)	Confidence Interval, 95%
<i>Thalassiosira Pseudonana</i>	Marine diatom	Moriches Bay, Long Island, NY	20°	6500	3.64	2.9-4.4
<i>Thalassiosira Pseudonana</i>	Marine diatom	Saragossa Sea	20°	6500	2.13	2.0-2.3

Table 43. Silicon half-saturation constant of two clones of the marine diatom *Thalassiosira Pseudonana* (Guillard et. al., 1973).

Species	Group	Source	Temperature (Celsius)	Light Intensity (lux)	Half-Saturation Constant (μM)	Confidence Interval, 95%
<i>Thalassiosira Pseudonana</i>	Marine diatom	Moriches Bay, Long Island, NY	20°	6500	0.98	0.28-1.95
<i>Thalassiosira Pseudonana</i>	Marine diatom	Saragossa Sea	20°	6500	0.19	0.09-0.29

Diatoms are not the only alga which require silicon. Klaveness and Guillard (1975) determined the maximum growth rate (Table 44) and silicon half-saturation coefficient (Table 45) for the golden-brown (Chrysophyceae) algae *Synura Petersenii*.

Golden brown algae are insignificant in the plankton of the sea but are abundant in freshwater lakes and ponds where they can form blooms. *Synura* spp. are known as an odor producing species.

Batch cultures were used to measure growth rate and half-saturation constant. Steady-state conditions are attained by maintaining very low algae populations which did not initially affect nutrient concentrations. Cultures were grown at 20° Celsius and light intensity was 9000 lux with 16 hour days.

The algae were obtained from a freshwater pond near Woods Hole, Massachusetts.

Table 44. Maximum growth rate of the golden-brown algae *Synura Petersenii* (Guillard and Klaveness, 1975).

Species	Group	Source	Temperature (Celsius)	Light Intensity (lux)	Maximum growth rate (divisions/day)
<i>Synura Petersenii</i>	Golden-brown algae (Chrysophyceae)	Fresh water pond, Massachusetts	20°	9000	1.12

Table 45. Silicon half-saturation constant of the golden-brown algae *Synura Petersenii* (Guillard and Klaveness, 1975).

Species	Group	Source	Temperature (Celsius)	Light Intensity (lux)	Silicon half-saturation constant (μM)
<i>Synura Petersenii</i>	Golden-brown algae (Chrysophyceae)	Fresh water pond, Massachusetts	20°	9000	0.23

Paasche (1973) measured the maximum growth rates of the marine diatom species *Skeletonema costatum*, *Thalassiosira pseudonana*, *Thalassiosira decipiens*, *Ditylum brightwellii*, and *Licmophora* sp. (Table 46). Cultures of *Skeletonema costatum*, *Thalassiosira decipiens*, and *Licmophora* were isolated from the Oslo Fjord.

Cultures were grown at 20 °C at a light intensity of about 25000 erg/cm²-sec. An 18 hour day was used for *D. brightwellii* whereas the other cultures were lit continuously.

Table 46. Maximum growth rates for five species of marine diatoms (Paasche, 1973).

Species	Group	Source	Temperature (Celsius)	Light Intensity (erg/cm ² -sec-ond)	Maximum growth rate (doublings/day)
<i>Skeletonema costatum</i>	Marine Diatom	Oslo Fjord	20°	25000	2.4
<i>Thalassiosira pseudonana</i>	Marine Diatom		20°	25000	4.0
<i>Thalassiosira decipiens</i>	Marine Diatom	Oslo Fjord	20°	25000	1.4
<i>Ditylum brightwellii</i>	Marine Diatom		20°	25000	3.2
<i>Licmophora</i> sp.	Marine Diatom	Oslo Fjord	20°	25000	1.3

Table 47 shows the maximum growth rate was determined for the marine diatom *Skeletonema Costatum costatum* (Sakshaug and Andresen, 1989). The culture temperature was 15° Celsius. *Skeletonema Costatum* is a prominent species in most coastal waters and fjords. At the maximum growth rate of 1.4 day⁻¹ the light intensity was 4.33 PAR, moles/m²-hour (PAR=photosynthetically available radiation). The culture was lit continuously at this growth rate.

Table 47. The maximum growth rate of the marine diatom *Skeletonema costatum* (Sakshaug and Andresen, 1989).

Species	Group	Temperature (Celsius)	Light Intensity (PAR, moles/m ² -hour)	Maximum growth rate (day ⁻¹)
<i>Skeletonema costatum</i>	Marine Diatom	15°	4.33	1.4

Maximum growth rate and dark respiration rate of the three marine diatom species *Skeletonema costatum*, *Olisthodiscus luteus* and *Gonyaulax tamarensis* measured by Langdon (1987) (Table 48-Table 49). Algae were grown using the batch culture method at 15° Celsius with a 14 hour day. Langdon developed a interspecies growth-irradiance model consisting of three variables:

cell carbon at maximum growth rate, carbon-chlorophyll a ratio, and dark respiration rate at zero growth rate. Cell growth was measured by counting cells.

Table 48. Maximum growth rate of the three marine diatom species *Skeletonema costatum*, *Olisthodiscus luteus* and *Gonyaulax tamarens* measured by Langdon (1987).

Species	Group	Temperature (Celsius)	Maximum growth rate (divisions/day)	Standard error of Maximum growth rate (divisions/day)
<i>Skeletonema costatum</i>	Marine Diatom	15°	2.41	0.02
<i>Olisthodiscus luteus</i>	Marine Diatom	15°	0.87	0.03
<i>Gonyaulax tamarens</i>	Marine Diatom	15°	0.56	0.02

Table 49. Dark respiration rate of the three marine diatom species *Skeletonema costatum*, *Olisthodiscus luteus* and *Gonyaulax tamarens* measured by Langdon (1987).

Species	Group	Temperature (Celsius)	Dark respiration at zero growth rate (divisions/day)	Standard error (divisions/day)
<i>Skeletonema costatum</i>	Marine Diatom	15°	0.04	0.03
<i>Olisthodiscus luteus</i>	Marine Diatom	15°	0.06	0.06
<i>Gonyaulax tamarens</i>	Marine Diatom	15°	0.17	0.17

Falkowski et. al. (1985) calculated the steady-state growth rates of three species of marine phytoplankton but did not determine maximum growth rates. They did determine that the *Isochrysis galbana* becomes light saturated at 200 $\mu\text{moles quanta/meter}^2\text{-second}$. Phytoplankton were grown at 18° Celsius.

Excretion rates of less than 5% of gross photosynthesis were observed in *Isochrysis galbana*, *Thalassiosira weissflogii*, and *Proocentrum micans*.

Table 50. Light saturation of *Isochrysis galbana* (Falkowski et. al., 1985).

Species	Group	Temperature (Celsius)	Light saturation ($\mu\text{moles quanta/meter}^2\text{-second}$)
<i>Isochrysis galbana</i>	Marine Chrysophyte	18°	200

Laws and Bannister (1981) measured the maximum growth rate of the marine diatom *Thalassiosira fluviatilis* using the carbon 14 labeling method. A continuous culture system was used to grow the phytoplankton. Temperature was maintained at 20° Celsius with a 12 hour light/12 hour dark cycle. Maximum growth was measured to be 1.22 day^{-1} .

Table 51. Maximum growth rate of *Thalassiosira fluviatilis* (Laws and Bannister, 1981).

Species	Group	Temperature (Celsius)	Maximum Growth Rate (day^{-1})
<i>Thalassiosira fluviatilis</i>	Marine Diatom	20°	1.22

Reay et al. (1999) measured maximum growth rates and optimal growth temperatures while studying the temperature effect of ammonia and nitrate uptake in algae and bacteria. The maximum growth rate and optimum growth temperatures for the algae are listed in Table 52. Also studied was dependence of ammonia and nitrate half-saturation coefficient on temperature.

Algae cultures were grown in chemostat and batch cultures and were illuminated using fluorescent tubes emitting 200 μmol of quanta/ $\text{m}^2\cdot\text{s}$.

Table 52. Maximum growth rates and optimum growth temperatures for phytoplankton studied by Reay et al. (1999).

Species	Group	Source	Optimum Growth Temperature (Celsius)	Maximum growth rate (day ⁻¹)
Chaetoceros sp.	Marine Diatom	Seawater Sample, Southern Ocean	6°	0.67
Chaetoceros curvisetum	Marine Diatom	Seawater Sample, North Sea	23°	0.48
Dinialiaella tertiolecta	Flagellate alga	Seawater Sample, Oslo Fjord, Norway	24°	2.50

Clark and Flynn (2000) determined maximum growth rates and inorganic carbon half-saturation coefficients of marine phytoplankton while studying the kinetics of inorganic carbon and the influence of nitrogen source. Batch cultures were grown in a 16° Celsius room under a photon intensity of 200 $\mu\text{mol m}^{-2} \text{s}^{-1}$ with a 12 hour light/ 12 hour dark cycle using cool-white fluorescent tubes. Half-saturation concentrations were estimated by fitting a growth curve to a rectangular hyperbolic (Michaelis-Menten type) function.

Table 53. Maximum growth rates and carbon half-saturation constants of marine phytoplankton studied by Clark and Flynn (2000).

Species	Group	Nitrogen Source	Carbon half-saturation constant (μM)	Maximum growth rate (day ⁻¹)
Phaedactylum tri-cornutum	Bacillariophyceae	NO ₂	30	0.80
Thalassiosira pseudonana	Bacillariophyceae	NO ₃	273	1.33
		NH ₄	233	1.75
Thalassiosira weissflogii	Bacillariophyceae	NO ₃	258	1.55
		NH ₄	135	1.52
Stichococcus Bacillaris	Chlorophyta	NO ₃	720	0.77
		NH ₄	568	0.83
Alexandrium fundyense	Dinophyta	NO ₃	468	0.36
Scrippsiella trochoidea	Dinophyta	NO ₃	280	0.40
Emiliana huxleyi	Prymnesiophyceae	NO ₃	150	1.19
		NH ₄	114	1.14
Isochrysis galbana	Prymnesiophyceae	NO ₂	81	0.48
Heterosigma carterae	Raphidophyceae	NO ₃	673	1.21
		NH ₄	663	1.62

Litchman (2000) compared the effect of constant light and fluctuating light on algae growth. Growth rate was shown to be species-specific and a diatom's *Nitzschia* sp. growth rate increased under fluctuating light at low average intensities. Maximum growth rates, metabolic loss rate (respiration) and light saturation intensity were measured for 4 freshwater species incubated in batch cultures at 20° Celsius (Table 54). The growth rates of the blue-greens *Anabaena* and *Phormidium* decreased at higher light intensities, whereas the growth rates of *Nitzschia* and the green alga *Sphaerocystis* were not inhibited at higher light intensities.

Table 54. Maximum growth rate, saturation intensity and respiration rate for 4 freshwater algae species (Litchman, 2000).

Species	Group	Saturating Light Intensity ($\mu\text{moles photons/m}^2\text{-s}$)	Respiration rate (day^{-1})	Maximum growth rate (day^{-1})
<i>Nitzschia</i> sp.	Diatom	35	0.24	1.31
<i>Anabaena</i>	Blue-green	25	0.1	1.19
<i>Sphaerocystis</i>	green	19	0.6	1.44
<i>Phormidium</i>	Blue-green	17	0.001	1.4

Maximum algal mortality rate [AM] is also temperature dependent. A general rule of thumb is the maximum algal mortality rate [AM] should be less than 10% of the maximum algal growth rate [AG]. Values ranging from 0.03 to 0.3 have been used in previous modeling studies, with the default value of 0.1 day^{-1} providing excellent results on a large number of systems.

[AE] is the maximum algal excretion (or photorespiration) rate that goes directly to the labile DOM compartment. The default value is 0.04 day^{-1} . [AR] is the maximum dark algal respiration rate. Respiration rates are often expressed as millilitres of oxygen consumed per milligram of organism dry weight per hour. To convert to model units ($\text{mg O}_2 \text{ mg}^{-1} \text{ organism dry weight day}^{-1}$), multiply dark respiration rates by $0.74 \text{ mg dry weight/1 ml O}_2$. Literature values are reported in [Table C-55](#) and [Table C-56](#). The default value is 0.04 day^{-1} .

Table C-55. Maximum Algal Excretion Rate Literature Values

Species	Excretion Rate, day^{-1}	Reference
<i>Actinastrum hantzschii</i>	0.044	Nalewajko, 1966
<i>Ankistrodesmus falcatus</i>	0.031	Nalewajko, 1966
<i>Asterococcus superbus</i>	0.036	Nalewajko, 1966
<i>Chlorella pyrenoidosa</i>	0.032	Nalewajko, 1966
<i>Eudorina elegans</i>	0.023	Nalewajko, 1966
<i>Micractinium pusillum</i>	0.014	Nalewajko, 1966

Table C-56. Algal Dark Respiration Rate Literature Values

Species	Respiration Rate, day^{-1}	Reference
<i>Anabaena variabilis</i>	0.10-0.92	Collins and Boylen, 1978
<i>Chlorella pyrenoidosa</i>	0.01-0.03	Myers and Graham, 1961
<i>Coscinodiscus excentricus</i>	0.07-0.11	Riley and von Aux, 1949
<i>Dunaliella teriolecta</i>	0.12-0.16	Laws and Wong, 1978
<i>Mesodinium rubrum</i>	0.05	Smith, 1979
<i>Monochrysis lutheri</i>	0.15-0.32	Laws and Wong, 1978

Thalassiosira allenii	0.05-0.59	Laws and Wong, 1978
-----------------------	-----------	---------------------

Literature value for algal settling velocities [AS] are given in [Table C-57](#), but care must be taken in their use. Laboratory and *in situ* methods for determining settling velocities each have their drawbacks when attempting to measure net settling velocities. The settling velocity is very dependent upon the type of algae present, so a single default value is not recommended. Previous studies have used a settling velocity of 0.2 m day^{-1} for diatoms, 0.1 m day^{-1} for greens, and $0.0\text{-}0.05 \text{ m day}^{-1}$ for cyanobacteria. Also, for cyanobacteria or other floating phytoplankton, one can specify a negative settling velocity.

Table C-57. Algal settling Velocity Literature Values

Species	Settling velocity, m day^{-1}	Reference
Diatoms		
Asterionella formosa	0.26-0.76	Smayda, 1974
Bacteriastrium hyalinum	0.39-1.27	Smayda & Boleyn, 1966
Chaetoceros didymus	0.85	Eppey Holmes, & Strickland, 1967b
Chaetoceros lauderi	0.46-1.54	Smayda & Boleyn, 1966
Chaetoceros spp.	0.85	Margalef, 1961
Chaetoceros spp.	4.00	Allen, 1932
Coscinodiscus wailesii	7.00-30.2	Eppey Holmes, & Strickland, 1967b
Coscinodiscus sp.	1.95-6.83	Eppey Holmes, & Strickland, 1967b
Cyclotella meneghiniana	0.08-0.24	Titman & Kilham, 1976
Cyclotella nana	0.16-0.76	Eppey Holmes, & Strickland, 1967b
Ditylum brightwellii	0.60-3.09	Eppey Holmes, & Strickland, 1967b
Fragilaria crotonensis	0.27	Burns & Rosa, 1980
Leptocylindrum danicus	0.08-0.42	Margalef, 1961
Melosira agassizii	0.67-1.87	Titman & Kilham, 1976
Nitzschia closterium	0.52	Margalef, 1961
Nitzschia seriata	0.35-0.50	Smayda & Boleyn, 1965
Phaeodactylum tricornutu	0.02-0.06	Riley, 1943
Rhizosolenia hebetata	0.22	Eppey, Holmes, & Strickland, 1967b
Rhizosolenia setigera	0.10-6.30	Smayda & Boleyn, 1974
Rhizosolenia stolterfothii	1.00-1.9	Eppey, Holmes, & Strickland, 1967b
Rhizosoleni sp.	0.00-0.72	Margalef, 1961
Skeletonema costatum	0.30-1.35	Smayda & Boleyn, 1974
Stephanopyxis turris	1.10	Eppey, Holmes, & Strickland, 1967b
Thalassionema nitzsoides	0.35-0.78	Smayda (unpublished)
Thalassiosira fluviatilis	0.60-1.10	Eppey, Holmes, & Strickland, 1967b
Thalassiosira nana	0.10-0.28	Smayda & Boleyn, 1966
Thalassiosira rotula	0.39-2.10	Smayda & Boleyn, 1966
Dinoflagellates		
Gonyaulax polyedra	2.80-6.10	Bramlette, 1961
Coccolithophorids		
Coccolithus huxleyi	0.28, 1.2	Eppey, Holmes, & Strickland, 1967b
Cricosphaera carterae	1.7	Eppey, Holmes, & Strickland, 1967b
Cricosphaera elongata	0.25	Eppey, Holmes, & Strickland, 1967b
Cycloccolitus fragilis	10.3-13.2	Bernard, 1963
Microflagellates		
Cryptomonas reosa	0.31	Burns & Rosa, 1980

[AHSP] is the algal half-saturation constant for phosphorus and is defined as the phosphorus concentration at which the uptake rate is one-half the maximum rate. This represents the upper concentration at which algal growth is directly proportional to phosphorus concentrations

Table C-58. Phosphorus Half-Saturation Constant Literature Values

Species	Half-Saturation Constant, $mg\ l^{-1}$	Reference
<i>Asterionella formosa</i>	0.002	Holm & Armstrong, 1981
<i>Asterionella japonica</i>	0.014	Thomas & Dodson, 1968
<i>Biddulphia sinensis</i>	0.016	Quasim, et al., 1973
<i>Cerataulina bergonii</i>	0.003	Finenko & Krupatkina, 1974
<i>Chaetoceros curvatus</i>	0.074-0.105	Finenko & Krupatkina, 1974
<i>Chaetoceros socialis</i>	0.001	Finenko & Krupatkina, 1974
<i>Chlorella pyrenoidosa</i>	0.380-0.475	Jeanjean, 1969
<i>Cyclotella nana</i>	0.055	Fuhs, et al., 1972
<i>Cyclotella nana</i>	0.001	Fogg, 1973
<i>Dinobryon cylindrium</i>	0.076	Lehman (unpublished)
<i>Dinobryon sociale</i>	0.047	Lehman (unpublished)
<i>Euglena gracilis</i>	1.520	Dlum, 1966
<i>Microcystis aeruginosa</i>	0.006	Holm & Armstrong, 1981
<i>Nitzschia actinastroides</i>	0.095	Von Muller, 1972
<i>Pediastrum duplex</i>	0.105	Lehman (unpublished)
<i>Pithophora oedogonia</i>	0.980	Spencer & Lembi, 1981
<i>Scenedesmus obliquus</i>	0.002	Fogg, 1973
<i>Scenedesmus sp.</i>	0.002-0.050	Rhee, 1973
<i>Thalassiosira fluviatilis</i>	0.163	Fogg, 1973

[AHSN] is the algal half-saturation constant for nitrogen and is defined as the nitrogen concentration (ammonium + nitrate/nitrite) at which the uptake rate is one-half the maximum rate. This represents the upper concentration at which algal growth is proportional to nitrogen. [Table C-59](#) gives literature values for the nitrogen half-saturation constant. To simulate algal nitrogen fixation, set AHSN equal to 0.0.

Table C-59. Nitrogen Half-Saturation Constant Literature Values

Species	Half saturation constant	N source	Reference
Diatoms			
<i>Biddulphia aurita</i>	0.056-0.197	NO ₃	Underhill, 1977
<i>Chaetoceros gracilis</i>	0.012	NO ₃	Eppley, Rogers, & McCarthy, 1969
	0.012	NH ₄	Eppley, Rogers, & McCarthy, 1969
<i>Coscinodiscus lineatus</i>	0.012	NO ₃	Eppley, Rogers, & McCarthy, 1969
	0.012	NH ₄	Eppley, Rogers, & McCarthy, 1969
<i>Cyclotella nana</i>	0.025-0.117	NO ₃	Carpenter & Guillard, 1971
	0.111		MacIsaac & Dugdale, 1969
	0.027		Caperon & Meyer, 1972
	0.031		Eppley, Rogers, & McCarthy, 1969
<i>Ditylum brightwellii</i>	0.037	NO ₃	Eppley, Rogers, & McCarthy, 1969
	0.020	NO ₃	Eppley, Rogers, & McCarthy, 1969
<i>Dunaliella teriolecta</i>	0.013	NO ₃	Caperon & Meyer, 1972
	0.013	NH ₄	Caperon & Meyer, 1972
	0.087	NO ₃	Eppley, Rogers, & McCarthy, 1969
<i>Fragilaria pinnata</i>	0.037-0.100	NO ₃	Carpenter & Guillard, 1971
<i>Leptocylindrus danicus</i>	0.078	NO ₃	Eppley, Rogers, & McCarthy, 1969
	0.013	NH ₄	Eppley, Rogers, & McCarthy, 1969
<i>Navicula pelliculosa</i>	0.923	NO ₃	Wallen & Cartier, 1975
<i>Phaeodactylum tricornutum</i>	0.161	NO ₃	Ketchum, 1939
<i>Rhizosolenia robusta</i>	0.186	NO ₃	Eppley, Rogers, & McCarthy, 1969
	0.135	NH ₄	Eppley, Rogers, & McCarthy, 1969
<i>Rhizosolenia stolterfothii</i>	0.105	NO ₃	Eppley, Rogers, & McCarthy, 1969
	0.009	NH ₄	Eppley, Rogers, & McCarthy, 1969
<i>Skeletonema costatum</i>	0.027	NO ₃	Eppley, Rogers, & McCarthy, 1969
	0.014	NH ₄	Eppley, Rogers, & McCarthy, 1969

Species	Half saturation constant	N source	Reference
Bluegreens			
Anabaena cylindrica	4.34	NO3	Hattori, 1962
	2.48	NO3	Hattori, 1962
Asterionella formosa	0.074-0.093	NO3	Eppey & Thomas, 1969
	0.062	NH4	Eppey & Thomas, 1969
Oscillatoria agardhii	0.22	NO3	van Lierre, 1977
Microflagellates			
Bellochia sp.	0.001-0.16	NO3	Carpenter & Guillard, 1971
Monochrysis lutheri	0.026	NO3	Caperon & Meyer, 1972
	0.052	NH4	Caperon & Meyer, 1972
	0.037	NO3	Eppey, Rogers, & McCarthy, 1969
	0.007	NH4	Eppey, Rogers, & McCarthy, 1969
Coccolithophorids			
Coccolithus huxleyi	0.006	NO3	Eppey, Rogers, & McCarthy, 1969
	0.002	NH4	Eppey, Rogers, & McCarthy, 1969
Greens			
Chlorella pyrenoidosa	0.006-0.14		Pickett, 1975
	1.15	NO3	Knudsen, 1965
Pithophora cedogonia	1.236	NO3	Spencer & Lembi, 1981
Dinoflagellates			
Gonyaulax polyedra	0.589	NO3	Eppey, Rogers, & McCarthy, 1969
	0.099	NH4	Eppey, Rogers, & McCarthy, 1969
Gymnodinium splendens	0.235	NO3	Eppey, Rogers, & McCarthy, 1969
	0.099	NH4	Eppey, Rogers, & McCarthy, 1969
Gymnodinium wailesii	0.223	NO3	Eppey, Rogers, & McCarthy, 1969
	0.088	NH4	Eppey, Rogers, & McCarthy, 1969
Chrysophytes			
Isochrysis galbana	0.006	NO3	Eppey, Rogers, & McCarthy, 1969

[ASAT] is the saturating light intensity at the maximum photosynthetic rate. Since phytoplankton adapt to low light regimes, saturation coefficients may be lower than those measured in the laboratory. [Table C-60](#) gives literature values for [ASAT]. EPA (1985) gives as a guideline that [ASAT] for total phytoplankton range between 200-350 Langley/day (about 100-170 W/m²).

Table C-60. Literature values for saturating light intensity

Species	Saturation, $W\ m^{-2}$	Reference
<i>Cryptomonas ovata</i>	12-36	Cloern, 1977
<i>Oscillatoria agardhii</i>	10	van Lierre, et al., 1978
<i>Oscillatoria rubescens</i>	36-61	Konopka, 1983
<i>Scenedesmus protuberans</i>	24	van Lierre, et al., 1978
Mixed diatoms	86	Belay, 1981
Mixed phytoplankton	36	Belay, 1981
Shade-adapted phytoplankton	18-29	Belay, 1981

Example

ALGAL RATE	AG	AR	AE	AM	AS	AHSP	AHSN	AHSSI	ASAT
Alg 1	1.5	0.04	0.04	0.15	0.20	0.003	0.014	0.003	75.0
Alg 2	2.5	0.04	0.04	0.10	0.10	0.003	0.014	0.000	75.0
Alg 3	0.5	0.04	0.04	0.05	0.02	0.003	0.010	0.000	75.0

KINETIC COEFFICIENTS

CONTROL FILE

Related Cards and Files

[Algal Extinction](#)

[Algal Temperature Rate Coefficients](#)

[Algal Stoichiometry](#)

Algal Temperature Rate Coefficients (ALG TEMP)

FIELD	NAME	VALUE	DEFAULT	DESCRIPTION
1				(Ignored by code)
2	AT1	Real	5.0	Lower temperature for algal growth, °C
3	AT2	Real	25.0	Lower temperature for maximum algal growth, °C
4	AT3	Real	35.0	Upper temperature for maximum algal growth, °C
5	AT4	Real	40.0	Upper temperature for algal growth, °C
6	AK1	Real	0.1	Fraction of algal growth rate at AT1
7	AK2	Real	0.99	Fraction of maximum algal growth rate at AT2
8	AK3	Real	0.99	Fraction of maximum algal growth rate at AT3
9	AK4	Real	0.1	Fraction of algal growth rate at AT4

This card specifies the lower, maximum lower, upper, and maximum upper temperatures used in defining the curve that determines effects of temperature on algal rates. Also specified is the fraction of maximum algal rates that occurs at the specified temperature. The default values are ones for a single algal assemblage used in Version 2. When including multiple algal groups, the temperature rate coefficients are one of the most important parameters determining algal succession. Diatoms would have much lower temperatures for AT1-AT4 and cyanobacteria would have higher values.

How temperature affects algae growth is shown below for the default values of AT1 through AT4 and AK1 through AK4.

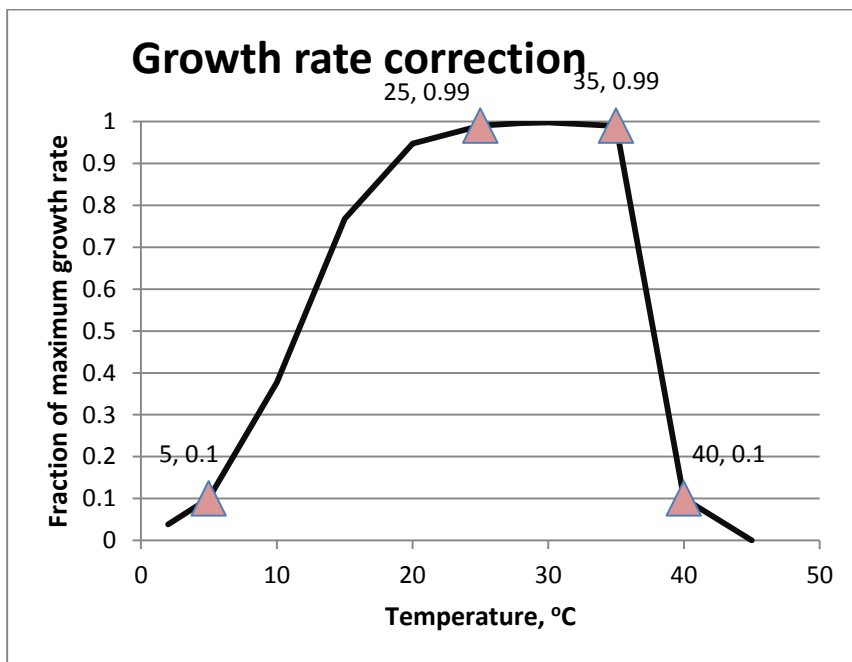


Figure 39. Growth rate as a function of temperature.

KINETIC COEFFICIENTS

CONTROL FILE

Example

ALGAL TEMP	AT1	AT2	AT3	AT4	AK1	AK2	AK3	AK4
Alg 1	5.0	18.0	20.0	24.0	0.1	0.99	0.99	0.01
Alg 2	10.0	30.0	35.0	40.0	0.1	0.99	0.99	0.01
Alg 3	10.0	35.0	40.0	50.0	0.1	0.99	0.99	0.01

Related Cards and Files

[Algal Rates](#)

[Algal Extinction](#)

[Algal Stoichiometry](#)

Algal Stoichiometry (ALG STOICH)

FIELD	NAME	VALUE	DEFAULT	DESCRIPTION
1				(Ignored by code)
2	AP	Real	0.005	Stoichiometric equivalent between algal biomass and phosphorus, fraction
3	AN	Real	0.08	Stoichiometric equivalent between algal biomass and nitrogen, fraction
4	AC	Real	0.45	Stoichiometric equivalent between algal biomass and carbon, fraction
5	ASI	Real	0.18	Stoichiometric equivalent between algal biomass and silica, fraction
6	ACHLA	Real	0.05	Ratio between algal biomass and chlorophyll a in terms of mg algae/μg chl a
7	APOM	Real	0.8	Fraction of algal biomass that is converted to particulate organic matter when algae die
8	ANEQN	Integer	2	Equation number for algal ammonium preference (either 1 or 2)
9	ANPR	Real	0.001	Algal half saturation constant for ammonium preference

This card specifies the stoichiometric equivalences used for determining the amount of nutrients in algal biomass. Numerous researchers have noted that these ratios are not constant over time and vary by algal species. In addition, the algal to chlorophyll *a* ratio [ACHLA] is known to be different for different algal species and is known to vary over time for a given algal species.

Table C-61 shows a summary of algal stoichiometry based on C, N, P, and Si percentages of dry-weight biomass from Reynolds (1984) for freshwater algae. EPA (1985) shows dry weight biomass fractions of C, N, and P ranging from 0.19-0.74 (typically 0.4-0.5), 0.006-0.16 (typically 0.08), and 0.0008 to 0.03 (typically 0.01), respectively, depending on algae type.

EPA(1985) reports percentages of chlorophyll *a* compared to dry weight algae biomass ranging from 0.25 to 3 for blue-green algae and from 2 to 10 for total phytoplankton. These correspond to a range in algae to chlorophyll *a* ratios (mg dry weight organic matter/μg chlorophyll *a*) [ACHLA] of from between 0.01 to 0.4. EPA(1985) also reports carbon:chlorophyll *a* ratios of from 10 to 100. Using a ratio of C:organic matter (OM) of about 1:2, this is approximately a range of 20-200 mg OM/mg chlorophyll *a*, or 0.02 to 0.2 mg OM/ μg chlorophyll *a*. Currently, the model does not include variable stoichiometry or biomass to chlorophyll *a*.

[APOM] is the fraction of algal biomass lost by mortality going into the detritus compartment with the remainder going to labile DOM. Otsuki and Hayna (1972) have reported a value of 0.8 for *Scenedesmus* sp. and this is the default value.

Certain algal groups are known to preferentially uptake ammonium over nitrate. If the equation number [ANEQN] for algal nitrogen uptake is set to 1, then the algal nitrogen preference factor for ammonium is computed using:

$$P_{NH4} = \frac{C_{NH4}}{(C_{NO3} + C_{NH4})}$$

and the preference for nitrate is:

$$P_{NO3} = \frac{C_{NO3}}{(C_{NO3} + C_{NH4})}$$

If the equation number [ANEQN] is set to 2, then the phytoplankton nitrogen preference for ammonium is computed using the following equation (Thomann and Fitzpatrick, 1982):

$$P_{NH4} = C_{NH4} \frac{C_{NOx}}{(K_{mN} + C_{NH4})(K_{mN} + C_{NOx})} + C_{NH4} \frac{K_{mN}}{(C_{NH4} + C_{NOx})(K_{mN} + C_{NOx})}$$

P_{NH4} = ammonium preference factor

K_{mN} = N half-saturation coefficient, $mg\ l^{-1}$

C_{NH4} = ammonium nitrogen concentration, $mg\ l^{-1}$

C_{NOx} = nitrate-nitrite nitrogen concentration, $mg\ l^{-1}$

The nitrite-nitrate nitrogen preference factor is then calculated from:

$$P_{NOx} = 1 - P_{NH4}$$

Table C-61. Freshwater algae minimum and optimum elemental contents in percentages of dry-weight (Reynolds, 1984).

Content	C	N	P	Si
Minimum				
<i>Anabaena flos-aquae</i>	49.7 ⁽¹⁾		0.40 ⁽²⁾	
<i>Microcystis aeruginosa</i>	46.5 ⁽¹⁾	3.8 ⁽³⁾	0.34 ⁽³⁾	
Various cyanobacteria		4.5 ⁽⁴⁾		
<i>Asterionella formosa</i>				32 ⁽⁴⁾
<i>Stephanodiscus hantzschii</i>				20 ⁽⁴⁾
<i>Asterionella Formosa</i> (percentages are ash-free dry weight)		3.4 ⁽⁵⁾	0.03 ⁽⁶⁾	
<i>Scenedesmus obliquus</i>	54.6 ⁽¹⁾			
<i>Scenedesmus quadricauda</i>			0.59 ⁽⁷⁾	
<i>Scenedesmus sp.</i>			0.10 ⁽⁸⁾	
Optimum				
Cyanobacteria	46-49 ⁽¹⁾	8-11 ⁽⁹⁾	0.7-1.1 ^(1,9)	
Chrysophytes		3.3-5 ⁽⁹⁾	2.1 ⁽⁹⁾	
Chlorophytes	49-56 ⁽¹⁾	6.6-1.9 ⁽⁹⁾	1.2-2.9 ^(1,9)	
In General ⁽¹⁰⁾	51-56	8.0-10.4	0.8-1.45	

References: (1) Anon (1968); (2) Healey (1973); (3) Gerloff & Skoog (1954); (4) Lund (1965); (5) Lund (1950); (6) Mackereth (1953); (7) Nalewajko & Lean (1978); (8) Rhee (1973); (9) Strickland (1965); (10) Reynolds (1984).

CONTROL FILE

KINETIC COEFFICIENTS

Example

ALG	STOICH	ALGP	ALGN	ALGC	ALGSI	ACHLA	APOM	ANEQN	ANPR
Alg 1		0.005	0.08	0.45	0.18	0.05	0.8	2	0.001
Alg 2		0.005	0.08	0.45	0.00	0.04	0.8	2	0.001
Alg 3		0.005	0.08	0.45	0.00	0.1000	0.8	2	0.001

Related Cards and Files

[Algal Rates](#)

[Algal Extinction](#)

[Algal Temperature Rate Coefficients](#)

Epiphyte/Periphyton Control (EPIPHYTE)

FIELD	NAME	VALUE	DEFAULT	DESCRIPTION
1				(Ignored by code)
2-10	EPIWBC	Character	OFF	Waterbody epiphyte/periphyton computations, ON or OFF

This card allows the user to turn ON/OFF epiphyton/periphyton computations and their effects on water quality for a given waterbody. This flexibility allows the user to decrease model complexity and computation time for waterbodies where epiphyton/periphyton impacts are not considered important.

Example

```
EPIPHYTE  EPIWBC  EPIWBC  EPIWBC  EPIWBC  EPIWBC  EPIWBC  EPIWBC  EPIWBC
Epi 1      ON      ON      ON      ON      ON      ON      ON      ON
```

Related Cards and Files

[Epiphyte Print](#)

[Epiphyte Initial Density](#)

[Epiphyte Rate](#)

[Epiphyte Half-Saturation](#)

[Epiphyte Temperature Rate Coefficients](#)

[Epiphyte Stoichiometry](#)

Epiphyte/Periphyton Print (EPI PRINT)

FIELD	NAME	VALUE	DEFAULT	DESCRIPTION
1				(Ignored by code)
2-10	EPRWBC	Character	OFF	epiphyte areal density output, ON or OFF

This card allows the user to turn ON/OFF epiphyton/periphyton biomass output in terms of areal density to the various output files for each waterbody.

Example

```
EPI PRINT EPRWBC  EPRWBC  EPRWBC  EPRWBC  EPRWBC  EPRWBC  EPRWBC  EPRWBC
Epi 1          ON      ON      ON      ON      ON      ON      ON      ON
```

Related Cards and Files

[Epiphyte Control](#)

[Epiphyte Initial Density](#)

[Epiphyte Rate](#)

[Epiphyte Half-Saturation](#)

[Epiphyte Temperature Rate Coefficients](#)

[Epiphyte Stoichiometry](#)

Epiphyte/Periphyton Initial Density (EPI INI)

FIELD	NAME	VALUE	DESCRIPTION
1			(Ignored by code)
2-10	EPIWBCI	Real	Initial areal density for each epiphyton//periphyton group, $g\ m^{-2}$

This card specifies the initial epiphyton/periphyton areal density for each waterbody.

Example

```
EPI INIT EPIWBCI EPIWBCI EPIWBCI EPIWBCI EPIWBCI EPIWBCI EPIWBCI EPIWBCI
Epi 1      10.0      10.0      10.0      10.0
```

Related Cards and Files

[Epiphyte Control](#)

[Epiphyte Print](#)

[Epiphyte Rate](#)

[Epiphyte Half-Saturation](#)

[Epiphyte Temperature Rate Coefficients](#)

[Epiphyte Stoichiometry](#)

Epiphyte/Periphyton Rate (EPI RATE)

FIELD	NAME	VALUE	DEFAULT	DESCRIPTION
1				(Ignored by code)
2	EG	Real	2.0	maximum epiphyton/periphyton growth rate, day^{-1}
3	ER	Real	0.04	maximum epiphyton/periphyton respiration rate, day^{-1}
4	EE	Real	0.04	maximum epiphyton/periphyton excretion rate, day^{-1}
5	EM	Real	0.1	maximum epiphyton/periphyton mortality rate, day^{-1}
6	EB	Real	0.001	epiphyton/periphyton burial rate, $m\ day^{-1}$
7	EHSP	Real	0.003	epiphyton half-saturation for phosphorus limited growth, $g\ m^{-3}$
8	EHSN	Real	0.014	epiphyton half-saturation for nitrogen limited growth, $g\ m^{-3}$
9	EHSSI	Real	-	epiphyton half-saturation for silica limited growth, $g\ m^{-3}$

This card specifies rates for epiphyton/periphyton growth, mortality, excretion, respiration, and burial. Additionally, values that affect the maximum epiphyton/periphyton growth rate including nutrient limited growth are also specified here. See the [Algal Rate](#) card for more detailed information, as the kinetic formulations are similar. Epiphyton/periphyton mortality becomes part of the LDOM and LPOM organic pool based on the variable EPOM (see EPI STOICH). The burial rate causes epiphyton/periphyton to be lost from the system and added to the first order sediment compartment.

Example

EPI RATE	EG	ER	EE	EM	EB	EHSP	EHSN	EHSSI
Epi 1	2.0	0.04	0.04	0.1	0.001	0.002	0.002	0.0

Related Cards and Files

[Epiphyte Control](#)
[Epiphyte Print](#)
[Epiphyte Initial Density](#)
[Epiphyte Half-Saturation](#)
[Epiphyte Temperature Rate Coefficients](#)
[Epiphyte Stoichiometry](#)

Epiphyte/Periphyton Half-Saturation (EPI HALF)

FIELD	NAME	VALUE	DEFAULT	DESCRIPTION
1				(Ignored by code)
2	ESAT	Real	75.0	light saturation intensity at maximum photosynthetic rate, $W\ m^{-2}$
3	EHS	Real	35.0	biomass limitation factor, $g\ m^{-2}$
4	ENEQN	Integer	2	ammonia preference factor equation for epiphyton/periphyton (1 or 2)
4	ENPR	Real	0.001	nitrogen half-saturation preference constant, mg/l - only used if ENEQN=2

This card specifies the light saturation intensity at maximum photosynthetic rate [ESAT], the half-saturation coefficient for epiphyton biomass limitation [EHS], and the nitrogen preference during epiphyton/periphyton growth [ENPR]. The ratio of nitrate-nitrite to ammonium taken up during epiphyton/periphyton growth increases as [ENPR] increases.

Field data during 2001 in the Spokane River have shown that biomass (dry weight) for epiphyton/periphyton can vary significantly from 13 to over 500 g/m^2 , with median values of about 40 g/m^2 (Annear, et al., 2005). Field data of periphyton biomass needs though to be examined to ensure that it is representative of active epiphyton, which CE-QUAL-W2 computes. For example in this model study, a value of EHS of 35 g/m^2 was used.

Certain epiphyton groups are known to preferentially uptake ammonium over nitrate. If the equation number [ANEQN] for algal nitrogen uptake is set to 1, then the epiphyton/periphyton nitrogen preference factor for ammonium is computed using:

$$P_{NH4} = \frac{C_{NH4}}{(C_{NO3} + C_{NH4})}$$

and the preference for nitrate is:

$$P_{NO3} = \frac{C_{NO3}}{(C_{NO3} + C_{NH4})}.$$

If the equation number [ANEQN] is set to 2, then the epiphyton/periphyton preference for ammonium is computed using the following equation (Thomann and Fitzpatrick, 1982):

$$P_{NH4} = C_{NH4} \frac{C_{NOx}}{(K_{mN} + C_{NH4})(K_{mN} + C_{NOx})} + C_{NH4} \frac{K_{mN}}{(C_{NH4} + C_{NOx})(K_{mN} + C_{NOx})}$$

P_{NH4} = ammonium preference factor

K_{mN} = N half-saturation coefficient, $mg\ l^{-1}$

C_{NH4} = ammonium nitrogen concentration. $mg\ l^{-1}$

C_{NOx} = nitrate-nitrite nitrogen concentration. $mg\ l^{-1}$

The nitrite-nitrate preference factor is then calculated from:

CONTROL FILE

KINETIC COEFFICIENTS

$$P_{NOx} = 1 - P_{NH4}$$

Example

EPI	HALF	ESAT	EHS	ENEQN	ENPR
Epi	1	150.00	35.0	2	0.001

Related Cards and Files

[Epiphyte Control](#)

[Epiphyte Print](#)

[Epiphyte Initial Density](#)

[Epiphyte Rate](#)

[Epiphyte Temperature Rate Coefficients](#)

[Epiphyte Stoichiometry](#)

Epiphyte/Periphyton Temperature Rate Coefficients (EPI TEMP)

FIELD	NAME	VALUE	DEFAULT	DESCRIPTION
1				(Ignored by code)
2	ET1	Real	5.0	Lower temperature for epiphyton growth, °C
3	ET2	Real	25.0	Lower temperature for maximum epiphyton/periphyton growth, °C
4	ET3	Real	35.0	Upper temperature for maximum epiphyton/periphyton growth, °C
5	ET4	Real	40.0	Upper temperature for epiphyton/periphyton growth, °C
6	EK1	Real	0.1	Fraction of epiphyton/periphyton growth rate at ET1
7	EK2	Real	0.99	Fraction of maximum epiphyton/periphyton growth rate at ET2
8	EK3	Real	0.99	Fraction of maximum epiphyton/periphyton growth rate at ET3
9	EK4	Real	0.1	Fraction of epiphyton/periphyton growth rate at ET4

This card specifies the lower, maximum lower, upper, and maximum upper temperatures used in defining the curve that determines effects of temperature on epiphyton/periphyton rates. Also specified is the fraction of maximum epiphyton/periphyton rates that occurs at the specified temperature. Since the epiphyton compartment was first introduced in V3.1, the default values have no basis other than these are the same default values used for algae in V2, so there is little experience in the use of these values.

How temperature affects epiphyton/periphyton growth is shown below for the default values of ET1 through ET4 and EK1 through EK4.

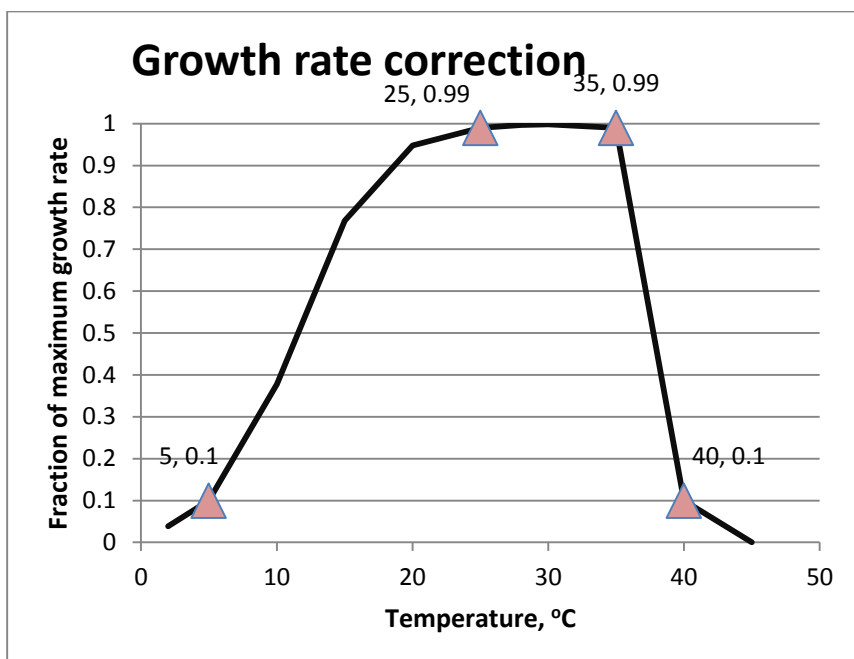


Figure 40. Growth rate as a function of temperature.

Example

EPI	TEMP	ET1	ET2	ET3	ET4	EK1	EK2	EK3	EK4
Epi 1		5.0	18.0	20.0	24.0	0.1	0.99	0.99	0.01
Epi 2		10.0	30.0	35.0	40.0	0.1	0.99	0.99	0.01
Epi 3		10.0	35.0	40.0	50.0	0.1	0.99	0.99	0.01

Related Cards and Files

[Epiphyte Control](#)

[Epiphyte Print](#)

[Epiphyte Initial Density](#)

[Epiphyte Rate](#)

[Epiphyte Half-Saturation](#)

[Epiphyte Stoichiometry](#)

Epiphyte/Periphyton Stoichiometry (EPI STOICH)

FIELD	NAME	VALUE	DEFAULT	DESCRIPTION
1				(Ignored by code)
2	EP	Real	0.005	Stoichiometric equivalent between epiphyton/periphyton biomass and phosphorus
3	EN	Real	0.08	Stoichiometric equivalent between epiphyton/periphyton biomass and nitrogen
4	EC	Real	0.45	Stoichiometric equivalent between epiphyton/periphyton biomass and carbon
5	ESI	Real	0.18	Stoichiometric equivalent between epiphyton/periphyton biomass and silica
6	ECHLA	Real	0.05	Ratio between epiphyton/periphyton biomass and chlorophyll a [Not used at present], mg biomass/ μ g chlorophyll a
7	EPOM	Real	0.8	Fraction of epiphyton/periphyton biomass that is converted to particulate organic matter when epiphyton/periphyton die

This card specifies the stoichiometric equivalences used for determining the amount of nutrients in epiphyton/periphyton biomass. These ratios are not constant over time and vary by epiphyton/periphyton species. The ratio of epiphyton biomass to chlorophyll a is currently not used in the model. This ratio will be used in the future to provide output in chlorophyll a rather than dry weight biomass. In addition, the epiphyton/periphyton to chlorophyll *a* ratio [ECHLA] is known to be different for different epiphyton/periphyton species and is known to vary over time for a given epiphyton/periphyton species. Currently, the model does not include variable stoichiometry or biomass to chlorophyll *a* ratios. This is an area that will be improved upon in the future. [EPOM] is the fraction of epiphyton/periphyton biomass lost by mortality going into the detritus compartment (labile POM) with the remainder going to labile DOM.

Example

EPI STOICH	EP	EN	EC	ESI	ECHLA	EPOM
Epi 1	0.005	0.08	0.45	0.18	0.05	0.8
Epi 2	0.005	0.08	0.45	0.00	0.05	0.8
Epi 3	0.005	0.08	0.45	0.00	0.05	0.8

Related Cards and Files

[Epiphyte Control](#)

[Epiphyte Print](#)

[Epiphyte Initial Density](#)

[Epiphyte Rate](#)

[Epiphyte Half-Saturation](#)

[Epiphyte Temperature Rate Coefficients](#)

Zooplankton Rate (ZOO RATE)

FIELD	NAME	VALUE	DEFAULT	DESCRIPTION
1				(Ignored by code)
2	ZG	Real	1.50	maximum zooplankton growth or ingestion rate, day^{-1}
3	ZR	Real	0.10	maximum zooplankton respiration rate, day^{-1}
4	ZM	Real	0.01	maximum zooplankton mortality (non-predatory) rate, day^{-1}
5	ZEFF	Real	0.50	Zooplankton assimilation efficiency or the proportion of food assimilated to food consumed (dimensionless), from 0 to 1.
6	PREFP	Real	0.50	Preference factor of zooplankton for detritus or LPOM (dimensionless), from 0 to 1.
7	ZOOMIN	Real	0.01	Threshold food concentration at which zooplankton feeding begins, $g\ m^{-3}$
8	ZS2P	Real	0.3	Zooplankton half-saturation constant for food (includes LPOM, algae, and zooplankton) ingestion, $g\ m^{-3}$

This card specifies rates for zooplankton growth, mortality and respiration. Additionally, the zooplankton assimilation efficiency and the preference factor of zooplankton for detritus are specified along with the threshold food concentration at which zooplankton feeding begins and the zooplankton half-saturation constant for food ingestion.

Example

ZOO RATE	ZG	ZR	ZM	ZEFFIC	PREFP	ZOOMIN	ZS2P
Zoo1	1.50	0.10	0.010	0.50	0.50	0.0100	0.30

Related Cards and Files

Zooplankton Algal Preference (ZOOPL ALGP)

FIELD	NAME	VALUE	DEFAULT	DESCRIPTION
1				(Ignored by code)
2-10	PREFA	Real	0.5	Preference factor of zooplankton for algae (dimensionless) from 0 to 1.

This card specifies the feeding preference of zooplankton for each algal species. For example, many zooplankton will avoid certain algae species as a food source, in that case the PREFA would be zero.

Note that the sum of the preference factors can be greater than 1 since the model normalizes them internally in the code.

Example

ZOOP ALGP	PREFA	PREFA	PREFA	PREFA	PREFA	PREFA	PREFA	PREFA	PREFA
Zoo1	1.00	0.50	0.50						

Related Cards and Files

Zooplankton Zooplankton Preference (ZOOZ ZOOZ)

FIELD	NAME	VALUE	DEFAULT	DESCRIPTION
1				(Ignored by code)
2-10	PREFZ	Real	0.0	Preference factor of zooplankton for zooplankton (dimensionless) from 0 to 1.

This card specifies the feeding preference of zooplankton for each zooplankton species. The card below shows that for the one zooplankton group, it does not feed on itself. Note that the sum of the preference factors can be greater than 1 since the model normalizes them internally in the code.

Example

ZOOZ ZOOZ	PREFZ	PREFZ	PREFZ	PREFZ	PREFZ	PREFZ	PREFZ	PREFZ	PREFZ	PREFZ
Zoo1	0.00									

Related Cards and Files

Zooplankton Temperature Rate Coefficients (ZOOPTMP)

FIELD	NAME	VALUE	DEFAULT	DESCRIPTION
1				(Ignored by code)
2	ZT1	Real	5.0	Lower temperature for zooplankton growth, °C
3	ZT2	Real	25.0	Lower temperature for maximum zooplankton growth, °C
4	ZT3	Real	35.0	Upper temperature for maximum zooplankton growth, °C
5	ZT4	Real	40.0	Upper temperature for zooplankton growth, °C
6	ZK1	Real	0.1	Fraction of zooplankton growth rate at ZT1
7	ZK2	Real	0.99	Fraction of maximum zooplankton growth rate at ZT2
8	ZK3	Real	0.99	Fraction of maximum zooplankton growth rate at ZT3
9	ZK4	Real	0.1	Fraction of zooplankton growth rate at ZT4

This card specifies the lower, maximum lower, upper, and maximum upper temperatures used in defining the curve that determines effects of temperature on zooplankton rates. Also specified is the fraction of maximum zooplankton rates that occurs at the specified temperature.

How temperature affects zooplankton growth is shown below for the default values of ZT1 through ZT4 and ZK1 through ZK4.

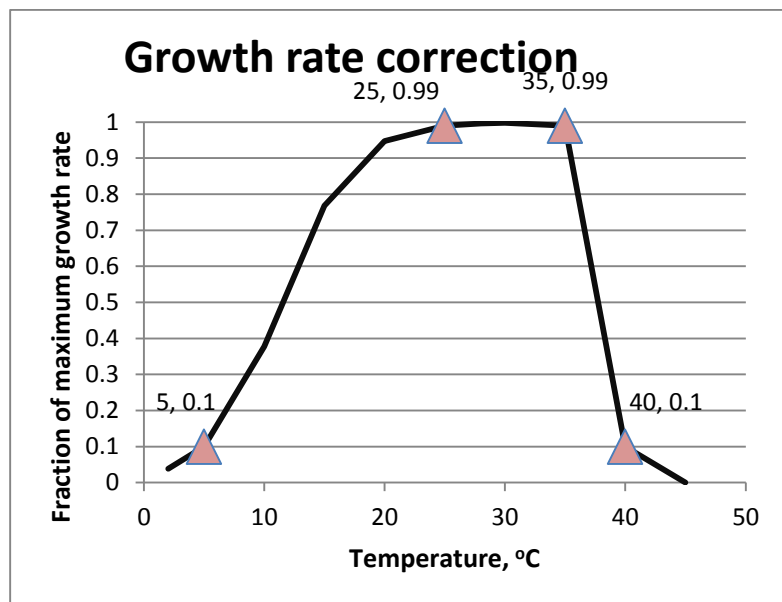


Figure 41. Growth rate as a function of temperature.

CONTROL FILE

KINETIC COEFFICIENTS

Example

ZOOP TEMP	ZT1	ZT2	ZT3	ZT4	ZK1	ZK2	ZK3	ZK4
Zoo1	0.0	15.0	20.0	36.0	0.1	0.9	0.98	0.100

Related Cards and Files

Zooplankton Stoichiometry (ZOO STOI)

FIELD	NAME	VALUE	DEFAULT	DESCRIPTION
1				(Ignored by code)
2	ZP	Real	0.005	Stoichiometric equivalent between zooplankton biomass and phosphorus
3	ZN	Real	0.08	Stoichiometric equivalent between zooplankton biomass and nitrogen
4	ZC	Real	0.45	Stoichiometric equivalent between zooplankton biomass and carbon

This card specifies the stoichiometric equivalences used for determining the amount of nutrients in zooplankton biomass. These ratios are not constant over time and vary by zooplankton species.

Example

```
ZOOP STOI      ZP      ZN      ZC
      0.01500 0.08000 0.45000
```

Related Cards and Files

Macrophyte Control (MACROPHYT)

FIELD	NAME	VALUE	DEFAULT	DESCRIPTION
1				(Ignored by code)
2-10	MACWBC	Character	OFF	Waterbody macrophyte computations, ON or OFF

This card allows the user to turn ON/OFF macrophyte computations and their effects on water quality for a given waterbody. This flexibility allows the user to decrease model complexity and computation time for waterbodies where macrophyte impacts are not considered important.

Example

MACROPHYT	MACWBC	MACWBC	MACWBC	MACWBC	MACWBC	MACWBC	MACWBC	MACWBC	MACWBC
Mac1	ON	OFF	OFF						

Related Cards and Files

Macrophyte Print (MAC PRINT)

FIELD	NAME	VALUE	DEFAULT	DESCRIPTION
1				(Ignored by code)
2-10	MPRWBC	Character	OFF	macrophyte concentration output, ON or OFF

This card allows the user to turn ON/OFF macrophyte biomass output to the SNP (snapshot) file and to the CPL file (only if TECPLOT='OFF') for each waterbody.

Example

```
MAC PRINT MPRWBC MPRWBC MPRWBC MPRWBC MPRWBC MPRWBC MPRWBC MPRWBC MPRWBC
Mac1      ON      OFF      OFF
```

Related Cards and Files

Macrophyte Initial Concentration (MAC INI)

FIELD	NAME	VALUE	DESCRIPTION
1			(Ignored by code)
2-10	MACWBCI	Real	Initial macrophyte concentration for each macrophyte group, gm^{-3}

This card specifies the initial macrophyte concentration for each waterbody. Without an initial concentration or seed, the macrophyte groups will not grow. The model currently does not have self-seeding of macrophytes.

Example

```
MAC INI  MACWBCI MACWBCI MACWBCI MACWBCI MACWBCI MACWBCI MACWBCI MACWBCI MACWBCI
Mac1      0.10000      0.1      0.5
```

Related Cards and Files

Macrophyte Rate (MAC RATE)

FIELD	NAME	VALUE	DEFAULT	DESCRIPTION
1				(Ignored by code)
2	MG	Real	0.3	maximum macrophyte growth rate, day^{-1}
3	MR	Real	0.05	maximum macrophyte respiration rate, day^{-1}
4	MM	Real	0.05	maximum macrophyte mortality rate, day^{-1}
5	MSAT	Real	30.0	light saturation intensity at maximum photosynthetic rate, W m^{-2}
6	MHSP	Real	0.0	macrophyte half-saturation for phosphorus limited growth, g m^{-3}
7	MHSN	Real	0.0	macrophyte half-saturation for nitrogen limited growth, g m^{-3}
8	MHSC	Real	0.0	macrophyte half-saturation for carbon limited growth, g m^{-3}
9	MPOM	Real	0.9	Fraction of macrophyte biomass that is converted to particulate organic matter when macrophytes die
10	LRPMAC	Real	0.2	Fraction of POM which originates as dead macrophytes becoming labile POM

This card specifies rates for macrophyte growth, mortality and respiration. Additionally, values that affect the maximum macrophyte growth rate including nutrient limited growth, light saturation, fraction of dead biomass converted to POM, and the fraction of POM originating from dead biomass becoming refractory POM are also specified here.

Light limitation was modeled with a hyperbolic equation which has the same form as the Michaelis-Menten function:

$$f(I) = \frac{I}{I + I_h}$$

where

I : solar radiation (W/m^2)

I_h : half-saturation coefficient for solar radiation (W/m^2)

The following table shows macrophyte coefficient values used in an application of CE-QUAL-R1 to Eau Galle Reservoir, Wisconsin (Collins and Wlosinski, 1989).

Table 62. Coefficients used in CE-QUAL-R1 to simulate macrophytes (from Collins and Wlosinski, 1989).

Description	Value	Reference
Carbon fraction of dry weight [MC] – see Macrophyte Stoichiometry	0.46	Soeder et al. (1969)
Maximum gross production rate [MG]	0.42 day^{-1}	Van et al. (1976)
Maximum dark respiration rate [MR]	0.05 day^{-1}	McGahee and Davis (1971)

CONTROL FILE

KINETIC COEFFICIENTS

Description	Value	Reference
Fraction of dead tissue to dissolved organic matter	0.2	Wetzel and Manny (1972)
Fraction of dead tissue to detritus [MPOM]	0.4	Godshalk and Wetzel (1978)
Fraction of dead tissue to sediments	0.4	Carpenter (1976)
Critical low temperature for metabolic processes [MT1] - See Macrophyte Temperature Rate Coefficients	7° C	Van et al. (1976)
Low optimum temperature for metabolic processes [MT2] - See Macrophyte Temperature Rate Coefficients	21° C	Barko et al. (1980)
High optimum temperature for metabolic processes [MT3] - See Macrophyte Temperature Rate Coefficients	24° C	Barko et al. (1980)
Critical high temperature [MT4] - See Macrophyte Temperature Rate Coefficients	34° C	Barko et al. (1980)
Volumetric density factor	40 g m ⁻³	Filbin and Barko (1985)

Example

MAC RATE	MG	MR	MM	MSAT	MHSP	MHSN	MHSC	MPOM	LRPMAC
Mac 1	0.30	0.05	0.05	30.0	0.0	0.0	0.0	0.9	0.2

Related Cards and Files

Macrophyte Sediments (MAC SED)

FIELD	NAME	VALUE	DEFAULT	DESCRIPTION
1				(Ignored by code)
2	PSED	Real	1.0	Fraction of phosphorus uptake by macrophytes obtained from sediments
3	NSED	Real	1.0	Fraction of nitrogen uptake by macrophytes obtained from sediments

This card specifies the fraction of phosphorus and nitrogen uptake obtained from the sediments. The remaining fraction of uptake will be obtained from the water column. Depending on the macrophyte species, nitrogen and phosphorus may be obtained from the sediments or the water column. If they are obtained from the sediments, the sediments are assumed to be an infinite pool that cannot limit growth.

Example

MAC SED	PSED	NSED
MAC 1	0.5	0.5

Related Cards and Files

Macrophyte Distribution (MAC DIST)

FIELD	NAME	VALUE	DEFAULT	DESCRIPTION
1				(Ignored by code)
2	MBMP	Real	40.0	Threshold macrophyte concentration for which growth is moved to the above layer, $g\ m^{-3}$
3	MMAX	Real	500.0	Maximum macrophyte concentration, $g\ m^{-3}$

This card specifies the concentration at which macrophyte growth will be moved to the above layer and the maximum macrophyte concentration. Plants grow upwards from the sediment through model layers. Growth upward is accomplished by moving the growth of a layer to the layer above if the concentration in the layer is greater than a threshold concentration and the concentration in the upper layer is less than the same threshold concentration.

Example

```
MAC DIST      MBMP      MMAX
Mac 1         40.0      500.0
```

Related Cards and Files

Macrophyte Drag (MAC DRAG)

FIELD	NAME	VALUE	DEFAULT	DESCRIPTION
1				(Ignored by code)
2	CDDRAG	Real	2.0	Macrophyte drag coefficient
3	DWV	Real	7.0e+04	Macrophyte dry weight to wet volume ratio, $g\ m^{-3}$
4	DWSA	Real	8.0	Macrophyte dry weight to surface area ratio, $g\ m^{-2}$
5	ANORM	Real	0.3	Fraction of macrophyte surface area normal to direction of flow

This card specifies the coefficients which simulate the frictional effects and porosity of macrophytes. The macrophyte drag coefficient, dry weight to wet volume ratio, dry weight to surface area ratio, and the fraction of macrophyte surface area facing the direction of flow are specified. Measured values for the ratio of dry weight to wet volume are shown in Table 63, and literature values for the ratio of dry weight to surface area are listed in Table 64.

Table 63. Values for the ratio between dry weight to wet volume ratio.

Species	Dry wt. to wet volume $g\ m^{-3}$	Reference
<i>Elodea Canadensis</i>	7.3e+04	Berger (2000)
<i>Ceratophyllum demersum</i>	5.4e+04	Berger (2000)

Table 64. Literature values for the ration of dry weight to surface area.

Species	Ratio of dry weight to wet surface area ($g\ m^{-2}$)	Reference
<i>Elodea canadensis</i>	7.97	Sher-Kaul et al. (1995)
<i>Myriophyllum spicatum</i>	8.30	Sher-Kaul et al. (1995)
<i>Nitellopsis obtuse</i>	17.86	Sher-Kaul et al. (1995)
<i>Potamogeton lucens</i>	15.75	Sher-Kaul et al. (1995)
<i>Potamogeton pectinatus</i>	20.00	Sher-Kaul et al. (1995)
<i>Potamogeton perfoliatus</i>	13.12	Sher-Kaul et al. (1995)

```
MAC DRAG  CDDRAG      DWV      DWSA  ANORM
Mac 1      3.0 7.0E+04      8.0      0.3
```

Related Cards and Files

Macrophyte Temperature Rate Coefficients (MAC TEMP)

FIELD	NAME	VALUE	DEFAULT	DESCRIPTION
1				(Ignored by code)
2	MT1	Real	5.0	Lower temperature for macrophyte growth, °C
3	MT2	Real	25.0	Lower temperature for maximum macrophyte growth, °C
4	MT3	Real	35.0	Upper temperature for maximum macrophyte growth, °C
5	MT4	Real	40.0	Upper temperature for macrophyte growth, °C
6	MK1	Real	0.1	Fraction of macrophyte growth rate at MT1
7	MK2	Real	0.99	Fraction of maximum macrophyte growth rate at MT2
8	MK3	Real	0.99	Fraction of maximum macrophyte growth rate at MT3
9	MK4	Real	0.1	Fraction of macrophyte growth rate at MT4

This card specifies the lower, maximum lower, upper, and maximum upper temperatures used in defining the curve that determines effects of temperature on macrophyte rates. Also specified is the fraction of maximum macrophyte rates that occurs at the specified temperature.

How temperature affects macrophyte growth is shown below for the default values of MT1 through MT4 and MK1 through MK4.

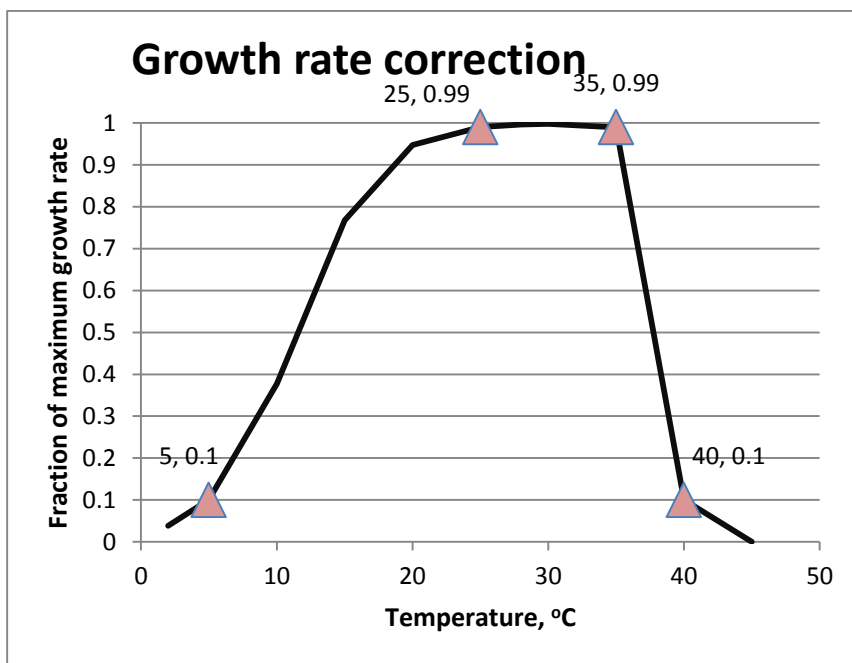


Figure 42. Growth rate as a function of temperature.

KINETIC COEFFICIENTS

CONTROL FILE

Example

MAC TEMP	MT1	MT2	MT3	MT4	MK1	MK2	MK3	MK4
Mac 1	7.0	15.0	24.0	34.0	0.1	0.99	0.99	0.01

Related Cards and Files

Macrophyte Stoichiometry (MAC STOICH)

FIELD	NAME	VALUE	DEFAULT	DESCRIPTION
1				(Ignored by code)
2	MP	Real	0.005	Stoichiometric equivalent between macrophyte biomass and phosphorus
3	MN	Real	0.08	Stoichiometric equivalent between macrophyte biomass and nitrogen
4	MC	Real	0.45	Stoichiometric equivalent between macrophyte biomass and carbon

This card specifies the stoichiometric equivalences used for determining the amount of nutrients in macrophyte biomass.

Example

```
MAC STOICH      MP      MN      MC
Mac 1          0.005    0.08    0.45
```

Related Cards and Files

Dissolved Organic Matter (DOM)

FIELD	NAME	VALUE	DEFAULT	DESCRIPTION
1				(Ignored by code)
2	LDOMDK	Real	0.1	Labile DOM decay rate, <i>day</i> ⁻¹
3	RDOMDK	Real	0.001	Refractory DOM decay rate, <i>day</i> ⁻¹
4	LRDDK	Real	0.01	Labile to refractory DOM decay rate, <i>day</i> ⁻¹

This card specifies decay rates associated with dissolved organic matter. Dissolved organic matter in the model is divided into labile and refractory partitions. The labile partition has a higher decay rate and generally consists of autochthonous inputs such as early products of algal decay. The refractory decay rate, [RDOMDK], is generally two orders of magnitude smaller than the labile decay rate [LDOMDK]. If BOD decay rates are available, then they should be used as a starting point for [LDOMDK].

Table C-65. Labile DOM Decay Rate Literature Values.

Compound	Decay Rate, <i>day</i> ⁻¹	Reference
Acetate	0.20	Wright, 1975
Amino acids	0.64	Williams et al., 1976
Glucose	0.24	Williams et al., 1976
Glucose	0.32-0.50	Toerien and Cavari, 1982
Glucose	0.11	Wright, 1975
Glutamate	0.11-0.63	Carney and Colwell, 1976
Glycine	0.31-0.45	Vaccaro, 1969
Glycolate	0.01-0.43	Wright, 1975

Example

DOM	LDOMDK	RDOMDK	LRDDK
Wb 1	0.12	0.001	0.001
Wb 2	0.12	0.001	0.001
Wb 3	0.12	0.001	0.001

Related Cards and Files

[Particulate Organic Matter](#)
[Organic Matter Stoichiometry](#)
[Organic Matter Temperature Rate Multipliers](#)
[Carbonaceous Biochemical Oxygen Demand](#)

Particulate Organic Matter (POM)

FIELD	NAME	VALUE	DEFAULT	DESCRIPTION
1				(Ignored by code)
2	LPOMDK	Real	0.08	Labile POM decay rate, day^{-1}
3	RPOMDK	Real	0.001	Refractory POM decay rate, day^{-1}
4	LRPDK	Real	0.01	Labile to refractory POM decay rate, day^{-1}
5	POMS	Real	0.1	POM settling rate, $m \text{ day}^{-1}$

Detritus in the model consists of autochthonous and allochthonous particulate organic matter (POM). The model uses a single decay rate [LPOMDK], but in reality, detritus is a heterogeneous mixture in various stages of decay. Allochthonous inputs are usually dominated by the refractory component while autochthonous inputs are initially labile becoming refractory over time. Literature values are given in the following tables.

Table C-66. Detritus Decay Rate Literature Values

Detritus Source	Detritus Decay Rate, day^{-1}	Reference
Cladophora glomerata	0.007	Piecznska, 1972
Gloeotrichia echinulata	0.001-0.007	Piecznska, 1972
Isoetes lancustris	0.003-0.015	Hanlon, 1982
Potamogeton crispus	0.002-0.004	Rogers & Breen, 1982
Potamogeton perfoliatus	0.002-0.007	Hanlon, 1982
Beech litter	0.001-0.004	Hanlon, 1982
Green algae	0.016-0.076	Otsuki & Hayna, 1972
Mixed algae	0.007-0.111	Jewell & McCarty, 1971
Mixed algae	0.007-0.060	Fitzgerald, 1964
Leaf packs	0.005-0.017	Sedell, Triska, and Triska, 1975

Detrital settling velocities [POMS] vary over a large range (0.001 to $> 20 m \text{ day}^{-1}$) depending upon the detritus. Again, the model allows for only a single value. Literature values are given in [Table C-67](#).

Table C-67. Detritus Settling Velocity Literature Values

Detritus Source	Settling Velocity, $m \text{ day}^{-1}$	Reference
Ceratium balticum	9.0	Apstein, 1910
Chaetoceros borealis	9.0	Apstein, 1910
Chaetoceros didymus	0.85	Eppley, Holmes, & Strickland, 1967
Cricosphaera carterae	1.70	Eppley, Holmes, & Strickland, 1967
Ditylum brightwellii	2.0	Apstein, 1910
Phaeodactylum tricornutum	0.02-0.04	Riley, 1943
Rhizosolenia herbata	0.22	Eppley, Holmes, & Strickland, 1967b
Stephanopyxis tunis	2.1	Eppley, Holmes, & Strickland, 1976b
Tabellaria flocculosa	0.46-1.5	Smayda, 1971
Thalassiosira pseudonana	0.85	Hecky & Kilham, 1974

Example

POM	LPOMDK	RPOMDK	LRPDK	POMS
WB 1	0.08	0.001	0.001	0.5
WB 2	0.08	0.001	0.001	0.5
WB 3	0.08	0.001	0.001	0.5

KINETIC COEFFICIENTS

CONTROL FILE

Related Cards and Files

[Dissolved Organic Matter](#)

[Organic Matter Stoichiometry](#)

[Organic Matter Temperature Rate Multipliers](#)

[Carbonaceous Biochemical Oxygen Demand](#)

Organic Matter Stoichiometry (OM STOICH)

FIELD	NAME	VALUE	DEFAULT	DESCRIPTION
1				(Ignored by code)
2	ORGP	Real	0.005	Stoichiometric equivalent between organic matter and phosphorus
3	ORGN	Real	0.08	Stoichiometric equivalent between organic matter and nitrogen
4	ORGC	Real	0.45	Stoichiometric equivalent between organic matter and carbon
5	ORGSi	Real	0.18	Stoichiometric equivalent between organic matter and silica

This card specifies the stoichiometric relationship between organic matter and inorganic nutrients. The user has the ability to change the relationship between waterbodies, although this option is not recommended. The values should not be changed from the defaults unless the user has the data to support the changes. If the variables: LDOM-P, RDOM-P, LPOM-P, and RPOM-P, are not active, the model does not track the dynamic stoichiometry of the organic P pool and uses the ORGP for the stoichiometric ratio between P and organic matter. If these variables are active, ORGP represents the initial P stoichiometry of organic matter set by the initial concentration of LDOM, RDOM, LPOM, and RPOM. Similarly, if the variables: LDOM-N, RDOM-N, LPOM-N, and RPOM-N, are not active, the model does not track the dynamic stoichiometry of the organic N pool and uses the ORGN for the stoichiometric ratio between N and organic matter. If these variables are active, ORGN represents the initial N stoichiometry of organic matter set by the initial concentration of LDOM, RDOM, LPOM, and RPOM.

Example

OM STOICH	ORGP	ORGN	ORGC	ORGSi
Wb 1	0.005	0.08	0.45	0.18
Wb 2	0.005	0.08	0.45	0.18
Wb 3	0.005	0.08	0.45	0.18

Related Cards and Files

[Dissolved Organic Matter](#)

[Particulate Organic Matter](#)

[Organic Matter Temperature Rate Multipliers](#)

[Carbonaceous Biochemical Oxygen Demand](#)

Organic Matter Temperature Rate Multipliers (OM RATE)

FIELD	NAME	VALUE	DEFAULT	DESCRIPTION
1				(Ignored by code)
2	OMT1	Real	4.0	Lower temperature for organic matter decay, °C
3	OMT2	Real	25.0	Upper temperature for organic matter decay, °C
4	OMK1	Real	0.1	Fraction of organic matter decay rate at OMT1
5	OMK2	Real	0.99	Fraction of organic matter decay rate at OMT2

This card specifies the lower and maximum temperatures used in defining the curve that determines effects of temperature on organic matter decay. Recommended values are given in the example.

The decay rate correction as a function of temperature is shown below for OMT1=5, OMK1=0.1, OMT2=25 and OMK2=0.99.

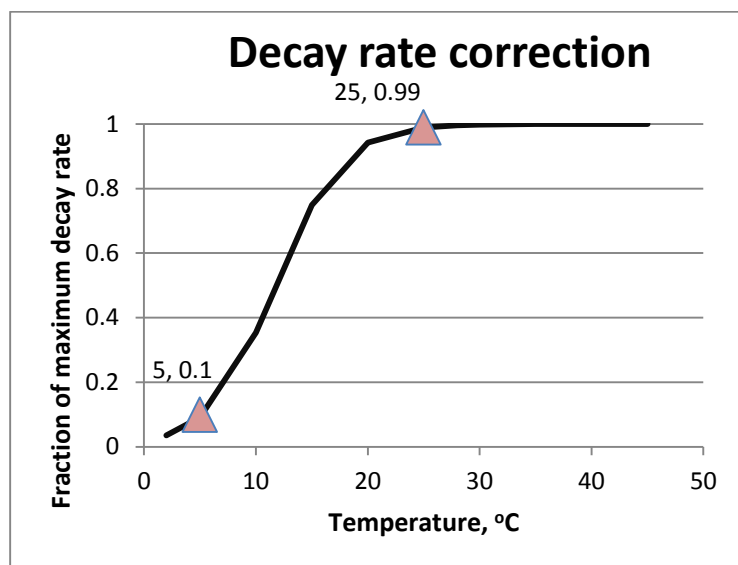


Figure 43. Organic matter decay as a function of temperature.

Example

OM RATE	OMT1	OMT2	OMK1	OMK2
Wb 1	4.0	25.0	0.1	0.99
Wb 2	4.0	25.0	0.1	0.99
Wb 3	4.0	25.0	0.1	0.99

Related Cards and Files

[Dissolved Organic Matter](#)
[Particulate Organic Matter](#)
[Organic Matter Stoichiometry](#)
[Carbonaceous Biochemical Oxygen Demand](#)

Carbonaceous Biochemical Oxygen Demand (CBOD)

FIELD	NAME	VALUE	DEFAULT	DESCRIPTION
1				(Ignored by code)
2	KBOD	Real	0.1	5-day decay rate @ 20°C, <i>day</i> ⁻¹
3	TBOD	Real	1.02	Temperature coefficient
4	RBOD	Real	1.85	Ratio of CBOD5 to ultimate CBOD
5	CBODS	Real	0.0	CBOD settling rate, <i>m day</i> ⁻¹

The model allows the user to include any number of CBOD groups (see [Constituent Dimensions](#) card). This allows the user to specify multiple point source loadings of CBOD with different rates associated with them and track them in the model over space and time.

[KBOD] is the first-order reaction rate for CBOD decay. [TBOD] is used to adjust the decay rate for temperature effects according to the following equation:

$$KBOD = KBOD_{20} * TBOD^{T-20}$$

where:

T = temperature, °C

$KBOD_{20}$ = decay rate at 20 °C

[RBOD] is used to convert 5-day CBOD values to ultimate CBOD. This formulation is included for applications that involve determining the effects of waste effluents on dissolved oxygen in which loadings are typically expressed in terms of CBOD. Note that if data are already in BOD-ultimate form, [RBOD]=1.0.

Settling rates for CBOD groups can be applied with [CBODS]. This allows for specification of particulate CBOD groups.

Example

CBOD	KBOD	TBOD	RBOD	CBODS
CBOD 1	0.25	1.0147	1.85	0.0
CBOD 2	0.25	1.0147	1.85	0.0
CBOD 3	0.25	1.0147	1.85	0.0

Related Cards and Files

[CBOD Stoichiometry](#)

CBOD Stoichiometry (CBOD STOICH)

FIELD	NAME	VALUE	DEFAULT	DESCRIPTION
1				(Ignored by code)
2	CBODP	Real	0.004	P stoichiometry for CBOD decay
3	CBODN	Real	0.06	N stoichiometry for CBOD decay
4	CBODC	Real	0.32	C stoichiometry for CBOD decay

The stoichiometric coefficients define the stoichiometry of BOD in terms of N, P, and C. Each coefficient expresses the fraction of N, P or C in terms of BOD. These are not the same as the organic matter stoichiometric coefficients defined in terms of N, P, or C in terms of organic matter. A typical conversion from organic matter to oxygen is about 1.4 (see [Oxygen Stoichiometry 1](#)). Note that if CBOD-P and CBOD-N are OFF in the CST ACTIVE card, CBODN and CBODP will represent the fixed stoichiometry of the CBOD group. If CBOD-P and CBOD-N are ON, then CBODN and CBODP are not used. The C stoichiometry for each CBOD group though is always fixed and is CBODC.

Example

CBOD	STOIC	CBODP	CBODN	CBODC
CBOD 1		0.004	0.06	0.32
CBOD 2		0.004	0.06	0.32
CBOD 3		0.004	0.06	0.32

Related Cards and Files

[Carbenaceous Biochemical Oxygen Demand](#)

Inorganic Phosphorus (PHOSPHOR)

FIELD	NAME	VALUE	DEFAULT	DESCRIPTION
1				(Ignored by code)
2	PO4R	Real	0.001	Sediment release rate of phosphorus, fraction of SOD
3	PARTP	Real	0.0	Phosphorus partitioning coefficient for suspended solids

[PO4R] is the sediment release rate of phosphorous under anaerobic conditions specified as a fraction of the sediment oxygen demand. Hence, the PO4 release rate under anaerobic conditions is [PO4R]*[SOD] in units of g/m²/day modified by the temperature multiplier for SOD. Hence the rate chosen is dependent on the SOD rate. Often, P release rates are very site-specific. Sen et al. (2004) determined an average anaerobic P release rate of 0.57 mg/m²/day for Beaver Lake, Arkansas. Auer et al. (1993) found rates in a hypereutrophic lake from 9-21 mg/m²/day (mean 13 mg/m²/day). Kim et al. (2004) found rates in the summer between 20-24°C up to 16 mg/m²/day. Spears et al. (2007) showed that for a large shallow lake recovering from high nutrient that the maximum P release was 12 mg/m²/day. James et al. (1995) found that P release rates for Lake Pepin, an impoundment on the upper Mississippi River, were between 3.8 and 15 mg/m²/day.

[PARTP] is the phosphorous partitioning coefficient for sorption onto suspended solids. In the current model formulations, it is not recommended to allow phosphorus to sorb onto inorganic suspended solids unless clear evidence for this mechanism is known, so [PARTP] should be set to zero. Note that concentrations of PO₄ in the model are in units of PO₄ as P. Note that the model does not have a mechanism for desorption of P from the inorganic suspended solids to the water column.

Example

PHOSPHOR	PO4R	PARTP
Wb 1	0.015	0.0
Wb 2	0.015	0.0
Wb 3	0.015	0.0

Ammonium (AMMONIUM)

FIELD	NAME	VALUE	DEFAULT	DESCRIPTION
1				(Ignored by code)
2	NH4REL	Real	0.001	Sediment release rate of ammonium, fraction of SOD
3	NH4DK	Real	0.12	Ammonium decay rate, day^{-1}

[NH4REL] is the sediment release rate of ammonium anaerobic conditions specified as a fraction of the sediment oxygen demand. Hence, when there is anoxia, the rate of ammonia release is approximately the (SOD rate)*(NH4REL) in units of g NH₄-N/m²/day or if divided by the layer height in m in units of g NH₄-N/m³/day. These rates are modified by the temperature multiplier for SOD. Beutel (2006) showed that release rates of ammonia-N can vary from less than 5 to more than 15 mg NH₄-N/m²/day between oligotrophic to hypereutrophic lakes, respectively.

[NH4DK] is the rate at which ammonium is oxidized to nitrate-nitrite. Since the model considers nitrate-nitrite as one compartment, the rate specified should be the rate for conversion of ammonium to nitrate. Literature values are given in the following table.

Note that concentrations of ammonia in the model are in terms of NH₄ as N.

Table C-68. Ammonium Decay Rate Literature Values

Site	Ammonium decay rate, day^{-1}	Reference
Grand River, IL	0.80	Bansal, 1976
Grasmerer Lake, UK	0.001-0.013	Hall, 1982
Truckee River, NV	0.09-1.30	Bansal, 1976
Mohawk River, NY	0.23-0.40	Bansal, 1976
Ohio River	0.25	Bansal, 1976
Big Blue River, NB	0.17-0.25	Bansal, 1976
Flint River, MI	0.76-0.95	Bansal, 1976

McCutcheon (1987) measured the difference in BOD between samples with and without a nitrification inhibitor in order to estimate nitrification rates. The measured rates are shown in Table 69. The measured streams were relatively deep with low velocities and lacked well-developed periphyton communities.

Table 69. Nitrification rates measured by McCutcheon (1987).

Reaction	Source	Nitrification rate (d^{-1})
Nitrification	Chattahoochee River, Georgia	0.26
Nitrification	West Fork Trinity River, Texas	0.50

Example

AMMONIUM	NH4R	NH4DK
Wb 1	0.001	0.12
Wb 2	0.001	0.12
Wb 3	0.001	0.12

CONTROL FILE

KINETIC COEFFICIENTS

Related Cards and Files

[Ammonium Temperature Rate Multipliers](#)

Ammonium Temperature Rate Multipliers (NH4 RATE)

FIELD	NAME	VALUE	DEFAULT	DESCRIPTION
1				(Ignored by code)
2	NH4T1	Real	5.0	Lower temperature for ammonia decay, °C
3	NH4T2	Real	25.0	Lower temperature for maximum ammonia decay, °C
4	NH4K1	Real	0.1	Fraction of nitrification rate at NH4T1
5	NH4K2	Real	0.99	Fraction of nitrification rate at NH4T2

This card specifies the lower and maximum lower temperatures used in defining the curve that determines the effect of temperature on ammonia nitrification. See Appendix B for more details on the mathematical formulation for the temperature coefficients. Recommended values are given in the example.

The ammonia decay rate correction as a function of temperature is shown below for NH4T1=5, NH4K1=0.1, NH4T2=25 and NH4K2=0.99.

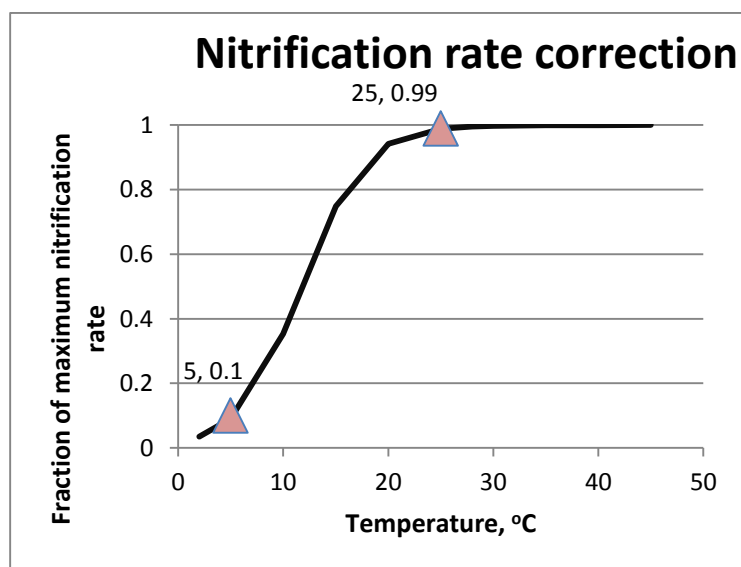


Figure 44. Ammonia decay as a function of temperature.

Example

NH4 RATE	NH4T1	NH4T2	NH4K1	NH4K2
Wb 1	5.0	25.0	0.1	0.99
Wb 2	5.0	25.0	0.1	0.99
Wb 3	5.0	25.0	0.1	0.99

Related Cards and Files

[Ammonium](#)

Nitrate (NITRATE)

FIELD	NAME	VALUE	DEFAULT	DESCRIPTION
1				(Ignored by code)
2	NO3DK	Real	0.03	Nitrate decay rate, day^{-1}
3	NO3S	Real	0.001	Denitrification rate from sediments, $m\ day^{-1}$
4	FNO3SED	Real	0.0	Fraction of NO_3 -N diffused into the sediments that becomes part of organic N in the sediments (The rest is denitrified.)

This card specifies the denitrification rates in the water column and from the water column to the sediments. Values used in previous modeling studies for the nitrate decay rate [NO3DK] have ranged from 0.05-0.15 day^{-1} . [NO3S] is analogous to a settling velocity and represents how fast nitrate is diffused into the sediments where it undergoes denitrification.

Of the NO_3 -N that is diffused into the sediments, a fraction of that, f_{NO_3-SED} , is incorporated into organic matter in the sediments. The rest, $1 - f_{NO_3-SED}$, is denitrified into N_2 . Wetzel shows that in one study 37% of the NO_3 -N of lake sediments was incorporated into bacterial organic matter. If 1st order sediments are not active, then all of the NO_3 -N diffused into the sediments is assumed to be denitrified. Be careful in using this term in conjunction with [NO3S] since the stoichiometry of sediments (C:N:P ratios) can be changed by allowing this to occur.

Note that concentrations of nitrate in the model are in terms of NO_3 as N.

Example

NITRATE	NO3DK	NO3S	FNO3SED
Wb 1	0.05	0.001	0.00
Wb 2	0.05	0.001	0.37
Wb 3	0.05	0.001	0.37

Related Cards and Files

[Nitrate Temperature Rate Multipliers](#)

Nitrate Temperature Rate Multipliers (NO3 RATE)

FIELD	NAME	VALUE	DEFAULT	DESCRIPTION
1				(Ignored by code)
2	NO3T1	Real	5.0	Lower temperature for nitrate decay, °C
3	NO3T2	Real	25.0	Lower temperature for maximum nitrate decay, °C
4	NO3K1	Real	0.1	Fraction of denitrification rate at NO3T1
5	NO3K2	Real	0.99	Fraction of denitrification rate at NO3T2

This card specifies the lower and maximum lower temperatures used in defining the curve that determines the effect of temperature on denitrification. See [Appendix B](#) for more details on the mathematical formulation for the temperature coefficients. Recommended values are given in the example.

The denitrification rate correction as a function of temperature is shown below for NO3T1=5, NO3K1=0.1, NO3T2=25 and NO3K2=0.99.

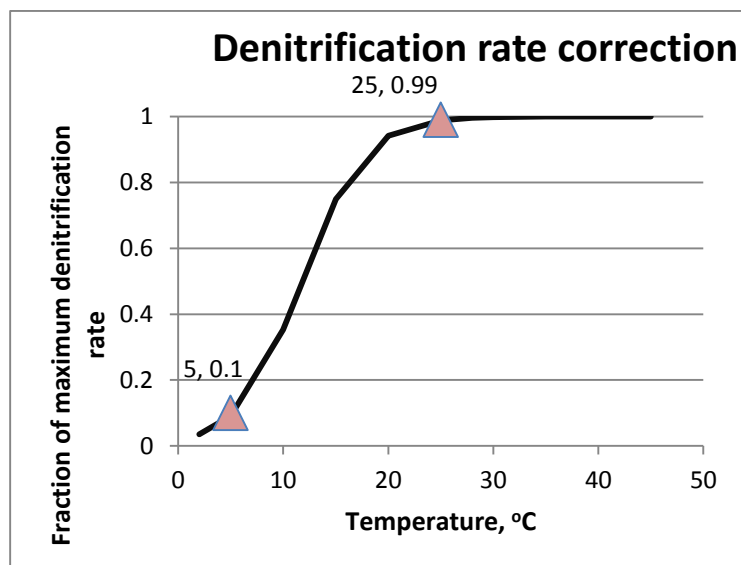


Figure 45. Denitrification as a function of temperature.

Example

NO3 RATE	NO3T1	NO3T2	NO3K1	NO3K2
Wb 1	5.0	25.0	0.1	0.99
Wb 2	5.0	25.0	0.1	0.99
Wb 3	5.0	25.0	0.1	0.99

Related Cards and Files

[Nitrate](#)

Silica (SILICA)

FIELD	NAME	VALUE	DEFAULT	DESCRIPTION
1				(Ignored by code)
2	DSIR	Real	0.1	Dissolved silica sediment release rate, fraction of SOD
3	PSIS	Real	1.0	Particulate biogenic settling rate, $m\ sec^{-1}$
4	PSIDK	Real	0.3	Particulate biogenic silica decay rate, day^{-1}
5	PARTSI	Real	0.0	Dissolved silica partitioning coefficient

This card specifies the relevant kinetic coefficient for silica kinetics. [DSIR] is the sediment release rate of dissolved silica from the zero-order sediment compartment. [PSIS] is the particulate biogenic settling rate and [PSIDK] is the particulate biogenic decay rate. Particulate biogenic silica represents the skeletal remains of diatoms. Dissolved silica is allowed to partition onto suspended solids and [PARTSI] is the value of the partitioning coefficient.

Example

SILICA	DSIR	PSIS	PSIDK	PARTSI
Wb 1	0.1	0.0	0.3	0.2
Wb 2	0.1	0.0	0.3	0.2
Wb 3	0.1	0.0	0.3	0.2

Related Cards and Files

[Algal Stoichiometry](#)

[Epiphyte Stoichiometry](#)

[Zero-Order Sediment Oxygen Demand](#)

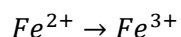
Iron (IRON)

FIELD	NAME	VALUE	DEFAULT	DESCRIPTION
1				(Ignored by code)
2	FEREL	Real	0.5	Iron sediment release rate, fraction of sediment oxygen demand
3	FESETL	Real	2.0	Iron settling velocity, $m\ day^{-1}$

[FER] specifies the iron release rate from the sediments as a fraction of the sediment oxygen demand. Values between 0.3 and 0.5 have been used in previous modeling studies, but this is a function of the 0-order SOD calibration values that should change from system to system.

[FES] is the particulate iron settling rate in the water column under oxic conditions. Values between 0.5 and 2.0 have been used in previous modeling studies.

This state variable can be thought of representing total metals. In an oxidizing environment reduced iron is oxidized as



The model uses [PARTP] to partition or sorb [PO4-P] onto the oxidized form. The model at present does not take up oxygen during the oxidation process.

Example

```
IRON      FER      FES
          0.5      2.0
```

Related Cards and Files

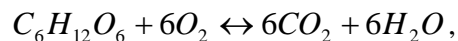
[Zero-Order Sediment Oxygen Demand](#)

Sediment Carbon Dioxide Release (SED CO2)

FIELD	NAME	VALUE	DEFAULT	DESCRIPTION
1				(Ignored by code)
2	CO2REL	Real	1.2	Sediment carbon dioxide release rate, fraction of sediment oxygen demand

This card specifies the carbon dioxide release rate from the sediments as a fraction of the 0-order sediment oxygen demand.

Values as high as 1.4 have been used in earlier modeling studies. If one considers the CO₂ release as a fraction of O₂ uptake from



the stoichiometric ratio of O₂ to CO₂ is 32 g O₂/44 g CO₂ or 0.8 g O₂/g CO₂ for a CO2REL of 1/0.8 or 1.25.

Example

```
SED CO2    CO2REL
          1.0
```

Related Cards and Files

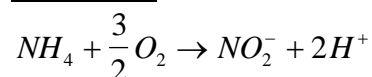
[Zero-Order Sediment Oxygen Demand](#)

Oxygen Stoichiometry 1 (STOICH 1)

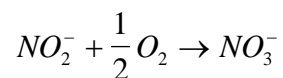
FIELD	NAME	VALUE	DEFAULT	DESCRIPTION
1				(Ignored by code)
2	O2NH4	Real	4.57	Oxygen stoichiometry for nitrification
3	O2OM	Real	1.4	Oxygen stoichiometry for organic matter decay

This card specifies the stoichiometric equivalents of oxygen for nitrification, organic matter decay. The default values should not be changed unless the user has data to support the change.

Nitrification



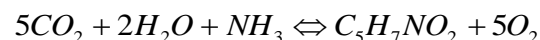
3.43 g O₂ required for 1 g N oxidized



1.14 g O₂ required for 1 g N oxidized for a total of 4.57 g O₂/g N. Gaudy and Gaudy (1980) recommend that the O₂ demand approaches 4.2 g O₂/g N because of cellular needs for N.

Organic matter

Assuming the organic matter represents average algal and bacterial composition (C₅H₇NO₂) (Golterman, 1975; Wang et al., 1978), the stoichiometric requirements are 1.4 g O₂/g organic matter from the following equation:



Example

STOICH 1	O2NH4	O2OM
Wb 1	4.57	1.4
Wb 2	4.57	1.4
Wb 3	4.57	1.4

Related Cards and Files

[Oxygen Stoichiometry 2](#)
[Oxygen Stoichiometry 3](#)

Oxygen Stoichiometry 2 (STOICH 2)

FIELD	NAME	VALUE	DEFAULT	DESCRIPTION
1				(Ignored by code)
2	O2AR	Real	1.1	Oxygen stoichiometry for algal respiration
3	O2AG	Real	1.4	Oxygen stoichiometry for algal primary production

This card specifies the stoichiometric equivalents of oxygen for algal respiration and algal primary production.

The biological oxygen requirement for respiration is based on converting carbohydrate to carbon dioxide and water, such as



or 1.1 g O₂/g organic matter. EPA (1985) reports model applications where [O2AR] varied from 0.95 to 2.3 mg O₂/mg dry weight algae biomass.

[O2AG] rates reported in modeling studies have varied from 1.24 to 1.8 mg O₂/mg dry weight algae biomass (EPA, 1985). Ruane (2014) reported that values from 1.8-2.0 were often required to produce supersaturation.

Example

STOICH 2	O2AR	O2AG
Alg 1	1.1	1.4
Alg 2	1.1	1.4
Alg 3	1.1	1.4

Related Cards and Files

[Oxygen Stoichiometry 1](#)
[Oxygen Stoichiometry 3](#)

Oxygen Stoichiometry 3 (STOICH 3)

FIELD	NAME	VALUE	DEFAULT	DESCRIPTION
1				(Ignored by code)
2	O2ER	Real	1.1	Oxygen stoichiometry for epiphyton/periphyton respiration
3	O2EG	Real	1.4	Oxygen stoichiometry for epiphyton/periphyton primary production

This card specifies the stoichiometric equivalents of oxygen for epiphyton/periphyton respiration and epiphyton/periphyton primary production. The default values should not be changed unless the user has data to support the change.

Example

```

STOICH 3      O2ER      O2EG
Ep 1          1.1       1.4
Ep 2          1.1       1.4
Ep 3          1.1       1.4

```

Related Cards and Files

[Oxygen Stoichiometry 1](#)
[Oxygen Stoichiometry 2](#)

Oxygen Stoichiometry 4 (STOICH 4)

FIELD	NAME	VALUE	DEFAULT	DESCRIPTION
1				(Ignored by code)
2	O2ZR	Real	1.1	Oxygen stoichiometry for zooplankton respiration

This card specifies the stoichiometric equivalents of oxygen for zooplankton respiration. The default values should not be changed unless the user has data to support the change.

Example

```
STOICH 4      O2ZR
ZOO1         1.10000
```

Related Cards and Files

[Oxygen Stoichiometry 1](#)

[Oxygen Stoichiometry 2](#)

Oxygen Stoichiometry 5 (STOICH 5)

FIELD	NAME	VALUE	DEFAULT	DESCRIPTION
1				(Ignored by code)
2	O2MR	Real	1.1	Oxygen stoichiometry for macrophyte respiration
3	O2MG	Real	1.4	Oxygen stoichiometry for macrophyte primary production

This card specifies the stoichiometric equivalents of oxygen for macrophyte respiration and macrophyte primary production. The default values should not be changed unless the user has data to support the change.

Example

```
STOICH 5      O2MR      O2MG
MAC1          1.1       1.4
```

Related Cards and Files

[Oxygen Stoichiometry 1](#)
[Oxygen Stoichiometry 2](#)

Oxygen Limit (O2 LIMIT)

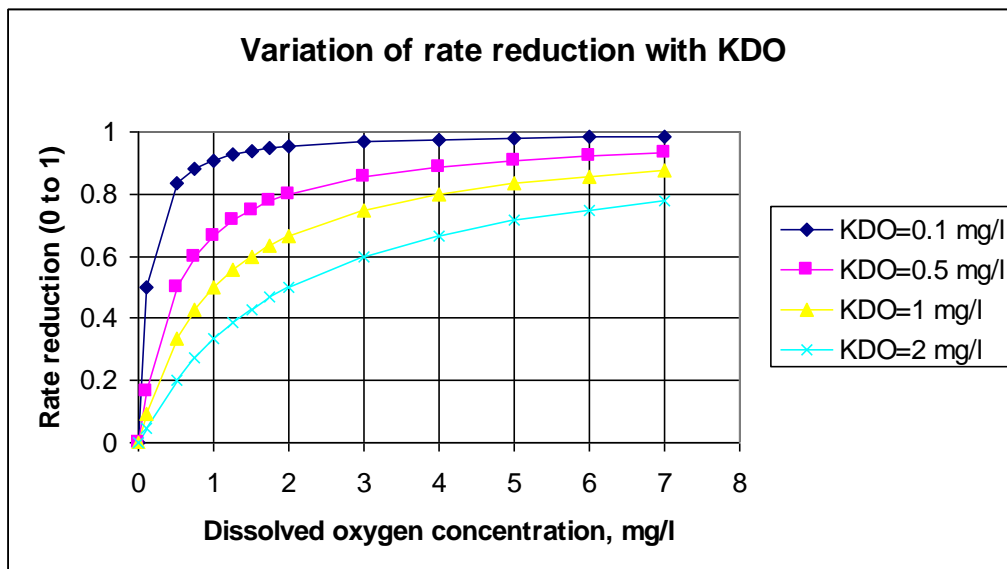
FIELD	NAME	VALUE	DEFAULT	DESCRIPTION
1				(Ignored by code)
2	KDO	Real	0.7	K _{DO} , Dissolved oxygen half-saturation constant or concentration at which aerobic processes are at 50% of their maximum, g m ⁻³

This card specifies the half-saturation constant or dissolved oxygen concentration at which oxic processes are at 50% of their normal oxic rates. Hence, sediment oxygen demand, nitrification, and other processes only occur when there is available oxygen. The change from aerobic to anaerobic processes occurs gradually by means of a Monod type formulation.

A Monod formulation is used though to move gradually from oxic to anoxic conditions. This reduction of oxic reactions as dissolved oxygen levels approach zero is based on specification of a dissolved oxygen half-saturation constant in the following equation:

$$\text{Rate Reduction} = \frac{\Phi_{DO}}{K_{DO} + \Phi_{DO}} \quad \text{where } \Phi_{DO} \text{ is the concentration of dissolved oxygen and } K_{DO} \text{ is}$$

a half-saturation dissolved oxygen concentration when oxic reactions are half of their maximum without limitation of oxygen conditions. Earlier versions of CE-QUAL-W2 used an ON-OFF oxygen limit for aerobic-anaerobic processes. Thomann and Mueller (1987) have used a value of K_{DO}=0.7 mg/l.



Example

```
O2 LIMIT      KDO
              0.7
```

Sediment Compartment (SEDIMENT)

FIELD	NAME	VALUE	DEFAULT	DESCRIPTION
1				(Ignored by code)
2	SEDC	Character	OFF	Turns ON/OFF the first-order sediment compartment
3	PRNSC	Character	OFF	Turns ON/OFF printing sediment organic matter concentrations to the snapshot file
4	SEDCI	Real	0.0	Initial sediment concentration, $g\ m^{-2}$
5	SEDK	Real	0.1	Sediment decay rate, day^{-1}
6	SEDS	Real	0.1	Sediment settling or focusing rate, $m\ day^{-1}$
7	FSOD	Real	1.0	Fraction of the zero-order SOD rate used
8	FSED	Real	1.0	Fraction of initial first-order sediment concentration
9	SEDBR	Real	0.01	Sediment burial rate, day^{-1}
10	DYNSEDK	Character	OFF	Turns ON/OFF dynamic calculation of the 1 st order sediment model decay rate

This card controls the behavior of the 0- and 1st-order sediment compartment. [SEDC] turns ON/OFF the 1st-order sediment compartment. The 1st-order sediment compartment is not a true sediment diagenesis compartment as it does not keep track of organic nutrient delivery to the sediments, their decay, and subsequent release back into the water column during hypoxic/anoxic conditions. However, it does keep track of organic matter delivery to the sediments via particulate organic matter and dead algal cells, and the subsequent water column oxygen demand that is exerted. The inclusion of the 1st-order sediment compartment makes the model more predictive in that any increase of organic matter delivery to the sediments will have an affect on the SOD.

[PRNSC] controls whether or not sediment organic matter concentrations that accumulate in the first-order SOD algorithm are output to the snapshot file. [SEDCI] specifies the initial “concentration(s)” for the 1st-order sediment compartment and its behavior is exactly the same as for setting the initial concentrations of any of the water column state variables, except that it is in units of mass per surface area or g/m^2 . Just as the algae are modeled as a dry weight of organic matter, the sediment concentration is also a dry weight of organic matter per bottom surface area.

The initial concentrations of Sediment-P, Sediment-N, and Sediment-C are based on the initial sediment concentration multiplied by the appropriate initial stoichiometric coefficient, [ORGP], [ORGN], and [ORGC], respectively. These nutrient ratios then are dynamically computed as organic matter accumulates and decays in the sediments. [SEDDK] specifies the sediment decay rate and should be somewhat less than the labile POM decay rate. [SEDS] is the velocity at which sediments that accumulate on each layer are settling or moving toward the bottom of the channel. In many systems turbulence tends to stir up and re-settle the sediments at lower and lower levels in the channel cross-section. In an earlier version (V3.2), the settling velocity of POM [POMS] was used to focus sediments toward the bottom. [FSOD] multiplies the values specified for the zero-order sediment compartment and can be used to rapidly adjust the SOD values during calibration. [FSED] is multiplied by the initial sediment concentration given either through the LPR, VPR or w2_con.npt files. [SEDBR] is the sediment burial rate. This allows sediments to effectively be bound and unavailable for further decay.

CONTROL FILE

KINETIC COEFFICIENTS

[DYNSEDK] allows the user to compute dynamically the sediment decay rate in the first order sediment model based on the organics that are deposited into the 1st order sediment compartment. If [DYNSEDK] is OFF, then the value of the maximum decay rate is [SEDDK]. It is then adjusted according to temperature. If [DYNSEDK] is turned ON, then the maximum sediment decay rate is computed based on the weighted mass average of the decay rates of material which has settled and the amount that is already residing in the sediments every time step for which kinetics are computed or updated.

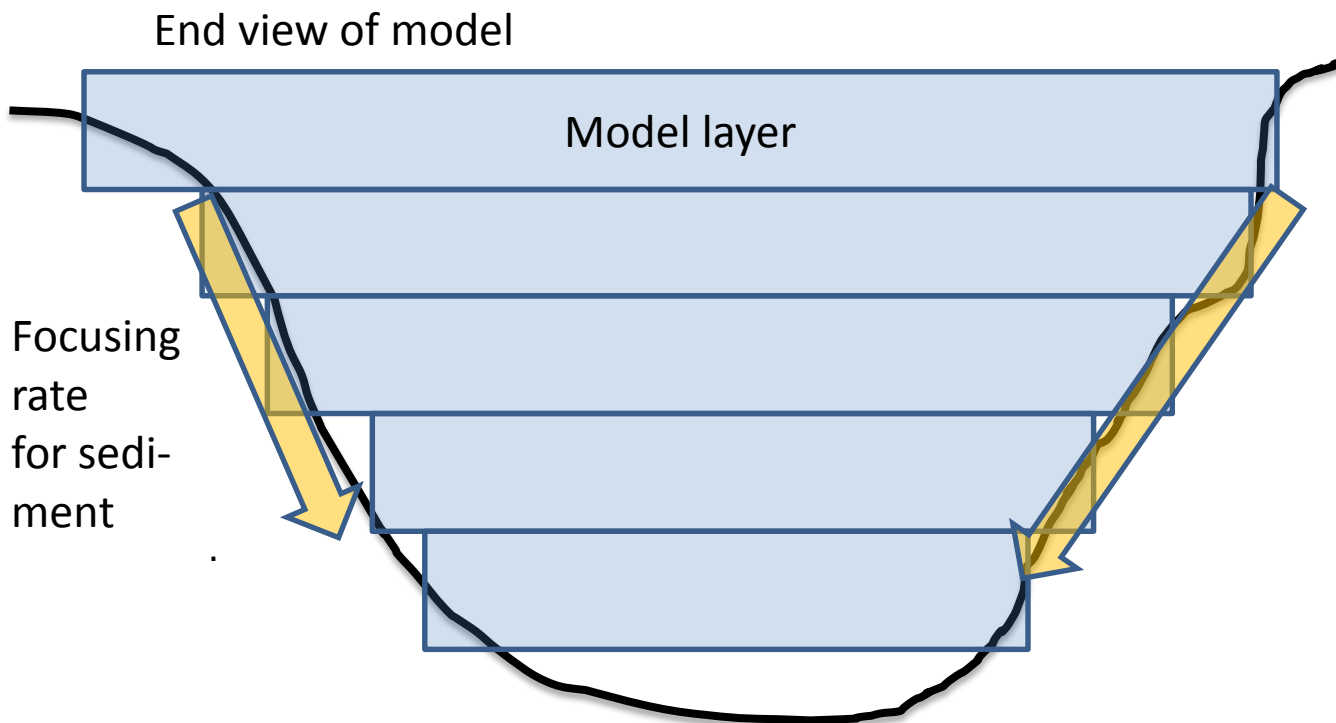


Figure 46. Illustration of sediment focusing rate.

Example

SEDIMENT	SEDC	PRNSC	SEDCI	SEDK	SEDS	FSOD	FSED	SEDBR	DYNSEDK
Wb 1	ON	ON	0.0	0.1	0.0	1.0	1.0	0.001	OFF
Wb 2	ON	ON	0.0	0.1	0.0	1.0	1.0	0.001	OFF
Wb 3	ON	ON	0.0	0.1	0.5	1.0	1.0	0.001	OFF

Related Cards and Files

[Zero-Order Sediment Oxygen Demand](#)
[SOD Temperature Rate Multipliers](#)

SOD Temperature Rate Multipliers (SOD RATE)

FIELD	NAME	VALUE	DEFAULT	DESCRIPTION
1				(Ignored by code)
2	SODT1	Real	4.0	Lower temperature for zero-order SOD or first-order sediment decay, °C
3	SODT2	Real	25.0	Upper temperature for zero-order SOD or first-order sediment decay, °C
4	SODK1	Real	0.1	Fraction of SOD or sediment decay rate at lower temperature
5	SODK2	Real	0.99	Fraction of SOD or sediment decay rate at upper temperature

This card specifies the temperature rate multipliers that adjust the 0-order SOD or 1st-order decay rate. The model is very sensitive to these values and they are an important calibration parameter for accurately reproducing the timing of water column oxygen decreases early during stratified periods. The SOD rate correction as a function of temperature is shown below for SODT1=5, SODK1=0.1, SODT2=25 and SODK2=0.99.

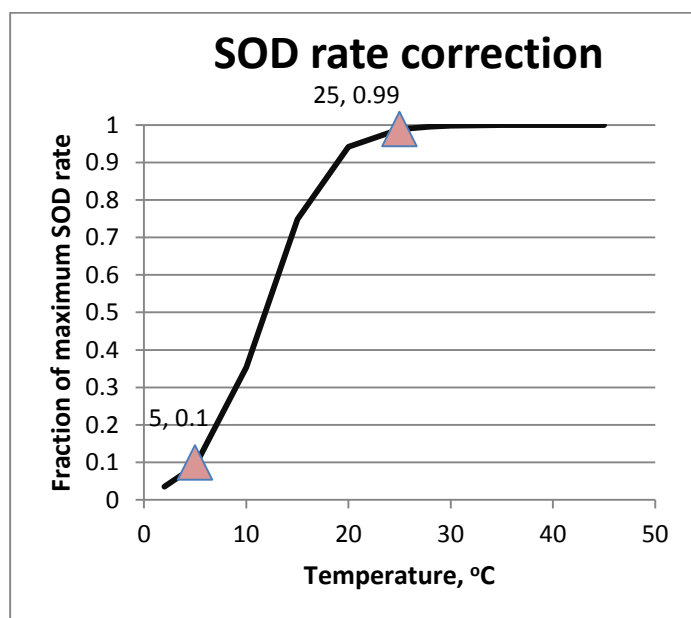


Figure 47. SOD rate as a function of temperature.

Example

SOD RATE	SODT1	SODT2	SODK1	SODK2
Wb 1	4.0	30.0	0.1	0.99
Wb 2	4.0	30.0	0.1	0.99
Wb 3	4.0	30.0	0.1	0.99

Related Cards and Files

[Sediment Compartment](#)

Zero-Order Sediment Oxygen Demand (S DEMAND)

FIELD	NAME	VALUE	DESCRIPTION
1			(Ignored by code)
2-10	SOD	Real	Zero-order sediment oxygen demand for each segment, $g\ O_2\ m^{-2}\ day^{-1}$

This card specifies the 0-order sediment oxygen demand for each segment (including boundary segments) in the computational grid. If there are *more* values than can be specified on one line, then they are continued on the next line without another **S DEMAND** card being specified.

Sediment oxygen demand is known to vary spatially in reservoirs due to differences in sedimentation patterns and algal production (Cole & Hannan, 1989). In the model, the user can specify a separate value of sediment oxygen demand [SOD] for each model segment. Sediment oxygen demand typically ranges from 0.1 to 1.0 $gO_2\ m^{-2}\ day^{-1}$, but can be higher (Newbold and Liggett, 1974). Additional information can be found in Gunnison, Chen, and Brannon (1983) and Chen, Brannon, and Gunnison (1984). Additional values are given in the following table.

Table C-70. Sediment Oxygen Demand Literature Values

Site	SOD, $g\ O_2\ m^{-2}\ day^{-1}$	Reference
Cayuga Lake, NY	0.3-1.0	Newbold & Liggett, 1974
Lake Sammamish, WA	1.0	Bella, 1970
Lake Lyndon B. Johnson, TX	1.7-5.8	Schnoor & Fruh, 1979
Saginaw River, MI	0.1-5.3	Chiaro & Burke, 1980

Example

S DEMAND	SOD	SOD	SOD	SOD	SOD	SOD	SOD	SOD	SOD
	0.3	0.3	0.3	0.3	0.3	0.3	0.3	0.3	0.3
	0.3	0.3	0.3	0.3	0.3	0.3	0.3	0.3	0.3
	0.3	0.3	0.3	0.3	0.3	0.3	0.3	0.3	0.3
	0.3	0.3	0.3	0.3	0.3	0.3	0.3	0.3	0.3
	0.3	0.3	0.3	0.3	0.3	0.3	0.3	0.3	0.3

Related Cards and Files

[Sediment Compartment](#)
[SOD Temperature Rate Multipliers](#)

Reaeration (REAERAT)

FIELD	NAME	VALUE	DEFAULT	DESCRIPTION
1				(Ignored by code)
2	REARC	Character	LAKE	Type of waterbody, RIVER, LAKE, or ESTUARY
3	EQN#	Integer	6 (if LAKE)	Equation number used for determining reaeration
4	COEF1	Real		User defined parameter
5	COEF2	Real		User defined parameter
6	COEF3	Real		User defined parameter
7	COEF4	Real		User defined parameter

This card allows the user to specify the appropriate reaeration formulation for the specific type of waterbody being simulated. [REARC] is used to specify the type of waterbody. [EQN#] is then used to specify the reaeration equation appropriate for the type of waterbody. The following table lists the equations for the RIVER waterbody type.

Table C-71. River Reaeration Equations

#	Equation	Comments	Applicability	Reference
0	Either Eq 1, 2 or 4	K_a is determined based on applicability criteria of each of these 3 formulations		Covar (1976)
1	$K_a = \frac{K_L}{H} = \frac{(D_{O_2} U)^{1/2}}{H^{3/2}}$	D_{O_2} = water molecular diffusion coefficient at 20°C, $8.1 \text{ E}^{-5} \text{ ft}^2 \text{ hr}^{-1}$ or $2.09 \text{ E}^{-5} \text{ cm}^2 \text{ s}^{-1}$ $D_{O_2} = 1.91 \text{ E}^{-3} (1.037)^{T-20}$, $\text{ft}^2 \text{ day}^{-1}$ U = velocity, ft/day H = depth, ft	Depths between 1-30 ft and velocities between 0.5-1.6 fps	O'Connor and Dobbins (1958)
2	$K_a = \frac{K_L}{H} = \frac{11.6U}{H^{1.67}}$	U = velocity, ft s^{-1} H = depth, ft K_a = reaeration rate, day^{-1}	Depths between 2-11 ft and velocities between 1.8-5 fps	Churchill, Elmore and Buckingham (1962)
3	$K_a = 0.88US \text{ for } 10 < Q < 300 \text{ cfs}$ $K_a = 1.8US \text{ for } 1 < Q < 10 \text{ cfs}$	S = slope, ft mile^{-1} U = velocity, ft s^{-1} K_a = reaeration rate, day^{-1}	Suggested for use when $Q < 10 \text{ cfs}$	Tsivoglou and Wallace (1972)
4	$K_a = \frac{K_L}{H} = \frac{21.6U^{0.67}}{H^{1.85}}$	U = velocity, ft s^{-1} H = depth, ft	Depths between 0.4-2.4 ft and velocities between 0.1-1.8 fps	Owens et al. (1964)
5	$K_a = \frac{K_L}{H} = \frac{25u^*}{H} (1 + F^{0.5})$	u^* = shear velocity, $(\text{HSg})^{0.5}$ S = energy grade line slope F = Froude number, $U/(gH)^{0.5}$		Thackston and Krenkel (1966)
6	$K_a = \frac{K_L}{H} = \frac{7.62U}{H^{1.33}}$	U = velocity, ft s^{-1} H = depth, ft		Langbien and Durum (1967)

#	Equation	Comments	Applicability	Reference
7	$K_a = 517(US)^{0.524}Q^{-0.242} \text{ for } Q < 0.556 \text{ m}^3 \text{ s}^{-1}$ $K_a = 596(US)^{0.528}Q^{-0.136} \text{ for } Q > 0.556 \text{ m}^3 \text{ s}^{-1}$	U = velocity, m s^{-1} S = slope, m m^{-1} Q = flow, $\text{m}^3 \text{ s}^{-1}$ K_a = reaeration rate, day^{-1}	For pool and riffle streams	Melching and Flores (1999)
8	$K_a = 88(US)^{0.313}D^{-0.353} \text{ for } Q < 0.556 \text{ m}^3 \text{ s}^{-1}$ $K_a = 142(US)^{0.333}D^{-0.66}W^{-0.243} \text{ for } Q > 0.556 \text{ m}^3 \text{ s}^{-1}$	U = velocity, m s^{-1} S = slope, m m^{-1} W = stream top width, m D = average depth, m K_a = reaeration rate, day^{-1}	For channel-control streams	Melching and Flores (1999)
9	$K_a = C_1 U^{C_2} H^{C_3} S^{C_4}$ <p>and if no channel slope:</p> $K_a = C_1 U^{C_2} H^{C_3}$	U = velocity, m s^{-1} H = depth, m S = slope [m/m or ft/ft] K_a = reaeration rate, day^{-1} C_1 = user defined C_2 = user defined C_3 = user defined C_4 = user defined	User defined relationship	
10	$K_a = \frac{K_L}{H} = \frac{5.0u^*}{H} (1 + 9F^{0.25})$	u^* = shear velocity, $(\text{HSg})^{0.5}$ S = slope of energy grade line F = Froude number, $U/(gH)^{0.5}$ K_a , day^{-1}		Thackston and Dawson (2001)

[Table C-72](#) lists the reaeration equations available for lakes, reservoirs, and estuaries in which it is assumed that wind is the dominant forcing function for reaeration.

Table C-72. Lake Reaeration Equations

#	Equation	Comments	Reference
1	$K_a = \frac{K_L}{H} = \frac{0.864W}{H}$	W = wind speed at 10 m , m s^{-1} H = depth, m K_L = reaeration velocity, m day^{-1}	Broecker et al (1978)
2	$K_a = \frac{K_L}{H} = \frac{\alpha W^\beta}{H}$	$\alpha=0.2$, $\beta=1.0$ for $W < 3.5 \text{ m s}^{-1}$ $\alpha=0.057$, $\beta=2.0$ for $W > 3.5 \text{ m s}^{-1}$ W = daily average wind speed, m s^{-1}	Gelda et al (1996)
3	$K_a = \frac{K_L}{H} = \frac{0.728W^{0.5} - 0.317W + 0.0372W^2}{H}$	W = wind speed at 10 m , m s^{-1} K_L = reaeration velocity, m day^{-1}	Banks and Herrera (1977)
4	$K_a = \frac{K_L}{H} = \frac{0.0986W^{1.64}}{H} \text{ at } T=20^\circ\text{C or}$ $K_a = \frac{K_L}{H} = \frac{0.0986W^{1.64}}{H} \left(\frac{600}{Sc} \right)^{0.5}$	W = wind speed at 10 m , m s^{-1} Sc = Schmidt number, $(\nu/D)=13750[0.10656 \exp(-0.0627T)+0.00495]$ T = temperature, $^\circ\text{C}$	Wanninkhof et al. (1991)
5	$K_a = \frac{K_L}{H} = \frac{\frac{D_{O_2}}{(200 - 60W^{0.5})10^{-6}}}{H}$	D_{O_2} = molecular diffusivity of oxygen, $\text{m}^2 \text{ s}^{-1}$, $2.1\text{E-}9 \text{ m}^2 \text{ s}^{-1}$ at 20°C W = wind speed, m s^{-1} K_L = reaeration velocity, m s^{-1}	Chen, Kanwisher (1963)
6	$K_a = \frac{K_L}{H} = \frac{0.5 + 0.05W^2}{H}$		Cole and Buchak (1995)

#	Equation	Comments	Reference
7	$K_a = \frac{K_L}{H} = \frac{0.362\sqrt{W}}{H} W < 5.5 \text{ m/s}$ $K_a = \frac{K_L}{H} = \frac{0.0277W^2}{H} W > 5.5 \text{ m/s}$		Banks (1975)
8	$K_a = \frac{K_L}{H} = \frac{0.64 + 0.128W^2}{H}$	Recommended form for WQRSS reservoir model	Smith (1978)
9	$K_a = \frac{K_L}{H} = \frac{0.156W^{0.63}}{H} W \leq 4.1 \text{ m s}^{-1}$ $K_a = \frac{K_L}{H} = \frac{0.0269W^{1.9}}{H} W > 4.1 \text{ m s}^{-1}$		Liss (1973)
10	$K_a = \frac{K_L}{H} = \frac{0.0276W^2}{H}$		Downing and Truesdale (1955)
11	$K_a = \frac{K_L}{H} = \frac{0.0432W^2}{H}$		Kanwisher (1963)
12	$K_a = \frac{K_L}{H} = \frac{0.319W}{H}$		Yu et al (1977)
13	$K_a = \frac{K_L}{H} = \frac{0.398}{H} W < 1.6 \text{ m s}^{-1}$ $K_a = \frac{K_L}{H} = \frac{0.155W^2}{H} W \geq 1.6 \text{ m s}^{-1}$		Weiler (1974)
14	$K_a = \frac{K_L}{H} = \frac{C_1 + C_2W^{C_3}}{H}$	W = wind speed, m s^{-1} at 10 m K_a = reaeration rate, day^{-1} C_1 = user defined C_2 = user defined C_3 = user defined	

For estuary systems, Thomann and Mueller (1987) and Chapra (1997) suggest using any of the wind formulations in [Table C-72](#) or Equation 1 in [Table C-71](#) (O'Connor-Dobbins formula) using the mean tidal velocity over a tidal cycle. [Table C-73](#) shows an additional formulation from Thomann and Fitzpatrick (1982) for estuaries, as well as the approach of Covar (1976) for rivers. Since many texts suggest using the mean tidal velocity, caution should be used in using these equations since they are based on the instantaneous velocity.

Table C-73. Estuarine Reaeration Equations

#	Equation	Comments	Reference
0	Either Eq 1, 2 or 4 from Table C-71	K_a is determined based on applicability criteria of each of these 3 formulations	Covar (1976)
1	$K_a = \frac{K_L}{H} = \frac{0.728W^{0.5} - 0.317W + 0.0372W^2}{H} + 3.93 \frac{\sqrt{U}}{H^{1.5}}$	U = mean tidal velocity, m s^{-1} W = wind speed, m s^{-1} H = depth, m K_L = reaeration velocity, m s^{-1} This formula combines the effect of wind from Banks and Herrera (1977) and estuary tidal flow	Thomann and Fitzpatrick (1982)

CONTROL FILE

KINETIC COEFFICIENTS

#	Equation	Comments	Reference
2	$K_a = C_1 U^{C_2} H^{C_3} + \frac{0.5 + C_4 W^2}{H}$	<i>U</i> = velocity, <i>m s</i> ⁻¹ <i>H</i> = depth, <i>m</i> <i>W</i> = wind speed at 10 <i>m</i> <i>K_a</i> = reaeration rate, <i>day</i> ⁻¹ <i>C</i> ₁ = user defined <i>C</i> ₂ = user defined <i>C</i> ₃ = user defined <i>C</i> ₄ = user defined	User defined relationship

In an estuary situation, a computation can be performed to evaluate whether wind shear or boundary shear controls the turbulence intensity at the surface. This algorithm will be added to the code in a future release version. For further information, see Appendix B.

Example

REAERAT	REARC	EQN#	COEF1	COEF2	COEF3	COEF4
Wb 1	RIVER	7				
Wb 2	LAKE	5				
Wb 3	ESTUARY	1				

Restart Input Filename (RSI FILE)

FIELD	NAME	VALUE	DESCRIPTION
1			(Ignored by code)
2-10	RSIFN	Character	Restart input data filename

This card specifies the filename used as input for restarts.

Example

```
RSI FILE.....RSIFN.....  
      rsi.npt
```

Withdrawal Filename (QWD FILE)

FIELD	NAME	VALUE	DESCRIPTION
1			(Ignored by code)
2-10	QWDFN	Character	Withdrawal filename

This card specifies the filename for withdrawal outflows. See a description of the [withdrawal file](#) for more information on data setup.

Example

```
QWD FILE.....QWDFN.....  
      qwd.npt
```

Gate Outflow Filename (QGT FILE)

FIELD	NAME	VALUE	DESCRIPTION
1			(Ignored by code)
2-10	QGTFN	Character	Gated outflow filename

This card specifies the filename(s) for branch outflows. See a description of the [gate outflow file](#) for more information on data setup.

Example

```
QGT FILE.....QGTFN.....  
      qgt.npt
```

Wind Sheltering Filename (WSC FILE)

FIELD	NAME	VALUE	DESCRIPTION
1			(Ignored by code)
2-10	WSCFN	Character	Wind sheltering Coefficient sheltering filename

This card specifies the filename containing the wind sheltering coefficients as a function of segment number and Julian date. One file contains all the wind sheltering coefficients for all waterbodies. See a description of the [wind-sheltering file](#) for more information on data setup.

Example

WSC FILE.....WSCFN.....
wsc.npt

Dynamic Shading Filename (SHD FILE)

FIELD	NAME	VALUE	DESCRIPTION
1			(Ignored by code)
2-10	SHDFN	Character	Dynamic shading filename

This card specifies the filename containing the wind sheltering coefficients as a function of segment number and Julian date. One file contains all the dynamic shading coefficients for all waterbodies. See a description of the [dynamic shading file](#) for more information on data setup.

Example

```
SHD FILE.....SHDFN.....  
      shd.npt
```

Bathymetry Filename (BTH FILE)

FIELD	NAME	VALUE	DESCRIPTION
1			(Ignored by code)
2-10	BTHFN	Character	Bathymetry filename

This card specifies the filename(s) containing the waterbody bathymetry. See a description of the [bathymetry file](#) for more information on the data setup.

Example

```
BTH FILE.....BTHFN.....  
Wb 1    bth_wb1.npt  
Wb 2    bth_wb2.npt  
Wb 3    bth_wb3.npt
```

Meteorology Filename (MET FILE)

FIELD	NAME	VALUE	DESCRIPTION
1			(Ignored by code)
2-10	METFN	Character	Meteorologic input data filename

This card specifies the filename(s) for time-varying meteorologic data. More information on data setup can be found in the description of the [meteorology input file](#).

Example

```
MET FILE.....METFN.....  
Wb 1    met_wb1.npt  
Wb 2    met_wb2.npt  
Wb 3    met_wb3.npt
```


Light Extinction Filename (EXT FILE)

FIELD	NAME	VALUE	DESCRIPTION
1			(Ignored by code)
2-10	EXTFN	Character	Light extinction input data filename

This card specifies the filename(s) for time-varying light extinction data in Julian day versus light extinction coefficient in m^{-1} . More information on data setup can be found in the description of the [light extinction file](#).

Example

```
EXT FILE.....EXTFN.....  
Wb 1      ext_wb1.npt - not used  
Wb 2      ext_wb2.npt - not used  
Wb 3      ext_wb3.npt - not used
```

Vertical Profile Filename (VPR FILE)

FIELD	NAME	VALUE	DESCRIPTION
1			(Ignored by code)
2-10	VPRFN	Character	Temperature and constituent vertical profile filename used for specifying initial conditions for the grid

This card specifies the filename(s) used to specify vertically varying initial temperatures and concentrations for the grid. More information on data setup can be found at the description of the [vertical profile file](#).

Example

```
VPR FILE.....VPRFN.....  
Wb 1      vpr_wb1.npt  
Wb 2      vpr_wb2.npt  
Wb 3      vpr_wb3.npt
```

Longitudinal Profile Filename (LPR FILE)

FIELD	NAME	VALUE	DESCRIPTION
1			(Ignored by code)
2-10	LPRFN	Character	Temperature and constituent longitudinal profile filename used for specifying initial conditions for the grid

This card specifies the filename(s) used to specify vertically and longitudinally varying initial temperatures and concentrations for the grid. More information on data setup can be found at the description of the [longitudinal profile file](#).

Example

```
LPR FILE.....LPRFN.....  
Wb 1      lpr_wb1.npt  
Wb 2      lpr_wb2.npt  
Wb 3      lpr_wb3.npt
```

Branch Inflow Filename (QIN FILE)

FIELD	NAME	VALUE	DESCRIPTION
1			(Ignored by code)
2-10	QINFN	Character	Inflow filename

This card specifies the filename(s) for branch inflows. More information on data setup can be found at the description of the [branch inflow file](#).

Example

```
QIN FILE.....QINFN.....  
Br 1    qin_br1.npt  
Br 2    qin_br2.npt  
Br 3    qin_br3.npt  
Br 4    qin_br4.npt
```

Branch Inflow Temperature Filename (TIN FILE)

FIELD	NAME	VALUE	DESCRIPTION
1			(Ignored by code)
2-10	TINFN	Character	Inflow temperature filename

This card specifies the filename(s) for branch inflow temperatures. More information on data setup can be found at the description of the [branch inflow temperature file](#).

Example

```
TIN FILE.....TINFN.....  
Br 1    tin_br1.npt  
Br 2    tin_br2.npt  
Br 3    tin_br3.npt  
Br 4    tin_br4.npt
```

Branch Inflow Constituent Filename (CIN FILE)

FIELD	NAME	VALUE	DESCRIPTION
1			(Ignored by code)
2-10	CINFN	Character	Inflow constituent filename

This card specifies the filename(s) for branch inflow concentrations. More information on data setup can be found at the description of the [branch inflow concentration file](#).

Example

```
CIN FILE.....CINFN.....  
Br 1    cin_br1.npt  
Br 2    cin_br2.npt  
Br 3    cin_br3.npt  
Br 4    cin_br4.npt
```

Branch Outflow Filename (QOT FILE)

FIELD	NAME	VALUE	DESCRIPTION
1			(Ignored by code)
2-10	QOTFN	Character	Outflow filename

This card specifies the filename(s) for branch outflows. More information on data setup can be found at the description of the [branch outflow file](#).

Example

```
QOT FILE.....QOTFN.....  
Br 1    qot_br1.npt  
Br 2    qot_br2.npt  
Br 3    qot_br3.npt  
Br 4    qot_br4.npt
```

Tributary Inflow Filename (QTR FILE)

FIELD	NAME	VALUE	DESCRIPTION
1			(Ignored by code)
2-10	QTRFN	Character	Tributary inflow filename

This card specifies the filename(s) for tributary inflows. There must be a separate file for each tributary. More information on data setup can be found at the description of the [tributary inflow file](#).

Example

```
QTR FILE.....QTRFN.....  
Tr 1      qtr_tr1.npt
```


Tributary Inflow Temperature Filename (TTR FILE)

FIELD	NAME	VALUE	DESCRIPTION
1			(Ignored by code)
2-10	TTRFN	Character	Tributary temperature filename

This card specifies the filename(s) for tributary inflow temperatures. There must be a separate file for each tributary. More information on data setup can be found at the description of the [tributary inflow temperature file](#).

Example

```
TTR FILE.....TTRFN.....  
Tr 1      ttr_tr1.npt
```

Tributary Inflow Concentration Filename (CTR FILE)

FIELD	NAME	VALUE	DESCRIPTION
1			(Ignored by code)
2-10	CTRFN	Character	Tributary inflow concentration filename

This card specifies the filename(s) for tributary inflow concentrations. There must be a separate file for each tributary. More information on data setup can be found at the description of the [tributary inflow concentration file](#).

Example

```
CTR FILE.....CTRFN.....  
Tr 1      ctr_tr1.npt
```

Distributed Tributary Inflow Filename (QDT FILE)

FIELD	NAME	VALUE	DESCRIPTION
1			(Ignored by code)
2-10	QDTFN	Character	Distributed tributary inflow filename

This card specifies the filename(s) for distributed tributary inflow. There must be a separate file for each branch. More information on data setup can be found at the description of the [distributed tributary inflow file](#).

Example

```
QDT FILE.....QDTFN.....  
Br 1    qdt_tr1.npt  
Br 2    qdt_tr2.npt  
Br 3    qdt_tr3.npt  
Br 4    qdt_tr4.npt
```

Distributed Tributary Inflow Temperature Filename (TDT FILE)

FIELD	NAME	VALUE	DESCRIPTION
1			(Ignored by code)
2-10	TDTFN	Character	Distributed tributary temperature filename

This card specifies the filename(s) for distributed tributary inflow temperatures. There must be a separate file for each branch. More information on data setup can be found at the description of the [distributed tributary inflow temperature file](#).

Example

```
TDT FILE.....TDTFN.....  
Br 1      tdt_tr1.npt  
Br 2      tdt_tr2.npt  
Br 3      tdt_tr3.npt  
Br 4      tdt_tr4.npt
```

Distributed Tributary Inflow Concentration Filename (CDT FILE)

FIELD	NAME	VALUE	DESCRIPTION
1			(Ignored by code)
2-10	CDTFN	Character	Distributed tributary inflow concentration filename

This card specifies the filename(s) for distributed tributary inflow concentrations. There must be a separate file for each branch. More information on data setup can be found at the description of the [distributed tributary inflow concentration file](#).

Example

```
CDT FILE.....CDTFN.....  
Br 1    cdt_tr1.npt  
Br 2    cdt_tr2.npt  
Br 3    cdt_tr3.npt  
Br 4    cdt_tr4.npt
```

Precipitation Filename (PRE FILE)

FIELD	NAME	VALUE	DESCRIPTION
1			(Ignored by code)
2-10	PREFN	Character	Precipitation filename

This card specifies the filename(s) for each branch precipitation. There must be a separate file for each branch. More information on data setup can be found at the description of the [precipitation file](#). The “ - not used” tag at the end of the filename is useful when looking at the echoing of input filenames in the [preprocessor output](#) and can alert the user to an input option that is or is not being used. If precipitation is turned ON for a branch, then the “ - not used” tag should be removed.

Example

```
PRE FILE.....PREFN.....
Br 1    pre_br1.npt - not used
Br 2    pre_br2.npt - not used
Br 3    pre_br3.npt - not used
Br 4    pre_br4.npt - not used
```

Precipitation Temperature Filename (TPR FILE)

FIELD	NAME	VALUE	DESCRIPTION
1			(Ignored by code)
2-10	TPRFN	Character	Precipitation temperature filename

This card specifies the filename(s) for branch precipitation temperatures. There must be a separate file for each branch. More information on data setup can be found at the description of the [precipitation temperature file](#). The “ - not used” tag at the end of the filename is useful when looking at the echoing of input filenames in the [preprocessor output](#) and can alert the user to an input option that is or is not being used. If precipitation is turned ON for a branch, then the “ - not used” tag should be removed.

Example

```
TPR FILE.....TPRFN.....
Br 1    tpr_br1.npt - not used
Br 2    tpr_br2.npt - not used
Br 3    tpr_br3.npt - not used
Br 4    tpr_br4.npt - not used
```

Precipitation Concentration Filename (CPR FILE)

FIELD	NAME	VALUE	DESCRIPTION
1			(Ignored by code)
2-10	CPRFN	Character	Precipitation concentration filename

This card specifies the filename(s) for branch precipitation constituent concentrations. There must be a separate file for each branch. More information on data setup can be found at the description of the [precipitation concentration file](#). The “ - not used” tag at the end of the filename is useful when looking at the echoing of input filenames in the [preprocessor output](#) and can alert the user to an input option that is or is not being used. If precipitation is turned ON for a branch, then the “ - not used” tag should be removed.

Example

```
CPR FILE.....CPRFN.....  
Br 1    cpr_br1.npt - not used  
Br 2    cpr_br2.npt - not used  
Br 3    cpr_br3.npt - not used  
Br 4    cpr_br4.npt - not used
```


External Upstream Head Filename (EUH FILE)

FIELD	NAME	VALUE	DESCRIPTION
1			(Ignored by code)
2-10	EUHFN	Character	External upstream head filename

This card specifies the filename(s) for branch external upstream heads. There must be a separate file for each branch. More information on data setup can be found at the description of the [upstream head file](#). The “ - not used” tag at the end of the filename is useful when looking at the echoing of input filenames in the [preprocessor output](#) and can alert the user to an input option that is or is not being used. If there is an external head for a branch, then the “ - not used” tag shown below should be removed.

Example

```
EUH FILE.....EUHFN.....  
Br 1    euh_br1.npt - not used  
Br 2    euh_br2.npt - not used  
Br 3    euh_br3.npt - not used  
Br 4    euh_br4.npt - not used
```

External Upstream Head Temperature Filename (TUH FILE)

FIELD	NAME	VALUE	DESCRIPTION
1			(Ignored by code)
2-10	TUHFN	Character	External upstream head temperature filename

This card specifies the filename(s) for branch external upstream head vertical temperatures. There must be a separate file for each branch. More information on data setup can be found at the description of the [upstream head temperature file](#). The “ - not used” tag at the end of the filename is useful when looking at the echoing of input filenames in the [preprocessor output](#) and can alert the user to an input option that is or is not being used. If there is an external head for a branch, then the “ - not used” tag shown below should be removed.

Example

```
TUH FILE.....TUHFN.....
Br 1    tuh_br1.npt - not used
Br 2    tuh_br2.npt - not used
Br 3    tuh_br3.npt - not used
Br 4    tuh_br4.npt - not used
```

External Upstream Head Concentration Filename (CUH FILE)

FIELD	NAME	VALUE	DESCRIPTION
1			(Ignored by code)
2-10	CUHFN	Character	External upstream head concentration filename

This card specifies the filename(s) for branch external upstream head constituent concentrations. There must be a separate file for each branch. More information on data setup can be found at the description of the [upstream head concentration file](#). The “ - not used” tag at the end of the filename is useful when looking at the echoing of input filenames in the [preprocessor output](#) and can alert the user to an input option that is or is not being used. If there is an external head for a branch, then the “ - not used” tag shown below should be removed.

Example

```
CUH FILE.....CUHFN.....
Br 1    cuh_br1.npt - not used
Br 2    cuh_br2.npt - not used
Br 3    cuh_br3.npt - not used
Br 4    cuh_br4.npt - not used
```

External Downstream Head Filename (EDH FILE)

FIELD	NAME	VALUE	DESCRIPTION
1			(Ignored by code)
2-10	EDHFN	Character	External downstream head filename

This card specifies the filename(s) for branch external downstream heads. There must be a separate file for each branch. More information on data setup can be found at the description of the [downstream head file](#). The “ - not used” tag at the end of the filename is useful when looking at the echoing of input filenames in the [preprocessor output](#) and can alert the user to an input option that is or is not being used. If there is an external head for a branch, then the “ - not used” tag shown below should be removed.

Example

```
EDH FILE.....EDHFN.....
Br 1    edh_br1.npt - not used
Br 2    edh_br2.npt - not used
Br 3    edh_br3.npt - not used
Br 4    edh_br4.npt
```

External Downstream Head Temperature Filename (TDH FILE)

FIELD	NAME	VALUE	DESCRIPTION
1			(Ignored by code)
2-10	TDHFN	Character	External downstream head temperature filename

This card specifies the filename(s) for branch external downstream head vertical temperatures. There must be a separate file for each branch. More information on data setup can be found at the description of the [downstream head temperature file](#). The “ - not used” tag at the end of the filename is useful when looking at the echoing of input filenames in the [preprocessor output](#) and can alert the user to an input option that is or is not being used. If there is an external head for a branch, then the “ - not used” tag shown below should be removed.

Example

```
TDH FILE.....TDHFN.....
Br 1    tdh_br1.npt - not used
Br 2    tdh_br2.npt - not used
Br 3    tdh_br3.npt - not used
Br 4    tdh_br4.npt
```

External Downstream Head Concentration Filename (CDH FILE)

FIELD	NAME	VALUE	DESCRIPTION
1			(Ignored by code)
2-10	CDHFN	Character	External downstream had concentration filename

This card specifies the filename(s) for branch external downstream head constituent concentrations. There must be a separate file for each branch. More information on data setup can be found at the description of the [downstream head concentration file](#). The “ - not used” tag at the end of the filename is useful when looking at the echoing of input filenames in the [preprocessor output](#) and can alert the user to an input option that is or is not being used. If there is an external head for a branch, then the “ - not used” tag shown below should be removed.

Example

```
CDH FILE.....CDHFN.....
Br 1    cdh_br1.npt - not used
Br 2    cdh_br2.npt - not used
Br 3    cdh_br3.npt - not used
Br 4    cdh_br4.npt
```

Snapshot Filename (SNP FILE)

FIELD	NAME	VALUE	DESCRIPTION
1			(Ignored by code)
2-10	SNPFN	Character	Snapshot filename

This card specifies the snapshot filename(s).

Example

```
SNP FILE.....SNPFN.....  
Wb 1      snp_wb1.opt  
Wb 2      snp_wb2.opt  
Wb 3      snp_wb3.opt
```

Profile Plot Filename (PRF FILE)

FIELD	NAME	VALUE	DESCRIPTION
1			(Ignored by code)
2-10	PRFFN	Character	Profile plot filename

This card specifies the vertical profile plot filename(s).

Example

```
PRF FILE.....PRFFN.....
Wb 1      prf_wb1.opt
Wb 2      prf_wb2.opt
Wb 3      prf_wb3.opt
```


W2 Linkage Output Filename (VPL FILE)

FIELD	NAME	VALUE	DESCRIPTION
1			(Ignored by code)
2-10	VPLFN	Character	Vector plot filename

Before version 3.71, this card specified the velocity vector plot filename(s). This card now specifies the W2 linkage file used in the w2-Post post-processor. Only the first file name for the first waterbody is used in the model. The post-processor is looking for a file with a file type: 'w2l'.

Example

```
VPL FILE.....VPLFN.....  
Wb 1      w2_post_output.w2l  
Wb 2      vpl_wb2.opt  
Wb 3      vpl_wb3.opt
```

Contour Plot Filename (CPL FILE)

FIELD	NAME	VALUE	DESCRIPTION
1			(Ignored by code)
2-10	CPLFN	Character	Contour plot filename

This card specifies the contour plot filename(s).

Example

```
CPL FILE.....CPLFN.....
Wb 1      cpl_wb1.opt
Wb 2      cpl_wb2.opt
Wb 3      cpl_wb3.opt
```

Spreadsheet Profile Plot Filename (SPR FILE)

FIELD	NAME	VALUE	DESCRIPTION
1			(Ignored by code)
2-10	SPRFN	Character	Spreadsheet plot filename

This card specifies the spreadsheet profile output filename(s). Output from this file is suitable for import into a spreadsheet or graphics package that uses a spreadsheet format for data management.

Example

```
SPR FILE.....SPRFN.....  
Wb 1      spr_wb1.opt  
Wb 2      spr_wb2.opt  
Wb 3      spr_wb3.opt
```

Flux Filename (FLX FILE)

FIELD	NAME	VALUE	DESCRIPTION
1			(Ignored by code)
2-10	FLXFN	Character	Flux filename

This card specifies the kinetic fluxes filename(s). Output from this file is suitable for import into a spreadsheet or graphics package that uses a spreadsheet format for data management.

Example

```
FLX FILE.....FLXFN.....  
Wb 1      flx_wb1.opt  
Wb 2      flx_wb2.opt  
Wb 3      flx_wb3.opt
```

Time Series Plot Filename (TSR FILE)

FIELD	NAME	VALUE	DESCRIPTION
1			(Ignored by code)
2-10	TSRFN	Character	Time series plot filename

This card specifies the time series plot filename(s).

Example

```
TSR FILE.....TSRFN.....  
      tsr.opt
```

Withdrawal Output Filename (WDO FILE)

FIELD	NAME	VALUE	DESCRIPTION
1			(Ignored by code)
2-10	WDOFN	Character	Withdrawal output filename

This card specifies the withdrawal output filename(s).

Example

```
WDO FILE.....WDOFN.....
      wdo.opt
```

Sample Control Input File

Spokane River/Long Lake Model Version 3.7

```

TITLE C .....TITLE.....
Card 1 Version 3.5 Spokane River/Long Lake application
Card 2 WB 1 - Sloping branches between State line and Upriver Pool
Card 3 WB 2 - Pool of Upriver DAm
Card 4 Wb 3 - Pool of Upper Falls Dam
Card 5 WB 4 - 2 sloping branches above 9-mile dam pool
Card 6 WB 5 - Nine Mile dam pool
Card 7 WB 6 - Long Lake
Card 8 Scott Wells, PSU
Card 9 Rob Annear, PSU; Chris Berger, PSU
Card 10 Tom Cole, WES

GRID          NWB      NBR      IMX      KMX      NPROC      CLOSEC
              6        12        189       47         2         OFF

IN/OUTFLOW    NTR      NST      NIW      NWD      NGT      NSP      NPI      NPU
              7        7         0         0         0         6         0         0

CONSTITU      NGC      NSS      NAL      NEP      NBOD      NMC      NZP
              3         1         3         1         1         0         1

MISCELL      NDAY  SELECTC  HABTATC  ENVIRPC  AERATEC  INITUWL
              100    OFF        ON        ON        ON        ON

TIME CON      TMSTRT   TMEND     YEAR
              1.0402  303.89    2000

DLT CON      NDLT    DLTMIN  DLTINTR
              6       0.1      ON

DLT DATE      DLTD     DLTD     DLTD     DLTD     DLTD     DLTD     DLTD     DLTD     DLTD
              1.00     1.2     172.0    225.0    231.0    251.0

DLT MAX      DLTMAX   DLTMAX   DLTMAX   DLTMAX   DLTMAX   DLTMAX   DLTMAX   DLTMAX   DLTMAX
              5.0     65.0    10.0     10.0     5.0     10.0

DLT FRN      DLTF     DLTF     DLTF     DLTF     DLTF     DLTF     DLTF     DLTF     DLTF
              0.90     0.90     0.90     0.90     0.90     0.90

DLT LIMIT      VISC     CELC
Wb 1           ON       ON
Wb 2           ON       ON
Wb 3           ON       ON
Wb 4           ON       ON
Wb 5           ON       ON
Wb 6           ON       ON

BRANCH G      US       DS       UHS      DHS      UQB      DQB      NL      SLOPE  SLOPEC
Br 1           2        10        0        13        0        0        1 0.00181 0.00181
Br 2           13       24        10       27        0        0        1 0.00152 0.00100
Br 3           27       36        24       39        0        0        1 0.00328 0.00200
Br 4           39       48        36        0        0        0        1 0.00142 0.00142
Br 5           51       64         0         0        0        0        1 0.00000 0.00000
Br 6           67       73       -64       76        0        0        1 0.00000 0.00000
Br 7           76       86        73         0        0        0        1 0.00000 0.00000
Br 8           89       94      -86       97        0        0        1 0.00256 0.00150
Br 9           97      128        94         0        0        0        1 0.00208 0.00100
Br 10          131     135         0       138        0        0        1 0.00000 0.00000
Br 11          138     151       135         0        0        0        1 0.00000 0.00000
Br 12          154     188     -151         0        0        0        1 0.00000 0.00000

```

SAMPLE CONTROL FILE

CONTROL FILE

LOCATION	LAT	LONG	EBOT	BS	BE	JBDN
WB 1	47.8	117.8	578.72	1	4	4
WB 2	47.8	117.8	571.00	5	5	5
WB 3	47.8	117.8	560.00	6	7	7
WB 4	47.8	117.8	485.51	8	9	9
WB 5	47.8	117.8	481.00	10	11	11
WB 6	47.8	117.8	422.10	12	12	12

INIT CND	T2I	ICEI	WTYPEC	GRIDC
Wb 1	4.0	0.0	FRESH	RECT
Wb 2	4.0	0.0	FRESH	RECT
Wb 3	4.0	0.0	FRESH	RECT
Wb 4	4.0	0.0	FRESH	RECT
Wb 5	4.0	0.0	FRESH	RECT
Wb 6	4.0	0.0	FRESH	RECT

CALCULAT	VBC	EBC	MBC	PQC	EVC	PRC
Wb 1	ON	ON	ON	OFF	OFF	OFF
Wb 2	ON	ON	ON	OFF	OFF	OFF
Wb 3	ON	ON	ON	OFF	OFF	OFF
Wb 4	ON	ON	ON	OFF	OFF	OFF
Wb 5	ON	ON	ON	OFF	OFF	OFF
Wb 6	ON	ON	ON	OFF	OFF	OFF

DEAD SEA	WINDC	QINC	QOUTC	HEATC
Wb 1	ON	ON	ON	ON
Wb 2	ON	ON	ON	ON
Wb 3	ON	ON	ON	ON
Wb 4	ON	ON	ON	ON
Wb 5	ON	ON	ON	ON
Wb 6	ON	ON	ON	ON

INTERPOL	QINIC	DTRIC	HDIC
Br 1	ON	OFF	ON
Br 2	ON	OFF	ON
Br 3	ON	OFF	ON
Br 4	ON	OFF	ON
Br 5	ON	OFF	ON
Br 6	ON	OFF	ON
Br 7	ON	OFF	ON
Br 8	ON	OFF	ON
Br 9	ON	OFF	ON
Br 10	ON	OFF	ON
Br 11	ON	OFF	ON
Br 12	ON	OFF	ON

HEAT EXCH	SLHTC	SROC	RHEVAP	METIC	FETCHC	AFW	BFW	CFW	WINDH
Wb 1	TERM	OFF	OFF	ON	OFF	9.2	0.46	2.0	2.0
Wb 2	TERM	OFF	OFF	ON	OFF	9.2	0.46	2.0	2.0
Wb 3	TERM	OFF	OFF	ON	OFF	9.2	0.46	2.0	2.0
Wb 4	TERM	OFF	OFF	ON	OFF	9.2	0.46	2.0	2.0
Wb 5	TERM	OFF	OFF	ON	OFF	9.2	0.46	2.0	2.0
Wb 6	TERM	OFF	OFF	ON	OFF	9.2	0.46	2.0	2.0

ICE COVER	ICEC	SLICEC	ALBEDO	HWICE	BICE	GICE	ICEMIN	ICET2
Wb 1	OFF	DETAIL	0.25	10.0	0.6	0.07	0.05	3.0
Wb 2	OFF	DETAIL	0.25	10.0	0.6	0.07	0.05	3.0
Wb 3	OFF	DETAIL	0.25	10.0	0.6	0.07	0.05	3.0
Wb 4	OFF	DETAIL	0.25	10.0	0.6	0.07	0.05	3.0
Wb 5	OFF	DETAIL	0.25	10.0	0.6	0.07	0.05	3.0
Wb 6	OFF	DETAIL	0.25	10.0	0.6	0.07	0.05	3.0

CONTROL FILE

SAMPLE CONTROL FILE

TRANSPORT	SLTRC	THETA
Wb 1	ULTIMATE	0.55
Wb 2	ULTIMATE	0.55
Wb 3	ULTIMATE	0.55
Wb 4	ULTIMATE	0.55
Wb 5	ULTIMATE	0.55
Wb 6	ULTIMATE	0.55

HYD COEF	AX	DX	CBHE	TSED	FI	TSEDF	FRICC	Z0
Wb 1	1.0	1.0	0.3	11.5	0.01	1.00	MANN	0.001
Wb 2	1.0	1.0	0.3	11.5	0.01	1.00	MANN	0.001
Wb 3	1.0	1.0	0.3	11.5	0.01	1.00	MANN	0.001
Wb 4	1.0	1.0	0.3	11.5	0.01	1.00	MANN	0.001
Wb 5	1.0	1.0	0.3	11.5	0.01	1.00	MANN	0.001
Wb 6	1.0	1.0	0.3	11.5	0.01	1.00	MANN	0.001

EDDY VISC	AZC	AZSLC	AZMAX	FBC	E	ARODI	STRCKLR	BOUNDFR	TKECAL
Wb 1	W2N	IMP	1.0	3	9.535	0.430	24.0	10.00	IMP
Wb 2	W2	IMP	1.0	3	9.535	0.430	24.0	10.00	IMP
Wb 3	W2	IMP	1.0	3	9.535	0.430	24.0	10.00	IMP
Wb 4	W2N	IMP	1.0	3	9.535	0.430	24.0	10.00	IMP
Wb 5	W2	IMP	1.0	3	9.535	0.430	24.0	10.00	IMP
Wb 6	W2	IMP	1.0	3	9.535	0.430	24.0	10.00	IMP

N STRUC	NSTR	DYNELEV
Br 1	0	OFF
Br 2	0	OFF
Br 3	0	OFF
Br 4	0	OFF
Br 5	2	OFF
Br 6	0	OFF
Br 7	2	ON
Br 8	0	OFF
Br 9	0	OFF
Br 10	0	OFF
Br 11	2	OFF
BRr 12	1	OFF

STR INT	STRIC	STRIC	STRIC	STRIC	STRIC	STRIC	STRIC	STRIC	STRIC
Br 1									
Br 2									
Br 3									
Br 4									
Br 5	OFF	OFF							
Br 6									
Br 7	OFF	OFF							
Br 8									
Br 9									
Br 10									
Br 11	OFF	OFF							
Br 12	OFF								

STR TOP	KTSTR	KTSTR	KTSTR	KTSTR	KTSTR	KTSTR	KTSTR	KTSTR	KTSTR
Br 1									
Br 2									
Br 3									
Br 4									
Br 5	2	2							
Br 6									
Br 7	2	2							
Br 8									
Br 9									
Br 10									
Br 11	2	2							
Br 12	2								

SAMPLE CONTROL FILE

CONTROL FILE

STR BOT	KBSTR	KBSTR	KBSTR	KBSTR	KBSTR	KBSTR	KBSTR	KBSTR	KBSTR	KBSTR
Br 1										
Br 2										
Br 3										
Br 4										
Br 5	41	41								
Br 6										
Br 7	38	38								
Br 8										
Br 9										
Br 10										
Br 11	39	39								
Br 12	46									
STR SINK	SINKC	SINKC	SINKC	SINKC	SINKC	SINKC	SINKC	SINKC	SINKC	SINKC
Br 1										
Br 2										
Br 3										
Br 4										
Br 5	POINT	LINE								
Br 6										
Br 7	POINT	POINT								
Br 8										
Br 9										
Br 10										
Br 11	POINT	POINT								
Br 12	POINT									
STR ELEV	ESTR	ESTR	ESTR	ESTR	ESTR	ESTR	ESTR	ESTR	ESTR	WSTR
Br 1										
Br 2										
Br 3										
Br 4										
Br 5	579.5	577.1								
Br 6										
Br 7	565.15	567.25								
Br 8										
Br 9										
Br 10										
Br 11	485.0	489.0								
Br 12	456.9									
STR WIDTH	WSTR	WSTR	WSTR	WSTR	WSTR	WSTR	WSTR	WSTR	WSTR	WSTR
Br 1										
Br 2										
Br 3										
Br 4										
Br 5		70.0								
Br 6										
Br 7										
Br 8										
Br 9										
Br 10										
Br 11										
Br 12										
PIPES	IUPI	IDPI	EUPI	EDPI	WPI	DLXPI	FPI	FMINPI	LATPIC	DYNPIPE
Pi 1	24	28	28.0	27.0	0.5	230.0	0.065	0.1	DOWN	ON
PIPE UP	PUPIC	ETUPI	EBUPI	KTUPI	KBUPI					
Pi 1	DISTR			2	23					
PIPE DOWN	PDPIC	ETDPI	EBDPI	KTDPI	KBDPI					
Pi 1	DISTR			2	23					

CONTROL FILE

SAMPLE CONTROL FILE

SPILLWAY	IUSP	IDSP	ESP	AISP	B1SP	A2SP	B2SP	LATSPC		
Spill 1	64	67	592.14	10000.0	1.5	20.00	1.5	DOWN		
Spill 2	86	89	580.14	7000.0	1.5	20.00	1.5	DOWN		
Spill 3	151	154	497.00	10000.0	1.5	20.00	1.5	DOWN		
Spill 4	188	0	469.00	20000.0	1.5	20.00	1.5	DOWN		
Spill 5	48	51	579.80	80.00	1.5	30.00	1.5	DOWN		
Spill 6	128	131	486.50	60.00	1.5	30.00	1.5	DOWN		
SPILL UP	PUSPC	ETUSP	EBUSP	KTUSP	KBUSP					
Spill1	DISTR			2	41					
Spill2	DISTR			2	38					
Spill3	DISTR			2	39					
Spill4	DISTR			2	46					
Spill5	DISTR			2	45					
Spill6	DISTR			2	46					
SPILL DOWN	PDSPC	ETDSP	EBDSP	KTDSP	KBDSP					
Spill1	DISTR			2	36					
Spill2	DISTR			2	45					
Spill3	DISTR			2	6					
Spill4	DISTR			2	46					
Spill5	DISTR			2	43					
Spill6	DISTR			2	39					
SPILL GAS	GASSP	EQSP	ASP	BSP	CSP					
Spill1	OFF									
Spill2	OFF									
Spill3	OFF									
Spill4	OFF									
Spill5	OFF									
Spill6	OFF									
GATES	IUGT	IDGT	EGT	A1GT	B1GT	G1GT	A2GT	B2GT	G2GT	LATGTC
Gt 1	27	33	44.0	10.00	1.0	1.0	10.0	2.5	0.0	DOWN
GATE WEIR	GA1	GB1	GA2	GB2	DYNGTC	GTIC				
Gt 1	10.0	1.5	10.0	1.5	B	ON				
GATE UP	PUGTC	ETUGT	EBUGT	KTUGT	KBUGT					
Gt 1	DISTR			3	23					
GATE DOWN	PDGTC	ETDGT	EBDGT	KT DGT	KBDGT					
Gt 1	DISTR			3	23					
GATE GAS	GASGT	EQGT	AGASG	BGASG	CGASG					
Gt 1	ON	1	10.0	120.00	1.0					
PUMPS 1	IUPU	IDPU	EPU	STRTPU	ENDPU	EONPU	EOFFPU	QPU	LATPUC	DYNPUMP
Pu 1	30	33	2.4	1.0	900.0	3.0	2.4	3.0	DOWN	OFF
PUMPS 2	PPUC	ETPU	EBPU	KTPU	KBPU					
Pu 1	DISTR			4	23					
WEIR SEG	IWR	IWR	IWR	IWR	IWR	IWR	IWR	IWR	IWR	
	27									
WEIR TOP	KTWR	KTWR	KTWR	KTWR	KTWR	KTWR	KTWR	KTWR	KTWR	
	9									
WEIR BOT	KBWR	KBWR	KBWR	KBWR	KBWR	KBWR	KBWR	KBWR	KBWR	
	23									
WD INT	WDIC	WDIC	WDIC	WDIC	WDIC	WDIC	WDIC	WDIC	WDIC	
WD SEG	IWD	IWD	IWD	IWD	IWD	IWD	IWD	IWD	IWD	

SAMPLE CONTROL FILE

CONTROL FILE

WD ELEV	EWD	EWD	EWD	EWD	EWD	EWD	EWD	EWD	EWD
WD TOP	ETWD	ETWD	ETWD	ETWD	ETWD	ETWD	ETWD	ETWD	ETWD
WD BOT	EBWD	EBWD	EBWD	EBWD	EBWD	EBWD	EBWD	EBWD	EBWD
TRIB PLACE	PTRC DISTR	PTRC DISTR	PTRC DISTR	PTRC DISTR	PTRC DISTR	PTRC DISTR	PTRC DISTR	PTRC	PTRC
TRIB INT	TRIC OFF	TRIC OFF	TRIC OFF	TRIC OFF	TRIC OFF	TRIC OFF	TRIC OFF	TRIC	TRIC
TRIB SEG	ITR 15	ITR 43	ITR 56	ITR 98	ITR 114	ITR 147	ITR 155	ITR	ITR
TRIB TOP	ETRT	ETRT	ETRT	ETRT	ETRT	ETRT	ETRT	ETRT	ETRT
TRIB BOT	ETRB	ETRB	ETRB	ETRB	ETRB	ETRB	ETRB	ETRB	ETRB
DST TRIB	DTRC								
Br 1	ON								
Br 2	ON								
Br 3	ON								
Br 4	ON								
Br 5	ON								
Br 6	ON								
Br 7	ON								
Br 8	ON								
Br 9	ON								
Br 10	ON								
Br 11	ON								
Br 12	ON								
HYD PRINT	HPRWBC	HPRWBC	HPRWBC	HPRWBC	HPRWBC	HPRWBC	HPRWBC	HPRWBC	HPRWBC
NLIM	ON	ON	ON	ON	ON	ON			
U	ON	ON	ON	ON	ON	ON			
W	ON	ON	ON	ON	ON	ON			
T	ON	ON	ON	ON	ON	ON			
RHO	OFF	OFF	OFF	OFF	OFF	OFF			
AZ	OFF	OFF	OFF	OFF	OFF	OFF			
SHEAR	OFF	OFF	OFF	OFF	OFF	OFF			
ST	OFF	OFF	OFF	OFF	OFF	OFF			
SB	OFF	OFF	OFF	OFF	OFF	OFF			
ADMX	OFF	OFF	OFF	OFF	OFF	OFF			
DM	OFF	OFF	OFF	OFF	OFF	OFF			
HDG	OFF	OFF	OFF	OFF	OFF	OFF			
ADMZ	OFF	OFF	OFF	OFF	OFF	OFF			
HPG	OFF	OFF	OFF	OFF	OFF	OFF			
GRAV	OFF	OFF	OFF	OFF	OFF	OFF			
SNP PRINT	SNPC	NSNP	NISNP						
Wb 1	ON	2	16						
Wb 2	ON	2	8						
Wb 3	ON	2	3						
Wb 4	ON	2	6						
Wb 5	ON	2	5						
Wb 6	ON	2	6						
SNP DATE	SNPD	SNPD	SNPD	SNPD	SNPD	SNPD	SNPD	SNPD	SNPD
Wb 1	1.0	1.6							
Wb 2	1.0	1.6							
Wb 3	1.0	1.6							
Wb 4	1.0	1.6							

CONTROL FILE

SAMPLE CONTROL FILE

Wb 5	1.0	1.6							
Wb 6	1.0	1.6							
SNP FREQ	SNPF	SNPF	SNPF	SNPF	SNPF	SNPF	SNPF	SNPF	SNPF
Wb 1	0.1	7.0							
Wb 2	0.1	7.0							
Wb 3	0.1	7.0							
Wb 4	0.1	7.0							
Wb 5	0.1	7.0							
Wb 6	0.1	7.0							
SNP SEG	ISNP	ISNP	ISNP	ISNP	ISNP	ISNP	ISNP	ISNP	ISN
Wb 1	2	10	13	24	27	36	39	40	41
	42	43	44	45	46	47	48		
Wb 2	51	53	55	57	59	61	63	64	
Wb 3	84	85	86						
Wb 4	89	90	92	122	123	124			
Wb 5	131	138	139	148	151				
Wb 6	154	155	156	175	187	188			
SCR PRINT	SCRC	NSCR							
Wb 1	OFF	1							
Wb 2	OFF	1							
Wb 3	OFF	1							
Wb 4	OFF	1							
Wb 5	OFF	1							
Wb 6	ON	1							
SCR DATE	SCRD	SCRD	SCRD	SCRD	SCRD	SCRD	SCRD	SCRD	SCRD
Wb 1	1.0								
Wb 2	1.0								
Wb 3	1.0								
Wb 4	1.0								
Wb 5	1.0								
Wb 6	1.0								
SCR FREQ	SCRF	SCRF	SCRF	SCRF	SCRF	SCRF	SCRF	SCRF	SCRF
Wb 1	0.05								
Wb 2	0.10								
Wb 3	0.10								
Wb 4	0.10								
Wb 5	0.10								
Wb 6	0.10								
PRF PLOT	PRFC	NPRF	NIPRF						
Wb 1	OFF	0	0						
Wb 2	ON	12	4						
Wb 3	OFF	0	0						
Wb 4	OFF	0	0						
Wb 5	ON	12	6						
Wb 6	ON	12	7						
PRF DATE	PRFD	PRFD	PRFD	PRFD	PRFD	PRFD	PRFD	PRFD	PRFD
Wb 1									
Wb 2	158.5	179.5	200.5	228.5	229.5	242.5	244.5	245.5	249.5
	257.5	270.5	271.5						
Wb 3									
Wb 4									
Wb 5	158.5	179.5	200.5	228.5	229.5	242.5	244.5	245.5	249.5
	257.0	270.0	271.0						
Wb 6	158.67	179.67	200.67	228.67	229.67	242.67	244.67	245.67	249.67
	257.67	270.67	271.67						
PRF FREQ	PRFF	PRFF	PRFF	PRFF	PRFF	PRFF	PRFF	PRFF	PRFF
Wb 1									
Wb 2	500.0	500.0	500.0	500.0	500.0	500.0	500.0	500.0	500.0
	500.0	500.0	500.0						
Wb 3									

SAMPLE CONTROL FILE

CONTROL FILE

Wb 4										
Wb 5	500.0	500.0	500.0	500.0	500.0	500.0	500.0	500.0	500.0	500.0
	500.0	500.0	500.0							
Wb 6	500.0	500.0	500.0	500.0	500.0	500.0	500.0	500.0	500.0	500.0
	500.0	500.0	500.0							
PRF SEG	IPRF	IPRF	IPRF	IPRF	IPRF	IPRF	IPRF	IPRF	IPRF	IPRF
Wb 1										
Wb 2	57	60	62	64						
Wb 3										
Wb 4										
Wb 5	135	139	141	143	147	150				
Wb 6	157	161	168	174	180	183	187			
SPR PLOT	SPRC	NSPR	NISPR							
Wb 1	OFF	0	0							
Wb 2	OFF	0	0							
Wb 3	OFF	0	0							
Wb 4	OFF	0	0							
Wb 5	OFF	0	0							
Wb 6	OFF	0	0							
SPR DATE	SPRD	SPRD	SPRD	SPRD	SPRD	SPRD	SPRD	SPRD	SPRD	SPRD
Wb 1										
Wb 2										
Wb 3										
Wb 4										
Wb 5										
Wb 6										
SPR FREQ	SPRF	SPRF	SPRF	SPRF	SPRF	SPRF	SPRF	SPRF	SPRF	SPRF
Wb 1										
Wb 2										
Wb 3										
Wb 4										
Wb 5										
Wb 6										
SPR SEG	ISPR	ISPR	ISPR	ISPR	ISPR	ISPR	ISPR	ISPR	ISPR	ISPR
Wb 1										
Wb 2										
Wb 3										
Wb 4										
Wb 5										
Wb 6										
VPL PLOT	VPLC	NVPL								
Wb 1	OFF	1								
Wb 2	OFF	1								
Wb 3	OFF	1								
Wb 4	OFF	1								
Wb 5	OFF	1								
Wb 6	OFF	1								
VPL DATE	VPLD	VPLD	VPLD	VPLD	VPLD	VPLD	VPLD	VPLD	VPLD	VPLD
Wb 1	63.5									
Wb 2	63.5									
Wb 3	63.5									
Wb 4	63.5									
Wb 5	63.5									
Wb 6	63.5									
VPL FREQ	VPLF	VPLF	VPLF	VPLF	VPLF	VPLF	VPLF	VPLF	VPLF	VPLF
Wb 1	1.0									
Wb 2	1.0									
Wb 3	1.0									
Wb 4	1.0									
Wb 5	1.0									

CONTROL FILE

SAMPLE CONTROL FILE

Wb 6	1.0								
CPL PLOT	CPLC	NCPL	TECPLOT						
Wb 1	ON	24	OFF						
Wb 2	ON	24	OFF						
Wb 3	ON	24	OFF						
Wb 4	ON	24	OFF						
Wb 5	ON	24	OFF						
Wb 6	ON	24	OFF						
CPL DATE	CPLD	CPLD	CPLD	CPLD	CPLD	CPLD	CPLD	CPLD	CPLD
Wb 1	9.67	37.67	72.75	100.6	128.67	163.75	187.6	191.6	208.4
	215.5	219.75	228.4	228.6	229.4	229.6	251.5	254.75	270.4
	270.6	271.4	271.6	284.4	319.35	347.35			
Wb 2	9.67	37.67	72.75	100.6	128.67	163.75	187.6	191.6	208.4
	215.5	219.75	228.4	228.6	229.4	229.6	251.5	254.75	270.4
	270.6	271.4	271.6	284.4	319.35	347.35			
Wb 3	9.67	37.67	72.75	100.6	128.67	163.75	187.6	191.6	208.4
	215.5	219.75	228.4	228.6	229.4	229.6	251.5	254.75	270.4
	270.6	271.4	271.6	284.4	319.35	347.35			
Wb 4	9.67	37.67	72.75	100.6	128.67	163.75	187.6	191.6	208.4
	215.5	219.75	228.4	228.6	229.4	229.6	251.5	254.75	270.4
	270.6	271.4	271.6	284.4	319.35	347.35			
Wb 5	9.67	37.67	72.75	100.6	128.67	163.75	187.6	191.6	208.4
	215.5	219.75	228.4	228.6	229.4	229.6	251.5	254.75	270.4
	270.6	271.4	271.6	284.4	319.35	347.35			
Wb 6	9.67	37.67	72.75	100.6	128.67	163.75	187.6	191.6	208.4
	215.5	219.75	228.4	228.6	229.4	229.6	251.5	254.75	270.4
	270.6	271.4	271.6	284.4	319.35	347.35			
CPL FREQ	CPLF	CPLF	CPLF	CPLF	CPLF	CPLF	CPLF	CPLF	CPLF
Wb 1	500.0	500.0	500.0	500.0	500.0	500.0	500.0	500.0	500.0
	500.0	500.0	500.0	500.0	500.0	500.0	500.0	500.0	500.0
	500.0	500.0	500.0	500.0	500.0	500.0			
Wb 2	500.0	500.0	500.0	500.0	500.0	500.0	500.0	500.0	500.0
	500.0	500.0	500.0	500.0	500.0	500.0	500.0	500.0	500.0
	500.0	500.0	500.0	500.0	500.0	500.0			
Wb 3	500.0	500.0	500.0	500.0	500.0	500.0	500.0	500.0	500.0
	500.0	500.0	500.0	500.0	500.0	500.0	500.0	500.0	500.0
	500.0	500.0	500.0	500.0	500.0	500.0			
Wb 4	500.0	500.0	500.0	500.0	500.0	500.0	500.0	500.0	500.0
	500.0	500.0	500.0	500.0	500.0	500.0	500.0	500.0	500.0
	500.0	500.0	500.0	500.0	500.0	500.0			
Wb 5	500.0	500.0	500.0	500.0	500.0	500.0	500.0	500.0	500.0
	500.0	500.0	500.0	500.0	500.0	500.0	500.0	500.0	500.0
	500.0	500.0	500.0	500.0	500.0	500.0			
Wb 6	500.0	500.0	500.0	500.0	500.0	500.0	500.0	500.0	500.0
	500.0	500.0	500.0	500.0	500.0	500.0	500.0	500.0	500.0
	500.0	500.0	500.0	500.0	500.0	500.0			
FLUXES	FLXC	NFLX							
Wb 1	OFF	0							
Wb 2	OFF	0							
Wb 3	OFF	0							
Wb 4	OFF	0							
Wb 5	OFF	0							
Wb 6	OFF	0							
FLX DATE	FLXD	FLXD	FLXD	FLXD	FLXD	FLXD	FLXD	FLXD	FLXD
Wb 1									
Wb 2									
Wb 3									
Wb 4									
Wb 5									
Wb 6									
FLX FREQ	FLXF	FLXF	FLXF	FLXF	FLXF	FLXF	FLXF	FLXF	FLXF
Wb 1									

SAMPLE CONTROL FILE

CONTROL FILE

Wb 2
Wb 3
Wb 4
Wb 5
Wb 6

TSR PLOT	TSRC ON	NTSR 1	NIKTSR 30						
TSR DATE	TSRD 1.0	TSRD	TSRD	TSRD	TSRD	TSRD	TSRD	TSRD	TSRD
TSR FREQ	TSRF 0.1	TSRF	TSRF	TSRF	TSRF	TSRF	TSRF	TSRF	TSRF
TSR SEG	ITSR 2 86 150 188	ITSR 13 89 151 128	ITSR 17 94 154 131	ITSR 24 97 155	ITSR 36 106 161	ITSR 48 114 168	ITSR 64 119 174	ITSR 67 135 180	ITSR 73 141 181
TSR ELEV	ETSR 0.1 0.1 0.1 0.1	ETSR 0.1 0.1 0.1 0.1	ETSR 0.1 0.1 0.1 0.1	ETSR 0.1 0.1 0.1 0.1	ETSR 0.1 0.1 0.1 0.1	ETSR 0.1 0.1 0.1 0.1	ETSR 0.1 0.1 0.1 0.1	ETSR 0.1 0.1 0.1 0.1	ETSR 0.1 0.1 0.1 0.1
WITH OUT	WDOC ON	NWDO 1	NIWDO 7						
WITH DATE	WDOD 1.0	WDOD	WDOD	WDOD	WDOD	WDOD	WDOD	WDOD	WDOD
WITH FREQ	WDOF 0.1	WDOF	WDOF	WDOF	WDOF	WDOF	WDOF	WDOF	WDOF
WITH SEG	IWDO 64	IWDO 86	IWDO 151	IWDO 188	IWDO 13	IWDO 24	IWDO 97	IWDO	IWDO
RESTART	RSOC OFF	NRSO 0	RSIC OFF						
RSO DATE	RSOD	RSOD	RSOD	RSOD	RSOD	RSOD	RSOD	RSOD	RSOD
RSO FREQ	RSOF	RSOF	RSOF	RSOF	RSOF	RSOF	RSOF	RSOF	RSOF
CST COMP	CCC ON	LIMC ON	CUF 10						

SAMPLE CONTROL FILE

CST	DERIV	CDWBC	CDWBC	CDWBC	CDWBC	CDWBC	CDWBC	CDWBC	CDWBC
DOC		ON	ON	ON	ON	ON	ON		!1
POC		OFF	OFF	OFF	OFF	OFF	OFF		!2
TOC		ON	ON	ON	ON	ON	ON		!3
DON		OFF	OFF	OFF	OFF	OFF	OFF		!4
PON		OFF	OFF	OFF	OFF	OFF	OFF		!5
TON		ON	ON	ON	ON	ON	ON		!6
TKN		ON	ON	ON	ON	ON	ON		!7
TN		ON	ON	ON	ON	ON	ON		!8
DOP		OFF	OFF	OFF	OFF	OFF	OFF		!9
POP		OFF	OFF	OFF	OFF	OFF	OFF		!10
TOP		ON	ON	ON	ON	ON	ON		!11
TP		ON	ON	ON	ON	ON	ON		!12
APR		OFF	OFF	OFF	OFF	OFF	OFF		!13
CHLA		ON	ON	ON	ON	ON	ON		!14
ATOT		OFF	OFF	OFF	OFF	OFF	OFF		!15
%DO		OFF	OFF	OFF	OFF	OFF	OFF		!16
TSS		ON	ON	ON	ON	ON	ON		!17
TISS		OFF	OFF	OFF	OFF	OFF	OFF		!18
CBODU		OFF	OFF	OFF	OFF	OFF	OFF		!19
pH		ON	ON	ON	ON	ON	ON		!20

SAMPLE CONTROL FILE

CONTROL FILE

CO2	OFF	OFF	OFF	OFF	OFF	OFF				!21
HCO3	OFF	OFF	OFF	OFF	OFF	OFF				!22
CO3	OFF	OFF	OFF	OFF	OFF	OFF				!23
CST FLUX	CFWBC	CFWBC	CFWBC	CFWBC	CFWBC	CFWBC	CFWBC	CFWBC	CFWBC	
TISSIN	OFF	OFF	OFF	OFF	OFF	OFF				!1
TISSOUT	OFF	OFF	OFF	OFF	OFF	OFF				!2
PO4AR	OFF	OFF	OFF	OFF	OFF	OFF				!3
PO4AG	OFF	OFF	OFF	OFF	OFF	OFF				!4
PO4AP	OFF	OFF	OFF	OFF	OFF	OFF				!5
PO4ER	OFF	OFF	OFF	OFF	OFF	OFF				!6
PO4EG	OFF	OFF	OFF	OFF	OFF	OFF				!7
PO4EP	OFF	OFF	OFF	OFF	OFF	OFF				!8
PO4POM	OFF	OFF	OFF	OFF	OFF	OFF				!9
PO4DOM	OFF	OFF	OFF	OFF	OFF	OFF				!10
PO4OM	OFF	OFF	OFF	OFF	OFF	OFF				!11
PO4SED	OFF	OFF	OFF	OFF	OFF	OFF				!12
PO4SOD	OFF	OFF	OFF	OFF	OFF	OFF				!13
PO4SET	OFF	OFF	OFF	OFF	OFF	OFF				!14
NH4NITR	OFF	OFF	OFF	OFF	OFF	OFF				!15
NH4AR	OFF	OFF	OFF	OFF	OFF	OFF				!16
NH4AG	OFF	OFF	OFF	OFF	OFF	OFF				!17
NH4AP	OFF	OFF	OFF	OFF	OFF	OFF				!18
NH4ER	OFF	OFF	OFF	OFF	OFF	OFF				!19
NH4EG	OFF	OFF	OFF	OFF	OFF	OFF				!20
NH4EP	OFF	OFF	OFF	OFF	OFF	OFF				!21
NH4POM	OFF	OFF	OFF	OFF	OFF	OFF				!22
NH4DOM	OFF	OFF	OFF	OFF	OFF	OFF				!23
NH4OM	OFF	OFF	OFF	OFF	OFF	OFF				!24
NH4SED	OFF	OFF	OFF	OFF	OFF	OFF				!25
NH4SOD	OFF	OFF	OFF	OFF	OFF	OFF				!26
NO3DEN	OFF	OFF	OFF	OFF	OFF	OFF				!27
NO3AG	OFF	OFF	OFF	OFF	OFF	OFF				!28
NO3EG	OFF	OFF	OFF	OFF	OFF	OFF				!29
NO3SED	OFF	OFF	OFF	OFF	OFF	OFF				!30
DSIAG	OFF	OFF	OFF	OFF	OFF	OFF				!31
DSIEG	OFF	OFF	OFF	OFF	OFF	OFF				!32
DSIPIS	OFF	OFF	OFF	OFF	OFF	OFF				!33
DSISED	OFF	OFF	OFF	OFF	OFF	OFF				!34
DSISOD	OFF	OFF	OFF	OFF	OFF	OFF				!35
DSISET	OFF	OFF	OFF	OFF	OFF	OFF				!36
PSIAM	OFF	OFF	OFF	OFF	OFF	OFF				!37
PSINET	OFF	OFF	OFF	OFF	OFF	OFF				!38
PSIDK	OFF	OFF	OFF	OFF	OFF	OFF				!39
FESET	OFF	OFF	OFF	OFF	OFF	OFF				!40
FESED	OFF	OFF	OFF	OFF	OFF	OFF				!41
LDOMDK	OFF	OFF	OFF	OFF	OFF	OFF				!42
LRDOM	OFF	OFF	OFF	OFF	OFF	OFF				!43
RDOMDK	OFF	OFF	OFF	OFF	OFF	OFF				!44
LDOMAP	OFF	OFF	OFF	OFF	OFF	OFF				!45
LDOMEK	OFF	OFF	OFF	OFF	OFF	OFF				!46
LPOMDK	OFF	OFF	OFF	OFF	OFF	OFF				!47
LRPOM	OFF	OFF	OFF	OFF	OFF	OFF				!48
RPOMDK	OFF	OFF	OFF	OFF	OFF	OFF				!49
LPOMAP	OFF	OFF	OFF	OFF	OFF	OFF				!50
LPOMEK	OFF	OFF	OFF	OFF	OFF	OFF				!51
LPOMSET	OFF	OFF	OFF	OFF	OFF	OFF				!52
RPOMSET	OFF	OFF	OFF	OFF	OFF	OFF				!53
CBODDK	OFF	OFF	OFF	OFF	OFF	OFF				!54
DOAP	OFF	OFF	OFF	OFF	OFF	OFF				!55
DOAR	OFF	OFF	OFF	OFF	OFF	OFF				!56
DOEP	OFF	OFF	OFF	OFF	OFF	OFF				!57
DOER	OFF	OFF	OFF	OFF	OFF	OFF				!58
DOPOM	OFF	OFF	OFF	OFF	OFF	OFF				!59
DODOM	OFF	OFF	OFF	OFF	OFF	OFF				!60
DOOM	OFF	OFF	OFF	OFF	OFF	OFF				!61
DONITR	OFF	OFF	OFF	OFF	OFF	OFF				!62
DOCBOD	OFF	OFF	OFF	OFF	OFF	OFF				!63

CONTROL FILE

SAMPLE CONTROL FILE

DOREAR	OFF	OFF	OFF	OFF	OFF	OFF				!64
DOSED	OFF	OFF	OFF	OFF	OFF	OFF				!65
DOSOD	OFF	OFF	OFF	OFF	OFF	OFF				!66
TICAG	OFF	OFF	OFF	OFF	OFF	OFF				!67
TICEG	OFF	OFF	OFF	OFF	OFF	OFF				!68
SEDDK	OFF	OFF	OFF	OFF	OFF	OFF				!69
SEDAS	OFF	OFF	OFF	OFF	OFF	OFF				!70
SEDLPOM	OFF	OFF	OFF	OFF	OFF	OFF				!71
SEDSET	OFF	OFF	OFF	OFF	OFF	OFF				!72
SODDK	OFF	OFF	OFF	OFF	OFF	OFF				!73

CST ICON	C2IWB	C2IWB	C2IWB	C2IWB	C2IWB	C2IWB	C2IWB	C2IWB	C2IWB	
TDS	0.0	0.0	0.0	0.0	0.0	0.0				!1
AGE	0.0	0.0	0.0	0.0	0.0	0.0				!2
TRACER	0.0	0.0	0.0	0.0	0.0	0.0				!3
COL1	0.0	0.0	0.0	0.0	0.0	0.0				!4
CONDUCT	0.0	0.0	0.0	0.0	0.0	0.0				!5
CHLORIDE	0.0	0.0	0.0	0.0	0.0	0.0				!6
ISS	0.0	0.0	0.0	0.0	0.0	0.0				!7
PO4	0.03	0.03	0.03	0.03	0.03	0.03				!8
NH4	0.01	0.01	0.01	0.01	0.01	0.01				!9
NOX	0.3	0.3	0.3	0.3	0.3	0.3				!10
DSI	0.0	0.0	0.0	0.0	0.0	0.0				!11
PSI	0.0	0.0	0.0	0.0	0.0	0.0				!12
TFE	0.0	0.0	0.0	0.0	0.0	0.0				!13
LDOM	0.1	0.1	0.1	0.1	0.1	0.1				!14
RDOM	0.1	0.1	0.1	0.1	0.1	0.1				!15
LPOM	0.1	0.1	0.1	0.1	0.1	0.1				!16
RPOM	0.1	0.1	0.1	0.1	0.1	0.1				!17
CBOD 1	0.0	0.0	0.0	0.0	0.0	0.0				!18
CBOD 2	0.0	0.0	0.0	0.0	0.0	0.0				!19
CBOD 3	0.0	0.0	0.0	0.0	0.0	0.0				!20
CBOD 4	0.0	0.0	0.0	0.0	0.0	0.0				!21
CBOD 5	0.0	0.0	0.0	0.0	0.0	0.0				!22
CBODP1	0.0	0.0	0.0	0.0	0.0	0.0				!23
CBODP2	0.0	0.0	0.0	0.0	0.0	0.0				!24
CBODP3	0.0	0.0	0.0	0.0	0.0	0.0				!25
CBODP4	0.0	0.0	0.0	0.0	0.0	0.0				!26
CBODP5	0.0	0.0	0.0	0.0	0.0	0.0				!27
CBODN1	0.0	0.0	0.0	0.0	0.0	0.0				!28
CBODN2	0.0	0.0	0.0	0.0	0.0	0.0				!29
CBODN3	0.0	0.0	0.0	0.0	0.0	0.0				!30
CBODN4	0.0	0.0	0.0	0.0	0.0	0.0				!31
CBODN5	0.0	0.0	0.0	0.0	0.0	0.0				!32
ALGAE	0.1	0.1	0.1	0.1	0.1	0.1				!33
DO	12.0	12.0	12.0	12.0	12.0	12.0				!34
TIC	5.0	5.0	5.0	5.0	5.0	5.0				!35
ALK	19.8	19.8	19.8	19.8	19.8	19.8				!36
ZOO1	0.1000	0.10	0.10	0.10	0.10	0.10				!37
LDOM_P	0.0005	0.005	0.005	0.0005	0.005	0.005				!38
RDOM_P	0.0005	0.005	0.005	0.0005	0.005	0.005				!39
LPOM_P	0.0005	0.005	0.005	0.0005	0.005	0.005				!40
RPOM_P	0.0005	0.005	0.005	0.0005	0.005	0.005				!41
LDOM_N	0.0080	0.080	0.080	0.0080	0.080	0.080				!42
RDOM_N	0.0080	0.080	0.080	0.0005	0.080	0.080				!43
LPOM_N	0.0080	0.080	0.080	0.0080	0.080	0.080				!44
RPOM_N	0.0080	0.080	0.080	0.0080	0.080	0.080				!45

CST PRINT	CPRWBC	CPRWBC	CPRWBC	CPRWBC	CPRWBC	CPRWBC	CPRWBC	CPRWBC	CPRWBC	
TDS	ON	ON	ON	ON	ON	ON				!1
AGE	ON	ON	ON	ON	ON	ON				!2
TRACER	ON	ON	ON	ON	ON	ON				!3
COLIFORM	ON	ON	ON	ON	ON	ON				!4
CONDUCT	ON	ON	ON	ON	ON	ON				!5
CHLORIDE	ON	ON	ON	ON	ON	ON				!6
ISS	ON	ON	ON	ON	ON	ON				!7
PO4	ON	ON	ON	ON	ON	ON				!8
NH4	ON	ON	ON	ON	ON	ON				!9

SAMPLE CONTROL FILE

CONTROL FILE

NOX	ON	ON	ON	ON	ON	ON	!10
DSI	OFF	OFF	OFF	OFF	OFF	OFF	!11
PSI	OFF	OFF	OFF	OFF	OFF	OFF	!12
TFE	OFF	OFF	OFF	OFF	OFF	OFF	!13
LDOM	ON	ON	ON	ON	ON	ON	!14
RDOM	ON	ON	ON	ON	ON	ON	!15
LPOM	ON	ON	ON	ON	ON	ON	!16
RPOM	ON	ON	ON	ON	ON	ON	!17
CBOD_1	ON	ON	ON	ON	ON	ON	!18
CBOD_2	ON	ON	ON	ON	ON	ON	!19
CBOD_3	ON	ON	ON	ON	ON	ON	!20
CBOD_4	ON	ON	ON	ON	ON	ON	!21
CBOD_5	ON	ON	ON	ON	ON	ON	!22
CBODP1	ON	ON	ON	ON	ON	ON	!18
CBODP2	ON	ON	ON	ON	ON	ON	!19
CBODP3	ON	ON	ON	ON	ON	ON	!20
CBODP4	ON	ON	ON	ON	ON	ON	!21
CBODP5	ON	ON	ON	ON	ON	ON	!22
CBODN1	ON	ON	ON	ON	ON	ON	
CBODN2	ON	ON	ON	ON	ON	ON	
CBODN3	ON	ON	ON	ON	ON	ON	
CBODN4	ON	ON	ON	ON	ON	ON	
CBODN5	ON	ON	ON	ON	ON	ON	
ALGAE	ON	ON	ON	ON	ON	ON	
DO	ON	ON	ON	ON	ON	ON	
TIC	ON	ON	ON	ON	ON	ON	!35
ALK	ON	ON	ON	ON	ON	ON	!36
ZOO1	ON	ON	ON	ON	ON	ON	!37
LDOM_P	ON	ON	ON	ON	ON	ON	!38
RDOM_P	ON	ON	ON	ON	ON	ON	!39
LPOM_P	ON	ON	ON	ON	ON	ON	!40
RPOM_P	ON	ON	ON	ON	ON	ON	!41
LDOM_N	ON	ON	ON	ON	ON	ON	!42
RDOM_N	ON	ON	ON	ON	ON	ON	!43
LPOM_N	ON	ON	ON	ON	ON	ON	!44
RPOM_N	ON	ON	ON	ON	ON	ON	!45

CIN CON	CINBRC	CINBRC	CINBRC	CINBRC	CINBRC	CINBRC	CINBRC	CINBRC	CINBRC	
TDS	ON	ON	ON	ON	ON	ON	ON	ON	ON	!1
AGE	OFF	OFF	OFF	OFF	OFF	OFF	OFF	OFF	OFF	!2
TRACER	ON	ON	ON	ON	ON	ON	ON	ON	ON	!3
COLIFORM	ON	ON	ON	ON	ON	ON	ON	ON	ON	!4
CONDUCT	ON	ON	ON	ON	ON	ON	ON	ON	ON	!5
CHLORIDE	ON	ON	ON	ON	ON	ON	ON	ON	ON	!6
ISS	ON	ON	ON	ON	ON	ON	ON	ON	ON	!7
PO4	ON	ON	ON	ON	ON	ON	ON	ON	ON	!8
NH4	ON	ON	ON	ON	ON	ON	ON	ON	ON	!9
NOX	ON	ON	ON	ON	ON	ON	ON	ON	ON	!10
DSI	OFF	OFF	OFF	OFF	OFF	OFF	OFF	OFF	OFF	!11
PSI	OFF	OFF	OFF	OFF	OFF	OFF	OFF	OFF	OFF	!12
TFE	OFF	OFF	OFF	OFF	OFF	OFF	OFF	OFF	OFF	!13
LDOM	ON	ON	ON	ON	ON	ON	ON	ON	ON	!14
RDOM	ON	ON	ON	ON	ON	ON	ON	ON	ON	!15

CONTROL FILE

SAMPLE CONTROL FILE

LPOM	ON	ON	ON	ON	ON	ON	ON	ON	ON	! 16
	ON	ON	ON							
RPOM	ON	ON	ON	ON	ON	ON	ON	ON	ON	! 17
	ON	ON	ON							
CBOD 1	ON	ON	ON	ON	ON	ON	ON	ON	ON	! 18
	ON	ON	ON							
CBOD 2	ON	ON	ON	ON	ON	ON	ON	ON	ON	! 19
	ON	ON	ON							
CBOD 3	ON	ON	ON	ON	ON	ON	ON	ON	ON	! 20
	ON	ON	ON							
CBOD 4	ON	ON	ON	ON	ON	ON	ON	ON	ON	! 21
	ON	ON	ON							
CBOD 5	ON	ON	ON	ON	ON	ON	ON	ON	ON	! 22
	ON	ON	ON							
CBODP1	ON	ON	ON	ON	ON	ON	ON	ON	ON	! 23
	ON	ON	ON							
CBODP2	ON	ON	ON	ON	ON	ON	ON	ON	ON	! 24
	ON	ON	ON							
CBODP3	ON	ON	ON	ON	ON	ON	ON	ON	ON	! 25
	ON	ON	ON							
CBODP4	ON	ON	ON	ON	ON	ON	ON	ON	ON	! 26
	ON	ON	ON							
CBODP5	ON	ON	ON	ON	ON	ON	ON	ON	ON	! 27
	ON	ON	ON							
CBODN1	ON	ON	ON	ON	ON	ON	ON	ON	ON	! 28
	ON	ON	ON							
CBODN2	ON	ON	ON	ON	ON	ON	ON	ON	ON	! 29
	ON	ON	ON							
CBODN3	ON	ON	ON	ON	ON	ON	ON	ON	ON	! 30
	ON	ON	ON							
CBODN4	ON	ON	ON	ON	ON	ON	ON	ON	ON	! 31
	ON	ON	ON							
CBODN5	ON	ON	ON	ON	ON	ON	ON	ON	ON	! 32
	ON	ON	ON							
ALGAE	ON	ON	ON	ON	ON	ON	ON	ON	ON	! 33
	ON	ON	ON							
DO	ON	ON	ON	ON	ON	ON	ON	ON	ON	! 34
	ON	ON	ON							
TIC	ON	ON	ON	ON	ON	ON	ON	ON	ON	! 35
	ON	ON	ON							
ALK	ON	ON	ON	ON	ON	ON	ON	ON	ON	! 36
	ON	ON	ON							
ZOO1	ON	ON	ON	ON	ON	ON	ON	ON	ON	! 37
	ON	ON	ON							
LDOM_P	ON	ON	ON	ON	ON	ON	ON	ON	ON	! 38
	ON	ON	ON							
RDOM_P	ON	ON	ON	ON	ON	ON	ON	ON	ON	! 39
	ON	ON	ON							
LPOM_P	ON	ON	ON	ON	ON	ON	ON	ON	ON	! 40
	ON	ON	ON							
RPOM_P	ON	ON	ON	ON	ON	ON	ON	ON	ON	! 41
	ON	ON	ON							
LDOM_N	ON	ON	ON	ON	ON	ON	ON	ON	ON	! 42
	ON	ON	ON							
RDOM_N	ON	ON	ON	ON	ON	ON	ON	ON	ON	! 43
	ON	ON	ON							
LPOM_N	ON	ON	ON	ON	ON	ON	ON	ON	ON	! 44
	ON	ON	ON							
RPOM_N	ON	ON	ON	ON	ON	ON	ON	ON	ON	! 45
	ON	ON	ON							
CTR CON	CTRTRC	CTRTRC	CTRTRC	CTRTRC	CTRTRC	CTRTRC	CTRTRC	CTRTRC	CTRTRC	
TDS	ON	ON	ON	ON	ON	ON	ON			! 1
AGE	OFF	OFF	OFF	OFF	OFF	OFF	OFF			! 2
TRACER	ON	ON	ON	ON	ON	ON	ON			! 3
COLIFORM	ON	ON	ON	ON	ON	ON	ON			! 4
CONDUCT	ON	ON	ON	ON	ON	ON	ON			! 5
CHLORIDE	ON	ON	ON	ON	ON	ON	ON			! 6

SAMPLE CONTROL FILE

CONTROL FILE

ISS	ON	ON	ON	ON	ON	ON	ON	!7
PO4	ON	ON	ON	ON	ON	ON	ON	!8
NH4	ON	ON	ON	ON	ON	ON	ON	!9
NOx	ON	ON	ON	ON	ON	ON	ON	!10
DSi	OFF	OFF	OFF	OFF	OFF	OFF	OFF	!11
PSi	OFF	OFF	OFF	OFF	OFF	OFF	OFF	!12
TFe	OFF	OFF	OFF	OFF	OFF	OFF	OFF	!13
LDOM	ON	ON	ON	ON	ON	ON	ON	!14
RDOM	ON	ON	ON	ON	ON	ON	ON	!15
LPOM	ON	ON	ON	ON	ON	ON	ON	!16
RPOM	ON	ON	ON	ON	ON	ON	ON	!17
CBOD_1	ON	ON	ON	ON	ON	ON	ON	!18
CBOD_2	ON	ON	ON	ON	ON	ON	ON	!19
CBOD_3	ON	ON	ON	ON	ON	ON	ON	!20
CBOD_4	ON	ON	ON	ON	ON	ON	ON	!21
CBOD_5	ON	ON	ON	ON	ON	ON	ON	!22
CBODP1	ON	ON	ON	ON	ON	ON	ON	!23
CBODP2	ON	ON	ON	ON	ON	ON	ON	!24
CBODP3	ON	ON	ON	ON	ON	ON	ON	!25
CBODP4	ON	ON	ON	ON	ON	ON	ON	!26
CBODP5	ON	ON	ON	ON	ON	ON	ON	!27
CBODN1	ON	ON	ON	ON	ON	ON	ON	!28
CBODN2	ON	ON	ON	ON	ON	ON	ON	!29
CBODN3	ON	ON	ON	ON	ON	ON	ON	!30
CBODN4	ON	ON	ON	ON	ON	ON	ON	!31
CBODN5	ON	ON	ON	ON	ON	ON	ON	!32
ALGAE	ON	ON	ON	ON	ON	ON	ON	!33
DO	ON	ON	ON	ON	ON	ON	ON	!34
TIC	ON	ON	ON	ON	ON	ON	ON	!35
ALK	ON	ON	ON	ON	ON	ON	ON	!36
ZOO1	ON	ON	ON	ON	ON	ON	ON	!37
LDOM_P	ON	ON	ON	ON	ON	ON	ON	!38
RDOM_P	ON	ON	ON	ON	ON	ON	ON	!39
LPOM_P	ON	ON	ON	ON	ON	ON	ON	!40
RPOM_P	ON	ON	ON	ON	ON	ON	ON	!41
LDOM_N	ON	ON	ON	ON	ON	ON	ON	!42
RDOM_N	ON	ON	ON	ON	ON	ON	ON	!43
LPOM_N	ON	ON	ON	ON	ON	ON	ON	!44
RPOM_N	ON	ON	ON	ON	ON	ON	ON	!45

CDT CON	CDTBRC	CDTBRC	CDTBRC	CDTBRC	CDTBRC	CDTBRC	CDTBRC	CDTBRC	CDTBRC	
TDS	ON	ON	ON	ON	ON	ON	ON	ON	ON	!1
AGE	OFF	OFF	OFF	OFF	OFF	OFF	OFF	OFF	OFF	!2
TRACER	ON	ON	ON	ON	ON	ON	ON	ON	ON	!3
COLIFORM	ON	ON	ON	ON	ON	ON	ON	ON	ON	!4
CONDUCT	ON	ON	ON	ON	ON	ON	ON	ON	ON	!5
CHLORIDE	ON	ON	ON	ON	ON	ON	ON	ON	ON	!6
ISS	ON	ON	ON	ON	ON	ON	ON	ON	ON	!7
PO4	ON	ON	ON	ON	ON	ON	ON	ON	ON	!8
NH4	ON	ON	ON	ON	ON	ON	ON	ON	ON	!9
NOX	ON	ON	ON	ON	ON	ON	ON	ON	ON	!10
DSI	OFF	OFF	OFF	OFF	OFF	OFF	OFF	OFF	OFF	!11
PSI	OFF	OFF	OFF	OFF	OFF	OFF	OFF	OFF	OFF	!12
TFE	OFF	OFF	OFF	OFF	OFF	OFF	OFF	OFF	OFF	!13
LDOM	ON	ON	ON	ON	ON	ON	ON	ON	ON	!14

CONTROL FILE

SAMPLE CONTROL FILE

RDOM	ON	ON	ON	ON	ON	ON	ON	ON	ON	!15
	ON	ON	ON							
LPOM	ON	ON	ON	ON	ON	ON	ON	ON	ON	!16
	ON	ON	ON							
RPOM	ON	ON	ON	ON	ON	ON	ON	ON	ON	!17
	ON	ON	ON							
CBOD 1	ON	ON	ON	ON	ON	ON	ON	ON	ON	!18
	ON	ON	ON							
CBOD 2	ON	ON	ON	ON	ON	ON	ON	ON	ON	!19
	ON	ON	ON							
CBOD 3	ON	ON	ON	ON	ON	ON	ON	ON	ON	!20
	ON	ON	ON							
CBOD 4	ON	ON	ON	ON	ON	ON	ON	ON	ON	!21
	ON	ON	ON							
CBOD 5	ON	ON	ON	ON	ON	ON	ON	ON	ON	!22
	ON	ON	ON							
CBODP1	ON	ON	ON	ON	ON	ON	ON	ON	ON	!23
	ON	ON	ON							
CBODP2	ON	ON	ON	ON	ON	ON	ON	ON	ON	!24
	ON	ON	ON							
CBODP3	ON	ON	ON	ON	ON	ON	ON	ON	ON	!25
	ON	ON	ON							
CBODP4	ON	ON	ON	ON	ON	ON	ON	ON	ON	!26
	ON	ON	ON							
CBODP5	ON	ON	ON	ON	ON	ON	ON	ON	ON	!27
	ON	ON	ON							
CBODN1	ON	ON	ON	ON	ON	ON	ON	ON	ON	!28
	ON	ON	ON							
CBODN2	ON	ON	ON	ON	ON	ON	ON	ON	ON	!29
	ON	ON	ON							
CBODN3	ON	ON	ON	ON	ON	ON	ON	ON	ON	!30
	ON	ON	ON							
CBODN4	ON	ON	ON	ON	ON	ON	ON	ON	ON	!31
	ON	ON	ON							
CBODN5	ON	ON	ON	ON	ON	ON	ON	ON	ON	!32
	ON	ON	ON							
ALGAE	ON	ON	ON	ON	ON	ON	ON	ON	ON	!33
	ON	ON	ON							
DO	ON	ON	ON	ON	ON	ON	ON	ON	ON	!34
	ON	ON	ON							
TIC	ON	ON	ON	ON	ON	ON	ON	ON	ON	!35
	ON	ON	ON							
ALK	ON	ON	ON	ON	ON	ON	ON	ON	ON	!36
	ON	ON	ON							
ZOO1	ON	ON	ON	ON	ON	ON	ON	ON	ON	!37
	ON	ON	ON							
LDOM_P	ON	ON	ON	ON	ON	ON	ON	ON	ON	!38
	ON	ON	ON							
RDOM_P	ON	ON	ON	ON	ON	ON	ON	ON	ON	!39
	ON	ON	ON							
LPOM_P	ON	ON	ON	ON	ON	ON	ON	ON	ON	!40
	ON	ON	ON							
RPOM_P	ON	ON	ON	ON	ON	ON	ON	ON	ON	!41
	ON	ON	ON							
LDOM_N	ON	ON	ON	ON	ON	ON	ON	ON	ON	!42
	ON	ON	ON							
RDOM_N	ON	ON	ON	ON	ON	ON	ON	ON	ON	!43
	ON	ON	ON							
LPOM_N	ON	ON	ON	ON	ON	ON	ON	ON	ON	!44
	ON	ON	ON							
RPOM_N	ON	ON	ON	ON	ON	ON	ON	ON	ON	!45
	ON	ON	ON							
CPR CON	CPRBRC	CPRBRC	CPRBRC	CPRBRC	CPRBRC	CPRBRC	CPRBRC	CPRBRC	CPRBRC	
TDS	ON	ON	ON	ON	ON	ON	ON	ON	ON	!1
	ON	ON	ON							
AGE	OFF	OFF	OFF	OFF	OFF	OFF	OFF	OFF	OFF	!2

SAMPLE CONTROL FILE

CONTROL FILE

	OFF	OFF	OFF							
TRACER	ON	ON	ON	ON	ON	ON	ON	ON	ON	!3
	ON	ON	ON							
COLIFORM	ON	ON	ON	ON	ON	ON	ON	ON	ON	!4
	ON	ON	ON							
CONDUCT	ON	ON	ON	ON	ON	ON	ON	ON	ON	!5
	ON	ON	ON							
CHLORIDE	ON	ON	ON	ON	ON	ON	ON	ON	ON	!6
	ON	ON	ON							
ISS1	ON	ON	ON	ON	ON	ON	ON	ON	ON	!7
	ON	ON	ON							
PO4	ON	ON	ON	ON	ON	ON	ON	ON	ON	!8
	ON	ON	ON							
NH4	ON	ON	ON	ON	ON	ON	ON	ON	ON	!9
	ON	ON	ON							
NOx	ON	ON	ON	ON	ON	ON	ON	ON	ON	!10
	ON	ON	ON							
DSI	OFF	OFF	OFF	OFF	OFF	OFF	OFF	OFF	OFF	!11
	OFF	OFF	OFF							
PSI	OFF	OFF	OFF	OFF	OFF	OFF	OFF	OFF	OFF	!12
	OFF	OFF	OFF							
TFE	OFF	OFF	OFF	OFF	OFF	OFF	OFF	OFF	OFF	!13
	OFF	OFF	OFF							
LDOM	ON	ON	ON	ON	ON	ON	ON	ON	ON	!14
	ON	ON	ON							
RDOM	ON	ON	ON	ON	ON	ON	ON	ON	ON	!15
	ON	ON	ON							
LPOM	ON	ON	ON	ON	ON	ON	ON	ON	ON	!16
	ON	ON	ON							
RPOM	ON	ON	ON	ON	ON	ON	ON	ON	ON	!17
	ON	ON	ON							
CBOD 1	ON	ON	ON	ON	ON	ON	ON	ON	ON	!18
	ON	ON	ON							
CBOD 2	ON	ON	ON	ON	ON	ON	ON	ON	ON	!19
	ON	ON	ON							
CBOD 3	ON	ON	ON	ON	ON	ON	ON	ON	ON	!20
	ON	ON	ON							
CBOD 4	ON	ON	ON	ON	ON	ON	ON	ON	ON	!21
	ON	ON	ON							
CBOD 5	ON	ON	ON	ON	ON	ON	ON	ON	ON	!22
	ON	ON	ON							
CBODP1	ON	ON	ON	ON	ON	ON	ON	ON	ON	!23
	ON	ON	ON							
CBODP2	ON	ON	ON	ON	ON	ON	ON	ON	ON	!24
	ON	ON	ON							
CBODP3	ON	ON	ON	ON	ON	ON	ON	ON	ON	!25
	ON	ON	ON							
CBODP4	ON	ON	ON	ON	ON	ON	ON	ON	ON	!26
	ON	ON	ON							
CBODP5	ON	ON	ON	ON	ON	ON	ON	ON	ON	!27
	ON	ON	ON							
CBODN1	ON	ON	ON	ON	ON	ON	ON	ON	ON	!28
	ON	ON	ON							
CBODN2	ON	ON	ON	ON	ON	ON	ON	ON	ON	!29
	ON	ON	ON							
CBODN3	ON	ON	ON	ON	ON	ON	ON	ON	ON	!30
	ON	ON	ON							
CBODN4	ON	ON	ON	ON	ON	ON	ON	ON	ON	!31
	ON	ON	ON							
CBODN5	ON	ON	ON	ON	ON	ON	ON	ON	ON	!32
	ON	ON	ON							
ALGAE	ON	ON	ON	ON	ON	ON	ON	ON	ON	!33
	ON	ON	ON							
DO	ON	ON	ON	ON	ON	ON	ON	ON	ON	!34
	ON	ON	ON							
TIC	ON	ON	ON	ON	ON	ON	ON	ON	ON	!35
	ON	ON	ON							
ALK	ON	ON	ON	ON	ON	ON	ON	ON	ON	!36

CONTROL FILE

SAMPLE CONTROL FILE

ZOO1	ON	ON	ON							
	ON	ON	ON	ON	ON	ON	ON	ON	ON	! 37
LDOM_P	ON	ON	ON	ON	ON	ON	ON	ON	ON	! 38
	ON	ON	ON							
RDOM_P	ON	ON	ON	ON	ON	ON	ON	ON	ON	! 39
	ON	ON	ON							
LPOM_P	ON	ON	ON	ON	ON	ON	ON	ON	ON	! 40
	ON	ON	ON							
RPOM_P	ON	ON	ON	ON	ON	ON	ON	ON	ON	! 41
	ON	ON	ON							
LDOM_N	ON	ON	ON	ON	ON	ON	ON	ON	ON	! 42
	ON	ON	ON							
RDOM_N	ON	ON	ON	ON	ON	ON	ON	ON	ON	! 43
	ON	ON	ON							
LPOM_N	ON	ON	ON	ON	ON	ON	ON	ON	ON	! 44
	ON	ON	ON							
RPOM_N	ON	ON	ON	ON	ON	ON	ON	ON	ON	! 45
	ON	ON	ON							
EX COEF	EXH2O	EXSS	EXOM	BETA	EXC	EXIC				
Wb 1	0.45	0.01	0.40	0.45	OFF	OFF				
Wb 2	0.45	0.01	0.40	0.45	OFF	OFF				
Wb 3	0.45	0.01	0.40	0.45	OFF	OFF				
Wb 4	0.45	0.01	0.40	0.45	OFF	OFF				
Wb 5	0.45	0.01	0.40	0.45	OFF	OFF				
Wb 6	0.45	0.01	0.40	0.45	OFF	OFF				
ALG EX	EXA	EXA	EXA	EXA	EXA	EXA				
	0.10	0.2	0.2	0.2	0.2	0.2				
ZOO EX	EXZ	EXZ	EXZ	EXZ	EXZ	EXZ				
	0.2	0.2	0.2							
MACRO EX	EXM	EXM	EXM	EXM	EXM	EXM				
	0.0100									
GENERIC	CGQ10	CGQDK	CG1DK	CGS						
AGE	0.00	-1.0	0.0	0.0						
TRACER	0.00	0.0	0.0	0.0						
COLIFORM	1.04	0.0	0.5	0.0						
CONDUCT	0.00	0.0	0.0	0.0						
CHLORIDE	0.00	0.0	0.0	0.0						
S SOLIDS	SSS	SEDRC	TAUCR							
SSS 1	1.5	OFF	0.0							
ALGAL RATE	AG	AR	AE	AM	AS	AHSP	AHSN	AHSSI	ASAT	
Alg 1	2.0	0.12	0.02	0.05	0.04	0.005	0.005	0.0	50.0	
ALGAL TEMP	AT1	AT2	AT3	AT4	AK1	AK2	AK3	AK4		
Alg 1	5.0	12.0	20.0	30.0	0.1	0.99	0.99	0.1		
ALG STOICH	ALGP	ALGN	ALGC	ALGSI	ACHLA	APOM	ANEQN	ANPR		
Alg 1	0.005	0.08	0.45	0.00	0.0500	0.8	2	0.001		
EPIPHYTE	EPIC	EPIC	EPIC	EPIC	EPIC	EPIC	EPIC	EPIC	EPIC	
Epi 1	ON	ON	ON	ON	ON	ON				
EPI PRINT	EPRC	EPRC	EPRC	EPRC	EPRC	EPRC	EPRC	EPRC	EPRC	
Epi 1	ON	ON	ON	ON	ON	ON				
EPI INIT	EPICI	EPICI	EPICI	EPICI	EPICI	EPICI	EPICI	EPICI	EPICI	
Epi 1	20.0	-1.0	-1.0	20.0	-1.0	-1.0				
EPI RATE	EG	ER	EE	EM	EB	EHSP	EHSN	EHSSI		
Epi 1	1.7	0.05	0.02	0.05	0.05	0.002	0.004	0.0		

SAMPLE CONTROL FILE

CONTROL FILE

EPI HALF	ESAT	EHS	ENEQN	ENPR						
Epi 1	150.00	40.0	2	0.001						
EPI TEMP	ET1	ET2	ET3	ET4	EK1	EK2	EK3	EK4		
Epi 1	2.0	5.0	20.0	30.0	0.1	0.99	0.99	0.1		
EPI STOICH	EP	EN	EC	ESI	ECHLA	EPOM				
Epi 1	0.005	0.08	0.45	0.0	65.0	0.8				
ZOOP RATE	ZG	ZR	ZM	ZEFF	PREFP	ZOOMIN	ZS2P			
Zoo1	1.50	0.10	0.010	0.50	0.50	0.0100	0.30			
ZOOP ALGP	PREFA	PREFA	PREFA	PREFA	PREFA	PREFA	PREFA	PREFA	PREFA	PREFA
Zoo1	1.00	0.50	0.50							
ZOOP ZOOP	PREFZ	PREFZ	PREFZ	PREFZ	PREFZ	PREFZ	PREFZ	PREFZ	PREFZ	PREFZ
Zoo1	0.00	0.00	0.00							
ZOOP TEMP	ZT1	ZT2	ZT3	ZT4	ZK1	ZK2	ZK3	ZK4		
	0.0	15.0	20.0	36.0	0.1	0.9	0.98	0.100		
ZOOP STOI	ZP	ZN	ZC							
	0.01500	0.08000	0.45000							
MACROPHYT	MACWBC	MACWBC	MACWBC	MACWBC	MACWBC	MACWBC	MACWBC	MACWBC	MACWBC	MACWBC
Mac1	ON	OFF	OFF							
MAC PRINT	MPRWBC	MPRWBC	MPRWBC	MPRWBC	MPRWBC	MPRWBC	MPRWBC	MPRWBC	MPRWBC	MPRWBC
Mac1	ON	OFF	OFF							
MAC INI	MACWBCI	MACWBCI	MACWBCI	MACWBCI	MACWBCI	MACWBCI	MACWBCI	MACWBCI	MACWBCI	MACWBCI
Mac1	0.00000	0.1	0.5							
MAC RATE	MG	MR	MM	MSAT	MHSP	MHSN	MHSC	MPOM	LRPMAC	
Mac 1	0.30	0.05	0.05	30.0	0.0	0.0	0.0	0.9	0.2	
MAC SED	PSED	NSED								
MAC 1	0.5	0.5								
MAC DIST	MBMP	MMAX								
Mac 1	40.0	500.0								
MAC DRAG	CDDRAG	DWV	DWSA	ANORM						
Mac 1	3.0	7.0E+04	8.0	0.3						
MAC TEMP	MT1	MT2	MT3	MT4	MK1	MK2	MK3	MK4		
Mac 1	7.0	15.0	24.0	34.0	0.1	0.99	0.99	0.01		
MAC STOICH	MP	MN	MC							
Mac 1	0.005	0.08	0.45							
DOM	LDOMDK	RDOMDK	LRDDK							
Wb 1	0.10	0.001	0.001							
Wb 2	0.10	0.001	0.001							
Wb 3	0.10	0.001	0.001							
Wb 4	0.10	0.001	0.001							
Wb 5	0.10	0.001	0.001							
Wb 6	0.10	0.001	0.001							
POM	LPOMDK	RPOMDK	LRPDK	POMS						
Wb 1	0.08	0.001	0.001	0.1						
Wb 2	0.08	0.001	0.001	0.1						
Wb 3	0.08	0.001	0.001	0.1						
Wb 4	0.08	0.001	0.001	0.1						
Wb 5	0.08	0.001	0.001	0.1						
Wb 6	0.08	0.001	0.001	0.1						

CONTROL FILE

SAMPLE CONTROL FILE

OM STOICH	ORGP	ORGN	ORGC	ORGS
Wb 1	0.005	0.08	0.45	0.18
Wb 2	0.005	0.08	0.45	0.18
Wb 3	0.005	0.08	0.45	0.18
Wb 4	0.005	0.08	0.45	0.18
Wb 5	0.005	0.08	0.45	0.18
Wb 6	0.005	0.08	0.45	0.18

OM RATE	OMT1	OMT2	OMK1	OMK2
Wb 1	4.0	30.0	0.1	0.99
Wb 2	4.0	30.0	0.1	0.99
Wb 3	4.0	30.0	0.1	0.99
Wb 4	4.0	30.0	0.1	0.99
Wb 5	4.0	30.0	0.1	0.99
Wb 6	4.0	30.0	0.1	0.99

CBOD	KBOD	TBOD	RBOD	CBODS
CBOD 1	0.0418	1.0147	1.0	0.0
CBOD 2	0.1302	1.0147	1.0	0.0
CBOD 3	0.0469	1.0147	1.0	0.0
CBOD 4	0.0880	1.0147	1.0	0.0
CBOD 5	0.050	1.0147	1.0	0.0

CBOD STOIC	CBODP	CBODN	CBODC
CBOD 1	0.005	0.08	0.45
CBOD 2	0.005	0.08	0.45
CBOD 3	0.005	0.08	0.45
CBOD 4	0.005	0.08	0.45
CBOD 5	0.005	0.08	0.45

PHOSPHOR	PO4R	PARTP
Wb 1	0.001	0.0
Wb 2	0.001	0.0
Wb 3	0.001	0.0
Wb 4	0.001	0.0
Wb 5	0.001	0.0
Wb 6	0.001	0.0

AMMONIUM	NH4R	NH4DK
Wb 1	0.001	0.50
Wb 2	0.001	0.50
Wb 3	0.001	0.50
Wb 4	0.001	0.50
Wb 5	0.001	0.50
Wb 6	0.001	0.50

NH4 RATE	NH4T1	NH4T2	NH4K1	NH4K2
Wb 1	5.0	25.0	0.1	0.99
Wb 2	5.0	25.0	0.1	0.99
Wb 3	5.0	25.0	0.1	0.99
Wb 4	5.0	25.0	0.1	0.99
Wb 5	5.0	25.0	0.1	0.99
Wb 6	5.0	25.0	0.1	0.99

NITRATE	NO3DK	NO3S	FNO3SED
Wb 1	0.05	0.0	0.00
Wb 2	0.05	0.0	0.00
Wb 3	0.05	0.0	0.00
Wb 4	0.05	0.0	0.00
Wb 5	0.05	0.0	0.00
Wb 6	0.05	0.0	0.00

NO3 RATE	NO3T1	NO3T2	NO3K1	NO3K2
Wb 1	5.0	25.0	0.1	0.99
Wb 2	5.0	25.0	0.1	0.99

SAMPLE CONTROL FILE

CONTROL FILE

Wb 3	5.0	25.0	0.1	0.99
Wb 4	5.0	25.0	0.1	0.99
Wb 5	5.0	25.0	0.1	0.99
Wb 6	5.0	25.0	0.1	0.99

SILICA	DSIR	PSIS	PSIDK	PARTSI
Wb 1	0.1	0.0	0.3	0.2
Wb 2	0.1	0.0	0.3	0.2
Wb 3	0.1	0.0	0.3	0.2
Wb 4	0.1	0.0	0.3	0.2
Wb 5	0.1	0.0	0.3	0.2
Wb 6	0.1	0.0	0.3	0.2

IRON	FEREL	FESETL
Wb 1	0.1	0.0
Wb 2	0.1	0.0
Wb 3	0.1	0.0
Wb 4	0.1	0.0
Wb 5	0.1	0.0
Wb 6	0.1	0.0

SED CO2	CO2R
Wb 1	0.1
Wb 2	0.1
Wb 3	0.1
Wb 4	0.1
Wb 5	0.1
Wb 6	0.1

STOICH 1	O2NH4	O2OM
Wb 1	4.570	1.400
Wb 2	4.570	1.400
Wb 3	4.570	1.400
Wb 4	4.570	1.400
Wb 5	4.570	1.400
Wb 6	4.570	1.400

STOICH 2	O2AR	O2AG
Alg 1	1.100	1.400

STOICH 3	O2ER	O2EG
Epi 1	1.100	1.400

STOICH 4	O2ZR
ZOO1	1.10000

STOICH 5	O2MR	O2MG
MAC1	1.1	1.4

O2 LIMIT	O2LIM
	0.1

SEDIMENT	SEDC	PRNSC	SEDCI	SEDK	SEDS	FSOD	FSOD	SEDBR	DYNSDK
Wb 1	ON	ON	0.0	0.1	0.0	1.0	1.0	0.001	OFF
Wb 2	ON	ON	0.0	0.1	0.0	1.0	1.0	0.001	OFF
Wb 3	ON	ON	0.0	0.1	0.0	1.0	1.0	0.001	OFF
Wb 4	ON	ON	0.0	0.1	0.0	1.0	1.0	0.001	OFF
Wb 5	ON	ON	0.0	0.1	0.0	1.0	1.0	0.001	OFF
Wb 6	ON	ON	0.0	0.1	0.0	1.0	1.0	0.001	OFF

SOD RATE	SODT1	SODT2	SODK1	SODK2
Wb 1	4.0	30.0	0.1	0.99
Wb 2	4.0	30.0	0.1	0.99
Wb 3	4.0	30.0	0.1	0.99
Wb 4	4.0	30.0	0.1	0.99
Wb 5	4.0	30.0	0.1	0.99
Wb 6	4.0	30.0	0.1	0.99

SAMPLE CONTROL FILE

REAERATION	TYPE	EQN#	COEF1	COEF2	COEF3	COEF4
Wb 1	RIVER	7				
Wb 2	LAKE	6				
Wb 3	LAKE	6				
Wb 4	RIVER	7				
Wb 5	LAKE	6				
Wb 6	LAKE	6				

```

BTH FILE.....BTHFN.....
Wb 1      bth_wb1.npt
Wb 2      bth_wb2.npt
Wb 3      bth_wb3.npt
Wb 4      bth_wb4.npt
Wb 5      bth_wb5.npt
Wb 6      bth_wb6.npt

```

```

EXT FILE.....EXTFN.....
Wb 1      ext_wb1.npt - not used
Wb 2      ext_wb2.npt - not used
Wb 3      ext_wb3.npt - not used
Wb 4      ext_wb3.npt - not used

```

SAMPLE CONTROL FILE

CONTROL FILE

Wb 5 ext_wb3.npt - not used
Wb 6 ext_wb3.npt - not used

VPR FILE.....VPRFN.....

Wb 1 vpr_wb1.npt
Wb 2 vpr_wb2.npt
Wb 3 vpr_wb3.npt
Wb 4 vpr_wb4.npt
Wb 5 vpr_wb5.npt
Wb 6 vpr_wb6.npt

LPR FILE.....LPRFN.....

Wb 1 lpr_wb1.npt - not used
Wb 2 lpr_wb2.npt - not used
Wb 3 lpr_wb3.npt - not used
Wb 4 lpr_wb4.npt - not used
Wb 5 lpr_wb5.npt - not used
Wb 6 lpr_wb6.npt - not used

QIN FILE.....QINFN.....

Br 1 qin_br1.npt
Br 2 qin_br2.npt - not used
Br 3 qin_br3.npt - not used
Br 4 qin_br4.npt - not used
Br 5 qin_br5.npt
Br 6 qin_br6.npt
Br 7 qin_br7.npt - not used
Br 8 qin_br8.npt
Br 9 qin_br9.npt - not used
Br 10 qin_br10.npt
Br 11 qin_br11.npt - not used
Br 12 qin_br12.npt

TIN FILE.....TINFN.....

Br 1 tin_br1.npt
Br 2 tin_br2.npt - not used
Br 3 tin_br3.npt - not used
Br 4 tin_br4.npt - not used
Br 5 tin_br5.npt
Br 6 tin_br6.npt
Br 7 tin_br7.npt - not used
Br 8 tin_br8.npt
Br 9 tin_br9.npt - not used
Br 10 tin_br10.npt
Br 11 tin_br11.npt - not used
Br 12 tin_br12.npt

CIN FILE.....CINFN.....

Br 1 cin_br1.npt
Br 2 cin_br2.npt - not used
Br 3 cin_br3.npt - not used
Br 4 cin_br4.npt - not used
Br 5 cin_br5.npt
Br 6 cin_br6.npt
Br 7 cin_br7.npt - not used
Br 8 cin_br8.npt
Br 9 cin_br9.npt - not used
Br 10 cin_br10.npt
Br 11 cin_br11.npt - not used
Br 12 cin_br12.npt

QOT FILE.....QOTFN.....

Br 1 qot_br1.npt - not used
Br 2 qot_br2.npt - not used
Br 3 qot_br3.npt - not used
Br 4 qot_br4.npt - not used
Br 5 qot_br5.npt
Br 6 qot_br6.npt - not used

CONTROL FILE

Br 7 qot_br7.npt
Br 8 qot_br8.npt - not used
Br 9 qot_br9.npt - not used
Br 10 qot_br10.npt - not used
Br 11 qot_br11.npt
Br 12 qot_br12.npt

QTR FILE.....QTRFN.....
Tr 1 qtr_tr1.npt
Tr 2 qtr_tr2.npt
Tr 3 qtr_tr3.npt
Tr 4 qtr_tr4.npt
Tr 5 qtr_tr5.npt
Tr 6 qtr_tr6.npt
Tr 7 qtr_tr7.npt

TTR FILE.....TTRFN.....
Tr 1 ttr_tr1.npt
Tr 2 ttr_tr2.npt
Tr 3 ttr_tr3.npt
Tr 4 ttr_tr4.npt
Tr 5 ttr_tr5.npt
Tr 6 ttr_tr6.npt
Tr 7 ttr_tr7.npt

CTR FILE.....CTRFN.....
Tr 1 ctr_tr1.npt
Tr 2 ctr_tr2.npt
Tr 3 ctr_tr3.npt
Tr 4 ctr_tr4.npt
Tr 5 ctr_tr5.npt
Tr 6 ctr_tr6.npt
Tr 7 ctr_tr7.npt

QDT FILE.....QDTFN.....
Br 1 qdt_br1.npt
Br 2 qdt_br2.npt
Br 3 qdt_br3.npt
Br 4 qdt_br4.npt
Br 5 qdt_br5.npt
Br 6 qdt_br6.npt
Br 7 qdt_br7.npt
Br 8 qdt_br8.npt
Br 9 qdt_br9.npt
Br 10 qdt_br10.npt
Br 11 qdt_br11.npt
Br 12 qdt_br12.npt

TDT FILE.....TDTFN.....
Br 1 tdt_br1.npt
Br 2 tdt_br2.npt
Br 3 tdt_br3.npt
Br 4 tdt_br4.npt
Br 5 tdt_br5.npt
Br 6 tdt_br6.npt
Br 7 tdt_br7.npt
Br 8 tdt_br8.npt
Br 9 tdt_br9.npt
Br 10 tdt_br10.npt
Br 11 tdt_br11.npt
Br 12 tdt_br12.npt

CDT FILE.....CDTFN.....
Br 1 cdt_br1.npt
Br 2 cdt_br2.npt
Br 3 cdt_br3.npt
Br 4 cdt_br4.npt
Br 5 cdt_br5.npt

SAMPLE CONTROL FILE

SAMPLE CONTROL FILE

CONTROL FILE

Br 6 cdt_br6.npt
Br 7 cdt_br7.npt
Br 8 cdt_br8.npt
Br 9 cdt_br9.npt
Br 10 cdt_br10.npt
Br 11 cdt_br11.npt
Br 12 cdt_br12.npt

PRE FILE.....PREFN.....

Br 1 pre_br1.npt - not used
Br 2 pre_br2.npt - not used
Br 3 pre_br3.npt - not used
Br 4 pre_br4.npt - not used
Br 5 pre_br5.npt - not used
Br 6 pre_br6.npt - not used
Br 7 pre_br7.npt - not used
Br 8 pre_br8.npt - not used
Br 9 pre_br9.npt - not used
Br 10 pre_br10.npt - not used
Br 11 pre_br11.npt - not used
Br 12 pre_br12.npt - not used

TPR FILE.....TPRFN.....

Br 1 tpr_br1.npt - not used
Br 2 tpr_br2.npt - not used
Br 3 tpr_br3.npt - not used
Br 4 tpr_br4.npt - not used
Br 5 tpr_br5.npt - not used
Br 6 tpr_br6.npt - not used
Br 7 tpr_br7.npt - not used
Br 8 tpr_br8.npt - not used
Br 9 tpr_br9.npt - not used
Br 10 tpr_br10.npt - not used
Br 11 tpr_br11.npt - not used
Br 12 tpr_br12.npt - not used

CPR FILE.....CPRFN.....

Br 1 cpr_br1.npt - not used
Br 2 cpr_br2.npt - not used
Br 3 cpr_br3.npt - not used
Br 4 cpr_br4.npt - not used
Br 5 cpr_br5.npt - not used
Br 6 cpr_br6.npt - not used
Br 7 cpr_br7.npt - not used
Br 8 cpr_br8.npt - not used
Br 9 cpr_br9.npt - not used
Br 10 cpr_br10.npt - not used
Br 11 cpr_br11.npt - not used
Br 12 cpr_br12.npt - not used

EUH FILE.....EUHFN.....

Br 1 euh_br1.npt - not used
Br 2 euh_br2.npt - not used
Br 3 euh_br3.npt - not used
Br 4 euh_br4.npt - not used
Br 5 euh_br5.npt - not used
Br 6 euh_br6.npt - not used
Br 7 euh_br7.npt - not used
Br 8 euh_br8.npt - not used
Br 9 euh_br9.npt - not used
Br 10 euh_br10.npt - not used
Br 11 euh_br11.npt - not used
Br 12 euh_br12.npt - not used

TUH FILE.....TUHFN.....

Br 1 tuh_br1.npt - not used
Br 2 tuh_br2.npt - not used

CONTROL FILE

SAMPLE CONTROL FILE

Br 3 tuh_br3.npt - not used
Br 4 tuh_br4.npt - not used
Br 5 tuh_br5.npt - not used
Br 6 tuh_br6.npt - not used
Br 7 tuh_br7.npt - not used
Br 8 tuh_br8.npt - not used
Br 9 tuh_br9.npt - not used
Br 10 tuh_br10.npt - not used
Br 11 tuh_br11.npt - not used
Br 12 tuh_br12.npt - not used

CUH FILE.....CUHFN.....

Br 1 cuh_br1.npt - not used
Br 2 cuh_br2.npt - not used
Br 3 cuh_br3.npt - not used
Br 4 cuh_br4.npt - not used
Br 5 cuh_br5.npt - not used
Br 6 cuh_br6.npt - not used
Br 7 cuh_br7.npt - not used
Br 8 cuh_br8.npt - not used
Br 9 cuh_br9.npt - not used
Br 10 cuh_br10.npt - not used
Br 11 cuh_br11.npt - not used
Br 12 cuh_br12.npt - not used

EDH FILE.....EDHFN.....

Br 1 edh_br1.npt - not used
Br 2 edh_br2.npt - not used
Br 3 edh_br3.npt - not used
Br 4 edh_br4.npt - not used
Br 5 edh_br5.npt - not used
Br 6 edh_br6.npt - not used
Br 7 edh_br7.npt - not used
Br 8 edh_br8.npt - not used
Br 9 edh_br9.npt - not used
Br 10 edh_br10.npt - not used
Br 11 edh_br11.npt - not used
Br 12 edh_br12.npt - not used

TDH FILE.....TDHFN.....

Br 1 tdh_br1.npt - not used
Br 2 tdh_br2.npt - not used
Br 3 tdh_br3.npt - not used
Br 4 tdh_br4.npt - not used
Br 5 tdh_br5.npt - not used
Br 6 tdh_br6.npt - not used
Br 7 tdh_br7.npt - not used
Br 8 tdh_br8.npt - not used
Br 9 tdh_br9.npt - not used
Br 10 tdh_br10.npt - not used
Br 11 tdh_br11.npt - not used
Br 12 tdh_br12.npt - not used

CDH FILE.....CDHFN.....

Br 1 cdh_br1.npt - not used
Br 2 cdh_br2.npt - not used
Br 3 cdh_br3.npt - not used
Br 4 cdh_br4.npt - not used
Br 5 cdh_br5.npt - not used
Br 6 cdh_br6.npt - not used
Br 7 cdh_br7.npt - not used
Br 8 cdh_br8.npt - not used
Br 9 cdh_br9.npt - not used
Br 10 cdh_br10.npt - not used
Br 11 cdh_br11.npt - not used
Br 12 cdh_br12.npt - not used

SNP FILE.....SNPFN.....

SAMPLE CONTROL FILE

CONTROL FILE

WB 1 snp_wb1.opt
WB 2 snp_wb2.opt
WB 3 snp_wb3.opt
WB 4 snp_wb4.opt
WB 5 snp_wb5.opt
WB 6 snp_wb6.opt

PRF FILE.....PRFFN.....
WB 1 prf_wb1.opt
WB 2 prf_wb2.opt
WB 3 prf_wb3.opt
WB 4 prf_wb4.opt
WB 5 prf_wb5.opt
WB 6 prf_wb6.opt

VPL FILE.....VPLFN.....
WB 1 vpl_wb1.opt
WB 2 vpl_wb2.opt
WB 3 vpl_wb3.opt
WB 4 vpl_wb4.opt
WB 5 vpl_wb5.opt
WB 6 vpl_wb6.opt

CPL FILE.....CPLFN.....
WB 1 cpl_wb1.opt
WB 2 cpl_wb2.opt
WB 3 cpl_wb3.opt
WB 4 cpl_wb4.opt
WB 5 cpl_wb5.opt
WB 6 cpl_wb6.opt

SPR FILE.....SPRFN.....
WB 1 spr_wb1.opt
WB 2 spr_wb2.opt
WB 3 spr_wb3.opt
WB 4 spr_wb4.opt
WB 5 spr_wb5.opt
WB 6 spr_wb6.opt

FLX FILE.....KFLFN.....
WB 1 kfl_wb1.opt
WB 2 kfl_wb2.opt
WB 3 kfl_wb3.opt
WB 4 kfl_wb4.opt
WB 5 kfl_wb5.opt
WB 6 kfl_wb6.opt

TSR FILE.....TSRFN.....
tsr.opt

WDO FILE.....WDOFN.....
wdo.opt

Bathymetry File

The bathymetry file(s) contains information specifying the segment lengths, water surface elevations, segment orientations, bottom friction, and layer heights for each segment, and average widths for each grid cell. The following is a list of guidelines for file preparation are shown below.

1. It is recommended the user number the branches starting with the mainstem as branch 1. The remaining branch numbers should be numbered consecutively starting with the most upstream branch followed by the remaining branches as one moves downstream.
2. Each branch is surrounded by a segment of boundary cells (cells with zero widths) on both the upstream and downstream ends. Note this requirement results in two segments of zero widths between each branch.
3. Boundary cells must also be included at the top and bottom of each segment.
4. Cell widths start at layer 1 and continue to the maximum number of layers [KMX]. The number of layers specified in this file must match the value of [KMX] in the control file.
5. Only cells that are potentially active have non-zero widths. The first layer, boundary segment cells, and cells below the reservoir bottom elevation at a given segment have zero widths.
6. A separate bathymetry file is required for each waterbody.
7. The segment angles are relative to N. Figure 48 shows an example of segment orientation.

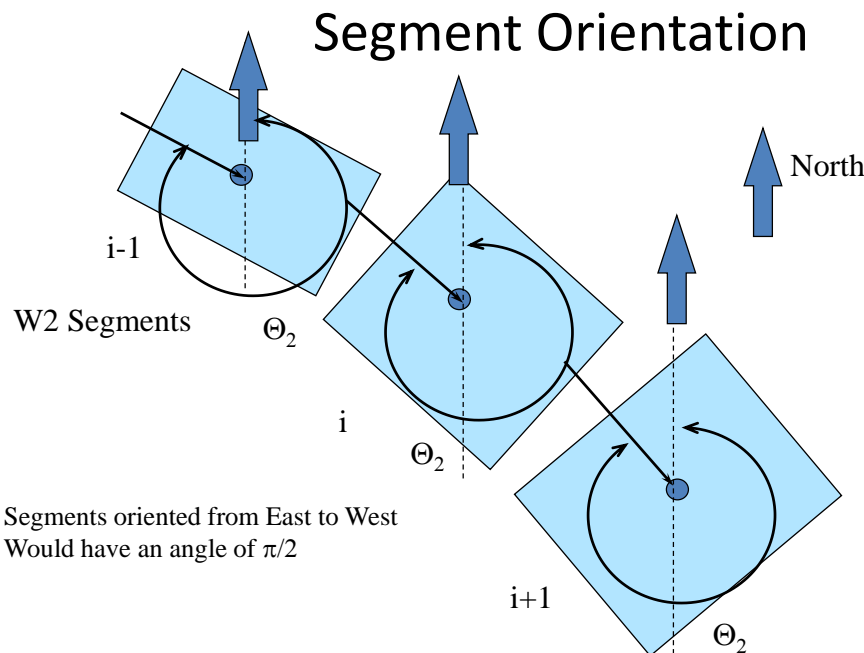


Figure 48. Illustration of segment angle orientation.

For the older bathymetry file format (the newer format is discussed below), the following additional guidelines must be followed:

1. The first three lines are ignored and can be used to comment the input file.
2. Segment lengths, water surface elevations, segment orientations, layer heights, and cell widths at each segment are preceded by two lines that are ignored. They can be used to comment each individual segment's bathymetry.
3. Input format for each cell width is F8.0 with 10 cell widths per line.
4. If there are more cell widths than can fit on one line, then they are continued immediately on the next line.

The following bathymetry files illustrate an example for a three-waterbody system with four branches involving a two-branch river system where the branches are connected in series with different bottom slopes, a reservoir, and an estuary. An alternate bathymetry input format is available since Version 3.7. The next section describes this new format that can be more easily developed in a spreadsheet using a comma delimited file format.

Example – 3 separate input files:

File **bth_wb1.npt**:

Waterbody 1 bathymetry

Segment lengths [DLX]

1200.00	1200.00	1200.00	1200.00	1200.00	1200.00	1200.00	1200.00	1200.00	1200.00	1200.00
1200.00	1200.00	1200.00	1200.00	1200.00						

Water surface elevation [WSEL]

49.80	49.20	48.00	46.80	45.60	44.40	43.20	44.40	43.20	42.96	
42.72	42.48	42.24	42.00	41.80						

Segment orientation [PHI0]

0.00	0.00	0.00	0.00	0.00	0.00	0.00	0.00	0.00	0.00	0.00
0.00	0.00	0.00	0.00	0.00						

Bottom friction [FRICTC]

0.04	0.04	0.04	0.04	0.04	0.04	0.04	0.04	0.04	0.04	0.04
0.04	0.04	0.04	0.04	0.04						

Layer heights [H]

2.00	2.00	2.00	2.00	2.00	2.00	2.00	2.00	2.00	2.00	2.00
2.00	2.00	2.00	1.00	1.00	1.00	1.00	1.00	1.00	1.00	1.00
1.00	1.00	1.00	1.00							

Segment 1 - branch 1

0.0	0.0	0.0	0.0	0.0	0.0	0.0	0.0	0.0	0.0	0.0
0.0	0.0	0.0	0.0	0.0	0.0	0.0	0.0	0.0	0.0	0.0
0.0	0.0	0.0	0.0							

Segment 2 - branch 1

0.0	300.0	300.0	300.0	300.0	300.0	300.0	300.0	300.0	300.0	300.0
300.0	300.0	300.0	300.0	300.0	300.0	300.0	300.0	300.0	300.0	300.0
250.0	200.0	050.0	0.0							

Segment 3 - branch 1

0.0	300.0	300.0	300.0	300.0	300.0	300.0	300.0	300.0	300.0	300.0
300.0	300.0	300.0	300.0	300.0	300.0	300.0	300.0	300.0	300.0	300.0
250.0	200.0	050.0	0.0							

Segment 4 - branch 1

0.0	300.0	300.0	300.0	300.0	300.0	300.0	300.0	300.0	300.0	300.0
300.0	300.0	300.0	300.0	300.0	300.0	300.0	300.0	300.0	300.0	300.0

INPUT FILES

BATHYMETRY

250.0	200.0	050.0	0.0							
Segment 5 - branch 1										
0.0	300.0	300.0	300.0	300.0	300.0	300.0	300.0	300.0	300.0	300.0
300.0	300.0	300.0	300.0	300.0	300.0	300.0	300.0	300.0	300.0	300.0
250.0	200.0	050.0	0.0							
Segment 6 - branch 1										
0.0	300.0	300.0	300.0	300.0	300.0	300.0	300.0	300.0	300.0	300.0
300.0	300.0	300.0	300.0	300.0	300.0	300.0	300.0	300.0	300.0	300.0
250.0	200.0	050.0	0.0							
Segment 7 - branch 1										
0.0	0.0	0.0	0.0	0.0	0.0	0.0	0.0	0.0	0.0	0.0
0.0	0.0	0.0	0.0	0.0	0.0	0.0	0.0	0.0	0.0	0.0
0.0	0.0	0.0	0.0							
Segment 8 - branch 2										
0.0	0.0	0.0	0.0	0.0	0.0	0.0	0.0	0.0	0.0	0.0
0.0	0.0	0.0	0.0	0.0	0.0	0.0	0.0	0.0	0.0	0.0
0.0	0.0	0.0	0.0							
Segment 9 - branch 2										
0.0	300.0	300.0	300.0	300.0	300.0	300.0	300.0	300.0	300.0	300.0
300.0	300.0	300.0	300.0	300.0	300.0	300.0	300.0	300.0	300.0	300.0
300.0	200.0	050.0	0.0							
Segment 10 - branch 2										
0.0	300.0	300.0	300.0	300.0	300.0	300.0	300.0	300.0	300.0	300.0
300.0	300.0	300.0	300.0	300.0	300.0	300.0	300.0	300.0	300.0	300.0
300.0	200.0	075.0	0.0							
Segment 11 - branch 2										
0.0	300.0	300.0	300.0	300.0	300.0	300.0	300.0	300.0	300.0	300.0
300.0	300.0	300.0	300.0	300.0	300.0	300.0	300.0	300.0	300.0	300.0
300.0	200.0	075.0	0.0							
Segment 12 - branch 2										
0.0	300.0	300.0	300.0	300.0	300.0	300.0	300.0	300.0	300.0	300.0
300.0	300.0	300.0	300.0	300.0	300.0	300.0	300.0	300.0	300.0	300.0
300.0	200.0	100.0	0.0							
Segment 13 - branch 2										
0.0	300.0	300.0	300.0	300.0	300.0	300.0	300.0	300.0	300.0	300.0
300.0	300.0	300.0	300.0	300.0	300.0	300.0	300.0	300.0	300.0	300.0
300.0	200.0	150.0	0.0							
Segment 14 - branch 2										
0.0	300.0	300.0	300.0	300.0	300.0	300.0	300.0	300.0	300.0	300.0
300.0	300.0	300.0	300.0	300.0	300.0	300.0	300.0	300.0	300.0	300.0
300.0	250.0	200.0	0.0							
Segment 15 - branch 2										
0.0	0.0	0.0	0.0	0.0	0.0	0.0	0.0	0.0	0.0	0.0
0.0	0.0	0.0	0.0	0.0	0.0	0.0	0.0	0.0	0.0	0.0
0.0	0.0	0.0	0.0							

File **bth_wb2.npt**:

Waterbody 2 bathymetry

Segment length [DLX]										
1200.0	1200.0	1200.0	1200.0	1200.0	1200.0	1200.0	1200.0	1200.0	1200.0	1200.0
1200.0	1200.0	1200.0	1200.0	1200.0	1200.0					
Water surface elevation [ELWS]										
42.00	42.00	42.00	42.00	42.00	42.00	42.00	42.00	42.00	42.00	42.00
42.00	42.00	42.00	42.00	42.00	42.00					

BATHYMETRY

INPUT FILES

Segment orientation [PHI0]									
0.00	0.00	0.00	0.00	0.00	0.00	0.00	0.00	0.00	0.00
0.00	0.00	0.00	0.00	0.00	0.00	0.00			
Bottom friction [MANN]									
0.04	0.04	0.04	0.04	0.04	0.04	0.04	0.04	0.04	0.04
0.04	0.04	0.04	0.04	0.04	0.04				
Layer height [H]									
2.00	2.00	2.00	2.00	2.00	2.00	2.00	2.00	2.00	2.00
2.00	2.00	2.00	2.00	2.00	2.00	2.00	2.00	2.00	2.00
2.00	2.00	2.00	2.00						
Width [B] - segment 16									
0.0	0.0	0.0	0.0	0.0	0.0	0.0	0.0	0.0	0.0
0.0	0.0	0.0	0.0	0.0	0.0	0.0	0.0	0.0	0.0
0.0	0.0	0.0	0.0						
Width [B] - segment 17									
0.0	300.0	300.0	300.0	300.0	300.0	300.0	300.0	300.0	300.0
300.0	300.0	300.0	0.0	0.0	0.0	0.0	0.0	0.0	0.0
0.0	0.0	0.0	0.0						
Width [B] - segment 18									
0.0	350.0	350.0	350.0	350.0	350.0	350.0	350.0	350.0	350.0
350.0	350.0	350.0	350.0	0.0	0.0	0.0	0.0	0.0	0.0
0.0	0.0	0.0	0.0						
Width [B] - segment 19									
0.0	500.0	500.0	500.0	500.0	500.0	500.0	500.0	500.0	500.0
500.0	500.0	500.0	500.0	500.0	0.0	0.0	0.0	0.0	0.0
0.0	0.0	0.0	0.0						
Width [B] - segment 20									
0.0	500.0	500.0	500.0	500.0	500.0	500.0	500.0	500.0	500.0
500.0	500.0	500.0	500.0	500.0	500.0	500.0	0.0	0.0	0.0
0.0	0.0	0.0	0.0						
Width [B] - segment 21									
0.0	500.0	500.0	500.0	500.0	500.0	500.0	500.0	500.0	500.0
500.0	500.0	500.0	500.0	500.0	500.0	500.0	500.0	0.0	0.0
0.0	0.0	0.0	0.0						
Width [B] - segment 22									
0.0	500.0	500.0	500.0	500.0	500.0	500.0	500.0	500.0	500.0
500.0	500.0	500.0	500.0	500.0	500.0	500.0	500.0	0.0	0.0
0.0	0.0	0.0	0.0						
Width [B] - segment 23									
0.0	500.0	500.0	500.0	500.0	500.0	500.0	500.0	500.0	500.0
500.0	500.0	500.0	500.0	500.0	500.0	500.0	500.0	500.0	0.0
0.0	0.0	0.0	0.0						
Width [B] - segment 24									
0.0	500.0	500.0	500.0	500.0	500.0	500.0	500.0	500.0	500.0
500.0	500.0	500.0	500.0	500.0	500.0	500.0	500.0	500.0	0.0
0.0	0.0	0.0	0.0						
Width [B] - segment 25									
0.0	600.0	600.0	600.0	600.0	600.0	600.0	600.0	600.0	600.0
600.0	600.0	600.0	600.0	600.0	600.0	600.0	600.0	600.0	600.0
0.0	0.0	0.0	0.0						
Width [B] - segment 26									
0.0	600.0	600.0	600.0	600.0	600.0	600.0	600.0	600.0	600.0
600.0	600.0	600.0	600.0	600.0	600.0	600.0	600.0	600.0	600.0
0.0	0.0	0.0	0.0						

INPUT FILES

BATHYMETRY

Width [B] - segment 27
 0.0 700.0 700.0 700.0 700.0 700.0 700.0 700.0 700.0 700.0
 700.0 700.0 700.0 700.0 700.0 700.0 700.0 700.0 700.0 700.0
 700.0 0.0 0.0 0.0

Width [B] - segment 28
 0.0 800.0 800.0 800.0 800.0 800.0 800.0 800.0 800.0 800.0
 800.0 800.0 800.0 800.0 800.0 800.0 800.0 800.0 800.0 800.0
 800.0 800.0 800.0 0.0

Width [B] - segment 29
 0.0 800.0 800.0 800.0 800.0 800.0 800.0 800.0 800.0 800.0
 800.0 800.0 800.0 800.0 800.0 800.0 800.0 800.0 800.0 800.0
 800.0 800.0 800.0 0.0

Width [B] - segment 30
 0.0 800.0 800.0 800.0 800.0 800.0 800.0 800.0 800.0 800.0
 800.0 800.0 800.0 800.0 800.0 800.0 800.0 800.0 800.0 800.0
 800.0 800.0 800.0 0.0

Width [B] - segment 31
 0.0 0.0 0.0 0.0 0.0 0.0 0.0 0.0 0.0 0.0
 0.0 0.0 0.0 0.0 0.0 0.0 0.0 0.0 0.0 0.0
 0.0 0.0 0.0 0.0

File bth_wb3.npt:

Waterbody 3 bathymetry

Width [B] - segment length [DLX]
 1200.0 1200.0 1200.0 1200.0 1200.0 1200.0 1200.0 1200.0 1200.0 1200.0
 1200.0 1200.0

Water surface elevation [ELWS]
 8.00 8.00 8.00 8.00 8.00 8.00 8.00 8.00 8.00 8.00
 8.00 8.00

Width [B] - segment orientation [PHI0]
 0.00 0.00 0.00 0.00 0.00 0.00 0.00 0.00 0.00 0.00
 0.00 0.00

Bottom friction [MANN]
 0.035 0.040 0.045 0.040 0.035 0.030 0.030 0.035 0.035 0.035
 0.040 0.040

Layer height [H]
 2.00 2.00 2.00 2.00 2.00 2.00 2.00 2.00 2.00 2.00
 2.00 2.00 2.00 2.00 2.00 2.00 2.00 2.00 2.00 2.00
 2.00 2.00 2.00 2.00

Width [B] - segment 32
 0.0 0.0 0.0 0.0 0.0 0.0 0.0 0.0 0.0 0.0
 0.0 0.0 0.0 0.0 0.0 0.0 0.0 0.0 0.0 0.0
 0.0 0.0 0.0 0.0

Width [B] - segment 33
 0.0 800.0 800.0 800.0 800.0 800.0 800.0 800.0 800.0 800.0
 800.0 800.0 800.0 800.0 800.0 800.0 800.0 800.0 800.0 800.0
 800.0 800.0 800.0 0.0

Width [B] - segment 34
 0.0 800.0 800.0 800.0 800.0 800.0 800.0 800.0 800.0 800.0
 800.0 800.0 800.0 800.0 800.0 800.0 800.0 800.0 800.0 800.0
 800.0 800.0 800.0 0.0

Width [B] - segment 35
 0.0 800.0 800.0 800.0 800.0 800.0 800.0 800.0 800.0 800.0
 800.0 800.0 800.0 800.0 800.0 800.0 800.0 800.0 800.0 800.0

BATHYMETRY

INPUT FILES

800.0	800.0	800.0	0.0							
Width [B] - segment 36										
0.0	800.0	800.0	800.0	800.0	800.0	800.0	800.0	800.0	800.0	800.0
800.0	800.0	800.0	800.0	800.0	800.0	800.0	800.0	800.0	800.0	800.0
800.0	800.0	800.0	0.0							
Width [B] - segment 37										
0.0	800.0	800.0	800.0	800.0	800.0	800.0	800.0	800.0	800.0	800.0
800.0	800.0	800.0	800.0	800.0	800.0	800.0	800.0	800.0	800.0	800.0
800.0	800.0	800.0	0.0							
Width [B] - segment 38										
0.0	800.0	800.0	800.0	800.0	800.0	800.0	800.0	800.0	800.0	800.0
800.0	800.0	800.0	800.0	800.0	800.0	800.0	800.0	800.0	800.0	800.0
800.0	800.0	800.0	0.0							
Width [B] - segment 39										
0.0	850.0	850.0	850.0	850.0	850.0	850.0	850.0	850.0	850.0	850.0
850.0	850.0	850.0	850.0	850.0	850.0	850.0	850.0	850.0	850.0	850.0
850.0	850.0	850.0	0.0							
Width [B] - segment 40										
0.0	900.0	900.0	900.0	900.0	900.0	900.0	900.0	900.0	900.0	900.0
900.0	900.0	900.0	900.0	900.0	900.0	900.0	900.0	900.0	900.0	900.0
900.0	900.0	900.0	0.0							
Width [B] - segment 41										
0.0	1000.0	1000.0	1000.0	1000.0	1000.0	1000.0	1000.0	1000.0	1000.0	1000.0
1000.0	1000.0	1000.0	1000.0	1000.0	1000.0	1000.0	1000.0	1000.0	1000.0	1000.0
1000.0	1000.0	1000.0	0.0							
Width [B] - segment 42										
0.0	1100.0	1100.0	1100.0	1100.0	1100.0	1100.0	1100.0	1100.0	1100.0	1100.0
1100.0	1100.0	1100.0	1100.0	1100.0	1100.0	1100.0	1100.0	1100.0	1100.0	1100.0
1100.0	1100.0	1100.0	0.0							
Width [B] - segment 43										
0.0	0.0	0.0	0.0	0.0	0.0	0.0	0.0	0.0	0.0	0.0
0.0	0.0	0.0	0.0	0.0	0.0	0.0	0.0	0.0	0.0	0.0
0.0	0.0	0.0	0.0							

INPUT FILES

Comma Delimited Bathymetry File Format

Starting in Version 3.7, the model user can input the bathymetry as a comma delimited file (csv format). This allows the user to assemble the file in a spreadsheet, such as Excel.

The new bathymetry format is shown below in Figure 49 using an Excel spreadsheet. The model reads the input format as a csv or a comma delimited file. The old format is still used, but if the model user has the '\$' character in the first line and first character of the bth file, the code will assume it is in the new format.

1st line: Include the '\$' character as the first character in line 1, the rest of this line is ignored and can be used for comments

\$1981 Bluestone Reservoir Bathymetry

2nd line: Title:Seg, followed by a header for each model segment, this is ignored

SEG: I	1	2	3	4	5	6	7
--------	---	---	---	---	---	---	---

3rd line: Title: DLX, followed by DLX in m for each segment

DLX	1046.4	1046.4	1046.4	965.9	965.9	764.7	764.7
-----	--------	--------	--------	-------	-------	-------	-------

4th line: Title: ELWS, followed by ELWS in m for each segment (initial water surface elevation)

ELWS	430.1	430.1	430.1	430.1	430.1	430.1	430.1
------	-------	-------	-------	-------	-------	-------	-------

5th line: Title: PHIO, followed by PHIO for each segment (orientation angle in radians)

PHIO	3.142	3.142	3.142	3.142	3.142	3.142	3.142
------	-------	-------	-------	-------	-------	-------	-------

6th line: Title: FRICT, followed by FRICT for each segment (Mannings or Chezy friction factor)

FRICT	70	70	70	70	70	70	70
-------	----	----	----	----	----	----	----

7th line: Titles that are ignored by the model

LAYERH		BR1						K
--------	--	-----	--	--	--	--	--	---

8th line to end of file: 1st column is layer height in m, 2nd column are segment widths for segment 1, 3rd column are segment widths for segment 2, etc. Note that the segment widths for the first segment and last segment are 0 and for the top layer K=1 and bottom layer are also 0. On the far right hand side there is a layer # specification

INPUT FILES

0.5	0	0	0	0	0	0	0	1
0.5	0	335	335	335	335	364	0	2
0.5	0	231	231	231	231	254	0	3
0.5	0	228	228	228	228	243	0	4
0.5	0	224	224	224	224	231	0	5
0.5	0	220	220	220	220	219	0	6
0.5	0	215	215	215	215	206	0	7
0.5	0	0	0	0	0	0	0	8

[illegible]

Figure 49. New bathymetry file format in csv format within Excel.

INPUT FILES

Fish Habitat Volumes and Volume-Weighted Averages of Eutrophication State Variables

This section describes how the model allows for the computation of

- Volume of fish habitat based on temperature and dissolved oxygen targets for various fish species
- Segment volume weighted averages of dissolved oxygen, $\text{NO}_3\text{-N}$, $\text{NH}_4\text{-N}$, $\text{PO}_4\text{-P}$, Total P, and chlorophyll a
- Surface volume weighted averages of dissolved oxygen, $\text{NO}_3\text{-N}$, $\text{NH}_4\text{-N}$, $\text{PO}_4\text{-P}$, Total P, and chlorophyll a

The input file, w2_habitat.npt, is read by the CE-QUAL-W2 model when 'HABTATC' is set to 'ON' in the control file, w2_con.npt. This file allows the model user to compute habitat volumes for various fish species and to evaluate volume-weighted averages of eutrophication parameters and examine first order sediment oxygen uptake as predicted by the model.

The file, w2_habitat, is set up as a text file in free format with commas delimiting fields with titles between lines explaining the following lines. Each fish species is given a temperature target, both a low and a high target, and a dissolved oxygen target not to go below. In case the model user is not modeling dissolved oxygen, the oxygen limits are ignored. Note that the time of output of all these variables and volumes are at the frequency of the time series frequency output (TSR files).

An example file is shown below:

```
FISH HABITAT AND WQ AVEREAGES INPUT FILE
#FISH CRITERIA, OUTPUTFILENAME
9, 'habitat3.opt'
NAMES OF FISH, TEMP-low, TEMP-high, DO limits [DO limits are ignored if
no water quality constituents]
RainbowTrout,0.0,18.0,5.0
StripedBass,10.0,24.0,5.0
Walleye,12.0,24.0,5.0
WhiteBass,0.0,28.0,3.0
SmallmouthBass,0.0,29.0,4.0
SpottedBass,0.0,24.4,6.0
GizzardShad,10.0,26.7,6.0
LargemouthBass,10.0,30.0,5.0
ChannelCatfish,18.0,31.0,5.0
VOLUME WEIGHTED AVERAGES AT THE FOLLOWING # OF SEGMENTS: NSEG [These
lines are ignored if no WQ constituents],Out.opt'putFileName for Vol
Weighted Avgs
3, 'volwgtavg.opt'
SEGMENT NUMBERS FOR VOL WEIGHTED AVERAGES
10,15,24
SURFACE WEIGHTED AVERAGES OVER THE FOLLOWING # OF SURFACE
LAYERS,OutputFileName for surface averages
4, 'surfvolwgtavg.opt'
OutputFileName for 1st order SED at all time and all segments
'sodsed.opt'
```

Fish habitat volumes

FISH HABITAT AND WQ AVEREAGES INPUT FILE

The first line is a title which is ignored by the model.

```
#FISH CRITERIA, OUTPUTFILENAME  
9, 'habitat3.opt'
```

The first line is a title which is ignored by the model. This variable tells the code to expect 9 fish temperature and dissolved oxygen criteria and specifies the output filename which must be in quotations. This output filename is only for the output of habitat volumes for the entire model grid. Other files are written out showing habitat volumes for each model branch and waterbody. Also, if TECPLOT is ON for CPL output, the habitat criteria can be animated – see CPL output file.

```
NAMES OF FISH, TEMP-low, TEMP-high, DO limits [DO limits are ignored if  
no water quality constituents]  
RainbowTrout,0.0,18.0,5.0  
StripedBass,10.0,24.0,5.0  
Walleye,12.0,24.0,5.0  
WhiteBass,0.0,28.0,3.0  
SmallmouthBass,0.0,29.0,4.0  
SpottedBass,0.0,24.4,6.0  
GizzardShad,10.0,26.7,6.0  
LargemouthBass,10.0,30.0,5.0  
ChannelCatfish,18.0,31.0,5.0
```

The first line (which is wrapped above) is ignored by the model. For each of the 9 species, a temperature in °C as a low and a high limit and a dissolved oxygen in mg/l target are used. These criteria can be selected for fish species in the reservoir or river system following the work of Cooke and Welch (2008) in

INPUT FILES

Table 74 or Hondzo and Stefan (1996) in Table 75. Note that the habitat volume uses the following criteria for acceptable habitat:

Model temperature $> \text{TEMP-low}$ and $\leq \text{TEMP-high}$ and dissolved oxygen $\geq \text{DO limit}$.

Table 74. Fish temperature and dissolved oxygen criteria from Cooke and Welch (2008).

TEMPERATURE AND DO REQUIREMENTS, SELECTED FISH SPECIES										
Species	Dissolved Oxygen (DO, mg/L)					Temperature (T, degrees C)				
	optimal DO ¹	Mean of optimal DO	Highest EC, DO	Effect	Reference	optimal T ¹	Mean of optimal T	Lowest EC, high T	Effect	Lowest Lethal T
rainbow trout	7.0 - 9.0	8.0	5.0	avoidance	USFWS HSI	12-18	15	18	avoidance	25
striped bass ²	6.0	6.0	5.0	ELS survival	USFWS HSI, USFWS SP (Optimal DO, juvenile)	20-21	20.5	24	avoidance	28
walleye	>5.0	none reported (est. 7.0)	<5.0	adult abundance, fry survival	USFWS HSI	20-24	22	>24	avoidance	29
white bass	>5.0	none reported (est. 7.0)	3.0	stress (decreased activity, increased ventilation)	USFWS HSI	19-28	23.5	>28	growth	27 (based on closely related white perch, <i>Morone americana</i>), dependent on acclimation T.
smallmouth bass	6.0	6.0	4.0	growth (20%)	USFWS HSI	21-27	24	29	growth	32.3
spotted bass	6.0	6.0	<6.0	growth	USFWS HSI	23.5-24.4	24	>24.4	reduced abundance	34
gizzard shad	6.0	6.0	6.0	other	USFWS HSI	22-29	25.5	26.7	repro. growth	36.5
largemouth bass	8.0	8.0	5.0	distress	USFWS HSI	24-30	27	30	embryo survival	35.0
channel catfish	7.0	7.0	5.0	reduced feeding	USFWS HSI	26-29	27.5	21	growth	33.5
EC = Effect Concentration (lowest of values of T> optimal and highest of values of DO <optimal)										
¹ based on field data (in preference to lab data)										
² except where indicated otherwise, data based on inland stocks (not coastal)										
Reference										
USFWS HSI - U.S. FWS Habitat Suitability Index (species specific)										
Grant et al. 2003 - Effects of Temperature on the Susceptibility of Largemouth Bass to Largemouth Bass Virus										
USFWS SP - Species Profile (Striped Bass, 1983)										

Table 75. General fish temperature criteria from Hondzo and Stefan (1996).

Fish type	Lower temperature (°C) good growth limit	Upper temperature (°C) good growth limit	Upper temperature (°C) lethal limit
Coldwater (examples include brook trout, Chinook salmon, coho salmon, mountain whitefish, rainbow trout)	9.0	18.5	23.4
Coolwater (examples include black crappie, northern pike, walleye, white crappie, white sucker, yellow perch)	16.3	28.2	30.4
Warmwater (examples include bluegill, carp, channel catfish, freshwater drum, gizzard shad, green sunfish, largemouth bass, rock bass, smallmouth bass, white bass)	19.7	32.3	> 32.3

Then based on these limits an output file for the entire waterbody is written out. The file is well-suited for importing into Excel or other graphics program.

A typical output file provides the following information:

Fish habitat analysis: CE-QUAL-W2 model results

```

Species, Temperature minimum, Temperature maximum, Dissolved oxygen minimum
RainbowTrout,           0.00,    18.00,    5.00
StripedBass,            10.00,    24.00,    5.00
Walleye,                 12.00,    24.00,    5.00
WhiteBass,               0.00,    28.00,    3.00
SmallmouthBass,         0.00,    29.00,    4.00

```

INPUT FILES

```
SpottedBass,          0.00,   24.40,   6.00
GizzardShad,         10.00,   26.70,   6.00
LargemouthBass,      10.00,   30.00,   5.00
ChannelCatfish,      18.00,   31.00,   5.00
```

```
JDAY,%VOL-RainbowTrout,HAB-VOL(m3)-RainbowTrout,%VOL-StripedBass,HAB-VOL(m3)-
StripedBass,%VOL-Walleye,HAB-VOL(m3)-Walleye,%VOL-WhiteBass,HAB-VOL(m3)-WhiteBass,%VOL-
SmallmouthBass,HAB-VOL(m3)-SmallmouthBass,%VOL-SpottedBass,HAB-VOL(m3)-SpottedBass,%VOL-
GizzardShad,HAB-VOL(m3)-GizzardShad,%VOL-LargemouthBass,HAB-VOL(m3)-LargemouthBass,%VOL-
ChannelCatfish,HAB-VOL(m3)-ChannelCatfish,
  61.532, 100.00, 0.1170E+09, 0.00, 0.0000E+00, 0.00, 0.0000E+00, 100.00,
0.1170E+09, 100.00, 0.1170E+09, 100.00, 0.1170E+09, 0.00, 0.0000E+00, 0.00,
0.0000E+00, 0.00, 0.0000E+00,
  61.542, 100.00, 0.1170E+09, 0.00, 0.0000E+00, 0.00, 0.0000E+00, 100.00,
0.1170E+09, 100.00, 0.1170E+09, 100.00, 0.1170E+09, 0.00, 0.0000E+00, 0.00,
0.0000E+00, 0.00, 0.0000E+00,
  61.566, 100.00, 0.1170E+09, 0.00, 0.0000E+00, 0.00, 0.0000E+00, 100.00,
0.1170E+09, 100.00, 0.1170E+09, 100.00, 0.1170E+09, 0.00, 0.0000E+00, 0.00,
0.0000E+00, 0.00, 0.0000E+00,
```

The output code reprints the original criteria and then at the output of the TSR FREQ, outputs JDAY (Julian day), % habitat volume for species 1, actual habitat volume in m³ for species 1, and then this is repeated for each species.

An example of this is shown below for DeGray Reservoir for small mouth bass and gizzard shad between March and September 1980 in Figure 50.

The model also writes out output for each branch and waterbody if this feature [HABITAC] is ON. For each waterbody the model will write out 'fish_habitat_wbX.opt' where X is the waterbody #. Also, for each branch the model will write out 'fish_habitat_brX.opt' where X is the branch #. These files allow the model user to explore fish habitat in smaller sections of the waterbody as required for the study. These files follow the output described above for the habitat volume % and habitat volume in that particular waterbody or branch.

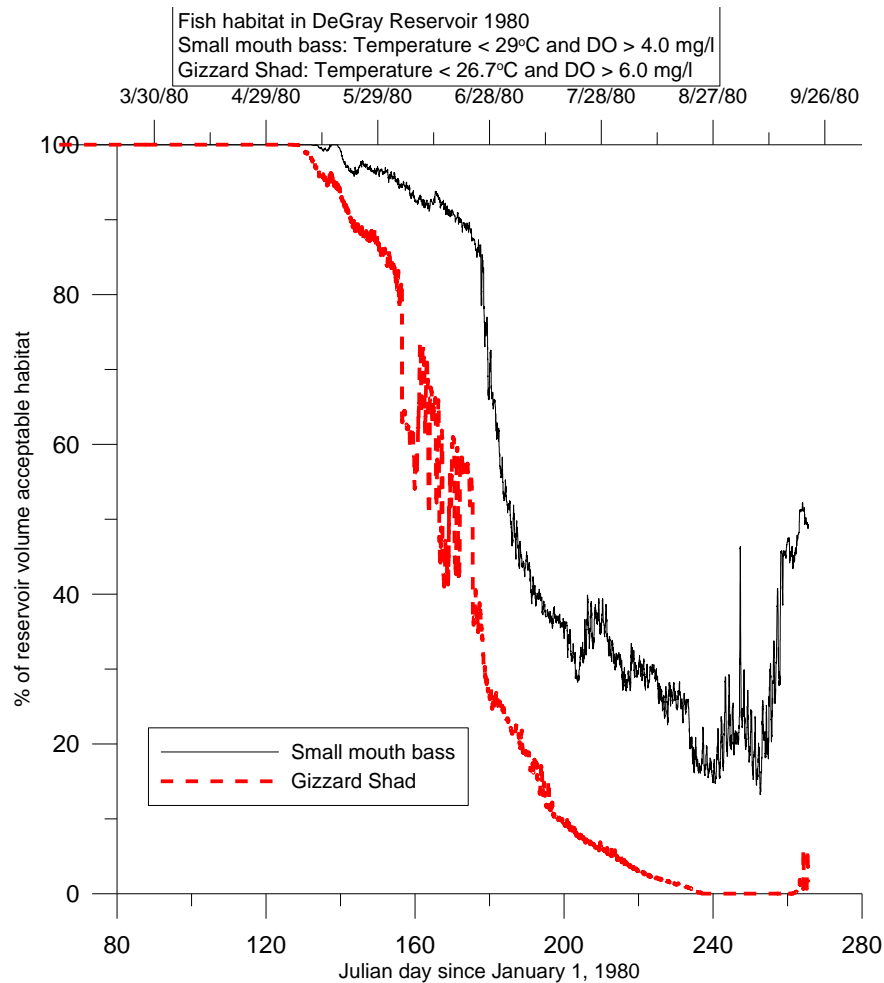


Figure 50. Small mouth bass habitat in DeGray reservoir for 1980.

Volume weighted segment and surface averages

VOLUME WEIGHTED AVERAGES AT THE FOLLOWING # OF SEGMENTS: NSEG [These lines are ignored if no WQ constituents], Out.opt'putFileName for Vol Weighted Avgs
 3, 'volwgtavg.opt'

The title is ignored in the model. The number of segments that the model will output volume weighted eutropication variables (dissolved oxygen, nutrients and chlorophyll a) and the file name are the next fields. The file name must be in quotations.

SEGMENT NUMBERS FOR VOL WEIGHTED AVERAGES
 10,15,24

The title is ignored in the model. The segment numbers are given separated by commas.

SURFACE WEIGHTED AVERAGES OVER THE FOLLOWING # OF SURFACE LAYERS, OutputFileName for surface averages
 4, 'surfvolwtavg.opt'

INPUT FILES

The title is ignored in the model. The number 4 gives the model the number of active surface layers to volume average. In many cases the model user wants just a surface or epilimnetic average of the water quality variables. The code also takes all dissolved oxygen greater than saturation and assigns it a value of 100% saturation for purposes of the average. Note that the model also for the surface average outputs the layer average light extinction coefficient that can be compared with field data. The file name of the surface averages is the next field and it must be in quotations.

Typical output file results are shown below for the volume weighted averages at the 3 segment numbers specified.

```
Volume weighted WQ parameters at segments: 10 15 24
JDAY, PO4- 10, NH4- 10, NO3- 10, DO- 10, TP- 10, CHLA- 10,
PO4- 15, NH4- 15, NO3- 15, DO- 15, TP- 15, CHLA- 15, PO4- 24,
NH4- 24, NO3- 24, DO- 24, TP- 24, CHLA- 24,
64.542, 0.0010, 0.0022, 0.1400, 11.0935, 0.0000, 0.0000, 0.0010,
0.0022, 0.1400, 11.0284, 0.0000, 0.0000, 0.0010, 0.0022, 0.1400,
10.6507, 0.0000, 0.0000,
64.583, 0.0010, 0.0023, 0.1400, 11.0934, 0.0000, 0.0000, 0.0010,
0.0023, 0.1400, 11.0276, 0.0000, 0.0000, 0.0010, 0.0023, 0.1400,
10.6486, 0.0000, 0.0000,
64.625, 0.0010, 0.0025, 0.1400, 11.0932, 0.0000, 0.0000, 0.0010,
0.0025, 0.1400, 11.0269, 0.0000, 0.0000, 0.0010, 0.0025, 0.1400,
10.6462, 0.0000, 0.0000,
64.667, 0.0010, 0.0026, 0.1400, 11.0929, 0.0000, 0.0000, 0.0010,
0.0026, 0.1400, 11.0259, 0.0000, 0.0000, 0.0010, 0.0026, 0.1400,
10.6437, 0.0000, 0.0000,
64.708, 0.0010, 0.0028, 0.1400, 11.0927, 0.0000, 0.0000, 0.0010,
0.0028, 0.1400, 11.0249, 0.0000, 0.0000, 0.0010, 0.0028, 0.1400,
10.6410, 0.0000, 0.0000,
64.750, 0.0010, 0.0029, 0.1400, 11.0926, 0.0000, 0.0000, 0.0010,
0.0029, 0.1400, 11.0240, 0.0000, 0.0000, 0.0010, 0.0029, 0.1400,
10.6380, 0.0000, 0.0000,
```

Typical output file results are shown below for the surface volume weighted averages at the 3 segment numbers specified.

```
Surface (upper 4 model layers) Volume weighted WQ parameters at segments: 10 15 24
JDAY, PO4- 10, NH4- 10, NO3- 10, DO- 10, TP- 10, CHLA-
10, Gamma (m-1)- 10, PO4- 15, NH4- 15, NO3- 15, DO- 15, TP- 15,
CHLA- 15, Gamma (m-1)- 15, PO4- 24, NH4- 24, NO3- 24, DO- 24, TP- 24,
CHLA- 24, Gamma (m-1)- 24,
64.542, 0.0010, 0.0022, 0.1400, 11.1004, 0.0000, 0.0000, 0.5100,
0.0010, 0.0022, 0.1400, 11.0998, 0.0000, 0.0000, 0.5100, 0.0010,
0.0022, 0.1400, 11.1001, 0.0000, 0.0000, 0.5100,
64.583, 0.0010, 0.0023, 0.1400, 11.1007, 0.0000, 0.0000, 0.5100,
0.0010, 0.0023, 0.1400, 11.0995, 0.0000, 0.0000, 0.5100, 0.0010,
0.0023, 0.1400, 11.1001, 0.0000, 0.0000, 0.5100,
64.625, 0.0010, 0.0025, 0.1400, 11.1012, 0.0000, 0.0000, 0.5100,
0.0010, 0.0025, 0.1400, 11.0992, 0.0000, 0.0000, 0.5100, 0.0010,
0.0025, 0.1400, 11.1000, 0.0000, 0.0000, 0.5100,
64.667, 0.0010, 0.0026, 0.1400, 11.1013, 0.0000, 0.0000, 0.5090,
0.0010, 0.0026, 0.1400, 11.0985, 0.0000, 0.0000, 0.5095, 0.0010,
0.0026, 0.1400, 11.0996, 0.0000, 0.0000, 0.5095,
64.708, 0.0010, 0.0028, 0.1400, 11.0998, 0.0000, 0.0000, 0.5090,
0.0010, 0.0028, 0.1400, 11.0977, 0.0000, 0.0000, 0.5095, 0.0010,
0.0028, 0.1400, 11.0991, 0.0000, 0.0000, 0.5095,
64.750, 0.0010, 0.0029, 0.1400, 11.1002, 0.0000, 0.0000, 0.5090,
0.0010, 0.0029, 0.1400, 11.0968, 0.0000, 0.0000, 0.5095, 0.0010,
0.0029, 0.1400, 11.0984, 0.0000, 0.0000, 0.5095,
```

INPUT FILES

Output of overall organic matter accumulation at the bottom of each layer and summed for each segment

OutputFileName for SOD+SED at all time and all segments
'sodsed.opt'

This output file prints the first order sediment organic matter accumulation at each segment as a function of time. It sums up all the sediment accumulated at all the vertical layers. The output is in grams of organic matter. This allows the model user to evaluate how changes in organic loading to the sediments affect the rate of accumulation of sediments and where they accumulate.

The output file is shown below where all entries are comma delimited and are for each segment and time of output. The values for each segment are grams of organic matter.

JDAY,	2,	3,	4,	5,	6,	7,	8,	9,	10,	11,	12,	13,	14,	15,	16,	17,	18,	19,	20,	21,	22,	23,	24,	25,	26,	27,	28,	29,	30,	31,
64.542,	0.2676E+03,	0.3751E+03,	0.5351E+03,	0.7376E+03,	0.1120E+04,	0.1630E+04,	0.1577E+04,	0.1288E+04,	0.1490E+04,	0.2253E+04,	0.2452E+04,	0.3120E+04,	0.4287E+04,	0.3824E+04,	0.2663E+04,	0.4700E+04,	0.5847E+04,	0.6447E+04,	0.1021E+05,	0.9486E+04,	0.1095E+05,	0.1289E+05,	0.7819E+04,	0.5235E+04,	0.5760E+04,	0.6320E+04,	0.6432E+04,	0.4698E+04,	0.2557E+04,	0.1682E+04,
64.583,	0.5577E+03,	0.7482E+03,	0.1067E+04,	0.1471E+04,	0.2236E+04,	0.3258E+04,	0.3150E+04,	0.2572E+04,	0.2976E+04,	0.4500E+04,	0.4898E+04,	0.6234E+04,	0.8565E+04,	0.7638E+04,	0.5316E+04,	0.9387E+04,	0.1168E+05,	0.1288E+05,	0.2039E+05,	0.1895E+05,	0.2189E+05,	0.2575E+05,	0.1562E+05,	0.1046E+05,	0.1150E+05,	0.1263E+05,	0.1285E+05,	0.9388E+04,	0.5109E+04,	0.3361E+04,
64.625,	0.8683E+03,	0.1121E+04,	0.1597E+04,	0.2201E+04,	0.3348E+04,	0.4886E+04,	0.4726E+04,	0.3853E+04,	0.4467E+04,	0.6745E+04,	0.7342E+04,	0.9346E+04,	0.1284E+05,	0.1145E+05,	0.7963E+04,	0.1407E+05,	0.1752E+05,	0.1931E+05,	0.3056E+05,	0.2841E+05,	0.3282E+05,	0.3860E+05,	0.2341E+05,	0.1567E+05,	0.1724E+05,	0.1892E+05,	0.1926E+05,	0.1407E+05,	0.7659E+04,	0.5037E+04,
64.667,	0.1194E+04,	0.1499E+04,	0.2125E+04,	0.2927E+04,	0.4458E+04,	0.6513E+04,	0.6300E+04,	0.5131E+04,	0.5956E+04,	0.8987E+04,	0.9782E+04,	0.1246E+05,	0.1711E+05,	0.1525E+05,	0.1060E+05,	0.1875E+05,	0.2334E+05,	0.2573E+05,	0.4072E+05,	0.3785E+05,	0.4375E+05,	0.5143E+05,	0.3119E+05,	0.2087E+05,	0.2296E+05,	0.2520E+05,	0.2567E+05,	0.1875E+05,	0.1021E+05,	0.6711E+04,

INPUT FILES

Automatic Port Selection and Reservoir Volumes at Specified Temperatures

The CE-QUAL-W2 model reads the file, w2_selective.npt', if the SELECTC control is 'ON' or set to 'USGS' in the w2_con.npt file. This input file allows the model user to

1. automatically choose a withdrawal port elevation based on meeting required temperature targets
2. print temperature of individual outlets rather than combining them together, and
3. print the volume of the reservoir at specified temperature targets.

SELECTC=' ON'

The input file is shown below for 'ON' and is named: 'w2_selective.npt'. A discussion of each line from the input file is included in the next sections.

```
Selective input control file
Temperature outlet control - frequency of output for temperature
OUT FREQ TFRQTMP
0.02083
Structure outlet control based on time and temperature and branch
DYNSTR1 CONTROL NUM FREQ
ON 2 0.50

DYNSTR2 WD/ST JB JS/NW YEARLY TSTR TEND TEMP NELEV ELEV1 ELEV2
1 ST 1 1 ON 010. 045. 15.0 2 210. 190.
2 ST 2 1 ON 180. 300. 20.0 1 95.0

MONITOR LOC ISEG ELEV DYNSEL
1 32 0 OFF
2 43 1 OFF

AUTO ELEVCONTROL
1 ON
2 OFF

SPLIT1 CNTR NUM
ON 1

SPLIT2 ST/WD JB YEARLY TSTR TEND TTARGET NOUTS JS1/NW1 JS2/NW2 ELCONT
1 ST 1 ON 010. 045. 12. 2 2 3 OFF

THRESH1 TEMPN
2

THRESH2 TCRTWB1 TCRTWB2 TCRTWB3 TCRTWB4 TCRTWB5
1 10.0 10.0
2 12.5 12.5
```

Temperature of outlet releases

Model Version 3.6 and earlier created an output file of the temperature of all withdrawals mixed together at a segment. For example, if there were 4 separate outlets at different elevations defining a structure withdrawal, the withdrawal output from W2 (specified in w2_con.npt) included the

INPUT FILES

mixed temperature of these outlets blended together. These were specified in the withdrawal outlet cards in the control file, w2_con.npt, starting with the card 'WITH OUT'.

When SELECTC='ON', the model allows printing each branch structure as a separate time series of outlet temperatures and flows for each individual outlet, in addition to the existing CE-QUAL-W2 combined temperature time series. The outlet files are named 'str_brX.opt' where X is the branch number. A similar file is written for withdrawals. The withdrawals are included in one file named: 'wd_out.opt'. The format for the structure and withdrawal output files is as follows:

Branch:	1	# of structures:	3			outlet temperatures					
JDAY	T (C)	T (C)	T (C)	Q (m3/s)	Q (m3/s)	Q (m3/s)	ELEVCL	ELEVCL	ELEVCL		
22920.000	0.00	9.52	7.20	0.00	69.27	17.91	300.23	280.42	173.74		
22921.000	0.00	9.76	7.20	0.00	68.36	17.57	300.23	280.42	173.74		
22922.000	0.00	9.81	7.20	0.00	67.46	17.23	300.23	280.42	173.74		
22923.000	0.00	9.90	7.20	0.00	66.55	16.90	300.23	280.42	173.74		

The first 2 lines are headers. The model output includes JDAY, the outlet temperature of each outlet in °C, the flow rate of each outlet in cms, and the elevation of each outlet in m. A '0' for temperature means that there was no outflow from that outlet. The frequency of the output of this file is determined from the input file called 'w2_selective.npt'. In this file, the variable TFRQTMP is the Julian day frequency of the output. For the example below (note that the value must be in columns 9-16 in F format), the 0.02083 Julian day is every 30 minutes.

```
Selective input control file
Temperature outlet control - frequency of output for temperature
OUT FREQ TFRQTMP
      0.02083
```

Out Freq

TFRQTMP: Real F8.0. This is the Julian day frequency of the output for the temperature for each structure outlet.

Automatic selection of outlet port to control temperature

The model code allows the user control over selective withdrawal structures and withdrawals. For each structure or withdrawal, the user can dynamically adjust the elevation of the discharge according to time and temperature of the outlet water. Hence, the model user does not need to add any more structures or withdrawals to the model to allow for a selective withdrawal tower. The model user will specify a beginning upper elevation ESTR for a structure or EWD for a withdrawal (in the w2_con.npt file) and supply the correct time series of flows (such as in a specified input file for structure outflows or withdrawal outflows). The model will then dynamically lower or raise the elevation of the outlet using as a starting point the starting elevation defined for the structure or withdrawal in w2_con.npt before the rule starts. Information supplied to the model is found in the file 'w2_selective.npt'. The relevant lines or card images from this file are shown below (note that fixed format is used; data are spaced every 8 columns; and there is no limit to the card length, i.e., the card images do not wrap around as in the other W2 files):

Dynstr1

```
DYNSTR1  CONTROL      NUM      FREQ
```

CONTROL: Character A8. This is set to 'ON' or 'OFF' (must be in all capitals) – this controls whether the algorithm is used. Turning it 'OFF' uses the normal W2 code.

INPUT FILES

NUM: Integer I8. This is the number of selective withdrawal structures. In the next set of lines, each line is for each selective withdrawal structure.

FREQ: Real F8.0. This is a real number that represents the Julian day frequency from the start time of the simulation to check the temperature criteria for the dynamic temperature control structure or the split temperature control. Hence, if one wanted to check the criteria every day and adjust the gates only once per day, FREQ=1.0. If every 12 hours, FREQ=0.5.

Dynstr2

DYNSTR2 ST/WD JB JS/NW YEARLY TSTR TEND TEMP NELEV ELEV1 ELEV2

ST/WD: Character A8. For a structure enter 'ST', for a withdrawal enter 'WD'. This specifies whether the dynamic withdrawal algorithm applies to a W2 'structure' or 'withdrawal' which are treated differently in the W2 model

JB: Integer I8. This is the branch number of the structure. This column is ignored for a withdrawal.

JS/NW: Integer I8. Outlet number of each selective withdrawal structure (if ST/WD='ST') or withdrawal number (if ST/WD='WD').

YEARLY: Character A8. This is a control that is ON or OFF. If it is ON, then the Julian days that follow TSTR and TEND are between 1 and 366 and are to be applied yearly during the simulation. If it is OFF, then TSTR and TEND are applied only once between the time period specified.

TSTR and TEND are the beginning Julian day and the ending Julian day for starting and ending selective withdrawal. The model will not lower the outlet until after TSTR. After TEND the outlet level will revert back to what was specified in the w2_con.npt file for the outlet elevation. Note that if YEARLY=ON, the Julian days must be between 1 and 366.

TEMP: Real F8.0. This is the temperature in C that is the criterion for lowering the structure elevation (or in practice – turning off one and opening up a lower one). If the TEMP is below the criterion and the temperature at the level of the outlet above the current outlet is also below the criterion, then the selective withdrawal structure will raise itself to a higher elevation until it reaches the top, or original elevation, as specified in the w2_con.npt file.

NELEV: Integer I8. This specifies model how many selective withdrawal elevations you will use in addition to the one supplied in the w2_con.npt file. Currently, this is limited to 10 values.

ELEV1, ELEV2...ELEV10: Real. These are the elevations in m of the selective withdrawal structures. Note that the model will use the value of the elevation in the control file as the initial elevation for the time before (<TSTR) and after (>TEND) the rule. It will raise the elevation if the temperature criterion, TEMP, is above the actual temperature; or it will lower the elevation if the actual temperature is above TEMP. There will be NELEV elevations specified. (The current limit on the number of elevations is set to 10 in the code.) These elevations must be ordered from a high to a low elevation.

Monitor

MONITOR LOC ISEG ELEV DYNSEL

ISEG: Integer I8. This can be <0 (use the summed flow weighted temperature of all structures and withdrawals at a withdrawal output segment defined in the WITH OUT card in the w2_con.npt file), =0 (use mixed outlet temperature of the particular structure or withdrawal defined in DYNSTR2), or >0 (use a model segment somewhere in the model domain as the monitoring point, such as a location downstream of a dam). If ISEG < 0, then the absolute value of ISEG must equal to the withdrawal number segment corresponding to IWDO(ABS(ISEG)) corresponding to the WITH OUT cards in the control file, w2_con.npt. At this segment all withdrawals will be combined and evaluated for temperature. If ISEG < 0, then you must specify the withdrawal output as ON

INPUT FILES

(WDOC=ON) and set up the withdrawal output to correspond to the monitor location. For example, if ISEG="3", then all withdrawals, hydraulic structures, and structure outlets from withdrawal #3 will be summed together at a set frequency (as specified in the WDOF card). If IWDO(3)=24, then the mixed temperature from all water withdrawals at segment 24 will be used to decide on whether to lower the outlet elevation. For this case, the value of ELEV is ignored.

For example, if in w2_con.npt, the WITH OUT cards are defined as follows:

WITH OUT	WDOC ON	NWDO 1	NIWDO 7						
WITH DATE	WDOD 1.0	WDOD	WDOD	WDOD	WDOD	WDOD	WDOD	WDOD	WDOD
WITH FREQ	WDOF 0.1	WDOF	WDOF	WDOF	WDOF	WDOF	WDOF	WDOF	WDOF
WITH SEG	IWDO 64	IWDO 86	IWDO 151	IWDO 188	IWDO 13	IWDO 24	IWDO 97	IWDO	IWDO

and in w2_selective.npt,

```
MONITOR LOC ISEG      ELEV
              -5
```

then the model will use the combined withdrawals from segment 13 (IWDO(ABS(ISEG))) as a temperature monitoring location. Note that the WDOF is 0.1 days. Be careful that FREQ in card DYNSTR1 is greater than WDOF since the code uses the value of the last mixed temperature however frequently it is updated as defined by WDOF (not FREQ). Hence if WDOF was every 20 days and FREQ was every 5 days, this would not be appropriate since WDOF > FREQ.

If ISEG=0, the model will use the mixed temperature of the specified structure or withdrawal as the control temperature (as defined in DYNSTR2). If ISEG > 0, the model uses this as the segment number for the temperature monitor location. This can be any active segment in the model domain. This would usually be used at a downstream location in a river below a dam structure.

ELEV: Real F8.0. This is the elevation of the temperature monitoring. Specifying a negative number results in the layer number being used for the vertical location. Hence, specifying '-5' results in specifying layer 5. Specifying '5.25' results in 5.25 m below the water surface. If ISEG=0 or ISEG<0, the elevation card is ignored.

DYNSEL: Character A8. This is either ON or OFF. This controls whether a time series file of temperature controls is read into the model. This allows the model user to use one selective withdrawal structure with a time varying temperature criterion. The file is named 'dynselectiveX.npt', where X is the # in the list of dynamic structures (hence the first line defining a dynamic structure would be '1'). This file is a time series that skips the first 3 lines, then includes a column of Julian day (F8.0), temperature criterion in °C (F8.0). *This time series is treated as a step function input*, i.e., there is no linear interpolation between successive values. An example input file is shown below.

```
Dynamic selective input temperature input file 'dynselective1.npt'
```

INPUT FILES

JDAY	TEMP
1.000	10.0
50.000	12.0
150.000	15.0
200.000	20.0
265.000	15.0
365.000	10.0

This card is repeated by the number of outlets (NUM in DYNSTR1 card).

Auto

AUTO ELEVCONTROL

ELEVCONTROL: Character A8. This is a switch that is either ON or OFF. This switch if 'ON' allows the elevation of the selective withdrawal structure to be reduced as the water level lowers. For example, if the water surface elevation is at an elevation of 259.9 m and the elevation of the withdrawal is at 260 m, the code then shifts the elevation of the outlet to the next lower elevation so that the water surface is always above the level of the outlet. If turned OFF, then W2 always takes water from the outlet at the surface if the elevation of the outlet is above the water surface elevation. This card is repeated by the number of outlets (NUM in DYNSTR1 card).

Split1

SPLIT1 CNTR NUM

This card specifies which of 2 outlets (current limitation is 2 outlets) to direct flow. The outlet structure must have defined at least 2 outlets in the control file. This algorithm combines the specified flows from these outlets (from qot.npt file) and decides how to apportion those flows between the 2 outlets.

CNTR: Character A8. Either 'OFF' or 'ON'. This specifies whether this algorithm is active ('ON') or not ('OFF').

NUM: Integer I8. This specifies the number of outlet pairs to consider. These have to be from the same branch, but can be any 2 already specified outlets in the w2-con.npt file.

Split2

SPLIT2 ST/WD JB YEARLY TSTR TEND TTARGET NOUTS JS1/NW1 JS2/NW2 ELCONT

ST/WD: Character A8. For a structure enter ' ST', for a withdrawal enter ' WD'. This specifies whether the dynamic withdrawal algorithm applies to a W2 'structure' or 'withdrawal' which are treated differently in the W2 model

JB: Integer I8. This is the branch number of the structure. This column is ignored for a withdrawal.

YEARLY: Character A8. This is a control that is ON or OFF. If it is ON, then the Julian days that follow TSTR and TEND are between 1 and 366 and are to be applied yearly during the simulation. If it is OFF, then TSTR and TEND are applied only once between the time period specified.

TSTR: Real F8.0 and **TEND: Real F8.0** are the beginning Julian day and the ending Julian day for starting and ending the splitting algorithm or rule. The model will not split the flow between outlets until after TSTR. After TEND the rule will end and there will be no more splitting. Note that if YEARLY=ON, the Julian days must be between 1 and 366.

TTARGET: Real F8.0. This is the temperature (°C) target for deciding where to apportion the flows. This is the temperature at the center line of the branch outlet, not the selective withdrawal mixed outlet temperature.

INPUT FILES

NOUTS: Integer I8. This is the number of outlets to apportion flows – **current limit is 2**. We may later increase this to more than 2 at a later date.

JS1/NW1: integer I8. Structure number (if ST/WD='ST') or withdrawal number (if ST/WD='WD') for upper outlet.

JS2/NW2: integer I8. Structure number (if ST/WD='ST') or withdrawal number (if ST/WD='WD') for lower outlet.

ELCONT: Character A8: Either ' ON' or ' OFF'. If this is ON, the top outlet elevation centerline will follow the water surface elevation if the centerline elevation of the outlet is below the existing water surface elevation. If OFF, the top outlet elevation is turned OFF when the water surface elevation is lowered below the centerline of the outlet level and all flow goes to the second outlet.

The decision rules for apportioning the flows between 2 outlets are shown in Table 76.

Table 76. Rules for selective withdrawal when there are 2 outlets where flow is being split.

Rule #	Rule
1	If $T_{JS1} > T_{target}$ and $T_{JS2} > T_{target}$, take all flow from lower outlet (JS2)
2	If $T_{JS1} < T_{target}$ and $T_{JS2} < T_{target}$, take all flow from upper outlet (JS1)
3	If $T_{JS1} > T_{target}$ and $T_{JS2} < T_{target}$, take apportion flow based on flow balance equation: $Q_{JS1} = \frac{(Q_{sum}(T_{target} - T_{JS2}))}{(T_{JS1} - T_{JS2})}$ and $Q_{JS2} = Q_{sum} - Q_{JS1}$ where Q_{sum} is the total flow from outlets at JS1 and JS2.
4	If water elevation is below outlet elevation for upper outlet (JS1), take all flow from lower outlet (JS2).

Figure 51 illustrates the use of this new code feature.

INPUT FILES

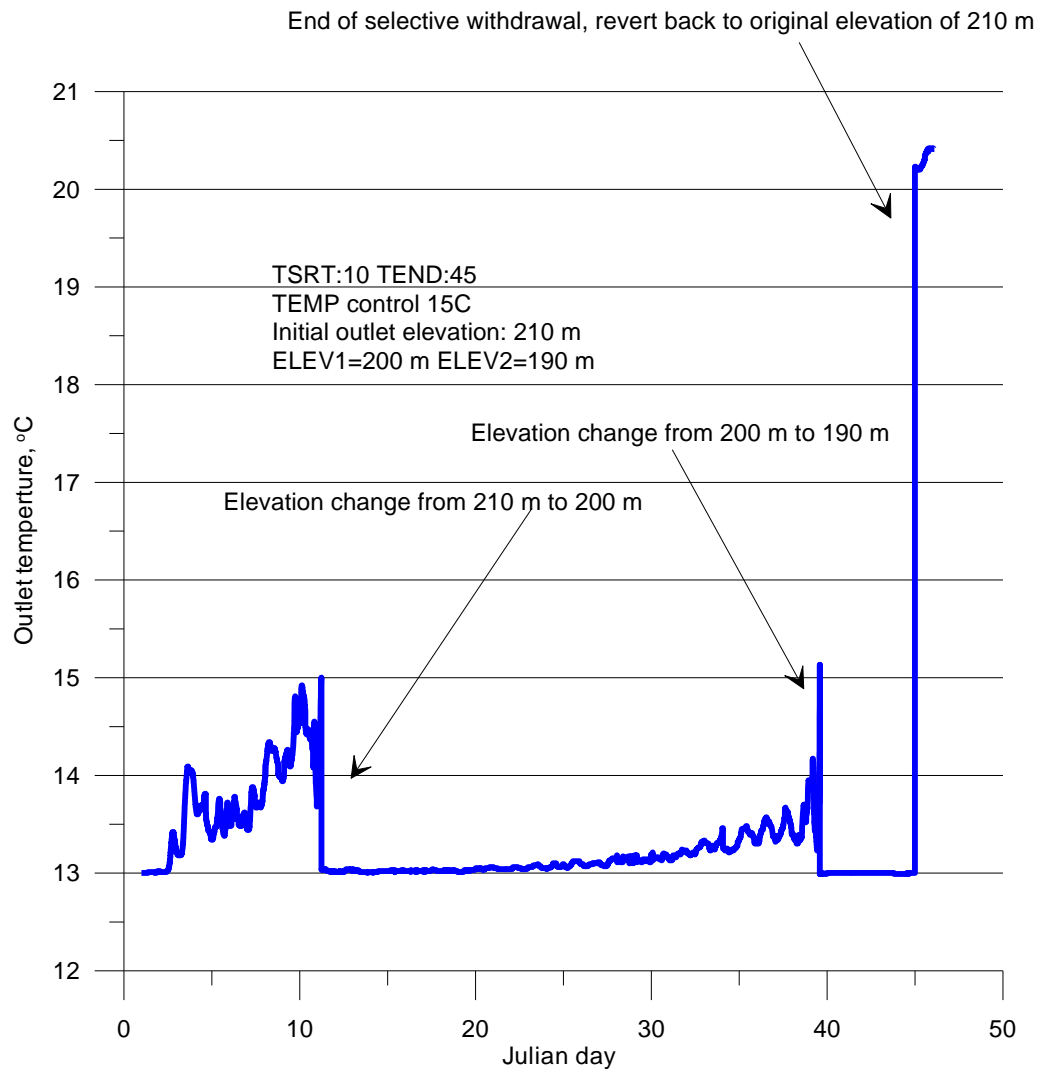


Figure 51. Outlet temperature as a function of time illustrating selective withdrawal meeting temperature target of 15°C between Julian day 1 and 45.

Volume of Reservoir at a Temperature Threshold

This feature is included in the file 'w2_selective.npt' in the last few lines of the input file. The lines that control this feature are shown below:

```
THRESH1      TEMPN
              2

THRESH2  TCRTWB1  TCRTWB2  TCRTWB3  TCRTWB4  TCRTWB5
1         10.0     10.0
2         12.5     12.5
```

THRESH1

```
THRESH1      TEMPN
              2
```

TEMPN: Integer I8. This is the number of temperature criteria for each water body

THRESH2

```
THRESH2  TCRTWB1  TCRTWB2  TCRTWB3  TCRTWB4  TCRTWB5
          11.11    11.11      ! 52 deg. F
          15.55    15.55      ! 60 deg. F
```

TCRTWBx: Real F8.0. This gives the temperature threshold for each waterbody for which to output the volume of the reservoir. In the example the first line corresponds to a temperature criterion of 11.11 degrees C for water bodies 1 and 2 (TCRTWB1, TCRTWB2), and the second line represents a second criterion of 15.55 degrees C for water bodies 1 and 2.

The output files are called 'Volume_wbX.opt', where X is the water body number. This file shows a time series of time (Julian day), total volume, and the volumes below the temperature thresholds. The number of values of TEMPCRIT are based on the number of waterbodies in the model domain. For example, the file Volume_wb1.opt contains the following output for time, total volume (m³), volume (m³) under 11.11°C, and volume (m³) under 15.55°C:

```
jday      Volume      Volcrit      Volcrit
22919.05   0.1650E+10   0.1565E+10   0.1650E+10
22919.09   0.1650E+10   0.1563E+10   0.1650E+10
22919.13   0.1650E+10   0.1561E+10   0.1650E+10
22919.17   0.1650E+10   0.1560E+10   0.1650E+10
22919.21   0.1650E+10   0.1557E+10   0.1650E+10
```

SELECTC=' USGS'

The input file is shown below for 'USGS' and is also named: 'w2_selective.npt' but has a somewhat different format than for SELECTC='ON'. Please consult the USGS report, Rounds and Buccola (2015), for details on the algorithm and example problems.

Below is a section from Rounds and Buccola (2015) describing the new variables and features.

In the w2_selective.npt file, two new inputs (TSFREQ, TSCONV) were added on the SPLIT1 input card. TSFREQ specifies the update frequency for the blending groups that are specified on the SPLIT2 input card, providing a means of separating the update frequency for blending groups and temperature control devices; previously, the

INPUT FILES

update frequency was set for both algorithms with the TCDFREQ input. TSCONV specifies the convergence criterion for the blending calculations in units that correspond to the fraction of the total flow assigned to the first-priority outlets; therefore, TSCONV should be in the neighborhood of 0.1 or less, but nonzero. The default value for TSCONV is 0.005.

Additional new inputs were added to the w2_selective.npt file, requiring some reformatting of that input file to accommodate the new blending inputs.... First, the maximum number of outlets in a blending group was increased from 2 to 10. With only two outlets, the blending solution is straightforward, but requires the user to determine which outlets should be blended at any time in the simulation prior to running the model. With up to 10 outlets specified, other constraints are used to select the outlets to be used and how flows in those outlets are balanced. The choice of outlets is controlled largely through the user-specified “priority” input, which is described later (see section, “Using the Priority Input To Choose Outlets”). The following sections describe the new user-specified constraints, all of which are in the w2_selective.npt input file and summarized in **Table 77**.

Dynamic Temperature Target (TSDYN on SPLIT2 input card).—Setting TSDYN to ON tells the model to override the temperature target (TTARGET) specified on the SPLIT2 input card and instead use a user-specified time-series of temperature targets from an external file named “dynsplit_selectiveX.npt” where X is the blending group number, starting at 1. This is implemented in much the same way that the original version 3.7 code allowed the user to set a time series of temperature targets for the single-structure temperature control device. This change simply allows a similar functionality to be applied for the blending of releases from two or more outlets.

Depth (DEPTHx on the DEPTH input card).—Specifying a nonzero depth for a particular outlet results in that outlet being treated as a floating outlet with a centerline elevation at DEPTH meters below the current water surface. This condition allows some outlets to be treated as floating outlets, an alternative to the original code that allowed one outlet to be “lowered” with the water surface if the ELCONT input was ON.

Minimum Head (MINHDx on the MINHEAD input card).—A nonzero minimum head criterion, specified for each blended outlet, is interpreted as the minimum depth in meters required for the outlet to be used. If the centerline outlet depth is shallower than this nonzero minimum head criterion, the outlet will not be used, regardless of any specified minimum flow criterion. This minimum head criterion is always honored. Inputs less than zero are changed to zero, which is interpreted as the absence of a minimum head criterion.

Maximum Head (MAXHDx on the MAXHEAD input card).—A nonzero maximum head criterion, specified for each blended outlet, is interpreted as the maximum depth in meters under which the outlet can be used. If the centerline outlet depth is

deeper than this nonzero maximum head criterion, the outlet will not be used, regardless of any specified minimum flow criterion. This maximum head criterion is always honored. Inputs less than zero are changed to zero, which is interpreted as the absence of a maximum head criterion. 6

Maximum Flow (MAXFLOx on the MAXFLOW input card).—A nonzero maximum flow criterion, specified for each blended outlet in cubic meters per second, is honored regardless of its effect on temperature or any other minimum flow criterion. Inputs less than zero are changed to zero, which is interpreted as the absence of a maximum flow criterion.

Minimum Flow or Minimum Flow Fraction (MINFRCx on the MINFRAC input card).—This input, specified for each outlet, can be used to specify a minimum flow rate or a minimum flow fraction. To specify a minimum flow rate, the input is negative and its absolute value is interpreted as a minimum flow rate in cubic meters per second. A minimum flow fraction is specified as a value between 0.0 and 1.0 and interpreted as the fraction of the total sum of all specified flows through outlets in the blending group. Values greater than 1.0 are set to 1.0. The blending algorithm attempts to honor all minimum flow criteria, but these criteria are subservient to the more important minimum head, maximum head, maximum flow, and priority inputs. If the priority is such that the outlet is not chosen to be used, the minimum flow criterion for that outlet is not honored. In addition, outlets that are high and dry (not under water) or that do not meet their minimum or maximum head criteria cannot have their minimum flows fulfilled.

INPUT FILES

Table 77. Description of user-specified inputs in the w2_selective.npt file for blending when SELECTC='USGS' (Rounds and Buccola, 2015)

Input variable	Card (name of input section)	Variable name in the code	Description
CNTR	SPLIT1	tspltc	Turns the blending calculations ON or OFF.
NUM	SPLIT1	numtsplt	Number of blending groups to specify, for different times of year or at different dams, etc.
TSFREQ	SPLIT1	tspltfreq	Frequency at which the blending calculations are updated, specified as a fraction of a day.
TSCONV	SPLIT1	tsconv	Convergence criterion for the iterative blending solution, constrained to be 0.1 or less, but nonzero.
ST/WD	SPLIT2	tspltcntr(j)	Specification of a group of either structures (ST) or withdrawals (WD) for blending.
JB	SPLIT2	tspltjb(j)	Branch number for the structures being blended (ignored if using withdrawals).
YEARLY	SPLIT2	tsyearly(j)	Specifies that starting and ending dates for blending should be repeated (ON) each year, or not (OFF).
TSTR	SPLIT2	tststrt(j)	Start date (Julian day) for blending calculations for that group (day 1 is the start of January 1).
TEND	SPLIT2	tstend(j)	End date (Julian day) for blending calculations for that group (day 1 is the start of January 1).
TTARGET	SPLIT2	tsplt(j)	Temperature target to try to meet for that period of dates, if not overridden by a time-series input.
TSDYN	SPLIT2	tsdynsel(j)	Specifies that a time-series of temperature targets is set (ON), with targets in the "dynsplit_selectiveX.npt" file where X is the group number designation.
ELCONT	SPLIT2	elcontspl(j)	Specifies whether an outlet should decrease its elevation to follow the water surface (ON/OFF); this is independent of specifying a floating outlet with the DEPTH parameter.
NOUTS	SPLIT2	nouts(j)	Number of outlets in this particular blending group, between 2 and 10.
TSSHARE	SPLIT2	tssshare	Specifies whether releases among set-2 outlets should be shared (ON) or whether the best single outlet should be chosen (OFF)—see section, “Blending to the Temperature Target”.
JSx/NWx	SPLITOUT	jtsplt(j,n)	Structure or outlet number.
DEPTHx	DEPTH	tsdepth(j,n)	A nonzero value specifies that the outlet is a floating structure with this depth defining its centerline distance from the water surface.
MINFRCx	MINFRAC	tsminfrac(j,n)	A minimum flow fraction (between 0 and 1) specifying that at least that fraction of the total release should go through that outlet. When specified as a negative number, this input is interpreted as a minimum flow rate in cubic meters per second.
PRIORx	PRIORITY	tsprior(j,n)	An integer designation of the "priority" setting for the outlet. A "-1" means the outlet is not blended and the specified flow release rates are unchanged, but the temperature effect is accounted for by the blending calculations. Values of 0 or greater are interpreted as higher priorities for lower input values.
MINHDx	MINHEAD	tsminhead(j,n)	A minimum head designation, in meters. The outlet must be at least this deep to be used. A zero input means that no criterion is specified.

INPUT FILES

[Input variable	Card (name of input section)	Variable name in the code	Description
MAXHDx	MAXHEAD	tsmaxhead(j,n)	A maximum head designation, in meters. The outlet must be shallower than this depth to be used. A zero input means that no criterion is specified.
MAXFLOx	MAXFLOW	tsmaxflow(j,n)	A maximum flow designation, in cubic meters per second. A zero input means that no criterion is specified.

Priority (PRIORx on the PRIORITY input card).—The priority input is an integer limited to values of -1 or greater. The priority input is used to distinguish among groups of both blended and nonblended outlets and to choose which outlets to use at any time. The details of how this input is used to select outlets for blending are provided later in section, “Using the Priority Input To Choose Outlets”.

Shared or Split Flows in Second Priority Group (TSSHARE on the SPLIT2 input card).—When at least two outlets are members of the same priority group and are being used in a blending scheme to meet a user-specified temperature target, by default the flow assigned to the priority groups is distributed among the members of the group equally, but while still fulfilling the minimum and maximum flow criteria set by the user. The TSSHARE input allows this default behavior to be modified for the second (lower) priority group. When turned OFF, the blending algorithm attempts to find the one preferred member of the second priority group that can best be used in conjunction with the first priority group to meet the user-specified temperature target. Minimum and maximum flow criteria are still honored.

An example of the ‘w2_seelctive.npt’ file is shown below for SELECTIVE=’USGS’. Note that older variables for SELECTC=’ON’ were described in the prior section.

```

Selective input control file for SELECTC='USGS'
Temperature outlet control - frequency of output for temperature
OUT FREQ TFRQTMP
    0.125
Structure outlet control based on time and temperature and branch
DYNSTR1  CONTROL      NUM TDCFREQ
        OFF           1    0.125

DYNSTR2    ST/WD      JB   JS/NW  YEARLY    TSTR    TEND    TEMP    NELEV    ELEV1    ELEV2
ELEV3     ELEV4     ELEV5  ELEV6   ELEV7    ELEV8    ELEV9   ELEV10
1          ST        1     1      ON       1.0    151.0   10.0      2      340.    330.

MONITOR LOC ISEG      ELEV  DYNCEL
1          0    -185    OFF

AUTO ELEVCONTROL
1          OFF

SPLIT1      CNTR      NUM  TSFREQ  TSCONV
            ON        1    0.125   0.005

SPLIT2      ST/WD      JB   YEARLY    TSTR    TEND  TTARGET  DYNSEL  ELCONT  NOUTS  TSSHARE
1          ST        1     ON       1.    99999   12.    ON     OFF    8      OFF

SPLITOUT JS1/NW1 JS2/NW2 JS3/NW3 JS4/NW4 JS5/NW5 JS6/NW6 JS7/NW7 JS8/NW8 JS9/NW9
JS0/NW0

```

INPUT FILES

1	1	2	3	4	5	6	7	8		
DEPTH	DEPTH1	DEPTH2	DEPTH3	DEPTH4	DEPTH5	DEPTH6	DEPTH7	DEPTH8	DEPTH9	DEPTH10
1	0	0	0	0	0	0	0	0	0	
MINFRAC	MINFRC1	MINFRC2	MINFRC3	MINFRC4	MINFRC5	MINFRC6	MINFRC7	MINFRC8	MINFRC9	MINFRC10
1	0	0	0	0	0	0	0	0	0	
PRIORITY	PRIOR1	PRIOR2	PRIOR3	PRIOR4	PRIOR5	PRIOR6	PRIOR7	PRIOR8	PRIOR9	PRIOR10
1	2	3	4	5	6	7	8		1	
MINHEAD	MINHD1	MINHD2	MINHD3	MINHD4	MINHD5	MINHD6	MINHD7	MINHD8	MINHD9	MINHD10
1	2	2	2	2	2	2	2	2	2	
MAXHEAD	MAXHD1	MAXHD2	MAXHD3	MAXHD4	MAXHD5	MAXHD6	MAXHD7	MAXHD8	MAXHD9	MAXHD10
1	0	0	0	0	0	0	0	0	0	
MAXFLOW	MAXFLO1	MAXFLO2	MAXFLO3	MAXFLO4	MAXFLO5	MAXFLO6	MAXFLO7	MAXFLO8	MAXFLO9	MAXFLO10
1	0	0	0	0	0	0	0	0	0	
THRESH1	TEMPN									
	2									
THRESH2	TEMPCRIT	TEMPCRIT								
1	11.11	11.11								
2	15.55	15.55								

There are also 4 example problems from the USGS that are described in the Rounds and Buccola (2015) report that are part of the download package. Error trapping is also included in this routine and has also been added to the CE-QUAL-W2 preprocessor. Some of these errors include the following:

- “At least 2 and no more than 10 outlets must be specified for the NOUTS input in each blending group on the SPLIT2 input card.
- Any single outlet can only be specified once in each blending group (SPLITOUT input card).
- Any single outlet can only be specified in one blending group or temperature control device at a time. (Start and end dates for each group are checked.)
- Integer priority specifications must be -1 or greater (PRIORITY input card).”

Environmental Performance Criteria

This section describes the environmental performance criteria which allow a model user to assess model predictions of state variables and how those can be affected by management changes to the waterbody system. The CE-QUAL-W2 model reads the file, w2_envirpf.npt, if the ENVIRPC control is ‘ON’ in the w2_con.npt file. This input file allows the model user to

1. Compute fraction of the reservoir volume and time associated with velocity and temperature levels
2. Compute fraction of the reservoir volume and time associated with CE-QUAL-W2 state variables for water quality

INPUT FILES

3. Compute fraction of the reservoir volume and time associated with CE-QUAL-W2 derived variables for water quality

These are very useful in assessing changes in water quality variables between model alternatives. The input file for these enhancements is shown below and is named: 'w2_envirpf.npt' which is shown below. A discussion of each line from the input file is included in the next sections.

```
ENVIRONMENTAL PERFORMANCE CRITERIA CE-QUAL-W2 MODEL
EPR COMP  INTVLS
      20

TEMP/VEL VELOCITY  VINCR  VTOP  TEMP  TINCR  TTOP
      OFF    0.050   0.50   ON     1.0   30.0

CST      ACTIVE INTSCLE TOPLMIT
TDS      OFF    1.00   20.00
WaterAge ON    1.00   20.00
Gen2     ON    1.00   20.00
GEN3     ON    1.00   20.00
ISS1     ON    1.00   20.00
PO4      OFF    1.00   20.00
NH4      OFF    1.00   20.00
NO3      OFF    1.00   20.00
DSI      OFF    1.00   20.00
PSI      OFF    1.00   20.00
FE       OFF    1.00   20.00
LDOM     OFF    1.00   20.00
RDOM     OFF    1.00   20.00
LPOM     OFF    1.00   20.00
RPOM     OFF    1.00   20.00
ALG1     OFF    1.00   20.00
DO       ON    1.00   20.00
TIC      OFF    1.00   20.00
ALK      OFF    1.00   20.00
ZOO1     OFF    1.00   20.00
LDOM-P   OFF    1.00   20.00
RDOM-P   OFF    1.00   20.00
LPOM-P   OFF    1.00   20.00
RPOM-P   OFF    1.00   20.00
LDOM-N   OFF    1.00   20.00
RDOM-N   OFF    1.00   20.00
LPOM-N   OFF    1.00   20.00
RPOM-N   OFF    1.00   20.00

CST DERI  ACTIVE INTSCLE TOPLMIT
DOC      OFF    1.00   20.00
POC      OFF    1.00   20.00
TOC      OFF    1.00   20.00
DON      OFF    1.00   20.00
PON      OFF    1.00   20.00
TON      OFF    1.00   20.00
TKN      OFF    1.00   20.00
TN       OFF    1.00   20.00
DOP      OFF    1.00   20.00
POP      OFF    1.00   20.00
TOP      OFF    1.00   20.00
TP       OFF    1.00   20.00
APR      OFF    1.00   20.00
CHLA     OFF    1.00   20.00
ATOT     OFF    1.00   20.00
%DO      OFF    1.00   20.00
TSS      OFF    1.00   20.00
TISS     OFF    1.00   20.00
CBOD     OFF    1.00   20.00
pH       OFF    1.00   20.00
```

! 26

! 14

INPUT FILES

CO2	OFF	1.00	20.00
HCO3	OFF	1.00	20.00
CO3	OFF	1.00	20.00

Description of each line of input file

The file is a formatted text file so the file format and spacing is important.

```
ENVIRONMENTAL PERFORMANCE CRITERIA CE-QUAL-W2 MODEL
EPR COMP INTVLS
      20
```

The first 2 lines are ignored and are titles. The **INTVLS**: Integer I8 are the number of intervals or bins on the histogram to use for the output file. There is a blank line after this line.

TEMP/VEL	VELOCITY	VINCR	VTOP	TEMP	TINCR	TTOP
	OFF	0.050	0.50	ON	1.0	30.0

The title line is ignored but they help set the correct spacing for the variables on the following line. **VELOCITY**: Character A8 is ON or OFF and allows a histogram of velocities. **VINCR**: Real F8.0 is the velocity increment in m/s and **VTOP**: Real F8.0 is the maximum velocity in the histogram. **TEMP**: Character A8 is ON/OFF and allows a histogram of temperatures. **TINCR**: Real F8.0 is the increment of the histogram bins and **TTOP**: Real F8.0 is the maximum temperature in °C for the histogram output.

CST	ACTIVE	INTSCLE	TOPLMIT
TDS	OFF	1.00	20.00
WaterAge	ON	1.00	20.00
Gen2	ON	1.00	20.00
GEN3	ON	1.00	20.00
ISS1	ON	1.00	20.00
PO4	OFF	1.00	20.00
NH4	OFF	1.00	20.00
NO3	OFF	1.00	20.00
DSI	OFF	1.00	20.00
PSI	OFF	1.00	20.00
FE	OFF	1.00	20.00
LDOM	OFF	1.00	20.00
RDOM	OFF	1.00	20.00
LPOM	OFF	1.00	20.00
RPOM	OFF	1.00	20.00
ALG1	OFF	1.00	20.00
DO	ON	1.00	20.00
TIC	OFF	1.00	20.00
ALK	OFF	1.00	20.00
ZOO1	OFF	1.00	20.00
LDOM-P	OFF	1.00	20.00
RDOM-P	OFF	1.00	20.00
LPOM-P	OFF	1.00	20.00
RPOM-P	OFF	1.00	20.00
LDOM-N	OFF	1.00	20.00
RDOM-N	OFF	1.00	20.00
LPOM-N	OFF	1.00	20.00
RPOM-N	OFF	1.00	20.00

! 26

The next line is a title line ignored by the code but the variable spacing format is shown. In the following lines, the same number of active constituents are required in this section as are in the w2_con.npt file under active constituents. The model user can decide which variables to output. The names of each state variable is ignored by the code. **ACTIVE: Character A8** is either

INPUT FILES

OFF/ON and indicates whether to turn this output ON or OFF. **INTSCLE: Real F8.0** is the interval scale for the output state variable – it is the bin interval in the units of the state variable.

TOPLMIT: Real F8.0 is the upper limit of the histogram output.

CST	DERI	ACTIVE	INTSCLE	TOPLMIT
DOC		OFF	1.00	20.00
POC		OFF	1.00	20.00
TOC		OFF	1.00	20.00
DON		OFF	1.00	20.00
PON		OFF	1.00	20.00
TON		OFF	1.00	20.00
TKN		OFF	1.00	20.00
TN		OFF	1.00	20.00
DOP		OFF	1.00	20.00
POP		OFF	1.00	20.00
TOP		OFF	1.00	20.00
TP		OFF	1.00	20.00
APR		OFF	1.00	20.00
CHLA		OFF	1.00	20.00
ATOT		OFF	1.00	20.00
%DO		OFF	1.00	20.00
TSS		OFF	1.00	20.00
TISS		OFF	1.00	20.00
CBOD		OFF	1.00	20.00
pH		OFF	1.00	20.00
CO2		OFF	1.00	20.00
HCO3		OFF	1.00	20.00
CO3		OFF	1.00	20.00

! 14

The next line is a title line ignored by the code but the variable spacing format is shown. In the following lines, the same number of active derived constituents are required in this section as are in the w2_con.npt file under derived constituents (these though are not variable as are the active constituents). The model user can decide which variables to output. The names of each state variable is ignored by the code. **ACTIVE: Character A8** is either OFF/ON and indicates whether to turn this output ON or OFF. **INTSCLE: Real F8.0** is the interval scale for the output state variable – it is the bin interval in the units of the state variable. **TOPLMIT: real F8.0** is the upper limit of the histogram output.

An example of this type of analysis is shown comparing alternatives in watershed loading for Lake Tenkiller in OK. Figure 52 shows the results for Total P for one sampling station for different modeling scenarios.

Typical output file format is shown below and is set up for graphing in Excel. The first series of output lines are a histogram of the fraction of volume and time that the water quality variable was in the specified interval. At the end of the column there is a sum of the fractions, which should sum to 1.0 and the last line is the temporal and volume weighted average over the entire model domain and simulation time period.

Gen1interval" "Fraction of volume" "		Gen2interval" "Fraction of volume" "	
Gen3interval" "Fraction of volume" "	ISS1interval" "Fraction of volume" "		
DOinterval" "Fraction of volume"			
20.00 0.1000E+01 20.00 0.1455E+00 20.00 0.3238E-02 20.00			
0.1047E-02 20.00 0.0000E+00			
19.00 0.0000E+00 19.00 0.4349E-01 19.00 0.1123E-03 19.00			
0.1258E-03 19.00 0.0000E+00			
18.00 0.0000E+00 18.00 0.4316E-01 18.00 0.9497E-04 18.00			
0.1211E-03 18.00 0.0000E+00			

INPUT FILES

17.00	0.0000E+00	17.00	0.4206E-01	17.00	0.1036E-03	17.00
0.1132E-03	17.00	0.0000E+00				
16.00	0.0000E+00	16.00	0.4335E-01	16.00	0.1092E-03	16.00
0.1605E-03	16.00	0.0000E+00				
15.00	0.0000E+00	15.00	0.4352E-01	15.00	0.1164E-03	15.00
0.1772E-03	15.00	0.0000E+00				
14.00	0.0000E+00	14.00	0.4367E-01	14.00	0.1325E-03	14.00
0.2543E-03	14.00	0.0000E+00				
13.00	0.0000E+00	13.00	0.4311E-01	13.00	0.1798E-03	13.00
0.2965E-03	13.00	0.8583E-04				
12.00	0.0000E+00	12.00	0.4296E-01	12.00	0.1926E-03	12.00
0.3453E-03	12.00	0.2429E-02				
11.00	0.0000E+00	11.00	0.4301E-01	11.00	0.1555E-03	11.00
0.3718E-03	11.00	0.6621E-01				
10.00	0.0000E+00	10.00	0.4291E-01	10.00	0.2083E-03	10.00
0.4882E-03	10.00	0.7014E+00				
9.00	0.0000E+00	9.00	0.4266E-01	9.00	0.3722E-02	9.00
0.5676E-03	9.00	0.2159E+00				
8.00	0.0000E+00	8.00	0.4296E-01	8.00	0.5889E-02	8.00
0.8105E-03	8.00	0.1384E-01				
7.00	0.0000E+00	7.00	0.4222E-01	7.00	0.6986E-02	7.00
0.9553E-03	7.00	0.6332E-04				
6.00	0.0000E+00	6.00	0.4215E-01	6.00	0.7670E-02	6.00
0.9875E-03	6.00	0.0000E+00				
5.00	0.0000E+00	5.00	0.4208E-01	5.00	0.9771E-02	5.00
0.1650E-02	5.00	0.0000E+00				
4.00	0.0000E+00	4.00	0.4211E-01	4.00	0.1175E-01	4.00
0.2712E-02	4.00	0.0000E+00				
3.00	0.0000E+00	3.00	0.4194E-01	3.00	0.1495E-01	3.00
0.4287E-02	3.00	0.0000E+00				
2.00	0.0000E+00	2.00	0.4228E-01	2.00	0.2231E-01	2.00
0.2022E-01	2.00	0.0000E+00				
1.00	0.0000E+00	1.00	0.8487E-01	1.00	0.9123E+00	1.00
0.9643E+00	1.00	0.0000E+00				
0	0.1000E+01	0	0.1000E+01	0	0.1000E+01	0
0	0.1000E+03	0	0.1177E+02	0	0.9146E+00	0
				0.1158E+01	0	0.1031E+02

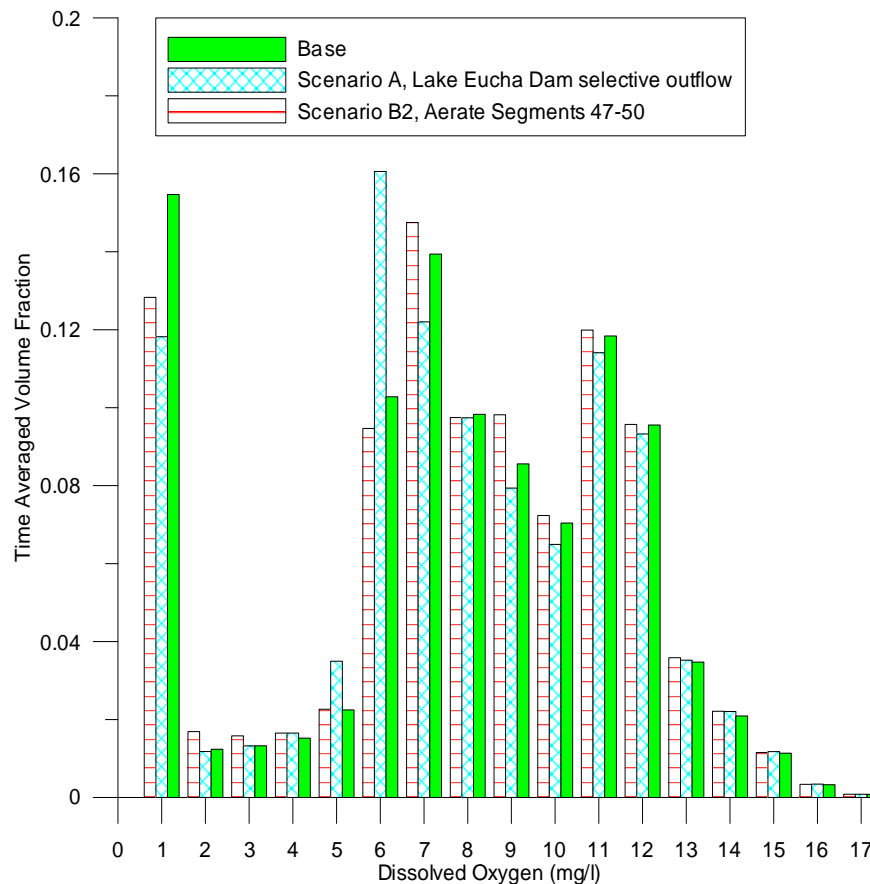


Figure 52. Environmental performance for 3 different scenario runs comparing dissolved oxygen in a eutrophic system Eucha Reservoir in OK.

Hypolimnetic Aeration

This section describes the hypolimnetic aeration algorithm which allow a model user to add oxygen and additional mixing to a section of a waterbody that is controlled by an oxygen probe. The CE-QUAL-W2 model reads the file, w2_aerate.npt', if the AERATEC control is 'ON' in the w2_con.npt file. This input file allows the model user to

1. Add oxygen mass to specified model segments and layers
2. Control the oxygen mass added by using oxygen probes located anywhere in the model domain
3. Affect the mixing associated with the oxygen input in a qualitative method

This algorithm does not model the dynamics of a bubble diffuser. It merely allows the user to experiment with delivering oxygen at given rates to parts of the reservoir domain. This is an excellent tool for planning since it does allow the model user to determine the amount of oxygen required to be delivered to meet a certain water quality target.

INPUT FILES

The input file for these enhancements is shown below and is named: 'w2_aerate.npt'. A discussion of each line from the input file is included in the next sections.

```
CONTROL FILE FOR Hypolimnetic aeration
NAER      OUTPUTFILE      # of aerators
  1      aeration.opt
                                kg O2/d
SEG#    KTOP#    KBOT#    MASSRT    TIMON    TIMOFF    DZFACT    O2OFF    O2ON    iprb    kprb
  31      25      30    1000.      1.0    125.0      5.      12.5    11.0     31     30
```

An explanation of each term in the input file is shown in the table below:

Parameter	Values (typical)	Description
AERATION	ON/OFF	Turn on or off aeration/mixing
NAER	Integer from 1 to the maximum number of aerators	There is no limit to the number of aerators. These can also be thought of as 1 aerator turned ON/OFF at different time, so each aerator would be a different cycle of the aerator
OUTPUTFILE	Output file name	
SEG#	Integer segment #	Location of aerator
KTOP#	Top layer #	Location of aerator – 1 aerator can span more than 1 vertical layer
KBOT#	Bottom layer #	Location of aerator - 1 aerator can span more than 1 vertical layer
MASSRT	Rate of mass injection of air in kg O2/day	Rate of mass injection of O2
TIMON	Julian day	Start date for aerator
TIMOFF	Julian day	End date for aerator
DZFACT	Factor to multiply the vertical mixing coefficient: 1-100	A factor of 1 means to use the model predicted vertical mixing coefficient. A value of 100, means to increase the mixing value by 100X. If DZFACT=1, this assumes the aerator does not mix the water column. If DZFACT>1, then DZ is increased as a result of additional vertical mixing induced by the aerator. One should use this as a sensitivity analysis to see if an increase in vertical mixing will affect the efficiency of the aerator or whether it is desired or not.
O2OFF	Dissolved oxygen concentration in mg/l	Assuming we have a DO probe located at iprb and kprb, this tells the model when to turn off the aerator based on DO measurements at a user defined location
O2ON	Dissolved oxygen concentration in mg/l	Assuming we have a DO probe located at iprb and kprb, this tells the model when to turn on the aerator based on DO measurements at a user defined location
iprb	Integer segment #	Location of DO probe for turning ON/OFF the aerator
kprb	Integer layer #	Location of DO probe for turning ON/OFF the aerator

INPUT FILES

An example of the use of a hypolimnetic aerator was inserted into for DeGray Lake during 1980 at segment 31 over K layers 25 to 30 (see Figure 53). A dissolved oxygen probe was set at segment 31 and layer 30. This probe controlled the aeration input – when the dissolved oxygen was below 11 mg/l it was turned ON and when it was at or above 12.5 mg/l it was turned OFF. Figure 54 shows the results of the cumulative dissolved oxygen input in kg and the dissolved oxygen concentration at the probe location.

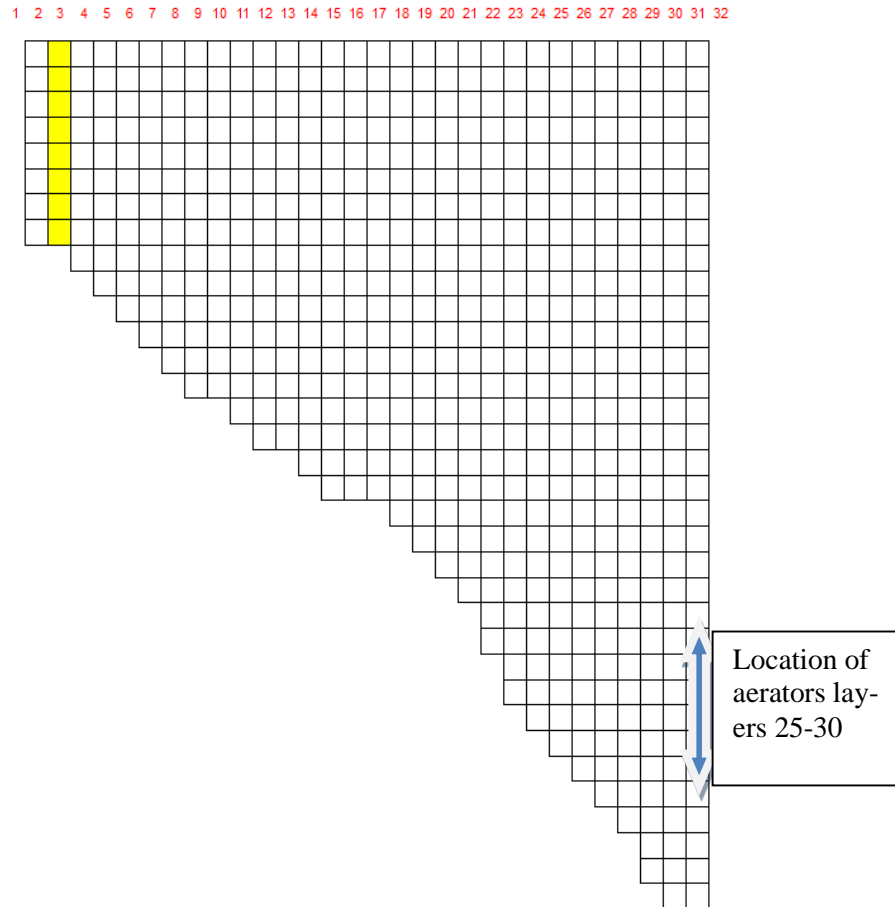


Figure 53. Side view of DeGray Lake grid used for hypolimnetic aeration.

INPUT FILES

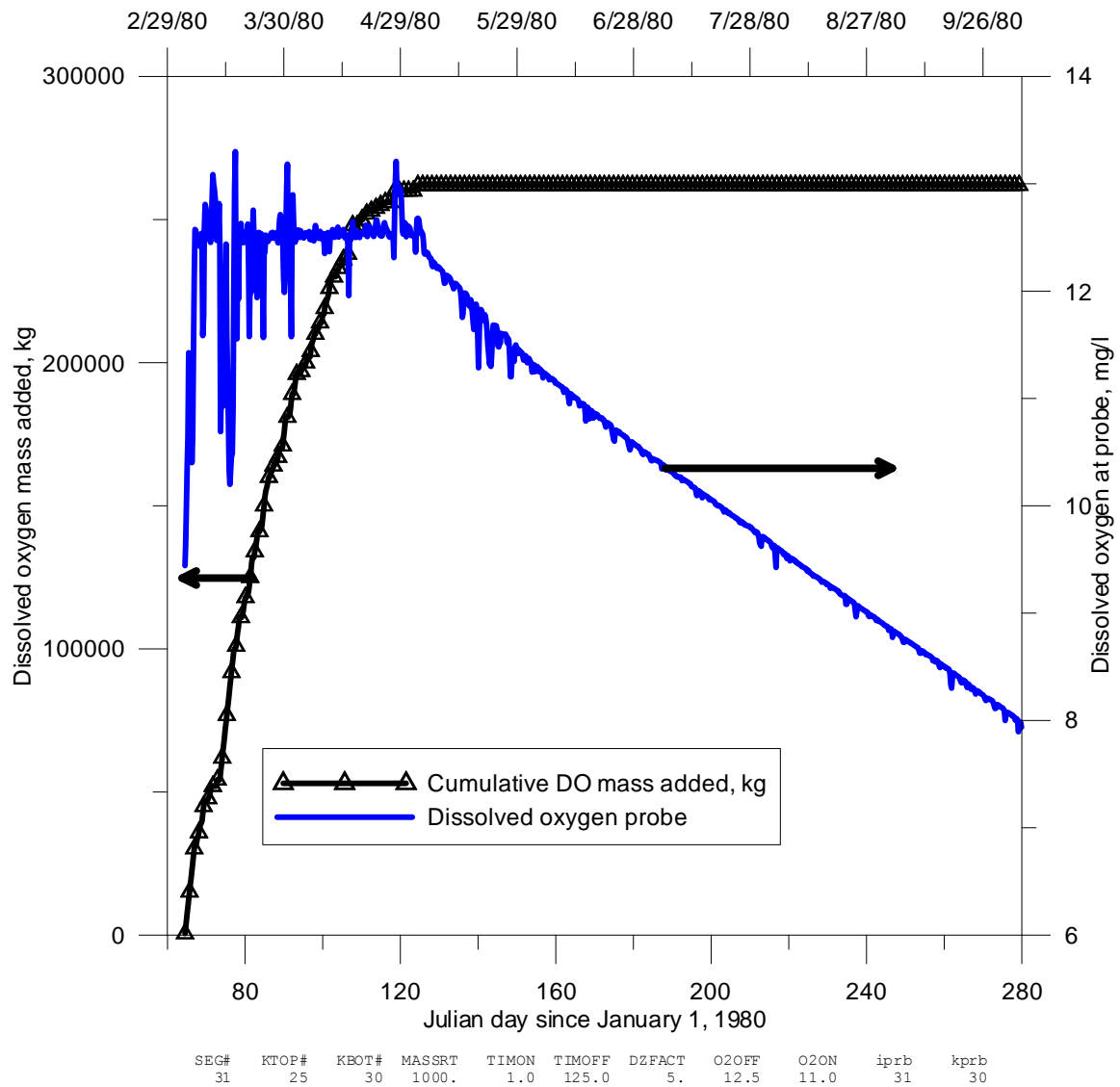


Figure 54. Dissolved oxygen at probe location and cumulative oxygen added in kg over period of aeration (Julian day 1-125). Target dissolved oxygen at probe location was between 11 and 12.5 mg/l.

Meteorology File

The meteorologic input file contains the following data:

Variable Description	Name	Format
Julian date	[JDAY]	F8.0
Air temperature, °C	[TAIR]	F8.0
Dewpoint temperature, °C	[TDEW]	F8.0
Wind speed, $m\ sec^{-1}$	[WIND]	F8.0
Wind direction, rad	[PHI]	F8.0
Cloud cover (0 to 10)	[CLOUD]	F8.0
Incident short wave solar radiation, $W\ m^{-2}$	[SRO]	F8.0

The following is a list of guidelines for file preparation:

1. Data is read in according to an F8.0 format which allows the user to override the decimal point location according to the location specified in the input file. The field widths must be the same as specified above.
2. The first two lines are ignored and can be used to comment the file.
3. The third line contains the variable names which are right justified according to the input field. This line is also ignored although the preprocessor checks to ensure the fields are aligned correctly.
4. Data can be input at any frequency and may vary during the simulation. The user need only specify the Julian date corresponding to the data.
5. Short wave solar radiation is required if the user has set [[SROC](#)] to ON in the [HEAT EXCH](#) card in the control file. Otherwise, this field is not required. This represents, not global radiation, but only the penetrating short-wave solar radiation component.
6. Cloud cover is provided in tenths between 0 (no clouds) and 10 (fully cloudy).

Example

Sample meteorologic input file

JDAY	TAIR	TDEW	WIND	PHI	CLOUD	SRO
1.0	7.8	-0.9	2.19	2.0	8.0	0.0
2.0	3.3	1.3	4.75	2.0	6.0	0.0
3.0	3.3	1.3	4.75	2.0	3.0	0.0
4.0	2.2	-3.5	3.33	2.0	4.0	0.0
5.0	6.4	-2.4	1.86	2.0	4.0	0.0
6.0	7.5	2.4	4.00	2.0	10.0	0.0
7.0	1.9	-4.9	4.83	2.0	2.0	0.0
8.0	1.7	-6.6	4.00	2.0	0.0	0.0

There is a new option starting with Version 3.71 to use a free-format file rather than the fixed format shown above. When the first character in the first line contains the '\$' symbol, the model will treat the file as being in free format. As in the fixed format file, the first 3 lines are ignored and the data fields are in the same order the fixed format file except that the user is no longer limited to 8 characters for each field. An example of a comma delimited file is shown below and the spreadsheet that was used to develop it.

Example

INPUT FILES

```
$Spokane International Airport met data 1/1/2001
Solar is from Odessa
JDAY,TAIR,TDEW,WIND,PHI,CLOUD,Solar,
1,-2.2,-3.3,2.57,2.62,10,0,
1.039,-2.2,-3.3,2.57,2.62,10,0,
1.081,-2.2,-3.9,3.09,1.75,10,0,
1.122,-2.2,-3.3,0,0,10,0,
1.164,-2.2,-3.3,2.06,0.87,10,0,
1.206,-2.2,-3.3,3.09,0.35,10,0,
1.247,-2.2,-2.8,3.09,0.35,10,0,
1.289,-2.2,-2.8,3.09,1.05,10,0,
1.331,-2.2,-2.8,3.09,1.05,10,0,
1.372,-1.7,-2.2,2.57,0.87,10,13.01,
1.414,-1.7,-1.7,0,0,10,64.47,
1.456,-1.1,-1.7,2.57,6.28,10,113.6,
1.497,-1.1,-1.1,2.57,0.7,10,152.29,
1.539,-0.6,-1.1,0,0,10,144.5,
1.581,-0.6,-1.1,0,0,10,100.71,
1.622,-1.1,-1.1,3.09,3.32,10,54.13,
1.664,-0.6,-1.1,0,0,10,20.68,
1.706,-1.1,-1.1,2.06,5.24,10,0,
```

In Excel this file looks like the following and can be written out as a csv file type.

	\$Spokane	Internatio	Airport	met	data,	1/1/2001	to	12/31/2001
	Solar	is	from	Odessa				
	JDAY	TAIR	TDEW	WIND	PHI	CLOUD	Solar	
	1	-2.2	-3.3	2.57	2.62	10	0	
	1.039	-2.2	-3.3	2.57	2.62	10	0	
	1.081	-2.2	-3.9	3.09	1.75	10	0	
	1.122	-2.2	-3.3	0	0	10	0	
	1.164	-2.2	-3.3	2.06	0.87	10	0	
	1.206	-2.2	-3.3	3.09	0.35	10	0	
	1.247	-2.2	-2.8	3.09	0.35	10	0	
	1.289	-2.2	-2.8	3.09	1.05	10	0	
	1.331	-2.2	-2.8	3.09	1.05	10	0	
	1.372	-1.7	-2.2	2.57	0.87	10	13.01	
	1.414	-1.7	-1.7	0	0	10	64.47	
	1.456	-1.1	-1.7	2.57	6.28	10	113.6	
	1.497	-1.1	-1.1	2.57	0.7	10	152.29	
	1.539	-0.6	-1.1	0	0	10	144.5	
	1.581	-0.6	-1.1	0	0	10	100.71	
	1.622	-1.1	-1.1	3.09	3.32	10	54.13	

Dynamic Elevation for Structure Outflows

Whenever DYNELEV is set to ON in the control file, w2_con.npt, the model looks for the file, **dynselevX.npt**, where X is the model branch #. This file contains the variable outlet elevation of one or more structures for that branch.

First line:	Ignored as header/title
Second line:	Integer, IJS, # of structures (outlets) for this branch that have variable ESTR. The following line is repeated IJS times (any text after IJS is ignored)
Third line:	Integer, NJS, Structure (Outlet) #, repeated IJS times showing the order of the structures to be read. (any text after NJS is ignored)
Fourth line	Ignored as header/title
Fifth line	JDAY, ESTR(NJS1),ESTR(NJS2),ESTR(NJS3),.... This is the Julian day and the centerline elevation of each structure in m. These are not interpolated in the model but are treated as step function changes in centerline elevation. There will be IJS columns of ESTR information provided.

An example input file is shown below.

```
$Dynamic structure withdrawal file for JB=1
2,# of outlets to for this branch that have a variable ESTR
17, Outlet number for this branch that has a variable ESTR, Repeat on different line.
18, Outlet number for this branch that has a variable ESTR
Jday since 2001,Elevation_m_17,Elev_m_18      Repeat columns for each JS
731.0,101.7129968,125.2
781.0,101.7129968,125.2
831.0,121.9214826,125.2
921.0,121.9214826,127.5
931.0,115.8254084,127.5
951.0,109.7293343,128.5
971.0,103.6332602,128.5
991.0,101.7129968,129.0
1096.0,101.7129968,129.0
```

The '\$' as the first character of the first line means that the JDAY and elevation values are in free format. Otherwise it is in 10f8.0:/(9f8.0) format.

Dynamic Pump Input File

Whenever DYNPUMP is set to ON in the control file, w2_con.npt, the model looks for the file, **dynpumpX.npt**, where X is the pump #. This file is a time series that skips the first 3 lines, then includes a column of Julian day (F8.0), elevation of the centerline of the pump withdrawal in m (F8.0), elevation for turning the pump ON in m (F8.0), elevation for turning OFF the pump in m (F8.0), and the pump flow rate in m³/s (F8.0). This file is treated as a step function input, i.e., there is no linear interpolation between successive values. An example input file is shown below.

Dynamic pump input file

JDAY	EPU	EONPU	EOFFPU	QPU
1.000	456.	460.0	459.0	1.0
60.000	456.	462.0	460.0	2.0
90.000	456.	463.0	461.0	3.0
160.000	457.5	464.0	462.0	5.0
365.000	458.	460.0	462.0	5.0

Dynamic Pipe Input File

Whenever DYNPIPE is set to ON in the control file, w2_con.npt, the model looks for the file, **dyn-pipe.npt**. This file is a time series that skips the first 3 lines, then includes a column of Julian day (F8.0), then every 8 columns it reads a number that is multiplied by the theoretical flow in the pipe. This allows for turning a pipe ON or OFF in case the number is 1 or 0, respectively. Or if the flow is throttled by closing a gate valve, the fraction of flow through the pipe can be given. This file is treated as a step function input, i.e., there is no linear interpolation between successive values. An example input file is shown below.

Chester Morse Lake Dynamic Pipe File. Pipe 1 = low level outlet, Pipe2 = Bypass valve

Jday	Pipe1	Pipe2
1.00	1.000	1
75.00	0.030	0
265.00	0.050	0
269.00	0.159	0
290.00	0.300	0
306.00	1.000	0
311.00	1.000	1
349.00	0.000	1
362.00	1.000	1
606.00	0.000	0
630.00	0.043	0
635.00	0.057	0
636.00	0.071	0
645.00	0.143	0
654.00	0.171	0
655.00	0.143	0
657.00	0.129	0
663.00	0.143	0
665.00	0.157	0
682.00	1.000	0
683.00	1.000	1
964.00	1.000	0
985.00	0.000	0
992.00	0.057	0
998.00	0.086	0
1002.00	0.286	0
1012.00	0.357	0
1063.00	1.000	0
1375.00	0.000	0
1382.00	0.129	0
1384.00	0.157	0
1390.00	0.143	0

Gate File

This file contains the dynamic gate height for each gate based on the rating curve supplied in the gates section in the control file. One file is required for all the gates specified in the control file and contains the following data for n gates:

Variable Description	Name	Format
Julian day	[JDAY]	F8.0
Gate#1 opening, m	[GATEH]	F8.0
Gate#2 opening, m	[GATEH]	F8.0
Gate#3 opening, m	[GATEH]	F8.0
Gate#4 opening, m	[GATEH]	F8.0
Gate#5 opening, m	[GATEH]	F8.0
....		
Gate# n opening, m	[GATEH]	F8.0

The following is a list of guidelines for file preparation:

1. Data is read in according to an F8.0 format which allows the user to override the decimal point location according to the location specified in the input file. The field widths must be the same as specified above.
2. The first two lines are ignored and can be used to comment the file.
3. The third line contains the variable names which are right justified according to the input field. This line is also ignored although the preprocessor checks to ensure the fields are aligned correctly.
4. Data can be input at any frequency and may vary during the simulation. The user need only specify the Julian date corresponding to the data.
5. After the Julian day field, there are n columns of F8.0 format corresponding to each gate
6. The gate height is always treated as a step function rather than interpolated between dates.

Example

Tainter gate opening, m

JDAY	GATEH
1.00	1.2
200.30	0
204.65	1.25
209.50	2.50
368.00	0

In some cases, gate openings can be used to open or close a valve or gate dynamically. In the following example, the dynamic opening is either closed (0) or fully open (1). In either case, the model uses the rating curve for the gate as specified in the control file.

Example

QGATE
simulating Willamette Falls 1999

GATE

INPUT FILES

Jday	Gate 1
1.00	1
200.30	0
204.65	1
209.50	0
368.00	0

Also, if the gate is specified as a dynamic weir ([DYNGC] is set to “ZGT”), then the bottom elevation is included in this file rather than the gate opening. For example, if flashboards are raised, the weir equations will be used but with the dynamic weir crest elevation. The example below shows a dynamic flashboard height.

Example

```
QGATE
Dynamic flashboards 1999
  Jday  Gate 1
    1.00   23.5
   200.30  25.5
   204.65  25.5
   209.50  23.5
   368.00  23.5
```

This file has also been used to predict the flow through needle valves where a rating curve based on the number of turns of the gate valve was developed. In this case, the dynamic height was interpreted as “turns” of a valve and is dependent on the supplied rating curve.

Also, if the gate is specified as a flow rate ([DYNGC] is set to “FLOW”), then the flow rate is included in this file rather than the gate opening. The example below shows a dynamic flow rate.

Example

```
QGATE
Flow rate for pumped storage between 2 reservoirs
  Jday  GATE 1  GATE 2
    1.00   23.5    0.0
    1.50    0.0   23.5
    2.00   12.5    0.0
    2.50    0.0   12.5
    3.00   20.0    0.0
```

The model user can also use the dynamic weir algorithm to achieve a target water level that changes over the year. When DYNGTC=ZGT, the elevation of the dynamic weir can be the target water level in the reservoir. The rating curve equations defining the gate describe the response of that weir/spillway. Under normal conditions, this would be a withdrawal at the vertical location of the dynamic weir elevation. In many cases it is desired that the target water level be achieved, but the flow is taken from a different target elevation. In that case the 2nd line in the gate file is not ignored. To turn this on, the model user must insert the following in the 2nd line:

Char 1-8: Title in all caps: EGT2ELEV

Char 9-16: Centerline elevation where the outflow will be removed in F8.0 format

This is repeated for the # of gates in F8.0 format. If you want to use the elevation specified in the dynamic weir elevations, just set the elevation above to 0.0. Note the example below for 2 gates both specified as dynamic weirs.

```
QGATE
```

INPUT FILES

GATE

```
EGT2ELEV    110.0    00.0
      Jday  GATE 1  GATE 2
      1.00   123.5   122.5
      3.00   140.0   123.0
```

GATE1 would compute flow based on the dynamic weir elevation, but it would take the centerline of the withdrawal at 110.0 m. GATE2 would compute the flow based on the dynamic weir elevation, and it would take the centerline of the withdrawal at elevation of the dynamic weir.

Light Extinction File

The light extinction input file contains the following data for each waterbody:

Variable Description	Name	Format
Julian date	[JDAY]	F8.0
Light extinction, m^{-1}	[EXH2O]	F8.0

These data are usually obtained by Secchi disk measurements. Due to inaccuracies in these measurements, a more appropriate method is the measurement of light extinction directly using a photometer. If dynamic light extinction is read in, all other internal calculations of light extinction are ignored. The following is a list of guidelines for file preparation:

1. Input format for each field is F8.0 that allows the user to specify the decimal point location.
2. The first two lines are ignored and can be used to comment the file.
3. The third line contains the variable name which is right justified according to the input field. This line is also ignored although the preprocessor checks to ensure the fields are aligned correctly.
4. The first field is the Julian date [JDAY], which can be entered at any frequency. The frequency between updates may vary during the simulation.
5. The second field contains values for observed light extinction, m^{-1} .

Example

Observed light extinction

```

JDAY    EXH2O
1.00    0.20
110.0   0.25
140.0   0.34
157.0   0.41
158.0   0.44
165.0   0.45
200.0   0.38
220.0   0.25
240.0   0.20
250.0   0.24
260.0   0.20
275.0   0.24
280.0   0.27
320.0   0.35
340.0   0.40
365.00  0.20
410.00  0.22
479.00  0.24
525.00  0.30
540.00  0.41
575.00  0.30
650.00  0.25

```


Wind Sheltering Coefficient File

The wind sheltering input file contains the following data:

Variable Description	Name	Format
Julian date	[JDAY]	F8.0
Wind-sheltering coefficient	[WSC]	F8.0

This file contains the wind-sheltering as a function of segment and time. This is a representation of having segment-by-segment wind velocity data, which is preferable if the data exist based on only one meteorological station. The following is a list of guidelines for file preparation:

1. Input format for each field is F8.0 that allows the user to specify the decimal point location.
2. The first two lines are ignored and can be used to comment the file.
3. The third line contains the variable name which is right justified according to the input field. This line is also ignored although the preprocessor checks to ensure the fields are aligned correctly.
4. The first field is the Julian date, which can be entered at any frequency. The frequency between updates may vary during the simulation.
5. The next fields are the wind-sheltering coefficients for all model segments including the boundary segments at the given Julian date.
6. The Julian date [JDAY] and wind-sheltering coefficient [WSC] are repeated as required to provide for dynamic wind sheltering.
7. Only one file is provided for all the model segments regardless of the number of waterbodies.

Example

Alum Creek wind sheltering coefficients

JDAY	WSC	WSC	WSC	WSC	WSC	WSC	WSC	WSC	WSC
1.0	0.1	0.2	0.3	0.4	0.5	0.6	0.7	0.8	0.9
	1.0	1.0	1.0	1.0	1.0	1.0	1.0	1.0	1.0
	1.0	1.0	1.0	1.0	1.0	1.0	1.0	1.0	1.0
	1.0	1.0	1.0	1.0	1.0	1.0	1.0	1.0	1.0
1.1	0.2	0.3	0.4	0.5	0.6	0.7	0.8	0.9	1.0
	1.0	1.0	1.0	1.0	1.0	1.0	1.0	1.0	1.0
	1.0	1.0	1.0	1.0	1.0	1.0	1.0	1.0	1.0
	1.0	1.0	1.0	1.0	1.0	1.0	1.0	1.0	1.0
365.0	1.0	1.0	1.0	1.0	1.0	1.0	1.0	1.0	1.0
	1.0	1.0	1.0	1.0	1.0	1.0	1.0	1.0	1.0
	1.0	1.0	1.0	1.0	1.0	1.0	1.0	1.0	1.0
	1.0	1.0	1.0	1.0	1.0	1.0	1.0	1.0	1.0

The model reads in a free format version of this file if the first character on the first line is '\$'. An example of this file type is shown below. The first 3 lines are ignored. Then each row starts with the Julian day followed by the WSC coefficient for each model segment including boundary/inactive segments.

WIND SHELTERING

INPUT FILES

Example free format file type

```
$wsc file,,,,,,,,,,,,,,,,,,,,,,,,,,,,,  
,Seg #s,,,,,,,,,,,,,,,,,,,,,,,,,,,,,  
JDAY,1,2,3,4,5,6,7,8,9,10,11,12,13,14,15,16,17,18,19,20  
1.0,1,1,1,1,1,1,1,1,1,1,1,1,1,1,1,1,1,1,1  
365.0,1,1,1,1,1,1,1,1,1,1,1,1,1,1,1,1,1,1,1
```

In Excel part of the file looks like this. There is no wrapping of lines of data as in the fixed format file. In this case the wind sheltering coefficient is 1.0. This file can then be written out as a csv file type.

Sws file																				
	Seg #s																			
JDAY	1	2	3	4	5	6	7	8	9	10	11	12	13	14	15	16	17	18	19	20
1	1	1	1	1	1	1	1	1	1	1	1	1	1	1	1	1	1	1	1	1
365	1	1	1	1	1	1	1	1	1	1	1	1	1	1	1	1	1	1	1	1

Shade Input File

The shade input file contains the following data (if in fixed format):

Variable Description	Name	Format
Segment Number	[SEG]	I8
Dynamic shading or static shading	[DYNOSH]	F8.0
Vegetative elevation left bank, m	[VEL]	F8.0
Vegetative elevation right bank, m	[VER]	F8.0
Distance to vegetation left bank, m	[DL]	F8.0
Distance to vegetation right bank, m	[DR]	F8.0
Shade reduction factor #1, left bank	[SRFL1]	F8.0
Shade reduction factor #2, left bank	[SRFL2]	F8.0
Shade reduction factor #1, right bank	[SRFR1]	F8.0
Shade reduction factor #2, right bank	[SRFR2]	F8.0
Topographic angle #1 at 0°, radians	[TOPO1]	F8.0
Topographic angle #2 at 20°, radians	[TOPO2]	F8.0
Topographic angle #3 at 40°, radians	[TOPO3]	F8.0
Topographic angle #4 at 60°, radians	[TOPO4]	F8.0
Topographic angle #5 at 80°, radians	[TOPO5]	F8.0
Topographic angle #6 at 100°, radians	[TOPO6]	F8.0
Topographic angle #7 at 120°, radians	[TOPO7]	F8.0
Topographic angle #8 at 140°, radians	[TOPO8]	F8.0
Topographic angle #9 at 160°, radians	[TOPO9]	F8.0
Topographic angle #10 at 180°, radians	[TOPO10]	F8.0
Topographic angle #11 at 200°, radians	[TOPO11]	F8.0
Topographic angle #12 at 220°, radians	[TOPO12]	F8.0
Topographic angle #13 at 240°, radians	[TOPO13]	F8.0
Topographic angle #14 at 260°, radians	[TOPO14]	F8.0
Topographic angle #15 at 280°, radians	[TOPO15]	F8.0
Topographic angle #16 at 300°, radians	[TOPO16]	F8.0
Topographic angle #17 at 320°, radians	[TOPO17]	F8.0
Topographic angle #18 at 340°, radians	[TOPO18]	F8.0
Starting date for SRF#1, Julian day	[JDSRF1]	F8.0
Starting date for SRF#2, Julian day	[JDSRF2]	F8.0

The file can also be written out as a comma delimited input file rather than fixed format. When the first character in line 1 is a '\$' character, the file format is in free format in the order listed above.

This file contains the shade information for computing the vegetative and topographic shading dynamically for a model segment. If the dynamic shading value [DYNOSH] is set from 0 to 1, then static shading is used and the shade factor takes on the specified value. This means that a dynamic shading value [DYNOSH] of 0.8 allows 80% of the incoming short-wave solar to reach the water surface of that segment – or 20% fully shaded. This would apply for all times. If dynamic shading [DYNOSH] is set to a negative value, then the remaining columns are read for dynamic shading information and the shade percentage is computed dynamically.

The shade file consists of four types of vegetative information for each bank of the river, topographic information, and the time for leaf growth and leaf fall if the trees are deciduous. More detailed information on the shading model and data preparation is given in Appendix A and Annear, et. al. (2001).

[Table C-78](#) provides a description of the input variables controlling dynamic shading.

Table C-78. Description of Dynamic Shading Input Variables

Heading	Description
SEG	Segment number in the model – include all segment numbers and leave blank those that are inactive.
DYN SH	If between 0 and 1, this is a non-dynamic constant shade reduction similar to that used in Version 3.0 and the columns to the right are ignored. If this number is negative, this means that the rest of the columns to the right will be read and dynamic shading will be implemented.
VEL	Tree top elevation on the left bank (m). The elevation of the left bank plus the height of the tree/vegetation are used to provide the tree top elevation. This is the absolute elevation that the entire model is referenced to. In most cases this is m, NGVD, or m MSL. This is not the elevation above the top of the bank.
VER	Tree top elevation on the right bank (m).
CDL	Distance from the centerline of the river segment to the shade controlling line of vegetation on the left bank (m).
CDR	Distance from the centerline of the river segment to the shade controlling line of vegetation on the right bank (m).
SRFL1	Shade reduction factor, left bank. This applies from SRFJD1 to SRFJD2 (and over multiple years for the same time period of the simulation goes over 360 days). It is based on the extent of vegetation along the length of the segment and the density of the vegetation (0 to 1).
SRFL2	Shade reduction factor, left bank (0 to 1). This applies from SRFJD2 to SRFJD1 (and over multiple years for the same time period of the simulation goes over 360 days). It is based on the extent of vegetation along the length of the segment and the density of the vegetation (0 to 1).
SRFR1	Shade reduction factor, right bank. This applies from SRFJD1 to SRFJD2 (and over multiple years for the same time period of the simulation goes over 360 days). It is based on the extent of vegetation along the length of the segment and the density of the vegetation (0 to 1).
SRFR2	Shade reduction factor, right bank (0 to 1). This applies from SRFJD2 to SRFJD1 (and over multiple years for the same time period if the simulation goes over 360 days). It is based on the extent of vegetation along the length of the segment and the density of the vegetation (0 to 1).
TOPO1 to TOPO18	Topographic inclination angle (radians) for every 20° around a segment starting with TOPO1 at 0° North and moving clockwise. The topographic angles are most easily computed using Digital Elevation Maps (DEMs) and using GIS or other programs to automatically compute controlling topographic angles from the DEM.
JDSRF1	Shading reduction factor Julian day for which SRF #1 starts to apply. This is typically thought of as “leaf-out” conditions for deciduous trees.
JDSRF2	Shading reduction factor Julian day for which SRF #2 starts to apply. This is typically thought of as when deciduous trees loose their leaves.

The following discussion provides an overview of data development for the dynamic shading file.

Vegetation Elevation

The algorithm uses elevations for the grid development so the vegetation's elevation is used instead of height. If shading is due to brush along side a river, the top elevation of the brush would be used in the model. The tree top elevation consists of the vegetation height and the bank surface elevation where the vegetation is standing as shown in [Figure C-1](#). The vegetation height can be obtained from field surveys or from a GIS vegetation coverage. The surface elevation of the banks can be obtained from field surveys or from the U.S. Geological Survey digital elevation model (DEM). The frequency of tree top elevation measurements along a river bank depends on the variability of the controlling vegetation. The more comprehensive the elevation information, the more accurately the model will simulate shade. Tree top elevations should be collected for both river banks.

Centerline Distance

The centerline distance is the distance between the river centerline and the controlling vegetation on each bank. As shown in [Figure C-1](#), the information will vary for each bank depending on the location of the river centerline and the offset of the vegetation from the wetted edge. The frequency of the distances should match the tree top elevation data and reflect the variability of the vegetation. Less frequent data may be acceptable if there is not much variability in the controlling vegetation and the stream width does not change much.

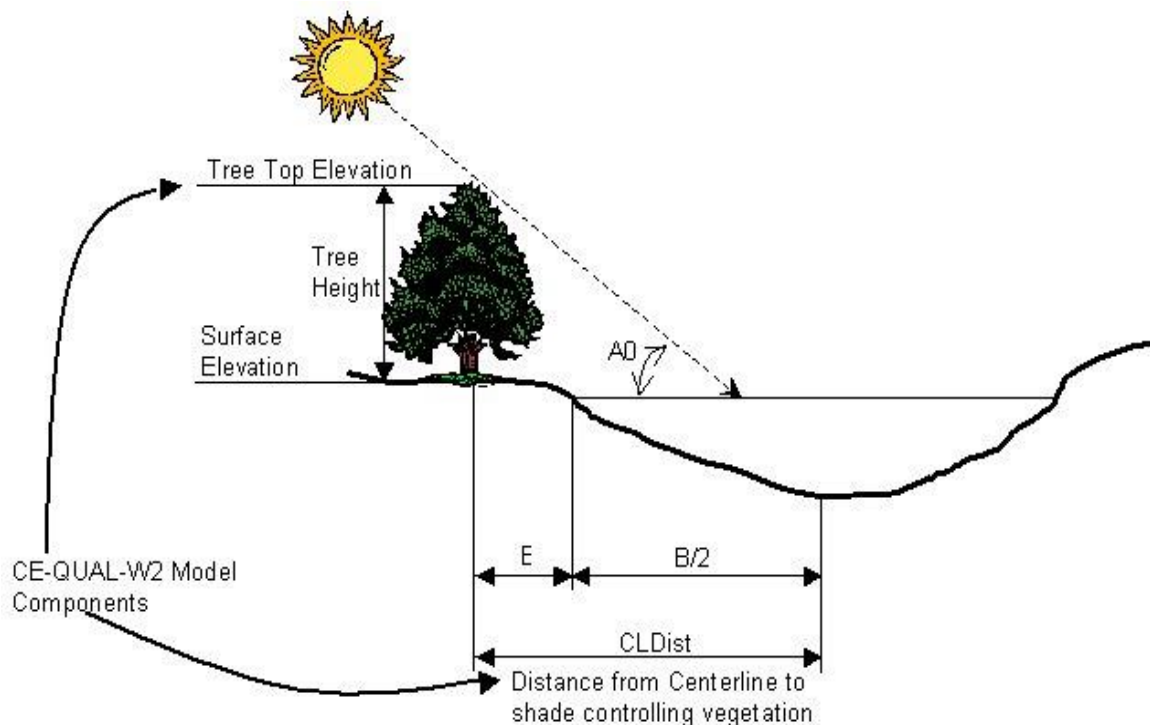


Figure C-1. Tree top elevation and vegetation offset from a river.

Shade reduction factor

The shade reduction factor is based on the density and extent of the vegetation along the length of each model segment. If shade producing vegetation exists along only half the length of a segment and was 100% opaque, a shade reduction factor of 0.50 would be used. If shade was due to vegetation along only half of the segment with 80% density, then a shade reduction factor of 0.40 would be used. The shade reduction factors, [SRFR1] and [SRFR2], are expressed as a fraction from 0.0 to 1.0.

The extent of the vegetation along the segment length will depend on the grid discretization and the amount of vegetation. Vegetation density can be obtained from field surveys or from GIS vegetation information. The shade reduction factor is designed to attenuate the shade since some short-wave solar radiation penetrates the vegetation. The shade reduction factor should be developed for both banks and can be used as a calibration parameter if field data is uncertain or incomplete.

Topographic Shading

In addition to the vegetation near a river, the local topography can influence the amount of solar radiation reaching the water surface. [Figure C-2](#) illustrates the influence of topographic shading on the water surface of a river.

The local topography around a river can be developed using survey information of the river channel or from a digital elevation map (DEM). To characterize the influence of the topography, inclination angles can be obtained every 20 degrees around each model segment center point as shown in [Figure C-3](#). For each 20-degree increment around a model segment, an array of elevation points and their distances from the center point are obtained from the DEM. The elevations and distances are then used to calculate the highest inclination angle relative to the center point. The distance away from each segment center point that should be analyzed to obtain the controlling inclination angle will vary depending on the terrain surrounding the river. Wide open channels will require larger distances away from the channel to be analyzed than if the river channel is in a deep, narrow canyon. Inclination angles are then generated that control topographic shading for each of the 20-degree increments around a segment's center point. The inclination angles are converted to radians and specified in the dynamic shading input file [SHDFN]. The first column of the topographic inclination angles represents the inclination angle at 0° north with subsequent inclination angles obtained by moving clockwise to the east.

The shade algorithm can be used in both the northern and southern hemispheres, so inclination angles are provided for 360 degrees around each segment. If there is no topographic shading in a specific direction due to the latitude or the surrounding terrain, zero can be used as the inclination angle. The model uses all 18 topographic inclination angles. Based on the position of the sun, the algorithm will interpolate between the two nearest inclination angles to obtain the most appropriate inclination angle. The inclination angles are then used in the shading algorithm to determine if vegetative or topographic shading dominates at a specific time during the day.

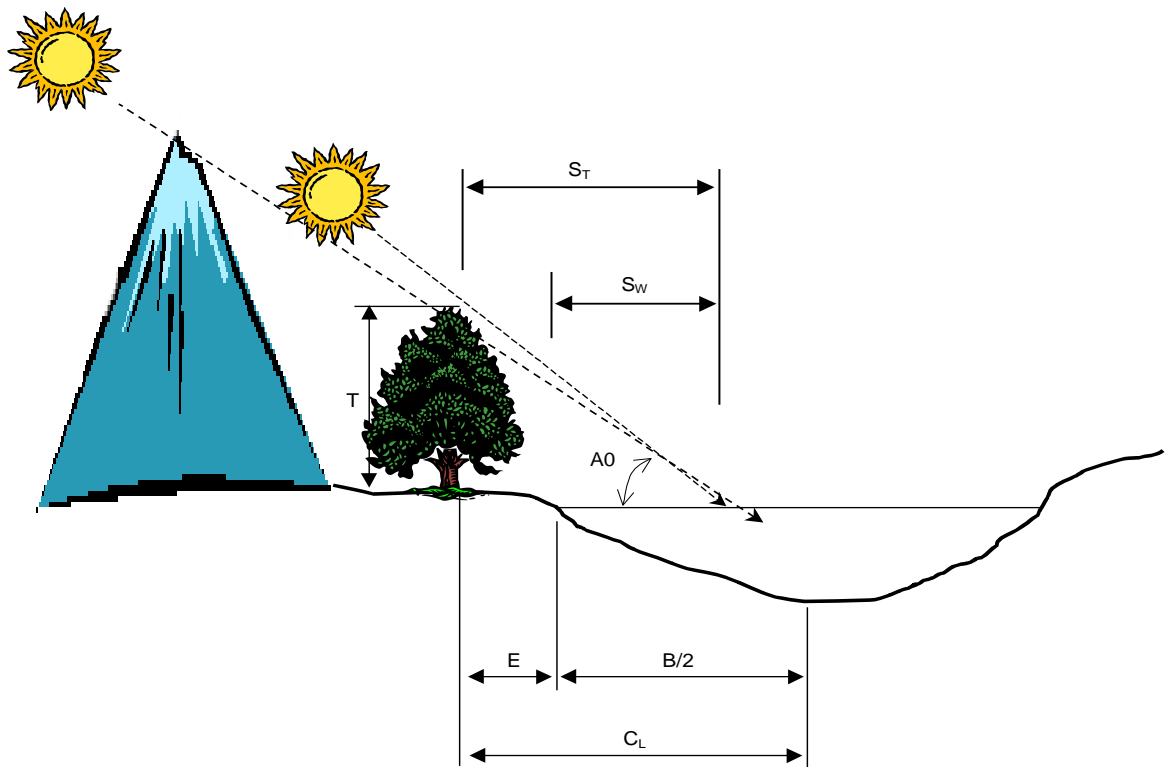


Figure C-2. The influence of topographic shading along a river.

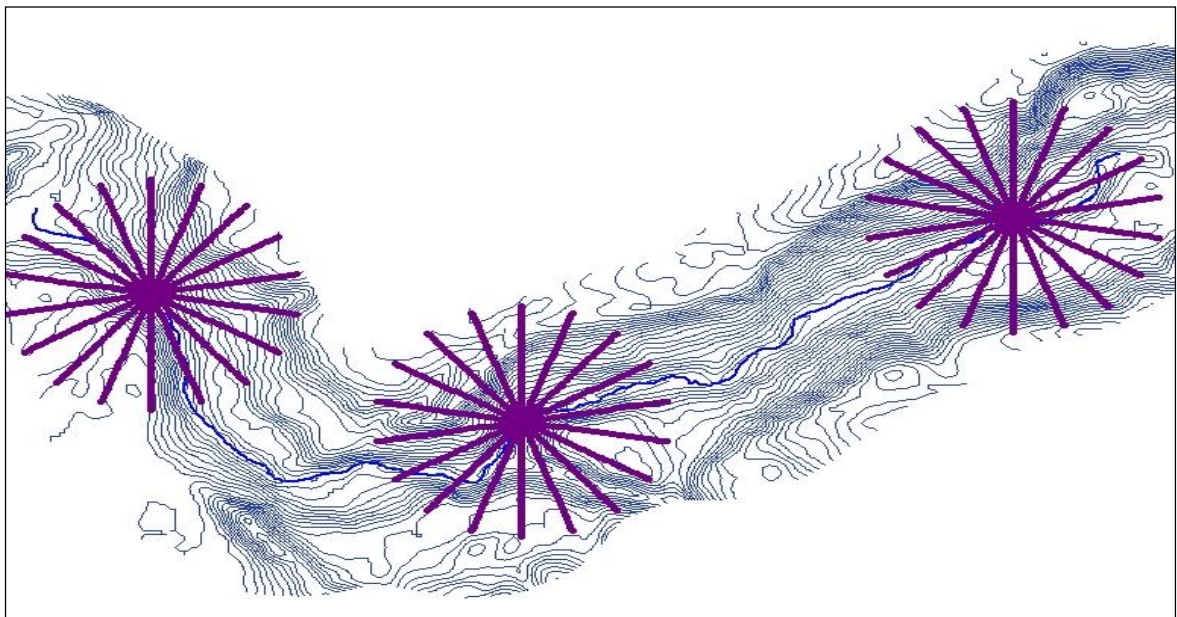


Figure C-3. Topographic slices at three segments along a river.

SHADE

INPUT FILES

Example

W2 Shading Input File, Vegetation and Topography, calibrated veg characteristics and corrected topography

SEGMENT	DYNSh	TTELeLB	TTELeRB	CLDisLB	CLDiRB	SRFLB1	SRFLB2	SRFRB1	SRFRB2	TOPO1	TOPO2	TOPO3	TOPO4	TOPO5	TOPO6	TOPO7	TOPO8	TOPO9	TOPO10	TOPO11	TOPO12	TOPO13	TOPO14	TOPO15	TOPO16	TOPO17	TOPO18	SRFJD1	SRFJD2
1																													
2	-1.0	233.37	224.39	33.22	12.50	0.00	0.57	0.00	0.50	0.486	0.490	0.414	0.295	0.191	0.149	0.134	0.296	0.353	0.359	0.329	0.250	0.120	0.123	0.242	0.298	0.310	0.414	80.00	288.00
3	-1.0	233.37	224.39	33.22	12.50	0.00	0.57	0.00	0.50	0.501	0.505	0.476	0.383	0.201	0.121	0.122	0.231	0.257	0.221	0.136	0.083	0.101	0.166	0.258	0.318	0.361	0.427	80.00	288.00
4	-1.0	233.37	224.39	33.22	12.50	0.00	0.57	0.00	0.50	0.599	0.583	0.566	0.458	0.478	0.469	0.409	0.296	0.246	0.221	0.180	0.077	0.137	0.289	0.350	0.433	0.530	0.588	80.00	288.00
5																													
6																													
7	-1.0	231.01	230.66	34.00	13.27	0.00	0.54	0.00	0.59	0.468	0.427	0.371	0.286	0.183	0.345	0.454	0.504	0.487	0.400	0.268	0.159	0.163	0.312	0.399	0.416	0.445	0.466	80.00	288.00
8	-1.0	227.30	240.49	35.22	14.49	0.00	0.55	0.00	0.53	0.468	0.418	0.332	0.251	0.127	0.185	0.230	0.255	0.247	0.197	0.102	0.134	0.253	0.427	0.522	0.536	0.534	0.500	80.00	288.00
9	-1.0	225.48	245.29	35.81	15.09	0.00	0.55	0.00	0.58	0.462	0.392	0.304	0.218	0.196	0.229	0.272	0.224	0.162	0.120	0.062	0.271	0.396	0.567	0.645	0.701	0.667	0.561	80.00	288.00
10																													
11																													
12	-1.0	225.00	237.01	28.08	15.14	0.00	0.51	0.00	0.58	0.393	0.310	0.236	0.216	0.228	0.228	0.250	0.222	0.169	0.119	0.283	0.558	0.736	0.809	0.770	0.699	0.668	0.564	80.00	288.00
13	-1.0	224.44	227.11	18.84	15.21	0.00	0.50	0.00	0.59	0.271	0.229	0.182	0.247	0.329	0.370	0.344	0.294	0.238	0.189	0.111	0.177	0.290	0.358	0.397	0.431	0.391	0.357	80.00	288.00
14	-1.0	225.46	222.71	16.11	16.02	0.00	0.59	0.00	0.58	0.243	0.190	0.215	0.346	0.394	0.425	0.428	0.405	0.372	0.287	0.162	0.068	0.210	0.288	0.297	0.308	0.324	0.302	80.00	288.00
15																													
16																													
17	-1.0	227.96	223.53	19.56	17.52	0.00	0.52	0.00	0.56	0.194	0.173	0.171	0.260	0.346	0.437	0.493	0.529	0.443	0.279	0.217	0.089	0.042	0.124	0.210	0.300	0.287	0.314	80.00	288.00
18	-1.0	230.47	224.35	23.00	19.02	0.00	0.55	0.00	0.54	0.184	0.162	0.103	0.187	0.280	0.392	0.365	0.271	0.299	0.311	0.246	0.128	0.051	0.155	0.197	0.300	0.281	0.285	80.00	288.00
19	-1.0	232.80	225.12	26.21	20.42	0.00	0.68	0.00	0.63	0.188	0.174	0.173	0.149	0.223	0.254	0.228	0.328	0.367	0.237	0.152	0.101	0.061	0.211	0.244	0.310	0.326	0.309	80.00	288.00
20																													
21																													

An example of a free format comma delimited file is shown below. The first character in line 1 must be a '\$'.

```
$W2 Shading InputFile Vegetation and Topography calibrated veg characteristics and corrected topography,,,,,,,,,,,,,
,,,,,,,,,,,,,,,,,,,,,,,,,,,,,
Segment, DynSh,TTLeLB,TTEeRB,CLDisLB,CLDiRB,SRFLB1,SRFLB2,SRFRB1,SRFRB2,TOPO1,TOPO2,TOPO3,TOPO4,TOPO5,TOPO6,TOPO7,TOPO8,TOPO9,TOPO10,TOPO11,
TOPO12,TOPO13,TOPO14,TOPO15,TOPO16,TOPO17,TOPO18,SRFJD1,SRFJD2,
1,,,,,,,,,,,,,,,,,,,,,,,,,,,,,
2,-1,575,580,70,70,0,0.57,0,0.5,0.486,0.49,0.414,0.295,0.191,0.149,0.134,0.296,0.353,0.359,0.329,0.25,0.12,0.123,0.242,0.298,0.31,0.414,80,288,
3,-
1,568,566,70,70,0,0.57,0,0.5,0.501,0.505,0.476,0.383,0.201,0.121,0.122,0.231,0.257,0.221,0.136,0.083,0.101,0.166,0.258,0.318,0.361,0.427,80,288,
4,-1,562,565,70,70,0,0.57,0,0.5,0.599,0.583,0.566,0.458,0.478,0.469,0.409,0.296,0.246,0.221,0.18,0.077,0.137,0.289,0.35,0.433,0.53,0.588,80,288,
5,-1,568,565,70,70,0,0.57,0,0.5,0.599,0.583,0.566,0.458,0.478,0.469,0.409,0.296,0.246,0.221,0.18,0.077,0.137,0.289,0.35,0.433,0.53,0.588,80,288,
6,-1,544,546,70,70,0,0.57,0,0.5,0.599,0.583,0.566,0.458,0.478,0.469,0.409,0.296,0.246,0.221,0.18,0.077,0.137,0.289,0.35,0.433,0.53,0.588,80,288,
7,-
1,548,567,70,70,0,0.54,0,0.59,0.468,0.427,0.371,0.286,0.183,0.345,0.454,0.504,0.487,0.4,0.268,0.159,0.163,0.312,0.399,0.416,0.445,0.466,80,288,
8,,,,,,,,,,,,,,,,,,,,,,,,,,,,,
```


Branch Inflow File

This file contains the inflow for a branch with an [upstream flow boundary condition](#). The following is a list of guidelines for file preparation:

1. A separate file is required for each branch with an upstream flow boundary condition. This allows the user to update inflows for one branch independent of another branch.
2. Input format for each field is F8.0 that allows the user to specify the decimal point location.
3. The first two lines are ignored and can be used to comment the file.
4. The third line contains the variable names which are right justified according to the input field. This line is also ignored although the preprocessor checks to ensure the fields are aligned correctly.
5. The first field is the Julian date that can be entered at any frequency. The frequency between updates may vary during the simulation.
6. The second field is the inflow rate, $m^3 \text{ sec}^{-1}$.
7. Note that the inflow file CANNOT handle negative inflows like the distributed inflow file or tributary inflows.

Note the following example takes advantage of the algorithm's capability to use data at varying frequencies.

Example

CE-QUAL-W2 sample inflow file

```

      JDAY      QIN
182.0000      0.0
182.5416    283.0
182.6250    566.0
182.6666   1699.0
182.7916    566.0
182.8333    283.0
182.9166      0.0
185.5416    283.0
185.6250    566.0
185.6666   1699.0
185.7916    566.0
185.8333    283.0
185.9166      0.0
186.5416    283.0

```

There is a new option starting with Version 3.71 to use a free-format file rather than the fixed format shown above. When the first character in the first line contains the '\$' symbol, the model will treat the file as being in free format. As in the fixed format file, the first 3 lines are ignored and the data fields are in the same order as the fixed format file except that the user is no longer limited to 8 characters for each field. An example of a comma delimited file is shown below.

```

$Flow data for 2012,,
,,
JDAY,q(m3/s),
1,9.12611182703854,
2,12.1179791828734,
3,4.2113553278442,
4,9.94341024175013E-03,
5,9.1933302008558E-03,
6,.011356298978275,
7,1.06203328212151E-02,

```

Branch Inflow Temperature File

This file contains the inflow temperatures for a branch with an [upstream flow boundary condition](#). The following is a list of guidelines for file preparation:

1. A separate file is required for each branch with an upstream flow boundary condition. This allows the user to update temperatures for one branch independent of another branch.
2. Input format for each field is F8.0 that allows the user to specify the decimal point location.
3. The first two lines are ignored and can be used to comment the file.
4. The third line contains the variable names which are right justified according to the input field. This line is also ignored although the preprocessor checks to ensure the fields are aligned correctly.
5. The first field is the Julian date that can be entered at any frequency. The frequency between updates may vary during the simulation.
6. The second field is the inflow temperature, °C.

Example

CE-QUAL-W2 sample inflow temperature file

JDAY	TIN
1.00	6.80
2.00	6.70
3.00	7.00
4.00	6.30
5.00	6.40
6.00	6.10
7.00	6.60
8.00	5.70
9.00	5.20
10.00	5.40
11.00	7.10
12.00	6.60
13.00	5.50
14.00	5.60
15.00	7.30
16.00	9.50

There is a new option starting with Version 3.71 to use a free-format file rather than the fixed format shown above. When the first character in the first line contains the '\$' symbol, the model will treat the file as being in free format. As in the fixed format file, the first 3 lines are ignored and the data fields are in the same order as the fixed format file except that the user is no longer limited to 8 characters for each field. An example of a comma delimited file is shown below.

```
$Temp data for 2012,,
,,
JDAY      ,Temp,
1,15.04924,
1.125,13.61301,
1.25,16.16824,
1.375,20.82835,
1.5,23.3214,
1.625,22.30952,
1.75,20.3509,
```

Branch Inflow Constituent Concentration File

This file contains the inflow concentrations for a branch with an [upstream flow boundary condition](#). The following is a list of guidelines for file preparation:

1. *If* constituents are being modeled, a separate file is required for each branch with an upstream flow boundary condition. This allows the user to update constituent concentrations for one branch independent of another branch.
2. Input format for all fields is F8.0 that allows the user to specify the decimal point location. The number of fields is determined by (6) below and they are always located on one line.
3. The first two lines are ignored and can be used to comment the file.
4. The next line contains the abbreviations for the constituent names that are right justified according to the input field. This line is also ignored although the preprocessor checks to ensure the fields are aligned correctly.
5. The first field is the Julian date that can be entered at any frequency. The frequency between updates may vary during the simulation.
6. The remaining fields contain the concentration for each constituent specified on the [Inflow Active Constituent Control](#) card. Only those constituents specified as active on the [Inflow Active Constituent Control](#) card are included in the constituent inflow concentration file.

There is also a free format option for this file. Whenever the first character on the first line is a '\$' character, the model assumes the input is in free format rather than fixed format. Besides allowing the use of Excel and easy exporting to a csv file type, this also allows one to not be constrained by the 8 column width of the concentration value. An example is shown below.

INPUT FILES

CE-QUAL-W2 constituent inflow concentration sample input file

JDAY	PO4	NH4	NOx	LDOM	RDOM	LPOM	RPOM	CBOD1	CBOD2	CBOD3	CBOD4	CBOD5	ALG1	DO
1.040	0.030	0.010	0.300	0.1000	0.1000	0.1000	0.1000	0.000	0.000	0.000	0.000	0.000	0.100	12.000
1.100	0.030	0.011	0.307	0.1040	0.0991	0.0989	0.0989	0.000	0.000	0.000	0.000	0.000	0.098	12.000
1.200	0.029	0.012	0.323	0.1100	0.0968	0.0963	0.0963	0.000	0.000	0.000	0.000	0.001	0.095	11.800
1.300	0.048	0.017	0.458	0.1250	0.0944	0.0935	0.0936	0.000	0.000	0.000	0.229	0.003	0.091	11.900
1.400	0.043	0.018	0.441	0.1360	0.0936	0.0924	0.0925	0.000	0.000	0.000	0.167	0.010	0.090	11.900
1.500	0.043	0.013	0.498	0.1430	0.0874	0.0861	0.0862	0.000	0.000	0.000	0.192	0.011	0.084	11.900
1.600	0.047	0.006	0.542	0.1530	0.0852	0.0837	0.0838	0.000	0.000	0.008	0.241	0.015	0.083	12.000
1.700	0.046	0.001	0.565	0.1690	0.0820	0.0804	0.0805	0.000	0.004	0.032	0.248	0.017	0.081	12.000
1.800	0.045	0.002	0.577	0.1730	0.0790	0.0773	0.0773	0.000	0.020	0.041	0.249	0.016	0.077	11.900
1.900	0.044	0.005	0.579	0.1790	0.0724	0.0705	0.0706	0.002	0.026	0.055	0.249	0.078	0.071	11.800
2.000	0.034	0.022	0.480	0.1230	0.0146	0.0142	0.0141	0.003	0.033	0.058	0.250	0.715	0.042	11.800

[Note the file below is wrapped for viewing convenience since it has 62 state variables]

\$Concentration file for segment 8,6,,,

```

JDAY,TDS,Conduct,ISS1,PO4,NH4,NOx,LDOM,RDOM,LPOM,RPOM,1CBOD,2CBOD,3CBOD,4CBOD,5CBOD,6CBOD,7CBOD,8CBOD,9CBOD,10CBO
D,1CBODP,2CBODP,3CBODP,4CBODP,5CBODP,6CBODP,7CBODP,8CBODP,9CBODP,10CBODP,1CBODN,2CBODN,3CBODN,4CBODN,5CBODN,6CBOD
N,7CBODN,8CBODN,9CBODN,10CBODN,ALG1,ALG2,ALG3,DO,TIC,ALK,LDOM_P,RDOM_P,LPOM_P,RPOM_P,LDOM_N,RDOM_N,LPOM_N,RPOM_N
1,0,0,0,3.00E-02,1.00E-
02,0.3,0.1,0.1,0.1,0.1,0,0,0,0,0,0,0,0,0,0,0,0,0,0,0,0,0,0,0,0,0,0,0,0,0,0,0,0,0.1,0.1,0.1,12,5,19.8,5.00E-
04,5.00E-04,5.00E-04,5.00E-04,8.00E-03,8.00E-03,8.00E-03,8.00E-03
1.01,0.118,0.208,.123-105,3.00E-02,1.02E-02,0.301,0.1,9.99E-02,0.102,9.99E-02,.330-233,.336-139,.389-
104,0,0,0,0,.449-319,.185-274,0,.679-235,.783-142,.912-107,0,0,0,0,.380-321,.539-277,0,.322-234,.369-140,.119-
105,0,0,0,0,.389-320,.539-277,0,9.98E-02,9.99E-02,9.99E-02,12,5.02,19.9,5.02E-04,5.00E-04,4.99E-04,4.99E-
04,8.04E-03,7.99E-03,7.99E-03,7.99E-03
1.02,0.235,0.413,3.18E-75,3.00E-02,1.03E-02,0.302,0.101,0.1,0.104,9.99E-02,.965-198,.279-107,1.01E-
73,0,0,0,0,.169-278,.332-233,0,.199-199,.650-110,2.37E-76,0,0,0,0,.143-280,.966-236,0,.943-199,.306-108,3.08E-
75,0,0,0,0,.146-279,.966-236,0,9.98E-02,9.98E-02,0.1,12,5.04,19.9,5.05E-04,5.00E-04,4.99E-04,5.00E-04,8.09E-
03,8.00E-03,7.99E-03,7.99E-03

```

Appendix C Input/Output Data Description

INPUT FILES

BRANCH INFLOW CONCENTRATION

Concentr	ation fi	le for s	egment 8	6														
JDAY	TDS	Conduct	ISS1	PO4	NH4	NOx	LDOM	RDOM	LPOM	RPOM	1CBOD	2CBOD	3CBOD	4CBOD	5CBOD	6CBOD	7CBOD	8CBOD
1	0	0	0	3.00E-02	1.00E-02	0.3	0.1	0.1	0.1	0.1	0	0	0	0	0	0	0	0
1.01	0.118	0.208	.123-105	3.00E-02	1.02E-02	0.301	0.1	9.99E-02	0.102	9.99E-02	.330-233	.336-139	.389-104	0	0	0	0	.449-319
1.02	0.235	0.413	3.18E-75	3.00E-02	1.03E-02	0.302	0.101	0.1	0.104	9.99E-02	.965-198	.279-107	1.01E-73	0	0	0	0	.169-278
1.03	0.311	0.547	4.09E-64	3.00E-02	1.04E-02	0.303	0.101	0.1	0.106	9.99E-02	.412-185	2.38E-97	1.32E-62	0	0	0	0	.921-260
1.04	0.383	0.674	5.12E-59	3.00E-02	1.05E-02	0.303	0.101	9.98E-02	0.106	9.97E-02	.203-176	2.82E-90	1.64E-57	0	0	0	0	.151-245
1.05	0.484	0.851	5.59E-55	2.99E-02	1.06E-02	0.303	0.102	9.96E-02	0.108	9.95E-02	.379-170	4.02E-85	1.79E-53	0	0	0	0	.289-235
1.06	0.619	1.09	5.58E-52	2.99E-02	1.08E-02	0.304	0.102	9.95E-02	0.112	9.94E-02	.407-164	2.29E-80	1.82E-50	0	0	0	0	.541-227
1.07	0.812	1.42	2.28E-49	2.99E-02	1.11E-02	0.305	0.103	9.94E-02	0.115	9.92E-02	.353-156	6.05E-76	7.03E-48	0	0	0	.855-320	.329-217
1.08	1.24	2.15	3.82E-47	2.99E-02	1.14E-02	0.308	0.104	9.91E-02	0.119	9.89E-02	.342-143	3.52E-71	1.43E-45	0	0	0	.295-309	.516-204
1.09	1.98	3.41	8.16E-44	2.98E-02	1.21E-02	0.313	0.105	9.87E-02	0.123	9.85E-02	.841-129	1.37E-67	7.75E-42	0	0	.101-316	.624-299	.766-190
1.1	3.54	6.06	9.85E-41	2.96E-02	1.31E-02	0.323	0.105	9.78E-02	0.126	9.75E-02	.381-117	7.12E-65	3.59E-39	0	0	.280-303	.151-285	.897-174
1.11	5.38	9.16	1.00E-33	2.94E-02	1.42E-02	0.335	0.105	9.68E-02	0.13	9.65E-02	.656-104	4.67E-62	3.68E-32	0	0	.145-288	.782-271	.502-162
1.12	7.25	12.3	7.49E-23	2.92E-02	1.53E-02	0.348	0.105	9.58E-02	0.133	9.55E-02	4.59E-94	5.22E-59	7.09E-23	0	0	.135-277	.729-260	.685-150

Branch Outflow File

This file contains the outflow for a branch with a [downstream flow boundary condition](#). The following is a list of guidelines for file preparation:

1. A separate file is required for each branch with a downstream flow boundary condition. This allows the user to update outflows for one branch independent of another branch.
2. Input format for each field is F8.0 that allows the user to specify the decimal point location. There are a maximum of 10 fields to a line. If there are more outflows than can be specified on one line, then they are continued on the next line with blanks inserted in the Julian date field.
3. The first two lines are ignored and can be used to comment the file.
4. The next line contains the variable names which are right justified according to the input field. This line is also ignored although the preprocessor checks to ensure the fields are aligned correctly.
5. The first field is the Julian date that can be entered at any frequency. The frequency between updates may vary during the simulation.
6. The remaining fields are the outflow rate, $m^3 sec^{-1}$.
7. A separate column of outflow values must be specified for each outlet structure.

There is also a free format option for this file. Whenever the first character on the first line is a '\$' character, the model assumes the input is in free format rather than fixed format. Besides allowing the use of Excel and easy exporting to a csv file type, this also allows one to not be constrained by the 8 column width of the concentration value nor be constrained by warpping lines when there are more than 9 outlets in a branch. An example is shown below.

Example

CE-QUAL-W2 sample outflow file

JDAY	QOUT	QOUT	QOUT	QOUT	QOUT	QOUT	QOUT	QOUT	QOUT
1.00	8.13	8.13	8.13						
2.00	6.77	6.77	6.77						
3.00	18.60	18.60	18.60						
4.00	0.60	0.60	0.60						
5.00	7.50	7.50	7.50						
6.00	2.87	2.87	2.87						

Free format example

[Note the file below is wrapped for viewing convenience since it has 17 outlets for 1 branch]

```
$Penstock flows and spill,,,,,% of lower leakage,,20%,,,,,,,,,,
,P1-O,P1-A,P1-U,P1-M,P1-L,P2-O,P2-A,P2-U,P2-M,P2-L,P3-O,P3-A,P3-U,P3-M,P3-L,,,
Julian
day,Q(m3/s),Q(m3/s),Q(m3/s),Q(m3/s),Q(m3/s),Q(m3/s),Q(m3/s),Q(m3/s),Q(m3/s),Q(m
3/s),Q(m3/s),Q(m3/s),Q(m3/s),Q(m3/s),Q(m3/s),QSPILL,QPP,
730.5,0.962772798,0,0,0,0,3.4093483788,0,0,0,13.6373935152,5.2839236502,0,0,0,2
1.1356946008,0,2.69009789124642,
```

INPUT FILES

BRANCH OUTFLOW

731.5,0.962772798,0,0,0,0,5.0007551802,0,20.0030207208,0,0,3.766140651,0,0,0,15.
 .064562604,0,2.63346425143071,
 732.5,0.962772798,0,0,0,0,3.5735860914,0,14.2943443656,0,0,5.040398766,0,0,0,20.
 .161595064,0,2.69009789124642,
 733.5,0.962772798,0,0,0,0,0.1925545596,0,0.7702182384,0,0,8.834856264,0,0,0,35.
 339425056,0,2.71841471115428,
 734.5,0.962772798,0,0,0,0,4.1172695538,0,16.4690782152,0,0,6.0484785192,0,0,0,2.
 4.1939140768,0,2.54851379170714,
 735.5,0.962772798,0,0,0,0,10.0977876402,0,40.3911505608,0,0,1.189307574,0,0,0,0.
 ,0,2.57683061161499,

In Excel this looks like the following:

SPenstock flows and spill				% of lower leakage		25.00 %												
	P1-O	P1-A	P1-U	P1-M	P1-L	P2-O	P2-A	P2-U	P2-M	P2-L	P3-O	P3-A	P3-U	P3-M	P3-L			
Julian day	Q(m3/s)	Q(m3/s)	Q(m3/s)	Q(m3/s)	Q(m3/s)	Q(m3/s)	Q(m3/s)	Q(m3/s)	Q(m3/s)	Q(m3/s)	Q(m3/s)	Q(m3/s)	Q(m3/s)	Q(m3/s)	Q(m3/s)	QSPILL	QPP	
730.50	0.96	0.00	0.00	0.00	0.00	0.00	4.26	0.00	0.00	0.00	12.79	6.60	0.00	0.00	0.00	19.81	0.00	2.69
731.50	0.96	0.00	0.00	0.00	0.00	0.00	6.25	0.00	18.75	0.00	0.00	4.71	0.00	0.00	0.00	14.12	0.00	2.63
732.50	0.96	0.00	0.00	0.00	0.00	0.00	4.47	0.00	13.40	0.00	0.00	6.30	0.00	0.00	0.00	18.90	0.00	2.69
733.50	0.96	0.00	0.00	0.00	0.00	0.00	0.24	0.00	0.72	0.00	0.00	11.04	0.00	0.00	0.00	33.13	0.00	2.72
734.50	0.96	0.00	0.00	0.00	0.00	0.00	5.15	0.00	15.44	0.00	0.00	7.56	0.00	0.00	0.00	22.68	0.00	2.55
735.50	0.96	0.00	0.00	0.00	0.00	0.00	12.62	0.00	37.87	0.00	0.00	1.19	0.00	0.00	0.00	0.00	0.00	2.58
736.50	0.96	0.00	0.00	0.00	0.00	0.00	11.31	0.00	33.94	0.00	0.00	1.19	0.00	0.00	0.00	0.00	0.00	2.46
737.50	0.96	0.00	0.00	0.00	0.00	0.00	10.70	0.00	32.11	0.00	0.00	1.19	0.00	0.00	0.00	0.00	0.00	2.41
738.50	0.96	0.00	0.00	0.00	0.00	0.00	11.47	0.00	34.40	0.00	0.00	1.19	0.00	0.00	0.00	0.00	0.00	2.46
739.50	0.96	0.00	0.00	0.00	0.00	0.00	12.97	0.00	38.91	0.00	0.00	1.19	0.00	0.00	0.00	0.00	0.00	2.41
740.50	0.96	0.00	0.00	0.00	0.00	0.00	13.95	0.00	41.86	0.00	0.00	1.19	0.00	0.00	0.00	0.00	0.00	2.41
741.50	0.96	0.00	0.00	0.00	0.00	0.00	15.26	0.00	45.77	0.00	0.00	1.19	0.00	0.00	0.00	0.00	0.00	2.46
742.50	0.96	0.00	0.00	0.00	0.00	0.00	19.28	0.00	57.85	0.00	0.00	1.19	0.00	0.00	0.00	0.00	0.00	2.61
743.50	0.96	0.00	0.00	0.00	0.00	0.00	20.01	0.00	60.02	0.00	0.00	1.19	0.00	0.00	0.00	0.00	0.00	3.06

Withdrawal File

This contains the outflow for each withdrawal specified on the [Inflow/Outflow Dimensions](#) card. The following is a list of guidelines for file preparation:

1. The order in which withdrawal outflows appear in the file **must** correspond with the order specified on the Withdrawal Segment and the [Withdrawal Elevation](#) cards.
2. Input format for each field is F8.0 with 10 fields to a line. The F8.0 input field allows the user to specify the decimal point location.
3. The first two lines are ignored and can be used to comment the file.
4. The third line contains the variable names which are right justified according to the input field. This line is also ignored although the preprocessor checks to ensure the fields are aligned correctly.
5. The first field is the Julian date that can be entered at any frequency. The frequency between updates may vary during the simulation.
6. The remaining fields are the withdrawal outflow rate, $m^3 sec^{-1}$
7. Outflows from a single withdrawal structure spanning more than one layer in the computational grid can be divided up into several outflows and the total outflow apportioned among them.
8. If there are **more** withdrawals than can be specified on one line, then they are continued on the next line with blanks inserted under the JDAY field.

There is also a free format option for this file. Whenever the first character on the first line is a '\$' character, the model assumes the input is in free format rather than fixed format. Besides allowing the use of Excel and easy exporting to a csv file type, this also allows one to not be constrained by the 8 column width of the concentration value nor be constrained by warpping lines when there are more than 9 outlets in a branch. See the branch outflow file as an example.

Example

CE-QUAL-W2 sample withdrawal outflow file

JDAY	QWD	QWD	QWD	QWD	QWD	QWD	QWD	QWD	QWD
182.0000	51.	51.	51.	51.	51.	51.	51.	51.	51.
	51.								
182.2500	0.	0.	0.	0.	0.	0.	0.	0.	0.
	0.								
183.0000	51.	51.	51.	51.	51.	51.	51.	51.	0.
	51.								
183.2500	0.	0.	0.	0.	0.	0.	0.	0.	0.
	0.								

Tributary Inflow File

This file contains the inflows for a tributary specified on the [Tributary Segment](#) card. The following is a list of guidelines for file preparation:

1. A separate file is required for each tributary. This allows the user to update inflows for one tributary independent of another tributary.
2. Input format for each field is F8.0 that allows the user to specify the decimal point location.
3. The first two lines are ignored and can be used to comment the file.
4. The third line contains the variable names which are right justified according to the input field. This line is also ignored although the preprocessor checks to ensure the fields are aligned correctly.
5. The first field is the Julian date that can be entered at any frequency. The frequency between updates may vary during the simulation.
6. The second field is the inflow rate, $m^3 \text{ sec}^{-1}$.

Example

CE-QUAL-W2 sample tributary inflow file

JDAY	QTR
1.0	22.8
5.0	44.5
12.0	31.2
23.0	80.4
35.0	50.6
74.5	103.0
74.7	185.6
75.0	212.3
75.5	178.6
80.0	123.4
80.5	78.3
90.0	46.5
112.0	35.9

There is a new option starting with Version 3.71 to use a free-format file rather than the fixed format shown above. When the first character in the first line contains the '\$' symbol, the model will treat the file as being in free format. As in the fixed format file, the first 3 lines are ignored and the data fields are in the same order as the fixed format file except that the user is no longer limited to 8 characters for each field. An example of a comma delimited file is shown in the Branch Inflow file description.

Tributary Inflow Temperature File

This file contains the inflow temperatures for a tributary specified on the [Tributary Segment](#) card. The following is a list of guidelines for file preparation:

1. A separate file is required for each tributary. This allows the user to update inflow temperatures for one tributary independent of another tributary.
2. Input format for each field is F8.0 that allows the user to specify the decimal point location.
3. The first two lines are ignored and can be used to comment the file.
4. The third line contains the variable names which are right justified according to the input field. This line is also ignored although the preprocessor checks to ensure the fields are aligned correctly.
5. The first field is the Julian date that can be entered at any frequency. The frequency between updates may vary during the simulation.
6. The second field is the inflow temperature, °C.

Example

CE-QUAL-W2 sample tributary inflow temperature file

JDAY	TTR
1.0	10.3
5.0	9.5
12.0	10.1
23.0	8.6
35.0	11.2
74.5	13.9
74.7	13.1
75.0	12.8
75.5	12.5
80.0	12.6
80.5	12.7
90.0	15.4

There is a new option starting with Version 3.71 to use a free-format file rather than the fixed format shown above. When the first character in the first line contains the '\$' symbol, the model will treat the file as being in free format. As in the fixed format file, the first 3 lines are ignored and the data fields are in the same order as the fixed format file except that the user is no longer limited to 8 characters for each field. An example of a comma delimited file is shown in the Branch Temperature Inflow file description.

Tributary Inflow Concentration File

This file contains the inflow constituent concentrations for each tributary specified on the [Tributary Segment](#) card. The following is a list of guidelines for file preparation:

1. *If* constituents are being modeled, a separate file is required for each tributary. This allows the user to update constituent inflow concentrations for one tributary independent of another tributary.
2. Input format for all fields is F8.0 that allows the user to specify the decimal point location. The number of fields is determined by (6) below and they are always located on one line.
3. The first two lines are ignored and can be used to comment the file.
4. The next line contains the abbreviations for the constituent names which are right justified according to the input field. This line is also ignored although the preprocessor checks to ensure the fields are aligned correctly.
5. The first field is the Julian date that can be entered at any frequency. The frequency between updates may vary during the simulation.
6. The remaining fields contain the concentration for each constituent specified on the [Tributary Active Constituent Control](#) card. Only those constituents specified as *active* on the [Tributary Active Constituent Control](#) card may be included in the tributary inflow concentration file.

There is also a free format option for this file. Whenever the first character on the first line is a '\$' character, the model assumes the input is in free format rather than fixed format. Besides allowing the use of Excel and easy exporting to a csv file type, this also allows one to not be constrained by the 8 column width of the concentration value. An example is shown in the Inflow concentration file section above.

Example

CE-QUAL-W2 sample tributary constituent inflow concentration file

JDAY	CLFORM	SSOLID	LDOM	RDOM	ALGAE	LPOM	PO4	NH4	NO3	O2	Fe
1.	17.	62.	7.333	17.111	0.0	0.9	0.02	0.10	0.42	13.9	0.4
8.	13.	0.0	8.000	18.667	0.0	0.4	0.01	0.03	0.37	14.0	0.2
15.	11.	17.	9.333	21.778	0.0	0.0	0.00	0.01	0.17	10.0	0.3
22.	14.	34.	10.000	23.333	0.0	0.0	0.05	0.00	0.20	10.4	1.6
29.	17.	38.	4.467	10.422	0.0	0.4	0.01	0.11	0.26	11.6	0.4
36.	101.	24.	3.867	9.022	0.0	0.2	0.01	0.00	0.23	12.2	0.3
43.	10.	11.	4.133	9.644	0.0	0.2	0.02	0.07	0.20	12.2	0.1

Branch Distributed Tributary Inflow File

This file contains the inflows for a distributed tributary specified on the [Distributed Tributary](#) card. The following is a list of guidelines for file preparation:

1. A separate file is required for each distributed tributary. This approach allows the user to update inflows for one distributed tributary independent of another distributed tributary.
2. Input format for each field is F8.0 that allows the user to specify the decimal point location.
3. The first two lines are ignored and can be used to comment the file.
4. The third line contains the variable names which are right justified according to the input field. This line is also ignored although the preprocessor checks to ensure the fields are aligned correctly.
5. The first field is the Julian date that can be entered at any frequency. The frequency between updates may vary during the simulation.
6. The second field is the inflow rate, $\text{m}^3 \text{sec}^{-1}$.

Example

CE-QUAL-W2 sample distributed tributary inflow file

JDAY	QDTR
1.0	22.8
5.0	44.5
12.0	31.2
23.0	80.4
35.0	50.6
74.5	103.0
74.7	185.6
75.0	212.3
75.5	178.6
80.0	123.4
80.5	78.3
90.0	46.5

There is a new option starting with Version 3.71 to use a free-format file rather than the fixed format shown above. When the first character in the first line contains the '\$' symbol, the model will treat the file as being in free format. As in the fixed format file, the first 3 lines are ignored and the data fields are in the same order as the fixed format file except that the user is no longer limited to 8 characters for each field. An example of a comma delimited file is shown in the Branch Inflow file description.

Branch Distributed Tributary Inflow Temperature File

This file contains the inflow temperatures for a distributed tributary specified on the [Distributed Tributary](#) card. The following is a list of guidelines for file preparation:

1. A separate file is required for each distributed tributary. This allows the user to update inflow temperatures for one distributed tributary independent of another distributed tributary.
2. Input format for each field is F8.0 that allows the user to specify the decimal point location.
3. The first two lines are ignored and can be used to comment the file.
4. The third line contains the variable names which are right justified according to the input field. This line is also ignored although the preprocessor checks to ensure the fields are aligned correctly.
5. The first field is the Julian date that can be entered at any frequency. The frequency between updates may vary during the simulation.
6. The second field is the inflow temperature, °C.

Example

CE-QUAL-W2 sample tributary inflow temperature file

JDAY	TDTR
1.0	10.3
5.0	9.5
12.0	10.1
23.0	8.6
35.0	11.2
74.5	13.9
74.7	13.1
75.0	12.8
75.5	12.5
80.0	12.6
80.5	12.7

There is a new option starting with Version 3.71 to use a free-format file rather than the fixed format shown above. When the first character in the first line contains the '\$' symbol, the model will treat the file as being in free format. As in the fixed format file, the first 3 lines are ignored and the data fields are in the same order as the fixed format file except that the user is no longer limited to 8 characters for each field. An example of a comma delimited file is shown in the Branch Temperature Inflow file description.

Branch Distributed Tributary Inflow Concentration File

This file contains the inflow concentrations for a distributed tributary specified on the [Distributed Tributary](#) card. The following is a list of guidelines for file preparation:

1. *If* constituents are being modeled, a separate file is required for each branch. This allows the user to update constituent inflow concentrations for one branch independent of another branch.
2. Input format for all fields is F8.0 that allows the user to specify the decimal point location. The number of fields is determined by (6) below and they are always located on one line.
3. The first two lines are ignored and can be used to comment the file.
4. The next line contains the abbreviations for the constituent names which are right justified according to the input field. This line is also ignored although the preprocessor checks to ensure the fields are aligned correctly.
5. The first field is the Julian date that can be entered at any frequency. The frequency between updates may vary during the simulation.
6. The remaining fields contain the concentration for each constituent specified on the [Distributed Tributary Active Constituent Control](#) card. Only those constituents specified as *active* on the [Distributed Tributary Active Constituent Control](#) card may be included in the distributed tributary inflow concentration file.

There is also a free format option for this file. Whenever the first character on the first line is a '\$' character, the model assumes the input is in free format rather than fixed format. Besides allowing the use of Excel and easy exporting to a csv file type, this also allows one to not be constrained by the 8 column width of the concentration value. An example is shown in the Inflow concentration file section above.

Example

```
CE-QUAL-W2 sample distributed tributary constituent inflow concentration file
JDAY CLFORM    ISS    LDOM    RDOM    ALGAE DETRIT    PO4    NH4    NO3    O2    Fe
 1.    17.    62.    7.333 17.111    0.0    0.9    0.02    0.10    0.42    13.9    0.4
 8.    13.    0.0    8.000 18.667    0.0    0.4    0.01    0.03    0.37    14.0    0.2
15.    11.    17.    9.333 21.778    0.0    0.0    0.00    0.01    0.17    10.0    0.3
22.    14.    34.   10.000 23.333    0.0    0.0    0.05    0.00    0.20    10.4    1.6
29.    17.    38.    4.467 10.422    0.0    0.4    0.01    0.11    0.26    11.6    0.4
```

Branch Precipitation File

This file contains the precipitation values for a branch and is needed only if the precipitation option [\[PRC\]](#) is turned on. The following is a list of guidelines for file preparation:

1. A separate file is required for each branch. This allows the user to update precipitation for one branch independent of another branch if needed.
2. Input format for each field is F8.0 that allows the user to specify the decimal point location.
3. The first two lines are ignored and can be used to comment the file.
4. The third line contains the variable names which are right justified according to the input field. This line is also ignored although the preprocessor checks to ensure the fields are aligned correctly.
5. The first field is the Julian date that can be entered at any frequency. The frequency between updates may vary during the simulation.
6. The second field is the precipitation rate, m sec^{-1} .

Note the following example takes advantage of the algorithm's capability to use data at varying frequencies.

Example

CE-QUAL-W2 sample precipitation file where Pre is in m/s

JDAY	PRE
182.0000	0.000
182.5416	1.E-6
182.6250	2.E-6
182.6666	0.000
188.475	2.E-6
189.500	0.000

Branch Precipitation Temperature File

This file contains the precipitation temperatures for a branch and is needed only if the precipitation option [[PRC](#)] is turned on. The following is a list of guidelines for file preparation:

1. A separate file is required for each branch. This allows the user to update temperatures for one branch independent of another branch.
2. Input format for each field is F8.0 that allows the user to specify the decimal point location.
3. The first two lines are ignored and can be used to comment the file.
4. The third line contains the variable names which are right justified according to the input field. This line is also ignored although the preprocessor checks to ensure the fields are aligned correctly.
5. The first field is the Julian date that can be entered at any frequency. The frequency between updates may vary during the simulation.
6. The second field is the precipitation temperature, °C.

Example

CE-QUAL-W2 sample precipitation temperature file

JDAY	TPR
1.00	6.80
2.00	6.70
3.00	7.00
4.00	6.30
5.00	6.40
6.00	6.10
7.00	6.60
8.00	5.70
9.00	5.20
10.00	5.40
11.00	7.10
12.00	6.60

Branch Precipitation Concentration File

This file contains the precipitation concentrations for a branch and is needed only if the precipitation option [[PRC](#)] is turned on. The following is a list of guidelines for file preparation:

1. *If* constituents are being modeled, a separate file is required for each branch. This allows the user to update constituent concentrations for one branch independent of another branch.
2. Input format for all fields is F8.0 that allows the user to specify the decimal point location. The number of fields is determined by (6) below and they are always located on one line.
3. The first two lines are ignored and can be used to comment the file.
4. The next line contains the abbreviations for the constituent names that are right justified according to the input field. This line is also ignored although the preprocessor checks to ensure the fields are aligned correctly.
5. The first field is the Julian date that can be entered at any frequency. The frequency between updates may vary during the simulation.
6. The remaining fields contain the concentration for each constituent specified on the [Precipitation Active Constituent Control](#) card. Only those constituents specified as *active* on the [Precipitation Active Constituent Control](#) card may be included in the constituent inflow concentration file. In the following example, only DO has been included.

There is also a free format option for this file. Whenever the first character on the first line is a '\$' character, the model assumes the input is in free format rather than fixed format. Besides allowing the use of Excel and easy exporting to a csv file type, this also allows one to not be constrained by the 8 column width of the concentration value. An example is shown in the Inflow concentration file section above.

Example

CE-QUAL-W2 constituent precipitation concentration sample input file

JDAY	DO
180.000	8.7
190.000	8.2
195.000	8.0
220.000	7.8

Branch External Upstream Head Elevation File

This file contains the elevations for a branch with an [external upstream head boundary condition](#). The following is a list of guidelines for file preparation:

1. A separate file is required for each branch with an external upstream head boundary condition. This allows the user to update elevations for one branch independent of another branch.
2. Input format for each field is F8.0 that allows the user to specify the decimal point location.
3. The first two lines are ignored and can be used to comment the file.
4. The next line contains the variable names which are right justified according to the input field. This line is also ignored although the preprocessor checks to ensure the fields are aligned correctly.
5. The first field is the Julian date that can be entered at any frequency. The frequency between updates may vary during the simulation.
6. The next field is the external head elevation (m above datum specified on the [LOCATION](#) card).

Example

CE-QUAL-W2 sample external head elevation file

JDAY	ELUH
180.000	431.12
180.050	431.15
180.100	431.20
180.150	431.25
180.200	431.30

Branch External Upstream Head Temperature File

This file contains the upstream temperature profiles for a branch with an [external upstream head boundary condition](#). The following is a list of guidelines for file preparation:

1. A separate file is required for each branch. This allows the user to update temperatures for one branch independent of another branch.
2. Input format for each field is F8.0 that allows the user to specify the decimal point location.
3. The first two lines are ignored and can be used to comment the file.
4. The third line contains the variable names which are right justified according to the input field. This line is also ignored although the preprocessor checks to ensure the fields are aligned correctly.
5. The first field is the Julian date that can be entered at any frequency. The frequency between updates may vary during the simulation.
6. The next fields are the upstream boundary temperatures, °C
7. Temperature values must be specified for each cell starting from layer two and extending to the bottom active layer at the upstream segment. If the values do not all fit on one line, then they are continued on the next line with the first field (corresponding to the Julian date field) left blank. The reason why the temperatures must start at layer two is the water surface may vary over many layers during the simulation and it is impossible to know beforehand exactly what time layers will be added or subtracted. When preparing the boundary temperature profiles, it is best to assign boundary temperatures starting from the bottom layer. Once the surface layer has been reached, then use this value to assign values up to layer two. In the following example, the surface layer [KT] starts out at layer six and the bottom is at layer 22. The first four values correspond to layers two through five and must be defined even if they are never used.

Example

CE-QUAL-W2 sample external upstream boundary temperature file

JDAY	TUH	TUH	TUH	TUH	TUH	TUH	TUH	TUH	TUH
180.500	19.3	19.3	19.3	19.3	19.3	19.0	18.8	18.7	18.6
	18.4	18.0	17.0	15.0	14.0	13.5	13.2	13.0	12.8
	12.8	12.8	12.8						
187.500	20.3	20.3	20.3	20.3	20.3	20.0	19.8	19.7	19.6
	19.4	19.0	18.0	15.5	14.0	13.5	13.2	13.0	12.8
	12.8	12.8	12.8						

Branch External Upstream Head Constituent Concentration File

This file contains the upstream constituent concentration profiles for a branch with an [external upstream head boundary condition](#). The following is a list of guidelines for file preparation:

1. *If* constituents are being modeled, then a separate file is required for each branch. This allows the user to update temperatures for one branch independent of another branch.
2. Input format for each field is F8.0 that allows the user to specify the decimal point location.
3. The first two lines are ignored and can be used to comment the file.
4. The third line contains the variable names which are right justified according to the input field. This line is also ignored although the preprocessor checks to ensure the fields are aligned correctly.
5. The first field is the Julian date that can be entered at any frequency. The frequency between updates may vary during the simulation.
6. The next fields are the upstream boundary constituent concentrations.
7. Constituents must appear in the same order as they are turned on in the [Active Constituent](#) card. A boundary concentration is *required for each* active constituent (except water age). If the constituent name is defined as 'AGE' in the 'CST ACTIVE' control file, concentrations for this constituent in the boundary condition will be assumed to be zero and will not be read by the model in the head boundary condition constituent files.
8. Concentration values must be specified for each cell starting from layer two and extending to the bottom active layer at the upstream segment. If the values do not all fit on one line, then they are continued on the next line with the first field (corresponding to the Julian date field) left blank. The reason why the concentrations must start at layer two is the water surface may vary over many layers during the simulation and it is impossible to know beforehand exactly what time layers will be added or subtracted. When preparing the boundary concentration profiles, it is best to assign concentrations starting from the bottom layer. Once the surface layer has been reached, then use this value to assign values up to layer two. In the following example, the surface layer [KT] starts out at layer six and the bottom is at layer 22. The first four values correspond to layers two through five and must be defined even if they are never used. Salinity and dissolved oxygen are the only values specified as active.

Example

CE-QUAL-W2 sample external upstream boundary constituent concentration file

JDAY	CUH	CUH	CUH	CUH	CUH	CUH	CUH	CUH	CUH	
180.000	23.5	23.5	23.5	23.5	23.5	23.9	24.5	25.0	26.0	!TDS
	27.0	28.0	29.0	29.5	30.0	30.2	30.4	30.6	30.6	
	30.6	30.6	30.6	30.6						
180.000	9.0	9.0	9.0	9.0	9.0	9.0	9.0	8.8	8.7	!DO
	8.6	8.4	8.0	7.5	7.0	6.0	5.5	5.5	5.5	
	5.5	5.5	5.5	5.5						
190.000	23.5	23.5	23.5	23.5	23.5	23.9	24.5	25.0	26.0	!TDS
	27.0	28.0	29.0	29.5	30.0	30.2	30.4	30.6	30.6	
	30.6	30.6	30.6	30.6						
190.000	9.0	9.0	9.0	9.0	9.0	9.0	9.0	8.8	8.7	!DO

UPSTREAM HEAD CONCENTRATION

INPUT FILES

8.6	8.4	8.0	7.0	6.0	5.0	5.0	5.0	5.0
5.0	5.0	5.0	5.0					

Branch External Downstream Head Elevation File

This file contains the elevations for a branch with an [external downstream head boundary condition](#). The following is a list of guidelines for file preparation:

1. A separate file is required for each branch with an external downstream head boundary condition. This allows the user to update elevations for one branch independent of another branch.
2. Input format for each field is F8.0 that allows the user to specify the decimal point location.
3. The first two lines are ignored and can be used to comment the file.
4. The next line contains the variable names which are right justified according to the input field. This line is also ignored although the preprocessor checks to ensure the fields are aligned correctly.
5. The first field is the Julian date that can be entered at any frequency. The frequency between updates may vary during the simulation.
6. The next field is the external head elevation (m above datum specified on the [Initial Condition](#) card.

Example

CE-QUAL-W2 sample external downstream head elevation file

JDAY	ELUH
180.000	431.12
180.050	431.15
180.100	431.20
180.150	431.25
180.200	431.30

Branch External Downstream Head Temperature File

This file contains the downstream temperature profiles for a branch with an [external downstream head boundary condition](#). The following is a list of guidelines for file preparation:

1. A separate file is required for each branch. This allows the user to update temperatures for one branch independent of another branch.
2. Input format for each field is F8.0 that allows the user to specify the decimal point location.
3. The first two lines are ignored and can be used to comment the file.
4. The third line contains the variable names which are right justified according to the input field. This line is also ignored although the preprocessor checks to ensure the fields are aligned correctly.
5. The first field is the Julian date that can be entered at any frequency. The frequency between updates may vary during the simulation.
6. The next fields are the downstream boundary temperatures, °C
7. Temperature values must be specified for each cell starting from layer two and extending to the bottom active layer at the downstream segment. If the values do not all fit on one line, then they are continued on the next line with the first field (corresponding to the Julian date field) left blank. The reason why the temperatures must start at layer two is the water surface may vary over many layers during the simulation and it is impossible to know beforehand exactly what time layers will be added or subtracted. When preparing the boundary temperature profiles, it is best to assign boundary temperatures starting from the bottom layer. Once the surface layer has been reached, then use this value to assign values up to layer two. In the following example, the surface layer [KT] starts out at layer six and the bottom is at layer 22. The first four values correspond to layers two through five and must be defined even if they are never used.

Example

CE-QUAL-W2 sample external downstream boundary temperature file

JDAY	TUH	TUH	TUH	TUH	TUH	TUH	TUH	TUH	TUH
180.500	19.3	19.3	19.3	19.3	19.3	19.0	18.8	18.7	18.6
	18.4	18.0	17.0	15.0	14.0	13.5	13.2	13.0	12.8
	12.8	12.8	12.8						
187.500	20.3	20.3	20.3	20.3	20.3	20.0	19.8	19.7	19.6
	19.4	19.0	18.0	15.5	14.0	13.5	13.2	13.0	12.8
	12.8	12.8	12.8						

Branch External Downstream Head Concentration File

This file contains the downstream constituent concentration profiles for a branch with an [external downstream head boundary condition](#). The following is a list of guidelines for file preparation:

1. A separate file is required for each branch. This allows the user to update temperatures for one branch independent of another branch.
2. Input format for each field is F8.0 that allows the user to specify the decimal point location.
3. The first two lines are ignored and can be used to comment the file.
4. The third line contains the variable names which are right justified according to the input field. This line is also ignored although the preprocessor checks to ensure the fields are aligned correctly.
5. The first field is the Julian date that can be entered at any frequency. The frequency between updates may vary during the simulation.
6. The next fields are the downstream boundary constituent concentrations.
7. Constituents must appear in the same order as they are turned on in the [Active Constituent](#) card. A boundary concentration profile is *required for each* active constituent (except water age). If the constituent name is defined as 'AGE' in the 'CST ACTIVE' control file, concentrations for this constituent in the boundary condition will be assumed to be zero and will not be read by the model in the head boundary condition constituent files.
8. Concentration values must be specified for each cell starting from layer two and extending to the bottom active layer at the downstream segment. If the values do not all fit on one line, then they are continued on the next line with the first field (corresponding to the Julian date field) left blank. The reason why the concentrations must start at layer two is the water surface may vary over many layers during the simulation and it is impossible to know beforehand exactly what time layers will be added or subtracted. When preparing the boundary concentration profiles, it is best to assign concentrations starting from the bottom layer. Once the surface layer has been reached, then use this value to assign values up to layer two. In the following example, the surface layer [KT] starts out at layer six and the bottom is at layer 22. The first four values correspond to layers two through five and must be defined even if they are never used. Salinity and dissolved oxygen are the only values specified as active.

Example

CE-QUAL-W2 sample external downstream boundary constituent concentration file

JDAY	CUH	CUH	CUH	CUH	CUH	CUH	CUH	CUH	CUH
180.000	23.5	23.5	23.5	23.5	23.5	23.9	24.5	25.0	26.0
Salinity	27.0	28.0	29.0	29.5	30.0	30.2	30.4	30.6	30.6
	30.6	30.6	30.6	30.6					
180.000	9.0	9.0	9.0	9.0	9.0	9.0	9.0	8.8	8.7
Temp	8.6	8.4	8.0	7.5	7.0	6.0	5.5	5.5	5.5
	5.5	5.5	5.5	5.5					
190.000	23.5	23.5	23.5	23.5	23.5	23.9	24.5	25.0	26.0
Salinity	27.0	28.0	29.0	29.5	30.0	30.2	30.4	30.6	30.6
	30.6	30.6	30.6	30.6					
190.000	9.0	9.0	9.0	9.0	9.0	9.0	9.0	8.8	8.7
Temp	8.6	8.4	8.0	7.0	6.0	5.0	5.0	5.0	5.0
	5.0	5.0	5.0	5.0					

Vertical Profile File

This file contains a single vertical profile used to specify initial conditions for temperatures and/or constituent concentrations. The vertically varying profile is then used to initialize all segments in the computational grid. This file is most commonly used for vertically stratified waterbodies with no longitudinal gradients. The following is a list of guidelines for file preparation:

1. An initial vertical profile is specified by inputting -1.0 for the initial temperature on the [Initial Conditions](#) card or a constituent's initial concentration on the [Initial Concentration](#) card. If temperature is included, then it *must* be the first profile in the file. Constituent profiles *must* be input in the same order as they are specified on the [Initial Concentration](#) card.
2. Input format for each field is F8.0 that allows the user to specify the decimal point location.
3. The first two lines are ignored and can be used to comment the file.
4. The third line contains in the first field a constituent identifier name to aid in creating and editing the file. The remaining fields contain the variable name which is right justified according to the input field. This line is also ignored although the preprocessor checks to ensure the fields are aligned correctly.
5. The first field is left blank or can be used for comments since it is ignored on input. The remaining fields are used for specifying the temperature or concentration at a given layer. If there are *more* values than can be specified on one line, then they are continued on the next line leaving the first field blank or using it for comments.
6. Values for the vertical profile start at the water surface layer [KT] and stop at the bottom layer. Boundary segments are *not* included in the file.

The following sample input file contains vertically varying initial temperature and dissolved oxygen profiles that correspond to the sample input bathymetry. The surface layer [KT] is located at layer five.

Example

```
CE-QUAL-W2 sample vertical profile initial conditions file

TEMP VPR      T1      T1      T1      T1      T1      T1      T1      T1      T1
              15.2    15.0    14.7    14.5    14.3    14.2    11.7    8.5    6.7
              6.2     6.0     6.0     6.0     6.0     6.0     6.0     6.0     6.0
              6.0     6.0

DO VPR        C1      C1      C1      C1      C1      C1      C1      C1      C1
              12.0    12.0    12.0    12.0    11.9    11.9    11.7    8.5    6.7
              6.2     6.0     6.0     6.0     6.0     6.0     6.0     6.0     6.0
              6.0     6.0
```

There is also a free format option for this file. Whenever the first character on the first line is a '\$' character, the model assumes the input is in free format rather than fixed format. Besides allowing the use of Excel and easy exporting to a csv file type, this also allows one not to be constrained by the 8 column width nor by wrapping temperature or concentration values. An example is shown below:

INPUT FILES

VERTICAL PROFILE

Free format example

```
$VPR file for Spokane River,,,KMX=47,Start at K=2 to 46,,,,,
Layer#,KT,,,,,,,,
Variable,37,38,39,40,41,42,43,44,45,46
TEMP,17.10,17.10,17.10,17.10,17.10,17.10,17.10,17.10,17.10,17.00
ALG1,0.10,0.10,0.10,0.10,0.10,0.10,0.10,0.10,0.10,0.11
DO,12.10,12.10,12.00,12.00,12.00,12.00,12.00,12.00,12.00,12.00
```

In Excel this looks like this where the first 3 lines are ignored by the code.

\$VPR file for Spokane River	KMX=47	Start at K=2 to 46								
Layer#	KT									
Variable	37	38	39	40	41	42	43	44	45	46
TEMP	17.10	17.10	17.10	17.10	17.10	17.10	17.10	17.10	17.10	17.10
ALG1	0.10	0.10	0.10	0.10	0.10	0.10	0.10	0.10	0.10	0.10
DO	12.10	12.10	12.00	12.00	12.00	12.00	12.00	12.00	12.00	12.00

Longitudinal Profile File

This file contains vertical profiles for each segment used to initialize temperature and/or constituent concentrations for each computational grid cell. It is useful when temperature or a constituent is both vertically and longitudinally stratified where a single value or profile is not representative of the initial conditions. The following is a list of guidelines for file preparation:

1. An initial longitudinal profile input is specified by inputting -2.0 for the initial temperature on the [Initial Conditions](#) card or a constituent's initial concentration on the [Initial Concentration](#) card. If temperature is included, then it *must* be the first series of profiles in the file. Constituent profiles *must* be input in the same order as they are specified on the [Initial Concentration](#) card.
2. Input format for each field is F8.0 that allows the user to specify the decimal point location.
3. The first two lines are ignored and can be used to comment the file.
4. The third line contains in the first field a constituent identifier name to aid in creating and editing the file. The remaining fields contain the variable name which is right justified according to the input field. This line is also ignored although the preprocessor checks to ensure the fields are aligned correctly.
5. The first field is left blank or can be used for comments since it is ignored on input. The remaining fields are used for specifying the temperature or concentration at a given layer. If there are *more* values than can be specified on one line, then they are continued on the next line leaving the first field blank or using it for comments.
6. Values for the vertical profile at each segment start at the water surface layer [KT] and stop at the bottom layer. Boundary segments are *not* included in the file.

The following sample input file includes vertically and longitudinally varying initial conditions for temperature and dissolved oxygen that corresponds to the sample input bathymetry. The surface layer [KT] is located at layer five.

Example

```

CE-QUAL-W2 sample longitudinal profile file

Segment 2
Temperature  T1      T1      T1      T1      T1      T1      T1      T1      T1
              15.0    14.8    14.5    14.3    14.2    14.1    11.5    8.2    6.5
              6.2      6.0      6.0

Segment 3
Temperature  T1      T1      T1      T1      T1      T1      T1      T1      T1
              15.0    14.8    14.5    14.3    14.2    14.1    11.5    8.2    6.5
              6.2      6.0

Segment 4
Temperature  T1      T1      T1      T1      T1      T1      T1      T1      T1
              15.0    14.8    14.5    14.3    14.2    14.1    11.5    8.2    6.5
              6.2

Segment 5
Temperature  T1      T1      T1      T1      T1      T1      T1      T1      T1
              15.0    14.8    14.5    14.3    14.2    14.1    11.5    8.2    6.5

Segment 6
Temperature  T1      T1      T1      T1      T1      T1      T1      T1      T1
              15.1    14.9    14.5    14.4    14.2    14.2    11.7    8.5    6.7
              6.2      6.0      6.0

Segment 7
Temperature  T1      T1      T1      T1      T1      T1      T1      T1      T1
              15.1    14.9    14.6    14.4    14.2    14.2    11.7    8.5    6.7
  
```

INPUT FILES

LONGITUDINAL PROFILE

	6.2	6.0	6.0	6.0	6.0	6.0			
Segment 8									
Temperature	T1	T1	T1	T1	T1	T1	T1	T1	T1
	15.2	15.0	14.7	14.5	14.3	14.2	11.7	8.5	6.7
	6.2	6.0	6.0	6.0	6.0	6.0	6.0	6.0	6.0
Segment 9									
Temperature	T1	T1	T1	T1	T1	T1	T1	T1	T1
	15.2	15.0	14.7	14.5	14.3	14.2	11.7	8.5	6.7
	6.2	6.0	6.0	6.0	6.0	6.0	6.0	6.0	6.0
	6.0	6.0							
Segment 12									
Temperature	T1	T1	T1	T1	T1	T1	T1	T1	T1
	15.5	15.3	14.8	14.5	14.3	14.2	10.6	7.2	
Segment 13									
Temperature	T1	T1	T1	T1	T1	T1	T1	T1	T1
	15.4	15.2	14.8	14.5	14.3	14.2	10.6	7.2	6.8
	6.2	6.0							
Segment 14									
Temperature	T1	T1	T1	T1	T1	T1	T1	T1	T1
	15.4	15.2	14.8	14.5	14.3	14.2	10.6	7.2	6.5
	6.2	6.0	6.0	6.0					
Segment 15									
Temperature	T1	T1	T1	T1	T1	T1	T1	T1	T1
	15.5	15.3	14.8	14.5	14.3	14.2	10.6	7.2	6.4
	6.2	6.0	6.0	6.0	6.0				
Segment 18									
Temperature	T1	T1	T1	T1	T1	T1	T1	T1	T1
	15.5	15.3	14.8	14.5	14.3	14.2	10.6	7.2	6.4
	6.2	6.0	6.0	6.0	6.0	6.0	6.0	6.0	
Segment 19									
Temperature	T1	T1	T1	T1	T1	T1	T1	T1	T1
	15.5	15.3	14.8	14.5	14.3	14.2	10.6	7.2	6.4
	6.2	6.0	6.0	6.0	6.0	6.0	6.0	6.0	6.0
	6.0								
Segment 2									
DO	C1	C1	C1	C1	C1	C1	C1	C1	C1
	12.0	12.0	12.0	12.0	11.9	11.9	11.5	8.2	6.5
	6.2	6.0	6.0						
Segment 3									
DO	C1	C1	C1	C1	C1	C1	C1	C1	C1
	12.0	12.0	12.0	12.0	11.9	11.9	11.5	8.2	6.5
	6.2	6.0							
Segment 4									
DO	C1	C1	C1	C1	C1	C1	C1	C1	C1
	12.0	12.0	12.0	12.0	11.9	11.9	11.5	8.2	6.5
	6.2								
Segment 5									
DO	C1	C1	C1	C1	C1	C1	C1	C1	C1
	12.0	12.0	12.0	12.0	11.9	11.9	11.5	8.3	6.5
	6.2	6.0							
Segment 6									
DO	C1	C1	C1	C1	C1	C1	C1	C1	C1
	12.0	12.0	12.0	12.0	11.9	11.9	11.6	8.4	6.7
	6.2	6.0	6.0						
Segment 7									
DO	C1	C1	C1	C1	C1	C1	C1	C1	C1
	12.0	12.0	12.0	12.0	11.9	11.9	11.6	8.5	6.7
	6.2	6.0	6.0	6.0	6.0	6.0			
Segment 8									
DO	C1	C1	C1	C1	C1	C1	C1	C1	C1
	12.0	12.0	12.0	12.0	11.9	11.9	11.6	8.5	6.7
	6.2	6.0	6.0	6.0	6.0	6.0	6.0	6.0	6.0
Segment 9									
DO	C1	C1	C1	C1	C1	C1	C1	C1	C1
	12.0	12.0	12.0	12.0	11.9	11.9	11.7	8.5	6.7
	6.2	6.0	6.0	6.0	6.0	6.0	6.0	6.0	6.0
	6.0	6.0							
Segment 12									

LONGITUDINAL PROFILE

INPUT FILES

DO	C1	C1	C1	C1	C1	C1	C1	C1	C1
	12.0	15.3	14.8	14.5	14.3	14.2	11.7	8.5	
Segment 13									
DO	C1	C1	C1	C1	C1	C1	C1	C1	C1
	12.0	12.0	12.0	12.0	11.9	11.9	11.7	8.5	6.8
	6.2	6.0							
Segment 14									
DO	C1	C1	C1	C1	C1	C1	C1	C1	C1
	12.0	12.0	12.0	12.0	11.9	11.9	11.7	8.5	6.5
	6.2	6.0	6.0	6.0					
Segment 15									
DO	C1	C1	C1	C1	C1	C1	C1	C1	C1
	12.0	12.0	12.0	12.0	11.9	11.9	11.7	8.5	6.4
	6.2	6.0	6.0	6.0	6.0				
Segment 18									
DO	C1	C1	C1	C1	C1	C1	C1	C1	C1
	12.0	12.0	12.0	12.0	11.9	11.9	11.7	8.5	6.4
	6.2	6.0	6.0	6.0	6.0	6.0	6.0	6.0	
Segment 19									
DO	C1	C1	C1	C1	C1	C1	C1	C1	C1
	12.0	12.0	12.0	12.0	11.9	11.9	11.7	8.5	6.4
	6.2	6.0	6.0	6.0	6.0	6.0	6.0	6.0	6.0
	6.0								

There is also a free format option for this file. Whenever the first character on the first line is a ‘\$’ character, the model assumes the input is in free format rather than fixed format. Besides allowing the use of Excel and easy exporting to a csv file type, this also allows one not to be constrained by the 8 column width nor by wrapping temperature or concentration values . An example is shown below:

Free Format example

[The free format example is in a similar structure as the fixed format shown above where layers are columns and rows are model segments.]

```
$LPR file,,,,,,,,,
,,,,,,,,,
PO4,KT:37,38,39,40,41,42,43,44,45,46,
Segment:2,0.03,0.03,0.03,0.03,0.03,0.03,0.03,0.03,0.03,0.03,
3,0.03,0.03,0.03,0.03,0.03,0.03,0.03,0.03,0.03,0.03,
4,0.03,0.03,0.03,0.03,0.03,0.03,0.03,0.03,0.03,0.03,
5,0.03,0.03,0.03,0.03,0.03,0.03,0.03,0.03,0.03,0.03,
6,0.03,0.03,0.03,0.03,0.03,0.03,0.03,0.03,0.03,0.03,
7,0.03,0.03,0.03,0.03,0.03,0.03,0.03,0.03,0.03,0.03,
10,0.03,0.03,0.03,0.03,0.03,0.03,0.03,0.03,0.03,0.03,
11,0.03,0.03,0.03,0.03,0.03,0.03,0.03,0.03,0.03,0.03,
12,0.03,0.03,0.03,0.03,0.03,0.03,0.03,0.03,0.03,0.03,
13,0.03,0.03,0.03,0.03,0.03,0.03,0.03,0.03,0.03,0.03,
14,0.03,0.03,0.03,0.03,0.03,0.03,0.03,0.03,0.03,0.03,
15,0.03,0.03,0.03,0.03,0.03,0.03,0.03,0.03,0.03,0.03,
16,0.03,0.03,0.03,0.03,0.03,0.03,0.03,0.03,0.03,0.03,
17,0.03,0.03,0.03,0.03,0.03,0.03,0.03,0.03,0.03,0.03,
18,0.03,0.03,0.03,0.03,0.03,0.03,0.03,0.03,0.03,0.03,
19,0.03,0.03,0.03,0.03,0.03,0.03,0.03,0.03,0.03,0.03,
20,0.03,0.03,0.03,0.03,0.03,0.03,0.03,0.03,0.03,0.03,
21,0.03,0.03,0.03,0.03,0.03,0.03,0.03,0.03,0.03,0.03,
22,0.03,0.03,0.03,0.03,0.03,0.03,0.03,0.03,0.03,0.03,
23,0.03,0.03,0.03,0.03,0.03,0.03,0.03,0.03,0.03,0.03,
24,0.03,0.03,0.03,0.03,0.03,0.03,0.03,0.03,0.03,0.03,
```

INPUT FILES

LONGITUDINAL PROFILE

```
25,0.03,0.03,0.03,0.03,0.03,0.03,0.03,0.03,0.03,0.03,
26,0.03,0.03,0.03,0.03,0.03,0.03,0.03,0.03,0.03,0.03,
27,0.03,0.03,0.03,0.03,0.03,0.03,0.03,0.03,0.03,0.03,
28,0.03,0.03,0.03,0.03,0.03,0.03,0.03,0.03,0.03,0.03,
29,0.03,0.03,0.03,0.03,0.03,0.03,0.03,0.03,0.03,0.03,
30,0.03,0.03,0.03,0.03,0.03,0.03,0.03,0.03,0.03,0.03,
31,0.03,0.03,0.03,0.03,0.03,0.03,0.03,0.03,0.03,0.03,
32,0.03,0.03,0.03,0.03,0.03,0.03,0.03,0.03,0.03,0.03,
33,0.03,0.03,0.03,0.03,0.03,0.03,0.03,0.03,0.03,0.03,
34,0.03,0.03,0.03,0.03,0.03,0.03,0.03,0.03,0.03,0.03,
35,0.03,0.03,0.03,0.03,0.03,0.03,0.03,0.03,0.03,0.03,
36,0.03,0.03,0.03,0.03,0.03,0.03,0.03,0.03,0.03,0.03,
37,0.03,0.03,0.03,0.03,0.03,0.03,0.03,0.03,0.03,0.03,
38,0.03,0.03,0.03,0.03,0.03,0.03,0.03,0.03,0.03,0.03,
39,0.04,0.03,0.03,0.03,0.03,0.03,0.03,0.03,0.03,0.03,
40,0.04,0.035,0.035,0.03,0.03,0.03,0.03,0.03,0.03,0.03,
41,0.05,0.04,0.03,0.02,0.03,0.03,0.03,0.03,0.03,0.03,
LDOM,KT:37,38,39,40,41,42,43,44,45,46,
Segment:2,0.015,0.015,0.01,0.01,0.01,0.01,0.01,0.01,0.01,0.01,
3,0.02,0.01,0.01,0.01,0.01,0.01,0.01,0.01,0.01,0.01,
4,0.02,0.01,0.01,0.01,0.01,0.01,0.01,0.01,0.01,0.01,
5,0.015,0.01,0.01,0.01,0.01,0.01,0.01,0.01,0.01,0.01,
6,0.01,0.01,0.01,0.01,0.01,0.01,0.01,0.01,0.01,0.01,
7,0.01,0.01,0.01,0.01,0.01,0.01,0.01,0.01,0.01,0.01,
10,0.01,0.01,0.01,0.01,0.01,0.01,0.01,0.01,0.01,0.01,
11,0.01,0.01,0.01,0.01,0.01,0.01,0.01,0.01,0.01,0.01,
12,0.01,0.01,0.01,0.01,0.01,0.01,0.01,0.01,0.01,0.01,
13,0.01,0.01,0.01,0.01,0.01,0.01,0.01,0.01,0.01,0.01,
14,0.01,0.01,0.01,0.01,0.01,0.01,0.01,0.01,0.01,0.01,
15,0.01,0.01,0.01,0.01,0.01,0.01,0.01,0.01,0.01,0.01,
16,0.01,0.01,0.01,0.01,0.01,0.01,0.01,0.01,0.01,0.01,
17,0.01,0.01,0.01,0.01,0.01,0.01,0.01,0.01,0.01,0.01,
18,0.01,0.01,0.01,0.01,0.01,0.01,0.01,0.01,0.01,0.01,
19,0.01,0.01,0.01,0.01,0.01,0.01,0.01,0.01,0.01,0.01,
20,0.01,0.01,0.01,0.01,0.01,0.01,0.01,0.01,0.01,0.01,
21,0.01,0.01,0.01,0.01,0.01,0.01,0.01,0.01,0.01,0.01,
22,0.01,0.01,0.01,0.01,0.01,0.01,0.01,0.01,0.01,0.01,
23,0.01,0.01,0.01,0.01,0.01,0.01,0.01,0.01,0.01,0.01,
24,0.01,0.01,0.01,0.01,0.01,0.01,0.01,0.01,0.01,0.01,
25,0.01,0.01,0.01,0.01,0.01,0.01,0.01,0.01,0.01,0.01,
26,0.01,0.01,0.01,0.01,0.01,0.01,0.01,0.01,0.01,0.01,
27,0.01,0.01,0.01,0.01,0.01,0.01,0.01,0.01,0.01,0.01,
28,0.01,0.01,0.01,0.01,0.01,0.01,0.01,0.01,0.01,0.01,
29,0.01,0.01,0.01,0.01,0.01,0.01,0.01,0.01,0.01,0.01,
30,0.01,0.01,0.01,0.01,0.01,0.01,0.01,0.01,0.01,0.01,
31,0.01,0.01,0.01,0.01,0.01,0.01,0.01,0.01,0.01,0.01,
32,0.01,0.01,0.01,0.01,0.01,0.01,0.01,0.01,0.01,0.01,
33,0.01,0.01,0.01,0.01,0.01,0.01,0.01,0.01,0.01,0.01,
34,0.01,0.01,0.01,0.01,0.01,0.01,0.01,0.01,0.01,0.01,
35,0.01,0.01,0.01,0.01,0.01,0.01,0.01,0.01,0.01,0.01,
36,0.01,0.01,0.01,0.01,0.01,0.01,0.01,0.01,0.01,0.01,
37,0.01,0.01,0.01,0.01,0.01,0.01,0.01,0.01,0.01,0.01,
38,0.01,0.01,0.01,0.01,0.01,0.01,0.01,0.01,0.01,0.01,
39,0.01,0.01,0.01,0.01,0.01,0.01,0.01,0.01,0.01,0.01,
40,0.01,0.01,0.01,0.01,0.01,0.01,0.01,0.01,0.01,0.01,
41,0.01,0.01,0.01,0.01,0.01,0.01,0.01,0.01,0.01,0.01,
```

Note that the Excel format is shown below. This file can then be exported as a csv file.

INPUT FILES

Appendix C Input/Output Data Description

Graph Input File

The file graph.npt is required for all model simulations of W2 on a PC using the downloadable executable. This file controls output formats for the model output variables.

The first section of the file contains a line for each active constituent defined in the control file. The concentration multiplier [CMULT] is a conversion factor and multiplies the output by the value specified. This is most useful when converting from $g\ m^{-3}$ to $mg\ m^{-3}$ for nutrient values. The concentration minimum [CMIN] and maximum [CMAX] *are no longer used* in Version 3.7 and later. For earlier versions they define the limits of the Array Viewer animation scaling. If [CMAX] is set to a negative number, the plots are scaled dynamically. The constituent plot control [CPLTC] turns on the Array Viewer animation for each variable. Note that severe performance degradation can occur depending upon output frequency and number of output windows open.

The second section contains hydraulic variables. The hydrodynamic format [HFMT] specifies the output variable format for the snapshot output file. The hydrodynamic minimum [HMIN] and maximum [HMAX] *are no longer used*. In earlier versions of the code they specify the plotting limits when viewing the output using Array Viewer. The hydrodynamic plot control [HPLTC] specifies whether the animation is turned ON or OFF during the simulation. The **HYD PR** card in the w2_con.npt control file defines which terms are printed and describes the output variables.

The third section contains derived constituent variables. The derived constituent multiplier [CDMULT] can be used to convert the output to units other than $g\ m^{-3}$. The derived constituent minimum [CDMIN] and maximum [CDMAX] concentration *are no longer used*. In earlier versions of the code they specify the plotting limits when viewing the output using Array Viewer. A negative value for [CDMAX] results in automatic scaling of the plot output. The derived constituent plot control [CDPLTC] specifies whether the animation is turned ON or OFF during the simulation.

Example

Hydrodynamic, constituent, and derived constituent names, formats, multipliers, and array viewer controls

.....HNAME.....	FMTH	HMULT	HMIN	HMAX	HPLTC	#
Timestep violations [NVIOL]	(I10)	1.0	-1.0	1.0	OFF	1
Horizontal velocity [U], m/s	(g10.3)	1.0	-.1000	0.25	OFF	2
Vertical velocity [W], m/s	(g10.3)	1.0	-.1E-6	-0.01	OFF	3
Temperature [T1], <o/>C	(g10.3)	1.0	-2.0	-30.0	ON	4
Density [RHO], kg/m ³	(g10.3)	1.0	997.0	1005.0	OFF	5
Vertical eddy viscosity [AZ], m ² /s	(g10.3)	1.0	-1E-08	0.01	OFF	6
Velocity shear stress [SHEAR], 1/s ²	(g10.3)	1.0	-1E-08	0.01	OFF	7
Internal shear [ST], m ³ /s ²	(g10.3)	1.0	-1E-08	0.01	OFF	8
Bottom shear [SB], m ³ /s ²	(g10.3)	1.0	-1E-08	0.01	OFF	9
Longitudinal momentum [ADMX], m ³ /s ²	(g10.3)	1.0	-1E-08	0.01	OFF	10
Longitudinal momentum [DM], m ³ /s ²	(g10.3)	1.0	-1E-08	0.01	OFF	11
Horizontal density gradient [HDG], m ³ /s ²	(g10.3)	1.0	-1E-08	0.01	OFF	12
Vertical momentum [ADMZ], m ³ /s ²	(g10.3)	1.0	-1E-08	0.01	OFF	13
Horizontal pressure gradient [HPG], m ³ /s ²	(g10.3)	1.0	-1E-08	10.0	OFF	14
Gravity term channel slope [GRAV], m ³ /s ²	(g10.3)	1.0	0.0	0.0	OFF	15
.....CNAME.....	FMTC	CMULT	CMIN	CMAX	CPLTC	#
TDS, g/m ³	(g10.3)	1.0	-1.0	200.0	OFF	1
Tracer, g/m ³	(g10.3)	1.0	-1.0	200.0	OFF	2
Age, days	(g10.3)	1.0	-1.0	-20.0	OFF	3
Coliform, g/m ³	(g10.3)	1.0	-1.0	200.0	OFF	4

GRAPH

INPUT FILES

Conductivity, g/m^3	(g10.3)	1.0	-1.0	-300.0	OFF	5
Chloride, g/m^3	(g10.3)	1.0	-1.0	6.0	OFF	6
ISS, g/m^3	(g10.3)	1.0	-20.000	15.0	OFF	7
Phosphate, mg/m^3	(g10.3)	1000.0	-1.0	-500.0	ON	8
Ammonium, mg/m^3	(g10.3)	1000.0	-0.1000	-300.0	OFF	9
Nitrate-Nitrite, g/m^3	(g10.3)	1.0	-0.1000	5.0	OFF	10
Dissolved silica, g/m^3	(g10.3)	1.0	-1.0	10.0	OFF	11
Particulate silica, g/m^3	(g10.3)	1.0	-0.2000	15.0	OFF	12
Total iron, g/m^3	(g10.3)	1.0	-0.1000	2.0	OFF	13
Labile DOM, g/m^3	(g10.3)	1.0	-0.1000	-3.0	OFF	14
Refractory DOM, g/m^3	(g10.3)	1.0	-0.1000	-4.0	OFF	15
Labile POM, g/m^3	(g10.3)	1.0	-0.1000	-3.0	OFF	16
Refractory POM, g/m^3	(g10.3)	1.0	-0.1000	-4.0	OFF	17
1CBOD, g/m^3	(g10.3)	1.0	-0.1	10.0	OFF	18
1CBODP, g/m^3	(g10.3)	1.0	-0.1	10.0	OFF	19
1CBODN, g/m^3	(g10.3)	1.0	-0.1	10.0	OFF	20
Algae1, g/m^3	(g10.3)	1.0	-0.0100	3.0	OFF	21
Algae2, g/m^3	(g10.3)	1.0	-0.0100	3.0	OFF	22
Algae3, g/m^3	(g10.3)	1.0	-0.0100	3.0	OFF	23
Algae4, g/m^3	(g10.3)	1.0	-0.0100	3.0	OFF	24
Dissolved oxygen, g/m^3	(g10.3)	1.0	-0.0100	-1.0	ON	25
Inorganic carbon, g/m^3	(g10.3)	1.0	-0.0100	3.0	OFF	26
Alkalinity, g/m^3	(g10.3)	1.0	-0.0100	3.0	OFF	27
zooplankton1, mg/m^3	(g10.3)	1000.0	-0.0100	1.0	OFF	28
LDOM P, mg/m^3	(g10.3)	1000.0	0.0	1.0	OFF	29
RDOM P, mg/m^3	(g10.3)	1000.0	0.0	1.0	OFF	30
LPOM P, mg/m^3	(g10.3)	1000.0	0.0	1.0	OFF	31
RPOM P, mg/m^3	(g10.3)	1000.0	0.0	1.0	OFF	32
LDOM N, mg/m^3	(g10.3)	1000.0	0.0	1.0	OFF	33
RDOM N, mg/m^3	(g10.3)	1000.0	0.0	1.0	OFF	34
LPOM N, mg/m^3	(g10.3)	1000.0	0.0	1.0	OFF	35
RPOM N, mg/m^3	(g10.3)	1000.0	0.0	1.0	OFF	36
.....CDNAME.....						
	FMTCD	CDMULT	CDMIN	CDMAX	CDPLTC	#
Dissolved organic carbon, g/m^3	(g10.3)	1.0	-1.0	25.0	OFF	1
Particulate organic carbon, g/m^3	(g10.3)	1.0	-1.0	50.0	OFF	2
Total organic carbon, g/m^3	(g10.3)	1.0	-1.0	25.0	OFF	3
Dissolved organic nitrogen, g/m^3	(g10.3)	1.0	-1.0	25.0	OFF	4
Particulate organic nitrogen, g/m^3	(g10.3)	1.0	-1.0	25.0	OFF	5
Total organic nitrogen, g/m^3	(g10.3)	1.0	-1.0	50.0	OFF	6
Total Kheldahl Nitrogen, g/m^3	(g10.3)	1.0	-1.0	15.0	OFF	7
Total nitrogen, g/m^3	(g10.3)	1.0	-1.0	15.0	OFF	8
Dissolved organic phosphorus, mg/m^3	(g10.3)	1000.0	-1.0	25.0	OFF	9
Particulate organic phosphorus, mg/m^3	(g10.3)	1000.0	-1.0	-1.0	OFF	10
Total organic phosphorus, mg/m^3	(g10.3)	1000.0	-1.0	5.0	OFF	11
Total phosphorus, mg/m^3	(g10.3)	1000.0	-1.0	20.0	OFF	12
Algal production, g/m^2/day	(g10.3)	1.0	-1.0	5.0	OFF	13
Chlorophyll a, mg/m^3	(g10.3)	1.0	-5.0	145.0	OFF	14
Total algae, g/m^3	(g10.3)	1.0	-1.0	60.0	OFF	15
Oxygen % Gas Saturation	(g10.3)	1.0	-1.0	50.0	OFF	16
Total suspended Solids, g/m^3	(g10.3)	1.0	-1.0	5.0	OFF	17
Total Inorganic Suspended Solids, g/m^3	(g10.3)	1.0	-1.0	20.0	OFF	18
Carbonaceous Ultimate BOD, g/m^3	(g10.3)	1.0	5.0	9.0	OFF	19
pH	(g10.3)	1.0	-1.0	10.0	OFF	20
CO2	(g10.3)	1.0	-1.0	10.0	OFF	21
HCO3	(g10.3)	1.0	-1.0	10.0	OFF	22
CO3	(g10.3)	1.0	-1.0	0.0	OFF	23

Output FilesSnapshot

The snapshot file was designed for output to a hard copy printer and contains useful information that can be utilized during model application. The file can also be pulled into a text editor such as “Notepad” that comes with Windows or any other text editor and quickly viewed and searched for specific information. A free text editor that is much more powerful than “Notepad” and that is available on many different platforms is “Notepad ++”.

Title Cards

The first lines of output contain the information specified in the **Title Card** for identifying the run plus the date and time that the run occurred. This information will appear everytime output is updated to the file based on the update dates [SNPD] and frequency [SNPF] specified in the control file. Following the title cards is information related to the progress of the run including the output date and timestep information.

EXAMPLE

```
CE-QUAL-W2 V3.1
Burnsville Reservoir - March 15 through December 11, 1992
Density placed inflow, point sink outflows
Default hydraulic coefficients
Default light absorption/extinction coefficients
Default kinetic coefficients
Temperature and water quality simulation
Run 8
Testing sensitivity to wind
Wind sheltering set to 0.75
Jim Stiles and Vince Marchese, USACE Huntington District
Model run at 16:58:03 on 07/22/02

Time Parameters
Gregorian date      [GDAY] =          March 15, 1992
Julian date         [JDAY] =          75 days 12.00 hours
Elapsed time        [ELTMJD] =         0 days 12.00 hours
Timestep            [DLT] =          356 sec
  at location       [KLOC,ILOC] = (26,47)
Minimum timestep    [MINDLT] =         378 sec
  at Julian day     [JDMIN] =         75 days  7.31 hours
  at location       [KMIN,IMIN] = (27,19)
Average timestep    [DLTAV] =         600 sec
Number of iterations [NIT] =           72
Number of violations [NV] =            5
```

Time Parameters

The time parameter information includes the date at which the information was output, the elapsed time of the simulation, and useful information about the timestep and its behavior. This includes the current timestep and where the computational cell is located that was used to determine the current timestep based on numerical stability criterion. The current minimum timestep that has occurred, the date at which it occurred, and the location is also given. The average timestep for the simulation up to this time, the total number of iterations, and the number of timestep violations that

required restoring variables and recomputing the water surface elevations and velocities is also output.

The timestep information can be very useful in providing information that can be analyzed to see where violations are occurring and possibly altering inputs or the bathymetry to increase the average timestep without impacting the results. For example, the location of the minimum timestep can be checked to see if the width can be increased without impacting results. The number of violations provides information as to whether or not the fraction of the computed timestep used needs to be decreased. If the number of violations exceeds 5% of the number of iterations, the fraction of the timestep [[DLTF](#)] should be decreased 5-10%.

Meteorological Parameters

The next information includes meteorological parameters used at the current timestep. This can be useful when trying to better understand temperature simulations such as “why is the model overpredicting epilimnetic temperatures on August 14?”. If the equilibrium temperature is $> 45^{\circ}\text{C}$ and there is no wind, then the model is behaving exactly as the user is telling it to behave. Running sensitivity analyses on meteorological forcing data during this time period can show that the model will reproduce observed data if the forcing data are more accurate.

EXAMPLE

```
Meteorological Parameters
Input
  Air temperature      [TAIR] =    0.55 °C
  Dewpoint temperature [TDEW] =   -8.59 °C
  Wind direction       [PHI] =    4.65 rad
  Cloud cover          [CLOUD] =    4.53
Calculated
  Equilibrium temperature [ET] =    0.00 °C
  Surface heat exchange [CSHE] = 0.00E+00 m/sec
  Short wave radiation   [SRO] = 0.14E-03 °C m/sec
```

Inflow/Outflow Parameters

Inflows, inflow placement, and inflow temperatures are then output to provide information as to what the model is seeing at all inflow boundaries during the current timestep. This information can be very useful in determining if the model is seeing what the user thinks he has input into the model and should always be checked once at the beginning of the simulation and whenever inflow boundary files are changed during the course of the simulation.

All outflows are also printed out including individual structure outflows, the layer-by-layer outflow computed from the selective withdrawal algorithm, and the total outflow. Again, this is useful to ensure that the model is seeing what the user thinks the model is seeing.

EXAMPLE

```
Inflows
Upstream inflows
  Branch 1
    Layer      [KQIN] = 23-23
    Inflow     [QIN] =   7.13 m^3/sec
    Temperature [TIN] =   3.59 °C
  Branch 2
```

OUTPUT FILES

SNAPSHOT

```

      Layer      [KQIN] = 29-29
      Inflow      [QIN] =   0.87 m^3/sec
      Temperature [TIN] =   5.10 øC
Branch 3
      Layer      [KQIN] = 35-35
      Inflow      [QIN] =   0.18 m^3/sec
      Temperature [TIN] =   5.10 øC
Branch 4
      Layer      [KQIN] = 28-28
      Inflow      [QIN] =   0.12 m^3/sec
      Temperature [TIN] =   5.10 øC
Branch 5
      Layer      [KQIN] = 28-28
      Inflow      [QIN] =   0.06 m^3/sec
      Temperature [TIN] =   5.10 øC
Branch 6
      Layer      [KQIN] = 24-24
      Inflow      [QIN] =   0.04 m^3/sec
      Temperature [TIN] =   5.10 øC

Tributaries
  Segment      [ITR] =    24
  Layer        [KTWB] = 23-38
  Inflow       [QTR] =   0.09
  Temperature  [TTR] =   5.10

Outflows

Structure outflows [QSTR]
  Branch 1 =    12.56    0.00    0.00

Total outflow [QOUT] =   12.56 m^3/s
Outlets
  Layer      [KOUT] =    23    24    25    26    27    28    29    30
31    32    33    34    35    36    37    38
      Outflow (m^3/sec) [QOUT] =   1.77   1.26   1.18   1.15   1.14   1.12   0.96   0.86
0.79   0.70   0.61   0.51   0.16   0.16   0.14   0.07

```

The final information regarding boundary forcing functions is output next and includes inflow constituent concentrations for all boundary inflows. A great deal of grief can be saved by checking to ensure that the concentrations are correct as it is very easy to get the inflow concentrations out of order.

EXAMPLE

```

Constituent Inflow Concentrations
Branch 1 [CIN]
  Dissolved solids = 43.004 g/m^3
  Suspended solids1 = 2.000 g/m^3
  Phosphate = 0.020 g/m^3
  Ammonium = 0.100 g/m^3
  Nitrate nitrite = 0.200 g/m^3
  Labile DOM = 0.382 g/m^3
  Refractory_DOM = 0.892 g/m^3
  Labile POM = 0.425 g/m^3
  Algae = 0.000 g/m^3
  Dissolved oxygen = 12.000 g/m^3
Tributary 1 [CTR]
  Dissolved solids = 161.196 g/m^3
  Suspended solids1 = 2.000 g/m^3
  Phosphate = 0.020 g/m^3
  Ammonium = 0.100 g/m^3
  Nitrate nitrite = 0.200 g/m^3
  Labile DOM = 0.405 g/m^3
  Refractory_DOM = 0.945 g/m^3

```

```

Labile POM          = 0.450 g/m^3
Algae               = 0.000 g/m^3
Dissolved oxygen    = 11.980 g/m^3
    
```

Balances

If volume, thermal, and/or constituent mass balances are turned on, then the balances are output next. They are computed separately for each branch and summed for each waterbody. Information includes the spatially and temporally integrated change in volume since the start of the simulation, the total volume error between the two, and the percent error based on the total volume change. Using the change in volume rather than the total volume is important for preventing roundoff error from masking the results of the balance. The volume balance is computed as:

$$\underbrace{\Delta S}_{\text{spatially integrated volume}} = \underbrace{\sum Q_{in} - \sum Q_{out}}_{\text{temporally integrated volume}}$$

where:

ΔS = change in volume, m^3
 $\sum Q_{in}$ = sum of all inflows, m^3
 $\sum Q_{out}$ = sum of all outflows, m^3

Energy and mass balances are computed similarly. Errors should be on the order of 10^{-8} to 10^{-13} percent, which means that the model is essentially conserving water to machine accuracy. Any model that cannot show this adherence to the fundamental principle of mass balance involved in hydrodynamic and water quality modeling should immediately be suspect. This computation is routinely used to debug and find errors in the code.

EXAMPLE

```

Water Balance
  Waterbody 1
    Spatial change [VOLSR] = -0.20089851E+06 m^3
    Temporal change [VOLTR] = -0.20089851E+06 m^3
    Volume error = 0.10186341E-08 m^3
    Percent error = -0.50703913E-12 %
  Branch 1
    Spatial change [VOLSBR] = -0.13863158E+06 m^3
    Temporal change [VOLTBR] = -0.13863158E+06 m^3
    Volume error = 0.10768417E-08 m^3
    Percent error = -0.77676510E-12 %
  Branch 2
    Spatial change [VOLSBR] = -0.28973777E+05 m^3
    Temporal change [VOLTBR] = -0.28973777E+05 m^3
    Volume error = -0.76397555E-10 m^3
    Percent error = 0.26367827E-12 %

Energy Balance
  Waterbody 1
    Spatially integrated energy [ESR] = 0.29332063E+12 kJ
    Temporally integrated energy [ETR] = 0.29332063E+12 kJ
    Energy error = -0.28701192E+01 kJ
    Percent error = -0.97849211E-09 %
  Branch 1
    Spatially integrated energy [ESBR] = 0.20810993E+12 kJ
    
```

OUTPUT FILES

SNAPSHOT

```

Temporally integrated energy [ETBR] = 0.20812486E+12 kJ
Energy error                      = 0.79701322E+01 kJ
Percent error                     = 0.38294956E-08 %
Branch 2
Spatially integrated energy [ESBR] = 0.46706347E+11 kJ
Temporally integrated energy [ETBR] = 0.46709696E+11 kJ
Energy error                      = -0.72348511E+01 kJ
Percent error                     = -0.15488971E-07 %

```

Mass Balance

```

Branch 1
Dissolved solids
  Spatially integrated mass [CMBRS] = 0.42683593E+09 g
  Temporally integrated mass [CMBRT] = 0.42683593E+09 g
  Mass error                  = -0.15495062E-01 g
  Percent error               = -0.36302150E-08 %
Residence time
  Spatially integrated mass [CMBRS] = 0.46090907E+07
  Temporally integrated mass [CMBRT] = 0.46090907E+07
  Mass error                  = -0.14215708E-04
  Percent error               = -0.30842760E-09 %
Suspended solids1
  Spatially integrated mass [CMBRS] = 0.10093689E+08 g
  Temporally integrated mass [CMBRT] = 0.10093689E+08 g
  Mass error                  = -0.31241588E-03 g
  Percent error               = -0.30951605E-08 %
Phosphate
  Spatially integrated mass [CMBRS] = 0.17123908E+06 g
  Temporally integrated mass [CMBRT] = 0.17123908E+06 g
  Mass error                  = -0.72119292E-05 g
  Percent error               = -0.42116142E-08 %
Ammonium
  Spatially integrated mass [CMBRS] = 0.48859061E+06 g
  Temporally integrated mass [CMBRT] = 0.48859061E+06 g
  Mass error                  = -0.20249572E-04 g
  Percent error               = -0.41444865E-08 %
Nitrate nitrite
  Spatially integrated mass [CMBRS] = 0.18775938E+07 g
  Temporally integrated mass [CMBRT] = 0.18775938E+07 g
  Mass error                  = -0.75169839E-04 g
  Percent error               = -0.40035198E-08 %
Labile DOM
  Spatially integrated mass [CMBRS] = 0.61793186E+07 g
  Temporally integrated mass [CMBRT] = 0.61793186E+07 g
  Mass error                  = -0.24503283E-03 g
  Percent error               = -0.39653698E-08 %
Refractory DOM
  Spatially integrated mass [CMBRS] = 0.14555086E+08 g
  Temporally integrated mass [CMBRT] = 0.14555086E+08 g
  Mass error                  = -0.57210773E-03 g
  Percent error               = -0.39306379E-08 %
Labile POM
  Spatially integrated mass [CMBRS] = 0.65861106E+07 g
  Temporally integrated mass [CMBRT] = 0.65861106E+07 g
  Mass error                  = -0.26675593E-03 g
  Percent error               = -0.40502802E-08 %
Algae
  Spatially integrated mass [CMBRS] = 0.57925594E+07 g
  Temporally integrated mass [CMBRT] = 0.57925594E+07 g
  Mass error                  = -0.22346061E-03 g
  Percent error               = -0.38577180E-08 %
Dissolved oxygen
  Spatially integrated mass [CMBRS] = 0.10224093E+09 g
  Temporally integrated mass [CMBRT] = 0.10224093E+09 g
  Mass error                  = -0.40865839E-02 g
  Percent error               = -0.39970136E-08 %
Branch 2

```

SNAPSHOT

OUTPUT FILES

```
Dissolved solids
  Spatially integrated mass [CMBRS] = 0.10016615E+09 g
  Temporally integrated mass [CMBRT] = 0.10016615E+09 g
  Mass error                  = 0.12986526E-01 g
  Percent error               = 0.12964984E-07 %
Residence time
  Spatially integrated mass [CMBRS] = 0.10294782E+07
  Temporally integrated mass [CMBRT] = 0.10294782E+07
  Mass error                  = 0.98625082E-04
  Percent error               = 0.95801035E-08 %
Suspended solids1
  Spatially integrated mass [CMBRS] = 0.21809107E+07 g
  Temporally integrated mass [CMBRT] = 0.21809107E+07 g
  Mass error                  = 0.29512448E-03 g
  Percent error               = 0.13532167E-07 %
Phosphate
  Spatially integrated mass [CMBRS] = 0.38423775E+05 g
  Temporally integrated mass [CMBRT] = 0.38423775E+05 g
  Mass error                  = 0.63260450E-05 g
  Percent error               = 0.16463882E-07 %
Ammonium
  Spatially integrated mass [CMBRS] = 0.10661579E+06 g
  Temporally integrated mass [CMBRT] = 0.10661579E+06 g
  Mass error                  = 0.16890146E-04 g
  Percent error               = 0.15842068E-07 %
Nitrate nitrite
  Spatially integrated mass [CMBRS] = 0.41545882E+06 g
  Temporally integrated mass [CMBRT] = 0.41545882E+06 g
  Mass error                  = 0.67292654E-04 g
  Percent error               = 0.16197190E-07 %
Labile DOM
  Spatially integrated mass [CMBRS] = 0.13767130E+07 g
  Temporally integrated mass [CMBRT] = 0.13767130E+07 g
  Mass error                  = 0.22568717E-03 g
  Percent error               = 0.16393189E-07 %
Refractory_DOM
  Spatially integrated mass [CMBRS] = 0.32433662E+07 g
  Temporally integrated mass [CMBRT] = 0.32433662E+07 g
  Mass error                  = 0.52960077E-03 g
  Percent error               = 0.16328738E-07 %
Labile POM
  Spatially integrated mass [CMBRS] = 0.14806668E+07 g
  Temporally integrated mass [CMBRT] = 0.14806668E+07 g
  Mass error                  = 0.24347263E-03 g
  Percent error               = 0.16443445E-07 %
Algae
  Spatially integrated mass [CMBRS] = 0.13063015E+07 g
  Temporally integrated mass [CMBRT] = 0.13063015E+07 g
  Mass error                  = 0.21586171E-03 g
  Percent error               = 0.16524647E-07 %
Dissolved oxygen
  Spatially integrated mass [CMBRS] = 0.22578360E+08 g
  Temporally integrated mass [CMBRT] = 0.22578360E+08 g
  Mass error                  = 0.36302954E-02 g
  Percent error               = 0.16078649E-07 %
```

Geometry

The water surface layer number, elevation at the downstream segment, and the current upstream segment number for each branch are then output. Note that in the example, the current upstream segment is located at segment 8.

EXAMPLE

Geometry

OUTPUT FILES

SNAPSHOT

```
Surface layer [KT] = 23
Elevation    [ELKT] = 238.575 m
```

```
Current upstream segment [CUS]
Branch 1 =8
Branch 2 =30
Branch 3 =41
Branch 4 =46
Branch 5 =51
Branch 6 =55
```

Water Surface

The water surface elevation and the water surface deviation from the top of the water surface layer number is output next. The water surface deviation uses the oceanographic convention in which the deviation downwards from the top of the surface layer is positive. The output includes information only for the segments specified on the [Snapshot Segments](#) card.

EXAMPLE

```
Water Surface, m
      8      9      10      11      12      13      14      15
238.574 238.573 238.574 238.573 238.574 238.574 238.574 238.574

Water Surface Deviation (positive downwards), m
      8      9      10      11      12      13      14      15
-0.2136 -0.2135 -0.2135 -0.2135 -0.2136 -0.2139 -0.2138 -0.2137
```

Temperature/Water Quality

The last information available from the snapshot file is information related to hydrodynamics and water quality. The user has complete control of how much information is output including which hydrodynamic and water quality variables are included in the output. The file can rapidly become quite large, so only variables of interest should be output. This information is useful for quickly looking at the results of a run to gain a feel for how the variables of concern are behaving over time. Title cards are printed on each new page for ease in identifying the simulation.

SNAPSHOT

OUTPUT FILES

EXAMPLE

Burnsville Reservoir - March 15 through December 11, 1992
 Density placed inflow, point sink outflows
 Default hydraulic coefficients
 Default light absorption/extinction coefficients
 Default kinetic coefficients
 Temperature and water quality simulation
 Run 8
 Testing sensitivity to wind
 Wind sheltering set to 0.75
 Jim Stiles and Vince Marchese, USACE Huntington District
 Model run at 08:25:31 on 07/23/02

March 15, 1992		Julian day = 75 days 12.00 hours		Temperature [T1], deg C								
Layer	Depth	8	9	10	11	12	13	14	15	16	17	18
23	0.41	3.74	3.77	4.19	5.02	5.53	5.62	5.49	5.51	5.50	5.55	5.58
24	1.13	3.81	3.77	4.19	4.96	5.32	5.43	5.26	5.34	5.29	5.34	5.35
25	1.74	3.83	3.76	4.19	5.03	5.27	5.31	5.17	5.30	5.23	5.28	5.29
26	2.35	3.81	3.76	4.19	5.07	5.26	5.22	5.11	5.25	5.19	5.24	5.30
27	2.96		3.76	4.19	5.08	5.27	5.14	5.05	5.27	5.17	5.24	5.33
28	3.57		3.76	4.19	5.08	5.26	5.14	5.01	5.29	5.20	5.26	5.31
29	4.18			4.19	5.11	5.23	5.14	5.01	5.32	5.36	5.31	5.33
30	4.79			4.19	5.21	5.22	5.14	5.19	5.31	5.35	5.34	5.33
31	5.40			4.63	5.21	5.22	5.14	5.23	5.31	5.33	5.33	5.32
32	6.01			5.06	5.32	5.24	5.14	5.24	5.31	5.31	5.31	5.31
33	6.62			5.31	5.34	5.26	5.14	5.26	5.31	5.30	5.31	5.31
34	7.23					5.32	5.22	5.30	5.31	5.30	5.30	5.31
35	7.84							5.33	5.32	5.30	5.29	5.31
36	8.45									5.30	5.29	5.31

Time Series

A time series history can be output for any number of cells in the computational grid with output for each cell written to a separate output file. Output is suitable for import into a spreadsheet program for analysis and plotting. The model takes the name of the time series file specified on the [TIME SERIES PLOT FILENAME](#) card and appends an “_x” to the filename where x is 1, 2, 3, etc., depending upon whether the cell is the first, second, third, etc. one specified on the [TIME SERIES SEGMENT](#) card. Title cards are included at the beginning of the output as an aid in identifying the particular model run. Information includes the Julian date, current time step (s), water surface elevation for the cell’s segment location (m), temperature (°C), velocity (m/s) at the layer and segment specified, total flow rate through the entire segment (m³/s, vertically integrated flow through the segment), net short wave solar radiation incident on the water surface (W/m², reflection is not included), light extinction coefficient in m⁻¹, depth from water surface to channel bottom (m), surface width (m), shade (shade factor multiplied by SRON, if SHADE =1, no shade, if shade =0, no short wave solar reaches the water surface), net radiation at surface of segment (W/m²), short wave solar net at surface (W/m²), long wave radiation in net at surface (W/m²), back radiation at surface (W/m²), evaporative heat flux at surface (W/m²), conductive heat flux at surface (W/m²), and active constituent concentrations, derived constituent concentrations, and instantaneous kinetic flux rates in kg/day.

Note that if SLHTC is set to ‘ET’ for equilibrium temperature approach (not recommended), then the radiation fluxes will all be set to zero.

TIME SERIES

OUTPUT FILES

Example

Version 3.5 Whatcom L. Model
 WB 1 : Basin III
 WB 2 : Basin I & II

Jing Liu & Bob Cusinamo, Department of Ecology
 Chris Berger and Scott Wells, Portland State University

Model run at 11:36:39 on 06/17/07

	JDAY	DLT	ELWS	T2	U	Q	SRON	ET	DEPTH	WIDTH	SHADE	Gen1	ISS1	PO4	NH4
02	45.607	600.00	95.11	5.04	0.01	0.00	435.43	0.00	21.11	605.66	1.00	0.520E-04	0.00	0.300E-02	0.301E-
02	45.647	294.54	95.09	5.15	0.01	0.00	303.69	0.00	21.09	605.66	1.00	0.254E-03	0.156E-06	0.301E-02	0.303E-
02	45.694	409.28	95.12	5.16	0.01	0.00	135.47	0.00	21.12	605.66	1.00	0.446E-03	0.949E-06	0.301E-02	0.305E-
02	45.742	326.10	95.09	5.08	0.01	0.00	19.69	0.00	21.09	605.66	0.00	0.444E-03	0.691E-05	0.301E-02	0.306E-
02	45.790	537.04	95.10	5.04	0.01	0.00	0.00	0.00	21.10	605.66	0.00	0.502E-03	0.836E-05	0.302E-02	0.309E-
02	45.837	360.06	95.11	5.01	0.01	0.00	0.00	0.00	21.11	605.66	0.00	0.482E-03	0.177E-04	0.303E-02	0.311E-
02	45.884	357.22	95.10	4.99	0.01	0.00	0.00	0.00	21.10	605.66	0.00	0.556E-03	0.297E-04	0.304E-02	0.313E-
02	45.931	431.23	95.13	4.96	0.01	0.00	0.00	0.00	21.13	605.66	0.00	0.728E-03	0.466E-04	0.305E-02	0.315E-
02	45.974	490.50	95.08	4.93	0.01	0.00	0.00	0.00	21.08	605.66	0.00	0.980E-03	0.785E-04	0.306E-02	0.317E-
02	46.025	459.69	95.10	4.91	0.01	0.00	0.00	0.00	21.10	605.66	0.00	0.115E-02	0.943E-04	0.307E-02	0.320E-
02	46.074	600.00	95.09	4.88	0.01	0.00	0.00	0.00	21.09	605.66	0.00	0.126E-02	0.994E-04	0.308E-02	0.322E-
02	46.118	479.46	95.12	4.86	0.01	0.00	0.00	0.00	21.12	605.66	0.00	0.151E-02	0.127E-03	0.309E-02	0.324E-
02	46.160	361.83	95.09	4.83	0.01	0.00	0.00	0.00	21.09	605.66	0.00	0.180E-02	0.162E-03	0.310E-02	0.326E-
02	46.208	376.46	95.07	4.80	0.01	0.00	0.00	0.00	21.07	605.66	0.00	0.200E-02	0.180E-03	0.311E-02	0.328E-
02	46.254	411.93	95.10	4.78	0.01	0.00	0.00	0.00	21.10	605.66	0.00	0.249E-02	0.241E-03	0.312E-02	0.330E-
02	46.301	110.15	95.12	4.75	0.01	0.00	0.00	0.00	21.12	605.66	0.00	0.283E-02	0.279E-03	0.313E-02	0.333E-
02	46.348	174.34	95.10	4.73	0.01	0.00	28.13	0.00	21.10	605.66	0.10	0.303E-02	0.296E-03	0.314E-02	0.335E-
02	46.398	495.28	95.10	4.71	0.01	0.00	140.03	0.00	21.10	605.66	1.00	0.320E-02	0.308E-03	0.314E-02	0.337E-

OUTPUT FILES

TIME SERIES

02	46.447	600.00	95.12	4.75	0.01	0.00	349.79	0.00	21.12	605.66	1.00	0.346E-02	0.302E-03	0.315E-02	0.340E-
02	46.487	204.07	95.09	4.87	0.01	0.00	507.84	0.00	21.09	605.66	1.00	0.414E-02	0.357E-03	0.314E-02	0.341E-
02	46.537	582.22	95.09	5.13	0.01	0.00	554.02	0.00	21.09	605.66	1.00	0.452E-02	0.331E-03	0.315E-02	0.345E-
02	46.583	297.55	95.08	5.36	0.01	0.00	470.29	0.00	21.08	605.66	1.00	0.483E-02	0.311E-03	0.316E-02	0.348E-
02	46.629	333.11	95.08	5.48	0.01	0.00	422.76	0.00	21.08	605.66	1.00	0.507E-02	0.312E-03	0.316E-02	0.350E-
02	46.678	311.76	95.09	5.53	0.01	0.00	242.76	0.00	21.09	605.66	1.00	0.534E-02	0.329E-03	0.318E-02	0.352E-
02	46.723	196.05	95.09	5.54	0.01	0.00	68.75	0.00	21.09	605.66	0.10	0.570E-02	0.319E-03	0.318E-02	0.356E-
02	46.768	124.77	95.09	5.49	0.01	0.00	0.00	0.00	21.09	605.66	0.00	0.605E-02	0.300E-03	0.319E-02	0.359E-
02	46.814	122.39	95.09	5.39	0.01	0.00	0.00	0.00	21.09	605.66	0.00	0.640E-02	0.284E-03	0.321E-02	0.363E-
02	46.862	93.39	95.09	5.28	0.01	0.00	0.00	0.00	21.09	605.66	0.00	0.669E-02	0.277E-03	0.322E-02	0.367E-
02	46.908	55.82	95.08	5.20	0.01	0.00	0.00	0.00	21.08	605.66	0.00	0.647E-02	0.334E-03	0.323E-02	0.367E-

Preprocessor

The preprocessor produces several output files including a file that echoes all control file inputs along with additional information (pre.opt), a warning file that attempts to alert the user to potential problems with inputs (pre.wrn), and an error file that points out serious problems in the input data that will probably prevent the model from running or running correctly. It is important to run the preprocessor periodically to ensure that changes made to various inputs during the course of the project have not introduced problems in the simulation.

Command-line working directory specification

In the windows version of the preprocessor, the user can now supply a command line argument that sets the working directory of the code. Hence, one does not need to copy the preprocessor into every directory. In a batch file, for example, one can execute the following command:

```
preW2_ivf.exe "C:\scott\w2workshop\2009 workshop\waterqual\problem3"
```

The preprocessor now uses the supplied directory (in double quotes) as the working directory for all the files. The command line argument has one blank space between the end of the executable and the first quote. The working directory is now displayed at the top of the window for the preprocessor.

Output (pre.opt)

As in nearly all output, the title cards are echoed at the beginning of the output followed by a complete echoing of all control file input. A description of the input, the FORTRAN variable name used in the control file, and the value of the variable are then output. The sequence of output tries to closely follow the sequence of input in the control file, but in some cases is different as certain types of output are more logically grouped together.

The first information includes variables affecting the time of simulation and the timestep for the simulation. Next is information that is used to set initial conditions and variables that are used to control certain calculations in the model.

EXAMPLE

```
Burnsville Reservoir - March 15 through December 11, 1992
Density placed inflow, point sink outflows
Default hydraulic coefficients
Default light absorption/extinction coefficients
Default kinetic coefficients
Temperature and water quality simulation
Run 8
Testing sensitivity to wind
Wind sheltering set to 0.75
Jim Stiles and Vince Marchese, USACE Huntington District

Time Control
Starting time (Julian day) [TMSTRT] = 75.00
Ending time (Julian day) [TMEND] = 320.00
Year [YEAR] = 1992
# Timestep intervals [NDLT] = 1
```

OUTPUT FILES

PREPROCESSOR

```
Minimum timestep (sec)      [DLTMIN] =    1.0
Timestep day (Julian day)   [DLTD]  =    1.0
Maximum timestep (sec)      [DLTMAX] =   1800.0
Fraction of timestep        [DLTF]   =    0.85
Timestep limitation
  Waterbody 1
    Vertical eddy viscosity [VISC] =  ON
    Internal gravity wave   [CELC] =  ON

Initial Conditions
  Waterbody 1
    Temperature      [T2I] = Downstream vertical profile
    Water type        [WTYPEC] = FRESH water
    Ice thickness     [ICEI] = 0.000 m

Calculations
  Waterbody 1
    Evaporation       [EVC] = OFF
    Precipitation     [PRC] = OFF
    Volume balance    [VBC] = ON
    Energy balance    [EBC] = ON
    Mass balance      [MBC] = ON
    Place inflows     [PQC] = ON
    Wind              [WINDC] = ON
    Inflow            [QINC] = ON
    Outflow           [QOUTC] = ON
    Heat exchange     [HEATC] = ON
    Heat exchange     [SLHTC] = TERM
  Waterbody 1
    read radiation     [SROC] =    OFF
    wind function coefficient a [AFW] =    9.20
    wind function coefficient b [BFW] =    0.46
    wind function coefficient c [CFW] =    2.00
    wind height        [WINDH] =   10.00
    Ryan-Harleman evaporation [RHEVC] =    OFF
```

The next output includes controls for all input interpolation. These are located at various places in the control file, but are grouped together in the output. These are then followed by meteorological parameters that affect wind and surface heat exchange.

EXAMPLE

```
Input Interpolations
  Branch 1
    Inflow              [QINIC] =  ON
    Distributed tributary [DTRIC] = OFF
    Head boundary       [HDIC]  = OFF
  Branch 2
    Inflow              [QINIC] =  ON
    Distributed tributary [DTRIC] = OFF
    Head boundary       [HDIC]  = OFF
  Branch 3
    Inflow              [QINIC] =  ON
    Distributed tributary [DTRIC] = OFF
    Head boundary       [HDIC]  = OFF
  Branch 4
    Inflow              [QINIC] =  ON
    Distributed tributary [DTRIC] = OFF
    Head boundary       [HDIC]  = OFF
  Branch 5
    Inflow              [QINIC] =  ON
    Distributed tributary [DTRIC] = OFF
    Head boundary       [HDIC]  = OFF
  Branch 6
    Inflow              [QINIC] =  ON
    Distributed tributary [DTRIC] = OFF
```

PREPROCESSOR

OUTPUT FILES

```

    Head boundary          [HDIC] = OFF
Waterbody 1
    Meteorology           [METIC] = ON
    Tributary 1           [TRIC] = ON
    Branch 1
        Structure 1       [STRIC] = ON
        Structure 2       [STRIC] = ON
        Structure 3       [STRIC] = ON

Meteorological Parameters
Waterbody 1
    Latitude               [LAT] = 38.80
    Longitude              [LONG] = 80.60
    Axis orientation
        Segment #         2      3      4      5      6      7      8      9      10     11     12     13     14     15
    [PHI0] (rads)          1.22  5.22  4.62  0.65  5.67  3.84  5.08  6.27  0.19  5.58  5.32  0.44  0.35  4.54
        Segment #         21     22     23     24     25     26     27     28     29     30     31     32     33     34
    [PHI0] (rads)          4.82  0.24  6.16  0.04  0.00  0.00  5.24  5.18  4.14  5.01  4.35  4.00  3.30  5.15
        Segment #         40     41     42     43     44     45     46     47     48     49     50     51     52     53
    [PHI0] (rads)          6.13  0.35  0.33  0.00  0.00  0.35  6.20  5.64  0.00  0.00  3.51  3.77  3.40  0.00

```

Variables affecting the transport solution and hydraulics are output next along with variables affecting ice cover.

EXAMPLE

```

Transport Solution
Waterbody 1
    Transport [SLTRC] = QUICKEST
    Theta    [THETA] = 0.55

Hydraulic coefficients
Waterbody 1
    Longitudinal eddy viscosity      [AX] = 1.00 m^2/sec
    Longitudinal eddy diffusivity    [DX] = 1.00 m^2/sec
    Sediment temperature             [TSED] = 11.80 °C
    Coefficient of bottom heat exchange [CBHE] = 0.3 W/m^2/°C

Ice cover
Waterbody 1
    Ice calculations                [ICEC] = OFF
    Solution                        [SLICEC] = DETAIL
    Albedo                          [ALBEDO] = 0.25
    Ice-water heat exchange         [HWI] = 10.00
    Light absorption                 [BETAI] = 0.60
    Light decay                     [GAMMAI] = 0.07

```

Output controls excluding constituents are output next. As in the control file, all constituent related variables are grouped together.

EXAMPLE

```

Output Control
Waterbody 1
    Timestep violations [NVIOL] = OFF
    Horizontal velocity [U], m/s = OFF
    Vertical velocity [W], m/s = OFF
    Temperature [T1], deg C = ON
    Density [RHO], kg/m^3 = OFF
    Vertical eddy viscosity [AZ], m^2/s = OFF
    Velocity shear stress [SHEAR], 1/s^2 = OFF
    Internal shear [ST], m^3/s^2 = OFF
    Bottom shear [SB], m^3/s^2 = OFF
    Longitudinal momentum [ADMX], m^3/s^2 = OFF

```

OUTPUT FILES

PREPROCESSOR

```

Longitudinal momentum [DM], m^3/s^2      = OFF
Horizontal density gradient [HDG], m^3/s^2= OFF
Vertical momentum [ADMZ], m^3/s^2        = OFF
Horizontal pressure gradient [HPG], m^3/s^2= OFF
Gravity term channel slope [GRAV], m^3/s^2= OFF
Waterbody 1
Snapshot      [SNPC] = ON
  Number of time intervals [NSNP] =      7
  Date (Julian day)       [SNPD] =  75.50 139.50 153.50 167.50 195.50 223.60 252.60
  Frequency (days)       [SNPF] = 100.00 100.00 100.00 100.00 100.00 100.00 100.00
Screen        [SCRC] = ON
  Number of time intervals [NSCR] =      1
  Date (Julian day)       [SCRD] =  75.50
  Frequency (days)       [SCRF] =   1.00
Fluxes        [FLXC] = ON
  Number of time intervals [NFLX] =      1
  Date (Julian day)       [FLXD] =  77.70
  Frequency (days)       [FLXF] = 100.00
Vector plot   [VPLC] = ON
  Number of time intervals [NVPL] =      1
  Date (Julian day)       [VPLD] =  75.70
  Frequency (days)       [VPLF] = 100.00
Profile plot   [PRFC] = ON
  Number of time intervals [NPRF] =      7
  Number of stations      [NIPRF] =      1
  Segment location        [IPRF] =     24
  Date (Julian day)       [PRFD] =  75.70 139.50 153.50 167.50 195.50 223.60 252.60
  Frequency (days)       [PRFF] = 100.00 100.00 100.00 100.00 100.00 100.00 100.00
Spreadsheet plot [SPRC] = ON
  Number of time intervals [NSPR] =      7
  Number of stations      [NISPR] =      1
  Segment location        [ISPR] =     24
  Date (Julian day)       [SPRD] =  75.70 139.50 153.50 167.50 195.50 223.60 252.60
  Frequency (days)       [SPRF] = 100.00 100.00 100.00 100.00 100.00 100.00 100.00
Contour plot   [CPLC] = ON
  Number of time intervals [NCPL] =      1
  Date (Julian day)       [CPLD] =  75.70
  Frequency (days)       [CPLF] =  15.00
Time series    [TSRC] = ON
  Number of time intervals [NTSR] =      1
  Date (Julian day)       [TSRD] =  75.70
  Frequency (days)       [TSRF] =   1.00
Restart out    [RSOC] = OFF
Restart in     [RSIC] = OFF

```

Inflow/outflow information is output next.

EXAMPLE

```

Inflow/Outflow
Selective Withdrawal
  Branch      # of structures [NSTR]
    1          3
    2          0
    3          0
    4          0
    5          0
    6          0
Branch 1
  Structure  Type  Width (m)  Elevation (m)  Bottom Layer
    1      POINT    0.0      237.7            38
    2      POINT    0.0      234.7            38
    3      LINE     6.1      231.9            38
Number of withdrawals [NWD] = 0
Number of tributaries [NTR] = 1
segment number      [ITR] =    24

```


PREPROCESSOR

OUTPUT FILES

```
Inflow placement [PTRC] = DISTR
Top elevation    [ETTR] = 2.00
Bottom elevation [EBTR] = 38.00
Distributed tributaries [DTRC]
Branch 1 = OFF
Branch 2 = OFF
Branch 3 = OFF
Branch 4 = OFF
Branch 5 = OFF
Branch 6 = OFF
```

Input and output filenames are then output.

EXAMPLE

```
Input Filenames
Control      = w2_con.npt
Restart      = rsl.npt - not used
Withdrawal   = qwd.npt - not used
Waterbody 1
  Bathymetry      = bth.npt
  Meteorology     = met.npt
  Vertical profile = vpr.npt
  Longitudinal profile = lpr.npt - not used
Branch 1
  Inflow                      = qin_br1.npt
  Inflow temperature         = tin_br1.npt
  Inflow concentrations      = cin_br1.npt
  Outflow                    = qot_br1.npt
  Distributed tributary inflows = qin_br1.npt - not used
  Distributed tributary temperatures = tdt_br1.npt - not used
  Distributed tributary concentrations = cdt_br1.npt - not used
  Precipitation              = pre_br1.npt - not used
  Precipitation temperatures = tpr_br1.npt - not used
  Precipitation concentrations = cpr_br1.npt - not used
  Upstream head              = euh_br1.npt - not used
  Upstream head temperatures = tuh_br1.npt - not used
  Upstream head concentrations = cuh_br1.npt - not used
  Downstream head            = edh_br1.npt - not used
  Downstream head temperatures = tdh_br1.npt - not used
  Downstream head concentrations = cdh_br1.npt - not used
Tributary 1
  Inflow                    = qtr_tr1.npt
  Inflow temperature        = ttr_tr1.npt
  Inflow concentration      = ctr_tr1.npt

Output Filenames
Error      = pre.err
Warning    = pre.wrn
Time series = tsr.opt
Withdrawal = wdo.opt
Waterbody 1
  Snapshot      = snp.opt
  Fluxes        = flx.opt
  Profile       = prf.opt
  Vector plot   = vpl.opt
  Contour plot  = cpl.opt
```

The next section includes all variables affecting water quality simulations including input/output controls, initial concentrations, active constituents, derived variables, kinetic fluxes, and kinetic rates constants.

OUTPUT FILES

PREPROCESSOR

EXAMPLE

Constituents [CCC] = ON
Algal limiting nutrient [LIMC] = OFF
Kinetics update frequency [CUF] = 2

Waterbody 1

State Variables

Constituent [CNAME]	Computation [CAC]	Initial Conc [C2IWB,g/m^3]	Fluxes [CFWBC]	Printout [CPRWBC]
Dissolved solids	ON	-1.000	OFF	ON
Residence time	ON	0.000	OFF	OFF
Suspended solids1	ON	-1.000	OFF	ON
Phosphate	ON	0.020	OFF	ON
Ammonium	ON	0.050	OFF	ON
Nitrate nitrite	ON	0.200	OFF	ON
Dissolved silica	OFF	0.000	OFF	OFF
Particulate silica	OFF	0.000	OFF	OFF
Total Iron	OFF	10.000	OFF	OFF
Labile DOM	ON	0.675	OFF	ON
Refractory_DOM	ON	1.575	OFF	ON
Labile POM	ON	0.750	OFF	ON
Refractory POM	OFF	0.000	OFF	OFF
Algae	ON	0.650	OFF	ON
Dissolved oxygen	ON	-1.000	OFF	ON
Inorganic carbon	OFF	11.910	OFF	OFF
Alkalinity	OFF	40.000	OFF	OFF
Sediments	OFF	0.000	OFF	OFF

Branch 1

State Variables

Constituent [CNAME]	Inflow [CINBRC]	Distributed trib [CDTBRC]	Precipitation [CPRBRC]
Dissolved solids	ON	OFF	OFF
Residence time	OFF	OFF	OFF
Suspended solids1	ON	OFF	OFF
Phosphate	ON	OFF	OFF
Ammonium	ON	OFF	OFF
Nitrate nitrite	ON	OFF	OFF
Dissolved silica	OFF	OFF	OFF
Particulate silica	OFF	OFF	OFF
Total Iron	OFF	OFF	OFF
Labile DOM	ON	OFF	OFF
Refractory_DOM	ON	OFF	OFF
Labile POM	ON	OFF	OFF
Refractory POM	OFF	OFF	OFF
Algae	ON	OFF	OFF
Dissolved oxygen	ON	OFF	OFF
Inorganic carbon	OFF	OFF	OFF
Alkalinity	OFF	OFF	OFF

Branch 2

State Variables

Constituent [CNAME]	Inflow [CINBRC]	Distributed trib [CDTBRC]	Precipitation [CPRBRC]
Dissolved solids	ON	OFF	OFF
Residence time	OFF	OFF	OFF
Suspended solids1	ON	OFF	OFF
Phosphate	ON	OFF	OFF
Ammonium	ON	OFF	OFF
Nitrate nitrite	ON	OFF	OFF
Dissolved silica	OFF	OFF	OFF
Particulate silica	OFF	OFF	OFF
Total Iron	OFF	OFF	OFF
Labile DOM	ON	OFF	OFF
Refractory_DOM	ON	OFF	OFF
Labile POM	ON	OFF	OFF

PREPROCESSOR

OUTPUT FILES

Refractory POM	OFF	OFF	OFF
Algae	ON	OFF	OFF
Dissolved oxygen	ON	OFF	OFF
Inorganic carbon	OFF	OFF	OFF
Alkalinity	OFF	OFF	OFF

Branch 3

State Variables

Constituent [CNAME]	Inflow [CINBRC]	Distributed trib [CDTBRC]	Precipitation [CPRBRC]
Dissolved solids	ON	OFF	OFF
Residence time	OFF	OFF	OFF
Suspended solids1	ON	OFF	OFF
Phosphate	ON	OFF	OFF
Ammonium	ON	OFF	OFF
Nitrate nitrite	ON	OFF	OFF
Dissolved silica	OFF	OFF	OFF
Particulate silica	OFF	OFF	OFF
Total Iron	OFF	OFF	OFF
Labile DOM	ON	OFF	OFF
Refractory_DOM	ON	OFF	OFF
Labile POM	ON	OFF	OFF
Refractory POM	OFF	OFF	OFF
Algae	ON	OFF	OFF
Dissolved oxygen	ON	OFF	OFF
Inorganic carbon	OFF	OFF	OFF
Alkalinity	OFF	OFF	OFF

Branch 4

State Variables

Constituent [CNAME]	Inflow [CINBRC]	Distributed trib [CDTBRC]	Precipitation [CPRBRC]
Dissolved solids	ON	OFF	OFF
Residence time	OFF	OFF	OFF
Suspended solids1	ON	OFF	OFF
Phosphate	ON	OFF	OFF
Ammonium	ON	OFF	OFF
Nitrate nitrite	ON	OFF	OFF
Dissolved silica	OFF	OFF	OFF
Particulate silica	OFF	OFF	OFF
Total Iron	OFF	OFF	OFF
Labile DOM	ON	OFF	OFF
Refractory_DOM	ON	OFF	OFF
Labile POM	ON	OFF	OFF
Refractory POM	OFF	OFF	OFF
Algae	ON	OFF	OFF
Dissolved oxygen	ON	OFF	OFF
Inorganic carbon	OFF	OFF	OFF
Alkalinity	OFF	OFF	OFF

Branch 5

State Variables

Constituent [CNAME]	Inflow [CINBRC]	Distributed trib [CDTBRC]	Precipitation [CPRBRC]
Dissolved solids	ON	OFF	OFF
Residence time	OFF	OFF	OFF
Suspended solids1	ON	OFF	OFF
Phosphate	ON	OFF	OFF
Ammonium	ON	OFF	OFF
Nitrate nitrite	ON	OFF	OFF
Dissolved silica	OFF	OFF	OFF
Particulate silica	OFF	OFF	OFF
Total Iron	OFF	OFF	OFF
Labile DOM	ON	OFF	OFF
Refractory_DOM	ON	OFF	OFF
Labile POM	ON	OFF	OFF
Refractory POM	OFF	OFF	OFF
Algae	ON	OFF	OFF

OUTPUT FILES

PREPROCESSOR

Dissolved oxygen	ON	OFF	OFF
Inorganic carbon	OFF	OFF	OFF
Alkalinity	OFF	OFF	OFF

Branch 6

State Variables

Constituent [CNAME]	Inflow [CINBRC]	Distributed trib [CDTBRC]	Precipitation [CPRBRC]
Dissolved solids	ON	OFF	OFF
Residence time	OFF	OFF	OFF
Suspended solids1	ON	OFF	OFF
Phosphate	ON	OFF	OFF
Ammonium	ON	OFF	OFF
Nitrate nitrite	ON	OFF	OFF
Dissolved silica	OFF	OFF	OFF
Particulate silica	OFF	OFF	OFF
Total Iron	OFF	OFF	OFF
Labile DOM	ON	OFF	OFF
Refractory_DOM	ON	OFF	OFF
Labile POM	ON	OFF	OFF
Refractory POM	OFF	OFF	OFF
Algae	ON	OFF	OFF
Dissolved oxygen	ON	OFF	OFF
Inorganic carbon	OFF	OFF	OFF
Alkalinity	OFF	OFF	OFF

Derived Variables

Constituent [CDNAME]	Computation [CDWBC]
Dissolved organic carbon, g/m ³	OFF
Particulate organic carbon, g/m ³	OFF
Total organic carbon, g/m ³	OFF
Dissolved organic nitrogen, g/m ³	OFF
Particulate organic nitrogen, g/m ³	OFF
Total organic nitrogen, g/m ³	OFF
Total nitrogen, g/m ³	OFF
Dissolved organic phosphorus, mg/m ³	OFF
Particulate organic phosphorus, mg/m ³	OFF
Total organic phosphorus, mg/m ³	OFF
Total phosphorus, mg/m ³	OFF
Algal production, g/m ² /day	OFF
Chlorophyll a, mg/m ³	OFF
Total algae, g/m ³	OFF
Oxygen gas saturation, %	OFF
Total suspended solids, g/m ³	OFF
Total inorganic suspended solids, g/m ³	OFF
Total Kheldahl nitrogen, g/m ³	OFF
Carbonaceous ultimate BOD, g/m ³	OFF
pH	OFF
Carbon dioxide, g/m ³	OFF
Bicarbonate, g/m ³	OFF
Carbonate, g/m ³	OFF

Tributary 1

State Variables

Constituent [CNAME]	Inflow [CINTRC]
Dissolved solids	ON
Residence time	OFF
Suspended solids1	ON
Phosphate	ON
Ammonium	ON
Nitrate nitrite	ON
Dissolved silica	OFF
Particulate silica	OFF
Total Iron	OFF
Labile DOM	ON
Refractory_DOM	ON

PREPROCESSOR

OUTPUT FILES

Labile POM	ON
Refractory POM	OFF
Algae	ON
Dissolved oxygen	ON
Inorganic carbon	OFF
Alkalinity	OFF

Waterbody 1

Constituent Rates

Constituent	Rate/Coefficient	
Residence time	Temperature mult	[CGQ10] = 0.000
	0-Order Decay	[CG0DK] = -1.000/day
	1-Order Decay	[CG1DK] = 0.000/day
	Settling	[CGS] = 0.000 m/day
Suspended solids	Settling	[SSS] = 1.000 m/day
Labile DOM	Decay	[LDOMDK] = 0.120 /day
	to refractory	[LRDDK] = 0.001 /day
Refractory DOM	Decay	[RDOMDK] = 0.001 /day
Labile POM	Decay	[LPOMDK] = 0.060 /day
	to refractory	[LRPDK] = 0.001 /day
	Settling	[POMS] = 0.350 m/day
Refractory POM	Decay	[RPOMDK] = 0.010 /day
Algal group 1	Growth	[AG] = 1.100 /day
	Mortality	[AM] = 0.010 /day
	Excretion	[AE] = 0.010 /day
	Respiration	[AR] = 0.020 /day
	Settling	[AS] = 0.140 m/day
	Org-P	[ALGP] = 0.011
	Org-N	[ALGN] = 0.080
	Org-C	[ALGC] = 0.450
	Org-Si	[ALGSI] = 0.000
	Chl a/algae ratio	[ACHLA] = 65.000 ug/mg
	Fraction algae to POM	[APOM] = 0.80
Phosphorous	Release	[PO4R] = 0.015 g/m^2/day
Ammonium	Decay	[NH4DK] = 0.120 /day
	Release	[NH4R] = 0.080 g/m^2/day
Nitrate-Nitrite	Decay	[NO3DK] = 0.102 /day
Silica	Decay	[PSIDK] = 0.100 /day
	Release	[DSIR] = 0.300 g/m^2/day
	Settling	[PSIS] = 0.100 m/day
Sediment	Decay	[SEDDK] = 0.080 /day
Iron	Settling	[FES] = 2.000 m/day
	Release	[FER] = 0.500 g/m^2/day
Oxygen	Sediment demand	[SOD] = 1.0 1.0 1.0 1.0 1.0 1.0 1.0
		1.0 1.0 1.0 1.0 1.0 1.0 1.0
		1.0 1.0 1.0 1.0 1.0 1.0 1.0
		1.0 1.0 1.0 1.0 1.0 1.0 1.0
		1.0 1.0 1.0 1.0
	SOD fraction	[FSOD] = 1.0
	Sediment fraction	[FSOD] = 1.0

Upper Temperature Bounds

Constituent	Rate	Upper	Max Upper
Ammonium	Decay	[NH4T1] = 5.0	[NH4T2] = 25.0
Nitrate	Decay	[NO3T1] = 5.0	[NO3T2] = 25.0
Organic	Decay	[OMT1] = 4.0	[OMT2] = 20.0
Sediment	Decay	[SEDT1] = 4.0	[SEDT2] = 20.0
Algal group 1	Growth	[AT1] = 10.0	[AT2] = 30.0

Lower Temperature Bounds

Constituent	Rate	Lower	Max Lower
Algal group 1	Growth	[AT3] = 35.0	[AT4] = 40.0

Stoichiometric Equivalence

Oxygen	
Ammonium	[O2NH4] = 4.57
Organic matter	[O2OM] = 1.40
Respiration	[O2AR] = 1.40
Algal growth	[O2AG] = 1.40
Organic Matter	

OUTPUT FILES

PREPROCESSOR

```
Carbon      [BIOC] = 0.450
Phosphorous [BIOP] = 0.011
Nitrogen    [BION] = 0.080
Silica      [BIOSI] = 0.180
Half Saturation
Algal group 1
Phosphorous [AHSP] = 0.009 g/m^3
Nitrogen    [AHSN] = 0.014 g/m^3
Silica      [AHSSI] = 0.000 g/m^3
Light
Attenuation
Surface layer [BETA] = 0.45
Water        [EXH2O] = 0.55 /m
Inorganic solids [EXSS] = 0.01 /m
Organic solids [EXOM] = 0.01 /m
Algal group 1 [EXA] = 0.20 /m
Saturation Intensity
Algal group 1 [ASAT] = 150.0 W/m^2
Diffusion
Oxygen       [DMO2] = 2.040E-09 m^2/g
Carbon dioxide [DMCO2] = 1.630E-09 m^2/g
Partitioning Coefficients
Phosphorous [PARTP] = 1.200 m^3/g
Silica      [PARTSI] = 0.200 m^3/g
Miscellaneous Constants
Aerobic half saturation coeff[KDO] = 0.20 g/m^3
CO2 sediment release [CO2R] = 0.10 g/m^2/day
```

The next section contains summary statistics regarding inflows, temperatures, and inflow constituent concentrations. This is useful for screening time-varying input files if the user has not already plotted up and screened them.

EXAMPLE

```
Water Balance Summary
Waterbody 1
  total inflows      total outflows
  average maximum    average maximum
  6.22  124.38      6.25  38.19

Branch 1
  Inflows
    total
    average maximum
    5.29  124.38
    upstream      tributaries      distributed tributaries      precipitation
    average maximum average maximum average maximum average maximum
    5.22  124.38   0.07  1.60      0.00  0.00      0.00  0.00
  Outflows
    outlets      withdrawals
    average maximum average maximum
    6.25  38.19   0.00  0.00

Branch Inflow Temperature Min/Max
Branch(JB)      Maximum Temp(C)      Minimum Temp(C)
1              0.200E+02              0.187E+01

Tributary Inflow Temperature Min/Max
Tributary(JT)    Maximum Temp(C)      Minimum Temp(C)
1              0.178E+02              0.320E+01
```

PREPROCESSOR

OUTPUT FILES

Inflow Constituent Statistics

Branch 1

Constituent name	Average	Maximum	Minimum
Dissolved solids	49.576	99.000	10.000
Suspended solids1	4.467	156.000	2.000
Phosphate	0.020	0.020	0.020
Ammonium	0.100	0.100	0.100
Nitrate nitrite	0.200	0.200	0.200
Labile DOM	0.382	0.382	0.382
Refractory_DOM	0.892	0.892	0.892
Labile POM	0.425	0.425	0.425
Algae	0.000	0.000	0.000
Dissolved oxygen	9.851	14.000	0.000

Geometric information follows including all information in the control and bathymetry file along with a computed area-volume-elevation table that also includes average width and depth. Theoretical hydraulic residence at each elevation is also included if the waterbody is a reservoir. The location of the surface layer is indicated by a [KT] next to the layer number. The computational grid showing cell widths is then output, at the top of which is the segment number and the distance to the end of the branch in m.

EXAMPLE

Geometry

Overall Grid

Total

```

segments [IMX] = 58
layers   [KMX] = 39
branches [NBR] = 6

```

Waterbody 1

```

Segments           = 1-58
Branches           = 1-6
Bottom elevation [ELBOT] = 228.60 m
Surface layer      [KT] = 23
Vertical spacing   [H]

```

Layer	1	2	3	4	5	6	7	8	9	10	11	12	13	14
	15	16	17	18	19									
Height (m)	0.6	0.6	0.6	0.6	0.6	0.6	0.6	0.6	0.6	0.6	0.6	0.6	0.6	0.6
	0.6	0.6	0.6	0.6	0.6									
Layer	20	21	22	23	24	25	26	27	28	29	30	31	32	33
	34	35	36	37	38									
Height (m)	0.6	0.6	0.6	0.6	0.6	0.6	0.6	0.6	0.6	0.6	0.6	0.6	0.6	0.6
	0.6	0.6	0.6	0.6	0.6									
Layer	39													
Height (m)	0.6													

Branch 1

```

Upstream segment [US] = 2      Downstream segment [DS] = 24
Upstream head segment [UHS] = 0 Downstream head segment [DHS] = 0

```

Branch 2

```

Upstream segment [US] = 27     Downstream segment [DS] = 36
Upstream head segment [UHS] = 0 Downstream head segment [DHS] = 19

```

Branch 3

```

Upstream segment [US] = 39     Downstream segment [DS] = 42
Upstream head segment [UHS] = 0 Downstream head segment [DHS] = 17

```

Branch 4

```

Upstream segment [US] = 45     Downstream segment [DS] = 47
Upstream head segment [UHS] = 0 Downstream head segment [DHS] = 21

```

Branch 5

```

Upstream segment [US] = 50     Downstream segment [DS] = 52
Upstream head segment [UHS] = 0 Downstream head segment [DHS] = 36

```

Branch 6

```

Upstream segment [US] = 55     Downstream segment [DS] = 57
Upstream head segment [UHS] = 0 Downstream head segment [DHS] = 32

```

OUTPUT FILES

PREPROCESSOR

Initial Branch Volume [VOLB] = 9495622.2 m³

Branch 1 Volume-Area-Elevation Table

Layer	Elevation (m)	Area (1.0E6 m ²)	Volume (1.0E6 m ³)	Active Cells	Average depth (m)	Average width (m)
2	251.17	5.171	58.316	630	11.3	262.48
3	250.56	5.002	55.162	607	11.0	253.90
4	249.95	4.923	52.111	584	10.6	249.88
5	249.34	4.828	49.108	563	10.2	245.09
6	248.73	4.706	46.163	542	9.8	238.89
7	248.12	4.624	43.292	521	9.4	234.74
8	247.51	4.522	40.471	500	9.0	229.52
9	246.90	4.350	37.713	479	8.7	220.84
10	246.29	4.191	35.059	458	8.4	212.73
11	245.68	4.059	32.503	437	8.0	206.02
12	245.07	3.835	30.027	417	7.8	194.70
13	244.46	3.661	27.688	397	7.6	185.86
14	243.85	3.570	25.454	378	7.1	181.21
15	243.24	3.476	23.277	359	6.7	176.45
16	242.63	3.363	21.156	341	6.3	170.73
17	242.02	3.083	19.104	323	6.2	156.48
18	241.41	2.972	17.224	305	5.8	150.88
19	240.80	2.878	15.411	287	5.4	146.07
20	240.19	2.777	13.655	269	4.9	140.96
21	239.58	2.626	11.962	251	4.6	133.29
22	238.97	2.485	10.360	233	4.2	126.14
23 KT	238.36	2.413	8.844	216	3.7	122.50
24	237.75	2.282	7.372	199	3.2	115.85
25	237.14	1.927	5.980	182	3.1	97.83
26	236.53	1.716	4.804	165	2.8	87.12
27	235.92	1.290	3.757	148	2.9	65.48
28	235.31	1.150	2.970	132	2.6	58.38
29	234.70	0.995	2.269	116	2.3	50.52
30	234.09	0.839	1.662	101	2.0	42.61
31	233.48	0.595	1.150	86	1.9	30.19
32	232.87	0.410	0.787	71	1.9	20.84
33	232.26	0.306	0.536	56	1.8	15.51
34	231.65	0.225	0.350	41	1.6	11.41
35	231.04	0.145	0.213	28	1.5	7.34
36	230.43	0.106	0.125	17	1.2	5.39
37	229.82	0.074	0.060	8	0.8	3.76
38	229.21	0.024	0.015	3	0.6	1.23

Initial Branch Volume [VOLB] = 2111233.1 m³

Branch 2 Volume-Area-Elevation Table

Layer	Elevation (m)	Area (1.0E6 m ²)	Volume (1.0E6 m ³)	Active Cells	Average depth (m)	Average width (m)
2	251.17	1.253	13.852	270	11.1	166.71
3	250.56	1.224	13.088	260	10.7	162.83
4	249.95	1.202	12.341	250	10.3	159.89
5	249.34	1.179	11.608	240	9.8	156.87
6	248.73	1.155	10.889	230	9.4	153.75
7	248.12	1.133	10.185	220	9.0	150.82
8	247.51	1.104	9.493	210	8.6	146.96
9	246.90	1.082	8.819	200	8.2	143.99
10	246.29	1.046	8.159	190	7.8	139.25
11	245.68	1.014	7.521	180	7.4	134.98
12	245.07	0.987	6.902	170	7.0	131.38
13	244.46	0.957	6.300	160	6.6	127.41
14	243.85	0.926	5.716	150	6.2	123.22
15	243.24	0.834	5.151	140	6.2	110.92
16	242.63	0.778	4.643	130	6.0	103.53

PREPROCESSOR

OUTPUT FILES

17	242.02	0.701	4.168	120	5.9	93.34
18	241.41	0.656	3.740	110	5.7	87.24
19	240.80	0.595	3.340	100	5.6	79.21
20	240.19	0.566	2.977	92	5.3	75.36
21	239.58	0.548	2.632	84	4.8	72.89
22	238.97	0.534	2.298	76	4.3	71.10
23 KT	238.36	0.517	1.972	68	3.8	68.81
24	237.75	0.488	1.656	60	3.4	64.89
25	237.14	0.471	1.359	53	2.9	62.69
26	236.53	0.447	1.071	46	2.4	59.53
27	235.92	0.370	0.798	39	2.2	49.26
28	235.31	0.339	0.573	32	1.7	45.10
29	234.70	0.216	0.366	25	1.7	28.68
30	234.09	0.153	0.234	18	1.5	20.31
31	233.48	0.094	0.141	14	1.5	12.52
32	232.87	0.074	0.084	10	1.1	9.82
33	232.26	0.035	0.039	7	1.1	4.61
34	231.65	0.024	0.018	4	0.7	3.18
35	231.04	0.005	0.003	1	0.6	0.69
36	230.43	0.000	0.000	0	0.0	0.00
37	229.82	0.000	0.000	0	0.0	0.00
38	229.21	0.000	0.000	0	0.0	0.00

OUTPUT FILES

PREPROCESSOR

Waterbody 1 Bathymetry [B], m											
	2	3	4	5	6	7	8	9	10	11	12
	19162	18000	16925	15787	14762	13925	13100	12337	11400	10400	9410
1	0.	0.	0.	0.	0.	0.	0.	0.	0.	0.	0.
2	23.	23.	59.	169.	169.	169.	137.	136.	216.	216.	442.
3	10.	14.	58.	168.	168.	168.	134.	131.	213.	213.	402.
4	0.	0.	56.	166.	166.	166.	130.	130.	212.	212.	401.
5	0.	0.	55.	163.	163.	163.	126.	126.	204.	204.	393.
6	0.	0.	52.	148.	148.	148.	123.	123.	201.	201.	387.
7	0.	0.	50.	140.	143.	143.	122.	120.	198.	198.	381.
8	0.	0.	33.	133.	140.	140.	119.	116.	195.	195.	378.
9	0.	0.	28.	128.	133.	133.	116.	113.	192.	192.	332.
10	0.	0.	26.	93.	131.	131.	114.	110.	187.	187.	320.
11	0.	0.	0.	73.	128.	128.	111.	105.	183.	183.	314.
12	0.	0.	0.	36.	93.	123.	108.	102.	180.	180.	277.
13	0.	0.	0.	0.	73.	120.	98.	98.	175.	175.	259.
14	0.	0.	0.	0.	36.	119.	96.	96.	172.	172.	256.
15	0.	0.	0.	0.	0.	119.	94.	94.	171.	171.	250.
16	0.	0.	0.	0.	0.	116.	93.	93.	168.	168.	219.
17	0.	0.	0.	0.	0.	111.	91.	81.	98.	98.	189.
18	0.	0.	0.	0.	0.	101.	90.	78.	85.	85.	186.
19	0.	0.	0.	0.	0.	93.	88.	73.	75.	75.	180.
20	0.	0.	0.	0.	0.	73.	84.	69.	64.	64.	177.
21	0.	0.	0.	0.	0.	36.	40.	67.	53.	53.	174.
22	0.	0.	0.	0.	0.	0.	32.	62.	46.	46.	155.
23 KT	0.	0.	0.	0.	0.	0.	30.	52.	43.	43.	152.
24	0.	0.	0.	0.	0.	0.	27.	49.	41.	41.	131.
25	0.	0.	0.	0.	0.	0.	16.	43.	37.	37.	125.
26	0.	0.	0.	0.	0.	0.	6.	24.	34.	34.	122.
27	0.	0.	0.	0.	0.	0.	0.	23.	30.	30.	37.
28	0.	0.	0.	0.	0.	0.	0.	18.	26.	26.	27.
29	0.	0.	0.	0.	0.	0.	0.	0.	20.	20.	18.
30	0.	0.	0.	0.	0.	0.	0.	0.	17.	17.	15.
31	0.	0.	0.	0.	0.	0.	0.	0.	15.	15.	12.
32	0.	0.	0.	0.	0.	0.	0.	0.	13.	13.	11.
33	0.	0.	0.	0.	0.	0.	0.	0.	10.	10.	9.
34	0.	0.	0.	0.	0.	0.	0.	0.	0.	0.	6.
35	0.	0.	0.	0.	0.	0.	0.	0.	0.	0.	0.
36	0.	0.	0.	0.	0.	0.	0.	0.	0.	0.	0.
37	0.	0.	0.	0.	0.	0.	0.	0.	0.	0.	0.
38	0.	0.	0.	0.	0.	0.	0.	0.	0.	0.	0.
39	0.	0.	0.	0.	0.	0.	0.	0.	0.	0.	0.

PREPROCESSOR

OUTPUT FILES

Finally, initial conditions for the water surface deviation, temperature, and constituent concentrations are output. The user should check these to ensure that the initial concentrations are correct, particularly when using the vertical and/or longitudinal profile files to set initial conditions. Inactive segments are output to ensure the user realizes that the initial water surface has caused upstream segments to be subtracted. The example illustrates this.

OUTPUT FILES

PREPROCESSOR

EXAMPLE

```
Water Surface [Z],
      2      3      4      5      6      7      8      9      10     11     12     13
    -0.2700 -0.2700 -0.2700 -0.2700 -0.2700 -0.2700 -0.2700 -0.2700 -0.2700 -0.2700 -0.2700 -0.2700

Temperature [T1], deg C
      2      3      4      5      6      7      8      9      10     11     12     13
23      5.500  5.500  5.500  5.500  5.500  5.500  5.500  5.500  5.500  5.500  5.500
24      5.500  5.500  5.500  5.500  5.500  5.500  5.500  5.500  5.500  5.500  5.500
25      5.500  5.500  5.500  5.500  5.500  5.500  5.500  5.500  5.500  5.500  5.500
26      5.400  5.400  5.400  5.400  5.400  5.400  5.400  5.400  5.400  5.400  5.400
27      5.400  5.400  5.400  5.400  5.400  5.400  5.400  5.400  5.400  5.400  5.400
28      5.500  5.500  5.500  5.500  5.500  5.500  5.500  5.500  5.500  5.500  5.500
29      5.400  5.400  5.400  5.400  5.400  5.400  5.400  5.400  5.400  5.400  5.400
30      5.300  5.300  5.300  5.300  5.300  5.300  5.300  5.300  5.300  5.300  5.300
31      5.300  5.300  5.300  5.300  5.300  5.300  5.300  5.300  5.300  5.300  5.300
32      5.400  5.400  5.400  5.400  5.400  5.400  5.400  5.400  5.400  5.400  5.400
33      5.300  5.300  5.300  5.300  5.300  5.300  5.300  5.300  5.300  5.300  5.300
34      5.200  5.200
```

Warning Messages (pre.wrn)

The preprocessor does an extensive check of inputs in order to determine if inputs “make sense”. For many cases, it is easy to determine if the input is valid or not. For these cases, information is written to the error output file (pre.err) if the information is invalid. For instance, an algal growth rate that is less than the respiration rate. However, because the model is so flexible, certain inputs are not necessarily errors, but should be flagged so that the user can check to ensure that what they have input is indeed what they mean to be doing. Additionally, when kinetic rates differ from valid ranges or a specific value that should not normally be changed, a warning message is also generated.

For example, the preprocessor warns the user that certain active constituents are given a zero initial concentration, are not included in branch inflows, or a number of other things that are okay to do, but need to be checked to see if this is what the user really wants to do. This is entirely analogous to a FORTRAN compiler that will issue warning and error messages. Warning messages are meant to alert the user to potential problems. Error messages are meant to alert the user that they cannot continue until the problem is fixed.

All warning messages include a concise statement in English showing what the problem is. Also included is the FORTRAN variable name as it appears in the input file header along with its value where appropriate. This is illustrated in the following example.

EXAMPLE

```
Epiphyton excretion rate [EE=0.000] < 0.001 for epiphyton group 1
Oxygen to algal respiration stoichiometry [O2AR=1.400] /= 1.1 for waterbody 1
Phosphorus/organic matter stoichiometry [ORGP=0.011] /= 0.005 for waterbody 1
Water surface elevation is below bottom elevation at segment 1
Water surface elevation is below bottom elevation at segment 2
Water surface elevation is below bottom elevation at segment 3
Water surface elevation is below bottom elevation at segment 4
Water surface elevation is below bottom elevation at segment 5
Water surface elevation is below bottom elevation at segment 6
Water surface elevation is below bottom elevation at segment 7
Water surface elevation is below bottom elevation at segment 26
Water surface elevation is below bottom elevation at segment 27
Water surface elevation is below bottom elevation at segment 28
Water surface elevation is below bottom elevation at segment 44
Water surface elevation is below bottom elevation at segment 45
Water surface elevation is below bottom elevation at segment 49
Water surface elevation is below bottom elevation at segment 50
```

In the above example, the user is warned that the epiphyton excretion rate is less than the recommended minimum value. Likewise, the stoichiometric relationships are flagged as these should not be changed from their default values unless the user has data that indicates a different stoichiometry. The remaining warning messages inform the user that part of the system is dry based on the given initial water surface elevation.

A very important point – the user should not assume that because there are no warnings generated that there are no problems with inputs. It is not possible to check all possible combinations of inputs, so there may be problems that were not flagged.

Error Messages (pre.err)

Input errors that will prevent the model from running correctly or running at all are extensively screened and, when found, are included in the preprocessor error output file. All error messages include a concise statement in English what the problem is along with the FORTRAN variable name as it appears in the input file header and its input value where appropriate. This is illustrated in the following example.

EXAMPLE

```
Starting time [TMSTRT=75.000] < ending time [TMEND=-320.000]
Timestep fraction [DLTF(1)=-0.850] <= 0.0
Internal gravity wave limitation control [CELC= on] /= " ON" or "OFF" for waterbody 1
Heat exchange solution control [SLHTC= term] /= " TERM" or " ET" for waterbody 1
Vertical advection time weighting [THETA=-0.550] < 0.0 for waterbody 1
Selective withdrawal elevation [ESTR=137.700] < the bottom active cell elevation
```

Spreadsheet Profile Plot

The spreadsheet profile output was designed to be easily imported into a spreadsheet program for plotting vertical profiles of temperature, constituents, and derived constituents. Output consists of the variable name, Julian date, depth below water surface, elevation, and temperature and/or concentrations for the output segment. Additional segments each contain a depth, elevation, and temperature/concentration column and are continued to the right. Whenever a depth or vertical layer is part of the channel bottom, a value of -99 is placed in the cell. Note that versions 3.5 and earlier had a negative depth for ease of plotting, but most graphics packages allow for reversing the axis and this was eliminated starting in V3.6.

EXAMPLE

Constituent	Julian_day	Depth	Elevation	Seg_24
Temperature	75.703	0.403	238.152	6.04
Temperature	75.703	1.110	237.444	5.86
Temperature	75.703	1.720	236.834	5.65
Temperature	75.703	2.330	236.224	5.50
Temperature	75.703	2.940	235.614	5.41
Temperature	75.703	3.550	235.004	5.34
Temperature	75.703	4.160	234.394	5.30
Temperature	75.703	4.770	233.784	5.28
Temperature	75.703	5.380	233.174	5.31
Temperature	75.703	5.990	232.564	5.34
Temperature	75.703	6.600	231.954	5.33
Temperature	75.703	7.210	231.344	5.32
Temperature	75.703	7.820	230.734	5.31
Temperature	75.703	8.430	230.124	5.31
Temperature	75.703	9.040	229.514	5.31
Temperature	75.703	9.650	228.904	5.31
Dissolved solids, g/m ³	75.703	0.403	238.152	0.42E+02
Dissolved solids, g/m ³	75.703	1.110	237.444	0.42E+02
Dissolved solids, g/m ³	75.703	1.720	236.834	0.42E+02
Dissolved solids, g/m ³	75.703	2.330	236.224	0.42E+02
Dissolved solids, g/m ³	75.703	2.940	235.614	0.42E+02
Dissolved solids, g/m ³	75.703	3.550	235.004	0.42E+02
Dissolved solids, g/m ³	75.703	4.160	234.394	0.42E+02
Dissolved solids, g/m ³	75.703	4.770	233.784	0.42E+02
Dissolved solids, g/m ³	75.703	5.380	233.174	0.47E+02
Dissolved solids, g/m ³	75.703	5.990	232.564	0.56E+02
Dissolved solids, g/m ³	75.703	6.600	231.954	0.61E+02
Dissolved solids, g/m ³	75.703	7.210	231.344	0.62E+02
Dissolved solids, g/m ³	75.703	7.820	230.734	0.62E+02
Dissolved solids, g/m ³	75.703	8.430	230.124	0.62E+02
Dissolved solids, g/m ³	75.703	9.040	229.514	0.62E+02
Dissolved solids, g/m ³	75.703	9.650	228.904	0.62E+02
Suspended solids1, g/m ³	75.703	0.403	238.152	0.60E+00
Suspended solids1, g/m ³	75.703	1.110	237.444	0.76E+00
Suspended solids1, g/m ³	75.703	1.720	236.834	0.83E+00
Suspended solids1, g/m ³	75.703	2.330	236.224	0.86E+00
Suspended solids1, g/m ³	75.703	2.940	235.614	0.87E+00
Suspended solids1, g/m ³	75.703	3.550	235.004	0.88E+00
Suspended solids1, g/m ³	75.703	4.160	234.394	0.88E+00
Suspended solids1, g/m ³	75.703	4.770	233.784	0.86E+00
Suspended solids1, g/m ³	75.703	5.380	233.174	0.90E+00
Suspended solids1, g/m ³	75.703	5.990	232.564	0.14E+01
Suspended solids1, g/m ³	75.703	6.600	231.954	0.22E+01
Suspended solids1, g/m ³	75.703	7.210	231.344	0.28E+01
Suspended solids1, g/m ³	75.703	7.820	230.734	0.29E+01
Suspended solids1, g/m ³	75.703	8.430	230.124	0.30E+01
Suspended solids1, g/m ³	75.703	9.040	229.514	0.30E+01
Suspended solids1, g/m ³	75.703	9.650	228.904	0.30E+01

Profile Plot

The profile plot output file was originally developed to provide data for a plotting package from Computer Associates called DISSPLA. This was a popular set of FORTRAN callable subroutines developed back in the 1970's for visualizing scientific computing. The vertical temperature plots with statistics presented in Chapter 3 were produced using a DISSPLA compatible software package developed for the PC. If the user should decide to develop their own plotting program, then the following describes the information located in the [profile plot output file](#).

As in most other output files, the card titles are included for identifying the run prior to plotting and also for including information about the run on the plot.

```
Burnsville Reservoir - March 15 through December 11, 1992
Density placed inflow, point sink outflows
Default hydraulic coefficients
Default light absorption/extinction coefficients
Default kinetic coefficients
Temperature and water quality simulation
Run 8
Testing sensitivity to wind
Wind sheltering set to 0.75
Jim Stiles and Vince Marchese, USACE Huntington District
Model run at 13:18:39 on 07/23/02
```

The next line reports:

1. maximum number of layers [KMX]
2. number of segments for which information is output [NIPRF]
3. total number of output dates [NDSP]
4. total number of constituents regardless of whether they are included in the simulations [NCT]
5. total number of derived constituents regardless of whether they are included in the output [NDC]
6. pointer to the profile date currently in effect [\[PRFDP\]](#)
7. waterbody surface layer [KTWB]
8. logical variable that is T if constituents are simulated, otherwise F

```
39      1      3      17      23      12      1      23 T
```

The next line reports the segment(s) output [\[IPRF\]](#):

```
18      24
```

The next three lines report which constituents are active:

```
ON  ON OFF  ON  ON  ON  ON OFF OFF OFF  ON  ON  ON OFF  ON  ON OFF OFF OFF OFF
OFF OFF OFF OFF OFF OFF OFF OFF OFF OFF OFF OFF OFF OFF OFF OFF OFF OFF OFF
OFF
```

Constituent and derived constituent names are included in the next 21 lines:

```
Temperature, °C          Dissolved solids, g/m^3
Residence time, days     Suspended solids1, g/m^3
Phosphate, mg/m^3        Ammonium, mg/m^3
```


PROFILE PLOT

OUTPUT FILES

```

Nitrate nitrite, g/m^3      Dissolved silica, g/m^3
Particulate silica, g/m^3  Total Iron, g/m^3
Labile DOM, g/m^3          Refractory DOM, g/m^3
Labile POM, g/m^3          Refractory POM, g/m^3
Algae, g/m^3               Dissolved oxygen, g/m^3
Inorganic carbon, g/m^3    Alkalinity, g/m^3
Dissolved organic carbon, g/m^3
Total organic carbon, g/m^3
Particulate organic nitrogen, g/m^3
Total nitrogen, g/m^3
Particulate organic phosphorus, mg/m^3
Total phosphorus, mg/m^3
Chlorophyll a, mg/m^3
Oxygen gas saturation, %
Total inorganic suspended solids, g/m^3
Carbonaceous ultimate BOD, g/m^3
Carbon dioxide, g/m^3
Carbonate, g/m^3
Particulate organic carbon, g/m^3
Dissolved organic nitrogen, g/m^3
Total organic nitrogen, g/m^3
Dissolved organic phosphorus, mg/m^3
Total organic phosphorus, mg/m^3
Algal production, g/m^2/day
Total algae, g/m^3
Total suspended solids, g/m^3
Total Kheldahl nitrogen, g/m^3
pH
Bicarbonate, g/m^3

```

The constituent and derived constituent numbers follow on the next line. Temperature is always considered constituent 1 and derived constituents continue increasing from the last constituent number.

```

1  2  3  4  5  6  7  11  12  13  15  16

```

The bottom active layer for each output segment is given on the next line.

```

36  38

```

Layer heights for layers 1 through the maximum [KMX] are output next.

```

0.61  0.61  0.61  0.61  0.61  0.61  0.61  0.61  0.61  0.61
0.61  0.61  0.61  0.61  0.61  0.61  0.61  0.61  0.61  0.61
0.61  0.61  0.61  0.61  0.61  0.61  0.61  0.61  0.61  0.61
0.61  0.61  0.61  0.61  0.61  0.61  0.61  0.61  0.61  0.61

```

Initial temperatures/constituent concentrations for each segment specified in the profile segment card are then output. Initial temperatures/constituent concentrations are always output in case the user wants to include these in their plot to show how much change has occurred over time. The first line contains the constituent abbreviation and the number of values corresponding to the number of active layers output. The next line(s) contain the temperatures/concentrations for a given segment.

```

TEMP      14
5.50      5.50      5.50      5.40      5.40      5.50      5.40      5.30
5.30      5.40      5.30      5.20      5.20      5.20
TEMP      16
5.50      5.50      5.50      5.40      5.40      5.50      5.40      5.30
5.30      5.40      5.30      5.20      5.20      5.20      5.20      5.20
TDS       14
0.400E+02 0.400E+02 0.400E+02 0.400E+02 0.450E+02 0.500E+02 0.550E+02 0.680E+02
0.700E+02 0.650E+02 0.600E+02 0.550E+02 0.500E+02 0.450E+02
TDS       16
0.400E+02 0.400E+02 0.400E+02 0.400E+02 0.450E+02 0.500E+02 0.550E+02 0.680E+02
0.700E+02 0.650E+02 0.600E+02 0.550E+02 0.500E+02 0.450E+02 0.400E+02 0.340E+02
ISS       14
0.100E+01 0.100E+01 0.100E+01 0.100E+01 0.100E+01 0.100E+01 0.100E+01 0.100E+01
0.100E+01 0.200E+01 0.200E+01 0.500E+01 0.500E+01 0.500E+01
ISS       16
0.100E+01 0.100E+01 0.100E+01 0.100E+01 0.100E+01 0.100E+01 0.100E+01 0.100E+01
0.100E+01 0.200E+01 0.200E+01 0.500E+01 0.500E+01 0.500E+01 0.150E+02 0.300E+02

```

OUTPUT FILES

PROFILE PLOT

```

PO4      14
 0.200E-01 0.200E-01 0.200E-01 0.200E-01 0.200E-01 0.200E-01 0.200E-01 0.200E-01
 0.200E-01 0.200E-01 0.200E-01 0.200E-01 0.200E-01 0.200E-01
PO4      16
 0.200E-01 0.200E-01 0.200E-01 0.200E-01 0.200E-01 0.200E-01 0.200E-01 0.200E-01
 0.200E-01 0.200E-01 0.200E-01 0.200E-01 0.200E-01 0.200E-01 0.200E-01 0.200E-01
NH4      14
 0.500E-01 0.500E-01 0.500E-01 0.500E-01 0.500E-01 0.500E-01 0.500E-01 0.500E-01
 0.500E-01 0.500E-01 0.500E-01 0.500E-01 0.500E-01 0.500E-01
NH4      16
 0.500E-01 0.500E-01 0.500E-01 0.500E-01 0.500E-01 0.500E-01 0.500E-01 0.500E-01
 0.500E-01 0.500E-01 0.500E-01 0.500E-01 0.500E-01 0.500E-01 0.500E-01 0.500E-01
NO3      14
 0.200E+00 0.200E+00 0.200E+00 0.200E+00 0.200E+00 0.200E+00 0.200E+00 0.200E+00
 0.200E+00 0.200E+00 0.200E+00 0.200E+00 0.200E+00 0.200E+00
NO3      16
 0.200E+00 0.200E+00 0.200E+00 0.200E+00 0.200E+00 0.200E+00 0.200E+00 0.200E+00
 0.200E+00 0.200E+00 0.200E+00 0.200E+00 0.200E+00 0.200E+00 0.200E+00 0.200E+00
LDOM      14
 0.675E+00 0.675E+00 0.675E+00 0.675E+00 0.675E+00 0.675E+00 0.675E+00 0.675E+00
 0.675E+00 0.675E+00 0.675E+00 0.675E+00 0.675E+00 0.675E+00
LDOM      16
 0.675E+00 0.675E+00 0.675E+00 0.675E+00 0.675E+00 0.675E+00 0.675E+00 0.675E+00
 0.675E+00 0.675E+00 0.675E+00 0.675E+00 0.675E+00 0.675E+00 0.675E+00 0.675E+00
RDOM      14
 0.157E+01 0.157E+01 0.157E+01 0.157E+01 0.157E+01 0.157E+01 0.157E+01 0.157E+01
 0.157E+01 0.157E+01 0.157E+01 0.157E+01 0.157E+01 0.157E+01
RDOM      16
 0.157E+01 0.157E+01 0.157E+01 0.157E+01 0.157E+01 0.157E+01 0.157E+01 0.157E+01
 0.157E+01 0.157E+01 0.157E+01 0.157E+01 0.157E+01 0.157E+01 0.157E+01 0.157E+01
LPOM      14
 0.750E+00 0.750E+00 0.750E+00 0.750E+00 0.750E+00 0.750E+00 0.750E+00 0.750E+00
 0.750E+00 0.750E+00 0.750E+00 0.750E+00 0.750E+00 0.750E+00
LPOM      16
 0.750E+00 0.750E+00 0.750E+00 0.750E+00 0.750E+00 0.750E+00 0.750E+00 0.750E+00
 0.750E+00 0.750E+00 0.750E+00 0.750E+00 0.750E+00 0.750E+00 0.750E+00 0.750E+00
ALG1      14
 0.650E+00 0.650E+00 0.650E+00 0.650E+00 0.650E+00 0.650E+00 0.650E+00 0.650E+00
 0.650E+00 0.650E+00 0.650E+00 0.650E+00 0.650E+00 0.650E+00
ALG1      16
 0.650E+00 0.650E+00 0.650E+00 0.650E+00 0.650E+00 0.650E+00 0.650E+00 0.650E+00
 0.650E+00 0.650E+00 0.650E+00 0.650E+00 0.650E+00 0.650E+00 0.650E+00 0.650E+00
DO      14
 0.108E+02 0.107E+02 0.107E+02 0.108E+02 0.108E+02 0.109E+02 0.109E+02 0.109E+02
 0.109E+02 0.110E+02 0.110E+02 0.110E+02 0.110E+02 0.110E+02
DO      16
 0.108E+02 0.107E+02 0.107E+02 0.108E+02 0.108E+02 0.109E+02 0.109E+02 0.109E+02
 0.109E+02 0.110E+02 0.110E+02 0.110E+02 0.110E+02 0.110E+02 0.110E+02 0.110E+02

```

The next output grouping consists of temperature/constituent concentrations output over time for the [dates](#) and [frequencies](#) specified in the control file. The first line includes:

1. Julian date [JDAY]
2. Gregorian date [GDAY]
3. water surface layer number [KTWB]
4. deviation of the water surface [Z] from the top of the surface layer [KT]
5. how many dates information has been written to the file

The next line contains the abbreviated constituent name and the number of active layers at the segment. This is also the number of values that have to be read in the following cards.

```

75.702 Mar 15, 1992 23 -0.1950 1
TEMP      14

```

PROFILE PLOT

OUTPUT FILES

	5.81	5.64	5.48	5.41	5.37	5.35	5.34	5.33
TEMP	5.32	5.32	5.32	5.32	5.32	5.32		
	16							
	6.07	5.89	5.67	5.52	5.41	5.34	5.30	5.29
	5.32	5.34	5.32	5.32	5.31	5.31	5.31	5.31
ISS	14							
	0.674E+00	0.850E+00	0.991E+00	0.116E+01	0.136E+01	0.148E+01	0.166E+01	0.191E+01
	0.208E+01	0.225E+01	0.239E+01	0.250E+01	0.255E+01	0.255E+01		
ISS	16							
	0.611E+00	0.771E+00	0.841E+00	0.873E+00	0.888E+00	0.893E+00	0.891E+00	0.870E+00
	0.877E+00	0.130E+01	0.217E+01	0.279E+01	0.296E+01	0.307E+01	0.307E+01	0.307E+01
PO4	14							
	0.157E-01	0.171E-01	0.182E-01	0.186E-01	0.188E-01	0.189E-01	0.191E-01	0.193E-01
	0.195E-01	0.196E-01	0.197E-01	0.198E-01	0.198E-01	0.198E-01		
PO4	16							
	0.155E-01	0.166E-01	0.177E-01	0.182E-01	0.185E-01	0.187E-01	0.189E-01	0.191E-01
	0.189E-01	0.181E-01	0.185E-01	0.193E-01	0.196E-01	0.199E-01	0.199E-01	0.199E-01
NH4	14							
	0.507E-01	0.507E-01	0.507E-01	0.507E-01	0.507E-01	0.507E-01	0.507E-01	0.507E-01
	0.507E-01	0.506E-01	0.506E-01	0.505E-01	0.503E-01	0.503E-01		
NH4	16							
	0.508E-01	0.508E-01	0.508E-01	0.508E-01	0.508E-01	0.508E-01	0.509E-01	0.509E-01
	0.509E-01	0.510E-01	0.510E-01	0.510E-01	0.510E-01	0.510E-01	0.510E-01	0.510E-01
NO3	14							
	0.200E+00	0.200E+00	0.200E+00	0.200E+00	0.200E+00	0.200E+00	0.200E+00	0.200E+00
	0.200E+00	0.200E+00	0.200E+00	0.200E+00	0.200E+00	0.200E+00		
NO3	16							
	0.200E+00	0.200E+00	0.200E+00	0.200E+00	0.200E+00	0.200E+00	0.200E+00	0.200E+00
	0.200E+00	0.200E+00	0.200E+00	0.200E+00	0.200E+00	0.200E+00	0.200E+00	0.200E+00
LDOM	14							
	0.665E+00	0.666E+00	0.666E+00	0.666E+00	0.666E+00	0.666E+00	0.666E+00	0.666E+00
	0.666E+00	0.666E+00	0.667E+00	0.667E+00	0.668E+00	0.668E+00		
LDOM	16							
	0.664E+00	0.665E+00	0.665E+00	0.665E+00	0.665E+00	0.665E+00	0.665E+00	0.665E+00
	0.665E+00	0.664E+00	0.664E+00	0.664E+00	0.664E+00	0.664E+00	0.664E+00	0.664E+00
RDOM	14							
	0.157E+01	0.157E+01	0.157E+01	0.157E+01	0.157E+01	0.158E+01	0.158E+01	0.158E+01
	0.158E+01	0.158E+01	0.158E+01	0.158E+01	0.158E+01	0.158E+01		
RDOM	16							
	0.157E+01	0.157E+01	0.157E+01	0.157E+01	0.157E+01	0.157E+01	0.157E+01	0.157E+01
	0.157E+01	0.157E+01	0.157E+01	0.157E+01	0.157E+01	0.157E+01	0.157E+01	0.157E+01
LPOM	14							
	0.641E+00	0.697E+00	0.717E+00	0.727E+00	0.732E+00	0.734E+00	0.739E+00	0.742E+00
	0.743E+00	0.744E+00	0.745E+00	0.746E+00	0.747E+00	0.747E+00		
LPOM	16							
	0.624E+00	0.683E+00	0.703E+00	0.711E+00	0.715E+00	0.718E+00	0.719E+00	0.721E+00
	0.728E+00	0.736E+00	0.742E+00	0.743E+00	0.743E+00	0.743E+00	0.743E+00	0.743E+00
ALG1	14							
	0.615E+00	0.636E+00	0.643E+00	0.646E+00	0.647E+00	0.648E+00	0.649E+00	0.650E+00
	0.650E+00	0.651E+00	0.652E+00	0.653E+00	0.655E+00	0.655E+00		
ALG1	16							
	0.607E+00	0.630E+00	0.637E+00	0.639E+00	0.640E+00	0.641E+00	0.641E+00	0.641E+00
	0.643E+00	0.645E+00	0.646E+00	0.646E+00	0.646E+00	0.646E+00	0.646E+00	0.646E+00
DO	14							
	0.110E+02	0.109E+02	0.108E+02	0.108E+02	0.108E+02	0.108E+02	0.108E+02	0.108E+02
	0.109E+02	0.109E+02	0.109E+02	0.109E+02	0.108E+02	0.108E+02		
DO	16							
	0.110E+02	0.109E+02	0.109E+02	0.108E+02	0.108E+02	0.108E+02	0.108E+02	0.108E+02
	0.108E+02	0.109E+02	0.109E+02	0.109E+02	0.109E+02	0.109E+02	0.109E+02	0.109E+02

Vector Plot

The vector plot output writes a binary file that is used by the W2_POST post-processor developed by DSI, Inc.

Contour Plot

As in the profile and vector plot output, this output was originally included for developing DISSPLA contour plots of model output using FORTRAN callable subroutines. The information is sufficient to develop contour plots of temperatures and constituents. Output consists initially of:

1. title cards
2. number of branches [NBR]
3. grid dimensions [KMX] and [IMX]
4. branch upstream and downstream segments [US] and [DS]
5. segment length [DLX]
6. layer heights [H]
7. number of active constituents
8. active constituent names

Each title card takes up a separate line in the output and each of the remaining item number is output on a single line. The user should refer to the code for the actual format of the output. The preceding information is time invariant and is used to set up the plotting grid. During simulations, the following information is output:

1. Julian date [JDAY] and Gregorian date [GDAY]
3. water surface layer [KTWB]
3. tributary inflows [QTR]
4. tributary inflow temperatures [TTR]
5. tributary inflow concentrations for each active constituent [CTR]
6. current upstream segment [CUS]
7. branch inflow [QIN] and the sum of the branch inflow [QSUM]
8. interfacial area (width times height) [BHRKT1] for all active segments in the surface layer [KT]
9. interfacial area [BHR] for all remaining active computational cells
10. horizontal velocities [U]
11. flows [QC]
12. water surface deviations [Z]
13. temperatures
14. constituent concentrations

Currently, the user must develop their own plotting program to use this feature, which will normally require “getting under the hood” of the model to customize model output.

When the TECPLOT option is ON, the output consists of elevation (m), longitudinal distance

CONTOUR PLOT

OUTPUT FILES

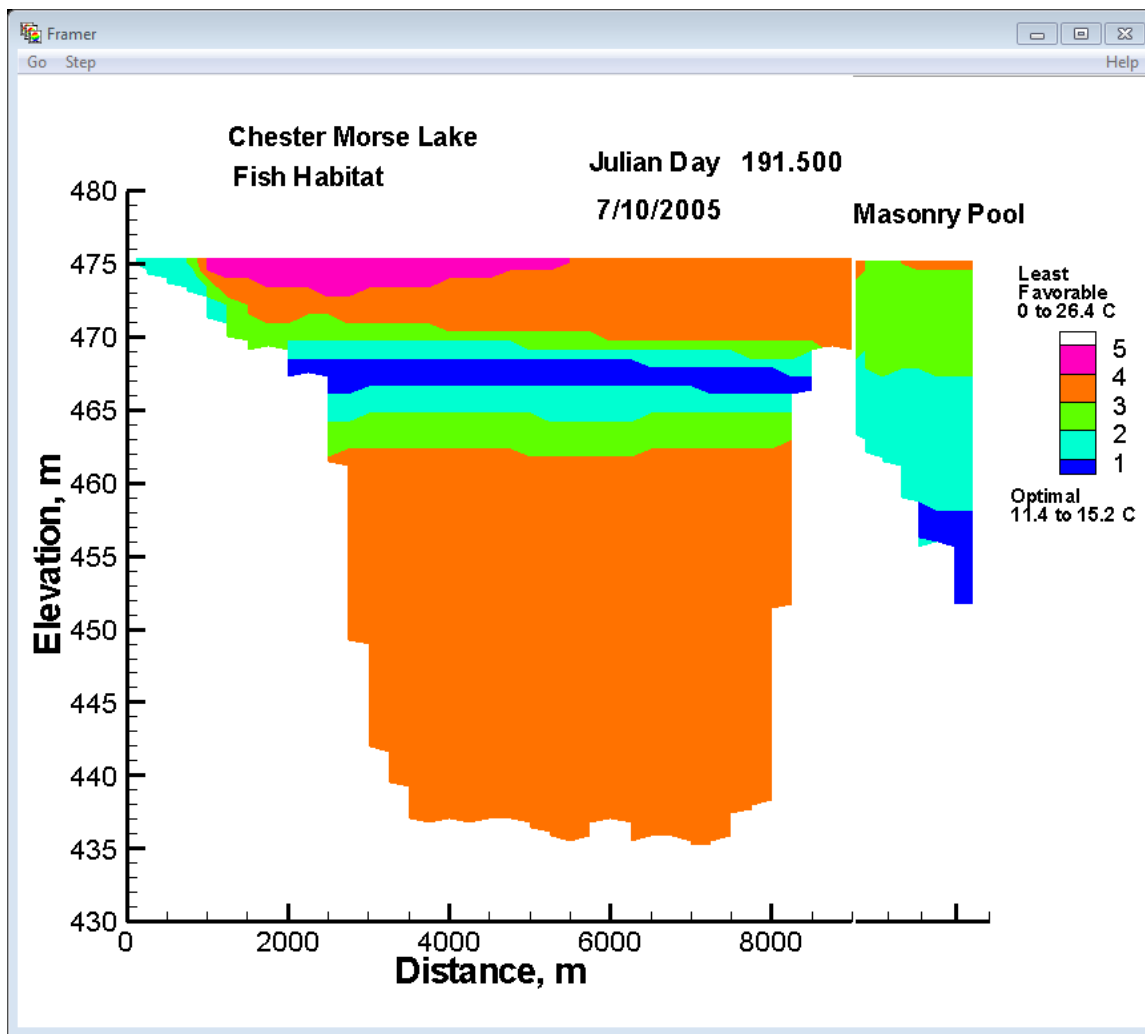
(m), U, W, T, RHO, Fish Habitat# (see below), and all active constituents for the entire grid at the time interval specified in CPL FREQ. For those users of TECPLOT, TECPLOT can read the file directly and the user can create contour animations of any of the variables including superimposed vector plots.

The Fish Habitat # is the fish criterion that is satisfied at that grid point (K,I). For example, consider defining fish criteria in the order of more restrictive to least restrictive. Consider 3 fish criteria defined as follows (See Fish Habitat input file):

```
OptimalFishX,12.0,18.0,5.0  
SuboptimalFishX,10.0,22.0,5.0  
NonOptimalFishX(Lethal),0.0,35.0,4.0
```

where the first 2 numbers are the lower and higher temperature criteria and the last number is the minimum dissolved oxygen level.

The first fish is given a #1, second fish #2, and 3rd fish group #3. In the Tecplot output for each grid point, the fish habitat criteria 1, 2, 3, or 100 (if outside the last range) is written to the Tecplot output file. You can then produce a dynamic movie of habitat areas that are optimal (1), suboptimal (2), not optimal perhaps lethal (3 to 100). An example is shown below for 5 criteria ranked from most favorable to least favorable.



The steps to making a useful contour animation in TECPLOT are as follows:

1. Import data (cpl.opt) file into Tecplot using the Tecplot Data Loader
2. Turn ON contours
3. Reset axes so that they are Independent (Tecplot default is dependent)
4. Turn on Value Blanking since any state variables outside the domain are set to -99. Set value blanking for temperature to any value less than 0.0.
5. Reset the contour intervals since Tecplot automatically uses the -99 as its minimum data value.
6. One can now go to the animation and view the zones (the model output frequency or time of output) to view the movie on screen or sent to an AVI or RM file.
7. Adding vectors is also easy. Turn on vectors and choose U and W as the vector variables. You will have to adjust the arrowhead size and length of the vector until the arrows appear correctly.

Kinetic Fluxes

The ability to compute kinetic fluxes was introduced first in Version 3.2. Two types of output are available. The first is similar to snapshot output and is specified by setting the kinetic flux control variable [\[KFLC\]](#) to ASCII. The segments that are output are currently controlled by the snapshot segments in the control file that are specified for output. The user must then develop a method for plotting up the output in whatever format they decide upon.

The other option for output is a binary format specified as BINARY for the kinetic flux control variable [\[KFLC\]](#). The only information currently output using this option is the entire kinetic source/sink flux array.

In addition another output file named internally in the model as “KFLUX_JW#.OPT” where # is the waterbody number is output for each waterbody. This sums up all the kinetic fluxes for all active cells at the frequency specified for the kinetic flux file (FLX_FREQ). Output format is JDAY, ELTM (elapsed time over which fluxes are summed in days), each active kinetic flux term in kg/day. Example output is shown below.

Example file output (fluxes are in units of kg/day):

JDAY,	ELTM,	PO4AR,	PO4AG,	PO4AP,	PO4ER,	PO4EG,	PO4EP,		
1.002,	0.002,	0.1262E+04,	0.0000E+00,	0.1262E+04,	0.0000E+00,	0.0000E+00,	0.0000E+00,	0.0000E+00,	
1.500,	0.498,	0.1212E+04,	0.1137E+04,	0.7486E+02,	0.1264E+04,	0.4886E+03,	0.7750E+03,		
2.000,	0.500,	0.1299E+04,	0.1720E+04,	-0.4210E+03,	0.1349E+04,	0.7735E+03,	0.5759E+03,		
2.500,	0.500,	0.1267E+04,	0.1291E+04,	-0.2459E+02,	0.1308E+04,	0.5881E+03,	0.7200E+03,		
3.000,	0.500,	0.1355E+04,	0.1966E+04,	-0.6102E+03,	0.1387E+04,	0.9324E+03,	0.4550E+03,		

Hence, the fluxes at JDAY=3.0 above represent the sum of all fluxes between JD 2.5 and JD 3.0 over the ELTM of 0.5 days.

Below is an example of the kinetic flux output in ASCII with a format similar to that of the SNP file.

Note also that the TSR file includes flux output on an instantaneous basis at a given cell location.

OUTPUT FILES

Burnsville Reservoir - March 15 through December 11, 1992
 Density placed inflow, point sink outflows
 Default hydraulic coefficients
 Default light absorption/extinction coefficients
 Default kinetic coefficients
 Temperature and water quality simulation
 Run 8
 Testing sensitivity to wind
 Wind sheltering set to 0.75
 Jim Stiles and Vince Marchese, USACE Huntington District
 Model run at 15:09:49 on 12/04/01

KINETIC FLUXES

	March 15, 1992	Julian Date = 75 days 16.86 hours		DO algal production - source, kg/day								
	2	3	4	5	6	7	8	9	10	11	12	13
23						0.232E-02	0.164E-01	0.558	1.34	7.22	8.22	
24						0.296E-02	0.237E-01	0.375	0.980	4.52	4.99	
25						0.195E-02	0.297E-01	0.316	0.898	4.21	4.38	
26						0.509E-03	0.220E-01	0.267	0.821	3.82	3.85	
27							0.259E-01	0.218	0.702	1.01	1.00	
28							0.201E-01	0.159	0.489	0.567	0.543	
29								0.944E-01	0.270	0.258	0.247	
30								0.569E-01	0.160	0.144	0.138	
31								0.746E-01	0.965E-01	0.770E-01	0.744E-01	
32								0.652E-01	0.583E-01	0.449E-01	0.434E-01	
33								0.431E-01	0.318E-01	0.254E-01	0.246E-01	
34										0.113E-01	0.139E-01	

Withdrawal Outflow

Withdrawal outflow files contain information for plotting any release or withdrawal temperatures and/or constituent concentrations as a time series. The files can also be used to externally link upstream waterbodies to downstream waterbodies so that waterbasins can be broken up into multiple waterbodies. This is an important feature when runtimes for the entire waterbasin become excessive. With this option, calibration can start at the most upstream waterbody and proceed sequentially downstream.

Output consists of up to four separate files for each segment [\[IWDO\]](#) specified in the control file. The files include an outflow, outflow temperature, constituent concentrations, and derived constituent concentrations. These files are for all the withdrawals specified at that segment lumped together if there are multiple withdrawals. The constituent concentration outflow file is only generated if constituent computations [\[CCC\]](#) are turned on. The derived constituent concentration outflow file is generated only if constituent computations [\[CCC\]](#) are turned on and one or more derived constituents [\[CDWBC\]](#) are turned on.

In addition, for the flow and temperature files, individual flows and outlet temperatures are provided to the right of the weighted average (temperature) or summed flow.

Also, whenever withdrawal output is ON (see in w2_con.npt file), a series of individual files are also output for each structure at the withdrawal segment. For example, if there are 2 spillways (weirs), 1 gate and 1 pump, all these withdrawal types are automatically output individually as separate files. They would be output with a fixed internally specified file name based on the hydraulic element and the segment number where it is located, such as: qwo_sp1_seg23.opt, qwo_sp2_seg23.opt, qwo_gt1_seg23.opt, and qwo_pmp1_seg23.opt. For further information, see the withdrawal output card description in w2_con.npt.

EXAMPLE

Flow file for segment 16

To the right of the sum of flows are individual flows starting with QWD then QSTR

JDAY	QWD				
1.002	14.84	0.40	0.00	7.22	7.22
1.200	14.88	0.40	0.00	7.24	7.24
1.400	14.92	0.40	0.00	7.26	7.26
1.600	14.96	0.40	0.00	7.28	7.28

Temperature file for segment 16

To the right of the sum of temperatures are individual temperatures starting with QWD then QSTR

JDAY	T				
1.002	5.00	5.00	0.00	5.00	5.00
1.200	4.98	4.98	0.00	4.98	4.98
1.400	4.96	4.96	0.00	4.96	4.96
1.600	5.00	4.96	0.00	4.99	5.02

Concentration file for segment 24

JDAY	AGE	PO4	NH4	NO3	LDOM	RDOM	LPOM	ALG1	DO
75.706	.696.201E-01	5.09E-01	.200	.665	1.57	.708	.638	46.6	
75.804	.793.202E-01	5.10E-01	.200	.663	1.57	.699	.634	46.0	
75.902	.890.202E-01	5.11E-01	.200	.662	1.57	.693	.632	45.6	
76.000	.987.202E-01	5.12E-01	.200	.660	1.57	.687	.630	45.2	

OUTPUT FILES

WITHDRAWAL OUTFLOW

76.102	1.09.202E-01.513E-01	.201	.659	1.57	.681	.628	44.8
76.201	1.18.202E-01.514E-01	.201	.657	1.57	.676	.626	44.5
76.300	1.29.203E-01.515E-01	.201	.656	1.57	.671	.624	44.1
76.402	1.39.203E-01.516E-01	.201	.655	1.57	.665	.623	43.8
76.500	1.48.203E-01.517E-01	.201	.653	1.57	.661	.622	43.5
76.604	1.59.203E-01.518E-01	.201	.652	1.57	.658	.622	43.2
76.703	1.69.203E-01.519E-01	.201	.651	1.57	.655	.621	43.0
76.806	1.79.204E-01.520E-01	.201	.649	1.57	.652	.621	42.8
76.902	1.89.204E-01.521E-01	.201	.648	1.57	.649	.619	42.5
77.000	1.99.204E-01.522E-01	.201	.647	1.57	.644	.618	42.1
77.102	2.08.204E-01.523E-01	.201	.645	1.57	.637	.616	41.7
77.201	2.18.204E-01.524E-01	.201	.644	1.57	.630	.613	41.3
77.300	2.28.205E-01.525E-01	.201	.642	1.57	.623	.610	40.9
77.400	2.38.205E-01.525E-01	.201	.641	1.57	.616	.608	40.5
77.500	2.48.205E-01.526E-01	.201	.639	1.57	.610	.607	40.1
77.606	2.59.205E-01.527E-01	.201	.638	1.57	.604	.605	39.7
77.702	2.68.205E-01.528E-01	.201	.637	1.57	.599	.604	39.3
77.804	2.78.206E-01.529E-01	.202	.635	1.57	.595	.602	39.0
77.902	2.88.206E-01.530E-01	.202	.634	1.57	.592	.601	38.8
78.000	2.98.206E-01.531E-01	.202	.632	1.57	.590	.600	38.6

Flow Balance Output File

When a Volume_Balance is turned ON, the model outputs a summary of the flow balance for each waterbody based on the output interval for CPL output. If CPL output is turned OFF or Volume-Balance is OFF, then no file will be written. The file name is 'flowbal.opt'. This file is useful in looking at waterbody overall flows. The output file consists of the following information: Julian day, water body #, inflow volume to waterbody from Qin files in m³, inflow volume from precipitation in m³, outflow volume from outlet structures in m³, output volume from withdrawals in m³, output volume from evaporation in m³, input volume from distributed tributaries in m³, and input volume from tributaries in m³. The volumes between Julian days are cumulative, not instantaneous, and are negative for an outflow and positive for an inflow.

An example file is shown below:

```
JDAY, WB, VOLIN (m3) , volpr (m3) , volout (m3) , volwd, volev, voldt, voltrb
1.000, 2, 0.19865109E+02, 0.00000000E+00, -0.59570259E+04, 0.00000000E+00, -
0.33811097E+01, 0.00000000E+00, 0.00000000E+00,
1.500, 2, 0.24879558E+06, 0.00000000E+00, -0.22578373E+07, 0.00000000E+00, -
0.20572546E+04, 0.00000000E+00, 0.00000000E+00,
2.000, 2, 0.39475582E+06, 0.00000000E+00, -0.28715176E+07, 0.00000000E+00, -
0.33273747E+04, 0.00000000E+00, 0.00000000E+00,
2.499, 2, 0.52130494E+06, 0.00000000E+00, -0.31609006E+07, 0.00000000E+00, -
0.37733181E+04, 0.00000000E+00, 0.00000000E+00,
3.000, 2, 0.64398975E+06, 0.00000000E+00, -0.33504191E+07, 0.00000000E+00, -
0.55960240E+04, 0.00000000E+00, 0.00000000E+00,
3.499, 2, 0.75950533E+06, 0.00000000E+00, -0.34985829E+07, 0.00000000E+00, -
0.81305637E+04, 0.00000000E+00, 0.00000000E+00,
3.999, 2, 0.86359619E+06, 0.00000000E+00, -0.36242731E+07, 0.00000000E+00, -
0.10630815E+05, 0.00000000E+00, 0.00000000E+00,
4.499, 2, 0.96960288E+06, 0.00000000E+00, -0.37364633E+07, 0.00000000E+00, -
0.13662457E+05, 0.00000000E+00, 0.00000000E+00,
5.000, 2, 0.10590140E+07, 0.00000000E+00, -0.38389353E+07, 0.00000000E+00, -
0.17216834E+05, 0.00000000E+00, 0.00000000E+00,
5.500, 2, 0.11696562E+07, 0.00000000E+00, -0.39345726E+07, 0.00000000E+00, -
0.20477682E+05, 0.00000000E+00, 0.00000000E+00,
```

Water Level Output File

A convenient file for plotting water level variations as a function of time and space is written out if the TIME_SERIES is ON. The water level at every model segment is written rather than those specified in the TIME_SERIES output. The output file name is 'wl.opt'. The file consists of Julian day followed by the water surface elevation at each model segment in m.

An example file is shown below:

```
JDAY, SEG  2, SEG  3, SEG  4, SEG  5, SEG  6, SEG  7, SEG  8, SEG  9, SEG 10, SEG 11, SEG
12, SEG 13, SEG 14, SEG 15, SEG 16, SEG 17, SEG 18, SEG 19, SEG 20, SEG 21, SEG 22, SEG
23, SEG 24, SEG 25, SEG 26, SEG 27, SEG 28, SEG 29, SEG 30, SEG 31, SEG 32, SEG 33, SEG
34, SEG 35, SEG 36, SEG 37, SEG 38, SEG 39, SEG 40, SEG 41, SEG 42, SEG 43, SEG 44, SEG
45, SEG 46, SEG 47, SEG 48, SEG 49, SEG 50, SEG 51, SEG 52, SEG 53, SEG 54, SEG 55, SEG
56, SEG 57, SEG 58, SEG 59, SEG 60, SEG 61, SEG 62, SEG 63, SEG 64, SEG 65, SEG
1.001, 1484.700, 1484.700, 1484.700, 1484.700, 1484.700, 1484.700, 1484.700, 1484.703, 1484.701, 1484.700, 14
84.700, 1484.700, 1484.700, 1484.700, 1484.700, 1484.699, 1484.698, 1484.696, 1484.691, 1484.691, 1
480.000, 1480.044, 1480.022, 1480.019, 1480.019, 1480.000, 1480.043, 1480.036, 1480.034, 1480.034,
1480.000, 1480.009, 1480.006, 1480.005, 1480.005, 1480.000, 1480.008, 1480.005, 1480.004, 1480.004
, 1473.700, 1473.701, 1473.700, 1473.700, 1473.700, 1470.900, 1470.900, 1470.900, 1470.900, 1470.90
0, 1470.900, 1466.500, 1466.500, 1466.500, 1466.500, 1466.500, 1464.500, 1464.500, 1464.500, 1464.5
00, 1464.500, 1464.000, 1464.000, 1464.000, 1464.000,
1.150, 1484.700, 1484.700, 1484.700, 1484.700, 1484.700, 1484.700, 1484.320, 1484.319, 1484.319, 14
84.319, 1484.700, 1484.317, 1484.317, 1484.317, 1484.317, 1484.317, 1484.317, 1484.317, 1484.317, 1
480.000, 1480.658, 1480.658, 1480.658, 1480.658, 1480.000, 1480.644, 1480.644, 1480.644, 1480.644,
1480.000, 1480.614, 1480.614, 1480.614, 1480.614, 1480.000, 1480.591, 1480.591, 1480.591, 1480.591
, 1473.700, 1474.226, 1474.226, 1474.226, 1474.226, 1470.900, 1470.900, 1470.900, 1470.900, 1470.90
0, 1470.900, 1466.500, 1466.500, 1466.500, 1466.500, 1466.500, 1464.500, 1464.500, 1464.500, 1464.5
00, 1464.500, 1464.000, 1464.000, 1464.000, 1464.000,
```

Run-time Warnings

The model generates the following run-time warnings that can be useful when setting up the model. These are output to the file: **w2.wrn**.

1. Water surface is above the top of layer 2 in segment 'x' at day 'y'

This message is output to inform the user that the water surface elevation has gone above the top of the computational grid. This may be okay or it might indicate that additional layers need to be added to the grid so that the surface layer does not become inappropriately thick. This is a common message when first calibrating the water surface in a reservoir if either the inflows are overestimated or the outflows are underestimated. An application of the model to Lake Roosevelt did not include water pumped to another reservoir and the water surface ended up 70 m above the top of the grid.

*2. Computational warning at Julian day = 'x',' at segment 'y' timestep = 'z'
water surface deviation [Z] = 'x' m layer thickness = 'y' m*

This message indicates that the water surface elevation solution is starting to go unstable and is generally a result of velocities approaching supercritical values. What is happening is that from one timestep to the next, the water surface elevation has gone from residing in layer [KT] to layer [KT]+1, which causes a negative surface layer thickness ([Figure C-4](#)). The surface layer thickness, HKT1, is the layer thickness, H, minus the water surface deviation, z, from the top layer [KT]. As can be seen, this is negative when the solution begins to go unstable.

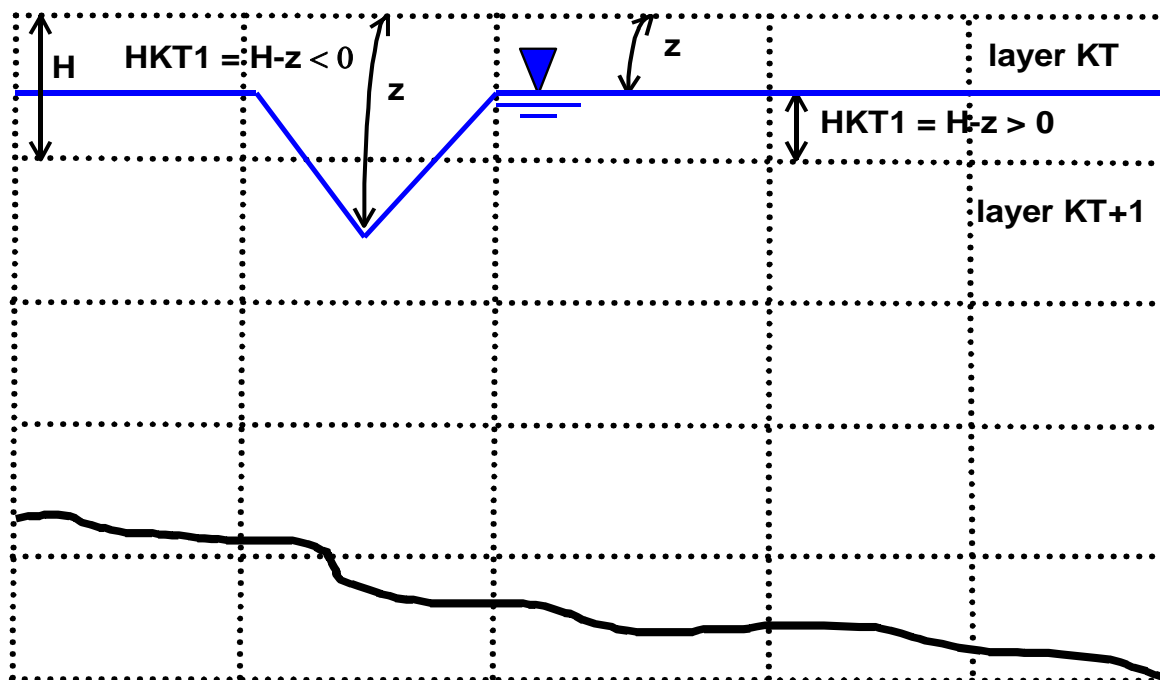


Figure C-4. Diagram illustrating unstable water surface elevation solution.

Normally, when the water surface elevation approaches the bottom of layer [KT], the model would subtract a layer thus allowing the water surface level to decline smoothly over time. However, if the water surface elevation jumps below the bottom of layer [KT] in one timestep, the layer subtraction algorithm does not have a chance to adjust the water surface layer before solving for the velocities.

The model attempts to recover from the instability by decreasing the timestep by 90% and recomputing the water surface elevation. If the current timestep is greater than the minimum timestep [DLTMIN], then the following warning message is then generated.

3. *Unstable water surface elevation on day 'x',
negative surface layer thickness using minimum timestep at iteration 'y'*

If the current timestep is less than or equal to the minimum timestep [DLTMIN], then an error message is output and the run is stopped. However, all is not lost. Based on the Julian date in the warning messages, the user can reduce the maximum timestep [DLTMAX] and/or the fraction of the timestep [DLTF] just prior to the instability and then increase back to the original value(s) sometime later in the simulation. Oftentimes, this allows the model to get through the time period that was generating the instability. This may need to be done for several time periods during the simulation in order to get the model to run to completion, especially for river applications.

If the instability is occurring during high inflow periods, the user also has the option of spreading inflows out over a greater time period in order to reduce the maximum velocities. Care must be taken to ensure that the total inflows remain the same, especially if inflow interpolation [QINIC] is turned on. Likewise, velocities can also be reduced through adjustments to the bathymetry such as making cells wider. If inflows are placed according to density [PQINC] and/or [PQTRC], velocities can also be reduced by using the “distribute evenly from top to bottom” option. Still another option is to increase the minimum number of layers [NLMIN] for a segment to remain active. This has a similar action as distributing the inflow evenly from top to bottom in that it provides more layers for the inflow to be distributed over thus reducing velocities.

Problems in model setup can also generate these warning messages. For instance, if an external head boundary condition is inadvertently set way off from the starting water surface elevation (or vice versa), then large velocities can be generated that result in a water surface instability. Extremely small widths ($<1\text{ m}$) can also cause the same problems.

4. *Low water in segment 'x' water surface deviation = 'y' at day 'z'*

This warning message is to alert the user that water is drying up in a segment with only one active layer. This may mean that more friction is required to hold back water in downstream segments or the segment in question, or that segments upstream may need to have less friction.

5. *Computational warning at Julian day = 'x'
spatial change = 'x' m^3 temporal change = 'y' m^3 volume error = 'z' m^3*

This message is to let the user now that the volume error is more than 1000 m^3 . This should not normally happen unless the user has incorrectly modified the code or the water surface elevation solution has become unstable. The message is more informational and does not require the user to do anything as the volume error is arbitrarily set to 1000 m^3 .

Run-time Errors

The model generates the following run-time error messages and outputs them to the file: **w2.err**

1. Unstable water surface elevation on day 'x' negative surface layer thickness using minimum timestep at iteration 'y'

As discussed in the [RUN-TIME WARNINGS](#) section, this error message is generated by an unstable water surface elevation solution. Refer to that section on methods for eliminating the instability. Additional information is output to the error message file and includes the segment number, the water surface elevation at that segment, the bottom elevation of that segment, and the elevation difference for all segments in the offending branch.

2. Fatal error - Insufficient segments in branch 'x' Julian day = 'y' water surface layer = 'z'

Currently in the model, if the number of segments in a branch becomes less than two due to drying out and subsequent subtraction of upstream segments from the active computational grid, then the model issues this error message and terminates. The reason why is that there must be at least two active segments in a branch for many of the computations to proceed. This error is most common in reservoir simulations. Future plans include bypassing this limitation so that the model runs using only active branches. However, this will involve major coding changes and will take some time to implement.

If this occurs during water surface calibration due to insufficient inflows or excessive outflows, then adjust the flows so that either more water comes in or less water flows out. The user will have to decide the appropriate inflow/outflow to adjust. If this problem occurs with a correct water balance, then one option is to remove the branch from the computational grid and include the branch inflows as a tributary. The missing branch volume should then be evenly distributed throughout the active computational grid cells to ensure that the project volume is conserved.

Another workaround is to add additional depth to the bottom of the branch so that water levels can drop without segments being subtracted. Similarly, the number of active layers required to prevent segment subtraction [\[NLMIN\]](#) can be set to one if it is not already set to that value, which may prevent the branch from going dry.

When the model goes unstable and stops running the code generates 2 files: w2.err and w2error-dump.opt. The first file was described above. The w2error-dump.opt file contains output of several important variables that allow an expert model user to discern what may have led the code to crash. Examples are shown below for each file.

An example of the w2.err file is shown below:

```
Unstable water surface elevation on day 200.039
negative surface layer thickness using minimum timestep at iteration 295
Segment, Surface layer thickness, m, Flow m3/s, U(KT,I) m/s, ELWS, m
37          3.15          92.69          0.63          495.73
38          3.09          95.95          0.76          494.66
39          3.00         -12781.80         -0.30          493.54
40         -88.37         3541556.07       -19427.77          401.16
41          9.73           0.00           0.02          498.24
```

OUTPUT FILES

[illegible]

RUN-TIME ERRORS

T2

OUTPUT FILES

[illegible]

In the windows version of the w2 model, the user can supply a command line argument that sets the working directory of the code. Hence, one does not need to copy the model executable into every directory. In a batch file, for example, one can execute the following command:

```
W2 ivf.exe "C:\scott\w2workshop\2009 workshop\waterqual\problem3"
```

The w2 code now uses the supplied directory (in double quotes) as the working directory for all the files. The command line argument has one blank space between the end of the executable and the first quote. The working directory is displayed in the text box of the window.